

# Final Report - ILAW PCT, VHT, Viscosity, and Electrical Conductivity Model Development, VSL-07R1230-1

Prepared for the U.S. Department of Energy  
Assistant Secretary for Environmental Management

**Office of River Protection**

P.O. Box 450  
Richland, Washington 99352

# Final Report - ILAW PCT, VHT, Viscosity, and Electrical Conductivity Model Development, VSL-07R1230-1

**A. A. Kruger**

Department of Energy - Office of River Protection

**S. K. Cooley**

Pacific Northwest National Laboratory

**I. Joseph**

The Catholic University of America

**I. L. Pegg**

The Catholic University of America

**G. F. Piepel**

Pacific Northwest National Laboratory

**H. Gan**

The Catholic University of America

**I. Muller**

The Catholic University of America

Date Published  
June 2007

Prepared for the U.S. Department of Energy  
Assistant Secretary for Environmental Management

**Office of River Protection**

**P.O. Box 450  
Richland, Washington 99352**

**APPROVED**

*By Julia Raymer at 4:01 pm, Dec 17, 2013*

Release Approval

Date

**Approved for Public Release;  
Further Dissemination Unlimited**

**TRADEMARK DISCLAIMER**

Reference herein to any specific commercial product, process, or service by tradename, trademark, manufacturer, or otherwise, does not necessarily constitute or imply its endorsement, recommendation, or favoring by the United States Government or any agency thereof or its contractors or subcontractors.

This report has been reproduced from the best available copy.

Printed in the United States of America

## **Final Report**

### **ILAW PCT, VHT, Viscosity, and Electrical Conductivity Model Development**

*prepared by*

**Greg F. Piepel and Scott K. Cooley<sup>(a)</sup>**

**Statistical Sciences  
Pacific Northwest National Laboratory  
Richland, WA 99352**

*and*

**Isabelle Muller, Hao Gan, Innocent Joseph, and Ian L. Pegg<sup>(b)</sup>**

**Vitreous State Laboratory  
The Catholic University of America  
Washington, DC 20064**

<sup>(a)</sup> **For the River Protection Project-Waste Treatment Plant  
Support Program for Bechtel National, Inc.**

<sup>(b)</sup> **For Duratek, Inc. and Bechtel National, Inc.**

**April 24, 2007**

***Rev. 0, 6/28/07***

**Document Title:** ILAW PCT, VHT, Viscosity, and Electrical Conductivity Model Development

**Document Number and Revision:** VSL-07R1230-1, Rev. 0

**Issue Date:** 6/28/07

**Performing Organizations:** Vitreous State Laboratory, The Catholic University of America (VSL), Pacific Northwest National Laboratory (PNNL)

**Test Specifications:** 24590-LAW-TSP-RT-01-013, Rev. 1 (VSL)  
24590-WTP-TSP-RT-02-001, Rev. 0 (PNNL)

**Test Exception:** 24590-WTP-TEF-RT-03-040 (PNNL)

**Test Plans:** VSL-02T4800-1, Rev. 1 (VSL)  
TP-RPP-WTP-179, Rev. 1 (PNNL)

**R&T Focus Area(s):** LAW Waste Form Qualification


**Test Scoping Statement(s):** VSL-21, LAW Glass Property Composition Modeling (VSL)  
VSL-22, LAW Processing Properties Models (VSL)  
B-66, Demonstrate Compliance with Glass Durability Requirements for LAW (PNNL)

**Completeness of Testing:**

This report describes the results of work and testing specified by the above-listed Test Specifications, Test Plans, and Text Exception. The work and any associated testing followed established quality assurance requirements and were conducted as authorized. The descriptions provided in this test report are an accurate account of both the conduct of the work and the data collected. Results required by the Test Plans are reported. Also reported are any unusual or anomalous occurrences that are different from the starting hypotheses. The test results and this report have been reviewed and verified.

**I.L. Pegg:**   
**VSL Program Director/Principal Investigator**

**Date:** 6/28/07

**I. Joseph:**   
**Duratek Sub-Contract Manager**

**Date:** 6/28/07

## TABLE OF CONTENTS

List of Appendices .....	vii
List of Tables .....	viii
List of Figures .....	xi
List of Abbreviations .....	xviii
SUMMARY OF TESTING .....	xx
SECTION 1 INTRODUCTION .....	1-1
1.1 Test Objectives.....	1-2
1.2 Test Overview.....	1-3
1.3 How Test Objectives Were Achieved.....	1-4
SECTION 2 DATA FOR LAW GLASS PROPERTY MODELING .....	2-1
2.1 Phase 1 Test Matrix Glasses .....	2-1
2.2 Existing Matrix Glasses .....	2-2
2.3 Phase 1a Augmentation Test Matrix Glasses.....	2-3
2.4 LAW Correlation and High Cr <sub>2</sub> O <sub>3</sub> Correlation Glasses .....	2-4
2.5 High Cr <sub>2</sub> O <sub>3</sub> and P <sub>2</sub> O <sub>5</sub> LAW Glasses .....	2-6
2.6 Remaining Actively Designed LAW Glasses.....	2-6
2.7 Actual LAW Glasses.....	2-8
2.8 Summary of LAW Glasses Available for Property Modeling.....	2-9
SECTION 3 EXPERIMENTAL PROCEDURES AND CALCULATIONS.....	3-1
3.1 Glass Batching and Preparation .....	3-1
3.1.1 Batching of Starting Materials .....	3-1
3.1.2 Glass Preparation .....	3-2
3.2 Analyses of Glass Compositions .....	3-3
3.3 Use of Analyzed SO <sub>3</sub> Values in Normalized Glass Compositions .....	3-4
3.4 Product Consistency Test.....	3-6
3.5 Vapor Hydration Test .....	3-7
3.6 Electrical Conductivity Testing .....	3-8
3.7 Viscosity Testing .....	3-8
3.8 Liquidus Temperature.....	3-8
3.9 Glass Density .....	3-9
SECTION 4 PCT, VHT, ELECTRICAL CONDUCTIVITY, AND VISCOSITY RESULTS... 4-1	
4.1 Product Consistency Test (PCT) Results and Discussion .....	4-1
4.1.1 PCT Results .....	4-1
4.1.2 Discussion of PCT Results.....	4-2
4.2 VHT Results and Discussion .....	4-4
4.2.1 VHT Results.....	4-4
4.2.2 Discussion of VHT Results.....	4-5
4.3 Electrical Conductivity Results and Discussion .....	4-6
4.3.1 Electrical Conductivity Results.....	4-6
4.3.2 Discussion of Electrical Conductivity Results.....	4-7

4.4	Viscosity Results and Discussion .....	4-8
4.4.1	Viscosity Results.....	4-8
4.4.2.	Discussion of Viscosity Results.....	4-9
4.5	Heat Treatment Results and Discussion .....	4-10
4.6	Glass Density Results and Discussion .....	4-12
<b>SECTION 5 MODELS RELATING PCT BORON AND SODIUM RELEASES TO LAW</b>		
	GLASS COMPOSITION.....	5-1
5.1	PCT Release Data Used for Model Development and Validation.....	5-1
5.1.1	PCT Release Model Development Data .....	5-1
5.1.2	Primary PCT Model Validation Approach and Data.....	5-4
5.1.3	Secondary PCT Model Validation Approach and Data.....	5-5
5.1.4	Limited Extrapolative PCT Model Validation Data .....	5-6
5.2	PCT Release Model Forms .....	5-6
5.2.1	PCT Mixture Experiment Model Forms .....	5-6
5.2.2	Normalization and Transformation of PCT Release Values.....	5-8
5.3	Property-Composition Model Results for PCT-B Release .....	5-9
5.3.1	Results from Full LM Model for ILAW PCT-B.....	5-9
5.3.2	Results from Reduced LM Model for ILAW PCT-B .....	5-11
5.3.3	Results from Reduced PQM Model for ILAW PCT-B .....	5-14
5.3.4	Results from Two-Part Reduced LM Model for ILAW PCT-B.....	5-17
5.3.5	Recommended ILAW PCT-B Model .....	5-19
5.4	Property-Composition Model Results for PCT-Na Release .....	5-20
5.4.1	Results from Full LM Model for ILAW PCT-Na.....	5-20
5.4.2	Results from Reduced LM Model for ILAW PCT-Na .....	5-21
5.4.3	Results from Reduced PQM Model for ILAW PCT-Na .....	5-24
5.4.4	Results from Two-Part Reduced LM Model for ILAW PCT-Na.....	5-27
5.4.5	Recommended ILAW PCT-Na Model .....	5-29
5.5	Example Illustrating PCT Model Predictions and Statistical Intervals .....	5-30
5.6	Suitability of the Recommended PCT-B and PCT-Na Models for Application by the WTP Project.....	5-32
<b>SECTION 6 MODELS RELATING VHT ALTERATION DEPTH TO LAW GLASS</b>		
	COMPOSITION .....	6-1
6.1	VHT Alteration Depth Data Used for Model Development and Validation .....	6-1
6.1.1	VHT Alteration Depth Model Development Data.....	6-1
6.1.2	Primary VHT Model Validation Approach and Data.....	6-4
6.1.3	Secondary VHT Model Validation Approach and Data.....	6-5
6.1.4	Limited Extrapolative VHT Model Validation Data .....	6-6
6.2	VHT Alteration Depth Model Forms.....	6-6
6.2.1	VHT Mixture Experiment Model Forms .....	6-6
6.2.2	Transformation of VHT Alteration Depth .....	6-7
6.3	Linear Mixture Model Results for LAW VHT Alteration Depth.....	6-8
6.3.1	Results for Full Linear Mixture Model on VHT Alteration Depth.....	6-9
6.3.2	Results for Reduced Linear Mixture Model on VHT Alteration Depth.....	6-10
6.4	Partial Quadratic Mixture Model Results for LAW VHT Alteration Depth .....	6-12

6.4.1	Results for VHT PQM Model Fit to Modeling Data .....	6-12
6.4.2	Validation Results for the VHT PQM Model .....	6-13
6.5	Two-Part Reduced Linear Mixture Model Results for LAW VHT Alteration Depth.....	6-15
6.6	Partial Cubic Mixture Model Results for LAW VHT Alteration Depth .....	6-16
6.6.1	Results for VHT PCM Model Fit to Modeling Data .....	6-17
6.6.2	Validation Results for the VHT PCM Model .....	6-18
6.7	Summary of Models Considered for LAW VHT Alteration Depth .....	6-19
6.7.1	Single Global Models Considered for VHT $\ln(D)$ .....	6-19
6.7.2	Local Linear Regression Model for VHT $\ln(D)$ .....	6-20
6.7.3	Other Approaches Considered for Modeling VHT Results.....	6-21
6.8	Comparison of VHT Models for $\ln(D)$ .....	6-22
6.9	Decision Process and Recommended Model for VHT Alteration Depth of LAW Glasses.....	6-25
6.10	Example Illustrating VHT Model Predictions and Statistical Intervals.....	6-26
6.11	Suitability of the Recommended VHT Alteration Depth Model for Application by the WTP Project.....	6-28

## SECTION 7 MODELS RELATING ELECTRICAL CONDUCTIVITY TO LAW GLASS

	COMPOSITION AND TEMPERATURE .....	7-1
7.1	Electrical Conductivity Data Used for Model Development and Validation .....	7-1
7.1.1	Electrical Conductivity Model Development Data.....	7-1
7.1.2	Primary Electrical Conductivity Model Validation Approach and Data .....	7-5
7.1.3	Secondary Electrical Conductivity Model Validation Approach and Data .....	7-6
7.1.4	Limited Extrapolative Electrical Conductivity Model Validation Data .....	7-6
7.2	Electrical Conductivity Model Forms.....	7-6
7.2.1	Temperature Dependence of Electrical Conductivity.....	7-7
7.2.2	Model Forms for the Temperature and Composition Dependence of Electrical Conductivity .....	7-7
7.2.3	Transformation of Electrical Conductivity .....	7-8
7.3	Model Results for ILAW Electrical Conductivity with the Arrhenius Equation Parameters Expanded as Linear Mixture Models .....	7-9
7.3.1	Results for 36-Term Electrical Conductivity Model with the Arrhenius Equation Parameters Expanded as 18-Component Linear Mixture Models .....	7-9
7.3.2	Results for 22-Term Electrical Conductivity Model with the Arrhenius Equation Parameters Expanded as Reduced 11-Component Linear Mixture Models .....	7-11
7.4	Investigation of Adding Three Crossproduct Terms to the 22-Term Arrhenius Linear Mixture Model.....	7-14
7.5	Results for the Recommended 25-Term Electrical Conductivity Model.....	7-15
7.5.1	Results for the Recommended 25-Term Electrical Conductivity Model Fitted to the 171-Glass Modeling Dataset .....	7-15
7.5.2	Validation Results for the Recommended 25-Term Electrical Conductivity Model .....	7-16
7.6	Example Illustrating Electrical Conductivity Model Predictions and Statistical Intervals.....	7-18



7.7	Suitability of the Recommended Electrical Conductivity Model for Application by the WTP Project.....	7-20
<b>SECTION 8 MODELS RELATING VISCOSITY TO LAW GLASS COMPOSITION AND TEMPERATURE .....</b>		
	TEMPERATURE .....	8-1
8.1	Viscosity Data Used for Model Development and Validation .....	8-1
8.1.1	Viscosity Model Development Data.....	8-1
8.1.2	Primary Viscosity Model Validation Approach and Data .....	8-3
8.1.3	Secondary Viscosity Model Validation Approach and Data .....	8-4
8.1.4	Limited Extrapolative Viscosity Model Validation Data .....	8-4
8.2	Viscosity Model Forms.....	8-5
8.2.1	Temperature Dependence of Viscosity.....	8-5
8.2.2	Model Forms for the Temperature and Composition Dependence of Viscosity .....	8-5
8.2.3	Transformation of Viscosity .....	8-7
8.3	Model Results for ILAW Viscosity with the Truncated-T2 Equation Parameters Expanded as Linear Mixture Models .....	8-7
8.3.1	Results for 36-Term Viscosity Model with the Truncated-T2 Equation Parameters Expanded as 18-Component Linear Mixture Models .....	8-8
8.3.2	Development of Viscosity Models with the Truncated-T2 Equation Parameters Expanded as Reduced Linear Mixture Models .....	8-10
8.3.3	Results for 24-Term and 22-Term Viscosity Models with the Truncated-T2 Equation Parameters Expanded as 12-Component and 11-Component Reduced Linear Mixture Models .....	8-11
8.4	Investigation of Adding Quadratic Terms to Truncated T2-Linear Mixture Models.....	8-14
8.5	Results for the Recommended 26-Term Viscosity Model.....	8-15
8.5.1	Results for the Recommended 26-Term Viscosity Model Fitted to the 171-Glass Modeling Dataset.....	8-16
8.5.2	Validation Results for the Recommended 26-Term Viscosity Model.....	8-17
8.6	Example Illustrating Viscosity Model Predictions and Statistical Intervals.....	8-19
8.7	Suitability of the Recommended Viscosity Model for Application by the WTP Project.....	8-21
<b>SECTION 9 REGIONS OF VALIDITY FOR LAW GLASS PROPERTY MODELS.....</b>		
9.1	Single-Component Composition and Temperature Constraints .....	9-2
9.2	Multiple-Component Composition and Temperature Constraints.....	9-3
9.2.1	Multiple-Component Property Constraints.....	9-3
9.2.2	Constraints on Pairs of Correlated LAW Glass Components.....	9-4
9.3	Summary and Discussion of LAW Glass Property Model Validity Regions.....	9-5
<b>SECTION 10 SUMMARY AND CONCLUSIONS FOR LAW GLASS PROPERTY-COMPOSITION MODELS.....</b>		
10.1	Summary of ILAW PCT Modeling .....	10-2
10.2	Summary of ILAW VHT Modeling .....	10-3
10.3	Summary of ILAW Electrical Conductivity Modeling .....	10-5
10.4	Summary of ILAW Viscosity Modeling.....	10-7

10.5	Summary of Model Validity Regions for Recommended LAW Glass Property Models.....	10-8
10.6	Suitability of Recommended LAW Glass Property Models for Use by the WTP Project.....	10-9
<b>SECTION 11 RECOMMENDATIONS FOR ANY FUTURE ILAW PROPERTY-COMPOSITION DATA COLLECTION, MODEL DEVELOPMENT, OR MODEL VALIDATION WORK .....</b>		
		11-1
11.1	Recommendations for ILAW PCT .....	11-1
11.2	Recommendations for ILAW VHT .....	11-2
11.3	Recommendations for ILAW Electrical Conductivity and Viscosity.....	11-3
11.4	General Recommendations .....	11-4
11.4.1	Recommendation for Additional Work to Assess Suitability of the Recommended LAW Glass Property Models.....	11-4
11.4.2	Recommendations for Replication.....	11-4
11.4.3	Recommendation to Investigate Local As Well As Global Modeling Approaches .....	11-5
11.4.4	Recommendation for Space-Filling Experimental Design .....	11-6
<b>SECTION 12 QUALITY ASSURANCE .....</b>		12-1
<b>SECTION 13 REFERENCES.....</b>		13-1

**List of Appendices**

Appendix A	Normalized Composition (in mol%) of 271 LAW Simulated and Actual Waste Glasses	A-1
Appendix B	Glass Melt Electrical Conductivity and Viscosity Values Calculated by Arrhenius Regression at a Temperature of 1150°C	B-1
Appendix C	Statistical Methods Used to Develop, Evaluate, and Validate Property-Composition Models	C-1
Appendix D	Variance-Covariance Matrices Associated With Coefficients of ILAW PCT, VHT, Electrical Conductivity, and Viscosity Models	D-1

## List of Tables

	<u>Page #</u>	
Table 2.1.	Components and Constraints <sup>(a)</sup> for ILAW Phase 1 Test Matrix.	T-1
Table 2.2.	Composition of the Grouped Component “Others” for ILAW Phase 1 Test Matrix.	T-2
Table 2.3.	Property Constraints for ILAW Phase 1 Test Matrix.	T-3
Table 2.4.	Model-Based <sup>(a)</sup> Glass Property Constraints for ILAW Phase 1 Test Matrix.	T-4
Table 2.5.	Target Compositions of ILAW Phase 1 Test Matrix Glasses (wt% ).	T-5
Table 2.6.	Target Glass Compositions of Existing Matrix LAW Glasses (wt%).	T-7
Table 2.7.	Target Compositions of LAW Phase 1a Augmentation Test Matrix Glasses (wt%).	T-8
Table 2.8.	Target Values of Others Components in LAW Phase 1a Augmentation Test Matrix Glasses.	T-9
Table 2.9.	Target Compositions of LAW Correlation and High Cr <sub>2</sub> O <sub>3</sub> Correlation Glasses.	T-10
Table 2.10.	Target Values of Others Components in LAW Correlation and High Cr <sub>2</sub> O <sub>3</sub> Correlation Glasses.	T-11
Table 2.11.	Target Compositions of LAW High Cr <sub>2</sub> O <sub>3</sub> and P <sub>2</sub> O <sub>5</sub> Glasses.	T-12
Table 2.12.	Target Values of Others Components in LAW High Cr <sub>2</sub> O <sub>3</sub> and P <sub>2</sub> O <sub>5</sub> Glasses.	T-12
Table 2.13.	Target Compositions of Remaining Actively Designed LAW Glasses (wt%).	T-13
Table 2.14.	Target Values of Others Components in Remaining Actively Designed LAW Glasses (wt%).	T-18
Table 2.15.	Target Compositions of Actual LAW Glasses.	T-23
Table 2.16.	Target Values of Others Components in Actual LAW Glasses.	T-23
Table 2.17.	Groups and Numbers of LAW Glasses with Property Data.	T-24
Table 3.1.	Glass IDs, Target SO <sub>3</sub> Values, and Estimates of Analyzed SO <sub>3</sub> Values for LAW Glasses Not Having SO <sub>3</sub> Analyses	T-25
Table 3.2.	Normalized Compositions (wt%) of 271 LAW Simulated and Actual Waste Glasses with XRF Analyzed or Estimated Values of SO <sub>3</sub> and Target Values of the Remaining Components.	T-26
Table 4.1.	LAW Glasses Having Data for PCT, VHT, Viscosity, and Electrical Conductivity.	T-35
Table 4.2.	PCT Results <sup>(a)</sup> for Simulated and Actual LAW Glasses.	T-39
Table 4.3.	VHT Results for Simulated and Actual LAW Glasses.	T-48
Table 4.4.	Melt Electrical Conductivity Data for Simulated LAW Glasses.	T-53
Table 4.5.	Melt Viscosity Data for Simulated LAW Glasses.	T-57
Table 5.1.	Twenty LAW Glasses Excluded from PCT Modeling Data Set.	T-62
Table 5.2.	Normalized <sup>(a)</sup> Compositions (mass fractions) of 244 LAW Glasses Used for PCT Model Development.	T-63
Table 5.3.	PCT Releases and Data Splitting Validation Sets of 244 LAW Glasses Used for PCT Model Development.	T-70
Table 5.4.	Variation in PCT-Boron and PCT-Sodium Responses for Replicate and Near-Replicate Pairs.	T-75
Table 5.5.	Normalized <sup>(a)</sup> Compositions (mass fractions) for 20 Outlying LAW Glasses Excluded from PCT Modeling Data.	T-76
Table 5.6.	PCT Releases for 20 Outlying LAW Glasses Excluded from the PCT Modeling Set.	T-77
Table 5.7.	Coefficients and Performance Summary for 18-Component Full Linear Mixture Model on the Natural Logarithm of ILAW PCT-B.	T-78
Table 5.8.	Coefficients and Performance Summary for 12-Component Reduced Linear Mixture Model on the Natural Logarithm of ILAW PCT-B.	T-79
Table 5.9.	Coefficients and Performance Summary for 17-Term Reduced Partial Quadratic Mixture Model on the Natural Logarithm of ILAW PCT-B.	T-80
Table 5.10.	Coefficients and Performance Summary for 24-Term Two-Part Reduced Linear Mixture Model on the Natural Logarithm of ILAW PCT-B.	T-81
Table 5.11.	Performance Summary of Four Models on the Natural Logarithm of ILAW PCT-B.	T-82

Table 5.12.	Coefficients and Performance Summary for 18-Component Full Linear Mixture Model on the Natural Logarithm of ILAW PCT-Na.	T-83
Table 5.13.	Coefficients and Performance Summary for 12-Component Reduced Linear Mixture Model on the Natural Logarithm of ILAW PCT-Na.	T-84
Table 5.14.	Coefficients and Performance Summary for 17-Term Reduced Partial Quadratic Mixture Model on the Natural Logarithm of ILAW PCT-Na.	T-85
Table 5.15.	Coefficients and Performance Summary for 24-Term Two-Part Reduced Linear Mixture Model on the Natural Logarithm of ILAW PCT-Na.	T-86
Table 5.16.	Performance Summary of Four Models for the Natural Logarithm of ILAW PCT-Na.	T-87
Table 5.17.	LAWA126 Composition in Formats Needed for Use in ILAW PCT Models.	T-88
Table 5.18.	Predicted PCT Releases and Corresponding 90% UCIs and 95% SUCIs for LAWA126 Composition Used in ILAW PCT Models.	T-89
Table 6.1.	Sixteen LAW Glasses Excluded from VHT Modeling Data Set.	T-90
Table 6.2.	Normalized(a) Compositions (mass fractions) of 165 LAW Glasses Used for VHT Model Development.	T-91
Table 6.3.	VHT Alteration Depths and Data Splitting Validation Sets of 165 LAW Glasses Used for VHT Model Development.	T-96
Table 6.4.	Variation in VHT Responses for Replicate and Near-Replicate Pairs.	T-100
Table 6.5.	Normalized(a) Compositions (mass fractions) for 16 LAW Glasses Excluded from VHT Modeling Data.	T-101
Table 6.6.	VHT Alteration Depths for 16 LAW Glasses Excluded from the VHT Modeling Set.	T-102
Table 6.7.	Coefficients and Performance Summary for 18-Component Full Linear Mixture Model on the Natural Logarithm of ILAW VHT Alteration Depth.	T-103
Table 6.8.	Coefficients and Performance Summary for 11-Component Reduced Linear Mixture Model on the Natural Logarithm of ILAW VHT Alteration Depth.	T-104
Table 6.9.	Coefficients and Performance Summary for 16-Term Reduced Partial Quadratic Mixture Model on the Natural Logarithm of ILAW VHT Alteration Depth.	T-105
Table 6.10.	Coefficients and Performance Summary for 22-Term Two-Part Reduced Linear Mixture Model on the Natural Logarithm of ILAW VHT Alteration Depth.	T-106
Table 6.11.	Terms Included in Models Investigated for VHT Alteration Depth.	T-107
Table 6.12.	Summary of LAW VHT Model Fit and Validation Statistics for 165 Glasses and 80%/20% Data Splits.	T-108
Table 6.13.	Summary of LAW VHT Model Fit (92 Glasses) and Validation Statistics (73 Glasses) from Partitioning the 165 Glasses with VHT Data.	T-109
Table 6.14.	Performance of Fitted Models Predicting (for the Modeling Data) Whether VHT Alteration Depths are Above or Below the Limit of 453 $\mu\text{m}$ Corresponding to 50 $\text{g}/\text{m}^2/\text{day}$	T-110
Table 6.15.	Performance of Fitted ILAW VHT Alteration Depth Models Below and Above a Cut-Off Value. <sup>(a)</sup>	T-111
Table 6.16.	Coefficients and Performance Summary for 15-Term Reduced Partial Cubic Mixture Model on the Natural Logarithm of ILAW VHT Alteration Depth.	T-112
Table 6.17.	LAWA126 Composition in Formats Needed for Use in ILAW VHT Models.	T-113
Table 6.18.	Predicted VHT Alteration Depths and Corresponding 90% UCIs and 95% SUCIs for LAWA126 Composition Used in ILAW VHT Models.	T-114
Table 7.1.	Ten LAW Glasses Excluded from the Electrical Conductivity and Viscosity Modeling Data Sets.	T-115
Table 7.2.	Normalized(a) Compositions (mass fractions) of 171 LAW Glasses Used for Electrical Conductivity and Viscosity Model Development.	T-116
Table 7.3.	Temperature and Electrical Conductivity Observations and Data-Splitting Validation Sets for Each of the 171 LAW Glasses Used for Electrical Conductivity Model Development.	T-122
Table 7.4.	Variation in Electrical Conductivity Values for Replicate and Near-Replicate Pairs.	T-126
Table 7.5.	Normalized(a) Compositions (mass fractions) for 10 Outlying LAW Glasses Excluded from the Electrical Conductivity and Viscosity Modeling Data.	T-127
Table 7.6.	Temperature and Electrical Conductivity Observations for 10 Outlying LAW Glasses Excluded from the Electrical Conductivity Modeling Set.	T-128

Table 7.7.	Coefficients and Performance Summary for 36-Term Arrhenius-Linear Mixture Model on the Natural Logarithm of ILAW Electrical Conductivity.	T-129
Table 7.8.	Coefficients and Performance Summary for 22-Term Reduced Arrhenius-Linear Mixture Model on the Natural Logarithm of ILAW Electrical Conductivity.	T-130
Table 7.9.	Summary Statistics for Various Models Fitted and Validated Using ILAW Electrical Conductivity Data.	T-131
Table 7.10.	Coefficients and Performance Summary for 25-Term Reduced Arrhenius-Linear Mixture Model with Three Crossproduct Terms on the Natural Logarithm of ILAW Electrical Conductivity.	T-132
Table 7.11.	LAWA126 Composition in Formats Needed for Use in ILAW Electrical Conductivity Models.	T-133
Table 7.12.	Predicted Electrical Conductivity and Corresponding 90% UCIs and 95% SUCIs for LAWA126 Composition Used in ILAW Electrical Conductivity Models.	T-134
Table 8.1.	Temperature and Viscosity Observations and Data-Splitting Validation Sets for Each of the 171 LAW Glasses Used for Viscosity Model Development.	T-135
Table 8.2.	Variation in Viscosity Values for Replicate and Near-Replicate Pairs.	T-140
Table 8.3.	Temperature and Viscosity Observations for 10 Outlying LAW Glasses Excluded from the Viscosity Modeling Set.	T-141
Table 8.4.	Coefficients and Performance Summary for 36-Term Truncated T2-Linear Mixture Model on the Natural Logarithm of ILAW Viscosity.	T-142
Table 8.5.	Summary Statistics for Various Models Fitted and Validated Using ILAW Viscosity Data.	T-143
Table 8.6.	Coefficients and Performance Summary for 24-Term Reduced Truncated T2-Linear Mixture Model on the Natural Logarithm of ILAW Viscosity.	T-144
Table 8.7.	Coefficients and Performance Summary for 22-Term Reduced Truncated T2-Linear Mixture Model on the Natural Logarithm of ILAW Viscosity.	T-145
Table 8.8.	Coefficients and Performance Summary for 26-Term Reduced Truncated T2-Linear Mixture Model with Four Quadratic Terms on the Natural Logarithm of ILAW Viscosity.	T-146
Table 8.9.	LAWA126 Composition in Formats Needed for Use in ILAW Viscosity Models.	T-147
Table 8.10.	Predicted Viscosity and Corresponding 90% UCIs and 95% SUCIs for LAWA126 Composition Used in ILAW Viscosity Models.	T-148
Table 9.1.	Minimums and Maximums of LAW Glass Components (in Mass Fractions) for Compositions in the Modeling Datasets for Each LAW Glass Property.	T-149
Table 9.2.	Lower and Upper Bounds on LAW Glass Components (in Mass Fractions) that Partially Define the Composition Validity Region for ILAW Property Models.	T-150
Table 9.3.	Minimum and Maximum Temperatures at Which Electrical Conductivity and Viscosity were Measured for LAW Glass Compositions in the Modeling Datasets Along with the Lower and Upper Bounds on Temperature that Partially Define the Validity Region for ILAW Electrical Conductivity and Viscosity Models.	T-151
Table 9.4.	Minimums and Maximums of LAW Glass Property Values for Compositions in the Modeling Dataset for Each LAW Glass Property.	T-151
Table 9.5.	Indirect Multiple-Component and Multiple-Variable Constraints Via Constraints on LAW Glass Properties(a) that Partially Define the Composition Validity Region for ILAW Property Models.	T-152
Table 9.6.	Summary of Constraints Specifying the Model Validity Region for each LAW Glass Property.	T-152

## List of Figures

	<u>Page #</u>	
Figure 3.1.	Centerline Canister Cooling Curve Used for Heat Treatment of LA137SRCCC	F-1
Figure 3.2.	Data and Regression Equations Relating Analyzed SO <sub>3</sub> to Target SO <sub>3</sub>	F-2
Figure 4.1.	Ranges of PCT Releases (B, Na, and Si, in g/m <sup>2</sup> ) for the 264 LAW Glasses with PCT Data, by Sub-Groups of Glasses.	F-3
Figure 4.2.	PCT Sodium and Silicon Releases (g/m <sup>2</sup> ) as a Function of PCT Boron Release for 264 LAW Glasses with PCT Data.	F-4
Figure 4.3.	Measured pH at 20°C in the 7-day PCT Leachate as a Function of the Sum of Alkali Oxides (Li <sub>2</sub> O+Na <sub>2</sub> O+K <sub>2</sub> O) in mol % for 262 LAW Glasses with PCT Data	F-5
Figure 4.4.	Plot of the PCT Boron Release as a Function of the pH Measured at 20°C in the 7-day PCT Leachate for 264 LAW Glasses with PCT Data.	F-6
Figure 4.5.	PCT Boron Release as a Function of the Sum of Alkali Oxides (Li <sub>2</sub> O+Na <sub>2</sub> O+K <sub>2</sub> O) in mol % for 264 LAW Glasses with PCT Data.	F-7
Figure 4.6.	PCT Sodium Release as a Function of the Sum of Alkali Oxides (Li <sub>2</sub> O+Na <sub>2</sub> O+K <sub>2</sub> O) in mol % for 264 LAW Glasses with PCT Data.	F-8
Figure 4.7.	PCT Boron Release as a Function of the Sum of Alkali and Alkaline Earth Oxides (Li <sub>2</sub> O+Na <sub>2</sub> O+K <sub>2</sub> O+CaO+MgO) in mol % for 264 LAW Glasses with PCT Data.	F-9
Figure 4.8.	PCT Boron Release as a Function of the Sum of Valence III, IV, and V Components (SiO <sub>2</sub> +ZrO <sub>2</sub> +P <sub>2</sub> O <sub>5</sub> +B <sub>2</sub> O <sub>3</sub> + Al <sub>2</sub> O <sub>3</sub> +Fe <sub>2</sub> O <sub>3</sub> ) in mol % for 264 LAW Glasses with PCT Data.	F-10
Figure 4.9.	PCT Boron Release as a Function of the Ratio of Alkali Oxides (Li <sub>2</sub> O+Na <sub>2</sub> O+K <sub>2</sub> O) to Glass Formers (SiO <sub>2</sub> +ZrO <sub>2</sub> +P <sub>2</sub> O <sub>5</sub> +B <sub>2</sub> O <sub>3</sub> + Al <sub>2</sub> O <sub>3</sub> +Fe <sub>2</sub> O <sub>3</sub> ) in mol % for 264 LAW Glasses with PCT Data.	F-11
Figure 4.10.	PCT Boron Release as a Function of the Ratio of Alkali and Alkaline Earth Oxides (Li <sub>2</sub> O+Na <sub>2</sub> O+K <sub>2</sub> O+CaO+MgO) to Glass Formers (SiO <sub>2</sub> +ZrO <sub>2</sub> +P <sub>2</sub> O <sub>5</sub> +B <sub>2</sub> O <sub>3</sub> + Al <sub>2</sub> O <sub>3</sub> +Fe <sub>2</sub> O <sub>3</sub> ) in mol % for 264 LAW Glasses with PCT Data.	F-12
Figure 4.11.	VHT Alteration Depth (in μm) as a Function of the Sum of Alkali Oxides (Li <sub>2</sub> O+Na <sub>2</sub> O+K <sub>2</sub> O) in mol % for 181 LAW Glasses with VHT Data.	F-13
Figure 4.12.	VHT Alteration Depth (in μm) as a Function of the Sum of Alkali and Alkaline Earth Oxides (Li <sub>2</sub> O+Na <sub>2</sub> O+K <sub>2</sub> O+CaO+MgO) in mol % for 181 LAW Glasses with VHT Data.	F-14
Figure 4.13.	VHT Alteration Depth (in μm) as a Function of the Sum of Valence III, IV, and V Components (SiO <sub>2</sub> +ZrO <sub>2</sub> +P <sub>2</sub> O <sub>5</sub> +B <sub>2</sub> O <sub>3</sub> + Al <sub>2</sub> O <sub>3</sub> +Fe <sub>2</sub> O <sub>3</sub> ) in mol % for 181 LAW Glasses with VHT Data	F-15
Figure 4.14.	VHT Alteration Depth (in μm) as a Function of the Ratio of Alkali Oxides (Li <sub>2</sub> O+Na <sub>2</sub> O+K <sub>2</sub> O) to Glass Formers (SiO <sub>2</sub> +ZrO <sub>2</sub> +P <sub>2</sub> O <sub>5</sub> +B <sub>2</sub> O <sub>3</sub> + Al <sub>2</sub> O <sub>3</sub> +Fe <sub>2</sub> O <sub>3</sub> ) in mol % for 181 LAW Glasses with VHT Data	F-16
Figure 4.15.	Distribution of Temperature Values for each of 181 LAW Glasses with Electrical Conductivity Data.	F-17
Figure 4.16.	Temperature Dependence of Electrical Conductivity for Each of 181 LAW Glasses with Electrical Conductivity Data.	F-17
Figure 4.17.	Glass Melt Electrical Conductivity Calculated by Arrhenius Equation Fit (in S/cm) at 1150°C as a Function of the Sum of Alkali Oxides (Li <sub>2</sub> O+Na <sub>2</sub> O+K <sub>2</sub> O) in mol % for 181 LAW Glasses with Electrical Conductivity Data.	F-18
Figure 4.18.	Glass Melt Electrical Conductivity Calculated by Arrhenius Equation Fit (in S/cm) at 1150°C as a Function of the Sum of Alkali and Alkaline Earth Oxides (Li <sub>2</sub> O+Na <sub>2</sub> O+K <sub>2</sub> O+CaO+MgO) in mol % for 181 LAW Glasses with Electrical Conductivity Data.	F-19

Figure 4.19.	Glass Melt Electrical Conductivity Calculated by Arrhenius Equation Fit (in S/cm) at 1150°C as a Function of the Sum of Valence III, IV, and V Components ( $\text{SiO}_2+\text{ZrO}_2+\text{P}_2\text{O}_5+\text{B}_2\text{O}_3+\text{Al}_2\text{O}_3+\text{Fe}_2\text{O}_3$ ) in mol % for 181 LAW Glasses with Electrical Conductivity Data.	F-19
Figure 4.20.	Distribution of Temperature Values for each of 181 LAW Glasses with Viscosity Data.	F-20
Figure 4.21.	Temperature Dependence of Viscosity for Each of 181 LAW Glasses with Viscosity Data.	F-20
Figure 4.22.	Glass Melt Viscosity Calculated by Arrhenius Equation Fit (in poise) at 1150°C as a Function of the Sum of Alkali Oxides ( $\text{Li}_2\text{O}+\text{Na}_2\text{O}+\text{K}_2\text{O}$ ) in mol % for 181 LAW Glasses with Melt Viscosity Data.	F-21
Figure 4.23.	Glass Melt Viscosity Calculated by Arrhenius Equation Fit (in poise) at 1150°C as a Function of the Sum of Alkali and Alkaline Earth Oxides ( $\text{Li}_2\text{O}+\text{Na}_2\text{O}+\text{K}_2\text{O}+\text{CaO}+\text{MgO}$ ) in mol % for 181 LAW Glasses with Melt Viscosity Data.	F-21
Figure 4.24.	Glass Melt Viscosity Calculated by Arrhenius Equation Fit (in poise) at 1150°C as a Function of the Sum of Alkali, Alkaline Earth and Boron Oxides ( $\text{Li}_2\text{O}+\text{Na}_2\text{O}+\text{K}_2\text{O}+\text{CaO}+\text{MgO}+\text{B}_2\text{O}_3$ ) in mol % for 181 LAW Glasses with Melt Viscosity Data.	F-22
Figure 4.25.	Glass Melt Viscosity Calculated by Arrhenius Equation Fit (in poise) at 1150°C as a Function of $\text{SiO}_2+\text{ZrO}_2+\text{P}_2\text{O}_5+\text{B}_2\text{O}_3+\text{Al}_2\text{O}_3+\text{Fe}_2\text{O}_3$ in mol % for 181 LAW Glasses with Melt Viscosity Data.	F-23
Figure 4.26.	Glass Melt Viscosity Calculated by Arrhenius Equation Fit (in poise) at 1150°C as a Function of the Ratio of Alkali and Alkaline Earth Oxides ( $\text{Li}_2\text{O}+\text{Na}_2\text{O}+\text{K}_2\text{O}+\text{CaO}+\text{MgO}+\text{B}_2\text{O}_3$ ) to Glass Former Oxides ( $\text{SiO}_2+\text{ZrO}_2+\text{P}_2\text{O}_5+\text{Al}_2\text{O}_3+\text{Fe}_2\text{O}_3$ ) in mol % for 181 LAW Glasses with Melt Viscosity Data.	F-24
Figure 4.27.	Densities of LAW Glasses.	F-25
Figure 5.1.	Plots Showing Ranges and Distributions of Values (mass fractions) for 14 Main Components in 264 LAW Glasses with PCT Data.	F-26
Figure 5.2.	Plots Showing Ranges and Distributions of Values (mass fractions) for 19 Minor Components in 264 LAW Glasses with PCT Data.	F-27
Figure 5.3.	Plots Showing Ranges and Distributions of Values (mass fractions) for 14 Main Components in 244 LAW Glasses Used for PCT Model Development (20 Outliers Excluded).	F-28
Figure 5.4.	Plots Showing Ranges and Distributions of Values (mass fractions) for 19 Minor Components in 244 LAW Glasses Used for PCT Model Development (20 Outliers Excluded).	F-29
Figure 5.5.	Scatterplot Matrix of 18 Components (mass fractions) for 244 LAW Glasses in the PCT Modeling Data Set	F-30
Figure 5.6.	Predicted Versus Measured Plot for 18-Component Full Linear Mixture Model on ILAW PCT-B.	F-31
Figure 5.7.	Response Trace Plot for 18-Component Full Linear Mixture Model on ILAW PCT-B.	F-31
Figure 5.8.	Predicted Versus Measured Plot for 12-Component Reduced Linear Mixture Model on ILAW PCT-B.	F-32
Figure 5.9.	Response Trace Plot for 12-Component Reduced Linear Mixture Model on ILAW PCT-B.	F-32
Figure 5.10.	Standardized Residuals Plot for 12-Component Reduced Linear Mixture Model on ILAW PCT-B.	F-33
Figure 5.11.	Predicted Versus Measured Plot for 12-Component Reduced Linear Mixture Model on ILAW PCT-B Fitted to Modeling Subset of 97 Glasses and Applied to Validation Subset of 147 Glasses. Error bars are 95% prediction intervals (PIs).	F-33

Figure 5.12.	Predicted Versus Measured Plot for 12-Component Reduced Linear Mixture Model on ILAW PCT-B Fitted to 244 Modeling Set Glasses and Applied to 20 Outlying Glasses. Error bars are 95% prediction intervals (PIs).	F-34
Figure 5.13.	Predicted Versus Measured Plot for 17-Term Reduced Partial Quadratic Mixture Model on ILAW PCT-B.	F-34
Figure 5.14.	Response Trace Plot for 17-Term Reduced Partial Quadratic Mixture Model on ILAW PCT-B.	F-35
Figure 5.15.	Standardized Residuals Plot for 17-Term Reduced Partial Quadratic Mixture Model on ILAW PCT-B.	F-35
Figure 5.16.	Predicted Versus Measured Plot for 17-Term Reduced Partial Quadratic Mixture Model on ILAW PCT-B Fitted to Modeling Subset of 97 Glasses and Applied to Validation Subset of 147 Glasses.	F-36
Figure 5.17.	Predicted Versus Measured Plot for 17-Term Reduced Partial Quadratic Mixture Model on ILAW PCT-B Fitted to 244 Modeling Set Glasses and Applied to 20 Outlying Glasses.	F-36
Figure 5.18.	Predicted Versus Measured Plot for 12-Term Reduced Linear Mixture Model on ILAW PCT-B Fitted to 244 Modeling Glasses.	F-37
Figure 5.19.	Predicted Versus Measured Plot for 24-Term Two-Part Reduced Linear Mixture Model on ILAW PCT-B Fitted to 244 Modeling Glasses	F-37
Figure 5.20.	Predicted Versus Measured Plot for 24-Term Two-Part Reduced Linear Mixture Model on ILAW PCT-B Fitted to 244 Modeling Set Glasses and Applied to 20 Outlying Glasses.	F-38
Figure 5.21.	Predicted Versus Measured Plot for 18-Component Full Linear Mixture Model on ILAW PCT-Na.	F-39
Figure 5.22.	Response Trace Plot for 18-Component Full Linear Mixture Model on ILAW PCT-Na.	F-39
Figure 5.23.	Predicted Versus Measured Plot for 12-Component Reduced Linear Mixture Model on ILAW PCT-Na.	F-40
Figure 5.24.	Response Trace Plot for 12-Component Reduced Linear Mixture Model on ILAW PCT-Na.	F-40
Figure 5.25.	Standardized Residuals Plot for 12-Component Reduced Linear Mixture Model on ILAW PCT-Na.	F-41
Figure 5.26.	Predicted Versus Measured Plot for 12-Component Reduced Linear Mixture Model on ILAW PCT-Na Fitted to Modeling Subset of 97 Glasses and Applied to Validation Subset of 147 Glasses.	F-41
Figure 5.27.	Predicted Versus Measured Plot for 12-Component Reduced Linear Mixture Model on ILAW PCT-Na Fitted to 244 Modeling Set Glasses and Applied to 20 Outlying Glasses.	F-42
Figure 5.28.	Predicted Versus Measured Plot for 17-Term Reduced Partial Quadratic Mixture Model on ILAW PCT-Na.	F-42
Figure 5.29.	Response Trace Plot for 17-Term Reduced Partial Quadratic Mixture Model on ILAW PCT-Na.	F-43
Figure 5.30.	Standardized Residuals Plot for 17-Term Reduced Partial Quadratic Mixture Model on ILAW PCT-Na.	F-43
Figure 5.31.	Predicted Versus Measured Plot for 17-Term Reduced Partial Quadratic Mixture Model on ILAW PCT-Na Fitted to Modeling Subset of 97 Glasses and Applied to Validation Subset of 147 Glasses.	F-44
Figure 5.32.	Predicted Versus Measured Plot for 17-Term Reduced Partial Quadratic Mixture Model on ILAW PCT-Na Fitted to 244 Modeling Set Glasses and Applied to 20 Outlying Glasses.	F-44
Figure 5.33.	Predicted Versus Measured Plot for 12-Component Reduced Linear Mixture Model on ILAW PCT-Na Fitted to 244 Modeling Glasses.	F-45
Figure 5.34.	Predicted Versus Measured Plot for 24-Term Two-Part Reduced Linear Mixture Model on ILAW PCT-Na Fitted to 244 Modeling Glasses.	F-45



Figure 5.35.	Predicted Versus Measured Plot for 24-Term Two-Part Reduced Linear Mixture Model on ILAW PCT-Na Fitted to 244 Modeling Set Glasses and Applied to 20 Outlying Glasses.	F-46
Figure 6.1.	Plots Showing Ranges and Distributions of Values (mass fractions) for 14 Main Components in 175 LAW Glasses with VHT Data.	F-47
Figure 6.2.	Plots Showing Ranges and Distributions of Values (mass fractions) for 19 Minor Components in 175 LAW Glasses with VHT Data.	F-48
Figure 6.3.	Plots Showing Ranges and Distributions of Values (mass fractions) for 14 Main Components in 165 LAW Glasses Used for VHT Model Development (10 Outliers Excluded).	F-49
Figure 6.4.	Plots Showing Ranges and Distributions of Values (mass fractions) for 19 Minor Components in 165 LAW Glasses Used for VHT Model Development (10 Outliers Excluded).	F-50
Figure 6.5.	Scatterplot Matrix of 18 Components (mass fractions) for 165 LAW Glasses in the VHT Modeling Data Set.	F-51
Figure 6.6.	Predicted Versus Measured Plot for 18-Component Full Linear Mixture Model on ILAW VHT Alteration Depth ( $D$ ).	F-52
Figure 6.7.	Response Trace Plot for 18-Component Full Linear Mixture Model on ILAW VHT Alteration Depth.	F-52
Figure 6.8.	Predicted Versus Measured Plot for 11-Component Reduced Linear Mixture Model on ILAW VHT Alteration Depth ( $D$ ).	F-53
Figure 6.9.	Response Trace Plot for 11-Component Reduced Linear Mixture Model on ILAW VHT Alteration Depth.	F-53
Figure 6.10.	Standardized Residuals Plot for 11-Component Reduced Linear Mixture Model on ILAW VHT Alteration Depth.	F-54
Figure 6.11.	Predicted Versus Measured Plot for 11-Component Reduced Linear Mixture Model on VHT Alteration Depth Fitted to Modeling Subset of 92 Glasses and Applied to Validation Subset of 73 Glasses.	F-54
Figure 6.12.	Predicted Versus Measured Plot for 11-Component Reduced Linear Mixture Model on ILAW VHT Alteration Depth Fitted to 165 Modeling Set Glasses and Applied to 10 Outlying Glasses.	F-55
Figure 6.13.	Predicted Versus Measured Plot for 16-Term Reduced Partial Quadratic Mixture Model on ILAW VHT Alteration Depth ( $D$ ).	F-55
Figure 6.14.	Response Trace Plot for 16-Term Reduced Partial Quadratic Mixture Model on ILAW VHT Alteration Depth.	F-56
Figure 6.15.	Standardized Residuals Plot for 16-Term Reduced Partial Quadratic Mixture Model on ILAW VHT Alteration Depth.	F-56
Figure 6.16.	Predicted Versus Measured Plot for 16-Term Reduced Partial Quadratic Mixture Model on ILAW VHT Alteration Depth Fitted to Modeling Subset of 92 Glasses and Applied to Validation Subset of 73 Glasses.	F-57
Figure 6.17.	Predicted Versus Measured Plot for 16-Term Reduced Partial Quadratic Mixture Model on ILAW VHT Alteration Depth Fitted to 165 Modeling Set Glasses and Applied to 10 Outlying Glasses.	F-57
Figure 6.18.	Predicted Versus Measured Plot for 11-Term Reduced Linear Mixture Model on ILAW VHT Alteration Depth Fitted to 165 Modeling Glasses.	F-58
Figure 6.19.	Predicted Versus Measured Plot for 22-Term Two-Part Reduced Linear Mixture Model on ILAW VHT Alteration Depth Fitted to 165 Modeling Glasses.	F-58
Figure 6.20.	Predicted Versus Measured Plot for 15-Term Reduced Partial Cubic Mixture Model on ILAW VHT Alteration Depth ( $D$ ).	F-59
Figure 6.21.	Response Trace Plot for 15-Term Reduced Partial Cubic Mixture Model on ILAW VHT Alteration Depth.	F-59
Figure 6.22.	Standardized Residuals Plot for 15-Term Reduced Partial Cubic Mixture Model on ILAW VHT Alteration Depth.	F-60

Figure 6.23.	Predicted Versus Measured Plot for 15-Term Reduced Partial Cubic Mixture Model on VHT Alteration Depth Fitted to Modeling Subset of 92 Glasses and Applied to Validation Subset of 73 Glasses.	F-60
Figure 6.24.	Predicted Versus Measured Plot for 15-Term Reduced Partial Cubic Mixture Model on ILAW VHT Alteration Depth Fitted to 165 Modeling Set Glasses and Applied to 10 Outlying Glasses.	F-61
Figure 7.1.	Distributions of 14 Main Components (in mass fractions) for 181 LAW Glass Compositions with Viscosity and Electrical Conductivity Data.	F-62
Figure 7.2.	Distributions of 19 Minor Components (in mass fractions) for 181 LAW Glass Compositions with Viscosity and Electrical Conductivity Data.	F-63
Figure 7.3.	Distributions of 14 Main Components (in mass fractions) for the 171 LAW Glass Compositions with Viscosity and Electrical Conductivity Data that Remain After Excluding 10 Glasses with “Outliers” in Individual Components.	F-64
Figure 7.4.	Distributions of 19 Minor Components (in mass fractions) for the 171 LAW Glass Compositions with Viscosity and Electrical Conductivity Data that Remain After Excluding 10 Glasses with “Outliers” in Individual Components.	F-65
Figure 7.5.	Scatterplot Matrix of 18 Components (mass fractions) for 171 LAW Glasses with Viscosity and Electrical Conductivity Data that Remain After Excluding 10 Glasses with “Outliers” in Individual Components.	F-66
Figure 7.6.	Predicted Versus Measured Plot for 36-Term ILAW Electrical Conductivity Model with the Two Parameters of the Arrhenius Equation Expressed as 18-Component Linear Mixture Models.	F-67
Figure 7.7.	Standardized Residuals Plot for 36-Term ILAW Electrical Conductivity Model with the Two Parameters of the Arrhenius Equation Expressed as 18-Component Linear Mixture Models.	F-67
Figure 7.8a.	Response Trace Plot for ILAW Electrical Conductivity at 950°C Constructed Using the 36-Term Arrhenius-Linear Mixture Model.	F-68
Figure 7.8b.	Response Trace Plot for ILAW Electrical Conductivity at 1050°C Constructed Using the 36-Term Arrhenius-Linear Mixture Model.	F-68
Figure 7.8c.	Response Trace Plot for ILAW Electrical Conductivity at 1150°C Constructed Using the 36-Term Arrhenius-Linear Mixture Model.	F-69
Figure 7.8d.	Response Trace Plot for ILAW Electrical Conductivity at 1250°C Constructed Using the 36-Term Arrhenius-Linear Mixture Model.	F-69
Figure 7.9.	Predicted Versus Measured Plot for 22-Term ILAW Electrical Conductivity Model with the Two Parameters of the Arrhenius Equation Expressed as Reduced 11-Component Linear Mixture Models.	F-70
Figure 7.10.	Standardized Residuals Plot for 22-Term ILAW Electrical Conductivity Model with the Two Parameters of the Arrhenius Equation Expressed as Reduced 11-Component Linear Mixture Models.	F-70
Figure 7.11a.	Response Trace Plot for ILAW Electrical Conductivity at 950°C Constructed Using the 22-Term Arrhenius-Linear Mixture Model.	F-71
Figure 7.11b.	Response Trace Plot for ILAW Electrical Conductivity at 1050°C Constructed Using the 22-Term Arrhenius-Linear Mixture Model.	F-71
Figure 7.11c.	Response Trace Plot for ILAW Electrical Conductivity at 1150°C Constructed Using the 22-Term Arrhenius-Linear Mixture Model.	F-72
Figure 7.11d.	Response Trace Plot for ILAW Electrical Conductivity at 1250°C Constructed Using the 22-Term Arrhenius-Linear Mixture Model.	F-72
Figure 7.12.	Predicted Versus Measured Plot for 22-Term Arrhenius-Linear Model on ILAW Electrical Conductivity Fitted to Modeling Subset of 86 Glasses and Applied to Validation Subset of 85 Glasses.	F-73
Figure 7.13.	Predicted Versus Measured Plot for 22-Term Arrhenius-Linear Model on ILAW Electrical Conductivity Fitted to 171 Modeling Set Glasses and Applied to 10 Outlying Glasses.	F-73
Figure 7.14.	Predicted Versus Measured Plot for 25-Term Arrhenius-Linear Mixture Model with Three Crossproduct Terms on ILAW Electrical Conductivity.	F-74

Figure 7.15.	Standardized Residuals Plot for 25-Term Arrhenius-Linear Mixture Model with Three Crossproduct Terms on ILAW Electrical Conductivity.	F-74
Figure 7.16a.	Response Trace Plot for ILAW Electrical Conductivity at 950°C Constructed Using the 25-Term Arrhenius-Linear Mixture Model with Three Crossproduct Terms.	F-75
Figure 7.16b.	Response Trace Plot for ILAW Electrical Conductivity at 1050°C Constructed Using the 25-Term Arrhenius-Linear Mixture Model with Three Crossproduct Terms.	F-75
Figure 7.16c.	Response Trace Plot for ILAW Electrical Conductivity at 1150°C Constructed Using the 25-Term Arrhenius-Linear Mixture Model with Three Crossproduct Terms.	F-76
Figure 7.16d.	Response Trace Plot for ILAW Electrical Conductivity at 1250°C Constructed Using the 25-Term Arrhenius-Linear Mixture Model with Three Crossproduct Terms.	F-76
Figure 7.17.	Predicted Versus Measured Plot for 25-Term Arrhenius-Linear Model with Three Crossproduct Terms on ILAW Electrical Conductivity Fitted to Modeling Subset of 86 Glasses and Applied to Validation Subset of 85 Glasses.	F-77
Figure 7.18.	Predicted Versus Measured Plot for 25-Term Arrhenius-Linear Model with Three Crossproduct Terms on ILAW Electrical Conductivity Fitted to 171 Modeling Set Glasses and Applied to 10 Outlying Glasses.	F-77
Figure 8.1.	Predicted Versus Measured Plot for 36-Term ILAW Viscosity Model with the Two Parameters of the Truncated-T2 Equation Expressed as 18-Component Linear Mixture Models.	F-78
Figure 8.2.	Standardized Residuals Plot for 36-Term ILAW Viscosity Model with the Two Parameters of the Truncated-T2 Equation Expressed as 18-Component Linear Mixture Models.	F-78
Figure 8.3a.	Response Trace Plot for ILAW Viscosity at 950°C Constructed Using the 36-Term Truncated T2-Linear Mixture Model.	F-79
Figure 8.3b.	Response Trace Plot for ILAW Viscosity at 1050°C Constructed Using the 36-Term Truncated T2-Linear Mixture Model.	F-79
Figure 8.3c.	Response Trace Plot for ILAW Viscosity at 1150°C Constructed Using the 36-Term Truncated T2-Linear Mixture Model.	F-80
Figure 8.3d.	Response Trace Plot for ILAW Viscosity at 1250°C Constructed Using the 36-Term Truncated T2-Linear Mixture Model.	F-80
Figure 8.4.	Plots of the Akaike Information Criterion (AIC) and Sum-of-Squared Errors (SSE) Versus the Number of Mixture Components in Truncated T2-Linear Mixture Models for ILAW Viscosity.	F-81
Figure 8.5.	Predicted Versus Measured Plot for 24-Term ILAW Viscosity Model with the Two Parameters of the Truncated-T2 Equation Expressed as Reduced 12-Component Linear Mixture Models.	F-82
Figure 8.6.	Standardized Residuals Plot for 24-Term ILAW Viscosity Model with the Two Parameters of the Truncated-T2 Equation Expressed as Reduced 12-Component Linear Mixture Models.	F-82
Figure 8.7a.	Response Trace Plot for ILAW Viscosity at 950°C Constructed Using the 24-Term Truncated T2-Linear Mixture Model.	F-83
Figure 8.7b.	Response Trace Plot for ILAW Viscosity at 1050°C Constructed Using the 24-Term Truncated T2-Linear Mixture Model.	F-83
Figure 8.7c.	Response Trace Plot for ILAW Viscosity at 1150°C Constructed Using the 24-Term Truncated T2-Linear Mixture Model.	F-84
Figure 8.7d.	Response Trace Plot for ILAW Viscosity at 1250°C Constructed Using the 24-Term Truncated T2-Linear Mixture Model.	F-84
Figure 8.8.	Predicted Versus Measured Plot for 24-Term Truncated T2-Linear Model on ILAW Viscosity Fitted to Modeling Subset of 86 Glasses and Applied to Validation Subset of 85 Glasses.	F-85
Figure 8.9.	Predicted Versus Measured Plot for 24-Term Truncated T2-Linear Model on ILAW Viscosity Fitted to 171 Modeling Set Glasses and Applied to 10 Outlying Glasses.	F-85
Figure 8.10.	Predicted Versus Measured Plot for 22-Term ILAW Viscosity Model with the Two Parameters of the Truncated-T2 Equation Expressed as Reduced 11-Component Linear Mixture Models.	F-86

Figure 8.11.	Standardized Residuals Plot for 22-Term ILAW Viscosity Model with the Two Parameters of the Truncated-T2 Equation Expressed as Reduced 11-Component Linear Mixture Models.	F-86
Figure 8.12.	Predicted Versus Measured Plot for 26-Term Reduced Truncated T2-Linear Mixture Model with Four Quadratic Terms on ILAW Viscosity.	F-87
Figure 8.13.	Standardized Residuals Plot for 26-Term Reduced Truncated T2-Linear Mixture Model with Four Quadratic Terms on ILAW Viscosity.	F-87
Figure 8.14a.	Response Trace Plot for ILAW Viscosity at 950°C Constructed Using the 26-Term Reduced Truncated T2-Linear Mixture Model with Four Quadratic Terms.	F-88
Figure 8.14b.	Response Trace Plot for ILAW Viscosity at 1050°C Constructed Using the 26-Term Reduced Truncated T2-Linear Mixture Model with Four Quadratic Terms.	F-88
Figure 8.14c.	Response Trace Plot for ILAW Viscosity at 1150°C Constructed Using the 26-Term Reduced Truncated T2-Linear Mixture Model with Four Quadratic Terms.	F-89
Figure 8.14d.	Response Trace Plot for ILAW Viscosity at 1250°C Constructed Using the 26-Term Reduced Truncated T2-Linear Mixture Model with Four Quadratic Terms.	F-89
Figure 8.15.	Predicted Versus Measured Plot for the 26-Term Reduced Truncated T2-Linear Model with Four Quadratic Terms on ILAW Viscosity Fitted to Modeling Subset of 86 Glasses and Applied to Validation Subset of 85 Glasses.	F-90
Figure 8.16.	Predicted Versus Measured Plot for the 26-Term Reduced Truncated T2-Linear Model with Four Quadratic Terms on ILAW Viscosity Fitted to 171 Modeling Set Glasses and Applied to 10 Outlying Glasses	F-90
Figure 9.1.	Lower and Upper Bound Lines on LAW Glass Electrical Conductivity as Functions of Temperature.	F-91
Figure 9.2.	Lower and Upper Bound Lines on LAW Glass Viscosity as Functions of Temperature.	F-92
Figure 9.3.	Lower and Upper Bound Constraints on LAW Glass Li <sub>2</sub> O and Na <sub>2</sub> O Values.	F-93

## List of Abbreviations

AA	Atomic Absorption
ANL-LRM	Argonne National Laboratory – Low Activity Reference Material
ASTM	American Society for Testing and Materials
BNFL	British Nuclear Fuels Limited
BNI	Bechtel National, Inc.
CCC	Container Centerline Cooling
CI	Confidence Interval (two-sided)
CUA	The Catholic University of America
DCP	Direct Current Plasma Emission Spectroscopy
DCP-AES	Direct Current Plasma Atomic Emission Spectroscopy
DOE	Department of Energy
GLS	Generalized Least Squares
HLW	High Level Waste
IC	Ion Chromatography
ICP-AES	Inductively Coupled Plasma Atomic Emission Spectroscopy
ID	Identification
IHLW	Immobilized High Level Waste
ILAW	Immobilized Low Activity Waste
LAW	Low Activity Waste
LCI	Lower Confidence Interval
LM	Linear Mixture
LOF	Lack of Fit
MAXR	Maximum R-Squared Improvement
MSE	Mean Squared Error (from regression)
NIST	National Institute of Standards and Technology
ORP	Office of River Protection
PCM	Partial Cubic Mixture
PCT	Product Consistency Test
PI	Prediction Interval
PNNL	Pacific Northwest National Laboratory
PNWD	Battelle–Pacific Northwest Division
PQM	Partial Quadratic Mixture
QA	Quality Assurance
QAPjP	Quality Assurance Project Plan for Testing Programs Generating Environmental Regulatory Data
R&T	Research & Technology
RCRA	Resource Conservation and Recovery Act
RMSE	Root Mean Squared Error
RPP	River Protection Project
RSD	Relative Standard Deviation
SD	Standard Deviation
SEM	Scanning Electron Microscopy
SRL-EA	Savannah River Laboratory-Environmental Assessment (Glass)
SRTC	Savannah River Technology Center
SSE	Sum of Squared Errors
SUCI	Simultaneous Upper Confidence Intervals
TCLP	Toxicity Characteristic Leaching Procedure
TFCOUP	Tank Farm Contractor Operation and Utilization Plan
TRU	Transuranic
UCI	Upper Confidence Interval
ULS	Unweighted Least Squares
VHT	Vapor Hydration Test
VSL	Vitreous State Laboratory

**List of Abbreviations (continued)**

WLS	Weighted Least Squares
WTP	Hanford Tank Waste Treatment and Immobilization Plant
XRF	X-Ray Fluorescence

## SUMMARY OF TESTING

### A) Objectives

This report is the last in a series of currently scheduled reports that presents the results from the Low Activity Waste (LAW) glass formulation development and testing work performed at the Vitreous State Laboratory (VSL) of the Catholic University of America (CUA) and the development of ILAW property-composition models performed jointly by Pacific Northwest National Laboratory (PNNL) and VSL for the Hanford Tank Waste Treatment and Immobilization Plant (WTP) Project. Specifically, this report presents results of glass testing at VSL and model development at PNNL for Product Consistency Test (PCT), Vapor Hydration Test (VHT), viscosity, and electrical conductivity. The models presented in this report may be augmented and additional validation work performed during any future ILAW model development work. Completion of the test objectives is addressed in Table S.1.

**Table S.1. Completion Status of Test Objectives.**

Test Objective	Objective Met (Y/N)	Discussion
Develop property-composition models and supporting data that relate ILAW performance on the PCT to ILAW composition and are suitable for predicting the PCT performance of ILAW glasses to be produced in the WTP.	Yes	The PCT models are described in Section 5. The supporting data and experimental methods are described in Sections 2, 3, and 4.
Develop property-composition models and supporting data that relate ILAW performance on the VHT to ILAW composition and are suitable for predicting the VHT performance of ILAW glasses to be produced in the WTP.	Yes	The VHT models are described in Section 6. The supporting data and experimental methods are described in Sections 2, 3, and 4.
Develop property-composition models that relate viscosity and electrical conductivity of glass melts to ILAW composition and are suitable for predicting the properties of ILAW glasses to be produced in the WTP.	Yes	The electrical conductivity models are described in Section 7. The viscosity models are described in Section 8. The supporting data and experimental methods are described in Sections 2, 3, and 4.

**Table S.1. Completion Status of Test Objectives (continued).**

Test Objective	Objective Met (Y/N)	Discussion
Develop bounding models for ILAW TCLP response. Such models are expected to be appropriate for LAW glasses as a result of the very low levels of RCRA elements in the LAW streams.	Yes	The bounding approach for ILAW TCLP response was developed and documented in a previous report (Kot et al. 2003).
Develop bounding models for ILAW liquidus temperature. Such models are expected to be appropriate for LAW glasses as a result of their consistently low liquidus values in comparison to the nominal melter operating temperature.	Yes; partially	Data on crystal content after heat treatment, which provide bounds on the liquidus temperature, are reported and discussed in Section 4.5. No model is proposed in view of the rare instances of crystallization. A bounding liquidus model is proposed which could be developed further, if so directed by the WTP Research and Technology (R&T) organization.
Develop property-composition models that relate density of ILAW glasses to composition in order to predict overall volumes of ILAW that would be produced from a given waste feed.	Yes; partially	Density data for a number of LAW glasses are reported and discussed in Section 4.6. WTP R&T concluded that it is not necessary to develop a property-composition model for ILAW density because all of the measured density values for LAW glasses are below the effective contract limit of 3.7 g/cc.

**B) Test Exceptions**

Test Exception 24590-WTP-TEF-RT-03-040 (Westsik 2003) applies to the PNNL Test Specification (Swanberg 2002) and Test Plan TP-RPP-WTP-179, Rev. 0. The Test Exception specifies that PNNL modeling of viscosity and electrical conductivity will only occur in Phase 2 (which is covered in this report), rather than both Phase 1 and Phase 2 as had been previously planned. The Test Exception was addressed by Rev. 1 of the Test Plan (Piepel and Cooley 2002).

**C) Results and Performance Against Success Criteria**

The subsequent subsections summarize the results for (i) property-composition data, (ii) modeling results for the PCT, VHT, electrical conductivity, and viscosity properties of LAW



glasses, and (iii) model validity region. Table S.2 summarizes the locations of the key results for the recommended model for each property as well as the alternative (second choice) model, if any.

**Table S.2. Locations of Results for Recommended LAW Glass Property Models.**

LAW Glass Property	Recommended Model		Second-Choice Model		Example Calculations
	Model Results	Variance-Covariance Matrix	Model Results	Variance-Covariance Matrix	
PCT-B	Table 5.9	Table D.2	N/A	N/A	Section 5.5
PCT-Na	Table 5.14	Table D.4	N/A	N/A	Section 5.5
VHT	Table 6.11	Table D.7	Table 6.9	Table D.6	Section 6.10
EC <sup>(a)</sup>	Table 7.10	Table D.9	N/A	N/A	Section 7.6
Viscosity	Table 8.8	Table D.11	N/A	N/A	Section 8.6

(a) EC = Electrical conductivity.

(b) N/A = Not applicable.

#### Property-Composition Data for Modeling ILAW Properties

The PCT boron releases of the glasses in the dataset varied from 0.08 g/m<sup>2</sup> to 17.83 g/m<sup>2</sup>, PCT sodium releases varied from 0.11 g/m<sup>2</sup> to 11.47 g/m<sup>2</sup>, and PCT silicon releases varied from 0.06 g/m<sup>2</sup> to 1.19 g/m<sup>2</sup>. The actively-designed glasses were designed to be compliant with ILAW performance requirements and, therefore, their PCT boron releases are less than 2 g/m<sup>2</sup>, which is the WTP contract limit. The statistically-designed glasses, however, were designed to cover a larger composition region and, accordingly, their PCT responses varied by a larger amount. It is desirable to have some glasses in the modeling dataset that have PCT releases ranging from somewhat below to somewhat above the limit. This allows for more confident use of the model in discerning between glasses with acceptable and unacceptable PCT releases. Of the 264 glasses with PCT data, nine had PCT boron releases above 2 g/m<sup>2</sup>, and eight had PCT sodium releases above 2 g/m<sup>2</sup>. All PCT silicon releases were below the contract limit of 2 g/m<sup>2</sup>. In general, the PCT releases increased as the alkali and alkaline earth oxide concentrations in the glass increased and the glass former oxide concentrations decreased.

The WTP PCT specification requires that the normalized mass losses of boron, sodium, and silicon in a seven-day PCT at 90°C individually be less than 2 g/m<sup>2</sup>. However, a review of the data showed that the normalized PCT mass losses for boron and sodium were *always* higher than the normalized PCT mass loss for silicon. Furthermore, for *every one* of the glasses in the dataset, the normalized PCT mass loss for silicon was below the WTP contract limit of 2 g/m<sup>2</sup>. These results are consistent with earlier conclusions that: (i) if the boron and sodium mass losses are below the WTP limit, so too will be the silicon mass loss, and (ii) the silicon mass loss does not exceed the WTP limit over the LAW glass composition region of interest. Therefore, similar to the conclusion reached in the earlier phase of ILAW model development, it was decided that a

model for silicon PCT response is not needed. Accordingly, with concurrence from the WTP Project, only PCT boron and sodium releases were modeled.

The VHT results for the LAW glasses in the modeling dataset varied from 0.1 g/m<sup>2</sup>/day to 108.2 g/m<sup>2</sup>/day, as compared to the contract requirement of < 50 g/m<sup>2</sup>/day. Six glasses were altered completely before the end of the 24-day test period so that only a greater-than value could be obtained for the alteration rate. Similar to the PCT results, the VHT alteration rates of the actively-designed glasses were generally below the contract limit by design, whereas the VHT alteration rates for the statistically-designed glasses showed larger variations with more glasses showing alteration rates above the WTP contract limit. It is desirable to have some glasses in the modeling dataset that have VHT alteration rates ranging from somewhat below to somewhat above the limit. This allows for more confident use of the model in discerning between glasses with acceptable and unacceptable VHT alteration rates. Of the 181 glasses with VHT data, 20 showed VHT alteration rates that are higher than the WTP contract limit of 50 g/m<sup>2</sup>/day. The VHT alteration rates, in general, increased as the alkali and alkaline earth oxide concentrations in the glass increased and the glass former oxide concentrations decreased, though the correlation was not as pronounced as in the case of PCT.

The electrical conductivity of the glass melts in the dataset ranges from 0.073 S/cm to 0.732 S/cm, as compared to the WTP specified range of 0.1 S/cm to 0.7 S/cm in the temperature range of 1100 to 1200°C. Of 188 electrical conductivity measurements taken in this temperature range, eight were outside that range, with five below and three above the respective limits. The electrical conductivity of the glasses increased with temperature. Among glass constituents, alkali oxide concentration had the most noticeable effect on electrical conductivity, which increased as the alkali oxide concentration increased. This is expected because electrical conductivity in these glasses is mostly ionic, and alkalis provide the most mobile ions.

The viscosity of the glass melts in the dataset ranges from 6 to 2329 poise, with smaller values at higher temperatures and higher values at lower temperatures. Five glasses had viscosities exceeding the recommended WTP upper limit of 150 poise at 1100°C with interpolated values in the range of 161 to 208 poise. The viscosity of the glasses decreased with increases in the concentrations of alkali, alkaline earth, and boron oxides and decreases in the concentrations of other glass former oxides.

### ILAW Property-Composition Model Development, Validation, and Performance

All data in the modeling dataset for a given property were used to develop models for that property. Model validation was accomplished by data-splitting, data-partitioning, and by applying the models to calculate the properties of outlying glass compositions. In the data-splitting approach, the modeling dataset was split into five sets of modeling and validation subsets, using roughly 80% of the data for modeling and 20% for validation. In the data partition approach, the modeling datasets were partitioned into a modeling dataset (comprised of the Existing, Phase 1 Test Matrix, and Phase 1a Augmentation subsets, which were statistically designed) and a validation subset (comprised of all remaining glasses, most or all of which were actively designed). Finally, property models fit to the full modeling dataset were applied to predict property values for the outlying glasses removed from the modeling dataset. This

provides a limited basis to judge the extrapolative capability of the LAW glass property models. Based on the performance of the models that were investigated, recommended models were selected.

The work in this report is limited to the development, validation, and quantification of uncertainty in property-composition models for LAW glasses. This work satisfied the success criteria of developing property-composition models suitable for predicting the properties of LAW glasses. However, it is outside the scope of work covered by this report to completely assess the suitability of the recommended property models. Ultimately, the WTP project needs to assess whether the recommended models, along with their corresponding uncertainties, are suitable for their various intended uses (e.g., glass formulation, addition of glass-forming chemicals to waste during LAW vitrification operations, and compliance with WTP contract specifications and processing constraints). Such assessments are within the scopes for algorithm development and verification (work being conducted by WTP project staff) and statistical compliance methodology development and demonstration (work under PNNL B-6069 scope). Initial statistical compliance methodology development and demonstration work was conducted for earlier versions of property-composition models (Piepel et al. 2005). That work is planned by the WTP project to be updated by PNNL in FY2009 for the models presented in this report. Similarly, the initial iteration of ILAW algorithm work that was performed (Muller et al. 2004b, Vienna 2005) is scheduled for a second iteration.

### PCT Modeling Results for LAW Glasses

For PCT-B and PCT-Na releases from LAW glasses, several model forms were investigated, including a linear mixture (LM) model, reduced LM models, partial quadratic mixture (PQM) models, and a two-part model consisting of two reduced LM models fitted above and below a PCT-B or PCT-Na release cutoff value selected to optimize the fit of the two-part model to the modeling data.

Based on model fitting and validation results, the 17-term PQM models are recommended for predicting PCT-B and PCT-Na releases from LAW glasses. The 12 linear terms ( $\text{Al}_2\text{O}_3$ ,  $\text{B}_2\text{O}_3$ ,  $\text{CaO}$ ,  $\text{Fe}_2\text{O}_3$ ,  $\text{K}_2\text{O}$ ,  $\text{Li}_2\text{O}$ ,  $\text{MgO}$ ,  $\text{Na}_2\text{O}$ ,  $\text{P}_2\text{O}_5$ ,  $\text{SiO}_2$ ,  $\text{ZrO}_2$ , and Others) are for the same components in each of the PCT-B and PCT-Na PQM models. The five quadratic terms in the PCT-B model are  $\text{CaO}\times\text{Li}_2\text{O}$ ,  $\text{B}_2\text{O}_3\times\text{MgO}$ ,  $\text{B}_2\text{O}_3\times\text{Li}_2\text{O}$ ,  $\text{Na}_2\text{O}\times\text{SiO}_2$ , and  $\text{CaO}\times\text{Fe}_2\text{O}_3$ . Results for the PCT-B 17-term PQM model are given in Table 5.9 and discussed in Section 5.3.3. The five quadratic terms in the PCT-Na model are  $\text{CaO}\times\text{Li}_2\text{O}$ ,  $\text{CaO}\times\text{Fe}_2\text{O}_3$ ,  $\text{B}_2\text{O}_3\times\text{MgO}$ ,  $\text{B}_2\text{O}_3\times\text{Na}_2\text{O}$ , and  $\text{K}_2\text{O}\times\text{K}_2\text{O}$ . Results for the PCT-Na 17-term PQM model are given in Table 5.14 and discussed in Section 5.4.3. Methods for making PCT-B and PCT-Na predictions and quantifying the uncertainties in the predictions are discussed and illustrated in Section 5.5.

The recommended 17-term PQM models for PCT-B and PCT-Na appear to reduce the tendency of the 12-term LM models to under-predict these releases near and above the 4 g/L (2 g/m<sup>2</sup>) WTP contract limit. However, the recommended 17-term models still tend to under-predict PCT-B and PCT-Na releases above approximately 2.7 g/L. The PCT modeling database contained an insufficient number of glasses with PCT-B and PCT-Na releases near and above the

contract limits to develop and validate models without this limitation. Hence, constraints were included in the model validity region to restrict the use of the recommended PCT-B and PCT-Na models to glasses with predicted releases below 2.7 g/L. The model validity region constraints are discussed in Section 9.

Because of the magnitudes of uncertainties in the PCT data (i.e., from making simulated LAW glasses, PCT testing, and chemical analysis of leachates), as well as some lack-of-fit of the recommended PCT-B and PCT-Na models, prediction uncertainties for the models are relatively large (see Section 5.6). Unless higher waste loadings are pursued, it is relatively easy to formulate LAW glasses with PCT-B and PCT-Na releases substantially below the contract limit, so the model limitations (under-predictions of releases near and above contract limits, as well as relatively large prediction uncertainties) may not unduly restrict WTP LAW vitrification operations. Separate work that will be performed to assess the impact of LAW glass composition and model uncertainties for the recommended PCT-B and PCT-Na models is discussed in Section 10.6.

### VHT Modeling Results for LAW Glasses

Several model forms were investigated for VHT alteration of LAW glasses including an LM model, reduced LM models, PQM models, a two-part model consisting of two reduced LM models fitted above and below a VHT alteration depth cutoff value selected to optimize the fit of the two-part model to the modeling data, and several mixture experiment models containing cubic terms, which are denoted partial cubic mixture (PCM) models. In addition, a preliminary investigation of local linear regression models was also performed.

Based on an extensive comparison of model fitting, validation, and other results, a 15-term PCM model consisting of 11 linear terms ( $\text{Al}_2\text{O}_3$ ,  $\text{B}_2\text{O}_3$ ,  $\text{CaO}$ ,  $\text{Fe}_2\text{O}_3$ ,  $\text{K}_2\text{O}$ ,  $\text{Li}_2\text{O}$ ,  $\text{MgO}$ ,  $\text{Na}_2\text{O}$ ,  $\text{SiO}_2$ ,  $\text{ZrO}_2$ , and Others) and four cubic terms [ $(\text{K}_2\text{O})^2 \times \text{Na}_2\text{O}$ ,  $(\text{Na}_2\text{O})^3$ ,  $\text{Li}_2\text{O} \times \text{Na}_2\text{O} \times \text{SiO}_2$ , and  $\text{B}_2\text{O}_3 \times \text{CaO} \times \text{Na}_2\text{O}$ ] was recommended for predicting the VHT alteration of LAW glasses. Results for this 15-term PCM model are given in Table 6.11 and discussed in Section 6.6. A second-choice alternate model containing quadratic but no cubic terms was also suggested. That 16-term PQM model consists of the same 11 linear terms and 5 quadratic terms ( $\text{CaO} \times \text{SiO}_2$ ,  $(\text{K}_2\text{O})^2$ ,  $\text{MgO} \times \text{Na}_2\text{O}$ ,  $\text{Al}_2\text{O}_3 \times \text{ZrO}_2$ , and  $\text{Na}_2\text{O} \times \text{ZrO}_2$ ). Results for this 16-term PQM model are given in Table 6.9 and discussed in Section 6.4. Methods for making VHT alteration depth predictions and quantifying the uncertainties in the predictions are discussed and illustrated in Section 6.10.

The inclusion of quadratic terms in the second-choice alternate model for VHT alteration appears to reduce the tendencies of the LM models to under-predict larger VHT alteration depths. The inclusion of cubic terms in the recommended model for VHT alteration appears to correct the tendency to under-predict larger VHT alterations. The inadequacy of linear mixture models is likely a reflection of the complexity of the VHT process, which tends to accentuate non-linear effects of glass composition. Thus, it is reasonable that non-linear terms would be needed in VHT models.

The recommended 15-term PCM model for VHT alteration depth appears to yield unbiased predictions over the full range of measured VHT alteration depth values in the modeling dataset, although there is relatively large scatter in data points about the fitted model (see Figure 6.20). This significant scatter results in a statistically significant LOF of the recommended model. Because of the magnitudes of uncertainties in the VHT data (i.e., from making simulated LAW glasses, VHT testing, and measuring alteration depths), as well as significant lack-of-fit of the recommended VHT model, prediction uncertainties for the recommended model are relatively large (see Section 6.11). While it may still be possible to formulate LAW glasses with VHT alteration depths sufficiently below the contract limit, so the relatively large prediction uncertainties do not unduly restrict WTP LAW vitrification operations, it is likely that there will be some impact on achievable waste loadings. Consequently, it is expected that additional effort in this area would be very beneficial. Separate work that will be performed to assess the impact of LAW glass composition and model uncertainties for the recommended VHT model is discussed in Section 10.6.

### Electrical Conductivity Modeling Results for LAW Glasses

Investigation of three equations (Arrhenius, “truncated T2”, and “T2”; see Appendix C.2.1) for the temperature dependence of the electrical conductivity (EC) showed that the Arrhenius equation was sufficient for the vast majority of the 171 glasses in the EC modeling dataset. Several property-composition-temperature model forms for EC were developed by expanding the two parameters of the Arrhenius equation as linear or partial quadratic mixture experiment models.

Based on model fitting and validation results, a 25-term Arrhenius-LM model with three additional crossproduct terms is the recommended model for EC of LAW glasses. This model has 11 linear composition terms of the form  $x_i$  ( $\text{Al}_2\text{O}_3$ ,  $\text{B}_2\text{O}_3$ ,  $\text{CaO}$ ,  $\text{Fe}_2\text{O}_3$ ,  $\text{K}_2\text{O}$ ,  $\text{Li}_2\text{O}$ ,  $\text{MgO}$ ,  $\text{Na}_2\text{O}$ ,  $\text{SiO}_2$ ,  $\text{ZrO}_2$ , and Others), three quadratic terms of the form  $x_i x_j$  (representing the crossproduct pairs  $\text{CaO} \times \text{Li}_2\text{O}$ ,  $\text{CaO} \times \text{Na}_2\text{O}$ , and  $\text{Li}_2\text{O} \times \text{Na}_2\text{O}$ ), and 11 composition-temperature terms of the form  $x_i/(T/1000)$ . The temperature ( $T$ , Kelvin) is scaled by 1000 so that the model coefficients for those terms are of comparable magnitudes to those of the linear-composition terms. Results for the recommended 25-term EC model are given in Table 7.10 and discussed in Section 7.5. Methods for making electrical conductivity predictions and quantifying the uncertainties in the predictions are discussed and illustrated in Section 7.6.

The recommended EC model provides unbiased predictions over the full range of measured EC values in the modeling dataset, with relatively tight scatter for most data points about the fitted model, and moderate scatter for some data points (see Figure 7.14). The recommended EC model does not have a statistically significant LOF, so that EC predictions can be expected to be within the uncertainty of what would be obtained by batching and melting glasses and measuring the EC. The magnitudes of uncertainties in EC model predictions should be small enough that they will not unduly restrict the formulation and processing of LAW glasses in the WTP facility. However, separate work to confirm this is planned, as discussed in Section 10.6.

## Viscosity Modeling Results for LAW Glasses

Investigation of three equations (Arrhenius, truncated T2, and T2; see Appendix C.2.1) for the temperature dependence of viscosity showed that the truncated-T2 equation was sufficient for the vast majority of the 171 glasses in the viscosity modeling dataset. Several property-composition-temperature model forms for viscosity were developed by expanding the two parameters of the truncated-T2 equation as linear or partial quadratic mixture experiment models.

Based on model fitting and validation results, a 26-term reduced truncated T2-LM model with four additional quadratic terms is the recommended model for viscosity of LAW glasses. This model has 12 linear composition terms of the form  $x_i$  ( $\text{Al}_2\text{O}_3$ ,  $\text{B}_2\text{O}_3$ ,  $\text{CaO}$ ,  $\text{Fe}_2\text{O}_3$ ,  $\text{K}_2\text{O}$ ,  $\text{Li}_2\text{O}$ ,  $\text{MgO}$ ,  $\text{Na}_2\text{O}$ ,  $\text{P}_2\text{O}_5$ ,  $\text{SiO}_2$ ,  $\text{ZrO}_2$ , and Others), four quadratic terms of the form  $x_i x_j$  or  $x_i^2$  [representing  $(\text{B}_2\text{O}_3)^2$ ,  $(\text{Li}_2\text{O})^2$ ,  $\text{Al}_2\text{O}_3 \times \text{Li}_2\text{O}$ ,  $(\text{MgO})^2$ ], and 10 composition-temperature terms of the form  $x_i/(T/1000)^2$  involving  $\text{Al}_2\text{O}_3$ ,  $\text{CaO}$ ,  $\text{Fe}_2\text{O}_3$ ,  $\text{Li}_2\text{O}$ ,  $\text{MgO}$ ,  $\text{Na}_2\text{O}$ ,  $\text{P}_2\text{O}_5$ ,  $\text{SiO}_2$ ,  $\text{ZrO}_2$ , and Others. The  $\text{B}_2\text{O}_3/(T/1000)^2$  and  $\text{K}_2\text{O}/(T/1000)^2$  terms were statistically non-significant and thus omitted from the model. The temperature ( $T$ , Kelvin) is scaled by 1000 so that the model coefficients for those terms are of comparable magnitudes to those of the linear-composition terms. Results for the recommended 26-term viscosity model are given in Table 8.8 and discussed in Section 8.5. Methods for making viscosity predictions and quantifying the uncertainties in the predictions are discussed and illustrated in Section 8.6.

The recommended viscosity model provides unbiased predictions over the full range of measured viscosity values in the modeling dataset, with relatively tight scatter for most data points about the fitted model, and moderate scatter for some data points (see Figure 8.12). The recommended viscosity model does not have a statistically significant LOF, so that viscosity predictions can be expected to be within the uncertainty of what would be obtained by batching and melting glasses and measuring the viscosity. The magnitudes of uncertainties in viscosity model predictions should be small enough that they will not unduly restrict the formulation and processing of LAW glasses in the WTP facility. However, separate work to confirm this is planned, as discussed in Section 10.6.

## Model Validity Region for LAW Glasses

The LAW glass property-composition models recommended in this report were obtained by estimating coefficients of models using least squares regression methods. PCT and VHT models developed in this way should only be applied to LAW glass compositions inside the composition region over which the models were developed and demonstrated to yield unbiased predictions. Similarly, EC and viscosity models developed in this way should only be applied to LAW glass compositions at melt temperatures inside the composition-temperature region over which the models were developed and demonstrated to yield unbiased predictions. Such regions are referred to as *model validity regions*, which are defined using single- and multiple-component constraints on LAW glass components. Single- and multiple-component constraints directly on LAW glass compositions are the same for each model validity region (i.e., PCT, VHT, electrical conductivity, and viscosity). Because electrical conductivity and viscosity also depend on melt temperature, there is a temperature aspect of the model validity region for those

properties. Finally, some multiple-component constraints are specific to the model validity region for a given LAW glass property. These multiple-component constraints involve limits on glass properties, and are implemented using the recommended property models. The model validity regions are discussed in Section 9, and the constraints defining them are summarized in Table 9.6.

#### **D) Quality Requirements**

The portions of this work that were performed at VSL were conducted under a quality assurance program based on NQA-1 (1989) and NQA-2a (1990) Part 2.7 that is in place at the VSL. This program is supplemented by a Quality Assurance Project Plan for WTP work that is conducted at VSL. Test and procedure requirements by which the testing activities are planned and controlled are also defined in this plan. The program is supported by VSL standard operating procedures (VSL 2006) that were used for this work. This work was not subject to DOE/RW-0333P (DOE-RW 2004). This work was not subject to the requirements of WTP QAPjP for environmental regulatory data (Blumenkranz 2001).

Eight of the existing glasses (LAWA44, LAWA44R10, LAWA54, LAWA56, LAWA88, LAWA88R1, LAWA102R1, and LAWA102R2) were prepared and characterized at VSL during Part B1 of the contract under BNFL. Two samples (GTSD-1126 and GTSD-1437) were prepared in the Duratek LAW Pilot Melter facility (Duratek 2003a, 2003b) and characterized at VSL. Two surrogate samples (AZ-102 Surr SRNL and AN-102 Surr LC Melter) and nine actual LAW samples (AN-103 Actual, AW-101 Actual, AP-101 Actual, AZ-101 Actual, AZ-102 Actual, AZ-102 Actual CCC, AN-107 Actual (LAWC15), AN-102 Actual LC Melter and AN-102 Actual) were prepared and characterized at SRTC and PNNL, according to procedures for control of measurement and testing equipment, tracking of radioactive samples, control of laboratory notebooks, and routine QA and QC, in compliance with the requirements of NQA-1. The remaining glasses were prepared and characterized at VSL during the Bechtel contract. An NQA-1 based QA program was in place during all of the work.

The QA requirements for the PNNL modeling work were met through the Quality Assurance Plan (PNNL 2007a) for the River Protection Project – Waste Treatment Plant Support Program (RPP-WTP Support Program). The RPP-WTP Support Program's quality assurance manual and its implementing procedures (PNNL 2007b) comply with the requirements of NQA-1 and NQA-2a Part 2.7.

#### **E) R&T Test Conditions**

The datasets used in the development of property-composition models included all data collected under the WTP project since 1998 that satisfy the applicable QA requirements. The datasets contained glasses from statistically-designed composition test matrices that cover a composition space, and actively-designed glasses where an iterative approach was used to develop glass compositions with desired properties. The statistically-designed glasses include the ILAW Phase 1 Test Matrix of 56 compositions and the Phase 1a Augmentation Test Matrix of 20

compositions. Different sets of actively-designed glasses that are in the dataset include: (i) 23 Existing Matrix Glasses (two of which are remakes of two of the other glasses), (ii) 21 LAW Correlation and High Cr<sub>2</sub>O<sub>3</sub> Correlation glasses, (iii) 7 High Cr<sub>2</sub>O<sub>3</sub> and P<sub>2</sub>O<sub>5</sub> glasses, (iv) a set of 135 glasses from simulant tests to develop suitable glass compositions for waste processing at WTP, melter testing at VSL and Duratek, and actual waste testing at PNNL and Savannah River Technology Center (SRTC), and (v) 9 actual LAW samples prepared and characterized at PNNL or SRTC. Of the 271 simulated and actual waste glasses in the dataset, 264 have PCT data, and 181 each have VHT, viscosity, and electrical conductivity data.

The majority of the glass samples are from crucible melts (about 400 g) prepared at the VSL by melting mixtures of reagent grade or higher purity chemicals in platinum-gold crucibles at 1200°C for 75 minutes. Mixing of the melt was accomplished mechanically using a platinum stirrer, beginning 15 minutes after the furnace temperature reached 1200°C and continuing for the next 60 minutes. Simulant glass samples to support actual waste testing at PNNL and SRTC were prepared at VSL by mixing appropriate amounts of glass forming chemicals with LAW simulants, drying the slurry slowly in platinum-gold crucibles, and melting as described above. Glass samples from melter tests were collected at VSL and Duratek from near the top of drums into which melter glass was discharged. Actual LAW glass samples were prepared at PNNL and SRTC by mixing appropriate amounts of glass forming chemicals with actual LAW followed by drying and melting in crucibles. Samples of the resulting simulant glasses were analyzed at VSL for composition directly by XRF, as well as by DCP-AES and IC on solutions resulting from microwave-assisted acid dissolution of solid samples. Glass composition analysis techniques at PNNL and SRTC included Inductively Coupled Plasma-Atomic Emission Spectroscopy (ICP-AES) and Atomic Absorption (AA) spectroscopy.

The PCT, at 90°C for seven days, was performed and the leachates were analyzed by DCP-AES at VSL or ICP-AES at PNNL and SRTC. The VHT, at 200°C for a nominal duration of 24 days, was performed at VSL. The alteration layer thicknesses were measured by Scanning Electron Microscopy (SEM). The electrical conductivity of each glass was determined at VSL by measuring the impedance of the glass melt at temperatures around 950, 1050, 1150 and 1250°C as a function of AC frequency using a calibrated platinum-rhodium electrode probe attached to a Hewlett-Packard model 4194A impedance analyzer. The collected impedance data were analyzed to obtain the DC electrical conductivity. The melt viscosity of each glass was measured at VSL using a Brookfield viscometer with platinum-rhodium spindle and crucible. The relative torque of a rotating spindle immersed in the molten glass was measured as a function of rotational velocity (revolutions per minute (RPM)) at temperatures around 950, 1050, 1150 and 1250°C. The viscosity of the molten glass was then calculated from the collected data of torque versus RPM. Glass crystallization behavior was assessed by performing various heat treatments at 700, 850, 950°C, or according to a container centerline cooling profile followed by optical microscopy and SEM-EDS evaluation. These data also provide bounding information on the liquidus temperature. Composition constraints to ensure less than 1 vol% crystals on heat treatment at 950°C were inferred from these data. The densities of the glasses were measured using a pycnometric method at 25°C.



## **F) Simulant Use**

The majority of the glasses used in model development were prepared at VSL from reagent grade chemicals in combinations designed to achieve the target compositions of the respective glasses. Glass samples to support actual waste testing at PNNL and SRTC were prepared at VSL using LAW simulants mixed with glass forming chemicals to achieve the desired target compositions. Melter glass samples were prepared at Duratek and VSL by mixing LAW simulants with the appropriate amounts of glass forming chemicals. Actual waste samples were prepared at PNNL and SRTC by mixing actual LAW with glass forming chemicals to obtain a known target glass composition.

## **G) Discrepancies and Follow-On Tests**

The models presented in this report may be augmented and additional validation work performed during any future ILAW model development work, especially if significant changes are anticipated in the compositions of the LAW streams or target glass compositions to be used in LAW processing.

## **SECTION 1 INTRODUCTION**

The United States Department of Energy's (DOE's) Hanford site in the State of Washington is the current storage location for about 50 million gallons of high-level mixed waste. This waste is stored in underground tanks at the Hanford site. The Hanford Tank Waste Treatment and Immobilization Plant (WTP) will provide DOE with a capability to treat the waste by vitrification for subsequent disposal. The tank waste will be partitioned into Low Activity Waste (LAW) and High Level Waste (HLW) fractions, which will then be vitrified, respectively, into Immobilized Low Activity Waste (ILAW) and Immobilized High Level Waste (IHLW) products. The ILAW product will be disposed of in an engineered facility on the Hanford site while the IHLW product will be directed to the national deep geological disposal facility for high-level nuclear waste. The ILAW and IHLW products must meet a variety of requirements with respect to protection of the environment before they can be accepted for disposal.

This report is the last in a series of currently scheduled reports for the WTP project that presents the results from the LAW glass formulation development and testing work performed at the Vitreous State Laboratory (VSL) of the Catholic University of America (CUA) and the development of ILAW property-composition models performed jointly by Pacific Northwest National Laboratory (PNNL) and VSL. Specifically, this report presents results of glass testing and model development for ILAW Product Consistency Test (PCT), Vapor Hydration Test (VHT), viscosity, and electrical conductivity. The data, model development, model validation, and model uncertainty results presented in this report are the last of this type of work currently planned for predicting the properties of LAW glasses. However, if the current LAW glass property-composition database is augmented with additional data in the future, additional model development and/or validation work could be performed at that time.

This report is responsive to the applicable Test Specifications (Swanberg 2001, Swanberg 2002), Test Exception (Westsik 2003), and Test Plans (Gan et al. 2002, Piepel and Cooley 2002) for LAW property-composition modeling. The purpose of the work described in these documents is to develop property-composition models to support LAW waste form qualification, processing, and compliance. The models are intended to provide the basis for defining operating ranges, developing target glass compositions, making operating decisions (e.g., glass former additions), and demonstrating compliance with applicable specifications during LAW vitrification operations at the WTP.

The test objectives, test overview, and discussion of how the objectives were met are presented in Sections 1.1, 1.2, and 1.3, respectively. The ILAW composition region of interest and the LAW glass data covering this compositional region are described in Section 2. Experimental procedures used in glass preparation, as well as sample preparations and analyses of PCT, VHT, viscosity, and electrical conductivity are described in Section 3. The PCT, VHT, electrical conductivity, and viscosity data and general features of their relationships to LAW glass composition are discussed in Section 4. Models relating PCT boron and sodium releases to LAW glass composition are presented and discussed in Section 5. Models relating VHT

alteration depth to LAW glass composition are presented and discussed in Section 6. Models relating electrical conductivity and viscosity to LAW glass composition and melt temperature are presented and discussed in Sections 7 and 8, respectively. The validity region for the ILAW property models is presented in Section 9. A summary and conclusions from the ILAW PCT, VHT, electrical conductivity, and viscosity model development and validation work are presented in Section 10. Recommendations for any future LAW property-composition data and model development or validation work that may be performed are presented in Section 11. The quality assurance requirements applied to the work presented in this report are described in Section 12. References are listed in Section 13. The mol% compositions of all the LAW glasses used in modeling are presented in Appendix A. The viscosity and electrical conductivity of the glass melts, calculated at a reference temperature of 1150°C using an Arrhenius relationship, are given in Appendix B. Appendix C discusses the statistical methods applied in the main body of the report. Appendix D presents the variance-covariance matrices for selected ILAW property-composition models, which are required to calculate uncertainties of model predictions.

## 1.1 Test Objectives

The objectives of the LAW glass property-composition modeling work as given in the Test Plans (Gan et al. 2002, Piepel and Cooley 2002) are listed below along with what has been done to address them.

- *Develop property-composition models and supporting data that relate ILAW performance on the PCT to ILAW composition and are suitable for predicting the PCT performance of ILAW glasses to be produced in the WTP.*
- *Develop property-composition models and supporting data that relate ILAW performance on the VHT to ILAW composition and are suitable for predicting the VHT performance of ILAW glasses to be produced in the WTP.*
- *Develop property-composition models that relate viscosity and electrical conductivity of glass melts to ILAW composition and are suitable for predicting the properties of ILAW glasses to be produced in the WTP.*

Data, model development, and model validation results for PCT, VHT, viscosity, and electrical conductivity property-composition models are presented in this report.

- *Develop bounding models for ILAW TCLP response. Such models are expected to be appropriate for LAW glasses as a result of the very low levels of RCRA elements in the LAW streams.*

The bounding approach for ILAW TCLP response was developed and reported earlier (Kot et al. 2003).

- *Develop bounding models for ILAW liquidus temperature. Such models are expected to be appropriate for LAW glasses as a result of their consistently low liquidus values in comparison to the nominal melter operating temperature.*

Data on crystal content after heat treatment, which provide bounds on the liquidus temperature, have been reported earlier for most of the LAW glasses prepared and tested at the VSL (Muller et al. 2001a, Muller and Pegg 2003, Muller and Pegg 2004, Rielley et al. 2004, Muller et al. 2006a, Muller et al. 2006b). The available data for all of the glasses employed in the present work are summarized in Section 4.5. From these data, composition constraints are provided to identify glasses that are expected to exhibit less than 1 vol% crystals after heat treatment at 950°C, which is effectively a bounding liquidus model.

- *Develop property-composition models that relate density of ILAW glasses to composition in order to predict overall volumes of ILAW that would be produced from a given waste feed.*

Density data for a number of LAW glasses have been reported earlier (Muller et al. 2001a, Muller and Pegg 2003, Muller and Pegg 2004, Reilley et al. 2004). The available data for all of the glasses employed in the present work are summarized in Section 4.6. WTP R&T concluded that it is not necessary to develop a property-composition model for ILAW density because all of the measured density values for LAW glasses are below the effective contract limit of 3.7 g/cc (DOE-ORP 2000).

See the “Summary of Testing” section for further discussion and summary of the objectives and the work performed to achieve them.

## 1.2 Test Overview

Databases of simulated and actual LAW waste glass compositions and property values have been compiled for the purpose of model development, model validation, and development of model uncertainty expressions for the following properties:

- PCT boron (B), sodium (Na), and silicon (Si) releases, in units of g/L
- VHT alteration depth ( $D$ ), in units of  $\mu\text{m}$
- viscosity ( $\eta$ ), in units of poise
- electrical conductivity, in units of S/cm

All LAW glass data developed under the WTP project dating back to 1998 that satisfy the relevant QA requirements have been included in a separate database for each of these four properties. The data included in these databases are discussed in Section 2.

The focus of the “testing” documented in this report was the development and validation of models for PCT B and Na releases<sup>1</sup>, VHT alteration depth, electrical conductivity, and viscosity. An additional focus was the development of expressions to quantify the uncertainty in property predictions made with the models. The work to develop, validate, and quantify prediction uncertainties for the PCT, VHT, electrical conductivity, and viscosity models is

---

<sup>1</sup> PCT Si release was not modeled for the reasons explained subsequently in Section 4.1.1.

discussed, respectively, in Sections 5, 6, 7, and 8. In addition to model development, the PCT, VHT, electrical conductivity, and viscosity data for the LAW glasses were analyzed to determine their dependences on glass composition in terms of the contribution of different constituents to the structure of the glass. These analyses are presented in Section 4. The generation of glass composition test matrices and measurement of glass properties have been documented in previous reports, as discussed in Sections 2 and 3.

Toxicity Characteristic Leach Procedure (TCLP) testing and modeling, which are part of the work scopes in the Test Specifications (Swanberg 2001, Swanberg 2002) and Test Plans (Gan et al. 2002, Piepel and Cooley 2002), were completed and reported earlier (Kot et al. 2003) using a separate composition matrix (Musick 2003). Because LAW glasses contain little or no RCRA metals, TCLP testing was limited to spiking a limited number of glasses with RCRA metals and subjecting the glasses to the TCLP in order to demonstrate that TCLP limits were not exceeded.

Heat treatment data, which provide bounds on the liquidus temperature, for all of the glasses employed in the present work are summarized in Section 4.5. From these data, composition constraints are provided to identify glasses that are expected to exhibit less than 1 vol% crystals after heat treatment at 950°C, which is effectively a bounding liquidus model. The available density data for all of the glasses employed in the present work are summarized in Section 4.6. WTP R&T concluded that it is not necessary to develop a property-composition model for ILAW density because all of the measured density values for LAW glasses are below the effective contract limit of 3.7 g/cc (DOE-ORP 2000).

### **1.3 How Test Objectives Were Achieved**

The test objectives in Section 1.1 were achieved by developing, validating, and quantifying uncertainty in property-composition models for LAW glasses. Recommended models are presented for PCT response (B and Na releases), VHT alteration, electrical conductivity, and viscosity. The recommended models for each property, being the best of the models considered in the development and validation process, are suitable for predicting properties of LAW glasses. However, it is outside the scope of work in this report to completely assess the suitability of the recommended property models. Ultimately, the WTP project needs to assess whether the recommended models, along with their corresponding uncertainties, are suitable for their various intended uses (e.g., glass formulation, addition of glass-forming chemicals to waste during LAW vitrification operations, and compliance with WTP contract specifications and processing constraints). Such assessments are within the scopes for algorithm development and verification (work being conducted by WTP project staff) and statistical compliance methodology development and demonstration (work under separate PNNL scope). Initial statistical compliance methodology development and demonstration work was conducted for earlier versions of property-composition models (Piepel et al. 2005). That work is tentatively planned by the WTP project to be updated by PNNL in FY2009 for the models presented in this report.

## SECTION 2 DATA FOR LAW GLASS PROPERTY MODELING

The databases used in the development of LAW glass property-composition models (PCT, VHT, electrical conductivity, and viscosity) include all data collected under the WTP project since 1998 that satisfy the applicable QA requirements. Some of the data are from statistically designed<sup>2</sup> composition matrices to cover the LAW glass composition regions of interest. Other data are from actively designed glass formulations that relied on glass science rather than statistical methods to develop glass compositions with desired properties. Property data from glasses made during scale melter tests are also included in the databases. The melter test glass compositions were selected from actively designed glass formulations that meet all WTP processing and product quality requirements. A limited number of data are from characterization of glasses made from actual LAW samples.

Sections 2.1 to 2.7 provide the identifications and target compositions of LAW glasses in the compiled property databases. Each section describes a series or group of glasses for which data on some or all of the properties were collected. References to the corresponding test matrix development reports and/or data summary reports are also provided. The property data that were collected from each set of glasses are identified in each section. Section 2.8 summarizes the groups of LAW glasses available for property modeling. Section 3 describes the experimental procedures used in data collection, while Section 4 presents and discusses the property data for the LAW glasses from a glass science perspective.

### 2.1 Phase 1 Test Matrix Glasses

The Phase 1 Test Matrix consists of a set of 56 glass formulations specified by a statistically-designed test matrix (Cooley et al. 2003) that was prepared and characterized to support Phase 1 of ILAW property-composition modeling. The focus of the ILAW Phase 1 Test Matrix was the first 11 LAW streams planned for the WTP at the time of the test matrix design: AP-101, AZ-101, AZ-102, AN-102, AN-103, AN-104, AN-105, AN-107, AW-101, AP-101 combined with SY-104 and SY-101 combined with AP-104. Beryllium and mercury were not included in the ILAW Phase 1 Test Matrix at the direction of WTP. The waste composition information considered in the development of the ILAW Phase 1 Test Matrix included Tank Farm Contractor Operation and Utilization Plan (TFCOUP) Rev. 3A (Kirkbride et al. 2001), TFCOUP Rev. 2 (Kirkbride et al. 2000), the WTP Test Specification for LAW melter testing (Morrey 2002), which also contained LAW actual waste characterization data, and prior VSL assessments of LAW waste composition (Muller et al. 2001a, Muller et al. 2001b).

---

<sup>2</sup> “Statistically designed” refers to a set of glass compositions designed using statistical experimental design methods to cover a composition space. “Actively designed” refers to glasses developed to meet certain specified requirements such as a glass composition to treat a LAW tank waste stream that has to meet all product quality and processing requirements. In this approach, information from characterization of one set of glasses is used to guide formulation of future glass compositions, with little or no intent to cover a composition space.

Design of the ILAW Phase 1 Test Matrix began with the selection of glass components and the development of constraints to define the glass composition region to be covered by the test matrix. The glass components and constraints were developed using information on Hanford LAW compositions, WTP pretreatment and recycle assumptions, existing WTP glass formulation data, glass science knowledge and experience, and statistical input. A total of 14 LAW glass components were chosen as design variables (including an “Others” component comprising all remaining minor glass components), as shown in Table 2.1. The composition of the “Others” component is shown in Table 2.2. The constraints were initially developed and then iterated by VSL based on inputs from the WTP Project and PNNL<sup>3</sup> (Cooley et al. 2003). The ILAW Phase 1 Test Matrix constraints are listed in Tables 2.1, 2.3, and 2.4. Table 2.1 lists the single-component constraints, while Table 2.3 lists the LAW glass properties and limits upon which some multi-component constraints were based. Note that no VHT constraint was used, because very few models existed for this property and the performance of the models was not good enough to be of practical use. Table 2.4 lists the multi-component property constraints.

The ILAW Phase 1 Test Matrix was developed by PNNL (with input from VSL and WTP) using a layered design approach (Piepel et al. 1993, Piepel et al. 2002). The design had one outer layer (containing 15 glasses), one middle layer (20 glasses), one inner layer (14 glasses), a center point, and 6 replicate glasses for a total of 56 glasses. These glasses were selected to augment 21 Existing Matrix glasses (see Section 2.2). Additional details of the test matrix development are discussed in a previous technical report (Cooley et al. 2003). The target compositions of the ILAW Phase 1 Test Matrix glasses are given in Table 2.5. Details of glass property measurements have been presented in an earlier report (Rielley et al. 2004). PCT, VHT, viscosity, and electrical conductivity data were collected on all 56 of the ILAW Phase 1 Test Matrix glasses, designated LAWM1 to LAWM56.

In addition to the 14 main glass components, Cl, Cr<sub>2</sub>O<sub>3</sub>, F, and P<sub>2</sub>O<sub>5</sub> have recently been identified as components that could affect waste loading in LAW glasses. As described later in Section 5.1, they also display sufficient concentration ranges and distributions of values within their ranges to support model terms so that these components are now considered as individual terms, and no longer as part of the “Others.” This increases the total number of components considered in this phase of modeling to 18.

## 2.2 Existing Matrix Glasses

A set of 21 Existing Matrix glasses representative of the range of working compositions at that time (early 2002) was chosen as the starting point for the ILAW Phase 1 Test Matrix development. These compositions for ILAW Test Matrix development were recommended by VSL and selected jointly by VSL, PNNL, and WTP (Cooley et al. 2003). Even though the

---

<sup>3</sup> Portions of the work in this report were conducted under Battelle’s government contract as Pacific Northwest National Laboratory (PNNL), while other work was conducted under the use permit of that contract as Battelle–Pacific Northwest Division (PNWD). For simplicity, all Battelle work will be referred to as being conducted at PNNL.

Existing Matrix consists of only 21 target glass compositions, 23 glass melts were prepared because the initial crucible melts of two of the glasses, LAWA88 and LAWA128, did not yield sufficient glass sample to perform all of the property measurements. Hence, additional melts LAWA88R1 and LAWA128R1 were prepared, where the suffix R1 indicates that the samples are remelts with the same target compositions<sup>4</sup>. PCT responses were measured using the samples LAWA88, LAWA88R1, and LAWA128; the VHT responses were measured using samples LAWA88R1 and LAWA128; and viscosity and electrical conductivity were measured using the samples LAWA88 and LAWA128R1. Preparation and characterization of six of these 23 samples (LAW Envelope A formulations LAWA44R10, LAWA53, LAWA56, LAWA88, LAWA88R1, and LAWA102R1) are reported in the Part B1 LAW glass formulation report (Muller et al. 2001a). The remaining 17 Existing Matrix glass samples consist of LAW Envelope A crucible glasses (LAWA126, LAWA128 for PCT and VHT testing, LAWA128R1 for viscosity and electrical conductivity testing, and LAWA130), LAW Envelope B crucible glasses (LAWB65, LAWB66, LAWB68, LAWB78, LAWB79, LAWB80, LAWB83, LAWB84, LAWB85, and LAWB86), LAW Envelope C crucible melts (LAWC27 and LAWC32) and one glass sample collected from a DuraMelter 100 Envelope C melter test (C100-G-136B). Details of the preparation and characterization of these samples have also been reported earlier (Muller and Pegg 2003a, 2003b, 2004). In subsequent sections, the abbreviation ExPh1 is used to denote the Existing Matrix glasses augmented by the ILAW Phase 1 Test Matrix glasses.

The target compositions of the 23 Existing Matrix glasses (two are remelts) are given in Table 2.6. The relevance of these glass compositions with respect to the composition ranges for LAW glass testing is discussed in a previous report (Muller et al. 2005a). Of the 23 glasses in this subset, 22 have PCT data, 21 have VHT data, and 21 have viscosity and electrical conductivity data.

### 2.3 Phase 1a Augmentation Test Matrix Glasses

In view of the large lack-of-fit in models for VHT alteration rates using Phase 1 data, 20 glass compositions, selected from a statistically-designed composition matrix, were formulated and tested with the primary objective of augmenting the LAW VHT data set available for modeling (Muller et al. 2006b). This augmentation matrix was designed with the objective of selecting 20 glass compositions for testing that have VHT alteration rates near the contractual limit of 50 g/m<sup>2</sup>/day (DOE-ORP 2000). In order to augment the capability of the VHT model, it was considered more important to obtain measurable VHT responses<sup>5</sup> near or above the contractual limit than to select glasses that are likely to meet the contractual requirement. The VHT alteration rate of 50 g/m<sup>2</sup>/day corresponds to an alteration depth of 453 μm for a 24-day test and an average glass density of 2.65 g/cc. The objective, therefore, was to select glass compositions that would show VHT alteration depths preferably in the range of about 200 to

---

<sup>4</sup> Note that for historical reasons, LAWA88 was counted as one of the “actively designed” group of glasses whereas the other three of these four glasses were counted in the “existing glasses” grouping.

<sup>5</sup> If the VHT alteration rate is too high, the test coupon is completely altered over the test duration and, therefore, the test yields only a “greater than” result, which is not amenable to property-composition modeling. Of the 56 Phase 1 Test Matrix glasses, 5 could not be used in modeling for that reason.



800  $\mu\text{m}$ , with the measurable upper limit being determined by the thickness of the VHT coupon. Given the lack of models that could reliably predict VHT responses in the high-alkali region of the LAW correlation, a two-step approach was used to select the 20 glasses for testing. Thirty glass compositions were generated using statistical experimental design software, from which 20 were selected manually through comparison with the few preexisting glass compositions with VHT responses in the desired range.

In view of the limited number of glass compositions available for VHT modeling and to avoid occurrences of unacceptably high (“greater than”) coupon alterations, emphasis was placed on selecting compositions close to those provided by the LAW correlation (Muller et al. 2004b). With this restriction, it is only glasses with high alkali content that can challenge the VHT limit, and, therefore, only such glasses were considered for the LAW augmentation matrix. A two-layer D-optimal mixture statistical design was employed, for which the major features of the design and the design constraints have been reported earlier (Muller et al. 2006b). Most importantly, the  $\text{Na}_2\text{O}$  and  $\text{K}_2\text{O}$  ranges were set beyond the upper bounds of the Phase 1 Test Matrix and varied from 20 to 23 wt% for  $\text{Na}_2\text{O}$  and 0 to 5.4 wt% for  $\text{K}_2\text{O}$ .

Twenty glasses were selected for testing from the 30 design compositions through additional screening aimed at decreasing the likelihood that the VHT alteration depths of the selected compositions would exceed the coupon thickness. Alkali content and the concentrations of four major components ( $\text{SiO}_2$ ,  $\text{ZrO}_2$ ,  $\text{Al}_2\text{O}_3$ , and  $\text{B}_2\text{O}_3$ ) were used for screening, based on past observations. In this composition region, increases in  $\text{SiO}_2$ ,  $\text{ZrO}_2$ , and  $\text{Al}_2\text{O}_3$  reduce VHT alteration rates, whereas increases in  $\text{B}_2\text{O}_3$  concentration increase VHT alteration rate.

The target compositions of the Phase 1a Augmentation Test Matrix glasses are listed in Table 2.7 for the 14 major components and Table 2.8 for the minor components. The glasses were designated LAW57 to LAW76, following the nomenclature used for the previous 56 LAW matrix glasses (Section 2.1). PCT and VHT data were collected on all 20 samples, whereas viscosity and electrical conductivity data were collected on only nine glasses selected to augment the corresponding property-composition databases.

## **2.4 LAW Correlation and High $\text{Cr}_2\text{O}_3$ Correlation Glasses**

A set of 21 LAW correlation glasses (denoted Corr) were formulated using a set of empirical relationships that define waste loadings and the concentrations of glass former additives for LAW wastes as a function of the molar ratio of sulfate to sodium ( $\text{SO}_4/\text{Na}$ ). These relationships together define the LAW Correlation (Muller et al. 2004b). The LAW Correlation is based on LAW glass compositions developed at the VSL and tested at various scales including the LAW Pilot Melter. The LAW Correlation algorithm uses a two-step process to calculate glass compositions for a given waste stream composition. First, waste loading (expressed as the alkali content of the waste  $\text{ALK} = \text{Na}_2\text{O (wt\%)} + 0.66 \text{K}_2\text{O (wt\%)}$ ) is calculated as the highest of three waste loading limiting constituents, leading to three types of formulations as follows:

Sodium limited formulations:

$$\text{Na}_2\text{O (wt\%)} \leq 21 \text{ (wt\%)} \quad (2.1)$$

Potassium limited formulations (for  $\text{ALK} = \text{Na}_2\text{O (wt\%)} + 0.66 \text{ K}_2\text{O (wt\%)}$ ):

$$\text{Na}_2\text{O (wt\%)} + 0.66 \text{ K}_2\text{O (wt\%)} \leq 21.5 \text{ (wt\%)} \quad (2.2)$$

Sulfate limited formulations:

$$\text{Na}_2\text{O (wt\%)} + 42.5 \text{ SO}_3 \text{ (wt\%)} \leq 35.875 \text{ (wt\%)} \quad (2.3)$$

Equation (2.3) can be rearranged and used as an equality to relate the  $\text{Na}_2\text{O}$  concentration to the  $\text{SO}_4/\text{Na}$  ratio for a given waste as:

$$\text{Na}_2\text{O (wt\%)} = \frac{35.875}{1 + \frac{80.06}{30.99} * 42.5 * \frac{\text{SO}_4}{\text{Na}}} \quad (2.4)$$

(the molecular weights of  $\text{SO}_3$  and  $\text{Na}_2\text{O}$  are 80.06 g/gmol and 61.98 g/gmol respectively; one mole of  $\text{SO}_3$  contributes one mole of  $\text{SO}_4$  and one mole of  $\text{Na}_2\text{O}$  contributes two moles of Na).

Amongst the glass former additives, concentrations of the following three components also vary with the waste loading (expressed as ALK):

$$\text{Li}_2\text{O (wt\%)} = 4.3 * \left(1 - \frac{(\text{ALK} - 5.4)^2}{12.75^2}\right)^{0.7} \quad (2.5)$$

$$\text{CaO (wt\%)} = 1.5 + 5.5 [1 + \exp((\text{ALK} - 17) / 2)]^{-1} \quad (2.6)$$

$$\text{MgO (wt\%)} = 1.48 + 1.49 [1 + \exp(\text{ALK} - 9)]^{-1} \quad (2.7)$$

Several of the added components ( $\text{Al}_2\text{O}_3$ ,  $\text{B}_2\text{O}_3$ ,  $\text{Fe}_2\text{O}_3$ ,  $\text{TiO}_2$ ,  $\text{ZnO}$ ,  $\text{ZrO}_2$ , and “Others”) are kept at fixed concentrations and the  $\text{SiO}_2$  concentration is calculated such that the glass composition in wt% sums to 100. “Others” is a component that captures the concentrations of all of the minor components in the glass. Minor variations in some of the above additives that were maintained at fixed values in most of the glasses were tested in glasses LAWE12 to LAWE16.

Additionally, four correlation glasses with increased  $\text{Cr}_2\text{O}_3$  concentrations (from 0.35 to 1.4 wt% based on currently predicted maximum  $\text{Cr}_2\text{O}_3$  concentrations in LAW waste streams) were prepared, subjected to container centerline cooling (CCC) heat treatment, and characterized. Property data from these glasses were included in the modeling dataset as part of the 21 LAW Correlation glasses. The target compositions of the LAW Correlation glasses are listed in Tables 2.9 and 2.10 for the major and minor components, respectively. Of the 21 glasses

in these two subsets, 18 have PCT data, 19 have VHT data, and 15 have viscosity and electrical conductivity data.

## **2.5 High Cr<sub>2</sub>O<sub>3</sub> and P<sub>2</sub>O<sub>5</sub> LAW Glasses**

A set of seven glasses with higher concentrations of Cr<sub>2</sub>O<sub>3</sub> and P<sub>2</sub>O<sub>5</sub> (in the range of 0.3 to 0.6 wt% Cr<sub>2</sub>O<sub>3</sub> and 1.3 to 2.4 wt% P<sub>2</sub>O<sub>5</sub> – see Muller et al. 2006a) were tested to determine the acceptable ranges for these components in LAW glasses formulated based on the LAW Correlation algorithm. These glasses are denoted by the label “HighCrP.” The target compositions of the HighCrP glasses are listed in Tables 2.11 and 2.12. Of the seven glasses in this subset, 7 have PCT data, 7 have VHT data, and 5 have viscosity and electrical conductivity data.

## **2.6 Remaining Actively Designed LAW Glasses**

This group consists of LAW glasses tested at VSL from 1998 to 2006 during Part B1 and subsequent contract phases. All of these glasses were "actively" rather than "statistically" designed and, therefore, compositional correlations are almost certainly present in the data, as described below.

Of the 135 glasses in this set, 39 were tested during Part B1 (Muller et al. 2001a) to support the development of glass formulations for LAW Envelope A (LAWA41 to LAWA105), LAW Envelope B (LAWB30 to LAWB41) and LAW Envelope C (LAWC12 to LAWC25), for which the primary source of tank waste compositional data was the Best Basis Inventory. The glass formulation TFA-Base is a glass sample prepared at VSL with the same composition as that of a PNNL composition used as the central glass composition of the initial Hanford Immobilized LAW Product Acceptance study (Vienna et al. 2000).

Subsequent changes to the tank waste compositions mentioned earlier (TFCOUP Rev. 2, Rev. 3 and Rev. 3A) were addressed in later glass formulation testing of each LAW Envelope (through LAWA136, LAWB96, and LAWC33 for waste envelopes A, B, and C, respectively). Of these, 51 glasses were subjected to the PCT with lesser numbers selected for VHT, viscosity, and electrical conductivity measurements. Details of the preparation and testing of these glasses have already been reported (Muller et al. 2003). Note that for three of these glasses (LAWA129, LAWB93 and LAWC31), the amounts of glass samples from the initial crucible melts were insufficient to complete all property measurements. The viscosity and electrical conductivity of these glasses were therefore measured using remelts designated LAWA129R1, LAWA93R1 and LAWC31R1.

For convenience in glass formulation development for the Hanford LAW tank wastes, the waste compositions were divided into seven LAW Sub-Envelopes, namely A1, A2, A3, B1, B2, C1, and C2. Glass formulations were developed and selected for melter testing of each of the LAW Sub-Envelope compositions, the results of which have been reported earlier (Muller and Pegg 2004). Thirty-five glasses from this group are included in the model data sets, of which

eight are crucible melts with the nominal composition of each of the selected glass formulations (the sample names are A1-AN105R2 for A1, A2-AP101 and A88-AP101R1 for A2, A3-AN104 for A3, B1-AZ101 for B1, C1-AN107 and C22AN107 for C1, and AN102C35 for C2). Four of the crucible glasses (A88Si+15, A88Si-15, C22Si+15 and C22Si-15) were prepared to study the effect of  $\pm 15\%$  variation in the blending of waste and glass former additives on their properties, and nine crucible melts (A1C1-1, A1C1-2, A1C1-3, A2B1-1, A2B1-2, A2B1-3, A3C2-1, A3C2-2, A3C2-3) were prepared and characterized to determine the effect of  $\frac{1}{4}$ ,  $\frac{1}{2}$ , and  $\frac{3}{4}$  composition changeovers on glass properties as the composition of the melt pool transitions from the glass compositions for one tank waste to another (Muller and Pegg 2004). Fourteen of the glass samples are from melter tests conducted at three different scales (Matlack et al. 2001, 2002a, 2002b, 2002c, 2002d, 2002e, 2002f, 2003a, 2003b, 2003c, 2003d, 2003e, Duratek 2003a and 2003b):

- DuraMelter 100 (WVF-G-21B and WVM-G-142C for Sub-Envelope A2, A100G115A, WVB-G-124B and WVR-G-127A for Sub-Envelope A3, WVJ-G-109D for Sub-Envelope B1 and WVH-G-57B for Sub-Envelope C2)
- DuraMelter 1200 (12U-G-86A for Sub-Envelope A1 and 12S-G-85C for Sub-Envelope C1)
- LAW Pilot Melter (GTSD-1126 for Sub-Envelope B1 and GTSD-1437 for Sub-Envelope C2).

Glass samples subjected to CCC heat treatment were also included in the database (A100CC, C100GCC and PLTC35CCC).

Simulant crucible glasses based on composition analysis of actual waste samples at PNNL and SRTC were also prepared and characterized at the VSL. Eight such samples were prepared at VSL from slurry feeds made by mixing waste simulants with glass former oxides. The crucible melts were prepared and subjected to CCC heat treatment before characterization. Property data from these glass samples, namely LA44PNCC (Muller et al. 2003d), PNLA126CC (Muller et al. 2003b), LA137SRCCC (Muller et al. 2004a), LB83PNCC (Muller et al. 2003c), LB83CCC-1, LA126CCC, LA44CCCR2, and LB88CCC (Muller et al. 2005b), are included in the database. In addition, simulant glass samples AN-102 Surr LC Melter (Zamecnik et al. 2002) prepared in a small-scale crucible-type melter system for actual waste vitrification, and a simulant crucible melt AZ-102 Surr (Crawford et al. 2004), both prepared at SRTC, are included in the modeling database. Further discussion concerning these glass samples is provided in Section 2.7. In all, this group is composed of 10 simulated glasses prepared from slurry feeds, eight of which were prepared at VSL and two of which were prepared at SRTC.

The target compositions of the remaining actively designed glasses are listed in Tables 2.13 and 2.14. Of the 135 glasses in this subset, 132 have PCT data, 58 have VHT data, and 75 have viscosity and electrical conductivity data. The property data are presented and discussed in subsequent sections.

## 2.7 Actual LAW Glasses

Glasses made from actual tank waste samples were characterized to demonstrate that glasses of similar compositions have similar properties, irrespective of their preparation method, or whether they are made from simulant or actual radioactive wastes. This comparison is used to validate the use of data that are obtained predominantly from simulants to predict the properties of ILAW to be produced at the WTP (Muller et al. 2005b). The results of the PCT on nine glasses made from actual radioactive waste samples were included in the database for development of PCT property-composition models.

Actual radioactive waste supernatant samples from seven underground storage tanks at the Hanford site were processed to remove most of the radioactivity according to the WTP project flow-sheet. These steps included dilution, removal of  $^{90}\text{Sr}/\text{TRU}$  by precipitation, ultrafiltration to remove entrained solids, ion exchange to remove  $^{137}\text{Cs}$  and  $^{99}\text{Tc}$ , and evaporation to re-concentrate the waste samples to the recommended level for vitrification, as required by the applicable waste envelope. Chemical analyses of these pretreated waste products were performed at PNNL or SRTC and provided to VSL, where glass formulations were developed and tested to identify suitable glass compositions for vitrification testing of the actual wastes. VSL then provided the crucible melt formulations to SRTC or PNNL where the actual waste glasses were prepared. Glasses were melted in Pt-alloy crucibles in high-temperature furnaces. Crucible melts were prepared from slurry feeds containing the prescribed amount of pretreated supernate and glass former blend. The crucible containing the slurry feed was placed in the furnace, heated slowly to dry the slurry, melted at  $1150^{\circ}\text{C}$ , and allowed to cool rapidly to produce a glass sample of a few hundred grams. Glass samples were then subjected to CCC heat treatment according to WTP supplied profiles (Petkus 2003) with the exception of one duplicate of Actual AZ-102 waste glass sample, which was tested both after quenching (AZ-102 Actual) and after CCC heat treatment (AZ-102 Actual CCC). The AN-102 Actual LC Melter sample was prepared at SRTC using a small-scale crucible-type melter where larger amounts of glass was prepared, from which about one kilogram was remelted and subjected to CCC heat treatment.

The tank waste samples were selected to be representative of all LAW Waste Sub-Envelopes, leading to the following nine samples:

- AN-103 Actual is a glass sample prepared at SRTC from an actual Tank 241-AN-103 waste sample (Crawford et al. 2001a), using VSL formulation LAWA44 and represents LAW Sub-Envelope A1.
- AW-101 Actual is a glass sample prepared at PNNL from an actual Tank 241-AW-101 waste sample (Smith et al. 2000), using VSL formulation LAWA88 for LAW Sub-Envelope A2. Differences in the measured potassium concentration in the waste, however, led to a revision of the glass composition selected for waste vitrification to VSL formulation LAWA170 (Muller et al. 2005b).
- AP-101 Actual is a glass sample prepared at PNNL from an actual Tank 241-AP-101 waste sample (Smith et al. 2004a), using VSL formulation LAWA126 for LAW Sub-Envelope A2.

- AZ-101 Actual is a glass sample prepared at PNNL from an actual Tank 241-AZ-101 waste sample (Smith et al. 2004b), using VSL formulation LAWB83 for LAW Sub-Envelope B1.
- AN-107 Actual (LAWC15) is a glass sample prepared at PNNL from an actual Tank 241-AN-107 waste sample (Smith et al. 2000), using VSL formulation LAWC15 for LAW Sub-Envelope C1.
- AZ-102 Actual and AZ-102 Actual CCC are glass samples prepared at SRTC from an actual Tank 241-AZ-102 waste sample (Crawford et al. 2004), quenched and container centerline-cooled, respectively, using VSL formulation LAWB88 for LAW Sub-Envelope B2. A non-radioactive simulant of this glass was prepared in parallel at SRTC, as mentioned earlier in Section 2.6.
- AN-102 Actual and AN-102 Actual LC Melter are glass samples prepared at SRTC from an actual Tank 241-AN-102 waste sample, at crucible-scale (Crawford et al. 2001b) and in the small-scale crucible-type melter system, respectively (Zamecnik et al. 2002), using VSL formulation LAWC21 for LAW Sub-Envelope C2. The SRTC melter system was first tested with a simulant of AN-102 waste, leading to glass AN-102 Surr LC Melter.

The target compositions of the Actual LAW glasses are listed in Tables 2.15 and 2.16. Of the nine glasses in this subset, all nine have PCT data. No other property measurements were conducted on these glasses.

## **2.8 Summary of LAW Glasses Available for Property Modeling**

As described in Sections 2.1 to 2.7, there are seven groups of LAW glasses available for developing property-composition models. Table 2.17 summarizes the groups of glasses, the group IDs, and the number of glasses in each group. In total, there are 271 LAW glasses with data for at least one of the four properties.

## **SECTION 3**

### **EXPERIMENTAL PROCEDURES AND CALCULATIONS**

The experimental procedures used in the preparation and characterization of the simulated LAW glasses are presented in this section. The procedures used in the preparation and testing of glasses made from actual LAW samples are discussed briefly.

For the simulated LAW glasses, the following subsections discuss the preparation of glass batches, crucible glass melting, glass composition analysis, normalization of target glass compositions with measured SO<sub>3</sub> values, and test procedures for PCT, VHT, electrical conductivity, and viscosity.

#### **3.1 Glass Batching and Preparation**

A total of 271 glass samples (some having the same target compositions) were prepared and characterized to support ILAW property-composition modeling. Four out of the 271 glass samples were remelts because the first crucible melts of these compositions did not yield sufficient glass sample to complete all of the property measurements. Of the 271 samples, 11 were prepared at SRTC or PNNL, 2 are glasses made with waste simulants, and 9 are actual LAW glasses, as discussed in Section 2. The remaining 260 samples were prepared at VSL. All simulant glasses were prepared using reagent grade or higher purity chemicals. Batching recipes were prepared to target the glass oxide compositions given in Tables 2.1 to 2.14 in Section 2. Section 3.1.1 describes the batching of starting materials, while Section 3.1.2 discusses glass preparation.

##### **3.1.1 Batching of Starting Materials**

Glass preparation began with a batching sheet that provided information on the required starting materials and their weights. The information included the chemicals needed, identification of the chemicals according to vendors and catalog numbers with the associated purity, and the amounts necessary to produce a given quantity of glass. Chemicals were weighed and batched according to the batching sheets. The batching and preparation of some of the LAW glasses was repeated as a result of the need for a larger amount of glass for additional testing and occasionally as a result of minor batching errors. Consequently, some glasses were prepared multiple times and are identified with an extension Rx (where x identifies the replicate number).

The information found in the batching sheets, including actual weights of chemicals used and their associated purities, can be used to calculate the composition of the glasses. The batching chemicals were determined such that the calculated compositions equaled the target compositions given in Section 2.

### 3.1.2 Glass Preparation

Preparation of all simulated LAW glasses at the VSL began with weighing and batching of chemicals according to the information in the batching sheets. The batches were prepared from reagent grade or higher purity chemicals to produce a batch size of approximately 400 to 450 g. A blender was used to mix and homogenize the starting materials before they were loaded into platinum-gold crucibles (Pt-Au) that were engraved with individual identification numbers. Note that for the ILAW Phase 1 Test Matrix (see Section 2.1), glass melts were prepared in the random order given in Table 2.5. Glass melts for the other test matrices (e.g., the Phase 1a Augmentation glasses, see Section 2.3) were typically prepared in the order of the Glass ID numbers. Generally Glass IDs are not assigned with glasses in any sort of compositional order, so that lack of explicit randomization is not a problem. Other crucible melts (e.g., the actively designed glasses discussed in Sections 2.2 and 2.6) were prepared at various times to support other activities such as melter testing, in addition to ILAW property-composition modeling.

After the batching was completed, the loaded platinum-gold crucibles were placed inside a Deltech DT-28 (or DT-29) furnace with a Eurotherm 2404 temperature controller. The glasses were melted for 75 minutes at 1200°C. Mixing of the melt was accomplished mechanically using a platinum stirrer, beginning 15 minutes after the furnace temperature reached 1200°C and continuing for the next 60 minutes. The molten glass was poured at the end of 75 minutes onto a graphite plate to cool.

Some of the simulated glass samples to support actual radioactive waste vitrification at PNNL or SRTC were prepared at VSL by melting slurry feeds made by mixing glass former additives to waste simulant solutions targeting the analyzed actual LAW compositions reported by SRTC or PNNL. The slurry feed was loaded into a Pt-Au crucible, dried in an oven at 110°C, heated slowly to 1150°C, and melted for four hours. The furnace temperature was then reduced to 1114°C, and most of the samples were cooled according to the CCC cooling profile provided by WTP (Petkus 2003). A typical CCC profile is given in Figure 3.1.

Crucible melts prepared at SRTC or PNNL from actual waste samples followed similar slurry preparation, melting in Pt-alloy crucibles, and CCC heat treatment procedures. The furnaces at PNNL and SRTC were, however, equipped with off-gas systems to collect the hazardous constituents. Four of the actual LAW samples were prepared at PNNL (Smith et al. 2000, 2004a, 2004b) and four at SRTC (Crawford et al. 2001a, 2001b, 2004). Another actual LAW sample was collected from a melter system (Zamecnik et al. 2002) at SRTC with a nominal melt temperature of 1135°C. This actual LAW waste melter sample was remelted and heat treated according to CCC profile before being subjected to PCT.

Samples from melter tests at the VSL and LAW Pilot Melter were collected from glass that had been air-lift discharged into drums. Pieces of broken glass were collected from the top part of the drums.



### 3.2 Analyses of Glass Compositions

The primary method used for glass composition analysis at VSL was x-ray fluorescence (XRF) on powdered glass samples. An ARL 9400 wavelength dispersive XRF spectrometer was used for this purpose. The XRF was calibrated over a range of glass compositions using standard reference materials traceable to the National Institute of Standards and Technology (NIST), as well as waste glasses such as Argonne National Laboratory – Low Activity Waste Reference Material (ANL-LRM) and Savannah River Laboratory – Environmental Assessment Glass (SRL-EA). XRF analysis provides data for most glass components of interest, except lithium and boron, which are analyzed by direct current plasma atomic emission spectroscopy (DCP-AES), as described below.

Glass samples for DCP-AES analysis were subjected to microwave-assisted total acid dissolution in Teflon vessels according to VSL standard operating procedures. Twenty milliliters of a 1:5 mixture of concentrated HF:HNO<sub>3</sub> were diluted to 50 ml and used for the dissolution. This procedure is similar to the ASTM Test Method C1412-99, which also employs a mixture of concentrated HF and HNO<sub>3</sub> in microwave digestion of pulverized glass samples. However, supplemental use of HCl/H<sub>3</sub>BO<sub>3</sub> is not included in the VSL procedure because boron is normally one of the analytes. The resulting solutions were analyzed by DCP-AES for all constituents except sulfur, for which Dionex Ion Chromatography was used. These results complement XRF, particularly for boron and lithium. DCP-AES was the only method of glass analysis used for early Part B1 glasses (Muller et al. 2001a).

Glasses prepared from actual LAW radioactive samples were analyzed by inductively coupled plasma atomic emission spectroscopy (ICP-AES) and atomic absorption (AA) spectroscopy using solutions from acid dissolution of ground glass or KOH or Na<sub>2</sub>O<sub>2</sub> fusion according to SRTC or PNNL operating procedures. If boric acid is one of the reagents used in acid dissolution, the analysis will not provide boron concentration in the glass. Similarly, if KOH or Na<sub>2</sub>O<sub>2</sub> is used as a reagent for fusion, or nickel and zirconium crucibles are used to hold the mixture, the analysis will not provide concentrations of the corresponding constituents.

The XRF detection limit for most components is about 0.01 wt%. The accuracy of the analysis is about  $\pm 10$  relative percent for major components ( $> 3.0$  wt% in the glass) or 1.0 wt% absolute, whichever is smaller. However, with the exception of volatile components such as SO<sub>3</sub>, the batched (target) glass compositions are expected to be more accurate than the analyzed compositions because the batched compositions are derived from simple weighing of pure chemicals. Hence, the target compositions for all major constituents, except SO<sub>3</sub>, are believed to provide the best compositional representations of the tested glasses. The principal role of the compositional analyses is, therefore, to confirm the target compositions.

Because SO<sub>3</sub> is a constituent that limits waste loading in LAW glasses and has a tendency to volatilize during glass preparation, the SO<sub>3</sub> concentration to be used in modeling LAW glass properties was of particular interest. Analysis of both crucible melts and melter discharge glass samples have shown SO<sub>3</sub> analyzed values to be consistently below target values due to volatilization (Pegg et al. 2000). The SO<sub>3</sub> retention in melter glasses varied from about 70% to 95% (Matlack et al. 2003a, 2003b and 2003d) depending on the SO<sub>3</sub> concentration in the glass,

LAW waste type, amount of reductants in the feed, etc. For this reason, it was decided that XRF analyzed  $\text{SO}_3$  values would better represent the glass composition. Accordingly, XRF measured  $\text{SO}_3$  values were used for modeling. A simple regression presented in Section 3.3 was used to estimate  $\text{SO}_3$  values to be used in modeling for about twenty glasses for which XRF measured  $\text{SO}_3$  values were not available.

In general, the chemical analysis results for non-volatile components were in good agreement with the corresponding target compositions. Chemical analyses of all glass samples used in modeling, along with discussions of the results are given in the references cited in Section 2 for each set of glasses.

### 3.3 Use of Analyzed $\text{SO}_3$ Values in Normalized Glass Compositions

As discussed in Section 3.2, analyzed  $\text{SO}_3$  values obtained by XRF are generally less than the target  $\text{SO}_3$  values to varying degrees because  $\text{SO}_3$  can be partially volatilized during glass melting. Thus, analyzed values of  $\text{SO}_3$  are expected to be more accurate than target values of  $\text{SO}_3$ . Therefore, for developing LAW property-composition models, it was decided to use simulated LAW glass compositions based on analyzed rather than target  $\text{SO}_3$  values. During production of WTP LAW glass, it is envisioned that  $\text{SO}_3$  volatility factors could be applied in calculating the estimated glass composition (after volatility) from process samples and measurements.

Hence, for the property-composition modeling database, it was decided to replace target  $\text{SO}_3$  values with analyzed  $\text{SO}_3$  values. In glasses where  $\text{SO}_3$  was not analyzed, analyzed  $\text{SO}_3$  values were estimated by interpolative regression. Specifically, 146 LAW glasses having target  $\text{SO}_3$  values less than or equal to 0.50 wt% and also having analyzed  $\text{SO}_3$  values were used<sup>6</sup> to fit two regression models of the form

$$A_{\text{SO}_3} = a_0 + a_1 T_{\text{SO}_3} \quad (3.1)$$

where

$A_{\text{SO}_3}$  = analyzed value of  $\text{SO}_3$  (wt%)

$T_{\text{SO}_3}$  = target value of  $\text{SO}_3$  (wt%)

$a_0, a_1$  = intercept ( $a_0$ ) and slope ( $a_1$ ) of the fitted regression equation.

The first regression equation was obtained for  $T_{\text{SO}_3} \leq 0.25$  wt% using 30 of the 146 glasses and is given by

---

<sup>6</sup> A total of 151 glasses had analyzed  $\text{SO}_3$  values with target  $\text{SO}_3$  values less than 0.50 wt%. However, a plot of the analyzed versus target  $\text{SO}_3$  values showed that five glasses (LAWM27, LAWM34, LAWM35, LAWA127R2, and LAWB86) were significant outliers to the relationship, and so the data on those five glasses were excluded from the regressions (so that only 146 were used).

$$A_{SO_3} = 0.0162 + 0.8092 T_{SO_3}, \quad (3.2)$$

while the second regression equation was obtained for  $0.25 \text{ wt}\% < T_{SO_3} \leq 0.50 \text{ wt}\%$  using 116 of the 146 glasses and is given by

$$A_{SO_3} = 0.1037 + 0.5680 T_{SO_3}. \quad (3.3)$$

Two linear regressions were selected as giving better approximations of the relationships between analyzed and target  $SO_3$  values over the ranges indicated.

Figure 3.2 shows the data points used and the resulting fitted regression lines. These regression equations were then applied to the 20 LAW glasses having target  $SO_3$  values but not analyzed  $SO_3$  values. Table 3.1 lists the glass IDs, target  $SO_3$  values, and estimated (predicted) analyzed  $SO_3$  values from the equations for these 20 LAW glasses.

The analyzed  $SO_3$  values (where available) or the estimated analyzed  $SO_3$  values (from Table 3.1) were substituted for the target  $SO_3$  values and then renormalized compositions of the LAW glasses were calculated using the equations

$$\begin{aligned} g_{ij} &= \frac{100T_{ij}}{A_{i,SO_3} + \sum_{j \neq SO_3} T_{ij}} \quad \text{for } j \neq SO_3 \\ &= A_{i,SO_3} \quad \text{for } j = SO_3 \end{aligned} \quad (3.4)$$

where

- $g_{ij}$  = normalized concentration of the  $j^{\text{th}}$  component in the  $i^{\text{th}}$  LAW glass (wt%)
- $T_{ij}$  = target value of the  $j^{\text{th}}$  component in the  $i^{\text{th}}$  LAW glass (wt%)
- $A_{i,SO_3}$  = analyzed or estimate of analyzed  $SO_3$  value for the  $i^{\text{th}}$  LAW glass (wt%)

The normalized LAW glass compositions (wt%) calculated per Equation (3.4) are listed in Table 3.2 for the 271 glasses discussed in Section 2.

The property-composition model forms used in Sections 5 to 8 are based on LAW glass compositions expressed in mass fractions rather than in wt%. Compositions are converted from wt% to mass fractions according to the formula

$$x_{ij} = \frac{g_{ij}}{100}, \quad j = 1, 2, \dots, q \quad (3.5)$$

where  $x_{ij}$  denotes the mass fraction of the  $j^{\text{th}}$  component in the  $i^{\text{th}}$  LAW glass and  $g_{ij}$  is as previously defined. Note that compositions expressed in mass fractions sum to 1.0 (i.e.,  $\sum_{j=1}^q x_{ij} = 1$ ) rather than to 100% as do compositions expressed in wt%.

### 3.4 Product Consistency Test

The Product Consistency Test (PCT) was conducted using 4 g of crushed glass (100-200 mesh, 75-149  $\mu\text{m}$ ) placed in 40 ml of test solution (de-ionized water) inside 304L stainless steel vessels. These test conditions result in a ratio of the glass surface area to the solution volume of about  $2000 \text{ m}^{-1}$ . PCT tests were performed at  $90^\circ\text{C}$  for 7 days according to ASTM (2002), in accordance with the current WTP contract requirement (DOE-ORP 2000). All tests were conducted in triplicate (or quadruplicate in the case of glasses made from actual LAW samples) in parallel with the ANL-LRM standard glass included in each test set. The leachates were sampled at seven days. One milliliter of sampled leachate was mixed with 20 ml of 1M  $\text{HNO}_3$  and the resulting solution was analyzed by DCP-AES. Another 3 ml of sampled leachate was used for pH measurement.

In addition to the leachate concentrations, it is convenient and conventional to also consider the normalized leachate concentrations. The normalization is performed by dividing the concentration measured in the leachate for any given component by its fraction in the glass. Thus, the *normalized concentration*  $C_i$  of element  $i$  (in g/L) is calculated from the elemental concentration  $c_i$  measured in the leachate (in ppm) as:

$$C_i = \frac{c_i}{f_i}, \quad (3.6)$$

where  $f_i$  is the mass fraction of element  $i$  in the glass.

The surface area of the glass sample tested and the volume of leachant used will also affect the measured leachate concentrations and, therefore, a standard value of their ratio ( $2000 \text{ m}^{-1}$ ) is specified in the PCT method (ASTM 2002). A further normalization for this effect is often considered by dividing the normalized concentration by the ratio of the surface area of glass exposed to the solution volume ( $S/V$ , in  $\text{m}^{-1}$ ). The *normalized mass loss* (in  $\text{g}/\text{m}^2$ ) is then obtained from

$$L_i = \frac{C_i}{(S/V)}, \quad (3.7)$$

where  $S/V$  is the ratio of the glass surface area to the volume of the leachant, which for the standard PCT is nominally  $2000 \text{ m}^{-1}$ . Assuming this value of  $S/V$ , if  $C_i$  is expressed in g/L, one need only divide by two to obtain  $L_i$  in  $\text{g}/\text{m}^2$  (because  $1 \text{ g}/\text{L} = 1000 \text{ g}/\text{m}^3$ ). Specification 2.2.2.17.2 in the WTP contract (DOE-ORP 2000) sets limits of  $2 \text{ g}/\text{m}^2$  for the normalized mass

losses of Na, B, and Si on the PCT. Thus, the WTP contract limit of a normalized mass loss of less than 2 g/m<sup>2</sup> corresponds to a normalized concentration of 4 g/L.

### 3.5 Vapor Hydration Test

The vapor hydration tests were run in Parr series 4700 screw-cap pressure vessels made of 304L stainless steel and having either 22 or 45 ml capacity, in accordance with VSL procedure. Glass coupons were fashioned about 5 to 10 mm square, about 2 mm thick, and with one cut and one fractured surface. A hole approximately 1.6 mm in diameter was drilled near one corner of the coupon to allow it to be suspended from a hanger made of 24 gauge stainless steel wire. Dimensional measurements were made to permit calculation of the area, and the coupon was weighed before and after the VHT on a balance having a resolution of 100 µg. The coupon was suspended vertically from the hanger in the pressure vessel and enough de-ionized water was added to the vessel to saturate the volume at the test temperature of 200°C and to allow for a non-dripping layer covering the coupon. The pressure vessels were flushed with argon, sealed, weighed, and placed in an oven held at 200°C. The temperature was monitored continuously with an independent thermocouple. At the completion of the test, the pressure vessels were removed and immediately partially immersed in an ice/water bath to condense the water vapor near the bottom of the vessel. Once cool, the vessels were weighed and opened, and then the coupons were removed and weighed. If the difference in the mass of the sealed pressure vessel before and after the test indicated a water loss in excess of 50% of the original amount, the test results were discarded. Otherwise, the coupons were examined using low-power optical microscopy and an X-ray diffraction pattern was taken directly off the surface of the coupon. Next, the coupons were sectioned and the pieces mounted separately to allow Scanning Electron Microscopy (SEM) examination, both of the cross section of the leached coupon and the leached surface itself, and to measure the layer thickness. For consistency with existing data, the nominal test duration was 24 days.

All of the VHT data used in this report were collected at VSL from tests performed at 200°C for a nominal duration of 24 days. The reacted glass samples were sectioned and examined by SEM to determine the altered layer thickness. For a layer thickness greater than 100 microns, the layer thickness (which can be uneven), was measured by subtracting the average remaining glass thickness measured at ten points throughout the coupon's cross-section from the original thickness of the coupon. The altered layer thickness, which (given certain assumptions) relates directly to the mean glass alteration rate over the test interval, was the variable that was used in this report. Thus, the dependence of the altered layer thickness on glass composition was investigated.

WTP Contract Specification 2 (DOE-ORP 2000) requires that the VHT alteration rate determined from tests of seven days or longer duration be below 50 g/m<sup>2</sup>/day. If it is assumed that the altered layer density is not appreciably different from that of the glass, the mean glass alteration rate over the test interval ( $r$  in g/m<sup>2</sup>/d) is related to the measured altered layer thickness  $D$  in microns by

$$r = \rho D/t, \quad (3.8)$$

where  $\rho$  is the glass density in  $\text{g/cm}^3$  and  $t$  is the test duration. Under this assumption, for a typical density of  $2.65 \text{ g/cm}^3$ , a layer thickness of 453 microns in a 24-day VHT would correspond to a mean glass alteration rate of  $50 \text{ g/m}^2/\text{day}$ .

Although in some previous VHT modeling work the test duration was included as a modeling variable (Gan et al. 2001b), the VHT modeling work in this report is similar to that in the preceding report (Muller et al. 2005a) in that modeling is restricted to VHT results obtained at a single test duration (24 days) because all of the more recent data have been collected at this test duration.

### **3.6 Electrical Conductivity Testing**

The electrical conductivity (EC) of each LAW glass was determined by measuring the impedance of the glass melt at temperatures around 950, 1050, 1150 and 1250°C as a function of AC frequency using a calibrated platinum-rhodium electrode probe attached to a Hewlett-Packard model 4194A impedance analyzer. The collected impedance data were analyzed to obtain the DC electrical conductivity. The probe (analyzer along with the crucible to assure that the geometry is replicated) was calibrated and checked using NIST traceable standard material periodically, as required by VSL technical procedure.

The current WTP requirement for glass melt EC limits is 0.1 to 0.7 Siemens/cm at 1100 - 1200 °C (Clark 2003).

### **3.7 Viscosity Testing**

The melt viscosity ( $\eta$ ) of each glass was measured using a Brookfield viscometer with a platinum-rhodium spindle and crucible. The relative torque of a rotating spindle immersed in molten glass was measured as a function of rotational velocity (revolutions per minute (RPM)) at temperatures around 950, 1050, 1150 and 1250°C. The viscosity of the molten glass was then calculated from the collected data of torque versus RPM. The equipment was calibrated using viscosity standard oils and checked using a NIST traceable standard glass periodically, per VSL technical procedure.

Per current WTP requirements glass melts should satisfy the viscosity limits of 10 to 150 poise at 1100 °C with the preferred range being 40-80 poise at 1150°C (Clark 2003).

### **3.8 Liquidus Temperature**

Bounds on the liquidus temperatures of LAW glasses were determined by examining heat-treated glass samples. Samples of about 1 to 5 g were melted in platinum-gold crucibles at a temperature of 1200°C for one hour to destroy any pre-existing nuclei, followed by heat treatment at 700°C, 850°C or 950°C. A heat treatment time of 20 hours was used. The

heat-treated glass sample was then quenched by submerging the outside of the crucible in cold water. This quenching freezes in the phase assemblage in equilibrium with the melt at the heat treatment temperature. If no crystals are observed in the cooled glass, then it is inferred that no crystals are present at the heat treatment temperature and that the liquidus temperature is below that temperature.

Because LAW glasses are designed to have a liquidus temperature of 950°C or less, and generally show little tendency to crystallize, in many cases, heat treatments were done at lower temperatures of 700°C or 850°C. In some cases, glasses were not subjected to any heat treatment, as mutually agreed with WTP, because prior experience had shown that LAW glasses did not have tendency to crystallize.

In addition to the isothermal heat treatments, many samples were subjected to container centerline cooling (CCC) heat treatment according to WTP supplied profiles (Petkus 2003). A typical CCC curve is given in Figure 3.1. The CCC heat treatment mimics the temperature profile experienced by the glass in the LAW container as it cools.

Optical microscopy and SEM were used to determine the amount of crystals and to characterize the microstructure of the glasses. Energy Dispersive X-ray Spectroscopy (EDS) was used to analyze the elemental composition of the glass and crystalline phases that were observed. Typical magnifications used ranged from 25× to 5,000×.

Digital imaging and analysis was used to determine the volume fractions of crystalline phases in both as-melted and heat-treated glasses. The accuracy of the volume percentage determinations is limited by uniformity of distribution and imaging characteristics of a phase. The accuracy of the volume percentage determination is estimated to be within 20% relative.

Optical microscopy with image analysis and quantitative X-ray Diffraction (XRD) were used in combination with the SEM/EDS measurements to characterize the secondary phases in heat treated LAW glass samples.

The current WTP requirement limits the amount of crystals to a maximum of 1 vol% at 950°C (Clark 2003).

### **3.9 Glass Density**

Density measurements were made on 5 to 15 grams of crushed glass using the pycnometric method described in ASTM D 854 (ASTM 2006). The densities of two NIST glasses (Lead Silicate Glass #1827a and Soda Lime Silica Glass #1826b) were measured as calibration checks. To confirm the reproducibility of the results, triplicate analyses of ten percent of the samples were performed, as required by the procedure.

WTP Contract Specification 2 (DOE-ORP 2000), for package dimension, weight and void fraction limits the glass density to 3.7 g/cc.

## SECTION 4

### PCT, VHT, ELECTRICAL CONDUCTIVITY, AND VISCOSITY RESULTS

Product Consistency Test (PCT), Vapor Hydration Test (VHT), electrical conductivity (EC), and viscosity results for the simulated and actual LAW glasses are presented and discussed in this section. In addition, general compositional trends in the data with respect to the expected roles of glass constituents (glass formers, modifiers, etc.) on the PCT, VHT, electrical conductivity, and viscosity responses are discussed. Quantitative statistical modeling of the respective property datasets are discussed in Sections 5, 6, 7, and 8.

#### 4.1 Product Consistency Test (PCT) Results and Discussion

The PCT results are presented in Section 4.1.1 and discussed in Section 4.1.2.

##### 4.1.1 PCT Results

Of the 271 simulated and actual LAW glasses discussed in Section 2, 264 glasses have data on PCT boron (PCT-B), sodium (PCT-Na), and silicon (PCT-Si) releases, as summarized in Table 4.1. The PCT was performed and results were obtained for these 264 LAW glasses using the procedure described in Section 3.4. Specifically, concentrations (ppm) of PCT-B, PCT-Na, and PCT-Si releases were obtained for the 264 LAW glasses. The PCT normalized concentration values (in g/L) and normalized mass loss values (in g/m<sup>2</sup>) were calculated from the PCT elemental concentrations (in ppm) using Equations (3.6) and (3.7), respectively, and the normalized glass compositions listed in Table 3.2.

The PCT-B, PCT-Na, and PCT-Si releases are given in Table 4.2 for the simulated and actual LAW glasses discussed in Section 2. The PCT releases vary from 0.152 g/L (0.076 g/m<sup>2</sup>) to 35.657 g/L (17.829 g/m<sup>2</sup>) for PCT-B, 0.209 g/L (0.105 g/m<sup>2</sup>) to 22.937 g/L (11.469 g/m<sup>2</sup>) for PCT-Na, and 0.114 g/L (0.057 g/m<sup>2</sup>) to 2.372 g/L (1.186 g/m<sup>2</sup>) for PCT-Si. The WTP contract (DOE-ORP 2000) limits for PCT-B, PCT-Na and PCT-Si releases are all 2.0 g/m<sup>2</sup> (4.0 g/L).

“Actively designed” glasses as well as the LAW Correlation glasses were designed to be in compliance with ILAW performance requirements. As can be seen in Figure 4.1, their PCT releases are indeed less than the contract limit of 2 g/m<sup>2</sup> (4.0 g/L). The ILAW Phase 1 and Augmentation Test Matrix glasses, however, were designed to cover a larger composition region and, accordingly, their PCT responses vary over a wider range. Of the 264 glasses with PCT results, 9 glasses have PCT-B releases greater than 2 g/m<sup>2</sup> (LAWM12, LAWM17, LAWM33R1, LAWM34, LAWM35, LAWM55, LAWM56, LAWM68, and LAWM71), and 8 have PCT-Na releases greater than 2 g/m<sup>2</sup> (LAWM12, LAWM13, LAWM17, LAWM33R1, LAWM34, LAWM35, LAWM55 and LAWM56). All of the glasses with PCT-B or PCT-Na releases above the contract limit are from the ILAW Phase 1 or Augmentation Test Matrices (see Figure 4.1)



and are on or near the boundary of the LAW glass composition region over which data were collected. Such compositions were expected to provide a wider range of PCT values to support modeling, but are not compositions that are likely to be selected for LAW processing at the WTP.

As can be seen from Figure 4.1 and Table 4.2, for every glass the normalized PCT mass losses for B and Na are higher than the normalized PCT mass loss for Si. Furthermore, for *every one* of the 264 glasses with PCT results, the normalized PCT mass loss for Si is below the WTP contract limit of 2 g/m<sup>2</sup>. These results suggest that: (i) if the B and Na mass losses are below the WTP limit, so too will be the Si mass loss, and (ii) the Si mass loss does not exceed the WTP limit over the composition region of interest. As discussed below, lower mass loss for silicon is expected because of the role that SiO<sub>2</sub> plays in the glass structure, the mechanism by which silicon is leached, and the chemistry of silicon in solution. It was therefore concluded that a model for PCT Si release is not needed. Accordingly, with concurrence from the WTP Project, only PCT B and Na releases were modeled.

#### 4.1.2 Discussion of PCT Results

In order to examine compositional trends in the PCT data with respect to the expected roles of the glass constituents, it is convenient to consider the glass compositions on a molar basis. The compositions of the glasses in mol% are given in Appendix A. Components such as SiO<sub>2</sub>, B<sub>2</sub>O<sub>3</sub>, and P<sub>2</sub>O<sub>5</sub> are known to be glass formers that easily form glasses themselves. Depending on the glass composition, these components also contribute to the network structure of multi-component glass matrices. Also depending on the glass composition, components such as Al<sub>2</sub>O<sub>3</sub>, Fe<sub>2</sub>O<sub>3</sub>, and ZrO<sub>2</sub> can act as glass formers and strengthen the glass network. In silicate glasses, trivalent species require charge compensation by cations such as alkalis in order to go into four-fold coordination and contribute to the network structure. Alkali oxides, such as Li<sub>2</sub>O, Na<sub>2</sub>O, and K<sub>2</sub>O, act as network modifiers (fluxes) by breaking Si-O-Si bonds and de-polymerizing the network structure. Alkaline earth oxides (CaO, MgO), play a similar role to the alkalis but generally to a lesser extent since their higher field strength and higher valence leads to more covalence in the glass network. In general, glasses that are high in network formers are more durable and those high in modifiers are more leachable. Among glass network formers, SiO<sub>2</sub> in higher concentration makes the glass more durable. Similar effects are seen for Al<sub>2</sub>O<sub>3</sub> and ZrO<sub>2</sub> and, to a lesser extent, for B<sub>2</sub>O<sub>3</sub>. Although boron, in the presence of sufficient alkali, does contribute to the network structure, it is highly soluble and, therefore, much of its beneficial effect on glass leaching is instead associated with pH buffering of the leachant.

The PCT results were reviewed with respect to glass composition, in terms of the molar concentrations of glass network formers and modifiers, to examine the extent to which general trends or relationships may be evident. This is made somewhat challenging by the fact that the ILAW Phase 1 and Phase 1a Augmentation test matrices were designed to cover specified composition regions and, therefore, include “many-at-a-time” variations in glass components. Systematic variation of the concentrations of a single component or a set of similar components (e.g., alkali oxides) was not the purpose. Trends are nevertheless observed and discussed here.

Boron forms few secondary phases that precipitate from the leachate and does not participate appreciably in ion exchange reactions. Consequently, its concentration in solution provides one of the best measures of the extent of the reaction of the glass with the leachant. For glasses that show little leaching (less than  $2 \text{ g/m}^2$ ), the observed sodium and boron releases are generally congruent, as can be seen in Figure 4.2. With increased leaching (greater extent of reaction), sodium-containing secondary phases are likely to form, which causes a deviation from congruent behavior. Glass LAWM13 (see Figure 4.2) with 22 wt%  $\text{Na}_2\text{O}$  and comparatively low concentrations of  $\text{Al}_2\text{O}_3$  and  $\text{SiO}_2$  is an exception in that sodium release is higher than that of boron or any other glass constituent. Sodium (and other alkalis) can be released into solution by ion exchange and diffusion processes, in addition to matrix hydrolysis. Depending on the relative rates of these processes for a given glass, the normalized sodium leachate concentration can be higher than that of boron. Silicon is not the object of ion exchange or diffusion and its leaching requires the slower hydrolysis of the Si-O- bonds in the glass matrix. Additionally, the lower solubility of silicon in the leaching solution makes it prone to forming alteration products rather than being found in solution. Consequently, as can be seen in Figure 4.2, the mass loss measured from Si is much lower than that of Na and B. Note that Si release remains below  $2 \text{ g/m}^2$  even for the markedly high leaching LAWM glasses identified in Figure 4.2.

The leachate pH is not only an indicator of the glass-water reaction, it is also a factor in determining the rate and path of subsequent reactions. Alkali ion exchange tends to rapidly increase the pH from neutral to basic. In addition, the rate of hydrolysis of the silicate matrix increases as the pH increases. Furthermore, the stability of alteration phases can be dependent on the solution pH. Certain glass constituents, such as boron, tend to buffer the solution and moderate the pH increase. It is, therefore, instructive to examine the relationships between the measured leachate pH values, the glass composition, and PCT boron and sodium releases.

As expected, leachate pH increases as the alkali concentration in the glass increases, as can be seen in Figure 4.3. The pH varies from about 9 to 12.5, while total alkali content in the glass varies from 9.3 mol% (for LAWM8) to 26.3 mol% (for LAWA105, LAWM12 and LAWM56). PCT boron release as a function of leachate pH is shown in Figure 4.4. Note that in Figure 4.4, the y-axis is limited to  $2.0 \text{ g/m}^2$  for clarity of display, but all data points including those with normalized release rates higher than  $2.0 \text{ g/m}^2$  were used to generate the fit. The boron release increases with pH but the relationship is markedly non-linear, as shown in the figure. Note that the glasses that fall farthest from the fitted curve are LAWB40 with very high lithium concentration and the Phase 1a augmentation glasses with the highest potassium concentrations, such as LAWM61, LAWM70 and LAWM72.

PCT boron release as a function of alkali concentration in the glasses is shown in Figure 4.5 and shows similar non-linearity to that seen in Figure 4.4, as would be expected in view of the linear relationship between pH and alkali content seen in Figure 4.3. In general, the PCT boron release increases as the alkali concentration in the glass increases indicating a greater de-polymerization of the glass network. A similar trend is observed for PCT sodium release as a function of alkali concentration, as shown in Figure 4.6. PCT boron release as a function of alkali and alkaline earth oxides concentration is shown in Figure 4.7. In general, as the sum of the alkali and alkaline earth oxides increases, the PCT release also increases, though the trend is not as clear as that for PCT boron release versus alkali oxide concentration. The data point at

about 40 mol% combined alkali and alkaline earth oxides and 0.4 g/m<sup>2</sup> PCT boron release is LAWM3, which contains about 19 mol% alkaline earth oxides and about 21 mol% alkali oxides. As mentioned previously, alkaline earth oxides are far less effective than alkali oxides in disrupting the glass network structure and, therefore, degrade glass durability to a lesser extent. PCT boron release as a function of the molar concentration of the glass network former oxides is shown in Figure 4.8. As expected, in general, the PCT boron release decreases as the concentration of network formers in the glass increases. It is difficult, however, to see any clear correlation as was evident with PCT B release as a function of alkali concentration. The five glasses in Figure 4.8 with very high boron releases all have high B<sub>2</sub>O<sub>3</sub> concentrations. The two glasses with the highest boron releases, LAWM12 and LAWM55, have the highest tested B<sub>2</sub>O<sub>3</sub> concentration of 12 wt%. PCT boron release is plotted as a function of the ratio of the concentration of alkali oxides to the concentration of network former oxides in Figure 4.9. As is evident from the figure, the PCT boron release increases as this ratio increases. This is expected because as the ratio increases, the concentration of glass network modifiers increases with respect to glass network formers resulting in less durable glasses. Figure 4.10 shows PCT boron release as a function of the ratio of the sum of the concentrations of alkali and alkaline earth oxides to the concentration of network former oxides. Again, the PCT boron release shows an increasing trend with increase in the ratio, but the correlation is not as clear as that for the ratio of alkali oxides to network former oxides.

A clear increasing trend of PCT boron and sodium release is observed as the alkali oxide content increases. This is expected because alkali oxides are the most effective modifiers in breaking up the glass structure. An increasing trend in PCT releases with increase in alkaline earth oxide concentration is less clear. Again, this is not unexpected because alkaline earth oxides have a lesser tendency to de-polymerize the glass structure as a result of their greater tendency towards covalent bonding. Finally, as expected, increases in the glass network former oxide concentrations lead to a decreasing trend in the PCT releases.

## 4.2 VHT Results and Discussion

The VHT results are presented in Section 4.2.1 and discussed in Section 4.2.2.

### 4.2.1 VHT Results

Of the 271 simulated and actual LAW glasses discussed in Section 2, 181 glasses have VHT results as summarized in Table 4.1. The VHT was performed and results obtained for these 181 LAW glasses using the procedure described in Section 3.5. Specifically, VHT alteration depths  $D$  (in  $\mu\text{m}$ ) were obtained for the 181 LAW glasses. The VHT alteration rates  $r$  (in g/m<sup>2</sup>/d) were calculated from the VHT alteration depths using Equation (3.8).

The VHT alteration depths (in  $\mu\text{m}$ ) and alteration rates (in g/m<sup>2</sup>/d) are given in Table 4.3 for the simulated and actual LAW glasses discussed in Section 2. The VHT alteration depths and rates for the 181 glasses vary from 1  $\mu\text{m}$  (0.1 g/m<sup>2</sup>/d) to 980  $\mu\text{m}$  (108.2 g/m<sup>2</sup>/d). This range

excludes the results for six glasses that were altered completely before the end of the 24-day test period (discussed further in the following paragraph).

The “actively designed” and the LAW Correlation glasses discussed in Section 2 were designed to be compliant with ILAW performance requirements. Therefore, the VHT alteration rates of the majority of them are expected to be less than the contract limit of 50 g/m<sup>2</sup>/d (453 μm). However, glasses in the ILAW Phase 1 Test Matrix and the Phase 1a Augmentation Test Matrix were designed to cover a large composition region. Accordingly, their VHT responses vary over a wider range. Also, some of the recent LAW Correlation glasses and all of the Augmentation Test Matrix glasses were formulated with the intent to approach or slightly exceed the VHT limit (see Sections 2.3 and 2.4). In total, 20 glasses have VHT alteration rates above the 50 g/m<sup>2</sup>/d limit. These glasses are generally on or near the boundary of the LAW glass compositional region studied. Such glasses were expected to provide a wider range of VHT values, but are not compositions that are likely to be selected for LAW processing at the WTP. The 20 glasses with VHT alteration rates above the 50 g/m<sup>2</sup>/d limit include six glasses whose extent of VHT alteration was so high that no rate could be calculated because the entire glass coupon was altered. Those glasses are LAWM12, LAWM13, LAWM14, LAWM32, LAWM55, and LAWE14. The VHT alteration rates for these glasses are listed as “greater than” values in Table 4.3.

#### 4.2.2 Discussion of VHT Results

The VHT results were reviewed in terms of the molar concentrations of glass network formers and modifiers in the glass composition to examine the extent to which general trends or relationships may be evident. The challenge offered by the large composition space is amplified by the fact that VHT is designed to assess relatively late-stage features of the glass corrosion. In late-stage glass corrosion, (i) the leachate (an absorbed aqueous film in the case of the VHT) is dominated by glass corrosion products which significantly modify the leachate properties, and (ii) secondary phases are formed in the leachate as reaction products. Consequently, VHT alteration is a complex process that is expected to exhibit complex dependencies on glass composition.

Figure 4.11 shows the VHT alteration depth as a function of the alkali oxide concentration (the five glasses with alterations greater than 1100 μm are displayed at the 1100 μm coordinate)<sup>7</sup>. Note that the number of glasses with alkali concentration exceeding 23 mol%, is now greatly increased by the addition of the Augmentation Matrix and LAW Correlation glasses. With these additional glasses, it is now apparent that the glass is more likely to fail VHT when the total alkali content is higher than 23 mol%. Figure 4.12 shows VHT alteration depth as a function of the sum of the alkali and alkaline earth oxide concentrations. No clear trend in VHT alteration rate is evident in this figure. The data point at 40.3 mol% alkali and alkaline earth oxides is LAWM3 in which alkali and alkaline earth oxides are almost equally distributed.

---

<sup>7</sup> In Figures 4.11 to 4.14, the plotting symbols overlap for two of the five glasses with alterations > 1100 μm.

VHT alteration depth as a function of the glass network former oxide concentration is given in Figure 4.13 on both linear and logarithmic scales. The highest VHT alteration depths tend to be for glasses that have lower glass network former oxide concentrations, which is consistent with expectations. In the logarithmic plot, a slight trend of decreasing VHT alteration depth with increasing glass network former oxide concentration is visible but not as distinct as was observed with PCT. Figure 4.14 shows VHT alteration depth as a function of the ratio of alkali oxide to glass network former oxide concentration on both linear and logarithmic scales. The highest VHT alteration depths occur at high ratios of alkali oxides to glass network former oxides, which is as would be expected. A clear increasing trend in VHT alteration depth as the ratio increases is evident in Figure 4.14, especially in the logarithmic plot, indicating a much higher slope in VHT alteration rate increase at the higher end of alkali concentration.

The VHT alteration depth data do not show simple correlations with either glass alkali oxide or network former oxide concentrations. There are, however, two noticeable effects related to the alkali content: a threshold at around 23 wt% alkali beyond which VHT alteration depths increase rapidly, and a correlation between the logarithm of VHT alteration depth and the ratio of alkali oxide to glass network former oxide concentration. This correlation is generally consistent from a glass structure perspective, where alkali oxides act as modifiers in breaking up the glass network structure and glass network former oxides act to strengthen it. Glasses with a more highly polymerized network, which results from having more network former oxides and less alkali oxides, tend to be more durable. As discussed previously, however, the overall VHT alteration mechanism is complex and a useful simple correlation to glass structural roles would seem to be unlikely.

### **4.3 Electrical Conductivity Results and Discussion**

The electrical conductivity results are presented in Section 4.3.1 and discussed in Section 4.3.2.

#### **4.3.1 Electrical Conductivity Results**

Of the 271 simulated and actual LAW glasses discussed in Section 2, 181 simulated glasses have electrical conductivity results as summarized in Table 4.1. As described in Section 3.6, electrical conductivity was generally measured at four temperatures for each LAW glass. The electrical conductivity versus temperature values are given in Table 4.4 for the 181 simulated glasses. Each row of Table 4.4 provides the electrical conductivity data for a given glass and four temperatures. There are four columns of data for each glass corresponding to the four temperatures at which electrical conductivity was measured.

The current WTP requirement (Clark 2003) for glass melt electrical conductivity is that it be within 0.1 to 0.7 S/cm in the temperature range of 1100 to 1200°C. For 188 measurements taken in this temperature range, the glass melts' electrical conductivity values were mostly within the acceptable range of 0.1 to 0.7 S/cm. Eight of the measurements were slightly outside of this range with values from 0.073 to 0.732 S/cm. The electrical conductivities of melts

LAWM7, LAWM8, LAWM9, LAWM28 and LAWM54R1 were slightly below the WTP recommended lower limit of 0.1 S/cm and the electrical conductivities of three melts LAWM13, LAWCrP2R and LAWCrP4R were slightly above the upper limit of 0.7 S/cm.

Figure 4.15 shows the distribution of temperature values at which data were collected for each LAW glass with electrical conductivity data. This figure shows that electrical conductivity was measured at temperatures not too far from the four nominal values (950, 1050, 1150, and 1250°C) for most LAW glasses. Selected glasses that have measurement temperatures much different than the nominal values are marked with the Glass ID in the figure. Only one temperature value is marked for each glass even if some/all temperature values differ much from the nominal values. Several glasses (C22AN107, C22Si-15, C22Si+15, LAWE7H, and several others) have maximum measurement temperatures of approximately 1200°C instead of around 1250°C. Also LAWB82, LAWM42, and LAWM48 have all four measurement temperatures noticeably below the nominal values. These observations are noted but they do not affect the suitability of the associated data for developing electrical conductivity models.

The electrical conductivity versus temperature values in Table 4.4 for the 181 LAW glasses vary from 0.020 to 0.961 S/cm, with smaller electrical conductivity values generally corresponding to lower temperatures and larger electrical conductivity values corresponding to higher temperatures. Figure 4.16 shows the electrical conductivity values plotted against  $1/T$  (with  $T$  in Kelvin), with a line corresponding to the fit of the Arrhenius equation

$$\ln(EC) = A + B(1/T) \quad (4.1)$$

for each LAW glass. The purpose of this figure is not to assess the adequacy of the Arrhenius equation for representing the temperature dependence of electrical conductivity, but to identify glasses that have different electrical conductivity versus temperature data or relationships. Figure 4.16 shows that most glasses have temperature dependences occurring within the same band, with several glasses (LAWM6, LAWM7, LAWM8, LAWM9, LAWM28, and LAWM54R1) falling below that band. LAWM6 has a somewhat different slope to its temperature dependence for electrical conductivity than the other glasses. However, there are no substantially different data or electrical conductivity-temperature relationships. Section 7.2.1 discusses the work performed to select the best equation to represent the dependence of electrical conductivity on temperature.

### 4.3.2 Discussion of Electrical Conductivity Results

The electrical conductivity results were reviewed in terms of the molar concentrations of glass network formers and modifiers in the glass composition to examine the extent to which general trends or relationships may be evident. In view of the differences in the temperature of measurement, the electrical conductivity was calculated at the nominal operating temperature of 1150°C for the WTP LAW glass melter using the Arrhenius relationship given in Equation (4.1). Appendix A provides the glass compositions in mol%, and Appendix B presents the values of electrical conductivity calculated at 1150°C.

Figure 4.17 shows the electrical conductivity at 1150°C as a function of the alkali oxide concentration of the glass. A strong correlation is observed, which is not surprising, given that ionic conduction dominates electrical conductivity of alkali borosilicate glasses, and that alkalis are the most mobile ions and as such are expected to contribute most to the electrical conductivity of the melt. On the contrary, the plots of electrical conductivity as a function of the sum of the alkali and alkaline earth oxide concentration (Figure 4.18) and as a function of the glass network former oxide concentration (Figure 4.19) indicate little discernable correlation. The alkali concentration of the glasses dominates the electrical conductivity.

#### 4.4 Viscosity Results and Discussion

The viscosity results are presented in Section 4.4.1 and discussed in Section 4.4.2.

##### 4.4.1 Viscosity Results

Of the 271 simulated and actual LAW glasses discussed in Section 2, 181 simulated glasses have viscosity results as summarized in Table 4.1. As described in Section 3.7, viscosity was generally measured at four temperatures for each LAW glass. The viscosity values at measurement temperatures are given in Table 4.5 for the 181 simulated LAW glasses. Each row of Table 4.5 provides the viscosity data for a given glass and four temperatures. There are four columns of data for each glass corresponding to the four temperatures at which viscosity was measured, with the exception of LAWM7 for which five measurements were taken.

Glasses LAWA51, LAWA128R1, LAWA129R1 and LAWM5 had viscosities exceeding the recommended WTP upper limit of 150 poise at 1100°C (Clark 2003) with interpolated values in the range of 161 to 208 poise.

Figure 4.20 shows the distribution of temperature values at which viscosity was measured for each LAW glass with viscosity data. This figure shows that viscosity was measured at temperatures not too far from the four nominal values (950, 1050, 1150, and 1250°C) for most LAW glasses. Selected glasses that have measurement temperatures much different than the nominal 950, 1050, 1150, and 1250°C values are marked with the Glass ID in the figure. Only one temperature value is marked for each glass even if some/all temperature values differ much from the nominal values. Note that LAWM7 has viscosity values at five temperatures, whereas the other glasses have values at only four temperatures. Of particular note are C22Si-15 and C22Si+15, which have maximum measurement temperatures of approximately 1200°C instead of around 1250°C. Also LAWE3H has all four measurement temperatures noticeably below the nominal values. To a lesser extent this occurs for LAWE7 and LAWM8. These observations are noted but they do not affect the suitability of the associated data for developing viscosity models.

The viscosity versus temperature values in Table 4.5 for the 181 LAW glasses vary from 5.99 to 2329.04 poise, with smaller viscosity values generally corresponding to higher temperatures and larger viscosity values corresponding to lower temperatures. Figure 4.21 shows the viscosity values plotted against  $1/T$  (with  $T$  in Kelvin), with a line corresponding to the fit of

the Arrhenius equation (given previously in Equation (4.1)) for each LAW glass. The purpose of this figure is not to assess the adequacy of the Arrhenius equation for modeling the temperature dependence of viscosity but to assess any glasses that appear to have “different” viscosity at temperature data or relationships. Figure 4.21 does not show any glasses with obviously different data or different viscosity-temperature relationships. Section 8.2.1 discusses the work performed to select the best equation to represent the dependence of viscosity on temperature.

#### 4.4.2. Discussion of Viscosity Results

As previously noted for electrical conductivity, because viscosity data were collected at different temperatures, it is convenient for comparison purposes to use the viscosity at 1150°C, calculated using the Arrhenius relationship given above in Equation (4.1). The glass compositions in mol% are provided in Appendix A and the calculated viscosity values at 1150°C are provided in Appendix B.

Figure 4.22 shows the calculated melt viscosity at 1150°C as a function of the alkali oxide concentration and Figure 4.23 as a function of the sum of alkali and alkaline earth oxide concentrations. While little correlation is observed in this case with alkali concentration, a better correlation is observed with the sum of alkali and alkaline earth oxide concentration. This indicates that the combined effect of alkali and alkaline earths, both contributing non-bridging oxygens in the glass structure, is responsible for much of the decrease in melt viscosity. Although less mobile (as evident in the electrical conductivity data), calcium and magnesium play an important role in the creation of non-bridging oxygens, and consequently affect the melt viscosity.

The role of boron in the glass structure has been often described as “anomalous” because of its changing coordination from triangular to tetrahedral with glass composition, especially alkali concentration. Details of the structural role of boron in glass, which is of critical importance for borosilicate glasses such as those studied here, can be found elsewhere (Pye et al. 1978). Because of the unique role of boron, the viscosity of the glass melt was examined as a function of the sum of concentrations of alkali, alkali earth and boron oxides. The plot of melt viscosity at 1150°C as a function of the sum of the alkali, alkaline earth oxide and boron oxide concentrations given in Figure 4.24 indeed shows good correlation, indicative of the role of boron along with alkali and alkaline earth oxides in decreasing the viscosity of glass melts. Conversely, the plot of melt viscosity as a function of glass former oxide concentrations was adjusted in this case by eliminating boron from this group so that Figure 4.25 shows melt viscosity as a function  $\text{SiO}_2 + \text{ZrO}_2 + \text{P}_2\text{O}_5 + \text{Al}_2\text{O}_3 + \text{Fe}_2\text{O}_3$  (mol%) concentration. Elimination of  $\text{B}_2\text{O}_3$  from the glass former group almost doubles  $R^2$  for the linear regression and shows increases in the viscosity values with increases in the concentrations of the glass former oxides. Figure 4.26 shows melt viscosity as a function of the ratio (alkali oxides + alkaline earth oxides + boron oxide)/ $\text{SiO}_2 + \text{ZrO}_2 + \text{P}_2\text{O}_5 + \text{Al}_2\text{O}_3 + \text{Fe}_2\text{O}_3$  in mol% and, as expected, the viscosity decreases as the magnitude of the ratio increases. Viscosity as a function of this ratio shows the best correlation of the viscosity relationships that were examined.



## 4.5 Heat Treatment Results and Discussion

Results of optical microscopy and SEM evaluation of as melted and heat treated LAW glass samples are summarized in Table 4.6 for the 271 samples studied in this report. Overall, about 550 as-melted and heat-treated LAW glass samples have been evaluated.

In general, the “as melted” glass samples were homogeneous, single phase solids varying in color for pale green or amber, to very dark brown for those containing higher amounts of iron oxide. In two instances (LAWB40 and LAWB41), a significant sulfate layer was noticed on the glass surface, which was removed with a mild acid wash before it was crushed and distributed for further testing. These two glasses were excluded from model development because of their very high sulfate content making them outliers with respect to sulfate concentration. The presence of a separate sulfate phase in the glass sample tested could artificially lower the pH in PCT testing, as was observed with LAWB40 (Figure 4.4)

Most of the as-melted and heat treated LAW glasses showed little or no crystallization. The three main crystals observed in these glasses are Cr-rich spinels, augite, and calcium phosphate.

Spinel crystals were identified in 28 of the 271 glasses, generally in small amounts (most often less than 0.1 vol% with higher amounts of up to 1 vol% in LAWE3Cr2CCC). The presence of spinel crystals in LAW glasses is almost always related to the addition of chromium to the glass (spinel has been identified in about two thirds of glasses containing more than 0.1 wt% Cr<sub>2</sub>O<sub>3</sub>) and is most likely a zinc-chromite (ZnCr<sub>2</sub>O<sub>4</sub>) in solid solution with spinel (MgAl<sub>2</sub>O<sub>4</sub>) and magnetite (Fe<sub>3</sub>O<sub>4</sub>). Only in high-chromium glasses (LAWCrP and high-chromium correlation glasses) has this spinel been seen in as-melted samples; it is seen after heat-treatments, with higher amounts in samples subjected to canister centerline cooling. With such small amounts present in the as-melted and heat treated glass samples, the spinel by itself is not a concern with respect to processing or product quality. However, rather large amounts of two other crystals seem to nucleate and grow from these spinels. These crystals are alumino-silicates of the pyroxene group (augite-aegirine) and a calcium phosphate (apatite).

Dendritic growth of pyroxene crystals nucleated from spinel, and when chromium is low, from minute platinum particles at the crucible contact surfaces have been observed. Based on EDS elemental analysis and XRD, these crystals have been identified as augite-aegirine of typical composition (Na, Ca, Mg)(Mg, Al, Fe<sup>3+</sup>, Ti, Cr, Zn)(Si, Al)<sub>2</sub>O<sub>6</sub>. Augite-aegirine is typically seen in heat treated LAW glass samples with low sodium contents. Among 33 samples in which it has been identified, 23 are low-sodium Envelope B glass samples, seven are low-sodium correlation glasses, and three are low-sodium matrix glasses. In five of the low-sodium correlation glasses, higher chromium content seems to enhance augite formation. All three of the above low-sodium matrix glasses (LAWM2, LAWM6 and LAWM7) have MgO concentrations in excess of 5 wt%. Overall, augite is observed in excess of 1 vol% in only 9 of 271 glasses: the five high-chromium, low-sodium correlation samples, the three high-magnesium, low-sodium matrix glasses, and LAWB94 in which sodium concentration is only 3.4 wt%.

Calcium phosphate crystals have been identified in 9 glasses in which  $P_2O_5$  concentration exceeded 2 wt% in the glass. In this case also, all are glasses with low sodium concentrations (5 to 9 wt%  $Na_2O$  in LAWB31 to LAWB38, LAWCrP6 and LAWCrP7). XRD results identify the crystals as calcium phosphates of formula  $Ca_3(PO_4)_2$  or apatite ( $Ca_5(PO_4)_3(OH,F,Cl)$ ). Spinel seems to also enhance crystallization of phosphate phases, which rose to 15.9 vol% in LAWCrP7 (with 0.64 wt %  $Cr_2O_3$  and 5.4 wt%  $Na_2O$ ) and 5.6 vol% in LAWCrP6 (with 0.64 wt %  $Cr_2O_3$  and 8.0 wt%  $Na_2O$ ). These and LAWB31 to LAWB38 (with 2.7 to 4.7 wt%  $P_2O_5$  and 7.9 wt%  $Na_2O$ ) are the only glasses that showed more than 1 vol% of phosphate crystals.

Overall, only 15 of the 271 glasses listed in Table 4.6 show more than 1 vol% of crystals upon heat treatment. Of these seven showed augite-aegirine, six showed calcium phosphate, and two showed both of these types of crystals. The data can be used to define the regions of compositions that give rise to more than 1 vol% of each of these phases after heat treatment, which effectively constitutes a bounding liquidus model. An example of this was used in the design of the LAW correlation (Muller et al. 2004b), which limits magnesium to 3 wt% at the low sodium range. None of the subsequently tested correlation glasses showed significant augite crystallization. Based on the glass compositions and crystallization data given in Table 4.6, a set of compositional boundaries to avoid more than 1 vol% crystals at 950°C can be estimated as follows:

- Limit the MgO concentration in LAW glasses to less than 3.7 wt%, which is the maximum concentration in all glasses that do not show more than 1 vol. % augite crystals.
- Limit the  $Cr_2O_3$  concentration to less than 0.3 wt%, particularly in low-sodium glass compositions ( $\approx 5.4$  wt%  $Na_2O$ ). Depending on the expected maximum  $Cr_2O_3$  concentrations in various LAW glasses, a more detailed analysis of the effect of  $Cr_2O_3$  concentration on low-sodium LAW glass crystallization may be needed as indicated by an earlier study of high chromium LAW glasses (Muller et al, 2006a).
- Limit the  $P_2O_5$  concentration to less than 2 wt%, which should eliminate calcium phosphate crystallization.

The LAW glass crystallization data presented in Table 4.6 indicate that a property-composition model for liquidus temperature is not necessary, provided glass compositions based on the current LAW correlation (Muller et al. 2004b) are used for waste processing. However, if new glass compositions are desired for higher waste loading or because of changes to the LAW compositions, the need for a property-composition model for LAW liquidus temperature should be reevaluated. Crystallization of LAW glasses will become more of a concern especially if compositions with higher CaO, MgO,  $P_2O_5$ , and  $Cr_2O_3$  contents and lower  $Na_2O$  contents are used.

#### **4.6 Glass Density Results and Discussion**

Of the 271 simulated and actual LAW glasses discussed in Section 2, densities were measured for 70, and the results are given in Table 4.3 (for those of the glasses for which VHT rate is calculated with the available measured density). The mode of these 70 density values is 2.65 g/cc, with a minimum of 2.48 g/cc and a maximum of 2.85 g/cc. As can be seen in Figure 4.27, the density of LAW glasses varies little: 39% of the glasses have density values between 2.64 g/cc and 2.68 g/cc. All density values are well below the contractual limit of 3.7 g/cc. Thus, the available density data for LAW glasses indicate that it is not necessary to develop a property-composition model to comply with contractual requirement for ILAW density.

## **SECTION 5**

### **MODELS RELATING PCT BORON AND SODIUM RELEASES TO LAW GLASS COMPOSITION**

This section documents the development and validation of property-composition models and corresponding uncertainty expressions for predicting the PCT-B and PCT-Na releases from low-activity waste (LAW) glasses. Specification 2.2.2.17.2 in the WTP Contract (DOE-ORP 2000) sets a 2 g/m<sup>2</sup> limit on PCT releases of B, Na, and Si from LAW glasses. However, as discussed in Section 4.1.1, PCT-Si releases were less than PCT-B and PCT-Na releases for all 264 of the simulated and actual LAW glasses having PCT results. Because PCT-B and PCT-Na releases dominate PCT-Si releases, it was directed by the WTP Project that only PCT-B and PCT-Na releases need be modeled. The property-composition models and corresponding uncertainty expressions for PCT-B and PCT-Na releases presented in this section were developed and validated using composition and PCT release data collected on 244 of the 264 simulated and actual LAW glasses having PCT results.

The 244 simulated and actual LAW glasses used for PCT model development and validation (from the database of 264 glasses) are discussed in Section 5.1. Section 5.2 presents the model forms for PCT-B and PCT-Na releases that were investigated. Sections 5.3 and 5.4, respectively, summarize the results for the PCT-B and PCT-Na model forms investigated and the model forms ultimately recommended. Using the recommended (and other) models and corresponding uncertainty equations for each of PCT-B and PCT-Na, Section 5.5 illustrates the calculation of PCT release predictions and the uncertainties in those predictions. Section 5.6 discusses the suitability of the recommended PCT-B and PCT-Na models for use by the WTP project. Appendix C discusses the statistical methods and summary statistics used to develop, evaluate, and validate the several model forms investigated, as well as statistical equations for quantifying the uncertainties in PCT release predictions made with the selected models.

#### **5.1 PCT Release Data Used for Model Development and Validation**

The data used for developing PCT-B and PCT-Na release models are discussed in Section 5.1.1. The approaches and data used for validating the models are discussed in Sections 5.1.2 to 5.1.4.

##### **5.1.1 PCT Release Model Development Data**

The data available for developing property-composition models for PCT-B and PCT-Na releases consist of composition and PCT release data from 264 LAW glasses. These glasses are discussed and their target compositions are presented in Section 2. The normalized compositions of these glasses based on analyzed (or estimated analyzed) SO<sub>3</sub> values are discussed in Section

3.3. The corresponding PCT-B and PCT-Na releases are presented in Table 4.2. The LAW PCT data are discussed in Section 4.1.

### Assessment of Available Glasses with PCT Releases

The database of 264 glasses with PCT releases contains statistically-designed as well as actively-designed glasses. Some actively-designed glasses are outside the composition region covered by the majority of the LAW compositions. Such glasses are not ideal for inclusion in a modeling set because they can be influential when fitting models to data. Hence, it was decided to (i) graphically assess the 264 simulated and actual LAW glass compositions and (ii) remove from the modeling set any compositions considered to be outlying or non-representative of LAW glasses of interest for the WTP.

Figure 5.1 displays plots of the mass fraction values for 14 “main components” in the 264 LAW glasses with PCT data. The “main components” are the ones that were varied in the ILAW Phase 1 Test Matrix and the Phase 1a Augmentation Test Matrix. Figure 5.2 displays similar plots for the remaining minor components. On each plot in Figures 5.1 and 5.2, the x-axis represents the mass fraction values of an LAW glass component. The y-axis shows an index value representing each LAW glass composition, which aids in spreading out the data points to avoid over-plotting. The plotting symbols correspond to the seven groups of LAW glass data discussed in Sections 2.1 to 2.7. For comparison purposes, the vertical bars in Figures 5.1 and 5.2 represent the ranges over which the components were varied in the ILAW Phase 1 Test Matrix.

Figure 5.1 shows several glasses have components with outlying mass fraction values compared to the remaining glasses and to the component ranges studied in the ILAW Phase 1 Test Matrix and the Phase 1a Augmentation Test Matrix. Figure 5.2 shows what appear to be outliers for some components, but the values and ranges of those components are small and hence the glass compositions were not considered to be outliers. Table 5.1 lists the 20 LAW glasses excluded from the ILAW PCT modeling set, and the reason each glass was excluded. The first 16 of the 20 glasses were excluded because of having outlying component values compared to the rest of the glasses. The last 4 of the 20 glasses were designed for a specific investigation, were high in  $\text{Cr}_2\text{O}_3$ , and were container-centerline-cooled. These glasses were considered non-representative and excluded from the PCT modeling dataset.

Figures 5.3 and 5.4 (corresponding to Figures 5.1 and 5.2, respectively) show plots of component distributions after the 20 outlying and non-representative glasses were removed from the PCT dataset. Figure 5.3 shows for the remaining 244 LAW glasses that all 13 of the specific LAW glass components ( $\text{Al}_2\text{O}_3$ ,  $\text{B}_2\text{O}_3$ ,  $\text{CaO}$ ,  $\text{Fe}_2\text{O}_3$ ,  $\text{K}_2\text{O}$ ,  $\text{Li}_2\text{O}$ ,  $\text{MgO}$ ,  $\text{Na}_2\text{O}$ ,  $\text{SO}_3$ ,  $\text{SiO}_2$ ,  $\text{TiO}_2$ ,  $\text{ZnO}$ , and  $\text{ZrO}_2$ ) have sufficient ranges and distributions of values within those ranges to support model terms. Similarly, Figure 5.4 shows that  $\text{Cl}$ ,  $\text{Cr}_2\text{O}_3$ ,  $\text{F}$ , and  $\text{P}_2\text{O}_5$  have sufficient ranges and distributions of values within their ranges to support model terms for those components. Hence, based on Figures 5.3 and 5.4, it was decided to use 18 components for initial PCT modeling work. These are  $\text{Al}_2\text{O}_3$ ,  $\text{B}_2\text{O}_3$ ,  $\text{CaO}$ ,  $\text{Cl}$ ,  $\text{Cr}_2\text{O}_3$ ,  $\text{F}$ ,  $\text{Fe}_2\text{O}_3$ ,  $\text{K}_2\text{O}$ ,  $\text{Li}_2\text{O}$ ,  $\text{MgO}$ ,  $\text{Na}_2\text{O}$ ,  $\text{P}_2\text{O}_5$ ,  $\text{SO}_3$ ,  $\text{SiO}_2$ ,  $\text{TiO}_2$ ,  $\text{ZnO}$ ,  $\text{ZrO}_2$ , and Others (the sum of all remaining components).

Figure 5.5 shows a scatterplot matrix of the 244 glasses remaining in the PCT modeling dataset after removing the 20 outlying compositions. High correlations between some pairs of components are evident, so pairwise correlation coefficients were calculated. These can vary from -1.0 (perfect negative correlation) to 0 (no correlation) to 1.0 (perfect positive correlation). The component pairs with correlations larger (in absolute value) than 0.60 are

Li <sub>2</sub> O and Na <sub>2</sub> O	-0.896
Na <sub>2</sub> O and CaO	-0.737
Li <sub>2</sub> O and CaO	0.687
Na <sub>2</sub> O and SO <sub>3</sub>	-0.679
Li <sub>2</sub> O and SO <sub>3</sub>	0.673
Na <sub>2</sub> O and SO <sub>2</sub>	-0.663

Such high pairwise correlations can make it difficult for regression methods to properly separate the effects of the components on the response variable (e.g., PCT releases). Thus, these high pairwise correlations need to be kept in mind in developing ILAW PCT property-composition models.

### PCT Modeling Dataset

Table 5.2 lists the Glass ID, Group ID, and normalized glass compositions for the 244 simulated and actual LAW glasses in the 18-component forms used for PCT model development. The Group ID column of Table 5.2 indicates the subset of data that each glass is associated with (see Sections 2.1 to 2.7). The glass compositions in Table 5.2 are the normalized mass fractions (mf) of the 18 components previously identified as having sufficient data to support a separate model term if needed. These components are Al<sub>2</sub>O<sub>3</sub>, B<sub>2</sub>O<sub>3</sub>, CaO, Cl, Cr<sub>2</sub>O<sub>3</sub>, F, Fe<sub>2</sub>O<sub>3</sub>, K<sub>2</sub>O, Li<sub>2</sub>O, MgO, Na<sub>2</sub>O, P<sub>2</sub>O<sub>5</sub>, SO<sub>3</sub>, SiO<sub>2</sub>, TiO<sub>2</sub>, ZnO, ZrO<sub>2</sub>, and Others. The mass fraction values of the 18 components shown in Table 5.2 were normalized so that they sum to 100% for each of the glasses (see Section 3.3).

Table 5.3 contains columns of measured (given in ppm units) and normalized (given in g/L units) versions of PCT-B and PCT-Na releases for the 244 glasses in the PCT modeling dataset. The normalized releases were calculated as described previously in Section 3.4. Table 5.3 also includes columns for PCT-Si release data. However, a PCT-Si model is not needed as discussed in the opening remarks of Section 5, so these columns were not used in the model development effort.

Of the 244 simulated and actual LAW glasses in the PCT modeling set, some had PCT releases (for B, Na, or both) that exceeded the limit of 4 g/L (equivalent to 2 g/m<sup>2</sup>, given in Specification 2.2.2.17.2 of the WTP Contract). It is desirable to have some glasses in the modeling dataset that have PCT releases ranging from somewhat below to somewhat above the limit. This allows for more confident use of the model in discerning between glasses with acceptable and unacceptable PCT releases. However, glass formulations that have PCT releases far beyond the limit may not be desirable for model development, because using such glasses to develop models could adversely affect model performance for the majority of the glasses. For this reason, dropping from the modeling dataset a few glasses with the highest PCT releases was

investigated. Specifically dropping the glasses with the two highest PCT releases (LAWM55 and LAWM12) was considered as one option. A second option of dropping the glasses with the five highest PCT releases (LAWM55, LAWM12, LAWM56, LAWM17, and LAWM35) was also considered. These sets of two and five glasses appeared as outliers during model development. However, comparison of model fits with and without these sets of glasses did not significantly change the predictive performance of models for the remaining glasses. Hence, the high PCT releases were outliers but not influential. This conclusion, along with the need to have glasses with higher PCT releases in the modeling dataset, led to the decision not to drop any LAW glasses from the PCT modeling dataset because of “too-large” PCT releases.

### Replicate and Near-Replicate PCT Data

The changes to the LAW glass compositions caused by the renormalization associated with using XRF analyzed (or estimates of XRF analyzed) SO<sub>3</sub> values (see Section 3.3) resulted in some replicate glasses not having exactly equal compositions. Such compositions are referred to as near-replicates. For ease of discussion, henceforth both replicates and near-replicates are referred to as replicates.

Table 5.4 lists the replicate sets of glasses in the ILAW PCT modeling data and the corresponding PCT-B and PCT-Na normalized releases. Table 5.4 also lists estimates of percent relative standard deviations (%RSDs) for each replicate set as well as pooled estimates over all the replicate sets. A pooled %RSD combines the separate %RSD estimates from each replicate set, so that a more accurate combined estimate of the %RSD is obtained. These pooled %RSDs include uncertainties due to fabricating glasses, performing the PCT, and chemically analyzing leachates to determine elemental releases.

The magnitudes of the pooled %RSDs in Table 5.4 are roughly twice the approximately 10 %RSD values for PCT-B and PCT-Na reported in Table F.5 of Hrma et al. (1994). The results from that Table F.5 were based on replicate sets of the same glasses fabricated and tested several times over several years. Hence, the approximately 10% RSD values for PCT-B and PCT-Na reported by Hrma et al. (1994) include an additional long-term source of variation not included in the replicate data of Table 5.4. This suggests that the PCT-B and PCT-Na data for the LAW glasses in Table 5.3 were subject to more experimental, testing, and measurement uncertainty than in the Hrma et al. glass composition variation study. The estimates of replicate uncertainty for PCT-B and PCT-Na releases in Table 5.4 are used subsequently to statistically assess lack-of-fit (LOF) of the various models considered.

### **5.1.2 Primary PCT Model Validation Approach and Data**

The primary model validation approach for PCT modeling was based on splitting the 244-glass dataset for model development into five modeling/validation subsets. Of the 244 model development glasses, 24 were intended to be replicates (12 replicate pairs). The five modeling/validation splits of the 244 glasses in the PCT modeling dataset were formed as follows.

- The 12 pairs of replicates (24 glasses) were set aside so they would always be included in each of the five model development datasets. This was done so that replicate pairs would not be split between modeling and validation subsets, thus negating the intent to have validation glasses different than model development glasses.
- The remaining  $244 - 24 = 220$  data points were ordered from smallest to largest according to their values of normalized PCT-Boron or PCT-Sodium release (g/L). The 220 data points were numbered 1, 2, 3, 4, 5, 1, 2, 3, 4, 5, etc. All of the 1's formed the first model validation set, while all of the remaining points formed the first model development dataset. Similarly, all of the 2's, 3's, 4's, and 5's respectively formed the second, third, fourth, and fifth model validation sets. In each case, the remaining non-2's, non-3's, non-4's, and non-5's formed the second, third, fourth, and fifth model development datasets. Accordingly, each of the five splits contained  $220/5 = 44$  glasses for validation and  $(4/5)220 = 176$  glasses for modeling.
- The 24 replicate glasses were added to each of the split modeling subsets so that each of the five splits contained 200 glasses for modeling and 44 glasses for validation. The last two columns of Table 5.3 specify the validation subsets for the five modeling/validation splits in the primary validation approach for both PCT-Boron and PCT-Sodium model development.

Data splitting was chosen as the primary validation approach because the PCT modeling dataset contains all compositions that (i) are in the ILAW composition region of interest, (ii) meet quality assurance (QA) requirements, and (iii) have PCT data. Having a separate validation dataset not used for modeling is desirable, but that desire was over-ridden by wanting PCT models developed with all appropriate data.

### 5.1.3 Secondary PCT Model Validation Approach and Data

The secondary model validation approach consisted of partitioning the 244-glass PCT modeling dataset into modeling and validation subsets. Included in the modeling subset were all glasses used in statistically-designed groups of the data. These included 21 glasses from the Existing Matrix<sup>8</sup>, the 56 glasses in the Phase 1 Test Matrix, and the 20 glasses in the Phase 1a Augmentation Test Matrix. Together, these yielded a modeling subset of 97 glasses. The remaining  $244 - 97 = 147$  glasses (which consist of actively-designed glasses and glasses made from actual LAW samples) were used as a validation subset.

The data-splitting approach discussed in Section 5.1.2 is considered the primary validation approach because it comes closer to validating the PCT models of interest, namely those fitted to all 244 modeling data points. The primary validation approach fits PCT models using 200 of the 244 modeling data points and validates with the remaining 44 data points, and does so five times. The secondary approach fits models with 97 glasses and validates with 147

---

<sup>8</sup> There are 22 Existing Matrix glasses with PCT data, but LAW88 was initially classified as an actively designed (ActDes) glass, and thus was not included in the modeling partition.



glasses. Hence, the primary validation approach comes closer to validating the PCT models of interest, namely those fitted to all 244 data points.

The secondary validation approach is desirable because it uses the statistically-designed glasses (and the Existing Matrix glasses that were factored into selecting the Phase 1 Test Matrix glasses) to fit models, and actively-designed glasses to validate the models. Actively-designed glasses tend to be more clustered in composition space, and can have strong or even perfect correlations between glass components. These aspects make actively-designed glasses somewhat less desirable for model development, but reasonable for model validation.

#### 5.1.4 Limited Extrapolative PCT Model Validation Data

The 20 glasses excluded from the PCT modeling set (see the discussion in Section 5.1.1) were used to perform a limited assessment of the extrapolative prediction performance of the PCT models. The normalized compositions of these 20 glasses are given in Table 5.5 and the corresponding PCT B, Na, and Si releases are given in Table 5.6.

### 5.2 PCT Release Model Forms

Ideally, a property-composition model for PCT would utilize known mechanisms of PCT release as a function of glass composition and aspects of the PCT. Several mechanistic modeling approaches have been investigated for predicting PCT releases. However, all are either reduced forms of a linear mixture model or can be well-approximated by such a model. Empirical model forms with coefficients estimated from model development data have been shown to perform as well or better than the mechanistic modeling approaches. The empirical model forms used are from the general class of *mixture experiment models* (Cornell 2002), which includes models linear in composition as well as non-linear in composition. Section C.1 of Appendix C discusses mixture experiments and several general forms of mixture experiment models. Section 5.2.1 discusses the forms of mixture experiment models used for PCT responses of LAW glasses. Section 5.2.2 discusses the choice between modeling unnormalized and normalized PCT releases and transformations thereof.

#### 5.2.1 PCT Mixture Experiment Model Forms

Linear mixture (LM) and partial quadratic mixture (PQM) model forms introduced in Section C.1.1 of Appendix C were chosen for use in modeling PCT-B and PCT-Na releases. For modeling PCT-B and PCT-Na, the specific LM model form is given by

$$\ln(C_B) \text{ or } \ln(C_{Na}) = \sum_{i=1}^q b_i x_i + E \quad (5.1)$$

while the specific PQM model form is given by

$$\ln(C_B) \text{ or } \ln(C_{Na}) = \sum_{i=1}^q b_i x_i + \text{Selected} \left\{ \sum_{i=1}^q b_{ii} x_i^2 + \sum_{i < j}^{q-1} b_{ij} x_i x_j \right\} + E . \quad (5.2)$$

In Equations (5.1) and (5.2):  $\ln(C_B)$  denotes the natural logarithm of the normalized PCT-B release (in g/L);  $\ln(C_{Na})$  denotes the natural logarithm of the normalized PCT-Na release (in g/L); the  $x_i$  ( $i = 1, 2, \dots, q$ ) are normalized mass fractions of  $q$  glass oxide or halogen components such that  $\sum_{i=1}^q x_i = 1$ ; the  $b_i$  ( $i = 1, 2, \dots, q$ ), the  $b_{ii}$  (selected), and the  $b_{ij}$  (selected) are coefficients to be estimated from data; and  $E$  is a random error for each data point. Many statistical methods exist for the case where the  $E$  are independent (i.e., not correlated) and normally distributed with mean 0 and standard deviation  $\sigma$ . In Equation (5.2), “Selected” means that only some of the terms in curly brackets are included in the model. The subset is selected using stepwise regression or other variable selection methods (Draper and Smith 1998, Montgomery et al. 2001). PQM models are discussed in more detail and illustrated by Piepel et al. (2002).

Cornell (2002) discusses many other empirical mixture model forms that could have been considered for PCT-composition modeling but were not investigated because of time constraints. However, models of the form in Equations (5.1) and (5.2) are widely used in many application areas (including waste glass property modeling) and often perform very well.

A two-part LM model of the following form was also considered

$$\ln(C_B) \text{ or } \ln(C_{Na}) = \sum_{i=1}^q b_i^B x_i J_i + \sum_{i=1}^q b_i^A x_i (1 - J_i) + E \quad (5.3)$$

where  $J_i = 1$  if  $C_B$  or  $C_{Na}$  is at or below a specified cutoff value, and  $J_i = 0$  if  $C_B$  or  $C_{Na}$  is above the specified cutoff value. The  $b_i^B$  are coefficients of the LM model below the cutoff value, while  $b_i^A$  are coefficients of the LM model above the cutoff value. The  $E$  is a random error for each data point, as previously discussed for the models in Equations (5.1) and (5.2). The two-part LM model form is appropriate in cases where two separate LM models are adequate to represent the property-composition relationship on either side of a cutoff value in the property (i.e., PCT-B or PCT-Na release). The cutoff value was chosen separately for PCT B and Na releases so that (i) all glasses with releases above the 4 g/L contract limit were included in the “above cutoff” model and (ii) glasses with tendencies to have their releases under-predicted were included in the “above cutoff” model. A series of cutoff values meeting these conditions were considered for each of PCT B and Na, and the cutoff value was selected that yielded the best fits for the “below cutoff” and “above cutoff” models. There is some concern that the number of data points above the cutoff values of PCT-B or PCT-Na release may be small enough to allow over-fitting of the “above cutoff” part of the model. However, because two-part models were outside the originally planned scope, reduction of the two-part models (e.g., some components may only need one term rather than two) was not pursued.

## 5.2.2 Normalization and Transformation of PCT Release Values

A transformation to “normalized” concentrations is widely employed in the data analysis and modeling of leaching data (Hrma et al. 1994, Gan et al. 2001a). The normalized PCT-B releases ( $C_B$ ) were calculated according to the formula

$$C_B \text{ (g/L)} = \frac{c_B \text{ (mg/L)}}{[1000 \text{ (mg/g)}][x_{B_2O_3} \text{ (g B}_2\text{O}_3\text{/g glass)}][0.3106 \text{ (g B/g B}_2\text{O}_3\text{)}]} \quad (5.4)$$

where  $c_B$  is the non-normalized boron release (concentration) from the 7-day PCT, and  $x_{B_2O_3}$  is the normalized mass fraction of  $B_2O_3$  in the glass. Normalized mass fraction compositions of glasses were calculated as discussed in Section 3.3. Similarly, normalized PCT-Na releases ( $C_{Na}$ ) were calculated according to the formula

$$C_{Na} \text{ (g/L)} = \frac{c_{Na} \text{ (mg/L)}}{[1000 \text{ (mg/g)}][x_{Na_2O} \text{ (g Na}_2\text{O/g glass)}][0.7419 \text{ (g Na/g Na}_2\text{O)}]} \quad (5.5)$$

As seen in Equations (5.4) and (5.5), normalizing involves dividing the measured leachate concentration for a given element by the corresponding mass fraction of that element in the glass. Mechanistically, this crudely takes into account the fact that, for a given amount of glass reacted, the concentration of a specific element in the leachate should be proportional to the mass fraction of the element in the glass. This is an approximation for a number of reasons, including the fact that the mass fraction of the element in question *affects* the amount of glass reacted, and not necessarily all of the constituents in the reacted glass are released to the solution. Nevertheless, factoring out this dependence by normalization has been empirically observed for many years to improve model fits to leaching data and to reduce the need for non-linear composition terms in the model.

Based on preliminary modeling work for ILAW PCT releases, Perez-Cardenas et al. (2003) suggested a slight preference for models based on PCT normalized elemental releases. The fact that Contract Specification 2.2.2.17.2 specifies a limit ( $2 \text{ g/m}^2 = 4 \text{ g/L}$ ) in terms of normalized releases was the deciding factor in the decision to model PCT normalized elemental releases in this work.

In modeling PCT elemental releases (unnormalized or normalized), it is advantageous to transform the PCT release concentrations in the leachate to the natural logarithm of the concentrations. The advantages of this transformation include:

- The PCT-B unnormalized releases for the 244 simulated and actual LAW glasses used for modeling range from 2.85 to 1440.000 ppm, while the normalized releases range from 0.152 to 35.657 g/L. The PCT-Na unnormalized releases range from 8.02 to 2426.00 ppm, while the normalized releases range from 0.209 to 22.937 g/L. The range (i.e., minimum to maximum values) for each normalized release spans more than an order-of-magnitude difference. In such cases, typically the uncertainty in making glasses,

performing the PCT, and analyzing the leachate leads to smaller absolute uncertainties for smaller normalized releases and larger absolute uncertainties for larger normalized releases. Hence, the unweighted least squares (ULS) regression assumption of equal variances for all response variable values (see Section C.3 of Appendix C) is violated. After a logarithmic transformation, variances of response values (PCT normalized releases, in this case) tend to be approximately equal as required for ULS regression.

- A logarithmic transformation tends to linearize the compositional dependence of leach test data and reduce the need for non-linear terms in the model form.
- A natural logarithm transformation is preferred over a common logarithm (or other base logarithm) transformation because of the approximate relationship

$$\text{SD} [\ln(y)] \cong \text{RSD} (y) \quad (5.6)$$

where SD denotes standard deviation, RSD denotes relative standard deviation (i.e., the standard deviation divided by the mean), and  $y$  denotes PCT-B or PCT-Na release. Equation (5.6) results from applying the first-order variance propagation formula [Equation (7-7) of Hahn and Shapiro (1967)] to the function  $z = \ln(y)$ . The relationship in Equation (5.6) is very useful, in that uncertainties of the natural logarithm of the response variable  $y$  can be interpreted as RSDs of the untransformed response variable  $y$ .

For these reasons, natural logarithmic transformations of PCT normalized releases (g/L) were used in modeling PCT-B and PCT-Na releases.

### 5.3 Property-Composition Model Results for PCT-B Release

This section discusses the results of fitting several different models using natural logarithms of ILAW PCT normalized boron release (g/L) as the response variable. Section 5.3.1 presents the results of modeling PCT-B using an 18-component LM model. Sections 5.3.2 and 5.3.3 present the results of modeling PCT-B using LM and PQM models based on a reduced set of 12 mixture components. Section 5.3.4 discusses the results from fitting a two-part model in which separate 12-term LM models were fit to glasses with PCT-B releases below and above a cutoff value. Finally, Section 5.3.5 compares the results from the four models and recommends a PCT-B model for future use and evaluation.

#### 5.3.1 Results from Full LM Model for ILAW PCT-B

As the initial step in PCT-B model development, a full LM model in the 18 components identified in Section 5.1.1 was fit to the modeling data (244 glasses) with the response being the natural logarithm of PCT-B normalized releases (g/L). This model form was a reasonable starting point based on the previous work modeling ILAW PCT releases (Perez-Cardenas et al. 2003, Muller et al. 2005) and provided a basis for appropriate model reductions.

Table 5.7 contains the results for the 18-component full LM model for ILAW PCT-B. Table 5.7 lists the model coefficients, standard deviations of the coefficients, and model performance summaries for the full LM model using the modeling dataset (244 glasses), the data-splitting approach (see Section 5.1.2), the modeling data partitioned into modeling (97 glasses) and validation (147 glasses) subsets (see Section 5.1.3), and the outlying glass dataset (see Section 5.1.4). In the data-splitting portion of results at the bottom of Table 5.7, the columns are labeled DS1, DS2, DS3, DS4, and DS5 to denote the five modeling/validation splits of the data as described in Section 5.1.2. The last column of this part of Table 5.7 shows the averages for the different statistics over the five splits.

The upper right corner of Table 5.7 contains the summary statistics that describe how well the 18-component LM model fits the 244-glass modeling data. The  $R^2 = 0.782$ ,  $R^2_A = 0.766$ , and  $R^2_P = 0.717$  statistics (see Section C.4 of Appendix C) indicate that the full 18-component LM model fits the PCT-B data in the 244-glass modeling dataset fairly well. However, the root mean squared error (RMSE) = 0.372 is noticeably larger than the glass batching and PCT-B measurement uncertainty (SD = 0.2267 in  $\ln(\text{g/L})$  units) estimated from replicates in Table 5.4. This indicates the full LM model for PCT-B has LOF, which was confirmed as statistically significant with  $p = 0.018$  as shown in Table 5.7 (see Section C.4 for discussion of the statistical test for model LOF).

The predicted versus measured plot in Figure 5.6 shows that the full LM model significantly under-predicts PCT-B release above the limit of 4 g/L (2 g/m<sup>2</sup>). The model also under-predicts PCT-B for most of the Phase 1a Augmentation Matrix glasses, many of which have PCT-B releases near but below the limit. Figure 5.6 also shows that the full LM model tends to under-predict glasses with the lowest PCT-B releases, although this is not of much concern for WTP application.

The PCT-B full LM model statistics from partitioning the 244-glass modeling set into subsets of 97 modeling glasses and 147 validation glasses (see Section 5.1.3) are given on the right side of Table 5.7. The fit statistics of  $R^2 = 0.857$ ,  $R^2_A = 0.826$ , and  $R^2_P = 0.747$  for the 97-glass subset are all better (i.e., larger) than the corresponding statistics for the full 244-glass modeling set. However, RMSE = 0.440 is worse (i.e., larger) for the 97-glass modeling subset. For the 147-glass validation subset,  $R^2_V$  is negative and  $\text{RMSE}_V = 0.795$ . This poor validation performance for the 18-component full LM model is because there is insufficient support in the 97-glass modeling subset to fit all 18 components.

At the bottom right of Table 5.7, the average statistics over the five data-splits are very close to the statistics obtained for fitting the PCT-B full LM model to all 244 glasses. This indicates that the model, despite its statistically significant LOF, maintains its performance for data not used to fit the model. The negative  $R^2_V$  and relatively large validation  $\text{RMSE}_V = 0.732$  for the 20 outlying glasses (see the right side of Table 5.7) indicate the full LM model for PCT-B does not have very good extrapolative predictive performance, but that is not a primary consideration.

Despite the statistically significant LOF of the full LM model for PCT-B, the model fits the data well enough to provide guidance for reducing the model (i.e., removing separate terms

for components that do not significantly influence PCT-B release). Hence, the full LM model was used to produce the response trace plot (see Section C.5.1) shown in Figure 5.7. The response trace plot shows that  $\text{Li}_2\text{O}$ ,  $\text{MgO}$ ,  $\text{Na}_2\text{O}$ ,  $\text{K}_2\text{O}$ , and  $\text{B}_2\text{O}_3$  tend to increase PCT-B release, while  $\text{Al}_2\text{O}_3$ ,  $\text{P}_2\text{O}_5$ , and  $\text{SiO}_2$  tend to decrease PCT-B release. The response trace for  $\text{Cr}_2\text{O}_3$  has the largest positive slope, suggesting that per unit increase  $\text{Cr}_2\text{O}_3$  has the strongest increasing effect on PCT-B release. However, this indication does not agree with glass science knowledge and experience. It appears to be an artifact resulting from small numbers of glasses with high  $\text{Cr}_2\text{O}_3$  and or  $\text{P}_2\text{O}_5$ .

### 5.3.2 Results from Reduced LM Model for ILAW PCT-B

The full 18-component LM model presented in Section 5.3.1 likely contains components that do not significantly contribute to predicting PCT-B release, so model reduction was the next step of the model development approach. Thus, LM models for PCT-B involving fewer than the 18 components were considered. The sequential F-test model reduction approach (see Section C.5.1 of Appendix C, Piepel and Cooley 2006) was used to develop a reduced LM model. Option (ii) discussed in Section C.5.1 was used to develop reduced LM models for all LAW glass properties considered in this report.

To reduce the full LM model for PCT-B, a significance level of 0.001<sup>9</sup> was used for the F-tests and non-significant components were always combined with the Others component. An option available with the F-test approach is to force certain terms to remain in the model during the model reduction process. For PCT-B,  $\text{Al}_2\text{O}_3$ ,  $\text{B}_2\text{O}_3$ ,  $\text{Li}_2\text{O}$ ,  $\text{Na}_2\text{O}$ ,  $\text{SiO}_2$ , and  $\text{ZrO}_2$  were forced into the reduced LM model. That is, they were not eligible to be combined during model reduction. Of these components,  $\text{Al}_2\text{O}_3$ ,  $\text{B}_2\text{O}_3$ ,  $\text{Li}_2\text{O}$ ,  $\text{Na}_2\text{O}$ , and  $\text{SiO}_2$  were significant at each step of the model reduction process and would have been retained in the reduced LM model without being forced to remain. However,  $\text{ZrO}_2$  would have been combined with other minor components if it were not forced into the reduced LM model. Forcing  $\text{ZrO}_2$  into the reduced LM model for PCT-B had very little impact on the model performance. Ultimately, the reduced LM model with  $\text{ZrO}_2$  was preferred because of glass-science knowledge and the importance of  $\text{ZrO}_2$  for other LAW glass properties.

The reduced LM model obtained for PCT-B using the F-test approach contained terms for 12 components:  $\text{Al}_2\text{O}_3$ ,  $\text{B}_2\text{O}_3$ ,  $\text{CaO}$ ,  $\text{Fe}_2\text{O}_3$ ,  $\text{K}_2\text{O}$ ,  $\text{Li}_2\text{O}$ ,  $\text{MgO}$ ,  $\text{Na}_2\text{O}$ ,  $\text{P}_2\text{O}_5$ ,  $\text{SiO}_2$ ,  $\text{ZrO}_2$ , and Others. Note that Others is the sum of all remaining components, and thus differs from the Others in the 18-component LM model discussed in Section 5.3.1. Table 5.8 gives the coefficients and coefficient standard deviations for the 12-component reduced LM model for  $\ln(\text{PCT-B})$ , as well as performance statistics for the (i) modeling data, (ii) 97/147 partition of the modeling data into modeling and validation subsets, (iii) data-split modeling data, and (iv) 20 outlying LAW glasses.

---

<sup>9</sup> Initially a value of 0.05 was used, but more than one group of combined minor components resulted. Choosing a smaller significance level allowed the minor components (including Others) to combine into a single group. This result better agreed with glass science knowledge and was of small impact statistically.

### Numerical Results for the Reduced Linear Mixture Model on $\ln(\text{PCT-B})$

In Table 5.8,  $R^2 = 0.766$  indicates that the reduced LM model for PCT-B accounts for roughly 77% of the variation in  $\ln(C_B)$  values in the 244-glass modeling dataset. While this is a reasonably large number, a larger value would be preferable. The value of  $R^2_A = 0.755$  is close to  $R^2$ , indicating that the model reduction was successful in removing unneeded components. The value for  $R^2_p = 0.720$  is not very far below the  $R^2$  and  $R^2_A$  values, indicating that there are not any highly influential data points in the PCT-B modeling dataset. In any case,  $R^2_p = 0.720$  provides an estimate of the fraction of variation in  $\ln(C_B)$  values for future glasses in the same glass composition region that might be accounted for by this reduced LM model.

The reduced LM model for PCT-B yielded somewhat different results for the partition of the modeling data into a modeling subset of 97 glasses and a validation subset of 147 glasses. As seen in Table 5.8, the fit statistics  $R^2 = 0.837$ ,  $R^2_A = 0.816$ , and  $R^2_p = 0.757$  for the 97-glass subset are all better (i.e., larger) than the corresponding statistics for the full 244-glass modeling set. However,  $\text{RMSE} = 0.452$  is worse (i.e., larger) for the 97-glass modeling subset. For the 147-glass validation subset,  $R^2_v$  is negative and  $\text{RMSE}_v = 0.726$ . The reasons for this less than ideal validation performance are explained subsequently when Figure 5.11 is discussed.

Over the five data splits of the PCT-B modeling data, Table 5.8 shows that the reduced LM model has average  $R^2$ ,  $R^2_A$ ,  $R^2_p$ , and  $\text{RMSE}$  values that are all close to their values from the 244-glass modeling dataset. The average  $R^2_v = 0.668$  from data-splitting is somewhat worse (i.e., smaller) than  $R^2_p = 0.720$  for the 244-glass modeling dataset. However, the average  $\text{RMSE}_v = 0.369$  from data-splitting is similar to  $\text{RMSE} = 0.380$  for the 244-glass modeling dataset. Hence, the data-splitting validation results are generally similar to those from fitting the 244-glass dataset.

For the set of 20 outlying LAW glasses, the reduced LM for PCT-B has  $R^2_v = 0.170$ , which is very small and indicates that the extrapolative prediction ability of the model is relatively poor. The  $\text{RMSE}_v = 0.566$  for these 20 glasses is worse than the average  $\text{RMSE}_v = 0.369$  for the five data-splits of the modeling data, but is better than  $\text{RMSE}_v = 0.726$  for the partitioned modeling data. Further insight to the extrapolative predictive performance of the reduced LM model for PCT-B is given subsequently when Figure 5.12 is discussed.

The  $\text{RMSE}$  in Table 5.8 is an estimate of the uncertainty [in  $\ln(C_B)$  units] in fabricating simulated LAW glasses and measuring  $C_B$  if the reduced LM model for PCT-B does not have statistically significant LOF. To judge the LOF, the  $\text{RMSE}$  value can be compared to uncertainty estimates based on replicate PCT-B release data. The  $\text{RMSE} = 0.380$  is much larger than the historical replicate  $\text{RSD}^{10}$  of  $\sim 0.10$  (from Appendix F of Hrma et al. 1994) in fabricating simulated waste glasses and measuring PCT-B release. It is also much larger than the replicate SD in  $\ln(\text{g/L})$  units of 0.2269 in Table 5.4 (which is discussed in the last subsection of Section 5.1.1). These observations suggest that the reduced LM model for  $\ln(\text{PCT-B})$  has a substantial LOF, which is confirmed by the LOF test p-value = 0.015 included in Table 5.8. This p-value

---

<sup>10</sup> Per Equation (5.6),  $\text{RSD}$  values calculated from replicate PCT-B releases approximate SDs calculated from natural logarithms of PCT-B releases.

indicates that the model LOF is significant at the 98.5% confidence level. See Section C.4 of Appendix C for further discussion of the LOF test.

### Graphical Results for the Reduced Linear Mixture Model on ln(PCT-B)

The predicted versus measured plot for the reduced LM model in Figure 5.8 is nearly identical to the one for the full LM model in Figure 5.6. Figure 5.8 shows that the reduced LM model significantly under-predicts PCT-B release above the limit of 4 g/L (2 g/m<sup>2</sup>). The reduced LM model also under-predicts PCT-B for most of the Phase 1a Augmentation Matrix glasses, many of which have PCT-B releases near but below the limit. Figure 5.8 also shows that the reduced LM model tends to under-predict glasses with the lowest PCT-B releases, although this is not of much concern for WTP application.

Figure 5.9 displays the response trace plot (see Section C.5.1) for the PCT-B reduced LM model. Figure 5.9 shows that Li<sub>2</sub>O, MgO, Na<sub>2</sub>O, K<sub>2</sub>O, and B<sub>2</sub>O<sub>3</sub> tend to increase PCT-B release, Al<sub>2</sub>O<sub>3</sub>, P<sub>2</sub>O<sub>5</sub>, and SiO<sub>2</sub> tend to decrease PCT-B release, and CaO, Fe<sub>2</sub>O<sub>3</sub>, ZrO<sub>2</sub>, and Others tend to have slight to negligible effects on PCT-B release.

Diagnostic plots for the reduced LM model (not included in this report) support that the assumption of normally distributed errors in the PCT-B data is reasonable (see Section C.3 of Appendix C). Figure 5.10 displays for the reduced LM model the standardized residuals plotted versus the data index (a sequential numbering of the modeling data points) with different plotting symbols representing the different groups of glasses discussed in Sections 2.1 to 2.7. Figure 5.10 shows a few glasses in the Phase 1 Test Matrix have standardized residuals greater than 3 in absolute value. Values this large should rarely occur if a model adequately fits the data. Hence, these large standardized residual values are additional indications of LOF for the PCT-B reduced LM model.

Figures 5.11 and 5.12 show predicted versus measured plots when the reduced LM model for ILAW PCT-B is applied to two validation datasets. Figure 5.11 results from fitting the reduced LM model to a subset of 97 out of 244 modeling glasses, and then applying the resulting model to the remaining subset of 147 glasses for validation (see Section 5.1.3). Figure 5.12 results from fitting the reduced LM model for PCT-B to all 244 glasses in the modeling set and then applying that model to the 20 outlying glasses (see Section 5.1.4). Also shown in Figures 5.11 and 5.12 are 95% prediction intervals (95% PIs) representing the model prediction uncertainty of single PCT-B determinations for each glass (see Sections C.6 and C.7 of Appendix C). If the error bar for a validation point overlaps the 45° line, that means the predicted and measured ln(PCT-B) values are within model and measurement uncertainty of each other.

Figure 5.11 shows that the reduced LM model for PCT-B fitted to the 97-glass modeling subset has varied predictive performance for the 147-glass validation subset. The PCT-B release is fairly accurately predicted for many of the 147 glasses, is somewhat over-predicted for some glasses, and is significantly over-predicted for several glasses. However, the 95% PIs overlap the 45° line (i.e., contain the measured values) for all but 13 of the 147 glasses in the validation subset. The 95% PIs are relatively wide, especially for the glasses on which PCT-B release is significantly over-predicted. The generally wide 95% PIs are partly due to: (i) any LOF of the



reduced LM model, and (ii) the inherent experimental uncertainty in fabricating glasses, performing the PCT, and analyzing B in the PCT leachates. The much wider 95% PIs for the significantly over-predicted glasses are a result of those glass compositions not having many other similar glass compositions in the modeling subset of 97 glasses.

Figure 5.12 shows that the reduced LM model for PCT-B fitted to the 244-glass modeling dataset has mixed predictive performance for the set of 20 outlying glasses excluded from the modeling dataset. The model over-predicts PCT-B for 16 of the 20 glasses. However, the 95% PIs are sufficiently wide that only two PIs do not contain the corresponding measured values.

### Summary of Reduced Linear Mixture Model for $\ln(\text{PCT-B})$

Summary statistics for the PCT-B reduced LM model (see Table 5.8) indicate that it performs as well or better than the full LM model (see Table 5.7). The reduced LM model is also expected to yield smaller uncertainties of PCT-B predictions because unnecessary terms have been removed from the model. However, the reduced LM model for PCT-B has significant LOF compared to the inherent uncertainty in batching and melting glasses, performing the PCT, and analyzing the leachate for B release.

### **5.3.3 Results from Reduced PQM Model for ILAW PCT-B**

In an effort to improve on the reduced LM model for PCT-B, PQM models (see Section 5.2.1) were also considered. Specifically, selected quadratic terms (squared and two-component crossproduct terms) were added to the linear terms of the reduced LM model to include important nonlinear blending effects of the glass components. PQM models are discussed in detail by Piepel et al. (2002).

Adding selected quadratic terms to a reduced LM model yields what are referred to as *reduced PQM models*. All possible quadratic terms were formed using the LAW glass components in the reduced LM model for PCT-B. The MAXR selection method (coded in R (Ihaka and Gentleman 1996, R Core Development Team 2006), but like the MAXR option of PROC REG in SAS 2005), was used to identify “best” subsets of quadratic terms to include in reduced PQM models. See Section C.5 of Appendix C for additional discussion.

Reduced PQM models were generated using the MAXR criterion to select from 3 to 9 quadratic terms to augment the 12 linear terms from the reduced LM model. Although statistical significance tests indicated up to 9 quadratic terms were statistically significant, past experience with developing and validating PQM models has indicated adding too many quadratic terms tends to over-fit the model development dataset and degrade predictive performance for new glasses. Ultimately, the 17-term PQM model with 12 linear terms and 5 quadratic terms was chosen as including enough quadratic terms to improve the model fit, hopefully without significantly over-fitting the model development data. Table 5.9 contains the coefficients of the 17-term PQM model for  $\ln(\text{PCT-B})$ , coefficient standard deviations, and performance statistics for the (i) modeling data, (ii) 97/147 partition of the modeling data into modeling and validation subsets, (iii) data-split modeling data, and (iv) 20 outlying LAW glasses.

### Numerical Results for the Reduced Partial Quadratic Mixture Model on $\ln(\text{PCT-B})$

In Table 5.9, the PCT-B model evaluation statistics  $R^2 = 0.866$ ,  $R^2_A = 0.857$ ,  $R^2_P = 0.835$ , and  $\text{RMSE} = 0.291$  are substantial improvements over the corresponding statistics for the 12-term reduced LM model (see Table 5.8). The small drop in values from  $R^2_A$  to  $R^2_P$  suggests that the PCT-B modeling dataset does not have any highly influential data points for the 17-term reduced PQM model. In any case,  $R^2_P = 0.835$  provides an estimate of the fraction of variation in  $\ln(C_B)$  values for future datasets over the same glass composition region that might be accounted for by this reduced PQM model.

The reduced PQM model for PCT-B yielded somewhat different results for the partition of the modeling data into a modeling subset of 97 glasses and a validation subset of 147 glasses. As seen in Table 5.9, the fit statistics  $R^2 = 0.923$ ,  $R^2_A = 0.908$ , and  $R^2_P = 0.870$  for the 97-glass subset are all better (i.e., larger) than the corresponding statistics for the full 244-glass modeling set. However,  $\text{RMSE} = 0.320$  is slightly worse (i.e., larger) for the 97-glass modeling subset. For the 147-glass validation subset,  $R^2_V = 0.071$  is very small and  $\text{RMSE}_V = 0.452$ . The reasons for this less than ideal validation performance are explained subsequently when Figure 5.16 is discussed.

Over the five data splits of the PCT-B modeling data, Table 5.9 shows that the reduced PQM model has average  $R^2$ ,  $R^2_A$ ,  $R^2_P$ , and  $\text{RMSE}$  values that are all close to their values from the 244-glass modeling dataset. The average  $R^2_V = 0.769$  from data-splitting is somewhat worse (i.e., smaller) than  $R^2_P = 0.835$  for the 244-glass modeling dataset. This suggests that either the reduced PQM model performance is not as good as represented by  $R^2_P = 0.835$ , or that the reduced PQM model form is not fitted as well using roughly 80% subsets of the complete modeling dataset. However, the average  $\text{RMSE}_V = 0.303$  from data-splitting is very close to the  $\text{RMSE} = 0.291$  for the 244-glass modeling dataset. Hence, the data-splitting validation results for the reduced PQM model are generally similar or slightly worse than those from fitting that model to the 244-glass dataset.

For the set of 20 outlying LAW glasses, the reduced PQM model for PCT-B has  $R^2_V = 0.446$ , indicating that the extrapolative prediction ability of the model is worse than for data included in the modeling set. The  $\text{RMSE}_V = 0.463$  for these 20 glasses is similar to the  $\text{RMSE}_V = 0.452$  for the partitioned modeling data, but not as good as the average  $\text{RMSE}_V = 0.303$  for the five data-splits of the modeling data. Additional explanation of the extrapolative validation performance of the reduced PQM model for PCT-B is provided subsequently when Figure 5.17 is discussed.

The  $\text{RMSE}$  in Table 5.9 is an estimate of the uncertainty [in  $\ln(C_B)$  units] in fabricating simulated LAW glasses and measuring  $C_B$  if the reduced PQM model for PCT-B does not have statistically significant LOF. Although  $\text{RMSE} = 0.291$  for the reduced PQM model is smaller than the corresponding value for the reduced LM model, it is still larger than the historical replicate RSD of  $\sim 0.10$  (from Appendix F of Hrma et al. 1994) in fabricating simulated waste glasses and measuring PCT-B release, as discussed at the end of Section 5.1.1. The  $\text{RMSE}$  value is also somewhat larger than the replicate SD in  $\ln(\text{g/L})$  units of 0.2269 in Table 5.4. These

observations suggest that the reduced PQM model may have a moderate to negligible LOF. This indication is confirmed by the  $p$ -value = 0.122 of the LOF test (see Section C.4 of Appendix C) for this model in Table 5.9. Although such a  $p$ -value does suggest some model LOF, it does not allow declaring a statistically significant model LOF with at least 90% confidence. However, it may be that the reduced PQM model for PCT-B does have a more substantial LOF that was not detected with higher confidence because of the relatively large uncertainty in the replicate PCT-B data.

### Graphical Results for the Reduced Partial Quadratic Mixture Model on ln(PCT-B)

Figure 5.13 displays the predicted versus measured plot for the PCT-B reduced PQM model. The distribution of points around the 45° line is substantially improved compared to the distribution for the reduced LM model in Figure 5.8. Figure 5.13 shows that the reduced PQM model still has some tendency to under-predict PCT-B releases near and above the limit of 4 g/L (2 g/m<sup>2</sup>). However, PCT-B predictions are improved compared to the reduced LM model for glasses with the five highest PCT-B releases as well as for the Phase 1a Augmentation Matrix glasses, many of which have PCT-B releases near but below the limit. Figure 5.13 also shows that the reduced PQM model has corrected the tendency of the reduced LM model to under-predict for glasses with the lowest PCT-B releases.

Figure 5.14 displays the response trace plot (see Section C.5.1) for the PCT-B reduced PQM model. Figure 5.14 shows that Li<sub>2</sub>O, MgO, Na<sub>2</sub>O, B<sub>2</sub>O<sub>3</sub> and K<sub>2</sub>O tend to increase PCT-B release, Al<sub>2</sub>O<sub>3</sub>, P<sub>2</sub>O<sub>5</sub>, and SiO<sub>2</sub> tend to decrease PCT-B release, and CaO, Fe<sub>2</sub>O<sub>3</sub>, ZrO<sub>2</sub>, and Others tend to have slight to negligible effects on PCT-B release.

Diagnostic plots for the reduced PQM model (not included in this report) support that the assumption of normally distributed errors in the PCT-B data is reasonable (see Section C.3 of Appendix C). The standardized residual plot for the PCT-B reduced PQM model in Figure 5.15 shows two or three glasses in the Phase 1 Test Matrix have standardized residuals greater than 3. Although outlying, these data points did not have much of an impact on the fitted model.

Figures 5.16 and 5.17 show predicted versus measured plots when the reduced PQM model for ILAW PCT-B is applied to two validation datasets. Figure 5.16 results from fitting the reduced PQM model to a subset of 97 out of 244 modeling glasses, and then applying the resulting model to the remaining subset of 147 glasses for validation (see Section 5.1.3). Figure 5.17 results from fitting the reduced PQM model for PCT-B to all 244 glasses in the modeling set and then applying that model to the 20 outlying glasses (see Section 5.1.4). Also shown in Figures 5.16 and 5.17 are 95% PIs representing the model prediction uncertainty of single PCT-B determinations for each glass (see Sections C.6 and C.7 of Appendix C). If the error bar for a validation point overlaps the 45° line, that means the predicted and measured ln(PCT-B) values are within model and measurement uncertainty of each other. The 95% PIs are relatively wide, which is partly due to: (i) any LOF of the reduced PQM model, and (ii) the inherent experimental uncertainty in fabricating glasses, performing the PCT, and analyzing B in the PCT leachates. However, note that the 95% PIs in Figures 5.16 and 5.17 are narrower for the reduced PQM model than for the reduced LM model in Figures 5.11 and 5.12. Separate work to assess the

consequences of LOF and prediction uncertainty for this PCT-B model is discussed in Section 5.6.

Figure 5.16 shows that the PCT-B reduced PQM model fitted to the 97-glass modeling subset has varied predictive performance for the 147-glass validation subset. The PCT-B release is fairly accurately predicted for many of the 147 glasses. However, it tends to be under-predicted for the largest and smallest values, and over-predicted for many intermediate values. Still, the over-predictions are not as severe for some glasses with the reduced PQM model compared to the reduced LM model. Also, the 95% PIs overlap the 45° line (i.e., contain the measured values) for all but 7 of the 147 glasses in the validation subset. Failure of  $100(7/147) = 4.8\%$  of the 95% PIs to include the corresponding measured values is about what would be expected by chance.

Figure 5.17 shows the predictive performance of the PCT-B reduced PQM model (fitted to the 244-glass modeling dataset) for the set of 20 outlying glasses excluded from the modeling dataset. The model predictions are scattered somewhat widely, but evenly, on either side of the 45° line representing perfect prediction. The 95% PIs, although narrower for the reduced PQM model than the reduced LM model, are sufficiently wide that only four of the twenty 95% PIs do not contain the corresponding measured values.

#### Summary of Reduced Partial Quadratic Mixture Model for ln(PCT-B)

Although the reduced PQM model for ln(PCT-B) still appears to have some LOF, it does fit the 244-glass modeling dataset better than the reduced LM model. The reduced PQM model also performs better on the data-splitting, data partitioning, and extrapolative validation assessments than does the reduced LM model.

#### **5.3.4 Results from Two-Part Reduced LM Model for ILAW PCT-B**

The two-part model form given by Equation (5.3) in Section 5.2.1 was fitted, evaluated, and validated for PCT-B releases. Separate 12-component reduced LM models were fit below and above a cutoff value of PCT B equal to 1.89 g/L, chosen using the approach described in Section 5.2.1. Figure 5.18 shows the cutoff value and PCT-B limit on the predicted versus measured plot of the reduced LM model. It can be seen from Figure 5.18 that all of the glasses for which the reduced LM model tends to under-predict PCT-B release are above the cutoff, which was the primary goal in selecting the cutoff value.

#### Numerical Results for the Two-Part Reduced Linear Mixture Model on ln(PCT-B)

Table 5.10 contains the coefficients of the 24-term, two-part model for ln(PCT-B), coefficient standard deviations, and performance statistics for the (i) modeling data, (ii) data-split modeling data, and (iii) 20 outlying LAW glasses. There were insufficient data in the modeling subset of the 97/147 partition of the 244-glass modeling dataset to fit and validate the two-part model with that approach. In Table 5.10, the modeling evaluation statistics  $R^2 = 0.897$ ,  $R^2_A = 0.886$ ,  $R^2_P = 0.862$ , and  $RMSE = 0.259$  are improvements over the corresponding statistics for

the 12-term reduced PQM model (see Table 5.9). The small drop in values from  $R^2_A$  to  $R^2_P$  suggests that the modeling dataset does not have any highly influential data points for the 24-term two-part model. In any case,  $R^2_P = 0.862$  provides an estimate of the fraction of variation in  $\ln(C_B)$  values for future datasets over the same glass composition region that might be accounted for by this two-part model.

Table 5.10 includes summary statistics from fitting each of the two parts of the model in addition to those discussed in the previous paragraph for the model taken as a whole. These statistics show that the part of the model above the PCT-B cutoff fits very well ( $R^2_{\text{Above}} = 0.889$ ) and performs better for this portion of the data than the reduced LM model ( $R^2_{\text{Above}} = 0.407$ ). The part of the model below the PCT-B cutoff does not fit as well ( $R^2_{\text{Below}} = 0.699$ ), but still accounts for a substantial fraction of the variability in lower PCT-B values, and performs better for this portion of the data than the reduced LM model ( $R^2_{\text{Below}} = 0.479$ ).

Over the five data splits of the PCT-B modeling data, Table 5.10 shows that the two-part reduced LM model has average  $R^2$ ,  $R^2_A$ ,  $R^2_P$ , and RMSE values that are all close to their values from the 244-glass modeling dataset. The average  $R^2_V = 0.675$  from data-splitting is significantly worse (i.e., smaller) than  $R^2_P = 0.862$  for the 244-glass modeling dataset. The average  $\text{RMSE}_V = 0.360$  from data-splitting is also noticeably worse (i.e., larger) than  $\text{RMSE} = 0.259$  for the 244-glass modeling dataset. This suggests that either the two-part model performance is not as good as represented by  $R^2_P = 0.862$  and  $\text{RMSE} = 0.259$ , or that the two-part model form is not fitted as well using roughly 80% subsets of the complete modeling dataset. Another potential explanation is discussed in the second following paragraph. The average  $R^2_V = 0.675$  from data splitting for the two-part model is also noticeably worse (i.e., smaller) than the average  $R^2_V = 0.769$  for the reduced PQM model.

For the set of 20 outlying LAW glasses, the two-part reduced LM model for PCT-B has  $R^2_V = 0.183$ , indicating that the extrapolative prediction ability of the model is poor. The  $\text{RMSE}_V = 0.562$  for the 20 glasses is not as good as the average  $\text{RMSE}_V = 0.360$  for the five data-splits of the modeling data. Also,  $\text{RMSE}_V = 0.562$  for the two-part model is worse than  $\text{RMSE}_V = 0.463$  for the reduced PQM model. Additional explanation of the extrapolative validation performance of the two-part reduced LM model for PCT-B is provided subsequently when Figure 5.20 is discussed.

The two-part model fits the 244-glass PCT-B modeling dataset very well, but it suffers compared to the reduced PQM model in the data-split validation performance. In applying the two-part model to new or validation data, the predicted PCT-B release from the “below cutoff” part of the model is used to determine whether the predicted PCT-B release is above or below the cutoff value. If above, then the “above cutoff” portion of the model is applied. Thus the performance of the two-part model for new or validation data is affected by how well the “below cutoff” part of the model determines which part of the model should be applied. This appears to be the reason for the degraded data-split validation performance of the two-part model for PCT-B.

The RMSE in Table 5.10 is an estimate of the uncertainty [in  $\ln(C_B)$  units] in fabricating simulated LAW glasses and measuring  $C_B$  if the two-part model does not have statistically

significant LOF. The RMSE = 0.259 for the two-part model is larger than the historical replicate RSD of ~0.10 (from Appendix F of Hrma et al. 1994) in fabricating simulated waste glasses and measuring PCT-B release, as discussed at the end of Section 5.1.1. The RMSE value is also marginally larger than replicate SD in  $\ln(\text{g/L})$  units of 0.2269 in Table 5.4. These observations suggest that the two-part model has a very small if not negligible LOF. This indication is confirmed by the  $p$ -value = 0.271 of the LOF test (see Section C.4 of Appendix C) for this model in Table 5.9. Such a  $p$ -value does not allow declaring a statistically significant model LOF with at least 90% confidence. However, it may be that the two-part model for PCT-B does have a LOF that was not detected with higher confidence because of the relatively large uncertainty in the replicate PCT-B data.

### Graphical Results for the Two-Part Reduced Linear Mixture Model on $\ln(\text{PCT-B})$

Figure 5.19 displays the predicted versus measured plot for the two-part model on  $\ln(\text{PCT-B})$ . The distribution of points around the 45° line is substantially improved compared to the distribution for the reduced LM model (see Figure 5.8). The distribution of points is also marginally improved compared to the distribution for the reduced PQM model (see Figure 5.18). Figure 5.19 shows that the two-part model has resolved the tendency to under-predict PCT-B releases near and above the limit of 4 g/L (2 g/m<sup>2</sup>). Figure 5.19 also shows that the two-part model has corrected the tendency of the reduced LM model to under-predict for glasses with the lowest PCT-B releases.

Figure 5.20 shows a predicted versus measured plot that results from fitting the two-part model for ILAW PCT-B to all 244 glasses in the modeling set and then applying that fitted model to the 20 outlying glasses (see Section 5.1.4). All except 5 of the 20 glasses have PCT-B over-predicted by the two-part reduced LM model. In this regard the two-part model has worse extrapolative validation performance than the reduced PQM model. Also shown in Figure 5.20 are 95% PIs representing the model prediction uncertainty of single PCT-B determinations for each glass (see Sections C.6 and C.7 of Appendix C). The 95% PIs are narrower for the “below cutoff” part of the model, and wider for the “above cutoff” part of the model. The narrower 95% PIs for the “below cutoff” part of the model do not include the corresponding measured  $\ln(\text{PCT-B})$  values for 6 of the 17 glasses for which the “below cutoff” part of the model was used.

### **5.3.5 Recommended ILAW PCT-B Model**

Table 5.11 summarizes the main PCT-B model evaluation and validation results for the

- PCT modeling data of 244 simulated and actual LAW glasses
- partition of the modeling dataset into subsets of 97 glasses for modeling and 147 for validation
- data-splitting approach to model validation

from Tables 5.7 to 5.10. Based on the summarized results in Table 5.11 and discussions in Sections 5.3.1 to 5.3.4, the 17-term reduced PQM model (listed in Table 5.9) is recommended for predicting PCT-B release of ILAW.

As a baseline for comparison, the 12-component reduced LM model (listed in Table 5.8) could be used. However, it is not recommended for primary use because of its tendency to under-predict PCT-B releases above and somewhat below the limit of 2 g/m<sup>2</sup> (4 g/L). Although the two-part model fits the 244-glass PCT-B modeling dataset better than the reduced PQM model, its data-split and outlier validation performances are worse than that of the reduced PQM model for reasons discussed in Section 5.3.4. This reason and the larger number of terms in the two-part model are why it was not recommended. However, the two-part model could be applied in the future to gain additional information on how well it predicts PCT-B for new glasses and whether it is competitive with the reduced PQM model.

## 5.4 Property-Composition Model Results for PCT-Na Release

This section discusses the results of fitting several different models using natural logarithms of ILAW PCT normalized sodium release (g/L) as the response variable. Section 5.4.1 presents the results of modeling PCT-Na using an 18-component LM model. Sections 5.4.2 and 5.4.3 present the results of modeling PCT-Na using LM and PQM models based on a reduced set of 12 mixture components. Section 5.4.4 discusses the results from fitting a two-part model in which separate 12-term LM models were fit to glasses with PCT-Na releases below and above a cutoff value. Finally, Section 5.4.5 compares the results from the four models and recommends a PCT-Na model for future use and evaluation.

### 5.4.1 Results from Full LM Model for ILAW PCT-Na

As the initial step in PCT-Na model development, a full LM model in the 18 components identified in Section 5.1.1 was fit to the modeling data (244 glasses) with the response being the natural logarithm of PCT-Na normalized releases (g/L). This is the same initial step as was used for the PCT-B model development.

Table 5.12 contains the results for the 18-component full LM model for ILAW PCT-Na. Table 5.12 lists the model coefficients, standard deviations of the coefficients, and model performance summaries for the full LM model using the modeling dataset (244 glasses), the data-splitting approach (see Section 5.1.2), the modeling data partitioned into modeling (97 glasses) and validation (147 glasses) subsets (see Section 5.1.3), and the outlying glass dataset (see Section 5.1.4). In the data-splitting portion of results at the bottom of Table 5.12, the columns are labeled DS1, DS2, DS3, DS4, and DS5 to denote the five modeling/validation splits of the data as described in Section 5.1.2. The last column of this part of Table 5.12 shows the averages for the different statistics over the five splits.

The  $R^2 = 0.798$ ,  $R^2_A = 0.783$ , and  $R^2_P = 0.740$  statistics in Table 5.12 show that the full LM model fits the PCT-Na data in the 244-glass modeling dataset fairly well. However, RMSE =

0.320 is noticeably larger than the glass batching and PCT-Na measurement uncertainty ( $SD = 0.1760$  in  $\ln(\text{g/L})$  units) estimated from replicates in Table 5.4. This indicates the full LM model has LOF, which was confirmed as statistically significant with  $p = 0.006$  as shown in Table 5.12 (see Section C.4 for discussion of the statistical test for model LOF).

The predicted versus measured plot in Figure 5.21 shows that the full LM model significantly under-predicts PCT-Na release above the limit of 4 g/L ( $2 \text{ g/m}^2$ ). The model also under-predicts PCT-Na for most of the Phase 1a Augmentation Matrix glasses, many of which have PCT-Na releases near but below the limit. Figure 5.21 also shows that the full LM model for PCT-Na tends to predict the lowest releases fairly well, without the tendency to under-predict seen with the full LM model for PCT-B.

The PCT-Na full LM model statistics from partitioning the 244-glass modeling set into subsets of 97 modeling glasses and 147 validation glasses (see Section 5.1.3) are given on the right side of Table 5.12. The fit statistics of  $R^2 = 0.858$ ,  $R^2_A = 0.827$ , and  $R^2_P = 0.740$  for the 97-glass subset are all better (i.e., larger) than the corresponding statistics for the full 244-glass modeling set. However,  $RMSE = 0.363$  is worse (i.e., larger) for the 97-glass modeling subset. For the 147-glass validation subset,  $R^2_V$  is negative and  $RMSE_V = 0.548$ . This poor validation performance for the 18-component full LM model is because there is insufficient support in the 97-glass modeling subset to fit all 18 components.

At the bottom right of Table 5.12, the average statistics over the five data-splits are very close to the statistics obtained for fitting the PCT-Na full LM model to all 244 glasses. This indicates that the model, despite its statistically significant LOF, maintains its performance for data not used to fit the model. The negative  $R^2_V$  and relatively large validation  $RMSE = 0.677$  for the 20 outlying glasses indicates the full LM model for PCT-Na does not have very good extrapolative predictive performance, but that is not a primary consideration.

Despite the statistically significant LOF of the full LM model for PCT-Na, the model fits the data well enough to provide guidance for reducing the model (i.e., removing separate terms for components that do not significantly influence PCT-Na release). Hence, the full LM model was used to produce the response trace plot (see Section C.5.1) shown in Figure 5.22. The response trace plot shows that  $\text{Li}_2\text{O}$ ,  $\text{MgO}$ ,  $\text{Na}_2\text{O}$ ,  $\text{K}_2\text{O}$ , and  $\text{B}_2\text{O}_3$  tend to increase PCT-Na release, while  $\text{Al}_2\text{O}_3$ ,  $\text{P}_2\text{O}_5$ , and  $\text{SiO}_2$  tend to decrease PCT-Na release. The response trace for  $\text{Cr}_2\text{O}_3$  has the largest positive slope, suggesting that per unit increase  $\text{Cr}_2\text{O}_3$  as the strongest increasing effect on PCT-Na release. However, this indication does not agree with glass science knowledge and experience, and appears to be an artifact resulting from small numbers of glasses with high  $\text{Cr}_2\text{O}_3$  and or  $\text{P}_2\text{O}_5$ .

#### 5.4.2 Results from Reduced LM Model for ILAW PCT-Na

The full 18-component LM model for PCT-Na presented in Section 5.4.2 likely contains components that do not significantly contribute to predicting PCT-Na release, so model reduction was the next step of the model development approach. Thus, LM models for PCT-Na involving fewer than the 18 components were considered. The sequential F-test model reduction



approach (see Section C.5.1 of Appendix C, Piepel and Cooley 2006) was used as previously described in Section 5.3.2 for developing the reduced LM model for PCT-B.

### Numerical Results for the Reduced Linear Mixture Model on $\ln(\text{PCT-Na})$

The reduced LM model obtained for PCT-Na using the F-test approach and a significance level of 0.001 (the same threshold used to obtain the reduced LM model for PCT-B) contained terms for 12 components:  $\text{Al}_2\text{O}_3$ ,  $\text{B}_2\text{O}_3$ ,  $\text{CaO}$ ,  $\text{Fe}_2\text{O}_3$ ,  $\text{K}_2\text{O}$ ,  $\text{Li}_2\text{O}$ ,  $\text{MgO}$ ,  $\text{Na}_2\text{O}$ ,  $\text{P}_2\text{O}_5$ ,  $\text{SiO}_2$ ,  $\text{ZrO}_2$ , and Others. Note that Others is the sum of all remaining components, and thus differs from the Others in the 18-component LM model discussed in Section 5.4.1. The reduced LM model form obtained for PCT-Na is the same as was obtained for PCT-B. Table 5.13 gives the coefficients and coefficient standard deviations for the 12-component reduced LM model for  $\ln(\text{PCT-Na})$ , as well as performance statistics for the (i) modeling data, (ii) 97/147 partition of the modeling data into modeling and validation subsets, (iii) data-split modeling data, and (iv) 20 outlying LAW glasses.

In Table 5.13,  $R^2 = 0.776$  indicates that the reduced LM model for PCT-Na accounts for roughly 78% of the variation in  $\ln(C_B)$  values in the 244-glass modeling dataset. While this is a reasonably large number, a larger value would be preferable. The value of  $R^2_A = 0.765$  is close to  $R^2$ , indicating that the model reduction was successful in removing unneeded components. The value for  $R^2_P = 0.732$  is not very far below the  $R^2$  and  $R^2_A$  values, indicating that there are not any highly influential data points in the PCT-Na modeling dataset. In any case,  $R^2_P = 0.732$  provides an estimate of the fraction of variation in  $\ln(C_B)$  values for future glasses in the same glass composition region that might be accounted for by this reduced LM model.

The reduced LM model for PCT-Na yielded somewhat different results for the partition of the modeling data into a modeling subset of 97 glasses and a validation subset of 147 glasses. As seen in Table 5.13, the fit statistics  $R^2 = 0.836$ ,  $R^2_A = 0.815$ , and  $R^2_P = 0.757$  for the 97-glass subset are all better (i.e., larger) than the corresponding statistics for the full 244-glass modeling set. However,  $\text{RMSE} = 0.376$  is slightly worse (i.e., larger) for the 97-glass modeling subset. For the 147-glass validation subset,  $R^2_V$  is negative and  $\text{RMSE}_V = 0.696$ . The reasons for this less than ideal validation performance are explained subsequently when Figure 5.26 is discussed.

Over the five data splits of the PCT-Na modeling data, Table 5.13 shows the reduced LM model for PCT-Na has average  $R^2$ ,  $R^2_A$ ,  $R^2_P$ , and  $\text{RMSE}$  values that are all close to their values from the 244-glass modeling dataset. The average  $R^2_V = 0.709$  from data-splitting is somewhat worse (i.e., smaller) than  $R^2_P = 0.732$  for the 244-glass modeling dataset. However, the average  $\text{RMSE}_V = 0.318$  from data-splitting is slightly better (i.e., smaller) than  $\text{RMSE} = 0.332$  for the 244-glass modeling dataset. Hence, the data-splitting validation results are generally similar to those from fitting the 244-glass dataset.

For the set of 20 outlying LAW glasses, the reduced LM for PCT-Na has  $R^2_V = 0.118$ , which is very small and indicates that the extrapolative prediction ability of the model is relatively poor. The  $\text{RMSE}_V = 0.518$  for these 20 glasses is worse than the average  $\text{RMSE}_V = 0.318$  for the five data-splits of the modeling data, but is better than  $\text{RMSE}_V = 0.696$  for the

partitioned modeling data. Further insight to the extrapolative predictive performance of the reduced LM model for PCT-Na is given subsequently when Figure 5.27 is discussed.

The RMSE in Table 5.13 is an estimate of the uncertainty [in  $\ln(C_{Na})$  units] in fabricating simulated LAW glasses and measuring  $C_{Na}$  if the reduced LM model does not have statistically significant LOF. To judge the LOF for the reduced LM model, the RMSE value can be compared to uncertainty estimates based on replicate PCT-Na release data. The RMSE = 0.3323 is much larger than the historical replicate RSD<sup>11</sup> of  $\sim 0.10$  (from Appendix F of Hrma et al. 1994) in fabricating simulated waste glasses and measuring PCT-Na release. It is also much larger than the replicate SD in  $\ln(\text{g/L})$  units of 0.1760 in Table 5.4 (which is discussed in the last subsection of Section 5.1.1). These observations suggest that the reduced LM model for  $\ln(\text{PCT-Na})$  has a substantial LOF, which is confirmed by the LOF test p-value = 0.006 included in Table 5.13. This p-value indicates that the model LOF is significant at the 99.4% confidence level. See Section C.4 of Appendix C for further discussion of the LOF test

#### Graphical Results for the Reduced Linear Mixture Model on $\ln(\text{PCT-Na})$

The predicted versus measured plot for the reduced LM model in Figure 5.23 is nearly identical to the one for the full LM model in Figure 5.21. Figure 5.23 shows that the reduced LM model significantly under-predicts PCT-Na release above the limit of 4 g/L (2 g/m<sup>2</sup>). The reduced LM model also under-predicts PCT-Na for most of the Phase 1a Augmentation Matrix glasses, many of which have PCT-Na releases near but below the limit. Figure 5.23 also shows that the reduced LM model for PCT-Na tends to predict the lowest releases fairly well, without the tendency to under-predict seen with the reduced LM model for PCT-B.

Figure 5.24 displays the response trace plot (see Section C.5.1) for the PCT-Na reduced LM model. Figure 5.24 shows that  $\text{Li}_2\text{O}$ ,  $\text{MgO}$ ,  $\text{Na}_2\text{O}$ ,  $\text{K}_2\text{O}$ , and  $\text{B}_2\text{O}_3$  tend to increase PCT-Na release,  $\text{Al}_2\text{O}_3$ ,  $\text{P}_2\text{O}_5$ , and  $\text{SiO}_2$  tend to decrease PCT-Na release, and  $\text{CaO}$ ,  $\text{Fe}_2\text{O}_3$ ,  $\text{ZrO}_2$ , and Others tend to have slight to negligible effects on PCT-Na release.

Diagnostic plots for the reduced LM model (not included in this report) support that the assumption of normally distributed errors in the PCT-Na data is reasonable (see Section C.3 of Appendix C). Figure 5.25 displays for the PCT-Na reduced LM model the standardized residuals plotted versus the data index (a sequential numbering of the modeling data points) with different plotting symbols representing the different groups of glasses discussed in Sections 2.1 to 2.7. Figure 5.25 shows a few glasses in the Phase 1 Test Matrix have standardized residuals greater than 3 in absolute value. Values this large should rarely occur if a model adequately fits the data. Hence, these large standardized residual values are additional indications of LOF for the PCT-Na reduced LM model.

Figures 5.26 and 5.27 show predicted versus measured plots when the reduced LM model for ILAW PCT-Na is applied to two validation datasets. Figure 5.26 results from fitting the reduced LM model to a subset of 97 out of 244 modeling glasses, and then applying the resulting

---

<sup>11</sup> Per Equation (5.6), RSD values calculated from replicate PCT-Na releases approximate SDs calculated from natural logarithms of PCT-Na releases.

model to the remaining subset of 147 glasses for validation (see Section 5.1.3). Figure 5.27 results from fitting the reduced LM model fitted to all 244 glasses in the modeling set and then applying that model to the 20 outlying glasses (see Section 5.1.4). Also shown in Figures 5.26 and 5.27 are 95% PIs representing the model prediction uncertainty of single PCT-Na determinations for each glass (see Sections C.6 and C.7 of Appendix C). If the error bar for a validation point overlaps the 45° line, that means the predicted and measured  $\ln(\text{PCT-Na})$  values are within model and measurement uncertainty of each other.

Figure 5.26 shows that the reduced LM model for PCT-Na fitted to the 97-glass modeling subset has varied predictive performance for the 147-glass validation subset. The PCT-Na release is fairly accurately predicted for many of the 147 glasses, is somewhat over-predicted for some glasses, and is significantly over-predicted for several glasses. However, the 95% PIs overlap the 45° line (i.e., contain the measured values) for all but 18 of the 147 glasses in the validation subset. The 95% PIs are relatively wide, especially for the glasses on which PCT-Na release is significantly over-predicted. The generally wide 95% PIs are partly due to: (i) any LOF of the reduced LM model, and (ii) the inherent experimental uncertainty in fabricating glasses, performing the PCT, and analyzing Na in the PCT leachates. The much wider 95% PIs for the significantly over-predicted glasses are a result of those glass compositions not having many other similar glass compositions in the modeling subset of 97 glasses.

#### Summary of Reduced Linear Mixture Model for $\ln(\text{PCT-Na})$

Summary statistics for the PCT-Na reduced LM model (see Table 5.13) indicate that it performs as well or better than the full LM model (see Table 5.12). The reduced LM model is also expected to yield smaller uncertainties of PCT-Na predictions because unnecessary terms have been removed from the model. However, the reduced LM model for PCT-Na has significant LOF compared to the inherent uncertainty in batching and melting glasses, performing the PCT, and analyzing the leachate for Na release.

### **5.4.3 Results from Reduced PQM Model for ILAW PCT-Na**

In an effort to improve on the reduced LM model for PCT-Na, reduced PQM models (see Section 5.2.1) were also considered in the same way as discussed in Section 5.3.3 for PCT-B. Reduced PQM models were generated using the MAXR criterion (see Section C.5 of Appendix C) to select from 3 to 9 quadratic terms to augment the 12 linear terms from the reduced LM model. Although statistical significance tests indicated up to nine quadratic terms were statistically significant, past experience with developing and validating PQM models has indicated that adding too many quadratic terms tends to over-fit the model development dataset and degrade predictive performance for new glasses. Ultimately, the 17-term PQM model with 12 linear terms and 5 quadratic terms was selected as including enough quadratic terms to improve the model fit, hopefully without significantly over-fitting the model development data. Table 5.14 contains the coefficients of the  $\ln(\text{PCT-Na})$  17-term PQM model, coefficient standard deviations, and performance statistics for the (i) modeling data, (ii) 97/147 partition of the modeling data into modeling and validation subsets, (iii) data-split modeling data, and (iv) 20 outlying LAW glasses.

### Numerical Results for the Reduced Partial Quadratic Mixture Model on ln(PCT-Na)

In Table 5.14, the PCT-Na model evaluation statistics  $R^2 = 0.870$ ,  $R^2_A = 0.861$ ,  $R^2_P = 0.840$ , and  $RMSE = 0.255$  are substantial improvements over the corresponding statistics for the 12-term reduced LM model (see Table 5.13). The small drop in values from  $R^2_A$  to  $R^2_P$  suggests that the PCT-Na modeling dataset does not have any highly influential data points for the 17-term reduced PQM model. In any case,  $R^2_P = 0.840$  provides an estimate of the fraction of variation in  $\ln(C_{Na})$  values for future datasets over the same glass composition region that might be accounted for by this reduced PQM model.

The reduced PQM model for PCT-Na yielded somewhat different results for the partition of the modeling data into a modeling subset of 97 glasses and a validation subset of 147 glasses. As seen in Table 5.14, the fit statistics  $R^2 = 0.919$ ,  $R^2_A = 0.903$ , and  $R^2_P = 0.869$  for the 97-glass subset are all better (i.e., larger) than the corresponding statistics for the full 244-glass modeling set. However,  $RMSE = 0.272$  is slightly worse (i.e., larger) for the 97-glass modeling subset. For the 147-glass validation subset,  $R^2_V = 0.425$  is moderate and  $RMSE_V = 0.363$ . The reasons for this less than ideal validation performance are explained subsequently when Figure 5.31 is discussed.

Over the five data splits of the PCT-Na modeling data, Table 5.14 shows that the reduced PQM model has average  $R^2$ ,  $R^2_A$ ,  $R^2_P$ , and  $RMSE$  values that are all close to their values from the 244-glass modeling dataset. The average  $R^2_V = 0.804$  from data-splitting is somewhat worse (i.e., smaller) than  $R^2_P = 0.840$  for the 244-glass modeling dataset. This suggests that either the reduced PQM model performance is not as good as represented by  $R^2_P = 0.840$ , or that the reduced PQM model form is not fitted as well using roughly 80% subsets of the complete modeling dataset. However, the average  $RMSE_V = 0.260$  from data-splitting is very close to the  $RMSE = 0.255$  for the 244-glass modeling dataset. Hence, the data-splitting validation results for the reduced PQM model are generally similar or slightly worse than those from fitting that model to the 244-glass dataset.

For the set of 20 outlying LAW glasses, the reduced PQM model for PCT-Na has  $R^2_V = 0.271$ , indicating that the extrapolative prediction ability of the model is relatively poor. The  $RMSE_V = 0.470$  for these 20 glasses is worse than  $RMSE_V = 0.363$  for the partitioned modeling data, and worse still than the average  $RMSE_V = 0.260$  for the five data-splits of the modeling data. Additional explanation of the extrapolative validation performance of the reduced PQM model for PCT-Na is provided subsequently when Figure 5.32 is discussed.

The  $RMSE$  in Table 5.14 is an estimate of the uncertainty [in  $\ln(C_{Na})$  units] in fabricating simulated LAW glasses and measuring  $C_{Na}$  if the reduced PQM model for PCT-Na does not have statistically significant LOF. Although  $RMSE = 0.255$  for the reduced PQM model is smaller than the corresponding value for the reduced LM model, it is still larger than the historical replicate RSD of  $\sim 0.10$  (from Appendix F of Hrma et al. 1994) in fabricating simulated waste glasses and measuring PCT-Na release, as discussed at the end of Section 5.1.1. The  $RMSE$  value is also somewhat larger than the replicate SD in  $\ln(g/L)$  units of 0.1760 in Table 5.4. These observations suggest that the reduced PQM model may have a moderate to significant LOF,

which is confirmed by the LOF test  $p$ -value = 0.055 included in Table 5.14. This  $p$ -value indicates that the model LOF is significant at the 94.5% confidence level. It may be that the reduced PQM model for PCT-Na has an even more significant LOF that is partially masked by relatively large uncertainty in the replicate PCT-Na data. See Section C.4 of Appendix C for further discussion of the LOF test.

#### Graphical Results for the Reduced Partial Quadratic Mixture Model on $\ln(\text{PCT-Na})$

Figure 5.28 displays the predicted versus measured plot for the PCT-Na reduced PQM model. The distribution of points around the 45° line is improved compared to the distribution for the reduced LM model in Figure 5.23. Figure 5.28 shows that the reduced PQM model still has some tendency to under-predict PCT-Na releases near and above the limit of 4 g/L (2 g/m<sup>2</sup>). However, PCT-Na predictions are improved compared to the reduced LM model for glasses with the five highest PCT-Na releases as well as for the Phase 1a Augmentation Matrix glasses, many of which have PCT-Na releases near but below the limit. Figure 5.28 also shows that the reduced PQM model has tightened the scatter of points with lower to moderate PCT-Na releases.

Figure 5.29 displays the response trace plot (see Section C.5.1) for the PCT-Na reduced PQM model. Figure 5.14 shows that Li<sub>2</sub>O, MgO, Na<sub>2</sub>O, K<sub>2</sub>O, and B<sub>2</sub>O<sub>3</sub> tend to increase PCT-Na release, Al<sub>2</sub>O<sub>3</sub>, P<sub>2</sub>O<sub>5</sub>, and SiO<sub>2</sub> tend to decrease PCT-Na release, and CaO, Fe<sub>2</sub>O<sub>3</sub>, ZrO<sub>2</sub>, and Others tend to have slight to negligible effects on PCT-Na release.

Diagnostic plots for the reduced PQM model (not included in this report) support that the assumption of normally distributed errors in the PCT-Na data is reasonable (see Section C.3 of Appendix C). The standardized residual plot for the PCT-Na reduced PQM model in Figure 5.30 shows two glasses in the Phase 1 Test Matrix have standardized residuals near 4. Although outlying, these data points did not have a major impact on the fitted model.

Figures 5.31 and 5.32 show predicted versus measured plots when the reduced PQM model for ILAW PCT-Na is applied to two validation datasets. Figure 5.31 results from fitting the reduced PQM model for PCT-Na to a subset of 97 out of 244 modeling glasses, and then applying the resulting model to the remaining subset of 147 glasses for validation (see Section 5.1.3). Figure 5.32 results from fitting the reduced PQM model for PCT-Na to all 244 glasses in the modeling set and then applying that model to the 20 outlying glasses (see Section 5.1.4). Also shown in Figures 5.31 and 5.32 are 95% PIs representing the model prediction uncertainty of single PCT-Na determinations for each glass (see Sections C.6 and C.7 of Appendix C). If the error bar for a validation point overlaps the 45° line, that means the predicted and measured  $\ln(D)$  values are within model and measurement uncertainty of each other. The 95% PIs are relatively wide, which is partly due to: (i) any LOF of the reduced PQM model, and (ii) the inherent experimental uncertainty in fabricating glasses, performing the PCT, and analyzing Na in the PCT leachates. However, note that the 95% PIs in Figures 5.31 and 5.32 are narrower for the reduced PQM model than for the reduced LM model in Figures 5.26 and 5.27. Separate work to assess the consequences of LOF and prediction uncertainties for this PCT-Na model is discussed in Section 5.6.

Figure 5.31 shows that the PCT-Na reduced PQM model fitted to the 97-glass subset has varied predictive performance for the 147-glass validation subset. The PCT-Na release is fairly accurately predicted for many of the 147 glasses. However, it tends to be over-predicted for the majority of glasses. Still, the over-predictions are not as severe for some glasses with the reduced PQM model compared to the reduced LM model. Also, the 95% PIs overlap the 45° line (i.e., contain the measured values) for all but 10 of the 147 glasses in the validation subset. Failure of  $100(10/147) = 6.8\%$  of the 95% PIs to include the corresponding measured values is only slightly worse than what would be expected by chance.

Figure 5.32 shows the predictive performance of the PCT-Na reduced PQM model (fitted to the 244-glass modeling dataset) for the set of 20 outlying glasses excluded from the modeling dataset. The model predictions are scattered somewhat widely, but evenly, on either side of the 45° line representing perfect prediction. The 95% PIs, although narrower for the reduced PQM model than the reduced LM model, are sufficiently wide that only five of the twenty 95% PIs do not contain the corresponding measured values.

#### Summary of Reduced Partial Quadratic Mixture Model for ln(PCT-Na)

Although the reduced PQM model for ln(PCT-Na) still appears to have a statistically significant LOF, it does fit the 244-glass modeling dataset better than the reduced LM model. The reduced PQM model also performs better on the data-splitting, data partitioning, and extrapolative validation assessments than does the reduced LM model.

#### **5.4.4 Results from Two-Part Reduced LM Model for ILAW PCT-Na**

The two-part model form given by Equation (5.3) in Section 5.2.1 was fitted, evaluated, and validated for PCT-Na releases. Separate 12-component reduced LM models were fit below and above a cutoff value of PCT Na equal to 1.80 g/L, chosen using the approach described in Section 5.2.1. Figure 5.33 shows the cutoff value and PCT-Na limit on the predicted versus measured plot of the reduced LM model. It can be seen from Figure 5.33 that all of the glasses for which the reduced LM model tends to under-predict PCT-Na release are above the cutoff, which was the primary goal in selecting the cutoff value.

#### Numerical Results for the Two-Part Reduced Linear Mixture Model on ln(PCT-Na)

Table 5.15 contains the coefficients of the 24-term, two-part model for ln(PCT-Na), coefficient standard deviations, and performance statistics for the (i) modeling data, (ii) data-split modeling data, and (iii) 20 outlying LAW glasses. There were insufficient data in the modeling subset of the 97/147 partition of the 244-glass modeling dataset to fit and validate the two-part model with that approach. In Table 5.15, the modeling evaluation statistics  $R^2 = 0.901$ ,  $R^2_A = 0.890$ ,  $R^2_P = 0.859$ , and  $RMSE = 0.227$  are improvements over the corresponding statistics for the 12-term reduced PQM model (see Table 5.14). The small drop in values from  $R^2_A$  to  $R^2_P$  suggests that the modeling dataset does not have any highly influential data points for the 24-term two-part model. In any case,  $R^2_P = 0.859$  provides an estimate of the fraction of

variation in  $\ln(C_{Na})$  values for future datasets over the same glass composition region that might be accounted for by this two-part model.

Table 5.15 includes summary statistics from fitting each of the two parts of the model in addition to those discussed in the previous paragraph for the model taken as a whole. These statistics show that the part of the model above the PCT-Na cutoff fits very well ( $R^2_{Above} = 0.910$ ) and performs much better for this portion of the data than the reduced LM model ( $R^2_{Above} = 0.293$ ). The part of the model below the PCT-Na cutoff does not fit as well ( $R^2_{Below} = 0.749$ ), but still accounts for a substantial fraction of the variability in lower PCT-Na values, and performs better for this portion of the data than the reduced LM model ( $R^2 = 0.590$ ).

Over the five data splits of the PCT-Na modeling data, Table 5.15 shows that the two-part reduced LM model has average  $R^2$ ,  $R^2_A$ ,  $R^2_P$ , and RMSE values that are all close to their values from the 244-glass modeling dataset. The average  $R^2_V = 0.712$  from data-splitting is significantly worse (i.e., smaller) than  $R^2_P = 0.859$  for the 244-glass modeling dataset. The average  $RMSE_V = 0.310$  from data-splitting is also noticeably worse (i.e., larger) than  $RMSE = 0.227$  for the 244-glass modeling dataset. This suggests that either the two-part model performance is not as good as represented by  $R^2_P = 0.859$  and  $RMSE = 0.227$ , or that the two-part model form is not fitted as well using roughly 80% subsets of the complete modeling dataset. Another potential explanation is discussed in the second following paragraph. The average  $R^2_V = 0.712$  from data splitting for the two-part model is also noticeably worse (i.e., smaller) than the average  $R^2_V = 0.804$  for the reduced PQM model.

For the set of 20 outlying LAW glasses, the two-part reduced LM model for PCT-Na has  $R^2_V = 0.212$ , indicating that the extrapolative prediction ability of the model is poor. The  $RMSE_V = 0.489$  is not as good as the average  $RMSE_V = 0.310$  for the five data-splits of the modeling data. However, the  $RMSE_V = 0.489$  for the two-part model is similar to the  $RMSE_V = 0.470$  for the reduced PQM model. Additional explanation of the extrapolative validation performance of the two-part reduced LM model for PCT-B is provided subsequently when Figure 5.35 is discussed

The two-part model fits the 244-glass PCT-Na modeling dataset very well, but it suffers compared to the reduced PQM model in the data-split validation performance. In applying the two-part model to new or validation data, the predicted PCT-Na release from the “below cutoff” part of the model is used to determine whether the predicted PCT-Na release is above or below the cutoff value. If above, then the “above cutoff” portion of the model is applied. Thus the performance of the two-part model for new or validation data is affected by how well the “below cutoff” part of the model determines which part of the model should be applied. This appears to be the reason for the degraded data-split validation performance of the two-part model for PCT-Na.

The RMSE in Table 5.15 is an estimate of the uncertainty [in  $\ln(C_{Na})$  units] in fabricating simulated LAW glasses and measuring  $C_{Na}$  if the two-part model does not have statistically significant LOF. The  $RMSE = 0.227$  for the two-part model is larger than the historical replicate RSD of  $\sim 0.10$  (from Appendix F of Hrma et al. 1994) in fabricating simulated waste glasses and measuring PCT-Na release, as discussed at the end of Section 5.1.1. The RMSE value is also

larger than replicate SD in  $\ln(\text{g/L})$  units of 0.1760 in Table 5.4. These observations suggest that the two-part model has a small to moderate LOF. This indication is confirmed by the  $p$ -value = 0.141 of the LOF test (see Section C.4 of Appendix C) for this model in Table 5.15. Such a  $p$ -value does not allow declaring a statistically significant model LOF with at least 90% confidence. However, it may be that the two-part model for PCT-Na does have a LOF that was not detected with higher confidence because of the relatively large uncertainty in the replicate PCT-Na data.

#### Graphical Results for the Two-Part Reduced Linear Mixture Model on $\ln(\text{PCT-Na})$

Figure 5.34 displays the predicted versus measured plot for the two-part model on  $\ln(\text{PCT-Na})$ . The distribution of points around the 45° line is substantially improved compared to the distribution for the reduced LM model (see Figure 5.33). The distribution of points is also notably improved compared to the distribution for the reduced PQM model (see Figure 5.28). Figure 5.34 shows that the two-part model has resolved the tendency to under-predict PCT-Na releases near and above the limit of 4 g/L (2 g/m<sup>2</sup>).

Figure 5.35 shows a predicted versus measured plot that results from fitting the two-part model for ILAW PCT-Na to all 244 glasses in the modeling set and then applying that fitted model to the 20 outlying glasses (see Section 5.1.4). The model tends to over-predict PCT-Na values below approximately 0.60 g/L, while above that value the predictions are more widely scattered on both sides of the 45° line representing perfect prediction. Also shown in Figure 5.35 are 95% PIs representing the model prediction uncertainty of single PCT-Na determinations for each glass (see Sections C.6 and C.7 of Appendix C). The 95% PIs are relatively wide, which is partly due to: (i) any LOF of the two-part model, and (ii) the inherent experimental uncertainty in fabricating glasses, performing the PCT, and analyzing Na in the PCT leachates. The 95% PIs for the two-part model are of similar width as those for the reduced PQM model. They are sufficiently wide that only six of the twenty 95% PIs do not contain the corresponding measured values.

#### **5.4.5 Recommended ILAW PCT-Na Model**

Table 5.16 summarizes the main PCT-Na model evaluation and validation results for the

- PCT modeling data of 244 simulated and actual LAW glasses
- partition of the modeling dataset into subsets of 97 glasses for modeling and 147 for validation
- data-splitting approach to model validation

from Tables 5.12 to 5.15. Based on the summarized results in Table 5.16 and discussions in Sections 5.4.1 to 5.4.4, the 17-term reduced PQM model (listed in Table 5.14) is recommended for predicting PCT-Na releases of LAW glasses.

As a baseline for comparison, the reduced LM model (listed in Table 5.13) could be used. However, it is not recommended for primary use because of its tendency to under-predict PCT-



Na releases above and somewhat below the limit of 2 g/m<sup>2</sup> (4 g/L). Although the two-part model fits the 244-glass PCT-Na modeling dataset better than the reduced PQM model, its data-split validation performance is worse than that of the reduced PQM model for reasons discussed in Section 5.4.4. This reason and the larger number of terms in the two-part model are why the two-part reduced LM model for PCT-Na was not recommended. However, the two-part model could be applied in the future to gain additional information on how well it predicts PCT-Na for new glasses and whether it is competitive with the reduced PQM model.

## 5.5 Example Illustrating PCT Model Predictions and Statistical Intervals

This section contains examples to illustrate using the recommended 17-term PQM models to obtain predicted PCT-B and PCT-Na releases and corresponding 90% UCIs and 95% SUCIs for a specific LAW glass composition. For comparison purposes the reduced LM models for PCT-B and PCT-Na (although not recommended) are also applied to obtain predicted values, 90% UCIs, and 95% SUCIs. The confidence levels associated with 90% UCIs and 95% SUCIs were chosen for illustration purposes only. The WTP project can use an appropriate confidence level depending on the use of the PCT-composition model and the type of statistical uncertainty expression.

The glass composition used in this example is LAWA126, which is one of the glasses in the ILAW Existing Matrix. The 18-component composition of LAWA126 for PCT modeling is given in Table 5.2 in mass fraction format. To apply the PCT models to this composition, the mass fractions of the 18 components must be converted to mass fractions (that sum to 1.0) of the 12 LAW glass components contained in the PCT-B and PCT-Na models. Mass fractions of the relevant components are then multiplied to obtain the quadratic terms of the PQM models. Table 5.17 contains the composition of LAWA126 prepared for use in the ILAW PCT-B and PCT-Na models.

For each of the PCT-B and PCT-Na models, predicted ln(PCT releases) are obtained by multiplying the composition in the format needed for that model by the coefficients for that model, then summing the results. That is, the predicted values are calculated by

$$\hat{y}(\mathbf{a}) = \mathbf{a}^T \mathbf{b}$$

where  $\mathbf{a}$  is the composition of LAWA126 formatted to match the terms in a given model (from Table 5.17), the superscript T represents a matrix transpose (or vector transpose in this case), and  $\mathbf{b}$  is the vector of coefficients for a given model. The predicted ln(PCT release) values from the PCT-B and PCT-Na models are listed in the second column of Table 5.18. The predicted ln(PCT releases) in ln(g/L) units are easily converted to the usual PCT release units of g/L by exponentiation. The third column of Table 5.18 contains the predicted PCT releases in g/L units. However, as discussed in Section C.7 of Appendix C, these back-transformed PCT release predictions in g/L units should be considered estimates of the true median (not the true mean) of the distribution of PCT releases that would result if the PCT were repeated multiple times using separately batched and melted samples of the LAWA126 glass composition.

Equation (C.27a) can be used to calculate a 90% UCI for the true mean of ln(PCT releases) from the LAWA126 glass composition for each of the ILAW PCT models. In the notation of Equation (C.27a):

- $100(1-\alpha)\% = 90\%$ , so that  $\alpha = 0.10$ .
- Vector  $\mathbf{a}$  contains entries corresponding to the terms in a given PCT model, which are calculated using the composition of LAWA126 in Table 5.17.
- Matrix  $\mathbf{A}$  is formed from the data matrix used in the regression that generated a given PCT model. Matrix  $\mathbf{A}$  has the number of rows in the PCT modeling dataset (244) and the number of columns corresponding to the number of terms in a given PCT-B or PCT-Na release model. Each column is calculated according to the corresponding term in the model using the LAW glass compositions in the PCT modeling dataset.

To obtain a 90% UCI in ln(PCT release) units of ln(g/L), the quantity  $t_{1-\alpha, n-p} RMSE \sqrt{\mathbf{a}^T (\mathbf{A}^T \mathbf{A})^{-1} \mathbf{a}}$  is added to the predicted ln(PCT release)  $\hat{y}(\mathbf{a})$  described above, as indicated by Equation (C.27a). The  $MSE[(\mathbf{A}^T \mathbf{A})^{-1}]$  portion of this expression is the variance-covariance matrix for the estimated model coefficients, as discussed near the end of Section C.7 of Appendix C. The variance-covariance matrices for the different PCT models are listed in Tables D.1 to D.4 of Appendix D. The quantity  $MSE$  is the mean squared error from regression,  $RMSE$  is the square root of  $MSE$ . The quantity  $RMSE \sqrt{\mathbf{a}^T (\mathbf{A}^T \mathbf{A})^{-1} \mathbf{a}}$  is the standard deviation of a model prediction; the value for each model is given in the fourth column of Table 5.18.

The 90% UCI values for the true mean ln(PCT release) in units of ln(g/L) for the LAWA126 composition based on the ILAW PCT-B and PCT-Na models are given in the fifth column of Table 5.18. Exponentiating the resulting 90% UCIs on the mean in ln(g/L) units yields 90% UCIs for the median in g/L units. For example, the 17-term reduced PQM model for PCT-B has 0.4168 ln(g/L) as the upper limit of the 90% UCI on the true mean ln(PCT-B release) for LAWA126. Then  $e^{0.4168} = 1.5171$  g/L is the upper limit of the 90% UCI on the true median PCT-B release. The sixth column of Table 5.18 contains 90% UCIs for the true median PCT releases from the LAWA126 glass composition based on the ILAW PCT models. Note that the 90% UCI values in g/L units for the ILAW PCT models are well below the PCT release limit of 4 g/L (2 g/m<sup>2</sup>).

As discussed in Section C.7 of Appendix C, there are times when a SUCI may be preferred rather than an UCI. This is particularly true when the regression model (composition-property model) is to be used a large number of times for various glass compositions from a specified composition region. Equation (C.30a) can be used, in much the same way as Equation (C.27a) is used to obtain UCIs, to calculate a 95% SUCI for the true mean of ln(PCT release) for glasses having a specified composition. The 95% SUCI values for the true mean ln(PCT release) in units of ln(g/L) for the LAWA126 composition based on the ILAW PCT models are given in the seventh column of Table 5.18. Exponentiating the resulting 95% SUCIs for the mean in

ln(g/L) units yields 95% SUCIs for the median in g/L. The eighth column of Table 5.18 contains 95% SUCIs for the true median PCT release from the LAWA126 glass composition based on the ILAW PCT models. Note that the 95% SUCI values in g/L for the different ILAW PCT models are well below the PCT release limit of 4 g/L (2 g/m<sup>2</sup>).

## 5.6 Suitability of the Recommended PCT-B and PCT-Na Models for Application by the WTP Project

The 17-term models for PCT-B discussed in Section 5.3.3 and for PCT-Na discussed in Section 5.4.3 are recommended for use by the WTP project as the best models currently available for predicting PCT releases from LAW glasses. These models appear to yield unbiased predictions of PCT-B and PCT-Na releases, except for tendencies to under-predict values above 1.0 ln(g/L) ~ 2.7 g/L, which is somewhat below the contract limit of 4 g/L (2 g/m<sup>2</sup>). The PCT modeling database contained an insufficient number of glasses with PCT-B and PCT-Na releases near and above the contract limits to develop and validate models without this limitation. Hence, constraints were included in the model validity region to restrict the use of the recommended PCT-B and PCT-Na models to predicted releases below 2.7 g/L. The model validity region constraints are discussed in Section 9.

Because of the magnitudes of uncertainties in the PCT data (i.e., from making simulated LAW glasses, PCT testing, and chemical analysis of leachates), as well as some lack-of-fit of the recommended PCT-B and PCT-Na models, prediction uncertainties for the models are relatively large. Figures 5.36 and 5.37 display the prediction standard deviations versus predicted values [both in ln(g/L) units] for the LAW glass compositions in the PCT-B and PCT-Na modeling datasets. The prediction standard deviations for modeling dataset glasses range from approximately 0.03 to 0.20 ln(g/L) for the recommended PCT-B model and from approximately 0.03 to 0.17 ln(g/L) for the recommended PCT-Na model. Note that prediction standard deviations will be larger for LAW glass compositions as their distance from glasses in the PCT modeling datasets increases. Also, the total uncertainty in predictions with the recommended PCT-B and PCT-Na models will depend on the type of statistical interval used (see Section C.7 of Appendix C).

Unless higher waste loadings are pursued, it is relatively easy to formulate LAW glasses with PCT-B and PCT-Na releases substantially below the contract limit, so the model limitations (under-predictions of releases near and above contract limits, as well as relatively large prediction uncertainties) do not unduly restrict use of the PCT models by the WTP project. The ultimate suitability of the recommended PCT-B and PCT-Na models for LAW glass formulation, glass former addition decisions during production, and demonstrating compliance with WTP Contract Specification 2.2.2.17.2 will be decided by separate WTP project work.

The impact of prediction uncertainties for ILAW Phase 1 PCT-B and PCT-Na models (Muller et al. 2005) on the ability to demonstrate compliance with WTP Contract Specification 2.2.2.17.2 was previously addressed in Section 7.4 of Piepel et al. (2005). In that work, the LAW glasses expected to be produced in the WTP LAW vitrification plant were shown to have PCT-B and PCT-Na releases sufficiently below the 2 g/m<sup>2</sup> (= 4 g/L) limit even after accounting for

conservative composition and model uncertainties. The impact of LAW glass composition and model uncertainties for the recommended PCT-B model (Section 5.3.3) and PCT-Na model (Section 5.4.3) on satisfying Contract Specification 2.2.2.17.2 is planned to be addressed as part of the Technical Scoping Statement (TSS) B-6069 work scope of the River Protection Project—Waste Treatment Plant Support Program at PNNL. The impacts are also planned to be addressed as part of the second iteration of LAW glass formulation algorithm development work planned by WTP project staff. The first iteration of that work (Vienna 2005) utilized the ILAW Phase 1 PCT-B and PCT-Na models (Muller et al. 2005) and the LAW glass formulation correlation (Muller et al. 2004b).

## **SECTION 6**

### **MODELS RELATING VHT ALTERATION DEPTH TO LAW GLASS COMPOSITION**

This section documents the development and validation of property-composition models and corresponding uncertainty expressions for predicting the alteration depth (denoted  $D$ ) for low-activity waste (LAW) glasses when subjected to the vapor hydration test (VHT). The property-composition models and corresponding uncertainty expressions for VHT alteration depth presented in this section were developed and validated using glass composition and VHT data collected on simulated LAW glasses. The VHT was not performed on any of the glasses made from actual waste samples that are discussed in Section 2.7.

The 165 simulated LAW glasses used for VHT model development and validation (from the database of 181 glasses) are discussed in Section 6.1. Section 6.2 presents the model forms for VHT alteration depth that were investigated. Sections 6.3 and 6.4 summarize the results for the selected linear and quadratic VHT model forms, respectively. Section 6.5 presents the results for a two-part model. Section 6.6 presents the detailed results for a partial cubic mixture model, which is ultimately the recommended model. Section 6.7 summarizes the VHT-composition model forms investigated. Section 6.8 uses model fit and validation statistics to compare the VHT-composition models investigated. Section 6.9 discusses the selection of the recommended and second-choice models. Section 6.10 illustrates the calculation of VHT alteration depth predictions and the uncertainties in those predictions using selected VHT models and corresponding uncertainty equations. Section 6.11 discusses the suitability of the recommended VHT models for use by the WTP project. Appendix C discusses the statistical methods and summary statistics used to develop, evaluate, and validate the several VHT model forms investigated, as well as statistical equations for quantifying the uncertainties in VHT alteration depth models.

#### **6.1 VHT Alteration Depth Data Used for Model Development and Validation**

The data used for developing VHT alteration depth models are discussed in Section 6.1.1. The approaches and data used for validating the models are discussed in Sections 6.1.2 to 6.1.4.

##### **6.1.1 VHT Alteration Depth Model Development Data**

The data available for developing property-composition models for VHT alteration depth consist of composition and alteration depth data on 181 LAW glasses. These glasses are discussed and their target compositions are presented in Section 2. The normalized compositions of these glasses based on analyzed (or estimated analyzed)  $\text{SO}_3$  values are discussed in Section 3.3. The corresponding VHT alteration depths ( $\mu\text{m}$ ) and alteration rates ( $\text{g}/\text{m}^2/\text{day}$ ) are presented in Table 4.4. The LAW VHT data are discussed in Section 4.2.

## Assessment of Available Glasses with VHT Alteration Data

The database of 181 glasses with VHT results contains statistically-designed as well as actively-designed glasses. Some actively-designed glasses are outside the composition region covered by the majority of the LAW compositions. Such glasses are not ideal for inclusion in a modeling set because they can be influential when fitting models to data. Hence, it was decided to (i) graphically assess the 181 simulated LAW glass compositions and (ii) remove from the modeling set any compositions considered to be outlying or non-representative of LAW glasses of interest for the WTP.

Figure 6.1 displays plots of the mass fraction values for 14 “main components” in 175 of the 181 LAW glasses with VHT data. The “main components” are the ones that were varied in the ILAW Phase 1 Test Matrix and the Phase 1a Augmentation Test Matrix. Figure 6.2 displays similar plots for the remaining minor components. Six glasses are excluded from Figures 6.1 and 6.2 because the VHT alteration depths were reported only as “greater than” values. On each plot in Figures 6.1 and 6.2, the x-axis represents the mass fraction values of an LAW glass component. The y-axis shows an index value representing each LAW glass composition, which aids in spreading out the data points to avoid over-plotting. The plotting symbols correspond to the six groups of LAW glass data discussed in Sections 2.1 to 2.6. The VHT test was not performed on any of the actual waste glasses discussed in Section 2.7. For comparison purposes, the vertical bars in Figures 6.1 and 6.2 represent the ranges over which the components were varied in the ILAW Phase 1 Test Matrix.

Figure 6.1 shows several glasses have components with outlying mass fraction values compared to the remaining glasses and to the component ranges studied in the ILAW Phase 1 Test Matrix and the Phase 1a Augmentation Test Matrix. Figure 6.2 shows what appear to be outliers for some components, but the values and ranges of those components are small and hence the glass compositions were not considered to be outliers. Table 6.1 lists the 16 LAW glasses excluded from the ILAW VHT modeling set, and the reason each glass was excluded. The first six of the 16 glasses were excluded because of having outlying component values compared to the rest of the glasses. The next four glasses in Table 6.1 were designed for a specific investigation, were high in  $\text{Cr}_2\text{O}_3$ , and were container-centerline-cooled. These glasses were considered non-representative and excluded from the VHT modeling dataset. The final six glasses in Table 6.1 were excluded from the modeling dataset because they have VHT alteration depths reported as “greater than” values. This was because the coupons used in VHT testing (see Section 3.5) were completely altered. Note that the first 10 glasses listed in Table 6.1 were 10 of the 20 glasses excluded from the PCT modeling dataset (see Table 5.1). The other 10 glasses excluded from the PCT modeling dataset did not have VHT data, or else they would have been excluded also.

Figures 6.3 and 6.4 (corresponding to Figures 6.1 and 6.2, respectively) show plots of component distributions after the 16 outlying and non-representative glasses were removed from the VHT dataset. Figure 6.3 shows for the remaining 165 LAW glasses that all 13 of the specific LAW glass components ( $\text{Al}_2\text{O}_3$ ,  $\text{B}_2\text{O}_3$ ,  $\text{CaO}$ ,  $\text{Fe}_2\text{O}_3$ ,  $\text{K}_2\text{O}$ ,  $\text{Li}_2\text{O}$ ,  $\text{MgO}$ ,  $\text{Na}_2\text{O}$ ,  $\text{SO}_3$ ,  $\text{SiO}_2$ ,  $\text{TiO}_2$ ,  $\text{ZnO}$ , and  $\text{ZrO}_2$ ) have sufficient ranges and distributions of values within those ranges to support model terms. Similarly, Figure 6.4 shows that  $\text{Cl}$ ,  $\text{Cr}_2\text{O}_3$ ,  $\text{F}$ , and  $\text{P}_2\text{O}_5$  have sufficient ranges and

distributions of values within their ranges to support model terms for those components. Of these four components, the support for a  $P_2O_5$  model term is somewhat tenuous, relying on the “HiCrP” glasses and an actively designed (ActDes) glass. Based on Figures 6.3 and 6.4, it was decided to use 18 components for initial VHT modeling work. These are  $Al_2O_3$ ,  $B_2O_3$ ,  $CaO$ ,  $Cl$ ,  $Cr_2O_3$ ,  $F$ ,  $Fe_2O_3$ ,  $K_2O$ ,  $Li_2O$ ,  $MgO$ ,  $Na_2O$ ,  $P_2O_5$ ,  $SO_3$ ,  $SiO_2$ ,  $TiO_2$ ,  $ZnO$ ,  $ZrO_2$ , and Others (the sum of all remaining components). Note that these are the same 18 components chosen for initial PCT modeling work.

Figure 6.5 shows a scatterplot matrix of the 165 glasses remaining in the VHT modeling dataset after removing the 16 outlying compositions. High correlations between some pairs of components are evident, so pairwise correlation coefficients were calculated. These can vary from  $-1.0$  (perfect negative correlation) to  $0$  (no correlation) to  $1.0$  (perfect positive correlation). The component pairs with correlations larger (in absolute value) than  $0.60$  are

$Li_2O$ and $Na_2O$	$-0.885$
$P_2O_5$ and $Cr_2O_3$	$0.746$
$Na_2O$ and $CaO$	$-0.734$
$Li_2O$ and $CaO$	$0.657$
$Li_2O$ and $SO_3$	$0.642$
$Na_2O$ and $SiO_2$	$-0.641$
$Na_2O$ and $SO_3$	$-0.622$

Such high pairwise correlations can make it difficult for regression methods to properly separate the effects of the components on the response variable (e.g., VHT alteration depths). Thus, these high pairwise correlations need to be kept in mind in developing ILAW VHT property-composition models.

### VHT Modeling Dataset

Table 6.2 lists the Glass ID, Group ID, and normalized glass compositions for the 165 simulated LAW glasses in the 18-component forms used for VHT model development. The Group ID column of Table 6.2 indicates the subset of data that each glass is associated with (see Sections 2.1 to 2.7). The glass compositions in Table 6.2 are the normalized mass fractions (mf) of the 18 components previously identified as having sufficient data to support a separate model term if needed. These components are  $Al_2O_3$ ,  $B_2O_3$ ,  $CaO$ ,  $Cl$ ,  $Cr_2O_3$ ,  $F$ ,  $Fe_2O_3$ ,  $K_2O$ ,  $Li_2O$ ,  $MgO$ ,  $Na_2O$ ,  $P_2O_5$ ,  $SO_3$ ,  $SiO_2$ ,  $TiO_2$ ,  $ZnO$ ,  $ZrO_2$ , and Others. The mass fraction values of the 18 components shown in Table 6.2 were normalized so that they sum to 100% for each of the glasses (see Section 3.3).

Table 6.3 contains a column of measured VHT alteration depths for the 165 glasses in the VHT modeling dataset. It also includes a column designating the data-splitting validation subsets for VHT modeling and validation. These subsets and the data-splitting validation approach are discussed in Section 6.1.2.

The values of  $D$  in Table 6.3 range from 1 to 980  $\mu m$ . Of the 165 simulated LAW glasses in the VHT modeling set, 14 had alteration depths that exceeded the limit of 453  $\mu m$  (equivalent

to 50 g/m<sup>2</sup>/day, given in Specification 2.2.2.17.3 of the WTP Contract). This number does not include the six glasses with “greater than” alteration depths that also exceed the contract limit. It is desirable to have some glasses in the modeling dataset that have VHT alteration depths ranging from somewhat below to somewhat above the limit. This allows for more confident use of the model in discerning between glasses with acceptable and unacceptable VHT results.

### Replicate and Near-Replicate VHT Data

The changes to the LAW glass compositions caused by the renormalization associated with using XRF analyzed (or estimates of XRF analyzed) SO<sub>3</sub> values (see Section 3.3) resulted in some replicate glasses not having exactly equal compositions. Such compositions are referred to as near-replicates. For ease of discussion, henceforth both replicates and near-replicates are referred to as replicates.

Table 6.4 lists the replicate sets of glasses in the ILAW VHT modeling data and the corresponding VHT alteration depths. Table 6.4 also lists estimates of %RSDs for each replicate set as well as pooled estimates over all the replicate sets. A pooled %RSD combines the separate %RSD estimates from each replicate set so that a more accurate combined estimate of the %RSD is obtained. These pooled %RSDs include uncertainties due to fabricating glasses, performing the VHT, and measuring alteration depths. The estimates of replicate uncertainty for VHT alteration depths in Table 6.4 are used subsequently to statistically assess lack-of-fit (LOF) of the various models considered.

The magnitudes of the pooled SD = 0.4493 [calculated from ln(μm) values] and %RSD = 41.87 [calculated from μm values] in Table 6.4 are quite large. However, these values are inflated significantly by the results for a single replicate pair (LAWM09 and LAW54R1), which have measured layer thicknesses of 1 and 3 μm, respectively. These thicknesses (which correspond to alteration rates of about 0.3% of the WTP contract limit) are approaching the resolution of the VHT. Furthermore, the relative error of the layer thickness measurement is larger for small layer thicknesses because of the effects of poor layer definition (i.e., the boundaries of the layer are not sharp and, on a relative basis, this diffuseness is increasingly important for thin layers). If this replicate pair is removed, the pooled %RSD for the four remaining pairs decreases to about 31%, while the SD in ln(μm) units decreases to about 0.32. Jiricka et al. (2001) reported %RSD's for replicated VHTs ranging from 14 to 99%, while Vienna et al. (2001) reported %RSDs ranging from 3 to 50%. Thus, 32 %RSD [0.32 SD in ln(μm) units] appears to be a reasonable estimate of the uncertainty in fabricating simulated LAW glasses, performing the VHT, and measuring the alteration depth. With such large relative uncertainty, it will be difficult to model VHT alteration depth well.

### **6.1.2 Primary VHT Model Validation Approach and Data**

The primary model validation approach for VHT modeling was based on splitting the 165-glass dataset for model development into five modeling/validation subsets. Of the 165 model development glasses, 10 were intended to be replicates (5 replicate pairs). The five



modeling/validation splits of the 165 glasses in the VHT modeling dataset were formed as follows.

- The five pairs of replicates (10 glasses) were set aside so they would always be included in each of the five model development datasets. This was done so that replicate pairs would not be split between modeling and validation subsets, thus negating the intent to have validation glasses different than model development glasses.
- The remaining  $165 - 10 = 155$  data points were ordered from smallest to largest according to their VHT alteration depths. The 155 data points were numbered 1, 2, 3, 4, 5, 1, 2, 3, 4, 5, etc. All of the 1's formed the first model validation set, while all of the remaining points formed the first model development dataset. Similarly, all of the 2's, 3's, 4's, and 5's respectively formed the second, third, fourth, and fifth model validation sets. In each case, the remaining non-2's, non-3's, non-4's, and non-5's formed the second, third, fourth, and fifth model development datasets. Accordingly, each of the five splits contained  $155/5 = 31$  glasses for validation and  $(4/5)155 = 124$  glasses for modeling.
- The 10 replicate glasses were added to each of the split modeling subsets so that each of the five splits contained 134 glasses for modeling and 31 glasses for validation. The last column of Table 6.3 specifies the validation subsets for the five modeling/validation splits in the primary validation approach for VHT model development.

Data splitting was chosen as the primary validation approach because the VHT modeling dataset contains all compositions that (i) are in the ILAW composition region of interest, (ii) meet quality assurance (QA) requirements, and (iii) have VHT data. Having a separate validation dataset not used for modeling is desirable, but that desire was over-ridden by wanting VHT models developed with all appropriate data.

### 6.1.3 Secondary VHT Model Validation Approach and Data

The secondary model validation approach consisted of partitioning the 165-glass VHT modeling dataset into modeling and validation subsets. Included in the modeling subset were all glasses used in statistically-designed groups of the data that had VHT results. Included are glasses in the Existing Matrix (23 glasses), the Phase 1 Test Matrix (56 glasses), and the Phase 1a Augmentation Test Matrix (20 glasses). Together, these comprise 99 glasses, but only 92 of them have VHT data. Hence, the modeling subset for this approach contains VHT results for 92 glasses. The remaining  $165 - 92 = 73$  glasses (all actively-designed) were used as a validation subset.

The data-splitting approach discussed in Section 6.1.2 is considered the primary validation approach because it comes closer to validating the VHT models of interest, namely those fitted to all 165 modeling data points. The primary validation approach fits VHT models using 134 of the 165 modeling data points and validates with the remaining 31 data points, and does so five times. The secondary approach fits models with 92 glasses and validates with 73

glasses. Hence, the primary validation approach comes closer to validating the VHT models of interest, namely those fitted to all 165 data points.

The secondary validation approach is desirable because it uses the statistically-designed glasses (and the Existing Matrix glasses that were factored into selecting the Phase 1 Test Matrix glasses) to fit models, and actively-designed glasses to validate the models. Actively-designed glasses tend to be more clustered in composition space, and can have strong or even perfect correlations between glass components. These aspects make actively-designed glasses somewhat less desirable for model development, but reasonable for model validation.

#### **6.1.4 Limited Extrapolative VHT Model Validation Data**

The 16 glasses excluded from the VHT modeling set (see the discussion in Section 6.1.1) were used to perform a limited assessment of the extrapolative prediction performance of the VHT models. The normalized compositions of these 16 glasses are given in Table 6.5 and the corresponding VHT alteration depths are given in Table 6.6. Typical summary statistics and predicted versus measured plots are used to assess the extrapolative performance of VHT models for the first 10 glasses listed in Tables 6.5 and 6.6. Because the last six glasses had alteration depths reported only as “greater than” values, the assessment for those glasses consists of whether a model correctly predicts alteration depths greater than the values listed in Table 6.6.

### **6.2 VHT Alteration Depth Model Forms**

Ideally, a property-composition model for VHT would utilize known mechanisms of VHT alteration as a function of glass composition and aspects of the VHT. However, no such mechanisms are known, so that mechanistic and semi-empirical model forms are not available. Hence, several empirical model forms with parameters to be estimated from model development data were considered. These model forms are from the general class of *mixture experiment models*. Section C.1 of Appendix C discusses mixture experiments and several general forms of mixture experiment models. Section 6.2.1 discusses the forms of mixture experiment models used for the VHT response of LAW glasses. Section 6.2.2 discusses the use of transformed VHT alteration depths as the response variable for VHT modeling.

#### **6.2.1 VHT Mixture Experiment Model Forms**

Linear mixture (LM) and partial quadratic mixture (PQM) model forms introduced in Section C.1.1 of Appendix C were initially chosen for use in modeling VHT alteration depths. The specific LM model form is given by

$$\ln(D) = \sum_{i=1}^q b_i x_i + E \quad (6.1)$$

while the specific PQM model form is given by

$$\ln(D) = \sum_{i=1}^q b_i x_i + \text{Selected} \left\{ \sum_{i=1}^q b_{ii} x_i^2 + \sum_{i < j}^{q-1} b_{ij} x_i x_j \right\} + E, \quad (6.2)$$

In Equations (6.1) and (6.2):  $\ln(D)$  denotes the natural logarithm of the VHT alteration depth,  $D$ , in microns; the  $x_i$  ( $i = 1, 2, \dots, q$ ) are mass fractions of  $q$  glass oxide or halogen components such that  $\sum_{i=1}^q x_i = 1$ ; the  $b_i$  ( $i = 1, 2, \dots, q$ ), the  $b_{ii}$  (selected), and the  $b_{ij}$  (selected) are coefficients to be estimated from data; and  $E$  is a random error for each data point. Many statistical methods exist for the case where the  $E$  are independent (i.e., not correlated) and normally distributed with mean 0 and standard deviation  $\sigma$ . In Equation (6.2), “Selected” means that only some of the terms in curly brackets are included in the model. The subset is selected using stepwise regression or other variable selection methods (Draper and Smith 1998, Montgomery et al. 2001). PQM models are discussed in more detail and illustrated by Piepel et al. (2002).

A two-part LM model of the following form was also considered

$$\ln(D) = \sum_{i=1}^q b_i^B x_i J_i + \sum_{i=1}^q b_i^A x_i (1 - J_i) + E \quad (6.3)$$

where the notation on the right hand side of the equation has the same explanation as following Equation (5.3) in Section 5.2.1.

Finally, partial cubic mixture (PCM) models of the form

$$\begin{aligned} \ln(D) = & \sum_{i=1}^q b_i x_i + \text{Selected} \left\{ \sum_{i=1}^q b_{ii} x_i^2 + \sum_{i < j}^{q-1} b_{ij} x_i x_j \right\} \\ & + \text{Selected} \left\{ \sum_{i=1}^q b_{iii} x_i^3 + \sum_{i < j}^{q-1} b_{ijj} x_i^2 x_j + \sum_{i < j < k}^{q-2} b_{ijk} x_i x_j x_k \right\} + E \end{aligned} \quad (6.4)$$

were also considered, where two kinds of quadratic terms ( $b_{ii} x_i^2$  and  $b_{ij} x_i x_j$ ) and three kinds of cubic terms ( $b_{iii} x_i^3$ ,  $b_{ijj} x_i^2 x_j$ , and  $b_{ijk} x_i x_j x_k$ ) can be selected using glass science knowledge, stepwise regression, or other variable selection methods. The other notation is as described previously.

## 6.2.2 Transformation of VHT Alteration Depth

In modeling VHT alteration depths, it is advantageous to use the natural logarithm of the alteration depths. The advantages of this transformation include:

- The VHT alteration depths for the 165 LAW glasses in the VHT modeling set range from 1 to 980 microns. This is a range of almost 3 orders of magnitude difference. In such cases, typically the uncertainty in making glasses, performing the VHT, and measuring the alteration depths leads to smaller absolute uncertainties for smaller alteration depths and larger absolute uncertainties for larger alteration depths. Hence, the unweighted least squares (ULS) regression assumption of equal variances for all response variable values (see Section C.3 of Appendix C) is violated. After a logarithmic transformation, variances of response values tend to be approximately equal as required for ULS regression.
- A logarithmic transformation tends to linearize the compositional dependence of VHT data and reduce the need for non-linear terms in the model form.
- A natural logarithm transformation is preferred over a common logarithm (or other base logarithm) transformation because of the approximate relationship

$$\text{SD} [\ln(y)] \cong \text{RSD} (y) \quad (6.5)$$

where SD denotes standard deviation, RSD denotes relative standard deviation (i.e., the standard deviation divided by the mean), and  $y$  denotes VHT alteration depth. Equation (6.5) results from applying the first-order variance propagation formula [Equation (7-7) of Hahn and Shapiro (1967)] to the function  $z = \ln(y)$ . The relationship in Equation (6.5) is very useful, in that uncertainties of the natural logarithm of the response variable  $y$  can be interpreted as RSDs of the untransformed response variable  $y$ .

For these reasons, the natural logarithmic transformation was employed for all VHT alteration model forms.

### 6.3 Linear Mixture Model Results for LAW VHT Alteration Depth

This section discusses the results of fitting two LM models using natural logarithms of LAW VHT alteration depths, denoted  $\ln(D)$ , as the response variable. Section 6.3.1 presents the results from fitting a full LM model containing linear terms for each of the 18 components determined to have sufficient support in the 165-glass modeling set. Section 6.3.2 presents the results from fitting a reduced 11-component LM model.

### 6.3.1 Results for Full Linear Mixture Model on VHT Alteration Depth

As the initial step in VHT model development, a full LM model in the 18 components identified in Section 6.1.1 was fit to the modeling data (165 glasses). The response was the natural logarithm of VHT alteration depth ( $\mu\text{m}$ ). This model form was a reasonable starting point based on the previous work modeling VHT alterations of LAW glasses (Muller et al. 2005, Perez-Cardenas et al. 2006) and provided a basis for appropriate model reductions.

Although not shown in this report, several regression diagnostic plots were produced to assess whether the full 18-component LM model fitted to the 165-glass VHT modeling set satisfies the assumptions for ULS regression (see Section C.4 of Appendix C). The diagnostic figures did not suggest any significant departures from normality for the distribution of standardized residuals<sup>12</sup> from the full LM model. Nor did they show any significant departure from the assumption of equal uncertainty in  $\ln(D)$  values over the modeling dataset. In summary, the ULS regression techniques were judged to be appropriate for the LM model development and evaluation.

Table 6.7 contains the results for the 18-component full LM model for ILAW VHT alteration depth. Table 6.7 lists the model coefficients, standard deviations of the coefficients, and model performance summaries for the full LM model using the modeling dataset (165 glasses), the data-splitting approach (see Section 6.1.2), the modeling data partitioned into modeling (92 glasses) and validation (73 glasses) subsets (see Section 6.1.3), and the 16 glasses excluded from the model dataset (see Section 6.1.4). In the data-splitting portion of results at the bottom of Table 6.7, the columns are labeled DS1, DS2, DS3, DS4, and DS5 to denote the five modeling/validation splits of the data as described in Section 6.1.2. The last column of this part of Table 6.7 shows the averages for the different statistics over the five splits.

In the upper right corner of Table 6.7 are the summary statistics that describe how well the 18-component LM model fits the 165-glass modeling data. The  $R^2 = 0.607$ ,  $R^2_A = 0.562$ , and  $R^2_P = 0.470$  statistics (see Section C.4 of Appendix C) indicate that the 18-component LM model offers only marginal predictive performance even when fitted to the modeling data. The root mean squared error (RMSE) in Table 6.7 is an estimate of the uncertainty [in  $\ln(D)$  units] in fabricating simulated LAW glasses, performing the VHT, and measuring  $D$  if the model does not have a significant LOF. To judge the LOF for the 18-component LM model, the RMSE value can be compared to uncertainty estimates based on replicate VHT  $D$  data. The  $\text{RMSE} = 1.060$  is much larger than the replicate SD in  $\ln(\mu\text{m})$  units of 0.32 from Table 6.4 (which is discussed in the last subsection of Section 6.1.1). This observation suggests that the 18-component LM model has a significant LOF, which is confirmed by the LOF test  $p$ -value = 0.014 included in Table 6.7. This  $p$ -value indicates that the model LOF is significant at the 98.6% confidence level. Thus, model lack-of-fit along with relatively large uncertainty in VHT  $D$  values appears to explain the large differences between measured and predicted VHT results. See Section C.4 of Appendix C for further explanations of the statistics and LOF test discussed in this paragraph.

---

<sup>12</sup> Standardized residuals are residuals [measured minus predicted  $\ln(D)$  values], divided by their standard deviations.

The VHT full LM model statistics from partitioning the 165-glass modeling set into subsets of 92 modeling glasses and 73 validation glasses (see Section 6.1.3) are given on the right side of Table 6.7. The fit statistics of  $R^2 = 0.699$  and  $R^2_A = 0.629$  are better (i.e., larger) than the corresponding statistics for the full 165-glass modeling set. However,  $R^2_P = 0.469$  and  $RMSE = 1.018$  are similar for the 97-glass modeling subset and the full 165-glass modeling set. For the 147-glass validation subset,  $R^2_V$  is a large negative value and  $RMSE_V$  is very large. This poor validation performance is because the 92-glass subset of data provided insufficient support for all 18 components in the full LM model, thus negatively affecting performance on the validation subset.

The predicted versus measured plot in Figure 6.6 for the 18-component full LM model shows a lot of scatter and some biased prediction behavior. The model tends to under-predict VHT alteration depths above approximately  $5 \ln(\mu\text{m}) = 148 \mu\text{m}$ . It also tends to over-predict for glasses with lower VHT alteration depths. Hence, the full 18-component LM model provides less than the desired performance for predicting VHT alteration depths.

Despite the shortcomings of the full LM model for VHT alteration depth, the model fits the data well enough to provide guidance for reducing the model (i.e., removing separate terms for components that do not significantly influence VHT alteration depth). Hence, the full LM model was used to produce the response trace plot (see Section C.5.1) shown in Figure 6.7. The response trace plot shows that  $\text{Li}_2\text{O}$ ,  $\text{Na}_2\text{O}$ , and  $\text{K}_2\text{O}$  have strong increasing effects on VHT alteration depth, while  $\text{ZrO}_2$ ,  $\text{Fe}_2\text{O}_3$ , and  $\text{SiO}_2$  have decreasing effects on VHT alteration depth. The response trace for  $\text{Cr}_2\text{O}_3$  has the largest positive slope, while F and Others have response traces with the largest negative slopes. However, these are artifacts resulting from larger uncertainties in determining the coefficients and hence the effects of these components.

### 6.3.2 Results for Reduced Linear Mixture Model on VHT Alteration Depth

The full 18-component LM model presented in Section 6.3.1 likely contains components that do not significantly contribute to predicting VHT alteration depth, so model reduction was the next step of the model development approach. Thus, LM models for VHT alteration depth involving fewer than the 18 components were considered. The sequential F-test model reduction approach (see Section C.5.1 of Appendix C, Piepel and Cooley 2006) was used to develop a reduced LM model. Option (ii) discussed in Section C.5.1 was used to develop reduced LM models for all LAW glass properties considered in this report.

To reduce the full LM model for VHT alteration depth, a significance level of 0.01 was used for the F-tests conducted by the model reduction algorithm. An option available with the F-test approach is to force certain terms to remain in the model during the model reduction process. For VHT alteration depth,  $\text{Al}_2\text{O}_3$ ,  $\text{B}_2\text{O}_3$ ,  $\text{CaO}$ ,  $\text{Fe}_2\text{O}_3$ ,  $\text{K}_2\text{O}$ ,  $\text{Li}_2\text{O}$ ,  $\text{MgO}$ ,  $\text{Na}_2\text{O}$ ,  $\text{SiO}_2$ , and  $\text{ZrO}_2$  were forced into the reduced LM model. That is, they were not eligible to be combined with other components or dropped from the model. The components Cl,  $\text{Cr}_2\text{O}_3$ , F,  $\text{P}_2\text{O}_5$ ,  $\text{SO}_3$ ,  $\text{TiO}_2$ ,  $\text{ZnO}$ , and Others were allowed to combine if having the combined-components term in the model rather than both individual component terms did not significantly decrease model performance. After an initial run of the model reduction algorithm, the resulting reduced model

contained two combined-components terms. This was considered an undesirable model form (based on glass science and a preference to keep similar model forms across glass properties), so the two combined-components terms were combined to form a new “Others” component in the reduced model.

The reduced LM model obtained for VHT alteration depth using the F-test approach contained terms for 11 components:  $\text{Al}_2\text{O}_3$ ,  $\text{B}_2\text{O}_3$ ,  $\text{CaO}$ ,  $\text{Fe}_2\text{O}_3$ ,  $\text{K}_2\text{O}$ ,  $\text{Li}_2\text{O}$ ,  $\text{MgO}$ ,  $\text{Na}_2\text{O}$ ,  $\text{SiO}_2$ ,  $\text{ZrO}_2$ , and Others. Note that Others is the sum of all remaining components, and thus differs from the Others in the 18-component LM model discussed in Section 6.3.1. Table 6.8 gives the coefficients and coefficient standard deviations for the 11-component reduced LM model for  $\ln(D)$ , as well as performance statistics for the (i) modeling data, (ii) partition of the modeling data into 92-glass modeling and 73-glass validation subsets, (iii) data-split modeling data, and (iv) 16 LAW glasses excluded from the VHT modeling set. The fit statistics in the upper right corner of Table 6.8 are somewhat worse than for the full 18-component LM model.

The predicted versus measured plot for the 11-component reduced LM model in Figure 6.8 is roughly similar to the one for the 18-component full LM model in Figure 6.6, although the under-prediction of larger VHT alteration depths is somewhat worse. The response trace plot in Figure 6.9 shows that the main components affecting VHT alteration depth are the same as for the full LM model, namely  $\text{Li}_2\text{O}$ ,  $\text{Na}_2\text{O}$ , and  $\text{K}_2\text{O}$  have strong increasing effects, while  $\text{ZrO}_2$ ,  $\text{Fe}_2\text{O}_3$ , and  $\text{SiO}_2$  have decreasing effects. The artifacts of  $\text{Cr}_2\text{O}_3$ , F, and Others having steep response traces seen in Figure 6.7 are gone in Figure 6.9 because of the model reduction.

Although the reduced LM model appears to fit the VHT modeling data somewhat worse than the full LM model, the data-splitting validation performances of the two models (see the average  $R^2_V$  and  $\text{RMSE}_V$  statistics in the bottom right portions of Tables 6.7 and 6.8) are nearly identical. This suggests that the appearance of a better fit for the full LM model may be a result of over-fitting the VHT data. Ultimately, the model reduction was carried out primarily to form a basis for adding non-linear blending terms to the model. The 11-component reduced LM model appears to be a reasonable starting point for adding non-linear blending terms.

Although the 11-term reduced LM model does not adequately fit the VHT modeling set, three figures are presented for baseline comparison purposes to those for subsequent models. Figure 6.10 shows the standardized residuals plotted versus the index numbers (a sequential numbering of the modeling data points) with different plotting symbols representing the different groups of glasses discussed in Sections 2.1 to 2.6. No strong outliers or patterns inconsistent with the ULS regression assumptions are seen in Figure 6.10.

Figures 6.11 and 6.12 show predicted versus measured plots when the reduced LM model for ILAW VHT alteration depth is applied to two validation datasets. Figure 6.11 results from fitting the reduced LM model to a subset of 92 out of 165 modeling glasses, and then applying the resulting model to the remaining subset of 73 glasses for validation (see Section 6.1.3). Figure 6.12 results from fitting the reduced LM model to all 165 glasses in the modeling set and then applying that model to the 10 outlying glasses with non-censored VHT results (see Section 6.1.4). Also shown in Figures 6.11 and 6.12 are 95% prediction intervals (95% PIs) representing the model prediction uncertainty of single VHT alteration depth determinations for each glass

(see Sections C.6 and C.7 of Appendix C). If the error bar for a validation point overlaps the 45° line, that means the predicted and measured  $\ln(D)$  values are within model and measurement uncertainty of each other. The 95% PIs in Figures 6.11 and 6.12 are very wide, due to: (i) the significant LOF of the reduced LM model, and (ii) the relatively large experimental uncertainty in fabricating glasses, performing the VHT, and measuring alteration depths. Thus, despite the tendencies toward biased predictions seen in Figure 6.11, the wide 95% PIs include (with one exception at a very low alteration) the measured  $\ln(D)$  values.

## 6.4 Partial Quadratic Mixture Model Results for LAW VHT Alteration Depth

As discussed in Section 6.3, the full and reduced LM models for VHT alteration depth provide only marginal predictive performance. Those models have statistically significant LOFs, with tendencies to under-predict larger VHT alteration depths and over-predict smaller VHT alteration depths. These results suggest that a model containing quadratic terms to represent non-linear blending effects of components might perform better. Therefore, PQM models of the general form in Equation (6.2) were considered for modeling VHT alteration depth. Section 6.4.1 presents the results for the PQM model fit to the 165 glasses of the modeling dataset. Section 6.4.2 presents the validation results for the PQM model.

### 6.4.1 Results for VHT PQM Model Fit to Modeling Data

Reduced PQM models were formed by adding selected quadratic terms to the 11-component reduced LM discussed in Section 6.3. Quadratic terms were selected using the MAXR criterion (see Section C.5 of Appendix C) from among all possible squared and two-component crossproduct terms formed using the 11 components in the reduced LM model for VHT alteration depth. Reduced PQM models containing from 3 to 9 quadratic terms were generated using the MAXR criterion. Although statistical significance tests indicated up to 9 quadratic terms were statistically significant, past experience with developing and validating PQM models has indicated adding too many quadratic terms tends to over-fit the model development dataset and degrade predictive performance for new glasses. Ultimately, the 16-term PQM model with 11 linear terms and 5 quadratic terms was chosen as including enough quadratic terms to improve the model fit, hopefully without significantly over-fitting the VHT modeling data.

Table 6.9 lists the fitted model coefficients and coefficient standard deviations for the 16-term PQM model. Table 6.9 also includes the summary statistics obtained by applying the model to the modeling dataset. The model fits the 165-glass modeling dataset with  $R^2 = 0.707$ , meaning that 70.7% of the variation in  $\ln(D)$  values is accounted for by the model.  $R^2_A = 0.677$  is fairly close to  $R^2$ , indicating that the model likely does not have unnecessary terms.  $R^2_P = 0.647$  being not too much less than  $R^2_A$  suggests that there are not many, if any, influential data points. Data points are influential if they impact the calculated values of the regression coefficients more than other points in the modeling dataset. That is, the calculated values of regression coefficients can differ significantly depending on whether influential data points (considered individually) are included or excluded when fitting the model.



The RMSE in Table 6.9 is an estimate of the uncertainty [in  $\ln(D)$  units] in fabricating LAW glasses, performing the VHT, and measuring  $D$  if the model does not have a statistically significant lack-of-fit. To judge the LOF for the 16-term PQM model, the RMSE value can be compared to uncertainty estimates based on replicate VHT  $D$  data. The RMSE = 0.909 value is much larger than the pooled standard deviation of 0.32 (see Table 6.4) obtained using the natural logarithm of VHT alteration depths for the four most-representative pairs of replicate VHT results included in the modeling dataset. This observation suggests that the 16-term PQM model has a significant LOF, which is confirmed by the LOF test p-value = 0.025 included in Table 6.9. This p-value indicates that the model LOF is significant at the 97.5% confidence level. See Section C.4 of Appendix C for further discussion of the LOF test.

A histogram and normal probability plot of the standardized residuals for the fit of the model in Table 6.9 to the 165-glass VHT modeling dataset were generated, although they are not shown in this report. These two plots do not show any significant departure from normality, which is required to utilize the statistical interval formulas for model prediction uncertainties that are discussed subsequently.

Figure 6.13 shows a predicted versus measured plot for the fit of the PQM model for  $\ln(D)$  in Table 6.9 to the 165-glass VHT modeling dataset. The plotted points in Figure 6.13 have relatively wide scatter about the 45° line corresponding to perfect prediction. Prediction of  $\ln(D)$  values above the contract limit is improved compared to the full and reduced LM models. However, Figure 6.13 still shows a tendency for  $\ln(D)$  values above 4  $\ln(\mu\text{m})$  [ $\sim 55 \mu\text{m}$ ] to be under-predicted. Although not as important, Figure 6.13 shows that the reduced PQM model better fits lower VHT alteration depths than did the full and reduced LM models.

Figure 6.14 displays the response trace plot for the reduced PQM model on  $\ln(D)$  given in Table 6.9. The response trace plot shows noticeable curvature in the response traces for  $\text{K}_2\text{O}$  (as a result of the  $(\text{K}_2\text{O})^2$  model term),  $\text{CaO}$  and  $\text{SiO}_2$  (as a result of the  $\text{CaO} \times \text{SiO}_2$  model term), and  $\text{Na}_2\text{O}$  (as a result of the  $\text{MgO} \times \text{Na}_2\text{O}$  and  $\text{Na}_2\text{O} \times \text{ZrO}_2$  model terms). Although  $\text{Al}_2\text{O}_3$ ,  $\text{MgO}$ , and  $\text{ZrO}_2$  appear in quadratic terms of the PQM model, the response traces for those components do not display noticeable curvature. Presumably this is because the quadratic effects of those components are mainly in combination with other components rather than individually.

Figure 6.15 displays a graph of the standardized residuals plotted versus the data index (a sequential numbering of the modeling data points) with different plotting symbols representing the different groups of glasses discussed in Sections 2.1 to 2.6. Typically, few if any standardized residuals beyond  $\pm 3.0$  is desirable, and none are seen in Figure 6.15.

#### 6.4.2 Validation Results for the VHT PQM Model

Performance statistics for the VHT PQM model when applied to the five modeling/validation splits formed from the 165-glass modeling dataset are given in Table 6.9. The columns in the lower portion of the table are labeled DS# to represent the five data-splitting subsets. The last column presents averages of the modeling  $R^2$ ,  $R^2_A$ ,  $R^2_P$ , RMSE,  $R^2_V$ , and

RMSE<sub>V</sub> statistics over the five data-splits. The average data-splitting  $R^2$ ,  $R^2_A$ ,  $R^2_P$ , and RMSE statistics are similar to those statistics calculated from the 165-glass VHT modeling dataset. The average  $R^2_V = 0.625$  from the data-splitting approach is slightly worse (i.e., smaller) than  $R^2_P = 0.647$  for the 165-glass modeling dataset. In general, the data-splitting results show that the PQM model in Table 6.9 maintains the level of its predictive performance when applied to validation data within the same composition region as used to develop the model.

Performance statistics from fitting the 16-term PQM model to the 92-glass modeling subset and validating using the remaining 73 glasses are given on the right hand side of Table 6.9. The  $R^2$ ,  $R^2_A$ ,  $R^2_P$ , and RMSE statistics from fitting the PQM model to the 92-glass subset are all improved compared to the statistics from fitting the model to the full 165-glass dataset. This indicates that the 73 actively-designed glasses in the validation subset are more difficult to model when they are included in the full 165-glass modeling set. The  $R^2_V = 0.561$  and  $RMSE_V = 0.999$  values for the 73-glass validation subset are worse than the average  $R^2_V = 0.625$  and  $RMSE_V = 0.959$  values for the data-splitting validation. This indicates that including the 73-actively designed glasses in the modeling set improves the fit and validation performance of the model for such glasses.

Figures 6.16 and 6.17 show predicted versus measured plots when the reduced PQM model for  $\ln(D)$  is applied to two validation datasets. Figure 6.16 results from fitting the reduced PQM model to a subset of 92 out of 165 modeling glasses, and then applying the resulting model to the remaining subset of 73 glasses for validation (see Section 6.1.3). Figure 6.17 results from fitting the reduced PQM model to all 165 glasses in the modeling set and then applying that model to the 10 outlying glasses with non-censored VHT results (see Section 6.1.4). Also shown in Figures 6.16 and 6.17 are 95% PIs representing the model prediction uncertainty of single VHT alteration determinations for each glass (see Sections C.6 and C.7 of Appendix C). If the error bar for a validation point overlaps the 45° line, that means the predicted and measured  $\ln(D)$  values are within model and measurement uncertainty of each other. The 95% PIs in Figures 6.16 and 6.17 are fairly wide, which is partly due to: (i) the significant LOF of the reduced PQM model, and (ii) the relatively large experimental uncertainty in fabricating glasses, performing the VHT, and measuring alteration depths. However, note that the 95% PIs in Figures 6.16 and 6.17 are narrower for the reduced PQM model than for the reduced LM model in Figures 6.11 and 6.12. Separate work to assess the consequences of LOF and prediction uncertainties for VHT models is discussed in Section 6.11.

Figure 6.16 shows that the reduced PQM model for  $\ln(D)$  fitted to the 92-glass modeling subset has varied predictive performance for the 73-glass validation subset. The VHT alteration depth is fairly accurately predicted for many of the 73 glasses. However, it tends to be under-predicted for some of the moderately large values, and over-predicted for the smallest values. Still, there are fewer biased predictions and they are not as severe with the reduced PQM model (Figure 6.16) compared to the reduced LM model (Figure 6.11). Also, the 95% PIs for the reduced PQM model overlap the 45° line (i.e., contain the measured values) for all but 8 of the 147 glasses in the validation subset. Failure of  $100(8/147) = 5.4\%$  of the 95% PIs to include the corresponding measured values is about what would be expected by chance.

Figure 6.17 shows the predictive performance of the reduced PQM model for  $\ln(D)$  fitted to the 165-glass modeling dataset and applied to the set of 10 outlying glasses with non-censored alteration depth values that were excluded from the modeling dataset. The model predictions are scattered somewhat widely, but evenly, on either side of the 45° line representing perfect prediction. The 95% PIs, although narrower for the reduced PQM model than the reduced LM model, are sufficiently wide that only one of the ten 95% PIs does not contain the corresponding measured value.

## 6.5 Two-Part Reduced Linear Mixture Model Results for LAW VHT Alteration Depth

The two-part model form given by Equation (6.3) in Section 6.2.1 was fitted, evaluated, and validated for natural logarithms of VHT alteration depth [ $\ln(D)$ ]. Separate 11-component reduced LM models were fit below and above a cutoff value of VHT alteration depth equal to 68.32  $\mu\text{m}$ . The cutoff value was chosen using an approach similar to that described in Section 5.2.1 for PCT-B. Figure 6.18 shows the cutoff value and VHT contract limit (50  $\text{g}/\text{m}^2/\text{d} \sim 453 \mu\text{m}$ ) on the predicted versus measured plot of the reduced LM model. It can be seen from Figure 6.18 that all of the glasses for which the reduced LM model tends to under-predict VHT alteration depth are above the cutoff, which was the primary goal in selecting the cutoff value.

Table 6.10 contains for the 22-term two-part model of  $\ln(D)$ : the coefficients, coefficient standard deviations, and performance statistics for the (i) 165-glass modeling data, (ii) the partition of the 165-glass modeling dataset into a 92-glass modeling subset and a 73-glass model validation subset, (iii) data-split modeling data, and (iv) 16 outlying LAW glasses.

In Table 6.10, the modeling evaluation statistics  $R^2 = 0.842$ ,  $R^2_A = 0.819$ ,  $R^2_P = 0.787$ , and  $\text{RMSE} = 0.682$  are improvements over the corresponding statistics for the 11-term reduced LM model (see Table 6.8) and the 16-term reduced PQM (see Table 6.9). Table 6.10 also includes summary statistics from fitting each of the two parts of the model in addition to those discussed in the previous paragraph for the model taken as a whole. These statistics show that the part of the model above the VHT  $D$  cutoff fits only marginally well ( $R^2_{\text{Above}} = 0.601$ ). The part of the model below the VHT  $D$  cutoff does not fit as well ( $R^2_{\text{Below}} = 0.383$ ). Both parts of the model fit their portions of the data better than the reduced LM model.

Over the five data splits of the VHT modeling data, Table 6.10 shows that the two-part reduced LM model for  $\ln(D)$  has average  $R^2$ ,  $R^2_A$ ,  $R^2_P$ , and  $\text{RMSE}$  values that are all close to their values from the 165-glass modeling dataset. The average  $R^2_V = 0.468$  from data-splitting is significantly worse (i.e., smaller) than  $R^2_P = 0.787$  for the 165-glass modeling dataset. The average  $\text{RMSE}_V = 1.136$  from data-splitting is also much worse (i.e., larger) than  $\text{RMSE} = 0.682$  for the 165-glass modeling dataset. This suggests that either the two-part model performance is not as good as represented by  $R^2_P = 0.787$  and  $\text{RMSE} = 0.682$ , or that the two-part model form is not fitted as well using roughly 80% subsets of the complete modeling dataset. Another potential explanation is discussed in the following paragraph. The average  $R^2_V = 0.468$  from data splitting for the two-part model is also noticeably worse (i.e., smaller) than the average  $R^2_V = 0.625$  for the reduced PQM model.

The modeling and validation statistics from partitioning the 165-glass VHT modeling dataset into a 92-glass modeling subset and a 73-glass validation subset are given on the right side of Table 6.10. There is some concern whether the 92-glass modeling subset is of sufficient size to fit the two-part model because there were only 32 glasses in the above-cutoff set and 60 glasses in the below-cutoff set. The results for the partitioned-data fit and validation of the two-part model for VHT  $\ln(D)$  are given on the right side of Table 6.10. The  $R^2$ ,  $R^2_A$ ,  $R^2_P$ , and RMSE values from the two-part model fit to the 92-glass modeling subset are close to their values from the 165-glass modeling dataset. The  $R^2_V = 0.338$  and the  $RMSE_V = 1.227$  for the 73-glass partitioned validation dataset are worse than the average  $R^2_V = 0.468$  and the average  $RMSE_V = 1.136$  values from the data-splitting validation. This could be a result of limitations in fitting the two-part model to the smaller partitioned dataset.

For the 10 of 16 outlying LAW glasses with measured VHT alteration depths, the two-part reduced LM model for  $\ln(D)$  has a negative value of  $R^2_V$ , indicating that the extrapolative prediction ability of the model is poor. The  $RMSE_V = 1.054$  is slightly better (i.e., smaller) than the average  $RMSE_V = 1.136$  for the five data-splits of the modeling data. For the 10 outliers the  $RMSE_V = 1.054$  for the two-part model is somewhat better (i.e., smaller) than to the  $RMSE_V = 1.273$  for the reduced PQM model.

Figure 6.19 shows the predicted versus measured plot for the fit of the two-part reduced LM model for  $\ln(D)$  to the 165-glass VHT modeling dataset. The plotted points in Figure 6.19 show several tendencies for biased and unbiased predictions (relative to the 45° line corresponding to perfect prediction). The two-part model tends to

- over-predict  $\ln(D)$  up to about  $2.5 \ln(\mu\text{m})$  [ $\sim D = 12.2 \mu\text{m}$ ]
- under-predict  $\ln(D)$  from 2.5 up to the cutoff of  $4.2 \ln(\mu\text{m})$  [ $\sim D = 68 \mu\text{m}$ ]
- predict without bias but significant scatter from  $4.2$  to  $6.0 \ln(\mu\text{m})$  [ $\sim D = 403 \mu\text{m}$ ]
- under-predict above  $6.0 \ln(\mu\text{m})$  [ $\sim D = 403 \mu\text{m}$ ], which is slightly below the contract limit value ( $453 \mu\text{m}$ ).

In summary, the two-part model has reasonable fit statistics for the 165-glass VHT modeling dataset, as summarized in Table 6.10. However, several aspects of the fit are seen to be undesirable in Figure 6.19, as discussed in the previous paragraph. Also, the two-part model suffers compared to the reduced PQM model in the data-split and data-partition validation performances.

## 6.6 Partial Cubic Mixture Model Results for LAW VHT Alteration Depth

Models containing selected cubic terms (referred to as partial cubic mixture (PCM) models) were investigated to see if improved fits of the VHT modeling dataset could be obtained. Four PCM models were formed by using the MAXR criterion (see Section C.5 of Appendix C) to statistically select the best subsets of 4, 5, 7, and 9 quadratic and/or cubic terms (formed from the 11 reduced LM model components) with which to augment the 11-component

reduced LM model. Although quadratic terms were allowed to be selected, only cubic terms were selected. Based on work reported in subsequent sections, the 15-term PCM model composed of the 11 linear terms and four cubic terms was selected for detailed investigation.

Section 6.6.1 presents the model coefficients, coefficient standard deviations, and other results for the 15-term PCM model fit to the 165 glasses of the modeling dataset. Section 6.6.2 presents the validation results for the 15-term PCM model.

### 6.6.1 Results for VHT PCM Model Fit to Modeling Data

Table 6.11 lists the fitted model coefficients and coefficient standard deviations for the 15-term PCM model. Table 6.11 also includes the summary statistics obtained by applying the model to the modeling dataset. The model fits the 165-glass modeling dataset with  $R^2 = 0.744$ , meaning that 74.4% of the variation in  $\ln(D)$  values is accounted for by the model.  $R^2_A = 0.720$  is fairly close to  $R^2$ , indicating that the model likely does not have unnecessary terms.  $R^2_P = 0.696$  being not too much less than  $R^2_A$  suggests that there are not many, if any, influential data points. Data points are influential if they impact the calculated values of the regression coefficients more than other points in the modeling dataset. That is, the calculated values of regression coefficients can differ significantly depending on whether influential data points (considered individually) are included or excluded when fitting the model.

The RMSE in Table 6.11 is an estimate of the uncertainty [in  $\ln(D)$  units] in fabricating LAW glasses, performing the VHT, and measuring  $D$  if the model does not have a statistically significant lack-of-fit. To judge the LOF for the 15-term PCM model, the RMSE value can be compared to uncertainty estimates based on replicate VHT  $D$  data. The  $\text{RMSE} = 0.848$  value is much larger than the pooled standard deviation of 0.32 (see Table 6.4) obtained using the natural logarithm of VHT alteration depths for the four most-representative pairs of replicate VHT results included in the modeling dataset. This observation suggests that the 15-term PCM model has a significant LOF, which is confirmed by the LOF test  $p$ -value = 0.032 included in Table 6.11. This  $p$ -value indicates that the model LOF is significant at the 96.8% confidence level. See Section C.4 of Appendix C for further discussion of the LOF test.

A histogram and normal probability plot of the standardized residuals for the fit of the model in Table 6.11 to the 165-glass VHT modeling dataset were generated, although they are not shown in this report. These two plots do not show any significant departure from normality, which is required to utilize the statistical interval formulas for model prediction uncertainties that are discussed subsequently.

Figure 6.20 shows a predicted versus measured plot for the fit of the PCM model for  $\ln(D)$  in Table 6.11 to the 165-glass VHT modeling dataset. The plotted points in Figure 6.20 have relatively wide scatter about the 45° line corresponding to perfect prediction. Prediction of  $\ln(D)$  values above the contract limit is improved compared to the full and reduced LM models and the PQM model. The tendency to under-predict larger  $\ln(D)$  values, as seen for LM and PQM models, seems to have mostly been corrected by the PCM model.

Figure 6.21 displays the response trace plot for the 15-term PCM model on  $\ln(D)$  given in Table 6.11. The response traces for most glass components are mainly linear with possibly a little curvature. However, the response traces for  $\text{Na}_2\text{O}$  and  $\text{K}_2\text{O}$  show significant curvature.

Figure 6.22 displays a graph of the standardized residuals plotted versus the data index (a sequential numbering of the modeling data points) with different plotting symbols representing the different groups of glasses discussed in Sections 2.1 to 2.6. Typically, few if any standardized residuals beyond  $\pm 3.0$  is desirable, and none are seen in Figure 6.22.

## 6.6.2 Validation Results for the VHT PCM Model

Performance statistics for the VHT 15-term PCM model when applied to the five modeling/validation splits formed from the 165-glass modeling dataset are given in the bottom portion of Table 6.11. The columns are labeled DS# to represent the five data-splitting subsets. The last column presents averages of the modeling  $R^2$ ,  $R^2_A$ ,  $R^2_P$ , RMSE,  $R^2_V$ , and  $\text{RMSE}_V$  statistics over the five data-splits. The average data-splitting  $R^2$ ,  $R^2_A$ ,  $R^2_P$ , and RMSE statistics are similar to those statistics calculated from the 165-glass VHT modeling dataset (shown in the top right portion of the table). The average  $R^2_V = 0.677$  from the data-splitting approach is slightly worse (i.e., smaller) than  $R^2_P = 0.696$  for the 165-glass modeling dataset. In general, the data-splitting results show that the 15-term PCM model in Table 6.11 maintains the level of its predictive performance when applied to validation data within the same composition region as used to develop the model.

Performance statistics from fitting the 15-term PCM model to the 92-glass modeling subset and validating using the remaining 73 glasses are given on the right hand side of Table 6.11. The  $R^2$ ,  $R^2_A$ ,  $R^2_P$ , and RMSE statistics from fitting the PCM model to the 92-glass subset are all improved compared to the statistics from fitting the model to the full 165-glass dataset. This indicates that the 73 actively-designed glasses in the validation subset are more difficult to model when they are included in the full 165-glass modeling set. The  $R^2_V = 0.629$  and  $\text{RMSE}_V = 0.919$  values for the 73-glass validation subset are worse than the average  $R^2_V = 0.677$  and  $\text{RMSE}_V = 0.893$  values for the data-splitting validation. This outcome could be a result of including some of the 73 actively designed glasses in the modeling subsets for data-splitting, thus improving the fit and validation performance of the model for such glasses. The outcome could also be a result of having fewer actively designed glasses in the validation subsets for data-splitting, thus improving the validation performance.

Figures 6.23 and 6.24 show predicted versus measured plots when the 15-term PCM model for  $\ln(D)$  is applied to two validation datasets. Figure 6.23 results from fitting the 15-term PCM model to a subset of 92 out of 165 modeling glasses, and then applying the resulting model to the remaining subset of 73 glasses for validation (see Section 6.1.3). Figure 6.24 results from fitting the 15-term PCM model to all 165 glasses in the modeling set and then applying that model to the 10 outlying glasses with non-censored VHT results (see Section 6.1.4). Also shown in Figures 6.23 and 6.24 are 95% PIs representing the model prediction uncertainty of single VHT alteration determinations for each glass (see Sections C.6 and C.7 of Appendix C). If the error bar for a validation point overlaps the 45° line, that means the predicted and measured  $\ln(D)$

values are within model and measurement uncertainty of each other. The 95% PIs in Figures 6.23 and 6.24 are fairly wide, which is partly due to: (i) the significant LOF of the 15-term PCM model, and (ii) the relatively large experimental uncertainty in fabricating glasses, performing the VHT, and measuring alteration depths. However, note that the 95% PIs in Figure 6.23 are narrower for the 15-term PCM model than for the reduced PQM model in Figure 6.16. The 95% PIs in Figure 6.24 for the 15-term PCM model have similar widths to those for the reduced PQM model in Figure 6.17. Separate work to assess the consequences of LOF and prediction uncertainties for VHT models is discussed further in Section 6.11.

Figure 6.23 shows that the 15-term PCM model for  $\ln(D)$  fitted to the 92-glass modeling subset has varied predictive performance for the 73-glass validation subset. The VHT alteration depth is fairly accurately predicted for many of the 73 glasses. However, it tends to be under-predicted for some of the moderately large values, and over-predicted for the smallest values. The validation prediction performance for the 15-term PCM model in Figure 6.23 is similar to validation performance for the reduced PQM model in Figure 6.16. Also, the 95% PIs for the 15-term PCM model overlap the 45° line (i.e., contain the measured values) for all but 4 of the 147 glasses in the validation subset. Failure of  $100(4/147) = 2.7\%$  of the 95% PIs to include the corresponding measured values is about what would be expected by chance.

Figure 6.24 shows the predictive performance of the 15-term PCM model for  $\ln(D)$  fitted to the 165-glass modeling dataset and applied to the set of 10 outlying glasses with non-censored alteration depth values that were excluded from the modeling dataset. The model predictions are scattered somewhat widely, with most being below the 45° line representing perfect prediction. This suggests a possible tendency to under-predict VHT alteration depth for these extrapolative outlying glasses. However, the 95% PIs are sufficiently wide that all ten contain the corresponding measured values.

## 6.7 Summary of Models Considered for LAW VHT Alteration Depth

This section summarizes and compares the four models on VHT  $\ln(D)$  discussed so far, as well as 11 other model forms considered. Section 6.7.1 summarizes the 14 single (“global”) models investigated. Section 6.7.2 describes the preliminary investigation of a local linear regression approach to ascertain whether local models might better model the  $\ln(D)$ -composition relationship than single “global” models. Section 6.7.3 briefly discusses some other modeling approaches considered.

### 6.7.1 Single Global Models Considered for VHT $\ln(D)$

The four models discussed in Sections 6.3, 6.4, and 6.5 include

- Model 1: An 18-component full LM model
- Model 2: An 11-component reduced LM model
- Model 3: A 16-term PQM model with 5 quadratic terms added to the 11 reduced LM model terms

- Model 4: A two-part model in which separate 11-component reduced LM models were fit below and above a cutoff value of VHT alteration depth.

Also considered were several model forms that were previously investigated by VSL (Perez-Cardenas et al. 2006) for a smaller set of data. In this work, some of those model forms were investigated using the 165-glass VHT dataset.

- Model 5: A PQM model containing 9 LM model terms and 8 squared terms.
- Model 6: A PQM model containing 14 LM model terms and 13 squared terms.
- Model 7: A PQM model containing 9 LM model terms and 7 quadratic terms.
- Model 8: A partial cubic mixture (PCM) model containing 14 LM model terms, 2 quadratic terms, and 2 cubic terms.
- Model 9: A PCM model containing 15 LM model terms, 3 quadratic terms, and 4 cubic terms.

Several other models including quadratic and cubic terms were considered in an attempt to better account for non-linear blending behavior of the LAW glass components on VHT alteration depth.

- Model 10: A PCM model containing the 11 terms in the reduced LM model, 2 quadratic terms, and 2 cubic terms. The quadratic and cubic terms are the same as for Model 8.
- Models 11 to 14: PCM models formed by using the MAXR criterion (see Section C.5 of Appendix C) to statistically select the best subsets of 4, 5, 7, and 9 quadratic and/or cubic terms (formed from the 11 reduced LM model components) with which to augment the 11-component reduced LM model. Although quadratic terms were allowed to be selected, only cubic terms were selected.

The specific terms in each of Models 1 to 14 are shown in Table 6.12. A detailed discussion of Model 11 is contained in Section 6.6.

### **6.7.2 Local Linear Regression Model for VHT $\ln(D)$**

A preliminary investigation of a local linear regression approach was conducted to determine whether it would better model the VHT  $\ln(D)$ -composition relationship than the single-model (“global regression”) approach. To greater or lesser extents, the various single models investigated for VHT  $\ln(D)$  tend to (i) under-predict higher alteration depths, and over-predict lower alteration depths. With the local regression approach, separate models fit to local subsets of the modeling data may better represent a more complicated true  $\ln(D)$ -composition relationship than a single “global” model can.

The local regression approach used in the preliminary investigation involved fitting separate 11-component reduced LM models (of the same form as discussed previously) around



the  $n$  closest glasses for each glass in the modeling dataset.<sup>13</sup> Thus, the predicted  $\ln(D)$  value for each glass in the modeling dataset is based on an 11-component LM model fitted to only the closest  $n$  glasses. A normalized distance measure from the statistical mixture experiment literature

$$d(\mathbf{x}_i, \mathbf{x}_j) = \sqrt{\sum_{r=1}^q \left( \frac{x_{ir} - x_{jr}}{U_r - L_r} \right)^2} \quad (6.6)$$

was used to calculate distances between pairs of glass compositions  $\mathbf{x}_i$  and  $\mathbf{x}_j$ , where  $L_r$  and  $U_r$  denote the lower and upper limits (in mass fractions) of the  $r^{\text{th}}$  glass component. The normalization by component ranges ( $U_r - L_r$ ) compensates for LAW glass components with smaller and larger ranges of values. Values of  $n$  ranging from 25 to 100 were investigated for the local model fits. In this interval, smaller values of  $n$  resulted in some regression estimation problems while larger values yielded results with shortcomings similar to those of global models. A value of  $n = 50$  was chosen because it avoided regression estimation problems and seemed to yield the highest improvements in  $R^2$ , the predicted-versus-measured plot, and performance in predicting glasses with VHT alterations above the 453  $\mu\text{m}$  limit.

The local regression modeling was performed as a fast, preliminary investigation to judge the potential value of local regression modeling in the future. This work was not intended to produce models to compete with global models and potentially be selected at this time. Hence, many of the regression statistics were not calculated and the data-splitting validation was not performed. Local regression modeling and validation was not performed on the partition of the 165-glass modeling set into 92-glass modeling and 73-glass validation subsets because of multiple issues.

### 6.7.3 Other Approaches Considered for Modeling VHT Results

A binary logistic model was investigated with the goal of predicting whether LAW glasses have VHT results above or below the WTP contract limit of 50  $\text{g/m}^2/\text{d} \sim 453 \mu\text{m}$ . The idea behind this investigation was that it may be easier to predict whether a glass would have VHT results below or above the contract limit than to accurately predict the alteration depth over the relatively wide LAW glass composition region of interest. The advantage of this approach is that it can use the “greater than” VHT results as data points, since all of those results were above the contract limit. However, even with this advantage, there were only 20 glasses with VHT alteration depth above the limiting value (453  $\mu\text{m}$ ) out of 171 glasses with VHT data. This was an insufficient number of glasses above the limit for the fits of the binary logistic model to converge using 18-, 14-, and 11-component linear mixture models to represent the compositional dependence.

---

<sup>13</sup> This is only one of many possible local regression methods available in the statistics and “machine learning” literature. The method used for the preliminary investigation was chosen because it could be quickly implemented, not because it is the best method. The goal was to quickly assess whether local regression might significantly outperform global regression, not to select the best local regression approach.

It is possible to supply starting parameter estimates for the iterative solution algorithm that might have resolved the non-convergence issues. Also, cutoff values lower than the WTP contract limit could have been used to increase the number of glasses having VHT results above the cutoff. However, investigation of binary prediction models was not planned as part of the scope, so no additional effort was expended trying to resolve the non-convergence problems for the binary logistic regression approach. Such work may be of value in the future if better prediction of whether VHT results are below or above the WTP contract limit is needed than is provided by the single (global) models recommended in Section 6.9.

Classification tree and/or regression tree models can often perform better than parametric models when the response takes on more “localized” patterns. These methods work by partitioning LAW glass composition space with successive binary partitions on individual components, with separate classifications or regression models for each partition. These methods were investigated during ILAW Phase 1 modeling (see Section 5.7.3 of Muller et al. 2005), but were not included in the scope for the current modeling effort.

## 6.8 Comparison of VHT Models for $\ln(D)$

Table 6.13 summarizes the (i) statistics from fitting (to the data from all 165 glasses) each of the 15 models considered, (ii) fitting and validation statistics averaged over the five 80%/20% data-splits, and (iii) extrapolative validation statistics for the 10 outlying LAW glasses. Table 6.14 summarizes the statistics from the 92-glass modeling subset and the 73-glass validation subset of the full set of 165 modeling glasses. Table 6.15 summarizes the performance of each model (fitted to the data from all 165 glasses) in predicting whether glasses have VHT results above or below the VHT alteration depth value of 453  $\mu\text{m}$  corresponding to the WTP contract limit of 50  $\text{g/m}^2/\text{d}$ . Notice the measures of predictive performance in Table 6.15 are for the data used to fit the model, and thus should be assumed to be optimistic compared to statistics that would be obtained for “new” data not used to fit the model. The results in Tables 6.13, 6.14, and 6.15 for Models 1 to 15 are discussed in the following paragraphs.

The full and reduced LM models (Models 1 and 2) provide inadequate fits of the data (see Table 6.13). They correctly predict only 4 and 1, respectively, out of the 14 glasses<sup>14</sup> that have VHT results above the WTP contract limit (see Table 6.15). These models, when fit to the subset of 92 modeling glasses, have poor validation performance for the remaining 73 glasses (see Table 6.14).

The PQM model (Model 3), by adding 5 quadratic terms to the 11 reduced linear terms, significantly improves the fit to the data. However, the model still has a statistically significant lack-of-fit (see Table 6.13). The PQM model has one of the best validation performances for the subset of 73 glasses after fitting with the subset of 92 glasses (see Table 6.14). The PQM model

---

<sup>14</sup> This number of glasses does not include the six glasses with “greater than” results for VHT alteration, which were not used for model development or validation.

correctly predicts 8 of the 14 glasses that have VHT results above the WTP contract limit (see Table 6.15).

The PQM model performs better than the three partial quadratic models investigated to represent the best of such models considered by VSL (Models 5, 6, and 7) in earlier preliminary VHT model development work (Perez-Cardenas et al. 2006). This is the case for the 165-glass fit, the data-split fitting and validation, and the 92-glass fit and 73-glass validation (see Tables 6.13, 6.14, and 6.15).

The two-part model (Model 4) has the highest  $R^2$  of all models fitted to the 165-glass modeling dataset, but its data-split validation results are only slightly better than the linear mixture models (see Table 6.13). The validation performance for the subset of 73 glasses after fitting with 92 glasses is poor for the two-part model (see Table 6.14), but this may be because 92 glasses is too few to fit with the two-part modeling approach. However, even when fitted to all 165 glasses, the two-part model only correctly predicts 3 of the 14 glasses that have VHT results above the limit (see Table 6.15). Thus the two-part modeling approach does not improve predictions of larger VHT results as it did for larger PCT results.

Adding cubic terms to models containing linear terms and possibly quadratic terms (referred to as partial cubic mixture (PCM) models) does seem to improve the fits of models to data compared to the PQM model (see Table 6.13). Two PCM models were investigated based on the VSL preliminary modeling work (Perez-Cardenas et al. 2006). These models (referred to as Models 8 and 9) did have the best extrapolative predictive performance on the 10 outlying/non-representative glasses (see last column of Table 6.13). However, little weight should be given to such performance except as a tie-breaker for all other things being about equal. The fits and data-splitting performance of Models 8 and 9 are comparable to those of the PQM model (Model 3) as seen in Table 6.13. However, the PQM model does better in the validation performance with 73 glasses based on fits with 92 glasses (see Table 6.14).

Another PCM model was obtained by adding the two quadratic and two cubic terms in Model 8 to the reduced LM model, thus forming Model 10. Model 10 has slightly improved performance compared to Model 8 for data-splitting validation (see Table 6.13) and shows more improvement for the 73-glass validation after the 92-glass fit (see Table 6.14). Compared to the PQM model (Model 3), Model 10 has decreased fit to the 92-glass modeling subset, but improved validation performance for the 73-glass validation subset (see Table 6.14).

Other PCM models (Models 11 to 14) were formed by adding 4, 5, 7, and 9 higher-order (quadratic or cubic) terms to the 11 reduced LM model terms by the MAXR statistical variable selection method (see Section C.5 of Appendix C). Only cubic terms were selected (based on model term selection using the 165 LAW glasses). These models have better fits and data-split validation performances than all of the LM models, PQM model, and PCM models discussed so far. Furthermore, the 73-glass validation performance for these models is better than for the best models considered so far (Models 3 and 10).

PCM models (Models 8 to 14) predicted 8 or 9 of 14 glasses that have VHT results above the WTP contract limit, compared to 8 for the PQM model (see Table 6.15). Hence, the PQM model and PCM models don't show much difference from this qualitative judgment standpoint.

Finally, the preliminary investigation of local regression by fitting local LM models using subsets of the closest 50 glasses out of 165 glasses in the modeling set (denoted Model 15) yielded results that appear to be comparable to (but with some tradeoffs versus) the best global regression model results. Specifically, the local LM model (Model 15) yielded  $R^2 = 0.761$  compared to 0.707 for the PQM model and 0.707 to 0.794 for several PCM models when fitting to all 165 glasses in the modeling set. The predicted-versus-measured plot for Model 15 shows generally unbiased prediction of higher VHT alterations (above and somewhat below the WTP contract limit), thus apparently correcting the tendency for under-prediction of higher VHT alteration values by global models. However, Model 15 still shows a tendency to over-predict lower VHT alteration depths with a few outlying over-predictions. Because of the preliminary nature of the local regression modeling work, explanations for the improved predictions of higher alteration depths without corresponding improvements for lower alteration depths were not investigated. However, these results suggest that more than local linear models (e.g., local PQM models) may be needed to improve predictive performance for smaller VHT alterations. Note however that for any of these models, prediction performance for lower values is less important as long as over-prediction is not so bad that false alarms (i.e., incorrectly predicting that the VHT alteration is above the WTP contract limit) would occur at an unacceptable rate. The performance of the local LM model approach in predicting VHT alteration depths above the WTP contract limit is the best of all models considered. Model 15 correctly predicts 10 of 14 such glasses (see Table 6.15). In conclusion, the results from fitting local LM models indicates that local regression methods have the potential to improve the prediction of VHT alteration depths (especially above and somewhat below the WTP contract limit) compared to global models. Hence, this approach to modeling may warrant additional investigation in the future if improved performance of VHT alteration predictions is required compared to that of the recommended global models. If this approach is investigated more in the future, it would be advisable to select additional glasses for modeling using a space-filling design approach (see Section 10.7.5 for further discussion of this topic).

As mentioned previously, Table 6.15 contains comparisons of measured and predicted VHT alteration depths to the WTP contract limit for the various models. The table also includes results of comparing predicted alteration depths plus uncertainty to the contract limit. The uncertainty accounted for in Table 6.15 is determined using two different approaches. For the first approach, the uncertainty is calculated using a 95% *simultaneous upper confidence interval* (SUCI) on the mean alteration depth for a given composition. The 95% confidence is simultaneous over multiple uses of the underlying VHT-composition model. For the second approach, the uncertainty is calculated using a 95% *upper prediction interval* (UPI) on a single alteration depth for a given composition. Both of these approaches are statistical interval statements that produce an interval upper bound by adding a calculated amount of uncertainty to the predicted VHT alteration depths [ $\ln(D)$  values, actually]. The amount of uncertainty added is based on a specified confidence level, in this case 95%, because it was considered appropriate for this aspect of comparing models. Of the two approaches, the UPI is more conservative in that it adds more uncertainty to the predicted alteration depth to determine the upper interval bound.

However, this is the case because a UPI is a statistical interval on single VHT result for a given composition, whereas a SUCI is a statistical interval on the mean alteration depth for a given composition. It is also possible to construct simultaneous UPIs, which would be even wider, but these are seldom used in practice. See Section C.7 of Appendix C for the equations and discussion of SUCIs and PIs.

In an attempt to better compare model predictive performance for glasses with “higher” VHT alteration depths, an RMSE value was calculated for each model applied to just the glasses with measured alteration depths greater than 68.3254  $\mu\text{m}$ , the cut-off specified for the two-part model. For completeness, a separate RMSE value was also calculated for each model applied to just the glasses below this specified cut-off. These statistics are listed in Table 6.16.

## **6.9 Decision Process and Recommended Model for VHT Alteration Depth of LAW Glasses**

Based on the model summaries presented in Tables 6.13 to 6.16, a first step in model selection was to identify models to consider as “final contenders”. Four models were identified as final contenders: Models 3, 10, 11, and 12. Rows representing these models are shaded in Tables 6.13 to 6.16 to aid in comparisons. These four models were selected as final contenders based on their respective performance statistics as well as their model forms. Note that Models 13 and 14 generally have better summary statistics than the four models selected as final contenders. However, there is concern that a model with 7 or 9 higher-order terms selected using statistical methods would likely over-fit the data. Past property-composition model development efforts have shown that such models do not perform as well as expected when applied to new glass compositions (glasses not included in the model development set). Hence, Models 13 and 14 were not considered as final contenders for this reason.

Among the four finalist models (Models 3, 10, 11, and 12), Model 10 ranks either third or fourth based on comparisons in Tables 6.13 to 6.16. Model 11 (the 15-term PCM model) ranks first or second on all comparisons and is thus the recommended model. Model 12 ranks higher than Model 11 based on Table 6.13, Table 6.14, and the “below cutoff” performance (predicting small-to-moderate VHT alteration depths) in Table 6.16. However, Model 11 ranks higher in Table 6.15 and the “above cutoff” performance (predicting moderate-to-larger VHT alteration depths) in Table 6.16, which are the more important considerations. In rankings based on Tables 6.13 to 6.16, Model 12 is a close competitor to Model 11. However, if a second model is to be recommended, it seems inadvisable to recommend Model 12 because of its similarity to Model 11 (both are PCM models with similar cubic terms). PCM models involving cubic terms have not been widely used to assess glass properties. It is possible that the cubic terms have helped improve model performance for the current modeling dataset, but that such terms will not be as effective when the model is applied to future glass compositions. Even the PQM models generated in past studies have sometimes been disappointing when applied to new glass compositions. However, Model 3 (the PQM model) is recommended here as a second-choice model because it has a model form that has been used fairly extensively in the past.

In summary, Model 11 (a 15-term partial cubic mixture model) listed in Table 6.11 is the recommended model for predicting VHT  $\ln(D)$ . As a second-choice alternate, Model 3 (a 16-term partial quadratic model) listed in Table 6.9 is suggested because it avoids cubic terms and has the second-best performance in predicting moderate-to-large VHT alteration depths. The full and reduced LM models (Model 1 and Model 2) are included (in Tables 6.7 and 6.8) as baselines for comparison. The full LM model (Model 1) and its reduced form (Model 2) are not recommended as final VHT models because of their relatively poor predictive performances.

As a final note of caution, recall that the first- and second-choice models (Models 11 and 3) still have statistically significant LOFs with greater than 90% confidence despite the relatively large uncertainty in the VHT alteration depth results (see Table 6.4). Together, these factors indicate that  $\ln(D)$  model predictions will be subject to relatively large uncertainty. Some indications of these uncertainties are given in Section 6.6 for the recommended Model 11 and in Section 6.4 for the second-choice Model 3. Section 6.10 also illustrates prediction uncertainties for these two models (as well as the reduced LM model for baseline comparison purposes) for the LAW glass composition considered in the example.

## 6.10 Example Illustrating VHT Model Predictions and Statistical Intervals

This section contains examples to illustrate using the (i) 11-term reduced LM model, (ii) 16-term PQM model, and (iii) 15-term PCM model to obtain predicted VHT alteration depths and corresponding 90% upper confidence intervals (UCIs) and 95% simultaneous upper confidence intervals (SUCIs) as described in Section C.7 of Appendix C. The 15-term PCM model is the one recommended in Section 6.9 and discussed in detail in Section 6.6. However, calculations are also performed in this section for the other two models for comparison purposes. The confidence levels associated with 90% UCIs and 95% SUCIs were chosen for illustration purposes only. The WTP project can use an appropriate confidence level depending on the use of the VHT-composition model and the type of statistical uncertainty expression.

The glass composition used in this example is LAWA126, which is one of the glasses in the ILAW Existing Matrix. The 18-component composition of LAWA126 for VHT modeling is given in Table 6.2 in mass fraction format. To apply the three VHT models to this composition, the mass fractions of the 18 components must be converted to mass fractions (that sum to 1.0) of the 11 LAW glass components contained in the models. Mass fractions of the relevant components are then multiplied to obtain the quadratic and cubic terms of the PQM and PCM models. Table 6.17 contains the composition of LAWA126 prepared for use in the three ILAW VHT models.

For each of the VHT models, predicted  $\ln(\text{VHT alteration depths})$  are obtained by multiplying the composition in the format needed for that model by the coefficients for that model, then summing the results. That is, the predicted values are calculated by

$$\hat{y}(a) = a^T b$$

where  $\mathbf{a}$  is the composition of LAWA126 formatted to match the terms in a given model (from Table 6.17), the superscript T represents a matrix transpose (or vector transpose in this case), and  $\mathbf{b}$  is the vector of coefficients for a given model. The predicted  $\ln(\text{VHT alteration depth})$  values from each of the ILAW VHT models are listed in the second column of Table 6.18. The predicted  $\ln(\text{VHT alteration depths})$  in  $\ln(\text{micron})$  units are easily converted to the usual VHT alteration depths in microns by exponentiation. The third column of Table 6.18 contains the predicted VHT alteration depths in microns. However, as discussed in Section C.7 of Appendix C, these back-transformed VHT alteration depth predictions in microns should be considered estimates of the true median (not the true mean) of the distribution of alteration depths that would result if the VHT were repeated multiple times using coupons of separately batched and melted samples of the LAWA126 glass composition.

The predicted VHT  $D$  values for LAWA126 in Table 6.18 vary significantly from 49.91  $\mu\text{m}$  for the 11-term LM model, 37.67  $\mu\text{m}$  for the 16-term PQM model, and 25.10  $\mu\text{m}$  for the recommended 15-term PCM model. The predicted value for the recommended PCM model is closest to the measured value of 22  $\mu\text{m}$  for LAWA126.

Equation (C.27a) can be used to calculate a 90% UCI for the true mean of  $\ln(D)$  from the LAWA126 glass composition for each of the ILAW VHT models. In the notation of Equation (C.27a):

- $100(1-\alpha)\% = 90\%$ , so that  $\alpha = 0.10$ .
- The vector  $\mathbf{a}$  contains entries corresponding to the terms in a given VHT model, which are calculated using the composition of LAWA126 in Table 6.17.
- Matrix  $\mathbf{A}$  is formed from the data matrix used in the regression that generated a given VHT model. Matrix  $\mathbf{A}$  has the number of rows in the VHT modeling dataset (165) and the number of columns corresponding to the number of terms in a given VHT model. Each column is calculated according to the corresponding term in the model using the LAW glass compositions in the VHT modeling dataset.

To obtain a 90% UCI in  $\ln(\text{VHT alteration depth})$  units of  $\ln(\text{microns})$ , the quantity  $t_{1-\alpha, n-p} RMSE \sqrt{\mathbf{a}^T (\mathbf{A}^T \mathbf{A})^{-1} \mathbf{a}}$  is added to the predicted  $\ln(\text{VHT alteration depth})$   $\hat{y}(\mathbf{a})$  described above, as indicated by Equation (C.27a). The  $MSE[(\mathbf{A}^T \mathbf{A})^{-1}]$  portion of this expression is the variance-covariance matrix for the estimated model coefficients, as discussed near the end of Section C.7 of Appendix C. The variance-covariance matrices for the VHT models are listed in Tables D.5, D.6, and D.7 of Appendix D. The quantity  $MSE$  is the mean squared error from regression,  $RMSE$  is the square root of  $MSE$ . The quantity  $RMSE \sqrt{\mathbf{a}^T (\mathbf{A}^T \mathbf{A})^{-1} \mathbf{a}}$  is the standard deviation of a model prediction; the value for each model is given in the fourth column of Table 6.18.

The 90% UCI values for the true mean  $\ln(\text{VHT alteration depth})$  in units of  $\ln(\text{microns})$  for the LAWA126 composition based on the ILAW VHT models are given in the fifth column of

Table 6.18. Exponentiating the resulting 90% UCIs for the mean in ln(micron) units yields 90% UCIs for the median in microns. For example, the 15-term PCM model for VHT has 3.4237 ln(microns) as the upper limit of the 90% UCI on the true mean ln(VHT alteration depth) for LAWA126. Then  $e^{3.4237} = 30.68$  microns is the upper limit of the 90% UCI on the true median VHT alteration depth. The sixth column of Table 6.18 contains 90% UCIs for the true median VHT alteration depth from the LAWA126 glass composition based on the ILAW VHT models. Note that the 90% UCI value of 30.68 microns for the PCM model for ILAW VHT is significantly below the VHT alteration depth limit of  $\approx 453$  microns for 24-day VHT and a glass density of  $2.65 \text{ g/cm}^3$ .

As discussed in Section C.7 of Appendix C, there are times when a SUCI may be preferred rather than an UCI. This is particularly true when the regression model (composition-property model) is to be used a large number of times for various glass compositions from a specified composition region. Equation (C.30a) can be used, in much the same way as how Equation (C.27a) is used to obtain UCIs, to calculate a 95% SUCI for the true mean of ln(VHT alteration depth) for glasses having a specified composition. The 95% SUCI values for the true mean ln(VHT alteration depth) in units of ln(microns) for the LAWA126 composition based on the ILAW VHT models are given in the seventh column of Table 6.18. Exponentiating the resulting 95% SUCIs for the mean in ln(micron) units yields 95% SUCIs for the median in microns. The eighth column of Table 6.18 contains 95% SUCIs for the true median VHT alteration depth from the LAWA126 glass composition based on the ILAW VHT models. Note that the 95% SUCI values of 109.53, 79.89, and 53.05 microns for the three ILAW VHT models are all significantly below the VHT alteration depth limit of  $\approx 453$  microns for 24-day VHT and a glass density of  $2.65 \text{ g/cm}^3$ .

### **6.11 Suitability of the Recommended VHT Alteration Depth Model for Application by the WTP Project**

The 15-term PCM model for VHT alteration depth discussed in Section 6.6 is recommended for use by the WTP project as the best model currently available for predicting VHT alteration for LAW glasses. This model appears to yield unbiased predictions of VHT alteration depth over the full range of measured VHT alteration depth values in the modeling dataset. The second-choice 16-term PQM model tended to under-predict the largest VHT alteration depths. There is relatively large scatter in data points about the recommended model (see Figure 6.20). One reason for the large scatter is the large uncertainty in VHT data (31 %RSD, see Table 6.4) from making simulated LAW glasses, VHT testing, and measuring alteration depths. Another reason is the significant lack-of-fit of the recommended VHT model.

Because of the large uncertainty in VHT data and the significant lack-of-fit of the recommended VHT model, prediction uncertainties for the model are relatively large. Figure 6.25 displays the ln(*D*) prediction standard deviations versus predicted values [both in ln( $\mu\text{m}$ ) units] for the LAW glass compositions in the VHT modeling dataset. The ln(*D*) prediction standard deviations for modeling dataset glasses range from approximately 0.13 to 0.56 ln( $\mu\text{m}$ ) for the recommended VHT alteration depth model. Note that prediction standard deviations will be larger for LAW glass compositions as their distance from glasses in the VHT modeling



dataset increases. Also, the total uncertainty in predictions with the recommended VHT alteration depth model will depend on the type of statistical interval used (see Section C.7 of Appendix C).

While it may still be possible to formulate LAW glasses with VHT alteration depths sufficiently below the contract limit, so the relatively large prediction uncertainties do not unduly restrict use of the recommended VHT model by the WTP project, it is likely that there will be some impact on achievable waste loadings. Consequently, it is expected that additional effort in this area would be very beneficial. The ultimate suitability of the recommended VHT model for LAW glass formulation, glass former addition decisions during production, and demonstrating compliance with WTP Contract Specification 2.2.2.17.3 will be decided by separate WTP project work.

The impact of prediction uncertainties for ILAW Phase 1 VHT alteration depth models (Muller et al. 2005) on the ability to demonstrate compliance with WTP Contract Specification 2.2.2.17.3 was previously addressed in Section 7.5 of Piepel et al. (2005). In that work, the LAW glasses expected to be produced in the WTP LAW vitrification plant were shown to have VHT alteration rates sufficiently below the  $50 \text{ g/m}^2/\text{day}$  ( $= 453 \text{ }\mu\text{m}$ ) limit even after accounting for conservative composition and model uncertainties. The impact of LAW glass composition and model uncertainties for the recommended VHT  $\ln(D)$  model (Section 6.6) on satisfying Contract Specification 2.2.2.17.3 is planned to be addressed as part of the Technical Scoping Statement (TSS) B-6069 work scope of the River Protection Project—Waste Treatment Plant Support Program at PNNL. The impacts are also planned to be addressed as part of the second iteration of the LAW glass formulation algorithm development work planned by WTP project staff. The first iteration of that work (Vienna 2005) utilized the ILAW Phase 1 VHT model (Muller 2005) and the LAW glass formulation correlation (Muller et al. 2004b).

## **SECTION 7**

### **MODELS RELATING ELECTRICAL CONDUCTIVITY TO LAW GLASS COMPOSITION AND TEMPERATURE**

This section documents the development and validation of property-composition-temperature models and corresponding uncertainty expressions for predicting the electrical conductivity (EC) for low-activity waste (LAW) glasses. Because EC is a property of a glass melt, it is a function of glass melt temperature as well as glass composition. The property-composition-temperature models and corresponding uncertainty expressions for EC presented in this section were developed and validated using glass composition, temperature, and EC data collected on simulated LAW glasses. Electrical conductivity was not measured on any of the glasses made from actual waste samples that are discussed in Section 2.7.

The 171 simulated LAW glasses used for EC model development and validation (from the database of 181 glasses) are discussed in Section 7.1. Section 7.2 lists the model forms for EC that were investigated. Section 7.3 presents the results for EC models with the two parameters of the Arrhenius equation (for temperature dependence) expressed as linear mixture models in composition. Section 7.4 presents the results for EC models of the form considered in Section 7.3 plus selected crossproduct terms. Section 7.5 presents the model fit and validation results for the recommended 25-term EC model. Section 7.6 illustrates the calculation of EC predictions and the uncertainties in those predictions using selected EC models and corresponding uncertainty equations. Section 7.7 discusses the suitability of the recommended EC model for use by the WTP project. Appendix C discusses the statistical methods and summary statistics used to develop, evaluate, and validate the several EC model forms investigated, as well as statistical equations for quantifying the uncertainties in EC models.

#### **7.1 Electrical Conductivity Data Used for Model Development and Validation**

The data used for developing EC models are discussed in Section 7.1.1. The approaches and data used for validating the models are discussed in Sections 7.1.2 to 7.1.4.

##### **7.1.1 Electrical Conductivity Model Development Data**

The data available for developing EC-composition-temperature models consist of composition, temperature, and EC data from 181 LAW glasses (see Section 4.3). These glasses are discussed and their target compositions are presented in Section 2. The normalized compositions of these glasses based on analyzed (or estimated analyzed) SO<sub>3</sub> values are discussed in Section 3.3. The corresponding EC (S/cm) at temperature values are presented in Table 4.5. The LAW EC data are discussed in Section 4.3.

As discussed subsequently in Section 8.1, the same 181 LAW glasses comprising the EC modeling set also comprise the viscosity modeling set. Hence, the assessment of glass compositions that follows applies to the EC and viscosity modeling sets.

### Assessment of Available Glasses with Electrical Conductivity Data

The database of 181 glasses with EC results contains statistically-designed as well as actively-designed glasses. Some actively-designed glasses are outside the composition region covered by the majority of the LAW compositions. Such glasses are not ideal for inclusion in a modeling set because they can be influential when fitting models to data. Hence, it was decided to (i) graphically assess the 181 simulated LAW glass compositions and (ii) remove from the modeling set any compositions considered to be outlying or non-representative of LAW glasses of interest for the WTP.

Figure 7.1 displays plots of the mass fraction values for 14 “main components” in the 181 LAW glasses with EC and viscosity data. The “main components” are the ones that were varied in the ILAW Phase 1 Test Matrix and the Phase 1a Augmentation Test Matrix. Figure 7.2 displays similar plots for the remaining minor components. On each plot in Figures 7.1 and 7.2, the x-axis represents the mass fraction values of an LAW glass component. The y-axis shows an index value representing each LAW glass composition, which aids in spreading out the data points to avoid over-plotting. The plotting symbols correspond to the six groups of LAW glass data discussed in Sections 2.1 to 2.6. Electrical conductivity was not measured on any of the actual waste glasses discussed in Section 2.7. For comparison purposes, the vertical bars in Figures 7.1 and 7.2 represent the ranges over which the components were varied in the ILAW Phase 1 Test Matrix.

Figure 7.1 shows several glasses have components with outlying mass fraction values compared to the remaining glasses and to the component ranges studied in the ILAW Phase 1 Test Matrix and the Phase 1a Augmentation Test Matrix. Figure 7.2 shows what appear to be outliers for some components, but the values and ranges of those components are small and hence the glass compositions were not considered to be outliers. Table 7.1 lists the 10 LAW glasses excluded from the ILAW EC and viscosity modeling sets, and the reason each glass was excluded. The first 6 of the 10 glasses were excluded because of having outlying component values compared to the rest of the glasses. The final 4 glasses in Table 7.1 were designed for a specific investigation, were high in  $\text{Cr}_2\text{O}_3$ , and were container-centerline-cooled. These glasses were considered non-representative and excluded from the EC modeling dataset. Note that the 10 glasses listed in Table 7.1 were 10 of the 20 glasses excluded from the PCT modeling dataset (see Table 5.1) and 10 of the 16 glasses excluded from the VHT modeling dataset (see Table 6.1). The other 10 glasses excluded from the PCT modeling dataset did not have EC or viscosity data, or else they would have been excluded from the modeling sets for these properties also.

Figures 7.3 and 7.4 (corresponding to Figures 7.1 and 7.2, respectively) show plots of component distributions after the 10 outlying and non-representative glasses were removed from the 181-glass set having EC and viscosity data. Figure 7.3 shows for the remaining 171 LAW glasses that all 13 of the specific LAW glass components ( $\text{Al}_2\text{O}_3$ ,  $\text{B}_2\text{O}_3$ ,  $\text{CaO}$ ,  $\text{Fe}_2\text{O}_3$ ,  $\text{K}_2\text{O}$ ,  $\text{Li}_2\text{O}$ ,  $\text{MgO}$ ,  $\text{Na}_2\text{O}$ ,  $\text{SO}_3$ ,  $\text{SiO}_2$ ,  $\text{TiO}_2$ ,  $\text{ZnO}$ , and  $\text{ZrO}_2$ ) have sufficient ranges and distributions of values

within those ranges to support model terms. Similarly, Figure 7.4 shows that Cl, Cr<sub>2</sub>O<sub>3</sub>, F, and P<sub>2</sub>O<sub>5</sub> have sufficient ranges and distributions of values within their ranges to support model terms for those components. Of these four components, the support for a P<sub>2</sub>O<sub>5</sub> model term is somewhat tenuous, relying on the “HiCrP” glasses and a few actively designed (ActDes) glasses. Based on Figures 7.3 and 7.4, it was decided to use 18 components for initial EC and viscosity modeling work. These are Al<sub>2</sub>O<sub>3</sub>, B<sub>2</sub>O<sub>3</sub>, CaO, Cl, Cr<sub>2</sub>O<sub>3</sub>, F, Fe<sub>2</sub>O<sub>3</sub>, K<sub>2</sub>O, Li<sub>2</sub>O, MgO, Na<sub>2</sub>O, P<sub>2</sub>O<sub>5</sub>, SO<sub>3</sub>, SiO<sub>2</sub>, TiO<sub>2</sub>, ZnO, ZrO<sub>2</sub>, and Others (the sum of all remaining components). Note that these are the same 18 components chosen for initial PCT and VHT modeling work.

Figure 7.5 shows a scatterplot matrix of the 171 glasses remaining in the EC and viscosity modeling datasets after removing the 10 outlying compositions. High correlations between some pairs of components are evident, so pairwise correlation coefficients were calculated. These can vary from -1.0 (perfect negative correlation) to 0 (no correlation) to 1.0 (perfect positive correlation). The component pairs with correlations larger (in absolute value) than 0.60 are

Li <sub>2</sub> O and Na <sub>2</sub> O	-0.878
CaO and Na <sub>2</sub> O	-0.703
CaO and Li <sub>2</sub> O	0.631
Na <sub>2</sub> O and SiO <sub>2</sub>	-0.631
Na <sub>2</sub> O and SO <sub>3</sub>	-0.617
Li <sub>2</sub> O and SO <sub>3</sub>	0.616

Such high pairwise correlations can make it difficult for regression methods to properly separate the effects of the components on the response variable (e.g., EC or viscosity). Thus, these high pairwise correlations need to be kept in mind in developing ILAW property-composition models for EC and viscosity.

### Electrical Conductivity Modeling Dataset

Table 7.2 lists the Glass ID, Group ID, and normalized glass compositions for the 171 simulated LAW glasses in the 18-component forms used for EC and viscosity model development. The Group ID column of Table 7.2 indicates the subset of data that each glass is associated with (see Sections 2.1 to 2.7). The glass compositions in Table 7.2 are the normalized mass fractions (mf) of the 18 components previously identified as having sufficient data to support a separate model term if needed. These components are Al<sub>2</sub>O<sub>3</sub>, B<sub>2</sub>O<sub>3</sub>, CaO, Cl, Cr<sub>2</sub>O<sub>3</sub>, F, Fe<sub>2</sub>O<sub>3</sub>, K<sub>2</sub>O, Li<sub>2</sub>O, MgO, Na<sub>2</sub>O, P<sub>2</sub>O<sub>5</sub>, SO<sub>3</sub>, SiO<sub>2</sub>, TiO<sub>2</sub>, ZnO, ZrO<sub>2</sub>, and Others. The mass fraction values of the 18 components shown in Table 7.2 were normalized so that they sum to 100% for each of the glasses (see Section 3.3).

Table 7.3 contains the measured EC at temperature pairs for the 171 glasses in the EC modeling dataset. It also includes a column designating the data-splitting validation subsets for EC modeling and validation. These subsets and the data-splitting validation approach are discussed in Section 7.1.2.

The values of EC in Table 7.3 range from 0.020 to 0.961 S/cm. Smaller values of EC tend to occur at lower temperatures and larger values tend to occur at higher temperatures.

### Replicate and Near-Replicate EC Data

The changes to the LAW glass compositions caused by the renormalization associated with using XRF analyzed (or estimates of XRF analyzed) SO<sub>3</sub> values (see Section 3.3) resulted in some replicate glasses not having exactly equal compositions. Such compositions are referred to as near-replicates. For ease of discussion, henceforth both replicates and near-replicates are referred to as replicates.

Table 7.4 lists the replicate sets of glasses in the ILAW EC modeling dataset and the corresponding EC values associated with the four temperatures at which EC was measured for each glass. The top portion of Table 7.4 lists the EC values corresponding to actual temperature values, which differ somewhat from the nominal values of 950, 1050, 1150, and 1250°C within replicate sets. The bottom portion of Table 7.4 lists interpolated values of EC at the four nominal temperature values. The interpolated values were obtained by fitting the T2 equation to the (temperature, EC) data for each glass (see Section C.2.1 of Appendix C) and then calculating EC at the nominal temperature values.

Table 7.4 also lists estimates of %RSDs [calculated using EC values in original S/cm units] and SDs [calculated from ln(EC) values in ln(S/cm) units] for each replicate set and nominal temperature. Pooled estimates of %RSDs and SDs are given over the (i) temperatures for a given replicate set, (ii) replicate sets for a given temperature, and (iii) all replicate sets and temperatures. A pooled %RSD or SD combines the separate %RSD or SD estimates so that a more accurate combined estimate of the %RSD or SD is obtained. These pooled %RSDs and SDs include uncertainties due to fabricating glasses and measuring EC. As discussed in Section 7.2.2, EC data are subject to two sources of uncertainty whose standard deviations are denoted  $\sigma_G$  and  $\sigma_T$ . These parameters are expressed in ln(S/cm) units because natural logarithms of EC values are modeled (see Section 7.2.2). The SDs given in Table 7.4 are estimates of  $\sqrt{\sigma_G^2 + \sigma_T^2}$ , the total standard deviation of an EC determination for a given glass and temperature. The pooled estimates of replicate uncertainty for EC in Table 7.4 are used subsequently to assess lack-of-fit (LOF) of the various models considered.

The %RSD and SD values in the top portion of Table 7.4 may over-estimate the uncertainty in EC values because the EC values of replicate sets are not exactly at the same temperature values. The %RSD and SD values in the bottom portion of Table 7.4 may underestimate the uncertainty in EC values because the interpolated EC values may “remove” some of the natural variation in the data that is the basis for uncertainty estimation. However, the %RSD and SD values in Table 7.4 are slightly larger in the bottom portion of the table compared to the top portion. In the subsequent discussion, only the uncertainty values from the bottom portion are discussed because they are more conservative (i.e., larger) estimates.

The magnitudes of the overall pooled SD = 0.164 [calculated from  $\ln(S/\text{cm})$  values] and %RSD = 16.2 [calculated from S/cm values] in Table 7.4 indicate roughly a 16% total relative uncertainty in the EC measurements over replicate glasses.

### 7.1.2 Primary Electrical Conductivity Model Validation Approach and Data

The primary model validation approach for EC modeling was based on splitting the 171-glass dataset for model development into five modeling/validation subsets. Of the 171 model development glasses, 12 were intended to be replicates (6 replicate pairs). The five modeling/validation splits of the 171 glasses in the EC modeling dataset were formed as follows.

- The six pairs of replicates (12 glasses) were set aside so they would always be included in each of the five model development datasets. This was done so that replicate pairs would not be split between modeling and validation subsets, thus negating the intent to have validation glasses different than model development glasses.
- The remaining  $171 - 12 = 159$  glasses were ordered from smallest to largest according to their average EC values across the four temperatures. The 159 glasses were numbered 1, 2, 3, 4, 5, 1, 2, 3, 4, 5, etc. All of the 1's formed the first model validation set, while all of the remaining points formed the first model development dataset. Similarly, all of the 2's, 3's, 4's, and 5's respectively formed the second, third, fourth, and fifth model validation sets. In each case, the remaining non-2's, non-3's, non-4's, and non-5's formed the second, third, fourth, and fifth model development datasets. Because 159 is not evenly divisible by 5, the five modeling and validation subsets did not all contain the same numbers of glasses. Four of the five splits contained 32 glasses for validation and 127 glasses for modeling. The fifth split contained 31 glasses for validation and 128 for modeling. Note that these numbers of glasses in the modeling subsets do not include the replicates.
- The 12 replicate glasses were added to each of the split modeling subsets. Including the replicates, four splits contained 139 glasses for modeling and 32 for validation, while the fifth split contains 140 glasses for modeling and 31 for validation. The last column of Table 7.3 specifies the validation subsets for the five modeling/validation splits in the primary validation approach for EC model development.

Data splitting was chosen as the primary validation approach because the EC modeling dataset contains all compositions that (i) are in the ILAW composition region of interest, (ii) meet quality assurance (QA) requirements, and (iii) have EC data. Having a separate validation dataset not used for modeling is desirable, but that desire was over-ridden by wanting EC models developed with all appropriate data.

### 7.1.3 Secondary Electrical Conductivity Model Validation Approach and Data

The secondary model validation approach consisted of partitioning the 171-glass EC modeling dataset into modeling and validation subsets. Included in the modeling subset were all glasses used in statistically-designed groups of the data that had EC results. Included are glasses in the Existing Matrix (23 glasses), the Phase 1 Test Matrix (56 glasses), and the Phase 1a Augmentation Test Matrix (20 glasses). Together, these comprise 99 glasses, but only 86 of them have EC data. Hence, the modeling subset for this approach contains EC results for 86 glasses. The remaining  $171 - 86 = 85$  glasses were used as a validation subset.

The data-splitting approach discussed in Section 7.1.2 is considered the primary validation approach because it comes closer to validating the EC models of interest, namely those fitted to all 171 glasses with EC data in the modeling dataset. The primary validation approach fits EC models using 139 or 140 of the 171 glasses in the modeling dataset and validates with the remaining 32 or 31 glasses, and does so five times. The secondary approach fits models with 86 glasses and validates with 85 glasses. Hence, the primary validation approach comes closer to validating the EC models of interest, namely those fitted to data on all 171 glasses.

The secondary validation approach is desirable because it uses the statistically-designed glasses (and the Existing Matrix glasses that were factored into selecting the Phase 1 Test Matrix glasses) to fit models, and correlation plus actively-designed glasses to validate the models. Actively-designed glasses tend to be more clustered in composition space, and can have strong or even perfect correlations between glass components. These aspects make actively-designed glasses somewhat less desirable for model development, but reasonable for model validation.

### 7.1.4 Limited Extrapolative Electrical Conductivity Model Validation Data

The 10 glasses excluded from the EC modeling set (see the discussion in Section 7.1.1) were used to perform a limited assessment of the extrapolative prediction performance of the EC models. The normalized compositions of these 10 glasses are given in Table 7.5 and the corresponding EC at temperature values are given in Table 7.6. Typical summary statistics and predicted versus measured plots are used to assess the extrapolative performance of EC models for the 10 glasses listed in Table 7.5 and their EC values listed in Table 7.6.

## 7.2 Electrical Conductivity Model Forms

Ideally, a property-composition-temperature model for EC would utilize known mechanisms of electrical conductivity as a function of glass composition and melt temperature. No such mechanisms are known, although there is considerable experience regarding the temperature dependence of EC over the range of 950 to 1250°C. Section 7.2.1 discusses the investigations performed to select an equation to represent the temperature dependence of EC. Sections C.1 and C.2 of Appendix C discuss mixture experiments and several general model forms in which mixture experiment models are used to expand the parameters of EC-temperature

equations. Section 7.2.2 discusses the forms of EC-temperature models investigated. Section 7.2.3 discusses the use of transformed EC values as the response variable for EC modeling.

### 7.2.1 Temperature Dependence of Electrical Conductivity

Three equations discussed in Section C.2.1 of Appendix C were considered for representing the temperature dependence of EC. These are the *Arrhenius equation* [Equation (C.8)], the *T2 equation* [Equation (C.9)], and the *truncated-T2 equation* [Equation (C.10)]. The EC at temperature observations for each of the 171 glasses in the EC modeling dataset were used to fit each of these three equations. Goodness of fit statistics were calculated and compared. There were only 12 to 15 out of 171 LAW glasses that showed sufficient curvature to warrant using the T2 or truncated-T2 equation instead of the Arrhenius equation (which represents a linear relationship between  $\ln(EC)$  and  $1/T$  (where  $T$  is temperature in Kelvin). The Arrhenius equation still provided a good fit for these glasses. Hence, it was decided that the Arrhenius equation was sufficient to represent the temperature dependence of EC for LAW glasses.

### 7.2.2 Model Forms for the Temperature and Composition Dependence of Electrical Conductivity

The model forms considered for EC start with a slightly modified version of the Arrhenius equation and expand its two parameters as functions of LAW glass composition. Linear mixture (LM) model forms and a special partial quadratic mixture (PQM) model form (see Section C.1.1 of Appendix C) were considered for use in expanding the parameters of the Arrhenius equation.

The EC model form with the parameters of a modified Arrhenius equation expanded as LM models is given by

$$\ln(EC) = \sum_{i=1}^q a_i x_i + E_G + \sum_{i=1}^q b_i \frac{x_i}{T/1000} + E_T. \quad (7.1)$$

The modification to the Arrhenius equation is that temperature ( $T$  in Kelvin) is divided by the scaling factor of 1000 so that the  $b_i$  coefficients are similar in magnitude to the  $a_i$  coefficients. Except for the scaling factor, this equation is the same one given as Equation (C.12) and discussed in Section C.2.2 of Appendix C. The remaining notation is discussed following the subsequent model forms.

The EC model form with the modified Arrhenius equation parameters expanded as LM models plus three alkali and alkaline earth crossproduct terms is given by



$$\ln(EC) = \sum_{i=1}^q a_i x_i + a_{CaOLi_2O} x_{CaO} x_{Li_2O} + a_{CaONa_2O} x_{CaO} x_{Na_2O} + a_{Li_2ONa_2O} x_{Li_2O} x_{Na_2O} + E_G + \sum_{i=1}^q b_i \frac{x_i}{T/1000} + E_T \quad (7.2)$$

Previous work (Feng et al. 2004) showed that these three crossproduct terms were beneficial in modeling EC. That previous work only considered adding these crossproduct terms in the composition portion of the model, so it was decided to also investigate whether these crossproduct effects are temperature dependent via the model

$$\ln(EC) = \sum_{i=1}^q a_i x_i + a_{CaOLi_2O} x_{CaO} x_{Li_2O} + a_{CaONa_2O} x_{CaO} x_{Na_2O} + a_{Li_2ONa_2O} x_{Li_2O} x_{Na_2O} + E_G + \sum_{i=1}^q b_i \frac{x_i}{T/1000} + b_{CaOLi_2O} \frac{x_{CaO} x_{Li_2O}}{T/1000} + b_{CaONa_2O} \frac{x_{CaO} x_{Na_2O}}{T/1000} + b_{Li_2ONa_2O} \frac{x_{Li_2O} x_{Na_2O}}{T/1000} + E_T \quad (7.3)$$

As with Equation (7.1), temperature (in Kelvin) is scaled by 1000 in Equations (7.2) and (7.3) for the reason discussed previously.

In Equations (7.1), (7.2), and (7.3):  $\ln(EC)$  denotes the natural logarithm of EC [in units of  $\ln(S/cm)$ ]; the  $x_i$  ( $i = 1, 2, \dots, q$ ) are mass fractions of  $q$  glass oxide or halogen components such that  $\sum_{i=1}^q x_i = 1$ ; the  $a_i$  and  $b_i$  ( $i = 1, 2, \dots, q$ ), and the  $a_{ij}$  and  $b_{ij}$  ( $ij = CaOLi_2O, CaONa_2O, \text{ and } Li_2ONa_2O$ ), are coefficients to be estimated from data;  $E_G$  is a random error associated with determining EC for each LAW glass; and  $E_T$  is a random error associated with determining EC at the temperature values of a given glass melt. The random errors  $E_G$  and  $E_T$  are assumed to be normally distributed with zero means and standard deviations  $\sigma_G$  and  $\sigma_T$ . These standard deviations and the model coefficients are estimated simultaneously using generalized least squares (GLS) regression. See Section C.2.1 in Appendix C for additional discussion of  $E_G$  and  $E_T$ . See Sections C.3.2 and C.3.3 for additional discussion of GLS regression.

### 7.2.3 Transformation of Electrical Conductivity

In modeling EC, it is advantageous to use the natural logarithm of the EC values. The advantages of this transformation include:

- The EC values for the 171 LAW glasses in the EC modeling dataset range from 0.020 to 0.961 S/cm. This is a range of approximately 1.5 orders of magnitude difference. In such cases, typically the uncertainty in making glasses and measuring EC leads to smaller absolute uncertainties for smaller EC values and larger absolute uncertainties for larger EC values. Hence, the unweighted least squares (ULS) regression assumption of equal variances for all response variable values (see Section C.3 of Appendix C) is violated.

After a logarithmic transformation, variances of response values tend to be approximately equal as required for ULS regression.

- A logarithmic transformation tends to linearize the compositional dependence of electrical conductivity data and reduce the need for non-linear terms in the model form.
- A natural logarithm transformation is preferred over a common logarithm (or other base logarithm) transformation because of the approximate relationship

$$\text{SD} [\ln(y)] \cong \text{RSD} (y) \quad (7.4)$$

where SD denotes standard deviation, RSD denotes relative standard deviation (i.e., the standard deviation divided by the mean), and  $y$  denotes EC. Equation (7.4) results from applying the first-order variance propagation formula [Equation (7-7) of Hahn and Shapiro (1967)] to the function  $z = \ln(y)$ . The relationship in Equation (7.4) is very useful, in that uncertainties of the natural logarithm of the response variable  $y$  can be interpreted as RSDs of the untransformed response variable  $y$ .

For these reasons, the natural logarithmic transformation was employed for all EC model forms.

### **7.3 Model Results for ILAW Electrical Conductivity with the Arrhenius Equation Parameters Expanded as Linear Mixture Models**

This section discusses the results of fitting two Arrhenius-linear mixture models using natural logarithms of LAW EC, denoted  $\ln(\text{EC})$ , as the response variable. These models are of the forms given in Equation (7.1). Section 7.3.1 presents the results from fitting a model consisting of the Arrhenius equation with its parameters expanded using LM terms for each of the 18 components determined to have sufficient support in the 171-glass modeling set. Section 7.3.2 presents the results from fitting a model consisting of the Arrhenius equation with its parameters expanded using reduced 11-component LM models.

To perform the GLS model fits (see Section 7.2.2 and Section C.3.2 of Appendix C), PROC MIXED in SAS (2005) was used. For each model fit, output files produced by SAS were used as input files to perform the remaining model evaluation and validation calculations using software codes written in R (Ihaka and Gentleman 1996, R Core Development Team 2006).

#### **7.3.1 Results for 36-Term Electrical Conductivity Model with the Arrhenius Equation Parameters Expanded as 18-Component Linear Mixture Models**

As the initial step in EC model development, the Arrhenius-LM model in Equation (7.1) with  $q = 18$  components identified in Section 7.1.1 was fit to the modeling data (171 glasses). The response was the natural logarithm of EC (S/cm). This 36-term model form was a reasonable starting point and provided a basis for appropriate model reductions.

Table 7.7 contains the results for the 36-term Arrhenius-LM model for ILAW EC. Table 7.7 lists the model coefficients, standard deviations of the coefficients, and estimates of the  $\sigma_G$  and  $\sigma_T$  error standard deviations (see Section 7.2.2). Table 7.7 also contains the model performance summaries for the 36-term model using the modeling dataset (171 glasses), the modeling data partitioned into modeling (86 glasses) and validation (85 glasses) subsets (see Section 7.1.3), and the 10 glasses excluded from the model dataset (see Section 7.1.4). The data-splitting approach was not used to validate this model because of the effort required to do so with GLS regression, and because it is just the first model in the EC model development process.

The summary statistics that describe how well the 36-term Arrhenius-LM model fits the 171-glass EC modeling dataset are given in the upper right corner of Table 7.7. Only the  $R^2$ , sum of squared errors (SSE), and root mean square error (RMSE) statistics were calculated because of using GLS regression (see Section C.4 in Appendix C). The  $R^2 = 0.931$  statistic indicates that the 36-term Arrhenius-LM model fits the EC modeling data reasonably well. For GLS regression, the  $SSE = 21.039$  and  $RMSE = 0.180$  statistics do not directly indicate the performance of the 36-term model, but are useful for comparison to the values for subsequently discussed models. The quantity  $\sqrt{\hat{\sigma}_G^2 + \hat{\sigma}_T^2} = \sqrt{(0.1760)^2 + (0.0565)^2} = 0.1848$  is an estimate of the total uncertainty in an EC determination for a given glass and temperature, under the assumption that the 36-term model does not have a significant LOF. A significant model LOF would inflate this quantity and it would over-estimate the true total uncertainty in an EC determination. However, it is only slightly larger than the overall pooled estimate of uncertainty  $SD = 0.164$  (in the bottom right corner of Table 7.4) calculated from replicate data that is not impacted by model LOF. Hence, the 36-term model does not seem to have a significant model LOF given the inherent uncertainty in the data.

The 36-term EC model statistics from partitioning the 171-glass modeling set into subsets of 86 modeling glasses and 85 validation glasses (see Section 7.1.3) are given on the right side of Table 7.7. The fit statistics of  $R^2 = 0.941$  and  $RMSE = 0.188$  for the 86-glass modeling subset are similar to those for the full 171-glass modeling set. For the 85-glass validation subset,  $R^2_v$  is a negative value and  $RMSE_v = 0.808$  is very large. This poor validation performance is because the 86-glass subset of data provided insufficient support for all 18 components in the full LM model expansions of the Arrhenius equation parameters, thus negatively affecting performance on the validation subset.

The statistics from fitting the 36-term EC model to the 171-glass modeling set and making extrapolative validation predictions for the 10 outlying glasses are given on the right side of Table 7.7. The statistic  $R^2_v = 0.900$  for the 10 outlying glasses is somewhat smaller than  $R^2_v = 0.941$  from data partitioning. The  $RMSE_v = 0.198$  for the 10 outlying glasses is not much worse than the  $RMSE = 0.180$  for fitting the 171-glass modeling set. Hence, the 36-term model appears to predict quite well for the 10 outlying glasses, even though the predictions are extrapolations.

The predicted versus measured plot and the standardized residual plot for the 36-term Arrhenius-LM model are given in Figures 7.6 and 7.7, respectively. Figure 7.6 shows moderate scatter about the 45° line representing perfect prediction, with significantly outlying data for

LAWM30 and moderately outlying data for LAW40. Figure 7.6 shows that low EC values (below about  $-3 \ln(\text{S/cm}) = 0.050 \text{ S/cm}$ ) tend to be over-predicted. Figure 7.7 does not show any strong tendencies of the 36-term EC model for biased prediction by groups of the modeling data discussed in Sections 2.1 to 2.6.

The 36-term Arrhenius-LM model for EC fits the 171-glass modeling dataset reasonably well and thus can provide guidance for reducing the model (i.e., removing separate terms for components that do not significantly influence EC). Hence, this model was used to produce a response trace plot (see Section C.5.1) at each of the four nominal temperatures at which EC was measured (950, 1050, 1150, and 1250°C) shown in Figures 7.8a to 7.8d. Note that the y-axis [predicted  $\ln(\text{EC}, \text{S/cm})$ ] does not have the same scale and tic marks on each of the four plots. Using the same scale would have greatly condensed the individual plots and made it even more difficult to differentiate response traces of individual components. The response trace plots show that  $\text{Li}_2\text{O}$  and  $\text{Na}_2\text{O}$  have dominant increasing effects on EC, while  $\text{SiO}_2$  has the strongest decreasing effect on EC. Figures 7.8a to 7.8d also show that  $\text{CaO}$  has a strong decreasing effect on EC for lower temperatures, but that the effect becomes less strong as temperature increases. Figures 7.8a to 7.8d also show the response trace for  $\text{Cr}_2\text{O}_3$  having a large positive slope, while F and Cl have response traces with the largest negative slopes. Minor components such as these are not expected to have significant effects on EC, and hence these may be artifacts resulting from larger uncertainties in determining the coefficients and hence the effects of these components. On the other hand,  $\text{Cr}_2\text{O}_3$  may play an important role in predicting the EC of the HiCrP glasses (see Section 2.5).

### **7.3.2 Results for 22-Term Electrical Conductivity Model with the Arrhenius Equation Parameters Expanded as Reduced 11-Component Linear Mixture Models**

In the 36-term Arrhenius-LM model presented in Section 7.3.1, some of the 18 components likely do not significantly contribute to predicting EC. Hence, model reduction was the next step of the model development approach. The two parameters of the Arrhenius equation were expanded using LM models involving fewer than the 18 components. The sequential F-test model reduction approach (see Section C.5.1 of Appendix C, Piepel and Cooley 2006) was used to develop reduced LM models for each of the two parameters treated as a separate response variable. Option (ii) discussed in Section C.5.1 was used to develop the reduced LM model for each parameter. Then, the two reduced parts of the model were fitted as a combined model of the form in Equation (7.1). The resulting model is of the same form as the 36-term model discussed in Section 7.3.1, but with fewer glass components.

To reduce the 18-component LM model for each of the two Arrhenius equation parameters, a significance level of 0.05 was used for the F-tests conducted by the model reduction algorithm. An option available with the F-test approach is to force certain terms to remain in the model during the model reduction process. For EC,  $\text{Al}_2\text{O}_3$ ,  $\text{B}_2\text{O}_3$ ,  $\text{CaO}$ ,  $\text{Fe}_2\text{O}_3$ ,  $\text{K}_2\text{O}$ ,  $\text{Li}_2\text{O}$ ,  $\text{MgO}$ ,  $\text{Na}_2\text{O}$ ,  $\text{SiO}_2$ , and  $\text{ZrO}_2$  were forced into the reduced LM model for each of the two Arrhenius equation parameters. That is, they were not eligible to be combined with other components or dropped from the model. The components Cl,  $\text{Cr}_2\text{O}_3$ , F,  $\text{P}_2\text{O}_5$ ,  $\text{SO}_3$ ,  $\text{TiO}_2$ , ZnO,

and Others were allowed to combine if having the combined-components term in the model rather than both individual component terms did not significantly decrease model performance. Running the model reduction algorithm with each of the two Arrhenius equation parameters used in turn as the response variable yielded the same reduced model form in which all of the components that were eligible for combining were combined into a new Others component. That is, the same reduced 11-component model form was chosen for each of the Arrhenius equation parameters for the dependence of EC on temperature. The 11 components were Al<sub>2</sub>O<sub>3</sub>, B<sub>2</sub>O<sub>3</sub>, CaO, Fe<sub>2</sub>O<sub>3</sub>, K<sub>2</sub>O, Li<sub>2</sub>O, MgO, Na<sub>2</sub>O, SiO<sub>2</sub>, ZrO<sub>2</sub>, and Others. Note that Others is the sum of all remaining components, and thus differs from the Others in the Arrhenius-LM model discussed in Section 7.3.1.

Table 7.8 gives the coefficients, coefficient standard deviations, and estimates of the  $\sigma_G$  and  $\sigma_T$  error standard deviations (see Section 7.2.2) for the 22-term Arrhenius-LM model of the form in Equation (7.1). This model was fitted to the EC data for the 171 glasses in the modeling set using the PROC MIXED procedure in SAS (2005). Table 7.8 also provides performance statistics for the (i) modeling data, (ii) partition of the modeling data into 86-glass modeling and 85-glass validation subsets, and (iii) 10 LAW glasses excluded from the EC modeling set. Data splitting was not performed for this model because of the extra work to do so with GLS regression.

The statistics from fitting the 22-term Arrhenius-LM model to the EC data from 171 glasses are given in the upper right corner of Table 7.8. The  $R^2 = 0.923$  and  $RMSE = 0.189$  statistics are only slightly worse than those for the full 36-term model. For the data partition into subsets of 86 modeling glasses and 85 validation glasses, the validation statistics  $R^2_V = 0.878$  and  $RMSE_V = 0.202$  are not much worse than the  $R^2$  and  $RMSE$  statistics from fitting the data from all 171 glasses. From entries in Table 7.8, the quantity  $\sqrt{\hat{\sigma}_G^2 + \hat{\sigma}_T^2} = \sqrt{(0.1829)^2 + (0.0569)^2} = 0.1915$  was calculated. It is an estimate of the total uncertainty in an EC determination for a given glass and temperature, under the assumption that the 22-term model does not have a significant LOF. A significant model LOF would inflate this quantity and it would over-estimate the true total uncertainty in an EC determination. However, this quantity for the 22-term model is only slightly larger than for the 36-term model. Also, it is only marginally larger than the overall pooled estimate of uncertainty  $SD = 0.164$  (in the bottom right corner of Table 7.4) calculated from replicate data that is not impacted by model LOF. Hence, the 22-term model does not seem to have a significant model LOF given the inherent uncertainty in the data. Together, these results indicate there is little consequence to reducing the Arrhenius-LM model form for EC from 36 terms to 22 terms.

The statistics from fitting the 22-term EC model to the 171-glass modeling set and making extrapolative validation predictions for the 10 outlying glasses are given on the right side of Table 7.8. The statistic  $R^2_V = 0.905$  for the 10 outlying glasses is slightly smaller than  $R^2_V = 0.929$  from data partitioning. The  $RMSE_V = 0.194$  for the 10 outlying glasses is similar to the  $RMSE = 0.189$  for fitting the 171-glass modeling set and to the  $RMSE_V = 0.202$  for the partitioned validation subset. Hence, the 22-term model appears to predict quite well for the 10 outlying glasses, even though the predictions are extrapolations.

The predicted versus measured plot and the standardized residual plot for the 22-term Arrhenius-LM model are given in Figures 7.9 and 7.10, respectively. Figure 7.9 shows moderate scatter about the 45° line representing perfect prediction, with significantly outlying data for LAWM30 and moderately outlying data for LAWM40. Figure 7.10 shows that low EC values (below about  $-3 \ln(\text{S/cm}) = 0.050 \text{ S/cm}$ ) tend to be over-predicted. Figure 7.10 does not show any strong tendencies of the 22-term EC model for biased prediction by groups of the modeling data discussed in Sections 2.1 to 2.6. In general, these figures are very similar to the ones for the 36-term model in Figures 7.6 and 7.7.

The response trace plots (see Section C.5.1) for EC at 950, 1050, 1150, and 1250°C produced using the 22-term Arrhenius-LM model are given in Figures 7.11a to 7.11d. These figures are very similar to the ones for the 36-term model, except the artifacts of minor components with steep response traces are no longer present because of combining those components into the Others component. The components Na<sub>2</sub>O and Li<sub>2</sub>O have very strong increasing effects on EC, while SiO<sub>2</sub> has a strong decreasing effect on EC. CaO also has a decreasing effect on EC, but it gets smaller as the temperature increases.

Figures 7.12 and 7.13 show predicted versus measured plots when the 22-term Arrhenius-LM model for ILAW EC is applied to two validation datasets. Figure 7.12 results from fitting the 22-term model to a subset of 86 out of 171 modeling glasses, and then applying the resulting model to the remaining subset of 85 glasses for validation (see Section 7.1.3). Figure 7.13 results from fitting the 22-term model to the data for all 171 glasses in the modeling set and then applying that model to the 10 outlying glasses with EC data (see Section 7.1.4). Also shown in Figures 7.12 and 7.13 are 95% prediction intervals (95% PIs) representing the model prediction uncertainty of single EC determinations for each glass at one temperature (see Sections C.6 and C.7 of Appendix C). If the error bar for a validation point overlaps the 45° line, that means the predicted and measured  $\ln(\epsilon)$  values are within model and measurement uncertainty of each other. Note that the error bars include the estimated uncertainties  $\hat{\sigma}_G$  and  $\hat{\sigma}_T$  resulting from the structure of the EC data. The 95% PIs in Figures 7.12 and 7.13 are moderately wide, due to: (i) the LOF of the 22-term Arrhenius-LM model, and (ii) the experimental uncertainty in fabricating glasses and measuring EC.

Figure 7.12 shows that the 22-term EC model for  $\ln(\epsilon)$  fitted to the 86-glass modeling subset has varied predictive performance for the 85-glass validation subset. The EC is fairly accurately predicted at the four nominal temperature values for many of the 85 glasses. However, it tends to be under-predicted for some of the smallest and largest values. Also, the 95% PIs for the 22-term model overlap the 45° line (i.e., contain the measured values) for all but 15 of the 340 (= 4 temperature values at each of 85 glasses) observations in the validation subset. Failure of  $100(15/340) = 4.4\%$  of the 95% PIs to include the corresponding measured values is about what would be expected by chance.

Figure 7.13 shows the predictive performance of the 22-term EC model for  $\ln(\epsilon)$  fitted to the 171-glass modeling dataset and applied to the set of 10 outlying glasses with EC data that were excluded from the modeling dataset. The 22-term model tends to under-predict most of the observations, but not significantly. The predictions are sufficiently close to the measured values

and the 95% PIs are sufficiently wide that all of the 95% PIs contain the corresponding measured values.

#### 7.4 Investigation of Adding Three Crossproduct Terms to the 22-Term Arrhenius Linear Mixture Model

Preliminary model development work conducted at VSL (Feng et al. 2004) indicated that crossproduct effects represented by the terms  $\text{CaO} \times \text{Li}_2\text{O}$ ,  $\text{CaO} \times \text{Na}_2\text{O}$ , and  $\text{Li}_2\text{O} \times \text{Na}_2\text{O}$  could help improve models for EC. This is based on glass science knowledge and that  $\text{Na}_2\text{O}$ ,  $\text{Li}_2\text{O}$ , and  $\text{CaO}$  have three of the four main effects on EC of LAW glasses (as shown in Figures 7.11a to 7.11d). Hence, it is reasonable that crossproduct terms of these three components could improve the predictive performance of the 22-term Arrhenius-LM model. The following model forms were investigated:

- Model 3: A 25-term model consisting of the 22-term Arrhenius-LM model plus the three terms involving  $\text{CaO} \times \text{Li}_2\text{O}$ ,  $\text{CaO} \times \text{Na}_2\text{O}$ , and  $\text{Li}_2\text{O} \times \text{Na}_2\text{O}$ . This model is represented by Equation (7.2).
- Model 4: A 28-term model consisting of the 22-term Arrhenius-LM model plus the six terms involving  $\text{CaO} \times \text{Li}_2\text{O}$ ,  $\text{CaO} \times \text{Na}_2\text{O}$ ,  $\text{Li}_2\text{O} \times \text{Na}_2\text{O}$ ,  $\text{CaO} \times \text{Li}_2\text{O}/(T/1000)$ ,  $\text{CaO} \times \text{Na}_2\text{O}/(T/1000)$ , and  $\text{Li}_2\text{O} \times \text{Na}_2\text{O}/(T/1000)$ . This model is represented by Equation (7.3).
- Model 5: A 27-term model that leaves out the  $\text{CaO} \times \text{Li}_2\text{O}/(T/1000)$  term from Model 4.
- Model 6: A 26-term model that leaves out the  $\text{CaO} \times \text{Li}_2\text{O}/(T/1000)$  and  $\text{CaO} \times \text{Na}_2\text{O}/(T/1000)$  terms from Model 4.

Models 5 and 6 were selected based on the statistical non-significance of those terms in Model 4. Table 7.9 summarizes key results for Models 3 to 6. Summarized are the results from fitting the models to the EC data from all 171 glasses as well as the results from fitting the models to the modeling subset of 86 glasses and validating with the remaining 85 glasses. For comparison purposes, the results for the two previously discussed models

- Model 1: A 36-term Arrhenius-LM model shown in Table 7.7
- Model 2: A 22-term Arrhenius-LM model shown in Table 7.8

are also shown in Table 7.9. Model 3 is seen to be a significant improvement over Model 2, with all three crossproduct terms having coefficients that are statistically significant (i.e., different from zero) with 95% confidence. This is the case for Model 3 fitted to the data from all 171 LAW glasses as well as fitted to the modeling subset of 86 glasses.

In the model development work, Model 4 was considered next to assess whether the three crossproduct effects are temperature dependent. However, Table 7.9 shows for the fit to the data

for all 171 LAW glasses that three of the six added crossproduct terms are statistically nonsignificant at the 95% confidence level. For the fit to the modeling subset of 86 glasses, five of the six crossproduct terms are statistically nonsignificant. Models 5 and 6 investigated dropping one and two, respectively, of the  $x_i x_j / (T/1000)$  terms with the goal of having all remaining  $x_i x_j$  and  $x_i x_j / (T/1000)$  terms statistically significant. This goal was achieved with the 26-term Model 6 when fitted to the data from all 171 LAW glasses, but not when fitted to the 86-glass modeling subset. Hence, it was decided that none of the three crossproduct terms were strongly temperature dependent, and that the 25-term Model 3 would be recommended. The results for this model are discussed in the following section.

## 7.5 Results for the Recommended 25-Term Electrical Conductivity Model

Section 7.5.1 presents the results for the recommended 25-term EC model fitted to the 171-glass modeling dataset. Section 7.5.2 presents the validation results for the 25-term model.

### 7.5.1 Results for the Recommended 25-Term Electrical Conductivity Model Fitted to the 171-Glass Modeling Dataset

The 25-term model of the form in Equation (7.2) was fitted to the EC data for the 171 glasses in the modeling set using the PROC MIXED procedure in SAS (2005) to perform the GLS regression required for the EC data structure. Table 7.10 lists the fitted model coefficients, the coefficient standard deviations, and estimates of the  $\sigma_G$  and  $\sigma_T$  error standard deviations (see Section 7.2.2).

The upper right portion of Table 7.10 shows that the 25-term EC model fits the 171-glass modeling dataset with  $R^2 = 0.951$ , meaning that 95.1% of the variation in  $\ln(\varepsilon)$  values is accounted for by the model. This  $R^2 = 0.951$  for the 25-term Model 3 is a noticeable improvement over the  $R^2 = 0.923$  for the 22-term Model 2 discussed in Section 7.3.2. The RMSE = 0.151 for Model 3 is smaller than the RMSE = 0.189 for Model 2. Hence, Model 3 in Table 7.10 clearly fits the modeling data better than does Model 2 in Table 7.8.

The quantity  $\sqrt{\hat{\sigma}_G^2 + \hat{\sigma}_T^2} = \sqrt{(0.1431)^2 + (0.0571)^2} = 0.1541$  is an estimate of the total uncertainty in an EC determination for a given glass and temperature, under the assumption that the 25-term model does not have a significant LOF. A significant model LOF would inflate this quantity and it would over-estimate the true total uncertainty in an EC determination. However, it is slightly less than the overall pooled estimate of uncertainty SD = 0.164 (in the bottom right corner of Table 7.4) calculated from replicate data that is not impacted by model LOF. Hence, the 25-term model does not seem to have a significant model LOF given the inherent uncertainty in the data.

A histogram and normal probability plot of the standardized residuals for the fit of the 25-term model in Table 7.10 to the 171-glass ILAW EC modeling dataset were generated, although they are not shown in this report. These two plots do not show any significant departure



from normality, which is required to utilize the statistical interval formulas for model prediction uncertainties that are discussed subsequently.

The predicted versus measured plot and the standardized residual plot for the 25-term  $\ln(\epsilon)$  model are given in Figures 7.14 and 7.15, respectively. Figure 7.14 shows relatively tight scatter about the 45° line representing perfect prediction, with significantly outlying data for LAWM30 and moderately outlying data for LAWM40. Figure 7.14 shows that the 22-term Model 2 problem of over-predicting low EC values (below about  $-3 \ln(\text{S/cm}) = 0.050 \text{ S/cm}$ ) has been corrected by the 25-term Model 3. Figure 7.15 shows a tendency for the 25-term EC model to under-predict EC (represented by positive standardized residuals<sup>15</sup>) for many of the HiCrP glasses (see Section 2.5). However, the prediction errors for those glasses are still within the applicable uncertainties.

The response trace plots (see Section C.5.1) for EC at 950, 1050, 1150, and 1250°C produced using the 25-term model are given in Figures 7.16a to 7.16d. These figures are very similar to the ones for the 22-term model, with Na<sub>2</sub> and Li<sub>2</sub>O having very strong increasing effects on EC and SiO<sub>2</sub> having a strong decreasing effect on EC. CaO also has a decreasing effect on EC, but it gets smaller as the temperature increases. These response trace plots for the 25-term model in Figures 7.16a to 7.16d look nearly identical to the ones for the 22-term model in Figures 7.11a to 7.11d. However, this is to be expected because response trace plots show the effects of changes in individual components on a response variable, not the effects of changing two components (which is what the crossproduct terms in 25-term model represent).

### 7.5.2 Validation Results for the Recommended 25-Term Electrical Conductivity Model

Performance statistics for the 25-term ILAW EC model when applied to the five modeling/validation splits formed from the 171-glass modeling dataset are given in the bottom part of Table 7.10. The columns are labeled DS1, DS2, DS3, DS4, and DS5 to denote the five modeling/validation splits of the data as described in Section 7.1.2. The last column of this part of Table 7.10 presents averages of the modeling ( $R^2$ , SSE, and RMSE) and validation ( $R^2_v$  and  $\text{RMSE}_v$ ) statistics over the five data-splits. The average modeling statistics  $R^2 = 0.952$  and  $\text{RMSE} = 0.149$  are similar to those statistics from fitting the model to the 171-glass EC modeling dataset. The average validation statistics  $R^2_v = 0.936$  and  $\text{RMSE} = 0.162$  from the data-splitting approach are only slightly worse (i.e., smaller and larger, respectively) than the values when fitting the EC data from all 171 glasses in the modeling set or the modeling subsets from data-splitting. In general, the data-splitting results show that the 25-term model in Table 7.10 maintains the level of its predictive performance when applied to validation data within the same composition region as used to develop the model.

Performance statistics from fitting the 25-term EC model to the 86-glass modeling subset and validating using the remaining 85 glasses are given on the right hand side of Table 7.10.

---

<sup>15</sup> It is long-term statistical practice, almost universally used in software, to define residuals as “measured – predicted”. That is why positive standardized residuals indicate that the model under-predicts the measured values.

Fitting the 25-term model to the 86-glass modeling subset yields  $R^2 = 0.947$ , which is similar to the  $R^2 = 0.951$  from fitting the model to the full 171-glass EC dataset. The  $RMSE = 0.175$  for the 86-glass modeling subset is somewhat worse than the  $RMSE = 0.151$  from the full 171-glass modeling dataset. The  $R^2_v = 0.939$  and  $RMSE_v = 0.142$  statistics for the 85-glass validation subset are, respectively, similar to and slightly better than, the corresponding values from data-splitting. Together, these results indicate that the 25-term EC model maintains its predictive performance fairly well even when partitioning the data in half for model fitting and validation.

Performance statistics from fitting the 25-term EC model to the 171-glass modeling subset and validating using the 10 outlying glasses are given on the right hand side of Table 7.10. The  $R^2_v = 0.920$  and  $RMSE_v = 0.178$  statistics for the 10 outlying glasses are only slightly worse than the corresponding average validation statistics from data-splitting and the corresponding data-partition validation statistics. Together, these results indicate that the 25-term EC model maintains its predictive performance fairly well even with some extrapolation in glass composition.

Figures 7.17 and 7.18 show predicted versus measured plots when the 25-term ILAW EC model for  $\ln(EC)$  is applied to two validation datasets. Figure 7.17 results from fitting the 25-term model to a subset of 86 out of 171 modeling glasses, and then applying the resulting model to the remaining subset of 85 glasses for validation (see Section 7.1.3). Figure 7.18 results from fitting the 25-term model to all 171 glasses in the EC modeling set and then applying that model to the 10 outlying glasses with EC results (see Section 7.1.4). Also shown in Figures 7.17 and 7.18 are 95% PIs representing the model prediction uncertainty of single EC determinations for each glass at one temperature (see Sections C.6 and C.7 of Appendix C). If the error bar for a validation point overlaps the 45° line, that means the predicted and measured  $\ln(\varepsilon)$  values are within model and measurement uncertainty of each other. Note that the error bars include the estimated uncertainties  $\hat{\sigma}_G$  and  $\hat{\sigma}_T$  resulting from the structure of the EC data. The 95% PIs in Figures 7.17 and 7.18 for the 25-term model are slightly narrower than the ones in Figures 7.12 and 7.13 for the 22-term model. The 25-term model does not appear to have a significant LOF, thus the width of the 95% PIs should be due primarily to the experimental uncertainty in fabricating glasses and measuring EC (and model uncertainty that results). Separate work to assess the consequences of LOF (if any) and prediction uncertainty for this recommended EC model is discussed further in Section 7.7.

Figure 7.17 shows that the 25-term EC model for  $\ln(EC)$  fitted to the 86-glass modeling subset predicts EC fairly accurately at the four temperatures each for nearly all of the 85-glass validation subset. The model tends to under-predict some of the largest EC values. The 25-term model has corrected the tendency of the 22-term model to under-predict the smallest EC values. Also, the 95% PIs for the 25-term model overlap the 45° line (i.e., contain the measured values) for all but 4 of the 340 (= 4 temperature values at each of 85 glasses) observations in the validation subset. Failure of  $100(4/340) = 1.2\%$  of the 95% PIs to include the corresponding measured values is even lower than what would be expected by chance. Hence, the 25-term model is validated very well using this data-partition approach.

Figure 7.18 shows the predictive performance of the 25-term EC model for  $\ln(EC)$  fitted to the 171-glass modeling dataset and applied to the set of 10 outlying glasses with EC data that

were excluded from the modeling dataset. The 25-term model tends to under-predict most of the observations, but not significantly. The predictions are sufficiently close to the measured values and the 95% PIs are sufficiently wide (despite being slightly narrower than for the 22-term model) that all but two of the 95% PIs contain the corresponding measured values.

## 7.6 Example Illustrating Electrical Conductivity Model Predictions and Statistical Intervals

This section contains examples to illustrate using the 22-term Arrhenius-LM model and the 25-term “Arrhenius-LM plus three crossproduct terms” model, to obtain predicted EC values and corresponding 90% lower confidence intervals (LCIs), 90% upper confidence intervals (UCIs), and two-sided 90% confidence intervals (CIs) as described in Section C.7 of Appendix C. The 25-term model is the one recommended in Section 7.4 and discussed in detail in Section 7.5. However, calculations are also performed in this section for the 22-term model for comparison purposes. The 90% confidence levels associated with LCIs, UCIs, and CIs were chosen for illustration purposes only. The WTP project can use an appropriate confidence level depending on the use of the EC-composition-temperature model and the type of statistical uncertainty expression desired.

The glass composition used in this example is LAWA126, which is one of the glasses in the ILAW Existing Matrix. The 18-component composition of LAWA126 for EC modeling is given in Table 7.2 in mass fraction format. To apply the two EC models to this composition, the mass fractions of the 18 components must be converted to mass fractions (that sum to 1.0) of the 11 LAW glass components contained in both models. Mass fractions of the relevant components are then multiplied to obtain the three crossproduct terms of the 25-term model. Table 7.11 contains the composition of LAWA126 prepared for use in the two ILAW EC models.

For each of the EC models, predicted  $\ln(\text{EC}, \text{S/cm})$  values are obtained by multiplying the composition in the format needed for that model by the coefficients for that model, then summing the results. That is, the predicted values are calculated by

$$\hat{y}(\mathbf{a}) = \mathbf{a}^T \mathbf{b}$$

where  $\mathbf{a}$  is a vector with entries corresponding to terms in a given model based on the LAWA126 composition and a specific temperature value (in Kelvin), the superscript T represents a matrix transpose (or vector transpose in this case), and  $\mathbf{b}$  is the vector of coefficients for a given model. The predicted  $\ln(\text{EC})$  values for LAWA126 at 1143°C<sup>16</sup> using each of the ILAW EC models are listed in the second column of Table 7.12. The predicted  $\ln(\text{EC})$  values in  $\ln(\text{S/cm})$  units are easily converted to EC values (S/cm) by exponentiation. The third column of Table 7.12 contains the predicted EC values (S/cm). However, as discussed in Section C.7 of Appendix C, these back-transformed EC predictions in S/cm should be considered estimates of the true median (not the true mean) of the distribution of EC values that would result if EC measurements at the

---

<sup>16</sup> The temperature of 1143°C was chosen because it was one of the temperatures at which the EC of LAWA126 was measured. This facilitates comparison of the predicted and measured values.

specific temperature were repeated multiple times on separately batched and melted samples of the LAWA126 glass composition.

The predicted ILAW EC values for LAWA126 at 1143°C in Table 7.12 are 0.376 S/cm for the 22-term EC model and 0.400 S/cm for the recommended 25-term model. The predicted value using the 22-term model is closest to the measured value of 0.373 S/cm for LAWA126 at 1143°C, although the predicted value using the recommended 25-term model is very close.

Equations (C.27c), (C.28c), and (C.29c) can be used to calculate, respectively, a 90% UCI, a 90% LCI, or a two-sided 90% CI for the true mean of  $\ln(\text{EC})$  values for the LAWA126 glass composition at a specific temperature with each of the ILAW EC models. In the notation of these equations:

- $100(1-\alpha)\% = 90\%$ , so that  $\alpha = 0.10$  for a 90% UCI, a 90% LCI, and a 90% CI in Equations (C.27c), (C.28c), and (C.29c), respectively.
- The vector  $\mathbf{a}$  contains entries corresponding to the terms in a given EC model, which are calculated using the composition of LAWA126 in Table 7.11 and a specific temperature value.
- Matrix  $\mathbf{A}$  is formed from the data matrix used in the regression that generated a given EC model. Matrix  $\mathbf{A}$  has the number of rows in the EC modeling dataset ( $684 = 171 \times 4$  temperatures each) and the number of columns corresponding to the number of terms in a given EC model. Each column is calculated according to the corresponding term in the model using the LAW glass compositions and the actual (not nominal or intended) temperatures in the EC modeling dataset.
- Matrix  $\hat{\mathbf{V}}$  is the estimated variance-covariance matrix for the vector of EC-at-temperature data used to fit an EC model. This matrix accounts for the two sources of uncertainty, as discussed in Section C.3.3 of Appendix C.

To calculate a 90% UCI or LCI in  $\ln(\text{EC})$  units of  $\ln(\text{S/cm})$ , the quantity  $t_{1-\alpha, n-p} \sqrt{\mathbf{a}^T (\mathbf{A}^T \hat{\mathbf{V}}^{-1} \mathbf{A})^{-1} \mathbf{a}}$  is added to (UCI) or subtracted from (LCI) the predicted  $\ln(\varepsilon)$  [denoted  $\hat{y}(\mathbf{a})$ ] described above. The calculations are given by Equation (C.27c) for an UCI and Equation (C.28c) for a LCI. To calculate a two-sided CI, the quantity  $t_{1-\alpha/2, n-p} \sqrt{\mathbf{a}^T (\mathbf{A}^T \hat{\mathbf{V}}^{-1} \mathbf{A})^{-1} \mathbf{a}}$  is subtracted from and added to the predicted  $\ln(\eta)$  [denoted  $\hat{y}(\mathbf{a})$ ], as indicated by Equation (C.29c). The  $(\mathbf{A}^T \hat{\mathbf{V}}^{-1} \mathbf{A})^{-1}$  portion of these expressions is an approximate estimate of variance-covariance matrix for the estimated model coefficients, as discussed near the end of Section C.7 of Appendix C. The variance-covariance matrices for the 22-term and 25-term EC models are respectively listed in Tables D.8 and D.9 of Appendix D. The quantity  $\sqrt{\mathbf{a}^T (\mathbf{A}^T \hat{\mathbf{V}}^{-1} \mathbf{A})^{-1} \mathbf{a}}$  is the standard deviation of a model prediction; the value for each model is given in the fourth column of Table 7.12.

The 90% LCI, 90% UCI, and 90% CI values for the true mean  $\ln(\text{EC})$  in units of  $\ln(\text{S/cm})$  for the LAWA126 composition at a temperature of 1143°C based on the two ILAW EC models are given in the fifth, seventh, and ninth columns of Table 7.12. Exponentiating the resulting 90% LCIs, UCIs, and CIs for the mean EC values in  $\ln(\text{S/cm})$  units yields 90% LCIs, UCIs, and CIs for the median EC (S/cm). These values are in the sixth, eighth, and tenth columns of Table 7.12. For example, the recommended 25-term EC model has  $(-0.962, -0.872)$   $\ln(\text{S/m})$  as the two-sided 90% CI on the true mean  $\ln(\text{EC})$  for LAWA126 at 1143°C. Then  $(e^{-0.962}, e^{-0.872}) = (0.382, 0.418)$  S/cm is the two-sided 90% CI on the true median EC for LAWA126 at 1143°C.

## 7.7 Suitability of the Recommended Electrical Conductivity Model for Application by the WTP Project

The 25-term model for EC discussed in Section 7.5 is recommended for use by the WTP project as the best model currently available for predicting EC for LAW glasses. This model appears to yield unbiased predictions of EC over the full range of measured EC values, with relatively tight scatter for most data points about the fitted model, and moderate scatter for some data points (see Figure 7.14). The recommended EC model does not appear to have a statistically significant LOF, so that EC predictions can be expected to be within the uncertainty of what would be obtained by batching and melting glasses and measuring the EC.

The magnitudes of uncertainties in EC model predictions should be small enough that they will not unduly restrict the formulation and processing of LAW glasses in the WTP facility. Figure 7.19 displays the  $\ln(\text{EC})$  prediction standard deviations versus predicted values [both in  $\ln(\text{S/cm})$  units] for the LAW glass compositions in the EC modeling dataset at temperatures of 950, 1050, 1150, and 1250°C. The  $\ln(\text{EC})$  prediction standard deviations for EC modeling dataset glasses at these temperatures range from approximately 0.02 to 0.10  $\ln(\text{S/cm})$  for the recommended EC model. Note that prediction standard deviations will be larger for LAW glass compositions as their distance from glasses in the EC modeling dataset increases. Also, the total uncertainty in predictions with the recommended EC model will depend on the type of statistical interval used (see Section C.7 of Appendix C).

Work to assess the impact of LAW glass composition and model uncertainties for the recommended EC  $\ln(\epsilon)$  model (Section 7.5) on satisfying WTP ILAW processing requirements is planned to be addressed as part of the Technical Scoping Statement (TSS) B-6069 work scope of the River Protection Project—Waste Treatment Plant Support Program at PNNL. The impacts of these uncertainties on glass formulation and processability are also planned to be addressed as part of the second iteration of the LAW glass formulation algorithm development work being conducted by WTP project staff. The impacts on glass formulation and processability are also planned to be addressed as part of the second iteration of the LAW glass formulation algorithm development work planned by WTP project staff. The first iteration of that work (Vienna 2005) utilized a preliminary EC model (Feng et al. 2004) and the LAW glass formulation correlation (Muller et al. 2004b).

## **SECTION 8 MODELS RELATING VISCOSITY TO LAW GLASS COMPOSITION AND TEMPERATURE**

This section documents the development and validation of property-composition-temperature models and corresponding uncertainty expressions for predicting the viscosity (denoted  $\eta$ ) for low-activity waste (LAW) glasses. Because viscosity is a property of a glass melt, it is a function of glass melt temperature as well as glass composition. The property-composition-temperature models and corresponding uncertainty expressions for viscosity presented in this section were developed and validated using glass composition, temperature, and viscosity data collected on simulated LAW glasses. Viscosity was not measured on any of the glasses made from actual waste samples that are discussed in Section 2.7.

The 171 simulated LAW glasses used for viscosity model development and validation (from the database of 181 glasses) are discussed in Section 8.1. Section 8.2 lists the model forms for viscosity that were investigated. Section 8.3 presents the results for viscosity models with the two parameters of the truncated-T2 equation (for temperature dependence) expressed as linear mixture models in composition. Section 8.4 presents the results for viscosity models of the form considered in Section 8.3 plus quadratic (squared and crossproduct) terms. Section 8.5 presents the model fit and validation results for the recommended 26-term viscosity model. Section 8.6 illustrates the calculation of viscosity predictions and the uncertainties in those predictions using selected viscosity models and corresponding uncertainty equations. Section 8.7 discusses the suitability of the recommended viscosity model for use by the WTP project. Appendix C discusses the statistical methods and summary statistics used to develop, evaluate, and validate the several viscosity model forms investigated, as well as statistical equations for quantifying the uncertainties in viscosity models.

### **8.1 Viscosity Data Used for Model Development and Validation**

The data used for developing viscosity models are discussed in Section 8.1.1. The approaches and data used for validating the models are discussed in Sections 8.1.2 to 8.1.4.

#### **8.1.1 Viscosity Model Development Data**

The data available for developing viscosity-composition-temperature models consist of composition, temperature, and viscosity data from 181 LAW glasses (see Section 4.3). These glasses are discussed and their target compositions are presented in Section 2. The normalized compositions of these glasses based on analyzed (or estimated analyzed) SO<sub>3</sub> values are discussed in Section 3.3. The corresponding viscosity (poise, P) at temperature values are presented in Table 4.6. The LAW viscosity data are discussed in Section 4.4.

## Assessment of Available Glasses with Viscosity Data

As mentioned in Section 7.1, the same 181 LAW glasses comprising the EC modeling set also comprise the viscosity modeling set. Hence, the assessment of available glass compositions with viscosity data is the same as the assessment for EC data in Section 7.1.1. As a brief summary, there are 181 simulated LAW glass compositions with viscosity and electrical conductivity data, 10 of which were identified as outlying or non-representative. Thus, the viscosity modeling set includes data on 171 LAW glasses. A total of 18 LAW glass components had sufficient ranges and distributions of values to support terms in initial viscosity modeling work. These components are Al<sub>2</sub>O<sub>3</sub>, B<sub>2</sub>O<sub>3</sub>, CaO, Cl, Cr<sub>2</sub>O<sub>3</sub>, F, Fe<sub>2</sub>O<sub>3</sub>, K<sub>2</sub>O, Li<sub>2</sub>O, MgO, Na<sub>2</sub>O, P<sub>2</sub>O<sub>5</sub>, SO<sub>3</sub>, SiO<sub>2</sub>, TiO<sub>2</sub>, ZnO, ZrO<sub>2</sub>, and Others (the sum of all remaining components). Note that these are the same 18 components chosen for initial PCT and VHT (as well as EC) modeling work. Several pairwise correlations (see Section 7.1.1) among these components are larger (in absolute value) than 0.60 and thus may make it difficult for regression methods to properly separate the effects of the components on viscosity. Thus, these high pairwise correlations need to be kept in mind in developing ILAW property-composition models for viscosity.

## Viscosity Modeling Dataset

The LAW glass compositions in the viscosity modeling dataset are the same as the EC modeling dataset, which are listed in Table 7.2. The table contains the Glass ID, Group ID, and normalized glass compositions for the 171 simulated LAW glasses in the 18-component forms used for EC and viscosity model development. The Group ID column of Table 7.2 indicates the subset of data that each glass is associated with (see Sections 2.1 to 2.7). The glass compositions in Table 7.2 are the normalized mass fractions (mf) of the 18 components previously identified as having sufficient data to support a separate model term if needed. The mass fraction values of the 18 components shown in Table 7.2 were normalized so that they sum to 100% for each of the glasses (see Section 3.3).

Table 8.1 contains the measured viscosity at temperature pairs for the 171 glasses in the viscosity modeling dataset. Viscosity was measured at four temperatures for all LAW glasses except for LAWM7, which had viscosity measured at five temperatures. Table 8.1 also includes a column designating the data-splitting validation subsets for viscosity modeling and validation. These subsets and the data-splitting validation approach are discussed in Section 8.1.2.

The values of viscosity in Table 8.1 range from 5.99 to 2329.04 P. Smaller values of viscosity tend to occur at higher temperatures and larger values tend to occur at lower temperatures.

## Replicate and Near-Replicate Viscosity Data

The changes to the LAW glass compositions caused by the renormalization associated with using XRF analyzed (or estimates of XRF analyzed) SO<sub>3</sub> values (see Section 3.3) resulted in some replicate glasses not having exactly equal compositions. Such compositions are referred to as near-replicates. For ease of discussion, henceforth both replicates and near-replicates are referred to as replicates.

Table 8.2 lists the replicate sets of glasses in the ILAW viscosity modeling dataset and the corresponding viscosity values associated with the four temperatures at which viscosity was measured for each glass. The top portion of Table 8.2 lists the viscosity values corresponding to actual temperature values, which differ somewhat from the nominal values of 950, 1050, 1150, and 1250°C within replicate sets. The bottom portion of Table 8.2 lists interpolated values of viscosity at the four nominal temperature values. The interpolated values were obtained by fitting the T2 equation to the (temperature, viscosity) data for each glass (see Section C.2.1 of Appendix C) and then calculating viscosity at the nominal temperature values.

Table 8.2 also lists estimates of %RSDs [calculated using viscosity values in original P units] and SDs [calculated from  $\ln(\eta)$  values in  $\ln(P)$  units] for each replicate set and nominal temperature. Pooled estimates of %RSDs and SDs are given over the (i) temperatures for a given replicate set, (ii) replicate sets for a given temperature, and (iii) all replicate sets and temperatures. A pooled %RSD or SD combines the separate %RSD or SD estimates so that a more accurate combined estimate of the %RSD or SD is obtained. These pooled %RSDs and SDs include uncertainties due to fabricating glasses and measuring viscosity. As discussed in Section 8.2.2, viscosity data are subject to two sources of uncertainty whose standard deviations are denoted  $\sigma_G$  and  $\sigma_T$ . These parameters are expressed in  $\ln(P)$  units because natural logarithms of viscosity values are modeled (see Section 8.2.2). The SDs given in Table 8.2 are estimates of  $\sqrt{\sigma_G^2 + \sigma_T^2}$ , the total standard deviation of a viscosity determination for a given glass and temperature. The pooled estimates of replicate uncertainty for viscosity in Table 8.2 are used subsequently to assess lack-of-fit (LOF) of the various models considered.

The %RSD and SD values in the top portion of Table 8.2 may over-estimate the uncertainty in viscosity values because the viscosity values of replicate sets are not exactly at the same temperature values. The %RSD and SD values in the bottom portion of Table 8.2 may under-estimate the uncertainty in viscosity values because the interpolated viscosity values may “remove” some of the natural variation in the data that is the basis for uncertainty estimation. The %RSD and SD values in Table 8.2 are noticeably larger in the top portion of the table compared to the bottom portion. In the top portion of Table 8.2, the overall pooled SD = 0.139 [calculated from  $\ln(P)$  values] and %RSD = 13.81 [calculated from P values]. In the bottom portion of Table 8.2, the overall pooled SD = 0.084 [calculated from  $\ln(P)$  values] and %RSD = 8.39 [calculated from P values]. These indicate that the relative uncertainty in viscosity measurements over replicate glasses is between 8.4 and 14%. In the subsequent discussion, compromise values of SD = 0.11 (%RSD = 11%) are used, chosen as being roughly half-way between the two estimates.

### 8.1.2 Primary Viscosity Model Validation Approach and Data

The primary model validation approach for viscosity modeling was based on splitting the 171-glass dataset for model development into five modeling/validation subsets. Of the 171 model development glasses, 12 were intended to be replicates (6 replicate pairs). The five



modeling/validation splits of the 171 glasses in the viscosity modeling dataset were formed as follows.

- The six pairs of replicates (12 glasses) were set aside so they would always be included in each of the five model development datasets. This was done so that replicate pairs would not be split between modeling and validation subsets, thus negating the intent to have validation glasses different than model development glasses.
- The remaining  $171 - 12 = 159$  glasses were ordered from smallest to largest according to their average viscosity values across the four temperatures (5 temperatures in the case of LAWM7). The 159 glasses were numbered 1, 2, 3, 4, 5, 1, 2, 3, 4, 5, etc. All of the 1's formed the first model validation set, while all of the remaining points formed the first model development dataset. Similarly, all of the 2's, 3's, 4's, and 5's respectively formed the second, third, fourth, and fifth model validation sets. In each case, the remaining non-2's, non-3's, non-4's, and non-5's formed the second, third, fourth, and fifth model development datasets. Because 159 is not evenly divisible by 5, the five modeling and validation subsets did not all contain the same numbers of glasses. Four of the five splits contained 32 glasses for validation and 127 glasses for modeling. The fifth split contained 31 glasses for validation and 128 for modeling. Note that these numbers of glasses in the modeling subsets do not include the replicates.
- The 12 replicate glasses were added to each of the split modeling subsets. Including the replicates, four splits contained 139 glasses for modeling and 32 for validation, while the fifth split contains 140 glasses for modeling and 31 for validation. The last column of Table 8.1 specifies the validation subsets for the five modeling/validation splits in the primary validation approach for viscosity model development.

Data splitting was chosen as the primary validation approach because the viscosity modeling dataset contains all compositions that (i) are in the ILAW composition region of interest, (ii) meet quality assurance (QA) requirements, and (iii) have viscosity data. Having a separate validation dataset not used for modeling is desirable, but that desire was over-ridden by wanting viscosity models developed with all appropriate data.

### **8.1.3 Secondary Viscosity Model Validation Approach and Data**

The secondary model validation approach consisted of partitioning the 171-glass viscosity modeling dataset into a modeling subset of 86 glasses and a validation subset of 85 glasses. The relevant discussion is the same as for electrical conductivity given in Section 7.1.3.

### **8.1.4 Limited Extrapolative Viscosity Model Validation Data**

The 10 glasses excluded from the viscosity and EC modeling sets (see the discussion in Section 7.1.1) were used to perform a limited assessment of the extrapolative prediction performance of the viscosity models. The normalized compositions of these 10 glasses are given

in Table 7.5 and the corresponding viscosity at temperature values are given in Table 8.3. Typical summary statistics and predicted versus measured plots are used to assess the extrapolative performance of viscosity models for the 10 glasses listed in Table 7.5 and their viscosity values listed in Table 8.3.

## 8.2 Viscosity Model Forms

Ideally, a property-composition-temperature model for viscosity would utilize known mechanisms of viscosity as a function of glass composition and melt temperature. No such mechanisms are known, although there is considerable experience regarding the temperature dependence of viscosity over the range of 950 to 1250°C. Section 8.2.1 discusses the investigations performed to select an equation to represent the temperature dependence of viscosity. Sections C.1 and C.2 of Appendix C discuss mixture experiments and several general model forms in which mixture experiment models are used to expand the parameters of viscosity-temperature equations. Section 8.2.2 discusses the forms of viscosity-temperature models investigated. Section 8.2.3 discusses the use of transformed viscosity values as the response variable for viscosity modeling.

### 8.2.1 Temperature Dependence of Viscosity

Three equations discussed in Section C.2.1 of Appendix C were considered for representing the temperature dependence of viscosity. These are the *Arrhenius equation* [Equation (C.8)], the *T2 equation* [Equation (C.9)], and the *truncated-T2 equation* [Equation (C.10)]. The viscosity at temperature observations for each of the 171 glasses in the viscosity modeling dataset were used to fit each of these three equations. Goodness of fit statistics were calculated and compared. The Arrhenius equation (which represents a linear relationship between  $\ln(\eta)$  and  $1/T$  (where  $T$  is temperature in Kelvin) was adequate for less than half of the glasses. The truncated-T2 equation was better for more than half of the glasses, because of curvature in plots of  $\ln(\eta)$  and  $1/T$  for many glasses. Only two glasses (LAWM33R1 and LAWM40) had sufficient curvature that the T2-equation was significantly better than the truncated-T2 equation. There were approximately 35 out of 171 LAW glasses that showed moderate improvement from using the T2 equation instead of the truncated-T2 equation. However, the curved fit of the truncated-T2 equation to the  $(1/T, \text{viscosity})$  values for those glasses were not much different than the curved fit of the T2 equation. Hence, it was decided that the truncated-T2 equation was sufficient to represent the temperature dependence of viscosity for LAW glasses.

### 8.2.2 Model Forms for the Temperature and Composition Dependence of Viscosity

The model forms considered for viscosity start with a slightly modified version of the truncated-T2 equation and expand its two parameters as functions of LAW glass composition. Linear mixture (LM) model forms and partial quadratic mixture (PQM) model forms (see

Section C.1.1 of Appendix C) were considered for use in expanding the parameters of the truncated-T2 equation.

The viscosity model form with the parameters of a modified truncated-T2 equation expanded as LM models is given by

$$\ln(\eta) = \sum_{i=1}^q a_i x_i + E_G + \sum_{i=1}^q b_i \frac{x_i}{(T/1000)^2} + E_T. \quad (8.1)$$

The modification to the truncated-T2 equation is that temperature ( $T$  in Kelvin) is divided by the scaling factor of 1000 so that the  $b_i$  coefficients are similar in magnitude to the  $a_i$  coefficients. Except for the scaling factor, this equation is the same one given as Equation (C.14) and discussed in Section C.2.2 of Appendix C. The remaining notation is discussed following the subsequent model forms.

The viscosity model form with the composition-only parameter of the modified truncated-T2 equation expanded as a PQM model is given by

$$\ln(\eta) = \sum_{i=1}^q a_i x_i + \text{Selected} \left\{ \sum_{i=1}^q a_{ii} x_i^2 + \sum_{i < j}^{q-1} \sum_j^q a_{ij} x_i x_j \right\} + E_G + \sum_{i=1}^q b_i \frac{x_i}{(T/1000)^2} + E_T. \quad (8.2)$$

The viscosity model form with both parameters of the modified truncated-T2 equation expanded as PQM models is given by

$$\begin{aligned} \ln(\eta) = & \sum_{i=1}^q a_i x_i + \text{Selected} \left\{ \sum_{i=1}^q a_{ii} x_i^2 + \sum_{i < j}^{q-1} \sum_j^q a_{ij} x_i x_j \right\} + E_G \\ & + \sum_{i=1}^q b_i \frac{x_i}{(T/1000)^2} + \text{Selected} \left\{ \sum_{i=1}^q b_{ii} \frac{x_i^2}{(T/1000)^2} + \sum_{i < j}^{q-1} \sum_j^q b_{ij} \frac{x_i x_j}{(T/1000)^2} \right\} + E_T \end{aligned} \quad (8.3)$$

Equation (8.2) would be appropriate if there are quadratic compositional effects on viscosity that are not temperature dependent, whereas Equation (8.3) would be appropriate if the quadratic composition effects on viscosity are temperature dependent. Temperature (in Kelvin) is scaled by 1000 in Equations (8.2) and (8.3) for the reason discussed previously for Equation (8.1).

In Equations (8.1), (8.2), and (8.3):  $\ln(\eta)$  denotes the natural logarithm of viscosity [in units of  $\ln(P)$ ]; the  $x_i$  ( $i = 1, 2, \dots, q$ ) are mass fractions of  $q$  glass oxide or halogen components such that  $\sum_{i=1}^q x_i = 1$ ; the  $a_i$  and  $b_i$  ( $i = 1, 2, \dots, q$ ), and the  $a_{ii}$ ,  $a_{ij}$ ,  $b_{ii}$ , and  $b_{ij}$  (selected), are coefficients to be estimated from data;  $E_G$  is a random error associated with determining viscosity for each LAW glass; and  $E_T$  is a random error associated with determining viscosity at the temperature values of a given glass melt. The random errors  $E_G$  and  $E_T$  are assumed to be normally distributed with zero means and standard deviations  $\sigma_G$  and  $\sigma_T$ . These standard

deviations and the model coefficients are estimated simultaneously using generalized least squares (GLS) regression. See Section C.2.1 in Appendix C for additional discussion of  $E_G$  and  $E_T$ . See Sections C.3.2 and C.3.3 for additional discussion of GLS regression.

### 8.2.3 Transformation of Viscosity

In modeling viscosity, it is advantageous to use the natural logarithm of the viscosity values. The advantages of this transformation include:

- The viscosity values for the 171 LAW glasses in the viscosity modeling dataset range from 5.99 to 2329.04 P. This is a range of approximately 2.5 orders of magnitude difference. In such cases, typically the uncertainty in making glasses and measuring viscosity leads to smaller absolute uncertainties for smaller viscosity values and larger absolute uncertainties for larger viscosity values. Hence, the unweighted least squares (ULS) regression assumption of equal variances for all response variable values (see Section C.3 of Appendix C) is violated. After a logarithmic transformation, variances of response values tend to be approximately equal as required for ULS regression.
- A logarithmic transformation tends to linearize the compositional dependence of viscosity data and reduce the need for non-linear terms in the model form.
- A natural logarithm transformation is preferred over a common logarithm (or other base logarithm) transformation because of the approximate relationship

$$\text{SD} [\ln(y)] \cong \text{RSD} (y) \quad (8.4)$$

where SD denotes standard deviation, RSD denotes relative standard deviation (i.e., the standard deviation divided by the mean), and  $y$  denotes viscosity. Equation (8.4) results from applying the first-order variance propagation formula [Equation (7-7) of Hahn and Shapiro (1967)] to the function  $z = \ln(y)$ . The relationship in Equation (8.4) is very useful, in that uncertainties of the natural logarithm of the response variable  $y$  can be interpreted as RSDs of the untransformed response variable  $y$ .

For these reasons, the natural logarithmic transformation was employed for all viscosity model forms.

## 8.3 Model Results for ILAW Viscosity with the Truncated-T2 Equation Parameters Expanded as Linear Mixture Models

This section discusses the results of fitting two truncated T2-linear mixture models using natural logarithms of LAW viscosity [denoted  $\ln(\eta)$ ] as the response variable. These models are of the forms given in Equation (8.1). Section 8.3.1 presents the results from fitting a model consisting of the truncated-T2 equation with its parameters expanded using LM terms for each of

the 18 components determined to have sufficient support in the 171-glass modeling set. Section 8.2.3 discusses the methods used to develop truncated T2-LM models with reduced numbers of LAW glass components. Section 8.3.3 presents the results from fitting two models consisting of the truncated-T2 equation with its parameters expanded using reduced 12-component and 11-component LM models.

To perform the GLS model fits (see Section 8.2.2 and Section C.3.2 of Appendix C), PROC MIXED in SAS (2005) was used. For each model fit, output files produced by SAS were used as an input file to perform the remaining model evaluation and validation calculations using software codes written in R (Ihaka and Gentleman 1996, R Core Development Team 2006).

### 8.3.1 Results for 36-Term Viscosity Model with the Truncated-T2 Equation Parameters Expanded as 18-Component Linear Mixture Models

As the initial step in viscosity model development, the truncated T2-LM model in Equation (8.1) with  $q = 18$  components identified in Section 8.1.1 was fit to the modeling data (171 glasses). The response was the natural logarithm of viscosity (P). This 36-term model form was a reasonable starting point and provided a basis for appropriate model reductions.

Table 8.4 contains the results for the 36-term truncated T2-LM model for ILAW viscosity. Table 8.4 lists the model coefficients, standard deviations of the coefficients, and estimates of the  $\sigma_G$  and  $\sigma_T$  error standard deviations (see Section 8.2.2). Table 8.4 also contains model performance summaries for the 36-term model using the modeling dataset (171 glasses), the modeling data partitioned into modeling (86 glasses) and validation (85 glasses) subsets (see Section 8.1.3), and the 10 glasses excluded from the model dataset (see Section 8.1.4). The data-splitting approach was not used to validate this model because of the effort required to do so with GLS regression, and because it is just the first model in the viscosity model development process.

The summary statistics that describe how well the 36-term truncated T2-LM model fits the 171-glass viscosity modeling dataset are given in the upper right corner of Table 8.4. Only the  $R^2$ , sum of squared errors (SSE), and root mean square error (RMSE) statistics were calculated because of using GLS regression (see Section C.4 in Appendix C). The  $R^2 = 0.987$  statistic indicates that the 36-term truncated T2-LM model fits the viscosity modeling data quite well. For GLS regression, the  $SSE = 15.443$  and  $RMSE = 0.154$  statistics do not directly indicate the performance of the 36-term model, but are useful for comparison to the values for subsequently discussed models. The quantity  $\hat{\sigma}_{Total} = \sqrt{\hat{\sigma}_G^2 + \hat{\sigma}_T^2} = \sqrt{(0.1457)^2 + (0.0607)^2} = 0.1578$  is an estimate of the total uncertainty in a viscosity determination for a given glass and temperature, under the assumption that the 36-term model does not have a significant LOF. A significant model LOF would inflate  $\hat{\sigma}_{Total}$  and it would over-estimate the true total uncertainty in a viscosity determination. However, it is about 43% larger than the compromise overall pooled estimate of uncertainty  $SD = 0.11$  (see Section 8.1.1) calculated from replicate data that is not impacted by model LOF. Hence, the 36-term model may have some LOF, but it does not appear to be to highly significant given the inherent uncertainty in the data.

The 36-term viscosity model statistics from partitioning the 171-glass modeling set into subsets of 86 modeling glasses and 85 validation glasses (see Section 8.1.3) are given on the right side of Table 8.4. The fit statistics of  $R^2 = 0.991$  and  $RMSE = 0.134$  for the 86-glass modeling subset are slightly better than those for the full 171-glass modeling set. For the 85-glass validation subset,  $R^2_v = 0.858$  is significantly less than  $R^2$  and  $RMSE_v = 0.469$  is significantly greater than  $RMSE = 0.134$ . This significantly reduced validation performance is because the 86-glass subset of data provided insufficient support for all 18 components in the full LM model expansions of the truncated-T2 equation parameters, thus negatively affecting performance on the validation subset.

The statistics from fitting the 36-term viscosity model to the 171-glass modeling set and making extrapolative validation predictions for the 10 outlying glasses are given on the right side of Table 8.4. The statistic  $R^2_v = 0.977$  for the 10 outlying glasses is noticeably larger than  $R^2_v = 0.858$  from data partitioning, but this is explained by footnote (g) of Table 8.4. The  $RMSE_v = 0.198$  for the 10 outlying glasses is not much worse than the  $RMSE = 0.154$  for fitting the 171-glass modeling set. Hence, the 36-term model appears to predict quite well for the 10 outlying glasses, even though the predictions are extrapolations.

The predicted versus measured plot and the standardized residual plot for the 36-term truncated T2-LM model are given in Figures 8.1 and 8.2, respectively. Figure 8.1 shows moderate scatter about the 45° line representing perfect prediction, with no significantly outlying data apparent. Figure 8.1 does not show any tendency to over- or under-predict viscosity within any range of values. Figure 8.2 shows that the data for glasses LAWB77, LAWM27, and LAWE7 have standardized residuals greater than 4.0 in absolute value for at least one temperature. Figure 8.2 also shows the 36-term viscosity model tends to over-predict viscosity<sup>17</sup> for the Corr glasses (see Section 2.4).

The 36-term truncated T2-LM model for viscosity fits the 171-glass modeling dataset reasonably well and thus can provide guidance for reducing the model (i.e., removing separate terms for components that do not significantly influence viscosity). Hence, this model was used to produce a response trace plot (see Section C.5.1) at each of the four nominal temperatures at which viscosity was measured (950, 1050, 1150, and 1250°C) shown in Figures 8.3a to 8.3d. Note that the y-axis [predicted  $\ln(\eta, P)$ ] does not have the same scale and tic marks on each of the four plots. Using the same scale would have greatly condensed the individual plots and made it even more difficult to differentiate response traces of individual components. The response trace plots show that  $Li_2O$  and  $Na_2O$  have dominant decreasing effects on viscosity, while  $SiO_2$  and  $Al_2O_3$  have the strongest increasing effect on viscosity. Figures 8.3a to 8.3d also show that  $CaO$ ,  $B_2O_3$ , and  $MgO$  have strong decreasing effects on viscosity, with the effects getting stronger as temperature increases. Figures 8.3a to 8.3d also show some minor components such as Others,  $Cr_2O_3$ , F and Cl have response traces with large positive and negative slopes. Minor components such as these are not expected to have significant effects on viscosity, and hence

---

<sup>17</sup> It is long-term statistical practice, almost universally used in software, to define residuals as “measured – predicted”. That is why negative standardized residuals indicate that the model over-predicts the measured values.

these may be artifacts resulting from larger uncertainties in determining the coefficients and hence the effects of these components.

### **8.3.2 Development of Viscosity Models with the Truncated-T2 Equation Parameters Expanded as Reduced Linear Mixture Models**

In the 36-term truncated T2-LM model presented in Section 8.3.1, the some of the 18 components likely do not significantly contribute to predicting viscosity. Hence, model reduction was the next step of the model development approach. The two parameters of the truncated-T2 equation were expanded using LM models involving fewer than the 18 components. Two approaches were considered in reducing the full 36-term viscosity model discussed in Section 8.3.1. Each of these approaches and brief summaries of results are discussed in turn.

The first approach was to compare summary statistics from the fits (using the PROC MIXED routine in SAS 2005) of progressively reduced models to see if a particular reduced model form could be considered “best”. For this approach, at each iteration the component (among Cl, Cr<sub>2</sub>O<sub>3</sub>, F, P<sub>2</sub>O<sub>5</sub>, SO<sub>3</sub>.XRF, TiO<sub>2</sub>, and ZnO) that appeared to have the least significance in the model was subsequently removed (combined into the Others component) until all of the minor components had been removed. At each reduction step, PROC MIXED in SAS was used to fit a model based on the viscosity data structure. The Akaike Information Criterion (AIC) and the sum of squared errors (SSE) were determined for each of these reduced models. The AIC includes a penalty for increasing the number of coefficients estimated from the data, whereas the SSE does not (see Akaike 1974 for more discussion of the AIC). The results of progressively reduced truncated T2-LM models are portrayed in Figure 8.4, where the vertical axis represents the summary statistic of interest (AIC or SSE) and the horizontal axis shows the number of LAW glass components in the reduced models. Lower values are better for both of these statistics. From these plots (which must be viewed from right to left as the number of components is reduced) it is seen that each of these statistics increase whenever a component is dropped from a model. However, the increase in these statistics (which indicates a worsening of how well the model fits the data) is larger moving from 14 to 13 components, and much larger moving from 12 to 11 components. There seems to be a clear benefit to including 12 components over 11 components. Therefore, Table 8.5 presents a summary of the results for the 14-component (28-term) model and the 12-component (24-term) model. These two models are denoted Model 2 and Model 3, respectively. For comparison purposes, Table 8.5 also includes the results for the 36-term model, denoted Model 1, and other models discussed subsequently.

The second approach used to determine potential reduced model forms for LAW viscosity involved a model reduction algorithm. An automated algorithm for reducing the number of components in a LM model (see Section C.5.1 of Appendix C, Piepel and Cooley 2006) was applied to develop reduced models for ILAW PCT and VHT. However, it would take additional work to extend the algorithm to situations such as viscosity and EC where the properties depend not only on composition but also temperature. In lieu of doing that, it was decided to make use of several inputs to guide reduction of the viscosity models.

One such input was to fit the  $\ln(\text{viscosity})$  data with the truncated-T2 equation for each glass, treat the resulting “intercepts” and “slopes” as separate responses, fit full (18-component) LM models to each response (intercept and slope), and then separately apply the existing automated model reduction algorithm to the full LM models for intercept and slope. The reduced forms of the viscosity intercept and slope LM models were determined using the sequential F-test algorithm in R with the stopping criterion for the reduction loop set at either 0.05 or 0.01. Only combinations of components (not removal and renormalization) were allowed as reductions. The set of components that were allowed to combine included the minor components Cl, Cr<sub>2</sub>O<sub>3</sub>, F, P<sub>2</sub>O<sub>5</sub>, SO<sub>3</sub>.XRF, TiO<sub>2</sub>, ZnO, and Others. The remaining “main” components, Al<sub>2</sub>O<sub>3</sub>, B<sub>2</sub>O<sub>3</sub>, CaO, Fe<sub>2</sub>O<sub>3</sub>, K<sub>2</sub>O, Li<sub>2</sub>O, MgO, Na<sub>2</sub>O, SiO<sub>2</sub>, and ZrO<sub>2</sub>, were not allowed to combine. For the model reduction run having “slope” as the response, all 8 components that were allowed to combine did so when the reduction stopping criterion was set to 0.01. If the criterion was 0.05, the resulting reduced model involved two combined components (which is not a preferred stopping point). For the model reduction run having “intercept” as the response, the resulting reduced model form involved terms for each of the 10 main components, a term for P<sub>2</sub>O<sub>5</sub>, and one combined component formed from the other 7 minor components. This was the result even when 0.01 was used as the reduction stopping criterion.

The reduced truncated T2-LM model for ILAW viscosity having P<sub>2</sub>O<sub>5</sub> as a separate component (not combined into Others) was previously denoted as Model 3. The reduced model having all 8 minor components combined into a new Others component is denoted as Model 4, with summary statistics included in Table 8.5. Based on the summary statistics in Table 8.5, Model 3 (24 terms) and Model 4 (22 terms) are discussed in more detail in the following subsection.

### **8.3.3 Results for 24-Term and 22-Term Viscosity Models with the Truncated-T2 Equation Parameters Expanded as 12-Component and 11-Component Reduced Linear Mixture Models**

Tables 8.6 and 8.7 give the coefficients, coefficient standard deviations, and estimates of the  $\sigma_G$  and  $\sigma_T$  error standard deviations (see Section 8.2.2) for the 24-term and 22-term truncated T2-LM models of the form in Equation (8.1). These models were fitted to the viscosity data for the 171 glasses in the modeling set using the PROC MIXED procedure in SAS (2005). Tables 8.6 and 8.7 also provide performance statistics for the (i) modeling data, (ii) partition of the modeling data into 86-glass modeling and 85-glass validation subsets, and (iii) 10 LAW glasses excluded from the viscosity modeling set. Data splitting was not performed for these models because of the extra work to do so with GLS regression. The results for the 24-term model in Table 8.6 are discussed first, followed by a discussion of the 22-term model results in Table 8.7.

The statistics from fitting the 24-term truncated T2-LM model to the viscosity data from 171 glasses are given in the upper right corner of Table 8.6. The  $R^2 = 0.985$  and  $\text{RMSE} = 0.163$  statistics are only slightly worse than those for the full 36-term model. For the data partition into subsets of 86 modeling glasses and 85 validation glasses, the validation statistics  $R^2_V = 0.971$  and  $\text{RMSE}_V = 0.210$  are not much worse than the  $R^2$  and  $\text{RMSE}$  statistics from fitting the data



from all 171 glasses. From entries in Table 8.6, the quantity  $\hat{\sigma}_{Total} = \sqrt{\hat{\sigma}_G^2 + \hat{\sigma}_T^2} = \sqrt{(0.1540)^2 + (0.0616)^2} = 0.1659$  was calculated. It is an estimate of the total uncertainty in a viscosity determination for a given glass and temperature, under the assumption that the 24-term model does not have a significant LOF. A significant model LOF would inflate this quantity and it would over-estimate the true total uncertainty in a viscosity determination. For the 24-term model,  $\hat{\sigma}_{Total} = 0.1659$  is only slightly larger than  $\hat{\sigma}_{Total} = 0.1578$  for the 36-term model. However, it is about 51% larger than the compromise overall pooled estimate of uncertainty SD = 0.11 (see Section 8.1.1) calculated from replicate data that is not impacted by model LOF. Hence, the 24-term model may have some LOF, but it does not appear to be to highly significant given the inherent uncertainty in the data. Therefore, the 24-term model does not seem to have a significant model LOF. Together, these results indicate there is little consequence to reducing the viscosity model from 36 terms to 24 terms.

The statistics from fitting the 24-term viscosity model to the 171-glass modeling set and making extrapolative validation predictions for the 10 outlying glasses are given on the right side of Table 8.6. The statistic  $R^2_v = 0.972$  for the 10 outlying glasses is nearly identical to the  $R^2_v = 0.971$  from data partitioning. The  $RMSE_v = 0.218$  for the 10 outlying glasses is somewhat larger than the  $RMSE = 0.163$  for fitting the 171-glass modeling set, but is similar to the  $RMSE_v = 0.210$  for the partitioned validation subset. Hence, the 24-term model appears to predict quite well for the 10 outlying glasses, even though the predictions are extrapolations.

The predicted versus measured plot and the standardized residual plot for the 24-term truncated T2-LM model are given in Figures 8.5 and 8.6, respectively. Figure 8.5 shows moderate scatter about the 45° line representing perfect prediction, with no significantly outlying data. Figure 8.5 does not show any tendency to over- or under-predict viscosity within any range of values. Figure 8.6 shows that the data for glasses LAWB77, LAWM27, and LAWE7 have standardized residuals greater than 4.0 in absolute value for at least one temperature. Figure 8.6 also shows the 24-term viscosity model tends to over-predict<sup>18</sup> viscosity for the Corr glasses (see Section 2.4). In general, Figures 8.5 and 8.6 are very similar to the ones for the 36-term model in Figures 8.1 and 8.2.

The response trace plots (see Section C.5.1) for viscosity at 950, 1050, 1150, and 1250°C produced using the 24-term truncated T2-LM model are given in Figures 8.7a to 8.7d. These figures are very similar to the ones for the 36-term model, except the artifacts of minor components with steep response traces are no longer present because of combining those components into the Others component. The components Na<sub>2</sub>O and Li<sub>2</sub>O have very strong decreasing effects on viscosity, while SiO<sub>2</sub> has a strong increasing effect on viscosity. CaO also has a decreasing effect on viscosity that gets stronger as the temperature increases. Al<sub>2</sub>O<sub>3</sub> and P<sub>2</sub>O<sub>5</sub> have moderate increasing effects on viscosity, while B<sub>2</sub>O<sub>3</sub>, MgO, K<sub>2</sub>O, and Fe<sub>2</sub>O<sub>3</sub> have moderate decreasing effects on viscosity.

---

<sup>18</sup> It is long-term statistical practice, almost universally used in software, to define residuals as “measured – predicted”. That is why negative standardized residuals indicate that the model over-predicts the measured values.

Figures 8.8 and 8.9 show predicted versus measured plots when the 24-term truncated T2-LM model for ILAW viscosity is applied to two validation datasets. Figure 8.8 results from fitting the 24-term model to a subset of 86 out of 171 modeling glasses, and then applying the resulting model to the remaining subset of 85 glasses for validation (see Section 8.1.3). Figure 8.9 results from fitting the 24-term model to the data for all 171 glasses in the modeling set and then applying that model to the 10 outlying glasses with viscosity data (see Section 8.1.4). Also shown in Figures 8.8 and 8.9 are 95% prediction intervals (95% PIs) representing the model prediction uncertainty of single viscosity determinations for each glass at one temperature (see Sections C.6 and C.7 of Appendix C). If the error bar for a validation point overlaps the 45° line, that means the predicted and measured  $\ln(\eta)$  values are within model and measurement uncertainty of each other. Note that the error bars include the estimated uncertainties  $\hat{\sigma}_G$  and  $\hat{\sigma}_T$  resulting from the structure of the viscosity data. The 95% PIs in Figures 8.8 and 8.9 are relatively narrow for most glass-temperature combinations, but somewhat wider for other combinations. The width of the PIs is due to (i) whatever LOF there is of the 24-term truncated T2-LM model, and (ii) the experimental uncertainty in fabricating glasses and measuring viscosity.

Figure 8.8 shows that the 24-term viscosity model for  $\ln(\eta)$  fitted to the 86-glass modeling subset has relatively accurate predictive performance for the 85-glass validation subset. However, there is some tendency to over-predict for some glasses (including the Correlation glasses discussed previously). The 95% PIs for the 24-term model overlap the 45° line (i.e., contain the measured values) for all but 31 of the 340 (= 4 temperature values at each of 85 glasses) observations in the validation subset. Failure of  $100(31/340) = 9.1\%$  of the 95% PIs to include the corresponding measured values is somewhat more than the 5% that would be expected by chance. Hence, this suggests that the 24-term model may have a LOF for some glasses.

Figure 8.9 shows the predictive performance of the 24-term viscosity model for  $\ln(\eta)$  fitted to the 171-glass modeling dataset and applied to the set of 10 outlying glasses with viscosity data that were excluded from the modeling dataset. The 24-term model tends to under-predict most of the observations, but not significantly. The predictions are sufficiently close to the measured values and the 95% PIs are sufficiently wide that all but 6 of the 40 glass-temperature combinations have 95% PIs that contain the corresponding measured values. Failure of  $100(6/40) = 15\%$  of the 95% PIs to include the corresponding measured values is more than the 5% expected by chance. So, the 24-term model does appear to have some LOF for these extrapolative predictions of viscosity.

Figures 8.10 and 8.11 show the predicted-versus-measured plot and the standardized residuals plot for the 22-term truncated T2-LM model listed in Table 8.7. Despite the noticeable increase in SSE for the 22-term model compared to the 24-term model (see Figure 8.4), there is not a lot of difference in Figures 8.10 and 8.11 for the 22-term model and Figures 8.5 and 8.6 for the 24-term model. The most noticeable difference is that the standardized residuals plot for the 22-term model in Figure 8.11 does not show the same tendency for over-prediction of the high- $\text{Cr}_2\text{O}_3$ - $\text{P}_2\text{O}_5$  glasses (HiCrP) as seen for the 24-term model in Figure 8.6. This result is somewhat perplexing, given that the 24-term model includes  $\text{P}_2\text{O}_5$  terms and the 22-term model does not.

The validation results in Tables 8.6 and 8.7 for data-partitioning and the 10 outlying glasses show the 22-term and 24-term models perform similarly.

#### 8.4 Investigation of Adding Quadratic Terms to Truncated T2-Linear Mixture Models

The standardized residual plots for the 36-term, 24-term, and 22-term truncated T2-LM models discussed in Section 8.3 show that those models tend to over-predict for the correlation and high-Cr<sub>2</sub>O<sub>3</sub> correlation glasses (denoted Corr) discussed in Section 2.4. The 24-term and 22-term models also have a slight tendency to over-predict for the ILAW Phase 1a Augmentation glasses (denoted Ph1aAug) discussed in Section 2.3. All of the models also under-predict for certain other glasses. The appearance of several “arms” sticking out of the main cloud of points in the standardized residual plots may indicate some degree of model inadequacy for certain LAW glasses. Hence, it was decided to explore adding quadratic (squared and/or crossproduct) terms to the 24-term and 22-term models to assess whether the tendencies toward biased prediction of viscosity for some glass compositions could be resolved.

Quadratic terms in the components Al<sub>2</sub>O<sub>3</sub>, B<sub>2</sub>O<sub>3</sub>, CaO, Li<sub>2</sub>O, MgO, Na<sub>2</sub>O, and SiO<sub>2</sub> were chosen for investigation for two reasons. First, several of these components have strong single-component linear effects on viscosity as shown in the response trace plots in Figures 8.7a to 8.7d. Hence, it is reasonable that quadratic (squared or crossproduct) terms involving these components could improve the predictive performance of the 24-term and 22-term truncated T2-LM models. Second, the statistically designed Phase 1 Test Matrix (see Section 2.1 and Cooley et al. 2003), was optimized for a PQM model including the 5 squared and 10 crossproduct terms involving Al<sub>2</sub>O<sub>3</sub>, B<sub>2</sub>O<sub>3</sub>, Li<sub>2</sub>O, Na<sub>2</sub>O, and SiO<sub>2</sub>. Hence, the Phase 1 Test Matrix provides good support for assessing the quadratic effects of terms involving these components. The scatterplot matrix in Figure 7.5 also indicates that the 171-glass modeling dataset provides good support for assessing quadratic effects of all seven of the listed components.

Stepwise regression methods (see Section C.5.2 of Appendix C) were used to select the best squared and crossproduct terms to include in a model of the form given by Equation (8.2). Initially, quadratic terms were considered for addition only to the composition part of the model as shown in Equation (8.2) under the expectation that strong quadratic compositional effects would be apparent in such terms, even if the quadratic effects also depended on temperature. Because stepwise regression capabilities are not built into the SAS routine PROC MIXED for implementing GLS regression, it was necessary to use the stepwise regression capability in SAS routine PROC REG that implements ULS regression. Such an implementation does not recognize the two-uncertainty structure of the viscosity data (as discussed in Section 8.2.2). However, the result is that the stepwise regression procedure would tend to select too many quadratic terms to include in the model. This tendency was compensated for by choosing a 0.01 significance level for implementing stepwise regression.

The following two models of the form in Equation (8.2) were obtained.

- Model 5: A 28-term model formed by adding four quadratic terms (B<sub>2</sub>O<sub>3</sub>)<sup>2</sup>, (Li<sub>2</sub>O)<sup>2</sup>, Al<sub>2</sub>O<sub>3</sub>×Li<sub>2</sub>O, and (MgO)<sup>2</sup> to the 24-term model (Model 3).

- **Model 6:** A 26-term model formed by adding four quadratic terms  $(\text{B}_2\text{O}_3)^2$ ,  $(\text{Li}_2\text{O})^2$ ,  $\text{B}_2\text{O}_3 \times \text{Li}_2\text{O}$ , and  $\text{Al}_2\text{O}_3 \times \text{Na}_2\text{O}$  to the 22-term model (Model 4).

Table 8.5 includes summary statistics for Models 5 and 6 (i) fitted to the 171-glass modeling dataset and (ii) fitted to the modeling subset of 86 glasses and validated with the remaining 85 glasses. Table 8.5 includes results for the 36-term model (Model 1), the 28-term model (Model 2), the 24-term model (Model 3), and the 22-term model (Model 4). Model 5 fits the 171-glass modeling dataset better than Models 1, 2, 3, 4, and 6. Model 2 fits the partitioned modeling subset slightly better than Model 5. However, the partitioned validation results for Model 2 are affected by the lack of support for all of the terms included in Model 2, and thus the comparison against Model 5 is not useful. Model 5 appears to be the best of Models 1 to 6 considered. Model 7 is a reduced version of Model 5 with two non-significant terms removed. It is discussed subsequently in Section 8.5.

Unfortunately, standardized residual plots for Models 5 and 6 (not included in the report) do not appear substantially different than the one for the 24-term model in Figure 8.6. Although the addition of four quadratic terms does improve the fits and validation performance of the 24-term model, it does not correct the over-prediction for the Corr (correlation and high- $\text{Cr}_2\text{O}_3$  glasses) or other over- and under-predictions for selected glasses as seen in Figure 8.6.

There are two likely reasons for the failure of quadratic terms to significantly improve the tendencies for biased predictions in some LAW glasses (in particular the Corr glasses). First, the Corr glasses were specifically designed with certain components fixed or calculated as a function of other components. This could result in multi-component effects on viscosity that could not be captured by quadratic terms. Similarly, the statistically designed subsets of glasses varied simultaneously the components investigated. Multi-component effects on viscosity would not be captured by quadratic terms.

In summary, it would have been desirable to develop viscosity model forms that improved or corrected some of the biased predictions seen for models of the form in Equation (8.1). However, ultimately the 28-term model formed by adding four quadratic terms to the 24-term model predicts reasonably well (generally within its uncertainties). Thus, a 26-term model obtained by dropping two non-significant terms from the 28-term model is discussed and recommended in the following subsection. The 24-term model discussed in Section 8.3.3 is an alternative, second-choice model.

## 8.5 Results for the Recommended 26-Term Viscosity Model

This section presents the results for the recommended 26-term ILAW viscosity model obtained by dropping the two statistically non-significant terms  $\text{B}_2\text{O}_3/(T/1000)^2$  and  $\text{K}_2\text{O}/(T/1000)^2$  from the 24-term model with four quadratic terms added. The non-significance of these terms indicates that the effects of  $\text{B}_2\text{O}_3$  and  $\text{K}_2\text{O}$  on viscosity do not depend substantially on temperature.

Section 8.5.1 presents the results for the recommended 26-term viscosity model fitted to the 171-glass modeling dataset. Section 8.5.2 presents the validation results for the 26-term model.

### 8.5.1 Results for the Recommended 26-Term Viscosity Model Fitted to the 171-Glass Modeling Dataset

The 26-term model of the form in Equation (8.2) after dropping the non-significant  $B_2O_3/(T/1000)^2$  and  $K_2O/(T/1000)^2$  terms was fitted to the viscosity data for the 171 glasses in the modeling set. The PROC MIXED procedure in SAS (2005) was used to perform the GLS regression required for the viscosity data structure. Table 8.8 lists the fitted model coefficients, the coefficient standard deviations, and estimates of the  $\sigma_G$  and  $\sigma_T$  error standard deviations (see Section 8.2.2). Selected summary statistics are also included in Table 8.5, where the 26-term model is denoted Model 7.

The upper right portion of Table 8.8 shows that the 26-term viscosity model fits the 171-glass modeling dataset with  $R^2 = 0.988$  and  $RMSE = 0.147$ . These statistics are improvements over those for the 24-term model in Table 8.6.

The quantity  $\hat{\sigma}_{Total} = \sqrt{\hat{\sigma}_G^2 + \hat{\sigma}_T^2} = \sqrt{(0.1375)^2 + (0.0615)^2} = 0.1506$  is an estimate of the total uncertainty in a viscosity determination for a given glass and temperature, under the assumption that the 26-term model does not have a significant LOF. A significant model LOF would inflate  $\hat{\sigma}_{Total}$  and it would over-estimate the true total uncertainty in a viscosity determination.

The quantity  $\hat{\sigma}_{Total}$  for the 26-term model is about 37% larger than the compromise overall pooled estimate of uncertainty  $SD = 0.11$  (see Section 8.1.1) calculated from replicate data that is not impacted by model LOF. Hence, the 26-term model may have some LOF, but it does not appear to be to highly significant given the inherent uncertainty in the data. Therefore, the 26-term model does not seem to have a significant model LOF.

A histogram and normal probability plot of the standardized residuals for the fit of the 26-term model in Table 8.8 to the 171-glass ILAW viscosity modeling dataset were generated, although they are not shown in this report. These two plots do not show any significant departure from normality, which is required to utilize the statistical interval formulas for model prediction uncertainties that are discussed subsequently.

The predicted versus measured plot and the standardized residual plot for the 26-term  $\ln(\eta)$  model are given in Figures 8.12 and 8.13, respectively. These figures are similar but slightly improved compared to those for the 24-term model shown in Figures 8.5 and 8.6. Figure 8.12 shows relatively tight scatter about the 45° line representing perfect prediction, with the Corr glasses tending to fall above the line (indicating slight over-prediction). Figure 8.13 shows that the data for glasses LAWB77, LAWM27, and LAWE7 have standardized residuals greater

than 4.0 in absolute value for at least one temperature. Figure 8.13 also shows the 26-term viscosity model tends to over-predict viscosity<sup>19</sup> for the Corr glasses (see Section 2.4) and many of the Ph1aAug glasses (see Section 2.3). However, the prediction errors for those glasses are still within the applicable uncertainties.

The response trace plots (see Section C.5.1) for viscosity at 950, 1050, 1150, and 1250°C produced using the 26-term model are given in Figures 8.14a to 8.14d. These figures are similar to the ones for the 24-term model in Figures 8.7a to 8.7d. However, additional curvature is seen in Figures 8.14a to 8.14d for the components involved in the quadratic terms. The response trace plots show that Li<sub>2</sub>O and Na<sub>2</sub>O have dominant decreasing effects on viscosity, while SiO<sub>2</sub> and Al<sub>2</sub>O<sub>3</sub> have the strongest increasing effects on viscosity. Figures 8.14a to 8.14d also show that CaO, B<sub>2</sub>O<sub>3</sub>, and MgO have strong decreasing effects on viscosity, with the effects getting stronger as temperature increases. Finally, ZrO<sub>2</sub> is seen to have a similar increasing effect on viscosity as Al<sub>2</sub>O<sub>3</sub> at 950 and 1050°C, but that its effect weakens relative to that of Al<sub>2</sub>O<sub>3</sub> at 1150 and 1250°C and has an effect similar to that of P<sub>2</sub>O<sub>5</sub> at those higher temperatures.

## 8.5.2 Validation Results for the Recommended 26-Term Viscosity Model

Performance statistics for the 26-term ILAW viscosity model when applied to the five modeling/validation splits formed from the 171-glass modeling dataset are given in the bottom part of Table 8.8. The columns are labeled DS1, DS2, DS3, DS4, and DS5 to denote the five modeling/validation splits of the data as described in Section 8.1.2. The last column of this part of Table 8.8 presents averages of the modeling ( $R^2$ , SSE, and RMSE) and validation ( $R^2_v$  and  $RMSE_v$ ) statistics over the five data-splits. The average modeling statistics  $R^2 = 0.988$  and  $RMSE = 0.145$  are similar to those statistics from fitting the model to the 171-glass viscosity modeling dataset. The average validation statistics  $R^2_v = 0.983$  and  $RMSE = 0.163$  from the data-splitting approach are only slightly worse (i.e., smaller and larger, respectively) than the values when fitting the viscosity data from all 171 glasses in the modeling set or the modeling subsets from data-splitting. In general, the data-splitting results show that the 26-term model in Table 8.8 maintains the level of its predictive performance when applied to validation data within the same composition region as used to develop the model.

Performance statistics from fitting the 26-term viscosity model to the 86-glass modeling subset and validating using the remaining 85 glasses are given on the right hand side of Table 8.8. Fitting the 26-term model to the 86-glass modeling subset yields  $R^2 = 0.990$  that is similar to the  $R^2 = 0.988$  from fitting the model to the full 171-glass viscosity dataset. The  $RMSE = 0.140$  for the 86-glass modeling subset is slightly better than the  $RMSE = 0.147$  from the full 171-glass modeling dataset. The  $R^2_v = 0.980$  and  $RMSE_v = 0.176$  statistics for the 85-glass validation subset are, respectively, similar to and slightly worse than, the corresponding values from data-splitting. Together, these results indicate that the 26-term viscosity model maintains its predictive performance fairly well even when partitioning the data in half for model fitting and validation.

---

<sup>19</sup> It is long-term statistical practice, almost universally used in software, to define residuals as “measured – predicted”. That is why negative standardized residuals indicate that the model over-predicts the measured values.

Performance statistics from fitting the 26-term viscosity model to the 171-glass modeling subset and validating using the 10 outlying glasses are given on the right hand side of Table 8.8. The  $R^2_V = 0.976$  and  $RMSE_V = 0.200$  statistics for the 10 outlying glasses are somewhat worse than the corresponding average validation statistics from data-splitting and the corresponding data-partition validation statistics. Together, these results indicate that the 26-term viscosity model has reduced predictive performance, but still performs fairly well even with some extrapolation in glass composition.

Figures 8.15 and 8.16 show predicted versus measured plots when the 26-term ILAW viscosity model for  $\ln(\eta)$  is applied to two validation datasets. Figure 8.15 results from fitting the 26-term model to a subset of 86 out of 171 modeling glasses, and then applying the resulting model to the remaining subset of 85 glasses for validation (see Section 8.1.3). Figure 8.16 results from fitting the 26-term model to all 171 glasses in the viscosity modeling set and then applying that model to the 10 outlying glasses with viscosity results (see Section 8.1.4). Also shown in Figures 8.15 and 8.16 are 95% PIs representing the model prediction uncertainty of single viscosity determinations for each glass at one temperature (see Sections C.6 and C.7 of Appendix C). If the error bar for a validation point overlaps the 45° line, that means the predicted and measured  $\ln(\eta)$  values are within model and measurement uncertainty of each other. Note that the error bars include the estimated uncertainties  $\hat{\sigma}_G$  and  $\hat{\sigma}_T$  resulting from the structure of the viscosity data. The 95% PIs in Figures 8.15 and 8.16 for the 26-term model have widths similar to those in Figures 8.8 and 8.9 for the 24-term model. The width of the 95% PIs is due to (i) whatever LOF there is of the 26-term viscosity model, and (ii) the experimental uncertainty in fabricating glasses and measuring viscosity. Separate work to assess the consequences of LOF and prediction uncertainty for this recommended viscosity model is discussed further in Section 8.7.

Figure 8.15 shows that the 26-term viscosity model for  $\ln(\eta)$  fitted to the 86-glass modeling subset predicts viscosity fairly accurately at the four temperatures each for nearly all of the 85-glass validation subset. Figure 8.15 for the 26-term model has a more even distribution of observations around the 45° line than does Figure 8.8 for the 24-term model. The 95% PIs for the 26-term model overlap the 45° line (i.e., contain the measured values) for all but 27 of the 340 (= 4 temperature values at each of 85 glasses) observations in the validation subset. Failure of  $100(27/340) = 7.9\%$  of the 95% PIs to include the corresponding measured values is not much higher than the 5% that would be expected by chance for a model with no LOF. Hence, the 26-term model may have some LOF but generally performs well based on this data-partition approach.

Figure 8.16 shows the predictive performance of the 26-term viscosity model for  $\ln(\eta)$  fitted to the 171-glass modeling dataset and applied to the set of 10 outlying glasses with viscosity data that were excluded from the modeling dataset. The 26-term model tends to under-predict most of the observations, but not significantly. The under-predictions are smaller than for the 24-term model (see Figure 8.9). The predictions are sufficiently close to the measured values and the 95% PIs are sufficiently wide that all but seven of the forty 95% PIs contain the corresponding measured values. Hence, the 26-term model does reasonably well predicting viscosity for the 10 outlying LAW glass compositions.

## 8.6 Example Illustrating Viscosity Model Predictions and Statistical Intervals

This section contains examples to illustrate using the 26-term truncated T2-LM model with four quadratic terms and the 24-term truncated T2-LM model to obtain predicted viscosity values and corresponding 90% lower confidence intervals (LCIs), 90% upper confidence intervals (UCIs), and two-sided 90% confidence intervals (CIs) as described in Section C.7 of Appendix C. The 26-term model is the one recommended in Section 8.4 and discussed in detail in Section 8.5. For comparison purposes, calculations are also performed in this section for the 24-term model discussed in Section 8.3.3. The 90% confidence levels associated with LCIs, UCIs, and CIs were chosen for illustration purposes only. The WTP project can use an appropriate confidence level depending on the use of the viscosity-composition-temperature model and the type of statistical uncertainty expression desired.

The glass composition used in this example is LAWA126, which is one of the glasses in the ILAW Existing Matrix. The 18-component composition of LAWA126 for viscosity modeling is given in Table 7.2 in mass fraction format. To apply the two viscosity models to this composition, the mass fractions of the 18 components must be converted to mass fractions (that sum to 1.0) of the 12 LAW glass components contained in the 24-term and 26-term models. Table 8.9 contains the composition of LAWA126 prepared for use in the two ILAW viscosity models.

For each of the viscosity models, predicted  $\ln(\eta, P)$  values are obtained by multiplying the composition in the format needed for that model by the coefficients for that model, then summing the results. That is, the predicted values are calculated by

$$\hat{y}(\mathbf{a}) = \mathbf{a}^T \mathbf{b}$$

where  $\mathbf{a}$  is a vector with entries corresponding to terms in a given model based on the LAWA126 composition and a specific temperature value (in Kelvin), the superscript T represents a matrix transpose (or vector transpose in this case), and  $\mathbf{b}$  is the vector of coefficients for a given model. The predicted  $\ln(\eta)$  values for LAWA126 at 1161°C<sup>20</sup> using each of the ILAW viscosity models are listed in the second column of Table 8.10. The predicted  $\ln(\eta)$  values in  $\ln(P)$  units are easily converted to viscosity values (P) by exponentiation. The third column of Table 8.10 contains the predicted viscosity values (P). However, as discussed in Section C.7 of Appendix C, these back-transformed viscosity predictions (P) should be considered estimates of the true median (not the true mean) of the distribution of viscosity values that would result if viscosity measurements at the specific temperature were repeated multiple times on separately batched and melted samples of the LAWA126 glass composition.

The predicted ILAW viscosity values for LAWA126 at 1161°C in Table 8.10 are 51.94 P for the 24-term viscosity model and 49.23 P for the recommended 26-term model. The predicted

---

<sup>20</sup> The temperature of 1161°C was chosen because it was one of the temperatures at which the viscosity of LAWA126 was measured. This facilitates comparison of the predicted and measured values.



value using the 24-term model is closest to the measured value of 55.81 P for LAWA126 at 1161°C.

Equations (C.27c), (C.28c), and (C.29c) can be used to calculate, respectively, a 90% UCI, a 90% LCI, or a two-sided 90% CI for the true mean of  $\ln(\eta)$  values for the LAWA126 glass composition at a specific temperature with each of the ILAW viscosity models. In the notation of these equations:

- $100(1-\alpha)\% = 90\%$ , so that  $\alpha = 0.10$  for a 90% UCI, a 90% LCI, and a 90% CI in Equations (C.27c), (C.28c), and (C.29c), respectively.
- The vector  $\mathbf{a}$  contains entries corresponding to the terms in a given viscosity model, which are calculated using the composition of LAWA126 in Table 8.8 and a specific temperature value.
- Matrix  $\mathbf{A}$  is formed from the data matrix used in the regression that generated a given viscosity model. Matrix  $\mathbf{A}$  has the number of rows in the viscosity modeling dataset (685 = 171 × 4 temperatures each + 1 additional measurement for LAWM7) and the number of columns corresponding to the number of terms in a given viscosity model. Each column is calculated according to the corresponding term in the model using the LAW glass compositions and the actual (not nominal or intended) temperatures in the viscosity modeling dataset.
- Matrix  $\hat{\mathbf{V}}$  is the estimated variance-covariance matrix for the vector of EC-at-temperature data used to fit an EC model. This matrix accounts for the two sources of uncertainty, as discussed in Section C.3.3 of Appendix C.

To calculate a 90% UCI or LCI in  $\ln(\eta)$  units of  $\ln(P)$ , the quantity  $t_{1-\alpha, n-p} \sqrt{\mathbf{a}^T (\mathbf{A}^T \hat{\mathbf{V}}^{-1} \mathbf{A})^{-1} \mathbf{a}}$  is added to (UCI) or subtracted from (LCI) the predicted  $\ln(\eta)$  [denoted  $\hat{y}(\mathbf{a})$ ] described above. The calculations are given by Equation (C.27c) for an UCI and Equation (C.28c) for a LCI. To calculate a two-sided CI, the quantity  $t_{1-\alpha/2, n-p} \sqrt{\mathbf{a}^T (\mathbf{A}^T \hat{\mathbf{V}}^{-1} \mathbf{A})^{-1} \mathbf{a}}$  is subtracted from and added to the predicted  $\ln(\eta)$  [denoted  $\hat{y}(\mathbf{a})$ ], as indicated by Equation (C.29c). The  $(\mathbf{A}^T \hat{\mathbf{V}}^{-1} \mathbf{A})^{-1}$  portion of these expressions is an approximate estimate of variance-covariance matrix for the estimated model coefficients, as discussed near the end of Section C.7 of Appendix C. The variance-covariance matrices for the 24-term and the recommended 26-term viscosity models are respectively listed in Tables D.10 and D.11 of Appendix D. The quantity  $\sqrt{\mathbf{a}^T (\mathbf{A}^T \hat{\mathbf{V}}^{-1} \mathbf{A})^{-1} \mathbf{a}}$  is the standard deviation of a model prediction; the value for each model is given in the fourth column of Table 8.10.

The 90% LCI, 90% UCI, and 90% CI values for the true mean  $\ln(\eta)$  in units of  $\ln(P)$  for the LAWA126 composition at a temperature of 1161°C based on the two ILAW viscosity models are given in the fifth, seventh, and ninth columns of Table 8.10. Exponentiating the resulting 90% UCIs, LCIs, and CIs for the mean viscosity values in  $\ln(P)$  units yields 90% LCIs, UCIs,

and CIs for the median viscosity (P). These values are in the sixth, eighth, and tenth columns of Table 8.10. For example, the recommended 26-term viscosity model has (3.852, 3.941)  $\ln(P)$  as the two-sided 90% CI on the true mean  $\ln(\eta)$  for LAWA126 at 1161°C. Then  $(e^{3.852}, e^{3.941}) = (47.09, 51.46)$  P is the two-sided 90% CI on the true median viscosity for LAWA126 at 1161°C.

## **8.7 Suitability of the Recommended Viscosity Model for Application by the WTP Project**

The 26-term model for viscosity discussed in Section 8.5 is recommended for use by the WTP project as the best model currently available for predicting this property for LAW glasses. This model appears to yield unbiased predictions of viscosity over the full range of measured viscosity values in the modeling dataset, with relatively tight scatter for most data points about the fitted model, and moderate scatter for some data points (see Figure 8.12). The recommended viscosity model does not have a statistically significant LOF, so that viscosity predictions can be expected to be within the uncertainty of what would be obtained by batching and melting glasses and measuring the viscosity.

The magnitudes of uncertainties in viscosity model predictions should be small enough that they will not unduly restrict the formulation and processing of LAW glasses in the WTP facility. Figure 8.17 displays the  $\ln(\eta)$  prediction standard deviations versus predicted values [both in  $\ln(\text{poise})$  units] for the LAW glass compositions in the viscosity modeling dataset at temperatures of 950, 1050, 1150, and 1250°C. The  $\ln(\eta)$  prediction standard deviations for viscosity modeling dataset glasses at these temperatures range from approximately 0.02 to 0.10  $\ln(\text{poise})$  for the recommended viscosity model. Note that prediction standard deviations will be larger for LAW glass compositions as their distance from glasses in the viscosity modeling dataset increases. Also, the total uncertainty in predictions with the recommended viscosity model will depend on the type of statistical interval used (see Section C.7 of Appendix C).

Work to assess the impact of LAW glass composition and model uncertainties for the recommended viscosity  $\ln(\eta)$  model (Section 8.5) on satisfying WTP ILAW processing requirements is planned to be addressed as part of the Technical Scoping Statement (TSS) B-6069 work scope of the River Protection Project—Waste Treatment Plant Support Program at PNNL. The impacts of these uncertainties on glass formulation and processability are also planned to be addressed as part of the second iteration of the LAW glass formulation algorithm development work planned by WTP project staff. The first iteration of that work (Vienna 2005) utilized a preliminary viscosity model (Feng et al. 2004) and the LAW glass formulation correlation (Muller et al. 2004b).

## SECTION 9 REGIONS OF VALIDITY FOR LAW GLASS PROPERTY MODELS

The LAW glass property models recommended in Sections 5 to 8 were fitted to experimental data using regression methods. These methods yield the optimal estimates of the model coefficients based on the modeling data provided the assumptions of the regression method are satisfied. In general, models obtained in this way should only be applied within appropriate composition regions of validity (or composition-temperature regions of validity in the case of viscosity and electrical conductivity). Such regions are referred to as *model validity regions*. The starting point for a model validity region is often the experimental region covered by the data used to develop the model. However, if a model yields biased predictions over some subregions, those subregions may be excluded from the model validity region. Extrapolations of models to compositions (or composition  $\times$  temperature combinations) slightly outside the experimental composition (or composition  $\times$  temperature) region are sometimes acceptable. However, such extrapolative uses of regression models should be validated before being applied.

For the PCT, VHT, melt electrical conductivity, and melt viscosity models on LAW glasses recommended in Sections 5 to 8, it was decided in consultation with the WTP Project to (i) specify the model validity regions as the regions covered by the modeling datasets, but (ii) exclude any subregions in which models yield unacceptably biased predictions. The modeling datasets for viscosity and electrical conductivity contain the same 171 glasses. However, the modeling datasets for PCT and VHT were different, containing 244 and 165 glasses, respectively. Mathematically, the convex hull of the compositions<sup>21</sup> comprising a modeling dataset could be the starting point for defining the model validity region for that property. However, we are unaware of any algorithm or software to identify all of the mathematical constraints that would specify the convex hull in high-dimensional LAW glass composition space.

The model validity regions for the recommended LAW glass property models are specified using (i) single-component constraints on LAW glass composition, (ii) single-variable constraints on LAW glass melt temperature (for viscosity and electrical conductivity models), (iii) multiple-component constraints for PCT and VHT properties, and (iv) multiple-variable constraints involving LAW glass composition and melt temperature for viscosity and electrical conductivity. The single-component (composition) constraints and single-variable (temperature) constraints are discussed in Section 9.1. The multiple-component constraints for PCT and VHT and the multiple-variable (composition and temperature) constraints for viscosity and electrical conductivity are discussed in Section 9.2. Section 9.3 summarizes and discusses the model validity regions.

---

<sup>21</sup> A convex hull of the LAW glass compositions in the modeling set would be the smallest convex polyhedral region enclosing all of the compositions.

## 9.1 Single-Component Composition and Temperature Constraints

The ranges (minimum and maximum values) of LAW glass components in the modeling dataset for each property were determined and are listed in Table 9.1. Table 9.1 lists values for the 18 components that had sufficient support for initial property modeling work, with one of those components being “Others”. The minimums and maximums for the specific components making up the Others component are listed in the bottom portion of Table 9.1. The last two columns of Table 9.1 list the minimum and maximum LAW glass component values across all of the property datasets.

The first step in specifying the composition region of validity for the ILAW PCT, VHT, viscosity, and electrical conductivity models is to list the lower and upper bounds on LAW glass components. The overall minimum and maximum columns in Table 9.1 are a starting place, but rounded values are preferred for practical use. Also, it is important to assess whether any of the recommended PCT, VHT, electrical conductivity, and viscosity models makes biased enough predictions at extremes of component ranges such that the lower and upper bounds for those components should be reduced from their minimums and maximums in the modeling datasets. Tendencies of recommended LAW glass property models (discussed in Sections 5 to 8) to yield biased predictions were not observed relating to low and high values of specific components. Because such tendencies for biased model predictions are likely to be a multiple-component phenomenon and not a single-component phenomenon, no narrowing of the LAW glass component overall ranges in Table 9.1 are proposed.

Table 9.2 lists rounded values of the minimums and maximums of the LAW glass components in the last two columns of Table 9.1. Minimum mass fraction values were rounded down to the nearest third decimal place (nearest 0.1 wt%). Maximum mass fraction values were rounded up to the nearest third decimal place (nearest 0.1 wt%). Rounding in this way provides for all of the LAW glass compositions in the property modeling datasets to satisfy the single-component constraints.<sup>22</sup> Choosing the lower and upper LAW glass component bounds in this way is not intended to limit other choices the WTP might decide to make. The WTP could decide to allow extrapolative use of LAW glass property models outside these lower and upper bounds. As an example, the decision could be made to expand the lower and upper bounds by 10% relative. Rather than making such decisions in this report, it was decided to merely list the rounded minimums and maximums for the combined modeling glasses in Table 9.2.

Because viscosity and electrical conductivity models depend on melt temperature as well as LAW glass composition, the validity regions for viscosity and electrical conductivity models must specify constraints on temperature as well as glass composition. Viscosity and electrical conductivity data were generally measured in the vicinity of four nominal temperatures: 950, 1050, 1150, and 1250°C. However, for some glasses measurements were made at nominal temperatures closer to 900 or 1200°C. Actual temperature values at which electrical conductivity was measured ranged from 917 to 1278°C. Actual temperature values at which viscosity was measured ranged from 903 to 1271°C. These ranges are from the property measurements for the

---

<sup>22</sup> Note, however, that the LAW glasses identified as outliers and excluded from each property-composition modeling dataset will be outside the lower and upper bounds selected.

171 LAW glasses in the viscosity and electrical conductivity modeling datasets. These temperature ranges and the rounded values of these ranges chosen as single-variable lower and upper bounds on temperature are summarized in Table 9.3.

## **9.2 Multiple-Component Composition and Temperature Constraints**

The lower and upper bounds on the LAW glass components in Table 9.2 are necessary but not sufficient to specify the composition region of validity for LAW glass property models. The lower and upper bounds in Table 9.2 allow LAW glass compositions with (i) combinations of components that are far from the compositions in a given LAW glass property modeling dataset, and/or (ii) property values that may be far outside of acceptable limits. Hence, it is necessary to develop multiple-component constraints that mathematically specify the allowable combinations of glass components in the composition region of validity for LAW glass property models.

It is difficult to directly develop multiple-component composition constraints. Instead, multiple-component constraints on LAW glass composition were specified indirectly via lower and upper bounds on properties of LAW glasses. The development of these constraints is discussed in Section 9.2.1. The development of several multiple-component constraints based on pairs of correlated LAW glass components is discussed in Section 9.2.2.

### **9.2.1 Multiple-Component Property Constraints**

The primary approach for developing multiple-component constraints was to specify lower and upper bounds on properties of LAW glasses. These lower and upper bounds are implemented using the recommended model for each property (see Sections 5 to 8). Because the models are functions of (i) LAW glass composition (for PCT-B, PCT-Na, and VHT alteration), and (ii) LAW glass composition and melt temperature (for electrical conductivity and viscosity), the lower and upper bounds on properties indirectly constrain the LAW glass composition region.

Table 9.4 lists the minimum and maximum values of measured and model-predicted LAW glass properties over the modeling dataset for each property. The minimum and maximum values of predicted PCT-B, PCT-Na, and VHT alteration depth in Table 9.4 were obtained as follows.

- For each of PCT-B and PCT-Na, the recommended model was used to predict property values for each LAW glass in that property's modeling dataset. Then the minimum and maximum of all predicted PCT-B and PCT-Na values were determined.
- For VHT alteration depth, the recommended model and second-choice model were used to predict VHT alteration depth values for each LAW glass in that property's modeling dataset. Then the minimum and maximum of all predicted values were determined.

Because the minimum values of PCT-B, PCT-Na, and VHT alteration depth in Table 9.4 are relatively small, it was decided that no lower limits were needed on these properties for the model validity region. This is shown in Table 9.5 by listing “None” under the lower bound column for these three properties.

As discussed in Section 5.6, upper bounds of 2.7 g/L are imposed on the validity region for PCT-B and PCT-Na models because of the tendency of those models to under-predict PCT releases above 2.7 g/L. Because the recommended model for VHT alteration depth yields relatively unbiased predictions, it was decided to set the upper limit for application of that model to the maximum alteration depth possible under the current VHT procedure, namely 1100  $\mu\text{m}$ . These upper bounds on PCT-B, PCT-Na, and VHT alteration depth for the model validity region of each property are shown in Table 9.5.

The lower and upper bounds on EC and viscosity for the model validity region of each property are listed in Table 9.5, and were obtained as follows. The recommended model for each property was used to predict property values for each LAW glass at the temperatures for which that property was measured. Then, bounding lines were determined to specify the lower and upper bounds for electrical conductivity and viscosity as a function of temperature. Specifically, the lower and upper bound lines for electrical conductivity and viscosity are of the form

$$\ln(\text{property}) = \text{intercept} + \text{slope} (1/T) \quad (9.1)$$

where  $T$  is temperature in  $^{\circ}\text{C}$ <sup>23</sup>. The lower and upper bound lines for electrical conductivity and viscosity are listed in Table 9.5 and displayed in Figures 9.1 and 9.2, respectively.

## 9.2.2 Constraints on Pairs of Correlated LAW Glass Components

It was noted in Sections 5.1.1, 6.1.1, 7.1.1, and 8.1.1 for each of the LAW glass property modeling datasets that several pairs of LAW glass components have strong correlation coefficients (i.e., above 0.60 in absolute value). The pairs of highly-correlated components and the ranges of their correlation coefficients across the four LAW glass properties are

Li <sub>2</sub> O and Na <sub>2</sub> O:	-0.878 to -0.896
Cr <sub>2</sub> O <sub>3</sub> and P <sub>2</sub> O <sub>5</sub> :	0.746 (VHT, below 0.60 for other properties)
Na <sub>2</sub> O and CaO:	-0.703 to -0.737
Li <sub>2</sub> O and CaO:	0.631 to 0.687
Na <sub>2</sub> O and SO <sub>3</sub> :	-0.617 to -0.679
Li <sub>2</sub> O and SO <sub>3</sub> :	0.616 to 0.673
Na <sub>2</sub> O and SiO <sub>2</sub> :	-0.622 to -0.663

The property-based multiple-component constraints discussed in Section 9.2.1 may not adequately represent the restrictions imposed by the higher correlations on these pairs of

---

<sup>23</sup> Note that this constraint was developed using temperature in  $^{\circ}\text{C}$  rather than K (which was used for electrical conductivity and viscosity models).

components. In that case, glass compositions outside the composition subregions represented by these stronger correlations would involve extrapolative use of the property models in this report. Because the models have not been validated for extrapolative use, pairwise constraints were developed to exclude such compositions from the model validity region of all property models.

Figure 9.3 shows a plot of  $\text{Li}_2\text{O}$  (y-axis) versus  $\text{Na}_2\text{O}$  (x-axis) for the combined set of LAW glasses having data for any of the four properties (PCT, VHT, electrical conductivity, and viscosity). Glasses having data for all four properties are shown with a filled circle, whereas glasses having data for fewer than all four properties are shown with an open circle. Also shown in the figure is the “best fit” regression line, which has a negative slope corresponding to the strong negative correlation between the two components. The upper constraint shown in Figure 9.3 is parallel to the “best fit” line, with intercept chosen so that all LAW glasses with values of all four properties (PCT, VHT, electrical conductivity, and viscosity) are inside the constraint. The lower constraint shown in Figure 9.3 was determined by two bounding glasses having values of all four properties. The equations for the two constraints on  $\text{Na}_2\text{O}$  and  $\text{Li}_2\text{O}$  are given in the bottom portion of Table 9.5.

As discussed in Section 4, jointly increasing  $\text{Li}_2\text{O}$  and  $\text{Na}_2\text{O}$  has the highest propensity to increase PCT, VHT, melt electrical conductivity and to lower melt viscosity. Consequently, no LAW glasses were formulated with the combined  $\text{Li}_2\text{O}$  and  $\text{Na}_2\text{O}$  concentrations exceeding 26 mol%. Considering the difference in the atomic masses of Na and Li ( $\text{Na}/\text{Li} = 3.3$ ), this limit can be written as  $\text{Na}_2\text{O} + 3.3 \text{Li}_2\text{O} < 30$  (wt%). Re-writing the upper limit constraint shown in Figure 9.3 in a similar format and using mass fractions (mf) yields  $\text{Na}_2\text{O} + 3.52 \text{Li}_2\text{O} < 0.29$  (mf). Hence, the upper constraint based on the modeling dataset correlation of  $\text{Li}_2\text{O}$  and  $\text{Na}_2\text{O}$  agrees very well with the one based on the glass formulation limit.

Constraints on the other pairs of LAW glass components with high correlations were developed with the same process used for  $\text{Li}_2\text{O}$  and  $\text{Na}_2\text{O}$ . Figures 9.4 to 9.9 display plots of the modeling datasets for the remaining pairs of strongly-correlated components. LAW glasses having values for all four properties are plotted with filled circles, while glasses having values for fewer than four properties are plotted with open circles. The best fit lines were developed and are shown as darker lines in Figures 9.4 to 9.9. Next, parallel lower and upper constraints were developed to include LAW glasses having values for all four properties. If a resulting lower or upper constraint was not very restrictive, it was eliminated. This occurred for the lower constraint involving  $\text{Li}_2\text{O}$  and  $\text{CaO}$  (see Figure 9.6). If a parallel lower or upper constraint was not representative of the pattern of points, it was replaced by a constraint determined by two bounding points. This occurred for the lower constraint involving  $\text{Cr}_2\text{O}_3$  and  $\text{P}_2\text{O}_5$  (see Figure 9.4). The equations for these constraints are given in the bottom portion of Table 9.5. The constraints are shown in Figures 9.4 to 9.9.

### 9.3 Summary and Discussion of LAW Glass Property Model Validity Regions

Table 9.6 summarizes the constraints defining the model validity region for each LAW glass property. The multiple-component and multiple-variable constraints implemented via lower and upper bounds on (i) LAW glass properties and (ii) pairs of highly-correlated components

eliminate LAW glass compositions (component combinations) that would otherwise be allowed by the single-component constraints. The resulting model validity region thus represents the LAW glass composition region and property data used to develop LAW glass property models. The PCT and VHT models developed in this report should only be used to predict property values and their uncertainties for LAW glass compositions within the model validity region summarized in Table 9.6. Similarly, the electrical conductivity and viscosity models should only be used to predict property values and their uncertainties for combinations of LAW glass compositions and melt temperatures within the model validity region summarized in Table 9.6.



## SECTION 10 SUMMARY AND CONCLUSIONS FOR LAW GLASS PROPERTY-COMPOSITION MODELS

This report documents the development of property models for LAW glasses and the data used to develop the models. Models have been developed to relate

- PCT responses for boron and sodium and the VHT response to the composition of WTP LAW glasses.
- Viscosity and electrical conductivity to the melt temperature and composition of WTP LAW glasses.

This work constitutes what has been denoted Phase 1a of the ILAW model development effort. The ILAW property models and formulas for uncertainties in model predictions resulting from this work can be used for numerous purposes, including (i) formulating LAW glasses for specific LAW waste compositions, (ii) developing LAW glass formulation algorithms to make process step decisions during operation of the LAW vitrification facility, (iii) assessing whether proposed LAW glass compositions or LAW glass compositions calculated by process simulation codes will satisfy property specifications (PCT and VHT) and processing requirements (viscosity and electrical conductivity), and (iv) as the basis for any future ILAW glass formulation and model development work, if needed.

The datasets available for developing ILAW PCT, VHT, viscosity, and electrical conductivity models are comprised of data from different LAW glass studies conducted over several years. The number of data points available for modeling varied by property because not every property was measured on every glass. The different studies from which data were drawn for ILAW property modeling are discussed in Section 2. Some of these studies used statistical experimental design methods to select some or all of the test matrix glasses. Glasses in parts or all of some studies were “actively designed” using glass science knowledge and experience to achieve the desired purpose for the study or individual glasses in the study. The various samples encompass the effects of testing scale (from crucible melts of a few hundred grams to samples collected from continuous melter tests producing many thousands of kilograms of glass), post-melt treatment such as canister cooling, and the use of actual radioactive waste as well as waste simulants. The datasets available for modeling LAW glass properties were assessed to remove outlying and non-representative compositions from the modeling datasets. The LAW glass compositions and their property values in the available dataset and modeling dataset for each property are presented in tables in this report.

All data in the modeling dataset for a given property were used to develop models for that property. Model validation was accomplished by data-splitting, data-partitioning, and by applying the models to calculate the properties of outlying glass compositions. In the data-splitting approach, the modeling dataset was split into five sets of modeling and validation subsets, using roughly 80% of the data for modeling and 20% for validation in each split of the dataset. In the data partition approach, the modeling dataset for a given property was partitioned

into a modeling dataset (comprised of the Existing, Phase 1 Test Matrix, and Phase 1a Augmentation subsets, which were statistically designed) and a validation subset (comprised of all remaining glasses, most or all of which were actively designed). Finally, property models fit to the full modeling dataset were applied to predict property values for the outlying glasses removed from the modeling dataset for each property. This provides a limited basis to judge the extrapolative capability of the LAW glass property models. Based on the performance of the models that were investigated, recommended models were selected.

Sections 10.1 to 10.4 summarize the model development data and work for PCT, VHT, electrical conductivity, and viscosity of LAW glasses. For each property, the recommended model is mentioned and any limitations of the model noted. Section 10.5 summarizes the model validity region for each of the four LAW glass properties modeled. Section 10.6 discusses the suitability of the recommended models for WTP applications. Section 10.7 makes recommendations for any future property-composition modeling work that may occur for LAW glasses.

## 10.1 Summary of ILAW PCT Modeling

Data on PCT boron (PCT-B), sodium (PCT-Na), and silicon (PCT-Si) releases were available for 264 LAW glasses from all seven of the data groups discussed in Sections 2.1 to 2.7. The PCT results vary from 0.152 g/L (0.076 g/m<sup>2</sup>) to 35.657 g/L (17.83 g/m<sup>2</sup>) for PCT-B release, 0.209 g/L (0.105 g/m<sup>2</sup>) to 22.937 g/L (11.469 g/m<sup>2</sup>) for PCT-Na release, and 0.114 g/L (0.057 g/m<sup>2</sup>) to 2.372 g/L (1.186 g/m<sup>2</sup>) for PCT-Si release.

The WTP contract specification for PCT results (DOE-ORP 2000) requires that the normalized releases of B, Na, and Si in a seven-day PCT at 90°C be less than 2 g/m<sup>2</sup>. A review of the data for all 264 LAW glasses with PCT results showed that the normalized PCT-B and PCT-Na releases were always higher than the normalized PCT-Si releases. These results suggest that if the PCT-B and PCT-Na releases are below the WTP limit, so too will be the PCT-Si release. We therefore concluded that a model for PCT-Si release is not needed. Accordingly, with concurrence from WTP project, only PCT-B and PCT-Na releases were modeled.

Assessment of the ranges and distributions of the component values over the 264 LAW glasses with PCT data led to designating 20 glasses as having outlying compositions. Hence, the PCT modeling dataset consisted of PCT release data for 244 LAW glasses. The LAW glass compositions and PCT data are listed in Tables 5.2 and 5.3, respectively. Over these 244 LAW glasses, the component ranges and distributions of 18 components (Al<sub>2</sub>O<sub>3</sub>, B<sub>2</sub>O<sub>3</sub>, CaO, Cl, Cr<sub>2</sub>O<sub>3</sub>, F, Fe<sub>2</sub>O<sub>3</sub>, K<sub>2</sub>O, Li<sub>2</sub>O, MgO, Na<sub>2</sub>O, P<sub>2</sub>O<sub>5</sub>, SO<sub>3</sub>, SiO<sub>2</sub>, TiO<sub>2</sub>, ZnO, ZrO<sub>2</sub>, and Others) were sufficient to support separate model terms if needed.

For PCT-B and PCT-Na releases from LAW glasses, several model forms were investigated.

- An 18-component linear mixture (LM) model using the 18 components listed in the previous paragraph.

- A reduced 12-component LM model involving  $\text{Al}_2\text{O}_3$ ,  $\text{B}_2\text{O}_3$ ,  $\text{CaO}$ ,  $\text{Fe}_2\text{O}_3$ ,  $\text{K}_2\text{O}$ ,  $\text{Li}_2\text{O}$ ,  $\text{MgO}$ ,  $\text{Na}_2\text{O}$ ,  $\text{P}_2\text{O}_5$ ,  $\text{SiO}_2$ ,  $\text{ZrO}_2$ , and Others. For both PCT-B and PCT-Na releases, this model had similar performance as the 18-component LM model.
- A series of a partial quadratic mixture (PQM) models, in which the reduced 12-component LM model was augmented with between three and nine quadratic (squared and/or crossproduct) terms, leading to PQM models of 15 to 21 terms.
- A two-part 24-term model consisting of two 12-term reduced LM models fitted above and below a PCT-B or PCT-Na release cutoff value selected to optimize the fit of the two-part model to the modeling data.

Based on model fitting and validation results, the 17-term PQM models are recommended for predicting PCT-B and PCT-Na releases from LAW glasses. The 12 linear terms ( $\text{Al}_2\text{O}_3$ ,  $\text{B}_2\text{O}_3$ ,  $\text{CaO}$ ,  $\text{Fe}_2\text{O}_3$ ,  $\text{K}_2\text{O}$ ,  $\text{Li}_2\text{O}$ ,  $\text{MgO}$ ,  $\text{Na}_2\text{O}$ ,  $\text{P}_2\text{O}_5$ ,  $\text{SiO}_2$ ,  $\text{ZrO}_2$ , and Others) are for the same components in each of the PCT-B and PCT-Na PQM models. The five quadratic terms in the PCT-B model are  $\text{CaO} \times \text{Li}_2\text{O}$ ,  $\text{B}_2\text{O}_3 \times \text{MgO}$ ,  $\text{B}_2\text{O}_3 \times \text{Li}_2\text{O}$ ,  $\text{Na}_2\text{O} \times \text{SiO}_2$ , and  $\text{CaO} \times \text{Fe}_2\text{O}_3$ . Results for the PCT-B 17-term PQM model are given in Table 5.9 and discussed in Section 5.3.3. The five quadratic terms in the PCT-Na model are  $\text{CaO} \times \text{Li}_2\text{O}$ ,  $\text{CaO} \times \text{Fe}_2\text{O}_3$ ,  $\text{B}_2\text{O}_3 \times \text{MgO}$ ,  $\text{B}_2\text{O}_3 \times \text{Na}_2\text{O}$ , and  $\text{K}_2\text{O} \times \text{K}_2\text{O}$ . Results for the PCT-Na 17-term PQM model are given in Table 5.14 and discussed in Section 5.4.3.

The recommended 17-term PQM models for PCT-B and PCT-Na appear to reduce the tendency of the 12-term LM models to under-predict these releases near and above the 4 g/L (2 g/m<sup>2</sup>) WTP contract limit. However, the recommended 17-term models still tend to under-predict PCT-B and PCT-Na releases above approximately 2.7 g/L. The PCT modeling database contained an insufficient number of glasses with PCT-B and PCT-Na releases near and above the contract limits to develop and validate models without this limitation. Hence, constraints were included in the model validity region to restrict the use of the recommended PCT-B and PCT-Na models to glasses with predicted releases below 2.7 g/L, as discussed in Section 9.

Because of the magnitudes of uncertainties in the PCT data (i.e., from making simulated LAW glasses, PCT testing, and chemical analysis of leachates), as well as moderate lack-of-fit of the recommended PCT-B and PCT-Na models, prediction uncertainties for the models are relatively large (see Section 5.6). Unless higher waste loadings are pursued, it is relatively easy to formulate LAW glasses with PCT-B and PCT-Na releases substantially below the contract limit, so the model limitations (under-predictions of releases near and above contract limits, as well as relatively large prediction uncertainties) may not unduly restrict WTP LAW vitrification operations. Separate work that will be performed to assess the impact of LAW glass composition and model uncertainties for the recommended PCT-B and PCT-Na models is discussed in Section 5.6.

## 10.2 Summary of ILAW VHT Modeling

Data on VHT alteration depth were available for 181 LAW glasses from the six data groups discussed in Sections 2.1 to 2.6. There were no VHT data on any of the LAW glasses

made from actual waste, which are discussed in Section 2.7. The VHT alteration data for six glasses were reported as “greater than” values of either  $>800$  or  $>1100$   $\mu\text{m}$ . Of the remaining 175 glasses, the VHT alteration results varied from 1  $\mu\text{m}$  ( $0.1$   $\text{g}/\text{m}^2/\text{day}$ ) to 980  $\mu\text{m}$  ( $108.2$   $\text{g}/\text{m}^2/\text{day}$ ), as compared to the contract requirement of  $< 50$   $\text{g}/\text{m}^2/\text{day}$ .

Assessment of the ranges and distributions of the component values over the 175 LAW glasses with non-censored VHT data led to designating 10 glasses as having outlying compositions. These 10 outlying compositions were 10 of the 20 outlying compositions for the PCT database (the other 10 outlying glass compositions that had PCT data did not have VHT data). Hence, the VHT modeling dataset consisted of VHT alteration data for 165 LAW glasses. These data are listed in Tables 6.2 and 6.3. Over these 165 LAW glasses, the component ranges and distributions of 18 components ( $\text{Al}_2\text{O}_3$ ,  $\text{B}_2\text{O}_3$ ,  $\text{CaO}$ ,  $\text{Cl}$ ,  $\text{Cr}_2\text{O}_3$ ,  $\text{F}$ ,  $\text{Fe}_2\text{O}_3$ ,  $\text{K}_2\text{O}$ ,  $\text{Li}_2\text{O}$ ,  $\text{MgO}$ ,  $\text{Na}_2\text{O}$ ,  $\text{P}_2\text{O}_5$ ,  $\text{SO}_3$ ,  $\text{SiO}_2$ ,  $\text{TiO}_2$ ,  $\text{ZnO}$ ,  $\text{ZrO}_2$ , and Others) were sufficient to support separate model terms if needed. These were the same 18 components selected for initial PCT modeling.

Several model forms were investigated for VHT alteration of LAW glasses.

- An 18-component LM model using the 18 components listed in the previous paragraph.
- A reduced 11-component LM model involving  $\text{Al}_2\text{O}_3$ ,  $\text{B}_2\text{O}_3$ ,  $\text{CaO}$ ,  $\text{Fe}_2\text{O}_3$ ,  $\text{K}_2\text{O}$ ,  $\text{Li}_2\text{O}$ ,  $\text{MgO}$ ,  $\text{Na}_2\text{O}$ ,  $\text{SiO}_2$ ,  $\text{ZrO}_2$ , and Others. This model had similar performance as the 18-component LM model.
- A series of PQM models, in which the reduced 11-component LM model was augmented using statistical variable selection methods with between three and nine quadratic (squared and/or crossproduct) terms. Three additional PQM models considered during previous preliminary VHT modeling work by VSL (Perez-Cardenas et al. 2006) consisting of (i) 9 linear plus 8 squared terms, (ii) 14 linear plus 13 squared terms, and (iii) 9 linear plus 7 quadratic terms) were also investigated.
- A two-part 22-term model consisting of two 11-term reduced LM models fitted above and below a VHT alteration depth cutoff value selected to optimize the fit of the two-part model to the modeling data.
- Several mixture experiment models containing cubic terms, which are denoted partial cubic mixture (PCM) models. Two of these PCM models were based on ones considered by VSL in previous preliminary modeling work. The first PCM model included 14 linear terms, 2 quadratic terms, and 2 cubic terms. The second included 14 linear terms, 3 quadratic terms, and 4 cubic terms. A third PCM model investigated in this work consisted of the 11 terms in the reduced LM model, plus the same two quadratic and two cubic terms as in the first PCM model. Finally, four additional PCM models were formed by augmenting the 11 terms in the reduced LM model with subsets of 4, 5, 7, or 9 cubic terms selected using statistical variable selection methods. Quadratic terms were allowed to be selected in addition to cubic terms, but only cubic terms were selected.
- A preliminary investigation of local linear regression models was also performed. This approach consisted of fitting separate 11-component LM models using the  $n$  closest LAW

glasses to any specific glass composition. Values of  $n$  ranging from 25 to 100 were investigated, with 50 selected as best.

More information about all of the VHT models considered and the results obtained is contained in Section 6.6.

Based on an extensive comparison of model fitting, validation, and other results in Sections 6.8 and 6.9, the 18-component and 11-component LM models were determined to have significant lack-of-fits (especially under-predicting larger VHT alteration depths). Ultimately, a 15-term PCM model consisting of 11 linear terms ( $\text{Al}_2\text{O}_3$ ,  $\text{B}_2\text{O}_3$ ,  $\text{CaO}$ ,  $\text{Fe}_2\text{O}_3$ ,  $\text{K}_2\text{O}$ ,  $\text{Li}_2\text{O}$ ,  $\text{MgO}$ ,  $\text{Na}_2\text{O}$ ,  $\text{SiO}_2$ ,  $\text{ZrO}_2$ , and Others) and four cubic terms [ $(\text{K}_2\text{O})^2 \times \text{Na}_2\text{O}$ ,  $(\text{Na}_2\text{O})^3$ ,  $\text{Li}_2\text{O} \times \text{Na}_2\text{O} \times \text{SiO}_2$ , and  $\text{B}_2\text{O}_3 \times \text{CaO} \times \text{Na}_2\text{O}$ ] was recommended for predicting the VHT alteration of LAW glasses. Results for this 15-term PCM model are given in Table 6.11 and discussed in Section 6.6. A second-choice alternate model containing quadratic but no cubic terms was also suggested. That 16-term PQM model consists of the same 11 linear terms and 5 quadratic terms ( $\text{CaO} \times \text{SiO}_2$ ,  $(\text{K}_2\text{O})^2$ ,  $\text{MgO} \times \text{Na}_2\text{O}$ ,  $\text{Al}_2\text{O}_3 \times \text{ZrO}_2$ , and  $\text{Na}_2\text{O} \times \text{ZrO}_2$ ). Results for this 16-term PQM model are given in Table 6.9 and discussed in Section 6.4.

The inclusion of quadratic terms in the second-choice alternate model for VHT alteration appears to reduce the tendencies of the LM models to under-predict larger VHT alteration depths. The inclusion of cubic terms in the recommended model for VHT alteration appears to correct the tendency to under-predict larger VHT alterations. The inadequacy of linear mixture models is likely a reflection of the complexity of the VHT process, which tends to accentuate non-linear effects of glass composition. Thus, it is reasonable that non-linear terms would be needed in VHT models.

The recommended 15-term PCM model for VHT alteration depth appears to yield unbiased predictions over the full range of measured VHT alteration depth values in the modeling dataset. However, there is some concern that this model may over-fit the data. Also, there is relatively large scatter in data points about the fitted model (see Figure 6.20). This significant scatter is a result of (i) relatively large uncertainties in the VHT data (i.e., from making simulated LAW glasses, VHT testing, and measuring alteration depths), and (ii) significant lack-of-fit of the recommended VHT model. Because of these reasons, prediction uncertainties for the model are relatively large (see Section 6.11). While it may still be possible to formulate LAW glasses with VHT alteration depths sufficiently below the contract limit, so the relatively large prediction uncertainties do not unduly restrict WTP LAW vitrification operations, it is likely that there will be some impact on achievable waste loadings. Consequently, it is expected that additional effort in this area would be very beneficial. Separate work that will be performed to assess the impact of LAW glass composition and model uncertainties for the recommended VHT model is discussed in Section 6.11.

### 10.3 Summary of ILAW Electrical Conductivity Modeling

Data on electrical conductivity (EC) were available for 181 LAW glasses from the six data groups discussed in Sections 2.1 to 2.6. There were no EC data on any of the LAW glasses

made from actual waste, which are discussed in Section 2.7. Electrical conductivity was measured for each LAW glass at four temperatures, generally in the vicinity of 950, 1050, 1150, and 1250°C. Actual temperatures at which EC was measured ranged from 917 to 1278°C. The EC results vary from 0.020 to 0.961 S/cm, with smaller values occurring at lower temperatures and larger values occurring at higher temperatures.

Assessment of the ranges and distributions of the component values over the 181 LAW glasses with EC data led to designating 10 glasses as having outlying compositions. These 10 outlying compositions were 10 of the 20 outlying compositions for the PCT database (the other 10 outlying glass compositions that had PCT data did not have EC data). Hence, the EC modeling dataset consisted of EC values at four temperatures for each of 171 LAW glasses. The LAW glass composition and EC data are listed in Tables 7.2 and 7.3, respectively. Over these 171 LAW glasses, the component ranges and distributions of 18 components (Al<sub>2</sub>O<sub>3</sub>, B<sub>2</sub>O<sub>3</sub>, CaO, Cl, Cr<sub>2</sub>O<sub>3</sub>, F, Fe<sub>2</sub>O<sub>3</sub>, K<sub>2</sub>O, Li<sub>2</sub>O, MgO, Na<sub>2</sub>O, P<sub>2</sub>O<sub>5</sub>, SO<sub>3</sub>, SiO<sub>2</sub>, TiO<sub>2</sub>, ZnO, ZrO<sub>2</sub>, and Others) were sufficient to support separate model terms if needed. These were the same 18 components selected for initial PCT and VHT modeling.

Investigation of three equations (Arrhenius, truncated T2, and T2; see Section C.2.1) for the temperature dependence of EC showed that the Arrhenius equation was sufficient for the vast majority of the 171 glasses in the EC modeling dataset. Several property-composition-temperature model forms for EC were developed by expanding the two parameters of the Arrhenius equation as linear or partial quadratic mixture experiment models.

- A 36-term Arrhenius-LM model involving 18  $x_i$  terms and 18  $x_i/(T/1000)$  terms based on the 18 components listed in the previous paragraph.
- A reduced 22-term Arrhenius-LM model involving 11  $x_i$  terms and 11  $x_i/(T/1000)$  terms based on the 11 components Al<sub>2</sub>O<sub>3</sub>, B<sub>2</sub>O<sub>3</sub>, CaO, Fe<sub>2</sub>O<sub>3</sub>, K<sub>2</sub>O, Li<sub>2</sub>O, MgO, Na<sub>2</sub>O, SiO<sub>2</sub>, ZrO<sub>2</sub>, and Others. (These are the same 11 components selected for the VHT reduced LM model.) This model had similar performance as the 36-term Arrhenius-LM model.
- A series of models adding three crossproduct terms (CaO×Li<sub>2</sub>O, CaO×Na<sub>2</sub>O, and Li<sub>2</sub>O×Na<sub>2</sub>O) to the “composition only” and/or “composition-temperature” portions of the 22-term Arrhenius-LM model. The number of terms in these models ranged from 25 to 28.

Based on model fitting and validation results, a 25-term Arrhenius-LM model with three additional crossproduct terms is the recommended model for EC of LAW glasses. This model has 11 linear composition terms of the form  $x_i$  (involving Al<sub>2</sub>O<sub>3</sub>, B<sub>2</sub>O<sub>3</sub>, CaO, Fe<sub>2</sub>O<sub>3</sub>, K<sub>2</sub>O, Li<sub>2</sub>O, MgO, Na<sub>2</sub>O, SiO<sub>2</sub>, ZrO<sub>2</sub>, and Others), three quadratic terms of the form  $x_i x_j$  (representing the crossproduct pairs CaO×Li<sub>2</sub>O, CaO×Na<sub>2</sub>O, and Li<sub>2</sub>O×Na<sub>2</sub>O), and 11 composition-temperature terms of the form  $x_i/(T/1000)$ . The temperature ( $T$ , Kelvin) is scaled by 1000 so that the model coefficients for those terms are of comparable magnitudes to those of the linear-composition terms. Results for the recommended 25-term EC model are given in Table 7.10 and discussed in Section 7.5. Methods for making electrical conductivity predictions and quantifying the uncertainties in the predictions are discussed and illustrated in Section 7.6.

The recommended EC model provides unbiased predictions over the full range of measured EC values in the modeling dataset, with relatively tight scatter for most data points about the fitted model, and moderate scatter for some data points (see Figure 7.14). The recommended EC model does not have a statistically significant LOF, so that EC predictions can be expected to be within the uncertainty of what would be obtained by batching and melting glasses and measuring the EC. The magnitudes of uncertainties in EC model predictions should be small enough that they will not unduly restrict the formulation and processing of LAW glasses in the WTP facility. However, separate work to confirm this is planned, as discussed in Section 7.7.

#### 10.4 Summary of ILAW Viscosity Modeling

Data on viscosity were available for 181 LAW glasses from the six data groups discussed in Sections 2.1 to 2.6. These were the same 181 glasses for which electrical conductivity data were available. There were no viscosity data on any of the LAW glasses made from actual waste, which are discussed in Section 2.7. Viscosity was measured for each LAW glass at four temperatures, generally in the vicinity of 950, 1050, 1150, and 1250°C. An exception was glass LAWM7, for which viscosity was measured at five temperatures. Actual temperatures at which viscosity was measured ranged from 903 to 1271°C. The viscosity results vary from 5.99 to 2329.04 poise, with smaller values occurring at higher temperatures and larger values occurring at lower temperatures.

Assessment of the ranges and distributions of the component values over the 181 LAW glasses with viscosity data led to designating 10 glasses as having outlying compositions. These 10 outlying compositions were the same 10 selected for EC, and 10 of the 20 outlying compositions for the PCT database (the other 10 outlying glass compositions that had PCT data did not have viscosity or EC data). Hence, the viscosity modeling dataset consisted of viscosity values at four temperatures for each of 171 LAW glasses, plus a viscosity value at the additional fifth temperature for glass LAWM7. The LAW glass composition and viscosity data are listed in Tables 7.2 and 8.1, respectively. Over these 171 LAW glasses, the component ranges and distributions of 18 components ( $\text{Al}_2\text{O}_3$ ,  $\text{B}_2\text{O}_3$ ,  $\text{CaO}$ ,  $\text{Cl}$ ,  $\text{Cr}_2\text{O}_3$ ,  $\text{F}$ ,  $\text{Fe}_2\text{O}_3$ ,  $\text{K}_2\text{O}$ ,  $\text{Li}_2\text{O}$ ,  $\text{MgO}$ ,  $\text{Na}_2\text{O}$ ,  $\text{P}_2\text{O}_5$ ,  $\text{SO}_3$ ,  $\text{SiO}_2$ ,  $\text{TiO}_2$ ,  $\text{ZnO}$ ,  $\text{ZrO}_2$ , and Others) were sufficient to support separate model terms if needed. These were the same 18 components selected for initial PCT, VHT, and EC modeling.

Investigation of three equations (Arrhenius, truncated T2, and T2; see Section C.2.1) for the temperature dependence of viscosity showed that the truncated-T2 equation was sufficient for the vast majority of the 171 glasses in the viscosity modeling dataset. Several property-composition-temperature model forms for viscosity were developed by expanding the two parameters of the truncated-T2 equation as linear or partial quadratic mixture experiment models.

- A 36-term truncated T2-LM model involving 18  $x_i$  terms and 18  $x_i/(T/1000)^2$  terms, each based on the 18 components listed in the previous paragraph.

- Two reduced truncated T2-LM models containing 22 or 24 terms involving 11 or 12  $x_i$  terms and 11 or 12  $x_i/(T/1000)$  terms. The 22-term model involved the 11 components  $\text{Al}_2\text{O}_3$ ,  $\text{B}_2\text{O}_3$ ,  $\text{CaO}$ ,  $\text{Fe}_2\text{O}_3$ ,  $\text{K}_2\text{O}$ ,  $\text{Li}_2\text{O}$ ,  $\text{MgO}$ ,  $\text{Na}_2\text{O}$ ,  $\text{SiO}_2$ ,  $\text{ZrO}_2$ , and Others, while the 24-term model also involved  $\text{P}_2\text{O}_5$ . These models had similar performances as the 36-term truncated T2-LM model.
- Two models adding four statistically-selected quadratic terms of the form  $x_i x_j$  to the 22-term and 24-term truncated T2-LM models. Hence, these models contained a total of 26 and 28 terms, respectively. A third model of this form containing 26 terms was obtained by dropping two statistically non-significant terms of the form  $x_i/(T/1000)^2$  from the 28-term model.

Based on model fitting and validation results, a 26-term reduced truncated T2-LM model with four additional quadratic terms is the recommended model for viscosity of LAW glasses. This model has 12 linear composition terms of the form  $x_i$  (involving  $\text{Al}_2\text{O}_3$ ,  $\text{B}_2\text{O}_3$ ,  $\text{CaO}$ ,  $\text{Fe}_2\text{O}_3$ ,  $\text{K}_2\text{O}$ ,  $\text{Li}_2\text{O}$ ,  $\text{MgO}$ ,  $\text{Na}_2\text{O}$ ,  $\text{P}_2\text{O}_5$ ,  $\text{SiO}_2$ ,  $\text{ZrO}_2$ , and Others), four quadratic terms of the form  $x_i x_j$  or  $x_i^2$  [representing  $(\text{B}_2\text{O}_3)^2$ ,  $(\text{Li}_2\text{O})^2$ ,  $\text{Al}_2\text{O}_3 \times \text{Li}_2\text{O}$ ,  $(\text{MgO})^2$ ], and 10 composition-temperature terms of the form  $x_i/(T/1000)^2$  involving  $\text{Al}_2\text{O}_3$ ,  $\text{CaO}$ ,  $\text{Fe}_2\text{O}_3$ ,  $\text{K}_2\text{O}$ ,  $\text{Li}_2\text{O}$ ,  $\text{MgO}$ ,  $\text{Na}_2\text{O}$ ,  $\text{P}_2\text{O}_5$ ,  $\text{SiO}_2$ ,  $\text{ZrO}_2$ , and Others. The  $\text{B}_2\text{O}_3/(T/1000)^2$  and  $\text{K}_2\text{O}/(T/1000)^2$  terms were statistically non-significant and thus omitted from the model. The temperature ( $T$ , Kelvin) is scaled by 1000 so that the model coefficients for those terms are of comparable magnitudes to those of the linear-composition terms. Results for the recommended 26-term viscosity model are given in Table 8.8 and discussed in Section 8.5. Methods for making viscosity predictions and quantifying the uncertainties in the predictions are discussed and illustrated in Section 8.6.

The recommended viscosity model provides unbiased predictions over the full range of measured viscosity values in the modeling dataset, with relatively tight scatter for most data points about the fitted model, and moderate scatter for some data points (see Figure 8.12). The recommended viscosity model does not have a statistically significant LOF, so that viscosity predictions can be expected to be within the uncertainty of what would be obtained by batching and melting glasses and measuring the viscosity. The magnitudes of uncertainties in viscosity model predictions should be small enough that they will not unduly restrict the formulation and processing of LAW glasses in the WTP facility. However, separate work to confirm this is planned, as discussed in Section 8.7.

## 10.5 Summary of Model Validity Regions for Recommended LAW Glass Property Models

The LAW glass property-composition models recommended in this report were obtained by estimating coefficients of models using least squares regression methods. PCT and VHT models developed in this way should only be applied to LAW glass compositions inside the composition region over which the models were developed and demonstrated to yield unbiased predictions. Similarly, EC and viscosity models developed in this way should only be applied to LAW glass compositions at melt temperatures inside the composition-temperature region over which the models were developed and demonstrated to yield unbiased predictions. Such regions



are referred to as *model validity regions*, which are defined using single- and multiple-component constraints on LAW glass components. Single- and multiple-component constraints directly on LAW glass compositions are the same for each model validity region (i.e., PCT, VHT, electrical conductivity, and viscosity). Because electrical conductivity and viscosity also depend on melt temperature, there is a temperature aspect of the model validity region for those properties. Finally, some multiple-component constraints are specific to the model validity region for a given LAW glass property. These multiple-component constraints involve limits on glass properties, and are implemented using the recommended property models. The model validity regions are discussed in Section 9, and the constraints defining them are summarized in Table 9.6.

## **10.6 Suitability of Recommended LAW Glass Property Models for Use by the WTP Project**

The test objectives for this work (see Section 1.1) were achieved by developing, validating, and quantifying uncertainty in property-composition models for LAW glasses. Recommended models are presented for PCT response (B and Na releases), VHT alteration, electrical conductivity, and viscosity. The recommended models for each property, being the best of the models considered in the development and validation process, are suitable for predicting properties of LAW glasses within the constraints of the model validity region for each property as discussed in Section 9.

The model validity region for the recommended PCT-B and PCT-Na models limits their use to LAW glasses with predicted normalized PCT releases below 2.7 g/L. These limitations were necessary because the recommended models for PCT-B and PCT-Na tend to under-predict releases above 2.7 g/L. These model limitations are attributed to insufficient data for glasses with releases higher than this value, and especially higher than the contract limit of 4 g/L (2 g/m<sup>2</sup>). Because it is relatively easy to formulate LAW glasses with lower PCT releases, the restriction on application of PCT-B and PCT-Na models to predicted releases below 2.7 g/L may not unduly limit WTP operations in the LAW vitrification facility. If the WTP project determines that these constraints on the PCT-B and PCT-Na models may be unduly restrictive, additional future work would then be necessary to address the issue (see Section 11.1).

Although the recommended VHT model appears to have corrected the problems of under-predicting higher VHT alterations seen with other models considered, it was not possible to demonstrate this definitively because of limited data near and above the contract limit of 50 g/m<sup>2</sup>/day. Also, the recommended VHT model is subject to relatively large prediction uncertainties because of (i) the magnitude of uncertainty in VHT alteration data and (ii) significant model lack-of-fit. Consequently, it is likely that there will be some impact on achievable waste loadings and therefore it is expected that additional effort in this area would be very beneficial. Planned future work to assess the suitability of the recommended models in this report (discussed subsequently in this section) will have to determine whether these limitations of the VHT property-composition dataset and recommended model are sufficient to unduly restrict operations of the LAW vitrification facility. If the WTP project determines that the

limitations of the recommended model for VHT alteration depth are unduly restrictive, additional future work would then be necessary to address the issue (see Section 11.2).

Electrical conductivity and viscosity models as functions of LAW glass composition and melt temperature fit their respective modeling datasets very well without bias or statistically significant lack-of-fit within the composition-temperature region represented by the modeling dataset. The only limitations of these models are the lack of data outside the processing ranges of their respective properties (see Section 11.3). Because viscosity and electrical conductivity models can often tolerate small to moderate extrapolation reasonably well, the lack of data outside the property processing ranges is not likely to be a major issue for the WTP project. However, if the WTP project decides this issue must be addressed, work would be needed to (i) validate the extrapolative performance of the recommended viscosity and electrical conductivity models, or (ii) expand the modeling dataset and update models to cover a larger desired region of applicability. In summary, the electrical conductivity and viscosity models for LAW glasses are well-suited for application by the WTP project as long as they are limited to application within the range of the modeling dataset

It is outside the scope of work in this report to completely assess the suitability of the recommended property models. Ultimately, the WTP project needs to assess whether the recommended models, along with their corresponding uncertainties, are suitable for their various intended uses (e.g., glass formulation, addition of glass-forming chemicals to waste during LAW vitrification operations, and compliance with WTP contract specifications and processing constraints). Such assessments are within the scopes for algorithm development and verification (work being conducted by WTP project staff) and statistical compliance methodology development and demonstration (work under separate PNNL scope).

Using earlier versions of property-composition models (Muller et al. 2005a) and the current LAW glass formulation correlation (Muller et al. 2004b), initial work has been previously conducted on algorithm development and verification (Vienna 2005) and on statistical compliance methodology development and demonstration (Piepel et al. 2005). The WTP project has future work planned to update the algorithm work (within the WTP project) and statistical compliance work (at PNNL).

## **SECTION 11**

### **RECOMMENDATIONS FOR ANY FUTURE ILAW PROPERTY-COMPOSITION DATA COLLECTION, MODEL DEVELOPMENT, OR MODEL VALIDATION WORK**

The work in this report to develop, validate, and quantify the uncertainty in property-composition models for LAW glasses is the last iteration of such work that is currently scheduled. However, there are many years between now and when the WTP LAW vitrification facility is scheduled to become operational. In that time, knowledge of tank waste compositions, blending scenarios, pretreatment outcomes, glass formulations, and desired waste loadings may improve. Improved knowledge could lead to a need to revise the LAW glass composition region of interest, and thus to additional glass property-composition data collection and model development and/or validation work. Further, the models recommended in this report have some limitations as discussed in Sections 10.1 to 10.4 and 10.6, which the WTP project may decide to address by collecting additional property-composition data and performing additional model development and/or validation work. It is in this context that the following discussion, suggestions, and recommendations are made.

An issue common to all four properties (PCT, VHT, electrical conductivity, and viscosity) is limited data outside contract or processing limits on the properties. One of the primary requirements for the ILAW property-composition models is that they be able to accurately predict, with acceptable uncertainty<sup>24</sup>, when an LAW glass would have property values outside WTP contract or processing limits. To achieve this goal, there must be sufficient LAW glasses with property values near and somewhat beyond the contract and processing limits.

Several recommendations are made in Sections 11.1 to 11.4 for any additional ILAW property-composition data collection and modeling work that may be performed in the future. A recommendation is made in each of Sections 11.1 to 11.3 to address the common issue discussed in the preceding paragraph. Sections 11.1 and 11.2 also make other recommendations for any future PCT and VHT property-composition data development, model development, or model validation work. Section 11.4 discusses some general recommendations.

#### **11.1 Recommendations for ILAW PCT**

The recommended models for PCT-B and PCT-Na releases of LAW glasses have two substantive limitations, as discussed in Sections 5.6 and 10.1. The first limitation is that the models tend to under-predict PCT-B and PCT-Na releases above 2.7 g/L, and hence model validity constraints were imposed limiting use of the models to glasses with predicted releases less than 2.7 g/L. The second limitation is that the PCT-B and PCT-Na models are subject to relatively large prediction uncertainties, resulting from uncertainty in the modeling data and from

---

<sup>24</sup> Here “acceptable uncertainty” refers to the uncertainty that will allow compliance and processing constraints to be met without overly restricting glass compositions or processing properties.

moderate model lack-of-fit. If the future work summarized in Section 10.6 concludes that these limitations are not unduly restrictive to operation of the WTP LAW vitrification facility, then no additional property-composition data and model development work will be needed. However, if the WTP project decides that such additional work is needed, the following recommendations are offered.

Collect Additional Data for LAW Glasses with Higher PCT Releases: For ILAW PCT-B and PCT-Na releases, the WTP contract limit is  $2 \text{ g/m}^2$  ( $4 \text{ g/L}$ ). However, only 9 of 264 LAW glasses with PCT data had PCT-B releases above the limit, and only 8 of 264 glasses had PCT-Na releases above the limit. These numbers of glasses with PCT-B and PCT-Na releases above the contract limits provide insufficient data to accurately predict (and validate such predictions) for higher PCT releases. Thus, if judged as necessary by the WTP project, it is recommended that additional higher PCT release data (ranging from somewhat below the contract limit to somewhat above) be collected to support development of new PCT-B and PCT-Na models with unbiased predictive performance above the model validity constraint of  $2.7 \text{ g/L}$  imposed for the models recommended in this report. Doing so would permit relaxing or removing that model validity constraint.

Investigate Other Model Development Approaches: The PCT-B and PCT-Na release data have relatively large uncertainties (i.e., %RSD of 23 for PCT-B and 18% for PCT-Na). Still, the recommended models have some lack-of-fit (meaning that the model prediction uncertainty is larger than can be accounted for by the uncertainty in PCT-B and PCT-Na data). This is presumably due to more complicated non-linear blending effects of LAW glass components on PCT releases over the LAW glass composition region of interest than can be captured by a single model equation with up to quadratic or even cubic terms. There are two classes of solutions to this situation. The first is to adopt other modeling approaches that provide for better capturing local dependence of PCT releases on LAW glass composition over the full glass composition region of interest. This option is discussed further in Sections 11.4.3 and 11.4.4. The second is to develop models of the forms considered so far, but over smaller LAW glass composition regions where they are likely to fit and predict better. The smaller glass composition regions might correspond to specific LAW wastes or groups of similar LAW wastes, for example.

## 11.2 Recommendations for ILAW VHT

The recommended model for VHT alteration of LAW glasses has an issue of moderate concern as well as a significant limitation. These are each briefly summarized and associated recommendations given.

The issue of moderate concern is whether the recommended VHT model accurately predicts near and above the WTP contract limit. The recommended VHT model (which contains up to cubic terms) appears to predict VHT alteration depths reasonably well near and above the WTP contract limit (see Figure 6.20). However, the second-choice VHT model (which contains up to quadratic terms) tends to under-predict VHT alteration rates near and above the limit (see

Figure 6.13). It is possible that the improved performance of the recommended VHT model for higher VHT alteration depths is a result of over-fitting (via the use of cubic terms) to the limited number of glasses with VHT alterations near and above the limit. The significant limitation is that the recommended VHT model is subject to relatively large prediction uncertainties, resulting from uncertainty in the modeling data and from significant model lack-of-fit. This topic was discussed in Sections 6.11 and 10.2.

If the future work summarized in Section 10.6 concludes that the concern and limitation are not unduly restrictive to operation of the WTP LAW vitrification facility, then no additional property-composition data and model development work will be needed. However, if the WTP project decides that such additional work is needed, the following recommendations are offered.

Collect Additional Data for LAW Glasses with Higher VHT Alterations: For ILAW VHT alteration rate, the WTP contract limit is 50 g/m<sup>2</sup>/day (which corresponds to a 453 μm alteration depth). However, only 20 of 171 LAW glasses with VHT data had alteration depths above the contract limit. Further, 6 of these were right-censored (i.e., greater-than values) and thus were not available as data points for VHT model development and validation. Thus, if judged as necessary by the WTP project, it is recommended that additional higher VHT alteration data (ranging from somewhat below the contract limit to somewhat above) be collected, possibly with replicate VHT testing of each glass to reduce uncertainties due to testing. The data could be used to first validate the model recommended in this report to determine if it accurately predicts higher VHT alterations. If the model is found to under-predict, then the data could be used to develop a new VHT model that would accurately predict larger values of VHT alteration depth.

Investigate Other Model Development Approaches: The VHT data have relatively large uncertainties (i.e., %RSD = 31), but the recommended model still has a statistically significant lack-of-fit (meaning that the model prediction uncertainty is larger than can be accounted for by the uncertainty in VHT data). This is presumably due to more complicated non-linear blending effects of LAW glass components on VHT alterations over the LAW glass composition region of interest than can be captured by a single model equation with up to cubic terms. There are two classes of solutions to this situation. The first is to adopt other modeling approaches that provide for better capturing local dependence of VHT alteration on LAW glass composition over the full glass composition region of interest. This option is discussed further in Sections 11.4.3 and 11.4.4. The second is to develop models of the forms considered so far, but over smaller LAW glass composition regions where they are likely to fit and predict better. The smaller glass composition regions might correspond to specific LAW wastes or groups of similar LAW wastes, for example.

### **11.3 Recommendations for ILAW Electrical Conductivity and Viscosity**

The recommended models for EC and viscosity of LAW glasses perform very well within the composition and temperature region represented by the modeling datasets. However, there are limited data outside of the processing ranges for these properties.

- The current WTP limits for glass melt electrical conductivity are 0.1 to 0.7 S/cm in the temperature range of 1100 to 1200°C. Only 8 of the 188 measurements made in this temperature range were outside of these limits.
- The current WTP limits for melt viscosity are 10 to 150 poise at 1100°C. Only 4 out of 181 glasses had viscosities outside of this range at this temperature.

The limited support for applying the electrical conductivity (EC) and viscosity models outside of their processing ranges could be improved with additional data. The WTP project will have to decide how likely it is that EC and viscosity may go outside their processing ranges, what the risks of such excursions would be, and the extent to which the risks could be acceptably addressed by extrapolative use of the recommended models. If the WTP project judges the risks are sufficient to need addressing, then additional data should be collected for LAW glasses with EC and viscosity outside the processing limits. Such data could first be used to validate the models recommended in this report, and if necessary to develop new models with improved predictive performance for EC and viscosity outside their processing ranges.

## **11.4 General Recommendations**

Sections 11.4.1 to 11.4.4 present general recommendations not specific to a given LAW glass property. Whether each recommendation is considered necessary or optional is discussed.

### **11.4.1 Recommendation for Additional Work to Assess Suitability of the Recommended LAW Glass Property Models**

Sections 5.6, 6.11, 7.7, and 8.7 discussed separate work that is planned to assess the impact on WTP operations and compliance of LAW glass composition and model uncertainties using the LAW glass property models recommended in this report. This separate work includes the second iterations of glass formulation algorithm development and verification work (planned to be performed by WTP project staff) and compliance methodology and verification work (planned to be conducted by PNNL). It is recommended that these planned future work scopes be completed as a necessary step in either (i) verifying the recommended LAW glass property models are sufficient for WTP needs, or (ii) deciding that additional property-composition data collection and model development and/or validation work is needed.

### **11.4.2 Recommendations for Replication**

In any future property-composition data and model development efforts, it is recommended that consideration be given to including the same glasses as replicates in each new study. At least one and up to five such replicate glasses should be included in each new study, depending on the number of glasses in the study. Including such replicate glasses would provide a better basis for directly assessing whether the new data are biased (i.e., impacted by systematic

effects). As an illustration, Figure 8.13 shows that the recommended viscosity model appears to over-predict viscosity for the “correlation” group of glasses discussed in Section 2.4. It is not clear whether this is due to model inadequacy or a bias in the data for the “correlation” group. Including replicates of the same three to five glasses in each new study would provide a direct basis for assessing and possibly correcting for any biases in data. However, the relative benefit of spending this effort (glass fabrication and testing) on replicates rather than new glass compositions should be assessed before proceeding. This recommendation should be considered as advisable for any future work to generate property-composition data for developing and/or validating LAW glass property-composition models.

Because of the restriction on randomization that occurs in measuring EC and viscosity data (see Sections C.3.2 and C.3.3 of Appendix C), it would be useful to collect replicate measurements of these properties at some temperature(s) for each glass. Currently, these properties are measured at four temperatures for each glass, without replication because the benefits of such replication have been judged to not justify the additional cost. Replication of viscosity and EC measurements at one or more temperature values would provide a basis for directly estimating the standard deviation of the uncertainty associated with measuring these properties. Currently, this can only be estimated indirectly, and is inflated by any lack-of-fit of the composition-temperature portion of the viscosity or EC model. Replication of viscosity and EC measurements at one or more temperatures would also provide for assessing the lack-of-fit of the portions of viscosity and EC models involving composition  $\times$  temperature terms. This recommendation would improve the ability to quantify viscosity and EC measurement uncertainty and to develop and future EC and viscosity models, but it is not necessary.

### **11.4.3 Recommendation to Investigate Local As Well As Global Modeling Approaches**

The approach of using a single “global” model to predict PCT releases and VHT alteration as functions of LAW glass composition may need to be revisited in the future under certain situations. One such situation would be collecting additional data with higher PCT releases and VHT alterations, as discussed in Sections 11.1 and 11.2. Another situation would be collecting additional ILAW property-composition data over a wider region of LAW glass compositions corresponding to a wider region of LAW compositions. Under such situations, a single global model may not be able to adequately approximate the changing relationship between the ILAW property and LAW glass composition over a wider composition region. It may be necessary to investigate in any future modeling work the use of “local” rather than “global” modeling approaches to obtain models having more accurate predictions of ILAW properties with smaller prediction uncertainties. One type of local modeling approach would be to develop multiple models over smaller, local regions of LAW glass composition space. Past experience has shown that linear mixture models or partial quadratic mixture models can be sufficiently accurate with lower uncertainties over less expansive compositions regions. Another type of local modeling approach would be to use so-called non-parametric regression methods such as local linear (or polynomial) regression, neural networks, or others. Such modeling methods are not restricted by requiring the same global model form to apply over all subregions of the glass composition region of interest. The non-parametric regression methods have the

disadvantage of requiring larger datasets with more evenly distributed data than does the global, parametric modeling approach. However, this issue could be addressed by collecting additional data as described in Section 11.4.4, and combining such data with data collected so far. This recommendation should be considered advisory rather than necessary at this point, pending the completion of work to assess the suitability of the PCT and VHT models recommended in this report given their limitations (as discussed in Sections 5.6 and 6.11).

#### **11.4.4 Recommendation for Space-Filling Experimental Design**

For the work in this report, glass compositions used to develop property-composition models were a combination of

- statistically designed test matrices developed using a layered design approach (Piepel et al. 1993, Piepel et al. 2002), which includes extreme compositions on the outer layer of a composition region, as well as more reasonable compositions on middle and/or inner layers of a composition region
- actively designed glasses developed using glass science methods for specific waste compositions or to achieve other specific goals.

This combined approach has worked well for the forms of models considered in this report. However, the limited data and associated limitations in PCT and VHT models for predicting values of those properties near and above their contract limits could be determined by the WTP Project to be too restrictive for WTP LAW vitrification operations. Also, in the future, glass composition regions may need to be expanded by adding additional components or expanding the ranges of components. In such cases, it may be necessary to consider more advanced property-composition modeling approaches (e.g., local or nonparametric modeling approaches as discussed in Section 11.4.3). A more even coverage of the LAW glass composition region would provide better support for such modeling approaches, which can better capture higher-order and/or local nonlinear composition effects. These types of more advanced modeling approaches may be necessary to more accurately predict ILAW properties.

*Space-filling designs* have as a goal the uniform coverage of the region of interest. Such designs should be considered for any future ILAW property-composition data collection and modeling work where advanced nonparametric or local regression methods may be investigated. This recommendation should be considered advisory rather than necessary at this point, pending the completion of work to assess the suitability of the PCT and VHT models recommended in this report given their limitations (as discussed in Sections 5.6 and 6.11).



## **SECTION 12 QUALITY ASSURANCE**

The portions of this work that were performed at VSL were conducted under a quality assurance program based on NQA-1 (1989) and NQA-2a (1990) Part 2.7 that is in place at the VSL. This program is supplemented by a Quality Assurance Project Plan for WTP work that is conducted at VSL. Test and procedure requirements by which the testing activities are planned and controlled are also defined in this plan. The program is supported by VSL standard operating procedures (VSL 2006) that were used for this work. This work was not subject to DOE/RW-0333P (DOE-RW 2004) nor to the requirements of WTP QAPjP for environmental regulatory data (Blumenkranz 2001).

Eight of the existing glasses (LAWA44, LAWA44R10, LAWA54, LAWA56, LAWA88, LAWA88R1, LAWA102R1, and LAWA102R2) were prepared and characterized at VSL during Part B1 of the contract under BNFL. Two samples (GTSD-1126 and GTSD-1437) were prepared in the Duratek LAW Pilot Melter facility (Duratek 2003a, 2003b) and characterized at VSL. Two surrogate samples (AZ-102 Surr SRNL and AN-102 Surr LC Melter) and nine actual LAW samples (AN-103 Actual, AW-101 Actual, AP-101 Actual, AZ-101 Actual, AZ-102 Actual, AZ-102 Actual CCC, AN-107 Actual (LAWC15), AN-102 Actual LC Melter and AN-102 Actual) were prepared and characterized at SRTC and PNNL, according to procedures for control of measurement and testing equipment, tracking of radioactive samples, control of laboratory notebooks, and routine QA and QC, in compliance with the requirements of NQA-1. The remaining glasses were prepared and characterized at VSL during the Bechtel contract. An NQA-1 based QA program was in place during all of the work.

The QA requirements for the PNNL modeling work were met through the Quality Assurance Plan (PNNL 2007a) for the River Protection Project – Waste Treatment Plant Support Program (RPP-WTP Support Program). The RPP-WTP Support Program's quality assurance manual and its implementing procedures (PNNL 2007b) comply with the requirements of NQA-1 and NQA-2a Part 2.7.

## SECTION 13 REFERENCES

Akaike, H. (1974), "A New Look at the Statistical Model Identification," *IEEE Transactions on Automatic Control*, 19, 716-723.

ASTM (2002), *Standard Test Methods for Determining Chemical Durability of Nuclear, Hazardous, and Mixed Waste Glasses and Multiphase Glass Ceramics: The Product Consistency Test (PCT)*, ASTM-C1285-02, American Society for Testing and Materials, West Conshohocken, PA, 2002.

ASTM (2006), *Standard Test Methods for Specific Gravity of Soil Solids by Water Pycnometer*, ASTM-D854-06, American Society for Testing and Materials, West Conshohocken, PA, 2006.

Blumenkranz, D. (2001), *Quality Assurance Project Plan for Testing Programs Generating Environmental Regulatory Data*, PL-24590-QA00001, Rev. 0 (RPP-WTP-QAPjP), River Protection Project, Waste Treatment Plant, Richland, WA, June 7, 2001.

Clark, K. (2003), *Engineering Specification for Low Activity Waste Melters*, 24590-LAW-3PS-AE00-T0001, River Protection Project – Waste Treatment Plant, Richland, WA, 2003.

Cooley, S. K., Piepel, G. F., Gan, H., Muller, I. S., and Pegg, I. L. (2003), *Test Matrix to Support Property-Composition Model Development for RPP-WTP LAW Glasses*, VSL-02S4600-3, Rev. 1, Vitreous State Laboratory, The Catholic University of America, Washington, DC, November 26, 2003. (Cleared for public release by Bechtel National, Inc. and Battelle–Pacific Northwest Division as PNWD-3714 in 2006)

Cornell, J. A. (2002), *Experiments with Mixtures*, Third Edition, John Wiley and Sons, NY, 2002.

Crawford, C. L., Ferrara, D. M., Schumacher, R. F., and Bibler, N. E. (2001a), *Crucible-Scale Active Vitrification Testing Envelope A, Tank 241-AN-103*, WSRC-TR-2000-00322, SRT-RPP-2000-00021, Rev. 1, Savannah River Technology Center, Aiken, SC, June 15, 2001.

Crawford, C. L., Ferrara, D. M., Schumacher, R. F., and Bibler, N. E. (2001b), *Crucible-Scale Active Vitrification Testing of a Hanford Envelope C Tank 241-AN-102 Sample*, WSRC-TR-2000-00371, Savannah River Technology Center, Aiken, SC, June 15, 2001.

Crawford, C. L., Schumacher, R. F., and Bibler, N. E. (2004), *Final Report For Crucible-Scale Radioactive Vitrification and Product Testing of Waste Envelope B (AZ-102) Low-Activity Waste Glass (U)*, WSRC-TR-2003-00536, Rev. 0, Savannah River Technology Center, Aiken, SC, April 2004.

DOE-ORP (2000), *Design, Construction, and Commissioning of the Hanford Tank Waste Treatment and Immobilization Plant*, Contract Number: DE-AC27-01RV14136, U. S. Department of Energy, Office of River Protection, Richland WA, 2001, as amended.

DOE-RW (2004), *Quality Assurance Requirements and Description*, DOE/RW-0333P, Revision 16, U. S. Department of Energy, Office of Civilian Radioactive Waste Management, Washington, DC, August 23, 2004.

Draper, N. R. and Smith, H. (1998), *Applied Regression Analysis*, Third Edition, John Wiley and Sons, Inc., New York, NY, 1998.

Duratek (2003a), *RPP-WTP Pilot Melter Sub-Envelope C2-A3 Changeover Test Results Report*, TRR-PLT-079, Rev. 0, Duratek, Inc., Columbia, MD, November 11, 2003.

Duratek (2003b), *RPP-WTP Pilot Melter Sub-Envelope B2 Variation Test Results Report*, TRR-PLT-073, Rev. 0, Duratek, Inc., Columbia, MD, October 27, 2003.

Feng, Z, Perez-Cardenas, F., Gan, H., and Pegg, I. L. (2004), *Summary and Recommendations on Viscosity and Electrical Conductivity Model Forms to Support LAW Vitrification*, VSL-03L4480-2, Rev. 1, Vitreous State Laboratory, The Catholic University of America, Washington, DC, October 22, 2004.

Freund, R. J. and Littell, R. C. (1995), *SAS System for Regression*, Second Edition, SAS Institute, Inc., Cary, NC, 1995.

Gan, H. and Pegg, I. L. (2001a), *Development of Property-Composition Models for RPP-WTP HLW Glasses*, VSL-01R3600-1, Rev. 0, Vitreous State Laboratory, The Catholic University of America, Washington, DC, July 30, 2001.

Gan, H. and Pegg, I. L. (2001b), *Development of Property-Composition Models for RPP-WTP LAW Glasses*, VSL-01R6600-1, Rev. 0, Vitreous State Laboratory, The Catholic University of America, Washington, DC, August 6, 2001.

Gan, H., and Pegg, I. L. (2002), *LAW Glass Property-Composition Modeling*, Test Plan, VSL-02T4800-1, Rev. 1, Vitreous State Laboratory, The Catholic University of America, Washington, DC, April 2002.

Gilbert, R. O. (1987), *Statistical Methods for Environmental Pollution Monitoring*, Van Nostrand Reinhold, New York, NY, 1987.

Hahn, G. J. and Shapiro, S. S. (1967), *Statistical Models in Engineering*, John Wiley and Sons, New York, 1967.

Hrma, P. R., Piepel, G. F., Schweiger, M. J., Smith, D. E., Kim, D. S., Redgate, P. E., Vienna, J. D., LoPresti, C. A., Simpson, D. B., Peeler, D. K., and Langowski, M. H. (1994), *Property/Composition Relationships for Hanford High-Level Waste Glasses Melting at 1150 °C*, PNL-10359, Volumes 1 and 2, Pacific Northwest Laboratory, Richland, WA, December 1994.

Ihaka, R. and Gentleman, R. (1996), “R: A Language for Data Analysis and Graphics,” *Journal of Computational and Graphical Statistics*, 5, 299-314, 1996.

Jiricka, A., Vienna, J. D., Hrma, P., and Strachan, D. M. (2001), “The Effect of Experimental Conditions and Evaluation Techniques on the Alteration of Low-Activity Waste Glasses by Vapor Hydration,” *Journal of Non-Crystalline Solids*, 292, 25-43.

Kirkbride, R. A., et. al. (2000), *Tank Farm Contractor Operations and Utilization Plan*, HNF-SD-WM-SP-012, Rev. 2, CH2M Hill Hanford Group, Richland, WA, April 2000.

Kirkbride, R. A., et. al. (2001), *Tank Farm Contractor Operations and Utilization Plan*, HNF-SD-WM-SP-012, Rev. 3A, CH2M Hill Hanford Group, Richland, WA, December 2001.

Kot, W., Klatt, K., Muller, I. S., Wilson, C. N., Pegg, I. L., Bates, D. J., Piepel, G. F., and Weier, D.R. (2003), *Regulatory Spike Testing of RPP-WTP LAW and HLW Glasses for Compliance with Land Disposal Restriction*, VSL-03R3760-1, Rev. 1, Vitreous State Laboratory, The Catholic University of America, Washington, DC, August 1, 2003.

Matlack, K. S., Morgan, S. P., and Pegg, I. L. (2001), *Melter Tests with LAW Envelope A and C Simulants to Support Enhanced Sulfate Incorporation*, VSL-01R3501-2, Rev. 0, Vitreous State Laboratory, The Catholic University of America, Washington, DC, January 26, 2001.

Matlack, K. S., Muller, I. S., and Pegg, I. L. (2002a), *Tests on DuraMelter 100 with LAW Sub-Envelope C2 Feed in Support of the LAW Pilot Melter*, VSL-02T62N0-1, Rev. 1, Vitreous State Laboratory, The Catholic University of America, Washington, DC, May 29, 2002.

Matlack, K. S., Gong, W., and Pegg, I. L. (2002b), *Compositional Variation Tests on DuraMelter 100 with LAW Sub-Envelope A1 Feed (LAWA44 Glass) in Support of the LAW Pilot Melter*, VSL-02R62N0-4, Rev. 0, Vitreous State Laboratory, The Catholic University of America, Washington, DC, June 18, 2002.

Matlack, K. S., Gong, W., and Pegg, I. L. (2002c), *Compositional Variation Tests on DuraMelter 100 with LAW Sub-Envelope A3 Feed in Support of the LAW Pilot Melter*, VSL-01R62N0-1, Rev. 1, Vitreous State Laboratory, The Catholic University of America, Washington, DC, July 15, 2002.

Matlack, K. S., Gong, W., Bardakci, T., D’Angelo, N., and Pegg, I. L. (2002d), *Integrated Off-Gas System Tests on the DMI200 Melter with RPP-WTP LAW Sub-Envelope C1 Simulants*, VSL-02R8800-1, Rev. 0, Vitreous State Laboratory, The Catholic University of America, Washington, DC, July 25, 2002.

Matlack, K. S., Gong, W., Bardakci, T., D'Angelo, N., and Pegg, I. L. (2002e), *Integrated Off-Gas System Tests on the DM1200 Melter with RPP-WTP LAW Sub-Envelope A1 Simulants*, VSL-02R8800-2, Rev. 0, Vitreous State Laboratory, The Catholic University of America, Washington, DC, September 3, 2002.

Matlack, K. S., Gong, W., and Pegg, I. L. (2002f), *Compositional Variation Tests on DuraMelter 100 with LAW Sub-Envelope A2 Feed (LAWA88) Glass in Support of the LAW Pilot Melter*, VSL-02R62N0-3, Rev. 0, Vitreous State Laboratory, The Catholic University of America, Washington, DC, November 1, 2002.

Matlack, K. S., Gong, W., Bardakci, T., D'Angelo, N., and Pegg, I. L. (2003a), *Integrated Off-Gas System Tests on the DM1200 Melter with RPP-WTP LAW Sub-Envelope B1 Simulants*, VSL-03R3851-1, Rev. 0, Vitreous State Laboratory, The Catholic University of America, Washington, DC, May 2, 2003.

Matlack, K. S., Gong, W., and Pegg, I. L. (2003b), *Compositional Variation Tests on DuraMelter 100 with LAW Sub-Envelope B1 Feed in Support of the LAW Pilot Melter*, VSL-02R62N0-5, Rev. 0, Vitreous State Laboratory, The Catholic University of America, Washington, DC, May 8, 2003.

Matlack, K. S., Gong, W., and Pegg, I. L. (2003c), *DuraMelter 100 Sub-Envelope Changeover Testing Using LAW Sub-Envelope A2 and B1 Feeds in Support of the LAW Pilot Melter*, VSL-03R3410-1, Rev. 0, Vitreous State Laboratory, The Catholic University of America, Washington, DC, August 22, 2003.

Matlack, K. S., Gong, W., and Pegg, I. L. (2003d), *DuraMelter 100 Sub-Envelope Changeover Testing Using LAW Sub-Envelope A1 and C1 Feeds in Support of the LAW Pilot Melter*, VSL-02R62N0-6, Rev. 0, Vitreous State Laboratory, The Catholic University of America, Washington, DC, September 9, 2003.

Matlack, K. S., Gong, W., and Pegg, I. L. (2003e), *DuraMelter 100 Sub-Envelope Changeover Testing Using LAW Sub-Envelope A3 and C2 Feeds in Support of the LAW Pilot Melter*, VSL-03R3410-3, Rev. 0, Vitreous State Laboratory, The Catholic University of America, Washington, DC, October 17, 2003.

Montgomery, D. C., Peck, E. A., and Vining, G. G. (2001), *Introduction to Linear Regression Analysis*, Third Edition, John Wiley and Sons, New York, NY 2001.

Morrey, E. V. (2002), *LAW Pilot Melter and DM100 Sub-Envelope Changeover Testing*, RPP-WTP Test Specification, 24590-LAW-TSP-RT-02-012, Rev 0, River Protection Project, Waste Treatment Plant, Richland, WA, August 13, 2002.

Muller, I. S., Buechele, A. C., and Pegg, I. L. (2001a), *Glass Formulation and Testing With RPP-WTP LAW Simulants*, VSL-01R3560-2, Rev. 0, Vitreous State Laboratory, The Catholic University of America, Washington, DC, February 23, 2001.

Muller, I. S., Gan, H., and Pegg, I. L. (2001b), *Physical and Rheological Properties of Waste Simulants and Melter Feeds for RPP-WTP LAW Vitrification*, VSL-01R3520-1, Rev. 0, Vitreous State Laboratory, The Catholic University of America, Washington, DC, January 16, 2001.

Muller, I. S. and Pegg, I. L. (2003), *Baseline LAW Glass Formulation Testing*, VSL-03R3460-1, Rev. 0, Vitreous State Laboratory, The Catholic University of America, Washington, DC, August 5, 2003.

Muller, I. S. and Pegg, I. L. (2003a), *LAW Glass Formulation to Support AZ-102 Actual Waste Testing*, VSL-03R3470-1, Rev. 0, Vitreous State Laboratory, The Catholic University of America, Washington, DC, August 15, 2003.

Muller, I. S. and Pegg, I. L. (2003b), *LAW Glass Formulation to Support AP-101 Actual Waste Testing*, VSL-03R3470-2, Rev. 0, Vitreous State Laboratory, The Catholic University of America, Washington, DC, August 13, 2003.

Muller, I. S. and Pegg, I. L. (2003c), *LAW Glass Formulation to Support AZ-101 Actual Waste Testing*, VSL-03R3470-3, Rev. 0, Vitreous State Laboratory, The Catholic University of America, Washington, DC, September 17, 2003.

Muller, I. S. and Pegg, I. L. (2003d), *LAW Glass Formulation to Support SY-101/AP-104 Actual Waste Testing*, VSL-03R4470-1, Rev. 0, Vitreous State Laboratory, The Catholic University of America, Washington, DC, December 17, 2003.

Muller, I. S. and Pegg, I. L. (2004), *Glass Formulations to Support Melter Testing*, VSL-03R3460-2, Rev. 0, Vitreous State Laboratory, The Catholic University of America, Washington, DC, February 5, 2004.

Muller, I. S., Goloski, L., and Pegg, I. L. (2004a), *LAW Glass Formulation to Support AN-104 Actual Waste Testing*, VSL-04R4470-1, Rev. 0, Vitreous State Laboratory, The Catholic University of America, Washington, DC, May 12, 2004.

Muller, I. S., Diener, G., Joseph, I., and Pegg, I. L. (2004b), *Proposed Approach for Development of LAW Glass Formulation Correlation*, VSL-04L4460-1, Rev. 2, Vitreous State Laboratory, The Catholic University of America, Washington, DC, October 29, 2004.

Muller, I. S., Gan, H., Pegg, I. L., Cooley, S. K., and Piepel, G. F. (2005a), *Phase 1 LAW PCT and VHT Model Development*, VSL-04R4480-2, Rev. 0, Vitreous State Laboratory, The Catholic University of America, Washington, DC, February 8, 2005.

Muller, I. S., Joseph, I., and Pegg, I. L. (2005b), *Comparison of LAW Simulant, Actual Waste, and Melter Glasses*, VSL-05R5460-1 Rev. 0 Vitreous State Laboratory, The Catholic University of America, Washington, DC, July 18, 2005.

Muller, I., Gan, H., Pegg, I. L., Cooley, S. K. and Piepel, G. F. (2005), *Phase I ILAW PCT and VHT Model Development*, VSL-04R4480-2, Rev. 0, Vitreous State Laboratory, The Catholic University of America, Washington, DC, February 2005. (Cleared for public release by Bechtel National, Inc. and Battelle–Pacific Northwest Division as PNWD-3718 in 2006)

Muller, I. S., Joseph, I., and Pegg, I. L. (2006a), *Preparation and Testing of LAW High-Phosphorous and High-Chromium Glasses*, VSL-06R6480-2 Rev. 0, Vitreous State Laboratory, The Catholic University of America, Washington, DC, July 27, 2006

Muller, I. S., Joseph, I., and Pegg, I. L. (2006b), *Preparation and Testing of LAW High-Alkali Correlation and Augmentation Matrix Glasses*, VSL-06R6480-3 Rev. 0, Vitreous State Laboratory, The Catholic University of America, Washington, DC, October 18, 2006

Musick, C.A. (2003), “Updated Instructions for ILAW Regulatory Spike Testing,” CCN 049799, River Protection Project, Waste Treatment Plant, Richland, WA, January 9, 2003.

Myers, R. H. and Montgomery, D. C. (1995), *Response Surface Methodology: Process and Product Optimization Using Designed Experiments*, John Wiley and Sons, New York, NY, 1995.

Myers, R. H., Montgomery, D. C., and Vining, G. G. (2002), *Generalized Linear Models: With Applications in Engineering and the Sciences*, John Wiley and Sons, New York, NY, 2002.

Pegg, I. L., Gan, H., Muller, I. S., McKeown, D. A., and Matlack, K. S. (2000), *Summary of Preliminary Results on Enhanced Sulfate Incorporation During Vitrification of LAW Feeds*, VSL-00R3630-1, Rev. 1, Vitreous State Laboratory, The Catholic University of America, Washington, DC, April 5, 2000.

Perez-Cardenas, F., Gan, H., and Pegg, I. L. (2003), *Summary and Recommendations on PCT Model Form to Support LAW Vitrification*, VSL-03L4480-1, Rev. 0, Vitreous State Laboratory, The Catholic University of America, Washington, DC, November 10, 2003.

Perez-Cardenas, F., Gan, H., and Pegg, I. L. (2006), *Summary and Recommendations on Phase II VHT Model Form to Support LAW Vitrification*, VSL-06L6480-1, Rev. 0, Vitreous State Laboratory, The Catholic University of America, Washington, DC, June 30, 2006.

Petkus, L. to Musick, C. (2003), “LAW Container Centerline Cooling Data,” RPP-WTP Memorandum, CCN# 074181, River Protection Project–Waste Treatment Plant, Richland, WA, October 16, 2003.

Piepel, G. F., Amidan, B. G., Heredia-Langner, A., Weier, D. R., and Cooley, S. K. (2005), *Statistical Methods and Results for WTP IHLW and ILAW Compliance*, PNWD-3568 (WTP-RPT-072), Rev. 1, Battelle–Pacific Northwest Division, Richland, WA, June 2005.

Piepel, G. F., Anderson, C. M., and Redgate, P. E. (1993), “Response Surface Designs for Irregularly-Shaped Regions” (Parts 1, 2, and 3), *1993 Proceedings of the Section on Physical and Engineering Sciences*, pp. 205-227, American Statistical Association, Alexandria, VA, 1993.

Piepel, G. F., and Cooley, S. K. (2002), *Statistics for IHLW and ILAW Property-Composition Modeling*, Test Plan TP-RPP-WTP-179, Rev. 1, Battelle–Pacific Northwest Division, Richland, WA, July 2002.

Piepel, G. F. and Cooley, S. K. (2006), “Automated Method for Reducing Scheffé Linear Mixture Experiment Models”, PNWD-SA-7469, Rev. 0, Battelle–Pacific Northwest Division, Richland, WA. (To appear in a special Response Surface Methodology issue of *Quality Technology and Quantitative Management*, December 2007).

Piepel, G. F., Cooley, S. K., Peeler, D. K., Vienna, J. D., and Edwards, T. B. (2002), “Augmenting a Waste Glass Mixture Experiment Study with Additional Glass Components and Experimental Runs,” *Quality Engineering*, 15, 91-111, 2002.

Piepel, G. and Redgate, T. (1997), “Mixture Experiment Techniques for Reducing the Number of Components Applied for Modeling Waste Glass Sodium Release,” *Journal of the American Ceramic Society*, 80, 3038-3044, 1997.

Piepel, G. F., Szychowski, J. M. and Loepky, J. L. (2002), “Augmenting Scheffé Linear Mixture Models with Squared and/or Crossproduct Terms,” *Journal of Quality Technology*, 34, 297-314, 2002.

PNNL (2007a), *River Protection Project – Waste Treatment Plant Support Program Quality Assurance Plan (QAP)*, RPP-WTP-QA-001, Rev. 0, Pacific Northwest National Laboratory, Richland, WA, February, 2007.

PNNL (2007b), *River Projection Project – Waste Treatment Plant Support Program Quality Assurance Manual (QAM)*, RPP-WTP-QA-003, Rev. 0, Pacific Northwest National Laboratory, Richland, WA, February 2007.

Pye, L. D., Frechette, V. D. and Kreidl, N. J. (1978), Editors, *Borate Glasses, Structure, Properties, Applications*, Plenum Press, New York, NY, 1978.

R Development Core Team (2006), *R: A Language and Environment for Statistical Computing*, R Foundation for Statistical Computing, Vienna, Austria. ISBN 3-900051-07-0, URL <http://www.R-project.org>.

Rielley, E., Muller, I. S., and Pegg, I. L. (2004), *Preparation and Testing of LAW Matrix Glasses to Support WTP Property-Composition Model Development*, VSL-04R4480-1, Rev. 0, Vitreous State Laboratory, The Catholic University of America, Washington, DC, April 21, 2004.

SAS (2005), *SAS Release 9.1.3*, SAS Institute, Inc., Cary, NC, 2005.

Smith G. L., Greenwood L. R., Piepel G. F., Schweiger M. J., Smith H. D., Urie M. W., and Wagner J. J. (2000), *Vitrification and Product Testing of AW-101 and AN-107 Pretreated Waste*, PNNL-13372 (WTP-RPT-003), Rev. 0, Pacific Northwest National Laboratory, Richland, WA, October 2000.



Smith H. D., Bates R. J., Bredt P. R., Greenwood L. R., Schweiger M. J., Urie M. W., and Weier D. R. (2004a), *Vitrification and Product Testing of AP-101 Pretreated LAW Envelope A Glass*, PNWD-3470 (WTP-RPT-092), Rev. 0, Battelle–Pacific Northwest Division, Richland, WA, June 2004.

Smith H. D., Bates R. J., Bredt P. R., Crum J. V., Hrma P. R., and Schweiger M. J. (2004b), *Vitrification and Product Testing of AZ-101 Pretreated LAW Envelope B Glass*, PNWD-3464 (WTP-RPT-106), Rev. 0, Battelle–Pacific Northwest Division, Richland, WA, June 2004.

Swanberg, D. J. (2001), *LAW Glass Property Composition Modeling*, BNI Test Specification, 24590-LAW-TSP-RT-01-013, Rev. 1, River Protection Project, Waste Treatment Plant, Richland, WA, November 27, 2001.

Swanberg, D. J. (2002), *Statistics for HLW & LAW Glass Property-Composition Modeling*, BNI Test Specification, 24590-WTP-TSP-RT-02-001, Rev. 0, River Protection Project, Waste Treatment Plant, Richland, WA, May 20, 2002.

Vienna, J. D. (2005), *Preliminary ILAW Formulation Algorithm Description*, 4590-LAW-RPT-RT-04-0003, Rev. 0, River Protection Project, Waste Treatment Plant, Richland, WA, May 18, 2005.

Vienna, J. D., Hrma, P., Jiricka, A., Smith, D. E., Lorier, T. H., Reamer, I. A., and Schulz, R. L. (2001), *Hanford Immobilized LAW Product Acceptance Testing: Tanks Focus Area Results*, PNNL-13744, Pacific Northwest National Laboratory, Richland, WA, December 2001.

VSL (2003), *Quality Assurance Project Plan for RPP-WTP Support Activities Conducted by VSL*, QAPP, Rev. 6, Vitreous State Laboratory, The Catholic University of America, Washington, DC, November 12, 2003.

VSL (2006), *Master List of Controlled VSL Manuals and Standard Operating Procedures in Use*, QA-MLCP, Rev. 19, Vitreous State Laboratory, The Catholic University of America, Washington, DC, September 20, 2006.

Weier, D. R. and Piepel, G. F. (2003), *Methodology for Adjusting and Normalizing Analyzed Glass Compositions*, PNWD-3260 (WTP-RPT-049), Battelle–Pacific Northwest Division, Richland, WA, March 2003.

Westsik Jr., J. H. (2003), *Test Exception to Test Specification 24590-WTP-TSP-RT-02-001 Rev. 0 and Test Plan TP-RPP-WTP-179*, 24590-WTP-TEF-RT-03-040, River Protection Project, Waste Treatment Plant, Richland, WA, July 23, 2003.

Zamecnik, J. R., Crawford, C. L., and Koopman, D. C. (2002), *Large Scale Vitrification of 241-AN-102 (Envelope C) Sample*, WSRC-TR-2002-00093, Rev. 0, Savannah River Technology Center, Aiken, SC, July 18, 2002.

**Table 2.1. Components and Constraints<sup>(a)</sup> for ILAW Phase 1 Test Matrix.**

Component	Inner Layer		Middle Layer		Outer Layer	
	Lower Bound (wt%)	Upper Bound (wt%)	Lower Bound (wt%)	Upper Bound (wt%)	Lower Bound (wt%)	Upper Bound (wt%)
Al <sub>2</sub> O <sub>3</sub>	6	7	5	8	3.5	9
B <sub>2</sub> O <sub>3</sub>	8	11	7	12	6	13
CaO	5	7	2	8	0	10
Fe <sub>2</sub> O <sub>3</sub>	3	5	2	6.5	0	8
K <sub>2</sub> O	0.1	0.3	0.1	2	0	4
Li <sub>2</sub> O	1	2.5	0.5	3	0	4.5
MgO	1.5	2.5	1	3.5	0	5
Na <sub>2</sub> O <sup>(b)</sup>	12 (Envelope C, Upper)	14 (Envelope A, Lower)	10 (Envelope C, Lower)	17 (Envelope A, Middle)	5 (Envelope B, Lower)	22 (Envelope A, Upper)
SiO <sub>2</sub>	45	48	42	50	40	52
SO <sub>3</sub>	0.1 <sup>(c)</sup>	1 <sup>(c)</sup>	0.1 <sup>(c)</sup>	1 <sup>(c)</sup>	0.1 <sup>(c)</sup>	1
TiO <sub>2</sub>	1	2	0.5	2.5	0	3
ZnO	3.5	4.6	2	5	1	5
ZrO <sub>2</sub>	2	3	1	3.5	0	4
Others <sup>(d)</sup>	0.05	2	0.05	2	0.05	2
Runs	14 plus the center-point of the inner layer		20		15 outer layer runs in addition to 21 existing LAW glasses.	
Cumulative number of glasses	15		35		71 (including the 21 existing glasses, but excluding the 6 replicates)	

(a) The wt% values of the components Al<sub>2</sub>O<sub>3</sub> to Others are constrained to sum to 100% for every glass.

(b) Na<sub>2</sub>O constraints were based on WTP Contract Specification 2 (DOE-ORP 2001):

Envelope A: Waste Na<sub>2</sub>O > 14.0 wt%

Envelope B: Waste Na<sub>2</sub>O > 5.0 wt%

Envelope C Waste Na<sub>2</sub>O > 10.0 wt%

It is important to note that the preceding Na<sub>2</sub>O minimums are for waste Na<sub>2</sub>O in LAW glass, not total Na<sub>2</sub>O. Also, the WTP contract was subsequently revised to allow a minimum waste Na<sub>2</sub>O loading for Envelope B waste from AZ-102 of 3 wt%. For Envelope B compositions, sodium is added either from the waste or as glass formers to provide at least 5 wt% Na<sub>2</sub>O in the glass.

(c) The achieved range of SO<sub>3</sub> is 0.346 – 0.425 wt% for the inner layer, 0.236 – 0.560 wt% for the middle layer, and 0.160 – 1.0 wt% for the outer layer.

(d) Others is a group of minor waste components (BaO, CdO, Cl, Cr<sub>2</sub>O<sub>3</sub>, F, NiO, PbO, and P<sub>2</sub>O<sub>5</sub>) in fixed relative proportions as listed in Table 2.2.

**Table 2.2. Composition of the Grouped Component “Others” for ILAW Phase 1 Test Matrix.**

<b>Components</b>	<b>Relative Amount (wt%)</b>	<b>Maximum Amount in Glass (wt%)</b>
BaO	0.50	0.01
CdO	0.50	0.01
Cl	40.01	0.80
Cr <sub>2</sub> O <sub>3</sub>	16.07	0.32
F	14.97	0.30
NiO	1.50	0.03
PbO	1.50	0.03
P <sub>2</sub> O <sub>5</sub>	24.95	0.50
Subtotal	100.00	2.00

**Table 2.3. Property Constraints for ILAW Phase 1 Test Matrix.**

<b>Property</b>	<b>Lower Limit<sup>(a)</sup></b>	<b>Upper Limit<sup>(a)</sup></b>
Viscosity at 1150°C ( $\eta_{1150}$ )	10 poise	100 poise
Electrical Conductivity at 1150°C ( $\sigma_{1150}$ )	0.2 S/cm (inner, middle layers) 0.1 S/cm (outer layer)	0.6 S/cm (inner, middle layers) 0.7 S/cm (outer layer)
7-Day B PCT ( $r_B^{PCT}$ )	(b)	2 g/l (inner, middle layers) 4 g/l (outer layer)
7-Day Na PCT ( $r_{Na}^{PCT}$ )	(b)	2 g/l (inner, middle layers) 4 g/l (outer layer)
7-Day Si PCT ( $r_{Si}^{PCT}$ )	(b)	2 g/l (inner, middle layers) 4 g/l (outer layer)
<b>Sulfur Incorporation</b>	<b>Lower Limit<sup>(c)</sup></b>	<b>Upper Limit<sup>(c)</sup></b>
Wt% SO <sub>3</sub> for Inner Layer	-0.02959 Na <sub>2</sub> O + 0.76	-0.02959 Na <sub>2</sub> O + 0.78
Wt% SO <sub>3</sub> for Middle Layer	-0.023529 Na <sub>2</sub> O + 0.635294	-0.032922 Na <sub>2</sub> O + 0.888888
Wt% SO <sub>3</sub> for Outer Layer	-0.014118 Na <sub>2</sub> O + 0.470588	-0.0453 Na <sub>2</sub> O + 1.52

- (a) Limits for viscosity and electrical conductivity are based on processing constraints (Clark 2003). Limits for PCT B, Na, and Si releases are based on a WTP contract constraint (DOE-ORP 2001).
- (b) No lower bound constraint imposed.
- (c) Based on sulfate incorporation constraints (Muller et. al. 2001a, Muller et. al. 2003a, Pegg et. al. 2000).

**Table 2.4. Model-Based<sup>(a)</sup> Glass Property Constraints for ILAW Phase 1 Test Matrix.**

Property		Viscosity	Electrical Conductivity	PCT-B	PCT-Na	PCT-Si
Modeled Response		$\ln(\eta_{1150})$	$\ln(\sigma_{1150})$	$\ln(r_B^{PCT})$	$\ln(r_{Na}^{PCT})$	$\ln(r_{Si}^{PCT})$
Units		ln(poise)	ln(S/cm)	ln(g/l)	ln(g/l)	ln(g/l)
Components (wt%)		Constraint Coefficients, Lower and Upper Bounds				
Al <sub>2</sub> O <sub>3</sub>		-0.18657	-0.01728	-0.118843	-0.136346	-0.07013
B <sub>2</sub> O <sub>3</sub>		-0.02217	+0.023548	+0.086761	-0.039907	-0.01172
CaO		-0.0361966	-0.02433	-0.042865	-0.032381	-0.0286
Fe <sub>2</sub> O <sub>3</sub>		+0.0390715	-0.01971	-0.012574	-0.085602	-0.00444
K <sub>2</sub> O		-0.0282883	-0.03656	+0.084951	+0.071036	+0.05056
Li <sub>2</sub> O		-0.290011	+0.206174	+0.333015	+0.234093	+0.20773
MgO		+0.0117262	-0.09654	+0.257082	+0.217455	+0.123
Na <sub>2</sub> O		-0.044155	+0.114266	+0.132831	+0.079692	+0.08841
SiO <sub>2</sub>		+0.1485	-0.01638	-0.070351	-0.10662	-0.01381
SO <sub>3</sub>		(b)	(b)	+0.105346	+0.006431	+0.09766
TiO <sub>2</sub>		-0.022756	(b)	+0.013925	-0.01047	+0.05648
ZnO		+0.05186	-0.01459	-0.15096	-0.264853	-0.09995
ZrO <sub>2</sub>		+0.09522	-0.07185	-0.218869	-0.259572	-0.13203
Others		+0.016989	(b)	-0.0624969	-0.065025	-0.102079
Lower Bound	Outer Layer	5.30295 (e),(f)	-0.577345	(c)	(c)	(c)
	Inner & Middle Layers		0.115802			
Upper Bound	Outer Layer	7.60553	1.36857	-0.267129	-4.635913	2.555237 (d)
	Inner & Middle Layers		1.21441 (f)	-0.426018 (f)	-5.32906 (f)	1.86209 (e),(f)

- (a) Intercepts in the original property-composition models of the form  $\ln(\text{property}) = A_0 + \sum A_i x_i$  are incorporated into the lower and upper bounds of the constraint expressions so that  $LB \leq \sum A_i x_i \leq UB$ .
- (b) A blank cell indicates the component has a minor effect on the property and is not included in the model used to form the constraint. The coefficients for these components were set to zero (i.e., they were simply not included in the regression).
- (c) No lower bounds were imposed for these properties.
- (d) Constraint unnecessary (i.e., unachievable) for the outer layer.
- (e) Constraint unnecessary (i.e., unachievable) for the middle layer.
- (f) Constraint unnecessary (i.e., unachievable) for the inner layer

**Table 2.5. Target Compositions of ILAW Phase 1 Test Matrix Glasses (wt%).**

Glass ID	Run Order <sup>(a)</sup>	Layer	Al <sub>2</sub> O <sub>3</sub>	B <sub>2</sub> O <sub>3</sub>	CaO	Fe <sub>2</sub> O <sub>3</sub>	K <sub>2</sub> O	Li <sub>2</sub> O	MgO	Na <sub>2</sub> O	SiO <sub>2</sub>	SO <sub>3</sub>	TiO <sub>2</sub>	ZnO	ZrO <sub>2</sub>	Others <sup>(b)</sup>	Sum
LAWM1	36	Outer	9.00	6.00	10.00	8.00	4.00	4.50	0.00	5.00	44.45	1.00	3.00	5.00	0.00	0.05	100
LAWM2	41	Outer	3.50	6.00	10.00	8.00	0.00	4.50	5.00	5.00	47.00	1.00	3.00	5.00	0.00	2.00	100
LAWM3	29	Outer	9.00	6.00	10.00	8.00	0.00	4.47	5.00	11.48	40.00	1.00	0.00	1.00	4.00	0.05	100
LAWM4	24	Outer	3.50	13.00	10.00	5.54	4.00	4.50	0.00	5.00	41.41	1.00	3.00	5.00	4.00	0.05	100
LAWM5	31	Outer	9.00	6.00	5.77	8.00	4.00	4.50	0.00	5.00	48.68	1.00	3.00	1.00	4.00	0.05	100
LAWM6	55	Outer	9.00	10.61	10.00	8.00	4.00	0.00	5.00	9.00	40.00	0.34	3.00	1.00	0.00	0.05	100
LAWM7	45	Outer	5.43	6.94	10.00	8.00	0.00	2.58	5.00	5.00	52.00	1.00	3.00	1.00	0.00	0.05	100
LAWM8	38	Outer	9.00	13.00	6.43	0.00	0.00	2.08	5.00	5.00	44.49	1.00	3.00	5.00	4.00	2.00	100
LAWM9	15	Outer	3.50	6.00	10.00	8.00	4.00	2.39	0.00	5.00	49.71	0.40	0.00	5.00	4.00	2.00	100
LAWM10	5	Outer	9.00	13.00	10.00	0.00	0.00	4.50	0.00	13.07	40.15	0.28	3.00	1.00	4.00	2.00	100
LAWM11	56	Outer	3.50	13.00	9.40	5.31	4.00	4.50	0.00	11.48	46.76	1.00	0.00	1.00	0.00	0.05	100
LAWM12	22	Outer	3.50	13.00	0.00	2.31	4.00	4.50	1.97	14.25	42.20	0.27	3.00	5.00	4.00	2.00	100
LAWM13	28	Outer	3.50	6.00	10.00	8.00	3.79	0.00	0.00	22.00	40.00	0.52	3.00	2.16	0.00	1.03	100
LAWM14	35	Outer	3.50	6.00	2.05	0.00	0.00	0.88	5.00	22.00	52.00	0.52	3.00	5.00	0.00	0.05	100
LAWM15	16	Outer	9.00	9.36	0.00	6.28	0.00	0.00	3.72	22.00	43.48	0.16	3.00	1.00	0.00	2.00	100
LAWM16	8	Middle	8.00	12.00	8.00	6.50	0.10	3.00	1.00	10.00	42.45	0.40	2.50	5.00	1.00	0.05	100
LAWM17	19	Middle	5.00	12.00	2.21	6.50	2.00	0.50	3.50	17.00	42.00	0.24	0.50	5.00	3.50	0.05	100
LAWM18	46	Middle	8.00	12.00	8.00	6.50	0.10	3.00	1.00	10.00	42.00	0.40	2.50	2.00	2.50	2.00	100
LAWM19	43	Middle	8.00	12.00	8.00	2.00	2.00	0.50	1.00	13.17	42.00	0.33	0.50	5.00	3.50	2.00	100
LAWM20	6	Middle	5.00	7.00	8.00	2.00	2.00	2.26	3.50	17.00	42.00	0.24	0.50	5.00	3.50	2.00	100
LAWM21	32	Middle	5.00	10.89	8.00	6.50	2.00	3.00	1.00	10.00	42.00	0.56	2.50	5.00	3.50	0.05	100
LAWM22	40	Middle	8.00	7.00	2.00	6.50	2.00	0.50	3.50	17.00	42.00	0.33	0.67	5.00	3.50	2.00	100
LAWM23	7	Middle	5.00	7.00	8.00	2.00	2.00	3.00	1.00	10.00	48.44	0.56	2.50	5.00	3.50	2.00	100
LAWM24	42	Middle	8.00	12.00	2.00	6.50	2.00	0.64	1.00	17.00	47.07	0.24	0.50	2.00	1.00	0.05	100
LAWM25	30	Middle	8.00	12.00	2.00	3.68	2.00	3.00	3.50	10.00	49.92	0.40	0.50	2.00	1.00	2.00	100
LAWM26	39	Middle	8.00	12.00	4.97	2.00	0.10	3.00	1.00	10.00	49.87	0.56	0.50	5.00	1.00	2.00	100
LAWM27	26	Middle	8.00	7.00	8.00	6.50	2.00	0.50	3.50	13.37	42.00	0.32	2.50	3.31	1.00	2.00	100
LAWM28	49	Middle	5.00	12.00	8.00	6.50	0.70	0.69	1.00	10.00	50.00	0.56	2.50	2.00	1.00	0.05	100
LAWM29	34	Middle	7.56	7.00	2.00	6.50	2.00	3.00	3.50	10.00	46.85	0.40	2.50	5.00	3.50	0.19	100
LAWM30	48	Middle	8.00	12.00	2.00	6.50	0.10	2.02	1.00	17.00	42.00	0.24	0.59	5.00	3.50	0.05	100

(a) Random order in which glasses were batched and melted.

(b) The composition of the “Others” component is given in Table 2.2.

**Table 2.5. Target Compositions of ILAW Phase 1 Test Matrix Glasses (wt%) (continued).**

Glass ID	Run Order <sup>(a)</sup>	Layer	Al <sub>2</sub> O <sub>3</sub>	B <sub>2</sub> O <sub>3</sub>	CaO	Fe <sub>2</sub> O <sub>3</sub>	K <sub>2</sub> O	Li <sub>2</sub> O	MgO	Na <sub>2</sub> O	SiO <sub>2</sub>	SO <sub>3</sub>	TiO <sub>2</sub>	ZnO	ZrO <sub>2</sub>	Others <sup>(b)</sup>	Sum
LAWM31	14	Middle	5.00	7.00	8.00	6.50	0.10	3.00	1.00	16.75	42.31	0.34	2.50	2.00	3.50	2.00	100
LAWM32	11	Middle	5.14	7.00	2.00	2.00	2.00	3.00	3.50	16.51	50.00	0.35	0.50	5.00	1.00	2.00	100
LAWM33	10	Middle	5.00	12.00	8.00	6.50	1.72	0.90	1.00	17.00	42.00	0.33	2.50	2.00	1.00	0.05	100
LAWM34	13	Middle	5.00	8.35	8.00	6.29	2.00	3.00	1.00	17.00	42.00	0.33	1.48	2.00	3.50	0.05	100
LAWM35	1	Middle	5.00	12.00	6.18	4.41	0.10	0.50	3.50	17.00	42.00	0.24	2.50	2.00	2.57	2.00	100
LAWM36	12	Inner	7.00	11.00	7.00	5.00	0.30	2.50	1.50	12.00	45.00	0.40	2.00	3.50	2.00	0.80	100
LAWM37	21	Inner	6.75	11.00	7.00	5.00	0.30	2.50	2.50	12.00	45.00	0.40	1.00	3.50	3.00	0.05	100
LAWM38	54	Inner	7.00	8.00	7.00	3.00	0.15	2.50	1.50	14.00	48.00	0.35	1.00	3.50	2.00	2.00	100
LAWM39	2	Inner	7.00	9.05	5.00	3.00	0.10	2.50	2.50	14.00	48.00	0.35	1.00	3.50	2.00	2.00	100
LAWM40	50	Inner	6.00	11.00	5.00	5.00	0.10	1.00	1.50	14.00	48.00	0.37	1.00	3.50	3.00	0.53	100
LAWM41	37	Inner	7.00	8.00	7.00	5.00	0.30	1.00	2.50	14.00	45.00	0.37	1.00	4.60	2.23	2.00	100
LAWM42	18	Inner	6.00	8.00	5.00	4.03	0.10	2.50	1.50	14.00	48.00	0.37	2.00	3.50	3.00	2.00	100
LAWM43	47	Inner	7.00	8.68	5.00	5.00	0.30	2.50	2.50	12.00	45.00	0.42	2.00	4.60	3.00	2.00	100
LAWM44	44	Inner	6.32	10.03	7.00	5.00	0.10	1.00	1.50	12.00	48.00	0.40	2.00	4.60	2.00	0.05	100
LAWM45	20	Inner	7.00	8.00	5.78	5.00	0.30	1.42	1.50	14.00	48.00	0.35	2.00	4.60	2.00	0.05	100
LAWM46	4	Inner	6.00	11.00	6.51	5.00	0.10	1.00	2.50	12.00	47.94	0.40	1.00	3.50	3.00	0.05	100
LAWM47	17	Inner	6.20	8.00	7.00	5.00	0.10	1.00	2.50	14.00	48.00	0.34	1.31	3.50	3.00	0.05	100
LAWM48	9	Inner	6.23	11.00	5.27	5.00	0.10	1.00	1.50	12.00	48.00	0.40	2.00	3.50	2.00	2.00	100
LAWM49	53	Inner	7.00	10.90	5.00	3.00	0.10	1.00	1.50	14.00	47.53	0.37	1.00	4.60	2.00	2.00	100
LAWM50	52	Center	6.52	9.69	6.10	4.11	0.20	1.67	2.03	13.08	46.94	0.38	1.53	4.10	2.53	1.12	100
<b>Replicates</b>		<b>Replicate Of</b>															
LAWM51	25	LAWM50	6.52	9.69	6.10	4.11	0.20	1.67	2.03	13.08	46.94	0.38	1.53	4.10	2.53	1.12	100
LAWM52	23	LAWA88 <sup>(c)</sup>	6.08	9.70	1.99	5.53	2.58	0.00	1.47	20.00	43.99	0.21	1.99	2.95	2.99	0.52	100
LAWM53	3	LAWM1	9.00	6.00	10.00	8.00	4.00	4.50	0.00	5.00	44.45	1.00	3.00	5.00	0.00	0.05	100
LAWM54	33	LAWM9	3.50	6.00	10.00	8.00	4.00	2.39	0.00	5.00	49.71	0.40	0.00	5.00	4.00	2.00	100
LAWM55	27	LAWM12	3.50	13.00	0.00	2.31	4.00	4.50	1.97	14.25	42.20	0.27	3.00	5.00	4.00	2.00	100
LAWM56	51	LAWM35	5.00	12.00	6.18	4.41	0.10	0.50	3.50	17.00	42.00	0.24	2.50	2.00	2.57	2.00	100

(a) Random order in which glasses were batched and melted.

(b) The composition of the “Others” component is given in Table 2.2.

(c) Two melts of this composition, LAWA88 and LAWA88R1, were prepared and characterized; they have the same measured (LAWA88R1) or estimated (LAWA88) SO<sub>3</sub> values. The target compositions are, therefore, identical.

**Table 2.6. Target Glass Compositions of Existing Matrix LAW Glasses (wt%).**

Glass ID	Al <sub>2</sub> O <sub>3</sub>	B <sub>2</sub> O <sub>3</sub>	CaO	Fe <sub>2</sub> O <sub>3</sub>	K <sub>2</sub> O	Li <sub>2</sub> O	MgO	Na <sub>2</sub> O	SiO <sub>2</sub>	SO <sub>3</sub>	TiO <sub>2</sub>	ZnO	ZrO <sub>2</sub>	Cl	Cr <sub>2</sub> O <sub>3</sub>	Cs <sub>2</sub> O	F	NiO	P <sub>2</sub> O <sub>5</sub>	Re <sub>2</sub> O	Sum
LAWA44R10	6.20	8.90	1.99	6.98	0.50	0.00	1.99	20.00	44.55	0.10	1.99	2.96	2.99	0.65	0.02	0.00	0.01	0.00	0.03	0.10	100
LAWA53	6.09	6.11	7.77	7.40	0.49	0.00	1.46	19.72	41.66	1.48 <sup>(a)</sup>	1.09	2.95	2.95	0.64	0.02	0.00	0.01	0.00	0.03	0.10	100
LAWA56	6.09	11.93	1.95	7.40	0.49	0.00	1.46	19.72	41.66	1.48 <sup>(a)</sup>	1.09	2.95	2.95	0.64	0.02	0.00	0.01	0.00	0.03	0.10	100
LAWA88 & LAW88R1	6.08	9.70	1.99	5.53	2.58	0.00	1.47	20.00	43.99	0.21	1.99	2.95	2.99	0.33	0.01	0.00	0.00	0.00	0.07	0.10	100
LAWA102R1	6.06	10.00	5.07	5.41	0.26	2.50	1.50	14.49	46.60	2.50 <sup>(a)</sup>	1.14	3.06	3.02	0.33	0.02	0.00	0.03	0.00	0.13	0.10	102 <sup>(b)</sup>
LAWA126	5.64	9.82	1.99	5.54	3.88	0.00	1.48	18.46	44.12	0.35	2.00	2.96	2.99	0.20	0.02	0.16	0.30	0.00	0.08	0.10	100
LAWA128 & LAW128R1	6.03	7.07	2.08	5.79	3.88	0.00	1.18	18.46	46.09	0.35	2.09	3.09	3.13	0.20	0.02	0.16	0.30	0.00	0.08	0.10	100
LAWA130	6.03	8.95	2.08	2.86	3.88	0.00	1.18	18.46	46.09	0.35	2.09	4.14	3.13	0.20	0.02	0.16	0.30	0.00	0.08	0.10	100
LAWB65	6.17	9.91	6.67	5.28	0.26	4.29	2.96	5.46	48.35	1.28 <sup>(a)</sup>	1.39	4.65	3.15	0.00	0.10	0.00	0.07	0.00	0.01	0.10	100
LAWB66	6.17	9.91	8.17	5.28	0.26	4.29	2.96	5.46	48.35	1.28 <sup>(a)</sup>	1.39	3.15	3.15	0.00	0.10	0.00	0.07	0.00	0.01	0.10	100
LAWB68	6.17	8.41	8.17	5.28	0.26	4.29	2.96	5.46	48.35	1.28 <sup>(a)</sup>	1.39	4.65	3.15	0.00	0.10	0.00	0.07	0.00	0.01	0.10	100
LAWB78	6.15	12.33	7.12	3.25	0.23	3.05	2.97	9.78	47.00	0.78	0.00	4.00	3.15	0.01	0.05	0.00	0.08	0.00	0.05	0.10	100
LAWB79	6.15	12.33	7.12	3.25	0.23	3.51	2.97	8.62	47.70	0.78	0.00	4.00	3.15	0.01	0.05	0.00	0.08	0.00	0.05	0.10	100
LAWB80	6.15	12.33	7.12	3.25	1.99	3.51	2.97	6.62	47.95	0.78	0.00	4.00	3.15	0.01	0.05	0.00	0.08	0.00	0.05	0.10	100
LAWB83	6.18	10.03	6.78	5.29	0.19	4.31	2.97	5.47	48.60	0.65	1.39	4.84	3.16	0.01	0.04	0.00	0.06	0.00	0.04	0.10	100
LAWB84	6.18	10.03	6.68	5.29	0.19	4.40	2.97	5.47	48.60	0.65	1.39	4.84	3.16	0.01	0.04	0.00	0.06	0.00	0.04	0.10	100
LAWB85	6.18	11.52	5.28	5.29	0.19	4.31	2.97	5.47	48.60	0.65	1.39	4.84	3.16	0.01	0.04	0.00	0.06	0.00	0.04	0.10	100
LAWB86	6.18	12.41	5.73	5.29	0.19	4.35	2.97	5.47	48.60	0.65	0.00	4.84	3.16	0.01	0.04	0.00	0.06	0.00	0.04	0.10	100
C100-G-136B	6.12	10.08	6.40	6.47	0.15	2.73	1.51	11.86	46.67	0.63	1.12	3.01	3.02	0.12	0.02	0.00	0.06	0.02	0.12	0.0	100
LAWC27	6.12	12.19	8.55	0.01	0.14	2.73	1.50	11.96	48.88	0.48	1.12	3.02	3.02	0.11	0.02	0.00	0.05	0.00	0.11	0.10	100
LAWC32	6.49	10.05	9.04	2.42	0.14	2.73	1.50	11.96	46.74	0.48	1.12	4.02	3.02	0.11	0.02	0.00	0.05	0.00	0.11	0.10	100

- (a) Excess SO<sub>3</sub> was added to test saturation sulfate solubility in the glass. For property-composition modeling, the SO<sub>3</sub> values as measured by XRF were used, which necessitated renormalizing the glass compositions. See Section 3.3 and Table 3.2.
- (b) LAW102R1 was batched with excess SO<sub>3</sub>. Because a large part of the SO<sub>3</sub> (~ 2 wt%) was expected to volatilize or form a separate phase, the excess SO<sub>3</sub> was treated differently making the sum 102 instead of 100.



**Table 2.7. Target Compositions of LAW Phase 1a Augmentation Test Matrix Glasses (wt%).**

Glass ID	Al <sub>2</sub> O <sub>3</sub>	B <sub>2</sub> O <sub>3</sub>	CaO	Fe <sub>2</sub> O <sub>3</sub>	K <sub>2</sub> O	Li <sub>2</sub> O	MgO	Na <sub>2</sub> O	SiO <sub>2</sub>	SO <sub>3</sub>	TiO <sub>2</sub>	ZnO	ZrO <sub>2</sub>	Others <sup>(a)</sup>	Sum
LAWM57	7.00	11.00	3.00	4.66	3.80	0.00	1.44	20.61	39.26	0.35	1.37	3.03	4.00	0.49	100
LAWM58	7.00	9.29	1.03	6.50	3.80	0.00	1.44	20.53	41.64	0.35	1.37	2.56	4.00	0.49	100
LAWM59	6.84	9.01	2.96	6.49	2.00	0.00	1.44	20.00	44.54	0.35	1.37	2.51	2.00	0.49	100
LAWM60	5.00	11.00	1.71	4.50	2.00	0.00	1.44	20.01	45.33	0.35	1.37	2.80	4.00	0.49	100
LAWM61	5.00	11.00	1.00	4.50	3.29	0.00	1.44	20.00	45.05	0.35	1.37	4.50	2.01	0.49	100
LAWM62	5.00	9.00	1.00	6.50	3.38	0.00	1.44	20.00	44.33	0.35	1.37	3.84	3.30	0.49	100
LAWM63	7.00	9.40	1.04	4.70	2.06	0.00	1.44	23.00	42.60	0.35	1.37	4.50	2.06	0.49	100
LAWM64	6.99	10.98	3.00	6.50	2.00	0.00	1.44	20.04	38.36	0.35	1.37	4.49	3.99	0.49	100
LAWM65	5.00	9.00	2.96	4.50	2.00	0.00	1.44	22.79	43.59	0.35	1.37	2.50	4.00	0.49	100
LAWM66	7.59	10.63	1.00	6.31	0.48	0.00	1.44	22.99	38.35	0.35	1.37	4.50	4.50	0.49	100
LAWM67	8.00	10.60	1.55	4.60	5.40	0.00	1.44	20.13	38.36	0.35	1.37	2.72	5.00	0.49	100
LAWM68	5.00	9.00	3.00	6.50	4.80	0.00	1.44	20.01	40.81	0.35	1.37	3.56	3.68	0.49	100
LAWM69	7.98	10.99	3.00	6.37	1.83	0.00	1.44	20.09	39.60	0.35	1.37	4.50	2.00	0.49	100
LAWM70	5.00	9.40	1.05	6.50	4.55	0.00	1.44	20.01	45.35	0.35	1.37	2.50	2.01	0.49	100
LAWM71	5.01	9.00	1.00	4.50	5.40	0.00	1.44	20.00	44.94	0.35	1.37	4.50	2.00	0.49	100
LAWM72	8.00	11.00	2.94	6.45	4.18	0.00	1.44	20.04	39.16	0.35	1.37	2.50	2.09	0.49	100
LAWM73	8.00	9.00	3.00	4.88	1.22	0.00	1.44	23.00	40.38	0.35	1.37	4.49	2.39	0.49	100
LAWM74	7.58	9.00	1.00	4.50	0.00	0.00	1.44	21.32	45.35	0.35	1.37	2.60	5.00	0.49	100
LAWM75	8.00	9.15	3.00	6.49	1.08	0.00	1.44	20.68	38.45	0.35	1.37	4.50	5.00	0.49	100
LAWM76	6.40	9.92	1.92	5.42	2.60	0.00	1.44	21.40	41.86	0.35	1.37	3.42	3.40	0.49	100

(a) See Table 2.8 for the compositions of the Others component.

**Table 2.8. Target Values of Others Components in LAW Phase 1a Augmentation Test Matrix Glasses.**

Glass ID	Cl	Cr <sub>2</sub> O <sub>3</sub>	F	NiO	P <sub>2</sub> O <sub>5</sub>	PbO
LAWM57	0.20	0.08	0.08	0.01	0.12	0.01
LAWM58	0.20	0.08	0.08	0.01	0.12	0.01
LAWM59	0.20	0.08	0.08	0.01	0.12	0.01
LAWM60	0.20	0.08	0.08	0.01	0.12	0.01
LAWM61	0.20	0.08	0.08	0.01	0.12	0.01
LAWM62	0.20	0.08	0.08	0.01	0.12	0.01
LAWM63	0.20	0.08	0.08	0.01	0.12	0.01
LAWM64	0.20	0.08	0.08	0.01	0.12	0.01
LAWM65	0.20	0.08	0.08	0.01	0.12	0.01
LAWM66	0.20	0.08	0.08	0.01	0.12	0.01
LAWM67	0.20	0.08	0.08	0.01	0.12	0.01
LAWM68	0.20	0.08	0.08	0.01	0.12	0.01
LAWM69	0.20	0.08	0.08	0.01	0.12	0.01
LAWM70	0.20	0.08	0.08	0.01	0.12	0.01
LAWM71	0.20	0.08	0.08	0.01	0.12	0.01
LAWM72	0.20	0.08	0.08	0.01	0.12	0.01
LAWM73	0.20	0.08	0.08	0.01	0.12	0.01
LAWM74	0.20	0.08	0.08	0.01	0.12	0.01
LAWM75	0.20	0.08	0.08	0.01	0.12	0.01
LAWM76	0.20	0.08	0.08	0.01	0.12	0.01

**Table 2.9. Target Compositions of LAW Correlation and High Cr<sub>2</sub>O<sub>3</sub> Correlation Glasses.**

GLASS	Al <sub>2</sub> O <sub>3</sub>	B <sub>2</sub> O <sub>3</sub>	CaO	Fe <sub>2</sub> O <sub>3</sub>	K <sub>2</sub> O	Li <sub>2</sub> O	MgO	Na <sub>2</sub> O	SiO <sub>2</sub>	SO <sub>3</sub>	TiO <sub>2</sub>	ZnO	ZrO <sub>2</sub>	Others <sup>(a)</sup>	Sum
LAWE2H	5.95	9.75	1.97	5.36	3.79	0.00	1.44	20.78	42.44	0.32	1.37	3.41	2.93	0.49	100
LAWE3	6.10	10.00	2.02	5.50	4.99	0.00	1.48	18.21	42.95	0.35	1.40	3.50	3.00	0.50	100
LAWE3H	5.94	9.74	1.97	5.36	5.41	0.00	1.44	19.74	41.85	0.37	1.36	3.41	2.92	0.49	100
LAWE4	6.10	10.00	2.52	5.50	0.50	0.00	1.48	19.64	45.48	0.38	1.40	3.50	3.00	0.50	100
LAWE4H	5.97	9.79	2.46	5.38	0.54	0.00	1.45	21.27	44.50	0.41	1.37	3.43	2.94	0.49	100
LAWE5	6.10	10.00	3.68	5.50	0.50	0.51	1.48	17.52	45.88	0.43	1.40	3.50	3.00	0.50	100
LAWE5H	5.99	9.81	3.61	5.40	0.54	0.49	1.45	18.97	45.05	0.46	1.37	3.43	2.94	0.49	100
LAWE7	6.10	10.00	6.39	5.50	0.50	3.22	1.51	12.50	45.33	0.55	1.40	3.50	3.00	0.50	100
LAWE7H	6.02	9.87	6.31	5.43	0.54	3.17	1.49	13.53	44.76	0.59	1.38	3.46	2.96	0.49	100
LAWE9H	6.05	9.92	6.86	5.45	0.54	4.08	2.36	8.93	46.80	0.69	1.39	3.47	2.97	0.49	100
LAWE10H	6.07	9.95	6.96	5.48	0.54	4.26	2.94	5.72	48.93	0.80	1.39	3.48	2.99	0.49	100
LAWE11	6.10	10.00	2.32	5.50	4.75	0.00	1.48	17.36	43.74	0.35	1.40	3.50	3.00	0.50	100
LAWE12	6.95	8.75	1.97	4.36	5.41	0.00	1.44	19.74	41.84	0.35	1.37	3.41	3.92	0.49	100
LAWE13	6.95	9.75	1.97	5.36	5.41	0.00	0.44	19.74	41.84	0.35	0.37	3.41	3.92	0.49	100
LAWE14	4.94	9.75	1.47	5.36	5.41	0.00	0.44	19.74	43.35	0.35	1.37	3.41	3.92	0.49	100
LAWE15	5.94	8.75	1.47	5.36	5.41	0.00	0.94	19.74	42.85	0.35	1.37	3.41	3.92	0.49	100
LAWE16	5.94	8.25	1.47	5.36	5.41	0.00	0.94	19.74	42.84	0.35	1.37	3.41	4.42	0.49	100
LAWE3Cr2	6.10	10.00	2.02	5.50	4.99	0.00	1.48	18.21	41.63	0.35	1.40	3.50	3.00	1.82	100
LAWE9HCr1	6.05	9.92	6.86	5.45	0.54	4.08	2.36	8.93	46.27	0.69	1.39	3.47	2.97	1.01	100
LAWE9HCr2	6.05	9.92	6.86	5.45	0.54	4.08	2.36	8.93	46.42	0.69	1.39	3.47	2.97	0.86	100
LAWE10HCr3	6.07	9.95	6.96	5.48	0.54	4.26	2.94	5.72	48.65	0.80	1.39	3.48	2.99	0.76	100

(a) See Table 2.10 for the compositions of the Others component.

**Table 2.10. Target Values of Others Components in LAW Correlation and High Cr<sub>2</sub>O<sub>3</sub> Correlation Glasses.**

Glass ID	Cl	Cr <sub>2</sub> O <sub>3</sub>	F	NiO	P <sub>2</sub> O <sub>5</sub>	PbO
LAWE2H	0.20	0.08	0.08	0.01	0.12	0.01
LAWE3	0.20	0.08	0.08	0.01	0.12	0.01
LAWE3H	0.20	0.08	0.08	0.01	0.12	0.01
LAWE4	0.20	0.08	0.08	0.01	0.12	0.01
LAWE4H	0.20	0.08	0.08	0.01	0.12	0.01
LAWE5	0.20	0.08	0.08	0.01	0.12	0.01
LAWE5H	0.20	0.08	0.08	0.01	0.12	0.01
LAWE7	0.20	0.08	0.08	0.01	0.12	0.01
LAWE7H	0.20	0.08	0.08	0.01	0.12	0.01
LAWE9H	0.20	0.08	0.08	0.01	0.12	0.01
LAWE10H	0.20	0.08	0.08	0.01	0.12	0.01
LAWE11	0.20	0.08	0.08	0.01	0.12	0.01
LAWE12	0.20	0.08	0.08	0.01	0.12	0.01
LAWE13	0.20	0.08	0.08	0.01	0.12	0.01
LAWE14	0.20	0.08	0.08	0.01	0.12	0.01
LAWE15	0.20	0.08	0.08	0.01	0.12	0.01
LAWE16	0.20	0.08	0.08	0.01	0.12	0.01
LAWE3Cr2	0.20	1.40	0.08	0.01	0.12	0.01
LAWE9HCr1	0.20	0.60	0.08	0.01	0.12	0.01
LAWE9HCr2	0.20	0.45	0.08	0.01	0.12	0.01
LAWE10HCr3	0.20	0.35	0.08	0.01	0.12	0.01

**Table 2.11. Target Compositions of LAW High Cr<sub>2</sub>O<sub>3</sub> and P<sub>2</sub>O<sub>5</sub> Glasses.**

Glass ID	Al <sub>2</sub> O <sub>3</sub>	B <sub>2</sub> O <sub>3</sub>	CaO	Fe <sub>2</sub> O <sub>3</sub>	K <sub>2</sub> O	Li <sub>2</sub> O	MgO	Na <sub>2</sub> O	SiO <sub>2</sub>	SO <sub>3</sub>	TiO <sub>2</sub>	ZnO	ZrO <sub>2</sub>	Others <sup>(a)</sup>	Sum
LAWCrP1R	6.10	10.00	2.76	5.50	0.13	0.00	1.48	19.34	44.39	0.39	1.40	3.50	3.00	2.01	100
LAWCrP2R	6.10	10.00	2.11	5.50	0.27	0.00	1.48	21.00	43.07	0.34	1.40	3.50	3.00	2.23	100
LAWCrP3R	6.10	10.00	2.76	5.50	0.13	0.00	1.48	19.34	43.45	0.39	1.40	3.50	3.00	2.95	100
LAWCrP4R	6.10	10.00	2.11	5.50	0.27	0.00	1.48	21.00	42.03	0.34	1.40	3.50	3.00	3.27	100
LAWCrP5	6.10	10.00	5.81	5.50	0.09	2.64	1.49	14.38	43.45	0.51	1.40	3.50	3.00	2.15	100
LAWCrP6	6.10	10.00	6.94	5.50	0.09	4.17	2.55	8.00	44.74	0.65	1.40	3.50	3.00	3.36	100
LAWCrP7	6.10	10.00	6.98	5.50	0.09	4.30	2.93	5.40	46.71	0.73	1.40	3.50	3.00	3.36	100

(a) See Table 2.12 for the compositions of the Others component.

**Table 2.12. Target Values of Others Components in LAW High Cr<sub>2</sub>O<sub>3</sub> and P<sub>2</sub>O<sub>5</sub> Glasses.**

Glass ID	Cl	Cr <sub>2</sub> O <sub>3</sub>	F	NiO	P <sub>2</sub> O <sub>5</sub>	PbO
LAWCrP1	0.12	0.33	0.11	0.00	1.44	0.00
LAWCrP2	0.19	0.59	0.10	0.00	1.33	0.00
LAWCrP3	0.12	0.33	0.11	0.00	2.38	0.00
LAWCrP4	0.19	0.59	0.10	0.00	2.38	0.00
LAWCrP5	0.14	0.59	0.07	0.01	1.33	0.01
LAWCrP6	0.14	0.63	0.07	0.01	2.51	0.01
LAWCrP7	0.14	0.63	0.07	0.01	2.51	0.01

**Table 2.13. Target Compositions of Remaining Actively Designed LAW Glasses (wt%).**

Glass ID	Al <sub>2</sub> O <sub>3</sub>	B <sub>2</sub> O <sub>3</sub>	CaO	Fe <sub>2</sub> O <sub>3</sub>	K <sub>2</sub> O	Li <sub>2</sub> O	MgO	Na <sub>2</sub> O	SO <sub>3</sub>	SiO <sub>2</sub>	TiO <sub>2</sub>	ZnO	ZrO <sub>2</sub>	Others <sup>(a)</sup>	Sum
LAWA41	6.20	7.50	2.00	6.98	3.10	0.00	1.99	20.00	0.10	43.41	1.99	2.99	2.99	0.72	100
LAWA42	6.20	9.03	2.40	8.41	3.10	0.00	2.40	20.00	0.10	38.00	2.40	3.60	3.61	0.71	100
LAWA43-1	12.00	7.39	1.97	6.88	3.10	0.00	1.96	20.00	0.10	38.00	1.97	2.95	2.95	0.71	100
LAWA44	6.20	8.90	1.99	6.98	0.50	0.00	1.99	20.00	0.10	44.55	1.99	2.97	2.99	0.81	100
LAWA45	6.20	11.90	0.00	6.98	0.50	0.00	1.48	20.00	0.10	44.55	1.99	2.48	2.99	0.83	100
LAWA49	6.20	8.90	0.00	9.98	0.50	0.00	1.48	20.00	0.10	44.55	1.99	2.48	2.99	0.83	100
LAWA50	6.20	8.90	0.00	11.98	0.50	0.00	1.48	20.00	0.10	42.55	1.99	2.48	2.99	0.83	100
LAWA51	6.20	11.97	0.00	7.00	0.45	0.00	1.48	18.00	0.09	46.57	2.00	2.49	3.00	0.75	100
LAWA52	6.18	6.19	7.88	7.51	0.50	0.00	1.48	20.00	0.10	42.25	1.11	2.99	2.99	0.83	100
LAWA60	8.53	11.23	4.32	0.00	0.50	0.00	1.99	20.00	0.10	44.55	1.99	2.96	2.99	0.83	100
LAWA65	6.09	6.11	3.26	7.40	0.49	0.00	5.97	19.72	1.48	41.66	1.09	2.95	2.95	0.81	100
LAWA76	6.09	10.85	7.77	7.40	0.49	4.95	1.46	10.03	1.48	41.66	1.09	2.95	2.95	0.81	100
LAWA81	6.20	8.90	3.99	6.98	0.50	0.00	1.99	20.00	0.10	44.55	0.00	2.96	2.99	0.83	100
LAWA82	6.20	8.90	0.00	6.98	0.50	0.00	1.99	20.00	0.10	44.55	3.99	2.96	2.99	0.83	100
LAWA83	6.20	8.90	1.99	4.99	0.50	0.00	1.99	20.00	0.10	44.55	1.99	2.96	2.99	2.82	100
LAWA84	6.20	8.90	1.99	2.99	0.50	0.00	1.99	20.00	0.10	44.55	1.99	2.96	2.99	4.81	100
LAWA87	4.48	8.87	1.99	6.97	2.58	0.00	1.99	20.00	0.21	44.46	1.99	2.96	2.99	0.51	100
LAWA89	6.08	9.70	0.00	5.53	2.58	0.00	1.47	20.00	0.21	43.99	3.98	2.95	2.99	0.51	100
LAWA90	6.08	9.70	3.98	5.53	2.58	0.00	1.47	20.00	0.21	43.99	0.00	2.95	2.99	0.51	100
LAWA93	6.18	11.10	7.88	7.51	0.50	5.07	1.48	10.03	0.10	42.25	1.11	2.99	2.99	0.83	100
LAWA96	6.20	7.90	3.99	2.99	0.50	0.00	1.99	20.00	0.10	43.56	1.99	2.96	2.99	4.81	100
LAWA102R2	6.05	10.00	5.06	5.40	0.26	2.50	1.50	14.48	0.44	46.58	1.14	3.06	3.02	0.51	100
LAWA104	6.61	8.59	1.92	6.73	0.55	0.00	1.92	22.00	0.10	42.99	1.92	2.86	2.89	0.90	100
LAWA105	7.03	8.28	1.85	6.49	0.60	0.00	1.85	24.00	0.11	41.42	1.85	2.76	2.78	0.97	100
LAWA112B14	6.10	9.87	7.65	0.00	1.89	0.00	1.48	20.00	0.17	44.26	2.00	2.97	3.01	0.70	100
LAWA112B15	6.16	9.81	7.61	0.00	2.41	0.00	1.48	20.00	0.11	44.02	1.99	2.95	2.99	0.56	100
LAWA125	5.64	9.55	1.94	5.39	4.21	0.00	1.44	20.00	0.38	42.91	1.94	2.88	2.91	0.93	100
LAWA127R1	5.65	10.20	2.07	5.76	3.43	0.00	1.54	16.31	0.31	45.82	2.07	3.07	3.11	0.78	100

(a) See Table 2.14 for the compositions of the Others component.

**Table 2.13. Target Compositions of Remaining Actively Designed LAW Glasses (wt%) (continued).**

Glass ID	Al <sub>2</sub> O <sub>3</sub>	B <sub>2</sub> O <sub>3</sub>	CaO	Fe <sub>2</sub> O <sub>3</sub>	K <sub>2</sub> O	Li <sub>2</sub> O	MgO	Na <sub>2</sub> O	SO <sub>3</sub>	SiO <sub>2</sub>	TiO <sub>2</sub>	ZnO	ZrO <sub>2</sub>	Others <sup>(a)</sup>	Sum
LAWA127R2	5.66	10.22	2.07	5.77	3.43	0.00	1.54	16.31	0.31	45.90	2.08	3.08	3.12	0.64	100
LAWA129	7.47	8.52	3.53	0.00	3.88	0.00	1.18	18.46	0.35	47.54	2.09	3.09	3.13	0.86	100
LAWA129R1	7.47	8.52	3.53	0.00	3.88	0.00	1.18	18.46	0.35	47.54	2.09	3.09	3.13	0.86	100
LAWA133	6.21	8.91	5.49	3.49	0.43	0.00	2.00	20.00	0.22	44.58	2.00	2.97	3.00	0.82	100
LAWA134	5.65	9.97	2.02	5.63	3.73	0.00	1.50	17.74	0.33	44.78	2.03	3.00	3.04	0.69	100
LAWA135	5.66	10.10	2.05	5.70	3.58	0.00	1.52	17.03	0.32	45.34	2.05	3.04	3.08	0.66	100
LAWA136	5.66	10.10	3.05	5.70	3.58	0.00	1.52	17.03	0.32	44.34	2.05	3.04	3.08	0.66	100
LAWA170	6.06	9.66	1.98	5.51	3.06	0.00	1.47	19.90	0.21	43.84	1.98	2.94	2.98	0.41	100
LAWB30	8.60	10.04	7.23	8.27	0.32	4.07	3.07	7.90	0.20	42.72	0.00	4.11	3.12	0.33	100
LAWB31	6.16	12.09	4.03	7.17	0.32	2.96	2.24	7.90	1.03	46.91	0.00	3.09	3.09	3.02	100
LAWB32	6.16	15.09	4.03	4.17	0.32	2.96	2.24	7.90	1.03	46.91	0.00	3.09	3.09	3.02	100
LAWB33	6.16	12.09	4.03	5.15	0.32	2.96	2.24	7.90	1.03	46.91	0.00	3.09	3.09	5.03	100
LAWB34	6.16	12.09	6.05	5.15	0.32	2.96	2.24	7.90	1.03	46.91	0.00	3.09	3.09	3.02	100
LAWB35	6.16	12.09	4.03	5.15	0.32	2.96	4.25	7.90	1.03	46.91	0.00	3.09	3.09	3.02	100
LAWB37	6.16	12.09	4.70	5.15	0.32	2.96	2.91	7.90	1.03	46.91	0.00	3.09	3.09	3.69	100
LAWB38	6.16	12.09	4.75	5.15	0.32	3.81	2.24	7.90	1.03	46.91	0.00	3.09	3.09	3.47	100
LAWB40	6.16	12.09	4.70	5.15	0.32	6.32	2.91	7.90	1.03	46.91	0.00	3.09	3.09	0.33	100
LAWB41	6.16	12.09	6.49	5.15	0.32	4.52	2.91	7.90	1.02	46.92	0.00	3.09	3.09	0.33	100
LAWB60	6.13	12.34	11.88	0.00	0.26	4.62	2.97	6.50	0.85	47.86	0.00	3.15	3.15	0.29	100
LAWB61	6.17	9.91	6.67	5.28	0.26	5.79	2.96	5.47	1.28	48.35	1.39	3.15	3.15	0.18	100
LAWB62	6.17	9.91	11.95	0.00	0.26	5.79	2.96	5.47	1.28	48.35	1.39	3.15	3.15	0.18	100
LAWB63	6.55	9.91	9.31	0.00	0.26	5.03	2.96	5.47	1.28	48.73	1.39	5.79	3.15	0.18	100
LAWB64	6.17	9.91	6.67	3.28	0.26	5.79	2.96	5.47	1.28	48.35	1.39	5.15	3.15	0.18	100
LAWB67	6.17	9.91	5.17	5.28	0.26	4.29	2.96	5.47	1.28	48.35	1.39	3.15	3.15	3.18	100
LAWB69	6.15	12.33	10.46	0.00	0.23	4.61	2.97	6.62	0.78	47.95	0.00	4.57	3.15	0.29	100
LAWB70	6.15	12.33	6.62	3.25	0.23	4.61	2.97	6.62	0.78	47.95	0.00	5.15	3.15	0.29	100
LAWB71	6.15	10.78	6.62	3.25	0.23	4.61	2.97	6.62	0.78	47.95	1.55	5.15	3.15	0.29	100
LAWB72	6.15	12.33	7.12	3.25	0.23	4.11	2.97	6.62	0.78	47.95	0.00	5.15	3.15	0.29	100

(a) See Table 2.14 for the compositions of the Others component.

**Table 2.13. Target Compositions of Remaining Actively Designed LAW Glasses (wt%) (continued).**

Glass ID	Al <sub>2</sub> O <sub>3</sub>	B <sub>2</sub> O <sub>3</sub>	CaO	Fe <sub>2</sub> O <sub>3</sub>	K <sub>2</sub> O	Li <sub>2</sub> O	MgO	Na <sub>2</sub> O	SO <sub>3</sub>	SiO <sub>2</sub>	TiO <sub>2</sub>	ZnO	ZrO <sub>2</sub>	Others <sup>(a)</sup>	Sum
LAWB73	6.17	9.91	9.31	1.90	0.26	5.03	2.96	5.47	1.28	48.35	1.39	4.65	3.15	0.18	100
LAWB74	6.17	10.03	8.66	1.90	0.26	5.29	2.96	5.47	1.28	48.35	1.39	4.65	3.15	0.18	100
LAWB75	6.17	11.76	8.66	1.90	0.26	5.29	1.50	5.47	1.28	48.35	1.39	4.65	3.15	0.18	100
LAWB76	6.17	11.76	8.66	1.90	0.26	5.79	1.50	5.47	1.28	49.24	0.00	4.65	3.15	0.18	100
LAWB77	6.15	12.33	6.62	2.20	0.23	4.11	2.97	6.62	0.78	47.95	1.55	5.15	3.15	0.29	100
LAWB81	6.15	12.33	7.12	3.25	0.23	4.26	2.97	6.62	0.78	47.95	0.00	5.00	3.15	0.29	100
LAWB82	6.15	10.08	7.12	9.50	0.23	4.26	1.48	6.62	0.78	45.44	0.00	5.00	3.15	0.29	100
LAWB87	6.48	12.99	6.10	5.02	0.20	4.69	1.41	5.00	0.81	49.10	0.00	4.88	3.19	0.14	100
LAWB88	6.48	12.99	7.98	2.20	0.20	4.69	1.41	5.00	0.81	50.04	0.00	4.88	3.19	0.14	100
LAWB89	6.18	10.03	6.78	5.29	0.19	5.00	2.97	4.08	0.65	49.30	1.39	4.84	3.16	0.25	100
LAWB90	6.18	10.03	6.78	5.29	0.19	3.61	2.97	6.87	0.65	47.90	1.39	4.84	3.16	0.25	100
LAWB91	6.18	10.03	6.78	5.29	0.19	2.92	2.97	8.72	0.65	46.74	1.39	4.84	3.16	0.25	100
LAWB92	6.18	10.03	6.78	5.29	0.19	2.22	2.97	10.11	0.65	46.05	1.39	4.84	3.16	0.25	100
LAWB93	6.18	10.03	6.78	5.29	0.19	4.66	2.97	4.78	0.65	48.94	1.39	4.84	3.16	0.25	100
LAWB93R1	6.18	10.03	6.78	5.29	0.19	4.66	2.97	4.78	0.65	48.94	1.39	4.84	3.16	0.25	100
LAWB94	6.18	10.03	6.78	5.29	0.19	5.36	2.97	3.38	0.65	49.64	1.39	4.84	3.16	0.25	100
LAWB95	6.18	10.03	6.78	5.29	0.19	5.76	2.97	2.45	0.65	50.17	1.39	4.84	3.16	0.25	100
LAWB96	6.16	10.01	6.76	5.28	0.12	4.29	2.97	5.47	0.65	48.66	1.39	4.85	3.17	0.22	100
LAWC12	11.97	9.13	1.59	5.71	0.14	0.00	1.38	20.00	0.20	39.33	3.41	4.27	2.45	0.29	100
LAWC15	6.23	8.95	2.01	7.02	0.14	0.00	2.01	20.00	0.13	44.80	2.00	3.00	3.01	0.79	100
LAWC21	6.13	10.09	6.41	6.48	0.15	2.74	1.51	11.88	0.42	46.70	1.12	3.02	3.02	0.32	100
LAWC21rev2	6.12	10.05	6.41	6.43	0.14	2.73	1.50	11.96	0.48	46.74	1.12	3.02	3.02	0.39	100
LAWC22	6.07	10.05	5.11	5.42	0.08	2.50	1.51	14.40	0.32	46.61	1.14	3.07	3.03	0.65	100
LAWC23	6.12	10.08	6.40	6.47	2.88	0.00	1.51	11.86	0.44	46.77	1.12	3.01	3.02	0.43	100
LAWC24	5.95	9.80	6.23	6.29	5.55	0.00	1.47	11.53	0.42	45.39	1.09	2.93	2.93	0.41	100
LAWC25	5.79	9.54	6.06	6.12	8.09	0.00	1.43	11.22	0.41	44.18	1.06	2.85	2.86	0.40	100
LAWC26	6.12	13.26	6.41	0.01	0.14	2.73	1.50	11.96	0.48	49.95	1.12	3.02	3.02	0.39	100
LAWC28	6.12	10.05	12.82	0.01	0.14	2.73	1.50	11.96	0.48	46.74	1.12	3.02	3.02	0.39	100

(a) See Table 2.14 for the compositions of the Others component.



**Table 2.13. Target Compositions of Remaining Actively Designed LAW Glasses (wt%) (continued).**

Glass ID	Al <sub>2</sub> O <sub>3</sub>	B <sub>2</sub> O <sub>3</sub>	CaO	Fe <sub>2</sub> O <sub>3</sub>	K <sub>2</sub> O	Li <sub>2</sub> O	MgO	Na <sub>2</sub> O	SO <sub>3</sub>	SiO <sub>2</sub>	TiO <sub>2</sub>	ZnO	ZrO <sub>2</sub>	Others <sup>(a)</sup>	Sum
LAWC29	6.55	10.05	9.62	0.01	0.14	2.73	1.50	11.96	0.48	47.18	1.12	5.36	3.02	0.39	100
LAWC30	6.12	10.05	6.41	4.10	0.14	2.73	1.50	11.96	0.48	46.74	1.12	5.35	3.02	0.39	100
LAWC31	6.12	10.05	7.41	4.43	0.14	2.73	1.50	11.96	0.48	46.74	1.12	4.02	3.02	0.39	100
LAWC31R1	6.12	10.05	7.41	4.43	0.14	2.73	1.50	11.96	0.48	46.74	1.12	4.02	3.02	0.39	100
LAWC33	6.14	10.09	6.94	4.44	0.14	2.75	1.51	12.00	0.48	46.93	1.13	4.04	3.03	0.39	100
TFA-BASE	7.00	10.00	0.01	5.50	0.41	0.00	1.50	20.00	0.07	49.07	3.00	1.50	1.50	0.44	100
A1-AN105R2	6.10	8.84	1.96	6.87	0.44	0.00	1.96	20.66	0.19	43.82	1.96	2.92	2.94	1.34	100
A2-AP101	5.62	9.82	1.99	5.53	3.81	0.00	1.48	18.46	0.40	43.99	1.99	2.94	2.96	1.02	100
A88AP101R1	6.10	9.83	2.00	5.55	2.14	0.00	1.48	20.00	0.28	44.13	2.00	2.96	3.00	0.55	100
A3-AN104	6.05	9.92	5.03	5.37	0.33	2.48	1.48	14.64	0.37	46.09	1.13	3.04	3.00	1.08	100
B1-AZ101	6.17	10.01	6.76	5.27	0.18	4.30	2.98	5.47	0.65	48.50	1.39	4.84	3.16	0.32	100
Cl-AN107	6.06	10.02	5.09	5.42	0.07	2.50	1.51	14.45	0.38	46.59	1.15	3.06	3.02	0.68	100
C22AN107	6.10	10.07	5.11	5.58	0.09	2.51	1.51	14.42	0.31	46.57	1.14	3.06	3.02	0.46	100
C2-AN102C35	6.07	9.42	7.35	3.60	0.09	3.25	1.49	11.97	0.63	47.24	1.08	3.99	3.00	0.83	100
A88Si+15	6.14	9.48	1.93	5.35	2.37	0.00	1.43	22.18	0.31	42.55	1.93	2.85	2.89	0.60	100
A88Si-15	6.05	10.21	2.07	5.76	1.88	0.00	1.54	17.66	0.25	45.83	2.07	3.07	3.11	0.48	100
C22Si+15	6.04	9.83	4.99	5.35	0.10	2.46	1.48	16.18	0.34	45.54	1.12	3.00	2.96	0.56	100
C22Si-15	6.16	10.28	5.21	5.55	0.08	2.57	1.55	12.80	0.27	47.64	1.17	3.14	3.09	0.45	100
A1C1-1	6.09	9.12	2.74	6.50	0.35	0.62	1.85	19.16	0.24	44.47	1.76	2.95	2.96	1.20	100
A1C1-2	6.07	9.41	3.52	6.13	0.25	1.25	1.73	17.66	0.28	45.11	1.55	2.98	2.97	1.06	100
A1C1-3	6.05	9.69	4.30	5.76	0.16	1.87	1.62	16.16	0.33	45.76	1.35	3.01	2.99	0.92	100
A2B1-1	5.75	9.87	3.18	5.47	2.90	1.07	1.85	15.21	0.46	45.12	1.84	3.41	3.01	0.84	100
A2B1-2	5.89	9.91	4.37	5.40	2.00	2.15	2.23	11.97	0.52	46.25	1.69	3.89	3.06	0.68	100
A2B1-3	6.03	9.96	5.57	5.34	1.09	3.22	2.60	8.72	0.59	47.38	1.54	4.36	3.11	0.50	100
A3C2-1	6.06	9.79	5.61	4.92	0.27	2.67	1.48	13.97	0.43	46.38	1.12	3.28	3.00	1.01	100
A3C2-2	6.06	9.67	6.19	4.48	0.21	2.86	1.48	13.31	0.50	46.66	1.11	3.51	3.00	0.96	100
A3C2-3	6.06	9.54	6.77	4.04	0.15	3.06	1.49	12.64	0.57	46.95	1.09	3.75	3.00	0.90	100
12S-G-85C	6.08	10.05	5.09	5.56	0.08	2.50	1.51	14.43	0.38	46.43	1.14	3.06	3.01	0.68	100
12U-G-86A	6.16	8.95	1.98	6.94	0.44	0.00	1.98	19.96	0.24	44.32	1.98	2.95	2.97	1.12	100

(a) See Table 2.14 for the compositions of the Others component.

**Table 2.13. Target Compositions of Remaining Actively Designed LAW Glasses (wt%) (continued).**

Glass ID	Al <sub>2</sub> O <sub>3</sub>	B <sub>2</sub> O <sub>3</sub>	CaO	Fe <sub>2</sub> O <sub>3</sub>	K <sub>2</sub> O	Li <sub>2</sub> O	MgO	Na <sub>2</sub> O	SO <sub>3</sub>	SiO <sub>2</sub>	TiO <sub>2</sub>	ZnO	ZrO <sub>2</sub>	Others <sup>(a)</sup>	Sum
A100G115A	6.06	10.00	5.06	5.41	0.26	2.50	1.49	14.46	0.44	46.58	1.14	3.07	3.03	0.51	100
A100CC	6.06	10.00	5.06	5.41	0.26	2.50	1.49	14.46	0.44	46.58	1.14	3.07	3.03	0.51	100
C100GCC	6.12	10.08	6.40	6.47	0.15	2.73	1.51	11.86	0.53	46.67	1.12	3.01	3.02	0.34	100
GTSD-1126	6.17	10.02	6.77	5.29	0.12	4.30	2.97	5.48	0.65	48.74	1.39	4.85	3.17	0.07	100
GTSD-1437	6.07	9.43	7.36	3.60	0.09	3.26	1.49	11.99	0.63	47.30	1.08	3.99	3.00	0.70	100
PLTC35CCC	6.07	9.43	7.36	3.60	0.09	3.26	1.49	11.99	0.63	47.30	1.08	3.99	3.00	0.70	100
WVB-G-124B	6.04	9.97	5.05	5.40	0.26	2.49	1.49	14.42	0.44	46.46	1.14	3.06	3.02	0.77	100
WVF-G-21B	6.08	9.80	1.99	5.54	2.13	0.00	1.48	20.01	0.35	44.00	1.99	2.95	2.99	0.72	100
WVH-G-57B	6.10	10.02	7.39	4.42	0.14	2.73	1.50	11.93	0.47	46.63	1.12	4.01	3.01	0.54	100
WVJ-G-109D	6.16	10.00	6.76	5.27	0.19	4.30	2.97	5.46	0.65	48.47	1.39	4.83	3.15	0.40	100
WVM-G-142C	5.61	9.81	1.99	5.53	3.81	0.00	1.47	18.44	0.40	43.94	1.98	2.94	2.96	1.12	100
WVR-G-127A	6.05	9.91	5.02	5.36	0.33	2.48	1.48	14.63	0.38	46.04	1.13	3.04	3.00	1.17	100
LA44PNCC	6.17	8.87	1.98	6.96	0.26	0.00	1.97	20.00	0.25	44.45	1.97	2.91	2.99	1.21	100
LA44CCCR2	6.17	8.87	1.98	6.96	0.26	0.00	1.97	20.00	0.25	44.45	1.97	2.91	2.99	1.21	100
PNLA126CC	5.65	9.85	2.00	5.56	3.88	0.00	1.48	18.46	0.35	44.22	2.00	2.96	3.00	0.61	100
LA126CCC	5.65	9.85	2.00	5.56	3.88	0.00	1.48	18.46	0.35	44.22	2.00	2.96	3.00	0.61	100
LA137SRCCC	6.05	9.91	5.03	5.36	0.62	2.48	1.48	14.64	0.28	46.06	1.13	3.04	3.00	0.92	100
LB83PNCC	6.21	10.04	6.79	5.29	0.18	4.31	2.99	5.37	0.55	48.68	1.40	4.85	3.17	0.16	100
LB83CCC-1	6.21	10.04	6.79	5.29	0.18	4.31	2.99	5.37	0.55	48.68	1.40	4.85	3.17	0.16	100
LB88CCC	6.50	12.97	7.97	2.20	0.20	4.69	1.41	5.00	0.81	50.04	0.00	4.88	3.19	0.14	100
AZ-102 Surr SRNL	6.43	13.00	7.97	2.20	0.20	4.69	1.41	5.08	0.77	50.00	0.00	4.88	3.19	0.18	100
AN-102 Surr LC Melter	6.14	10.14	6.42	6.50	0.07	2.75	1.52	11.80	0.29	46.77	1.13	3.03	3.03	0.38	100

(a) See Table 2.14 for the compositions of the Others component.

**Table 2.14. Target Values of Others Components in Remaining Actively Designed LAW Glasses (wt%).**

Glass ID	BaO	Br	CdO	Cl	Cr <sub>2</sub> O <sub>3</sub>	Cs <sub>2</sub> O	F	I	MnO	MoO <sub>3</sub>	NiO	P <sub>2</sub> O <sub>5</sub>	PbO	Re <sub>2</sub> O <sub>7</sub>	SeO <sub>2</sub>	SrO	Unknown
LAWA41	- <sup>(a)</sup>	-	-	0.58	0.02	-	0.04	-	-	-	-	0.08	0.00	0.00	-	-	-
LAWA42	-	-	-	0.58	0.02	-	0.04	-	-	-	0.00	0.08	0.00	0.00	-	-	-
LAWA43-1	-	-	-	0.58	0.02	-	0.04	-	-	-	0.00	0.08	0.00	0.00	-	-	-
LAWA44	-	-	-	0.65	0.02	-	0.01	-	-	-	-	0.03	-	0.10	-	-	-
LAWA45	-	-	-	0.65	0.02	-	0.01	-	-	0.01	0.00	0.03	0.00	0.10	-	-	-
LAWA49	-	-	-	0.65	0.02	0.00	0.01	-	-	0.01	0.00	0.03	0.00	0.10	-	-	-
LAWA50	-	-	-	0.65	0.02	-	0.01	-	-	0.01	0.00	0.03	0.00	0.10	-	-	-
LAWA51	-	-	-	0.59	0.02	0.00	0.01	-	-	0.01	0.00	0.03	0.00	0.10	-	-	-
LAWA52	-	-	-	0.65	0.02	0.00	0.01	-	-	0.01	0.00	0.03	0.00	0.10	-	-	-
LAWA60	-	-	-	0.65	0.02	0.00	0.01	-	-	0.01	0.00	0.03	0.00	0.10	-	-	-
LAWA65	-	-	-	0.64	0.02	-	0.01	-	-	0.01	0.00	0.03	0.00	0.10	-	-	-
LAWA76	-	-	-	0.64	0.02	-	0.01	-	-	0.01	0.00	0.03	0.00	0.10	-	-	-
LAWA81	-	-	-	0.65	0.02	-	0.01	-	-	0.01	0.00	0.03	0.00	0.10	-	-	-
LAWA82	-	-	-	0.65	0.02	-	0.01	-	-	0.01	0.00	0.03	0.00	0.10	-	-	-
LAWA83	-	-	-	0.65	0.02	-	0.01	-	-	0.01	0.00	2.03	0.00	0.10	-	-	-
LAWA84	-	-	-	0.65	0.02	-	0.01	-	-	0.01	0.00	4.02	0.00	0.10	-	-	-
LAWA87	-	-	-	0.33	0.01	-	0.00	-	-	-	0.00	0.07	0.00	0.10	-	-	-
LAWA89	-	-	-	0.33	0.01	-	0.00	-	-	-	0.00	0.07	0.00	0.10	-	-	-
LAWA90	-	-	-	0.33	0.01	-	0.00	-	-	-	0.00	0.07	0.00	0.10	-	-	-
LAWA93	-	-	-	0.65	0.02	0.00	0.01	-	-	0.01	0.00	0.03	0.00	0.10	-	-	-
LAWA96	-	-	-	0.65	0.02	-	0.01	-	-	0.01	0.00	4.02	0.00	0.10	-	-	-
LAWA102R2	-	-	-	0.33	0.02	-	0.03	-	-	-	-	0.13	-	-	-	-	-
LAWA104	-	-	-	0.72	0.02	0.00	0.01	-	-	0.01	0.00	0.04	0.00	0.10	-	-	-
LAWA105	-	-	-	0.78	0.02	0.00	0.01	-	-	0.01	0.00	0.04	0.00	0.10	-	-	-
LAWA112B14	-	-	-	0.38	0.02	-	0.10	-	-	-	-	0.10	-	0.10	-	-	-
LAWA112B15	-	-	-	0.31	0.01	-	0.09	-	-	-	-	0.05	-	0.10	-	-	-
LAWA125	-	-	-	0.22	0.02	0.18	0.32	-	-	-	-	0.09	-	0.10	-	-	-

(a) A dash (-) denotes an empty data cell.

**Table 2.14. Target Values of Others Components in Remaining Actively Designed LAW Glasses (wt%) (continued).**

Glass ID	BaO	Br	CdO	Cl	Cr <sub>2</sub> O <sub>3</sub>	Cs <sub>2</sub> O	F	I	MnO	MoO <sub>3</sub>	NiO	P <sub>2</sub> O <sub>5</sub>	PbO	Re <sub>2</sub> O <sub>7</sub>	SeO <sub>2</sub>	SrO	Unknown
LAWA127R2	- <sup>(a)</sup>	-	-	0.18	0.02	-	0.27	-	-	-	-	0.07	-	0.10	-	-	-
LAWA129	-	-	-	0.20	0.02	0.16	0.30	-	-	-	-	0.08	-	0.10	-	-	-
LAWA129R1	-	-	-	0.20	0.02	0.16	0.30	-	-	-	-	0.08	-	0.10	-	-	-
LAWA133	-	-	-	0.56	0.02	-	0.04	-	-	-	-	0.10	-	0.10	-	-	-
LAWA134	-	-	-	0.20	0.02	-	0.29	-	-	-	-	0.08	-	0.10	-	-	-
LAWA135	-	-	-	0.19	0.02	-	0.28	-	-	-	-	0.07	-	0.10	-	-	-
LAWA136	-	-	-	0.19	0.02	-	0.28	-	-	-	-	0.07	-	0.10	-	-	-
LAWA170	-	-	-	0.33	0.01	-		-	-	-	-	0.07	-	-	-	-	-
LAWB30	-	-	-	0.01	0.09	0.00	0.10	-	-	-	-	0.04	-	0.10	-	-	-
LAWB31	-	-	-	0.01	0.09	0.00	0.10	-	-	-	-	2.72	-	0.10	-	-	-
LAWB32	-	-	-	0.01	0.09	0.00	0.10	-	-	-	-	2.72	-	0.10	-	-	-
LAWB33	-	-	-	0.01	0.09	0.00	0.10	-	-	-	-	4.74	-	0.10	-	-	-
LAWB34	-	-	-	0.01	0.09	0.00	0.10	-	-	-	-	2.72	-	0.10	-	-	-
LAWB35	-	-	-	0.01	0.09	0.00	0.10	-	-	-	-	2.72	-	0.10	-	-	-
LAWB37	-	-	-	0.01	0.09	0.00	0.10	-	-	-	-	3.40	-	0.10	-	-	-
LAWB38	-	-	-	0.01	0.09	0.00	0.10	-	-	-	-	3.17	-	0.10	-	-	-
LAWB40	-	-	-	0.01	0.09	0.00	0.10	-	-	-	-	0.04	-	0.10	-	-	-
LAWB41	-	-	-	0.01	0.09	0.00	0.10	-	-	-	-	0.04	-	0.10	-	-	-
LAWB60	-	-	-	0.01	0.07	-	0.08	-	-	-	-	0.03	-	0.10	-	-	-
LAWB61	-	-	-	-	0.10	-	0.07	-	-	-	-	0.01	-	-	-	-	-
LAWB62	-	-	-	-	0.10	-	0.07	-	-	-	-	0.01	-	-	-	-	-
LAWB63	-	-	-	-	0.10	-	0.07	-	-	-	-	0.01	-	-	-	-	-
LAWB64	-	-	-	-	0.10	-	0.07	-	-	-	-	0.01	-	-	-	-	-
LAWB67	-	-	-	-	0.10	-	0.07	-	-	-	-	3.01	-	-	-	-	-
LAWB69	-	-	-	0.01	0.05	-	0.08	-	-	-	-	0.05	-	0.10	-	-	-
LAWB70	-	-	-	0.01	0.05	-	0.08	-	-	-	-	0.05	-	0.10	-	-	-
LAWB71	-	-	-	0.01	0.05	-	0.08	-	-	-	-	0.05	-	0.10	-	-	-
LAWB72	-	-	-	0.01	0.05	-	0.08	-	-	-	-	0.05	-	0.10	-	-	-

(a) A dash (-) denotes an empty data cell.

**Table 2.14. Target Values of Others Components in Remaining Actively Designed LAW Glasses (wt%) (continued).**

Glass ID	BaO	Br	CdO	Cl	Cr <sub>2</sub> O <sub>3</sub>	Cs <sub>2</sub> O	F	I	MnO	MoO <sub>3</sub>	NiO	P <sub>2</sub> O <sub>5</sub>	PbO	Re <sub>2</sub> O <sub>7</sub>	SeO <sub>2</sub>	SrO	Unknown
LAWB73	- (a)	-	-	-	0.10	-	0.07	-	-	-	-	0.01	-	-	-	-	-
LAWB74	-	-	-	-	0.10	-	0.07	-	-	-	-	0.01	-	-	-	-	-
LAWB75	-	-	-	-	0.10	-	0.07	-	-	-	-	0.01	-	-	-	-	-
LAWB76	-	-	-	-	0.10	-	0.07	-	-	-	-	0.01	-	-	-	-	-
LAWB77	-	-	-	0.01	0.05	-	0.08	-	-	-	-	0.05	-	0.10	-	-	-
LAWB81	-	-	-	0.01	0.05	-	0.08	-	-	-	-	0.05	-	0.10	-	-	-
LAWB82	-	-	-	0.01	0.05	-	0.08	-	-	-	-	0.05	-	0.10	-	-	-
LAWB87	-	-	-	0.01	0.06	-	0.05	-	-	-	-	0.02	-	-	-	-	-
LAWB88	-	-	-	0.01	0.06	-	0.05	-	-	-	-	0.02	-	-	-	-	-
LAWB89	-	-	-	0.01	0.04	-	0.06	-	-	-	-	0.04	-	0.10	-	-	-
LAWB90	-	-	-	0.01	0.04	-	0.06	-	-	-	-	0.04	-	0.10	-	-	-
LAWB91	-	-	-	0.01	0.04	-	0.06	-	-	-	-	0.04	-	0.10	-	-	-
LAWB92	-	-	-	0.01	0.04	-	0.06	-	-	-	-	0.04	-	0.10	-	-	-
LAWB93	-	-	-	0.01	0.04	-	0.06	-	-	-	-	0.04	-	0.10	-	-	-
LAWB93R1	-	-	-	0.01	0.04	-	0.06	-	-	-	-	0.04	-	0.10	-	-	-
LAWB94	-	-	-	0.01	0.04	-	0.06	-	-	-	-	0.04	-	0.10	-	-	-
LAWB95	-	-	-	0.01	0.04	-	0.06	-	-	-	-	0.04	-	0.10	-	-	-
LAWB96	-	-	-	0.01	0.03	0.15	0.02	-	-	-	-	0.01	-	-	-	-	-
LAWC12	-	-	-	0.12	0.02	-	0.01	-	0.05	0.00	0.04	0.03	0.03	-	-	-	-
LAWC15	-	0.08	-	0.08	0.00	-	0.47	-	-	0.00	0.04	0.02	0.00	0.10	-	-	-
LAWC21	-	-	-	0.12	0.02	-	0.06	-	-	-	-	0.12	-	-	-	-	-
LAWC21rev2	-	-	-	0.11	0.02	-	0.05	-	-	-	-	0.11	-	0.10	-	-	-
LAWC22	-	0.05	-	0.05	0.01	-	0.34	-	-	0.00	0.03	0.07	0.01	0.10	-	-	-
LAWC23	-	-	-	0.12	0.02	0.00	0.06	-	0.00	-	-	0.12	-	0.10	-	-	-
LAWC24	-	-	-	0.12	0.02	0.00	0.06	-	0.00	-	-	0.11	-	0.10	-	-	-
LAWC25	-	-	-	0.12	0.02	0.00	0.06	-	-	-	-	0.11	-	0.09	-	-	-
LAWC26	-	-	-	0.11	0.02	-	0.05	-	-	-	-	0.11	-	0.10	-	-	-
LAWC28	-	-	-	0.11	0.02	-	0.05	-	-	-	-	0.11	-	0.10	-	-	-

(a) A dash (-) denotes an empty data cell.

**Table 2.14. Target Values of Others Components in Remaining Actively Designed LAW Glasses (wt%) (continued).**

Glass ID	BaO	Br	CdO	Cl	Cr <sub>2</sub> O <sub>3</sub>	Cs <sub>2</sub> O	F	I	MnO	MoO <sub>3</sub>	NiO	P <sub>2</sub> O <sub>5</sub>	PbO	Re <sub>2</sub> O <sub>7</sub>	SeO <sub>2</sub>	SrO	Unknown
LAWC29	- <sup>(a)</sup>	-	-	0.11	0.02	-	0.05	-	-	-	-	0.11	-	0.10	-	-	-
LAWC30	-	-	-	0.11	0.02	-	0.05	-	-	-	-	0.11	-	0.10	-	-	-
LAWC31	-	-	-	0.11	0.02	-	0.05	-	-	-	-	0.11	-	0.10	-	-	-
LAWC31R1	-	-	-	0.11	0.02	-	0.05	-	-	-	-	0.11	-	0.10	-	-	-
LAWC33	-	-	-	0.11	0.02	-	0.05	-	-	-	-	0.11	-	0.10	-	-	-
TFA-BASE	-	-	-	0.28	-	-	0.01	-	-	-	-	0.06	-	0.09	-	-	-
A1-AN105R2	-	-	-	1.17	0.02	0.15	-	-	-	-	-	-	-	-	-	-	-
A2-AP101	-	-	-	0.42	0.02	0.15	0.35	-	-	-	-	0.08	-	-	-	-	-
A88AP101R1	-	-	-	0.13	0.02	-	0.23	-	-	-	-	0.07	-	0.10	-	-	-
A3-AN104	-	-	-	0.79	0.02	0.15	0.01	-	-	-	-	0.11	-	-	-	-	-
B1-AZ101	-	-	-	0.02	0.03	0.15	0.08	-	-	-	-	0.04	-	-	-	-	-
CI-AN107	-	-	-	0.07	0.01	0.15	0.28	-	-	-	0.03	0.13	0.02	-	-	-	-
C22AN107	-	-	-	0.08	0.02	-	0.14	-	-	-	-	0.12	-	0.10	-	-	-
C2-AN102C35	-	-	-	0.39	0.01	0.15	0.11	-	-	-	-	0.16	0.01	-	-	-	-
A88Si+15	-	-	-	0.14	0.02	-	0.25	-	-	-	-	0.08	-	0.11	-	-	-
A88Si-15	-	-	-	0.12	0.01	-	0.20	-	-	-	-	0.06	-	0.09	-	-	-
C22Si+15	-	-	-	0.09	0.02	-	0.16	-	-	-	0.03	0.13	0.02	0.11	-	-	-
C22Si-15	-	-	-	0.07	0.02	-	0.13	-	-	-	-	0.14	-	0.09	-	-	-
A1C1-1	-	-	-	0.91	0.02	0.15	0.09	-	-	-	0.01	0.03	-	-	-	-	-
A1C1-2	-	-	-	0.65	0.01	0.15	0.17	-	-	-	0.01	0.07	-	-	-	-	-
A1C1-3	-	-	-	0.39	0.01	0.15	0.25	-	-	-	0.02	0.10	-	-	-	-	-
A2B1-1	-	-	-	0.32	0.02	0.15	0.28	-	-	-	-	0.07	-	-	-	-	-
A2B1-2	-	-	-	0.22	0.03	0.15	0.22	-	-	-	-	0.06	-	-	-	-	-
A2B1-3	-	-	-	0.12	0.03	0.15	0.15	-	-	-	-	0.05	-	-	-	-	-
A3C2-1	-	-	-	0.69	0.02	0.15	0.03	-	-	-	-	0.12	-	-	-	-	-
A3C2-2	-	-	-	0.59	0.02	0.15	0.06	-	-	-	-	0.14	-	-	-	-	-
A3C2-3	-	-	-	0.49	0.01	0.15	0.09	-	-	-	-	0.15	0.01	-	-	-	-
12S-G-85C	-	-	-	0.08	0.02	0.16	0.14	0.10	-	-	0.03	0.12	0.02	-	-	-	0.01
12U-G-86A	-	-	0.10	0.56	0.02	0.14	0.02	0.10	-	-	0.01	0.07	-	-	0.10	-	-

(a) A dash (-) denotes an empty data cell.

**Table 2.14. Target Values of Others Components in Remaining Actively Designed LAW Glasses (wt%) (continued).**

Glass ID	BaO	Br	CdO	Cl	Cr <sub>2</sub> O <sub>3</sub>	Cs <sub>2</sub> O	F	I	MnO	MoO <sub>3</sub>	NiO	P <sub>2</sub> O <sub>5</sub>	PbO	Re <sub>2</sub> O <sub>7</sub>	SeO <sub>2</sub>	SrO	Unknown
A100CC	- (a)	-	-	0.33	0.02	-	0.03	-	-	-	-	0.13	-	-	-	-	-
C100GCC	-	-	-	0.12	0.02	-	0.06	-	-	-	0.02	0.12	-	-	-	-	-
GTSD-1126	-	-	-	0.01	0.03	-	0.02	-	-	-	-	0.01	-	-	-	-	-
GTSD-1437	-	-	-	0.39	0.01	-	0.11	-	-	-	0.02	0.16	0.01	-	-	-	-
PLTC35CCC	-	-	-	0.39	0.01	-	0.11	-	-	-	0.02	0.16	0.01	-	-	-	-
WVB-G-124B	-	-	-	0.33	0.02	0.16	0.03	0.10	-	-	-	0.13	-	-	-	-	-
WVF-G-21B	-	-	-	0.13	0.02	0.15	0.23	0.10	-	-	0.01	0.07	0.01	-	-	-	-
WVH-G-57B	-	-	-	0.11	0.02	0.15	0.05	0.10	-	-	0.01	0.10	-	-	-	-	-
WVJ-G-109D	-	-	-	0.01	0.04	0.15	0.06	0.10	-	-	-	0.04	-	-	-	-	-
WVM-G-142C	-	-	-	0.42	0.02	0.15	0.35	0.10	-	-	-	0.08	-	-	-	-	-
WVR-G-127A	-	-	-	0.79	0.02	0.15	0.00	0.10	-	-	-	0.11	-	-	-	-	-
LA44PNCC	-	-	-	0.57	0.07	-	0.22	-	-	-	-	0.35	-	-	-	-	-
LA44CCCR2	-	-	-	0.57	0.07	-	0.22	-	-	-	-	0.35	-	-	-	-	-
PNLA126CC	-	-	-	0.20	0.02	-	0.30	-	-	-	-	0.08	-	-	-	-	0.01
LA126CCC	-	-	-	0.20	0.02	-	0.30	-	-	-	-	0.08	-	-	-	-	0.01
LA137SRCCC	-	-	-	0.76	0.03	-	0.02	-	-	-	-	0.11	-	-	-	-	-
LB83PNCC	-	-	-	-	0.03	-	0.08	-	-	-	-	0.05	-	-	-	-	-
LB83CCC-1	-	-	-	-	0.03	-	0.08	-	-	-	-	0.05	-	-	-	-	-
LB88CCC	-	-	-	0.01	0.06	-	0.05	-	-	-	-	0.02	-	-	-	-	-
AZ-102 Surr SRNL	-	-	-	-	0.06	-	0.10	-	-	-	-	0.02	-	-	-	-	-
AN-102 Surr LC Melter	-	-	-	0.21	0.02	-	0.06	-	-	-	0.01	0.08	-	-	-	-	-

(a) A dash (-) denotes an empty data cell.

**Table 2.15. Target Compositions of Actual LAW Glasses.**

Glass ID	Al <sub>2</sub> O <sub>3</sub>	B <sub>2</sub> O <sub>3</sub>	CaO	Fe <sub>2</sub> O <sub>3</sub>	K <sub>2</sub> O	Li <sub>2</sub> O	MgO	Na <sub>2</sub> O	SO <sub>3</sub>	SiO <sub>2</sub>	TiO <sub>2</sub>	ZnO	ZrO <sub>2</sub>	Others <sup>(a)</sup>	Sum
AN-103 Actual	6.22	8.95	2.01	7.02	0.60	0.00	2.01	20.00	0.10	44.68	2.01	3.00	3.01	0.39	100
AW-101 Actual	6.08	9.71	1.99	5.54	2.58	0.00	1.48	20.00	0.21	44.05	1.99	2.95	2.99	0.42	100
AP-101 Actual	5.66	9.85	2.00	5.56	3.82	0.00	1.49	18.46	0.31	44.27	2.01	2.97	3.01	0.59	100
AZ-101 Actual	6.21	10.04	6.79	5.29	0.18	4.31	2.99	5.35	0.55	48.70	1.40	4.85	3.17	0.17	100
AZ-102 Actual	6.50	13.00	8.00	2.20	0.21	4.69	1.41	5.00	0.86	50.00	0.00	4.87	3.19	0.14	100
AZ-102 Actual CCC	6.50	13.00	8.00	2.20	0.21	4.69	1.41	5.00	0.86	50.00	0.00	4.87	3.19	0.14	100
AN-107 Actual (LAWC15)	6.23	8.94	2.01	7.02	0.14	0.00	2.01	20.00	0.13	44.78	2.00	2.99	3.01	0.72	100
AN-102 Actual LC Melter	6.15	10.10	6.43	6.50	0.07	2.75	1.52	11.80	0.32	46.80	1.13	3.04	3.04	0.35	100
AN-102 Actual	6.15	10.13	6.42	6.49	0.09	2.74	1.52	11.80	0.36	46.75	1.13	3.03	3.03	0.36	100

(a) See Table 2.16 for the compositions of the Others component.

**Table 2.16. Target Values of Others Components in Actual LAW Glasses.**

Glass ID	BaO	Br	CdO	Cl	Cr <sub>2</sub> O <sub>3</sub>	Cs <sub>2</sub> O	F	MoO <sub>3</sub>	NiO	P <sub>2</sub> O <sub>5</sub>	PbO	SrO
AN-103 Actual	-(a)	-	-	0.31	0.01	-	0.02	-	-	0.05	-	-
AW-101 Actual	-	-	-	0.08	0.01	0.00	-	-	-	0.07	-	-
AP-101 Actual	-	-	-	0.17	0.03	-	0.27	-	-	0.09	-	-
AZ-101 Actual	-	-	-	-	0.03	-	0.08	-	-	0.05	-	-
AZ-102 Actual	-	-	-	0.01	0.06	-	0.05	-	-	0.02	-	-
AZ-102 Actual CCC	-	-	-	0.01	0.06	-	0.05	-	-	0.02	-	-
AN-107 Actual (LAWC15)	0.02	0.08	0.00	0.08	0.00	-	0.47	0.00	0.04	0.02	0.00	0.00
AN-102 Actual LC Melter	-	-	-	0.09	0.02	-	0.05	-	0.01	0.08	-	-
AN-102 Actual	-	-	-	0.12	0.02	-	0.06	-	0.01	0.13	-	-

(a) A dash (-) denotes an empty data cell.



**Table 2.17. Groups and Numbers of LAW Glasses with Property Data.**

<b>Group of LAW Glasses</b>	<b>Group ID</b>	<b>Number of LAW Glasses</b>	<b>Statistically or Actively Designed</b>
Existing	ExPh1	23	Actively
Phase 1	Ph1	56	Statistically
Phase 1 Augmentation	Ph1aAug	20	Statistically
Correlation & High Cr <sub>2</sub> O <sub>3</sub> Correlation	Corr	21	Actively
High Cr <sub>2</sub> O <sub>3</sub> & P <sub>2</sub> O <sub>5</sub>	HiCrP	7	Actively
Actively Designed	ActDes	135	Actively
Actual Waste	Actual	7	Actively
<b>Total</b>		<b>271</b>	

**Table 3.1. Glass IDs, Target SO<sub>3</sub> Values, and Estimates of Analyzed SO<sub>3</sub> Values for LAW Glasses Not Having SO<sub>3</sub> Analyses**

<b>Glass ID</b>	<b>Target SO<sub>3</sub> (wt%)</b>	<b>Estimate of Analyzed SO<sub>3</sub> (wt%)<sup>(a)</sup></b>
LAWA41	0.10	0.10
LAWA42	0.10	0.10
LAWA43-1	0.10	0.10
LAWA45	0.10	0.10
LAWA50	0.10	0.10
LAWA81	0.10	0.10
LAWA82	0.10	0.10
LAWA83	0.10	0.10
LAWA84	0.10	0.10
LAWA87	0.21	0.19
LAWA88	0.21	0.19
LAWA89	0.21	0.19
LAWA90	0.21	0.19
LAWA93	0.10	0.10
LAWA96	0.10	0.10
LAWB30	0.20	0.18
LAWC12	0.20	0.18
LAWC22	0.32	0.29
LAWC23	0.44	0.35
LAWC24	0.42	0.34

(a) Estimates with target values  $\leq 0.25$  wt% were predicted using the regression model in Equation (3.2), while estimates with target values between 0.25 wt% and 0.50 wt% were predicted using the regression model in Equation (3.3).

**Table 3.2. Normalized Compositions (wt%) of 271 LAW Simulated and Actual Waste Glasses with XRF Analyzed or Estimated Values of SO<sub>3</sub> and Target Values of the Remaining Components.**

Glass ID	Al <sub>2</sub> O <sub>3</sub>	B <sub>2</sub> O <sub>3</sub>	CaO	Cl	Cr <sub>2</sub> O <sub>3</sub>	F	Fe <sub>2</sub> O <sub>3</sub>	K <sub>2</sub> O	Li <sub>2</sub> O	MgO	Na <sub>2</sub> O	P <sub>2</sub> O <sub>5</sub>	SO <sub>3</sub> <sup>(a)</sup>	SiO <sub>2</sub>	TiO <sub>2</sub>	ZnO	ZrO <sub>2</sub>	Others	Sum
LAWA44R10	6.202	8.903	1.991	0.650	0.020	0.010	6.982	0.500	0.000	1.991	20.006	0.030	0.090	44.563	1.991	2.971	2.991	0.110	100.000
LAWA53	6.145	6.165	7.840	0.646	0.020	0.010	7.467	0.494	0.000	1.473	19.898	0.030	0.620	42.036	1.100	2.977	2.977	0.101	100.000
LAWA56	6.151	12.050	1.970	0.646	0.020	0.010	7.474	0.495	0.000	1.475	19.918	0.030	0.520	42.079	1.101	2.980	2.980	0.101	100.000
LAWA88	6.082	9.700	1.992	0.329	0.009	0.000	5.533	2.583	0.000	1.475	20.005	0.070	<b>0.190*</b>	44.002	1.992	2.951	2.988	0.100	100.000
LAWA88R1	6.082	9.700	1.991	0.330	0.010	0.000	5.532	2.581	0.000	1.475	20.006	0.070	0.190	44.004	1.991	2.951	2.987	0.100	100.000
LAWA102R1	6.040	9.968	5.044	0.329	0.020	0.030	5.383	0.259	2.492	1.485	14.503	0.130	0.670	46.350	1.136	3.050	3.010	0.101	100.000
LAWA126	5.637	9.815	1.989	0.200	0.020	0.300	5.537	3.878	0.000	1.479	18.451	0.080	0.310	44.098	1.999	2.959	2.989	0.260	100.000
LAWA128	6.027	7.066	2.079	0.200	0.020	0.300	5.787	3.878	0.000	1.179	18.451	0.080	0.300	46.067	2.089	3.088	3.128	0.260	100.000
LAWA128R1	6.026	7.065	2.079	0.200	0.020	0.300	5.786	3.877	0.000	1.179	18.447	0.080	0.320	46.058	2.089	3.088	3.128	0.260	100.000
LAWA130	6.025	8.943	2.078	0.200	0.020	0.300	2.858	3.877	0.000	1.179	18.445	0.080	0.330	46.053	2.088	4.137	3.127	0.260	100.000
LAWB65	6.188	9.939	6.690	0.000	0.100	0.070	5.295	0.261	4.303	2.969	5.476	0.010	0.890	48.492	1.394	4.664	3.159	0.100	100.000
LAWB66	6.203	9.963	8.214	0.000	0.101	0.070	5.308	0.261	4.313	2.976	5.489	0.010	0.650	48.609	1.397	3.167	3.167	0.101	100.000
LAWB68	6.192	8.440	8.199	0.000	0.100	0.070	5.299	0.261	4.305	2.970	5.479	0.010	0.830	48.521	1.395	4.666	3.161	0.100	100.000
LAWB78	6.161	12.351	7.132	0.010	0.050	0.080	3.256	0.230	3.055	2.975	9.797	0.050	0.510	47.080	0.000	4.007	3.155	0.100	100.000
LAWB79	6.156	12.342	7.127	0.010	0.050	0.080	3.253	0.230	3.514	2.973	8.629	0.050	0.580	47.748	0.000	4.004	3.153	0.100	100.000
LAWB80	6.156	12.341	7.126	0.010	0.050	0.080	3.253	1.992	3.513	2.973	6.626	0.050	0.580	47.993	0.000	4.004	3.153	0.100	100.000
LAWB83	6.183	10.035	6.783	0.010	0.040	0.060	5.293	0.190	4.312	2.971	5.473	0.040	0.490	48.624	1.391	4.842	3.162	0.100	100.000
LAWB84	6.187	10.041	6.687	0.010	0.040	0.060	5.296	0.190	4.405	2.973	5.476	0.040	0.440	48.654	1.392	4.845	3.163	0.100	100.000
LAWB85	6.184	11.527	5.283	0.010	0.040	0.060	5.293	0.190	4.313	2.972	5.473	0.040	0.490	48.629	1.391	4.843	3.162	0.100	100.000
LAWB86	6.188	12.426	5.737	0.010	0.040	0.060	5.297	0.190	4.356	2.974	5.477	0.040	0.430	48.664	0.000	4.846	3.164	0.100	100.000
C100-G-136B	6.127	10.092	6.408	0.120	0.020	0.060	6.478	0.150	2.733	1.512	11.874	0.120	0.400	46.726	1.121	3.014	3.024	0.020	100.000
LAWC27	6.117	12.183	8.544	0.111	0.018	0.054	0.009	0.136	2.733	1.500	11.953	0.106	0.410	48.868	1.121	3.018	3.018	0.101	100.000
LAWC32	6.490	10.047	9.038	0.111	0.018	0.054	2.424	0.136	2.734	1.501	11.956	0.106	0.380	46.744	1.121	4.019	3.019	0.101	100.000
LAWM1	9.044	6.029	10.048	0.020	0.008	0.008	8.039	4.019	4.522	0.000	5.024	0.013	0.520	44.666	3.015	5.024	0.000	0.002	100.000
LAWM2	3.512	6.020	10.033	0.803	0.322	0.300	8.027	0.000	4.515	5.017	5.017	0.501	0.670	47.157	3.010	5.017	0.000	0.080	100.000
LAWM3	9.033	6.022	10.036	0.020	0.008	0.008	8.029	0.000	4.487	5.018	11.521	0.013	0.640	40.145	0.000	1.004	4.015	0.002	100.000
LAWM4	3.516	13.058	10.044	0.020	0.008	0.008	5.560	4.018	4.520	0.000	5.022	0.013	0.560	41.599	3.013	5.022	4.018	0.002	100.000
LAWM5	9.041	6.027	5.794	0.020	0.008	0.008	8.036	4.018	4.520	0.000	5.023	0.013	0.550	48.903	3.014	1.005	4.018	0.002	100.000
LAWM6	9.002	10.612	10.002	0.020	0.008	0.007	8.002	4.001	0.000	5.001	8.999	0.012	0.320	40.009	3.001	1.000	0.000	0.002	100.000
LAWM7	5.441	6.966	10.028	0.020	0.008	0.008	8.023	0.000	2.585	5.014	5.014	0.013	0.720	52.147	3.008	1.003	0.000	0.002	100.000

(a) SO<sub>3</sub> values that were interpolated are in boldface and marked with an asterisk – all others were measured by XRF.

**Table 3.2. Normalized Compositions (wt%) of 271 LAW Simulated and Actual Waste Glasses with XRF Analyzed or Estimated Values of SO<sub>3</sub> and Target Values of Remaining Components (continued).**

Glass ID	Al <sub>2</sub> O <sub>3</sub>	B <sub>2</sub> O <sub>3</sub>	CaO	Cl	Cr <sub>2</sub> O <sub>3</sub>	F	Fe <sub>2</sub> O <sub>3</sub>	K <sub>2</sub> O	Li <sub>2</sub> O	MgO	Na <sub>2</sub> O	P <sub>2</sub> O <sub>5</sub>	SO <sub>3</sub> <sup>(a)</sup>	SiO <sub>2</sub>	TiO <sub>2</sub>	ZnO	ZrO <sub>2</sub>	Others	Sum
LAWM8	9.027	13.039	6.448	0.803	0.322	0.300	0.000	0.000	2.087	5.015	5.015	0.501	0.700	44.626	3.009	5.015	4.012	0.080	100.000
LAWM9	3.506	6.010	10.016	0.801	0.322	0.300	8.013	4.006	2.392	0.000	5.008	0.500	0.240	49.792	0.000	5.008	4.006	0.080	100.000
LAWM10	9.005	13.007	10.006	0.801	0.322	0.300	0.000	0.000	4.503	0.000	13.074	0.499	0.230	40.170	3.002	1.001	4.002	0.080	100.000
LAWM11	3.504	13.013	9.413	0.020	0.008	0.007	5.317	4.004	4.505	0.000	11.491	0.012	0.900	46.804	0.000	1.001	0.000	0.002	100.000
LAWM12	3.501	13.005	0.000	0.801	0.322	0.300	2.310	4.002	4.502	1.971	14.259	0.499	0.230	42.215	3.001	5.002	4.002	0.080	100.000
LAWM13	3.501	6.001	10.002	0.412	0.165	0.154	8.002	3.785	0.000	0.000	22.005	0.257	0.500	40.009	3.001	2.164	0.000	0.041	100.000
LAWM14	3.500	6.000	2.045	0.020	0.008	0.007	0.000	0.000	0.881	5.000	21.999	0.012	0.530	51.997	3.000	5.000	0.000	0.002	100.000
LAWM15	8.999	9.356	0.000	0.800	0.321	0.299	6.283	0.000	0.000	3.724	21.998	0.499	0.170	43.471	3.000	1.000	0.000	0.080	100.000
LAWM16	8.006	12.008	8.006	0.020	0.008	0.007	6.505	0.100	3.002	1.001	10.007	0.012	0.330	42.480	2.502	5.004	1.001	0.002	100.000
LAWM17	5.002	12.004	2.215	0.020	0.008	0.007	6.502	2.001	0.500	3.501	17.006	0.012	0.200	42.015	0.500	5.002	3.501	0.002	100.000
LAWM18	8.005	12.007	8.005	0.801	0.322	0.300	6.504	0.100	3.002	1.001	10.006	0.499	0.340	42.025	2.502	2.001	2.501	0.080	100.000
LAWM19	7.997	11.996	7.997	0.800	0.321	0.299	1.999	1.999	0.500	1.000	13.170	0.499	0.360	41.986	0.500	4.998	3.499	0.080	100.000
LAWM20	5.001	7.002	8.002	0.800	0.321	0.299	2.001	2.001	2.265	3.501	17.004	0.499	0.210	42.011	0.500	5.001	3.501	0.080	100.000
LAWM21	5.005	10.901	8.008	0.020	0.008	0.007	6.507	2.002	3.003	1.001	10.010	0.012	0.460	42.042	2.503	5.005	3.504	0.002	100.000
LAWM22	7.990	6.992	1.998	0.799	0.321	0.299	6.492	1.998	0.499	3.496	16.979	0.498	0.450	41.949	0.670	4.994	3.496	0.080	100.000
LAWM23	5.011	7.015	8.018	0.802	0.322	0.300	2.004	2.004	3.007	1.002	10.022	0.500	0.340	48.547	2.506	5.011	3.508	0.080	100.000
LAWM24	8.000	12.001	2.000	0.020	0.008	0.007	6.500	2.000	0.641	1.000	17.001	0.012	0.230	47.076	0.500	2.000	1.000	0.002	100.000
LAWM25R1	8.011	12.017	2.003	0.801	0.322	0.300	3.684	2.003	3.004	3.505	10.014	0.500	0.260	49.991	0.501	2.003	1.001	0.080	100.000
LAWM26	8.006	12.008	4.970	0.801	0.322	0.300	2.001	0.100	3.002	1.001	10.007	0.499	0.490	49.909	0.500	5.004	1.001	0.080	100.000
LAWM27	8.006	7.005	8.006	0.801	0.322	0.300	6.505	2.001	0.500	3.502	13.381	0.499	0.250	42.030	2.502	3.309	1.001	0.080	100.000
LAWM28	5.010	12.024	8.016	0.020	0.008	0.008	6.513	0.703	0.690	1.002	10.020	0.013	0.360	50.101	2.505	2.004	1.002	0.002	100.000
LAWM29	7.565	7.006	2.002	0.077	0.031	0.029	6.506	2.002	3.003	3.503	10.009	0.048	0.310	46.892	2.502	5.005	3.503	0.008	100.000
LAWM30	8.003	12.004	2.001	0.020	0.008	0.007	6.502	0.100	2.023	1.000	17.006	0.012	0.200	42.015	0.592	5.002	3.501	0.002	100.000
LAWM31	5.002	7.003	8.003	0.801	0.322	0.300	6.502	0.100	3.001	1.000	16.758	0.499	0.300	42.327	2.501	2.001	3.501	0.080	100.000
LAWM32	5.146	7.002	2.001	0.800	0.321	0.299	2.001	2.001	3.001	3.501	16.514	0.499	0.320	50.013	0.500	5.001	1.000	0.080	100.000
LAWM33R1	5.002	12.005	8.003	0.020	0.008	0.007	6.503	1.722	0.899	1.000	17.007	0.012	0.290	42.017	2.501	2.001	1.000	0.002	100.000
LAWM34	5.001	8.356	8.002	0.020	0.008	0.007	6.295	2.001	3.001	1.000	17.005	0.012	0.300	42.012	1.474	2.001	3.501	0.002	100.000
LAWM35	5.003	12.007	6.182	0.801	0.322	0.300	4.413	0.100	0.500	3.502	17.010	0.499	0.180	42.023	2.501	2.001	2.576	0.080	100.000
LAWM36	7.002	11.004	7.002	0.318	0.128	0.119	5.002	0.300	2.501	1.501	12.004	0.198	0.370	45.016	2.001	3.501	2.001	0.032	100.000
LAWM37	6.751	11.009	7.006	0.020	0.008	0.007	5.004	0.300	2.502	2.502	12.010	0.012	0.320	45.038	1.001	3.503	3.003	0.002	100.000

(a) SO<sub>3</sub> values that were interpolated are in boldface and marked with an asterisk – all others were measured by XRF.

**Table 3.2. Normalized Compositions (wt%) of 271 LAW Simulated and Actual Waste Glasses with XRF Analyzed or Estimated Values of SO<sub>3</sub> and Target Values of Remaining Components (continued).**

Glass ID	Al <sub>2</sub> O <sub>3</sub>	B <sub>2</sub> O <sub>3</sub>	CaO	Cl	Cr <sub>2</sub> O <sub>3</sub>	F	Fe <sub>2</sub> O <sub>3</sub>	K <sub>2</sub> O	Li <sub>2</sub> O	MgO	Na <sub>2</sub> O	P <sub>2</sub> O <sub>5</sub>	SO <sub>3</sub> <sup>(a)</sup>	SiO <sub>2</sub>	TiO <sub>2</sub>	ZnO	ZrO <sub>2</sub>	Others	Sum
LAWM38	6.998	7.998	6.998	0.800	0.321	0.299	2.999	0.154	2.499	1.500	13.997	0.499	0.370	47.988	1.000	3.499	2.000	0.080	100.000
LAWM39	7.007	9.063	5.005	0.801	0.322	0.300	3.003	0.100	2.502	2.502	14.013	0.499	0.250	48.046	1.001	3.503	2.002	0.080	100.000
LAWM40	6.003	11.006	5.003	0.214	0.086	0.080	5.003	0.100	1.001	1.501	14.008	0.133	0.310	48.027	1.001	3.502	3.002	0.021	100.000
LAWM41	7.002	8.002	7.002	0.800	0.321	0.299	5.001	0.300	1.000	2.501	14.004	0.499	0.340	45.012	1.000	4.601	2.235	0.080	100.000
LAWM42	6.004	8.005	5.003	0.801	0.322	0.300	4.037	0.100	2.502	1.501	14.009	0.499	0.300	48.032	2.001	3.502	3.002	0.080	100.000
LAWM43	7.002	8.678	5.002	0.800	0.322	0.300	5.002	0.300	2.501	2.501	12.004	0.499	0.390	45.016	2.001	4.602	3.001	0.080	100.000
LAWM44	6.325	10.039	7.008	0.020	0.008	0.007	5.006	0.100	1.001	1.502	12.014	0.012	0.290	48.055	2.002	4.605	2.002	0.002	100.000
LAWM45	7.003	8.003	5.784	0.020	0.008	0.007	5.002	0.300	1.423	1.501	14.005	0.012	0.310	48.017	2.001	4.602	2.001	0.002	100.000
LAWM46	6.012	11.023	6.523	0.020	0.008	0.008	5.010	0.100	1.002	2.505	12.025	0.013	0.200	48.034	1.002	3.507	3.006	0.002	100.000
LAWM47	6.200	8.003	7.003	0.020	0.008	0.007	5.002	0.100	1.000	2.501	14.005	0.012	0.310	48.017	1.307	3.501	3.001	0.002	100.000
LAWM48	6.234	11.016	5.277	0.801	0.322	0.300	5.007	0.100	1.001	1.502	12.017	0.500	0.260	48.070	2.003	3.505	2.003	0.080	100.000
LAWM49	7.001	10.906	5.001	0.800	0.321	0.299	3.000	0.100	1.000	1.500	14.002	0.499	0.350	47.538	1.000	4.601	2.000	0.080	100.000
LAWM50	6.530	9.700	6.109	0.446	0.179	0.167	4.111	0.204	1.668	2.032	13.095	0.278	0.290	46.982	1.528	4.104	2.533	0.045	100.000
LAWM51	6.528	9.697	6.107	0.446	0.179	0.167	4.110	0.204	1.667	2.031	13.091	0.278	0.320	46.968	1.528	4.102	2.533	0.045	100.000
LAWM52	6.088	9.711	1.994	0.329	0.009	0.000	5.538	2.586	0.000	1.477	20.027	0.070	0.180	44.051	1.994	2.954	2.991	0.000	100.000
LAWM53	9.031	6.021	10.034	0.020	0.008	0.008	8.027	4.014	4.515	0.000	5.017	0.013	0.660	44.603	3.010	5.017	0.000	0.002	100.000
LAWM54R1	3.505	6.008	10.014	0.801	0.322	0.300	8.011	4.006	2.391	0.000	5.007	0.500	0.260	49.782	0.000	5.007	4.006	0.080	100.000
LAWM55	3.501	13.004	0.000	0.800	0.321	0.299	2.310	4.001	4.501	1.971	14.257	0.499	0.240	42.211	3.001	5.001	4.001	0.080	100.000
LAWM56	4.990	11.975	6.166	0.799	0.321	0.299	4.402	0.100	0.499	3.493	16.965	0.498	0.440	41.914	2.495	1.996	2.570	0.080	100.000
LAWM57	6.997	11.000	3.000	0.196	0.078	0.078	4.659	3.801	0.000	1.440	20.620	0.122	0.320	39.274	1.370	3.026	4.001	0.016	100.000
LAWM58	7.002	9.294	1.028	0.196	0.078	0.078	6.500	3.800	0.000	1.440	20.536	0.122	0.320	41.654	1.370	2.563	4.001	0.016	100.000
LAWM59	6.847	9.009	2.965	0.196	0.078	0.078	6.492	2.004	0.000	1.441	20.008	0.122	0.310	44.558	1.371	2.506	2.001	0.016	100.000
LAWM60	5.003	11.006	1.714	0.196	0.078	0.078	4.503	2.004	0.000	1.441	20.015	0.122	0.300	45.351	1.371	2.804	3.998	0.016	100.000
LAWM61	5.002	11.001	1.001	0.196	0.078	0.078	4.502	3.293	0.000	1.440	20.004	0.122	0.330	45.060	1.370	4.501	2.005	0.016	100.000
LAWM62	5.004	9.004	1.002	0.196	0.078	0.078	6.500	3.380	0.000	1.440	20.006	0.122	0.320	44.341	1.370	3.842	3.300	0.016	100.000
LAWM63	7.001	9.402	1.044	0.196	0.078	0.078	4.695	2.059	0.000	1.440	22.998	0.122	0.340	42.601	1.370	4.500	2.058	0.016	100.000
LAWM64	6.991	10.989	3.002	0.196	0.078	0.078	6.503	2.001	0.000	1.441	20.051	0.122	0.300	38.379	1.371	4.490	3.993	0.016	100.000
LAWM65	5.001	9.001	2.964	0.196	0.078	0.078	4.503	2.001	0.000	1.440	22.791	0.122	0.340	43.599	1.370	2.501	3.997	0.016	100.000
LAWM66	7.587	10.637	1.003	0.196	0.078	0.078	6.315	0.479	0.000	1.440	22.996	0.122	0.320	38.362	1.370	4.500	4.498	0.016	100.000
LAWM67	8.002	10.601	1.545	0.196	0.078	0.078	4.603	5.402	0.000	1.440	20.134	0.122	0.320	38.370	1.370	2.720	5.001	0.016	100.000

(a) SO<sub>3</sub> values that were interpolated are in boldface and marked with an asterisk – all others were measured by XRF.

**Table 3.2. Normalized Compositions (wt%) of 271 LAW Simulated and Actual Waste Glasses with XRF Analyzed or Estimated Values of SO<sub>3</sub> and Target Values of Remaining Components (continued).**

Glass ID	Al <sub>2</sub> O <sub>3</sub>	B <sub>2</sub> O <sub>3</sub>	CaO	Cl	Cr <sub>2</sub> O <sub>3</sub>	F	Fe <sub>2</sub> O <sub>3</sub>	K <sub>2</sub> O	Li <sub>2</sub> O	MgO	Na <sub>2</sub> O	P <sub>2</sub> O <sub>5</sub>	SO <sub>3</sub> <sup>(a)</sup>	SiO <sub>2</sub>	TiO <sub>2</sub>	ZnO	ZrO <sub>2</sub>	Others	Sum
LAWM68	5.003	9.002	2.999	0.196	0.078	0.078	6.500	4.803	0.000	1.440	20.009	0.122	0.330	40.815	1.370	3.562	3.677	0.016	100.000
LAWM69	7.976	10.990	2.997	0.196	0.078	0.078	6.370	1.829	0.000	1.440	20.095	0.122	0.340	39.601	1.370	4.499	2.002	0.016	100.000
LAWM70	5.002	9.397	1.047	0.196	0.078	0.078	6.498	4.550	0.000	1.440	20.011	0.122	0.330	45.357	1.370	2.501	2.006	0.016	100.000
LAWM71	5.006	9.001	1.003	0.196	0.078	0.078	4.501	5.401	0.000	1.440	20.004	0.122	0.340	44.943	1.370	4.498	2.002	0.016	100.000
LAWM72	8.002	11.002	2.937	0.196	0.078	0.078	6.449	4.177	0.000	1.440	20.042	0.122	0.320	39.173	1.370	2.501	2.095	0.016	100.000
LAWM73	8.002	9.006	2.996	0.196	0.078	0.078	4.878	1.221	0.000	1.440	23.002	0.122	0.320	40.391	1.370	4.494	2.388	0.016	100.000
LAWM74	7.589	9.009	1.001	0.196	0.078	0.078	4.504	0.000	0.000	1.441	21.329	0.122	0.290	45.377	1.371	2.598	5.002	0.016	100.000
LAWM75	8.003	9.157	2.996	0.196	0.078	0.078	6.497	1.082	0.000	1.441	20.691	0.122	0.310	38.461	1.371	4.500	5.001	0.016	100.000
LAWM76	6.403	9.926	1.923	0.196	0.078	0.078	5.424	2.599	0.000	1.441	21.409	0.122	0.310	41.881	1.371	3.423	3.401	0.016	100.000
LAWE2H	5.951	9.751	1.970	0.196	0.078	0.078	5.365	3.790	0.000	1.440	20.782	0.122	0.310	42.440	1.370	3.410	2.930	0.016	100.000
LAWE3	6.102	10.003	2.021	0.200	0.080	0.080	5.502	4.992	0.000	1.480	18.215	0.124	0.320	42.963	1.400	3.501	3.001	0.016	100.000
LAWE3H	5.942	9.743	1.971	0.196	0.078	0.078	5.366	5.412	0.000	1.440	19.746	0.122	0.340	41.859	1.360	3.411	2.921	0.016	100.000
LAWE4	6.107	10.012	2.523	0.200	0.080	0.080	5.507	0.501	0.000	1.482	19.664	0.124	0.260	45.535	1.402	3.504	3.004	0.016	100.000
LAWE4H	5.974	9.796	2.461	0.196	0.078	0.078	5.383	0.540	0.000	1.451	21.283	0.122	0.350	44.527	1.371	3.432	2.942	0.016	100.000
LAWE5	6.106	10.009	3.683	0.200	0.080	0.080	5.505	0.500	0.510	1.481	17.536	0.124	0.340	45.921	1.401	3.503	3.003	0.016	100.000
LAWE5H	5.997	9.821	3.614	0.196	0.078	0.078	5.410	0.541	0.491	1.452	18.991	0.122	0.350	45.096	1.372	3.434	2.943	0.016	100.000
LAWE7	6.110	10.017	6.401	0.200	0.080	0.080	5.509	0.501	3.226	1.513	12.521	0.124	0.380	45.407	1.402	3.506	3.005	0.016	100.000
LAWE7H	6.027	9.882	6.318	0.196	0.078	0.078	5.441	0.541	3.174	1.492	13.546	0.122	0.470	44.810	1.382	3.464	2.964	0.016	100.000
LAWE9H	6.066	9.946	6.878	0.197	0.079	0.079	5.468	0.541	4.091	2.366	8.953	0.122	0.430	46.919	1.394	3.479	2.978	0.016	100.000
LAWE10H	6.086	9.976	6.978	0.197	0.079	0.079	5.498	0.541	4.271	2.948	5.735	0.122	0.540	49.054	1.394	3.489	2.998	0.016	100.000
LAWE11	6.106	10.010	2.322	0.200	0.080	0.080	5.506	4.755	0.000	1.481	17.377	0.124	0.250	43.784	1.401	3.504	3.003	0.016	100.000
LAWE12	6.952	8.753	1.971	0.196	0.078	0.078	4.361	5.412	0.000	1.440	19.746	0.122	0.320	41.853	1.370	3.411	3.921	0.016	100.000
LAWE13	6.952	9.753	1.971	0.196	0.078	0.078	5.362	5.412	0.000	0.440	19.746	0.122	0.320	41.853	0.370	3.411	3.921	0.016	100.000
LAWE14	4.942	9.754	1.471	0.196	0.078	0.078	5.366	5.412	0.000	0.440	19.748	0.122	0.310	43.363	1.371	3.411	3.922	0.016	100.000
LAWE15	5.942	8.754	1.471	0.196	0.078	0.078	5.366	5.412	0.000	0.940	19.748	0.122	0.310	42.863	1.371	3.411	3.922	0.016	100.000
LAWE16	5.934	8.241	1.468	0.196	0.078	0.078	5.358	5.404	0.000	0.939	19.719	0.122	0.460	42.798	1.369	3.406	4.415	0.016	100.000
LAWE3Cr2CCC	6.103	10.005	2.021	0.200	1.401	0.080	5.503	4.992	0.000	1.481	18.219	0.124	0.300	41.651	1.401	3.502	3.002	0.016	100.000
LAWE9HCr1CCC	6.059	9.934	6.870	0.196	0.601	0.079	5.462	0.541	4.086	2.363	8.943	0.122	0.551	46.339	1.392	3.475	2.974	0.016	100.000
LAWE9HCr2CCC	6.060	9.937	6.872	0.196	0.451	0.079	5.463	0.541	4.087	2.364	8.945	0.122	0.521	46.503	1.392	3.476	2.975	0.016	100.000
LAWE10HCr3CCC	6.081	9.968	6.973	0.196	0.351	0.079	5.494	0.541	4.268	2.945	5.730	0.122	0.621	48.742	1.393	3.486	2.995	0.016	100.000

(a) SO<sub>3</sub> values that were interpolated are in boldface and marked with an asterisk – all others were measured by XRF.

**Table 3.2. Normalized Compositions (wt%) of 271 LAW Simulated and Actual Waste Glasses with XRF Analyzed or Estimated Values of SO<sub>3</sub> and Target Values of Remaining Components (continued).**

Glass ID	Al <sub>2</sub> O <sub>3</sub>	B <sub>2</sub> O <sub>3</sub>	CaO	Cl	Cr <sub>2</sub> O <sub>3</sub>	F	Fe <sub>2</sub> O <sub>3</sub>	K <sub>2</sub> O	Li <sub>2</sub> O	MgO	Na <sub>2</sub> O	P <sub>2</sub> O <sub>5</sub>	SO <sub>3</sub> <sup>(a)</sup>	SiO <sub>2</sub>	TiO <sub>2</sub>	ZnO	ZrO <sub>2</sub>	Others	Sum
LAWCrPIR	6.101	10.002	2.761	0.124	0.328	0.112	5.501	0.125	0.000	1.480	19.347	1.442	0.370	44.401	1.400	3.501	3.001	0.004	100.000
LAWCrP2R	6.099	9.998	2.105	0.193	0.591	0.103	5.499	0.275	0.000	1.480	20.996	1.333	0.360	43.065	1.400	3.499	2.999	0.006	100.000
LAWCrP3R	6.101	10.001	2.761	0.124	0.328	0.111	5.500	0.125	0.000	1.480	19.345	2.380	0.380	43.458	1.400	3.500	3.000	0.004	100.000
LAWCrP4R	6.098	9.997	2.104	0.192	0.591	0.103	5.498	0.275	0.000	1.480	20.994	2.379	0.370	42.014	1.400	3.499	2.999	0.006	100.000
LAWCrP5	6.108	10.013	5.813	0.136	0.591	0.067	5.507	0.087	2.642	1.488	14.395	1.335	0.380	43.505	1.402	3.504	3.004	0.021	100.000
LAWCrP6	6.104	10.007	6.945	0.136	0.630	0.067	5.504	0.087	4.173	2.552	8.006	2.512	0.580	44.770	1.401	3.502	3.002	0.021	100.000
LAWCrP7	6.104	10.007	6.985	0.136	0.630	0.067	5.504	0.087	4.303	2.932	5.404	2.512	0.660	46.741	1.401	3.502	3.002	0.021	100.000
LAWA41	6.203	7.501	2.000	0.580	0.017	0.040	6.983	3.101	0.000	1.995	20.002	0.078	<b>0.100*</b>	43.414	1.995	2.993	2.995	0.004	100.000
LAWA42	6.204	9.034	2.404	0.579	0.017	0.036	8.411	3.101	0.001	2.402	20.004	0.078	<b>0.100*</b>	38.007	2.403	3.605	3.607	0.005	100.000
LAWA43-1	12.002	7.391	1.967	0.579	0.017	0.036	6.881	3.101	0.001	1.965	20.004	0.078	<b>0.100*</b>	38.007	1.966	2.949	2.951	0.005	100.000
LAWA44	6.202	8.903	1.991	0.650	0.020	0.010	6.982	0.500	0.000	1.991	20.006	0.030	0.100	44.563	1.991	2.971	2.991	0.100	100.000
LAWA45	6.201	11.901	0.000	0.652	0.020	0.010	6.980	0.501	0.000	1.477	20.000	0.034	<b>0.100*</b>	44.552	1.994	2.477	2.992	0.111	100.000
LAWA49	6.203	8.904	0.000	0.652	0.020	0.010	9.982	0.501	0.000	1.478	20.005	0.034	0.070	44.565	1.995	2.478	2.992	0.112	100.000
LAWA50	6.201	8.902	0.000	0.652	0.020	0.010	11.981	0.501	0.000	1.477	20.000	0.034	<b>0.100*</b>	42.550	1.994	2.477	2.992	0.111	100.000
LAWA51	6.203	11.976	0.000	0.587	0.018	0.009	6.998	0.451	0.000	1.484	18.003	0.030	0.070	46.579	1.996	2.488	2.998	0.111	100.000
LAWA52	6.179	6.191	7.882	0.652	0.020	0.010	7.505	0.501	0.000	1.477	19.999	0.034	0.100	42.247	1.108	2.994	2.992	0.112	100.000
LAWA60	8.528	11.228	4.321	0.652	0.020	0.010	0.000	0.501	0.000	1.994	19.999	0.034	0.100	44.551	1.994	2.965	2.992	0.112	100.000
LAWA65	6.155	6.167	3.289	0.649	0.020	0.010	7.476	0.499	0.000	6.034	19.924	0.034	0.480	42.087	1.104	2.983	2.980	0.109	100.000
LAWA76	6.132	10.916	7.822	0.647	0.019	0.010	7.448	0.497	4.985	1.466	10.098	0.033	0.860	41.919	1.100	2.971	2.969	0.108	100.000
LAWA81	6.201	8.902	3.989	0.652	0.020	0.010	6.980	0.501	0.000	1.994	20.000	0.034	<b>0.100*</b>	44.552	0.000	2.965	2.992	0.111	100.000
LAWA82	6.201	8.902	0.000	0.652	0.020	0.010	6.980	0.501	0.000	1.994	20.000	0.034	<b>0.100*</b>	44.552	3.989	2.965	2.992	0.111	100.000
LAWA83	6.201	8.902	1.994	0.652	0.020	0.010	4.986	0.501	0.000	1.994	20.000	2.028	<b>0.100*</b>	44.552	1.994	2.965	2.992	0.111	100.000
LAWA84	6.201	8.902	1.994	0.652	0.020	0.010	2.992	0.501	0.000	1.994	20.000	4.023	<b>0.100*</b>	44.552	1.994	2.965	2.992	0.111	100.000
LAWA87	4.481	8.874	1.992	0.329	0.009	0.000	6.971	2.583	0.000	1.992	20.005	0.070	<b>0.190*</b>	44.467	1.992	2.958	2.988	0.100	100.000
LAWA89	6.082	9.700	0.000	0.329	0.009	0.000	5.533	2.583	0.000	1.475	20.005	0.070	<b>0.190*</b>	44.002	3.983	2.951	2.988	0.100	100.000
LAWA90	6.082	9.700	3.983	0.329	0.009	0.000	5.533	2.583	0.000	1.475	20.005	0.070	<b>0.190*</b>	44.002	0.000	2.951	2.988	0.100	100.000
LAWA93	6.179	11.095	7.882	0.652	0.020	0.010	7.505	0.501	5.067	1.477	10.027	0.034	<b>0.100*</b>	42.247	1.108	2.994	2.992	0.112	100.000
LAWA96	6.201	7.904	3.989	0.652	0.020	0.010	2.992	0.501	0.000	1.994	20.000	4.023	<b>0.100*</b>	43.555	1.994	2.965	2.992	0.111	100.000
LAWA102R2	6.057	10.011	5.066	0.330	0.020	0.030	5.406	0.260	2.503	1.502	14.496	0.130	0.330	46.631	1.141	3.063	3.023	0.000	100.000
LAWA104	6.614	8.591	1.924	0.717	0.022	0.011	6.735	0.551	0.000	1.924	22.001	0.037	0.100	42.989	1.924	2.861	2.886	0.113	100.000

(a) SO<sub>3</sub> values that were interpolated are in boldface and marked with an asterisk – all others were measured by XRF.

**Table 3.2. Normalized Compositions (wt%) of 271 LAW Simulated and Actual Waste Glasses with XRF Analyzed or Estimated Values of SO<sub>3</sub> and Target Values of Remaining Components (continued).**

Glass ID	Al <sub>2</sub> O <sub>3</sub>	B <sub>2</sub> O <sub>3</sub>	CaO	Cl	Cr <sub>2</sub> O <sub>3</sub>	F	Fe <sub>2</sub> O <sub>3</sub>	K <sub>2</sub> O	Li <sub>2</sub> O	MgO	Na <sub>2</sub> O	P <sub>2</sub> O <sub>5</sub>	SO <sub>3</sub> <sup>(a)</sup>	SiO <sub>2</sub>	TiO <sub>2</sub>	ZnO	ZrO <sub>2</sub>	Others	Sum
LAWA105	7.027	8.281	1.854	0.782	0.024	0.012	6.490	0.602	0.000	1.854	24.006	0.040	0.090	41.430	1.854	2.757	2.782	0.114	100.000
LAWA112B14	6.095	9.861	7.643	0.380	0.020	0.100	0.000	1.888	0.000	1.479	19.982	0.100	0.160	44.220	1.998	2.967	3.007	0.100	100.000
LAWA112B15	6.154	9.801	7.603	0.310	0.010	0.090	0.000	2.408	0.000	1.479	19.982	0.050	0.110	43.980	1.988	2.947	2.987	0.100	100.000
LAWA125	5.637	9.545	1.939	0.220	0.020	0.320	5.387	4.208	0.000	1.439	19.990	0.090	0.310	42.888	1.939	2.879	2.909	0.280	100.000
LAWA127R1	5.651	10.205	2.068	0.181	0.019	0.265	5.758	3.430	0.000	1.536	16.312	0.070	0.180	45.828	2.073	3.071	3.110	0.245	100.000
LAWA127R2	5.658	10.217	2.069	0.180	0.020	0.270	5.768	3.429	0.000	1.540	16.305	0.070	0.210	45.886	2.079	3.079	3.119	0.100	100.000
LAWA129	7.466	8.515	3.528	0.200	0.020	0.300	0.000	3.878	0.000	1.179	18.449	0.080	0.310	47.511	2.089	3.088	3.128	0.260	100.000
LAWA129R1	7.466	8.515	3.528	0.200	0.020	0.300	0.000	3.878	0.000	1.179	18.449	0.080	0.310	47.511	2.089	3.088	3.128	0.260	100.000
LAWA133	6.204	8.901	5.485	0.559	0.020	0.040	3.487	0.430	0.000	1.998	19.980	0.100	0.200	44.535	1.998	2.967	2.997	0.100	100.000
LAWA134	5.647	9.964	2.019	0.200	0.020	0.290	5.627	3.728	0.000	1.499	17.729	0.080	0.280	44.753	2.029	2.998	3.038	0.100	100.000
LAWA135	5.655	10.092	2.048	0.190	0.020	0.280	5.695	3.577	0.000	1.519	17.016	0.070	0.270	45.304	2.048	3.038	3.078	0.100	100.000
LAWA136	5.655	10.092	3.048	0.190	0.020	0.280	5.695	3.577	0.000	1.519	17.016	0.070	0.270	44.304	2.048	3.038	3.078	0.100	100.000
LAWA170	6.056	9.664	1.980	0.327	0.009	0.000	5.513	3.055	0.000	1.473	19.905	0.070	0.210	43.841	1.984	2.936	2.976	0.000	100.000
LAWB30	8.604	10.039	7.235	0.007	0.086	0.097	8.276	0.323	4.070	3.075	7.902	0.038	<b>0.180*</b>	42.730	0.000	4.115	3.120	0.102	100.000
LAWB31	6.183	12.141	4.047	0.007	0.089	0.099	7.195	0.320	2.968	2.248	7.932	2.734	0.630	47.101	0.000	3.103	3.103	0.102	100.000
LAWB32	6.180	15.146	4.045	0.007	0.089	0.099	4.180	0.320	2.966	2.247	7.928	2.733	0.680	47.077	0.000	3.101	3.101	0.102	100.000
LAWB33	6.175	12.125	4.042	0.007	0.089	0.099	5.164	0.320	2.964	2.245	7.921	4.752	0.760	47.039	0.000	3.099	3.099	0.102	100.000
LAWB34	6.178	12.131	6.065	0.007	0.089	0.099	5.167	0.320	2.965	2.246	7.925	2.732	0.710	47.063	0.000	3.100	3.100	0.102	100.000
LAWB35	6.178	12.132	4.044	0.007	0.089	0.099	5.167	0.320	2.966	4.269	7.926	2.732	0.700	47.067	0.000	3.100	3.100	0.102	100.000
LAWB37	6.166	12.108	4.709	0.007	0.089	0.099	5.157	0.319	2.960	2.915	7.910	3.400	0.900	46.973	0.000	3.094	3.094	0.102	100.000
LAWB38	6.156	12.088	4.746	0.007	0.088	0.099	5.149	0.319	3.806	2.239	7.897	3.170	1.060	46.897	0.000	3.089	3.089	0.102	100.000
LAWB40	6.137	12.052	4.687	0.007	0.088	0.098	5.133	0.318	6.294	2.901	7.873	0.036	1.360	46.755	0.000	3.080	3.080	0.102	100.000
LAWB41	6.145	12.067	6.481	0.007	0.088	0.099	5.140	0.318	4.514	2.905	7.884	0.036	1.230	46.816	0.000	3.084	3.084	0.102	100.000
LAWB60	6.143	12.366	11.905	0.010	0.070	0.080	0.000	0.261	4.630	2.976	6.514	0.030	0.640	47.961	0.000	3.157	3.157	0.100	100.000
LAWB61	6.205	9.966	6.708	0.000	0.101	0.070	5.310	0.261	5.823	2.977	5.501	0.010	0.710	48.624	1.398	3.168	3.168	0.000	100.000
LAWB62	6.194	9.948	11.996	0.000	0.100	0.070	0.000	0.261	5.812	2.971	5.491	0.010	0.890	48.536	1.395	3.162	3.162	0.000	100.000
LAWB63	6.579	9.953	9.351	0.000	0.100	0.070	0.000	0.261	5.052	2.973	5.494	0.010	0.840	48.942	1.396	5.815	3.164	0.000	100.000
LAWB64	6.207	9.969	6.710	0.000	0.101	0.070	3.300	0.262	5.825	2.978	5.503	0.010	0.680	48.639	1.398	5.181	3.169	0.000	100.000
LAWB67	6.189	9.940	5.186	0.000	0.100	0.070	5.296	0.261	4.303	2.969	5.487	3.019	0.970	48.497	1.394	3.160	3.160	0.000	100.000
LAWB69	6.151	12.332	10.462	0.010	0.050	0.080	0.000	0.230	4.611	2.971	6.621	0.050	0.650	47.960	0.000	4.571	3.151	0.100	100.000
LAWB70	6.159	12.347	6.629	0.010	0.050	0.080	3.255	0.230	4.616	2.974	6.629	0.050	0.540	48.018	0.000	5.157	3.154	0.100	100.000

(a) values that were interpolated are in boldface and marked with an asterisk – all others were measured by XRF.



**Table 3.2. Normalized Compositions (wt%) of 271 LAW Simulated and Actual Waste Glasses with XRF Analyzed or Estimated Values of SO<sub>3</sub> and Target Values of Remaining Components (continued).**

Glass ID	Al <sub>2</sub> O <sub>3</sub>	B <sub>2</sub> O <sub>3</sub>	CaO	Cl	Cr <sub>2</sub> O <sub>3</sub>	F	Fe <sub>2</sub> O <sub>3</sub>	K <sub>2</sub> O	Li <sub>2</sub> O	MgO	Na <sub>2</sub> O	P <sub>2</sub> O <sub>5</sub>	SO <sub>3</sub> <sup>(a)</sup>	SiO <sub>2</sub>	TiO <sub>2</sub>	ZnO	ZrO <sub>2</sub>	Others	Sum
LAWB71	6.162	10.802	6.633	0.010	0.050	0.080	3.257	0.230	4.619	2.976	6.633	0.050	0.480	48.047	1.553	5.160	3.156	0.100	100.000
LAWB72	6.154	12.339	7.125	0.010	0.050	0.080	3.252	0.230	4.113	2.972	6.625	0.050	0.610	47.984	0.000	5.154	3.152	0.100	100.000
LAWB73	6.193	9.947	9.345	0.000	0.100	0.070	1.907	0.261	5.049	2.971	5.490	0.010	0.900	48.531	1.395	4.667	3.162	0.000	100.000
LAWB74	6.218	10.108	8.728	0.000	0.101	0.071	1.915	0.262	5.331	2.983	5.513	0.010	0.770	48.728	1.401	4.686	3.175	0.000	100.000
LAWB75	6.187	11.792	8.684	0.000	0.100	0.070	1.905	0.261	5.304	1.504	5.485	0.010	1.000	48.482	1.394	4.663	3.159	0.000	100.000
LAWB76	6.186	11.790	8.682	0.000	0.100	0.070	1.905	0.261	5.805	1.504	5.484	0.010	1.020	49.365	0.000	4.662	3.158	0.000	100.000
LAWB77	6.160	12.350	6.631	0.010	0.050	0.080	2.204	0.230	4.117	2.975	6.631	0.050	0.520	48.027	1.552	5.158	3.155	0.100	100.000
LAWB81	6.155	12.340	7.126	0.010	0.050	0.080	3.253	0.230	4.263	2.972	6.625	0.050	0.600	47.989	0.000	5.004	3.153	0.100	100.000
LAWB82	6.162	10.100	7.134	0.010	0.050	0.080	9.519	0.230	4.269	1.483	6.633	0.050	0.480	45.532	0.000	5.010	3.156	0.100	100.000
LAWB87	6.495	13.020	6.114	0.010	0.060	0.050	5.032	0.200	4.701	1.413	5.012	0.020	0.570	49.214	0.000	4.891	3.197	0.000	100.000
LAWB88	6.488	13.006	7.990	0.010	0.060	0.050	2.203	0.200	4.696	1.412	5.006	0.020	0.680	50.101	0.000	4.886	3.194	0.000	100.000
LAWB89	6.186	10.040	6.787	0.010	0.040	0.060	5.295	0.190	5.005	2.973	4.084	0.040	0.440	49.350	1.391	4.845	3.163	0.100	100.000
LAWB90	6.192	10.050	6.794	0.010	0.040	0.060	5.301	0.190	3.617	2.976	6.884	0.040	0.340	47.996	1.393	4.850	3.166	0.100	100.000
LAWB91	6.191	10.047	6.792	0.010	0.040	0.060	5.299	0.190	2.925	2.975	8.735	0.040	0.370	46.820	1.392	4.848	3.165	0.100	100.000
LAWB92	6.187	10.041	6.787	0.010	0.040	0.060	5.296	0.190	2.222	2.973	10.121	0.040	0.430	46.101	1.392	4.845	3.163	0.100	100.000
LAWB93	6.186	10.039	6.786	0.010	0.040	0.060	5.295	0.190	4.664	2.973	4.784	0.040	0.450	48.984	1.391	4.844	3.163	0.100	100.000
LAWB93R1	6.187	10.042	6.788	0.010	0.040	0.060	5.296	0.190	4.666	2.974	4.786	0.040	0.420	48.999	1.392	4.846	3.164	0.100	100.000
LAWB94	6.186	10.031	6.780	0.007	0.039	0.064	5.295	0.194	5.359	2.972	3.385	0.037	0.500	49.662	1.393	4.839	3.158	0.100	100.000
LAWB95	6.189	10.035	6.783	0.007	0.039	0.064	5.297	0.194	5.761	2.973	2.457	0.037	0.460	50.211	1.394	4.841	3.159	0.100	100.000
LAWB96	6.171	10.027	6.772	0.010	0.030	0.020	5.289	0.120	4.297	2.975	5.479	0.010	0.480	48.743	1.392	4.858	3.175	0.150	100.000
LAWC12	11.989	9.142	1.596	0.119	0.017	0.009	5.716	0.141	0.000	1.387	20.026	0.027	<b>0.180*</b>	39.384	3.416	4.274	2.458	0.121	100.000
LAWC15	6.221	8.929	2.006	0.078	0.003	0.469	7.007	0.142	0.000	2.009	19.963	0.015	0.230	44.713	2.001	2.990	3.005	0.220	100.000
LAWC21	6.139	10.104	6.419	0.120	0.020	0.060	6.489	0.150	2.744	1.512	11.897	0.120	0.290	46.766	1.122	3.024	3.024	0.000	100.000
LAWC21rev2	6.125	10.058	6.415	0.110	0.020	0.050	6.435	0.140	2.732	1.501	11.970	0.110	0.290	46.778	1.121	3.022	3.022	0.100	100.000
LAWC22	6.076	10.056	5.110	0.048	0.012	0.336	5.426	0.083	2.506	1.514	14.408	0.067	<b>0.290*</b>	46.642	1.144	3.071	3.028	0.183	100.000
LAWC23	6.118	10.076	6.401	0.123	0.020	0.060	6.470	2.881	0.000	1.507	11.856	0.118	<b>0.350*</b>	46.763	1.122	3.014	3.017	0.105	100.000
LAWC24	5.955	9.808	6.231	0.120	0.019	0.058	6.297	5.558	0.000	1.467	11.541	0.115	<b>0.340*</b>	45.429	1.090	2.934	2.937	0.102	100.000
LAWC25	5.784	9.526	6.052	0.117	0.019	0.057	6.116	8.079	0.000	1.425	11.209	0.111	0.530	44.122	1.058	2.850	2.852	0.095	100.000
LAWC26	6.121	13.263	6.411	0.110	0.020	0.050	0.010	0.140	2.731	1.500	11.962	0.110	0.350	49.960	1.120	3.021	3.021	0.100	100.000
LAWC28	6.117	10.045	12.814	0.110	0.020	0.050	0.010	0.140	2.729	1.499	11.954	0.110	0.430	46.717	1.119	3.018	3.018	0.100	100.000

(a) SO<sub>3</sub> values that were interpolated are in boldface and marked with an asterisk – all others were measured by XRF.

**Table 3.2. Normalized Compositions (wt%) of 271 LAW Simulated and Actual Waste Glasses with XRF Analyzed or Estimated Values of SO<sub>3</sub> and Target Values of Remaining Components (continued).**

Glass ID	Al <sub>2</sub> O <sub>3</sub>	B <sub>2</sub> O <sub>3</sub>	CaO	Cl	Cr <sub>2</sub> O <sub>3</sub>	F	Fe <sub>2</sub> O <sub>3</sub>	K <sub>2</sub> O	Li <sub>2</sub> O	MgO	Na <sub>2</sub> O	P <sub>2</sub> O <sub>5</sub>	SO <sub>3</sub> <sup>(a)</sup>	SiO <sub>2</sub>	TiO <sub>2</sub>	ZnO	ZrO <sub>2</sub>	Others	Sum
LAWC29	6.551	10.049	9.617	0.112	0.018	0.054	0.009	0.136	2.734	1.501	11.958	0.106	0.370	47.181	1.121	5.365	3.019	0.100	100.000
LAWC30	6.122	10.053	6.412	0.110	0.020	0.050	4.101	0.140	2.731	1.500	11.964	0.110	0.340	46.754	1.120	5.352	3.021	0.100	100.000
LAWC31	6.119	10.048	7.409	0.110	0.020	0.050	4.429	0.140	2.729	1.500	11.958	0.110	0.390	46.731	1.120	4.019	3.019	0.100	100.000
LAWC31R1	6.122	10.053	7.412	0.110	0.020	0.050	4.431	0.140	2.731	1.500	11.964	0.110	0.340	46.754	1.120	4.021	3.021	0.100	100.000
LAWC33	6.146	10.100	6.947	0.110	0.020	0.050	4.444	0.140	2.753	1.512	12.012	0.110	0.370	46.977	1.131	4.044	3.033	0.100	100.000
TFA-BASE	6.999	9.999	0.010	0.280	0.000	0.010	5.499	0.410	0.000	1.500	19.998	0.060	0.080	49.065	3.000	1.500	1.500	0.090	100.000
C22AN107	6.106	10.079	5.115	0.080	0.020	0.140	5.585	0.090	2.512	1.511	14.433	0.120	0.270	46.612	1.141	3.063	3.023	0.100	100.000
A88AP101R1	6.102	9.834	1.999	0.130	0.016	0.227	5.552	2.136	0.000	1.480	20.011	0.073	0.230	44.153	1.999	2.961	2.998	0.100	100.000
A88Si+15	6.141	9.481	1.930	0.140	0.020	0.250	5.351	2.370	0.000	1.430	22.182	0.080	0.290	42.554	1.930	2.850	2.890	0.110	100.000
A88Si-15	6.055	10.218	2.072	0.120	0.010	0.200	5.765	1.882	0.000	1.541	17.674	0.060	0.190	45.867	2.072	3.072	3.112	0.090	100.000
C22Si+15	6.043	9.837	4.994	0.090	0.020	0.160	5.358	0.095	2.459	1.484	16.197	0.130	0.310	45.581	1.121	3.001	2.960	0.160	100.000
C22Si-15	6.160	10.291	5.218	0.071	0.017	0.129	5.555	0.076	2.572	1.551	12.812	0.138	0.230	47.680	1.175	3.139	3.096	0.090	100.000
A1C1-1	6.088	9.126	2.742	0.913	0.015	0.086	6.501	0.347	0.623	1.850	19.167	0.033	0.210	44.480	1.759	2.951	2.956	0.153	100.000
A1C1-2	6.073	9.415	3.521	0.654	0.013	0.169	6.135	0.255	1.247	1.735	17.673	0.066	0.230	45.142	1.554	2.984	2.974	0.160	100.000
A1C1-3	6.057	9.701	4.299	0.395	0.011	0.252	5.766	0.161	1.871	1.619	16.170	0.099	0.290	45.787	1.348	3.017	2.991	0.167	100.000
C1-AN107	6.066	10.031	5.098	0.065	0.009	0.283	5.421	0.069	2.506	1.510	14.465	0.132	0.290	46.636	1.147	3.062	3.020	0.189	100.000
A2-AP101	5.622	9.824	1.991	0.420	0.020	0.350	5.532	3.812	0.000	1.481	18.467	0.080	0.350	44.008	1.991	2.941	2.961	0.150	100.000
A2B1-1	5.758	9.883	3.184	0.320	0.020	0.280	5.477	2.904	1.071	1.852	15.230	0.070	0.350	45.179	1.842	3.414	3.014	0.150	100.000
A2B1-2	5.895	9.919	4.374	0.220	0.030	0.220	5.405	2.002	2.152	2.232	11.981	0.060	0.420	46.292	1.692	3.894	3.063	0.150	100.000
B1-AZ101	6.180	10.026	6.771	0.020	0.030	0.080	5.278	0.180	4.307	2.985	5.479	0.040	0.490	48.578	1.392	4.848	3.165	0.150	100.000
C2-AN102C35	6.075	9.428	7.356	0.390	0.010	0.110	3.603	0.090	3.253	1.491	11.980	0.160	0.540	47.278	1.081	3.993	3.002	0.160	100.000
A3-AN104	6.051	9.921	5.031	0.790	0.020	0.010	5.371	0.330	2.480	1.480	14.641	0.110	0.350	46.095	1.130	3.040	3.000	0.150	100.000
A2B1-3	6.037	9.971	5.576	0.120	0.030	0.150	5.346	1.091	3.224	2.603	8.730	0.050	0.470	47.432	1.542	4.365	3.113	0.150	100.000
A3C2-1	6.064	9.796	5.613	0.690	0.020	0.030	4.923	0.270	2.672	1.481	13.978	0.120	0.380	46.408	1.121	3.282	3.002	0.150	100.000
A3C2-2	6.066	9.680	6.196	0.591	0.020	0.060	4.485	0.210	2.863	1.481	13.323	0.140	0.400	46.707	1.111	3.514	3.003	0.150	100.000
A3C2-3	6.064	9.547	6.775	0.490	0.010	0.090	4.043	0.150	3.062	1.491	12.649	0.150	0.490	46.983	1.091	3.753	3.002	0.160	100.000
A1-AN105R2	6.101	8.841	1.960	1.170	0.020	0.000	6.871	0.440	0.000	1.960	20.662	0.000	0.180	43.824	1.960	2.920	2.940	0.150	100.000
12U-G-86A	6.161	8.952	1.980	0.560	0.020	0.020	6.941	0.440	0.000	1.980	19.964	0.070	0.230	44.329	1.980	2.951	2.971	0.450	100.000
LA44PNCC	6.173	8.874	1.981	0.570	0.070	0.220	6.963	0.260	0.000	1.971	20.010	0.350	0.210	44.472	1.971	2.911	2.991	0.000	100.000
LA44CCCR2	6.173	8.874	1.981	0.570	0.070	0.220	6.963	0.260	0.000	1.971	20.010	0.350	0.210	44.472	1.971	2.911	2.991	0.000	100.000

(a) SO<sub>3</sub> values that were interpolated are in boldface and marked with an asterisk – all others were measured by XRF.

**Table 3.2. Normalized Compositions (wt%) of 271 LAW Simulated and Actual Waste Glasses with XRF Analyzed or Estimated Values of SO<sub>3</sub> and Target Values of Remaining Components (continued).**

Glass ID	Al <sub>2</sub> O <sub>3</sub>	B <sub>2</sub> O <sub>3</sub>	CaO	Cl	Cr <sub>2</sub> O <sub>3</sub>	F	Fe <sub>2</sub> O <sub>3</sub>	K <sub>2</sub> O	Li <sub>2</sub> O	MgO	Na <sub>2</sub> O	P <sub>2</sub> O <sub>5</sub>	SO <sub>3</sub> <sup>(a)</sup>	SiO <sub>2</sub>	TiO <sub>2</sub>	ZnO	ZrO <sub>2</sub>	Others	Sum
WVF-G-21B	6.079	9.799	1.990	0.130	0.020	0.230	5.539	2.130	0.000	1.480	20.008	0.070	0.330	43.996	1.990	2.950	2.990	0.270	100.000
PNLA126CC	5.652	9.854	2.001	0.200	0.020	0.300	5.562	3.882	0.000	1.481	18.467	0.080	0.290	44.238	2.001	2.961	3.001	0.010	100.000
LA126CCC	5.652	9.854	2.001	0.200	0.020	0.300	5.562	3.882	0.000	1.481	18.467	0.080	0.290	44.238	2.001	2.961	3.001	0.010	100.000
WVM-G-142C	5.618	9.825	1.993	0.421	0.020	0.351	5.538	3.816	0.000	1.472	18.468	0.080	0.250	44.006	1.983	2.944	2.964	0.250	100.000
A100G115A	6.063	10.005	5.063	0.330	0.020	0.030	5.413	0.260	2.501	1.491	14.467	0.130	0.380	46.603	1.141	3.072	3.032	0.000	100.000
A100CC	6.064	10.007	5.064	0.330	0.020	0.030	5.414	0.260	2.502	1.491	14.470	0.130	0.360	46.613	1.141	3.072	3.032	0.000	100.000
WVB-G-124B	6.039	9.969	5.049	0.330	0.020	0.030	5.399	0.260	2.490	1.490	14.419	0.130	0.440	46.455	1.140	3.060	3.020	0.260	100.000
LA137SRCCC	6.051	9.911	5.031	0.760	0.030	0.020	5.361	0.620	2.480	1.480	14.641	0.110	0.270	46.065	1.130	3.040	3.000	0.000	100.000
WVR-G-127A	6.049	9.908	5.019	0.790	0.020	0.000	5.359	0.330	2.480	1.480	14.627	0.110	0.380	46.031	1.130	3.039	2.999	0.250	100.000
LB83PNCC	6.214	10.047	6.795	0.000	0.030	0.080	5.294	0.180	4.313	2.992	5.374	0.050	0.490	48.714	1.401	4.853	3.172	0.000	100.000
LB83CCC-1	6.214	10.047	6.795	0.000	0.030	0.080	5.294	0.180	4.313	2.992	5.374	0.050	0.490	48.714	1.401	4.853	3.172	0.000	100.000
WVJ-G-109D	6.174	10.022	6.775	0.010	0.040	0.060	5.282	0.190	4.310	2.977	5.472	0.040	0.430	48.577	1.393	4.841	3.157	0.251	100.000
GTSD-1126	6.183	10.041	6.784	0.010	0.030	0.020	5.301	0.120	4.309	2.976	5.492	0.010	0.450	48.843	1.393	4.860	3.177	0.000	100.000
LB88CCC	6.505	12.980	7.976	0.010	0.060	0.050	2.202	0.200	4.694	1.411	5.004	0.020	0.730	50.080	0.000	4.884	3.193	0.000	100.000
AZ-102 Surr SRNL	6.420	12.979	7.957	0.000	0.060	0.100	2.196	0.200	4.682	1.408	5.072	0.020	0.930	49.919	0.000	4.872	3.185	0.000	100.000
12S-G-85C	6.080	10.050	5.090	0.080	0.020	0.140	5.560	0.080	2.500	1.510	14.430	0.120	0.380	46.430	1.140	3.060	3.010	0.320	100.000
C100GCC	6.127	10.092	6.408	0.120	0.020	0.060	6.478	0.150	2.733	1.512	11.874	0.120	0.400	46.726	1.121	3.014	3.024	0.020	100.000
AN-102 Surr LC Melter	6.142	10.143	6.422	0.210	0.020	0.060	6.502	0.070	2.751	1.520	11.804	0.080	0.290	46.784	1.130	3.031	3.031	0.010	100.000
WVH-G-57B	6.102	10.023	7.392	0.110	0.020	0.050	4.421	0.140	2.731	1.500	11.934	0.100	0.430	46.644	1.120	4.011	3.011	0.260	100.000
GTSD-1437	6.091	9.463	7.386	0.391	0.010	0.110	3.613	0.090	3.271	1.495	12.032	0.161	0.290	47.467	1.084	4.004	3.011	0.030	100.000
PLTC35CCC	6.091	9.463	7.386	0.391	0.010	0.110	3.613	0.090	3.271	1.495	12.032	0.161	0.290	47.467	1.084	4.004	3.011	0.030	100.000
AN-103 Actual	6.220	8.950	2.010	0.310	0.010	0.020	7.020	0.600	0.000	2.010	20.000	0.050	0.100	44.680	2.010	3.000	3.010	0.000	100.000
AW-101 Actual	6.080	9.710	1.990	0.078	0.009	0.000	5.540	2.580	0.000	1.480	20.001	0.070	0.210	44.052	1.994	2.950	2.990	0.265	100.000
AP-101 Actual	5.660	9.850	2.000	0.170	0.030	0.270	5.560	3.820	0.000	1.490	18.460	0.090	0.310	44.270	2.010	2.970	3.010	0.030	100.000
AZ-101 Actual	6.210	10.040	6.790	0.000	0.030	0.080	5.290	0.180	4.310	2.990	5.350	0.050	0.550	48.700	1.400	4.850	3.170	0.010	100.000
AZ-102 Actual	6.496	12.992	7.995	0.010	0.060	0.050	2.199	0.210	4.687	1.409	4.997	0.020	0.850	49.970	0.000	4.867	3.188	0.000	100.000
AZ-102 Actual CCC	6.496	12.992	7.995	0.010	0.060	0.050	2.199	0.210	4.687	1.409	4.997	0.020	0.850	49.970	0.000	4.867	3.188	0.000	100.000
AN-107 Actual (LAWC15)	6.231	8.943	2.010	0.078	0.003	0.470	7.018	0.142	0.000	2.012	20.000	0.015	0.130	44.784	2.004	2.995	3.010	0.155	100.000
AN-102 Actual LC Melter	6.148	10.096	6.427	0.090	0.020	0.050	6.497	0.070	2.749	1.519	11.795	0.080	0.360	46.781	1.130	3.039	3.039	0.110	100.000
AN-102 Actual	6.150	10.130	6.420	0.120	0.020	0.060	6.490	0.090	2.740	1.520	11.800	0.130	0.360	46.750	1.130	3.030	3.030	0.030	100.000

(a) SO<sub>3</sub> values that were interpolated are in boldface and marked with an asterisk – all others were measured by XRF.

**Table 4.1. LAW Glasses Having Data for PCT, VHT, Viscosity, and Electrical Conductivity.**

Glass ID	Group ID <sup>(a)</sup>	PCT <sup>(b)</sup>	VHT <sup>(b)</sup>	Viscosity <sup>(b)</sup>	Electrical <sup>(b)</sup> Conductivity	Glass ID	Group ID	PCT	VHT	Viscosity	Electrical Conductivity
LAWA44R10	ExPh1	1	1	1	1	LAWM16	Ph1	1	1	1	1
LAWA53	ExPh1	1	1	1	1	LAWM17	Ph1	1	1	1	1
LAWA56	ExPh1	1	1	1	1	LAWM18	Ph1	1	1	1	1
LAWA88	ExPh1 <sup>(c)</sup>	1	0	1	1	LAWM19	Ph1	1	1	1	1
LAWA88R1	ExPh1	1	1	0	0	LAWM20	Ph1	1	1	1	1
LAWA102R1	ExPh1	1	1	1	1	LAWM21	Ph1	1	1	1	1
LAWA126	ExPh1	1	1	1	1	LAWM22	Ph1	1	1	1	1
LAWA128	ExPh1	1	1	0	0	LAWM23	Ph1	1	1	1	1
LAWA128R1	ExPh1	0	0	1	1	LAWM24	Ph1	1	1	1	1
LAWA130	ExPh1	1	1	1	1	LAWM25R1	Ph1	1	1	1	1
LAWB65	ExPh1	1	1	1	1	LAWM26	Ph1	1	1	1	1
LAWB66	ExPh1	1	1	1	1	LAWM27	Ph1	1	1	1	1
LAWB68	ExPh1	1	1	1	1	LAWM28	Ph1	1	1	1	1
LAWB78	ExPh1	1	1	1	1	LAWM29	Ph1	1	1	1	1
LAWB79	ExPh1	1	1	1	1	LAWM30	Ph1	1	1	1	1
LAWB80	ExPh1	1	1	1	1	LAWM31	Ph1	1	1	1	1
LAWB83	ExPh1	1	1	1	1	LAWM32	Ph1	1	1	1	1
LAWB84	ExPh1	1	1	1	1	LAWM33R1	Ph1	1	1	1	1
LAWB85	ExPh1	1	1	1	1	LAWM34	Ph1	1	1	1	1
LAWB86	ExPh1	1	1	1	1	LAWM35	Ph1	1	1	1	1
C100-G-136B	ExPh1	1	1	1	1	LAWM36	Ph1	1	1	1	1
LAWC27	ExPh1	1	1	1	1	LAWM37	Ph1	1	1	1	1
LAWC32	ExPh1	1	1	1	1	LAWM38	Ph1	1	1	1	1
LAWM1	Ph1	1	1	1	1	LAWM39	Ph1	1	1	1	1
LAWM2	Ph1	1	1	1	1	LAWM40	Ph1	1	1	1	1
LAWM3	Ph1	1	1	1	1	LAWM41	Ph1	1	1	1	1
LAWM4	Ph1	1	1	1	1	LAWM42	Ph1	1	1	1	1
LAWM5	Ph1	1	1	1	1	LAWM43	Ph1	1	1	1	1
LAWM6	Ph1	1	1	1	1	LAWM44	Ph1	1	1	1	1
LAWM7	Ph1	1	1	1	1	LAWM45	Ph1	1	1	1	1
LAWM8	Ph1	1	1	1	1	LAWM46	Ph1	1	1	1	1
LAWM9	Ph1	1	1	1	1	LAWM47	Ph1	1	1	1	1
LAWM10	Ph1	1	1	1	1	LAWM48	Ph1	1	1	1	1
LAWM11	Ph1	1	1	1	1	LAWM49	Ph1	1	1	1	1
LAWM12	Ph1	1	1	1	1	LAWM50	Ph1	1	1	1	1
LAWM13	Ph1	1	1	1	1	LAWM51	Ph1	1	1	1	1
LAWM14	Ph1	1	1	1	1	LAWM52	Ph1	1	1	1	1
LAWM15	Ph1	1	1	1	1	LAWM53	Ph1	1	1	1	1

- (a) ExPh1 denotes existing LAW glasses that were selected to be augmented by Phase 1 glasses. Ph1 denotes the Phase 1 test matrix glasses. See Sections 2.1 and 2.2 for more information about these groups of glasses.
- (b) An entry of 1 indicates data is available for that property on that glass, while an entry of 0 indicates no data is available for that property on that glass.
- (c) LAWA88 was previously classified in the actively designed (ActDes) group for the PCT response, with that classification used for the plotting symbols in Section 5.

**Table 4.1. LAW Glasses Having Data for PCT, VHT, Viscosity, and Electrical Conductivity (continued).**

Glass ID	Group ID <sup>(a)</sup>	PCT	VHT	Viscosity	Electrical Conductivity
LAWM54R1	Ph1	1	1	1	1
LAWM55	Ph1	1	1	1	1
LAWM56	Ph1	1	1	1	1
LAWM57	Ph1aAug	1	1	1	1
LAWM58	Ph1aAug	1	1	0	0
LAWM59	Ph1aAug	1	1	1	1
LAWM60	Ph1aAug	1	1	1	1
LAWM61	Ph1aAug	1	1	0	0
LAWM62	Ph1aAug	1	1	0	0
LAWM63	Ph1aAug	1	1	1	1
LAWM64	Ph1aAug	1	1	0	0
LAWM65	Ph1aAug	1	1	0	0
LAWM66	Ph1aAug	1	1	1	1
LAWM67	Ph1aAug	1	1	0	0
LAWM68	Ph1aAug	1	1	1	1
LAWM69	Ph1aAug	1	1	0	0
LAWM70	Ph1aAug	1	1	0	0
LAWM71	Ph1aAug	1	1	1	1
LAWM72	Ph1aAug	1	1	0	0
LAWM73	Ph1aAug	1	1	1	1
LAWM74	Ph1aAug	1	1	0	0
LAWM75	Ph1aAug	1	1	1	1
LAWM76	Ph1aAug	1	1	0	0
LAWE2H	Corr	1	1	1	1
LAWE3	Corr	1	1	1	1
LAWE3H	Corr	1	1	1	1
LAWE4	Corr	0	0	1	1
LAWE4H	Corr	1	1	1	1
LAWE5	Corr	0	0	1	1
LAWE5H	Corr	1	1	1	1
LAWE7	Corr	0	1	1	1
LAWE7H	Corr	1	1	1	1
LAWE9H	Corr	1	1	1	1
LAWE10H	Corr	1	1	1	1
LAWE11	Corr	1	1	1	1
LAWE12	Corr	1	1	1	1
LAWE13	Corr	1	1	1	1
LAWE14	Corr	1	1	0	0
LAWE15	Corr	1	1	0	0
LAWE16	Corr	1	1	1	1
LAWE3Cr2CCC	Corr	1	1	0	0
LAWE9HCr1CCC	Corr	1	1	0	0
LAWE9HCr2CCC	Corr	1	1	0	0
LAWE10HCr3CCC	Corr	1	1	0	0
LAWCrP1R	HiCrP	1	1	1	1
LAWCrP2R	HiCrP	1	1	1	1
LAWCrP3R	HiCrP	1	1	1	1
LAWCrP4R	HiCrP	1	1	1	1
LAWCrP5	HiCrP	1	1	1	1
LAWCrP6	HiCrP	1	1	0	0
LAWCrP7	HiCrP	1	1	0	0
LAWA41	ActDes	1	0	1	1
LAWA42	ActDes	1	0	1	1
LAWA43-1	ActDes	1	0	1	1
LAWA44	ActDes	1	0	0	0
LAWA45	ActDes	1	0	1	1
LAWA49	ActDes	1	1	1	1
LAWA50	ActDes	1	0	1	1
LAWA51	ActDes	1	1	1	1
LAWA52	ActDes	1	1	1	1
LAWA60	ActDes	1	1	1	1
LAWA65	ActDes	1	0	0	0
LAWA76	ActDes	1	0	0	0
LAWA81	ActDes	1	0	1	1
LAWA82	ActDes	1	0	1	1
LAWA83	ActDes	1	0	1	1
LAWA84	ActDes	1	0	0	0
LAWA87	ActDes	1	0	0	0
LAWA89	ActDes	1	0	1	1
LAWA90	ActDes	1	0	1	1
LAWA93	ActDes	1	0	1	1
LAWA96	ActDes	1	0	1	1
LAWA102R2	ActDes	1	0	0	0
LAWA104	ActDes	1	1	0	0
LAWA105	ActDes	1	1	0	0
LAWA112B14	ActDes	1	0	0	0

- (a) Ph1 denotes the Phase 1 test matrix glasses. Ph1aAug denotes the Phase 1a augmentation test matrix glasses. Corr denotes the correlation glasses. HiCrP denotes the glasses with high Cr<sub>2</sub>O<sub>3</sub> and P<sub>2</sub>O<sub>5</sub> levels. ActDes denotes actively designed glasses. See Sections 2.2 to 2.6 for more information about these groups of glasses.
- (b) An entry of 1 indicates data is available for that property on that glass, while an entry of 0 indicates no data is available for that property on that glass.

**Table 4.1. LAW Glasses Having Data for PCT, VHT, Viscosity, and Electrical Conductivity (continued).**

Glass ID	Group ID <sup>(a)</sup>	PCT	VHT	Viscosity	Electrical Conductivity
LAWA112B15	ActDes	1	0	0	0
LAWA125	ActDes	1	1	1	1
LAWA127R1	ActDes	1	0	1	1
LAWA127R2	ActDes	1	0	0	0
LAWA129	ActDes	1	0	0	0
LAWA129R1	ActDes	0	0	1	1
LAWA133	ActDes	1	1	0	0
LAWA134	ActDes	1	1	1	1
LAWA135	ActDes	1	1	1	1
LAWA136	ActDes	1	1	1	1
LAWA170	ActDes	1	0	0	0
LAWB30	ActDes	1	0	1	1
LAWB31	ActDes	1	0	0	0
LAWB32	ActDes	1	0	0	0
LAWB33	ActDes	1	0	0	0
LAWB34	ActDes	1	0	1	1
LAWB35	ActDes	1	0	0	0
LAWB37	ActDes	1	0	1	1
LAWB38	ActDes	1	0	1	1
LAWB40	ActDes	1	0	0	0
LAWB41	ActDes	1	0	0	0
LAWB60	ActDes	1	1	1	1
LAWB61	ActDes	1	0	1	1
LAWB62	ActDes	1	1	1	1
LAWB63	ActDes	1	1	1	1
LAWB64	ActDes	1	1	1	1
LAWB67	ActDes	1	1	1	1
LAWB69	ActDes	1	1	1	1
LAWB70	ActDes	1	1	1	1
LAWB71	ActDes	1	1	1	1
LAWB72	ActDes	1	1	1	1
LAWB73	ActDes	1	1	1	1
LAWB74	ActDes	1	1	1	1
LAWB75	ActDes	1	1	1	1
LAWB76	ActDes	1	1	1	1
LAWB77	ActDes	1	1	1	1
LAWB81	ActDes	1	1	1	1
LAWB82	ActDes	1	1	1	1

Glass ID	Group ID	PCT	VHT	Viscosity	Electrical Conductivity
LAWB87	ActDes	1	0	1	1
LAWB88	ActDes	1	0	1	1
LAWB89	ActDes	1	1	1	1
LAWB90	ActDes	1	1	1	1
LAWB91	ActDes	1	1	0	0
LAWB92	ActDes	1	1	1	1
LAWB93	ActDes	1	1	0	0
LAWB93R1	ActDes	0	0	1	1
LAWB94	ActDes	1	1	1	1
LAWB95	ActDes	1	1	1	1
LAWB96	ActDes	1	0	0	0
LAWC12	ActDes	1	0	1	1
LAWC15	ActDes	1	1	0	0
LAWC21	ActDes	1	0	0	0
LAWC21rev2	ActDes	1	0	1	1
LAWC22	ActDes	1	0	0	0
LAWC23	ActDes	1	0	0	0
LAWC24	ActDes	1	0	0	0
LAWC25	ActDes	1	0	0	0
LAWC26	ActDes	1	1	0	0
LAWC28	ActDes	1	1	0	0
LAWC29	ActDes	1	1	1	1
LAWC30	ActDes	1	1	1	1
LAWC31	ActDes	1	1	0	0
LAWC31R1	ActDes	0	0	1	1
LAWC33	ActDes	1	1	0	0
TFA-BASE	ActDes	1	1	0	0
C22AN107	ActDes	1	1	1	1
A88AP101R1	ActDes	1	1	0	0
A88Si+15	ActDes	1	1	1	1
A88Si-15	ActDes	1	1	1	1
C22Si+15	ActDes	1	1	1	1
C22Si-15	ActDes	1	1	1	1
A1C1-1	ActDes	1	1	1	1
A1C1-2	ActDes	1	1	1	1
A1C1-3	ActDes	1	1	0	0
C1-AN107	ActDes	1	1	1	1
A2-AP101	ActDes	1	1	1	1

- (a) ActDes denotes actively designed glasses. See Section 2.6 for more information about this group of glasses.  
 (b) An entry of 1 indicates data is available for that property on that glass, while an entry of 0 indicates no data is available for that property on that glass.

**Table 4.1. LAW Glasses Having Data for PCT, VHT, Viscosity, and Electrical Conductivity (continued).**

Glass ID	Group ID <sup>(a)</sup>	PCT	VHT	Viscosity	Electrical Conductivity
A2B1-1	ActDes	1	1	1	1
A2B1-2	ActDes	1	1	1	1
B1-AZ101	ActDes	1	1	1	1
C2-AN102C35	ActDes	1	1	1	1
A3-AN104	ActDes	1	1	1	1
A2B1-3	ActDes	1	0	1	1
A3C2-1	ActDes	1	0	1	1
A3C2-2	ActDes	1	0	1	1
A3C2-3	ActDes	1	0	1	1
A1-AN105R2	ActDes	1	0	1	1
12U-G-86A	ActDes	1	0	0	0
LA44PNCC	ActDes	1	0	0	0
LA44CCCR2	ActDes	1	0	0	0
WVF-G-21B	ActDes	1	0	0	0
PNLA126CC	ActDes	1	0	0	0
LA126CCC	ActDes	1	0	0	0
WVM-G-142C	ActDes	1	0	0	0
A100G115A	ActDes	1	0	0	0
A100CC	ActDes	1	0	0	0
WVB-G-124B	ActDes	1	0	0	0
LA137SRCCC	ActDes	1	0	0	0
WVR-G-127A	ActDes	1	0	0	0

Glass ID	Group ID	PCT	VHT	Viscosity	Electrical Conductivity
LB83PNCC	ActDes	1	0	0	0
LB83CCC-1	ActDes	1	0	0	0
WVJ-G-109D	ActDes	1	0	0	0
GTSD-1126	ActDes	1	0	0	0
LB88CCC	ActDes	1	0	0	0
AZ-102 Surr SRNL	ActDes	1	0	0	0
12S-G-85C	ActDes	1	0	0	0
C100GCC	ActDes	1	0	0	0
AN-102 Surr LC Melter	ActDes	1	0	0	0
WVH-G-57B	ActDes	1	0	0	0
GTSD-1437	ActDes	1	0	0	0
PLTC35CCC	ActDes	1	0	0	0
AN-103 Actual	Actual	1	0	0	0
AW-101 Actual	Actual	1	0	0	0
AP-101 Actual	Actual	1	0	0	0
AZ-101 Actual	Actual	1	0	0	0
AZ-102 Actual	Actual	1	0	0	0
AZ-102 Actual CCC	Actual	1	0	0	0
AN-107 Actual (LAWC15)	Actual	1	0	0	0
AN-102 Actual LC Melter	Actual	1	0	0	0
AN-102 Actual	Actual	1	0	0	0
<b>Totals</b>	<b># Glasses = 271</b>	<b>264</b>	<b>181</b>	<b>181</b>	<b>181</b>

- (a) ActDes denotes actively designed glasses. Actual denotes glasses made from actual tank waste samples. See Sections 2.6 and 2.7 for more information about these groups of glasses.
- (b) An entry of 1 indicates data is available for that property on that glass, while an entry of 0 indicates no data is available for that property on that glass.

**Table 4.2. PCT Results<sup>(a)</sup> for Simulated and Actual LAW Glasses.**

Glass ID	Group ID <sup>(b)</sup>	Concentration (ppm)			Normalized Concentration (g/L)			Normalized Mass Loss (g/m <sup>2</sup> )		
		B	Na	Si	B	Na	Si	B	Na	Si
LAWA44R10	ExPh1	29.81	139.90	90.30	1.078	0.943	0.434	0.539	0.471	0.217
LAWA53	ExPh1	15.40	156.30	68.32	0.804	1.059	0.348	0.402	0.529	0.174
LAWA56	ExPh1	64.39	172.30	64.02	1.721	1.166	0.325	0.860	0.583	0.163
LAWA88	ExPh1 <sup>(c)</sup>	26.11	126.50	70.24	0.867	0.852	0.342	0.433	0.426	0.171
LAWA88R1	ExPh1	49.18	192.20	93.01	1.633	1.295	0.452	0.816	0.647	0.226
LAWA102R1	ExPh1	26.74	78.61	78.43	0.864	0.731	0.362	0.432	0.365	0.181
LAWA126	ExPh1	36.47	143.50	68.28	1.196	1.048	0.331	0.598	0.524	0.166
LAWA128	ExPh1	13.80	118.90	75.55	0.629	0.869	0.351	0.314	0.434	0.175
LAWA130	ExPh1	25.59	126.50	76.74	0.921	0.924	0.356	0.461	0.462	0.178
LAWB65	ExPh1	17.14	19.39	46.73	0.555	0.477	0.206	0.278	0.239	0.103
LAWB66	ExPh1	18.11	22.20	48.55	0.585	0.545	0.214	0.293	0.273	0.107
LAWB68	ExPh1	13.18	19.27	44.78	0.503	0.474	0.197	0.251	0.237	0.099
LAWB78	ExPh1	46.94	80.68	70.59	1.224	1.110	0.321	0.612	0.555	0.160
LAWB79	ExPh1	41.78	62.59	67.28	1.090	0.978	0.301	0.545	0.489	0.151
LAWB80	ExPh1	33.76	35.79	56.41	0.881	0.728	0.251	0.440	0.364	0.126
LAWB83	ExPh1	19.06	21.38	52.35	0.612	0.527	0.230	0.306	0.263	0.115
LAWB84	ExPh1	21.02	22.72	55.73	0.674	0.559	0.245	0.337	0.280	0.123
LAWB85	ExPh1	23.29	20.30	55.69	0.651	0.500	0.245	0.325	0.250	0.122
LAWB86	ExPh1	48.31	41.00	75.22	1.252	1.009	0.331	0.626	0.505	0.165
C100-G-136B	ExPh1	23.01	61.38	58.30	0.734	0.697	0.267	0.367	0.348	0.133
LAWC27	ExPh1	14.27	39.02	41.86	0.377	0.440	0.183	0.189	0.220	0.092
LAWC32	ExPh1	13.05	49.04	45.34	0.418	0.553	0.207	0.209	0.276	0.104
LAWM1	Ph1	2.85	10.81	27.31	0.152	0.290	0.131	0.076	0.145	0.065
LAWM2	Ph1	12.57	31.74	67.17	0.672	0.853	0.305	0.336	0.426	0.152
LAWM3	Ph1	14.86	98.87	47.31	0.795	1.157	0.252	0.397	0.578	0.126
LAWM4	Ph1	18.59	22.32	36.68	0.458	0.599	0.189	0.229	0.300	0.094
LAWM5	Ph1	4.59	10.40	36.38	0.245	0.279	0.159	0.123	0.140	0.080
LAWM6	Ph1	18.04	47.66	36.07	0.547	0.714	0.193	0.274	0.357	0.096

(a) 7-Day PCT, stainless steel vessel with S/V = 2000 m<sup>-1</sup>. The PCT concentrations (ppm) are as measured from the PCTs on the glasses. Normalized concentrations (g/L) and normalized mass losses (g/m<sup>2</sup>) are normalized based on the normalized compositions discussed in Section 3.3.

(b) The Group IDs are described in Sections 2.1 to 2.7.

(c) LAWA88 was previously classified in the actively designed (ActDes) group for the PCT response, with that classification used for the plotting symbols in Section 5.



**Table 4.2. PCT Results<sup>(a)</sup> for Simulated and Actual LAW Glasses (continued).**

Glass ID	Group ID <sup>(b)</sup>	Concentration (ppm)			Normalized Concentration (g/L)			Normalized Mass Loss (g/m <sup>2</sup> )		
		B	Na	Si	B	Na	Si	B	Na	Si
LAWM7	Ph1	5.39	15.97	52.08	0.249	0.429	0.214	0.125	0.215	0.107
LAWM8	Ph1	13.00	10.30	29.21	0.321	0.277	0.140	0.161	0.138	0.070
LAWM9	Ph1	3.92	19.07	31.50	0.210	0.513	0.135	0.105	0.257	0.068
LAWM10	Ph1	9.78	42.94	26.25	0.242	0.443	0.140	0.121	0.221	0.070
LAWM11	Ph1	46.93	120.40	120.30	1.161	1.412	0.550	0.581	0.706	0.275
LAWM12	Ph1	1199.00	1701.00	468.10	29.686	16.081	2.372	14.843	8.040	1.186
LAWM13	Ph1	46.12	804.90	223.00	2.475	4.931	1.192	1.237	2.465	0.596
LAWM14	Ph1	37.17	352.80	276.30	1.995	2.162	1.137	0.997	1.081	0.568
LAWM15	Ph1	63.09	251.30	101.20	2.171	1.540	0.498	1.086	0.770	0.249
LAWM16	Ph1	10.62	30.79	31.34	0.285	0.415	0.158	0.142	0.207	0.079
LAWM17	Ph1	467.00	1006.00	179.00	12.527	7.974	0.911	6.263	3.987	0.456
LAWM18	Ph1	16.12	37.77	37.39	0.432	0.509	0.190	0.216	0.254	0.095
LAWM19	Ph1	18.80	54.12	36.13	0.505	0.554	0.184	0.252	0.277	0.092
LAWM20	Ph1	58.05	343.60	147.50	2.670	2.724	0.751	1.335	1.362	0.376
LAWM21	Ph1	30.16	70.94	61.49	0.891	0.955	0.313	0.445	0.478	0.156
LAWM22	Ph1	8.53	78.57	56.35	0.393	0.624	0.287	0.196	0.312	0.144
LAWM23	Ph1	6.06	37.94	45.74	0.278	0.510	0.202	0.139	0.255	0.101
LAWM24	Ph1	39.26	103.80	62.85	1.053	0.823	0.286	0.527	0.412	0.143
LAWM25R1	Ph1	30.37	42.73	61.98	0.814	0.575	0.265	0.407	0.288	0.133
LAWM26	Ph1	15.77	26.37	48.99	0.423	0.355	0.210	0.211	0.178	0.105
LAWM27	Ph1	15.00	84.37	49.29	0.690	0.850	0.251	0.345	0.425	0.125
LAWM28	Ph1	13.77	39.23	49.44	0.369	0.528	0.211	0.184	0.264	0.106
LAWM29	Ph1	10.96	36.31	60.93	0.504	0.489	0.278	0.252	0.245	0.139
LAWM30	Ph1	43.96	129.00	60.51	1.179	1.023	0.308	0.590	0.511	0.154
LAWM31	Ph1	49.43	272.20	146.40	2.273	2.190	0.740	1.136	1.095	0.370
LAWM32	Ph1	43.46	225.00	202.30	1.999	1.837	0.865	0.999	0.918	0.433
LAWM33R1	Ph1	159.50	518.70	179.50	4.278	4.111	0.914	2.139	2.056	0.457
LAWM34	Ph1	135.50	538.00	234.40	5.221	4.265	1.194	2.611	2.132	0.597
LAWM35	Ph1	392.50	836.00	168.90	10.526	6.625	0.860	5.263	3.313	0.430
LAWM36	Ph1	16.70	54.06	49.52	0.489	0.607	0.235	0.244	0.304	0.118

(a) 7-Day PCT, stainless steel vessel with S/V = 2000 m<sup>-1</sup>. The PCT concentrations (ppm) are as measured from the PCTs on the glasses. Normalized concentrations (g/L) and normalized mass losses (g/m<sup>2</sup>) are normalized based on the normalized compositions discussed in Section 3.3.

(b) The Group IDs are described in Sections 2.1 to 2.7.

**Table 4.2. PCT Results<sup>(a)</sup> for Simulated and Actual LAW Glasses (continued).**

Glass ID	Group ID <sup>(b)</sup>	Concentration (ppm)			Normalized Concentration (g/L)			Normalized Mass Loss (g/m <sup>2</sup> )		
		B	Na	Si	B	Na	Si	B	Na	Si
LAWM37	Ph1	42.29	87.79	65.99	1.237	0.985	0.313	0.618	0.493	0.157
LAWM38	Ph1	9.50	71.16	58.99	0.383	0.685	0.263	0.191	0.343	0.131
LAWM39	Ph1	15.11	48.09	47.67	0.537	0.463	0.212	0.268	0.231	0.106
LAWM40	Ph1	26.25	75.38	65.45	0.768	0.725	0.292	0.384	0.363	0.146
LAWM41	Ph1	8.95	60.85	49.26	0.360	0.586	0.234	0.180	0.293	0.117
LAWM42	Ph1	13.23	60.31	60.31	0.532	0.580	0.269	0.266	0.290	0.134
LAWM43	Ph1	17.73	58.03	58.02	0.658	0.652	0.276	0.329	0.326	0.138
LAWM44	Ph1	15.50	50.46	52.35	0.497	0.566	0.233	0.249	0.283	0.117
LAWM45	Ph1	10.60	60.82	51.51	0.426	0.585	0.229	0.213	0.293	0.115
LAWM46	Ph1	16.35	41.60	40.86	0.478	0.466	0.182	0.239	0.233	0.091
LAWM47	Ph1	12.96	75.99	60.47	0.521	0.731	0.269	0.261	0.366	0.135
LAWM48	Ph1	16.01	50.77	51.75	0.468	0.569	0.230	0.234	0.285	0.115
LAWM49	Ph1	18.16	52.35	47.81	0.536	0.504	0.215	0.268	0.252	0.108
LAWM50	Ph1	19.49	61.17	55.67	0.647	0.630	0.253	0.324	0.315	0.127
LAWM51	Ph1	20.84	69.67	57.32	0.692	0.717	0.261	0.346	0.359	0.131
LAWM52	Ph1	43.56	172.50	84.73	1.444	1.161	0.411	0.722	0.581	0.206
LAWM53	Ph1	3.34	9.95	23.67	0.178	0.267	0.114	0.089	0.134	0.057
LAWM54R1	Ph1	6.94	13.64	32.05	0.372	0.367	0.138	0.186	0.184	0.069
LAWM55	Ph1	1440.00	2426.00	441.80	35.657	22.937	2.239	17.829	11.469	1.120
LAWM56	Ph1	543.10	1233.00	209.50	14.603	9.797	1.069	7.302	4.898	0.535
LAWM57	Ph1aAug	89.86	315.50	77.19	2.630	2.062	0.420	1.315	1.031	0.210
LAWM58	Ph1aAug	63.64	250.30	77.06	2.205	1.643	0.396	1.102	0.821	0.198
LAWM59	Ph1aAug	21.54	133.40	71.36	0.770	0.899	0.343	0.385	0.449	0.171
LAWM60	Ph1aAug	80.87	265.50	106.00	2.366	1.788	0.500	1.183	0.894	0.250
LAWM61	Ph1aAug	125.00	409.30	163.20	3.659	2.758	0.775	1.829	1.379	0.387
LAWM62	Ph1aAug	41.95	185.90	83.63	1.500	1.253	0.403	0.750	0.626	0.202
LAWM63	Ph1aAug	72.72	326.70	108.50	2.491	1.915	0.545	1.245	0.957	0.272
LAWM64	Ph1aAug	66.74	231.80	69.64	1.956	1.558	0.388	0.978	0.779	0.194
LAWM65	Ph1aAug	73.73	384.90	167.70	2.638	2.276	0.823	1.319	1.138	0.411
LAWM66	Ph1aAug	72.76	267.50	71.33	2.203	1.568	0.398	1.101	0.784	0.199

(a) 7-Day PCT, stainless steel vessel with S/V = 2000 m<sup>-1</sup>. The PCT concentrations (ppm) are as measured from the PCTs on the glasses. Normalized concentrations (g/L) and normalized mass losses (g/m<sup>2</sup>) are normalized based on the normalized compositions discussed in Section 3.3.

(b) The Group IDs are described in Sections 2.1 to 2.7.

**Table 4.2. PCT Results<sup>(a)</sup> for Simulated and Actual LAW Glasses (continued).**

Glass ID	Group ID <sup>(b)</sup>	Concentration (ppm)			Normalized Concentration (g/L)			Normalized Mass Loss (g/m <sup>2</sup> )		
		B	Na	Si	B	Na	Si	B	Na	Si
LAWM67	Ph1aAug	88.73	296.20	62.95	2.695	1.983	0.351	1.348	0.992	0.175
LAWM68	Ph1aAug	135.70	519.20	182.90	4.854	3.498	0.959	2.427	1.749	0.479
LAWM69	Ph1aAug	54.23	198.20	70.75	1.589	1.330	0.382	0.794	0.665	0.191
LAWM70	Ph1aAug	93.88	387.30	149.50	3.217	2.609	0.705	1.608	1.304	0.353
LAWM71	Ph1aAug	122.60	521.60	216.50	4.386	3.515	1.031	2.193	1.757	0.515
LAWM72	Ph1aAug	107.90	390.80	86.34	3.158	2.628	0.472	1.579	1.314	0.236
LAWM73	Ph1aAug	55.56	361.50	108.90	1.987	2.118	0.577	0.993	1.059	0.288
LAWM74	Ph1aAug	29.64	180.90	78.97	1.059	1.143	0.372	0.530	0.572	0.186
LAWM75	Ph1aAug	31.92	180.20	64.77	1.122	1.174	0.360	0.561	0.587	0.180
LAWM76	Ph1aAug	73.17	310.50	90.66	2.374	1.955	0.463	1.187	0.978	0.232
LAWE2H	Corr	75.57	301.10	97.86	2.495	1.953	0.493	1.248	0.977	0.247
LAWE3	Corr	59.18	191.00	73.49	1.905	1.413	0.366	0.953	0.707	0.183
LAWE3H	Corr	87.08	326.10	99.90	2.878	2.226	0.511	1.439	1.113	0.255
LAWE4H	Corr	38.34	189.70	87.92	1.260	1.201	0.422	0.630	0.601	0.211
LAWE5H	Corr	23.95	129.80	78.42	0.785	0.921	0.372	0.393	0.461	0.186
LAWE7H	Corr	32.72	103.20	81.85	1.066	1.027	0.391	0.533	0.513	0.195
LAWE9H	Corr	20.45	46.46	63.16	0.662	0.699	0.288	0.331	0.350	0.144
LAWE10H	Corr	14.08	18.38	47.87	0.454	0.432	0.209	0.227	0.216	0.104
LAWE11	Corr	34.03	116.80	64.50	1.095	0.906	0.315	0.547	0.453	0.158
LAWE12	Corr	65.27	310.40	92.75	2.401	2.119	0.474	1.201	1.059	0.237
LAWE13	Corr	76.16	289.60	77.66	2.514	1.977	0.397	1.257	0.988	0.198
LAWE14	Corr	90.46	352.40	99.31	2.986	2.405	0.490	1.493	1.203	0.245
LAWE15	Corr	61.81	300.50	90.10	2.274	2.051	0.450	1.137	1.026	0.225
LAWE16	Corr	42.48	238.80	83.97	1.660	1.632	0.420	0.830	0.816	0.210
LAWE3Cr2CCC	Corr	36.28	148.40	67.82	1.168	1.098	0.348	0.584	0.549	0.174
LAWE9HCr1CCC	Corr	12.50	30.18	42.25	0.405	0.455	0.195	0.203	0.227	0.098
LAWE9HCr2CCC	Corr	15.54	32.43	41.86	0.504	0.489	0.193	0.252	0.244	0.096
LAWE10HCr3CCC	Corr	8.21	12.14	32.85	0.265	0.286	0.144	0.133	0.143	0.072
LAWCrP1R	HiCrP	17.55	94.13	61.09	0.565	0.656	0.294	0.283	0.328	0.147
LAWCrP2R	HiCrP	34.65	161.78	76.04	1.116	1.039	0.378	0.558	0.519	0.189

(a) 7-Day PCT, stainless steel vessel with S/V = 2000 m<sup>-1</sup>. The PCT concentrations (ppm) are as measured from the PCTs on the glasses. Normalized concentrations (g/L) and normalized mass losses (g/m<sup>2</sup>) are normalized based on the normalized compositions discussed in Section 3.3.

(b) The Group IDs are described in Sections 2.1 to 2.7.

**Table 4.2. PCT Results<sup>(a)</sup> for Simulated and Actual LAW Glasses (continued).**

Glass ID	Group ID <sup>(b)</sup>	Concentration (ppm)			Normalized Concentration (g/L)			Normalized Mass Loss (g/m <sup>2</sup> )		
		B	Na	Si	B	Na	Si	B	Na	Si
LAWCrP3R	HiCrP	23.31	121.59	73.34	0.751	0.847	0.361	0.375	0.424	0.181
LAWCrP4R	HiCrP	27.14	136.18	76.89	0.874	0.874	0.392	0.437	0.437	0.196
LAWCrP5	HiCrP	45.53	156.60	102.50	1.464	1.466	0.504	0.732	0.733	0.252
LAWCrP6	HiCrP	20.81	34.18	58.18	0.670	0.576	0.278	0.335	0.288	0.139
LAWCrP7	HiCrP	15.03	14.22	49.94	0.484	0.355	0.229	0.242	0.177	0.114
LAWA41	ActDes	21.95	154.10	80.83	0.942	1.039	0.398	0.471	0.519	0.199
LAWA42	ActDes	43.65	206.40	77.24	1.556	1.391	0.435	0.778	0.695	0.217
LAWA43-1	ActDes	17.59	127.80	57.66	0.766	0.861	0.325	0.383	0.431	0.162
LAWA44	ActDes	20.51	106.10	68.11	0.742	0.715	0.327	0.371	0.357	0.163
LAWA45	ActDes	56.83	152.40	64.00	1.538	1.027	0.307	0.769	0.514	0.154
LAWA49	ActDes	17.18	86.71	63.38	0.621	0.584	0.304	0.311	0.292	0.152
LAWA50	ActDes	17.28	88.98	61.00	0.625	0.600	0.307	0.313	0.300	0.153
LAWA51	ActDes	26.24	69.32	52.5	0.706	0.519	0.241	0.353	0.260	0.121
LAWA52	ActDes	16.36	163.60	67.82	0.851	1.103	0.343	0.425	0.551	0.172
LAWA60	ActDes	20.11	92.50	47.72	0.577	0.623	0.229	0.288	0.312	0.115
LAWA65	ActDes	27.02	194.70	93.65	1.411	1.317	0.476	0.705	0.659	0.238
LAWA76	ActDes	47.77	98.61	76.23	1.409	1.316	0.389	0.705	0.658	0.195
LAWA81	ActDes	21.54	124.30	61.73	0.779	0.838	0.296	0.390	0.419	0.148
LAWA82	ActDes	18.83	99.37	69.19	0.681	0.670	0.332	0.341	0.335	0.166
LAWA83	ActDes	17.09	100.80	66.95	0.618	0.679	0.321	0.309	0.340	0.161
LAWA84	ActDes	16.33	99.20	66.25	0.591	0.669	0.318	0.295	0.334	0.159
LAWA87	ActDes	32.85	163.70	102.10	1.192	1.103	0.491	0.596	0.552	0.246
LAWA89	ActDes	35.12	138.10	74.45	1.166	0.931	0.362	0.583	0.465	0.181
LAWA90	ActDes	29.35	144.50	73.74	0.974	0.974	0.359	0.487	0.487	0.179
LAWA93	ActDes	36.25	79.66	67.04	1.052	1.071	0.339	0.526	0.535	0.170
LAWA96	ActDes	15.14	111.40	70.07	0.617	0.751	0.344	0.308	0.375	0.172
LAWA102R2	ActDes	23.56	94.62	73.07	0.758	0.880	0.335	0.379	0.440	0.168
LAWA104	ActDes	30.99	171.50	84.59	1.162	1.051	0.421	0.581	0.525	0.210
LAWA105	ActDes	49.27	282.30	108.4	1.916	1.585	0.560	0.958	0.793	0.280
LAWA112B14	ActDes	23.83	160.10	75.49	0.778	1.080	0.365	0.389	0.540	0.183

(a) 7-Day PCT, stainless steel vessel with S/V = 2000 m<sup>-1</sup>. The PCT concentrations (ppm) are as measured from the PCTs on the glasses. Normalized concentrations (g/L) and normalized mass losses (g/m<sup>2</sup>) are normalized based on the normalized compositions discussed in Section 3.3.

(b) The Group IDs are described in Sections 2.1 to 2.7.

**Table 4.2. PCT Results<sup>(a)</sup> for Simulated and Actual LAW Glasses (continued).**

Glass ID	Group ID <sup>(b)</sup>	Concentration (ppm)			Normalized Concentration (g/L)			Normalized Mass Loss (g/m <sup>2</sup> )		
		B	Na	Si	B	Na	Si	B	Na	Si
LAWA112B15	ActDes	23.71	154.80	72.46	0.779	1.044	0.352	0.389	0.522	0.176
LAWA125	ActDes	57.18	239.90	88.74	1.929	1.618	0.443	0.964	0.809	0.221
LAWA127R1	ActDes	21.13	82.72	58.43	0.667	0.684	0.273	0.333	0.342	0.136
LAWA127R2	ActDes	23.17	85.36	62.08	0.730	0.706	0.289	0.365	0.353	0.145
LAWA129	ActDes	14.30	101.70	62.28	0.541	0.743	0.280	0.270	0.372	0.140
LAWA133	ActDes	29.89	168.3	92.72	1.081	1.135	0.445	0.541	0.568	0.223
LAWA134	ActDes	28.39	102.5	63.06	0.917	0.779	0.301	0.459	0.390	0.151
LAWA135	ActDes	27.2	93.78	62.68	0.868	0.743	0.296	0.434	0.371	0.148
LAWA136	ActDes	23.85	89.44	61.15	0.761	0.709	0.295	0.380	0.354	0.148
LAWA170	ActDes	39.28	188.80	77.72	1.309	1.279	0.379	0.654	0.639	0.190
LAWB30	ActDes	15.09	27.90	35.13	0.484	0.476	0.176	0.242	0.238	0.088
LAWB31	ActDes	15.65	12.32	44.22	0.415	0.209	0.201	0.208	0.105	0.100
LAWB32	ActDes	23.15	16.70	46.28	0.492	0.284	0.210	0.246	0.142	0.105
LAWB33	ActDes	14.29	13.65	43.22	0.379	0.232	0.197	0.190	0.116	0.098
LAWB34	ActDes	16.22	14.69	43.77	0.431	0.250	0.199	0.215	0.125	0.099
LAWB35	ActDes	37.43	40.06	62.19	0.993	0.681	0.283	0.497	0.341	0.141
LAWB37	ActDes	19.16	20.79	47.44	0.510	0.354	0.216	0.255	0.177	0.108
LAWB38	ActDes	18.72	20.73	49.79	0.499	0.354	0.227	0.249	0.177	0.114
LAWB40	ActDes	119.20	137.60	142.10	3.185	2.356	0.650	1.592	1.178	0.325
LAWB41	ActDes	63.73	82.37	83.63	1.701	1.408	0.382	0.850	0.704	0.191
LAWB60	ActDes	16.95	21.83	42.83	0.441	0.452	0.191	0.221	0.226	0.096
LAWB61	ActDes	24.13	27.36	63.49	0.780	0.670	0.279	0.390	0.335	0.140
LAWB62	ActDes	10.02	14.47	37.81	0.324	0.355	0.167	0.162	0.178	0.083
LAWB63	ActDes	11.15	14.12	37.7	0.361	0.346	0.165	0.180	0.173	0.082
LAWB64	ActDes	17.25	19.89	47.79	0.557	0.487	0.210	0.279	0.244	0.105
LAWB67	ActDes	14.98	11.51	50.91	0.485	0.283	0.225	0.243	0.141	0.112
LAWB69	ActDes	18.82	23.44	44.25	0.491	0.477	0.197	0.246	0.239	0.099
LAWB70	ActDes	42.81	46.00	69.01	1.116	0.935	0.307	0.558	0.468	0.154
LAWB71	ActDes	21.50	27.19	52.44	0.641	0.553	0.233	0.320	0.276	0.117
LAWB72	ActDes	33.65	37.78	58.14	0.878	0.769	0.259	0.439	0.384	0.130

(a) 7-Day PCT, stainless steel vessel with S/V = 2000 m<sup>-1</sup>. The PCT concentrations (ppm) are as measured from the PCTs on the glasses. Normalized concentrations (g/L) and normalized mass losses (g/m<sup>2</sup>) are normalized based on the normalized compositions discussed in Section 3.3.

(b) The Group IDs are described in Sections 2.1 to 2.7.

**Table 4.2. PCT Results<sup>(a)</sup> for Simulated and Actual LAW Glasses (continued).**

Glass ID	Group ID <sup>(b)</sup>	Concentration (ppm)			Normalized Concentration (g/L)			Normalized Mass Loss (g/m <sup>2</sup> )		
		B	Na	Si	B	Na	Si	B	Na	Si
LAWB73	ActDes	12.74	15.47	39.51	0.412	0.380	0.174	0.206	0.190	0.087
LAWB74	ActDes	14.50	16.34	41.88	0.462	0.400	0.184	0.231	0.200	0.092
LAWB75	ActDes	12.57	11.73	36.10	0.343	0.288	0.159	0.172	0.144	0.080
LAWB76	ActDes	15.37	14.64	42.69	0.420	0.360	0.185	0.210	0.180	0.093
LAWB77	ActDes	27.73	29.53	52.03	0.723	0.600	0.232	0.362	0.300	0.116
LAWB81	ActDes	34.46	38.59	59.15	0.899	0.785	0.264	0.450	0.393	0.132
LAWB82	ActDes	15.58	22.43	39.85	0.497	0.456	0.187	0.248	0.228	0.094
LAWB87	ActDes	21.40	15.47	50.52	0.529	0.416	0.220	0.265	0.208	0.110
LAWB88	ActDes	15.86	11.90	43.30	0.393	0.320	0.185	0.196	0.160	0.092
LAWB89	ActDes	18.60	14.08	58.47	0.597	0.465	0.253	0.298	0.232	0.127
LAWB90	ActDes	19.41	27.78	57.26	0.622	0.544	0.255	0.311	0.272	0.128
LAWB91	ActDes	24.65	44.92	62.79	0.790	0.693	0.287	0.395	0.347	0.143
LAWB92	ActDes	28.43	59.63	64.66	0.912	0.794	0.300	0.456	0.397	0.150
LAWB93	ActDes	26.69	17.55	52.00	0.856	0.494	0.227	0.428	0.247	0.114
LAWB94	ActDes	22.12	11.75	52.87	0.710	0.468	0.228	0.355	0.234	0.114
LAWB95	ActDes	20.85	8.02	51.49	0.669	0.440	0.219	0.335	0.220	0.110
LAWB96	ActDes	17.14	22.96	54.92	0.550	0.565	0.241	0.275	0.282	0.121
LAWC12	ActDes	23.81	121.40	67.79	0.839	0.817	0.368	0.419	0.409	0.184
LAWC15	ActDes	18.29	99.49	67.59	0.660	0.672	0.323	0.330	0.336	0.162
LAWC21	ActDes	20.47	62.94	56.73	0.652	0.713	0.260	0.326	0.357	0.130
LAWC21rev2	ActDes	21.63	63.84	60.18	0.692	0.719	0.275	0.346	0.359	0.138
LAWC22	ActDes	32.32	100.20	78.92	1.035	0.937	0.362	0.517	0.469	0.181
LAWC23	ActDes	14.98	48.19	41.75	0.479	0.548	0.191	0.239	0.274	0.096
LAWC24	ActDes	13.45	48.22	38.94	0.442	0.563	0.183	0.221	0.282	0.092
LAWC25	ActDes	18.93	64.06	45.12	0.640	0.770	0.219	0.320	0.385	0.109
LAWC26	ActDes	28.16	58.95	50.07	0.684	0.664	0.214	0.342	0.332	0.107
LAWC28	ActDes	8.92	38.91	35.72	0.286	0.439	0.164	0.143	0.219	0.082
LAWC29	ActDes	9.46	36.73	36.23	0.303	0.414	0.164	0.152	0.207	0.082
LAWC30	ActDes	18.64	58.26	56.64	0.597	0.656	0.259	0.299	0.328	0.130
LAWC31	ActDes	17.14	55.568	52.25	0.549	0.626	0.239	0.275	0.313	0.120

(a) 7-Day PCT, stainless steel vessel with S/V = 2000 m<sup>-1</sup>. The PCT concentrations (ppm) are as measured from the PCTs on the glasses. Normalized concentrations (g/L) and normalized mass losses (g/m<sup>2</sup>) are normalized based on the normalized compositions discussed in Section 3.3.

(b) The Group IDs are described in Sections 2.1 to 2.7.

**Table 4.2. PCT Results<sup>(a)</sup> for Simulated and Actual LAW Glasses (continued).**

Glass ID	Group ID <sup>(b)</sup>	Concentration (ppm)			Normalized Concentration (g/L)			Normalized Mass Loss (g/m <sup>2</sup> )		
		B	Na	Si	B	Na	Si	B	Na	Si
LAWC33	ActDes	21.97	67.90	66.05	0.700	0.762	0.301	0.350	0.381	0.150
TFA-BASE	ActDes	24.39	96.56	73.52	0.785	0.651	0.321	0.393	0.325	0.160
C22AN107	ActDes	35.50	119.10	89.75	1.134	1.112	0.412	0.567	0.556	0.206
A88AP101R1	ActDes	41.9	173.50	84.97	1.372	1.169	0.412	0.686	0.584	0.206
A88Si+15	ActDes	73.03	329.40	113.80	2.480	2.002	0.572	1.240	1.001	0.286
A88Si-15	ActDes	20.58	85.62	65.56	0.649	0.653	0.306	0.324	0.327	0.153
C22Si+15	ActDes	40.8	154.60	103.50	1.336	1.287	0.486	0.668	0.643	0.243
C22Si-15	ActDes	28.27	83.41	75.62	0.885	0.878	0.339	0.442	0.439	0.170
A1C1-1	ActDes	24.89	119.60	80.57	0.878	0.841	0.388	0.439	0.421	0.194
A1C1-2	ActDes	24.22	113.80	78.19	0.828	0.868	0.371	0.414	0.434	0.185
A1C1-3	ActDes	27.52	98.33	78.73	0.913	0.820	0.368	0.457	0.410	0.184
C1-AN107	ActDes	32.01	113.80	89.64	1.028	1.060	0.411	0.514	0.530	0.206
A2-AP101	ActDes	47.46	152.90	81.65	1.556	1.116	0.397	0.778	0.558	0.198
A2B1-1	ActDes	21.89	73.11	68.79	0.713	0.647	0.326	0.357	0.324	0.163
A2B1-2	ActDes	21.03	53.68	65.29	0.683	0.604	0.302	0.341	0.302	0.151
B1-AZ101	ActDes	24.30	21.52	58.04	0.780	0.529	0.256	0.390	0.265	0.128
C2-AN102C35	ActDes	19.82	66.86	64.19	0.677	0.752	0.290	0.338	0.376	0.145
A3-AN104	ActDes	33.32	115.10	84.50	1.081	1.060	0.392	0.541	0.530	0.196
A2B1-3	ActDes	25.69	42.45	66.61	0.830	0.655	0.300	0.415	0.328	0.150
A3C2-1	ActDes	33.46	110.60	85.04	1.100	1.067	0.392	0.550	0.533	0.196
A3C2-2	ActDes	32.84	109.30	83.64	1.092	1.106	0.383	0.546	0.553	0.192
A3C2-3	ActDes	24.46	80.38	70.98	0.825	0.857	0.323	0.413	0.428	0.162
A1-AN105R2	ActDes	29.15	153.60	81.50	1.062	1.002	0.398	0.531	0.501	0.199
12U-G-86A	ActDes	22.43	113.80	75.10	0.807	0.768	0.362	0.403	0.384	0.181
LA44PNCC	ActDes	18.36	99.80	69.67	0.666	0.672	0.335	0.333	0.336	0.168
LA44CCCR2	ActDes	18.19	107.30	79.34	0.660	0.723	0.382	0.330	0.361	0.191
WVF-G-21B	ActDes	25.39	108.80	66.35	0.834	0.733	0.323	0.417	0.367	0.161
PNLA126CC	ActDes	27.40	107.50	64.91	0.895	0.785	0.314	0.448	0.392	0.157
LA126CCC	ActDes	28.93	116.90	67.41	0.945	0.853	0.326	0.473	0.427	0.163
WVM-G-142C	ActDes	34.98	140.80	73.34	1.146	1.028	0.357	0.573	0.514	0.178

(a) 7-Day PCT, stainless steel vessel with S/V = 2000 m<sup>-1</sup>. The PCT concentrations (ppm) are as measured from the PCTs on the glasses. Normalized concentrations (g/L) and normalized mass losses (g/m<sup>2</sup>) are normalized based on the normalized compositions discussed in Section 3.3.

(b) The Group IDs are described in Sections 2.1 to 2.7.

**Table 4.2. PCT Results<sup>(a)</sup> for Simulated and Actual LAW Glasses (continued).**

Glass ID	Group ID <sup>(b)</sup>	Concentration (ppm)			Normalized Concentration (g/L)			Normalized Mass Loss (g/m <sup>2</sup> )		
		B	Na	Si	B	Na	Si	B	Na	Si
A100G115A	ActDes	30.03	96.27	74.41	0.966	0.897	0.342	0.483	0.448	0.171
A100CC	ActDes	22.14	70.02	67.77	0.712	0.652	0.311	0.356	0.326	0.156
WVB-G-124B	ActDes	24.96	88.79	72.99	0.806	0.830	0.336	0.403	0.415	0.168
LA137SRCCC	ActDes	33.31	104.90	89.68	1.082	0.966	0.416	0.541	0.483	0.208
WVR-G-127A	ActDes	24.82	85.78	73.30	0.807	0.791	0.341	0.403	0.395	0.170
LB83PNCC	ActDes	14.55	18.47	47.09	0.466	0.463	0.207	0.233	0.232	0.103
LB83CCC-1	ActDes	16.30	17.68	50.92	0.522	0.443	0.224	0.261	0.222	0.112
WVJ-G-109D	ActDes	15.35	17.72	44.33	0.493	0.437	0.195	0.247	0.218	0.098
GTSD-1126	ActDes	17.92	22.49	53.44	0.575	0.552	0.234	0.287	0.276	0.117
LB88CCC	ActDes	11.64	10.07	41.19	0.289	0.271	0.176	0.144	0.136	0.088
AZ-102 Surr SRNL	ActDes	17.70	15.29	45.30	0.439	0.406	0.194	0.220	0.203	0.097
12S-G-85C	ActDes	21.13	71.15	68.34	0.677	0.665	0.315	0.338	0.332	0.157
C100GCC	ActDes	14.51	42.65	46.28	0.463	0.484	0.212	0.231	0.242	0.106
AN-102 Surr LC Melter	ActDes	13.40	43.70	51.90	0.425	0.499	0.237	0.213	0.250	0.119
WVH-G-57B	ActDes	14.97	43.01	44.52	0.481	0.486	0.204	0.240	0.243	0.102
GTSD-1437	ActDes	20.71	65.32	65.34	0.705	0.732	0.294	0.352	0.366	0.147
PLTC35CCC	ActDes	14.86	54.98	63.92	0.506	0.616	0.288	0.253	0.308	0.144
AN-103 Actual	Actual	20.00	113.20	69.60	0.720	0.763	0.333	0.360	0.381	0.167
AW-101 Actual	Actual	33.27	154.33	77.27	1.103	1.040	0.375	0.552	0.520	0.188
AP-101 Actual	Actual	39.83	177.00	87.77	1.302	1.292	0.424	0.651	0.646	0.212
AZ-101 Actual	Actual	16.07	20.47	50.77	0.515	0.516	0.223	0.258	0.258	0.112
AZ-102 Actual	Actual	16.10	11.80	42.40	0.399	0.318	0.182	0.200	0.159	0.091
AZ-102 Actual CCC	Actual	12.80	10.10	37.10	0.317	0.272	0.159	0.159	0.136	0.079
AN-107 Actual (LAWC15)	Actual	18.77	114.67	76.50	0.676	0.773	0.365	0.338	0.386	0.183
AN-102 Actual LC Melter	Actual	12.60	35.70	50.50	0.402	0.408	0.231	0.201	0.204	0.115
AN-102 Actual	Actual	19.40	62.90	57.10	0.617	0.719	0.261	0.308	0.359	0.131

(a) 7-Day PCT, stainless steel vessel with S/V = 2000 m<sup>-1</sup>. The PCT concentrations (ppm) are as measured from the PCTs on the glasses. Normalized concentrations (g/L) and normalized mass losses (g/m<sup>2</sup>) are normalized based on the normalized compositions discussed in Section 3.3.

(b) The Group IDs are described in Sections 2.1 to 2.7.



**Table 4.3. VHT Results for Simulated and Actual LAW Glasses.**

Glass ID	Group ID <sup>(a)</sup>	Alteration Depth (µm)	Days	Measured Density (g/cc)	Rate (g/m <sup>2</sup> /d) Calculated for Measured Density or Estimated Average Value of 2.65 g/cc	Comparison to Limit of 50 g/m <sup>2</sup> /d
LAWA44R10	ExPh1	9	24.0	2.67	1.0	2%
LAWA53	ExPh1	7	23.5	(b)	0.8	2%
LAWA56	ExPh1	15	23.5	(b)	1.7	3%
LAWA88R1	ExPh1	13	24.0	2.67	1.4	3%
LAWA102R1	ExPh1	34	24.0	2.61	3.7	7%
LAWA126	ExPh1	22	24.0	2.687	2.5	5%
LAWA128	ExPh1	8	24.0	(b)	0.9	2%
LAWA130	ExPh1	6	24.0	(b)	0.7	1%
LAWB65	ExPh1	10	24.0	(b)	1.1	2%
LAWB66	ExPh1	17	24.0	(b)	1.9	4%
LAWB68	ExPh1	18	24.0	(b)	2.0	4%
LAWB78	ExPh1	23	24.0	(b)	2.5	5%
LAWB79	ExPh1	11	24.0	(b)	1.2	2%
LAWB80	ExPh1	10	24.0	(b)	1.1	2%
LAWB83	ExPh1	16	24.0	2.75	1.8	4%
LAWB84	ExPh1	15	24.0	(b)	1.7	3%
LAWB85	ExPh1	11	24.0	(b)	1.2	2%
LAWB86	ExPh1	15	24.0	(b)	1.7	3%
C100G136B	ExPh1	23	24.0	2.65	2.5	5%
LAWC27	ExPh1	177	24.0	(b)	19.5	39%
LAWC32	ExPh1	206	24.0	(b)	22.7	45%
LAWM1	Ph1	82	24.0	2.74	9.4	19%
LAWM2	Ph1	75	24.0	2.76	8.6	17%
LAWM3	Ph1	34	24.0	2.65	3.8	8%
LAWM4	Ph1	5	24.0	2.72	0.6	1%
LAWM5	Ph1	7	24.0	2.80	0.8	2%
LAWM6	Ph1	19	24.0	2.66	2.1	4%
LAWM7	Ph1	26	24.0	2.66	2.9	6%
LAWM8	Ph1	13	24.0	2.85	1.5	3%
LAWM9	Ph1	1	24.0	2.66	0.1	0%
LAWM10	Ph1	114	24.0	2.65	12.6	25%
LAWM11	Ph1	700	24.0	2.62	76.5	153%
LAWM12	Ph1	> 1100	24.0	2.68	> 122	> 246%
LAWM13	Ph1	> 1100	24.0	2.61	> 119	> 239%
LAWM14	Ph1	> 1000	24.0	2.62	> 120	> 241%
LAWM15	Ph1	856	24.0	2.67	95.1	190%
LAWM16	Ph1	71	24.0	2.65	7.8	16%
LAWM17	Ph1	3	24.0	2.65	0.3	1%
LAWM18	Ph1	15	24.0	2.57	1.6	3%
LAWM19	Ph1	1	24.0	2.58	0.1	0%
LAWM20	Ph1	116	24.0	2.83	13.7	27%
LAWM21	Ph1	9	24.0	2.77	1.0	2%

(a) The Group IDs are described in Sections 2.1 to 2.6.

(b) Density was not measured and an estimated average value of 2.65 was used (note that the calculated rate may differ slightly from previous reports where a density of 2.655 was used).

**Table 4.3. VHT Results for Simulated and Actual LAW Glasses (continued).**

Glass ID	Group ID <sup>(a)</sup>	Alteration Depth (μm)	Days	Measured Glass Density (g/cc)	Rate (g/m <sup>2</sup> /d) Calculated for Measured Density or Estimated Average Value of 2.65 g/cc	Comparison to Limit of 50 g/m <sup>2</sup> /d
LAWM22	Ph1	2	24.0	2.70	0.2	0%
LAWM23	Ph1	9	24.0	2.70	1.0	2%
LAWM24	Ph1	123	24.0	2.67	13.7	27%
LAWM25R1	Ph1	41	24.0	2.48	4.2	8%
LAWM26	Ph1	31	24.0	2.62	3.4	7%
LAWM27	Ph1	45	24.0	2.70	5.1	10%
LAWM28	Ph1	6	24.0	2.58	0.7	1%
LAWM29	Ph1	9	24.0	2.67	1.0	2%
LAWM30	Ph1	181	24.0	2.72	21.3	43%
LAWM31	Ph1	48	24.0	2.73	5.5	11%
LAWM32	Ph1	> 1100	24.0	2.63	> 120	> 241%
LAWM33R1	Ph1	34	24.0	2.67	3.8	8%
LAWM34	Ph1	420	24.0	2.78	48.7	97%
LAWM35	Ph1	4	24.0	2.53	1.0	2%
LAWM36	Ph1	107	24.0	2.54	11.3	23%
LAWM37	Ph1	10	24.0	2.58	1.1	2%
LAWM38	Ph1	171	24.0	2.76	19.7	39%
LAWM39	Ph1	112	24.0	2.65	12.4	25%
LAWM40	Ph1	3	24.0	2.49	0.3	1%
LAWM41	Ph1	43	24.0	2.65	4.8	9%
LAWM42	Ph1	7	24.0	2.65	0.8	2%
LAWM43	Ph1	9	24.0	2.66	1.0	2%
LAWM44	Ph1	20	24.0	2.55	2.2	4%
LAWM45	Ph1	44	24.0	2.70	5.0	10%
LAWM46	Ph1	3	24.0	2.66	0.3	1%
LAWM47	Ph1	25	24.0	2.77	2.9	6%
LAWM48	Ph1	5	24.0	2.85	0.6	1%
LAWM49	Ph1	23	24.0	2.57	2.5	5%
LAWM50	Ph1	4	24.0	2.66	0.4	1%
LAWM51	Ph1	5	24.0	2.59	0.5	1%
LAWM52	Ph1	28	24.0	2.65	3.1	6%
LAWM53	Ph1	90	24.0	2.73	10.2	20%
LAWM54R1	Ph1	3	24.0	2.52	0.3	1%
LAWM55	Ph1	> 1100	24.0	2.73	> 125	> 250%
LAWM56	Ph1	6	24.0	2.73	0.7	1%
LAWM57	Ph1aAug	142	24.0	(b)	15.7	31%
LAWM58	Ph1aAug	157	24.0	(b)	17.3	35%
LAWM59	Ph1aAug	134	24.0	(b)	14.8	30%
LAWM60	Ph1aAug	30	24.0	(b)	3.3	7%
LAWM61	Ph1aAug	361	24.0	(b)	39.9	80%
LAWM62	Ph1aAug	115	24.0	(b)	12.7	25%
LAWM63	Ph1aAug	655	24.0	(b)	72.3	145%

(a) The Group IDs are described in Sections 2.1 to 2.6.

(b) Density was not measured and an estimated average value of 2.65 was used (note that the calculated rate may differ slightly from previous reports where a density of 2.655 was used).

**Table 4.3. VHT Results for Simulated and Actual LAW Glasses (continued).**

Glass ID	Group ID <sup>(a)</sup>	Alteration Depth (μm)	Days	Measured Glass Density (g/cc)	Rate (g/m <sup>2</sup> /d) Calculated for Measured Density or Estimated Average Value of 2.65 g/cc	Comparison to Limit of 50 g/m <sup>2</sup> /d
LAWM64	Ph1aAug	27	24.0	(b)	3.0	6%
LAWM65	Ph1aAug	522	24.0	(b)	57.6	115%
LAWM66	Ph1aAug	445	24.0	(b)	49.1	98%
LAWM67	Ph1aAug	260	24.0	(b)	28.7	57%
LAWM68	Ph1aAug	234	24.0	(b)	25.8	52%
LAWM69	Ph1aAug	283	24.0	(b)	31.2	62%
LAWM70	Ph1aAug	813	24.0	(b)	89.8	180%
LAWM71	Ph1aAug	980	24.0	(b)	108.2	216%
LAWM72	Ph1aAug	495	24.0	(b)	54.7	109%
LAWM73	Ph1aAug	472	24.0	(b)	52.1	104%
LAWM74	Ph1aAug	14	24.0	(b)	1.5	3%
LAWM75	Ph1aAug	7	24.0	(b)	0.8	2%
LAWM76	Ph1aAug	90	24.0	(b)	9.9	20%
LAWA104	ActDes	59	24.0	(b)	6.5	13%
LAWA105	ActDes	359	24.0	(b)	39.6	79%
LAWA49	ActDes	30	23.5	2.64	3.4	7%
LAWA51	ActDes	5	23.5	(b)	0.6	1%
LAWA52	ActDes	67	23.5	(b)	7.6	15%
LAWA60	ActDes	56	24.0	2.64	6.2	12%
LAWC15	ActDes	5	24.0	2.68	0.6	1%
TFA-BASE	ActDes	86	23.5	(b)	9.7	19%
LAWA133	ActDes	5	24.0	(b)	0.6	1%
LAWA134	ActDes	2	24.0	(b)	0.2	0%
LAWA135	ActDes	3	24.0	(b)	0.3	1%
LAWA136	ActDes	3	24.0	(b)	0.3	1%
LAWB60	ActDes	68	24.0	(b)	7.5	15%
LAWB62	ActDes	37	24.0	(b)	4.1	8%
LAWB63	ActDes	72	24.0	(b)	8.0	16%
LAWB64	ActDes	15	24.0	(b)	1.7	3%
LAWB67	ActDes	15	24.0	(b)	1.7	3%
LAWB69	ActDes	128	24.0	(b)	14.1	28%
LAWB70	ActDes	31	24.0	(b)	3.4	7%
LAWB71	ActDes	12	24.0	(b)	1.3	3%
LAWB72	ActDes	23	24.0	(b)	2.5	5%
LAWB73	ActDes	31	24.0	(b)	3.4	7%
LAWB74	ActDes	52	24.0	(b)	5.7	11%
LAWB75	ActDes	59	24.0	(b)	6.5	13%
LAWB76	ActDes	78	24.0	(b)	8.6	17%
LAWB77	ActDes	17	24.0	(b)	1.9	4%
LAWB81	ActDes	24	24.0	(b)	2.7	5%
LAWB82	ActDes	32	24.0	(b)	3.5	7%
LAWB89	ActDes	16	24.0	(b)	1.8	4%

(a) The Group IDs are described in Sections 2.1 to 2.6.

(b) Density was not measured and an estimated average value of 2.65 was used (note that the calculated rate may differ slightly from previous reports where a density of 2.655 was used).

**Table 4.3. VHT Results for Simulated and Actual LAW Glasses (continued).**

Glass ID	Group ID <sup>(a)</sup>	Alteration Depth (μm)	Days	Measured Glass Density (g/cc)	Rate (g/m <sup>2</sup> /d) Calculated for Measured Density or Estimated Average Value of 2.65 g/cc	Comparison to Limit of 50 g/m <sup>2</sup> /d
LAWB90	ActDes	14	24.0	(b)	1.5	3%
LAWB91	ActDes	12	24.0	(b)	1.3	3%
LAWB92	ActDes	10	24.0	(b)	1.1	2%
LAWB93	ActDes	15	24.0	(b)	1.7	3%
LAWB94	ActDes	14	24.0	(b)	1.5	3%
LAWB95	ActDes	11	24.0	(b)	1.2	2%
C22AN107	ActDes	9	24.0	(b)	1.0	2%
LAWC26	ActDes	22	24.0	(b)	2.4	5%
LAWC28	ActDes	92	24.0	(b)	10.2	20%
LAWC29	ActDes	106	24.0	(b)	11.7	23%
LAWC30	ActDes	60	24.0	(b)	6.6	13%
LAWC31	ActDes	110	24.0	2.71	12.4	25%
LAWC33	ActDes	17	24.0	(b)	1.9	4%
A88AP101R1	ActDes	13	24.0	(b)	1.4	3%
A88Si+15	ActDes	290	24.0	(b)	32.0	64%
A88Si-15	ActDes	4	24.0	(b)	0.4	1%
C22Si+15	ActDes	23	24.0	(b)	2.5	5%
C22Si-15	ActDes	29	24.0	(b)	3.2	6%
A1C1-1	ActDes	6	24.0	(b)	0.7	1%
A1C1-2	ActDes	31	24.0	(b)	3.4	7%
A1C1-3	ActDes	6	24.0	(b)	0.7	1%
C1-AN107	ActDes	80	24.0	(b)	8.8	18%
A2-AP101	ActDes	7	24.0	2.69	0.8	2%
A2B1-1	ActDes	5	24.7	(b)	0.5	1%
A2B1-2	ActDes	6	24.7	(b)	0.6	1%
B1-AZ101	ActDes	14	24.7	(b)	1.5	3%
C2-AN102C35	ActDes	154	24.0	2.68	17.2	34%
A3-AN104	ActDes	6	24.0	2.68	0.7	1%
LAWE2H	Corr	588	24.0	(b)	64.9	130%
LAWE3H	Corr	644	24.0	(b)	71.1	142%
LAWE3	Corr	129	24.0	(b)	14.2	28%
LAWE4H	Corr	147	24.0	(b)	16.2	32%
LAWE5H	Corr	15	24.0	(b)	1.7	3%
LAWE7	Corr	191	24.0	(b)	21.1	42%
LAWE7H	Corr	152	24.0	(b)	16.8	34%
LAWE9H	Corr	131	24.0	(b)	14.5	29%
LAWE10H	Corr	17	24.0	(b)	1.9	4%
LAWE11	Corr	33	24.0	(b)	3.6	7%
LAWE12	Corr	737	24.0	(b)	81.4	163%
LAWE13	Corr	615	24.0	(b)	67.9	136%
LAWE14	Corr	>800	24.0	(b)	>88	>177%
LAWE15	Corr	485	24.0	(b)	53.6	107%

(a) The Group IDs are described in Sections 2.1 to 2.6.

(b) Density was not measured and an estimated average value of 2.65 was used (note that the calculated rate may differ slightly from previous reports where a density of 2.655 was used).

**Table 4.3. VHT Results for Simulated and Actual LAW Glasses (continued).**

Glass ID	Group ID <sup>(a)</sup>	Alteration Depth (µm)	Days	Measured Glass Density (g/cc)	Rate (g/m <sup>2</sup> /d) Calculated for Measured Density or Estimated Average Value of 2.65 g/cc	Comparison to Limit of 50 g/m <sup>2</sup> /d
LAWE16	Corr	459	24.0	(b)	50.7	101%
LAWA125	ActDes	343	24.0	(b)	37.9	76%
LAWCrP1R	HiCrP	32	23.8	(b)	3.6	7%
LAWCrP2R	HiCrP	216	23.8	(b)	24.1	48%
LAWCrP3R	HiCrP	79	23.8	(b)	8.8	18%
LAWCrP4R	HiCrP	200	23.8	(b)	22.3	45%
LAWB94	ActDes	14	24.0	(b)	1.5	3%
LAWB95	ActDes	11	24.0	(b)	1.2	2%
C22AN107	ActDes	9	24.0	(b)	1.0	2%
LAWC26	ActDes	22	24.0	(b)	2.4	5%
LAWC28	ActDes	92	24.0	(b)	10.2	20%
LAWC29	ActDes	106	24.0	(b)	11.7	23%
LAWC30	ActDes	60	24.0	(b)	6.6	13%
LAWC31	ActDes	110	24.0	2.71	12.4	25%

(a) The Group IDs are described in Sections 2.1 to 2.6.

(b) Density was not measured and an estimated average value of 2.65 was used (note that the calculated rate may differ slightly from previous reports where a density of 2.655 was used).

**Table 4.4. Melt Electrical Conductivity Data for Simulated LAW Glasses.**

Glass ID	Group ID <sup>(a)</sup>	Temp1 (°C)	EC1 (S/cm)	Temp2 (°C)	EC2 (S/cm)	Temp3 (°C)	EC3 (S/cm)	Temp4 (°C)	EC4 (S/cm)
LAWA44R10	ExPh1	1245	0.389	1144	0.274	1053	0.211	957	0.142
LAWA53	ExPh1	1240	0.568	1142	0.426	1045	0.262	946	0.163
LAWA56	ExPh1	1239	0.567	1142	0.426	1044	0.285	946	0.178
LAWA88	ExPh1	1251	0.765	1143	0.554	1044	0.370	949	0.248
LAWA102R1	ExPh1	1240	0.523	1142	0.368	1043	0.238	945	0.156
LAWA126	ExPh1	1240	0.550	1143	0.373	1042	0.258	949	0.171
LAWA128R1	ExPh1	1236	0.530	1146	0.383	1046	0.264	947	0.167
LAWA130	ExPh1	1246	0.557	1157	0.416	1061	0.292	965	0.188
LAWB65	ExPh1	1228	0.305	1127	0.195	1034	0.125	939	0.063
LAWB66	ExPh1	1232	0.368	1137	0.253	1043	0.151	948	0.084
LAWB68	ExPh1	1255	0.325	1156	0.222	1057	0.132	959	0.069
LAWB78	ExPh1	1239	0.352	1141	0.228	1046	0.149	951	0.085
LAWB79	ExPh1	1239	0.338	1142	0.217	1045	0.142	949	0.079
LAWB80	ExPh1	1239	0.264	1138	0.172	1040	0.105	943	0.054
LAWB83	ExPh1	1239	0.323	1141	0.215	1044	0.128	949	0.067
LAWB84	ExPh1	1245	0.339	1147	0.227	1049	0.139	953	0.076
LAWB85	ExPh1	1255	0.353	1157	0.251	1058	0.148	961	0.089
LAWB86	ExPh1	1251	0.338	1153	0.220	1055	0.147	959	0.080
C100-G-136B	ExPh1	1245	0.443	1145	0.299	1045	0.194	944	0.105
LAWC27	ExPh1	1240	0.346	1142	0.246	1045	0.162	954	0.093
LAWC32	ExPh1	1242	0.444	1147	0.315	1051	0.199	958	0.109
LAWM1	Ph1	1253	0.243	1156	0.169	1058	0.101	959	0.052
LAWM2	Ph1	1253	0.284	1162	0.213	1066	0.112	970	0.058
LAWM3	Ph1	1236	0.513	1145	0.357	1051	0.229	957	0.128
LAWM4	Ph1	1252	0.289	1155	0.199	1058	0.119	960	0.062
LAWM5	Ph1	1224	0.248	1127	0.183	1027	0.117	929	0.059
LAWM6	Ph1	1216	0.185	1120	0.113	1022	0.056	923	0.026
LAWM7	Ph1	1238	0.118	1140	0.074	1052	0.042	958	0.021
LAWM8	Ph1	1223	0.140	1124	0.073	1024	0.041	931	0.020
LAWM9	Ph1	1248	0.139	1154	0.097	1057	0.054	963	0.027
LAWM10	Ph1	1244	0.580	1150	0.425	1054	0.289	960	0.166
LAWM11	Ph1	1215	0.609	1117	0.429	1015	0.276	923	0.166
LAWM12	Ph1	1253	0.721	1161	0.553	1068	0.385	973	0.249
LAWM13	Ph1	1242	0.945	1143	0.708	1045	0.498	946	0.284
LAWM14	Ph1	1244	0.693	1151	0.458	1056	0.340	960	0.239
LAWM15	Ph1	1241	0.691	1143	0.573	1044	0.411	946	0.276
LAWM16	Ph1	1238	0.399	1140	0.289	1042	0.182	944	0.094
LAWM17	Ph1	1230	0.628	1132	0.380	1034	0.235	940	0.133
LAWM18	Ph1	1237	0.406	1140	0.281	1043	0.175	947	0.115
LAWM19	Ph1	1227	0.321	1131	0.231	1034	0.135	938	0.069
LAWM20	Ph1	1235	0.699	1138	0.467	1040	0.311	942	0.187
LAWM21	Ph1	1228	0.501	1130	0.318	1032	0.182	934	0.109
LAWM22	Ph1	1231	0.389	1134	0.267	1036	0.181	939	0.112
LAWM23	Ph1	1227	0.374	1131	0.252	1035	0.146	939	0.083
LAWM24	Ph1	1225	0.475	1128	0.345	1030	0.247	933	0.161

(a) The Group IDs are described in Sections 2.1 to 2.6.

**Table 4.4. Melt Electrical Conductivity Data for Simulated LAW Glasses (continued).**

Glass ID	Group ID <sup>(a)</sup>	Temp1 (°C)	EC1 (S/cm)	Temp2 (°C)	EC2 (S/cm)	Temp3 (°C)	EC3 (S/cm)	Temp4 (°C)	EC4 (S/cm)
LAWM25R1	Ph1	1220	0.325	1123	0.220	1028	0.147	927	0.085
LAWM26	Ph1	1239	0.377	1142	0.232	1043	0.142	945	0.085
LAWM27	Ph1	1235	0.282	1137	0.189	1039	0.111	942	0.061
LAWM28	Ph1	1249	0.136	1155	0.096	1060	0.060	966	0.032
LAWM29	Ph1	1236	0.334	1136	0.235	1038	0.136	941	0.081
LAWM30	Ph1	1219	0.282	1123	0.187	1027	0.114	929	0.059
LAWM31	Ph1	1230	0.711	1132	0.536	1034	0.331	937	0.197
LAWM32	Ph1	1248	0.516	1154	0.417	1059	0.296	964	0.190
LAWM33R1	Ph1	1243	0.563	1145	0.506	1046	0.346	949	0.175
LAWM34	Ph1	1230	0.707	1130	0.535	1032	0.365	936	0.195
LAWM35	Ph1	1246	0.425	1152	0.306	1056	0.205	961	0.126
LAWM36	Ph1	1244	0.421	1145	0.293	1047	0.178	949	0.103
LAWM37	Ph1	1237	0.390	1140	0.267	1042	0.165	943	0.101
LAWM38	Ph1	1243	0.484	1145	0.312	1046	0.231	948	0.117
LAWM39	Ph1	1248	0.473	1150	0.335	1050	0.225	951	0.105
LAWM40	Ph1	1249	0.619	1152	0.453	1053	0.297	949	0.094
LAWM41	Ph1	1245	0.348	1148	0.243	1050	0.159	952	0.089
LAWM42	Ph1	1198	0.336	1108	0.236	1017	0.167	927	0.097
LAWM43	Ph1	1243	0.390	1147	0.270	1050	0.183	953	0.108
LAWM44	Ph1	1239	0.267	1142	0.182	1043	0.108	946	0.058
LAWM45	Ph1	1236	0.386	1139	0.285	1041	0.179	944	0.111
LAWM46	Ph1	1252	0.208	1157	0.143	1062	0.091	965	0.052
LAWM47	Ph1	1238	0.354	1141	0.234	1043	0.145	945	0.082
LAWM48	Ph1	1199	0.280	1106	0.182	1015	0.111	926	0.062
LAWM49	Ph1	1238	0.331	1141	0.215	1041	0.139	946	0.088
LAWM50	Ph1	1239	0.399	1143	0.260	1044	0.168	947	0.101
LAWM51	Ph1	1230	0.347	1133	0.245	1036	0.157	939	0.091
LAWM52	Ph1	1234	0.568	1137	0.421	1038	0.280	942	0.176
LAWM53	Ph1	1237	0.379	1141	0.241	1043	0.144	945	0.074
LAWM54R1	Ph1	1236	0.146	1146	0.092	1047	0.048	949	0.023
LAWM55	Ph1	1236	0.742	1139	0.588	1042	0.388	944	0.248
LAWM56	Ph1	1235	0.481	1138	0.331	1041	0.223	947	0.123
LAWM57	Ph1aAug	1251	0.769	1160	0.550	1068	0.402	975	0.247
LAWM59	Ph1aAug	1228	0.632	1136	0.440	1043	0.338	952	0.214
LAWM60	Ph1aAug	1236	0.586	1144	0.460	1050	0.290	958	0.218
LAWM63	Ph1aAug	1245	0.871	1153	0.665	1060	0.493	967	0.317
LAWM66	Ph1aAug	1243	0.783	1150	0.619	1057	0.461	965	0.320
LAWM68	Ph1aAug	1243	0.654	1150	0.497	1057	0.344	963	0.239
LAWM71	Ph1aAug	1238	0.622	1145	0.483	1051	0.348	959	0.239
LAWM73	Ph1aAug	1239	0.633	1145	0.506	1052	0.388	960	0.289
LAWM75	Ph1aAug	1247	0.583	1156	0.457	1062	0.326	970	0.209
LAWE2H	Corr	1197	0.592	1115	0.446	1022	0.350	931	0.199
LAWE3	Corr	1208	0.456	1116	0.325	1026	0.243	934	0.152
LAWE3H	Corr	1214	0.617	1122	0.470	1027	0.318	932	0.203
LAWE4	Corr	1213	0.497	1119	0.386	1025	0.268	930	0.173

(a) The Group IDs are described in Sections 2.1 to 2.6.

**Table 4.4. Melt Electrical Conductivity Data for Simulated LAW Glasses (continued).**

Glass ID	Group ID <sup>(a)</sup>	EC1 (S/cm)	Vis1 (P)	EC2 (S/cm)	Vis2 (P)	EC3 (S/cm)	Vis3 (P)	EC4 (S/cm)	Vis4 (P)
LAW4H	Corr	1234	0.567	1140	0.444	1048	0.323	957	0.219
LAW5	Corr	1208	0.489	1116	0.349	1026	0.261	934	0.163
LAW5H	Corr	1201	0.500	1107	0.361	1015	0.257	917	0.151
LAW7	Corr	1210	0.465	1120	0.312	1024	0.217	930	0.128
LAW7H	Corr	1182	0.471	1099	0.298	1009	0.207	919	0.115
LAW9H	Corr	1204	0.414	1114	0.288	1023	0.171	934	0.105
LAW10H	Corr	1208	0.269	1118	0.169	1036	0.109	934	0.063
LAW11	Corr	1207	0.402	1117	0.327	1024	0.223	933	0.146
LAW12	Corr	1234	0.611	1138	0.483	1046	0.353	954	0.238
LAW13	Corr	1238	0.676	1147	0.514	1054	0.393	962	0.255
LAW16	Corr	1220	0.575	1128	0.477	1042	0.322	952	0.215
LAWCrP1R	HiCrP	1274	0.787	1179	0.562	1081	0.414	982	0.270
LAWCrP2R	HiCrP	1275	0.924	1176	0.712	1078	0.514	980	0.339
LAWCrP3R	HiCrP	1278	0.693	1179	0.559	1081	0.422	982	0.287
LAWCrP4R	HiCrP	1271	0.961	1172	0.732	1073	0.557	978	0.357
LAWCrP5	HiCrP	1222	0.435	1136	0.349	1044	0.231	953	0.144
LAWA41	ActDes	1243	0.713	1154	0.529	1052	0.369	951	0.238
LAWA42	ActDes	1240	0.710	1152	0.561	1054	0.393	956	0.248
LAWA43-1	ActDes	1250	0.704	1153	0.537	1054	0.364	957	0.254
LAWA45	ActDes	1249	0.643	1149	0.527	1050	0.366	948	0.242
LAWA49	ActDes	1248	0.683	1150	0.521	1050	0.369	951	0.242
LAWA50	ActDes	1248	0.657	1151	0.514	1051	0.380	953	0.248
LAWA51	ActDes	1248	0.550	1150	0.408	1049	0.290	951	0.186
LAWA52	ActDes	1247	0.657	1141	0.439	1043	0.305	945	0.186
LAWA60	ActDes	1257	0.543	1148	0.415	1050	0.293	950	0.197
LAWA81	ActDes	1250	0.637	1138	0.538	1039	0.320	942	0.211
LAWA82	ActDes	1250	0.705	1139	0.499	1044	0.358	944	0.244
LAWA83	ActDes	1249	0.613	1142	0.450	1043	0.315	944	0.201
LAWA89	ActDes	1250	0.697	1147	0.542	1046	0.390	947	0.260
LAWA90	ActDes	1244	0.653	1150	0.511	1051	0.350	955	0.233
LAWA93	ActDes	1244	0.558	1139	0.432	1041	0.297	947	0.183
LAWA96	ActDes	1244	0.748	1162	0.533	1052	0.307	951	0.204
LAWA125	ActDes	1247	0.646	1148	0.474	1048	0.295	949	0.204
LAWA127R1	ActDes	1239	0.390	1139	0.293	1038	0.188	940	0.126
LAWA129R1	ActDes	1238	0.454	1146	0.323	1035	0.184	945	0.131
LAWA134	ActDes	1241	0.518	1147	0.372	1052	0.260	958	0.165
LAWA135	ActDes	1245	0.479	1150	0.357	1056	0.238	961	0.157
LAWA136	ActDes	1237	0.475	1145	0.353	1049	0.240	957	0.153
LAWB30	ActDes	1244	0.424	1137	0.276	1040	0.163	925	0.084
LAWB34	ActDes	1237	0.361	1143	0.218	1045	0.141	947	0.070
LAWB37	ActDes	1247	0.297	1139	0.229	1042	0.144	947	0.083
LAWB38	ActDes	1245	0.386	1141	0.283	1043	0.163	944	0.101
LAWB60	ActDes	1237	0.355	1143	0.244	1045	0.147	946	0.077
LAWB61	ActDes	1229	0.401	1132	0.284	1035	0.170	938	0.098
LAWB62	ActDes	1237	0.479	1142	0.342	1045	0.212	939	0.111

(a) The Group IDs are described in Sections 2.1 to 2.6.



**Table 4.4. Melt Electrical Conductivity Data for Simulated LAW Glasses (continued).**

Glass ID	Group ID <sup>(a)</sup>	Temp1 (°C)	EC1 (S/cm)	Temp2 (°C)	EC2 (S/cm)	Temp3 (°C)	EC3 (S/cm)	Temp4 (°C)	EC4 (S/cm)
LAWB63	ActDes	1240	0.364	1142	0.239	1043	0.141	947	0.075
LAWB64	ActDes	1242	0.437	1148	0.290	1046	0.186	950	0.102
LAWB67	ActDes	1236	0.296	1140	0.206	1040	0.130	954	0.073
LAWB69	ActDes	1238	0.349	1143	0.249	1046	0.145	951	0.073
LAWB70	ActDes	1229	0.387	1135	0.265	1040	0.147	945	0.098
LAWB71	ActDes	1218	0.387	1126	0.265	1030	0.173	936	0.097
LAWB72	ActDes	1247	0.338	1150	0.246	1050	0.135	954	0.074
LAWB73	ActDes	1244	0.418	1147	0.284	1055	0.178	962	0.117
LAWB74	ActDes	1224	0.433	1135	0.305	1043	0.197	947	0.110
LAWB75	ActDes	1231	0.457	1142	0.300	1041	0.171	949	0.095
LAWB76	ActDes	1246	0.516	1148	0.361	1050	0.250	952	0.135
LAWB77	ActDes	1249	0.382	1150	0.254	1049	0.131	948	0.071
LAWB81	ActDes	1252	0.502	1153	0.292	1053	0.184	955	0.099
LAWB82	ActDes	1208	0.402	1113	0.219	1022	0.143	930	0.077
LAWB87	ActDes	1229	0.379	1134	0.277	1041	0.176	946	0.102
LAWB88	ActDes	1227	0.372	1132	0.256	1039	0.160	947	0.093
LAWB89	ActDes	1223	0.359	1131	0.252	1038	0.157	945	0.090
LAWB90	ActDes	1240	0.306	1147	0.207	1053	0.130	964	0.069
LAWB92	ActDes	1238	0.316	1143	0.216	1049	0.135	955	0.073
LAWB93R1	ActDes	1257	0.314	1162	0.213	1068	0.141	969	0.083
LAWB94	ActDes	1243	0.344	1150	0.231	1054	0.149	958	0.083
LAWB95	ActDes	1239	0.389	1146	0.277	1052	0.180	958	0.101
LAWC12	ActDes	1252	0.793	1150	0.600	1050	0.409	950	0.266
LAWC21rev2	ActDes	1245	0.370	1151	0.264	1054	0.171	960	0.101
LAWC29	ActDes	1242	0.421	1144	0.264	1046	0.166	949	0.088
LAWC30	ActDes	1238	0.527	1142	0.329	1045	0.197	950	0.117
LAWC31R1	ActDes	1238	0.401	1140	0.271	1043	0.167	947	0.100
C22AN107	ActDes	1200	0.416	1151	0.339	1052	0.228	953	0.131
A88Si+15	ActDes	1242	0.777	1144	0.569	1045	0.399	946	0.278
A88Si-15	ActDes	1241	0.433	1142	0.334	1042	0.238	944	0.135
C22Si+15	ActDes	1206	0.508	1157	0.426	1058	0.290	959	0.172
C22Si-15	ActDes	1193	0.346	1144	0.302	1046	0.206	948	0.121
A1C1-1	ActDes	1236	0.578	1143	0.426	1049	0.304	955	0.195
A1C1-2	ActDes	1247	0.555	1153	0.402	1058	0.272	963	0.178
C1-AN107	ActDes	1248	0.439	1154	0.324	1057	0.218	962	0.136
A2-AP101	ActDes	1247	0.474	1153	0.356	1057	0.253	962	0.157
A2B1-1	ActDes	1237	0.427	1145	0.311	1049	0.206	957	0.132
A2B1-2	ActDes	1243	0.342	1151	0.251	1057	0.158	963	0.094
B1-AZ101	ActDes	1246	0.286	1152	0.204	1056	0.126	961	0.070
C2-AN102C35	ActDes	1248	0.378	1154	0.274	1059	0.175	963	0.105
A3-AN104	ActDes	1250	0.413	1155	0.299	1060	0.205	964	0.126
A2B1-3	ActDes	1244	0.354	1151	0.236	1056	0.150	963	0.086
A3C2-1	ActDes	1240	0.418	1147	0.326	1051	0.211	955	0.130
A3C2-2	ActDes	1248	0.392	1154	0.278	1058	0.188	963	0.114
A3C2-3	ActDes	1249	0.378	1154	0.270	1058	0.179	963	0.098
A1-AN105R2	ActDes	1246	0.484	1149	0.375	1053	0.288	958	0.180

(a) The Group IDs are described in Sections 2.1 to 2.6.

**Table 4.5. Melt Viscosity Data for Simulated LAW Glasses.**

Glass ID	Group ID <sup>(a)</sup>	Temp1 (°C)	Vis1 (P)	Temp2 (°C)	Vis2 (P)	Temp3 (°C)	Vis3 (P)	Temp4 (°C)	Vis4 (P)
LAWA44R10	ExPh1	1233	34.89	1134	83.13	1034	247.19	935	1001.77
LAWA53	ExPh1	1250	23.16	1153	54.10	1057	158.10	961	644.90
LAWA56	ExPh1	1254	22.26	1156	48.29	1058	133.71	961	489.26
LAWA88	ExPh1	1244	27.27	1133	71.10	1032	198.05	931	750.05
LAWA102R1	ExPh1	1241	24.23	1145	52.83	1050	142.49	954	515.05
LAWA126	ExPh1	1261	24.12	1161	55.81	1061	161.83	960	598.57
LAWA128R1	ExPh1	1261	34.29	1161	83.05	1061	258.87	961	1049.25
LAWA130	ExPh1	1228	35.41	1126	91.30	1023	281.27	921	1241.71
LAWB65	ExPh1	1264	19.61	1164	46.05	1064	137.88	964	530.89
LAWB66	ExPh1	1265	16.96	1162	39.48	1060	119.18	959	473.33
LAWB68	ExPh1	1264	21.11	1164	49.66	1064	150.84	964	599.38
LAWB78	ExPh1	1256	18.28	1156	40.12	1056	109.81	971	374.92
LAWB79	ExPh1	1241	18.92	1141	44.62	1041	122.63	951	456.78
LAWB80	ExPh1	1252	22.77	1152	53.00	1052	155.45	952	614.12
LAWB83	ExPh1	1253	22.13	1155	49.86	1058	148.96	962	562.98
LAWB84	ExPh1	1268	18.67	1168	42.54	1068	124.70	968	470.71
LAWB85	ExPh1	1255	22.50	1155	51.79	1055	149.43	957	552.70
LAWB86	ExPh1	1250	21.52	1149	50.37	1049	135.84	968	478.21
C100-G-136B	ExPh1	1271	21.36	1169	46.28	1067	130.19	965	463.82
LAWC27	ExPh1	1246	23.59	1146	54.06	1046	145.68	946	543.51
LAWC32	ExPh1	1255	15.44	1162	34.91	1062	96.79	963	331.64
LAWM1	Ph1	1252	16.91	1152	35.00	1053	94.14	953	376.96
LAWM2	Ph1	1244	9.60	1147	21.38	1051	59.90	953	253.24
LAWM3	Ph1	1249	8.29	1152	17.88	1053	45.54	956	162.10
LAWM4	Ph1	1254	6.02	1154	13.03	1054	32.10	954	110.63
LAWM5	Ph1	1246	52.13	1149	126.97	1052	363.81	956	1562.29
LAWM6	Ph1	1244	21.08	1144	52.45	1044	173.14	944	872.14
LAWM7 <sup>(b)</sup>	Ph1	1252	41.88	1152	113.87	1052	386.83	952	1996.66
LAWM8	Ph1	1225	35.17	1128	93.96	1030	328.41	932	1626.62
LAWM9	Ph1	1252	43.77	1150	126.36	1048	462.35	946	2329.04
LAWM10	Ph1	1238	7.23	1143	15.04	1047	36.31	952	114.91
LAWM11	Ph1	1239	7.48	1142	13.73	1045	29.09	948	73.40
LAWM12	Ph1	1246	6.82	1148	14.24	1049	32.05	951	90.07
LAWM13	Ph1	1246	7.60	1148	14.67	1051	32.41	954	91.38
LAWM14	Ph1	1234	25.14	1138	51.91	1042	131.85	945	430.55
LAWM15	Ph1	1245	30.81	1148	67.56	1051	176.27	955	624.02
LAWM16	Ph1	1247	12.50	1150	25.81	1052	64.58	955	214.94

(a) The Group IDs are described in Sections 2.1 to 2.6.

(b) This glass had a fifth viscosity measurement of 894.15 poise at 1002°C that was also used in the data set modeled.

**Table 4.5. Melt Viscosity Data for Simulated LAW Glasses (continued).**

<b>Glass ID</b>	<b>Group ID<sup>(a)</sup></b>	<b>Temp1 (°C)</b>	<b>Vis1 (P)</b>	<b>Temp2 (°C)</b>	<b>Vis2 (P)</b>	<b>Temp3 (°C)</b>	<b>Vis3 (P)</b>	<b>Temp4 (°C)</b>	<b>Vis4 (P)</b>
LAWM17	Ph1	1237	15.81	1143	35.08	1049	94.19	955	331.97
LAWM18	Ph1	1243	14.38	1141	31.26	1039	85.32	939	306.52
LAWM19	Ph1	1243	30.72	1146	71.70	1049	271.86	952	1146.71
LAWM20	Ph1	1240	10.52	1142	22.47	1045	58.37	948	195.96
LAWM21	Ph1	1242	10.62	1145	22.26	1048	58.19	952	198.85
LAWM22	Ph1	1245	40.06	1144	106.27	1043	353.28	943	1696.57
LAWM23	Ph1	1238	27.31	1139	64.40	1040	191.57	942	797.88
LAWM24	Ph1	1238	39.99	1142	84.18	1046	218.17	951	751.15
LAWM25R1	Ph1	1240	40.81	1142	92.69	1044	255.56	947	891.03
LAWM26	Ph1	1236	37.82	1139	82.92	1043	239.14	946	836.07
LAWM27	Ph1	1243	18.12	1147	36.12	1051	90.31	957	290.01
LAWM28	Ph1	1241	43.34	1143	103.26	1044	309.25	945	2130.74
LAWM29	Ph1	1248	34.20	1150	78.11	1052	228.45	955	860.19
LAWM30	Ph1	1246	17.29	1149	34.17	1052	87.17	955	277.22
LAWM31	Ph1	1247	10.05	1149	20.10	1050	56.94	952	158.91
LAWM32	Ph1	1248	20.41	1149	42.21	1050	105.79	951	345.60
LAWM33R1	Ph1	1245	9.67	1148	19.16	1051	45.65	954	139.60
LAWM34	Ph1	1244	8.67	1147	16.67	1050	36.48	954	104.88
LAWM35	Ph1	1249	11.17	1149	25.02	1050	68.28	950	269.85
LAWM36	Ph1	1237	18.99	1140	39.77	1044	106.51	947	385.10
LAWM37	Ph1	1237	15.79	1142	34.38	1047	90.46	951	318.00
LAWM38	Ph1	1234	26.60	1138	60.50	1042	166.84	945	596.59
LAWM39	Ph1	1230	25.27	1135	56.11	1041	151.89	946	531.87
LAWM40	Ph1	1236	34.33	1140	79.30	1044	231.63	947	929.51
LAWM41	Ph1	1241	28.68	1143	73.02	1046	222.56	948	1021.93
LAWM42	Ph1	1233	27.50	1134	63.19	1036	183.30	937	721.23
LAWM43	Ph1	1244	19.75	1147	45.52	1051	126.69	954	467.08
LAWM44	Ph1	1246	31.45	1149	74.85	1052	217.52	956	901.07
LAWM45	Ph1	1240	30.05	1146	69.01	1052	193.15	959	717.82
LAWM46	Ph1	1243	32.80	1144	80.94	1045	254.48	945	1159.85
LAWM47	Ph1	1235	31.99	1143	75.82	1051	227.57	960	941.10
LAWM48	Ph1	1249	36.63	1151	86.21	1053	257.34	956	1143.07
LAWM49	Ph1	1249	32.43	1149	75.11	1048	222.00	948	879.38
LAWM50	Ph1	1243	26.82	1146	60.43	1049	173.87	953	721.01
LAWM51	Ph1	1248	26.09	1154	59.03	1060	171.04	966	624.53
LAWM52	Ph1	1246	24.16	1149	51.50	1052	138.67	955	531.45
LAWM53	Ph1	1248	16.84	1150	39.95	1056	105.13	958	314.34
LAWM54R1	Ph1	1254	41.43	1155	105.91	1056	347.39	957	1659.86
LAWM55	Ph1	1259	5.99	1158	11.23	1057	24.47	956	65.90

(a) The Group IDs are described in Sections 2.1 to 2.6.

**Table 4.5. Melt Viscosity Data for Simulated LAW Glasses (continued).**

<b>Glass ID</b>	<b>Group ID<sup>(a)</sup></b>	<b>Temp1 (°C)</b>	<b>Vis1 (P)</b>	<b>Temp2 (°C)</b>	<b>Vis2 (P)</b>	<b>Temp3 (°C)</b>	<b>Vis3 (P)</b>	<b>Temp4 (°C)</b>	<b>Vis4 (P)</b>
LAWM56	Ph1	1245	11.82	1148	25.79	1052	69.99	956	262.73
LAWM57	Ph1aAug	1247	12.94	1150	27.95	1054	72.11	958	245.32
LAWM59	Ph1aAug	1255	25.18	1156	54.13	1059	137.18	961	487.70
LAWM60	Ph1aAug	1257	20.39	1157	44.43	1057	119.32	958	433.64
LAWM63	Ph1aAug	1256	18.97	1156	37.79	1057	95.96	958	296.69
LAWM66	Ph1aAug	1254	13.70	1155	30.03	1056	79.27	958	277.89
LAWM68	Ph1aAug	1257	14.83	1156	30.17	1054	76.86	954	262.88
LAWM71	Ph1aAug	1258	19.20	1157	40.96	1054	104.61	955	337.67
LAWM73	Ph1aAug	1260	14.32	1159	30.53	1057	77.71	957	257.01
LAWM75	Ph1aAug	1254	18.23	1153	40.45	1053	115.74	953	449.45
LAWE2H	Corr	1242	16.32	1142	34.08	1040	84.78	939	271.78
LAWE3	Corr	1249	23.74	1149	52.79	1051	143.69	952	525.82
LAWE3H	Corr	1211	21.28	1109	46.05	1006	120.37	903	419.24
LAWE4	Corr	1255	22.73	1159	49.41	1062	130.73	966	451.51
LAWE4H	Corr	1255	19.43	1159	41.03	1062	103.82	965	335.99
LAWE5	Corr	1253	26.04	1158	53.86	1062	141.51	967	470.58
LAWE5H	Corr	1252	17.08	1157	36.58	1062	92.54	966	295.17
LAWE7	Corr	1226	13.94	1124	28.57	1021	70.66	917	222.91
LAWE7H	Corr	1245	11.32	1145	22.20	1045	51.83	944	154.24
LAWE9H	Corr	1243	12.68	1147	25.89	1051	62.80	954	194.75
LAWE10H	Corr	1248	18.37	1153	39.54	1057	105.64	951	357.57
LAWE11	Corr	1251	26.08	1150	59.47	1049	167.75	949	636.57
LAWE12	Corr	1260	19.88	1158	43.90	1057	119.58	956	412.71
LAWE13	Corr	1258	21.60	1157	47.88	1057	127.53	957	439.36
LAWE16	Corr	1260	24.48	1159	54.64	1058	151.15	956	554.83
LAWCrP1R	HiCrP	1263	25.07	1163	55.71	1063	155.47	964	598.52
LAWCrP2R	HiCrP	1249	20.59	1149	45.39	1050	126.24	951	476.61
LAWCrP3R	HiCrP	1248	24.93	1151	55.49	1052	156.94	954	608.55
LAWCrP4R	HiCrP	1259	18.39	1157	41.80	1056	116.76	955	439.69
LAWCrP5	HiCrP	1252	14.23	1151	29.21	1051	73.72	951	262.10
LAWA41	ActDes	1248	28.37	1150	68.23	1050	198.18	950	737.09
LAWA42	ActDes	1257	12.95	1150	30.61	1050	85.64	950	306.13
LAWA43-1	ActDes	1249	35.31	1150	85.20	1050	270.22	950	1100.89
LAWA45	ActDes	1250	28.10	1150	63.89	1050	183.46	950	683.85
LAWA49	ActDes	1252	35.66	1150	86.39	1050	256.51	950	978.16
LAWA50	ActDes	1251	30.48	1150	71.69	1050	210.42	950	787.40
LAWA51	ActDes	1243	47.46	1150	105.86	1050	320.66	950	1284.25
LAWA52	ActDes	1250	21.52	1139	57.87	1039	177.65	939	773.68
LAWA60	ActDes	1248	30.28	1130	77.64	1029	227.03	945	911.46

(a) The Group IDs are described in Sections 2.1 to 2.6.

**Table 4.5. Melt Viscosity Data for Simulated LAW Glasses (continued).**

Glass ID	Group ID <sup>(a)</sup>	Temp1 (°C)	Vis1 (P)	Temp2 (°C)	Vis2 (P)	Temp3 (°C)	Vis3 (P)	Temp4 (°C)	Vis4 (P)
LAWA81	ActDes	1252	26.58	1152	68.91	1053	209.55	953	816.83
LAWA82	ActDes	1253	39.40	1142	103.06	1043	309.49	943	1262.72
LAWA83	ActDes	1254	36.37	1145	98.08	1044	293.21	944	1237.99
LAWA89	ActDes	1268	24.96	1167	56.31	1065	154.95	965	568.48
LAWA90	ActDes	1256	26.60	1157	60.78	1055	171.12	956	609.53
LAWA93	ActDes	1249	7.46	1139	17.49	1041	40.74	940	128.09
LAWA96	ActDes	1252	30.67	1152	73.34	1052	223.42	953	905.47
LAWA125	ActDes	1257	17.54	1157	38.99	1057	107.12	957	367.95
LAWA127R1	ActDes	1256	32.81	1156	78.49	1056	245.11	957	1031.48
LAWA129R1	ActDes	1248	44.48	1148	111.31	1048	330.40	948	1370.72
LAWA134	ActDes	1239	30.60	1143	71.16	1046	198.22	950	771.55
LAWA135	ActDes	1233	37.10	1138	87.17	1042	257.58	948	962.96
LAWA136	ActDes	1230	26.94	1133	66.46	1034	192.85	936	826.33
LAWB30	ActDes	1255	13.82	1155	29.01	1056	77.89	946	328.04
LAWB34	ActDes	1257	31.64	1156	80.72	1056	248.68	955	993.47
LAWB37	ActDes	1246	39.21	1145	94.88	1045	288.12	945	1168.09
LAWB38	ActDes	1254	27.60	1143	70.03	1043	195.22	943	722.92
LAWB60	ActDes	1258	12.03	1159	26.76	1056	72.25	956	257.94
LAWB61	ActDes	1230	18.43	1155	34.43	1058	92.83	958	332.53
LAWB62	ActDes	1225	14.45	1131	33.16	1038	83.87	945	301.99
LAWB63	ActDes	1243	19.28	1143	43.64	1043	123.34	943	497.38
LAWB64	ActDes	1257	15.12	1156	33.33	1056	88.14	957	345.61
LAWB67	ActDes	1266	27.31	1166	64.80	1066	197.14	967	805.21
LAWB69	ActDes	1247	16.61	1147	38.14	1047	102.80	947	373.54
LAWB70	ActDes	1239	17.57	1141	41.28	1043	114.17	946	421.57
LAWB71	ActDes	1238	19.09	1140	43.12	1042	113.53	945	405.23
LAWB72	ActDes	1250	19.39	1150	41.06	1050	116.03	950	422.00
LAWB73	ActDes	1246	15.35	1146	37.48	1046	107.53	947	430.54
LAWB74	ActDes	1257	13.46	1159	30.56	1059	86.62	958	322.40
LAWB75	ActDes	1261	13.75	1159	29.98	1057	81.52	956	306.58
LAWB76	ActDes	1270	13.39	1168	28.66	1066	75.45	963	259.89
LAWB77	ActDes	1252	32.91	1152	60.06	1052	169.14	967	572.51
LAWB81	ActDes	1253	16.54	1153	37.03	1053	106.98	946	425.89
LAWB82	ActDes	1269	12.58	1169	27.49	1069	74.50	969	254.33

(a) The Group IDs are described in Sections 2.1 to 2.6.

**Table 4.5. Melt Viscosity Data for Simulated LAW Glasses (continued).**

Glass ID	Group ID <sup>(a)</sup>	Temp1 (°C)	Vis1 (P)	Temp2 (°C)	Vis2 (P)	Temp3 (°C)	Vis3 (P)	Temp4 (°C)	Vis4 (P)
LAWB88	ActDes	1255	21.87	1155	48.65	1056	140.31	956	525.15
LAWB89	ActDes	1256	18.91	1156	44.34	1055	132.68	955	522.71
LAWB90	ActDes	1244	23.60	1144	58.93	1043	166.75	943	703.81
LAWB92	ActDes	1227	28.53	1131	64.65	1036	187.26	941	757.05
LAWB93R1	ActDes	1250	20.68	1152	47.57	1053	140.69	955	554.31
LAWB94	ActDes	1245	22.01	1146	50.13	1047	141.21	948	578.08
LAWB95	ActDes	1244	24.77	1144	58.67	1043	172.31	942	739.97
LAWC12	ActDes	1255	23.48	1151	54.28	1050	157.66	948	601.64
LAWC21rev2	ActDes	1251	21.85	1151	47.41	1052	133.96	953	478.86
LAWC29	ActDes	1243	18.43	1143	41.95	1043	116.52	943	437.15
LAWC30	ActDes	1258	17.65	1159	38.88	1059	110.00	959	400.48
LAWC31R1	ActDes	1261	16.26	1161	36.47	1061	103.94	961	378.47
C22AN107	ActDes	1253	19.30	1153	41.64	1053	115.57	953	396.25
A88Si+15	ActDes	1251	19.18	1151	40.53	1051	112.08	951	390.39
A88Si-15	ActDes	1262	33.46	1162	80.99	1062	262.09	962	1114.95
C22Si+15	ActDes	1192	24.41	1143	38.09	1044	95.76	944	314.32
C22Si-15	ActDes	1189	39.02	1085	101.57	985	331.96	935	677.87
A1C1-1	ActDes	1251	24.32	1152	56.59	1052	164.16	953	615.46
A1C1-2	ActDes	1253	21.82	1153	46.42	1051	129.84	950	458.57
C1-AN107	ActDes	1220	25.84	1126	56.90	1032	151.51	938	558.46
A2-AP101	ActDes	1251	25.09	1153	57.76	1053	165.07	955	595.97
A2B1-1	ActDes	1251	25.78	1152	59.98	1052	173.00	952	638.01
A2B1-2	ActDes	1241	25.47	1139	60.90	1037	171.95	935	708.67
B1-AZ101	ActDes	1247	22.95	1149	52.76	1051	151.27	953	607.75
C2-AN102C35	ActDes	1249	16.21	1150	34.86	1051	90.80	952	322.86
A3-AN104	ActDes	1244	16.61	1146	35.69	1048	92.50	950	309.47
A2B1-3	ActDes	1225	26.24	1128	66.36	1031	205.08	935	901.60
A3C2-1	ActDes	1220	23.32	1125	50.74	1031	132.81	936	461.77
A3C2-2	ActDes	1241	17.23	1144	36.37	1047	94.11	950	318.79
A3C2-3	ActDes	1239	16.62	1141	35.69	1043	95.54	945	333.94
A1-AN105R2	ActDes	1250	29.37	1151	68.88	1051	209.02	952	845.32

(a) The Group IDs are described in Sections 2.1 to 2.6.

**Table 4.6 Optical Microscopy and SEM Evaluation of 271 LAW Simulated and Actual Waste Glasses.**

Glass ID	As Melted	Optical and SEM evaluation of glass sample heat treated at 950°C and quenched.	Optical and SEM evaluation of glass sample heat treated at 850°C and quenched.	Optical and SEM evaluation of glass sample subjected to Canister Centerline Cooling (CCC).
LAWA44 <sup>(a)</sup>	Clear glass	Clear glass	Clear glass	Clear glass
LAWA44R10	Clear glass	Clear glass	Clear glass	Clear glass
LAWA53	Clear glass	– <sup>(b)</sup>	–	–
LAWA56	Clear glass	–	–	–
LAWA88	Clear glass	Clear glass	Clear glass	Clear glass
LAWA88R1	Clear glass	Clear glass	–	–
LAWA102R1	Clear glass	Clear glass	–	Clear glass
LAWA126	Clear glass	–	Clear glass	Clear glass (see PNLA126CC)
LAWA128	Clear glass	–	Clear glass	–
LAWA128R1	Clear glass	–	–	–
LAWA130	Clear glass	–	Clear glass	–
LAWB65	Clear glass	–	< 0.1 vol% Augite – aegirine crystals along crucible contact.	–
LAWB66	Clear glass	–	< 0.1 vol% Augite – aegirine crystals along crucible contact.	–
LAWB68	Clear glass	–	< 0.1 vol% Augite – aegirine crystals along crucible contact.	–
LAWB78	Clear glass	–	Clear glass	–
LAWB79	Clear glass	–	< 0.1 vol% Augite – aegirine crystals along crucible contact.	–
LAWB80	Clear glass	–	Clear glass	–
LAWB83	Clear glass	–	≈ 0.2 vol% Augite – aegirine crystals along crucible contact.	–
LAWB84	Clear glass	–	≈ 0.1 vol% Augite – aegirine crystals along crucible contact.	–
LAWB85	Clear glass	–	Clear glass (≈ 0.1 vol% Augite seen in sample heat treated at 700 °C)	–
LAWB86	Clear glass	–	Clear glass (≈ 0.1 vol% Augite seen in sample heat treated at 700 °C)	–
C100-G-136B	Clear glass	–	Clear glass	–
LAWC27	Clear glass	–	Clear glass	–
LAWC32	Clear glass	–	Clear glass	–

(a) A TTT diagram prepared for this glass between 500°C and 900°C and up to 72 hours heat treatment time did not show any crystals.

(b) A dash (–) indicates that this glass was not subjected to the described heat treatment.

**Table 4.6 Optical Microscopy and SEM Evaluation of 271 LAW Simulated and Actual Waste Glasses (continued).**

Glass ID	As Melted	Optical and SEM evaluation of glass sample heat treated at 950°C and quenched.	Optical and SEM evaluation of glass sample heat treated at 850°C and quenched.	Optical and SEM evaluation of glass sample subjected to Canister Centerline Cooling (CCC).
LAWM1	Clear glass	Clear glass	– <sup>(a)</sup>	–
LAWM2	Clear glass	≈ 18 vol% of augite crystals throughout the glass + Cr Fe Zn Mg Ti spinel crystals	–	–
LAWM3	Clear glass	Clear glass	–	–
LAWM4	Clear glass	Clear glass	–	–
LAWM5	Clear glass	<<0.1 vol% black crystals at the crucible contact; possibly a contamination	–	–
LAWM6	Clear glass	≈ 5 vol% of augite and Ti Fe Mg spinel crystals	–	–
LAWM7	Mostly clear glass - one crystal observed	≈ 22 vol% of acicular and fibrous bundles of augite crystals	–	–
LAWM8	≈ 0.6 vol% zircon, possibly undissolved batch material	≈ 0.1 vol% Ti, Cr, Fe, Ni, Zn spinel crystals at the crucible contact.	–	–
LAWM9	Clear glass	Clear glass	–	–
LAWM10	Clear glass	Clear glass	–	–
LAWM11	Clear glass	Clear glass	–	–
LAWM12	Clear glass	Clear glass	–	–
LAWM13	Clear glass	< 0.1 vol% of cubic semi-transparent crystals (probably Na <sub>2</sub> Ca <sub>3</sub> Si <sub>5</sub> O <sub>15</sub> )	–	–
LAWM14	Clear glass	Clear glass	–	–
LAWM15	Clear glass	<<0.1 vol% Cr Fe Ni Zn spinel crystals – No characteristic crystalline peaks observed in XRD.	–	–
LAWM16	Clear glass	Clear glass	–	–
LAWM17	Clear glass	Clear glass	–	–
LAWM18	Clear glass	<<0.1% vol% Ti Cr Fe Ni Zn spinel at crucible contact.	–	–
LAWM19	Clear glass	Clear glass	–	–

(a) A dash (–) indicates that this glass was not subjected to the described heat treatment.



**Table 4.6 Optical Microscopy and SEM Evaluation of 271 LAW Simulated and Actual Waste Glasses (continued).**

Glass ID	As Melted	Optical and SEM evaluation of glass sample heat treated at 950°C and quenched.	Optical and SEM evaluation of glass sample heat treated at 850°C and quenched.	Optical and SEM evaluation of glass sample subjected to Canister Centerline Cooling (CCC).
LAWM20	Clear glass	Clear glass	– <sup>(a)</sup>	–
LAWM21	Clear glass	Clear glass	–	–
LAWM22	<<0.1 vol% Cr Zn Fe Mg spinel	<<0.1 vol% Cr Fe Ni Zn spinel	–	–
LAWM23	Clear glass	Clear glass	–	–
LAWM24	Clear glass	Clear glass	–	–
LAWM25R1	Clear glass	<<0.1% vol% spinel	–	–
LAWM26	<<0.1% vol% spinel at crucible contact.	<<0.1% vol% Ti Cr Fe Ni Zn spinel at crucible contact.	–	–
LAWM27	Clear glass	Clear glass	–	–
LAWM28	Clear glass	Clear glass	–	–
LAWM29	Clear glass	Clear glass	–	–
LAWM30	Clear glass	Clear glass	–	–
LAWM31	Clear glass	Clear glass	–	–
LAWM32	Clear glass	Clear glass	–	–
LAWM33R1	Clear glass	Clear glass	–	–
LAWM34	Clear glass	Clear glass	–	–
LAWM35	Clear glass	<< 0.1 vol% crystals. No characteristic crystalline peaks observed in XRD.	–	–
LAWM36	Clear glass	Clear glass	–	–
LAWM37	Clear glass	Clear glass	–	–
LAWM38	Clear glass	Clear glass	–	–
LAWM39	Clear glass	Mostly clear glass << 0.1 vol% minute crystals	–	–
LAWM40	Clear glass	Clear glass	–	–
LAWM41	Clear glass	<<0.1% vol% Ti Cr Fe Ni Zn spinel at crucible contact.	–	–
LAWM42	Clear glass	Clear glass	–	–

(a) A dash (–) indicates that this glass was not subjected to the described heat treatment.

**Table 4.6 Optical Microscopy and SEM Evaluation of 271 LAW Simulated and Actual Waste Glasses (continued).**

Glass ID	As Melted	Optical and SEM evaluation of glass sample heat treated at 950°C and quenched.	Optical and SEM evaluation of glass sample heat treated at 850°C and quenched.	Optical and SEM evaluation of glass sample subjected to Canister Centerline Cooling (CCC).
LAWM43	Clear glass	<<0.1% vol% Ti Cr Fe Ni Zn spinel at crucible contact.	–	–
LAWM44	Clear glass	Clear glass	–	–
LAWM45	Clear glass	Clear glass	–	–
LAWM46	Clear glass	Clear glass	–	–
LAWM47	Clear glass	Clear glass	–	–
LAWM48	Clear glass	Clear glass	–	–
LAWM49	Clear glass	<<0.1% vol% Ti Cr Fe Ni Zn spinel at crucible contact.	–	–
LAWM50	Clear glass	Clear glass	–	–
LAWM51	Clear glass	Clear glass	–	–
LAWM52	Clear glass	Clear glass	–	–
LAWM53	Clear glass	Clear glass	–	–
LAWM54R1	Clear glass	<<0.1% vol% Ti Cr Fe Ni Zn spinel at crucible contact.	–	–
LAWM55	Clear glass	Clear glass	–	–
LAWM56	Clear glass	Clear glass	–	–
LAWM57	Clear glass	– <sup>(a)</sup>	–	–
LAWM58	Clear glass	–	–	–
LAWM59	Clear glass	–	–	–
LAWM60	Clear glass	–	–	–
LAWM61	Clear glass	–	–	–
LAWM62	Clear glass	–	–	–
LAWM63	Clear glass	–	–	–
LAWM64	Clear glass	–	–	–
LAWM65	Clear glass	–	–	–
LAWM66	Clear glass	–	–	–
LAWM67	Clear glass	–	–	–
LAWM68	Clear glass	–	–	–
LAWM69	Clear glass	–	–	–
LAWM70	Clear glass	–	–	–
LAWM71	Clear glass	–	–	–
LAWM72	Clear glass	–	–	–

(a) A dash (–) indicates that this glass was not subjected to the described heat treatment.

**Table 4.6 Optical Microscopy and SEM Evaluation of 271 LAW Simulated and Actual Waste Glasses (continued).**

Glass ID	As Melted	Optical and SEM evaluation of glass sample heat treated at 950°C and quenched.	Optical and SEM evaluation of glass sample heat treated at 850°C and quenched.	Optical and SEM evaluation of glass sample subjected to Canister Centerline Cooling (CCC).
LAWM73	Clear glass	– <sup>(a)</sup>	–	–
LAWM74	Clear glass	–	–	–
LAWM75	Clear glass	–	–	–
LAWM76	Clear glass	–	–	–
LAWE2H	Clear glass	–	Clear glass	Clear glass
LAWE3	Clear glass	–	Clear glass	–
LAWE3H	Clear glass	–	Clear glass	Clear glass
LAWE4	Clear glass	–	Clear glass	Clear glass
LAWE4H	Clear glass	–	Clear glass	Clear glass
LAWE5	Clear glass	–	Clear glass	Clear glass
LAWE5H	Clear glass	–	Clear glass	Clear glass
LAWE7	Clear glass	–	Clear glass	Clear glass
LAWE7H	Clear glass	–	Clear glass	Clear glass
LAWE9H	Clear glass	–	≈ 0.2 vol% of augite crystals at the crucible contact	≈ 0.1 vol% of augite crystals at the crucible contact
LAWE10H	Clear glass	–	≈ 0.6 vol% of augite crystals at the crucible contact	≈ 0.1 vol% of augite crystals at the crucible contact
LAWE11	Clear glass	–	Clear glass	–
LAWE12	Clear glass	–	Clear glass	–
LAWE13	Clear glass	–	Clear glass	–
LAWE14	Clear glass	–	Clear glass	–
LAWE15	Clear glass	–	Clear glass	–
LAWE16	Clear glass	–	Clear glass	–
LAWE3Cr2CCC	Not applicable	Not applicable	Not applicable	≈ 1.1 vol% of very fine (1-5 μm) Cr-rich spinels with Zn, Fe and Ti dispersed throughout the glass.
LAWE9HCr1CCC	Not applicable	Not applicable	Not applicable	≈ 24.7 vol% crystals; mainly augite-aegirine (about 95% of crystals) forming along Cr-rich spinels with Zn, Fe and Ti. Remaining glass shows no detectable Cr <sub>2</sub> O <sub>3</sub> .
LAWE9HCr2CCC	Not applicable	Not applicable	Not applicable	≈ 23.5 vol% of crystals; mainly augite-aegirine (about 98% of crystals) forming along Cr-rich ZnFeTi spinels.
LAWE10HCr3CCC	Not applicable	Not applicable	Not applicable	≈ 5.8 vol% crystals; mostly large augite-aegirine along Cr-rich ZnFeTi spinels (negligible amount compared to augite-aegirine) ~0.3 wt% Cr <sub>2</sub> O <sub>3</sub> in remaining glass.

(a) A dash (–) indicates that this glass was not subjected to the described heat treatment.

**Table 4.6 Optical Microscopy and SEM Evaluation of 271 LAW Simulated and Actual Waste Glasses (continued).**

Glass ID	As Melted	Optical and SEM evaluation of glass sample heat treated at 950°C and quenched.	Optical and SEM evaluation of glass sample heat treated at 850°C and quenched.	Optical and SEM evaluation of glass sample subjected to Canister Centerline Cooling (CCC).
LAWCrP1R	Clear glass	Clear glass	–	Clear glass
LAWCrP2R	≈ 0.1 vol% of small Cr-rich spinels	< 0.1 vol% of small Cr-rich spinels	–	< 0.1 vol% of small Cr-rich spinels
LAWCrP3R	Clear glass	≈ 0.1 vol% of Na Ca Phosphate crystals.	–	< 0.1 vol% of Na Ca Phosphate crystals clustered at crucible contact.
LAWCrP4R	≈ 0.1 vol% of small Cr-rich spinels	< 0.1 vol% of small Cr-rich spinels	–	≈ 0.2 vol.% of small Cr-rich spinels
LAWCrP5	≈ 0.2 vol% of small (~1 μm) Cr-rich ZnFeTi spinels.	≈ 0.3 vol% of small (5 to 20 μm) Cr-rich ZnFeTi spinels distributed uniformly throughout the sample.	–	≈ 0.2 vol% of small (5 to 20 μm) Cr-rich ZnFeTi spinels.
LAWCrP6	≈ 0.2 vol% of small Cr-rich ZnFeTi spinels + a small silica phosphate glassy nodule in the crucible.	≈ 0.7 vol% of small (~1 to 10 μm) Cr-rich ZnFeTi spinels throughout the sample with heavy crystallization along the crucible contact surfaces.	–	≈ 5.6 vol% of crystals concentrated along the crucible contact and up to 5mm deep. Augite-aegirine (Ca,Na)(Mg,Fe,Al) silicate nucleating around Cr-rich Fe-Zn spinels; also some needle shaped Ca phosphate (apatite) crystals.
LAWCrP7	≈ 0.2 vol% of small Cr-rich ZnFeTi spinels.	≈ 0.7 vol% of Cr-rich ZnFeTi spinels and some apatite.	–	≈ 15.9 vol% crystals on average - same as LAWCrP6 and ranging from ~12 vol% in the bulk of the glass to ~24 vol% at the crucible contact.
LAWA41	Clear glass	Clear glass	–	–
LAWA42	Clear glass	Clear glass	–	–
LAWA43-1	Clear glass	Trace (~0.01 vol%) of ZrO <sub>2</sub>	–	–
LAWA45	Clear glass	Clear glass	–	–
LAWA49	Clear glass	Clear glass	–	–
LAWA50	Clear glass	Clear glass	–	–
LAWA51	Clear glass	Clear glass	–	–
LAWA52	Clear glass	– <sup>(a)</sup>	–	–
LAWA60	Clear glass	–	–	–
LAWA65	Clear glass	–	–	–
LAWA76	Clear glass	–	–	–
LAWA81	Clear glass	Clear glass	–	–
LAWA82	Clear glass	Clear glass	–	–
LAWA83	Clear glass	Clear glass	–	–
LAWA84	Clear glass	Clear glass	–	–
LAWA87	Clear glass	Clear glass	–	–
LAWA89	Clear glass	Clear glass	–	–
LAWA90	Clear glass	Clear glass	–	–

(a) A dash (–) indicates that this glass was not subjected to the described heat treatment.

**Table 4.6 Optical Microscopy and SEM Evaluation of 271 LAW Simulated and Actual Waste Glasses (continued).**

Glass ID	As Melted	Optical and SEM evaluation of glass sample heat treated at 950°C and quenched.	Optical and SEM evaluation of glass sample heat treated at 850°C and quenched.	Optical and SEM evaluation of glass sample subjected to Canister Centerline Cooling (CCC).
LAWA93	Clear glass	Clear glass	–	–
LAWA96	Clear glass	< 0.1 vol% white dendritic crystals		
LAWA102R2	Clear glass	Clear glass		
LAWA104	Clear glass	– <sup>(a)</sup>	Clear glass	
LAWA105	Clear glass	–	Clear glass	–
LAWA112B14	Clear glass	–	–	–
LAWA112B15	Clear glass	–	–	–
LAWA125	Clear glass	–	Clear glass	–
LAWA127R1	Clear glass	–	Clear glass	–
LAWA127R2	Clear glass	–	–	–
LAWA129	Clear glass	–	Clear glass	–
LAWA129R1	Clear glass	–	–	–
LAWA133	Clear glass	–	Clear glass	–
LAWA134	Clear glass	–	Clear glass	–
LAWA135	Clear glass	–	Clear glass	–
LAWA136	Clear glass	–	Clear glass	–
LAWA170	Clear glass	–	Clear glass	–
LAWB30	Clear glass	<< 0.1 vol% high-Fe spinel crystals	–	–
LAWB31	Some undissolved or crystallized material	–	≈ 2.4 vol% of calcium phosphate crystals either Ca <sub>3</sub> (PO <sub>4</sub> ) <sub>2</sub> or apatite (Ca <sub>5</sub> (PO <sub>4</sub> ) <sub>3</sub> (OH,F,Cl)).	–
LAWB32	Some crystallized material	–	≈ 2.9 vol% of calcium phosphate crystals, same as above	–
LAWB33	Some crystallized material noted in the recovered glass.	–	≈ 6.2 vol% phosphate, same as above	–
LAWB34	Clear glass	–	≈ 4.8 vol% phosphate, same as above	–
LAWB35	Clear glass	–	≈ 0.26 vol% phosphate, same as above	–
LAWB37	Clear glass (undissolved material required an additional 60 min. melt time)	–	≈ 4.8 vol% phosphate, same as above	≈ 3.3 vol% calcium phosphate and trace amounts of TiO <sub>2</sub> , ZrSiO <sub>4</sub> , Al and Zn silicates.
LAWB38	Clear glass	–	≈ 4.0 vol% phosphate, same as above	–
LAWB40	Clear glass with sulfate layer	–	One small submicron crystal	–
LAWB41	Clear glass with sulfate layer	–	Clear glass	< 0.1 vol% Augite, spodumene and spinel crystals at crucible contact.
LAWB60	Clear glass	–	Clear glass	–

(a) A dash (–) indicates that this glass was not subjected to the described heat treatment.

**Table 4.6 Optical Microscopy and SEM Evaluation of 271 LAW Simulated and Actual Waste Glasses (continued).**

Glass ID	As Melted	Optical and SEM evaluation of glass sample heat treated at 950°C and quenched.	Optical and SEM evaluation of glass sample heat treated at 850°C and quenched.	Optical and SEM evaluation of glass sample subjected to Canister Centerline Cooling (CCC).
LAWB61	Clear glass	– <sup>(a)</sup>	<< 0.1 vol% Augite observed near meniscus .or crucible contact	–
LAWB62	Clear glass	–	Clear glass (<< 0.1 vol% Augite observed in sample heat treated at 700 °C)	–
LAWB63	Clear glass	–	Clear glass (<< 0.1 vol% Augite observed in sample heat treated at 700 °C)	–
LAWB64	Clear glass	–	<< 0.1 vol% Augite observed near meniscus .or crucible contact	–
LAWB67	Clear glass	–	<< 0.1 vol% Augite observed near meniscus .or crucible contact	–
LAWB69	Clear glass	–	Clear glass	–
LAWB70	Clear glass	–	Clear glass (<< 0.1 vol% Augite observed in sample heat treated at 700 °C)	–
LAWB71	Clear glass	–	Clear glass	–
LAWB72	Clear glass	–	Clear glass	–
LAWB73	Clear glass	–	< 0.1 vol% Augite (2.6 vol% Augite observed in sample heat treated at 700 °C)	–
LAWB74	Clear glass	–	Clear glass	–
LAWB75	Clear glass	–	Clear glass	–
LAWB76	Clear glass	–	Clear glass	–
LAWB77	Clear glass	–	Clear glass	–
LAWB81	Clear glass	–	<< 0.1 vol% Augite and one CrZnMg spinel crystal.	–
LAWB82	Clear glass	–	≈ 0.3 vol% Augite-aegirine along crucible interface + some clusters in bulk glass + small amount of spinels (similar observations in sample heat treated at 700 °C)	–
LAWB87	Clear glass	–	Clear glass	Clear glass
LAWB88	Clear glass	–	Clear glass	Clear glass
LAWB89	Clear glass	–	< 1 vol% Augite at air and crucible contact	–
LAWB90	Clear glass	–	< 1 vol% Augite at air and crucible contact	–
LAWB91	Clear glass	–	< 1 vol% Augite at air and crucible contact	–
LAWB92	Clear glass	–	< 1 vol% Augite at air and crucible contact	–
LAWB93	Clear glass	–	< 1 vol% Augite at air and crucible contact	–
LAWB93R1	Clear glass	–	–	–

(a) A dash (–) indicates that this glass was not subjected to the described heat treatment.

**Table 4.6 Optical Microscopy and SEM Evaluation of 271 LAW Simulated and Actual Waste Glasses (continued).**

Glass ID	As Melted	Optical and SEM evaluation of glass sample heat treated at 950°C and quenched.	Optical and SEM evaluation of glass sample heat treated at 850°C and quenched.	Optical and SEM evaluation of glass sample subjected to Canister Centerline Cooling (CCC).
LAWB94	Crystallized opaque glass.	– <sup>(a)</sup>	< 5 vol% Augite at air and crucible contact	–
LAWB95	Crystallized opaque glass.	–	≈ 1 vol% Augite at air and crucible contact (also spodumene detected in sample heat treated at 700°C)	–
LAWB96	Clear glass	–	≈ 0.9 vol% Augite at air and crucible contact.	–
LAWC12	Clear glass	–	Clear glass	–
LAWC15	Clear glass	–	Clear glass	–
LAWC21	Clear glass	Clear glass	–	–
LAWC21rev2	Clear glass	–	<< 0.1 vol% - two crystals	–
LAWC22	Clear glass	Clear glass	Clear glass	–
LAWC23	Clear glass	Clear glass	–	–
LAWC24	Clear glass	Clear glass + white granular nodules at crucible contact	–	–
LAWC25	Clear glass	Clear glass + white granular nodules at crucible contact	–	–
LAWC26	Clear glass	–	Clear glass	–
LAWC28	Clear glass	–	Clear glass	–
LAWC29	Clear glass	–	Clear glass	–
LAWC30	Clear glass	–	Clear glass	–
LAWC31	Clear glass	–	Clear glass	–
LAWC31R1	Clear glass	–	Clear glass	–
LAWC33	Clear glass	–	Clear glass	–
TFA-BASE	Clear glass	–	–	–
C22AN107	Clear glass	–	Clear glass	–
A88AP101R1	Clear glass	–	Clear glass	–
A88Si+15	Clear glass	–	Clear glass	–
A88Si-15	Clear glass	–	Clear glass	–
C22Si+15	Clear glass	–	Clear glass	–
C22Si-15	Clear glass	–	Clear glass	–
A1C1-1	Clear glass	–	Clear glass	–
A1C1-2	Clear glass	–	Clear glass	–
A1C1-3	Clear glass	–	Clear glass	–
C1-AN107	Clear glass	–	Clear glass	–

(a) A dash (–) indicates that this glass was not subjected to the described heat treatment.

**Table 4.6 Optical Microscopy and SEM Evaluation of 271 LAW Simulated and Actual Waste Glasses (continued).**

Glass ID	As Melted	Optical and SEM evaluation of glass sample heat treated at 950°C and quenched.	Optical and SEM evaluation of glass sample heat treated at 850°C and quenched.	Optical and SEM evaluation of glass sample subjected to Canister Centerline Cooling (CCC).
A2-AP101	Clear glass	– <sup>(a)</sup>	Clear glass	–
A2B1-1	Clear glass	–	Clear glass	–
A2B1-2	Clear glass	–	Clear glass	–
B1-AZ101	Clear glass	–	<< 1 vol% Augite at crucible contact	–
C2-AN102C35	Clear glass	–	Clear glass	–
A3-AN104	Clear glass	–	Clear glass	–
A2B1-3	Clear glass	–	Clear glass	–
A3C2-1	Clear glass	–	Clear glass	–
A3C2-2	Clear glass	–	Clear glass	–
A3C2-3	Clear glass	–	Clear glass	–
A1-AN105R2	Clear glass	–	Clear glass	–
12U-G-86A	Clear glass	–	–	Clear glass
LA44PNCC	Not applicable	Not applicable	Not applicable	Clear glass
LA44CCCR2	Not applicable	Not applicable	Not applicable	Clear glass
WVF-G-21B	Clear Glass	–	–	–
PNLA126CC	Not applicable	Not applicable	Not applicable	Clear glass
LA126CCC	Not applicable	Not applicable	Not applicable	Clear glass
WVM-G-142C	Clear Glass	–	–	–
A100G115A	Clear Glass	–	–	(sample A100CC described below)
A100CC	Not applicable	Not applicable	Not applicable	Clear glass
WVB-G-124B	Clear Glass	–	–	–
LA137SRCCC	Not applicable	Not applicable	Not applicable	Clear glass
WVR-G-127A	Clear Glass	–	–	–
LB83PNCC	Not applicable	Not applicable	Not applicable	Clear glass
LB83CCC-1	Not applicable	Not applicable	Not applicable	Clear glass
WVJ-G-109D	Clear Glass	–	–	–
GTSD-1126	Clear Glass	–	–	–
LB88CCC	Not applicable	Not applicable	Not applicable	Clear glass
AZ-102 Surr SRNL	Not applicable	Not applicable	Not applicable	Clear glass
12S-G-85C	Clear Glass	–	–	–
C100GCC	Not applicable	Not applicable	Not applicable	Clear glass
AN-102 Surr LC Melter	–	–	–	Clear glass
WVH-G-57B	Clear Glass	–	–	–
GTSD-1437	Clear Glass	–	–	–
PLTC35CCC	Not applicable	Not applicable	Not applicable	Clear glass

(a) A dash (–) indicates that this glass was not subjected to the described heat treatment.



**Table 4.6 Optical Microscopy and SEM Evaluation of 271 LAW Simulated and Actual Waste Glasses (continued).**

Glass ID	As Melted	Optical and SEM evaluation of glass sample heat treated at 950°C and quenched.	Optical and SEM evaluation of glass sample heat treated at 850°C and quenched.	Optical and SEM evaluation of glass sample subjected to Canister Centerline Cooling (CCC).
AN-103 Actual <sup>(a)</sup>	Not applicable	Not applicable	Not applicable	Clear glass
AW-101 Actual <sup>(a)</sup>	Not applicable	Not applicable	Not applicable	Clear glass
AP-101 Actual <sup>(a)</sup>	Not applicable	Not applicable	Not applicable	Clear glass
AZ-101 Actual <sup>(a)</sup>	Clear glass	–	–	≈ 0.8 vol% augite and few spinels, mostly zinc-chromite (ZnCr <sub>2</sub> O <sub>4</sub> ) in solid solution with spinel (MgAl <sub>2</sub> O <sub>4</sub> ) and magnetite (Fe <sub>3</sub> O <sub>4</sub> ). Augite dendrites of the average composition Na <sub>0.08</sub> Ca <sub>0.81</sub> Mg <sub>0.49</sub> Zn <sub>0.07</sub> Al <sub>0.08</sub> Fe <sub>0.35</sub> Cr <sub>0.01</sub> Si <sub>1.92</sub> Ti <sub>0.08</sub> O <sub>6</sub> nucleated on and branched from bubbles and spinels.
AZ-102 Actual <sup>(a)</sup>	Clear glass	–	–	Clear glass (Note that this is the sample “AZ-102 Actual CCC” described below)
AZ-102 Actual CCC <sup>(a)</sup>	Not applicable	Not applicable	Not applicable	Clear glass
AN-107 Actual <sup>(a)</sup> (LAWC15)	Not applicable	Not applicable	Not applicable	Clear glass
AN-102 Actual LC Melter <sup>(a)</sup>	–	–	–	Clear glass
AN-102 Actual <sup>(a)</sup>	Not applicable	Not applicable	Not applicable	Clear glass

(a) These samples were prepared at SRTC or PNNL from actual radioactive waste samples; all but one (AZ -102 Actual) were subjected to CCC.

(b) A dash (–) indicates that this glass was not subjected to the described heat treatment.

**Table 5.1. Twenty LAW Glasses Excluded from PCT Modeling Data Set.**

<b>Class ID</b>	<b>Reason Glass Excluded from PCT Modeling Set</b>
LAWA43-1	Outlying composition ( $\text{Al}_2\text{O}_3 = 12 \text{ wt}\%$ )
LAWA49	Outlying composition ( $\text{Fe}_2\text{O}_3 = 9.98 \text{ wt}\%$ )
LAWA50	Outlying composition ( $\text{Fe}_2\text{O}_3 = 11.98 \text{ wt}\%$ )
LAWA65	Outlying composition ( $\text{MgO} = 6.03 \text{ wt}\%$ )
LAWA82	Outlying composition ( $\text{TiO}_2 = 3.99 \text{ wt}\%$ )
LAWA89	Outlying composition ( $\text{TiO}_2 = 3.98 \text{ wt}\%$ )
LAWB32	Outlying composition ( $\text{B}_2\text{O}_3 = 15.15 \text{ wt}\%$ )
LAWB40	Outlying composition (XRF $\text{SO}_3 = 1.36 \text{ wt}\%$ )
LAWB41	Outlying composition (XRF $\text{SO}_3 = 1.23 \text{ wt}\%$ )
LAWB60	Outlying composition ( $\text{CaO} = 11.91 \text{ wt}\%$ )
LAWB62	Outlying composition ( $\text{CaO} = 12.00 \text{ wt}\%$ )
LAWB63	Outlying composition ( $\text{ZnO} = 5.82 \text{ wt}\%$ )
LAWB82	Outlying composition ( $\text{Fe}_2\text{O}_3 = 9.52 \text{ wt}\%$ )
LAWC12	Outlying composition ( $\text{Al}_2\text{O}_3 = 11.99 \text{ wt}\%$ , $\text{TiO}_2 = 3.42 \text{ wt}\%$ )
LAWC25	Outlying composition ( $\text{K}_2\text{O} = 8.08 \text{ wt}\%$ )
LAWC28	Outlying composition ( $\text{CaO} = 12.81 \text{ wt}\%$ )
LAWE3Cr2CCC	Non-representative composition & heat treatment
LAWE9HCr1CCC	Non-representative composition & heat treatment
LAWE9HCr2CCC	Non-representative composition & heat treatment
LAWE10HCr3CCC	Non-representative composition & heat treatment

**Table 5.2. Normalized<sup>(a)</sup> Compositions (mass fractions) of 244 LAW Glasses Used for PCT Model Development.**

Glass ID	Group ID <sup>(b)</sup>	Al <sub>2</sub> O <sub>3</sub>	B <sub>2</sub> O <sub>3</sub>	CaO	Cl	Cr <sub>2</sub> O <sub>3</sub>	F	Fe <sub>2</sub> O <sub>3</sub>	K <sub>2</sub> O	Li <sub>2</sub> O	MgO	Na <sub>2</sub> O	P <sub>2</sub> O <sub>5</sub>	XRF SO <sub>3</sub> <sup>(c)</sup>	SiO <sub>2</sub>	TiO <sub>2</sub>	ZnO	ZrO <sub>2</sub>	Others	Sum <sup>(d)</sup>
LAWA44R10	ExPh1	.06202	.08903	.01991	.00650	.00020	.00010	.06982	.00500	.00000	.01991	.20006	.00030	.00090	.44563	.01991	.02971	.02991	.00110	1.00000
LAWA53	ExPh1	.06145	.06165	.07840	.00646	.00020	.00010	.07467	.00494	.00000	.01473	.19898	.00030	.00620	.42036	.01100	.02977	.02977	.00101	1.00000
LAWA56	ExPh1	.06151	.12050	.01970	.00646	.00020	.00010	.07474	.00495	.00000	.01475	.19918	.00030	.00520	.42079	.01101	.02980	.02980	.00101	1.00000
LAWA88	ExPh1 <sup>(e)</sup>	.06082	.09700	.01992	.00329	.00009	.00000	.05533	.02583	.00000	.01475	.20005	.00070	.00190	.44002	.01992	.02951	.02988	.00100	1.00000
LAWA88R1	ExPh1	.06082	.09700	.01991	.00330	.00010	.00000	.05532	.02581	.00000	.01475	.20006	.00070	.00190	.44004	.01991	.02951	.02987	.00100	1.00000
LAWA102R1	ExPh1	.06040	.09968	.05044	.00329	.00020	.00030	.05383	.00259	.02492	.01485	.14503	.00130	.00670	.46350	.01136	.03050	.03010	.00101	1.00000
LAWA126	ExPh1	.05637	.09815	.01989	.00200	.00020	.00300	.05537	.03878	.00000	.01479	.18451	.00080	.00310	.44098	.01999	.02959	.02989	.00260	1.00000
LAWA128	ExPh1	.06027	.07066	.02079	.00200	.00020	.00300	.05787	.03878	.00000	.01179	.18451	.00080	.00300	.46067	.02089	.03088	.03128	.00260	1.00000
LAWA130	ExPh1	.06025	.08943	.02078	.00200	.00020	.00300	.02858	.03877	.00000	.01179	.18445	.00080	.00330	.46053	.02088	.04137	.03127	.00260	1.00000
LAWB65	ExPh1	.06188	.09939	.06690	.00000	.00100	.00070	.05295	.00261	.04303	.02969	.05476	.00010	.00890	.48492	.01394	.04664	.03159	.00100	1.00000
LAWB66	ExPh1	.06203	.09963	.08214	.00000	.00101	.00070	.05308	.00261	.04313	.02976	.05489	.00010	.00650	.48609	.01397	.03167	.03167	.00101	1.00000
LAWB68	ExPh1	.06192	.08440	.08199	.00000	.00100	.00070	.05299	.00261	.04305	.02970	.05479	.00010	.00830	.48521	.01395	.04666	.03161	.00100	1.00000
LAWB78	ExPh1	.06161	.12351	.07132	.00010	.00050	.00080	.03256	.00230	.03055	.02975	.09797	.00050	.00510	.47080	.00000	.04007	.03155	.00100	1.00000
LAWB79	ExPh1	.06156	.12342	.07127	.00010	.00050	.00080	.03253	.00230	.03514	.02973	.08629	.00050	.00580	.47748	.00000	.04004	.03153	.00100	1.00000
LAWB80	ExPh1	.06156	.12341	.07126	.00010	.00050	.00080	.03253	.01992	.03513	.02973	.06626	.00050	.00580	.47993	.00000	.04004	.03153	.00100	1.00000
LAWB83	ExPh1	.06183	.10035	.06783	.00010	.00040	.00060	.05293	.00190	.04312	.02971	.05473	.00040	.00490	.48624	.01391	.04842	.03162	.00100	1.00000
LAWB84	ExPh1	.06187	.10041	.06687	.00010	.00040	.00060	.05296	.00190	.04405	.02973	.05476	.00040	.00440	.48654	.01392	.04845	.03163	.00100	1.00000
LAWB85	ExPh1	.06184	.11527	.05283	.00010	.00040	.00060	.05293	.00190	.04313	.02972	.05473	.00040	.00490	.48629	.01391	.04843	.03162	.00100	1.00000
LAWB86	ExPh1	.06188	.12426	.05737	.00010	.00040	.00060	.05297	.00190	.04356	.02974	.05477	.00040	.00430	.48664	.00000	.04846	.03164	.00100	1.00000
C100-G-136B	ExPh1	.06127	.10092	.06408	.00120	.00020	.00060	.06478	.00150	.02733	.01512	.11874	.00120	.00400	.46726	.01121	.03014	.03024	.00020	1.00000
LAWC27	ExPh1	.06117	.12183	.08544	.00111	.00018	.00054	.00009	.00136	.02733	.01500	.11953	.00106	.00410	.48868	.01121	.03018	.03018	.00101	1.00000
LAWC32	ExPh1	.06490	.10047	.09038	.00111	.00018	.00054	.02424	.00136	.02734	.01501	.11956	.00106	.00380	.46744	.01121	.04019	.03019	.00101	1.00000
LAWM1	Ph1	.09044	.06029	.10048	.00020	.00008	.00008	.08039	.04019	.04522	.00000	.05024	.00013	.00520	.44666	.03015	.05024	.00000	.00002	1.00000
LAWM2	Ph1	.03512	.06020	.10033	.00803	.00322	.00300	.08027	.00000	.04515	.05017	.05017	.00501	.00670	.47157	.03010	.05017	.00000	.00080	1.00000
LAWM3	Ph1	.09033	.06022	.10036	.00020	.00008	.00008	.08029	.00000	.04487	.05018	.11521	.00013	.00640	.40145	.00000	.01004	.04015	.00002	1.00000
LAWM4	Ph1	.03516	.13058	.10044	.00020	.00008	.00008	.05560	.04018	.04520	.00000	.05022	.00013	.00560	.41599	.03013	.05022	.04018	.00002	1.00000
LAWM5	Ph1	.09041	.06027	.05794	.00020	.00008	.00008	.08036	.04018	.04520	.00000	.05023	.00013	.00550	.48903	.03014	.01005	.04018	.00002	1.00000
LAWM6	Ph1	.09002	.10612	.10002	.00020	.00008	.00007	.08002	.04001	.00000	.05001	.08999	.00012	.00320	.40009	.03001	.01000	.00000	.00002	1.00000
LAWM7	Ph1	.05441	.06966	.10028	.00020	.00008	.00008	.08023	.00000	.02585	.05014	.05014	.00013	.00720	.52147	.03008	.01003	.00000	.00002	1.00000
LAWM8	Ph1	.09027	.13039	.06448	.00803	.00322	.00300	.00000	.00000	.02087	.05015	.05015	.00501	.00700	.44626	.03009	.05015	.04012	.00080	1.00000
LAWM9	Ph1	.03506	.06010	.10016	.00801	.00322	.00300	.08013	.04006	.02392	.00000	.05008	.00500	.00240	.49792	.00000	.05008	.04006	.00080	1.00000
LAWM10	Ph1	.09005	.13007	.10006	.00801	.00322	.00300	.00000	.00000	.04503	.00000	.13074	.00499	.00230	.40170	.03002	.01001	.04002	.00080	1.00000
LAWM11	Ph1	.03504	.13013	.09413	.00020	.00008	.00007	.05317	.04004	.04505	.00000	.11491	.00012	.00900	.46804	.00000	.01001	.00000	.00002	1.00000
LAWM12	Ph1	.03501	.13005	.00000	.00801	.00322	.00300	.02310	.04002	.04502	.01971	.14259	.00499	.00230	.42215	.03001	.05002	.04002	.00080	1.00000
LAWM13	Ph1	.03501	.06001	.10002	.00412	.00165	.00154	.08002	.03785	.00000	.00000	.22005	.00257	.00500	.40009	.03001	.02164	.00000	.00041	1.00000
LAWM14	Ph1	.03500	.06000	.02045	.00020	.00008	.00007	.00000	.00000	.00881	.05000	.21999	.00012	.00530	.51997	.03000	.05000	.00000	.00002	1.00000

- (a) The compositions listed in this table are normalized mass fraction versions of target compositions of the glasses, after replacing the target values of SO<sub>3</sub> by XRF analyzed (or estimated analyzed) values. See Section 3.3 for the details.
- (b) The Group IDs are described in Sections 2.1 to 2.7.
- (c) XRF SO<sub>3</sub> denotes that the SO<sub>3</sub> composition is based on chemical analysis by XRF. For most glasses SO<sub>3</sub> was directly measured by XRF, but for some glasses estimated XRF values were used (see Section 3.3).
- (d) The normalized component mass fractions listed in this table were rounded to five decimals, and may not sum exactly to 1.00000 as listed. However, complete compositions listed to more decimal places and summing to 1.0000 were used for property-composition modeling.
- (e) LAW88 was previously classified in the actively designed (ActDes) group for the PCT response, with that classification used for the plotting symbols in Section 5.

**Table 5.2. Normalized<sup>(a)</sup> Compositions (mass fractions) of 244 LAW Glasses Used for PCT Model Development (continued).**

Glass ID	Group ID <sup>(b)</sup>	Al <sub>2</sub> O <sub>3</sub>	B <sub>2</sub> O <sub>3</sub>	CaO	Cl	Cr <sub>2</sub> O <sub>3</sub>	F	Fe <sub>2</sub> O <sub>3</sub>	K <sub>2</sub> O	Li <sub>2</sub> O	MgO	Na <sub>2</sub> O	P <sub>2</sub> O <sub>5</sub>	XRF SO <sub>3</sub> <sup>(c)</sup>	SiO <sub>2</sub>	TiO <sub>2</sub>	ZnO	ZrO <sub>2</sub>	Others	Sum <sup>(d)</sup>
LAWM15	Ph1	.08999	.09356	.00000	.00800	.00321	.00299	.06283	.00000	.00000	.03724	.21998	.00499	.00170	.43471	.03000	.01000	.00000	.00080	1.00000
LAWM16	Ph1	.08006	.12008	.08006	.00020	.00008	.00007	.06505	.00100	.03002	.01001	.10007	.00012	.00330	.42480	.02502	.05004	.01001	.00002	1.00000
LAWM17	Ph1	.05002	.12004	.02215	.00020	.00008	.00007	.06502	.02001	.00500	.03501	.17006	.00012	.00200	.42015	.00500	.05002	.03501	.00002	1.00000
LAWM18	Ph1	.08005	.12007	.08005	.00801	.00322	.00300	.06504	.00100	.03002	.01001	.10006	.00499	.00340	.42025	.02502	.02001	.02501	.00080	1.00000
LAWM19	Ph1	.07997	.11996	.07997	.00800	.00321	.00299	.01999	.01999	.00500	.01000	.13170	.00499	.00360	.41986	.00500	.04998	.03499	.00080	1.00000
LAWM20	Ph1	.05001	.07002	.08002	.00800	.00321	.00299	.02001	.02001	.02265	.03501	.17004	.00499	.00210	.42011	.00500	.05001	.03501	.00080	1.00000
LAWM21	Ph1	.05005	.10901	.08008	.00020	.00008	.00007	.06507	.02002	.03003	.01001	.10010	.00012	.00460	.42042	.02503	.05005	.03504	.00002	1.00000
LAWM22	Ph1	.07990	.06992	.01998	.00799	.00321	.00299	.06492	.01998	.00499	.03496	.16979	.00498	.00450	.41949	.00670	.04994	.03496	.00080	1.00000
LAWM23	Ph1	.05011	.07015	.08018	.00802	.00322	.00300	.02004	.02004	.03007	.01002	.10022	.00500	.00340	.48547	.02506	.05011	.03508	.00080	1.00000
LAWM24	Ph1	.08000	.12001	.02000	.00020	.00008	.00007	.06500	.02000	.00641	.01000	.17001	.00012	.00230	.47076	.00500	.02000	.01000	.00002	1.00000
LAWM25R1	Ph1	.08011	.12017	.02003	.00801	.00322	.00300	.03684	.02003	.03004	.03505	.10014	.00500	.00260	.49991	.00501	.02003	.01001	.00080	1.00000
LAWM26	Ph1	.08006	.12008	.04970	.00801	.00322	.00300	.02001	.00100	.03002	.01001	.10007	.00499	.00490	.49909	.00500	.05004	.01001	.00080	1.00000
LAWM27	Ph1	.08006	.07005	.08006	.00801	.00322	.00300	.06505	.02001	.00500	.03502	.13381	.00499	.00250	.42030	.02502	.03309	.01001	.00080	1.00000
LAWM28	Ph1	.05010	.12024	.08016	.00020	.00008	.00008	.06513	.00703	.00690	.01002	.10020	.00013	.00360	.50101	.02505	.02004	.01002	.00002	1.00000
LAWM29	Ph1	.07565	.07006	.02002	.00077	.00031	.00029	.06506	.02002	.03003	.03503	.10009	.00048	.00310	.46892	.02502	.05005	.03503	.00008	1.00000
LAWM30	Ph1	.08003	.12004	.02001	.00020	.00008	.00007	.06502	.00100	.02023	.01000	.17006	.00012	.00200	.42015	.00592	.05002	.03501	.00002	1.00000
LAWM31	Ph1	.05002	.07003	.08003	.00801	.00322	.00300	.06502	.00100	.03001	.01000	.16758	.00499	.00300	.42327	.02501	.02001	.03501	.00080	1.00000
LAWM32	Ph1	.05146	.07002	.02001	.00800	.00321	.00299	.02001	.02001	.03001	.03501	.16514	.00499	.00320	.50013	.00500	.05001	.01000	.00080	1.00000
LAWM33R1	Ph1	.05002	.12005	.08003	.00020	.00008	.00007	.06503	.01722	.00899	.01000	.17007	.00012	.00290	.42017	.02501	.02001	.01000	.00002	1.00000
LAWM34	Ph1	.05001	.08356	.08002	.00020	.00008	.00007	.06295	.02001	.03001	.01000	.17005	.00012	.00300	.42012	.01474	.02001	.03501	.00002	1.00000
LAWM35	Ph1	.05003	.12007	.06182	.00801	.00322	.00300	.04413	.00100	.00500	.03502	.17010	.00499	.00180	.42023	.02501	.02001	.02576	.00080	1.00000
LAWM36	Ph1	.07002	.11004	.07002	.00318	.00128	.00119	.05002	.00300	.02501	.01501	.12004	.00198	.00370	.45016	.02001	.03501	.02001	.00032	1.00000
LAWM37	Ph1	.06751	.11009	.07006	.00020	.00008	.00007	.05004	.00300	.02502	.02502	.12010	.00012	.00320	.45038	.01001	.03503	.03003	.00002	1.00000
LAWM38	Ph1	.06998	.07998	.06998	.00800	.00321	.00299	.02999	.00154	.02499	.01500	.13997	.00499	.00370	.47988	.01000	.03499	.02000	.00080	1.00000
LAWM39	Ph1	.07007	.09063	.05005	.00801	.00322	.00300	.03003	.00100	.02502	.02502	.14013	.00499	.00250	.48046	.01001	.03503	.02002	.00080	1.00000
LAWM40	Ph1	.06003	.11006	.05003	.00214	.00086	.00080	.05003	.00100	.01001	.01501	.14008	.00133	.00310	.48027	.01001	.03502	.03002	.00021	1.00000
LAWM41	Ph1	.07002	.08002	.07002	.00800	.00321	.00299	.05001	.00300	.01000	.02501	.14004	.00499	.00340	.45012	.01000	.04601	.02235	.00080	1.00000
LAWM42	Ph1	.06004	.08005	.05003	.00801	.00322	.00300	.04037	.00100	.02502	.01501	.14009	.00499	.00300	.48032	.02001	.03502	.03002	.00080	1.00000
LAWM43	Ph1	.07002	.08678	.05002	.00800	.00322	.00300	.05002	.00300	.02501	.02501	.12004	.00499	.00390	.45016	.02001	.04602	.03001	.00080	1.00000
LAWM44	Ph1	.06325	.10039	.07008	.00020	.00008	.00007	.05006	.00100	.01001	.01502	.12014	.00012	.00290	.48055	.02002	.04605	.02002	.00002	1.00000
LAWM45	Ph1	.07003	.08003	.05784	.00020	.00008	.00007	.05002	.00300	.01423	.01501	.14005	.00012	.00310	.48017	.02001	.04602	.02001	.00002	1.00000
LAWM46	Ph1	.06012	.11023	.06523	.00020	.00008	.00008	.05010	.00100	.01002	.02505	.12025	.00013	.00200	.48034	.01002	.03507	.03006	.00002	1.00000
LAWM47	Ph1	.06200	.08003	.07003	.00020	.00008	.00007	.05002	.00100	.01000	.02501	.14005	.00012	.00310	.48017	.01307	.03501	.03001	.00002	1.00000
LAWM48	Ph1	.06234	.11016	.05277	.00801	.00322	.00300	.05007	.00100	.01001	.01502	.12017	.00500	.00260	.48070	.02003	.03505	.02003	.00080	1.00000
LAWM49	Ph1	.07001	.10906	.05001	.00800	.00321	.00299	.03000	.00100	.01000	.01500	.14002	.00499	.00350	.47538	.01000	.04601	.02000	.00080	1.00000

- (a) The compositions listed in this table are normalized mass fraction versions of target compositions of the glasses, after replacing the target values of SO<sub>3</sub> by XRF analyzed (or estimated analyzed) values. See Section 3.3 for the details.
- (b) The Group IDs are described in Sections 2.1 to 2.7.
- (c) XRF SO<sub>3</sub> denotes that the SO<sub>3</sub> composition is based on chemical analysis by XRF. For most glasses SO<sub>3</sub> was directly measured by XRF, but for some glasses estimated XRF values were used (see Section 3.3).
- (d) The normalized component mass fractions listed in this table were rounded to five decimals, and may not sum exactly to 1.00000 as listed. However, complete compositions listed to more decimal places and summing to 1.0000 were used for property-composition modeling.

**Table 5.2. Normalized<sup>(a)</sup> Compositions (mass fractions) of 244 LAW Glasses Used for PCT Model Development (continued).**

Glass ID	Group ID <sup>(b)</sup>	Al <sub>2</sub> O <sub>3</sub>	B <sub>2</sub> O <sub>3</sub>	CaO	Cl	Cr <sub>2</sub> O <sub>3</sub>	F	Fe <sub>2</sub> O <sub>3</sub>	K <sub>2</sub> O	Li <sub>2</sub> O	MgO	Na <sub>2</sub> O	P <sub>2</sub> O <sub>5</sub>	XRF SO <sub>3</sub> <sup>(c)</sup>	SiO <sub>2</sub>	TiO <sub>2</sub>	ZnO	ZrO <sub>2</sub>	Others	Sum <sup>(d)</sup>
LAWM50	Ph1	.06530	.09700	.06109	.00446	.00179	.00167	.04111	.00204	.01668	.02032	.13095	.00278	.00290	.46982	.01528	.04104	.02533	.00045	1.00000
LAWM51	Ph1	.06528	.09697	.06107	.00446	.00179	.00167	.04110	.00204	.01667	.02031	.13091	.00278	.00320	.46968	.01528	.04102	.02533	.00045	1.00000
LAWM52	Ph1	.06088	.09711	.01994	.00329	.00009	.00000	.05538	.02586	.00000	.01477	.20027	.00070	.00180	.44051	.01994	.02954	.02991	.00000	1.00000
LAWM53	Ph1	.09031	.06021	.10034	.00020	.00008	.00008	.08027	.04014	.04515	.00000	.05017	.00013	.00660	.44603	.03010	.05017	.00000	.00002	1.00000
LAWM54R1	Ph1	.03505	.06008	.10014	.00801	.00322	.00300	.08011	.04006	.02391	.00000	.05007	.00500	.00260	.49782	.00000	.05007	.04006	.00080	1.00000
LAWM55	Ph1	.03501	.13004	.00000	.00800	.00321	.00299	.02310	.04001	.04501	.01971	.14257	.00499	.00240	.42211	.03001	.05001	.04001	.00080	1.00000
LAWM56	Ph1	.04990	.11975	.06166	.00799	.00321	.00299	.04402	.00100	.00499	.03493	.16965	.00498	.00440	.41914	.02495	.01996	.02570	.00080	1.00000
LAWM57	Ph1aAug	.06997	.11000	.03000	.00196	.00078	.00078	.04659	.03801	.00000	.01440	.20620	.00122	.00320	.39274	.01370	.03026	.04001	.00016	1.00000
LAWM58	Ph1aAug	.07002	.09294	.01028	.00196	.00078	.00078	.06500	.03800	.00000	.01440	.20536	.00122	.00320	.41654	.01370	.02563	.04001	.00016	1.00000
LAWM59	Ph1aAug	.06847	.09009	.02965	.00196	.00078	.00078	.06492	.02004	.00000	.01441	.20008	.00122	.00310	.44558	.01371	.02506	.02001	.00016	1.00000
LAWM60	Ph1aAug	.05003	.11006	.01714	.00196	.00078	.00078	.04503	.02004	.00000	.01441	.20015	.00122	.00300	.45351	.01371	.02804	.03998	.00016	1.00000
LAWM61	Ph1aAug	.05002	.11001	.01001	.00196	.00078	.00078	.04502	.03293	.00000	.01440	.20004	.00122	.00330	.45060	.01370	.04501	.02005	.00016	1.00000
LAWM62	Ph1aAug	.05004	.09004	.01002	.00196	.00078	.00078	.06500	.03380	.00000	.01440	.20006	.00122	.00320	.44341	.01370	.03842	.03300	.00016	1.00000
LAWM63	Ph1aAug	.07001	.09402	.01044	.00196	.00078	.00078	.04695	.02059	.00000	.01440	.22998	.00122	.00340	.42601	.01370	.04500	.02058	.00016	1.00000
LAWM64	Ph1aAug	.06991	.10989	.03002	.00196	.00078	.00078	.06503	.02001	.00000	.01441	.20051	.00122	.00300	.38379	.01371	.04490	.03993	.00016	1.00000
LAWM65	Ph1aAug	.05001	.09001	.02964	.00196	.00078	.00078	.04503	.02001	.00000	.01440	.22791	.00122	.00340	.43599	.01370	.02501	.03997	.00016	1.00000
LAWM66	Ph1aAug	.07587	.10637	.01003	.00196	.00078	.00078	.06315	.00479	.00000	.01440	.22996	.00122	.00320	.38362	.01370	.04500	.04498	.00016	1.00000
LAWM67	Ph1aAug	.08002	.10601	.01545	.00196	.00078	.00078	.04603	.05402	.00000	.01440	.20134	.00122	.00320	.38370	.01370	.02720	.05001	.00016	1.00000
LAWM68	Ph1aAug	.05003	.09002	.02999	.00196	.00078	.00078	.06500	.04803	.00000	.01440	.20009	.00122	.00330	.40815	.01370	.03562	.03677	.00016	1.00000
LAWM69	Ph1aAug	.07976	.10990	.02997	.00196	.00078	.00078	.06370	.01829	.00000	.01440	.20095	.00122	.00340	.39601	.01370	.04499	.02002	.00016	1.00000
LAWM70	Ph1aAug	.05002	.09397	.01047	.00196	.00078	.00078	.06498	.04550	.00000	.01440	.20011	.00122	.00330	.45357	.01370	.02501	.02006	.00016	1.00000
LAWM71	Ph1aAug	.05006	.09001	.01003	.00196	.00078	.00078	.04501	.05401	.00000	.01440	.20004	.00122	.00340	.44943	.01370	.04498	.02002	.00016	1.00000
LAWM72	Ph1aAug	.08002	.11002	.02937	.00196	.00078	.00078	.06449	.04177	.00000	.01440	.20042	.00122	.00320	.39173	.01370	.02501	.02095	.00016	1.00000
LAWM73	Ph1aAug	.08002	.09006	.02996	.00196	.00078	.00078	.04878	.01221	.00000	.01440	.23002	.00122	.00320	.40391	.01370	.04494	.02388	.00016	1.00000
LAWM74	Ph1aAug	.07589	.09009	.01001	.00196	.00078	.00078	.04504	.00000	.00000	.01441	.21329	.00122	.00290	.45377	.01371	.02598	.05002	.00016	1.00000
LAWM75	Ph1aAug	.08003	.09157	.02996	.00196	.00078	.00078	.06497	.01082	.00000	.01441	.20691	.00122	.00310	.38461	.01371	.04500	.05001	.00016	1.00000
LAWM76	Ph1aAug	.06403	.09926	.01923	.00196	.00078	.00078	.05424	.02599	.00000	.01441	.21409	.00122	.00310	.41881	.01371	.03423	.03401	.00016	1.00000
LAWE2H	Corr	.05951	.09751	.01970	.00196	.00078	.00078	.05365	.03790	.00000	.01440	.20782	.00122	.00310	.42440	.01370	.03410	.02930	.00016	1.00000
LAWE3	Corr	.06102	.10003	.02021	.00200	.00080	.00080	.05502	.04992	.00000	.01480	.18215	.00124	.00320	.42963	.01400	.03501	.03001	.00016	1.00000
LAWE3H	Corr	.05942	.09743	.01971	.00196	.00078	.00078	.05366	.05412	.00000	.01440	.19746	.00122	.00340	.41859	.01360	.03411	.02921	.00016	1.00000
LAWE4H	Corr	.05974	.09796	.02461	.00196	.00078	.00078	.05383	.00540	.00000	.01451	.21283	.00122	.00350	.44527	.01371	.03432	.02942	.00016	1.00000
LAWE5H	Corr	.05997	.09821	.03614	.00196	.00078	.00078	.05410	.00541	.00491	.01452	.18991	.00122	.00350	.45096	.01372	.03434	.02943	.00016	1.00000
LAWE7H	Corr	.06027	.09882	.06318	.00196	.00078	.00078	.05441	.00541	.03174	.01492	.13546	.00122	.00470	.44810	.01382	.03464	.02964	.00016	1.00000
LAWE9H	Corr	.06066	.09946	.06878	.00197	.00079	.00079	.05468	.00541	.04091	.02366	.08953	.00122	.00430	.46919	.01394	.03479	.02978	.00016	1.00000
LAWE10H	Corr	.06086	.09976	.06978	.00197	.00079	.00079	.05498	.00541	.04271	.02948	.05735	.00122	.00540	.49054	.01394	.03489	.02998	.00016	1.00000

- (a) The compositions listed in this table are normalized mass fraction versions of target compositions of the glasses, after replacing the target values of SO<sub>3</sub> by XRF analyzed (or estimated analyzed) values. See Section 3.3 for the details.
- (b) The Group IDs are described in Sections 2.1 to 2.7.
- (c) XRF SO<sub>3</sub> denotes that the SO<sub>3</sub> composition is based on chemical analysis by XRF. For most glasses SO<sub>3</sub> was directly measured by XRF, but for some glasses estimated XRF values were used (see Section 3.3).
- (d) The normalized component mass fractions listed in this table were rounded to five decimals, and may not sum exactly to 1.00000 as listed. However, complete compositions listed to more decimal places and summing to 1.0000 were used for property-composition modeling.

**Table 5.2. Normalized<sup>(a)</sup> Compositions (mass fractions) of 244 LAW Glasses Used for PCT Model Development (continued).**

Glass ID	Group ID <sup>(b)</sup>	Al <sub>2</sub> O <sub>3</sub>	B <sub>2</sub> O <sub>3</sub>	CaO	Cl	Cr <sub>2</sub> O <sub>3</sub>	F	Fe <sub>2</sub> O <sub>3</sub>	K <sub>2</sub> O	Li <sub>2</sub> O	MgO	Na <sub>2</sub> O	P <sub>2</sub> O <sub>5</sub>	XRF SO <sub>3</sub> <sup>(c)</sup>	SiO <sub>2</sub>	TiO <sub>2</sub>	ZnO	ZrO <sub>2</sub>	Others	Sum <sup>(d)</sup>
LAWE11	Corr	.06106	.10010	.02322	.00200	.00080	.00080	.05506	.04755	.00000	.01481	.17377	.00124	.00250	.43784	.01401	.03504	.03003	.00016	1.00000
LAWE12	Corr	.06952	.08753	.01971	.00196	.00078	.00078	.04361	.05412	.00000	.01440	.19746	.00122	.00320	.41853	.01370	.03411	.03921	.00016	1.00000
LAWE13	Corr	.06952	.09753	.01971	.00196	.00078	.00078	.05362	.05412	.00000	.00440	.19746	.00122	.00320	.41853	.00370	.03411	.03921	.00016	1.00000
LAWE14	Corr	.04942	.09754	.01471	.00196	.00078	.00078	.05366	.05412	.00000	.00440	.19748	.00122	.00310	.43363	.01371	.03411	.03922	.00016	1.00000
LAWE15	Corr	.05942	.08754	.01471	.00196	.00078	.00078	.05366	.05412	.00000	.00940	.19748	.00122	.00310	.42863	.01371	.03411	.03922	.00016	1.00000
LAWE16	Corr	.05934	.08241	.01468	.00196	.00078	.00078	.05358	.05404	.00000	.00939	.19719	.00122	.00460	.42798	.01369	.03406	.04415	.00016	1.00000
LAWCrP1R	HiCrP	.06101	.10002	.02761	.00124	.00328	.00112	.05501	.00125	.00000	.01480	.19347	.01442	.00370	.44401	.01400	.03501	.03001	.00004	1.00000
LAWCrP2R	HiCrP	.06099	.09998	.02105	.00193	.00591	.00103	.05499	.00275	.00000	.01480	.20996	.01333	.00360	.43065	.01400	.03499	.02999	.00006	1.00000
LAWCrP3R	HiCrP	.06101	.10001	.02761	.00124	.00328	.00111	.05500	.00125	.00000	.01480	.19345	.02380	.00380	.43458	.01400	.03500	.03000	.00004	1.00000
LAWCrP4R	HiCrP	.06098	.09997	.02104	.00192	.00591	.00103	.05498	.00275	.00000	.01480	.20994	.02379	.00370	.42014	.01400	.03499	.02999	.00006	1.00000
LAWCrP5	HiCrP	.06108	.10013	.05813	.00136	.00591	.00067	.05507	.00087	.02642	.01488	.14395	.01335	.00380	.43505	.01402	.03504	.03004	.00021	1.00000
LAWCrP6	HiCrP	.06104	.10007	.06945	.00136	.00630	.00067	.05504	.00087	.04173	.02552	.08006	.02512	.00580	.44770	.01401	.03502	.03002	.00021	1.00000
LAWCrP7	HiCrP	.06104	.10007	.06985	.00136	.00630	.00067	.05504	.00087	.04303	.02932	.05404	.02512	.00660	.46741	.01401	.03502	.03002	.00021	1.00000
LAWA41	ActDes	.06203	.07501	.02000	.00580	.00017	.00040	.06983	.03101	.00000	.01995	.20002	.00078	.00100	.43414	.01995	.02993	.02995	.00004	1.00000
LAWA42	ActDes	.06204	.09034	.02404	.00579	.00017	.00036	.08411	.03101	.00001	.02402	.20004	.00078	.00100	.38007	.02403	.03605	.03607	.00005	1.00000
LAWA44	ActDes	.06202	.08903	.01991	.00650	.00020	.00010	.06982	.00500	.00000	.01991	.20006	.00030	.00100	.44563	.01991	.02971	.02991	.00100	1.00000
LAWA45	ActDes	.06201	.11901	.00000	.00652	.00020	.00010	.06980	.00501	.00000	.01477	.20000	.00034	.00100	.44552	.01994	.02477	.02992	.00111	1.00000
LAWA51	ActDes	.06203	.11976	.00000	.00587	.00018	.00009	.06998	.00451	.00000	.01484	.18003	.00030	.00070	.46579	.01996	.02488	.02998	.00111	1.00000
LAWA52	ActDes	.06179	.06191	.07882	.00652	.00020	.00010	.07505	.00501	.00000	.01477	.19999	.00034	.00100	.42247	.01108	.02994	.02992	.00112	1.00000
LAWA60	ActDes	.08528	.11228	.04321	.00652	.00020	.00010	.00000	.00501	.00000	.01994	.19999	.00034	.00100	.44551	.01994	.02965	.02992	.00112	1.00000
LAWA76	ActDes	.06132	.10916	.07822	.00647	.00019	.00010	.07448	.00497	.04985	.01466	.10098	.00033	.00860	.41919	.01100	.02971	.02969	.00108	1.00000
LAWA81	ActDes	.06201	.08902	.03989	.00652	.00020	.00010	.06980	.00501	.00000	.01994	.20000	.00034	.00100	.44552	.00000	.02965	.02992	.00111	1.00000
LAWA83	ActDes	.06201	.08902	.01994	.00652	.00020	.00010	.04986	.00501	.00000	.01994	.20000	.02028	.00100	.44552	.01994	.02965	.02992	.00111	1.00000
LAWA84	ActDes	.06201	.08902	.01994	.00652	.00020	.00010	.02992	.00501	.00000	.01994	.20000	.04023	.00100	.44552	.01994	.02965	.02992	.00111	1.00000
LAWA87	ActDes	.04481	.08874	.01992	.00329	.00009	.00000	.06971	.02583	.00000	.01992	.20005	.00070	.00190	.44467	.01992	.02958	.02988	.00100	1.00000
LAWA90	ActDes	.06082	.09700	.03983	.00329	.00009	.00000	.05533	.02583	.00000	.01475	.20005	.00070	.00190	.44002	.00000	.02951	.02988	.00100	1.00000
LAWA93	ActDes	.06179	.11095	.07882	.00652	.00020	.00010	.07505	.00501	.05067	.01477	.10027	.00034	.00100	.42247	.01108	.02994	.02992	.00112	1.00000
LAWA96	ActDes	.06201	.07904	.03989	.00652	.00020	.00010	.02992	.00501	.00000	.01994	.20000	.04023	.00100	.43555	.01994	.02965	.02992	.00111	1.00000
LAWA102R2	ActDes	.06057	.10011	.05066	.00330	.00020	.00030	.05406	.00260	.02503	.01502	.14496	.00130	.00330	.46631	.01141	.03063	.03023	.00000	1.00000
LAWA104	ActDes	.06614	.08591	.01924	.00717	.00022	.00011	.06735	.00551	.00000	.01924	.22001	.00037	.00100	.42989	.01924	.02861	.02886	.00113	1.00000
LAWA105	ActDes	.07027	.08281	.01854	.00782	.00024	.00012	.06490	.00602	.00000	.01854	.24006	.00040	.00090	.41430	.01854	.02757	.02782	.00114	1.00000
LAWA112B14	ActDes	.06095	.09861	.07643	.00380	.00020	.00100	.00000	.01888	.00000	.01479	.19982	.00100	.00160	.44220	.01998	.02967	.03007	.00100	1.00000
LAWA112B15	ActDes	.06154	.09801	.07603	.00310	.00010	.00090	.00000	.02408	.00000	.01479	.19982	.00050	.00110	.43980	.01988	.02947	.02987	.00100	1.00000
LAWA125	ActDes	.05637	.09545	.01939	.00220	.00020	.00320	.05387	.04208	.00000	.01439	.19990	.00090	.00310	.42888	.01939	.02879	.02909	.00280	1.00000

- (a) The compositions listed in this table are normalized mass fraction versions of target compositions of the glasses, after replacing the target values of SO<sub>3</sub> by XRF analyzed (or estimated analyzed) values. See Section 3.3 for the details.
- (b) The Group IDs are described in Sections 2.1 to 2.7.
- (c) XRF SO<sub>3</sub> denotes that the SO<sub>3</sub> composition is based on chemical analysis by XRF. For most glasses SO<sub>3</sub> was directly measured by XRF, but for some glasses estimated XRF values were used (see Section 3.3).
- (d) The normalized component mass fractions listed in this table were rounded to five decimals, and may not sum exactly to 1.00000 as listed. However, complete compositions listed to more decimal places and summing to 1.0000 were used for property-composition modeling.

**Table 5.2. Normalized<sup>(a)</sup> Compositions (mass fractions) of 244 LAW Glasses Used for PCT Model Development (continued).**

Glass ID	Group ID <sup>(b)</sup>	Al <sub>2</sub> O <sub>3</sub>	B <sub>2</sub> O <sub>3</sub>	CaO	Cl	Cr <sub>2</sub> O <sub>3</sub>	F	Fe <sub>2</sub> O <sub>3</sub>	K <sub>2</sub> O	Li <sub>2</sub> O	MgO	Na <sub>2</sub> O	P <sub>2</sub> O <sub>5</sub>	XRF SO <sub>3</sub> <sup>(c)</sup>	SiO <sub>2</sub>	TiO <sub>2</sub>	ZnO	ZrO <sub>2</sub>	Others	Sum <sup>(d)</sup>
LAWA127R1	ActDes	.05651	.10205	.02068	.00181	.00019	.00265	.05758	.03430	.00000	.01536	.16312	.00070	.00180	.45828	.02073	.03071	.03110	.00245	1.00000
LAWA127R2	ActDes	.05658	.10217	.02069	.00180	.00020	.00270	.05768	.03429	.00000	.01540	.16305	.00070	.00210	.45886	.02079	.03079	.03119	.00100	1.00000
LAWA129	ActDes	.07466	.08515	.03528	.00200	.00020	.00300	.00000	.03878	.00000	.01179	.18449	.00080	.00310	.47511	.02089	.03088	.03128	.00260	1.00000
LAWA133	ActDes	.06204	.08901	.05485	.00559	.00020	.00040	.03487	.00430	.00000	.01998	.19980	.00100	.00200	.44535	.01998	.02967	.02997	.00100	1.00000
LAWA134	ActDes	.05647	.09964	.02019	.00200	.00020	.00290	.05627	.03728	.00000	.01499	.17729	.00080	.00280	.44753	.02029	.02998	.03038	.00100	1.00000
LAWA135	ActDes	.05655	.10092	.02048	.00190	.00020	.00280	.05695	.03577	.00000	.01519	.17016	.00070	.00270	.45304	.02048	.03038	.03078	.00100	1.00000
LAWA136	ActDes	.05655	.10092	.03048	.00190	.00020	.00280	.05695	.03577	.00000	.01519	.17016	.00070	.00270	.44304	.02048	.03038	.03078	.00100	1.00000
LAWA170	ActDes	.06056	.09664	.01980	.00327	.00009	.00000	.05513	.03055	.00000	.01473	.19905	.00070	.00210	.43841	.01984	.02936	.02976	.00000	1.00000
LAWB30	ActDes	.08604	.10039	.07235	.00007	.00086	.00097	.08276	.00323	.04070	.03075	.07902	.00038	.00180	.42730	.00000	.04115	.03120	.00102	1.00000
LAWB31	ActDes	.06183	.12141	.04047	.00007	.00089	.00099	.07195	.00320	.02968	.02248	.07932	.02734	.00630	.47101	.00000	.03103	.03103	.00102	1.00000
LAWB33	ActDes	.06175	.12125	.04042	.00007	.00089	.00099	.05164	.00320	.02964	.02245	.07921	.04752	.00760	.47039	.00000	.03099	.03099	.00102	1.00000
LAWB34	ActDes	.06178	.12131	.06065	.00007	.00089	.00099	.05167	.00320	.02965	.02246	.07925	.02732	.00710	.47063	.00000	.03100	.03100	.00102	1.00000
LAWB35	ActDes	.06178	.12132	.04044	.00007	.00089	.00099	.05167	.00320	.02966	.04269	.07926	.02732	.00700	.47067	.00000	.03100	.03100	.00102	1.00000
LAWB37	ActDes	.06166	.12108	.04709	.00007	.00089	.00099	.05157	.00319	.02960	.02915	.07910	.03400	.00900	.46973	.00000	.03094	.03094	.00102	1.00000
LAWB38	ActDes	.06156	.12088	.04746	.00007	.00088	.00099	.05149	.00319	.03806	.02239	.07897	.03170	.01060	.46897	.00000	.03089	.03089	.00102	1.00000
LAWB61	ActDes	.06205	.09966	.06708	.00000	.00101	.00070	.05310	.00261	.05823	.02977	.05501	.00010	.00710	.48624	.01398	.03168	.03168	.00000	1.00000
LAWB64	ActDes	.06207	.09969	.06710	.00000	.00101	.00070	.03300	.00262	.05825	.02978	.05503	.00010	.00680	.48639	.01398	.05181	.03169	.00000	1.00000
LAWB67	ActDes	.06189	.09940	.05186	.00000	.00100	.00070	.05296	.00261	.04303	.02969	.05487	.03019	.00970	.48497	.01394	.03160	.03160	.00000	1.00000
LAWB69	ActDes	.06151	.12332	.10462	.00010	.00050	.00080	.00000	.00230	.04611	.02971	.06621	.00050	.00650	.47960	.00000	.04571	.03151	.00100	1.00000
LAWB70	ActDes	.06159	.12347	.06629	.00010	.00050	.00080	.03255	.00230	.04616	.02974	.06629	.00050	.00540	.48018	.00000	.05157	.03154	.00100	1.00000
LAWB71	ActDes	.06162	.10802	.06633	.00010	.00050	.00080	.03257	.00230	.04619	.02976	.06633	.00050	.00480	.48047	.01553	.05160	.03156	.00100	1.00000
LAWB72	ActDes	.06154	.12339	.07125	.00010	.00050	.00080	.03252	.00230	.04113	.02972	.06625	.00050	.00610	.47984	.00000	.05154	.03152	.00100	1.00000
LAWB73	ActDes	.06193	.09947	.09345	.00000	.00100	.00070	.01907	.00261	.05049	.02971	.05490	.00010	.00900	.48531	.01395	.04667	.03162	.00000	1.00000
LAWB74	ActDes	.06218	.10108	.08728	.00000	.00101	.00071	.01915	.00262	.05331	.02983	.05513	.00010	.00770	.48728	.01401	.04686	.03175	.00000	1.00000
LAWB75	ActDes	.06187	.11792	.08684	.00000	.00100	.00070	.01905	.00261	.05304	.01504	.05485	.00010	.01000	.48482	.01394	.04663	.03159	.00000	1.00000
LAWB76	ActDes	.06186	.11790	.08682	.00000	.00100	.00070	.01905	.00261	.05805	.01504	.05484	.00010	.01020	.49365	.00000	.04662	.03158	.00000	1.00000
LAWB77	ActDes	.06160	.12350	.06631	.00010	.00050	.00080	.02204	.00230	.04117	.02975	.06631	.00050	.00520	.48027	.01552	.05158	.03155	.00100	1.00000
LAWB81	ActDes	.06155	.12340	.07126	.00010	.00050	.00080	.03253	.00230	.04263	.02972	.06625	.00050	.00600	.47989	.00000	.05004	.03153	.00100	1.00000
LAWB87	ActDes	.06495	.13020	.06114	.00010	.00060	.00050	.05032	.00200	.04701	.01413	.05012	.00020	.00570	.49214	.00000	.04891	.03197	.00000	1.00000
LAWB88	ActDes	.06488	.13006	.07990	.00010	.00060	.00050	.02203	.00200	.04696	.01412	.05006	.00020	.00680	.50101	.00000	.04886	.03194	.00000	1.00000
LAWB89	ActDes	.06186	.10040	.06787	.00010	.00040	.00060	.05295	.00190	.05005	.02973	.04084	.00040	.00440	.49350	.01391	.04845	.03163	.00100	1.00000
LAWB90	ActDes	.06192	.10050	.06794	.00010	.00040	.00060	.05301	.00190	.03617	.02976	.06884	.00040	.00340	.47996	.01393	.04850	.03166	.00100	1.00000
LAWB91	ActDes	.06191	.10047	.06792	.00010	.00040	.00060	.05299	.00190	.02925	.02975	.08735	.00040	.00370	.46820	.01392	.04848	.03165	.00100	1.00000
LAWB92	ActDes	.06187	.10041	.06787	.00010	.00040	.00060	.05296	.00190	.02222	.02973	.10121	.00040	.00430	.46101	.01392	.04845	.03163	.00100	1.00000
LAWB93	ActDes	.06186	.10039	.06786	.00010	.00040	.00060	.05295	.00190	.04664	.02973	.04784	.00040	.00450	.48984	.01391	.04844	.03163	.00100	1.00000

- (a) The compositions listed in this table are normalized mass fraction versions of target compositions of the glasses, after replacing the target values of SO<sub>3</sub> by XRF analyzed (or estimated analyzed) values. See Section 3.3 for the details.
- (b) The Group IDs are described in Sections 2.1 to 2.7.
- (c) XRF SO<sub>3</sub> denotes that the SO<sub>3</sub> composition is based on chemical analysis by XRF. For most glasses SO<sub>3</sub> was directly measured by XRF, but for some glasses estimated XRF values were used (see Section 3.3).
- (d) The normalized component mass fractions listed in this table were rounded to five decimals, and may not sum exactly to 1.00000 as listed. However, complete compositions listed to more decimal places and summing to 1.0000 were used for property-composition modeling.

**Table 5.2. Normalized<sup>(a)</sup> Compositions (mass fractions) of 244 LAW Glasses Used for PCT Model Development (continued).**

Glass ID	Group ID <sup>(b)</sup>	Al <sub>2</sub> O <sub>3</sub>	B <sub>2</sub> O <sub>3</sub>	CaO	Cl	Cr <sub>2</sub> O <sub>3</sub>	F	Fe <sub>2</sub> O <sub>3</sub>	K <sub>2</sub> O	Li <sub>2</sub> O	MgO	Na <sub>2</sub> O	P <sub>2</sub> O <sub>5</sub>	XRF SO <sub>3</sub> <sup>(c)</sup>	SiO <sub>2</sub>	TiO <sub>2</sub>	ZnO	ZrO <sub>2</sub>	Others	Sum <sup>(d)</sup>
LAWB94	ActDes	.06186	.10031	.06780	.00007	.00039	.00064	.05295	.00194	.05359	.02972	.03385	.00037	.00500	.49662	.01393	.04839	.03158	.00100	1.00000
LAWB95	ActDes	.06189	.10035	.06783	.00007	.00039	.00064	.05297	.00194	.05761	.02973	.02457	.00037	.00460	.50211	.01394	.04841	.03159	.00100	1.00000
LAWB96	ActDes	.06171	.10027	.06772	.00010	.00030	.00020	.05289	.00120	.04297	.02975	.05479	.00010	.00480	.48743	.01392	.04858	.03175	.00150	1.00000
LAWC15	ActDes	.06221	.08929	.02006	.00078	.00003	.00469	.07007	.00142	.00000	.02009	.19963	.00015	.00230	.44713	.02001	.02990	.03005	.00220	1.00000
LAWC21	ActDes	.06139	.10104	.06419	.00120	.00020	.00060	.06489	.00150	.02744	.01512	.11897	.00120	.00290	.46766	.01122	.03024	.03024	.00000	1.00000
LAWC21rev2	ActDes	.06125	.10058	.06415	.00110	.00020	.00050	.06435	.00140	.02732	.01501	.11970	.00110	.00290	.46778	.01121	.03022	.03022	.00100	1.00000
LAWC22	ActDes	.06076	.10056	.05110	.00048	.00012	.00336	.05426	.00083	.02506	.01514	.14408	.00067	.00290	.46642	.01144	.03071	.03028	.00183	1.00000
LAWC23	ActDes	.06118	.10076	.06401	.00123	.00020	.00060	.06470	.02881	.00000	.01507	.11856	.00118	.00350	.46763	.01122	.03014	.03017	.00105	1.00000
LAWC24	ActDes	.05955	.09808	.06231	.00120	.00019	.00058	.06297	.05558	.00000	.01467	.11541	.00115	.00340	.45429	.01090	.02934	.02937	.00102	1.00000
LAWC26	ActDes	.06121	.13263	.06411	.00110	.00020	.00050	.00010	.00140	.02731	.01500	.11962	.00110	.00350	.49960	.01120	.03021	.03021	.00100	1.00000
LAWC29	ActDes	.06551	.10049	.09617	.00112	.00018	.00054	.00009	.00136	.02734	.01501	.11958	.00106	.00370	.47181	.01121	.05365	.03019	.00100	1.00000
LAWC30	ActDes	.06122	.10053	.06412	.00110	.00020	.00050	.04101	.00140	.02731	.01500	.11964	.00110	.00340	.46754	.01120	.05352	.03021	.00100	1.00000
LAWC31	ActDes	.06119	.10048	.07409	.00110	.00020	.00050	.04429	.00140	.02729	.01500	.11958	.00110	.00390	.46731	.01120	.04019	.03019	.00100	1.00000
LAWC33	ActDes	.06146	.10100	.06947	.00110	.00020	.00050	.04444	.00140	.02753	.01512	.12012	.00110	.00370	.46977	.01131	.04044	.03033	.00100	1.00000
TFA-BASE	ActDes	.06999	.09999	.00010	.00280	.00000	.00010	.05499	.00410	.00000	.01500	.19998	.00060	.00080	.49065	.03000	.01500	.01500	.00090	1.00000
C22AN107	ActDes	.06106	.10079	.05115	.00080	.00020	.00140	.05585	.00090	.02512	.01511	.14433	.00120	.00270	.46612	.01141	.03063	.03023	.00100	1.00000
A88AP101R1	ActDes	.06102	.09834	.01999	.00130	.00016	.00227	.05552	.02136	.00000	.01480	.20011	.00073	.00230	.44153	.01999	.02961	.02998	.00100	1.00000
A88Si+15	ActDes	.06141	.09481	.01930	.00140	.00020	.00250	.05351	.02370	.00000	.01430	.22182	.00080	.00290	.42554	.01930	.02850	.02890	.00110	1.00000
A88Si-15	ActDes	.06055	.10218	.02072	.00120	.00010	.00200	.05765	.01882	.00000	.01541	.17674	.00060	.00190	.45867	.02072	.03072	.03112	.00090	1.00000
C22Si+15	ActDes	.06043	.09837	.04994	.00090	.00020	.00160	.05358	.00095	.02459	.01484	.16197	.00130	.00310	.45581	.01121	.03001	.02960	.00160	1.00000
C22Si-15	ActDes	.06160	.10291	.05218	.00071	.00017	.00129	.05555	.00076	.02572	.01551	.12812	.00138	.00230	.47680	.01175	.03139	.03096	.00090	1.00000
A1C1-1	ActDes	.06088	.09126	.02742	.00913	.00015	.00086	.06501	.00347	.00623	.01850	.19167	.00033	.00210	.44480	.01759	.02951	.02956	.00153	1.00000
A1C1-2	ActDes	.06073	.09415	.03521	.00654	.00013	.00169	.06135	.00255	.01247	.01735	.17673	.00066	.00230	.45142	.01554	.02984	.02974	.00160	1.00000
A1C1-3	ActDes	.06057	.09701	.04299	.00395	.00011	.00252	.05766	.00161	.01871	.01619	.16170	.00099	.00290	.45787	.01348	.03017	.02991	.00167	1.00000
C1-AN107	ActDes	.06066	.10031	.05098	.00065	.00009	.00283	.05421	.00069	.02506	.01510	.14465	.00132	.00290	.46636	.01147	.03062	.03020	.00189	1.00000
A2-AP101	ActDes	.05622	.09824	.01991	.00420	.00020	.00350	.05532	.03812	.00000	.01481	.18467	.00080	.00350	.44008	.01991	.02941	.02961	.00150	1.00000
A2B1-1	ActDes	.05758	.09883	.03184	.00320	.00020	.00280	.05477	.02904	.01071	.01852	.15230	.00070	.00350	.45179	.01842	.03414	.03014	.00150	1.00000
A2B1-2	ActDes	.05895	.09919	.04374	.00220	.00030	.00220	.05405	.02002	.02152	.02232	.11981	.00060	.00420	.46292	.01692	.03894	.03063	.00150	1.00000
B1-AZ101	ActDes	.06180	.10026	.06771	.00020	.00030	.00080	.05278	.00180	.04307	.02985	.05479	.00040	.00490	.48578	.01392	.04848	.03165	.00150	1.00000
C2-AN102C35	ActDes	.06075	.09428	.07356	.00390	.00010	.00110	.03603	.00090	.03253	.01491	.11980	.00160	.00540	.47278	.01081	.03993	.03002	.00160	1.00000
A3-AN104	ActDes	.06051	.09921	.05031	.00790	.00020	.00100	.05371	.00330	.02480	.01480	.14641	.00110	.00350	.46095	.01130	.03040	.03000	.00150	1.00000
A2B1-3	ActDes	.06037	.09971	.05576	.00120	.00030	.00150	.05346	.01091	.03224	.02603	.08730	.00050	.00470	.47432	.01542	.04365	.03113	.00150	1.00000
A3C2-1	ActDes	.06064	.09796	.05613	.00690	.00020	.00030	.04923	.00270	.02672	.01481	.13978	.00120	.00380	.46408	.01121	.03282	.03002	.00150	1.00000
A3C2-2	ActDes	.06066	.09680	.06196	.00591	.00020	.00060	.04485	.00210	.02863	.01481	.13323	.00140	.00400	.46707	.01111	.03514	.03003	.00150	1.00000
A3C2-3	ActDes	.06064	.09547	.06775	.00490	.00010	.00090	.04043	.00150	.03062	.01491	.12649	.00150	.00490	.46983	.01091	.03753	.03002	.00160	1.00000

- (a) The compositions listed in this table are normalized mass fraction versions of target compositions of the glasses, after replacing the target values of SO<sub>3</sub> by XRF analyzed (or estimated analyzed) values. See Section 3.3 for the details.
- (b) The Group IDs are described in Sections 2.1 to 2.7.
- (c) XRF SO<sub>3</sub> denotes that the SO<sub>3</sub> composition is based on chemical analysis by XRF. For most glasses SO<sub>3</sub> was directly measured by XRF, but for some glasses estimated XRF values were used (see Section 3.3).
- (d) The normalized component mass fractions listed in this table were rounded to five decimals, and may not sum exactly to 1.00000 as listed. However, complete compositions listed to more decimal places and summing to 1.0000 were used for property-composition modeling.



**Table 5.2. Normalized<sup>(a)</sup> Compositions (mass fractions) of 244 LAW Glasses Used for PCT Model Development (continued).**

Glass ID	Group ID <sup>(b)</sup>	Al <sub>2</sub> O <sub>3</sub>	B <sub>2</sub> O <sub>3</sub>	CaO	Cl	Cr <sub>2</sub> O <sub>3</sub>	F	Fe <sub>2</sub> O <sub>3</sub>	K <sub>2</sub> O	Li <sub>2</sub> O	MgO	Na <sub>2</sub> O	P <sub>2</sub> O <sub>5</sub>	XRF SO <sub>3</sub> <sup>(c)</sup>	SiO <sub>2</sub>	TiO <sub>2</sub>	ZnO	ZrO <sub>2</sub>	Others	Sum <sup>(d)</sup>
A1-AN105R2	ActDes	.06101	.08841	.01960	.01170	.00020	.00000	.06871	.00440	.00000	.01960	.20662	.00000	.00180	.43824	.01960	.02920	.02940	.00150	1.00000
12U-G-86A	ActDes	.06161	.08952	.01980	.00560	.00020	.00020	.06941	.00440	.00000	.01980	.19964	.00070	.00230	.44329	.01980	.02951	.02971	.00450	1.00000
LA44PNCC	ActDes	.06173	.08874	.01981	.00570	.00070	.00220	.06963	.00260	.00000	.01971	.20010	.00350	.00210	.44472	.01971	.02911	.02991	.00000	1.00000
LA44CCCR2	ActDes	.06173	.08874	.01981	.00570	.00070	.00220	.06963	.00260	.00000	.01971	.20010	.00350	.00210	.44472	.01971	.02911	.02991	.00000	1.00000
WVF-G-21B	ActDes	.06079	.09799	.01990	.00130	.00020	.00230	.05539	.02130	.00000	.01480	.20008	.00070	.00330	.43996	.01990	.02950	.02990	.00270	1.00000
PNLA126CC	ActDes	.05652	.09854	.02001	.00200	.00020	.00300	.05562	.03882	.00000	.01481	.18467	.00080	.00290	.44238	.02001	.02961	.03001	.00010	1.00000
LA126CCC	ActDes	.05652	.09854	.02001	.00200	.00020	.00300	.05562	.03882	.00000	.01481	.18467	.00080	.00290	.44238	.02001	.02961	.03001	.00010	1.00000
WVM-G-142C	ActDes	.05618	.09825	.01993	.00421	.00020	.00351	.05538	.03816	.00000	.01472	.18468	.00080	.00250	.44006	.01983	.02944	.02964	.00250	1.00000
A100G115A	ActDes	.06063	.10005	.05063	.00330	.00020	.00030	.05413	.00260	.02501	.01491	.14467	.00130	.00380	.46603	.01141	.03072	.03032	.00000	1.00000
A100CC	ActDes	.06064	.10007	.05064	.00330	.00020	.00030	.05414	.00260	.02502	.01491	.14470	.00130	.00360	.46613	.01141	.03072	.03032	.00000	1.00000
WVB-G-124B	ActDes	.06039	.09969	.05049	.00330	.00020	.00030	.05399	.00260	.02490	.01490	.14419	.00130	.00440	.46455	.01140	.03060	.03020	.00260	1.00000
LA137SRCCC	ActDes	.06051	.09911	.05031	.00760	.00030	.00020	.05361	.00620	.02480	.01480	.14641	.00110	.00270	.46065	.01130	.03040	.03000	.00000	1.00000
WVR-G-127A	ActDes	.06049	.09908	.05019	.00790	.00020	.00000	.05359	.00330	.02480	.01480	.14627	.00110	.00380	.46031	.01130	.03039	.02999	.00250	1.00000
LB83PNCC	ActDes	.06214	.10047	.06795	.00000	.00030	.00080	.05294	.00180	.04313	.02992	.05374	.00050	.00490	.48714	.01401	.04853	.03172	.00000	1.00000
LB83CCC-1	ActDes	.06214	.10047	.06795	.00000	.00030	.00080	.05294	.00180	.04313	.02992	.05374	.00050	.00490	.48714	.01401	.04853	.03172	.00000	1.00000
WVJ-G-109D	ActDes	.06174	.10022	.06775	.00010	.00040	.00060	.05282	.00190	.04310	.02977	.05472	.00040	.00430	.48577	.01393	.04841	.03157	.00251	1.00000
GTSD-1126	ActDes	.06183	.10041	.06784	.00010	.00030	.00020	.05301	.00120	.04309	.02976	.05492	.00010	.00450	.48843	.01393	.04860	.03177	.00000	1.00000
LB88CCC	ActDes	.06505	.12980	.07976	.00010	.00060	.00050	.02202	.00200	.04694	.01411	.05004	.00020	.00730	.50080	.00000	.04884	.03193	.00000	1.00000
AZ-102 Surr SRNL	ActDes	.06420	.12979	.07957	.00000	.00060	.00100	.02196	.00200	.04682	.01408	.05072	.00020	.00930	.49919	.00000	.04872	.03185	.00000	1.00000
12S-G-85C	ActDes	.06080	.10050	.05090	.00080	.00020	.00140	.05560	.00080	.02500	.01510	.14430	.00120	.00380	.46430	.01140	.03060	.03010	.00320	1.00000
C100GCC	ActDes	.06127	.10092	.06408	.00120	.00020	.00060	.06478	.00150	.02733	.01512	.11874	.00120	.00400	.46726	.01121	.03014	.03024	.00020	1.00000
AN-102 Surr LC Melter	ActDes	.06142	.10143	.06422	.00210	.00020	.00060	.06502	.00070	.02751	.01520	.11804	.00080	.00290	.46784	.01130	.03031	.03031	.00010	1.00000
WVH-G-57B	ActDes	.06102	.10023	.07392	.00110	.00020	.00050	.04421	.00140	.02731	.01500	.11934	.00100	.00430	.46644	.01120	.04011	.03011	.00260	1.00000
GTSD-1437	ActDes	.06091	.09463	.07386	.00391	.00010	.00110	.03613	.00090	.03271	.01495	.12032	.00161	.00290	.47467	.01084	.04004	.03011	.00030	1.00000
PLTC35CCC	ActDes	.06091	.09463	.07386	.00391	.00010	.00110	.03613	.00090	.03271	.01495	.12032	.00161	.00290	.47467	.01084	.04004	.03011	.00030	1.00000
AN-103 Actual	Actual	.06220	.08950	.02010	.00310	.00010	.00020	.07020	.00600	.00000	.02010	.20000	.00050	.00100	.44680	.02010	.03000	.03010	.00000	1.00000
AW-101 Actual	Actual	.06080	.09710	.01990	.00078	.00009	.00000	.05540	.02580	.00000	.01480	.20001	.00070	.00210	.44052	.01994	.02950	.02990	.00265	1.00000
AP-101 Actual	Actual	.05660	.09850	.02000	.00170	.00030	.00270	.05560	.03820	.00000	.01490	.18460	.00090	.00310	.44270	.02010	.02970	.03010	.00030	1.00000
AZ-101 Actual	Actual	.06210	.10040	.06790	.00000	.00030	.00080	.05290	.00180	.04310	.02990	.05350	.00050	.00550	.48700	.01400	.04850	.03170	.00010	1.00000
AZ-102 Actual	Actual	.06496	.12992	.07995	.00010	.00060	.00050	.02199	.00210	.04687	.01409	.04997	.00020	.00850	.49970	.00000	.04867	.03188	.00000	1.00000
AZ-102 Actual CCC	Actual	.06496	.12992	.07995	.00010	.00060	.00050	.02199	.00210	.04687	.01409	.04997	.00020	.00850	.49970	.00000	.04867	.03188	.00000	1.00000
AN-107 Actual (LAWC15)	Actual	.06231	.08943	.02010	.00078	.00003	.00470	.07018	.00142	.00000	.02012	.20000	.00015	.00130	.44784	.02004	.02995	.03010	.00155	1.00000
AN-102 Actual LC Melter	Actual	.06148	.10096	.06427	.00090	.00020	.00050	.06497	.00070	.02749	.01519	.11795	.00080	.00360	.46781	.01130	.03039	.03039	.00110	1.00000
AN-102 Actual	Actual	.06150	.10130	.06420	.00120	.00020	.00060	.06490	.00090	.02740	.01520	.11800	.00130	.00360	.46750	.01130	.03030	.03030	.00030	1.00000

- (a) The compositions listed in this table are normalized mass fraction versions of target compositions of the glasses, after replacing the target values of SO<sub>3</sub> by XRF analyzed (or estimated analyzed) values. See Section 3.3 for the details.
- (b) The Group IDs are described in Sections 2.1 to 2.7.
- (c) XRF SO<sub>3</sub> denotes that the SO<sub>3</sub> composition is based on chemical analysis by XRF. For most glasses SO<sub>3</sub> was directly measured by XRF, but for some glasses estimated XRF values were used (see Section 3.3).
- (d) The normalized component mass fractions listed in this table were rounded to five decimals, and may not sum exactly to 1.00000 as listed. However, complete compositions listed to more decimal places and summing to 1.0000 were used for property-composition modeling.

**Table 5.3. PCT Releases and Data Splitting Validation Sets of 244 LAW Glasses Used for PCT Model Development.**

Glass ID	Group ID <sup>(a)</sup>	Replicate <sup>(b)</sup>	B (ppm)	Na (ppm)	Si (ppm)	B (g/L)	Na (g/L)	Si (g/L)	B Data Splitting Validation Set <sup>(c)</sup>	Na Data Splitting Validation Set <sup>(c)</sup>
LAWA44R10	ExPh1	NO	29.81	139.90	90.30	1.078	0.943	0.434	1	5
LAWA53	ExPh1	NO	15.40	156.30	68.32	0.804	1.059	0.348	1	3
LAWA56	ExPh1	NO	64.39	172.30	64.02	1.721	1.166	0.325	2	3
LAWA88 <sup>(e)</sup>	ExPh1	LAWM52 <sup>(d)</sup>	26.11	126.50	70.24	0.867	0.852	0.342	NA	NA
LAWA88R1	ExPh1	<sup>(d)</sup>	49.18	192.20	93.01	1.633	1.295	0.452	5 <sup>(d)</sup>	1 <sup>(d)</sup>
LAWA102R1	ExPh1	NO	26.74	78.61	78.43	0.864	0.731	0.362	2	3
LAWA126	ExPh1	NO	36.47	143.50	68.28	1.196	1.048	0.331	4	1
LAWA128	ExPh1	NO	13.80	118.90	75.55	0.629	0.869	0.351	3	4
LAWA130	ExPh1	NO	25.59	126.50	76.74	0.921	0.924	0.356	4	2
LAWB65	ExPh1	NO	17.14	19.39	46.73	0.555	0.477	0.206	4	1
LAWB66	ExPh1	NO	18.11	22.20	48.55	0.585	0.545	0.214	4	2
LAWB68	ExPh1	NO	13.18	19.27	44.78	0.503	0.474	0.197	5	3
LAWB78	ExPh1	NO	46.94	80.68	70.59	1.224	1.110	0.321	5	2
LAWB79	ExPh1	NO	41.78	62.59	67.28	1.090	0.978	0.301	5	4
LAWB80	ExPh1	NO	33.76	35.79	56.41	0.881	0.728	0.251	2	2
LAWB83	ExPh1	NO	19.06	21.38	52.35	0.612	0.527	0.230	3	3
LAWB84	ExPh1	NO	21.02	22.72	55.73	0.674	0.559	0.245	5	3
LAWB85	ExPh1	NO	23.29	20.30	55.69	0.651	0.500	0.245	1	2
LAWB86	ExPh1	NO	48.31	41.00	75.22	1.252	1.009	0.331	2	2
C100G136B	ExPh1	NO	23.01	61.38	58.30	0.734	0.697	0.267	NA	NA
LAWC27	ExPh1	NO	14.27	39.02	41.86	0.377	0.440	0.183	3	2
LAWC32	ExPh1	NO	13.05	49.04	45.34	0.418	0.553	0.207	1	1
LAWM1	Ph1	LAWM53	2.85	10.81	27.31	0.152	0.290	0.131	NA	NA
LAWM2	Ph1	NO	12.57	31.74	67.17	0.672	0.853	0.305	4	1
LAWM3	Ph1	NO	14.86	98.87	47.31	0.795	1.157	0.252	5	2
LAWM4	Ph1	NO	18.59	22.32	36.68	0.458	0.599	0.189	1	3
LAWM5	Ph1	NO	4.59	10.40	36.38	0.245	0.279	0.159	3	2
LAWM6	Ph1	NO	18.04	47.66	36.07	0.547	0.714	0.193	1	2
LAWM7	Ph1	NO	5.39	15.97	52.08	0.249	0.429	0.214	4	3
LAWM8	Ph1	NO	13.00	10.30	29.21	0.321	0.277	0.140	4	1
LAWM9	Ph1	LAWM54R1	3.92	19.07	31.50	0.210	0.513	0.135	NA	NA
LAWM10	Ph1	NO	9.78	42.94	26.25	0.242	0.443	0.140	2	3
LAWM11	Ph1	NO	46.93	120.40	120.30	1.161	1.412	0.550	5	5
LAWM12	Ph1	LAWM55	1199.00	1701.00	468.10	29.686	16.081	2.372	NA	NA
LAWM13	Ph1	NO	46.12	804.90	223.00	2.475	4.931	1.192	3	5
LAWM14	Ph1	NO	37.17	352.80	276.30	1.995	2.162	1.137	3	2
LAWM15	Ph1	NO	63.09	251.30	101.20	2.171	1.540	0.498	5	3
LAWM16	Ph1	NO	10.62	30.79	31.34	0.285	0.415	0.158	1	1
LAWM17	Ph1	NO	467.00	1006.00	179.00	12.527	7.974	0.911	1	1
LAWM18	Ph1	NO	16.12	37.77	37.39	0.432	0.509	0.190	2	4
LAWM19	Ph1	NO	18.80	54.12	36.13	0.505	0.554	0.184	2	2
LAWM20	Ph1	NO	58.05	343.60	147.50	2.670	2.724	0.751	5	4
LAWM21	Ph1	NO	30.16	70.94	61.49	0.891	0.955	0.313	4	1
LAWM22	Ph1	NO	8.53	78.57	56.35	0.393	0.624	0.287	2	3
LAWM23	Ph1	NO	6.06	37.94	45.74	0.278	0.510	0.202	5	5
LAWM24	Ph1	NO	39.26	103.80	62.85	1.053	0.823	0.286	2	5
LAWM25R1	Ph1	NO	30.37	42.73	61.98	0.814	0.575	0.265	5	3

- (a) Group IDs are described in Sections 2.1 to 2.7.
- (b) If a given glass has a replicate, the glass ID is listed. If not, NO is listed.
- (c) Numbers from 1 to 5 denote the five split validation subsets. NA denotes “not applicable”, because these replicate glasses were forced into the modeling subsets, and thus were not parts of the validation subsets.
- (d) LAW88R1 is a replicate of LAW52 and LAW88. However, it was mistakenly not identified as such for the data-splitting approach to model validation. The impact of this oversight is negligible.
- (e) LAW88 was previously classified in the actively designed (ActDes) group for the PCT response, with that classification used for the plotting symbols in Section 5.

**Table 5.3. PCT Releases and Data Splitting Validation Sets for 244 LAW Glasses Used for PCT Model Development (continued).**

Glass ID	Group ID <sup>(a)</sup>	Replicate <sup>(b)</sup>	B (ppm)	Na (ppm)	Si (ppm)	B (g/L)	Na (g/L)	Si (g/L)	B Data Splitting Validation Set <sup>(c)</sup>	Na Data Splitting Validation Set <sup>(c)</sup>
LAWM26	Ph1	NO	15.77	26.37	48.99	0.423	0.355	0.210	3	4
LAWM27	Ph1	NO	15.00	84.37	49.29	0.690	0.850	0.251	1	5
LAWM28	Ph1	NO	13.77	39.23	49.44	0.369	0.528	0.211	2	4
LAWM29	Ph1	NO	10.96	36.31	60.93	0.504	0.489	0.278	1	4
LAWM30	Ph1	NO	43.96	129.00	60.51	1.179	1.023	0.308	2	3
LAWM31	Ph1	NO	49.43	272.20	146.40	2.273	2.190	0.740	3	3
LAWM32	Ph1	NO	43.46	225.00	202.30	1.999	1.837	0.865	4	1
LAWM33R1	Ph1	NO	159.50	518.70	179.50	4.278	4.111	0.914	2	3
LAWM34	Ph1	NO	135.50	538.00	234.40	5.221	4.265	1.194	5	4
LAWM35	Ph1	LAWM56	392.50	836.00	168.90	10.526	6.625	0.860	NA	NA
LAWM36	Ph1	NO	16.70	54.06	49.52	0.489	0.607	0.235	5	1
LAWM37	Ph1	NO	42.29	87.79	65.99	1.237	0.985	0.313	1	5
LAWM38	Ph1	NO	9.50	71.16	58.99	0.383	0.685	0.263	5	1
LAWM39	Ph1	NO	15.11	48.09	47.67	0.537	0.463	0.212	4	4
LAWM40	Ph1	NO	26.25	75.38	65.45	0.768	0.725	0.292	5	1
LAWM41	Ph1	NO	8.95	60.85	49.26	0.360	0.586	0.234	1	2
LAWM42	Ph1	NO	13.23	60.31	60.31	0.532	0.580	0.269	2	5
LAWM43	Ph1	NO	17.73	58.03	58.02	0.658	0.652	0.276	3	2
LAWM44	Ph1	NO	15.50	50.46	52.35	0.497	0.566	0.233	3	1
LAWM45	Ph1	NO	10.60	60.82	51.51	0.426	0.585	0.229	5	1
LAWM46	Ph1	NO	16.35	41.60	40.86	0.478	0.466	0.182	4	1
LAWM47	Ph1	NO	12.96	75.99	60.47	0.521	0.731	0.269	5	4
LAWM48	Ph1	NO	16.01	50.77	51.75	0.468	0.569	0.230	3	2
LAWM49	Ph1	NO	18.16	52.35	47.81	0.536	0.504	0.215	3	3
LAWM50	Ph1	LAWM51	19.49	61.17	55.67	0.647	0.630	0.253	NA	NA
LAWM51	Ph1	LAWM50	20.84	69.67	57.32	0.692	0.717	0.261	NA	NA
LAWM52	Ph1	LAWA88R1	43.56	172.50	84.73	1.444	1.161	0.411	NA	NA
LAWM53	Ph1	LAWM01	3.34	9.95	23.67	0.178	0.267	0.114	NA	NA
LAWM54R1	Ph1	LAWM09	6.94	13.64	32.05	0.372	0.367	0.138	NA	NA
LAWM55	Ph1	LAWM12	1440.00	2426.00	441.80	35.657	22.937	2.239	NA	NA
LAWM56	Ph1	LAWM35	543.10	1233.00	209.50	14.603	9.797	1.069	NA	NA
LAWM57	Ph1aAug	NO	89.86	315.50	77.19	2.630	2.062	0.420	3	4
LAWM58	Ph1aAug	NO	63.64	250.30	77.06	2.205	1.643	0.396	2	4
LAWM59	Ph1aAug	NO	21.54	133.40	71.36	0.770	0.899	0.343	1	4
LAWM60	Ph1aAug	NO	80.87	265.50	106.00	2.366	1.788	0.500	5	5
LAWM61	Ph1aAug	NO	125.00	409.30	163.20	3.659	2.758	0.775	1	5
LAWM62	Ph1aAug	NO	41.95	185.90	83.63	1.500	1.253	0.403	5	2
LAWM63	Ph1aAug	NO	72.72	326.70	108.50	2.491	1.915	0.545	5	2
LAWM64	Ph1aAug	NO	66.74	231.80	69.64	1.956	1.558	0.388	1	4
LAWM65	Ph1aAug	NO	73.73	384.90	167.70	2.638	2.276	0.823	4	5
LAWM66	Ph1aAug	NO	72.76	267.50	71.33	2.203	1.568	0.398	1	5
LAWM67	Ph1aAug	NO	88.73	296.20	62.95	2.695	1.983	0.351	1	1
LAWM68	Ph1aAug	NO	135.70	519.20	182.90	4.854	3.498	0.959	4	1
LAWM69	Ph1aAug	NO	54.23	198.20	70.75	1.589	1.330	0.382	4	3
LAWM70	Ph1aAug	NO	93.88	387.30	149.50	3.217	2.609	0.705	5	2
LAWM71	Ph1aAug	NO	122.60	521.60	216.50	4.386	3.515	1.031	3	2
LAWM72	Ph1aAug	NO	107.90	390.80	86.34	3.158	2.628	0.472	4	3
LAWM73	Ph1aAug	NO	55.56	361.50	108.90	1.987	2.118	0.577	2	5
LAWM74	Ph1aAug	NO	29.64	180.90	78.97	1.059	1.143	0.372	3	1
LAWM75	Ph1aAug	NO	31.92	180.20	64.77	1.122	1.174	0.360	2	5
LAWM76	Ph1aAug	NO	73.17	310.50	90.66	2.374	1.955	0.463	1	4

- (a) Group IDs are described in Sections 2.1 to 2.7.  
 (b) If a given glass has a replicate, the glass ID is listed. If not, NO is listed.  
 (c) Numbers from 1 to 5 denote the five split validation subsets. NA denotes “not applicable”, because these replicate glasses were forced into the modeling subsets, and thus were not parts of the validation subsets.

**Table 5.3. PCT Releases and Data Splitting Validation Sets for 244 LAW Glasses Used for PCT Model Development (continued).**

Glass ID	Group ID <sup>(a)</sup>	Replicate <sup>(b)</sup>	B (ppm)	Na (ppm)	Si (ppm)	B (g/L)	Na (g/L)	Si (g/L)	B Data Splitting Validation Set <sup>(c)</sup>	Na Data Splitting Validation Set <sup>(c)</sup>
LAW2H	Corr	NO	75.57	301.10	97.86	2.495	1.953	0.493	1	3
LAW3	Corr	NO	59.18	191.00	73.49	1.905	1.413	0.366	3	1
LAW3H	Corr	NO	87.08	326.10	99.90	2.878	2.226	0.511	2	4
LAW4H	Corr	NO	38.34	189.70	87.92	1.260	1.201	0.422	3	1
LAW5H	Corr	NO	23.95	129.80	78.42	0.785	0.921	0.372	2	1
LAW7H	Corr	NO	32.72	103.20	81.85	1.066	1.027	0.391	5	4
LAW9H	Corr	NO	20.45	46.46	63.16	0.662	0.699	0.288	5	3
LAW10H	Corr	NO	14.08	18.38	47.87	0.454	0.432	0.209	5	4
LAW11	Corr	NO	34.03	116.80	64.50	1.095	0.906	0.315	2	5
LAW12	Corr	NO	65.27	310.40	92.75	2.401	2.119	0.474	2	1
LAW13	Corr	NO	76.16	289.60	77.66	2.514	1.977	0.397	2	5
LAW14	Corr	NO	90.46	352.40	99.31	2.986	2.405	0.490	3	1
LAW15	Corr	NO	61.81	300.50	90.10	2.274	2.051	0.450	4	3
LAW16	Corr	NO	42.48	238.80	83.97	1.660	1.632	0.420	1	3
LAWCrP1R	HiCrP	NO	17.55	94.13	61.09	0.565	0.656	0.294	1	1
LAWCrP2R	HiCrP	NO	34.65	161.78	76.04	1.116	1.039	0.378	5	3
LAWCrP3R	HiCrP	NO	23.31	121.59	73.34	0.751	0.847	0.361	2	4
LAWCrP4R	HiCrP	NO	27.14	136.18	76.89	0.874	0.874	0.392	4	5
LAWCrP5	HiCrP	NO	45.53	156.60	102.50	1.464	1.466	0.504	4	2
LAWCrP6	HiCrP	NO	20.81	34.18	58.18	0.670	0.576	0.278	3	4
LAWCrP7	HiCrP	NO	15.03	14.22	49.94	0.484	0.355	0.229	2	3
LAWA41	ActDes	NO	21.95	154.10	80.83	0.942	1.039	0.398	5	2
LAWA42	ActDes	NO	43.65	206.40	77.24	1.556	1.391	0.435	3	4
LAWA44	ActDes	NO	20.51	106.10	68.11	0.742	0.715	0.327	1	3
LAWA45	ActDes	NO	56.83	152.40	64.00	1.538	1.027	0.307	1	5
LAWA51	ActDes	NO	26.24	69.32	52.5	0.706	0.519	0.241	4	2
LAWA52	ActDes	NO	16.36	163.6	67.82	0.851	1.103	0.343	5	4
LAWA60	ActDes	NO	20.11	92.5	47.72	0.577	0.623	0.229	3	2
LAWA76	ActDes	NO	47.77	98.61	76.23	1.409	1.316	0.389	3	2
LAWA81	ActDes	NO	21.54	124.30	61.73	0.779	0.838	0.296	4	2
LAWA83	ActDes	NO	17.09	100.80	66.95	0.618	0.679	0.321	1	3
LAWA84	ActDes	NO	16.33	99.20	66.25	0.591	0.669	0.318	5	5
LAWA87	ActDes	NO	32.85	163.70	102.10	1.192	1.103	0.491	3	5
LAWA90	ActDes	NO	29.35	144.50	73.74	0.974	0.974	0.359	2	3
LAWA93	ActDes	NO	36.25	79.66	67.04	1.052	1.071	0.339	1	2
LAWA96	ActDes	NO	15.14	111.40	70.07	0.617	0.751	0.344	5	3
LAWA102R2	ActDes	NO	23.56	94.62	73.07	0.758	0.880	0.335	3	2
LAWA104	ActDes	NO	30.99	171.5	84.59	1.162	1.051	0.421	1	2
LAWA105	ActDes	NO	49.27	282.3	108.4	1.916	1.585	0.560	4	1
LAWA112B14	ActDes	NO	23.83	160.10	75.49	0.778	1.080	0.365	2	3
LAWA112B15	ActDes	NO	23.71	154.80	72.46	0.779	1.044	0.352	3	5
LAWA125	ActDes	NO	57.18	239.90	88.74	1.929	1.618	0.443	5	2
LAWA127R1	ActDes	NO	21.13	82.72	58.43	0.667	0.684	0.273	1	5
LAWA127R2	ActDes	NO	23.17	85.36	62.08	0.730	0.706	0.289	5	4
LAWA129	ActDes	NO	14.30	101.70	62.28	0.541	0.743	0.280	5	2
LAWA133	ActDes	NO	29.89	168.3	92.72	1.081	1.135	0.445	2	5
LAWA134	ActDes	NO	28.39	102.5	63.06	0.917	0.779	0.301	3	5
LAWA135	ActDes	NO	27.2	93.78	62.68	0.868	0.743	0.296	3	1
LAWA136	ActDes	NO	23.85	89.44	61.15	0.761	0.709	0.295	4	5
LAWA170	ActDes	NO	39.28	188.80	77.72	1.309	1.279	0.379	5	3
LAWB30	ActDes	NO	15.09	27.90	35.13	0.484	0.476	0.176	3	4
LAWB31	ActDes	NO	15.65	12.32	44.22	0.415	0.209	0.201	5	2

- (a) Group IDs are described in Sections 2.1 to 2.7.
- (b) If a given glass has a replicate, the glass ID is listed. If not, NO is listed.
- (c) Numbers from 1 to 5 denote the five split validation subsets. NA denotes “not applicable”, because these replicate glasses were forced into the modeling subsets, and thus were not parts of the validation subsets.

**Table 5.3. PCT Releases and Data Splitting Validation Sets for 244 LAW Glasses Used for PCT Model Development (continued).**

Glass ID	Group ID <sup>(a)</sup>	Replicate <sup>(b)</sup>	B (ppm)	Na (ppm)	Si (ppm)	B (g/L)	Na (g/L)	Si (g/L)	B Data Splitting Validation Set <sup>(c)</sup>	Na Data Splitting Validation Set <sup>(c)</sup>
LAWB33	ActDes	NO	14.29	13.65	43.22	0.379	0.232	0.197	4	3
LAWB34	ActDes	NO	16.22	14.69	43.77	0.431	0.250	0.199	1	4
LAWB35	ActDes	NO	37.43	40.06	62.19	0.993	0.681	0.283	3	4
LAWB37	ActDes	NO	19.16	20.79	47.44	0.510	0.354	0.216	3	2
LAWB38	ActDes	NO	18.72	20.73	49.79	0.499	0.354	0.227	4	1
LAWB61	ActDes	NO	24.13	27.36	63.49	0.780	0.670	0.279	5	1
LAWB64	ActDes	NO	17.25	19.89	47.79	0.557	0.487	0.210	5	3
LAWB67	ActDes	NO	14.975	11.511	50.906	0.485	0.283	0.225	4	3
LAWB69	ActDes	NO	18.82	23.44	44.25	0.491	0.477	0.197	1	5
LAWB70	ActDes	NO	42.81	46	69.01	1.116	0.935	0.307	1	3
LAWB71	ActDes	NO	21.5	27.19	52.44	0.641	0.553	0.233	4	5
LAWB72	ActDes	NO	33.65	37.78	58.14	0.878	0.769	0.259	5	3
LAWB73	ActDes	NO	12.74	15.47	39.51	0.412	0.380	0.174	4	1
LAWB74	ActDes	NO	14.5	16.34	41.88	0.462	0.400	0.184	2	2
LAWB75	ActDes	NO	12.57	11.73	36.1	0.343	0.288	0.159	5	4
LAWB76	ActDes	NO	15.37	14.64	42.69	0.420	0.360	0.185	2	5
LAWB77	ActDes	NO	27.73	29.53	52.03	0.723	0.600	0.232	4	4
LAWB81	ActDes	NO	34.46	38.59	59.15	0.899	0.785	0.264	5	1
LAWB87	ActDes	NO	21.40	15.47	50.52	0.529	0.416	0.220	1	2
LAWB88	ActDes	NO	15.86	11.90	43.30	0.393	0.320	0.185	1	5
LAWB89	ActDes	NO	18.60	14.08	58.47	0.597	0.465	0.253	1	5
LAWB90	ActDes	NO	19.41	27.78	57.26	0.622	0.544	0.255	2	1
LAWB91	ActDes	NO	24.65	44.92	62.79	0.790	0.693	0.287	4	2
LAWB92	ActDes	NO	28.43	59.63	64.66	0.912	0.794	0.300	1	3
LAWB93	ActDes	NO	26.69	17.55	52	0.856	0.494	0.227	1	5
LAWB94	ActDes	NO	22.12	11.75	52.87	0.710	0.468	0.228	5	2
LAWB95	ActDes	NO	20.85	8.02	51.49	0.669	0.440	0.219	2	1
LAWB96	ActDes	NO	17.14	22.96	54.92	0.550	0.565	0.241	3	5
LAWC15	ActDes	NO	18.29	99.49	67.59	0.660	0.672	0.323	4	2
LAWC21	ActDes	NO	20.47	62.94	56.73	0.652	0.713	0.260	2	1
LAWC21rev2	ActDes	NO	21.63	63.84	60.18	0.692	0.719	0.275	2	5
LAWC22	ActDes	NO	32.32	100.20	78.92	1.035	0.937	0.362	5	4
LAWC23	ActDes	NO	14.98	48.19	41.75	0.479	0.548	0.191	5	3
LAWC24	ActDes	NO	13.45	48.22	38.94	0.442	0.563	0.183	4	4
LAWC26	ActDes	NO	28.16	58.95	50.07	0.684	0.664	0.214	5	3
LAWC29	ActDes	NO	9.457	36.73	36.23	0.303	0.414	0.164	3	5
LAWC30	ActDes	NO	18.64	58.26	56.64	0.597	0.656	0.259	2	2
LAWC31	ActDes	NO	17.137	55.568	52.245	0.549	0.626	0.239	2	4
LAWC33	ActDes	NO	21.97	67.9	66.05	0.700	0.762	0.301	3	5
TFA-BASE	ActDes	NO	24.39	96.56	73.52	0.785	0.651	0.321	3	1
C22AN107	ActDes	NO	35.5	119.1	89.75	1.134	1.112	0.412	3	3
A88AP101R1	ActDes	NO	41.9	173.5	84.97	1.372	1.169	0.412	2	4
A88Si+15	ActDes	NO	73.03	329.4	113.8	2.480	2.002	0.572	4	2
A88Si-15	ActDes	NO	20.58	85.62	65.56	0.649	0.653	0.306	5	4
C22Si+15	ActDes	NO	40.8	154.6	103.5	1.336	1.287	0.486	1	4
C22Si-15	ActDes	NO	28.27	83.41	75.62	0.885	0.878	0.339	3	1
A1C1-1	ActDes	NO	24.89	119.6	80.57	0.878	0.841	0.388	1	3
A1C1-2	ActDes	NO	24.22	113.8	78.19	0.828	0.868	0.371	2	3
A1C1-3	ActDes	NO	27.52	98.33	78.73	0.913	0.820	0.368	2	4
C1-AN107	ActDes	NO	32.01	113.8	89.64	1.028	1.060	0.411	4	5

(a) Group IDs are described in Sections 2.1 to 2.7.

(b) If a given glass has a replicate, the glass ID is listed. If not, NO is listed.

(c) Numbers from 1 to 5 denote the five split validation subsets. NA denotes “not applicable”, because these replicate glasses were forced into the modeling subsets, and thus were not parts of the validation subsets.

**Table 5.3. PCT Releases and Data Splitting Validation Sets for 244 LAW Glasses Used for PCT Model Development (continued).**

Glass ID	Group ID <sup>(a)</sup>	Replicate <sup>(b)</sup>	B (ppm)	Na (ppm)	Si (ppm)	B (g/L)	Na (g/L)	Si (g/L)	B Data Splitting Validation Set <sup>(c)</sup>	Na Data Splitting Validation Set <sup>(c)</sup>
A2-API01	ActDes	NO	47.46	152.9	81.65	1.556	1.116	0.397	2	4
A2B1-1	ActDes	NO	21.89	73.11	68.79	0.713	0.647	0.326	2	5
A2B1-2	ActDes	NO	21.03	53.68	65.29	0.683	0.604	0.302	4	5
B1-AZ101	ActDes	NO	24.3	21.52	58.04	0.780	0.529	0.256	1	5
C2-AN102C35	ActDes	NO	19.82	66.86	64.19	0.677	0.752	0.290	2	4
A3-AN104	ActDes	NO	33.32	115.1	84.5	1.081	1.060	0.392	3	4
A2B1-3	ActDes	NO	25.69	42.45	66.61	0.830	0.655	0.300	3	5
A3C2-1	ActDes	NO	33.46	110.60	85.04	1.100	1.067	0.392	3	1
A3C2-2	ActDes	NO	32.84	109.30	83.64	1.092	1.106	0.383	1	1
A3C2-3	ActDes	NO	24.46	80.38	70.98	0.825	0.857	0.323	1	2
A1-AN105R2	ActDes	NO	29.15	153.60	81.50	1.062	1.002	0.398	4	1
I2U-G-86A	ActDes	NO	22.43	113.80	75.10	0.807	0.768	0.362	4	2
LA44PNCC	ActDes	LA44CCCR2	18.36	99.80	69.67	0.666	0.672	0.335	NA	NA
LA44CCCR2	ActDes	LA44PNCC	18.19	107.30	79.34	0.660	0.723	0.382	NA	NA
WVF-G-21B	ActDes	NO	25.39	108.80	66.35	0.834	0.733	0.323	4	5
PNLA126CC	ActDes	LA126CCC	27.40	107.50	64.91	0.895	0.785	0.314	NA	NA
LA126CCC	ActDes	PNLA126CC	28.93	116.90	67.41	0.945	0.853	0.326	NA	NA
WVM-G-142C	ActDes	NO	34.98	140.80	73.34	1.146	1.028	0.357	4	1
A100G115A	ActDes	NO	30.03	96.27	74.41	0.966	0.897	0.342	1	3
A100CC	ActDes	NO	22.14	70.02	67.77	0.712	0.652	0.311	1	3
WVB-G-124B	ActDes	NO	24.96	88.79	72.99	0.806	0.830	0.336	2	1
LA137SRCCC	ActDes	NO	33.31	104.90	89.68	1.082	0.966	0.416	4	2
WVR-G-127A	ActDes	NO	24.82	85.78	73.30	0.807	0.791	0.341	3	2
LB83PNCC	ActDes	LB83CCC-1	14.55	18.47	47.09	0.466	0.463	0.207	NA	NA
LB83CCC-1	ActDes	LB83PNCC	16.30	17.68	50.92	0.522	0.443	0.224	NA	NA
WVJ-G-109D	ActDes	NO	15.35	17.72	44.33	0.493	0.437	0.195	2	5
GTSD-1126	ActDes	NO	17.92	22.49	53.44	0.575	0.552	0.234	2	4
LB88CCC	ActDes	NO	11.64	10.07	41.19	0.289	0.271	0.176	2	5
AZ-102 Surr SRNL	ActDes	NO	17.70	15.29	45.30	0.439	0.406	0.194	3	3
I2S-G-85C	ActDes	NO	21.13	71.15	68.34	0.677	0.665	0.315	3	4
C100GCC	ActDes	C100-G-136B	14.51	42.65	46.28	0.463	0.484	0.212	NA	NA
AN-102 Surr LC Melter	ActDes	NO	13.40	43.70	51.90	0.425	0.499	0.237	4	1
WVH-G-57B	ActDes	NO	14.97	43.01	44.52	0.481	0.486	0.204	1	2
GTSD-1437	ActDes	PLTC35CCC	20.71	65.32	65.34	0.705	0.732	0.294	NA	NA
PLTC35CCC	ActDes	GTSD-1437	14.86	54.98	63.92	0.506	0.616	0.288	NA	NA
AN-103 Actual	Actual	NO	20.00	113.20	69.60	0.720	0.763	0.333	3	1
AW-101 Actual	Actual	NO	33.27	154.33	77.27	1.103	1.040	0.375	4	4
AP-101 Actual	Actual	NO	39.83	177.00	87.77	1.302	1.292	0.424	4	5
AZ-101 Actual	Actual	NO	16.07	20.47	50.77	0.515	0.516	0.223	4	1
AZ-102 Actual	Actual	102 Actual CCC	16.10	11.80	42.40	0.399	0.318	0.182	NA	NA
AZ-102 Actual CCC	Actual	AZ-102 Actual	12.80	10.10	37.10	0.317	0.272	0.159	NA	NA
AN-107 Actual (LAWC15)	Actual	NO	18.77	114.67	76.50	0.676	0.773	0.365	1	4
AN-102 Actual LC Melter	Actual	NO	12.60	35.70	50.50	0.402	0.408	0.231	3	4
AN-102 Actual	Actual	NO	19.40	62.90	57.10	0.617	0.719	0.261	4	4

- (a) Group IDs are described in Sections 2.1 to 2.7.
- (b) If a given glass has a replicate, the glass ID is listed. If not, NO is listed.
- (c) Numbers from 1 to 5 denote the five split validation subsets. NA denotes “not applicable”, because these replicate glasses were forced into the modeling subsets, and thus were not parts of the validation subsets.

**Table 5.4. Variation in PCT-Boron and PCT-Sodium Responses for Replicate and Near-Replicate Pairs.**

Glass IDs of Replicate and Near-Replicate Pairs <sup>(a)</sup>	In PCT Modeling Data?	PCT-Boron		PCT-Sodium	
		g/L	ln(g/L)	g/L	ln(g/L)
LAWM01	Yes	0.152	-1.88387	0.290	-1.23787
LAWM53	Yes	0.178	-1.72597	0.267	-1.32051
		<b>%RSD<sup>(b)</sup> = 11.14</b>	<b>SD = 0.1117</b>	<b>%RSD = 5.84</b>	<b>SD = 0.0584</b>
LAWM09	Yes	0.210	-1.56065	0.513	-0.66748
LAWM54R1	Yes	0.372	-0.98886	0.367	-1.00239
		<b>%RSD = 39.36</b>	<b>SD = 0.4043</b>	<b>%RSD = 23.46</b>	<b>SD = 0.2368</b>
LAWM12	Yes	29.686	3.39068	16.081	2.77764
LAWM55	Yes	35.657	3.57395	22.937	3.13275
		<b>%RSD = 12.92</b>	<b>SD = 0.1296</b>	<b>%RSD = 24.85</b>	<b>SD = 0.2511</b>
LAWM35	Yes	10.526	2.35385	6.625	1.89085
LAWM56	Yes	14.603	2.68123	9.797	2.28208
		<b>%RSD = 22.94</b>	<b>SD = 0.2315</b>	<b>%RSD = 27.32</b>	<b>SD = 0.2766</b>
LAWM50	Yes	0.647	-0.43541	0.630	-0.46204
LAWM51	Yes	0.692	-0.36817	0.717	-0.33268
		<b>%RSD = 4.75</b>	<b>SD = 0.0475</b>	<b>%RSD = 9.13</b>	<b>SD = 0.0915</b>
LAWM52	Yes	1.444	0.36742	1.161	0.14928
LAWA88R1 <sup>(c)</sup>	Yes	1.633	0.49042	1.295	0.25851
LAWA88	Yes	0.867	-0.14272	0.852	-0.16017
		<b>%RSD = 30.35</b>	<b>SD = 0.3357</b>	<b>%RSD = 20.60</b>	<b>SD = 0.2172</b>
C100-G-136B	Yes	0.734	-0.30925	0.697	-0.36097
C100GCC <sup>(d)</sup>	Yes	0.463	-0.77003	0.484	-0.72567
		<b>%RSD = 32.02</b>	<b>SD = 0.3258</b>	<b>%RSD = 25.51</b>	<b>SD = 0.2579</b>
LA44PNCC <sup>(e)</sup>	Yes	0.666	-0.40647	0.672	-0.39750
LA44CCCR2 <sup>(e)</sup>	Yes	0.660	-0.51552	0.723	-0.32435
		<b>%RSD = 0.64</b>	<b>SD = 0.0064</b>	<b>%RSD = 5.17</b>	<b>SD = 0.0517</b>
PNLA126CC <sup>(f)</sup>	Yes	0.895	-0.11093	0.785	-0.24207
LA126CCC <sup>(f)</sup>	Yes	0.945	-0.05657	0.853	-0.15900
		<b>%RSD = 3.84</b>	<b>SD = 0.0384</b>	<b>%RSD = 5.87</b>	<b>SD = 0.0587</b>
LB83PNCC <sup>(g)</sup>	Yes	0.466	-0.76357	0.463	-0.77003
LB83CCC-1 <sup>(g)</sup>	Yes	0.522	-0.65009	0.443	-0.81419
		<b>%RSD = 8.02</b>	<b>SD = 0.0802</b>	<b>%RSD = 3.12</b>	<b>SD = 0.0312</b>
AZ-102 Actual <sup>(h)</sup>	Yes	0.399	-0.91879	0.318	-1.14570
AZ-102 Actual CCC <sup>(h)</sup>	Yes	0.317	-1.14885	0.272	-1.30195
		<b>%RSD = 16.20</b>	<b>SD = 0.1627</b>	<b>%RSD = 11.03</b>	<b>SD = 0.1105</b>
GTSD-1437	Yes	0.705	-0.34956	0.732	-0.31197
PLTC35CCC <sup>(i)</sup>	Yes	0.506	-0.68122	0.616	-0.48451
		<b>%RSD = 23.24</b>	<b>SD = 0.2345</b>	<b>%RSD = 12.17</b>	<b>SD = 0.1220</b>
<b>Pooled Over 12 Replicate Pairs</b>		<b>%RSD = 21.73</b>	<b>SD = 0.2269</b>	<b>%RSD = 17.23</b>	<b>SD = 0.1760</b>

- (a) Because glass compositions were renormalized based on analyzed (or estimates of analyzed) SO<sub>3</sub> values, the compositions of replicate pairs may not match exactly. However, they were still treated as replicate pairs for statistical data analyses.
- (b) %RSD = 100×(Standard Deviation / Mean)
- (c) LAWA88R1 was accidentally not treated as a replicate in model lack-of-fit tests. The impact of this oversight is negligible.
- (d) Container centerline cooled (CCC) sample of C100-G-136B (which was a DM100 melter glass).
- (e) Crucible glasses with the same target glass composition but independently batched and melted. A CCC curve was used for LA44PNCC, while a slightly different cooling curve was used for LA44CCCR2.
- (f) Crucible glasses with the same target glass composition but independently batched and melted. A CCC curve was used for PNLA126CC, while a slightly different cooling curve was used for LA126CCC.
- (g) Crucible glasses with the same target glass composition but independently batched and melted. A CCC curve was used for LB83PNCC, while a slightly different cooling curve was used for LB83CCC-1.
- (h) Crucible glass made from AZ-102 waste, with a sample of the glass subjected to a CCC curve.
- (i) A CCC sample of GTSD-1437, which was a LAW pilot melter glass.

**Table 5.5. Normalized<sup>(a)</sup> Compositions (mass fractions) for 20 Outlying LAW Glasses Excluded from PCT Modeling Data.**

Glass ID	Group ID <sup>(b)</sup>	Al <sub>2</sub> O <sub>3</sub>	B <sub>2</sub> O <sub>3</sub>	CaO	Cl	Cr <sub>2</sub> O <sub>3</sub>	F	Fe <sub>2</sub> O <sub>3</sub>	K <sub>2</sub> O	Li <sub>2</sub> O	MgO	Na <sub>2</sub> O	P <sub>2</sub> O <sub>5</sub>	XRF SO <sub>3</sub> <sup>(c)</sup>	SiO <sub>2</sub>	TiO <sub>2</sub>	ZnO	ZrO <sub>2</sub>	Others	Sum <sup>(d)</sup>
LAWA43-1	ActDes	.12002	.07391	.01967	.00579	.00017	.00036	.06881	.03101	.00001	.01965	.20004	.00078	.00100	.38007	.01966	.02949	.02951	.00005	1.00000
LAWA49	ActDes	.06203	.08904	.00000	.00652	.00020	.00010	.09982	.00501	.00000	.01478	.20005	.00034	.00070	.44565	.01995	.02478	.02992	.00112	1.00000
LAWA50	ActDes	.06201	.08902	.00000	.00652	.00020	.00010	.11981	.00501	.00000	.01477	.20000	.00034	.00100	.42550	.01994	.02477	.02992	.00111	1.00000
LAWA65	ActDes	.06155	.06167	.03289	.00649	.00020	.00010	.07476	.00499	.00000	.06034	.19924	.00034	.00480	.42087	.01104	.02983	.02980	.00109	1.00000
LAWA82	ActDes	.06201	.08902	.00000	.00652	.00020	.00010	.06980	.00501	.00000	.01994	.20000	.00034	.00100	.44552	.03989	.02965	.02992	.00111	1.00000
LAWA89	ActDes	.06082	.09700	.00000	.00329	.00009	.00000	.05533	.02583	.00000	.01475	.20005	.00070	.00190	.44002	.03983	.02951	.02988	.00100	1.00000
LAWB32	ActDes	.06180	.15146	.04045	.00007	.00089	.00099	.04180	.00320	.02966	.02247	.07928	.02733	.00680	.47077	.00000	.03101	.03101	.00102	1.00000
LAWB40	ActDes	.06137	.12052	.04687	.00007	.00088	.00098	.05133	.00318	.06294	.02901	.07873	.00036	.01360	.46755	.00000	.03080	.03080	.00102	1.00000
LAWB41	ActDes	.06145	.12067	.06481	.00007	.00088	.00099	.05140	.00318	.04514	.02905	.07884	.00036	.01230	.46816	.00000	.03084	.03084	.00102	1.00000
LAWB60	ActDes	.06143	.12366	.11905	.00010	.00070	.00080	.00000	.00261	.04630	.02976	.06514	.00030	.00640	.47961	.00000	.03157	.03157	.00100	1.00000
LAWB62	ActDes	.06194	.09948	.11996	.00000	.00100	.00070	.00000	.00261	.05812	.02971	.05491	.00010	.00890	.48536	.01395	.03162	.03162	.00000	1.00000
LAWB63	ActDes	.06579	.09953	.09351	.00000	.00100	.00070	.00000	.00261	.05052	.02973	.05494	.00010	.00840	.48942	.01396	.05815	.03164	.00000	1.00000
LAWB82	ActDes	.06162	.10100	.07134	.00010	.00050	.00080	.09519	.00230	.04269	.01483	.06633	.00050	.00480	.45532	.00000	.05010	.03156	.00100	1.00000
LAWC12	ActDes	.11989	.09142	.01596	.00119	.00017	.00009	.05716	.00141	.00000	.01387	.20026	.00027	.00180	.39384	.03416	.04274	.02458	.00121	1.00000
LAWC25	ActDes	.05784	.09526	.06052	.00117	.00019	.00057	.06116	.08079	.00000	.01425	.11209	.00111	.00530	.44122	.01058	.02850	.02852	.00095	1.00000
LAWC28	ActDes	.06117	.10045	.12814	.00110	.00020	.00050	.00010	.00140	.02729	.01499	.11954	.00110	.00430	.46717	.01119	.03018	.03018	.00100	1.00000
LAWE3Cr2CCC	Corr	.06103	.10005	.02021	.00200	.01401	.00080	.05503	.04992	.00000	.01481	.18219	.00124	.00300	.41651	.01401	.03502	.03002	.00016	1.00000
LAWE9HCr1CCC	Corr	.06059	.09934	.06870	.00196	.00601	.00079	.05462	.00541	.04086	.02363	.08943	.00122	.00551	.46339	.01392	.03475	.02974	.00016	1.00000
LAWE9HCr2CCC	Corr	.06060	.09937	.06872	.00196	.00451	.00079	.05463	.00541	.04087	.02364	.08945	.00122	.00521	.46503	.01392	.03476	.02975	.00016	1.00000
LAWE10HCr3CCC	Corr	.06081	.09968	.06973	.00196	.00351	.00079	.05494	.00541	.04268	.02945	.05730	.00122	.00621	.48742	.01393	.03486	.02995	.00016	1.00000

- (a) The compositions listed in this table are normalized versions of target compositions of the glasses, after replacing the target values of SO<sub>3</sub> by XRF analyzed (or estimated analyzed) values. See Section 3.3 for the details.
- (b) The Group IDs are described in Sections 2.1 to 2.7.
- (c) XRF SO<sub>3</sub> denotes that the SO<sub>3</sub> composition is based on chemical analysis by XRF. For most glasses SO<sub>3</sub> was directly measured by XRF, but for some glasses estimated XRF values were used (see Section 3.3).
- (d) The normalized component mass fractions listed in this table were rounded to five decimals, and may not sum exactly to 1.00000 as listed. However, complete compositions listed to more decimal places and summing to 1.0000 were used for property-composition modeling.



**Table 5.6. PCT Releases for 20 Outlying LAW Glasses Excluded from the PCT Modeling Set.**

<b>Glass ID</b>	<b>Group ID<sup>(a)</sup></b>	<b>B (ppm)</b>	<b>Na (ppm)</b>	<b>Si (ppm)</b>	<b>B (g/L)</b>	<b>Na (g/L)</b>	<b>Si (g/L)</b>
LAWA43-1	ActDes	17.59	127.80	57.66	0.766	0.861	0.325
LAWA49	ActDes	17.18	86.71	63.38	0.621	0.584	0.304
LAWA50	ActDes	17.28	88.98	61.00	0.625	0.600	0.307
LAWA65	ActDes	27.02	194.70	93.65	1.411	1.317	0.476
LAWA82	ActDes	18.83	99.37	69.19	0.681	0.670	0.332
LAWA89	ActDes	35.12	138.10	74.45	1.166	0.931	0.362
LAWB32	ActDes	23.15	16.70	46.28	0.492	0.284	0.210
LAWB40	ActDes	119.20	137.60	142.10	3.185	2.356	0.650
LAWB41	ActDes	63.73	82.37	83.63	1.701	1.408	0.382
LAWB60	ActDes	16.95	21.83	42.83	0.441	0.452	0.191
LAWB62	ActDes	10.02	14.47	37.81	0.324	0.355	0.167
LAWB63	ActDes	11.15	14.12	37.7	0.361	0.346	0.165
LAWB82	ActDes	15.58	22.43	39.85	0.497	0.456	0.187
LAWC12	ActDes	23.81	121.40	67.79	0.839	0.817	0.368
LAWC25	ActDes	18.93	64.06	45.12	0.640	0.770	0.219
LAWC28	ActDes	8.92	38.91	35.72	0.286	0.439	0.164
LAW E3Cr2CCC	Corr	36.28	148.40	67.82	1.168	1.098	0.348
LAW E9HCr1CCC	Corr	12.50	30.18	42.25	0.405	0.455	0.195
LAW E9HCr2CCC	Corr	15.54	32.43	41.86	0.504	0.489	0.193
LAW E10HCr3CCC	Corr	8.21	12.14	32.85	0.265	0.286	0.144

(a) The Group IDs are described in Sections 2.1 to 2.7.

**Table 5.7. Coefficients and Performance Summary for 18-Component Full Linear Mixture Model on the Natural Logarithm of ILAW PCT-B.**

In(PCT-B) Full LM Model Term	Coefficient Estimate	Coefficient Stand. Dev.	Modeling Data Statistic, 244 Glasses <sup>(a)</sup>				Value
Al <sub>2</sub> O <sub>3</sub>	-26.4769	2.3175	R <sup>2</sup>				0.782
B <sub>2</sub> O <sub>3</sub>	14.9463	1.6070	R <sup>2</sup> Adjusted (R <sup>2</sup> <sub>A</sub> )				0.766
CaO	-3.0631	1.3529	R <sup>2</sup> Predicted (R <sup>2</sup> <sub>p</sub> )				0.717
Cl	-2.0430	11.4519	RMSE				0.372
Cr <sub>2</sub> O <sub>3</sub>	81.9917	28.5122	Model LOF p-value				0.018
F	-31.5827	29.4419					
Fe <sub>2</sub> O <sub>3</sub>	3.0626	1.4003	<b>Extrapolative Validation Statistic, 20 Outlying Glasses<sup>(a,b)</sup></b>				<b>Value</b>
K <sub>2</sub> O	15.3902	1.8903	R <sup>2</sup> Validation (R <sup>2</sup> <sub>v</sub> )				-0.385
Li <sub>2</sub> O	32.4843	3.1637	RMSE Validation (RMSE <sub>v</sub> )				0.732
MgO	31.2856	2.9636					
Na <sub>2</sub> O	14.0572	0.9206	<b>Data Partition Statistic, 97 Modeling &amp; 147 Validation<sup>(a,c)</sup></b>				<b>Value</b>
P <sub>2</sub> O <sub>5</sub>	-14.2353	4.0086	R <sup>2</sup>				0.857
SO <sub>3</sub>	-29.8705	18.9715	R <sup>2</sup> Adjusted (R <sup>2</sup> <sub>A</sub> )				0.826
SiO <sub>2</sub>	-6.8866	0.6551	R <sup>2</sup> Predicted (R <sup>2</sup> <sub>p</sub> )				0.747
TiO <sub>2</sub>	-4.1040	3.6205	RMSE				0.440
ZnO	0.8193	2.9049	R <sup>2</sup> Validation (R <sup>2</sup> <sub>v</sub> )				-1.875
ZrO <sub>2</sub>	-1.5452	3.1277	RMSE Validation (RMSE <sub>v</sub> )				0.795
Others <sup>(e)</sup>	-28.7854	38.3016					
<b>Data Splitting Statistic<sup>(a,d)</sup></b>							
	<b>DS1</b>	<b>DS2</b>	<b>DS3</b>	<b>DS4</b>	<b>DS5</b>	<b>Average</b>	
R <sup>2</sup>	0.797	0.798	0.801	0.781	0.793	0.794	
R <sup>2</sup> Adjusted (R <sup>2</sup> <sub>A</sub> )	0.778	0.779	0.783	0.761	0.773	0.775	
R <sup>2</sup> Predicted (R <sup>2</sup> <sub>p</sub> )	0.722	0.727	0.723	0.694	0.716	0.717	
RMSE	0.369	0.375	0.371	0.389	0.379	0.377	
R <sup>2</sup> Validation (R <sup>2</sup> <sub>v</sub> )	0.666	0.603	0.547	0.749	0.645	0.642	
RMSE Validation (RMSE <sub>v</sub> )	0.406	0.391	0.421	0.316	0.378	0.382	

- (a) The model evaluation statistics are defined in Section C.3 of Appendix C. Model validation statistics are defined in Section C.5 of Appendix C. A negative value for R<sup>2</sup><sub>v</sub> means that the sum of squares of model prediction errors is larger than if the mean response value over the validation data set were used as the predicted value for each glass. In other words, the model predicts worse for the validation data than the mean response value does.
- (b) The 20 outlying LAW glass compositions are discussed in Section 5.1.4.
- (c) The partition of the PCT-B modeling data set into modeling and validation subsets is described in Section 5.1.3.
- (d) The evaluation and validation statistics calculated for data-splits are defined the same as for separate modeling and validation sets. Section 5.1.2 describes how the data-splitting was accomplished.
- (e) For the full LM model, the “Others” component includes Ag<sub>2</sub>O, BaO, Br, CdO, Cs<sub>2</sub>O, I, La<sub>2</sub>O<sub>3</sub>, MnO, MoO<sub>3</sub>, NiO, PbO, Re<sub>2</sub>O<sub>7</sub>, SeO<sub>2</sub>, SrO, and “Unknown”.

**Table 5.8. Coefficients and Performance Summary for 12-Component Reduced Linear Mixture Model on the Natural Logarithm of ILAW PCT-B.**

In(PCT-B) Reduced LM Model Term	Coefficient Estimate	Coefficient Stand. Dev.	Modeling Data Statistic, 244 Glasses <sup>(a)</sup>				Value
Al <sub>2</sub> O <sub>3</sub>	-26.1173	2.3603	R <sup>2</sup>				0.766
B <sub>2</sub> O <sub>3</sub>	14.9224	1.6198	R <sup>2</sup> Adjusted (R <sup>2</sup> <sub>A</sub> )				0.755
CaO	-2.7909	1.3389	R <sup>2</sup> Predicted (R <sup>2</sup> <sub>p</sub> )				0.720
Fe <sub>2</sub> O <sub>3</sub>	2.8886	1.3886	RMSE				0.380
K <sub>2</sub> O	14.5517	1.8118	Model LOF p-value				0.015
Li <sub>2</sub> O	32.4088	3.0590					
MgO	31.0061	3.0031	<b>Extrapolative Validation Statistic, 20 Outlying Glasses<sup>(a,b)</sup></b>				<b>Value</b>
Na <sub>2</sub> O	14.3303	0.8762	R <sup>2</sup> Validation (R <sup>2</sup> <sub>v</sub> )				0.170
P <sub>2</sub> O <sub>5</sub>	-10.1386	3.4724	RMSE Validation (RMSE <sub>v</sub> )				0.566
SiO <sub>2</sub>	-7.5000	0.6313					
ZrO <sub>2</sub>	-1.1337	3.0180					
Others <sup>(e)</sup>	1.2500	2.1078	<b>Data Partition Statistic, 97 Modeling &amp; 147 Validation<sup>(a,c)</sup></b>				<b>Value</b>
			R <sup>2</sup>				0.837
			R <sup>2</sup> Adjusted (R <sup>2</sup> <sub>A</sub> )				0.816
			R <sup>2</sup> Predicted (R <sup>2</sup> <sub>p</sub> )				0.757
			RMSE				0.452
			R <sup>2</sup> Validation (R <sup>2</sup> <sub>v</sub> )				-1.397
			RMSE Validation (RMSE <sub>v</sub> )				0.726
<b>Data Splitting Statistic<sup>(a,d)</sup></b>	<b>DS1</b>	<b>DS2</b>	<b>DS3</b>	<b>DS4</b>	<b>DS5</b>	<b>Average</b>	
R <sup>2</sup>	0.781	0.777	0.783	0.766	0.771	0.776	
R <sup>2</sup> Adjusted (R <sup>2</sup> <sub>A</sub> )	0.768	0.764	0.770	0.753	0.758	0.763	
R <sup>2</sup> Predicted (R <sup>2</sup> <sub>p</sub> )	0.727	0.725	0.721	0.706	0.718	0.719	
RMSE	0.377	0.387	0.382	0.396	0.391	0.386	
R <sup>2</sup> Validation (R <sup>2</sup> <sub>v</sub> )	0.660	0.653	0.588	0.730	0.709	0.668	
RMSE Validation (RMSE <sub>v</sub> )	0.410	0.365	0.402	0.328	0.342	0.369	

- (a) The model evaluation statistics are defined in Section C.3 of Appendix C. Model validation statistics are defined in Section C.5 of Appendix C. A negative value for R<sup>2</sup><sub>v</sub> means that the sum of squares of model prediction errors is larger than if the mean response value over the validation data set were used as the predicted value for each glass. In other words, the model predicts worse for the validation data than the mean response value does.
- (b) The 20 outlying LAW glass compositions are discussed in Section 5.1.4.
- (c) The partition of the PCT-B modeling data set into modeling and validation subsets is described in Section 5.1.3.
- (d) The evaluation and validation statistics calculated for data-splits are defined the same as for separate modeling and validation sets. Section 5.1.2 describes how the data-splitting was accomplished.
- (e) For the reduced LM model, the “Others” component includes the original “Others” component (which contains Ag<sub>2</sub>O, BaO, Br, CdO, Cs<sub>2</sub>O, I, La<sub>2</sub>O<sub>3</sub>, MnO, MoO<sub>3</sub>, NiO, PbO, Re<sub>2</sub>O<sub>7</sub>, SeO<sub>2</sub>, SrO, and “Unknown”) plus Cl, Cr<sub>2</sub>O<sub>3</sub>, F, SO<sub>3</sub>, TiO<sub>2</sub>, and ZnO.

**Table 5.9. Coefficients and Performance Summary for 17-Term Reduced Partial Quadratic Mixture Model on the Natural Logarithm of ILAW PCT-B.**

In(PCT-B) Reduced PQM Model Term	Coefficient Estimate	Coefficient Stand. Dev.	Modeling Data Statistic, 244 Glasses <sup>(a)</sup>				Value
Al <sub>2</sub> O <sub>3</sub>	-31.3612	2.1310	R <sup>2</sup>				0.866
B <sub>2</sub> O <sub>3</sub>	11.8101	2.5505	R <sup>2</sup> Adjusted (R <sup>2</sup> <sub>A</sub> )				0.857
CaO	-13.8404	3.0142	R <sup>2</sup> Predicted (R <sup>2</sup> <sub>p</sub> )				0.835
Fe <sub>2</sub> O <sub>3</sub>	-16.5948	3.2161	RMSE				0.291
K <sub>2</sub> O	7.9687	1.7452	Model LOF p-value				0.122
Li <sub>2</sub> O	83.3036	8.4889					
MgO	-21.2343	8.2492	<b>Extrapolative Validation Statistic, 20 Outlying Glasses<sup>(a,b)</sup></b>				<b>Value</b>
Na <sub>2</sub> O	46.1599	5.2140	R <sup>2</sup> Validation (R <sup>2</sup> <sub>v</sub> )				0.446
P <sub>2</sub> O <sub>5</sub>	-19.2540	2.8180	RMSE Validation (RMSE <sub>v</sub> )				0.463
SiO <sub>2</sub>	-1.6161	1.1133					
ZrO <sub>2</sub>	-6.6289	2.7866					
Others <sup>(c)</sup>	-5.1690	1.8573	<b>Data Partition Statistic, 97 Modeling &amp; 147 Validation<sup>(a,c)</sup></b>				<b>Value</b>
CaO×Li <sub>2</sub> O	-251.2654	53.4354	R <sup>2</sup>				0.923
B <sub>2</sub> O <sub>3</sub> ×MgO	488.8612	89.5443	R <sup>2</sup> Adjusted (R <sup>2</sup> <sub>A</sub> )				0.908
B <sub>2</sub> O <sub>3</sub> ×Li <sub>2</sub> O	-374.9533	72.1448	R <sup>2</sup> Predicted (R <sup>2</sup> <sub>p</sub> )				0.870
Na <sub>2</sub> O×SiO <sub>2</sub>	-74.3462	13.1157	RMSE				0.320
CaO×Fe <sub>2</sub> O <sub>3</sub>	212.0947	46.0965	R <sup>2</sup> Validation (R <sup>2</sup> <sub>v</sub> )				0.071
			RMSE Validation (RMSE <sub>v</sub> )				0.452
<b>Data Splitting Statistic<sup>(a,d)</sup></b>							
	<b>DS1</b>	<b>DS2</b>	<b>DS3</b>	<b>DS4</b>	<b>DS5</b>	<b>Average</b>	
R <sup>2</sup>	0.871	0.869	0.890	0.871	0.874	0.875	
R <sup>2</sup> Adjusted (R <sup>2</sup> <sub>A</sub> )	0.860	0.858	0.881	0.859	0.863	0.864	
R <sup>2</sup> Predicted (R <sup>2</sup> <sub>p</sub> )	0.833	0.831	0.857	0.832	0.835	0.837	
RMSE	0.293	0.300	0.275	0.298	0.294	0.292	
R <sup>2</sup> Validation (R <sup>2</sup> <sub>v</sub> )	0.829	0.827	0.595	0.802	0.790	0.769	
RMSE Validation (RMSE <sub>v</sub> )	0.291	0.258	0.398	0.280	0.290	0.303	

- (a) The model evaluation statistics are defined in Section C.3 of Appendix C. Model validation statistics are defined in Section C.5 of Appendix C. A negative value for R<sup>2</sup><sub>v</sub> means that the sum of squares of model prediction errors is larger than if the mean response value over the validation data set were used as the predicted value for each glass. In other words, the model predicts worse for the validation data than the mean response value does.
- (b) The 20 outlying LAW glass compositions are discussed in Section 5.1.4.
- (c) The partition of the PCT-B modeling data set into modeling and validation subsets is described in Section 5.1.3.
- (d) The evaluation and validation statistics calculated for data-splits are defined the same as for separate modeling and validation sets. Section 5.1.2 describes how the data-splitting was accomplished.
- (e) For the reduced PQM model, the “Others” component includes the original “Others” component (which contains Ag<sub>2</sub>O, BaO, Br, CdO, Cs<sub>2</sub>O, I, La<sub>2</sub>O<sub>3</sub>, MnO, MoO<sub>3</sub>, NiO, PbO, Re<sub>2</sub>O<sub>7</sub>, SeO<sub>2</sub>, SrO, and “Unknown”) plus Cl, Cr<sub>2</sub>O<sub>3</sub>, F, SO<sub>3</sub>, TiO<sub>2</sub>, and ZnO.

**Table 5.10. Coefficients and Performance Summary for 24-Term Two-Part Reduced Linear Mixture Model on the Natural Logarithm of ILAW PCT-B.**

ln(PCT-B) Two-Part Reduced LM Model Term	Below Cutoff (1.89 g/L)		Above Cutoff (1.89 g/L)		Modeling Data Statistic, 244 Glasses <sup>(a)</sup>		Value	
	Coefficient Estimate	Coefficient Stand. Dev.	Coefficient Estimate	Coefficient Stand. Dev.				
Al <sub>2</sub> O <sub>3</sub>	-15.9172	1.9626	-31.1589	5.9720	R <sup>2</sup>			0.897
B <sub>2</sub> O <sub>3</sub>	7.7970	1.2637	28.4019	3.5981	R <sup>2</sup> Adjusted (R <sup>2</sup> <sub>A</sub> )			0.886
CaO	-4.7349	1.0715	0.1542	2.4495	R <sup>2</sup> Predicted (R <sup>2</sup> <sub>p</sub> )			0.862
Fe <sub>2</sub> O <sub>3</sub>	2.4580	1.0336	8.5760	4.9620	RMSE			0.259
K <sub>2</sub> O	4.5612	1.5694	12.6861	4.1629	Model LOF p-value			0.271
Li <sub>2</sub> O	18.5072	2.5157	33.4697	8.8289				
MgO	19.0852	2.3049	35.9553	9.1489				
Na <sub>2</sub> O	8.4183	0.7660	11.2872	4.8894	<b>Extrapolative Validation Statistic, 20 Outlying Glasses<sup>(a,b)</sup></b>			
P <sub>2</sub> O <sub>5</sub>	-11.6088	2.3496	57.4524	44.1003	R <sup>2</sup> Validation (R <sup>2</sup> <sub>v</sub> )			0.183
SiO <sub>2</sub>	-3.7785	0.5134	-7.6604	2.0505	RMSE Validation (RMSE <sub>v</sub> )			0.562
ZrO <sub>2</sub>	1.8070	2.5312	-4.0158	5.0063				
Others <sup>(c)</sup>	-3.4009	1.5710	-5.8429	7.2751				
					<b>Data Partition Statistic, 97 Modeling &amp; 147 Validation<sup>(a,c)</sup></b>		<b>Value</b>	
<b>Summary Statistic</b>					Insufficient data in the modeling subset to fit the two-part model and perform these assessments			
	<b>Below Cutoff Data</b>	<b>Based on Reduced LM Model</b>	<b>Above Cutoff Data</b>	<b>Based on Reduced LM Model</b>				
R <sup>2</sup>	0.699	0.479	0.889	0.407				
R <sup>2</sup> Adjusted (R <sup>2</sup> <sub>A</sub> )	0.682		0.842					
R <sup>2</sup> Predicted (R <sup>2</sup> <sub>p</sub> )	0.649		0.741					
RMSE	0.254		0.292					
					<b>Data Splitting Statistic<sup>(a,d)</sup></b>			
R <sup>2</sup>	<b>DS1</b>	<b>DS2</b>	<b>DS3</b>	<b>DS4</b>	<b>DS5</b>	<b>Average</b>		
R <sup>2</sup>	0.909	0.911	0.902	0.905	0.902	0.906		
R <sup>2</sup> Adjusted (R <sup>2</sup> <sub>A</sub> )	0.897	0.900	0.889	0.893	0.889	0.894		
R <sup>2</sup> Predicted (R <sup>2</sup> <sub>p</sub> )	0.864	0.873	0.834	0.844	0.860	0.855		
RMSE	0.251	0.252	0.265	0.260	0.265	0.259		
R <sup>2</sup> Validation (R <sup>2</sup> <sub>v</sub> )	0.800	0.564	0.684	0.762	0.565	0.675		
RMSE Validation (RMSE <sub>v</sub> )	0.314	0.409	0.352	0.308	0.418	0.360		

(a) to (e) The footnotes in this table are the same as in Tables 5.7 to 5.9.

**Table 5.11. Performance Summary of Four Models on the Natural Logarithm of ILAW PCT-B.**

Summary Statistic from Model Fit to 244 Glasses <sup>(a)</sup>	ln(PCT-B) Models			
	Full LM	Reduced LM	Reduced PQM	Two-Part
R <sup>2</sup>	0.782	0.766	0.866	0.897
R <sup>2</sup> Adjusted (R <sup>2</sup> <sub>A</sub> )	0.766	0.755	0.857	0.886
R <sup>2</sup> Predicted (R <sup>2</sup> <sub>p</sub> )	0.717	0.720	0.835	0.862
RMSE	0.372	0.380	0.291	0.259
LOF p-value	0.018	0.015	0.122	0.271
<b>Linear Terms</b>	See Table 5.7	Al <sub>2</sub> O <sub>3</sub> , B <sub>2</sub> O <sub>3</sub> , CaO, Fe <sub>2</sub> O <sub>3</sub> , K <sub>2</sub> O, Li <sub>2</sub> O, MgO, Na <sub>2</sub> O, P <sub>2</sub> O <sub>5</sub> , SiO <sub>2</sub> , ZrO <sub>2</sub> , Others		
<b>Selected Quadratic Terms in Model</b>	N/A	N/A	CaO×Li <sub>2</sub> O B <sub>2</sub> O <sub>3</sub> ×MgO B <sub>2</sub> O <sub>3</sub> ×Li <sub>2</sub> O Na <sub>2</sub> O×SiO <sub>2</sub> CaO×Fe <sub>2</sub> O <sub>3</sub>	N/A
<b># Model Terms</b>	18	12	17	24
<b>Summary Statistic for Partition of PCT-B Data into Modeling (97 Glasses) and Validation (147 Glasses) Subsets<sup>(a)</sup></b>				
R <sup>2</sup>	0.857	0.837	0.923	(b)
R <sup>2</sup> Adjusted (R <sup>2</sup> <sub>A</sub> )	0.826	0.816	0.908	(b)
R <sup>2</sup> Predicted (R <sup>2</sup> <sub>p</sub> )	0.747	0.757	0.870	(b)
RMSE	0.440	0.452	0.320	(b)
R <sup>2</sup> Validation (R <sup>2</sup> <sub>v</sub> )	-1.875	-1.397	0.071	(b)
RMSE Validation (RMSE <sub>v</sub> )	0.795	0.726	0.452	(b)
<b>Summary Statistic Averaged Over 5 Data-Splitting Sets<sup>(a)</sup></b>				
R <sup>2</sup>	0.794	0.776	0.875	0.906
R <sup>2</sup> Adjusted (R <sup>2</sup> <sub>A</sub> )	0.775	0.763	0.864	0.894
R <sup>2</sup> Predicted (R <sup>2</sup> <sub>p</sub> )	0.717	0.719	0.837	0.855
RMSE	0.377	0.386	0.292	0.259
R <sup>2</sup> Validation (R <sup>2</sup> <sub>v</sub> )	0.642	0.668	0.769	0.675
RMSE Validation (RMSE <sub>v</sub> )	0.382	0.369	0.303	0.360

- (a) The model evaluation statistics are defined in Section C.3 of Appendix C. Model validation statistics are defined in Section C.5 of Appendix C. A negative value for R<sup>2</sup><sub>v</sub> means that the sum of squares of model prediction errors is larger than if the mean response value over the validation data set were used as the predicted value for each glass. In other words, the model predicts worse for the validation data than the mean response value does.
- (b) There were insufficient data in the 97-glass modeling subset to adequately fit the two-part model.

**Table 5.12. Coefficients and Performance Summary for 18-Component Full Linear Mixture Model on the Natural Logarithm of ILAW PCT-Na.**

In(PCT-Na) Full LM Model Term	Coefficient Estimate	Coefficient Stand. Dev.	Modeling Data Statistic, 244 Glasses <sup>(a)</sup>				Value
Al <sub>2</sub> O <sub>3</sub>	-23.5367	1.9927	R <sup>2</sup>				0.798
B <sub>2</sub> O <sub>3</sub>	9.2019	1.3817	R <sup>2</sup> Adjusted (R <sup>2</sup> <sub>A</sub> )				0.783
CaO	3.1515	1.1633	R <sup>2</sup> Predicted (R <sup>2</sup> <sub>P</sub> )				0.740
Cl	-1.8369	9.8468	RMSE				0.320
Cr <sub>2</sub> O <sub>3</sub>	78.5606	24.5159	Model LOF p-value				0.008
F	-18.1706	25.3152					
Fe <sub>2</sub> O <sub>3</sub>	1.8575	1.2040	<b>Extrapolative Validation Statistic, 20 Outlying Glasses<sup>(a,b)</sup></b>				<b>Value</b>
K <sub>2</sub> O	14.3140	1.6253	R <sup>2</sup> Validation (R <sup>2</sup> <sub>V</sub> )				-0.510
Li <sub>2</sub> O	28.0550	2.7203	RMSE Validation (RMSE <sub>V</sub> )				0.677
MgO	24.6999	2.5482					
Na <sub>2</sub> O	14.1650	0.7916	<b>Data Partition Statistic, 97 Modeling &amp; 147 Validation<sup>(a,c)</sup></b>				<b>Value</b>
P <sub>2</sub> O <sub>5</sub>	-14.5435	3.4467	R <sup>2</sup>				0.858
SO <sub>3</sub>	-44.0369	16.3125	R <sup>2</sup> Adjusted (R <sup>2</sup> <sub>A</sub> )				0.827
SiO <sub>2</sub>	-6.0965	0.5632	R <sup>2</sup> Predicted (R <sup>2</sup> <sub>P</sub> )				0.754
TiO <sub>2</sub>	-1.0927	3.1130	RMSE				0.363
ZnO	1.2945	2.4977	R <sup>2</sup> Validation (R <sup>2</sup> <sub>V</sub> )				-0.306
ZrO <sub>2</sub>	-3.6409	2.6893	RMSE Validation (RMSE <sub>V</sub> )				0.548
Others <sup>(e)</sup>	-38.2225	32.9332					
<b>Data Splitting Statistic<sup>(a,d)</sup></b>							
	<b>DS1</b>	<b>DS2</b>	<b>DS3</b>	<b>DS4</b>	<b>DS5</b>	<b>Average</b>	
R <sup>2</sup>	0.802	0.804	0.813	0.797	0.808	0.805	
R <sup>2</sup> Adjusted (R <sup>2</sup> <sub>A</sub> )	0.784	0.786	0.796	0.778	0.790	0.787	
R <sup>2</sup> Predicted (R <sup>2</sup> <sub>P</sub> )	0.725	0.733	0.753	0.724	0.740	0.735	
RMSE	0.324	0.327	0.319	0.333	0.323	0.325	
R <sup>2</sup> Validation (R <sup>2</sup> <sub>V</sub> )	0.742	0.710	0.634	0.786	0.686	0.712	
RMSE Validation (RMSE <sub>V</sub> )	0.320	0.310	0.352	0.269	0.329	0.316	

- (a) The model evaluation statistics are defined in Section C.3 of Appendix C. Model validation statistics are defined in Section C.5 of Appendix C. A negative value for R<sup>2</sup><sub>V</sub> means that the sum of squares of model prediction errors is larger than if the mean response value over the validation data set were used as the predicted value for each glass. In other words, the model predicts worse for the validation data than the mean response value does.
- (b) The 20 outlying LAW glass compositions are discussed in Section 5.1.4.
- (c) The partition of the PCT-Na modeling data set into modeling and validation subsets is described in Section 5.1.3.
- (d) The evaluation and validation statistics calculated for data-splits are defined the same as for separate modeling and validation sets. Section 5.1.2 describes how the data-splitting was accomplished.
- (e) For the full LM model, the “Others” component includes Ag<sub>2</sub>O, BaO, Br, CdO, Cs<sub>2</sub>O, I, La<sub>2</sub>O<sub>3</sub>, MnO, MoO<sub>3</sub>, NiO, PbO, Re<sub>2</sub>O<sub>7</sub>, SeO<sub>2</sub>, SrO, and “Unknown”.

**Table 5.13. Coefficients and Performance Summary for 12-Component Reduced Linear Mixture Model on the Natural Logarithm of ILAW PCT-Na.**

In(PCT-Na) Reduced LM Model Term	Coefficient Estimate	Coefficient Stand. Dev.	Modeling Data Statistic, 244 Glasses <sup>(a)</sup>				Value
Al <sub>2</sub> O <sub>3</sub>	-23.1138	2.0636	R <sup>2</sup>				0.776
B <sub>2</sub> O <sub>3</sub>	8.9587	1.4162	R <sup>2</sup> Adjusted (R <sup>2</sup> <sub>A</sub> )				0.765
CaO	3.2758	1.1706	R <sup>2</sup> Predicted (R <sup>2</sup> <sub>p</sub> )				0.732
Fe <sub>2</sub> O <sub>3</sub>	1.8399	1.2141	RMSE				0.332
K <sub>2</sub> O	13.3474	1.5841	Model LOF p-value				0.006
Li <sub>2</sub> O	27.0258	2.6745					
MgO	24.1833	2.6256	<b>Extrapolative Validation Statistic, 20 Outlying Glasses<sup>(a,b)</sup></b>				<b>Value</b>
Na <sub>2</sub> O	14.5538	0.7661	R <sup>2</sup> Validation (R <sup>2</sup> <sub>v</sub> )				0.118
P <sub>2</sub> O <sub>5</sub>	-11.5267	3.0359	RMSE Validation (RMSE <sub>v</sub> )				0.518
SiO <sub>2</sub>	-6.8100	0.5520					
ZrO <sub>2</sub>	-3.6502	2.6387					
Others <sup>(c)</sup>	2.9069	1.8428	<b>Data Partition Statistic, 97 Modeling &amp; 147 Validation<sup>(a,c)</sup></b>				<b>Value</b>
			R <sup>2</sup>				0.836
			R <sup>2</sup> Adjusted (R <sup>2</sup> <sub>A</sub> )				0.815
			R <sup>2</sup> Predicted (R <sup>2</sup> <sub>p</sub> )				0.757
			RMSE				0.376
			R <sup>2</sup> Validation (R <sup>2</sup> <sub>v</sub> )				-1.108
			RMSE Validation (RMSE <sub>v</sub> )				0.696
<b>Data Splitting Statistic<sup>(a,d)</sup></b>	<b>DS1</b>	<b>DS2</b>	<b>DS3</b>	<b>DS4</b>	<b>DS5</b>	<b>Average</b>	
R <sup>2</sup>	0.782	0.783	0.783	0.771	0.787	0.781	
R <sup>2</sup> Adjusted (R <sup>2</sup> <sub>A</sub> )	0.770	0.770	0.770	0.757	0.774	0.768	
R <sup>2</sup> Predicted (R <sup>2</sup> <sub>p</sub> )	0.724	0.726	0.736	0.717	0.736	0.728	
RMSE	0.335	0.339	0.338	0.348	0.335	0.339	
R <sup>2</sup> Validation (R <sup>2</sup> <sub>v</sub> )	0.709	0.692	0.684	0.800	0.661	0.709	
RMSE Validation (RMSE <sub>v</sub> )	0.340	0.320	0.327	0.260	0.342	0.318	

- (a) The model evaluation statistics are defined in Section C.3 of Appendix C. Model validation statistics are defined in Section C.5 of Appendix C. A negative value for R<sup>2</sup><sub>v</sub> means that the sum of squares of model prediction errors is larger than if the mean response value over the validation data set were used as the predicted value for each glass. In other words, the model predicts worse for the validation data than the mean response value does.
- (b) The 20 outlying LAW glass compositions are discussed in Section 5.1.4.
- (c) The partition of the PCT-Na modeling data set into modeling and validation subsets is described in Section 5.1.3.
- (d) The evaluation and validation statistics calculated for data-splits are defined the same as for separate modeling and validation sets. Section 5.1.2 describes how the data-splitting was accomplished.
- (e) For the reduced LM model, the “Others” component includes the original “Others” component (which contains Ag<sub>2</sub>O, BaO, Br, CdO, Cs<sub>2</sub>O, I, La<sub>2</sub>O<sub>3</sub>, MnO, MoO<sub>3</sub>, NiO, PbO, Re<sub>2</sub>O<sub>7</sub>, SeO<sub>2</sub>, SrO, and “Unknown”) plus Cl, Cr<sub>2</sub>O<sub>3</sub>, F, SO<sub>3</sub>, TiO<sub>2</sub>, and ZnO.



**Table 5.14. Coefficients and Performance Summary for 17-Term Reduced Partial Quadratic Mixture Model on the Natural Logarithm of ILAW PCT-Na.**

In(PCT-Na) Reduced PQM Model Term	Coefficient Estimate	Coefficient Stand. Dev.	Modeling Data Statistic, 244 Glasses <sup>(a)</sup>				Value
Al <sub>2</sub> O <sub>3</sub>	-20.7142	1.6238	R <sup>2</sup>				0.870
B <sub>2</sub> O <sub>3</sub>	-6.5489	2.7610	R <sup>2</sup> Adjusted (R <sup>2</sup> <sub>A</sub> )				0.861
CaO	0.0151	2.5591	R <sup>2</sup> Predicted (R <sup>2</sup> <sub>p</sub> )				0.840
Fe <sub>2</sub> O <sub>3</sub>	-8.4617	2.6039	RMSE				0.255
K <sub>2</sub> O	-0.8724	3.9729	Model LOF p-value				0.055
Li <sub>2</sub> O	44.7604	3.5466					
MgO	-13.8667	7.2503	<b>Extrapolative Validation Statistic, 20 Outlying Glasses<sup>(a,b)</sup></b>				<b>Value</b>
Na <sub>2</sub> O	9.9942	1.6770	R <sup>2</sup> Validation (R <sup>2</sup> <sub>v</sub> )				0.271
P <sub>2</sub> O <sub>5</sub>	-14.5324	2.4027	RMSE Validation (RMSE <sub>v</sub> )				0.470
SiO <sub>2</sub>	-4.8834	0.5143					
ZrO <sub>2</sub>	-0.6200	2.2096					
Others <sup>(c)</sup>	3.3450	1.4341	<b>Data Partition Statistic, 97 Modeling &amp; 147 Validation<sup>(a,c)</sup></b>				<b>Value</b>
CaO×Li <sub>2</sub> O	-232.1695	46.7097	R <sup>2</sup>				0.919
CaO×Fe <sub>2</sub> O <sub>3</sub>	182.6191	40.4128	R <sup>2</sup> Adjusted (R <sup>2</sup> <sub>A</sub> )				0.903
B <sub>2</sub> O <sub>3</sub> ×MgO	437.4267	77.8463	R <sup>2</sup> Predicted (R <sup>2</sup> <sub>p</sub> )				0.869
B <sub>2</sub> O <sub>3</sub> ×Na <sub>2</sub> O	87.6716	19.0092	RMSE				0.272
K <sub>2</sub> O×K <sub>2</sub> O	315.6867	83.2397	R <sup>2</sup> Validation (R <sup>2</sup> <sub>v</sub> )				0.425
			RMSE Validation (RMSE <sub>v</sub> )				0.363
<b>Data Splitting Statistic<sup>(a,d)</sup></b>							
	<b>DS1</b>	<b>DS2</b>	<b>DS3</b>	<b>DS4</b>	<b>DS5</b>	<b>Average</b>	
R <sup>2</sup>	0.875	0.885	0.875	0.876	0.877	0.878	
R <sup>2</sup> Adjusted (R <sup>2</sup> <sub>A</sub> )	0.865	0.875	0.864	0.865	0.866	0.867	
R <sup>2</sup> Predicted (R <sup>2</sup> <sub>p</sub> )	0.836	0.851	0.839	0.837	0.837	0.840	
RMSE	0.256	0.250	0.260	0.260	0.258	0.257	
R <sup>2</sup> Validation (R <sup>2</sup> <sub>v</sub> )	0.830	0.727	0.826	0.824	0.813	0.804	
RMSE Validation (RMSE <sub>v</sub> )	0.260	0.301	0.243	0.244	0.254	0.260	

- (a) The model evaluation statistics are defined in Section C.3 of Appendix C. Model validation statistics are defined in Section C.5 of Appendix C. A negative value for R<sup>2</sup><sub>v</sub> means that the sum of squares of model prediction errors is larger than if the mean response value over the validation data set were used as the predicted value for each glass. In other words, the model predicts worse for the validation data than the mean response value does.
- (b) The 20 outlying LAW glass compositions are discussed in Section 5.1.4.
- (c) The partition of the PCT-Na modeling data set into modeling and validation subsets is described in Section 5.1.3.
- (d) The evaluation and validation statistics calculated for data-splits are defined the same as for separate modeling and validation sets. Section 5.1.2 describes how the data-splitting was accomplished.
- (e) For the reduced PQM model, the “Others” component includes the original “Others” component (which contains Ag<sub>2</sub>O, BaO, Br, CdO, Cs<sub>2</sub>O, I, La<sub>2</sub>O<sub>3</sub>, MnO, MoO<sub>3</sub>, NiO, PbO, Re<sub>2</sub>O<sub>7</sub>, SeO<sub>2</sub>, SrO, and “Unknown”) plus Cl, Cr<sub>2</sub>O<sub>3</sub>, F, SO<sub>3</sub>, TiO<sub>2</sub>, and ZnO.

**Table 5.15. Coefficients and Performance Summary for 24-Term Two-Part Reduced Linear Mixture Model on the Natural Logarithm of ILAW PCT-Na.**

In(PCT-Na) Two-Part Reduced LM Model Term	Below Cutoff (1.80 g/L)		Above Cutoff (1.80 g/L)		Modeling Data Statistic, 244 Glasses <sup>(a)</sup>		Value
	Coefficient Estimate	Coefficient Stand. Dev.	Coefficient Estimate	Coefficient Stand. Dev.			
Al <sub>2</sub> O <sub>3</sub>	-12.8277	1.6993	-23.8756	5.6807	R <sup>2</sup>		0.901
B <sub>2</sub> O <sub>3</sub>	2.6897	1.0984	19.7509	3.3762	R <sup>2</sup> Adjusted (R <sup>2</sup> <sub>A</sub> )		0.890
CaO	2.0502	0.9334	3.7598	2.7885	R <sup>2</sup> Predicted (R <sup>2</sup> <sub>p</sub> )		0.859
Fe <sub>2</sub> O <sub>3</sub>	1.6490	0.9040	11.8603	5.3956	RMSE		0.227
K <sub>2</sub> O	5.4650	1.3287	8.2602	4.3692	Model LOF p-value		0.141
Li <sub>2</sub> O	15.1916	2.1885	18.0580	9.3096			
MgO	14.9427	2.0121	23.4389	9.2263			
Na <sub>2</sub> O	9.9840	0.6620	5.1598	5.1022			
P <sub>2</sub> O <sub>5</sub>	-13.2071	2.0737	0.1769	47.1381			
SiO <sub>2</sub>	-3.9226	0.4327	-6.2206	2.1058			
ZrO <sub>2</sub>	-0.5254	2.0953	-2.2911	5.6782			
Others <sup>(e)</sup>	-2.1827	1.3705	13.0504	8.2384			
					<b>Extrapolative Validation Statistic, 20 Outlying Glasses<sup>(a,b)</sup></b>		<b>Value</b>
					R <sup>2</sup> Validation (R <sup>2</sup> <sub>v</sub> )		0.212
					RMSE Validation (RMSE <sub>v</sub> )		0.489
					<b>Data Partition Statistic, 97 Modeling &amp; 147 Validation<sup>(a,c)</sup></b>		<b>Value</b>
					Insufficient data in the modeling subset to fit the two-part model and perform these assessments		
<b>Summary Statistic</b>		<b>Below Cutoff Data</b>	<b>Based on Reduced LM Model</b>	<b>Above Cutoff Data</b>	<b>Based on Reduced LM Model</b>		
R <sup>2</sup>		0.749	0.590	0.910	0.293		
R <sup>2</sup> Adjusted (R <sup>2</sup> <sub>A</sub> )		0.736		0.855			
R <sup>2</sup> Predicted (R <sup>2</sup> <sub>p</sub> )		0.719		0.631			
RMSE		0.225		0.252			
<b>Data Splitting Statistic<sup>(a,d)</sup></b>		<b>DS1</b>	<b>DS2</b>	<b>DS3</b>	<b>DS4</b>	<b>DS5</b>	<b>Average</b>
R <sup>2</sup>		0.899	0.916	0.908	0.911	0.906	0.908
R <sup>2</sup> Adjusted (R <sup>2</sup> <sub>A</sub> )		0.885	0.904	0.896	0.900	0.894	0.896
R <sup>2</sup> Predicted (R <sup>2</sup> <sub>p</sub> )		0.804	0.826	0.871	0.880	0.835	0.843
RMSE		0.236	0.219	0.227	0.224	0.229	0.227
R <sup>2</sup> Validation (R <sup>2</sup> <sub>v</sub> )		0.861	0.763	0.753	0.654	0.530	0.712
RMSE Validation (RMSE <sub>v</sub> )		0.235	0.280	0.289	0.342	0.402	0.310

(a) to (e) The footnotes in this table are the same as in Tables 5.7 to 5.9.

**Table 5.16. Performance Summary of Four Models for the Natural Logarithm of ILAW PCT-Na.**

Summary Statistic from Model Fit to 244 Glasses <sup>(a)</sup>	ln(PCT-Na) Models			
	Full LM	Reduced LM	Reduced PQM	Two-Part
R <sup>2</sup>	0.798	0.776	0.870	0.901
R <sup>2</sup> Adjusted (R <sup>2</sup> <sub>A</sub> )	0.783	0.765	0.861	0.890
R <sup>2</sup> Predicted (R <sup>2</sup> <sub>p</sub> )	0.740	0.732	0.840	0.859
RMSE	0.320	0.332	0.255	0.227
LOF p-value	0.008	0.006	0.055	0.141
<b>Linear Terms</b>	See Table 5.7	Al <sub>2</sub> O <sub>3</sub> , B <sub>2</sub> O <sub>3</sub> , CaO, Fe <sub>2</sub> O <sub>3</sub> , K <sub>2</sub> O, Li <sub>2</sub> O, MgO, Na <sub>2</sub> O, P <sub>2</sub> O <sub>5</sub> , SiO <sub>2</sub> , ZrO <sub>2</sub> , Others		
<b>Selected Quadratic Terms in Model</b>	N/A	N/A	CaO×Li <sub>2</sub> O CaO×Fe <sub>2</sub> O <sub>3</sub> B <sub>2</sub> O <sub>3</sub> ×MgO B <sub>2</sub> O <sub>3</sub> ×Na <sub>2</sub> O K <sub>2</sub> O×K <sub>2</sub> O	N/A
<b># Model Terms</b>	18	12	17	24
<b>Summary Statistic for Partition of PCT-Na Data into Modeling (97 Glasses) and Validation (147 Glasses) Subsets<sup>(a)</sup></b>				
R <sup>2</sup>	0.858	0.836	0.919	(b)
R <sup>2</sup> Adjusted (R <sup>2</sup> <sub>A</sub> )	0.827	0.815	0.903	(b)
R <sup>2</sup> Predicted (R <sup>2</sup> <sub>p</sub> )	0.754	0.757	0.869	(b)
RMSE	0.363	0.376	0.272	(b)
R <sup>2</sup> Validation (R <sup>2</sup> <sub>v</sub> )	-0.306	-1.108	0.425	(b)
RMSE Validation (RMSE <sub>v</sub> )	0.548	0.696	0.363	(b)
<b>Summary Statistic Averaged Over 5 Data-Splitting Sets<sup>(a)</sup></b>				
R <sup>2</sup>	0.805	0.781	0.878	0.908
R <sup>2</sup> Adjusted (R <sup>2</sup> <sub>A</sub> )	0.787	0.768	0.867	0.896
R <sup>2</sup> Predicted (R <sup>2</sup> <sub>p</sub> )	0.735	0.728	0.840	0.843
RMSE	0.325	0.339	0.257	0.227
R <sup>2</sup> Validation (R <sup>2</sup> <sub>v</sub> )	0.712	0.709	0.804	0.712
RMSE Validation (RMSE <sub>v</sub> )	0.316	0.318	0.260	0.310

- (a) The model evaluation statistics are defined in Section C.3 of Appendix C. Model validation statistics are defined in Section C.5 of Appendix C. A negative value for R<sup>2</sup><sub>v</sub> means that the sum of squares of model prediction errors is larger than if the mean response value over the validation data set were used as the predicted value for each glass. In other words, the model predicts worse for the validation data than the mean response value does.
- (b) There were insufficient data in the 97-glass modeling subset to adequately fit the two-part model.

**Table 5.17. LAWA126 Composition in Formats Needed for Use in ILAW PCT Models.**

<b>Model Term</b>	<b>LAWA126 Composition<sup>(a)</sup> (wt%)</b>	<b>LAWA126 Composition (mass fractions) for Use in PCT-B LM Model<sup>(b)</sup></b>	<b>LAWA126 Composition (mass fractions) for Use in PCT-B PQM Model<sup>(c)</sup></b>	<b>LAWA126 Composition (mass fractions) for Use in PCT-Na LM Model<sup>(d)</sup></b>	<b>LAWA126 Composition (mass fractions) for Use in PCT-Na PQM Model<sup>(e)</sup></b>
Al <sub>2</sub> O <sub>3</sub>	0.05637	0.05637	0.05637	0.05637	0.05637
B <sub>2</sub> O <sub>3</sub>	0.09815	0.09815	0.09815	0.09815	0.09815
CaO	0.01989	0.01989	0.01989	0.01989	0.01989
Cl	0.00200	NA <sup>(f)</sup>	NA	NA	NA
Cr <sub>2</sub> O <sub>3</sub>	0.00020	NA	NA	NA	NA
F	0.00300	NA	NA	NA	NA
Fe <sub>2</sub> O <sub>3</sub>	0.05537	0.05537	0.05537	0.05537	0.05537
K <sub>2</sub> O	0.03878	0.03878	0.03878	0.03878	0.03878
Li <sub>2</sub> O	0.00000	0.00000	0.00000	0.00000	0.00000
MgO	0.01479	0.01479	0.01479	0.01479	0.01479
Na <sub>2</sub> O	0.18451	0.18451	0.18451	0.18451	0.18451
P <sub>2</sub> O <sub>5</sub>	0.00080	0.00080	0.00080	0.00080	0.00080
SO <sub>3</sub>	0.00310	NA	NA	NA	NA
SiO <sub>2</sub>	0.44098	0.44098	0.44098	0.44098	0.44098
TiO <sub>2</sub>	0.01999	NA	NA	NA	NA
ZnO	0.02959	NA	NA	NA	NA
ZrO <sub>2</sub>	0.02989	0.02989	0.02989	0.02989	0.02989
Others	0.00260	0.06047	0.06047	0.06047	0.06047
CaO×Li <sub>2</sub> O	NA	NA	0.0000000	NA	0.0000000
B <sub>2</sub> O <sub>3</sub> ×MgO	NA	NA	0.0014519	NA	0.0014519
B <sub>2</sub> O <sub>3</sub> ×Li <sub>2</sub> O	NA	NA	0.0000000	NA	NA
Na <sub>2</sub> O×SiO <sub>2</sub>	NA	NA	0.0813639	NA	NA
CaO×Fe <sub>2</sub> O <sub>3</sub>	NA	NA	0.0011014	NA	0.0011014
B <sub>2</sub> O <sub>3</sub> ×Na <sub>2</sub> O	NA	NA	NA	NA	0.0181095
K <sub>2</sub> O×K <sub>2</sub> O	NA	NA	NA	NA	0.0015039

- (a) The composition in mass fractions is from Table 5.2.  
 (b) See Table 5.8.  
 (c) See Table 5.9.  
 (d) See Table 5.13.  
 (e) See Table 5.14.  
 (f) NA = not applicable, because the model does not contain this term.

**Table 5.18. Predicted PCT Releases and Corresponding 90% UCIs and 95% SUCIs for LAWA126 Composition Used in ILAW PCT Models.**

Model <sup>(a)</sup>	Predicted ln(PCT) [ln(g/L)]	Predicted PCT [g/L]	Standard Deviation of Predicted ln(PCT) <sup>(b)</sup> [ln(g/L)]	90% UCI on Mean ln(PCT) [ln(g/L)]	90% UCI on Median PCT [g/L]	95% SUCI on Mean ln(PCT) [ln(g/L)]	95% SUCI on Median PCT [g/L]
12-Term PCT-B LM Model	0.4901 <sup>(c)</sup>	1.632	0.0506	0.5551	1.742	0.7102	2.034
17-Term PCT-B PQM Model	0.3644	1.440	0.0408	0.4168	1.517	0.5697	1.768
12-Term PCT-Na LM Model	0.3584	1.431	0.0443	0.4154	1.515	0.5511	1.735
17-Term PCT-Na PQM Model	0.2436	1.276	0.0357	0.2895	1.336	0.4232	1.527

- (a) The four models in this column are given in Tables 5.8, 5.9, 5.13, and 5.14, respectively. Note that LM = linear mixture and PQM = partial quadratic mixture.
- (b) The standard deviation is for the ln(PCT) prediction considered to be the mean of such values for the LAWA126 glass.
- (c) All calculations were performed using the LAWA126 glass composition, model coefficients, and variance-covariance matrix values given in tables of this report. The calculated ln(g/L) values were rounded to four decimal places in this table. The g/L values were calculated by exponentiating the ln(g/L) values before rounding, then rounding the resulting values to three decimal places in this table.

**Table 6.1. Sixteen LAW Glasses Excluded from VHT Modeling Data Set.**

<b>Glass ID</b>	<b>Reason Glass Excluded from VHT Modeling Set</b>
LAWA49	Outlying composition ( $\text{Fe}_2\text{O}_3 = 9.98 \text{ wt}\%$ )
LAWB60	Outlying composition ( $\text{CaO} = 11.91 \text{ wt}\%$ )
LAWB62	Outlying composition ( $\text{CaO} = 12.00 \text{ wt}\%$ )
LAWB63	Outlying composition ( $\text{ZnO} = 5.82 \text{ wt}\%$ )
LAWB82	Outlying composition ( $\text{Fe}_2\text{O}_3 = 9.52 \text{ wt}\%$ )
LAWC28	Outlying composition ( $\text{CaO} = 12.81 \text{ wt}\%$ )
LAWE3Cr2CCC	Non-representative composition & heat treatment
LAWE9HCr1CCC	Non-representative composition & heat treatment
LAWE9HCr2CCC	Non-representative composition & heat treatment
LAWE10HCr3CCC	Non-representative composition & heat treatment
LAWM12	Alteration depth > 1100 $\mu\text{m}$
LAWM13	Alteration depth > 1100 $\mu\text{m}$
LAWM14	Alteration depth > 1100 $\mu\text{m}$
LAWM32	Alteration depth > 1100 $\mu\text{m}$
LAWM55	Alteration depth > 1100 $\mu\text{m}$
LAWE14	Alteration depth > 800 $\mu\text{m}$

**Table 6.2. Normalized<sup>(a)</sup> Compositions (mass fractions) of 165 LAW Glasses Used for VHT Model Development.**

Glass ID	Group ID <sup>(b)</sup>	Al <sub>2</sub> O <sub>3</sub>	B <sub>2</sub> O <sub>3</sub>	CaO	Cl	Cr <sub>2</sub> O <sub>3</sub>	F	Fe <sub>2</sub> O <sub>3</sub>	K <sub>2</sub> O	Li <sub>2</sub> O	MgO	Na <sub>2</sub> O	P <sub>2</sub> O <sub>5</sub>	XRF SO <sub>3</sub> <sup>(c)</sup>	SiO <sub>2</sub>	TiO <sub>2</sub>	ZnO	ZrO <sub>2</sub>	Others	Sum <sup>(d)</sup>
LAWA44R10	ExPh1	.06202	.08903	.01991	.00650	.00020	.00010	.06982	.00500	.00000	.01991	.20006	.00030	.00090	.44563	.01991	.02971	.02991	.00110	1.00000
LAWA53	ExPh1	.06145	.06165	.07840	.00646	.00020	.00010	.07467	.00494	.00000	.01473	.19898	.00030	.00620	.42036	.01100	.02977	.02977	.00101	1.00000
LAWA56	ExPh1	.06151	.12050	.01970	.00646	.00020	.00010	.07474	.00495	.00000	.01475	.19918	.00030	.00520	.42079	.01101	.02980	.02980	.00101	1.00000
LAWA88R1	ExPh1	.06082	.09700	.01991	.00330	.00010	.00000	.05532	.02581	.00000	.01475	.20006	.00070	.00190	.44004	.01991	.02951	.02987	.00100	1.00000
LAWA102R1	ExPh1	.06040	.09968	.05044	.00329	.00020	.00030	.05383	.00259	.02492	.01485	.14503	.00130	.00670	.46350	.01136	.03050	.03010	.00101	1.00000
LAWA126	ExPh1	.05637	.09815	.01989	.00200	.00020	.00300	.05537	.03878	.00000	.01479	.18451	.00080	.00310	.44098	.01999	.02959	.02989	.00260	1.00000
LAWA128	ExPh1	.06027	.07066	.02079	.00200	.00020	.00300	.05787	.03878	.00000	.01179	.18451	.00080	.00300	.46067	.02089	.03088	.03128	.00260	1.00000
LAWA130	ExPh1	.06025	.08943	.02078	.00200	.00020	.00300	.02858	.03877	.00000	.01179	.18445	.00080	.00330	.46053	.02088	.04137	.03127	.00260	1.00000
LAWB65	ExPh1	.06188	.09939	.06690	.00000	.00100	.00070	.05295	.00261	.04303	.02969	.05476	.00010	.00890	.48492	.01394	.04664	.03159	.00100	1.00000
LAWB66	ExPh1	.06203	.09963	.08214	.00000	.00101	.00070	.05308	.00261	.04313	.02976	.05489	.00010	.00650	.48609	.01397	.03167	.03167	.00101	1.00000
LAWB68	ExPh1	.06192	.08440	.08199	.00000	.00100	.00070	.05299	.00261	.04305	.02970	.05479	.00010	.00830	.48521	.01395	.04666	.03161	.00100	1.00000
LAWB78	ExPh1	.06161	.12351	.07132	.00010	.00050	.00080	.03256	.00230	.03055	.02975	.09797	.00050	.00510	.47080	.00000	.04007	.03155	.00100	1.00000
LAWB79	ExPh1	.06156	.12342	.07127	.00010	.00050	.00080	.03253	.00230	.03514	.02973	.08629	.00050	.00580	.47748	.00000	.04004	.03153	.00100	1.00000
LAWB80	ExPh1	.06156	.12341	.07126	.00010	.00050	.00080	.03253	.01992	.03513	.02973	.06626	.00050	.00580	.47993	.00000	.04004	.03153	.00100	1.00000
LAWB83	ExPh1	.06183	.10035	.06783	.00010	.00040	.00060	.05293	.00190	.04312	.02971	.05473	.00040	.00490	.48624	.01391	.04842	.03162	.00100	1.00000
LAWB84	ExPh1	.06187	.10041	.06687	.00010	.00040	.00060	.05296	.00190	.04405	.02973	.05476	.00040	.00440	.48654	.01392	.04845	.03163	.00100	1.00000
LAWB85	ExPh1	.06184	.11527	.05283	.00010	.00040	.00060	.05293	.00190	.04313	.02972	.05473	.00040	.00490	.48629	.01391	.04843	.03162	.00100	1.00000
LAWB86	ExPh1	.06188	.12426	.05737	.00010	.00040	.00060	.05297	.00190	.04356	.02974	.05477	.00040	.00430	.48664	.00000	.04846	.03164	.00100	1.00000
C100-G-136B	ExPh1	.06127	.10092	.06408	.00120	.00020	.00060	.06478	.00150	.02733	.01512	.11874	.00120	.00400	.46726	.01121	.03014	.03024	.00020	1.00000
LAWC27	ExPh1	.06117	.12183	.08544	.00111	.00018	.00054	.00009	.00136	.02733	.01500	.11953	.00106	.00410	.48868	.01121	.03018	.03018	.00101	1.00000
LAWC32	ExPh1	.06490	.10047	.09038	.00111	.00018	.00054	.02424	.00136	.02734	.01501	.11956	.00106	.00380	.46744	.01121	.04019	.03019	.00101	1.00000
LAWM1	Ph1	.09044	.06029	.10048	.00020	.00008	.00008	.08039	.04019	.04522	.00000	.05024	.00013	.00520	.44666	.03015	.05024	.00000	.00002	1.00000
LAWM2	Ph1	.03512	.06020	.10033	.00803	.00322	.00300	.08027	.00000	.04515	.05017	.05017	.00501	.00670	.47157	.03010	.05017	.00000	.00080	1.00000
LAWM3	Ph1	.09033	.06022	.10036	.00020	.00008	.00008	.08029	.00000	.04487	.05018	.11521	.00013	.00640	.40145	.00000	.01004	.04015	.00002	1.00000
LAWM4	Ph1	.03516	.13058	.10044	.00020	.00008	.00008	.05560	.04018	.04520	.00000	.05022	.00013	.00560	.41599	.03013	.05022	.04018	.00002	1.00000
LAWM5	Ph1	.09041	.06027	.05794	.00020	.00008	.00008	.08036	.04018	.04520	.00000	.05023	.00013	.00550	.48903	.03014	.01005	.04018	.00002	1.00000
LAWM6	Ph1	.09002	.10612	.10002	.00020	.00008	.00007	.08002	.04001	.00000	.05001	.08999	.00012	.00320	.40009	.03001	.01000	.00000	.00002	1.00000
LAWM7	Ph1	.05441	.06966	.10028	.00020	.00008	.00008	.08023	.00000	.02585	.05014	.05014	.00013	.00720	.52147	.03008	.01003	.00000	.00002	1.00000
LAWM8	Ph1	.09027	.13039	.06448	.00803	.00322	.00300	.00000	.00000	.02087	.05015	.05015	.00501	.00700	.44626	.03009	.05015	.04012	.00080	1.00000
LAWM9	Ph1	.03506	.06010	.10016	.00801	.00322	.00300	.08013	.04006	.02392	.00000	.05008	.00500	.00240	.49792	.00000	.05008	.04006	.00080	1.00000
LAWM10	Ph1	.09005	.13007	.10006	.00801	.00322	.00300	.00000	.00000	.04503	.00000	.13074	.00499	.00230	.40170	.03002	.01001	.04002	.00080	1.00000
LAWM11	Ph1	.03504	.13013	.09413	.00020	.00008	.00007	.05317	.04004	.04505	.00000	.11491	.00012	.00900	.46804	.00000	.01001	.00000	.00002	1.00000
LAWM15	Ph1	.08999	.09356	.00000	.00800	.00321	.00299	.06283	.00000	.00000	.03724	.21998	.00499	.00170	.43471	.03000	.01000	.00000	.00080	1.00000
LAWM16	Ph1	.08006	.12008	.08006	.00020	.00008	.00007	.06505	.00100	.03002	.01001	.10007	.00012	.00330	.42480	.02502	.05004	.01001	.00002	1.00000

- (a) The compositions listed in this table are normalized mass fraction versions of target compositions of the glasses, after replacing the target values of SO<sub>3</sub> by XRF analyzed (or estimated analyzed) values. See Section 3.3 for the details.
- (b) The Group IDs are described in Sections 2.1 to 2.6.
- (c) XRF SO<sub>3</sub> denotes that the SO<sub>3</sub> composition is based on chemical analysis by XRF. For most glasses SO<sub>3</sub> was directly measured by XRF, but for some glasses estimated XRF values were used (see Section 3.3).
- (d) The normalized component mass fractions listed in this table were rounded to five decimals, and may not sum exactly to 1.00000 as listed. However, complete compositions listed to more decimal places and summing to 1.00000 were used for property-composition modeling.

**Table 6.2. Normalized<sup>(a)</sup> Compositions (mass fractions) of 165 LAW Glasses Used for VHT Model Development (continued).**

Glass ID	Group ID <sup>(b)</sup>	Al <sub>2</sub> O <sub>3</sub>	B <sub>2</sub> O <sub>3</sub>	CaO	Cl	Cr <sub>2</sub> O <sub>3</sub>	F	Fe <sub>2</sub> O <sub>3</sub>	K <sub>2</sub> O	Li <sub>2</sub> O	MgO	Na <sub>2</sub> O	P <sub>2</sub> O <sub>5</sub>	XRF SO <sub>3</sub> <sup>(c)</sup>	SiO <sub>2</sub>	TiO <sub>2</sub>	ZnO	ZrO <sub>2</sub>	Others	Sum <sup>(d)</sup>
LAWM17	Ph1	.05002	.12004	.02215	.00020	.00008	.00007	.06502	.02001	.00500	.03501	.17006	.00012	.00200	.42015	.00500	.05002	.03501	.00002	1.00000
LAWM18	Ph1	.08005	.12007	.08005	.00801	.00322	.00300	.06504	.00100	.03002	.01001	.10006	.00499	.00340	.42025	.02502	.02001	.02501	.00080	1.00000
LAWM19	Ph1	.07997	.11996	.07997	.00800	.00321	.00299	.01999	.01999	.00500	.01000	.13170	.00499	.00360	.41986	.00500	.04998	.03499	.00080	1.00000
LAWM20	Ph1	.05001	.07002	.08002	.00800	.00321	.00299	.02001	.02001	.02265	.03501	.17004	.00499	.00210	.42011	.00500	.05001	.03501	.00080	1.00000
LAWM21	Ph1	.05005	.10901	.08008	.00020	.00008	.00007	.06507	.02002	.03003	.01001	.10010	.00012	.00460	.42042	.02503	.05005	.03504	.00002	1.00000
LAWM22	Ph1	.07990	.06992	.01998	.00799	.00321	.00299	.06492	.01998	.00499	.03496	.16979	.00498	.00450	.41949	.00670	.04994	.03496	.00080	1.00000
LAWM23	Ph1	.05011	.07015	.08018	.00802	.00322	.00300	.02004	.02004	.03007	.01002	.10022	.00500	.00340	.48547	.02506	.05011	.03508	.00080	1.00000
LAWM24	Ph1	.08000	.12001	.02000	.00020	.00008	.00007	.06500	.02000	.00641	.01000	.17001	.00012	.00230	.47076	.00500	.02000	.01000	.00002	1.00000
LAWM25R1	Ph1	.08011	.12017	.02003	.00801	.00322	.00300	.03684	.02003	.03004	.03505	.10014	.00500	.00260	.49991	.00501	.02003	.01001	.00080	1.00000
LAWM26	Ph1	.08006	.12008	.04970	.00801	.00322	.00300	.02001	.00100	.03002	.01001	.10007	.00499	.00490	.49909	.00500	.05004	.01001	.00080	1.00000
LAWM27	Ph1	.08006	.07005	.08006	.00801	.00322	.00300	.06505	.02001	.00500	.03502	.13381	.00499	.00250	.42030	.02502	.03309	.01001	.00080	1.00000
LAWM28	Ph1	.05010	.12024	.08016	.00020	.00008	.00008	.06513	.00703	.00690	.01002	.10020	.00013	.00360	.50101	.02505	.02004	.01002	.00002	1.00000
LAWM29	Ph1	.07565	.07006	.02002	.00077	.00031	.00029	.06506	.02002	.03003	.03503	.10009	.00048	.00310	.46892	.02502	.05005	.03503	.00008	1.00000
LAWM30	Ph1	.08003	.12004	.02001	.00020	.00008	.00007	.06502	.00100	.02023	.01000	.17006	.00012	.00200	.42015	.00592	.05002	.03501	.00002	1.00000
LAWM31	Ph1	.05002	.07003	.08003	.00801	.00322	.00300	.06502	.00100	.03001	.01000	.16758	.00499	.00300	.42327	.02501	.02001	.03501	.00080	1.00000
LAWM33R1	Ph1	.05002	.12005	.08003	.00020	.00008	.00007	.06503	.01722	.00899	.01000	.17007	.00012	.00290	.42017	.02501	.02001	.01000	.00002	1.00000
LAWM34	Ph1	.05001	.08356	.08002	.00020	.00008	.00007	.06295	.02001	.03001	.01000	.17005	.00012	.00300	.42012	.01474	.02001	.03501	.00002	1.00000
LAWM35	Ph1	.05003	.12007	.06182	.00801	.00322	.00300	.04413	.00100	.00500	.03502	.17010	.00499	.00180	.42023	.02501	.02001	.02576	.00080	1.00000
LAWM36	Ph1	.07002	.11004	.07002	.00318	.00128	.00119	.05002	.00300	.02501	.01501	.12004	.00198	.00370	.45016	.02001	.03501	.02001	.00032	1.00000
LAWM37	Ph1	.06751	.11009	.07006	.00020	.00008	.00007	.05004	.00300	.02502	.02502	.12010	.00012	.00320	.45038	.01001	.03503	.03003	.00002	1.00000
LAWM38	Ph1	.06998	.07998	.06998	.00800	.00321	.00299	.02999	.00154	.02499	.01500	.13997	.00499	.00370	.47988	.01000	.03499	.02000	.00080	1.00000
LAWM39	Ph1	.07007	.09063	.05005	.00801	.00322	.00300	.03003	.00100	.02502	.02502	.14013	.00499	.00250	.48046	.01001	.03503	.02002	.00080	1.00000
LAWM40	Ph1	.06003	.11006	.05003	.00214	.00086	.00080	.05003	.00100	.01001	.01501	.14008	.00133	.00310	.48027	.01001	.03502	.03002	.00021	1.00000
LAWM41	Ph1	.07002	.08002	.07002	.00800	.00321	.00299	.05001	.00300	.01000	.02501	.14004	.00499	.00340	.45012	.01000	.04601	.02235	.00080	1.00000
LAWM42	Ph1	.06004	.08005	.05003	.00801	.00322	.00300	.04037	.00100	.02502	.01501	.14009	.00499	.00300	.48032	.02001	.03502	.03002	.00080	1.00000
LAWM43	Ph1	.07002	.08678	.05002	.00800	.00322	.00300	.05002	.00300	.02501	.02501	.12004	.00499	.00390	.45016	.02001	.04602	.03001	.00080	1.00000
LAWM44	Ph1	.06325	.10039	.07008	.00020	.00008	.00007	.05006	.00100	.01001	.01502	.12014	.00012	.00290	.48055	.02002	.04605	.02002	.00002	1.00000
LAWM45	Ph1	.07003	.08003	.05784	.00020	.00008	.00007	.05002	.00300	.01423	.01501	.14005	.00012	.00310	.48017	.02001	.04602	.02001	.00002	1.00000
LAWM46	Ph1	.06012	.11023	.06523	.00020	.00008	.00008	.05010	.00100	.01002	.02505	.12025	.00013	.00200	.48034	.01002	.03507	.03006	.00002	1.00000
LAWM47	Ph1	.06200	.08003	.07003	.00020	.00008	.00007	.05002	.00100	.01000	.02501	.14005	.00012	.00310	.48017	.01307	.03501	.03001	.00002	1.00000
LAWM48	Ph1	.06234	.11016	.05277	.00801	.00322	.00300	.05007	.00100	.01001	.01502	.12017	.00500	.00260	.48070	.02003	.03505	.02003	.00080	1.00000
LAWM49	Ph1	.07001	.10906	.05001	.00800	.00321	.00299	.03000	.00100	.01000	.01500	.14002	.00499	.00350	.47538	.01000	.04601	.02000	.00080	1.00000
LAWM50	Ph1	.06530	.09700	.06109	.00446	.00179	.00167	.04111	.00204	.01668	.02032	.13095	.00278	.00290	.46982	.01528	.04104	.02533	.00045	1.00000
LAWM51	Ph1	.06528	.09697	.06107	.00446	.00179	.00167	.04110	.00204	.01667	.02031	.13091	.00278	.00320	.46968	.01528	.04102	.02533	.00045	1.00000

- (a) The compositions listed in this table are normalized mass fraction versions of target compositions of the glasses, after replacing the target values of SO<sub>3</sub> by XRF analyzed (or estimated analyzed) values. See Section 3.3 for the details.
- (b) The Group IDs are described in Sections 2.1 to 2.6.
- (c) XRF SO<sub>3</sub> denotes that the SO<sub>3</sub> composition is based on chemical analysis by XRF. For most glasses SO<sub>3</sub> was directly measured by XRF, but for some glasses estimated XRF values were used (see Section 3.3).
- (d) The normalized component mass fractions listed in this table were rounded to five decimals, and may not sum exactly to 1.00000 as listed. However, complete compositions listed to more decimal places and summing to 1.0000 were used for property-composition modeling.



**Table 6.2. Normalized<sup>(a)</sup> Compositions (mass fractions) of 165 LAW Glasses Used for VHT Model Development (continued).**

Glass ID	Group ID <sup>(b)</sup>	Al <sub>2</sub> O <sub>3</sub>	B <sub>2</sub> O <sub>3</sub>	CaO	Cl	Cr <sub>2</sub> O <sub>3</sub>	F	Fe <sub>2</sub> O <sub>3</sub>	K <sub>2</sub> O	Li <sub>2</sub> O	MgO	Na <sub>2</sub> O	P <sub>2</sub> O <sub>5</sub>	XRF SO <sub>3</sub> <sup>(c)</sup>	SiO <sub>2</sub>	TiO <sub>2</sub>	ZnO	ZrO <sub>2</sub>	Others	Sum <sup>(d)</sup>
LAWM52	Ph1	.06088	.09711	.01994	.00329	.00009	.00000	.05538	.02586	.00000	.01477	.20027	.00070	.00180	.44051	.01994	.02954	.02991	.00000	1.00000
LAWM53	Ph1	.09031	.06021	.10034	.00020	.00008	.00008	.08027	.04014	.04515	.00000	.05017	.00013	.00660	.44603	.03010	.05017	.00000	.00002	1.00000
LAWM54R1	Ph1	.03505	.06008	.10014	.00801	.00322	.00300	.08011	.04006	.02391	.00000	.05007	.00500	.00260	.49782	.00000	.05007	.04006	.00080	1.00000
LAWM56	Ph1	.04990	.11975	.06166	.00799	.00321	.00299	.04402	.00100	.00499	.03493	.16965	.00498	.00440	.41914	.02495	.01996	.02570	.00080	1.00000
LAWM57	Ph1aAug	.06997	.11000	.03000	.00196	.00078	.00078	.04659	.03801	.00000	.01440	.20620	.00122	.00320	.39274	.01370	.03026	.04001	.00016	1.00000
LAWM58	Ph1aAug	.07002	.09294	.01028	.00196	.00078	.00078	.06500	.03800	.00000	.01440	.20536	.00122	.00320	.41654	.01370	.02563	.04001	.00016	1.00000
LAWM59	Ph1aAug	.06847	.09009	.02965	.00196	.00078	.00078	.06492	.02004	.00000	.01441	.20008	.00122	.00310	.44558	.01371	.02506	.02001	.00016	1.00000
LAWM60	Ph1aAug	.05003	.11006	.01714	.00196	.00078	.00078	.04503	.02004	.00000	.01441	.20015	.00122	.00300	.45351	.01371	.02804	.03998	.00016	1.00000
LAWM61	Ph1aAug	.05002	.11001	.01001	.00196	.00078	.00078	.04502	.03293	.00000	.01440	.20004	.00122	.00330	.45060	.01370	.04501	.02005	.00016	1.00000
LAWM62	Ph1aAug	.05004	.09004	.01002	.00196	.00078	.00078	.06500	.03380	.00000	.01440	.20006	.00122	.00320	.44341	.01370	.03842	.03300	.00016	1.00000
LAWM63	Ph1aAug	.07001	.09402	.01044	.00196	.00078	.00078	.04695	.02059	.00000	.01440	.22998	.00122	.00340	.42601	.01370	.04500	.02058	.00016	1.00000
LAWM64	Ph1aAug	.06991	.10989	.03002	.00196	.00078	.00078	.06503	.02001	.00000	.01441	.20051	.00122	.00300	.38379	.01371	.04490	.03993	.00016	1.00000
LAWM65	Ph1aAug	.05001	.09001	.02964	.00196	.00078	.00078	.04503	.02001	.00000	.01440	.22791	.00122	.00340	.43599	.01370	.02501	.03997	.00016	1.00000
LAWM66	Ph1aAug	.07587	.10637	.01003	.00196	.00078	.00078	.06315	.00479	.00000	.01440	.22996	.00122	.00320	.38362	.01370	.04500	.04498	.00016	1.00000
LAWM67	Ph1aAug	.08002	.10601	.01545	.00196	.00078	.00078	.04603	.05402	.00000	.01440	.20134	.00122	.00320	.38370	.01370	.02720	.05001	.00016	1.00000
LAWM68	Ph1aAug	.05003	.09002	.02999	.00196	.00078	.00078	.06500	.04803	.00000	.01440	.20009	.00122	.00330	.40815	.01370	.03562	.03677	.00016	1.00000
LAWM69	Ph1aAug	.07976	.10990	.02997	.00196	.00078	.00078	.06370	.01829	.00000	.01440	.20095	.00122	.00340	.39601	.01370	.04499	.02002	.00016	1.00000
LAWM70	Ph1aAug	.05002	.09397	.01047	.00196	.00078	.00078	.06498	.04550	.00000	.01440	.20011	.00122	.00330	.45357	.01370	.02501	.02006	.00016	1.00000
LAWM71	Ph1aAug	.05006	.09001	.01003	.00196	.00078	.00078	.04501	.05401	.00000	.01440	.20004	.00122	.00340	.44943	.01370	.04498	.02002	.00016	1.00000
LAWM72	Ph1aAug	.08002	.11002	.02937	.00196	.00078	.00078	.06449	.04177	.00000	.01440	.20042	.00122	.00320	.39173	.01370	.02501	.02095	.00016	1.00000
LAWM73	Ph1aAug	.08002	.09006	.02996	.00196	.00078	.00078	.04878	.01221	.00000	.01440	.23002	.00122	.00320	.40391	.01370	.04494	.02388	.00016	1.00000
LAWM74	Ph1aAug	.07589	.09009	.01001	.00196	.00078	.00078	.04504	.00000	.00000	.01441	.21329	.00122	.00290	.45377	.01371	.02598	.05002	.00016	1.00000
LAWM75	Ph1aAug	.08003	.09157	.02996	.00196	.00078	.00078	.06497	.01082	.00000	.01441	.20691	.00122	.00310	.38461	.01371	.04500	.05001	.00016	1.00000
LAWM76	Ph1aAug	.06403	.09926	.01923	.00196	.00078	.00078	.05424	.02599	.00000	.01441	.21409	.00122	.00310	.41881	.01371	.03423	.03401	.00016	1.00000
LAWE2H	Corr	.05951	.09751	.01970	.00196	.00078	.00078	.05365	.03790	.00000	.01440	.20782	.00122	.00310	.42440	.01370	.03410	.02930	.00016	1.00000
LAWE3	Corr	.06102	.10003	.02021	.00200	.00080	.00080	.05502	.04992	.00000	.01480	.18215	.00124	.00320	.42963	.01400	.03501	.03001	.00016	1.00000
LAWE3H	Corr	.05942	.09743	.01971	.00196	.00078	.00078	.05366	.05412	.00000	.01440	.19746	.00122	.00340	.41859	.01360	.03411	.02921	.00016	1.00000
LAWE4H	Corr	.05974	.09796	.02461	.00196	.00078	.00078	.05383	.00540	.00000	.01451	.21283	.00122	.00350	.44527	.01371	.03432	.02942	.00016	1.00000
LAWE5H	Corr	.05997	.09821	.03614	.00196	.00078	.00078	.05410	.00541	.00491	.01452	.18991	.00122	.00350	.45096	.01372	.03434	.02943	.00016	1.00000
LAWE7	Corr	.06110	.10017	.06401	.00200	.00080	.00080	.05509	.00501	.03226	.01513	.12521	.00124	.00380	.45407	.01402	.03506	.03005	.00016	1.00000
LAWE7H	Corr	.06027	.09882	.06318	.00196	.00078	.00078	.05441	.00541	.03174	.01492	.13546	.00122	.00470	.44810	.01382	.03464	.02964	.00016	1.00000
LAWE9H	Corr	.06066	.09946	.06878	.00197	.00079	.00079	.05468	.00541	.04091	.02366	.08953	.00122	.00430	.46919	.01394	.03479	.02978	.00016	1.00000
LAWE10H	Corr	.06086	.09976	.06978	.00197	.00079	.00079	.05498	.00541	.04271	.02948	.05735	.00122	.00540	.49054	.01394	.03489	.02998	.00016	1.00000
LAWE11	Corr	.06106	.10010	.02322	.00200	.00080	.00080	.05506	.04755	.00000	.01481	.17377	.00124	.00250	.43784	.01401	.03504	.03003	.00016	1.00000

- (a) The compositions listed in this table are normalized mass fraction versions of target compositions of the glasses, after replacing the target values of SO<sub>3</sub> by XRF analyzed (or estimated analyzed) values. See Section 3.3 for the details.
- (b) The Group IDs are described in Sections 2.1 to 2.6.
- (c) XRF SO<sub>3</sub> denotes that the SO<sub>3</sub> composition is based on chemical analysis by XRF. For most glasses SO<sub>3</sub> was directly measured by XRF, but for some glasses estimated XRF values were used (see Section 3.3).
- (d) The normalized component mass fractions listed in this table were rounded to five decimals, and may not sum exactly to 1.00000 as listed. However, complete compositions listed to more decimal places and summing to 1.0000 were used for property-composition modeling.

**Table 6.2. Normalized<sup>(a)</sup> Compositions (mass fractions) of 165 LAW Glasses Used for VHT Model Development (continued).**

Glass ID	Group ID <sup>(b)</sup>	Al <sub>2</sub> O <sub>3</sub>	B <sub>2</sub> O <sub>3</sub>	CaO	Cl	Cr <sub>2</sub> O <sub>3</sub>	F	Fe <sub>2</sub> O <sub>3</sub>	K <sub>2</sub> O	Li <sub>2</sub> O	MgO	Na <sub>2</sub> O	P <sub>2</sub> O <sub>5</sub>	XRF SO <sub>3</sub> <sup>(c)</sup>	SiO <sub>2</sub>	TiO <sub>2</sub>	ZnO	ZrO <sub>2</sub>	Others	Sum <sup>(d)</sup>
LAWE12	Corr	.06952	.08753	.01971	.00196	.00078	.00078	.04361	.05412	.00000	.01440	.19746	.00122	.00320	.41853	.01370	.03411	.03921	.00016	1.00000
LAWE13	Corr	.06952	.09753	.01971	.00196	.00078	.00078	.05362	.05412	.00000	.00440	.19746	.00122	.00320	.41853	.00370	.03411	.03921	.00016	1.00000
LAWE15	Corr	.05942	.08754	.01471	.00196	.00078	.00078	.05366	.05412	.00000	.00940	.19748	.00122	.00310	.42863	.01371	.03411	.03922	.00016	1.00000
LAWE16	Corr	.05934	.08241	.01468	.00196	.00078	.00078	.05358	.05404	.00000	.00939	.19719	.00122	.00460	.42798	.01369	.03406	.04415	.00016	1.00000
LAWCrP1R	HiCrP	.06101	.10002	.02761	.00124	.00328	.00112	.05501	.00125	.00000	.01480	.19347	.01442	.00370	.44401	.01400	.03501	.03001	.00004	1.00000
LAWCrP2R	HiCrP	.06099	.09998	.02105	.00193	.00591	.00103	.05499	.00275	.00000	.01480	.20996	.01333	.00360	.43065	.01400	.03499	.02999	.00006	1.00000
LAWCrP3R	HiCrP	.06101	.10001	.02761	.00124	.00328	.00111	.05500	.00125	.00000	.01480	.19345	.02380	.00380	.43458	.01400	.03500	.03000	.00004	1.00000
LAWCrP4R	HiCrP	.06098	.09997	.02104	.00192	.00591	.00103	.05498	.00275	.00000	.01480	.20994	.02379	.00370	.42014	.01400	.03499	.02999	.00006	1.00000
LAWCrP5	HiCrP	.06108	.10013	.05813	.00136	.00591	.00067	.05507	.00087	.02642	.01488	.14395	.01335	.00380	.43505	.01402	.03504	.03004	.00021	1.00000
LAWCrP6	HiCrP	.06104	.10007	.06945	.00136	.00630	.00067	.05504	.00087	.04173	.02552	.08006	.02512	.00580	.44770	.01401	.03502	.03002	.00021	1.00000
LAWCrP7	HiCrP	.06104	.10007	.06985	.00136	.00630	.00067	.05504	.00087	.04303	.02932	.05404	.02512	.00660	.46741	.01401	.03502	.03002	.00021	1.00000
LAWA51	ActDes	.06203	.11976	.00000	.00587	.00018	.00009	.06998	.00451	.00000	.01484	.18003	.00030	.00070	.46579	.01996	.02488	.02998	.00111	1.00000
LAWA52	ActDes	.06179	.06191	.07882	.00652	.00020	.00010	.07505	.00501	.00000	.01477	.19999	.00034	.00100	.42247	.01108	.02994	.02992	.00112	1.00000
LAWA60	ActDes	.08528	.11228	.04321	.00652	.00020	.00010	.00000	.00501	.00000	.01994	.19999	.00034	.00100	.44551	.01994	.02965	.02992	.00112	1.00000
LAWA104	ActDes	.06614	.08591	.01924	.00717	.00022	.00011	.06735	.00551	.00000	.01924	.22001	.00037	.00100	.42989	.01924	.02861	.02886	.00113	1.00000
LAWA105	ActDes	.07027	.08281	.01854	.00782	.00024	.00012	.06490	.00602	.00000	.01854	.24006	.00040	.00090	.41430	.01854	.02757	.02782	.00114	1.00000
LAWA125	ActDes	.05637	.09545	.01939	.00220	.00020	.00320	.05387	.04208	.00000	.01439	.19990	.00090	.00310	.42888	.01939	.02879	.02909	.00280	1.00000
LAWA133	ActDes	.06204	.08901	.05485	.00559	.00020	.00040	.03487	.00430	.00000	.01998	.19980	.00100	.00200	.44535	.01998	.02967	.02997	.00100	1.00000
LAWA134	ActDes	.05647	.09964	.02019	.00200	.00020	.00290	.05627	.03728	.00000	.01499	.17729	.00080	.00280	.44753	.02029	.02998	.03038	.00100	1.00000
LAWA135	ActDes	.05655	.10092	.02048	.00190	.00020	.00280	.05695	.03577	.00000	.01519	.17016	.00070	.00270	.45304	.02048	.03038	.03078	.00100	1.00000
LAWA136	ActDes	.05655	.10092	.03048	.00190	.00020	.00280	.05695	.03577	.00000	.01519	.17016	.00070	.00270	.44304	.02048	.03038	.03078	.00100	1.00000
LAWB64	ActDes	.06207	.09969	.06710	.00000	.00101	.00070	.03300	.00262	.05825	.02978	.05503	.00010	.00680	.48639	.01398	.05181	.03169	.00000	1.00000
LAWB67	ActDes	.06189	.09940	.05186	.00000	.00100	.00070	.05296	.00261	.04303	.02969	.05487	.03019	.00970	.48497	.01394	.03160	.03160	.00000	1.00000
LAWB69	ActDes	.06151	.12332	.10462	.00010	.00050	.00080	.00000	.00230	.04611	.02971	.06621	.00050	.00650	.47960	.00000	.04571	.03151	.00100	1.00000
LAWB70	ActDes	.06159	.12347	.06629	.00010	.00050	.00080	.03255	.00230	.04616	.02974	.06629	.00050	.00540	.48018	.00000	.05157	.03154	.00100	1.00000
LAWB71	ActDes	.06162	.10802	.06633	.00010	.00050	.00080	.03257	.00230	.04619	.02976	.06633	.00050	.00480	.48047	.01553	.05160	.03156	.00100	1.00000
LAWB72	ActDes	.06154	.12339	.07125	.00010	.00050	.00080	.03252	.00230	.04113	.02972	.06625	.00050	.00610	.47984	.00000	.05154	.03152	.00100	1.00000
LAWB73	ActDes	.06193	.09947	.09345	.00000	.00100	.00070	.01907	.00261	.05049	.02971	.05490	.00010	.00900	.48531	.01395	.04667	.03162	.00000	1.00000
LAWB74	ActDes	.06218	.10108	.08728	.00000	.00101	.00071	.01915	.00262	.05331	.02983	.05513	.00010	.00770	.48728	.01401	.04686	.03175	.00000	1.00000
LAWB75	ActDes	.06187	.11792	.08684	.00000	.00100	.00070	.01905	.00261	.05304	.01504	.05485	.00010	.01000	.48482	.01394	.04663	.03159	.00000	1.00000
LAWB76	ActDes	.06186	.11790	.08682	.00000	.00100	.00070	.01905	.00261	.05805	.01504	.05484	.00010	.01020	.49365	.00000	.04662	.03158	.00000	1.00000
LAWB77	ActDes	.06160	.12350	.06631	.00010	.00050	.00080	.02204	.00230	.04117	.02975	.06631	.00050	.00520	.48027	.01552	.05158	.03155	.00100	1.00000
LAWB81	ActDes	.06155	.12340	.07126	.00010	.00050	.00080	.03253	.00230	.04263	.02972	.06625	.00050	.00600	.47989	.00000	.05004	.03153	.00100	1.00000
LAWB89	ActDes	.06186	.10040	.06787	.00010	.00040	.00060	.05295	.00190	.05005	.02973	.04084	.00040	.00440	.49350	.01391	.04845	.03163	.00100	1.00000

- (a) The compositions listed in this table are normalized mass fraction versions of target compositions of the glasses, after replacing the target values of SO<sub>3</sub> by XRF analyzed (or estimated analyzed) values. See Section 3.3 for the details.
- (b) The Group IDs are described in Sections 2.1 to 2.6.
- (c) XRF SO<sub>3</sub> denotes that the SO<sub>3</sub> composition is based on chemical analysis by XRF. For most glasses SO<sub>3</sub> was directly measured by XRF, but for some glasses estimated XRF values were used (see Section 3.3).
- (d) The normalized component mass fractions listed in this table were rounded to five decimals, and may not sum exactly to 1.00000 as listed. However, complete compositions listed to more decimal places and summing to 1.0000 were used for property-composition modeling.

**Table 6.2. Normalized<sup>(a)</sup> Compositions (mass fractions) of 165 LAW Glasses Used for VHT Model Development (continued).**

Glass ID	Group ID <sup>(b)</sup>	Al <sub>2</sub> O <sub>3</sub>	B <sub>2</sub> O <sub>3</sub>	CaO	Cl	Cr <sub>2</sub> O <sub>3</sub>	F	Fe <sub>2</sub> O <sub>3</sub>	K <sub>2</sub> O	Li <sub>2</sub> O	MgO	Na <sub>2</sub> O	P <sub>2</sub> O <sub>5</sub>	XRF SO <sub>3</sub> <sup>(c)</sup>	SiO <sub>2</sub>	TiO <sub>2</sub>	ZnO	ZrO <sub>2</sub>	Others	Sum <sup>(d)</sup>
LAWB90	ActDes	.06192	.10050	.06794	.00010	.00040	.00060	.05301	.00190	.03617	.02976	.06884	.00040	.00340	.47996	.01393	.04850	.03166	.00100	1.00000
LAWB91	ActDes	.06191	.10047	.06792	.00010	.00040	.00060	.05299	.00190	.02925	.02975	.08735	.00040	.00370	.46820	.01392	.04848	.03165	.00100	1.00000
LAWB92	ActDes	.06187	.10041	.06787	.00010	.00040	.00060	.05296	.00190	.02222	.02973	.10121	.00040	.00430	.46101	.01392	.04845	.03163	.00100	1.00000
LAWB93	ActDes	.06186	.10039	.06786	.00010	.00040	.00060	.05295	.00190	.04664	.02973	.04784	.00040	.00450	.48984	.01391	.04844	.03163	.00100	1.00000
LAWB94	ActDes	.06186	.10031	.06780	.00007	.00039	.00064	.05295	.00194	.05359	.02972	.03385	.00037	.00500	.49662	.01393	.04839	.03158	.00100	1.00000
LAWB95	ActDes	.06189	.10035	.06783	.00007	.00039	.00064	.05297	.00194	.05761	.02973	.02457	.00037	.00460	.50211	.01394	.04841	.03159	.00100	1.00000
LAWC15	ActDes	.06221	.08929	.02006	.00078	.00003	.00469	.07007	.00142	.00000	.02009	.19963	.00015	.00230	.44713	.02001	.02990	.03005	.00220	1.00000
LAWC26	ActDes	.06121	.13263	.06411	.00110	.00020	.00050	.00010	.00140	.02731	.01500	.11962	.00110	.00350	.49960	.01120	.03021	.03021	.00100	1.00000
LAWC29	ActDes	.06551	.10049	.09617	.00112	.00018	.00054	.00009	.00136	.02734	.01501	.11958	.00106	.00370	.47181	.01121	.05365	.03019	.00100	1.00000
LAWC30	ActDes	.06122	.10053	.06412	.00110	.00020	.00050	.04101	.00140	.02731	.01500	.11964	.00110	.00340	.46754	.01120	.05352	.03021	.00100	1.00000
LAWC31	ActDes	.06119	.10048	.07409	.00110	.00020	.00050	.04429	.00140	.02729	.01500	.11958	.00110	.00390	.46731	.01120	.04019	.03019	.00100	1.00000
LAWC33	ActDes	.06146	.10100	.06947	.00110	.00020	.00050	.04444	.00140	.02753	.01512	.12012	.00110	.00370	.46977	.01131	.04044	.03033	.00100	1.00000
TFA-BASE	ActDes	.06999	.09999	.00010	.00280	.00000	.00010	.05499	.00410	.00000	.01500	.19998	.00060	.00080	.49065	.03000	.01500	.01500	.00090	1.00000
C22AN107	ActDes	.06106	.10079	.05115	.00080	.00020	.00140	.05585	.00090	.02512	.01511	.14433	.00120	.00270	.46612	.01141	.03063	.03023	.00100	1.00000
A88AP101R1	ActDes	.06102	.09834	.01999	.00130	.00016	.00227	.05552	.02136	.00000	.01480	.20011	.00073	.00230	.44153	.01999	.02961	.02998	.00100	1.00000
A88Si+15	ActDes	.06141	.09481	.01930	.00140	.00020	.00250	.05351	.02370	.00000	.01430	.22182	.00080	.00290	.42554	.01930	.02850	.02890	.00110	1.00000
A88Si-15	ActDes	.06055	.10218	.02072	.00120	.00010	.00200	.05765	.01882	.00000	.01541	.17674	.00060	.00190	.45867	.02072	.03072	.03112	.00090	1.00000
C22Si+15	ActDes	.06043	.09837	.04994	.00090	.00020	.00160	.05358	.00095	.02459	.01484	.16197	.00130	.00310	.45581	.01121	.03001	.02960	.00160	1.00000
C22Si-15	ActDes	.06160	.10291	.05218	.00071	.00017	.00129	.05555	.00076	.02572	.01551	.12812	.00138	.00230	.47680	.01175	.03139	.03096	.00090	1.00000
A1C1-1	ActDes	.06088	.09126	.02742	.00913	.00015	.00086	.06501	.00347	.00623	.01850	.19167	.00033	.00210	.44480	.01759	.02951	.02956	.00153	1.00000
A1C1-2	ActDes	.06073	.09415	.03521	.00654	.00013	.00169	.06135	.00255	.01247	.01735	.17673	.00066	.00230	.45142	.01554	.02984	.02974	.00160	1.00000
A1C1-3	ActDes	.06057	.09701	.04299	.00395	.00011	.00252	.05766	.00161	.01871	.01619	.16170	.00099	.00290	.45787	.01348	.03017	.02991	.00167	1.00000
C1-AN107	ActDes	.06066	.10031	.05098	.00065	.00009	.00283	.05421	.00069	.02506	.01510	.14465	.00132	.00290	.46636	.01147	.03062	.03020	.00189	1.00000
A2-AP101	ActDes	.05622	.09824	.01991	.00420	.00020	.00350	.05532	.03812	.00000	.01481	.18467	.00080	.00350	.44008	.01991	.02941	.02961	.00150	1.00000
A2B1-1	ActDes	.05758	.09883	.03184	.00320	.00020	.00280	.05477	.02904	.01071	.01852	.15230	.00070	.00350	.45179	.01842	.03414	.03014	.00150	1.00000
A2B1-2	ActDes	.05895	.09919	.04374	.00220	.00030	.00220	.05405	.02002	.02152	.02232	.11981	.00060	.00420	.46292	.01692	.03894	.03063	.00150	1.00000
B1-AZ101	ActDes	.06180	.10026	.06771	.00020	.00030	.00080	.05278	.00180	.04307	.02985	.05479	.00040	.00490	.48578	.01392	.04848	.03165	.00150	1.00000
C2-AN102C35	ActDes	.06075	.09428	.07356	.00390	.00010	.00110	.03603	.00090	.03253	.01491	.11980	.00160	.00540	.47278	.01081	.03993	.03002	.00160	1.00000
A3-AN104	ActDes	.06051	.09921	.05031	.00790	.00020	.00010	.05371	.00330	.02480	.01480	.14641	.00110	.00350	.46095	.01130	.03040	.03000	.00150	1.00000

- (a) The compositions listed in this table are normalized mass fraction versions of target compositions of the glasses, after replacing the target values of SO<sub>3</sub> by XRF analyzed (or estimated analyzed) values. See Section 3.3 for the details.
- (b) The Group IDs are described in Sections 2.1 to 2.6.
- (c) XRF SO<sub>3</sub> denotes that the SO<sub>3</sub> composition is based on chemical analysis by XRF. For most glasses SO<sub>3</sub> was directly measured by XRF, but for some glasses estimated XRF values were used (see Section 3.3).
- (d) The normalized component mass fractions listed in this table were rounded to five decimals, and may not sum exactly to 1.00000 as listed. However, complete compositions listed to more decimal places and summing to 1.00000 were used for property-composition modeling.

**Table 6.3. VHT Alteration Depths and Data Splitting Validation Sets of 165 LAW Glasses Used for VHT Model Development.**

<b>Glass</b>	<b>Group ID<sup>(a)</sup></b>	<b>Replicate<sup>(b)</sup></b>	<b>VHT Alteration Depth (<math>\mu\text{m}</math>)</b>	<b>VHT Data Splitting Validation Set<sup>(c)</sup></b>
LAWA44R10	ExPh1	No	9	5
LAWA53	ExPh1	No	7	3
LAWA56	ExPh1	No	15	3
LAWA88R1	ExPh1	LAWM52	13	NA
LAWA102R1	ExPh1	No	34	4
LAWA126	ExPh1	No	22	5
LAWA128	ExPh1	No	8	3
LAWA130	ExPh1	No	6	2
LAWB65	ExPh1	No	10	1
LAWB66	ExPh1	No	17	3
LAWB68	ExPh1	No	18	2
LAWB78	ExPh1	No	23	2
LAWB79	ExPh1	No	11	5
LAWB80	ExPh1	No	10	2
LAWB83	ExPh1	No	16	1
LAWB84	ExPh1	No	15	4
LAWB85	ExPh1	No	11	1
LAWB86	ExPh1	No	15	5
C100G136B	ExPh1	No	23	3
LAWC27	ExPh1	No	177	3
LAWC32	ExPh1	No	206	2
LAWM1	Ph1	LAWM53	82	NA
LAWM2	Ph1	No	75	4
LAWM3	Ph1	No	34	5
LAWM4	Ph1	No	5	1
LAWM5	Ph1	No	7	4
LAWM6	Ph1	No	19	3
LAWM7	Ph1	No	26	4
LAWM8	Ph1	No	13	1
LAWM9	Ph1	LAWM54R1	1	NA
LAWM10	Ph1	No	114	4
LAWM11	Ph1	No	700	2
LAWM15	Ph1	No	856	5
LAWM16	Ph1	No	71	3
LAWM17	Ph1	No	3	5
LAWM18	Ph1	No	15	1
LAWM19	Ph1	No	1	2
LAWM20	Ph1	No	116	1
LAWM21	Ph1	No	9	1
LAWM22	Ph1	No	2	3
LAWM23	Ph1	No	9	2
LAWM24	Ph1	No	123	2
LAWM25R1	Ph1	No	41	2
LAWM26	Ph1	No	31	3
LAWM27	Ph1	No	45	5

- (a) Group IDs are described in Sections 2.1 to 2.6.  
 (b) If a given glass has a replicate, the glass ID is listed. If not, No is listed.  
 (c) Numbers from 1 to 5 denote the five split validation subsets. NA denotes “not applicable”, because these replicate glasses were forced into the modeling subsets, and thus were not parts of the validation subsets.

**Table 6.3. VHT Alteration Depths and Data Splitting Validation Sets of 165 LAW Glasses Used for VHT Model Development (continued).**

Glass	Group ID <sup>(a)</sup>	Replicate <sup>(b)</sup>	VHT Alteration Depth (μm)	VHT Data Splitting Validation Set <sup>(c)</sup>
LAWM28	Ph1	No	6	3
LAWM29	Ph1	No	9	3
LAWM30	Ph1	No	181	4
LAWM31	Ph1	No	48	1
LAWM33R1	Ph1	No	34	1
LAWM34	Ph1	No	420	1
LAWM35	Ph1	LAWM56	4	NA
LAWM36	Ph1	No	107	1
LAWM37	Ph1	No	10	3
LAWM38	Ph1	No	171	2
LAWM39	Ph1	No	112	3
LAWM40	Ph1	No	3	1
LAWM41	Ph1	No	43	3
LAWM42	Ph1	No	7	5
LAWM43	Ph1	No	9	4
LAWM44	Ph1	No	20	4
LAWM45	Ph1	No	44	4
LAWM46	Ph1	No	3	2
LAWM47	Ph1	No	25	3
LAWM48	Ph1	No	5	2
LAWM49	Ph1	No	23	4
LAWM50	Ph1	LAWM51	4	NA
LAWM51	Ph1	LAWM50	5	NA
LAWM52	Ph1	LAWA88R1	28	NA
LAWM53	Ph1	LAWM01	90	NA
LAWM54R1	Ph1	LAWM09	3	NA
LAWM56	Ph1	LAWM35	6	NA
LAWM57	Ph1aAug	No	142	2
LAWM58	Ph1aAug	No	157	1
LAWM59	Ph1aAug	No	134	1
LAWM60	Ph1aAug	No	30	2
LAWM61	Ph1aAug	No	361	5
LAWM62	Ph1aAug	No	115	5
LAWM63	Ph1aAug	No	655	1
LAWM64	Ph1aAug	No	27	5
LAWM65	Ph1aAug	No	522	2
LAWM66	Ph1aAug	No	445	2
LAWM67	Ph1aAug	No	260	5
LAWM68	Ph1aAug	No	234	4
LAWM69	Ph1aAug	No	283	1
LAWM70	Ph1aAug	No	813	4
LAWM71	Ph1aAug	No	980	1
LAWM72	Ph1aAug	No	495	1
LAWM73	Ph1aAug	No	472	4
LAWM74	Ph1aAug	No	14	4

- (a) Group IDs are described in Sections 2.1 to 2.6.
- (b) If a given glass has a replicate, the glass ID is listed. If not, No is listed.
- (c) Numbers from 1 to 5 denote the five split validation subsets. NA denotes “not applicable”, because these replicate glasses were forced into the modeling subsets, and thus were not parts of the validation subsets.

**Table 6.3. VHT Alteration Depths and Data Splitting Validation Sets of 165 LAW Glasses Used for VHT Model Development (continued).**

<b>Glass</b>	<b>Group ID<sup>(a)</sup></b>	<b>Replicate<sup>(b)</sup></b>	<b>VHT Alteration Depth (μm)</b>	<b>VHT Data Splitting Validation Set<sup>(c)</sup></b>
LAWM75	Ph1aAug	No	7	1
LAWM76	Ph1aAug	No	90	4
LAWE2H	Corr	No	588	3
LAWE3H	Corr	No	644	5
LAWE3	Corr	No	129	4
LAWE4H	Corr	No	147	3
LAWE5H	Corr	No	15	5
LAWE7	Corr	No	191	5
LAWE7H	Corr	No	152	4
LAWE9H	Corr	No	131	5
LAWE10H	Corr	No	17	1
LAWE11	Corr	No	33	3
LAWE12	Corr	No	737	3
LAWE13	Corr	No	615	4
LAWE15	Corr	No	485	5
LAWE16	Corr	No	459	3
LAWCrP1R	HiCrP	No	32	2
LAWCrP2R	HiCrP	No	216	3
LAWCrP3R	HiCrP	No	79	1
LAWCrP4R	HiCrP	No	200	1
LAWCrP5	HiCrP	No	8	4
LAWCrP6	HiCrP	No	13	3
LAWCrP7	HiCrP	No	12	5
LAWA51	ActDes	No	5	3
LAWA52	ActDes	No	67	2
LAWA60	ActDes	No	56	3
LAWA104	ActDes	No	59	4
LAWA105	ActDes	No	359	4
LAWA125	ActDes	No	343	3
LAWA133	ActDes	No	5	5
LAWA134	ActDes	No	2	4
LAWA135	ActDes	No	3	3
LAWA136	ActDes	No	3	4
LAWB64	ActDes	No	15	2
LAWB67	ActDes	No	15	3
LAWB69	ActDes	No	128	3
LAWB70	ActDes	No	31	4
LAWB71	ActDes	No	12	3
LAWB72	ActDes	No	23	5
LAWB73	ActDes	No	31	5
LAWB74	ActDes	No	52	2
LAWB75	ActDes	No	59	5
LAWB76	ActDes	No	78	5
LAWB77	ActDes	No	17	4

- (a) Group IDs are described in Sections 2.1 to 2.6.
- (b) If a given glass has a replicate, the glass ID is listed. If not, No is listed.
- (c) Numbers from 1 to 5 denote the five split validation subsets. NA denotes “not applicable”, because these replicate glasses were forced into the modeling subsets, and thus were not parts of the validation subsets.

**Table 6.3. VHT Alteration Depths and Data Splitting Validation Sets of 165 LAW Glasses Used for VHT Model Development (continued).**

<b>Glass</b>	<b>Group ID<sup>(a)</sup></b>	<b>Replicate<sup>(b)</sup></b>	<b>VHT Alteration Depth (μm)</b>	<b>VHT Data Splitting Validation Set<sup>(c)</sup></b>
LAWB81	ActDes	No	24	2
LAWB89	ActDes	No	16	2
LAWB90	ActDes	No	14	5
LAWB91	ActDes	No	12	4
LAWB92	ActDes	No	10	4
LAWB93	ActDes	No	15	4
LAWB94	ActDes	No	14	1
LAWB95	ActDes	No	11	2
LAWC15	ActDes	No	5	4
LAWC26	ActDes	No	22	1
LAWC29	ActDes	No	106	5
LAWC30	ActDes	No	60	1
LAWC31	ActDes	No	110	2
LAWC33	ActDes	No	17	5
TFA-BASE	ActDes	No	86	3
C22AN107	ActDes	No	9	5
A88AP101R1	ActDes	No	13	2
A88Si+15	ActDes	No	290	2
A88Si-15	ActDes	No	4	5
C22Si+15	ActDes	No	23	1
C22Si-15	ActDes	No	29	1
A1C1-1	ActDes	No	6	4
A1C1-2	ActDes	No	31	1
A1C1-3	ActDes	No	6	5
C1-AN107	ActDes	No	80	2
A2-AP101	ActDes	No	7	2
A2B1-1	ActDes	No	5	1
A2B1-2	ActDes	No	6	1
B1-AZ101	ActDes	No	14	2
C2-AN102C35	ActDes	No	154	5
A3-AN104	ActDes	No	6	2

- (a) Group IDs are described in Sections 2.1 to 2.6.
- (b) If a given glass has a replicate, the glass ID is listed. If not, No is listed.
- (c) Numbers from 1 to 5 denote the five split validation subsets. NA denotes “not applicable”, because these replicate glasses were forced into the modeling subsets, and thus were not parts of the validation subsets.

**Table 6.4. Variation in VHT Responses for Replicate and Near-Replicate Pairs.**

Glass IDs of Replicate and Near-Replicate Pairs	Included in VHT Modeling Data?	VHT Alteration Depth	
		$\mu\text{m}$	$\ln(\mu\text{m})$
LAWM01	Yes	82	4.4067
LAWM53	Yes	90	4.4998
		<b>%RSD<sup>(a)</sup> = 6.58</b>	<b>SD = 0.0658</b>
LAWM09	Yes	1	0.0000
LAWM54R1	Yes	3	1.0986
		<b>%RSD = 70.71</b>	<b>SD = 0.7768</b>
LAWM12	No	>1100	>7.0030
LAWM55	No	>1100	>7.0030
		<b>%RSD = NA</b>	<b>SD = NA</b>
LAWM35	Yes	4	1.3863
LAWM56	Yes	6	1.7916
		<b>%RSD = 28.28</b>	<b>SD = 0.2867</b>
LAWM50	Yes	4	1.3863
LAWM51	Yes	5	1.6094
		<b>%RSD = 15.71</b>	<b>SD = 0.1578</b>
LAWM52	Yes	28	3.3322
LAWA88R1	Yes	13	2.5649
		<b>%RSD = 51.74</b>	<b>SD = 0.5425</b>
<b>Pooled Over All 5 Replicate Pairs Used for Modeling</b>		<b>%RSD = 41.87</b>	<b>SD = 0.4493</b>
<b>Pooled Over 4 Replicate Pairs (Excluding the LAWM09 and LAWM54R1 pair)</b>		<b>%RSD = 30.69</b>	<b>SD = 0.3185</b>

(a) %RSD = 100×(Standard Deviation / Mean).



**Table 6.5. Normalized<sup>(a)</sup> Compositions (mass fractions) for 16 LAW Glasses Excluded from VHT Modeling Data.**

Glass ID	Group ID <sup>(b)</sup>	Al <sub>2</sub> O <sub>3</sub>	B <sub>2</sub> O <sub>3</sub>	CaO	Cl	Cr <sub>2</sub> O <sub>3</sub>	F	Fe <sub>2</sub> O <sub>3</sub>	K <sub>2</sub> O	Li <sub>2</sub> O	MgO	Na <sub>2</sub> O	P <sub>2</sub> O <sub>5</sub>	XRF SO <sub>3</sub> <sup>(c)</sup>	SiO <sub>2</sub>	TiO <sub>2</sub>	ZnO	ZrO <sub>2</sub>	Others	Sum <sup>(d)</sup>
LAWA49	ActDes	.06203	.08904	.00000	.00652	.00020	.00010	.09982	.00501	.00000	.01478	.20005	.00034	.00070	.44565	.01995	.02478	.02992	.00112	1.00000
LAWB60	ActDes	.06143	.12366	.11905	.00010	.00070	.00080	.00000	.00261	.04630	.02976	.06514	.00030	.00640	.47961	.00000	.03157	.03157	.00100	1.00000
LAWB62	ActDes	.06194	.09948	.11996	.00000	.00100	.00070	.00000	.00261	.05812	.02971	.05491	.00010	.00890	.48536	.01395	.03162	.03162	.00000	1.00000
LAWB63	ActDes	.06579	.09953	.09351	.00000	.00100	.00070	.00000	.00261	.05052	.02973	.05494	.00010	.00840	.48942	.01396	.05815	.03164	.00000	1.00000
LAWB82	ActDes	.06162	.10100	.07134	.00010	.00050	.00080	.09519	.00230	.04269	.01483	.06633	.00050	.00480	.45532	.00000	.05010	.03156	.00100	1.00000
LAWC28	ActDes	.06117	.10045	.12814	.00110	.00020	.00050	.00010	.00140	.02729	.01499	.11954	.00110	.00430	.46717	.01119	.03018	.03018	.00100	1.00000
LAWE3Cr2CCC	Corr	.06103	.10005	.02021	.00200	.01401	.00080	.05503	.04992	.00000	.01481	.18219	.00124	.00300	.41651	.01401	.03502	.03002	.00016	1.00000
LAWE9HCr1CCC	Corr	.06059	.09934	.06870	.00196	.00601	.00079	.05462	.00541	.04086	.02363	.08943	.00122	.00551	.46339	.01392	.03475	.02974	.00016	1.00000
LAWE9HCr2CCC	Corr	.06060	.09937	.06872	.00196	.00451	.00079	.05463	.00541	.04087	.02364	.08945	.00122	.00521	.46503	.01392	.03476	.02975	.00016	1.00000
LAWE10HCr3CCC	Corr	.06081	.09968	.06973	.00196	.00351	.00079	.05494	.00541	.04268	.02945	.05730	.00122	.00621	.48742	.01393	.03486	.02995	.00016	1.00000
LAWM12	Ph1	.03501	.13005	.00000	.00801	.00322	.00300	.02310	.04002	.04502	.01971	.14259	.00499	.00230	.42215	.03001	.05002	.04002	.00080	1.00000
LAWM13	Ph1	.03501	.06001	.10002	.00412	.00165	.00154	.08002	.03785	.00000	.00000	.22005	.00257	.00500	.40009	.03001	.02164	.00000	.00041	1.00000
LAWM14	Ph1	.03500	.06000	.02045	.00020	.00008	.00007	.00000	.00000	.00881	.05000	.21999	.00012	.00530	.51997	.03000	.05000	.00000	.00002	1.00000
LAWM32	Ph1	.05146	.07002	.02001	.00800	.00321	.00299	.02001	.02001	.03001	.03501	.16514	.00499	.00320	.50013	.00500	.05001	.01000	.00080	1.00000
LAWM55	Ph1	.03501	.13004	.00000	.00800	.00321	.00299	.02310	.04001	.04501	.01971	.14257	.00499	.00240	.42211	.03001	.05001	.04001	.00080	1.00000
LAWE14	Corr	.04942	.09754	.01471	.00196	.00078	.00078	.05366	.05412	.00000	.00440	.19748	.00122	.00310	.43363	.01371	.03411	.03922	.00016	1.00000

- (a) The compositions listed in this table are normalized mass-fraction versions of target compositions of the glasses, after replacing the target values of SO<sub>3</sub> by XRF analyzed (or estimated analyzed) values. See Section 3.3 for the details.
- (b) The Group IDs are described in Sections 2.1 to 2.6.
- (c) XRF SO<sub>3</sub> denotes that the SO<sub>3</sub> composition is based on chemical analysis by XRF. For most glasses SO<sub>3</sub> was directly measured by XRF, but for some glasses estimated XRF values were used (see Section 3.3).
- (d) The normalized component mass fractions listed in this table were rounded to five decimals, and may not sum exactly to 1.00000 as listed. However, complete compositions listed to more decimal places and summing to 1.0000 were used for property-composition modeling.

**Table 6.6. VHT Alteration Depths for 16 LAW Glasses Excluded from the VHT Modeling Set.**

<b>Glass ID</b>	<b>Group ID<sup>(a)</sup></b>	<b>VHT Alteration Depth (μm)</b>
LAWA49	ActDes	30
LAWB60	ActDes	68
LAWB62	ActDes	37
LAWB63	ActDes	72
LAWB82	ActDes	32
LAWC28	ActDes	92
LAWE3Cr2CCC	Corr	186
LAWE9HCr1CCC	Corr	68
LAWE9HCr2CCC	Corr	92
LAWE10HCr3CCC	Corr	28
LAWM12	Ph1	> 1100
LAWM13	Ph1	> 1100
LAWM14	Ph1	> 1100
LAWM32	Ph1	> 1100
LAWM55	Ph1	> 1100
LAWE14	Corr	> 800

(a) The Group IDs are described in Sections 2.1 to 2.6.

**Table 6.7. Coefficients and Performance Summary for 18-Component Full Linear Mixture Model on the Natural Logarithm of ILAW VHT Alteration Depth.**

In(D) Full LM Model Term	Coefficient Estimate	Coefficient Stand. Dev.	Modeling Data Statistic, 165 Glasses <sup>(a)</sup>				Value
Al <sub>2</sub> O <sub>3</sub>	12.6056	7.6617	R <sup>2</sup>				0.607
B <sub>2</sub> O <sub>3</sub>	-9.0658	5.4035	R <sup>2</sup> Adjusted (R <sup>2</sup> <sub>A</sub> )				0.562
CaO	1.6150	4.6890	R <sup>2</sup> Predicted (R <sup>2</sup> <sub>p</sub> )				0.470
Cl	-77.3733	45.8666	RMSE				1.060
Cr <sub>2</sub> O <sub>3</sub>	162.7379	136.6976	Model LOF p-value				0.014
F	-269.6950	127.5691					
Fe <sub>2</sub> O <sub>3</sub>	-22.2568	5.4625	<b>Extrapolative Validation Statistic, 16 Outlying Glasses<sup>(a,b)</sup></b>				<b>Value</b>
K <sub>2</sub> O	35.6904	6.5566	R <sup>2</sup> Validation (R <sup>2</sup> <sub>v</sub> ) <sup>(f)</sup>				-2.120
Li <sub>2</sub> O	89.2858	11.9792	RMSE Validation (RMSE <sub>v</sub> ) <sup>(f)</sup>				1.030
MgO	11.9115	9.7255	# Correct predicted > Values <sup>(g)</sup>				2 of 6
Na <sub>2</sub> O	37.9075	3.2219					
P <sub>2</sub> O <sub>5</sub>	-8.9889	31.1194	<b>Data Partition Statistic, 92 Modeling &amp; 73 Validation<sup>(a,c)</sup></b>				<b>Value</b>
SO <sub>3</sub>	39.5908	70.7652	R <sup>2</sup>				0.699
SiO <sub>2</sub>	-1.6730	2.1842	R <sup>2</sup> Adjusted (R <sup>2</sup> <sub>A</sub> )				0.629
TiO <sub>2</sub>	-16.7208	12.7560	R <sup>2</sup> Predicted (R <sup>2</sup> <sub>p</sub> )				0.469
ZnO	5.9267	8.8853	RMSE				1.018
ZrO <sub>2</sub>	-65.0768	9.8510	R <sup>2</sup> Validation (R <sup>2</sup> <sub>v</sub> )				-17.971
Others <sup>(e)</sup>	-244.6475	205.8114	RMSE Validation (RMSE <sub>v</sub> )				6.570
<b>Data Splitting Statistic<sup>(a,d)</sup></b>							
	<b>DS1</b>	<b>DS2</b>	<b>DS3</b>	<b>DS4</b>	<b>DS5</b>	<b>Average</b>	
R <sup>2</sup>	0.598	0.638	0.628	0.613	0.627	0.621	
R <sup>2</sup> Adjusted (R <sup>2</sup> <sub>A</sub> )	0.539	0.585	0.573	0.556	0.572	0.565	
R <sup>2</sup> Predicted (R <sup>2</sup> <sub>p</sub> )	0.363	0.478	0.423	0.438	0.461	0.433	
RMSE	1.092	1.032	1.052	1.070	1.053	1.060	
R <sup>2</sup> Validation (R <sup>2</sup> <sub>v</sub> )	0.532	0.345	0.428	0.441	0.460	0.441	
RMSE Validation (RMSE <sub>v</sub> )	1.071	1.290	1.182	1.182	1.143	1.174	

- (a) The model evaluation statistics are defined in Section C.3 of Appendix C. Model validation statistics are defined in Section C.5 of Appendix C. A negative value for R<sup>2</sup><sub>v</sub> means that the sum of squares of model prediction errors is larger than if the mean response value over the validation data set were used as the predicted value for each glass. In other words, the model predicts worse for the validation data than the mean response value does.
- (b) The 10 outlying LAW glass compositions are discussed in Section 6.1.4.
- (c) The partition of the VHT modeling data set into modeling and validation subsets is described in Section 6.1.3.
- (d) The evaluation and validation statistics calculated for data-splits are defined the same as for separate modeling and validation sets. Section 6.1.2 describes how the data-splitting was accomplished.
- (e) For the full LM model, the “Others” component includes Ag<sub>2</sub>O, BaO, Br, CdO, Cs<sub>2</sub>O, I, La<sub>2</sub>O<sub>3</sub>, MnO, MoO<sub>3</sub>, NiO, PbO, Re<sub>2</sub>O<sub>7</sub>, SeO<sub>2</sub>, SrO, and “Unknown”.
- (f) Based on the 10 outlying glasses for which there were specific VHT alteration depths reported.
- (g) The number of VHT alteration depths, out of the six with reported “greater than” results, which were correctly predicted to be greater than the reported value.

**Table 6.8. Coefficients and Performance Summary for 11-Component Reduced Linear Mixture Model on the Natural Logarithm of ILAW VHT Alteration Depth.**

In(D) Reduced LM Model Term	Coefficient Estimate	Coefficient Stand. Dev.	Modeling Data Statistic, 165 Glasses <sup>(a)</sup>				Value
Al <sub>2</sub> O <sub>3</sub>	12.5230	8.0899	R <sup>2</sup>				0.514
B <sub>2</sub> O <sub>3</sub>	-2.6871	5.6945	R <sup>2</sup> Adjusted (R <sup>2</sup> <sub>A</sub> )				0.482
CaO	1.0430	4.8347	R <sup>2</sup> Predicted (R <sup>2</sup> <sub>P</sub> )				0.434
Fe <sub>2</sub> O <sub>3</sub>	-18.2629	5.5928	RMSE				1.152
K <sub>2</sub> O	37.4436	6.3782	Model LOF p-value				0.010
Li <sub>2</sub> O	102.1677	11.8551					
MgO	11.3749	10.1889	<b>Extrapolative Validation Statistic, 16 Outlying Glasses<sup>(a,b)</sup></b>				<b>Value</b>
Na <sub>2</sub> O	36.7381	3.4025	R <sup>2</sup> Validation (R <sup>2</sup> <sub>V</sub> ) <sup>(f)</sup>				-1.575
SiO <sub>2</sub>	-4.0480	2.2429	RMSE Validation (RMSE <sub>V</sub> ) <sup>(f)</sup>				0.935
ZrO <sub>2</sub>	-59.3073	10.1312	# Correct predicted > Values <sup>(g)</sup>				2 of 6
Others <sup>(e)</sup>	-6.2478	6.7119					
			<b>Data Partition Statistic, 92 Modeling &amp; 73 Validation<sup>(a,c)</sup></b>				<b>Value</b>
			R <sup>2</sup>				0.608
			R <sup>2</sup> Adjusted (R <sup>2</sup> <sub>A</sub> )				0.560
			R <sup>2</sup> Predicted (R <sup>2</sup> <sub>P</sub> )				0.477
			RMSE				1.109
			R <sup>2</sup> Validation (R <sup>2</sup> <sub>V</sub> )				0.337
			RMSE Validation (RMSE <sub>V</sub> )				1.228
<b>Data Splitting Statistic<sup>(a,d)</sup></b>							
	<b>DS1</b>	<b>DS2</b>	<b>DS3</b>	<b>DS4</b>	<b>DS5</b>	<b>Average</b>	
R <sup>2</sup>	0.501	0.551	0.529	0.528	0.524	0.527	
R <sup>2</sup> Adjusted (R <sup>2</sup> <sub>A</sub> )	0.460	0.514	0.491	0.490	0.485	0.488	
R <sup>2</sup> Predicted (R <sup>2</sup> <sub>P</sub> )	0.382	0.462	0.422	0.429	0.430	0.425	
RMSE	1.181	1.117	1.149	1.147	1.156	1.150	
R <sup>2</sup> Validation (R <sup>2</sup> <sub>V</sub> )	0.486	0.258	0.402	0.354	0.408	0.381	
RMSE Validation (RMSE <sub>V</sub> )	1.122	1.373	1.209	1.271	1.198	1.235	

- (a) The model evaluation statistics are defined in Section C.3 of Appendix C. Model validation statistics are defined in Section C.5 of Appendix C. A negative value for R<sup>2</sup><sub>V</sub> means that the sum of squares of model prediction errors is larger than if the mean response value over the validation data set were used as the predicted value for each glass. In other words, the model predicts worse for the validation data than the mean response value does.
- (b) The 10 outlying LAW glass compositions are discussed in Section 6.1.4.
- (c) The partition of the VHT modeling data set into modeling and validation subsets is described in Section 6.1.3.
- (d) The evaluation and validation statistics calculated for data-splits are defined the same as for separate modeling and validation sets. Section 6.1.2 describes how the data-splitting was accomplished.
- (e) For the reduced LM model, the “Others” component includes the original “Others” component (which contains Ag<sub>2</sub>O, BaO, Br, CdO, Cs<sub>2</sub>O, I, La<sub>2</sub>O<sub>3</sub>, MnO, MoO<sub>3</sub>, NiO, PbO, Re<sub>2</sub>O<sub>7</sub>, SeO<sub>2</sub>, SrO, and “Unknown”) plus Cl, Cr<sub>2</sub>O<sub>3</sub>, F, SO<sub>3</sub>, TiO<sub>2</sub>, and ZnO.
- (f) Based on the 10 outlying glasses for which there were specific VHT alteration depths reported.
- (g) The number of VHT alteration depths, out of the six with reported “greater than” results, which were correctly predicted to be greater than the reported value.

**Table 6.9. Coefficients and Performance Summary for 16-Term Reduced Partial Quadratic Mixture Model on the Natural Logarithm of ILAW VHT Alteration Depth.**

In(D) Reduced PQM Model Term	Coefficient Estimate	Coefficient Stand. Dev.	Modeling Data Statistic, 165 Glasses <sup>(a)</sup>				Value
Al <sub>2</sub> O <sub>3</sub>	66.1577	13.3921	R <sup>2</sup>				0.707
B <sub>2</sub> O <sub>3</sub>	5.2229	5.3054	R <sup>2</sup> Adjusted (R <sup>2</sup> <sub>A</sub> )				0.677
CaO	-233.0861	39.6386	R <sup>2</sup> Predicted (R <sup>2</sup> <sub>p</sub> )				0.647
Fe <sub>2</sub> O <sub>3</sub>	-5.2172	5.1010	RMSE				0.909
K <sub>2</sub> O	-33.5013	17.2534	Model LOF p-value				0.025
Li <sub>2</sub> O	111.8417	9.7959					
MgO	111.5235	18.2736					
Na <sub>2</sub> O	75.4548	6.4807	<b>Extrapolative Validation Statistic, 16 Outlying Glasses<sup>(a,b)</sup></b>				<b>Value</b>
SiO <sub>2</sub>	-29.0882	3.9323	R <sup>2</sup> Validation (R <sup>2</sup> <sub>v</sub> ) <sup>(f)</sup>				-3.770
ZrO <sub>2</sub>	77.6908	35.6541	RMSE Validation (RMSE <sub>v</sub> ) <sup>(f)</sup>				1.273
Others <sup>(c)</sup>	1.7371	5.8183	# Correct predicted > Values <sup>(g)</sup>				1 of 6
CaO×SiO <sub>2</sub>	556.6025	93.1812					
K <sub>2</sub> O×K <sub>2</sub> O	1605.6605	346.6207					
MgO×Na <sub>2</sub> O	-920.4672	171.9162					
Al <sub>2</sub> O <sub>3</sub> ×ZrO <sub>2</sub>	-1479.4599	479.4755					
Na <sub>2</sub> O×ZrO <sub>2</sub>	-336.1985	135.8857					
			<b>Data Partition Statistic, 92 Modeling &amp; 73 Validation<sup>(a,c)</sup></b>				<b>Value</b>
			R <sup>2</sup>				0.782
			R <sup>2</sup> Adjusted (R <sup>2</sup> <sub>A</sub> )				0.739
			R <sup>2</sup> Predicted (R <sup>2</sup> <sub>p</sub> )				0.681
			RMSE				0.854
			R <sup>2</sup> Validation (R <sup>2</sup> <sub>v</sub> )				0.561
			RMSE Validation (RMSE <sub>v</sub> )				0.999
<b>Data Splitting Statistic<sup>(a,d)</sup></b>							
	<b>DS1</b>	<b>DS2</b>	<b>DS3</b>	<b>DS4</b>	<b>DS5</b>	<b>Average</b>	
R <sup>2</sup>	0.697	0.737	0.710	0.711	0.723	0.716	
R <sup>2</sup> Adjusted (R <sup>2</sup> <sub>A</sub> )	0.659	0.704	0.673	0.675	0.688	0.680	
R <sup>2</sup> Predicted (R <sup>2</sup> <sub>p</sub> )	0.613	0.678	0.630	0.632	0.634	0.637	
RMSE	0.939	0.872	0.920	0.916	0.899	0.909	
R <sup>2</sup> Validation (R <sup>2</sup> <sub>v</sub> )	0.695	0.503	0.671	0.649	0.608	0.625	
RMSE Validation (RMSE <sub>v</sub> )	0.865	1.124	0.897	0.937	0.974	0.959	

- (a) The model evaluation statistics are defined in Section C.3 of Appendix C. Model validation statistics are defined in Section C.5 of Appendix C. A negative value for R<sup>2</sup><sub>v</sub> means that the sum of squares of model prediction errors is larger than if the mean response value over the validation data set were used as the predicted value for each glass. In other words, the model predicts worse for the validation data than the mean response value does.
- (b) The 10 outlying LAW glass compositions are discussed in Section 6.1.4.
- (c) The partition of the VHT modeling data set into modeling and validation subsets is described in Section 6.1.3.
- (d) The evaluation and validation statistics calculated for data-splits are defined the same as for separate modeling and validation sets. Section 6.1.2 describes how the data-splitting was accomplished.
- (e) For the reduced PQM model, the “Others” component includes the original “Others” component (which contains Ag<sub>2</sub>O, BaO, Br, CdO, Cs<sub>2</sub>O, I, La<sub>2</sub>O<sub>3</sub>, MnO, MoO<sub>3</sub>, NiO, PbO, Re<sub>2</sub>O<sub>7</sub>, SeO<sub>2</sub>, SrO, and “Unknown”) plus Cl, Cr<sub>2</sub>O<sub>3</sub>, F, SO<sub>3</sub>, TiO<sub>2</sub>, and ZnO.
- (f) Based on the 10 outlying glasses for which there were specific VHT alteration depths reported.
- (g) The number of VHT alteration depths, out of the six with reported “greater than” results, which were correctly predicted to be greater than the reported value.

**Table 6.10. Coefficients and Performance Summary for 22-Term Two-Part Reduced Linear Mixture Model on the Natural Logarithm of ILAW VHT Alteration Depth.**

ln(D) Two-Part Reduced LM Model Term	Below Cutoff (68.32 μm)		Above Cutoff (68.32 μm)		Modeling Data Statistic, 165 Glasses <sup>(a)</sup>		Value	
	Coefficient Estimate	Coefficient Stand. Dev.	Coefficient Estimate	Coefficient Stand. Dev.				
Al <sub>2</sub> O <sub>3</sub>	16.4460	7.5938	-0.8366	6.3122	R <sup>2</sup>			0.842
B <sub>2</sub> O <sub>3</sub>	-2.8297	4.3366	4.1860	5.7642	R <sup>2</sup> Adjusted (R <sup>2</sup> <sub>A</sub> )			0.819
CaO	6.3287	3.8290	-0.7089	6.4030	R <sup>2</sup> Predicted (R <sup>2</sup> <sub>p</sub> )			0.787
Fe <sub>2</sub> O <sub>3</sub>	-8.0141	4.7980	-5.3237	5.0702	RMSE			0.682
K <sub>2</sub> O	-0.3897	6.5885	24.3276	4.5937	Model LOF p-value			0.073
Li <sub>2</sub> O	52.6206	10.2419	47.5823	16.1605				
MgO	4.7055	8.6503	11.6210	10.9608				
Na <sub>2</sub> O	16.7874	3.1376	22.7643	3.7933				
SiO <sub>2</sub>	0.3389	1.8229	1.4056	2.0285				
ZrO <sub>2</sub>	-42.4660	10.7633	-18.4703	7.9208				
Others <sup>(c)</sup>	-5.7934	5.5882	0.2794	6.4240				
Summary Statistic	Below Cutoff Data	Based on Reduced LM Model	Above Cutoff Data	Based on Reduced LM Model	Extrapolative Validation Statistic, 16 Outlying Glasses <sup>(a,b)</sup>			
	R <sup>2</sup>	-0.490	0.601	-1.317	R <sup>2</sup> Validation (R <sup>2</sup> <sub>v</sub> )			-2.271
	R <sup>2</sup> Adjusted (R <sup>2</sup> <sub>A</sub> )	0.320	0.512		RMSE Validation (RMSE <sub>v</sub> ) <sup>(f)</sup>			1.054
	R <sup>2</sup> Predicted (R <sup>2</sup> <sub>p</sub> )	0.211	0.348		# Correct predicted > Values <sup>(g)</sup>			0 of 6
	RMSE	0.739	0.537		Data Partition Statistic, 92 Modeling & 73 Validation <sup>(a,c)</sup>			
					R <sup>2</sup>			0.857
					R <sup>2</sup> Adjusted (R <sup>2</sup> <sub>A</sub> )			0.814
					R <sup>2</sup> Predicted (R <sup>2</sup> <sub>p</sub> )			0.749
					RMSE			0.722
					R <sup>2</sup> Validation (R <sup>2</sup> <sub>v</sub> )			0.338
					RMSE Validation (RMSE <sub>v</sub> )			1.227
Data Splitting Statistic <sup>(a,d)</sup>	DS1	DS2	DS3	DS4	DS5	Average		
R <sup>2</sup>	0.835	0.862	0.844	0.844	0.848	0.846		
R <sup>2</sup> Adjusted (R <sup>2</sup> <sub>A</sub> )	0.804	0.836	0.814	0.814	0.819	0.818		
R <sup>2</sup> Predicted (R <sup>2</sup> <sub>p</sub> )	0.760	0.803	0.770	0.752	0.777	0.772		
RMSE	0.711	0.650	0.694	0.692	0.685	0.686		
R <sup>2</sup> Validation (R <sup>2</sup> <sub>v</sub> )	0.479	0.380	0.259	0.679	0.544	0.468		
RMSE Validation (RMSE <sub>v</sub> )	1.130	1.255	1.345	0.896	1.051	1.136		

(a) to (g) The footnotes in this table are the same as in Tables 6.7 to 6.9.

**Table 6.11. Coefficients and Performance Summary for 15-Term Reduced Partial Cubic Mixture Model on the Natural Logarithm of ILAW VHT Alteration Depth.**

In(D) Reduced Partial Cubic Mixture Model Term	Coefficient Estimate	Coefficient Stand. Dev.	Modeling Data Statistic, 165 Glasses <sup>(a)</sup>				Value
Al <sub>2</sub> O <sub>3</sub>	19.5685	6.0850	R <sup>2</sup>				0.744
B <sub>2</sub> O <sub>3</sub>	18.5336	5.9232	R <sup>2</sup> Adjusted (R <sup>2</sup> <sub>A</sub> )				0.720
CaO	38.2412	9.4479	R <sup>2</sup> Predicted (R <sup>2</sup> <sub>p</sub> )				0.696
Fe <sub>2</sub> O <sub>3</sub>	-8.4126	4.7225	RMSE				0.848
K <sub>2</sub> O	-39.3124	10.7075	Model LOF p-value				0.032
Li <sub>2</sub> O	-17.8250	20.0670					
MgO	-8.3068	8.0413					
Na <sub>2</sub> O	-20.6518	10.4755	<b>Extrapolative Validation Statistic, 16 Outlying Glasses<sup>(a,b)</sup></b>				<b>Value</b>
SiO <sub>2</sub>	-0.5137	2.2871	R <sup>2</sup> Validation (R <sup>2</sup> <sub>v</sub> ) <sup>(f)</sup>				-1.367
ZrO <sub>2</sub>	-62.8457	7.5911	RMSE Validation (RMSE <sub>v</sub> ) <sup>(f)</sup>				0.897
Others <sup>(e)</sup>	-0.4293	5.3481	# Correct predicted > Values <sup>(g)</sup>				2 of 6
(K <sub>2</sub> O) <sup>2</sup> ×Na <sub>2</sub> O	10138.2817	1198.5167					
(Na <sub>2</sub> O) <sup>3</sup>	872.6563	130.6419					
Li <sub>2</sub> O×Na <sub>2</sub> O×SiO <sub>2</sub>	2139.8048	387.6038	<b>Data Partition Statistic, 92 Modeling &amp; 73 Validation<sup>(a,c)</sup></b>				<b>Value</b>
B <sub>2</sub> O <sub>3</sub> ×CaO×Na <sub>2</sub> O	-1943.0687	773.3618	R <sup>2</sup>				0.799
			R <sup>2</sup> Adjusted (R <sup>2</sup> <sub>A</sub> )				0.762
			R <sup>2</sup> Predicted (R <sup>2</sup> <sub>p</sub> )				0.719
			RMSE				0.815
			R <sup>2</sup> Validation (R <sup>2</sup> <sub>v</sub> )				0.629
			RMSE Validation (RMSE <sub>v</sub> )				0.919
<b>Data Splitting Statistic<sup>(a,d)</sup></b>							
	<b>DS1</b>	<b>DS2</b>	<b>DS3</b>	<b>DS4</b>	<b>DS5</b>	<b>Average</b>	
R <sup>2</sup>	0.741	0.750	0.748	0.752	0.764	0.751	
R <sup>2</sup> Adjusted (R <sup>2</sup> <sub>A</sub> )	0.711	0.721	0.719	0.722	0.736	0.722	
R <sup>2</sup> Predicted (R <sup>2</sup> <sub>p</sub> )	0.674	0.695	0.680	0.693	0.707	0.690	
RMSE	0.864	0.847	0.854	0.846	0.828	0.848	
R <sup>2</sup> Validation (R <sup>2</sup> <sub>v</sub> )	0.730	0.676	0.694	0.656	0.628	0.677	
RMSE Validation (RMSE <sub>v</sub> )	0.813	0.908	0.865	0.928	0.950	0.893	

- (a) The model evaluation statistics are defined in Section C.3 of Appendix C. Model validation statistics are defined in Section C.5 of Appendix C. A negative value for R<sup>2</sup><sub>v</sub> means that the sum of squares of model prediction errors is larger than if the mean response value over the validation data set were used as the predicted value for each glass. In other words, the model predicts worse for the validation data than the mean response value does.
- (b) The 10 outlying LAW glass compositions are discussed in Section 6.1.4.
- (c) The partition of the VHT modeling data set into modeling and validation subsets is described in Section 6.1.3.
- (d) The evaluation and validation statistics calculated for data-splits are defined the same as for separate modeling and validation sets. Section 6.1.2 describes how the data-splitting was accomplished.
- (e) For the reduced partial cubic mixture model, the “Others” component includes the original “Others” component (which contains Ag<sub>2</sub>O, BaO, Br, CdO, Cs<sub>2</sub>O, I, La<sub>2</sub>O<sub>3</sub>, MnO, MoO<sub>3</sub>, NiO, PbO, Re<sub>2</sub>O<sub>7</sub>, SeO<sub>2</sub>, SrO, and “Unknown”) plus Cl, Cr<sub>2</sub>O<sub>3</sub>, F, SO<sub>3</sub>, TiO<sub>2</sub>, and ZnO.
- (f) Based on the 10 outlying glasses for which there were specific VHT alteration depths reported.
- (g) The number of VHT alteration depths, out of the six with reported “greater than” results, which were correctly predicted to be greater than the reported value.

**Table 6.12. Terms Included in Models Investigated for VHT Alteration Depth.**

Model Term <sup>(b)</sup>	Model Number <sup>(a)</sup>														
	1	2	3	4 <sup>(c)</sup>	5	6	7	8	9	10	11	12	13	14	15 <sup>(e)</sup>
Al <sub>2</sub> O <sub>3</sub>	x	x	x	x	x	x	x	x	x	x	x	x	x	x	x
B <sub>2</sub> O <sub>3</sub>	x	x	x	x	x	x	x	x	x	x	x	x	x	x	x
CaO	x	x	x	x	x	x	x	x	x	x	x	x	x	x	x
Cl	x	- <sup>(f)</sup>	-	-	-	-	-	-	-	-	-	-	-	-	-
Cr <sub>2</sub> O <sub>3</sub>	x	-	-	-	-	-	-	-	-	-	-	-	-	-	-
F	x	-	-	-	-	-	-	-	-	-	-	-	-	-	-
Fe <sub>2</sub> O <sub>3</sub>	x	x	x	x	-	x	-	x	x	x	x	x	x	x	x
K <sub>2</sub> O	x	x	x	x	x	x	x	x	x	x	x	x	x	x	x
Li <sub>2</sub> O	x	x	x	x	x	x	x	x	x	x	x	x	x	x	x
MgO	x	x	x	x	x	x	x	x	x	x	x	x	x	x	x
Na <sub>2</sub> O	x	x	x	x	x	x	x	x	x	x	x	x	x	x	x
P <sub>2</sub> O <sub>5</sub>	x	-	-	-	-	-	-	-	-	-	-	-	-	-	-
SO <sub>3</sub>	x	-	-	-	-	x	-	x	x	-	-	-	-	-	-
SiO <sub>2</sub>	x	x	x	x	x	x	x	x	x	x	x	x	x	x	x
TiO <sub>2</sub>	x	-	-	-	-	x	-	x	x	-	-	-	-	-	-
ZnO	x	-	-	-	-	x	-	x	x	-	-	-	-	-	-
ZrO <sub>2</sub>	x	x	x	x	-	x	-	x	x	x	x	x	x	x	x
Others18	x	-	-	-	-	-	-	-	-	-	-	-	-	-	-
Others14	-	-	-	-	-	x	-	x	x	-	-	-	-	-	-
Others11	-	x	x	x	-	-	-	-	-	x	x	x	x	x	x
Others9	-	-	-	-	x	-	x	-	-	-	-	-	-	-	-
(Al <sub>2</sub> O <sub>3</sub> ) <sup>2</sup>	-	-	-	-	x <sup>(d)</sup>	x <sup>(d)</sup>	-	-	-	-	-	-	-	-	-
(B <sub>2</sub> O <sub>3</sub> ) <sup>2</sup>	-	-	-	-	x	x <sup>(d)</sup>	-	-	-	-	-	-	-	-	-
(CaO) <sup>2</sup>	-	-	-	-	x	x	-	-	-	-	-	-	-	-	-
(Fe <sub>2</sub> O <sub>3</sub> ) <sup>2</sup>	-	-	-	-	-	x <sup>(d)</sup>	-	-	-	-	-	-	-	-	-
(K <sub>2</sub> O) <sup>2</sup>	-	-	x	-	x	x	x	x	x <sup>(d)</sup>	x	-	-	-	-	-
(Li <sub>2</sub> O) <sup>2</sup>	-	-	-	-	x	x	x	-	x <sup>(d)</sup>	-	-	-	-	-	-
(MgO) <sup>2</sup>	-	-	-	-	x <sup>(d)</sup>	x <sup>(d)</sup>	-	-	-	-	-	-	-	-	-
(Na <sub>2</sub> O) <sup>2</sup>	-	-	-	-	x	x	-	x	x <sup>(d)</sup>	x	-	-	-	-	-
(SO <sub>3</sub> ) <sup>2</sup>	-	-	-	-	-	x <sup>(d)</sup>	-	-	-	-	-	-	-	-	-
(SiO <sub>2</sub> ) <sup>2</sup>	-	-	-	-	x <sup>(d)</sup>	x <sup>(d)</sup>	x <sup>(d)</sup>	-	-	-	-	-	-	-	-
(TiO <sub>2</sub> ) <sup>2</sup>	-	-	-	-	-	x <sup>(d)</sup>	-	-	-	-	-	-	-	-	-
(ZnO) <sup>2</sup>	-	-	-	-	-	x <sup>(d)</sup>	-	-	-	-	-	-	-	-	-
(ZrO <sub>2</sub> ) <sup>2</sup>	-	-	-	-	-	x <sup>(d)</sup>	-	-	-	-	-	-	-	-	-
Al <sub>2</sub> O <sub>3</sub> ×K <sub>2</sub> O	-	-	-	-	-	-	x <sup>(d)</sup>	-	-	-	-	-	-	-	-
Al <sub>2</sub> O <sub>3</sub> ×SiO <sub>2</sub>	-	-	-	-	-	-	x <sup>(d)</sup>	-	-	-	-	-	-	-	-
Al <sub>2</sub> O <sub>3</sub> ×ZrO <sub>2</sub>	-	-	x	-	-	-	-	-	-	-	-	-	-	-	-
CaO×SiO <sub>2</sub>	-	-	x	-	-	-	-	-	-	-	-	-	-	-	-
K <sub>2</sub> O×SiO <sub>2</sub>	-	-	-	-	-	-	x	-	-	-	-	-	-	-	-
MgO×Na <sub>2</sub> O	-	-	x	-	-	-	-	-	-	-	-	-	-	-	-

- (a) The models associated with the model numbers are discussed in Section 6.7.
- (b) Mixed-component cubic terms are displayed as Al×Ca×Mg (denoting Al<sub>2</sub>O<sub>3</sub>×CaO×MgO) for space reasons.
- (c) The same 11 linear terms are used in both parts of the model for a total of 22 terms.
- (d) Nonsignificant quadratic terms based on single-term t-tests at 5% significance level. In a given model, removing some of such terms may result in others becoming statistically significant.
- (e) The same 11 linear terms are used to fit a local linear mixture model in the neighborhood of each glass in the modeling set.
- (f) Empty cell.



**Table 6.12. Terms Included in Models Investigated for VHT Alteration Depth (continued).**

Model Term <sup>(b)</sup>	Model Number <sup>(a)</sup>														
	1	2	3	4 <sup>(c)</sup>	5	6	7	8	9	10	11	12	13	14	15 <sup>(e)</sup>
Na <sub>2</sub> O×SiO <sub>2</sub>	-	-	-	-	-	-	x <sup>(d)</sup>	-	-	-	-	-	-	-	-
Na <sub>2</sub> O×ZrO <sub>2</sub>	-	-	x	-	-	-	-	-	-	-	-	-	-	-	-
(K <sub>2</sub> O) <sup>3</sup>	- <sup>(f)</sup>	-	-	-	-	-	-	-	x <sup>(d)</sup>	-	-	x	x	x	-
(Li <sub>2</sub> O) <sup>3</sup>	-	-	-	-	-	-	-	-	x <sup>(d)</sup>	-	-	-	-	-	-
(Na <sub>2</sub> O) <sup>3</sup>	-	-	-	-	-	-	-	x	x	x	x	-	-	-	-
Al×Ca×Mg	-	-	-	-	-	-	-	-	-	-	-	-	-	x	-
Al×K×Na	-	-	-	-	-	-	-	x	x	x	-	x	-	-	-
B×Ca×Na	-	-	-	-	-	-	-	-	-	-	x	x	x	x	-
B×Ca×Si	-	-	-	-	-	-	-	-	-	-	-	-	X	x	-
B×Na×Na	-	-	-	-	-	-	-	-	-	-	-	-	X	x	-
Ca×Ca×Na	-	-	-	-	-	-	-	-	-	-	-	-	-	x	-
Ca×Li×Li	-	-	-	-	-	-	-	-	-	-	-	x	x	x	-
Fe×K×Na	-	-	-	-	-	-	-	-	-	-	-	x	x	x	-
K×Li×Mg	-	-	-	-	-	-	-	-	-	-	-	-	x	x	-
K×K×Na	-	-	-	-	-	-	-	-	-	-	x	-	-	-	-
Li×Na×Si	-	-	-	-	-	-	-	-	-	-	x	-	-	-	-
<b># Terms</b>	18	11	16	22	17	27	16	18	21	15	15	16	18	20	11

- (a) The models associated with the model numbers are discussed in Section 6.7.
- (b) Mixed-component cubic terms are displayed as Al×Ca×Mg (denoting Al<sub>2</sub>O<sub>3</sub>×CaO×MgO) for space reasons.
- (c) The same 11 linear terms are used in both parts of the model for a total of 22 terms.
- (d) Nonsignificant quadratic terms based on single-term t-tests at 5% significance level. In a given model, removing some of such terms may result in others becoming statistically significant.
- (e) The same 11 linear terms are used to fit a local linear mixture model in the neighborhood of each glass in the modeling set.
- (f) Empty cell.

**Table 6.13. Summary of LAW VHT Model Fit and Validation Statistics for 165 Glasses and 80%/20% Data Splits.**

Model #	Model <sup>(a)</sup>	# Terms	Fit to Data for 165 LAW Glasses					Average over Five 80%/20% Data Splits					10 Outliers RMSE <sub>V</sub> <sup>(b)</sup>
			R <sup>2</sup>	R <sup>2</sup> <sub>A</sub>	R <sup>2</sup> <sub>P</sub>	RMSE	LOF p	R <sup>2</sup>	R <sup>2</sup> <sub>A</sub>	R <sup>2</sup> <sub>P</sub>	R <sup>2</sup> <sub>V</sub>	RMSE <sub>V</sub>	
1	Full LMM (18)	18	0.607	0.562	0.470	1.060	0.014	0.621	0.565	0.433	0.441	1.174	1.030
2	Reduced LMM (11)	11	0.514	0.482	0.434	1.152	0.010	0.527	0.488	0.425	0.381	1.235	0.935
3	PQMM (11 + 5)	16	0.707	0.677	0.647	0.909	0.025	0.716	0.680	0.637	0.625	0.959	1.273
4	Two-Part (11+ 11)	22	0.842	0.819	0.787	0.682	0.073	0.846	0.818	0.772	0.468	1.136	1.054
<b>VSL Preliminary Model Forms, with pre-selected (not statistically selected) higher-order terms</b>													
5	9 LMM + 8 Squared	17	0.633	0.594	0.533	1.021	0.016	0.644	0.595	0.512	0.534	1.060	1.701
6	14 LMM + 13 Squared	27	0.732	0.681	0.579	0.904	0.025	0.744	0.682	0.529	0.587	1.009	1.516
7	9 LMM + 7 Quadratic	16	0.594	0.553	0.474	1.070	0.013	0.610	0.561	0.464	0.399	1.214	1.062
8	14 LMM, 2 Quad, 2 Cubic	18	0.707	0.674	0.624	0.915	0.024	0.718	0.676	0.612	0.600	0.993	0.793
9	14 LMM, 3 Quad, 4 Cubic	21	0.727	0.689	0.640	0.893	0.026	0.737	0.691	0.624	0.616	0.972	0.787
<b>Partial Cubic Mixture Models</b>													
10	11 LMM, 2 Quad, 2 Cubic <sup>(c)</sup>	15	0.697	0.668	0.631	0.922	0.023	0.705	0.670	0.622	0.611	0.979	0.810
11	11 LMM + 4 Cubic <sup>(d)</sup>	15	0.744	0.720	0.696	0.848	0.032	0.751	0.722	0.690	0.677	0.893	0.897
12	11 LMM + 5 Cubic <sup>(d)</sup>	16	0.756	0.731	0.708	0.830	0.035	0.762	0.732	0.701	0.695	0.864	0.909
13	11 LMM + 7 Cubic <sup>(d)</sup>	18	0.780	0.754	0.725	0.794	0.041	0.787	0.756	0.716	0.702	0.856	1.024
14	11 LMM + 9 Cubic <sup>(d)</sup>	20	0.794	0.767	0.741	0.773	0.045	0.802	0.769	0.731	0.709	0.845	1.197
<b>Local Reduced Linear Mixture Models</b>													
15	Local Reduced LMMs	11 <sup>(e)</sup>	0.761	NC <sup>(f)</sup>	NC <sup>(f)</sup>	0.808	NC <sup>(f)</sup>	NC <sup>(f)</sup>	NC <sup>(f)</sup>	NC <sup>(f)</sup>	NC <sup>(f)</sup>	NC <sup>(f)</sup>	NC <sup>(f)</sup>

- (a) See Table 6.12 for the terms in each model. The following acronyms are used: LMM = linear mixture model and PQMM = partial quadratic mixture model.  
 (b) Based on the 10 outlying and non-representative glasses with VHT results that were left out of the modeling data set.  
 (c) This model contains the same quadratic and cubic terms as in Model 8 but with the reduced LMM terms.  
 (d) Quadratic terms were candidates (along with cubic terms) but were not selected by the statistical “variable selection” method.  
 (e) The reduced LMM (Model 2) form using 11 components was fit locally to the 50 closest glasses around each LAW glass.  
 (f) NC = not calculated. See Section 6.6.2 for discussion.

**Table 6.14. Summary of LAW VHT Model Fit (92 Glasses) and Validation Statistics (73 Glasses) from Partitioning the 165 Glasses with VHT Data.**

Model #	Model <sup>(a)</sup>	# Terms	Fit to Data for 92 LAW Glasses					Validation Statistics for 73 Glasses	
			R <sup>2</sup>	R <sup>2</sup> <sub>A</sub>	R <sup>2</sup> <sub>P</sub>	RMSE	LOF p	R <sup>2</sup> <sub>V</sub>	RMSE <sub>V</sub>
1	Full LMM (18)	18	0.699	0.629	0.469	1.018	0.016	-17.971	6.570
2	Reduced LMM (11)	11	0.608	0.560	0.477	1.109	0.011	0.337	1.228
3	PQMM (11 + 5)	16	0.782	0.739	0.681	0.854	0.030	0.561	0.999
4	Two-Part (11+ 11)	22	0.857	0.814	0.749	0.722	0.055	0.338	1.227
<b>VSL Preliminary Model Forms, with pre-selected (not statistically selected) higher-order terms</b>									
5	9 LMM + 8 Squared	17	0.680	0.612	0.497	1.042	0.014	0.497	1.070
6	14 LMM + 13 Squared	27	0.824	0.753	0.573	0.831	0.033	0.303	1.259
7	9 LMM + 7 Quadratic	16	0.652	0.584	0.452	1.079	0.013	0.463	1.105
8	14 LMM, 2 Quad, 2 Cubic	18	0.753	0.697	0.598	0.921	0.023	0.552	1.010
9	14 LMM, 3 Quad, 4 Cubic	21	0.789	0.730	0.643	0.869	0.028	0.496	1.071
<b>Partial Cubic Mixture Models</b>									
10	11 LMM, 2 Quad, 2 Cubic <sup>(b)</sup>	15	0.736	0.688	0.616	0.935	0.022	0.605	0.949
11	11 LMM + 4 Cubic <sup>(c)</sup>	15	0.799	0.762	0.719	0.815	0.036	0.629	0.919
12	11 LMM + 5 Cubic <sup>(c)</sup>	16	0.825	0.791	0.749	0.765	0.045	0.629	0.919
13	11 LMM + 7 Cubic <sup>(c)</sup>	18	0.847	0.812	0.765	0.725	0.054	0.641	0.904
14	11 LMM + 9 Cubic <sup>(c)</sup>	20	0.859	0.822	0.780	0.705	0.060	0.658	0.882
<b>Local Reduced Linear Mixture Models</b>									
15	Local Reduced LMMs	11 <sup>(d)</sup>	NC <sup>(e)</sup>	NC <sup>(e)</sup>	NC <sup>(e)</sup>	NC <sup>(e)</sup>	NC <sup>(e)</sup>	NC <sup>(e)</sup>	NC <sup>(e)</sup>

- (a) See Table 6.12 for the terms in each model. The following acronyms are used: LMM = linear mixture model and PQMM = partial quadratic mixture model.
- (b) This model contains the same quadratic and cubic terms as in Model 8 but with the reduced LMM terms.
- (c) The cubic terms included in the model are the same ones selected using all 165 LAW glasses as described in the corresponding model of Table 6.13. See Table 6.12 for a listing of the cubic terms. Note that because the cubic terms were not optimally selected based on the 92 Phase 1 glasses, some of the terms were non-significant in some of these models.
- (d) The local reduced LMM using 11 components was not fitted (using the 50 closest glasses around each glass) and validated because of insufficient data and impact on the results with the 92-glass subset of the modeling set.
- (e) NC = not calculated.

**Table 6.15. Performance of Fitted Models Predicting (for the Modeling Data) Whether VHT Alteration Depths are Above or Below the Limit of 453  $\mu\text{m}$  Corresponding to 50  $\text{g}/\text{m}^2/\text{day}$**

Model #	Model <sup>(d)</sup>	# Terms	Model Predictions <sup>(a)</sup>				95% SUCIs <sup>(b)</sup>				95% UPIs <sup>(c)</sup>				
			# Below Limit		# Above Limit		# Below Limit		# Above Limit		# Below Limit		# Above Limit		
			Predicted Below	Predicted Above	Predicted Below	Predicted Above	Predicted Below	Predicted Above	Predicted Below	Predicted Above	Predicted Below	Predicted Above	Predicted Below	Predicted Above	
1	Full LMM (18)	18	151	0	10	4	148	3	9	5	121	30	0	14	
2	Reduced LMM (11)	11	151	0	13	1	147	4	10	4	121	30	0	14	
3	PQMM (11 + 5)	16	151	0	6	8	150	1	4	10	132	19	1	13	
4	Two-Part (11+ 11)	22	151	0	11	3	148	3	6	8	125	26	0	14	
<b>VSL Preliminary Model Forms, with pre-selected (not statistically selected) higher-order terms</b>															
5	9 LMM + 8 Squared	17	149	2	8	6	148	3	5	9	128	23	0	14	
6	14 LMM + 13 Squared	27	150	1	7	7	148	3	4	10	131	20	0	14	
7	9 LMM + 7 Quadratic	16	149	2	11	3	147	4	5	9	127	24	0	14	
8	14 LMM, 2 Quad, 2 Cubic	18	149	2	5	9	149	2	5	9	134	17	0	14	
9	14 LMM, 3 Quad, 4 Cubic	21	149	2	5	9	149	2	4	10	136	15	0	14	
<b>Partial Cubic Mixture Models</b>															
10	11 LMM, 2 Quad, 2 Cubic <sup>(e)</sup>	15	149	2	5	9	149	2	5	9	136	15	0	14	
11	11 LMM + 4 Cubic <sup>(f)</sup>	15	149	2	6	8	149	2	3	11	135	16	0	14	
12	11 LMM + 5 Cubic <sup>(f)</sup>	16	150	1	6	8	148	3	4	10	136	15	0	14	
13	11 LMM + 7 Cubic <sup>(f)</sup>	18	149	2	6	8	147	4	4	10	135	16	1	13	
14	11 LMM + 9 Cubic <sup>(f)</sup>	20	149	2	5	9	148	3	4	10	135	16	1	13	
<b>Local Reduced Linear Mixture Models</b>															
15	Local Reduced LMMs	11 <sup>(g)</sup>	148	3	4	10	NC <sup>(h)</sup>	NC	NC	NC	NC	NC	NC	NC	

- (a) The results are based on model predicted values without accounting for model uncertainty.  
 (b) The results are based on 95% simultaneous upper confidence intervals (95% SUCIs) to account for model uncertainty. See Section C.7 of Appendix C.  
 (c) The results are based on 95% upper prediction intervals (95% UPIs) to account for model uncertainty. See Section C.7 of Appendix C.  
 (d) See Table 6.12 for the terms in each model. The following acronyms are used: LMM = linear mixture model and PQMM = partial quadratic mixture model.  
 (e) This model contains the same quadratic and cubic terms as in Model 8 but with the reduced LMM terms.  
 (f) Quadratic terms were candidates (along with cubic terms) but were not selected by the statistical “variable selection” method.  
 (g) Separate 11-term reduced LMMs were fit using the 50 closest points to each glass in the modeling set to obtain the model-predicted  $D$  values and determine whether they are below or above the limit.  
 (h) NC = not calculated.

**Table 6.16. Performance of Fitted ILAW VHT Alteration Depth Models Below and Above a Cut-Off Value.<sup>(a)</sup>**

Model #	Model <sup>(b)</sup>	# Terms	RMSE	
			Below Cutoff	Above Cutoff
1	Full LMM (18)	18	0.9804	1.0380
2	Reduced LMM (11)	11	1.0887	1.1595
3	PQMM (11 + 5)	16	0.8611	0.8703
4	Two-Part (11+ 11)	22	0.7390	0.5369
<b>VSL Preliminary Model Forms, with pre-selected (not statistically selected) higher-order terms</b>				
5	9 LMM + 8 Squared	17	0.9319	1.0317
6	14 LMM + 13 Squared	27	0.8236	0.8335
7	9 LMM + 7 Quadratic	16	0.9309	1.1668
8	14 LMM, 2 Quad, 2 Cubic	18	0.8004	0.9750
9	14 LMM, 3 Quad, 4 Cubic	21	0.7690	0.9476
<b>Partial Cubic Mixture Models</b>				
10	11 LMM, 2 Quad, 2 Cubic	15	0.8095	1.0015
11	11 LMM + 4 Cubic	15	0.7651	0.8867
12	11 LMM + 5 Cubic	16	0.7585	0.8448
13	11 LMM + 7 Cubic	18	0.7193	0.8039
14	11 LMM + 9 Cubic	20	0.6904	0.7866
<b>Local Reduced Linear Mixture Models</b>				
15	Local Reduced LMMs	11	NC <sup>(c)</sup>	NC

- (a) The cutoff value for VHT alteration depth ( $D$ ) is 68.3254  $\mu\text{m}$ , which was selected for the two-part model. For this investigation, the cutoff represents the value above which most models tend to under predict the VHT alteration depth. Hence, it is desirable to see how different models perform below and above the cutoff value.
- (b) The models are the same as described in Tables 6.13, 6.14, and 6.15. The following acronyms are used: LMM = linear mixture model and PQMM = partial quadratic mixture model.
- (c) NC = not calculated.

**Table 6.17. LAWA126 Composition in Formats Needed for Use in ILAW VHT Models.**

<b>Model Term</b>	<b>LAWA126 Composition<sup>(a)</sup> (wt%)</b>	<b>LAWA126 Composition (mass fractions) for Use in VHT LM Model<sup>(b)</sup></b>	<b>LAWA126 Composition (mass fractions) for Use in VHT PQM Model<sup>(c)</sup></b>	<b>LAWA126 Composition (mass fractions) for Use in VHT PCM Model<sup>(d)</sup></b>
Al <sub>2</sub> O <sub>3</sub>	0.05637	0.05637	0.05637	0.05637
B <sub>2</sub> O <sub>3</sub>	0.09815	0.09815	0.09815	0.09815
CaO	0.01989	0.01989	0.01989	0.01989
Cl	0.00200	NA <sup>(e)</sup>	NA	NA
Cr <sub>2</sub> O <sub>3</sub>	0.00020	NA	NA	NA
F	0.00300	NA	NA	NA
Fe <sub>2</sub> O <sub>3</sub>	0.05537	0.05537	0.05537	0.05537
K <sub>2</sub> O	0.03878	0.03878	0.03878	0.03878
Li <sub>2</sub> O	0.00000	0.00000	0.00000	0.00000
MgO	0.01479	0.01479	0.01479	0.01479
Na <sub>2</sub> O	0.18451	0.18451	0.18451	0.18451
P <sub>2</sub> O <sub>5</sub>	0.00080	NA	NA	NA
SO <sub>3</sub>	0.00310	NA	NA	NA
SiO <sub>2</sub>	0.44098	0.44098	0.44098	0.44098
TiO <sub>2</sub>	0.01999	NA	NA	NA
ZnO	0.02959	NA	NA	NA
ZrO <sub>2</sub>	0.02989	0.02989	0.02989	0.02989
Others	0.00260	0.06127	0.06127	0.06127
CaO×SiO <sub>2</sub>	NA	NA	0.0087711	NA
K <sub>2</sub> O×K <sub>2</sub> O	NA	NA	0.0015039	NA
MgO×Na <sub>2</sub> O	NA	NA	0.0027293	NA
Al <sub>2</sub> O <sub>3</sub> ×ZrO <sub>2</sub>	NA	NA	0.0016847	NA
NaO <sub>2</sub> ×ZrO <sub>2</sub>	NA	NA	0.0055140	NA
(K <sub>2</sub> O) <sup>2</sup> ×Na <sub>2</sub> O	NA	NA	NA	0.0002775
(Na <sub>2</sub> O) <sup>3</sup>	NA	NA	NA	0.0062812
Li <sub>2</sub> O×Na <sub>2</sub> O×SiO <sub>2</sub>	NA	NA	NA	0.0000000
B <sub>2</sub> O <sub>3</sub> ×CaO×Na <sub>2</sub> O	NA	NA	NA	0.0003602

- (a) The composition in mass fractions is from Table 6.2.  
 (b) See Table 6.8.  
 (c) See Table 6.9.  
 (d) See Table 6.11.  
 (e) NA = not applicable, because the model does not contain this term.

**Table 6.18. Predicted VHT Alteration Depths and Corresponding 90% UCIs and 95% SUCIs for LAWA126 Composition Used in ILAW VHT Models.**

<b>Model<sup>(a)</sup></b>	<b>Predicted VHT <math>\ln(D)</math> [<math>\ln(\mu\text{m})</math>]</b>	<b>Predicted VHT <math>D</math><sup>(b)</sup> [<math>\mu\text{m}</math>]</b>	<b>Standard Deviation of Predicted VHT <math>\ln(D)</math><sup>(c)</sup> [<math>\ln(\mu\text{m})</math>]</b>	<b>90% UCI on Mean VHT <math>\ln(D)</math> [<math>\ln(\mu\text{m})</math>]</b>	<b>90% UCI on Median VHT <math>D</math> [<math>\mu\text{m}</math>]</b>	<b>95% SUCI on Mean VHT <math>\ln(D)</math> [<math>\ln(\mu\text{m})</math>]</b>	<b>95% SUCI on Median VHT <math>D</math> [<math>\mu\text{m}</math>]</b>
11-Term VHT LM Model	3.9100 <sup>(d)</sup>	49.90	0.1866	4.1502	63.45	4.6961	109.52
16-Term VHT PQM Model	3.6287	37.66	0.1526	3.8251	45.84	4.3807	79.90
15-Term VHT PCM Model	3.2227	25.09	0.1561	3.4236	30.68	3.9712	53.05

- (a) The three models in this column are given in Tables 6.8, 6.9, and 6.16, respectively. Note that LM = linear mixture, PQM = partial quadratic mixture, and PCM = partial cubic mixture.
- (b) Of the three models, the one with the predicted VHT  $D$  value closest to the measured value of 22  $\mu\text{m}$  is the 15-term PCM model.
- (c) The standard deviation is for the VHT  $\ln(D)$  prediction considered to be the mean of such values for the LAWA126 glass.
- (d) All calculations were performed using the LAWA126 glass composition, model coefficients, and variance-covariance matrix values given in tables of this report. The calculated  $\ln(\mu\text{m})$  values were rounded to four decimal places in this table. The  $\mu\text{m}$  values were calculated by exponentiating the  $\ln(\mu\text{m})$  values before rounding, then rounding the resulting values to two decimal places in this table.

**Table 7.1. Ten LAW Glasses Excluded from the Electrical Conductivity and Viscosity Modeling Data Sets.**

<b>Glass ID</b>	<b>Reason Glass Excluded from Electrical Conductivity and Viscosity Modeling Sets</b>
LAWA43-1	Outlying composition ( $\text{Al}_2\text{O}_3 = 12 \text{ wt}\%$ )
LAWA49	Outlying composition ( $\text{Fe}_2\text{O}_3 = 9.98 \text{ wt}\%$ )
LAWA50	Outlying composition ( $\text{Fe}_2\text{O}_3 = 11.98 \text{ wt}\%$ )
LAWA82	Outlying composition ( $\text{TiO}_2 = 3.99 \text{ wt}\%$ )
LAWA89	Outlying composition ( $\text{TiO}_2 = 3.98 \text{ wt}\%$ )
LAWB60	Outlying composition ( $\text{CaO} = 11.91 \text{ wt}\%$ )
LAWB62	Outlying composition ( $\text{CaO} = 12.00 \text{ wt}\%$ )
LAWB63	Outlying composition ( $\text{ZnO} = 5.82 \text{ wt}\%$ )
LAWB82	Outlying composition ( $\text{Fe}_2\text{O}_3 = 9.52 \text{ wt}\%$ )
LAWC12	Outlying composition ( $\text{Al}_2\text{O}_3 = 11.99 \text{ wt}\%$ , $\text{TiO}_2 = 3.42 \text{ wt}\%$ )



**Table 7.2. Normalized<sup>(a)</sup> Compositions (mass fractions) of 171 LAW Glasses Used for Electrical Conductivity and Viscosity Model Development.**

Glass ID	Group ID <sup>(b)</sup>	Al <sub>2</sub> O <sub>3</sub>	B <sub>2</sub> O <sub>3</sub>	CaO	Cl	Cr <sub>2</sub> O <sub>3</sub>	F	Fe <sub>2</sub> O <sub>3</sub>	K <sub>2</sub> O	Li <sub>2</sub> O	MgO	Na <sub>2</sub> O	P <sub>2</sub> O <sub>5</sub>	XRF SO <sub>3</sub> <sup>(c)</sup>	SiO <sub>2</sub>	TiO <sub>2</sub>	ZnO	ZrO <sub>2</sub>	Others	Sum <sup>(d)</sup>
LAWA44R10	ExPh1	.06202	.08903	.01991	.00650	.00020	.00010	.06982	.00500	.00000	.01991	.20006	.00030	.00090	.44563	.01991	.02971	.02991	.00110	1.00000
LAWA53	ExPh1	.06145	.06165	.07840	.00646	.00020	.00010	.07467	.00494	.00000	.01473	.19898	.00030	.00620	.42036	.01100	.02977	.02977	.00101	1.00000
LAWA56	ExPh1	.06151	.12050	.01970	.00646	.00020	.00010	.07474	.00495	.00000	.01475	.19918	.00030	.00520	.42079	.01101	.02980	.02980	.00101	1.00000
LAWA88	ExPh1	.06082	.09700	.01991	.00330	.00010	.00000	.05532	.02581	.00000	.01475	.20006	.00070	.00190	.44004	.01991	.02951	.02987	.00100	1.00000
LAWA102R1	ExPh1	.06040	.09968	.05044	.00329	.00020	.00030	.05383	.00259	.02492	.01485	.14503	.00130	.00670	.46350	.01136	.03050	.03010	.00101	1.00000
LAWA126	ExPh1	.05637	.09815	.01989	.00200	.00020	.00300	.05537	.03878	.00000	.01479	.18451	.00080	.00310	.44098	.01999	.02959	.02989	.00260	1.00000
LAWA128R1	ExPh1	.06026	.07065	.02079	.00200	.00020	.00300	.05786	.03877	.00000	.01179	.18447	.00080	.00320	.46058	.02089	.03088	.03128	.00260	1.00000
LAWA130	ExPh1	.06025	.08943	.02078	.00200	.00020	.00300	.02858	.03877	.00000	.01179	.18445	.00080	.00330	.46053	.02088	.04137	.03127	.00260	1.00000
LAWB65	ExPh1	.06188	.09939	.06690	.00000	.00100	.00070	.05295	.00261	.04303	.02969	.05476	.00010	.00890	.48492	.01394	.04664	.03159	.00100	1.00000
LAWB66	ExPh1	.06203	.09963	.08214	.00000	.00101	.00070	.05308	.00261	.04313	.02976	.05489	.00010	.00650	.48609	.01397	.03167	.03167	.00101	1.00000
LAWB68	ExPh1	.06192	.08440	.08199	.00000	.00100	.00070	.05299	.00261	.04305	.02970	.05479	.00010	.00830	.48521	.01395	.04666	.03161	.00100	1.00000
LAWB78	ExPh1	.06161	.12351	.07132	.00010	.00050	.00080	.03256	.00230	.03055	.02975	.09797	.00050	.00510	.47080	.00000	.04007	.03155	.00100	1.00000
LAWB79	ExPh1	.06156	.12342	.07127	.00010	.00050	.00080	.03253	.00230	.03514	.02973	.08629	.00050	.00580	.47748	.00000	.04004	.03153	.00100	1.00000
LAWB80	ExPh1	.06156	.12341	.07126	.00010	.00050	.00080	.03253	.01992	.03513	.02973	.06626	.00050	.00580	.47993	.00000	.04004	.03153	.00100	1.00000
LAWB83	ExPh1	.06183	.10035	.06783	.00010	.00040	.00060	.05293	.00190	.04312	.02971	.05473	.00040	.00490	.48624	.01391	.04842	.03162	.00100	1.00000
LAWB84	ExPh1	.06187	.10041	.06687	.00010	.00040	.00060	.05296	.00190	.04405	.02973	.05476	.00040	.00440	.48654	.01392	.04845	.03163	.00100	1.00000
LAWB85	ExPh1	.06184	.11527	.05283	.00010	.00040	.00060	.05293	.00190	.04313	.02972	.05473	.00040	.00490	.48629	.01391	.04843	.03162	.00100	1.00000
LAWB86	ExPh1	.06188	.12426	.05737	.00010	.00040	.00060	.05297	.00190	.04356	.02974	.05477	.00040	.00430	.48664	.00000	.04846	.03164	.00100	1.00000
C100-G-136B	ExPh1	.06127	.10092	.06408	.00120	.00020	.00060	.06478	.00150	.02733	.01512	.11874	.00120	.00400	.46726	.01121	.03014	.03024	.00020	1.00000
LAWC27	ExPh1	.06117	.12183	.08544	.00111	.00018	.00054	.00009	.00136	.02733	.01500	.11953	.00106	.00410	.48868	.01121	.03018	.03018	.00101	1.00000
LAWC32	ExPh1	.06490	.10047	.09038	.00111	.00018	.00054	.02424	.00136	.02734	.01501	.11956	.00106	.00380	.46744	.01121	.04019	.03019	.00101	1.00000
LAWM1	Ph1	.09044	.06029	.10048	.00020	.00008	.00008	.08039	.04019	.04522	.00000	.05024	.00013	.00520	.44666	.03015	.05024	.00000	.00002	1.00000
LAWM2	Ph1	.03512	.06020	.10033	.00803	.00322	.00300	.08027	.00000	.04515	.05017	.05017	.00501	.00670	.47157	.03010	.05017	.00000	.00080	1.00000
LAWM3	Ph1	.09033	.06022	.10036	.00020	.00008	.00008	.08029	.00000	.04487	.05018	.11521	.00013	.00640	.40145	.00000	.01004	.04015	.00002	1.00000
LAWM4	Ph1	.03516	.13058	.10044	.00020	.00008	.00008	.05560	.04018	.04520	.00000	.05022	.00013	.00560	.41599	.03013	.05022	.04018	.00002	1.00000
LAWM5	Ph1	.09041	.06027	.05794	.00020	.00008	.00008	.08036	.04018	.04520	.00000	.05023	.00013	.00550	.48903	.03014	.01005	.04018	.00002	1.00000
LAWM6	Ph1	.09002	.10612	.10002	.00020	.00008	.00007	.08002	.04001	.00000	.05001	.08999	.00012	.00320	.40009	.03001	.01000	.00000	.00002	1.00000
LAWM7	Ph1	.05441	.06966	.10028	.00020	.00008	.00008	.08023	.00000	.02585	.05014	.05014	.00013	.00720	.52147	.03008	.01003	.00000	.00002	1.00000
LAWM8	Ph1	.09027	.13039	.06448	.00803	.00322	.00300	.00000	.00000	.02087	.05015	.05015	.00501	.00700	.44626	.03009	.05015	.04012	.00080	1.00000
LAWM9	Ph1	.03506	.06010	.10016	.00801	.00322	.00300	.08013	.04006	.02392	.00000	.05008	.00500	.00240	.49792	.00000	.05008	.04006	.00080	1.00000
LAWM10	Ph1	.09005	.13007	.10006	.00801	.00322	.00300	.00000	.00000	.04503	.00000	.13074	.00499	.00230	.40170	.03002	.01001	.04002	.00080	1.00000
LAWM11	Ph1	.03504	.13013	.09413	.00020	.00008	.00007	.05317	.04004	.04505	.00000	.11491	.00012	.00900	.46804	.00000	.01001	.00000	.00002	1.00000
LAWM12	Ph1	.03501	.13005	.00000	.00801	.00322	.00300	.02310	.04002	.04502	.01971	.14259	.00499	.00230	.42215	.03001	.05002	.04002	.00080	1.00000

- (a) The compositions listed in this table are normalized mass fraction versions of target compositions of the glasses, after replacing the target values of SO<sub>3</sub> by XRF analyzed (or estimated analyzed) values. See Section 3.3 for the details.
- (b) The Group IDs are described in Sections 2.1 to 2.6.
- (c) XRF SO<sub>3</sub> denotes that the SO<sub>3</sub> composition is based on chemical analysis by XRF. For most glasses SO<sub>3</sub> was directly measured by XRF, but for some glasses estimated XRF values were used (see Section 3.3).
- (d) The normalized component mass fractions listed in this table were rounded to five decimals, and may not sum exactly to 1.00000 as listed. However, complete compositions listed to more decimal places and summing to 1.0000 were used for property-composition modeling.

**Table 7.2. Normalized<sup>(a)</sup> Compositions (mass fractions) of 171 LAW Glasses Used for Electrical Conductivity and Viscosity Model Development (continued).**

Glass ID	Group ID <sup>(b)</sup>	Al <sub>2</sub> O <sub>3</sub>	B <sub>2</sub> O <sub>3</sub>	CaO	Cl	Cr <sub>2</sub> O <sub>3</sub>	F	Fe <sub>2</sub> O <sub>3</sub>	K <sub>2</sub> O	Li <sub>2</sub> O	MgO	Na <sub>2</sub> O	P <sub>2</sub> O <sub>5</sub>	XRF SO <sub>3</sub> <sup>(c)</sup>	SiO <sub>2</sub>	TiO <sub>2</sub>	ZnO	ZrO <sub>2</sub>	Others	Sum <sup>(d)</sup>
LAWM13	Ph1	.03501	.06001	.10002	.00412	.00165	.00154	.08002	.03785	.00000	.00000	.22005	.00257	.00500	.40009	.03001	.02164	.00000	.00041	1.00000
LAWM14	Ph1	.03500	.06000	.02045	.00020	.00008	.00007	.00000	.00000	.00881	.05000	.21999	.00012	.00530	.51997	.03000	.05000	.00000	.00002	1.00000
LAWM15	Ph1	.08999	.09356	.00000	.00800	.00321	.00299	.06283	.00000	.00000	.03724	.21998	.00499	.00170	.43471	.03000	.01000	.00000	.00080	1.00000
LAWM16	Ph1	.08006	.12008	.08006	.00020	.00008	.00007	.06505	.00100	.03002	.01001	.10007	.00012	.00330	.42480	.02502	.05004	.01001	.00002	1.00000
LAWM17	Ph1	.05002	.12004	.02215	.00020	.00008	.00007	.06502	.02001	.00500	.03501	.17006	.00012	.00200	.42015	.00500	.05002	.03501	.00002	1.00000
LAWM18	Ph1	.08005	.12007	.08005	.00801	.00322	.00300	.06504	.00100	.03002	.01001	.10006	.00499	.00340	.42025	.02502	.02001	.02501	.00080	1.00000
LAWM19	Ph1	.07997	.11996	.07997	.00800	.00321	.00299	.01999	.01999	.00500	.01000	.13170	.00499	.00360	.41986	.00500	.04998	.03499	.00080	1.00000
LAWM20	Ph1	.05001	.07002	.08002	.00800	.00321	.00299	.02001	.02001	.02265	.03501	.17004	.00499	.00210	.42011	.00500	.05001	.03501	.00080	1.00000
LAWM21	Ph1	.05005	.10901	.08008	.00020	.00008	.00007	.06507	.02002	.03003	.01001	.10010	.00012	.00460	.42042	.02503	.05005	.03504	.00002	1.00000
LAWM22	Ph1	.07990	.06992	.01998	.00799	.00321	.00299	.06492	.01998	.00499	.03496	.16979	.00498	.00450	.41949	.00670	.04994	.03496	.00080	1.00000
LAWM23	Ph1	.05011	.07015	.08018	.00802	.00322	.00300	.02004	.02004	.03007	.01002	.10022	.00500	.00340	.48547	.02506	.05011	.03508	.00080	1.00000
LAWM24	Ph1	.08000	.12001	.02000	.00020	.00008	.00007	.06500	.02000	.00641	.01000	.17001	.00012	.00230	.47076	.00500	.02000	.01000	.00002	1.00000
LAWM25R1	Ph1	.08011	.12017	.02003	.00801	.00322	.00300	.03684	.02003	.03004	.03505	.10014	.00500	.00260	.49991	.00501	.02003	.01001	.00080	1.00000
LAWM26	Ph1	.08006	.12008	.04970	.00801	.00322	.00300	.02001	.00100	.03002	.01001	.10007	.00499	.00490	.49909	.00500	.05004	.01001	.00080	1.00000
LAWM27	Ph1	.08006	.07005	.08006	.00801	.00322	.00300	.06505	.02001	.00500	.03502	.13381	.00499	.00250	.42030	.02502	.03309	.01001	.00080	1.00000
LAWM28	Ph1	.05010	.12024	.08016	.00020	.00008	.00008	.06513	.00703	.00690	.01002	.10020	.00013	.00360	.50101	.02505	.02004	.01002	.00002	1.00000
LAWM29	Ph1	.07565	.07006	.02002	.00077	.00031	.00029	.06506	.02002	.03003	.03503	.10009	.00048	.00310	.46892	.02502	.05005	.03503	.00008	1.00000
LAWM30	Ph1	.08003	.12004	.02001	.00020	.00008	.00007	.06502	.00100	.02023	.01000	.17006	.00012	.00200	.42015	.00592	.05002	.03501	.00002	1.00000
LAWM31	Ph1	.05002	.07003	.08003	.00801	.00322	.00300	.06502	.00100	.03001	.01000	.16758	.00499	.00300	.42327	.02501	.02001	.03501	.00080	1.00000
LAWM32	Ph1	.05146	.07002	.02001	.00800	.00321	.00299	.02001	.02001	.03001	.03501	.16514	.00499	.00320	.50013	.00500	.05001	.01000	.00080	1.00000
LAWM33R1	Ph1	.05002	.12005	.08003	.00020	.00008	.00007	.06503	.01722	.00899	.01000	.17007	.00012	.00290	.42017	.02501	.02001	.01000	.00002	1.00000
LAWM34	Ph1	.05001	.08356	.08002	.00020	.00008	.00007	.06295	.02001	.03001	.01000	.17005	.00012	.00300	.42012	.01474	.02001	.03501	.00002	1.00000
LAWM35	Ph1	.05003	.12007	.06182	.00801	.00322	.00300	.04413	.00100	.00500	.03502	.17010	.00499	.00180	.42023	.02501	.02001	.02576	.00080	1.00000
LAWM36	Ph1	.07002	.11004	.07002	.00318	.00128	.00119	.05002	.00300	.02501	.01501	.12004	.00198	.00370	.45016	.02001	.03501	.02001	.00032	1.00000
LAWM37	Ph1	.06751	.11009	.07006	.00020	.00008	.00007	.05004	.00300	.02502	.02502	.12010	.00012	.00320	.45038	.01001	.03503	.03003	.00002	1.00000
LAWM38	Ph1	.06998	.07998	.06998	.00800	.00321	.00299	.02999	.00154	.02499	.01500	.13997	.00499	.00370	.47988	.01000	.03499	.02000	.00080	1.00000
LAWM39	Ph1	.07007	.09063	.05005	.00801	.00322	.00300	.03003	.00100	.02502	.02502	.14013	.00499	.00250	.48046	.01001	.03503	.02002	.00080	1.00000
LAWM40	Ph1	.06003	.11006	.05003	.00214	.00086	.00080	.05003	.00100	.01001	.01501	.14008	.00133	.00310	.48027	.01001	.03502	.03002	.00021	1.00000
LAWM41	Ph1	.07002	.08002	.07002	.00800	.00321	.00299	.05001	.00300	.01000	.02501	.14004	.00499	.00340	.45012	.01000	.04601	.02235	.00080	1.00000
LAWM42	Ph1	.06004	.08005	.05003	.00801	.00322	.00300	.04037	.00100	.02502	.01501	.14009	.00499	.00300	.48032	.02001	.03502	.03002	.00080	1.00000
LAWM43	Ph1	.07002	.08678	.05002	.00800	.00322	.00300	.05002	.00300	.02501	.02501	.12004	.00499	.00390	.45016	.02001	.04602	.03001	.00080	1.00000
LAWM44	Ph1	.06325	.10039	.07008	.00020	.00008	.00007	.05006	.00100	.01001	.01502	.12014	.00012	.00290	.48055	.02002	.04605	.02002	.00002	1.00000
LAWM45	Ph1	.07003	.08003	.05784	.00020	.00008	.00007	.05002	.00300	.01423	.01501	.14005	.00012	.00310	.48017	.02001	.04602	.02001	.00002	1.00000

- (a) The compositions listed in this table are normalized mass fraction versions of target compositions of the glasses, after replacing the target values of SO<sub>3</sub> by XRF analyzed (or estimated analyzed) values. See Section 3.3 for the details.
- (b) The Group IDs are described in Sections 2.1 to 2.6.
- (c) XRF SO<sub>3</sub> denotes that the SO<sub>3</sub> composition is based on chemical analysis by XRF. For most glasses SO<sub>3</sub> was directly measured by XRF, but for some glasses estimated XRF values were used (see Section 3.3).
- (d) The normalized component mass fractions listed in this table were rounded to five decimals, and may not sum exactly to 1.00000 as listed. However, complete compositions listed to more decimal places and summing to 1.0000 were used for property-composition modeling.

**Table 7.2. Normalized<sup>(a)</sup> Compositions (mass fractions) of 171 LAW Glasses Used for Electrical Conductivity and Viscosity Model Development (continued).**

Glass ID	Group ID <sup>(b)</sup>	Al <sub>2</sub> O <sub>3</sub>	B <sub>2</sub> O <sub>3</sub>	CaO	Cl	Cr <sub>2</sub> O <sub>3</sub>	F	Fe <sub>2</sub> O <sub>3</sub>	K <sub>2</sub> O	Li <sub>2</sub> O	MgO	Na <sub>2</sub> O	P <sub>2</sub> O <sub>5</sub>	XRF SO <sub>3</sub> <sup>(c)</sup>	SiO <sub>2</sub>	TiO <sub>2</sub>	ZnO	ZrO <sub>2</sub>	Others	Sum <sup>(d)</sup>
LAWM46	Ph1	.06012	.11023	.06523	.00020	.00008	.00008	.05010	.00100	.01002	.02505	.12025	.00013	.00200	.48034	.01002	.03507	.03006	.00002	1.00000
LAWM47	Ph1	.06200	.08003	.07003	.00020	.00008	.00007	.05002	.00100	.01000	.02501	.14005	.00012	.00310	.48017	.01307	.03501	.03001	.00002	1.00000
LAWM48	Ph1	.06234	.11016	.05277	.00801	.00322	.00300	.05007	.00100	.01001	.01502	.12017	.00500	.00260	.48070	.02003	.03505	.02003	.00080	1.00000
LAWM49	Ph1	.07001	.10906	.05001	.00800	.00321	.00299	.03000	.00100	.01000	.01500	.14002	.00499	.00350	.47538	.01000	.04601	.02000	.00080	1.00000
LAWM50	Ph1	.06530	.09700	.06109	.00446	.00179	.00167	.04111	.00204	.01668	.02032	.13095	.00278	.00290	.46982	.01528	.04104	.02533	.00045	1.00000
LAWM51	Ph1	.06528	.09697	.06107	.00446	.00179	.00167	.04110	.00204	.01667	.02031	.13091	.00278	.00320	.46968	.01528	.04102	.02533	.00045	1.00000
LAWM52	Ph1	.06088	.09711	.01994	.00329	.00009	.00000	.05538	.02586	.00000	.01477	.20027	.00070	.00180	.44051	.01994	.02954	.02991	.00000	1.00000
LAWM53	Ph1	.09031	.06021	.10034	.00020	.00008	.00008	.08027	.04014	.04515	.00000	.05017	.00013	.00660	.44603	.03010	.05017	.00000	.00002	1.00000
LAWM54R1	Ph1	.03505	.06008	.10014	.00801	.00322	.00300	.08011	.04006	.02391	.00000	.05007	.00500	.00260	.49782	.00000	.05007	.04006	.00080	1.00000
LAWM55	Ph1	.03501	.13004	.00000	.00800	.00321	.00299	.02310	.04001	.04501	.01971	.14257	.00499	.00240	.42211	.03001	.05001	.04001	.00080	1.00000
LAWM56	Ph1	.04990	.11975	.06166	.00799	.00321	.00299	.04402	.00100	.00499	.03493	.16965	.00498	.00440	.41914	.02495	.01996	.02570	.00080	1.00000
LAWM57	Ph1aAug	.06997	.11000	.03000	.00196	.00078	.00078	.04659	.03801	.00000	.01440	.20620	.00122	.00320	.39274	.01370	.03026	.04001	.00016	1.00000
LAWM59	Ph1aAug	.06847	.09009	.02965	.00196	.00078	.00078	.06492	.02004	.00000	.01441	.20008	.00122	.00310	.44558	.01371	.02506	.02001	.00016	1.00000
LAWM60	Ph1aAug	.05003	.11006	.01714	.00196	.00078	.00078	.04503	.02004	.00000	.01441	.20015	.00122	.00300	.45351	.01371	.02804	.03998	.00016	1.00000
LAWM63	Ph1aAug	.07001	.09402	.01044	.00196	.00078	.00078	.04695	.02059	.00000	.01440	.22998	.00122	.00340	.42601	.01370	.04500	.02058	.00016	1.00000
LAWM66	Ph1aAug	.07587	.10637	.01003	.00196	.00078	.00078	.06315	.00479	.00000	.01440	.22996	.00122	.00320	.38362	.01370	.04500	.04498	.00016	1.00000
LAWM68	Ph1aAug	.05003	.09002	.02999	.00196	.00078	.00078	.06500	.04803	.00000	.01440	.20009	.00122	.00330	.40815	.01370	.03562	.03677	.00016	1.00000
LAWM71	Ph1aAug	.05006	.09001	.01003	.00196	.00078	.00078	.04501	.05401	.00000	.01440	.20004	.00122	.00340	.44943	.01370	.04498	.02002	.00016	1.00000
LAWM73	Ph1aAug	.08002	.09006	.02996	.00196	.00078	.00078	.04878	.01221	.00000	.01440	.23002	.00122	.00320	.40391	.01370	.04494	.02388	.00016	1.00000
LAWM75	Ph1aAug	.08003	.09157	.02996	.00196	.00078	.00078	.06497	.01082	.00000	.01441	.20691	.00122	.00310	.38461	.01371	.04500	.05001	.00016	1.00000
LAWE2H	Corr	.05951	.09751	.01970	.00196	.00078	.00078	.05365	.03790	.00000	.01440	.20782	.00122	.00310	.42440	.01370	.03410	.02930	.00016	1.00000
LAWE3	Corr	.06102	.10003	.02021	.00200	.00080	.00080	.05502	.04992	.00000	.01480	.18215	.00124	.00320	.42963	.01400	.03501	.03001	.00016	1.00000
LAWE3H	Corr	.05942	.09743	.01971	.00196	.00078	.00078	.05366	.05412	.00000	.01440	.19746	.00122	.00340	.41859	.01360	.03411	.02921	.00016	1.00000
LAWE4	Corr	.06107	.10012	.02523	.00200	.00080	.00080	.05507	.00501	.00000	.01482	.19664	.00124	.00260	.45535	.01402	.03504	.03004	.00015	1.00000
LAWE4H	Corr	.05974	.09796	.02461	.00196	.00078	.00078	.05383	.00540	.00000	.01451	.21283	.00122	.00350	.44527	.01371	.03432	.02942	.00016	1.00000
LAWE5	Corr	.06106	.10009	.03683	.00200	.00080	.00080	.05505	.00500	.00510	.01481	.17536	.00124	.00340	.45921	.01401	.03503	.03003	.00018	1.00000
LAWE5H	Corr	.05997	.09821	.03614	.00196	.00078	.00078	.05410	.00541	.00491	.01452	.18991	.00122	.00350	.45096	.01372	.03434	.02943	.00016	1.00000
LAWE7	Corr	.06110	.10017	.06401	.00200	.00080	.00080	.05509	.00501	.03226	.01513	.12521	.00124	.00380	.45407	.01402	.03506	.03005	.00018	1.00000
LAWE7H	Corr	.06027	.09882	.06318	.00196	.00078	.00078	.05441	.00541	.03174	.01492	.13546	.00122	.00470	.44810	.01382	.03464	.02964	.00016	1.00000
LAWE9H	Corr	.06066	.09946	.06878	.00197	.00079	.00079	.05468	.00541	.04091	.02366	.08953	.00122	.00430	.46919	.01394	.03479	.02978	.00016	1.00000
LAWE10H	Corr	.06086	.09976	.06978	.00197	.00079	.00079	.05498	.00541	.04271	.02948	.05735	.00122	.00540	.49054	.01394	.03489	.02998	.00016	1.00000
LAWE11	Corr	.06106	.10010	.02322	.00200	.00080	.00080	.05506	.04755	.00000	.01481	.17377	.00124	.00250	.43784	.01401	.03504	.03003	.00016	1.00000
LAWE12	Corr	.06952	.08753	.01971	.00196	.00078	.00078	.04361	.05412	.00000	.01440	.19746	.00122	.00320	.41853	.01370	.03411	.03921	.00016	1.00000

- (a) The compositions listed in this table are normalized mass fraction versions of target compositions of the glasses, after replacing the target values of SO<sub>3</sub> by XRF analyzed (or estimated analyzed) values. See Section 3.3 for the details.
- (b) The Group IDs are described in Sections 2.1 to 2.6.
- (c) XRF SO<sub>3</sub> denotes that the SO<sub>3</sub> composition is based on chemical analysis by XRF. For most glasses SO<sub>3</sub> was directly measured by XRF, but for some glasses estimated XRF values were used (see Section 3.3).
- (d) The normalized component mass fractions listed in this table were rounded to five decimals, and may not sum exactly to 1.00000 as listed. However, complete compositions listed to more decimal places and summing to 1.0000 were used for property-composition modeling.

**Table 7.2. Normalized<sup>(a)</sup> Compositions (mass fractions) of 171 LAW Glasses Used for Electrical Conductivity and Viscosity Model Development (continued).**

Glass ID	Group ID <sup>(b)</sup>	Al <sub>2</sub> O <sub>3</sub>	B <sub>2</sub> O <sub>3</sub>	CaO	Cl	Cr <sub>2</sub> O <sub>3</sub>	F	Fe <sub>2</sub> O <sub>3</sub>	K <sub>2</sub> O	Li <sub>2</sub> O	MgO	Na <sub>2</sub> O	P <sub>2</sub> O <sub>5</sub>	XRF SO <sub>3</sub> <sup>(c)</sup>	SiO <sub>2</sub>	TiO <sub>2</sub>	ZnO	ZrO <sub>2</sub>	Others	Sum <sup>(d)</sup>
LAWE13	Corr	.06952	.09753	.01971	.00196	.00078	.00078	.05362	.05412	.00000	.00440	.19746	.00122	.00320	.41853	.00370	.03411	.03921	.00016	1.00000
LAWE16	Corr	.05934	.08241	.01468	.00196	.00078	.00078	.05358	.05404	.00000	.00939	.19719	.00122	.00460	.42798	.01369	.03406	.04415	.00016	1.00000
LAWCrP1R	HiCrP	.06101	.10002	.02761	.00124	.00328	.00112	.05501	.00125	.00000	.01480	.19347	.01442	.00370	.44401	.01400	.03501	.03001	.00004	1.00000
LAWCrP2R	HiCrP	.06099	.09998	.02105	.00193	.00591	.00103	.05499	.00275	.00000	.01480	.20996	.01333	.00360	.43065	.01400	.03499	.02999	.00006	1.00000
LAWCrP3R	HiCrP	.06101	.10001	.02761	.00124	.00328	.00111	.05500	.00125	.00000	.01480	.19345	.02380	.00380	.43458	.01400	.03500	.03000	.00004	1.00000
LAWCrP4R	HiCrP	.06098	.09997	.02104	.00192	.00591	.00103	.05498	.00275	.00000	.01480	.20994	.02379	.00370	.42014	.01400	.03499	.02999	.00006	1.00000
LAWCrP5	HiCrP	.06108	.10013	.05813	.00136	.00591	.00067	.05507	.00087	.02642	.01488	.14395	.01335	.00380	.43505	.01402	.03504	.03004	.00021	1.00000
LAWA41	ActDes	.06203	.07501	.02000	.00580	.00017	.00040	.06983	.03101	.00000	.01995	.20002	.00078	.00100	.43414	.01995	.02993	.02995	.00004	1.00000
LAWA42	ActDes	.06204	.09034	.02404	.00579	.00017	.00036	.08411	.03101	.00001	.02402	.20004	.00078	.00100	.38007	.02403	.03605	.03607	.00005	1.00000
LAWA45	ActDes	.06201	.11901	.00000	.00652	.00020	.00010	.06980	.00501	.00000	.01477	.20000	.00034	.00100	.44552	.01994	.02477	.02992	.00111	1.00000
LAWA51	ActDes	.06203	.11976	.00000	.00587	.00018	.00009	.06998	.00451	.00000	.01484	.18003	.00030	.00070	.46579	.01996	.02488	.02998	.00111	1.00000
LAWA52	ActDes	.06179	.06191	.07882	.00652	.00020	.00010	.07505	.00501	.00000	.01477	.19999	.00034	.00100	.42247	.01108	.02994	.02992	.00112	1.00000
LAWA60	ActDes	.08528	.11228	.04321	.00652	.00020	.00010	.00000	.00501	.00000	.01994	.19999	.00034	.00100	.44551	.01994	.02965	.02992	.00112	1.00000
LAWA81	ActDes	.06201	.08902	.03989	.00652	.00020	.00010	.06980	.00501	.00000	.01994	.20000	.00034	.00100	.44552	.00000	.02965	.02992	.00111	1.00000
LAWA83	ActDes	.06201	.08902	.01994	.00652	.00020	.00010	.04986	.00501	.00000	.01994	.20000	.02028	.00100	.44552	.01994	.02965	.02992	.00111	1.00000
LAWA90	ActDes	.06082	.09700	.03983	.00329	.00009	.00000	.05533	.02583	.00000	.01475	.20005	.00070	.00190	.44002	.00000	.02951	.02988	.00100	1.00000
LAWA93	ActDes	.06179	.11095	.07882	.00652	.00020	.00010	.07505	.00501	.05067	.01477	.10027	.00034	.00100	.42247	.01108	.02994	.02992	.00112	1.00000
LAWA96	ActDes	.06201	.07904	.03989	.00652	.00020	.00010	.02992	.00501	.00000	.01994	.20000	.04023	.00100	.43555	.01994	.02965	.02992	.00111	1.00000
LAWA125	ActDes	.05637	.09545	.01939	.00220	.00020	.00320	.05387	.04208	.00000	.01439	.19990	.00090	.00310	.42888	.01939	.02879	.02909	.00280	1.00000
LAWA127R1	ActDes	.05651	.10205	.02068	.00181	.00019	.00265	.05758	.03430	.00000	.01536	.16312	.00070	.00180	.45828	.02073	.03071	.03110	.00245	1.00000
LAWA129R1	ActDes	.07466	.08515	.03528	.00200	.00020	.00300	.00000	.03878	.00000	.01179	.18449	.00080	.00310	.47511	.02089	.03088	.03128	.00260	1.00000
LAWA134	ActDes	.05647	.09964	.02019	.00200	.00020	.00290	.05627	.03728	.00000	.01499	.17729	.00080	.00280	.44753	.02029	.02998	.03038	.00100	1.00000
LAWA135	ActDes	.05655	.10092	.02048	.00190	.00020	.00280	.05695	.03577	.00000	.01519	.17016	.00070	.00270	.45304	.02048	.03038	.03078	.00100	1.00000
LAWA136	ActDes	.05655	.10092	.03048	.00190	.00020	.00280	.05695	.03577	.00000	.01519	.17016	.00070	.00270	.44304	.02048	.03038	.03078	.00100	1.00000
LAWB30	ActDes	.08604	.10039	.07235	.00007	.00086	.00097	.08276	.00323	.04070	.03075	.07902	.00038	.00180	.42730	.00000	.04115	.03120	.00102	1.00000
LAWB34	ActDes	.06178	.12131	.06065	.00007	.00089	.00099	.05167	.00320	.02965	.02246	.07925	.02732	.00710	.47063	.00000	.03100	.03100	.00102	1.00000
LAWB37	ActDes	.06166	.12108	.04709	.00007	.00089	.00099	.05157	.00319	.02960	.02915	.07910	.03400	.00900	.46973	.00000	.03094	.03094	.00102	1.00000
LAWB38	ActDes	.06156	.12088	.04746	.00007	.00088	.00099	.05149	.00319	.03806	.02239	.07897	.03170	.01060	.46897	.00000	.03089	.03089	.00102	1.00000
LAWB61	ActDes	.06205	.09966	.06708	.00000	.00101	.00070	.05310	.00261	.05823	.02977	.05501	.00010	.00710	.48624	.01398	.03168	.03168	.00000	1.00000
LAWB64	ActDes	.06207	.09969	.06710	.00000	.00101	.00070	.03300	.00262	.05825	.02978	.05503	.00010	.00680	.48639	.01398	.05181	.03169	.00000	1.00000
LAWB67	ActDes	.06189	.09940	.05186	.00000	.00100	.00070	.05296	.00261	.04303	.02969	.05487	.03019	.00970	.48497	.01394	.03160	.03160	.00000	1.00000
LAWB69	ActDes	.06151	.12332	.10462	.00010	.00050	.00080	.00000	.00230	.04611	.02971	.06621	.00050	.00650	.47960	.00000	.04571	.03151	.00100	1.00000
LAWB70	ActDes	.06159	.12347	.06629	.00010	.00050	.00080	.03255	.00230	.04616	.02974	.06629	.00050	.00540	.48018	.00000	.05157	.03154	.00100	1.00000

- (a) The compositions listed in this table are normalized mass fraction versions of target compositions of the glasses, after replacing the target values of SO<sub>3</sub> by XRF analyzed (or estimated analyzed) values. See Section 3.3 for the details.
- (b) The Group IDs are described in Sections 2.1 to 2.6.
- (c) XRF SO<sub>3</sub> denotes that the SO<sub>3</sub> composition is based on chemical analysis by XRF. For most glasses SO<sub>3</sub> was directly measured by XRF, but for some glasses estimated XRF values were used (see Section 3.3).
- (d) The normalized component mass fractions listed in this table were rounded to five decimals, and may not sum exactly to 1.00000 as listed. However, complete compositions listed to more decimal places and summing to 1.0000 were used for property-composition modeling.

**Table 7.2. Normalized<sup>(a)</sup> Compositions (mass fractions) of 171 LAW Glasses Used for Electrical Conductivity and Viscosity Model Development (continued).**

Glass ID	Group ID <sup>(b)</sup>	Al <sub>2</sub> O <sub>3</sub>	B <sub>2</sub> O <sub>3</sub>	CaO	Cl	Cr <sub>2</sub> O <sub>3</sub>	F	Fe <sub>2</sub> O <sub>3</sub>	K <sub>2</sub> O	Li <sub>2</sub> O	MgO	Na <sub>2</sub> O	P <sub>2</sub> O <sub>5</sub>	XRF SO <sub>3</sub> <sup>(c)</sup>	SiO <sub>2</sub>	TiO <sub>2</sub>	ZnO	ZrO <sub>2</sub>	Others	Sum <sup>(d)</sup>
LAWB71	ActDes	.06162	.10802	.06633	.00010	.00050	.00080	.03257	.00230	.04619	.02976	.06633	.00050	.00480	.48047	.01553	.05160	.03156	.00100	1.00000
LAWB72	ActDes	.06154	.12339	.07125	.00010	.00050	.00080	.03252	.00230	.04113	.02972	.06625	.00050	.00610	.47984	.00000	.05154	.03152	.00100	1.00000
LAWB73	ActDes	.06193	.09947	.09345	.00000	.00100	.00070	.01907	.00261	.05049	.02971	.05490	.00010	.00900	.48531	.01395	.04667	.03162	.00000	1.00000
LAWB74	ActDes	.06218	.10108	.08728	.00000	.00101	.00071	.01915	.00262	.05331	.02983	.05513	.00010	.00770	.48728	.01401	.04686	.03175	.00000	1.00000
LAWB75	ActDes	.06187	.11792	.08684	.00000	.00100	.00070	.01905	.00261	.05304	.01504	.05485	.00010	.01000	.48482	.01394	.04663	.03159	.00000	1.00000
LAWB76	ActDes	.06186	.11790	.08682	.00000	.00100	.00070	.01905	.00261	.05805	.01504	.05484	.00010	.01020	.49365	.00000	.04662	.03158	.00000	1.00000
LAWB77	ActDes	.06160	.12350	.06631	.00010	.00050	.00080	.02204	.00230	.04117	.02975	.06631	.00050	.00520	.48027	.01552	.05158	.03155	.00100	1.00000
LAWB81	ActDes	.06155	.12340	.07126	.00010	.00050	.00080	.03253	.00230	.04263	.02972	.06625	.00050	.00600	.47989	.00000	.05004	.03153	.00100	1.00000
LAWB87	ActDes	.06495	.13020	.06114	.00010	.00060	.00050	.05032	.00200	.04701	.01413	.05012	.00020	.00570	.49214	.00000	.04891	.03197	.00000	1.00000
LAWB88	ActDes	.06488	.13006	.07990	.00010	.00060	.00050	.02203	.00200	.04696	.01412	.05006	.00020	.00680	.50101	.00000	.04886	.03194	.00000	1.00000
LAWB89	ActDes	.06186	.10040	.06787	.00010	.00040	.00060	.05295	.00190	.05005	.02973	.04084	.00040	.00440	.49350	.01391	.04845	.03163	.00100	1.00000
LAWB90	ActDes	.06192	.10050	.06794	.00010	.00040	.00060	.05301	.00190	.03617	.02976	.06884	.00040	.00340	.47996	.01393	.04850	.03166	.00100	1.00000
LAWB92	ActDes	.06187	.10041	.06787	.00010	.00040	.00060	.05296	.00190	.02222	.02973	.10121	.00040	.00430	.46101	.01392	.04845	.03163	.00100	1.00000
LAWB93R1	ActDes	.06187	.10042	.06788	.00010	.00040	.00060	.05296	.00190	.04666	.02974	.04786	.00040	.00420	.48999	.01392	.04846	.03163	.00100	1.00000
LAWB94	ActDes	.06186	.10031	.06780	.00007	.00039	.00064	.05295	.00194	.05359	.02972	.03385	.00037	.00500	.49662	.01393	.04839	.03158	.00100	1.00000
LAWB95	ActDes	.06189	.10035	.06783	.00007	.00039	.00064	.05297	.00194	.05761	.02973	.02457	.00037	.00460	.50211	.01394	.04841	.03159	.00100	1.00000
LAWC21rev2	ActDes	.06125	.10058	.06415	.00110	.00020	.00050	.06435	.00140	.02732	.01501	.11970	.00110	.00290	.46778	.01121	.03022	.03022	.00100	1.00000
LAWC29	ActDes	.06551	.10049	.09617	.00112	.00018	.00054	.00009	.00136	.02734	.01501	.11958	.00106	.00370	.47181	.01121	.05365	.03019	.00100	1.00000
LAWC30	ActDes	.06122	.10053	.06412	.00110	.00020	.00050	.04101	.00140	.02731	.01500	.11964	.00110	.00340	.46754	.01120	.05352	.03021	.00100	1.00000
LAWC31R1	ActDes	.06122	.10053	.07412	.00110	.00020	.00050	.04431	.00140	.02731	.01500	.11964	.00110	.00340	.46754	.01120	.04021	.03021	.00100	1.00000
C22AN107	ActDes	.06106	.10079	.05115	.00080	.00020	.00140	.05585	.00090	.02512	.01511	.14433	.00120	.00270	.46612	.01141	.03063	.03023	.00100	1.00000
A88Si+15	ActDes	.06141	.09481	.01930	.00140	.00020	.00250	.05351	.02370	.00000	.01430	.22182	.00080	.00290	.42554	.01930	.02850	.02890	.00110	1.00000
A88Si-15	ActDes	.06055	.10218	.02072	.00120	.00010	.00200	.05765	.01882	.00000	.01541	.17674	.00060	.00190	.45867	.02072	.03072	.03112	.00090	1.00000
C22Si+15	ActDes	.06043	.09837	.04994	.00090	.00020	.00160	.05358	.00095	.02459	.01484	.16197	.00130	.00310	.45581	.01121	.03001	.02960	.00160	1.00000
C22Si-15	ActDes	.06160	.10291	.05218	.00071	.00017	.00129	.05555	.00076	.02572	.01551	.12812	.00138	.00230	.47680	.01175	.03139	.03096	.00090	1.00000
A1C1-1	ActDes	.06088	.09126	.02742	.00913	.00015	.00086	.06501	.00347	.00623	.01850	.19167	.00033	.00210	.44480	.01759	.02951	.02956	.00153	1.00000
A1C1-2	ActDes	.06073	.09415	.03521	.00654	.00013	.00169	.06135	.00255	.01247	.01735	.17673	.00066	.00230	.45142	.01554	.02984	.02974	.00160	1.00000
C1-AN107	ActDes	.06066	.10031	.05098	.00065	.00009	.00283	.05421	.00069	.02506	.01510	.14465	.00132	.00290	.46636	.01147	.03062	.03020	.00189	1.00000
A2-AP101	ActDes	.05622	.09824	.01991	.00420	.00020	.00350	.05532	.03812	.00000	.01481	.18467	.00080	.00350	.44008	.01991	.02941	.02961	.00150	1.00000
A2B1-1	ActDes	.05758	.09883	.03184	.00320	.00020	.00280	.05477	.02904	.01071	.01852	.15230	.00070	.00350	.45179	.01842	.03414	.03014	.00150	1.00000
A2B1-2	ActDes	.05895	.09919	.04374	.00220	.00030	.00220	.05405	.02002	.02152	.02232	.11981	.00060	.00420	.46292	.01692	.03894	.03063	.00150	1.00000
B1-AZ101	ActDes	.06180	.10026	.06771	.00020	.00030	.00080	.05278	.00180	.04307	.02985	.05479	.00040	.00490	.48578	.01392	.04848	.03165	.00150	1.00000
C2-AN102C35	ActDes	.06075	.09428	.07356	.00390	.00010	.00110	.03603	.00090	.03253	.01491	.11980	.00160	.00540	.47278	.01081	.03993	.03002	.00160	1.00000

- (a) The compositions listed in this table are normalized mass fraction versions of target compositions of the glasses, after replacing the target values of SO<sub>3</sub> by XRF analyzed (or estimated analyzed) values. See Section 3.3 for the details.
- (b) The Group IDs are described in Sections 2.1 to 2.6.
- (c) XRF SO<sub>3</sub> denotes that the SO<sub>3</sub> composition is based on chemical analysis by XRF. For most glasses SO<sub>3</sub> was directly measured by XRF, but for some glasses estimated XRF values were used (see Section 3.3).
- (d) The normalized component mass fractions listed in this table were rounded to five decimals, and may not sum exactly to 1.00000 as listed. However, complete compositions listed to more decimal places and summing to 1.0000 were used for property-composition modeling.

**Table 7.2. Normalized<sup>(a)</sup> Compositions (mass fractions) of 171 LAW Glasses Used for Electrical Conductivity and Viscosity Model Development (continued).**

Glass ID	Group ID <sup>(b)</sup>	Al <sub>2</sub> O <sub>3</sub>	B <sub>2</sub> O <sub>3</sub>	CaO	Cl	Cr <sub>2</sub> O <sub>3</sub>	F	Fe <sub>2</sub> O <sub>3</sub>	K <sub>2</sub> O	Li <sub>2</sub> O	MgO	Na <sub>2</sub> O	P <sub>2</sub> O <sub>5</sub>	XRF SO <sub>3</sub> <sup>(c)</sup>	SiO <sub>2</sub>	TiO <sub>2</sub>	ZnO	ZrO <sub>2</sub>	Others	Sum <sup>(d)</sup>
A3-AN104	ActDes	.06051	.09921	.05031	.00790	.00020	.00010	.05371	.00330	.02480	.01480	.14641	.00110	.00350	.46095	.01130	.03040	.03000	.00150	1.00000
A2B1-3	ActDes	.06037	.09971	.05576	.00120	.00030	.00150	.05346	.01091	.03224	.02603	.08730	.00050	.00470	.47432	.01542	.04365	.03113	.00150	1.00000
A3C2-1	ActDes	.06064	.09796	.05613	.00690	.00020	.00030	.04923	.00270	.02672	.01481	.13978	.00120	.00380	.46408	.01121	.03282	.03002	.00150	1.00000
A3C2-2	ActDes	.06066	.09680	.06196	.00591	.00020	.00060	.04485	.00210	.02863	.01481	.13323	.00140	.00400	.46707	.01111	.03514	.03003	.00150	1.00000
A3C2-3	ActDes	.06064	.09547	.06775	.00490	.00010	.00090	.04043	.00150	.03062	.01491	.12649	.00150	.00490	.46983	.01091	.03753	.03002	.00160	1.00000
A1-AN105R2	ActDes	.06101	.08841	.01960	.01170	.00020	.00000	.06871	.00440	.00000	.01960	.20662	.00000	.00180	.43824	.01960	.02920	.02940	.00150	1.00000

- (a) The compositions listed in this table are normalized mass fraction versions of target compositions of the glasses, after replacing the target values of SO<sub>3</sub> by XRF analyzed (or estimated analyzed) values. See Section 3.3 for the details.
- (b) The Group IDs are described in Sections 2.1 to 2.6.
- (c) XRF SO<sub>3</sub> denotes that the SO<sub>3</sub> composition is based on chemical analysis by XRF. For most glasses SO<sub>3</sub> was directly measured by XRF, but for some glasses estimated XRF values were used (see Section 3.3).
- (d) The normalized component mass fractions listed in this table were rounded to five decimals, and may not sum exactly to 1.00000 as listed. However, complete compositions listed to more decimal places and summing to 1.0000 were used for property-composition modeling.

**Table 7.3. Temperature and Electrical Conductivity Observations and Data-Splitting Validation Sets for Each of the 171 LAW Glasses Used for Electrical Conductivity Model Development.**

<b>Glass ID</b>	<b>Group ID<sup>(a)</sup></b>	<b>Temp1 (°C)</b>	<b>EC1 (S/cm)</b>	<b>Temp2 (°C)</b>	<b>EC2 (S/cm)</b>	<b>Temp3 (°C)</b>	<b>EC3 (S/cm)</b>	<b>Temp4 (°C)</b>	<b>EC4 (S/cm)</b>	<b>EC Data Splitting Validation Set<sup>(b)</sup></b>
LAWA44R10	ExPh1	1245	0.389	1144	0.274	1053	0.211	957	0.142	5
LAWA53	ExPh1	1240	0.568	1142	0.426	1045	0.262	946	0.163	4
LAWA56	ExPh1	1239	0.567	1142	0.426	1044	0.285	946	0.178	2
LAWA88	ExPh1	1251	0.765	1143	0.554	1044	0.370	949	0.248	NA
LAWA102R1	ExPh1	1240	0.523	1142	0.368	1043	0.238	945	0.156	3
LAWA126	ExPh1	1240	0.550	1143	0.373	1042	0.258	949	0.171	1
LAWA128R1	ExPh1	1236	0.530	1146	0.383	1046	0.264	947	0.167	2
LAWA130	ExPh1	1246	0.557	1157	0.416	1061	0.292	965	0.188	1
LAWB65	ExPh1	1228	0.305	1127	0.195	1034	0.125	939	0.063	1
LAWB66	ExPh1	1232	0.368	1137	0.253	1043	0.151	948	0.084	4
LAWB68	ExPh1	1255	0.325	1156	0.222	1057	0.132	959	0.069	1
LAWB78	ExPh1	1239	0.352	1141	0.228	1046	0.149	951	0.085	4
LAWB79	ExPh1	1239	0.338	1142	0.217	1045	0.142	949	0.079	4
LAWB80	ExPh1	1239	0.264	1138	0.172	1040	0.105	943	0.054	5
LAWB83	ExPh1	1239	0.323	1141	0.215	1044	0.128	949	0.067	2
LAWB84	ExPh1	1245	0.339	1147	0.227	1049	0.139	953	0.076	5
LAWB85	ExPh1	1255	0.353	1157	0.251	1058	0.148	961	0.089	5
LAWB86	ExPh1	1251	0.338	1153	0.220	1055	0.147	959	0.080	5
C100-G-136B	ExPh1	1245	0.443	1145	0.299	1045	0.194	944	0.105	1
LAWC27	ExPh1	1240	0.346	1142	0.246	1045	0.162	954	0.093	5
LAWC32	ExPh1	1242	0.444	1147	0.315	1051	0.199	958	0.109	3
LAWM1	Ph1	1253	0.243	1156	0.169	1058	0.101	959	0.052	NA
LAWM2	Ph1	1253	0.284	1162	0.213	1066	0.112	970	0.058	3
LAWM3	Ph1	1236	0.513	1145	0.357	1051	0.229	957	0.128	1
LAWM4	Ph1	1252	0.289	1155	0.199	1058	0.119	960	0.062	2
LAWM5	Ph1	1224	0.248	1127	0.183	1027	0.117	929	0.059	2
LAWM6	Ph1	1216	0.185	1120	0.113	1022	0.056	923	0.026	2
LAWM7	Ph1	1238	0.118	1140	0.074	1052	0.042	958	0.021	5
LAWM8	Ph1	1223	0.140	1124	0.073	1024	0.041	931	0.020	4
LAWM9	Ph1	1248	0.139	1154	0.097	1057	0.054	963	0.027	NA
LAWM10	Ph1	1244	0.580	1150	0.425	1054	0.289	960	0.166	1
LAWM11	Ph1	1215	0.609	1117	0.429	1015	0.276	923	0.166	5
LAWM12	Ph1	1253	0.721	1161	0.553	1068	0.385	973	0.249	NA
LAWM13	Ph1	1242	0.945	1143	0.708	1045	0.498	946	0.284	4
LAWM14	Ph1	1244	0.693	1151	0.458	1056	0.340	960	0.239	5
LAWM15	Ph1	1241	0.691	1143	0.573	1044	0.411	946	0.276	5
LAWM16	Ph1	1238	0.399	1140	0.289	1042	0.182	944	0.094	4
LAWM17	Ph1	1230	0.628	1132	0.380	1034	0.235	940	0.133	1
LAWM18	Ph1	1237	0.406	1140	0.281	1043	0.175	947	0.115	2
LAWM19	Ph1	1227	0.321	1131	0.231	1034	0.135	938	0.069	4
LAWM20	Ph1	1235	0.699	1138	0.467	1040	0.311	942	0.187	3
LAWM21	Ph1	1228	0.501	1130	0.318	1032	0.182	934	0.109	2
LAWM22	Ph1	1231	0.389	1134	0.267	1036	0.181	939	0.112	2

(a) The Group IDs are described in Sections 2.1 to 2.6.

(b) Numbers from 1 to 5 denote the five split validation subsets. NA denotes “not applicable”, because these replicate glasses were forced into the modeling subsets, and thus were not parts of the validation subsets.

**Table 7.3. Temperature and Electrical Conductivity Observations and Data-Splitting Validation Sets for Each of the 171 LAW Glasses Used for Electrical Conductivity Model Development (continued).**

Glass ID	Group ID <sup>(a)</sup>	Temp1 (°C)	EC1 (S/cm)	Temp2 (°C)	EC2 (S/cm)	Temp3 (°C)	EC3 (S/cm)	Temp4 (°C)	EC4 (S/cm)	EC Data Splitting Validation Set <sup>(b)</sup>
LAWM23	Ph1	1227	0.374	1131	0.252	1035	0.146	939	0.083	1
LAWM24	Ph1	1225	0.475	1128	0.345	1030	0.247	933	0.161	1
LAWM25R1	Ph1	1220	0.325	1123	0.220	1028	0.147	927	0.085	4
LAWM26	Ph1	1239	0.377	1142	0.232	1043	0.142	945	0.085	3
LAWM27	Ph1	1235	0.282	1137	0.189	1039	0.111	942	0.061	4
LAWM28	Ph1	1249	0.136	1155	0.096	1060	0.060	966	0.032	3
LAWM29	Ph1	1236	0.334	1136	0.235	1038	0.136	941	0.081	2
LAWM30	Ph1	1219	0.282	1123	0.187	1027	0.114	929	0.059	5
LAWM31	Ph1	1230	0.711	1132	0.536	1034	0.331	937	0.197	3
LAWM32	Ph1	1248	0.516	1154	0.417	1059	0.296	964	0.190	4
LAWM33R1	Ph1	1243	0.563	1145	0.506	1046	0.346	949	0.175	5
LAWM34	Ph1	1230	0.707	1130	0.535	1032	0.365	936	0.195	3
LAWM35	Ph1	1246	0.425	1152	0.306	1056	0.205	961	0.126	NA
LAWM36	Ph1	1244	0.421	1145	0.293	1047	0.178	949	0.103	3
LAWM37	Ph1	1237	0.390	1140	0.267	1042	0.165	943	0.101	2
LAWM38	Ph1	1243	0.484	1145	0.312	1046	0.231	948	0.117	2
LAWM39	Ph1	1248	0.473	1150	0.335	1050	0.225	951	0.105	5
LAWM40	Ph1	1249	0.619	1152	0.453	1053	0.297	949	0.094	5
LAWM41	Ph1	1245	0.348	1148	0.243	1050	0.159	952	0.089	3
LAWM42	Ph1	1198	0.336	1108	0.236	1017	0.167	927	0.097	4
LAWM43	Ph1	1243	0.390	1147	0.270	1050	0.183	953	0.108	3
LAWM44	Ph1	1239	0.267	1142	0.182	1043	0.108	946	0.058	4
LAWM45	Ph1	1236	0.386	1139	0.285	1041	0.179	944	0.111	5
LAWM46	Ph1	1252	0.208	1157	0.143	1062	0.091	965	0.052	1
LAWM47	Ph1	1238	0.354	1141	0.234	1043	0.145	945	0.082	5
LAWM48	Ph1	1199	0.280	1106	0.182	1015	0.111	926	0.062	1
LAWM49	Ph1	1238	0.331	1141	0.215	1041	0.139	946	0.088	1
LAWM50	Ph1	1239	0.399	1143	0.260	1044	0.168	947	0.101	NA
LAWM51	Ph1	1230	0.347	1133	0.245	1036	0.157	939	0.091	NA
LAWM52	Ph1	1234	0.568	1137	0.421	1038	0.280	942	0.176	NA
LAWM53	Ph1	1237	0.379	1141	0.241	1043	0.144	945	0.074	NA
LAWM54R1	Ph1	1236	0.146	1146	0.092	1047	0.048	949	0.023	NA
LAWM55	Ph1	1236	0.742	1139	0.588	1042	0.388	944	0.248	NA
LAWM56	Ph1	1235	0.481	1138	0.331	1041	0.223	947	0.123	NA
LAWM57	Ph1aAug	1251	0.769	1160	0.550	1068	0.402	975	0.247	1
LAWM59	Ph1aAug	1228	0.632	1136	0.440	1043	0.338	952	0.214	1
LAWM60	Ph1aAug	1236	0.586	1144	0.460	1050	0.290	958	0.218	1
LAWM63	Ph1aAug	1245	0.871	1153	0.665	1060	0.493	967	0.317	5
LAWM66	Ph1aAug	1243	0.783	1150	0.619	1057	0.461	965	0.320	1
LAWM68	Ph1aAug	1243	0.654	1150	0.497	1057	0.344	963	0.239	4
LAWM71	Ph1aAug	1238	0.622	1145	0.483	1051	0.348	959	0.239	1

(a) The Group IDs are described in Sections 2.1 to 2.6.

(b) Numbers from 1 to 5 denote the five split validation subsets. NA denotes “not applicable”, because these replicate glasses were forced into the modeling subsets, and thus were not parts of the validation subsets.



**Table 7.3. Temperature and Electrical Conductivity Observations and Data-Splitting Validation Sets for Each of the 171 LAW Glasses Used for Electrical Conductivity Model Development (continued).**

Glass ID	Group ID <sup>(a)</sup>	Temp1 (°C)	EC1 (S/cm)	Temp2 (°C)	EC2 (S/cm)	Temp3 (°C)	EC3 (S/cm)	Temp4 (°C)	EC4 (S/cm)	EC Data Splitting Validation Set <sup>(b)</sup>
LAWM73	Ph1aAug	1239	0.633	1145	0.506	1052	0.388	960	0.289	3
LAWM75	Ph1aAug	1247	0.583	1156	0.457	1062	0.326	970	0.209	2
LAWE2H	Corr	1197	0.592	1115	0.446	1022	0.350	931	0.199	1
LAWE3	Corr	1208	0.456	1116	0.325	1026	0.243	934	0.152	5
LAWE3H	Corr	1214	0.617	1122	0.470	1027	0.318	932	0.203	4
LAWE4	Corr	1213	0.497	1119	0.386	1025	0.268	930	0.173	3
LAWE4H	Corr	1234	0.567	1140	0.444	1048	0.323	957	0.219	3
LAWE5	Corr	1208	0.489	1116	0.349	1026	0.261	934	0.163	2
LAWE5H	Corr	1201	0.500	1107	0.361	1015	0.257	917	0.151	4
LAWE7	Corr	1210	0.465	1120	0.312	1024	0.217	930	0.128	3
LAWE7H	Corr	1182	0.471	1099	0.298	1009	0.207	919	0.115	4
LAWE9H	Corr	1204	0.414	1114	0.288	1023	0.171	934	0.105	1
LAWE10H	Corr	1208	0.269	1118	0.169	1036	0.109	934	0.063	3
LAWE11	Corr	1207	0.402	1117	0.327	1024	0.223	933	0.146	4
LAWE12	Corr	1234	0.611	1138	0.483	1046	0.353	954	0.238	4
LAWE13	Corr	1238	0.676	1147	0.514	1054	0.393	962	0.255	4
LAWE16	Corr	1220	0.575	1128	0.477	1042	0.322	952	0.215	2
LAWCrP1R	HiCrP	1274	0.787	1179	0.562	1081	0.414	982	0.270	2
LAWCrP2R	HiCrP	1275	0.924	1176	0.712	1078	0.514	980	0.339	3
LAWCrP3R	HiCrP	1278	0.693	1179	0.559	1081	0.422	982	0.287	4
LAWCrP4R	HiCrP	1271	0.961	1172	0.732	1073	0.557	978	0.357	2
LAWCrP5	HiCrP	1222	0.435	1136	0.349	1044	0.231	953	0.144	2
LAWA41	ActDes	1243	0.713	1154	0.529	1052	0.369	951	0.238	5
LAWA42	ActDes	1240	0.710	1152	0.561	1054	0.393	956	0.248	2
LAWA45	ActDes	1249	0.643	1149	0.527	1050	0.366	948	0.242	1
LAWA51	ActDes	1248	0.550	1150	0.408	1049	0.290	951	0.186	3
LAWA52	ActDes	1247	0.657	1141	0.439	1043	0.305	945	0.186	2
LAWA60	ActDes	1257	0.543	1148	0.415	1050	0.293	950	0.197	5
LAWA81	ActDes	1250	0.637	1138	0.538	1039	0.320	942	0.211	5
LAWA83	ActDes	1249	0.613	1142	0.450	1043	0.315	944	0.201	4
LAWA90	ActDes	1244	0.653	1150	0.511	1051	0.350	955	0.233	2
LAWA93	ActDes	1244	0.558	1139	0.432	1041	0.297	947	0.183	4
LAWA96	ActDes	1244	0.748	1162	0.533	1052	0.307	951	0.204	2
LAWA125	ActDes	1247	0.646	1148	0.474	1048	0.295	949	0.204	5
LAWA127R1	ActDes	1239	0.390	1139	0.293	1038	0.188	940	0.126	5
LAWA129R1	ActDes	1238	0.454	1146	0.323	1035	0.184	945	0.131	3
LAWA134	ActDes	1241	0.518	1147	0.372	1052	0.260	958	0.165	4
LAWA135	ActDes	1245	0.479	1150	0.357	1056	0.238	961	0.157	2
LAWA136	ActDes	1237	0.475	1145	0.353	1049	0.240	957	0.153	4
LAWB30	ActDes	1244	0.424	1137	0.276	1040	0.163	925	0.084	1
LAWB34	ActDes	1237	0.361	1143	0.218	1045	0.141	947	0.070	3
LAWB37	ActDes	1247	0.297	1139	0.229	1042	0.144	947	0.083	1
LAWB38	ActDes	1245	0.386	1141	0.283	1043	0.163	944	0.101	5

(a) The Group IDs are described in Sections 2.1 to 2.6.

(b) Numbers from 1 to 5 denote the five split validation subsets. NA denotes “not applicable”, because these replicate glasses were forced into the modeling subsets, and thus were not parts of the validation subsets.

**Table 7.3. Temperature and Electrical Conductivity Observations and Data-Splitting Validation Sets for Each of the 171 LAW Glasses Used for Electrical Conductivity Model Development (continued).**

Glass ID	Group ID <sup>(a)</sup>	Temp1 (°C)	EC1 (S/cm)	Temp2 (°C)	EC2 (S/cm)	Temp3 (°C)	EC3 (S/cm)	Temp4 (°C)	EC4 (S/cm)	EC Data Splitting Validation Set <sup>(b)</sup>
LAWB61	ActDes	1229	0.401	1132	0.284	1035	0.170	938	0.098	2
LAWB64	ActDes	1242	0.437	1148	0.290	1046	0.186	950	0.102	5
LAWB67	ActDes	1236	0.296	1140	0.206	1040	0.130	954	0.073	3
LAWB69	ActDes	1238	0.349	1143	0.249	1046	0.145	951	0.073	2
LAWB70	ActDes	1229	0.387	1135	0.265	1040	0.147	945	0.098	2
LAWB71	ActDes	1218	0.387	1126	0.265	1030	0.173	936	0.097	3
LAWB72	ActDes	1247	0.338	1150	0.246	1050	0.135	954	0.074	3
LAWB73	ActDes	1244	0.418	1147	0.284	1055	0.178	962	0.117	4
LAWB74	ActDes	1224	0.433	1135	0.305	1043	0.197	947	0.110	4
LAWB75	ActDes	1231	0.457	1142	0.300	1041	0.171	949	0.095	4
LAWB76	ActDes	1246	0.516	1148	0.361	1050	0.250	952	0.135	3
LAWB77	ActDes	1249	0.382	1150	0.254	1049	0.131	948	0.071	3
LAWB81	ActDes	1252	0.502	1153	0.292	1053	0.184	955	0.099	2
LAWB87	ActDes	1229	0.379	1134	0.277	1041	0.176	946	0.102	3
LAWB88	ActDes	1227	0.372	1132	0.256	1039	0.160	947	0.093	3
LAWB89	ActDes	1223	0.359	1131	0.252	1038	0.157	945	0.090	1
LAWB90	ActDes	1240	0.306	1147	0.207	1053	0.130	964	0.069	4
LAWB92	ActDes	1238	0.316	1143	0.216	1049	0.135	955	0.073	5
LAWB93R1	ActDes	1257	0.314	1162	0.213	1068	0.141	969	0.083	2
LAWB94	ActDes	1243	0.344	1150	0.231	1054	0.149	958	0.083	1
LAWB95	ActDes	1239	0.389	1146	0.277	1052	0.180	958	0.101	5
LAWC21rev2	ActDes	1245	0.370	1151	0.264	1054	0.171	960	0.101	4
LAWC29	ActDes	1242	0.421	1144	0.264	1046	0.166	949	0.088	5
LAWC30	ActDes	1238	0.527	1142	0.329	1045	0.197	950	0.117	4
LAWC31R1	ActDes	1238	0.401	1140	0.271	1043	0.167	947	0.100	4
C22AN107	ActDes	1200	0.416	1151	0.339	1052	0.228	953	0.131	1
A88Si+15	ActDes	1242	0.777	1144	0.569	1045	0.399	946	0.278	3
A88Si-15	ActDes	1241	0.433	1142	0.334	1042	0.238	944	0.135	3
C22Si+15	ActDes	1206	0.508	1157	0.426	1058	0.290	959	0.172	3
C22Si-15	ActDes	1193	0.346	1144	0.302	1046	0.206	948	0.121	3
A1C1-1	ActDes	1236	0.578	1143	0.426	1049	0.304	955	0.195	3
A1C1-2	ActDes	1247	0.555	1153	0.402	1058	0.272	963	0.178	2
C1-AN107	ActDes	1248	0.439	1154	0.324	1057	0.218	962	0.136	5
A2-AP101	ActDes	1247	0.474	1153	0.356	1057	0.253	962	0.157	5
A2B1-1	ActDes	1237	0.427	1145	0.311	1049	0.206	957	0.132	2
A2B1-2	ActDes	1243	0.342	1151	0.251	1057	0.158	963	0.094	2
B1-AZ101	ActDes	1246	0.286	1152	0.204	1056	0.126	961	0.070	5
C2-AN102C35	ActDes	1248	0.378	1154	0.274	1059	0.175	963	0.105	1
A3-AN104	ActDes	1250	0.413	1155	0.299	1060	0.205	964	0.126	1
A2B1-3	ActDes	1244	0.354	1151	0.236	1056	0.150	963	0.086	2
A3C2-1	ActDes	1240	0.418	1147	0.326	1051	0.211	955	0.130	1
A3C2-2	ActDes	1248	0.392	1154	0.278	1058	0.188	963	0.114	1
A3C2-3	ActDes	1249	0.378	1154	0.270	1058	0.179	963	0.098	1
A1-AN105R2	ActDes	1246	0.484	1149	0.375	1053	0.288	958	0.180	5

(a) The Group IDs are described in Sections 2.1 to 2.6.

(b) Numbers from 1 to 5 denote the five split validation subsets. NA denotes “not applicable”, because these replicate glasses were forced into the modeling subsets, and thus were not parts of the validation subsets.

**Table 7.4. Variation in Electrical Conductivity Values for Replicate and Near-Replicate Pairs.**

Glass IDs of Replicate Pairs <sup>(a)</sup>	EC Values For Exact Temperatures at Each Nominal Temperature <sup>(b)</sup>								Pooled Over Temp.	
	950°C		1050°C		1150°C		1250°C		%RSD	SD
	T (°C)	S/cm	T (°C)	S/cm	T (°C)	S/cm	T (°C)	S/cm	S/cm	ln(S/cm)
LAWM01	959	0.052	1058	0.101	1156	0.169	1253	0.243		
LAWM53	945	0.074	1043	0.144	1141	0.241	1237	0.379		
<b>%RSD<sup>(c)</sup>, SD<sup>(d)</sup></b>	<b>24.69<sup>(e)</sup></b>	<b>0.249<sup>(e)</sup></b>	<b>24.82</b>	<b>0.251</b>	<b>24.83</b>	<b>0.251</b>	<b>30.92</b>	<b>0.314</b>	<b>26.45</b>	<b>0.268</b>
LAWM09	963	0.027	1057	0.054	1154	0.097	1248	0.139		
LAWM54R1	949	0.023	1047	0.048	1146	0.092	1236	0.146		
<b>%RSD<sup>(c)</sup>, SD<sup>(d)</sup></b>	<b>11.31</b>	<b>0.113</b>	<b>8.32</b>	<b>0.083</b>	<b>3.74</b>	<b>0.037</b>	<b>3.47</b>	<b>0.035</b>	<b>7.47</b>	<b>0.075</b>
LAWM12	973	0.249	1068	0.385	1161	0.553	1253	0.721		
LAWM55	944	0.248	1042	0.388	1139	0.588	1236	0.742		
<b>%RSD<sup>(c)</sup>, SD<sup>(d)</sup></b>	<b>0.28</b>	<b>0.003</b>	<b>0.55</b>	<b>0.005</b>	<b>4.34</b>	<b>0.043</b>	<b>2.03</b>	<b>0.020</b>	<b>2.41</b>	<b>0.024</b>
LAWM35	961	0.126	1056	0.205	1152	0.306	1246	0.425		
LAWM56	947	0.123	1041	0.223	1138	0.331	1235	0.481		
<b>%RSD<sup>(c)</sup>, SD<sup>(d)</sup></b>	<b>1.70</b>	<b>0.017</b>	<b>5.95</b>	<b>0.060</b>	<b>5.55</b>	<b>0.056</b>	<b>8.74</b>	<b>0.088</b>	<b>6.03</b>	<b>0.060</b>
LAWM50	947	0.101	1044	0.168	1143	0.260	1239	0.399		
LAWM51	939	0.091	1036	0.157	1133	0.245	1230	0.347		
<b>%RSD<sup>(c)</sup>, SD<sup>(d)</sup></b>	<b>7.37</b>	<b>0.074</b>	<b>4.79</b>	<b>0.048</b>	<b>4.20</b>	<b>0.042</b>	<b>9.86</b>	<b>0.099</b>	<b>6.93</b>	<b>0.069</b>
LAWM52	942	0.176	1038	0.280	1137	0.421	1234	0.568		
LAWA88R1	957	0.142	1053	0.211	1144	0.274	1245	0.389		
<b>%RSD<sup>(c)</sup>, SD<sup>(d)</sup></b>	<b>24.01</b>	<b>0.242</b>	<b>19.58</b>	<b>0.197</b>	<b>19.29</b>	<b>0.194</b>	<b>20.90</b>	<b>0.211</b>	<b>21.03</b>	<b>0.212</b>
<b>Pooled Over 6 Replicate Pairs<sup>(e)</sup></b>	<b>15.12</b>	<b>0.153</b>	<b>13.71</b>	<b>0.138</b>	<b>13.36</b>	<b>0.135</b>	<b>16.24</b>	<b>0.164</b>	<b>14.65</b>	<b>0.148</b>
Glass IDs of Replicate Pairs <sup>(a)</sup>	Electrical Conductivity Values at Nominal Temperatures <sup>(g)</sup>								Pooled Over Temp.	
	950°C		1050°C		1150°C		1250°C		%RSD	SD
	S/cm	ln(S/cm)	S/cm	ln(S/cm)	S/cm	ln(S/cm)	S/cm	ln(S/cm)	S/cm	ln(S/cm)
LAWM01	0.048	-3.030	0.097	-2.333	0.163	-1.813	0.241	-1.422		
LAWM53	0.077	-2.564	0.149	-1.906	0.255	-1.368	0.398	-0.921		
<b>%RSD<sup>(c)</sup>, SD<sup>(d)</sup></b>	<b>32.38</b>	<b>0.330</b>	<b>29.74</b>	<b>0.302</b>	<b>30.99</b>	<b>0.315</b>	<b>34.69</b>	<b>0.354</b>	<b>32.00</b>	<b>0.326</b>
LAWM09	0.024	-3.735	0.053	-2.946	0.093	-2.374	0.141	-1.958		
LAWM54R1	0.023	-3.767	0.050	-3.005	0.093	-2.376	0.157	-1.850		
<b>%RSD<sup>(c)</sup>, SD<sup>(d)</sup></b>	<b>2.24</b>	<b>0.022</b>	<b>4.16</b>	<b>0.042</b>	<b>0.14</b>	<b>0.001</b>	<b>7.58</b>	<b>0.076</b>	<b>4.47</b>	<b>0.045</b>
LAWM12	0.219	-1.517	0.359	-1.024	0.528	-0.638	0.717	-0.332		
LAWM55	0.255	-1.368	0.412	-0.887	0.591	-0.526	0.777	-0.253		
<b>%RSD<sup>(c)</sup>, SD<sup>(d)</sup></b>	<b>10.54</b>	<b>0.106</b>	<b>9.64</b>	<b>0.097</b>	<b>7.88</b>	<b>0.079</b>	<b>5.60</b>	<b>0.056</b>	<b>8.62</b>	<b>0.086</b>
LAWM35	0.118	-2.134	0.199	-1.613	0.304	-1.191	0.430	-0.843		
LAWM56	0.126	-2.068	0.228	-1.477	0.356	-1.033	0.498	-0.697		
<b>%RSD<sup>(c)</sup>, SD<sup>(d)</sup></b>	<b>4.67</b>	<b>0.047</b>	<b>9.65</b>	<b>0.097</b>	<b>11.14</b>	<b>0.112</b>	<b>10.35</b>	<b>0.104</b>	<b>9.30</b>	<b>0.093</b>
LAWM50	0.103	-2.273	0.171	-1.766	0.272	-1.303	0.415	-0.879		
LAWM51	0.097	-2.329	0.169	-1.779	0.261	-1.343	0.371	-0.993		
<b>%RSD<sup>(c)</sup>, SD<sup>(d)</sup></b>	<b>3.91</b>	<b>0.039</b>	<b>0.89</b>	<b>0.009</b>	<b>2.86</b>	<b>0.029</b>	<b>8.00</b>	<b>0.080</b>	<b>4.70</b>	<b>0.047</b>
LAWM52	0.183	-1.696	0.297	-1.213	0.437	-0.828	0.597	-0.516		
LAWA88R1	0.248	-1.394	0.385	-0.955	0.558	-0.583	0.767	-0.265		
<b>%RSD<sup>(c)</sup>, SD<sup>(d)</sup></b>	<b>21.16</b>	<b>0.213</b>	<b>18.18</b>	<b>0.183</b>	<b>17.26</b>	<b>0.173</b>	<b>17.70</b>	<b>0.178</b>	<b>18.64</b>	<b>0.188</b>
<b>Pooled Over 6 Replicate Pairs<sup>(f)</sup></b>	<b>16.58</b>	<b>0.168</b>	<b>15.38</b>	<b>0.155</b>	<b>15.56</b>	<b>0.157</b>	<b>17.21</b>	<b>0.175</b>	<b>16.20</b>	<b>0.164</b>

- (a) Because glass compositions were renormalized based on analyzed (or estimates of analyzed) SO<sub>3</sub> values, the compositions of replicate pairs may not match exactly. However, they were still treated as replicate pairs for statistical data analyses.
- (b) Electrical conductivity values are listed at the exact temperatures corresponding to the nominal temperature values.
- (c) %RSD = 100 × (Standard Deviation / Mean), calculated using the S/cm values.
- (d) Calculated using ln(S/cm) values.
- (e) The %RSD and SD values in the top part of the table are uncertainties of EC values, not temperature values. Because EC values at actual temperatures were used in the top part of the table, temperature and EC columns are listed.
- (f) The individual and pooled SDs estimate  $\sqrt{\sigma_G^2 + \sigma_T^2}$  in ln(S/cm) units (see Section C.2.2 of Appendix C).
- (g) Electrical conductivity values were interpolated at the nominal temperature values using a T2-equation (see Section C.2.1) fit for each glass.

**Table 7.5. Normalized<sup>(a)</sup> Compositions (mass fractions) for 10 Outlying LAW Glasses Excluded from the Electrical Conductivity and Viscosity Modeling Data.**

Glass ID	Group ID <sup>(b)</sup>	Al <sub>2</sub> O <sub>3</sub>	B <sub>2</sub> O <sub>3</sub>	CaO	Cl	Cr <sub>2</sub> O <sub>3</sub>	F	Fe <sub>2</sub> O <sub>3</sub>	K <sub>2</sub> O	Li <sub>2</sub> O	MgO	Na <sub>2</sub> O	P <sub>2</sub> O <sub>5</sub>	XRF SO <sub>3</sub> <sup>(c)</sup>	SiO <sub>2</sub>	TiO <sub>2</sub>	ZnO	ZrO <sub>2</sub>	Others	Sum <sup>(d)</sup>
LAWA43-1	ActDes	.12002	.07391	.01967	.00579	.00017	.00036	.06881	.03101	.00001	.01965	.20004	.00078	.00100	.38007	.01966	.02949	.02951	.00005	1.00000
LAWA49	ActDes	.06203	.08904	.00000	.00652	.00020	.00010	.09982	.00501	.00000	.01478	.20005	.00034	.00070	.44565	.01995	.02478	.02992	.00112	1.00000
LAWA50	ActDes	.06201	.08902	.00000	.00652	.00020	.00010	.11981	.00501	.00000	.01477	.20000	.00034	.00100	.42550	.01994	.02477	.02992	.00111	1.00000
LAWA82	ActDes	.06201	.08902	.00000	.00652	.00020	.00010	.06980	.00501	.00000	.01994	.20000	.00034	.00100	.44552	.03989	.02965	.02992	.00111	1.00000
LAWA89	ActDes	.06082	.09700	.00000	.00329	.00009	.00000	.05533	.02583	.00000	.01475	.20005	.00070	.00190	.44002	.03983	.02951	.02988	.00100	1.00000
LAWB60	ActDes	.06143	.12366	.11905	.00010	.00070	.00080	.00000	.00261	.04630	.02976	.06514	.00030	.00640	.47961	.00000	.03157	.03157	.00100	1.00000
LAWB62	ActDes	.06194	.09948	.11996	.00000	.00100	.00070	.00000	.00261	.05812	.02971	.05491	.00010	.00890	.48536	.01395	.03162	.03162	.00000	1.00000
LAWB63	ActDes	.06579	.09953	.09351	.00000	.00100	.00070	.00000	.00261	.05052	.02973	.05494	.00010	.00840	.48942	.01396	.05815	.03164	.00000	1.00000
LAWB82	ActDes	.06162	.10100	.07134	.00010	.00050	.00080	.09519	.00230	.04269	.01483	.06633	.00050	.00480	.45532	.00000	.05010	.03156	.00100	1.00000
LAWC12	ActDes	.11989	.09142	.01596	.00119	.00017	.00009	.05716	.00141	.00000	.01387	.20026	.00027	.00180	.39384	.03416	.04274	.02458	.00121	1.00000

- (a) The compositions listed in this table are normalized versions of target compositions of the glasses, after replacing the target values of SO<sub>3</sub> by XRF analyzed (or estimated analyzed) values. See Section 3.3 for the details.
- (b) The Group IDs are described in Sections 2.1 to 2.6.
- (c) XRF SO<sub>3</sub> denotes that the SO<sub>3</sub> composition is based on chemical analysis by XRF. For most glasses SO<sub>3</sub> was directly measured by XRF, but for some glasses estimated XRF values were used (see Section 3.3).
- (d) The normalized component mass fractions listed in this table were rounded to five decimals, and may not sum exactly to 1.00000 as listed. However, complete compositions listed to more decimal places and summing to 1.00000 were used for property-composition modeling.

**Table 7.6. Temperature and Electrical Conductivity Observations for 10 Outlying LAW Glasses Excluded from the Electrical Conductivity Modeling Set.**

<b>Glass ID</b>	<b>Group ID<sup>(a)</sup></b>	<b>Temp1 (°C)</b>	<b>EC1 (S/cm)</b>	<b>Temp2 (°C)</b>	<b>EC2 (S/cm)</b>	<b>Temp3 (°C)</b>	<b>EC3 (S/cm)</b>	<b>Temp4 (°C)</b>	<b>EC4 (S/cm)</b>
LAWA43-1	ActDes	1250	0.704	1153	0.537	1054	0.364	957	0.254
LAWA49	ActDes	1248	0.683	1150	0.521	1050	0.369	951	0.242
LAWA50	ActDes	1248	0.657	1151	0.514	1051	0.380	953	0.248
LAWA82	ActDes	1250	0.705	1139	0.499	1044	0.358	944	0.244
LAWA89	ActDes	1250	0.697	1147	0.542	1046	0.390	947	0.260
LAWB60	ActDes	1237	0.355	1143	0.244	1045	0.147	946	0.077
LAWB62	ActDes	1237	0.479	1142	0.342	1045	0.212	939	0.111
LAWB63	ActDes	1240	0.364	1142	0.239	1043	0.141	947	0.075
LAWB82	ActDes	1208	0.402	1113	0.219	1022	0.143	930	0.077
LAWC12	ActDes	1252	0.793	1150	0.600	1050	0.409	950	0.266

(a) The Group IDs are described in Sections 2.1 to 2.6.

**Table 7.7. Coefficients and Performance Summary for 36-Term Arrhenius-Linear Mixture Model on the Natural Logarithm of ILAW Electrical Conductivity.**

Mixture Terms ( $x_i$ )	Coefficient Estimate	Coefficient Stand. Dev.	Mixture-Temp. Terms [ $x_i/(T/1000)$ ]	Coefficient Estimate	Coefficient Stand. Dev.	t-value = Coeff/SD	p-value	Modeling Data Statistic, 171 Glasses <sup>(a)</sup>	Value		
Al <sub>2</sub> O <sub>3</sub>	2.9942	2.6225	Al <sub>2</sub> O <sub>3</sub> /(T/1000)	-8.8630	3.1836	-2.78	0.0056	R <sup>2</sup>	0.931		
B <sub>2</sub> O <sub>3</sub>	6.9687	1.8088	B <sub>2</sub> O <sub>3</sub> /(T/1000)	-11.7268	2.1918	-5.35	< 0.0001	SSE	21.039		
CaO	18.3598	1.5980	CaO/(T/1000)	-31.3265	1.9348	-16.19	< 0.0001	RMSE	0.180		
Cl	-4.1068	14.8679	Cl/(T/1000)	-21.2807	18.1517	-1.17	0.2416	<b>Extrapolative Validation Statistic, 10 Outlying Glasses<sup>(a,c)</sup></b>			
Cr <sub>2</sub> O <sub>3</sub>	-37.3878	45.0171	Cr <sub>2</sub> O <sub>3</sub> /(T/1000)	90.7468	55.3137	1.64	0.1015	R <sup>2</sup> Validation (R <sup>2</sup> <sub>v</sub> )	0.900		
F	86.8192	52.4921	F/(T/1000)	-165.5948	64.1204	-2.58	0.0101	RMSE Validation (RMSE <sub>v</sub> )	0.198		
Fe <sub>2</sub> O <sub>3</sub>	5.0372	1.7948	Fe <sub>2</sub> O <sub>3</sub> /(T/1000)	-10.4961	2.1813	-4.81	< 0.0001	<b>Data Partition Statistic, 86 Modeling &amp; 85 Validation<sup>(a,d)</sup></b>			
K <sub>2</sub> O	5.8881	2.5028	K <sub>2</sub> O/(T/1000)	-9.2665	3.0356	-3.05	0.0024	R <sup>2</sup>	0.941		
Li <sub>2</sub> O	-1.4398	3.6326	Li <sub>2</sub> O/(T/1000)	29.1695	4.4086	6.62	< 0.0001	SSE	10.878		
MgO	14.8230	3.3667	MgO/(T/1000)	-25.7152	4.0814	-6.30	< 0.0001	RMSE	0.188		
Na <sub>2</sub> O	0.3480	1.0866	Na <sub>2</sub> O/(T/1000)	11.9228	1.3186	9.04	< 0.0001	R <sup>2</sup> Validation (R <sup>2</sup> <sub>v</sub> )	-0.953 <sup>(g)</sup>		
P <sub>2</sub> O <sub>5</sub>	10.3075	5.7603	P <sub>2</sub> O <sub>5</sub> /(T/1000)	-14.8917	6.9923	-2.13	0.0337	RMSE Validation (RMSE <sub>v</sub> )	0.808 <sup>(g)</sup>		
SO <sub>3</sub>	-5.8104	22.9176	SO <sub>3</sub> /(T/1000)	19.1452	27.7842	0.69	0.4911	(e) See Section 7.1.2. (f) These statistics require extra effort to calculate for GLS regression (see Section C.3.2 in Appendix C) and were only calculated for the recommended model. (g) The partitioned data does not adequately support all 18 components, which leads to poor validation performance.			
SiO <sub>2</sub>	2.9629	0.8044	SiO <sub>2</sub> /(T/1000)	-9.8004	0.9774	-10.03	< 0.0001				
TiO <sub>2</sub>	5.6800	4.0961	TiO <sub>2</sub> /(T/1000)	-12.8484	4.9649	-2.59	0.0099				
ZnO	15.8354	3.4316	ZnO/(T/1000)	-25.2166	4.1607	-6.06	< 0.0001				
ZrO <sub>2</sub>	7.1839	3.6708	ZrO <sub>2</sub> /(T/1000)	-14.4117	4.4522	-3.24	0.0013				
Others <sup>(b)</sup>	-87.4387	72.5525	Others/(T/1000)	158.1939	88.3547	1.79	0.0740				
$\hat{\sigma}_G = 0.1760$			$\hat{\sigma}_T = 0.0565$								
<b>Data Splitting Statistic<sup>(a,e)</sup></b>		<b>DS1</b>	<b>DS2</b>	<b>DS3</b>	<b>DS4</b>	<b>DS5</b>	<b>Average</b>				
R <sup>2</sup>		(f)	(f)	(f)	(f)	(f)	(f)				
SSE		(f)	(f)	(f)	(f)	(f)	(f)				
RMSE		(f)	(f)	(f)	(f)	(f)	(f)				
R <sup>2</sup> Validation (R <sup>2</sup> <sub>v</sub> )		(f)	(f)	(f)	(f)	(f)	(f)				
RMSE Validation (RMSE <sub>v</sub> )		(f)	(f)	(f)	(f)	(f)	(f)				

- (a) The model evaluation statistics are defined in Section C.3 of Appendix C. Model validation statistics are defined in Section C.5 of Appendix C. A negative value for R<sup>2</sup><sub>v</sub> means that the sum of squares of model prediction errors is larger than if the mean response value over the validation data set were used as the predicted value for each glass. In other words, the model predicts worse for the validation data than the mean response value does.
- (b) The “Others” component includes Ag<sub>2</sub>O, BaO, Br, CdO, Cs<sub>2</sub>O, I, La<sub>2</sub>O<sub>3</sub>, MnO, MoO<sub>3</sub>, NiO, PbO, Re<sub>2</sub>O<sub>7</sub>, SeO<sub>2</sub>, SrO, and “Unknown”.
- (c) See Section 7.1.4.
- (d) See Section 7.1.3.

**Table 7.8. Coefficients and Performance Summary for 22-Term Reduced Arrhenius-Linear Mixture Model on the Natural Logarithm of ILAW Electrical Conductivity.**

Mixture Terms ( $x_i$ )	Coefficient Estimate	Coefficient Stand. Dev.	Mixture-Temp. Terms [ $x_i/(T/1000)$ ]	Coefficient Estimate	Coefficient Stand. Dev.	t-value = Coeff/SD	p-value	Modeling Data Statistic, 171 Glasses <sup>(a)</sup>	Value	
Al <sub>2</sub> O <sub>3</sub>	2.9948	2.6421	Al <sub>2</sub> O <sub>3</sub> /(T/1000)	-9.1229	3.1856	-2.86	0.0044	R <sup>2</sup>	0.923	
B <sub>2</sub> O <sub>3</sub>	7.0161	1.8111	B <sub>2</sub> O <sub>3</sub> /(T/1000)	-11.1910	2.1810	-5.13	< 0.0001	SSE	23.547	
CaO	17.8262	1.5561	CaO/(T/1000)	-30.7267	1.8732	-16.40	< 0.0001	RMSE	0.189	
Fe <sub>2</sub> O <sub>3</sub>	4.2374	1.7082	Fe <sub>2</sub> O <sub>3</sub> /(T/1000)	-9.3310	2.0629	-4.52	< 0.0001			
K <sub>2</sub> O	7.2429	2.2404	K <sub>2</sub> O/(T/1000)	-11.6388	2.7047	-4.30	< 0.0001			
Li <sub>2</sub> O	-1.9447	3.5025	Li <sub>2</sub> O/(T/1000)	30.6582	4.2256	7.26	< 0.0001			
MgO	14.6695	3.3664	MgO/(T/1000)	-25.2760	4.0580	-6.23	< 0.0001	<b>Extrapolative Validation Statistic, 10 Outlying Glasses<sup>(a,c)</sup></b>	<b>Value</b>	
Na <sub>2</sub> O	-0.3871	1.0335	Na <sub>2</sub> O/(T/1000)	12.4238	1.2473	9.96	< 0.0001	R <sup>2</sup> Validation (R <sup>2</sup> <sub>v</sub> )	0.905	
SiO <sub>2</sub>	3.2756	0.7456	SiO <sub>2</sub> /(T/1000)	-10.1179	0.9016	-11.22	< 0.0001	RMSE Validation (RMSE <sub>v</sub> )	0.194	
ZrO <sub>2</sub>	9.0672	3.4583	ZrO <sub>2</sub> /(T/1000)	-16.4492	4.1707	-3.94	< 0.0001			
Others <sup>(b)</sup>	9.7634	2.1667	Others/(T/1000)	-17.7342	2.6165	-6.78	< 0.0001			
$\hat{\sigma}_G = 0.1829$			$\hat{\sigma}_T = 0.0569$							
<b>Data Splitting Statistic<sup>(a,e)</sup></b>		<b>DS1</b>	<b>DS2</b>	<b>DS3</b>	<b>DS4</b>	<b>DS5</b>	<b>Average</b>	<b>Data Partition Statistic, 86 Modeling &amp; 85 Validation<sup>(a,d)</sup></b>	<b>Value</b>	
R <sup>2</sup>		(f)	(f)	(f)	(f)	(f)	(f)	R <sup>2</sup>	0.929	
SSE		(f)	(f)	(f)	(f)	(f)	(f)	SSE	13.241	
RMSE		(f)	(f)	(f)	(f)	(f)	(f)	RMSE	0.203	
R <sup>2</sup> Validation (R <sup>2</sup> <sub>v</sub> )		(f)	(f)	(f)	(f)	(f)	(f)	R <sup>2</sup> Validation (R <sup>2</sup> <sub>v</sub> )	0.878	
RMSE Validation (RMSE <sub>v</sub> )		(f)	(f)	(f)	(f)	(f)	(f)	RMSE Validation (RMSE <sub>v</sub> )	0.202	

- (a) The model evaluation statistics are defined in Section C.3 of Appendix C. Model validation statistics are defined in Section C.5 of Appendix C. A negative value for R<sup>2</sup><sub>v</sub> means that the sum of squares of model prediction errors is larger than if the mean response value over the validation data set were used as the predicted value for each glass. In other words, the model predicts worse for the validation data than the mean response value does.
- (b) The “Others” component includes Ag<sub>2</sub>O, BaO, Br, CdO, Cs<sub>2</sub>O, I, La<sub>2</sub>O<sub>3</sub>, MnO, MoO<sub>3</sub>, NiO, PbO, Re<sub>2</sub>O<sub>7</sub>, SeO<sub>2</sub>, SrO, and “Unknown” as well as the reduced components Cl, Cr<sub>2</sub>O<sub>3</sub>, F, P<sub>2</sub>O<sub>5</sub>, SO<sub>3</sub>, TiO<sub>2</sub>, and ZnO.
- (c) The 10 outlying LAW glass compositions are discussed in Section 7.1.4.
- (d) The partition of the EC modeling data set into modeling and validation subsets is described in Section 7.1.3.
- (e) The evaluation and validation statistics calculated for data-splits are defined the same as for separate modeling and validation sets. Section 7.1.2 describes how the data-splitting was accomplished.
- (f) These statistics require extra effort to calculate for GLS regression (see Section C.3.2 in Appendix C) and were only calculated for the recommended model.

**Table 7.9. Summary Statistics for Various Models Fitted and Validated Using ILAW Electrical Conductivity Data.**

<b>Results Using all 171 LAW Glasses with Electrical Conductivity Data</b>						
<b>Statistic</b>	<b>Model 1</b>	<b>Model 2</b>	<b>Model 3<sup>(a)</sup></b>	<b>Model 4</b>	<b>Model 5</b>	<b>Model 6</b>
# Model Terms	36	22	25	28	27	26
R <sup>2</sup>	0.931	0.923	0.951	0.951	0.951	0.951
SSE	21.039	23.547	15.010	14.908	14.914	14.927
RMSE	0.180	0.189	0.151	0.151	0.151	0.151
<b>Model Term</b>	<b>p-value</b>	<b>p-value</b>	<b>p-value<sup>(b)</sup></b>	<b>p-value</b>	<b>p-value</b>	<b>p-value</b>
CaO×Li <sub>2</sub> O	NA	NA	0.0013	0.6065	0.0013	0.0013
CaO×Na <sub>2</sub> O	NA	NA	< 0.0001	0.4918	0.4699	< 0.0001
Li <sub>2</sub> O×Na <sub>2</sub> O	NA	NA	< 0.0001	0.0468	0.0054	0.0506
CaO×Li <sub>2</sub> O/(T/1000)	NA	NA	NA	0.0518	NA	NA
CaO×Na <sub>2</sub> O/(T/1000)	NA	NA	NA	0.0026	0.0209	NA
Li <sub>2</sub> O×Na <sub>2</sub> O/(T/1000)	NA	NA	NA	< 0.0001	< 0.0001	< 0.0001
<b>Results Using 86 LAW Glasses for Modeling and 85 for Validation<sup>(c)</sup></b>						
<b>Statistic</b>	<b>Model 1</b>	<b>Model 2</b>	<b>Model 3</b>	<b>Model 4</b>	<b>Model 5</b>	<b>Model 6</b>
R <sup>2</sup>	0.941	0.929	0.947	0.948	0.948	0.947
SSE	10.878	13.241	9.788	9.733	9.733	9.736
RMSE	0.188	0.203	0.175	0.176	0.175	0.175
R <sup>2</sup> <sub>v</sub>	-0.953 <sup>(d)</sup>	0.878	0.939	0.940	0.940	0.940
RMSE <sub>v</sub>	0.808 <sup>(d)</sup>	0.202	0.142	0.141	0.141	0.142
<b>Model Term</b>	<b>p-value</b>	<b>p-value</b>	<b>p-value</b>	<b>p-value</b>	<b>p-value</b>	<b>p-value</b>
CaO×Li <sub>2</sub> O	NA	NA	0.0489	0.4293	0.0480	0.0479
CaO×Na <sub>2</sub> O	NA	NA	0.0001	0.5140	0.3790	0.0001
Li <sub>2</sub> O×Na <sub>2</sub> O	NA	NA	0.0022	0.0730	0.0481	0.1271
CaO×Li <sub>2</sub> O/(T/1000)	NA	NA	NA	0.9569	NA	NA
CaO×Na <sub>2</sub> O/(T/1000)	NA	NA	NA	0.2547	0.1293	NA
Li <sub>2</sub> O×Na <sub>2</sub> O/(T/1000)	NA	NA	NA	0.0007	0.0001	0.0005

- (a) Model 3 is the recommended model, indicated by gray shading in the column.
- (b) A p-value less than 0.05 indicates the coefficient of the corresponding model term is significantly different from zero with 95% confidence.
- (c) There were 86 glasses in the ILAW Existing Matrix, Phase 1 Test Matrix, and Phase 1a Augmentation Test Matrix that have data for electrical conductivity. The remaining 85 glasses were used as a validation subset.
- (d) There is less support, or potentially even inadequate support, for fitting the 36-term full model using the partitioned modeling data set of 86 LAW glasses. That portion of the data set was designed to support 14 rather than 18 components. Hence, the model performance was poor for some of the validation glasses.



**Table 7.10. Coefficients and Performance Summary for 25-Term Reduced Arrhenius-Linear Mixture Model with Three Crossproduct Terms on the Natural Logarithm of ILAW Electrical Conductivity.**

Mixture Terms ( $x_i$ )	Coefficient Estimate	Coefficient Stand. Dev.	Mixture-Temp. Terms [ $x_i/(T/1000)$ ]	Coefficient Estimate	Coefficient Stand. Dev.	t-value = Coeff/SD	p-value	Modeling Data Statistic, 171 Glasses <sup>(a)</sup>	Value	
Al <sub>2</sub> O <sub>3</sub>	2.3854	2.5456	Al <sub>2</sub> O <sub>3</sub> /(T/1000)	-9.0593	3.1966	-2.83	0.0048	R <sup>2</sup>	0.951	
B <sub>2</sub> O <sub>3</sub>	7.9750	1.7536	B <sub>2</sub> O <sub>3</sub> /(T/1000)	-11.0983	2.1885	-5.07	< 0.0001	SSE	15.010	
CaO	5.2093	3.0161	CaO/(T/1000)	-30.6535	1.8797	-16.31	< 0.0001	RMSE	0.151	
Fe <sub>2</sub> O <sub>3</sub>	4.3935	1.6656	Fe <sub>2</sub> O <sub>3</sub> /(T/1000)	-9.2407	2.0700	-4.46	< 0.0001			
K <sub>2</sub> O	7.6774	2.1834	K <sub>2</sub> O/(T/1000)	-11.5299	2.7137	-4.25	< 0.0001			
Li <sub>2</sub> O	4.2464	5.0291	Li <sub>2</sub> O/(T/1000)	30.4827	4.2400	7.19	< 0.0001			
MgO	15.1675	3.2610	MgO/(T/1000)	-25.0634	4.0719	-6.16	< 0.0001			
Na <sub>2</sub> O	-2.0291	1.2653	Na <sub>2</sub> O/(T/1000)	12.3822	1.2516	9.89	< 0.0001	<b>Extrapolative Validation Statistic, 10 Outlying Glasses<sup>(a,c)</sup></b>	<b>Value</b>	
SiO <sub>2</sub>	3.6811	0.7384	SiO <sub>2</sub> /(T/1000)	-10.1563	0.9047	-11.23	< 0.0001	R <sup>2</sup> Validation (R <sup>2</sup> <sub>v</sub> )	0.920	
ZrO <sub>2</sub>	7.8740	3.3302	ZrO <sub>2</sub> /(T/1000)	-16.5390	4.1850	-3.95	< 0.0001	RMSE Validation (RMSE <sub>v</sub> )	0.178	
Others <sup>(b)</sup>	11.2069	2.1288	Others/(T/1000)	-17.7117	2.6254	-6.75	< 0.0001			
CaO×Li <sub>2</sub> O	144.9519	44.2208								
CaO×Na <sub>2</sub> O	79.0190	14.6533								
Li <sub>2</sub> O×Na <sub>2</sub> O	-130.1441	17.2032								
$\hat{\sigma}_G = 0.1431$			$\hat{\sigma}_T = 0.0571$							
<b>Data-Splitting Statistic<sup>(a,e)</sup></b>		<b>DS1</b>	<b>DS2</b>	<b>DS3</b>	<b>DS4</b>	<b>DS5</b>	<b>Average</b>	<b>Data Partition Statistic, 86 Modeling &amp; 85 Validation<sup>(a,d)</sup></b>		
R <sup>2</sup>		0.950	0.952	0.949	0.947	0.964	0.952	R <sup>2</sup>	0.947	
SSE		12.943	11.900	12.647	13.192	8.976	11.932	SSE	9.788	
RMSE		0.156	0.150	0.154	0.158	0.130	0.149	RMSE	0.175	
R <sup>2</sup> Validation (R <sup>2</sup> <sub>v</sub> )		0.949	0.929	0.952	0.962	0.887	0.936	R <sup>2</sup> Validation (R <sup>2</sup> <sub>v</sub> )	0.939	
RMSE Validation (RMSE <sub>v</sub> )		0.138	0.173	0.142	0.131	0.226	0.162	RMSE Validation (RMSE <sub>v</sub> )	0.142	

- (a) The model evaluation statistics are defined in Section C.3 of Appendix C. Model validation statistics are defined in Section C.5 of Appendix C. A negative value for R<sup>2</sup><sub>v</sub> means that the sum of squares of model prediction errors is larger than if the mean response value over the validation data set were used as the predicted value for each glass. In other words, the model predicts worse for the validation data than the mean response value does.
- (b) The “Others” component includes Ag<sub>2</sub>O, BaO, Br, CdO, Cs<sub>2</sub>O, I, La<sub>2</sub>O<sub>3</sub>, MnO, MoO<sub>3</sub>, NiO, PbO, Re<sub>2</sub>O<sub>7</sub>, SeO<sub>2</sub>, SrO, and “Unknown” as well as the reduced components Cl, Cr<sub>2</sub>O<sub>3</sub>, F, P<sub>2</sub>O<sub>5</sub>, SO<sub>3</sub>, TiO<sub>2</sub>, and ZnO.
- (c) The 10 outlying LAW glass compositions are discussed in Section 7.1.4.
- (d) The partition of the EC modeling data set into modeling and validation subsets is described in Section 7.1.3.
- (e) The evaluation and validation statistics calculated for data-splits are defined the same as for separate modeling and validation sets. Section 7.1.2 describes how the data-splitting was accomplished.

**Table 7.11. LAWA126 Composition in Formats Needed for Use in ILAW Electrical Conductivity Models.**

<b>Model Term<sup>(a)</sup></b>	<b>LAWA126 Composition<sup>(b)</sup> (wt%)</b>	<b>LAWA126 Composition (mass fractions) for Use in 22-Term EC Model 2<sup>(c)</sup></b>	<b>LAWA126 Composition (mass fractions) for Use in 25-Term EC Model 3<sup>(d)</sup></b>
Al <sub>2</sub> O <sub>3</sub>	0.05637	0.05637	0.05637
B <sub>2</sub> O <sub>3</sub>	0.09815	0.09815	0.09815
CaO	0.01989	0.01989	0.01989
Cl	0.00200	NA <sup>(e)</sup>	NA
Cr <sub>2</sub> O <sub>3</sub>	0.00020	NA	NA
F	0.00300	NA	NA
Fe <sub>2</sub> O <sub>3</sub>	0.05537	0.05537	0.05537
K <sub>2</sub> O	0.03878	0.03878	0.03878
Li <sub>2</sub> O	0.00000	0.00000	0.00000
MgO	0.01479	0.01479	0.01479
Na <sub>2</sub> O	0.18451	0.18451	0.18451
P <sub>2</sub> O <sub>5</sub>	0.00080	NA	NA
SO <sub>3</sub>	0.00310	NA	NA
SiO <sub>2</sub>	0.44098	0.44098	0.44098
TiO <sub>2</sub>	0.01999	NA	NA
ZnO	0.02959	NA	NA
ZrO <sub>2</sub>	0.02989	0.02989	0.02989
Others	0.00260	0.06127	0.06127
CaO×Li <sub>2</sub> O	NA	NA	0.00000
CaO×Na <sub>2</sub> O	NA	NA	0.00367
Li <sub>2</sub> O×Na <sub>2</sub> O	NA	NA	0.00000

- (a) The electrical conductivity models contain  $x_i/(T/1000)$  terms in addition to the  $x_i$  and  $x_i x_j$  terms shown in this column. The purpose of this table is to show the compositional forms needed for model predictions, so the temperature-containing terms are not shown.
- (b) The composition in mass fractions is from Table 7.2.
- (c) See Table 7.8.
- (d) See Table 7.9.
- (e) NA = not applicable, because the model does not contain this term.

**Table 7.12. Predicted Electrical Conductivity, Standard Deviation, and Statistical Intervals for LAWA126 Composition Used in ILAW Electrical Conductivity Models.**

Model <sup>(a)</sup>	Predicted ln(EC) [ln(S/cm)]	Predicted EC <sup>(c)</sup> [S/cm]	Standard Deviation of Predicted ln(EC) <sup>(d)</sup> [ln(S/cm)]	90% LCI <sup>(e)</sup> on Mean ln(EC) [ln(S/cm)]	90% LCI <sup>(e)</sup> on Median EC [S/cm]	90% UCI <sup>(e)</sup> on Mean ln(EC) [ln(S/cm)]	90% UCI <sup>(e)</sup> on Median EC [S/cm]	90% CI <sup>(e)</sup> on Mean ln(EC) [ln(S/cm)]	90% CI <sup>(e)</sup> on Median EC [S/cm]
22-Term EC Model at 1143°C <sup>(b)</sup>	-0.9775 <sup>(f)</sup>	0.376	0.0304	-1.0167	0.362	-0.9383	0.391	(-1.0279, -0.9271)	(0.358, 0.396)
25-Term EC Model at 1143°C <sup>(b)</sup>	-0.9168	0.400	0.0273	-0.9520	0.386	-0.8816	0.414	(-0.9620, -0.8716)	(0.382, 0.418)

- (a) The two models in this column are given in Tables 7.8 and 7.10, respectively.
- (b) The temperature of 1143°C was chosen because it was one of the temperatures at which the EC of LAWA126 was measured. This facilitates comparison of the predicted and measured values.
- (c) Of the two models, the one with the predicted EC value at 1143°C closest to the measured value of 0.373 S/cm is the 22-term EC model. However, the prediction using the 25-term model is very close.
- (d) The standard deviation is for the ln(EC) prediction at 1143°C considered to be the mean of such values for the LAWA126 glass.
- (e) UCI = upper confidence interval, LCI = lower confidence interval, and CI = two-sided confidence interval (see Section C.7 of Appendix C).
- (f) All calculations were performed using the LAWA126 glass composition, model coefficients, and variance-covariance matrix values given in tables of this report. The calculated ln(S/cm) values were rounded to four decimal places in this table. The S/cm values were calculated by exponentiating the ln(S/cm) values before rounding, then rounding the resulting values to three decimal places in this table.

**Table 8.1. Temperature and Viscosity Observations and Data-Splitting Validation Sets for Each of the 171 LAW Glasses Used for Viscosity Model Development.**

Glass ID	Group ID <sup>(a)</sup>	Temp1 (°C)	Vis1 (P)	Temp2 (°C)	Vis2 (P)	Temp3 (°C)	Vis3 (P)	Temp4 (°C)	Vis4 (P)	Viscosity Data Splitting Validation Set <sup>(b)</sup>
LAWA44R10	ExPh1	1233	34.89	1134	83.13	1034	247.19	935	1001.77	4
LAWA53	ExPh1	1250	23.16	1153	54.10	1057	158.10	961	644.90	3
LAWA56	ExPh1	1254	22.26	1156	48.29	1058	133.71	961	489.26	3
LAWA88	ExPh1	1244	27.27	1133	71.10	1032	198.05	931	750.05	NA
LAWA102R1	ExPh1	1241	24.23	1145	52.83	1050	142.49	954	515.05	3
LAWA126	ExPh1	1261	24.12	1161	55.81	1061	161.83	960	598.57	1
LAWA128R1	ExPh1	1261	34.29	1161	83.05	1061	258.87	961	1049.25	3
LAWA130	ExPh1	1228	35.41	1126	91.30	1023	281.27	921	1241.71	1
LAWB65	ExPh1	1264	19.61	1164	46.05	1064	137.88	964	530.89	1
LAWB66	ExPh1	1265	16.96	1162	39.48	1060	119.18	959	473.33	3
LAWB68	ExPh1	1264	21.11	1164	49.66	1064	150.84	964	599.38	1
LAWB78	ExPh1	1256	18.28	1156	40.12	1056	109.81	971	374.92	5
LAWB79	ExPh1	1241	18.92	1141	44.62	1041	122.63	951	456.78	4
LAWB80	ExPh1	1252	22.77	1152	53.00	1052	155.45	952	614.12	5
LAWB83	ExPh1	1253	22.13	1155	49.86	1058	148.96	962	562.98	5
LAWB84	ExPh1	1268	18.67	1168	42.54	1068	124.70	968	470.71	1
LAWB85	ExPh1	1255	22.50	1155	51.79	1055	149.43	957	552.70	5
LAWB86	ExPh1	1250	21.52	1149	50.37	1049	135.84	968	478.21	2
C100-G-136B	ExPh1	1271	21.36	1169	46.28	1067	130.19	965	463.82	3
LAWC27	ExPh1	1246	23.59	1146	54.06	1046	145.68	946	543.51	4
LAWC32	ExPh1	1255	15.44	1162	34.91	1062	96.79	963	331.64	5
LAWM1	Ph1	1252	16.91	1152	35.00	1053	94.14	953	376.96	NA
LAWM2	Ph1	1244	9.60	1147	21.38	1051	59.90	953	253.24	3
LAWM3	Ph1	1249	8.29	1152	17.88	1053	45.54	956	162.10	4
LAWM4	Ph1	1254	6.02	1154	13.03	1054	32.10	954	110.63	4
LAWM5	Ph1	1246	52.13	1149	126.97	1052	363.81	956	1562.29	3
LAWM6	Ph1	1244	21.08	1144	52.45	1044	173.14	944	872.14	4
LAWM7 <sup>(c)</sup>	Ph1	1252	41.88	1152	113.87	1052	386.83	952	1996.66	2
LAWM8	Ph1	1225	35.17	1128	93.96	1030	328.41	932	1626.62	3
LAWM9	Ph1	1252	43.77	1150	126.36	1048	462.35	946	2329.04	NA
LAWM10	Ph1	1238	7.23	1143	15.04	1047	36.31	952	114.91	2
LAWM11	Ph1	1239	7.48	1142	13.73	1045	29.09	948	73.40	5
LAWM12	Ph1	1246	6.82	1148	14.24	1049	32.05	951	90.07	NA
LAWM13	Ph1	1246	7.60	1148	14.67	1051	32.41	954	91.38	3
LAWM14	Ph1	1234	25.14	1138	51.91	1042	131.85	945	430.55	5
LAWM15	Ph1	1245	30.81	1148	67.56	1051	176.27	955	624.02	1
LAWM16	Ph1	1247	12.50	1150	25.81	1052	64.58	955	214.94	1
LAWM17	Ph1	1237	15.81	1143	35.08	1049	94.19	955	331.97	4
LAWM18	Ph1	1243	14.38	1141	31.26	1039	85.32	939	306.52	4
LAWM19	Ph1	1243	30.72	1146	71.70	1049	271.86	952	1146.71	5
LAWM20	Ph1	1240	10.52	1142	22.47	1045	58.37	948	195.96	5

- (a) The Group IDs are described in Sections 2.1 to 2.6.  
 (b) Numbers from 1 to 5 denote the five split validation subsets. NA denotes “not applicable”, because these replicate glasses were forced into the modeling subsets, and thus were not parts of the validation subsets.  
 (c) This glass had a fifth viscosity measurement of 894.15 poise at 1002°C.

**Table 8.1. Temperature and Viscosity Observations and Data-Splitting Validation Sets for Each of the 171 LAW Glasses Used for Viscosity Model Development (continued).**

Glass ID	Group ID <sup>(a)</sup>	Temp1 (°C)	Vis1 (P)	Temp2 (°C)	Vis2 (P)	Temp3 (°C)	Vis3 (P)	Temp4 (°C)	Vis4 (P)	Viscosity Data Splitting Validation Set <sup>(b)</sup>
LAWM21	Ph1	1242	10.62	1145	22.26	1048	58.19	952	198.85	4
LAWM22	Ph1	1245	40.06	1144	106.27	1043	353.28	943	1696.57	5
LAWM23	Ph1	1238	27.31	1139	64.40	1040	191.57	942	797.88	3
LAWM24	Ph1	1238	39.99	1142	84.18	1046	218.17	951	751.15	5
LAWM25R1	Ph1	1240	40.81	1142	92.69	1044	255.56	947	891.03	4
LAWM26	Ph1	1236	37.82	1139	82.92	1043	239.14	946	836.07	3
LAWM27	Ph1	1243	18.12	1147	36.12	1051	90.31	957	290.01	1
LAWM28	Ph1	1241	43.34	1143	103.26	1044	309.25	945	2130.74	4
LAWM29	Ph1	1248	34.20	1150	78.11	1052	228.45	955	860.19	1
LAWM30	Ph1	1246	17.29	1149	34.17	1052	87.17	955	277.22	2
LAWM31	Ph1	1247	10.05	1149	20.10	1050	56.94	952	158.91	2
LAWM32	Ph1	1248	20.41	1149	42.21	1050	105.79	951	345.60	2
LAWM33R1	Ph1	1245	9.67	1148	19.16	1051	45.65	954	139.60	3
LAWM34	Ph1	1244	8.67	1147	16.67	1050	36.48	954	104.88	1
LAWM35	Ph1	1249	11.17	1149	25.02	1050	68.28	950	269.85	NA
LAWM36	Ph1	1237	18.99	1140	39.77	1044	106.51	947	385.10	3
LAWM37	Ph1	1237	15.79	1142	34.38	1047	90.46	951	318.00	5
LAWM38	Ph1	1234	26.60	1138	60.50	1042	166.84	945	596.59	2
LAWM39	Ph1	1230	25.27	1135	56.11	1041	151.89	946	531.87	1
LAWM40	Ph1	1236	34.33	1140	79.30	1044	231.63	947	929.51	4
LAWM41	Ph1	1241	28.68	1143	73.02	1046	222.56	948	1021.93	4
LAWM42	Ph1	1233	27.50	1134	63.19	1036	183.30	937	721.23	5
LAWM43	Ph1	1244	19.75	1147	45.52	1051	126.69	954	467.08	2
LAWM44	Ph1	1246	31.45	1149	74.85	1052	217.52	956	901.07	1
LAWM45	Ph1	1240	30.05	1146	69.01	1052	193.15	959	717.82	3
LAWM46	Ph1	1243	32.80	1144	80.94	1045	254.48	945	1159.85	2
LAWM47	Ph1	1235	31.99	1143	75.82	1051	227.57	960	941.10	2
LAWM48	Ph1	1249	36.63	1151	86.21	1053	257.34	956	1143.07	2
LAWM49	Ph1	1249	32.43	1149	75.11	1048	222.00	948	879.38	5
LAWM50	Ph1	1243	26.82	1146	60.43	1049	173.87	953	721.01	NA
LAWM51	Ph1	1248	26.09	1154	59.03	1060	171.04	966	624.53	NA
LAWM52	Ph1	1246	24.16	1149	51.50	1052	138.67	955	531.45	NA
LAWM53	Ph1	1248	16.84	1150	39.95	1056	105.13	958	314.34	NA
LAWM54R1	Ph1	1254	41.43	1155	105.91	1056	347.39	957	1659.86	NA
LAWM55	Ph1	1259	5.99	1158	11.23	1057	24.47	956	65.90	NA
LAWM56	Ph1	1245	11.82	1148	25.79	1052	69.99	956	262.73	NA
LAWM57	Ph1aAug	1247	12.94	1150	27.95	1054	72.11	958	245.32	4
LAWM59	Ph1aAug	1255	25.18	1156	54.13	1059	137.18	961	487.70	1
LAWM60	Ph1aAug	1257	20.39	1157	44.43	1057	119.32	958	433.64	5
LAWM63	Ph1aAug	1256	18.97	1156	37.79	1057	95.96	958	296.69	5
LAWM66	Ph1aAug	1254	13.70	1155	30.03	1056	79.27	958	277.89	4
LAWM68	Ph1aAug	1257	14.83	1156	30.17	1054	76.86	954	262.88	5

(a) The Group IDs are described in Sections 2.1 to 2.6.

(b) Numbers from 1 to 5 denote the five split validation subsets. NA denotes “not applicable”, because these replicate glasses were forced into the modeling subsets, and thus were not parts of the validation subsets.

**Table 8.1. Temperature and Viscosity Observations and Data-Splitting Validation Sets for Each of the 171 LAW Glasses Used for Viscosity Model Development (continued).**

Glass ID	Group ID <sup>(a)</sup>	Temp1 (°C)	Vis1 (P)	Temp2 (°C)	Vis2 (P)	Temp3 (°C)	Vis3 (P)	Temp4 (°C)	Vis4 (P)	Viscosity Data Splitting Validation Set <sup>(b)</sup>
LAWM71	Ph1aAug	1258	19.20	1157	40.96	1054	104.61	955	337.67	4
LAWM73	Ph1aAug	1260	14.32	1159	30.53	1057	77.71	957	257.01	1
LAWM75	Ph1aAug	1254	18.23	1153	40.45	1053	115.74	953	449.45	1
LAWE2H	Corr	1242	16.32	1142	34.08	1040	84.78	939	271.78	3
LAWE3	Corr	1249	23.74	1149	52.79	1051	143.69	952	525.82	2
LAWE3H	Corr	1211	21.28	1109	46.05	1006	120.37	903	419.24	3
LAWE4	Corr	1255	22.73	1159	49.41	1062	130.73	966	451.51	5
LAWE4H	Corr	1255	19.43	1159	41.03	1062	103.82	965	335.99	3
LAWE5	Corr	1253	26.04	1158	53.86	1062	141.51	967	470.58	4
LAWE5H	Corr	1252	17.08	1157	36.58	1062	92.54	966	295.17	2
LAWE7	Corr	1226	13.94	1124	28.57	1021	70.66	917	222.91	5
LAWE7H	Corr	1245	11.32	1145	22.20	1045	51.83	944	154.24	1
LAWE9H	Corr	1243	12.68	1147	25.89	1051	62.80	954	194.75	2
LAWE10H	Corr	1248	18.37	1153	39.54	1057	105.64	951	357.57	5
LAWE11	Corr	1251	26.08	1150	59.47	1049	167.75	949	636.57	5
LAWE12	Corr	1260	19.88	1158	43.90	1057	119.58	956	412.71	2
LAWE13	Corr	1258	21.60	1157	47.88	1057	127.53	957	439.36	5
LAWE16	Corr	1260	24.48	1159	54.64	1058	151.15	956	554.83	2
LAWCrP1R	HiCrP	1263	25.07	1163	55.71	1063	155.47	964	598.52	2
LAWCrP2R	HiCrP	1249	20.59	1149	45.39	1050	126.24	951	476.61	1
LAWCrP3R	HiCrP	1248	24.93	1151	55.49	1052	156.94	954	608.55	5
LAWCrP4R	HiCrP	1259	18.39	1157	41.80	1056	116.76	955	439.69	3
LAWCrP5	HiCrP	1252	14.23	1151	29.21	1051	73.72	951	262.10	2
LAWA41	ActDes	1248	28.37	1150	68.23	1050	198.18	950	737.09	5
LAWA42	ActDes	1257	12.95	1150	30.61	1050	85.64	950	306.13	1
LAWA45	ActDes	1250	28.10	1150	63.89	1050	183.46	950	683.85	2
LAWA51	ActDes	1243	47.46	1150	105.86	1050	320.66	950	1284.25	2
LAWA52	ActDes	1250	21.52	1139	57.87	1039	177.65	939	773.68	1
LAWA60	ActDes	1248	30.28	1130	77.64	1029	227.03	945	911.46	3
LAWA81	ActDes	1252	26.58	1152	68.91	1053	209.55	953	816.83	2
LAWA83	ActDes	1254	36.37	1145	98.08	1044	293.21	944	1237.99	4
LAWA90	ActDes	1256	26.60	1157	60.78	1055	171.12	956	609.53	3
LAWA93	ActDes	1249	7.46	1139	17.49	1041	40.74	940	128.09	5
LAWA96	ActDes	1252	30.67	1152	73.34	1052	223.42	953	905.47	2
LAWA125	ActDes	1257	17.54	1157	38.99	1057	107.12	957	367.95	1
LAWA127R1	ActDes	1256	32.81	1156	78.49	1056	245.11	957	1031.48	1
LAWA129R1	ActDes	1248	44.48	1148	111.31	1048	330.40	948	1370.72	1
LAWA134	ActDes	1239	30.60	1143	71.16	1046	198.22	950	771.55	5
LAWA135	ActDes	1233	37.10	1138	87.17	1042	257.58	948	962.96	5
LAWA136	ActDes	1230	26.94	1133	66.46	1034	192.85	936	826.33	4
LAWB30	ActDes	1255	13.82	1155	29.01	1056	77.89	946	328.04	3
LAWB34	ActDes	1257	31.64	1156	80.72	1056	248.68	955	993.47	2
LAWB37	ActDes	1246	39.21	1145	94.88	1045	288.12	945	1168.09	5

(a) The Group IDs are described in Sections 2.1 to 2.6.

(b) Numbers from 1 to 5 denote the five split validation subsets. NA denotes “not applicable”, because these replicate glasses were forced into the modeling subsets, and thus were not parts of the validation subsets.

**Table 8.1. Temperature and Viscosity Observations and Data-Splitting Validation Sets for Each of the 171 LAW Glasses Used for Viscosity Model Development (continued).**

Glass ID	Group ID <sup>(a)</sup>	Temp1 (°C)	Vis1 (P)	Temp2 (°C)	Vis2 (P)	Temp3 (°C)	Vis3 (P)	Temp4 (°C)	Vis4 (P)	Viscosity Data Splitting Validation Set <sup>(b)</sup>
LAWB38	ActDes	1254	27.60	1143	70.03	1043	195.22	943	722.92	2
LAWB61	ActDes	1230	18.43	1155	34.43	1058	92.83	958	332.53	1
LAWB64	ActDes	1257	15.12	1156	33.33	1056	88.14	957	345.61	1
LAWB67	ActDes	1266	27.31	1166	64.80	1066	197.14	967	805.21	1
LAWB69	ActDes	1247	16.61	1147	38.14	1047	102.80	947	373.54	3
LAWB70	ActDes	1239	17.57	1141	41.28	1043	114.17	946	421.57	5
LAWB71	ActDes	1238	19.09	1140	43.12	1042	113.53	945	405.23	2
LAWB72	ActDes	1250	19.39	1150	41.06	1050	116.03	950	422.00	5
LAWB73	ActDes	1246	15.35	1146	37.48	1046	107.53	947	430.54	2
LAWB74	ActDes	1257	13.46	1159	30.56	1059	86.62	958	322.40	5
LAWB75	ActDes	1261	13.75	1159	29.98	1057	81.52	956	306.58	2
LAWB76	ActDes	1270	13.39	1168	28.66	1066	75.45	963	259.89	3
LAWB77	ActDes	1252	32.91	1152	60.06	1052	169.14	967	572.51	3
LAWB81	ActDes	1253	16.54	1153	37.03	1053	106.98	946	425.89	2
LAWB87	ActDes	1235	30.70	1139	72.46	1043	200.91	948	760.82	4
LAWB88	ActDes	1255	21.87	1155	48.65	1056	140.31	956	525.15	3
LAWB89	ActDes	1256	18.91	1156	44.34	1055	132.68	955	522.71	4
LAWB90	ActDes	1244	23.60	1144	58.93	1043	166.75	943	703.81	1
LAWB92	ActDes	1227	28.53	1131	64.65	1036	187.26	941	757.05	4
LAWB93R1	ActDes	1250	20.68	1152	47.57	1053	140.69	955	554.31	4
LAWB94	ActDes	1245	22.01	1146	50.13	1047	141.21	948	578.08	2
LAWB95	ActDes	1244	24.77	1144	58.67	1043	172.31	942	739.97	5
LAWC21rev2	ActDes	1251	21.85	1151	47.41	1052	133.96	953	478.86	4
LAWC29	ActDes	1243	18.43	1143	41.95	1043	116.52	943	437.15	4
LAWC30	ActDes	1258	17.65	1159	38.88	1059	110.00	959	400.48	4
LAWC31R1	ActDes	1261	16.26	1161	36.47	1061	103.94	961	378.47	4
C22AN107	ActDes	1253	19.30	1153	41.64	1053	115.57	953	396.25	4
A88Si+15	ActDes	1251	19.18	1151	40.53	1051	112.08	951	390.39	1
A88Si-15	ActDes	1262	33.46	1162	80.99	1062	262.09	962	1114.95	1
C22Si+15	ActDes	1192	24.41	1143	38.09	1044	95.76	944	314.32	1
C22Si-15	ActDes	1189	39.02	1085	101.57	985	331.96	935	677.87	3
A1C1-1	ActDes	1251	24.32	1152	56.59	1052	164.16	953	615.46	4
A1C1-2	ActDes	1253	21.82	1153	46.42	1051	129.84	950	458.57	2
C1-AN107	ActDes	1220	25.84	1126	56.90	1032	151.51	938	558.46	4
A2-AP101	ActDes	1251	25.09	1153	57.76	1053	165.07	955	595.97	3
A2B1-1	ActDes	1251	25.78	1152	59.98	1052	173.00	952	638.01	2
A2B1-2	ActDes	1241	25.47	1139	60.90	1037	171.95	935	708.67	4
B1-AZ101	ActDes	1247	22.95	1149	52.76	1051	151.27	953	607.75	3
C2-AN102C35	ActDes	1249	16.21	1150	34.86	1051	90.80	952	322.86	4
A3-AN104	ActDes	1244	16.61	1146	35.69	1048	92.50	950	309.47	3
A2B1-3	ActDes	1225	26.24	1128	66.36	1031	205.08	935	901.60	1

(a) The Group IDs are described in Sections 2.1 to 2.6.

(b) Numbers from 1 to 5 denote the five split validation subsets. NA denotes “not applicable”, because these replicate glasses were forced into the modeling subsets, and thus were not parts of the validation subsets.

**Table 8.1. Temperature and Viscosity Observations and Data-Splitting Validation Sets for Each of the 171 LAW Glasses Used for Viscosity Model Development (continued).**

<b>Glass ID</b>	<b>Group ID<sup>(a)</sup></b>	<b>Temp1 (°C)</b>	<b>Vis1 (P)</b>	<b>Temp2 (°C)</b>	<b>Vis2 (P)</b>	<b>Temp3 (°C)</b>	<b>Vis3 (P)</b>	<b>Temp4 (°C)</b>	<b>Vis4 (P)</b>	<b>Viscosity Data Splitting Validation Set<sup>(b)</sup></b>
A3C2-1	ActDes	1220	23.32	1125	50.74	1031	132.81	936	461.77	1
A3C2-2	ActDes	1241	17.23	1144	36.37	1047	94.11	950	318.79	3
A3C2-3	ActDes	1239	16.62	1141	35.69	1043	95.54	945	333.94	2
A1-AN105R2	ActDes	1250	29.37	1151	68.88	1051	209.02	952	845.32	3

- (a) The Group IDs are described in Sections 2.1 to 2.6.  
 (b) Numbers from 1 to 5 denote the five split validation subsets. NA denotes “not applicable”, because these replicate glasses were forced into the modeling subsets, and thus were not parts of the validation subsets.



**Table 8.2. Variation in Viscosity Values for Replicate and Near-Replicate Pairs.**

Glass IDs of Replicate Pairs <sup>(a)</sup>	Viscosity Values For Exact Temperatures at Each Nominal Temperature <sup>(b)</sup>								Pooled Over Temp.	
	950°C		1050°C		1150°C		1250°C		%RSD	SD
	T (°C)	P	T (°C)	P	T (°C)	P	T (°C)	P	P	ln(P)
LAWM01	953	376.96	1053	94.14	1152	35.00	1252	16.91		
LAWM53	958	314.34	1056	105.13	1150	39.95	1248	16.84		
<b>%RSD<sup>(c)</sup>, SD<sup>(d)</sup></b>	<b>12.81</b>	<b>0.128</b>	<b>7.80</b>	<b>0.078</b>	<b>9.34</b>	<b>0.094</b>	<b>0.29</b>	<b>0.003</b>	<b>8.84</b>	<b>0.089</b>
LAWM09	946	2329.04	1048	462.35	1150	126.36	1252	43.77		
LAWM54R1	957	1659.86	1056	347.39	1155	105.91	1254	41.43		
<b>%RSD<sup>(c)</sup>, SD<sup>(d)</sup></b>	<b>23.72</b>	<b>0.240</b>	<b>20.08</b>	<b>0.202</b>	<b>12.45</b>	<b>0.125</b>	<b>3.88</b>	<b>0.039</b>	<b>16.85</b>	<b>0.170</b>
LAWM12	951	90.07	1049	32.05	1148	14.24	1246	6.82		
LAWM55	956	65.90	1057	24.47	1158	11.23	1259	5.99		
<b>%RSD<sup>(c)</sup>, SD<sup>(d)</sup></b>	<b>21.92</b>	<b>0.221</b>	<b>18.97</b>	<b>0.191</b>	<b>16.71</b>	<b>0.168</b>	<b>9.16</b>	<b>0.092</b>	<b>17.34</b>	<b>0.175</b>
LAWM35	950	269.85	1050	68.28	1149	25.02	1249	11.17		
LAWM56	956	262.73	1052	69.99	1148	25.79	1245	11.82		
<b>%RSD<sup>(c)</sup>, SD<sup>(d)</sup></b>	<b>1.89</b>	<b>0.019</b>	<b>1.75</b>	<b>0.017</b>	<b>2.14</b>	<b>0.021</b>	<b>4.00</b>	<b>0.040</b>	<b>2.61</b>	<b>0.026</b>
LAWM50	953	721.01	1049	173.87	1146	60.43	1243	26.82		
LAWM51	966	624.53	1060	171.04	1154	59.03	1248	26.09		
<b>%RSD<sup>(c)</sup>, SD<sup>(d)</sup></b>	<b>10.14</b>	<b>0.102</b>	<b>1.16</b>	<b>0.012</b>	<b>1.66</b>	<b>0.017</b>	<b>1.95</b>	<b>0.020</b>	<b>5.26</b>	<b>0.053</b>
LAWM52	955	531.45	1052	138.67	1149	51.50	1246	24.16		
LAWA88R1	931	750.05	1032	198.05	1133	71.10	1244	27.27		
<b>%RSD<sup>(c)</sup>, SD<sup>(d)</sup></b>	<b>24.12</b>	<b>0.244</b>	<b>24.94</b>	<b>0.252</b>	<b>22.61</b>	<b>0.228</b>	<b>8.55</b>	<b>0.086</b>	<b>21.14</b>	<b>0.213</b>
<b>Pooled Over 6 Replicate Pairs<sup>(e)</sup></b>	<b>17.77</b>	<b>0.179</b>	<b>15.55</b>	<b>0.157</b>	<b>13.17</b>	<b>0.132</b>	<b>5.66</b>	<b>0.057</b>	<b>13.81</b>	<b>0.139</b>

Glass IDs of Replicate Pairs <sup>(a)</sup>	Viscosity Values at Nominal Temperatures <sup>(f)</sup>								Pooled Over Temp.	
	950°C		1050°C		1150°C		1250°C		%RSD	SD
	P	ln(P)	P	ln(P)	P	ln(P)	P	ln(P)	P	ln(P)
LAWM01	395.865	5.981	97.592	4.581	35.572	3.572	17.126	2.841		
LAWM53	347.297	5.850	110.907	4.709	40.436	3.700	16.483	2.802		
<b>%RSD<sup>(c)</sup>, SD<sup>(d)</sup></b>	<b>9.24</b>	<b>0.093</b>	<b>9.03</b>	<b>0.090</b>	<b>9.05</b>	<b>0.091</b>	<b>2.71</b>	<b>0.027</b>	<b>8.00</b>	<b>0.080</b>
LAWM09	2169.885	7.682	449.653	6.108	126.308	4.839	44.611	3.798		
LAWM54R1	1882.911	7.541	379.032	5.938	111.184	4.711	42.918	3.759		
<b>%RSD<sup>(c)</sup>, SD<sup>(d)</sup></b>	<b>10.01</b>	<b>0.100</b>	<b>12.05</b>	<b>0.121</b>	<b>9.01</b>	<b>0.090</b>	<b>2.74</b>	<b>0.027</b>	<b>9.14</b>	<b>0.092</b>
LAWM12	90.643	4.507	32.310	3.475	13.739	2.620	6.693	1.901		
LAWM55	70.436	4.255	26.040	3.260	11.858	2.473	6.304	1.841		
<b>%RSD<sup>(c)</sup>, SD<sup>(d)</sup></b>	<b>17.74</b>	<b>0.178</b>	<b>15.20</b>	<b>0.153</b>	<b>10.39</b>	<b>0.104</b>	<b>4.23</b>	<b>0.042</b>	<b>12.96</b>	<b>0.130</b>
LAWM35	269.197	5.595	68.868	4.232	24.552	3.201	11.134	2.410		
LAWM56	288.933	5.666	71.826	4.274	25.268	3.230	11.425	2.436		
<b>%RSD<sup>(c)</sup>, SD<sup>(d)</sup></b>	<b>5.00</b>	<b>0.050</b>	<b>2.97</b>	<b>0.030</b>	<b>2.03</b>	<b>0.020</b>	<b>1.82</b>	<b>0.018</b>	<b>3.21</b>	<b>0.032</b>
LAWM50	757.875	6.631	172.592	5.151	57.836	4.058	25.576	3.242		
LAWM51	809.817	6.697	191.577	5.255	62.245	4.131	25.548	3.241		
<b>%RSD<sup>(c)</sup>, SD<sup>(d)</sup></b>	<b>4.69</b>	<b>0.047</b>	<b>7.37</b>	<b>0.074</b>	<b>5.19</b>	<b>0.052</b>	<b>0.08</b>	<b>0.001</b>	<b>5.08</b>	<b>0.051</b>
LAWM52	575.443	6.355	142.518	4.959	50.834	3.929	23.561	3.160		
LAWA88R1	569.817	6.345	163.696	5.098	59.826	4.091	26.211	3.266		
<b>%RSD<sup>(c)</sup>, SD<sup>(d)</sup></b>	<b>0.69</b>	<b>0.007</b>	<b>9.78</b>	<b>0.098</b>	<b>11.49</b>	<b>0.115</b>	<b>7.53</b>	<b>0.075</b>	<b>8.44</b>	<b>0.085</b>
<b>Pooled Over 6 Replicate Pairs<sup>(e)</sup></b>	<b>9.56</b>	<b>0.096</b>	<b>10.14</b>	<b>0.102</b>	<b>8.51</b>	<b>0.085</b>	<b>3.93</b>	<b>0.039</b>	<b>8.39</b>	<b>0.084</b>

- (a) Because glass compositions were renormalized based on analyzed (or estimates of analyzed) SO<sub>3</sub> values, the compositions of replicate pairs may not match exactly. However, they were still treated as replicate pairs for statistical data analyses.
- (b) Viscosity values are listed at the exact temperatures corresponding to the nominal temperature values.
- (c) %RSD = 100×(Standard Deviation / Mean), calculated using the P values.
- (d) Calculated using ln(P) values.
- (e) The individual and pooled SDs estimate  $\sqrt{\sigma_G^2 + \sigma_T^2}$  in ln(P) units (see Section C.2.2 of Appendix C).
- (f) Viscosity values were interpolated at the nominal temperature values using a T2-equation (see Section C.2.1) fit for each glass.

**Table 8.3. Temperature and Viscosity Observations for 10 Outlying LAW Glasses Excluded from the Viscosity Modeling Set.**

<b>Glass ID</b>	<b>Group ID<sup>(a)</sup></b>	<b>Temp1 (°C)</b>	<b>Vis1 (P)</b>	<b>Temp2 (°C)</b>	<b>Vis2 (P)</b>	<b>Temp3 (°C)</b>	<b>Vis3 (P)</b>	<b>Temp4 (°C)</b>	<b>Vis4 (P)</b>
LAWA43-1	ActDes	1249	35.31	1150	85.20	1050	270.22	950	1100.89
LAWA49	ActDes	1252	35.66	1150	86.39	1050	256.51	950	978.16
LAWA50	ActDes	1251	30.48	1150	71.69	1050	210.42	950	787.40
LAWA82	ActDes	1253	39.40	1142	103.06	1043	309.49	943	1262.72
LAWA89	ActDes	1268	24.96	1167	56.31	1065	154.95	965	568.48
LAWB60	ActDes	1258	12.03	1159	26.76	1056	72.25	956	257.94
LAWB62	ActDes	1225	14.45	1131	33.16	1038	83.87	945	301.99
LAWB63	ActDes	1243	19.28	1143	43.64	1043	123.34	943	497.38
LAWB82	ActDes	1269	12.58	1169	27.49	1069	74.50	969	254.33
LAWC12	ActDes	1255	23.48	1151	54.28	1050	157.66	948	601.64

(a) The Group IDs are described in Sections 2.1 to 2.6.

**Table 8.4. Coefficients and Performance Summary for 36-Term Truncated T2-Linear Mixture Model on the Natural Logarithm of ILAW Viscosity.**

Mixture Terms ( $x_i$ )	Coefficient Estimate	Coefficient Stand. Dev.	Mixture-Temp. Terms [ $x_i/(T/1000)^2$ ]	Coefficient Estimate	Coefficient Stand. Dev.	t-value = Coeff/SD	p-value	Modeling Data Statistic, 171 Glasses <sup>(a)</sup>	Value		
Al <sub>2</sub> O <sub>3</sub>	0.2801	1.5837	Al <sub>2</sub> O <sub>3</sub> /(T/1000) <sup>2</sup>	24.8478	2.2922	10.84	< 0.0001	R <sup>2</sup>	0.987		
B <sub>2</sub> O <sub>3</sub>	-4.5934	1.0935	B <sub>2</sub> O <sub>3</sub> /(T/1000) <sup>2</sup>	0.1531	1.5831	0.10	0.9230	SSE	15.443		
CaO	-11.7356	0.9688	CaO/(T/1000) <sup>2</sup>	13.0443	1.4029	9.30	< 0.0001	RMSE	0.154		
Cl	-7.6758	8.8934	Cl/(T/1000) <sup>2</sup>	47.5763	12.8429	3.70	0.0002	<b>Extrapolative Validation Statistic, 10 Outlying Glasses<sup>(a,c)</sup></b>			
Cr <sub>2</sub> O <sub>3</sub>	-17.7928	26.5385	Cr <sub>2</sub> O <sub>3</sub> /(T/1000) <sup>2</sup>	12.0939	38.3851	0.32	0.7528	R <sup>2</sup> Validation (R <sup>2</sup> <sub>v</sub> )	0.977		
F	-20.5317	31.2450	F/(T/1000) <sup>2</sup>	-6.6504	45.0346	-0.13	0.9002	RMSE Validation (RMSE <sub>v</sub> )	0.198		
Fe <sub>2</sub> O <sub>3</sub>	-6.2146	1.0805	Fe <sub>2</sub> O <sub>3</sub> /(T/1000) <sup>2</sup>	15.4093	1.5554	9.91	< 0.0001	<b>Data Partition Statistic, 86 Modeling &amp; 85 Validation<sup>(a,d)</sup></b>			
K <sub>2</sub> O	-0.0159	1.4902	K <sub>2</sub> O/(T/1000) <sup>2</sup>	-0.7124	2.1504	-0.33	0.7405	R <sup>2</sup>	0.991		
Li <sub>2</sub> O	8.8841	2.1805	Li <sub>2</sub> O/(T/1000) <sup>2</sup>	-83.0404	3.1432	-26.42	< 0.0001	SSE	5.514		
MgO	-14.2255	2.0276	MgO/(T/1000) <sup>2</sup>	21.6229	2.9293	7.38	< 0.0001	RMSE	0.134		
Na <sub>2</sub> O	-0.2871	0.6524	Na <sub>2</sub> O/(T/1000) <sup>2</sup>	-15.1903	0.9419	-16.13	< 0.0001	R <sup>2</sup> Validation (R <sup>2</sup> <sub>v</sub> )	0.858 <sup>(g)</sup>		
P <sub>2</sub> O <sub>5</sub>	0.1277	3.4817	P <sub>2</sub> O <sub>5</sub> /(T/1000) <sup>2</sup>	20.5631	5.0331	4.09	< 0.0001	RMSE Validation (RMSE <sub>v</sub> )	0.469 <sup>(g)</sup>		
SO <sub>3</sub>	-14.2162	13.8266	SO <sub>3</sub> /(T/1000) <sup>2</sup>	53.7040	20.0225	2.68	0.0076	(e) See Section 8.1.2. (f) These statistics require extra effort to calculate for GLS regression (see Section C.3.2 in Appendix C) and were only calculated for the recommended model. (g) The partitioned data does not adequately support all 18 components, which leads to poor validation performance.			
SiO <sub>2</sub>	-0.5173	0.4823	SiO <sub>2</sub> /(T/1000) <sup>2</sup>	24.2955	0.6967	34.87	< 0.0001				
TiO <sub>2</sub>	-12.7592	2.4731	TiO <sub>2</sub> /(T/1000) <sup>2</sup>	20.3122	3.5713	5.69	< 0.0001				
ZnO	-7.6264	2.0701	ZnO/(T/1000) <sup>2</sup>	12.4643	3.0007	4.15	< 0.0001				
ZrO <sub>2</sub>	-15.4787	2.2172	ZrO <sub>2</sub> /(T/1000) <sup>2</sup>	49.5611	3.2146	15.42	< 0.0001				
Others <sup>(b)</sup>	-19.4536	43.3323	Others/(T/1000) <sup>2</sup>	143.6633	62.7302	2.29	0.0224				
$\hat{\sigma}_G = 0.1457$			$\hat{\sigma}_T = 0.0607$								
<b>Data Splitting Statistic<sup>(a,e)</sup></b>		<b>DS1</b>	<b>DS2</b>	<b>DS3</b>	<b>DS4</b>	<b>DS5</b>	<b>Average</b>				
R <sup>2</sup>		(f)	(f)	(f)	(f)	(f)	(f)				
SSE		(f)	(f)	(f)	(f)	(f)	(f)				
RMSE		(f)	(f)	(f)	(f)	(f)	(f)				
R <sup>2</sup> Validation (R <sup>2</sup> <sub>v</sub> )		(f)	(f)	(f)	(f)	(f)	(f)				
RMSE Validation (RMSE <sub>v</sub> )		(f)	(f)	(f)	(f)	(f)	(f)				

- (a) The model evaluation statistics are defined in Section C.3 of Appendix C. Model validation statistics are defined in Section C.5 of Appendix C. A negative value for R<sup>2</sup><sub>v</sub> means that the sum of squares of model prediction errors is larger than if the mean response value over the validation data set were used as the predicted value for each glass. In other words, the model predicts worse for the validation data than the mean response value does.
- (b) The “Others” component includes Ag<sub>2</sub>O, BaO, Br, CdO, Cs<sub>2</sub>O, I, La<sub>2</sub>O<sub>3</sub>, MnO, MoO<sub>3</sub>, NiO, PbO, Re<sub>2</sub>O<sub>7</sub>, SeO<sub>2</sub>, SrO, and “Unknown”.
- (c) See Section 8.1.4.
- (d) See Section 8.1.3.

**Table 8.5. Summary Statistics for Various Models Fitted and Validated Using ILAW Viscosity Data.**

Info/Statistic	Model 1	Model 2	Model 3	Model 4	Model 5	Model 6	Model 7
# $x_i$ Terms	18	14	12	11	12	11	12
# $x_i/(T/1000)^2$ Terms	18	14	12	11	12	11	10
# Quadratic Terms <sup>(a)</sup>	0	0	0	0	4	4	4
# Terms Total	36	28	24	22	28	26	26
Components Combined with Others	None	F, Cl, Cr <sub>2</sub> O <sub>3</sub> , SO <sub>3</sub>	F, Cl, Cr <sub>2</sub> O <sub>3</sub> , SO <sub>3</sub> , TiO <sub>2</sub> , ZnO	F, Cl, Cr <sub>2</sub> O <sub>3</sub> , P <sub>2</sub> O <sub>5</sub> , SO <sub>3</sub> , TiO <sub>2</sub> , ZnO	F, Cl, Cr <sub>2</sub> O <sub>3</sub> , SO <sub>3</sub> , TiO <sub>2</sub> , ZnO	F, Cl, Cr <sub>2</sub> O <sub>3</sub> , P <sub>2</sub> O <sub>5</sub> , SO <sub>3</sub> , TiO <sub>2</sub> , ZnO	F, Cl, Cr <sub>2</sub> O <sub>3</sub> , SO <sub>3</sub> , TiO <sub>2</sub> , ZnO
Quadratic Terms	None	None	None	None	(B <sub>2</sub> O <sub>3</sub> ) <sup>2</sup> (Li <sub>2</sub> O) <sup>2</sup> Al <sub>2</sub> O <sub>3</sub> ×Li <sub>2</sub> O (MgO) <sup>2</sup>	(B <sub>2</sub> O <sub>3</sub> ) <sup>2</sup> (Li <sub>2</sub> O) <sup>2</sup> B <sub>2</sub> O <sub>3</sub> ×Li <sub>2</sub> O Al <sub>2</sub> O <sub>3</sub> ×Na <sub>2</sub> O	(B <sub>2</sub> O <sub>3</sub> ) <sup>2</sup> (Li <sub>2</sub> O) <sup>2</sup> Al <sub>2</sub> O <sub>3</sub> ×Li <sub>2</sub> O (MgO) <sup>2</sup>
<b>Results Using all 171 LAW Glasses with Viscosity Data</b>							
R <sup>2</sup>	0.987	0.985	0.985	0.982	0.988	0.985	0.988
SSE	15.443	16.895	17.658	20.938	14.287	17.359	14.291
RMSE	0.154	0.160	0.163	0.178	0.147	0.162	0.147
<b>Results Using 86 LAW Glasses for Modeling and 85 for Validation<sup>(b)</sup></b>							
R <sup>2</sup>	0.991	0.990	0.989	0.988	0.990	0.989	0.990
SSE	5.514	5.940	7.003	7.577	6.222	6.729	6.222
RMSE	0.134	0.137	0.148	0.153	0.140	0.145	0.140
R <sup>2</sup> <sub>v</sub>	0.858 <sup>(c)</sup>	0.847 <sup>(c)</sup>	0.971	0.973	0.980	0.977	0.980
RMSE <sub>v</sub>	0.469 <sup>(c)</sup>	0.486 <sup>(c)</sup>	0.210	0.205	0.176	0.190	0.176

- (a) Quadratic terms include squared ( $x_i^2$ ) and/or crossproduct ( $x_i x_j$ ) terms.
- (b) There were 86 glasses in the ILAW Existing Matrix, Phase 1 Test Matrix, and Phase 1a Augmentation Test Matrix that have data for viscosity. The remaining 85 glasses were used as a validation subset.
- (c) The partitioned modeling data set of 86 LAW glasses is from the portion of the data that was designed to support 14 rather than 18 components. Hence, the model performance was poor for some of the validation glasses.

**Table 8.6. Coefficients and Performance Summary for 24-Term Reduced Truncated T2-Linear Mixture Model on the Natural Logarithm of ILAW Viscosity.**

Mixture Terms ( $x_i$ )	Coefficient Estimate	Coefficient Stand. Dev.	Mixture-Temp. Terms [ $x_i/(T/1000)^2$ ]	Coefficient Estimate	Coefficient Stand. Dev.	t-value = Coeff/SD	p-value	Modeling Data Statistic, 171 Glasses <sup>(a)</sup>	Value	
Al <sub>2</sub> O <sub>3</sub>	0.1559	1.6272	Al <sub>2</sub> O <sub>3</sub> /(T/1000) <sup>2</sup>	24.6640	2.3205	10.63	< 0.0001	R <sup>2</sup>	0.985	
B <sub>2</sub> O <sub>3</sub>	-4.6415	1.1172	B <sub>2</sub> O <sub>3</sub> /(T/1000) <sup>2</sup>	-0.3877	1.5925	-0.24	0.8078	SSE	17.658	
CaO	-11.9086	0.9628	CaO/(T/1000) <sup>2</sup>	13.6377	1.3729	9.93	< 0.0001	RMSE	0.163	
Fe <sub>2</sub> O <sub>3</sub>	-6.3228	1.0476	Fe <sub>2</sub> O <sub>3</sub> /(T/1000) <sup>2</sup>	15.2930	1.4845	10.30	< 0.0001			
K <sub>2</sub> O	-0.4171	1.3967	K <sub>2</sub> O/(T/1000) <sup>2</sup>	-1.1260	1.9837	-0.57	0.5705			
Li <sub>2</sub> O	8.9298	2.1510	Li <sub>2</sub> O/(T/1000) <sup>2</sup>	-82.6484	3.0571	-27.03	< 0.0001			
MgO	-14.4812	2.0639	MgO/(T/1000) <sup>2</sup>	22.2768	2.9354	7.59	< 0.0001	<b>Extrapolative Validation Statistic, 10 Outlying Glasses<sup>(a,c)</sup></b>	<b>Value</b>	
Na <sub>2</sub> O	-0.4259	0.6327	Na <sub>2</sub> O/(T/1000) <sup>2</sup>	-14.5565	0.9004	-16.17	< 0.0001	R <sup>2</sup> Validation (R <sup>2</sup> <sub>v</sub> )	0.972	
P <sub>2</sub> O <sub>5</sub>	-1.0643	3.0256	P <sub>2</sub> O <sub>5</sub> /(T/1000) <sup>2</sup>	23.6740	4.3038	5.50	< 0.0001	RMSE Validation (RMSE <sub>v</sub> )	0.218	
SiO <sub>2</sub>	-0.4123	0.4565	SiO <sub>2</sub> /(T/1000) <sup>2</sup>	24.5176	0.6490	37.78	< 0.0001			
ZrO <sub>2</sub>	-14.3140	2.1234	ZrO <sub>2</sub> /(T/1000) <sup>2</sup>	48.4882	3.0281	16.01	< 0.0001			
Others <sup>(b)</sup>	-10.2058	1.4843	Others/(T/1000) <sup>2</sup>	17.5441	2.1159	8.29	< 0.0001			
$\hat{\sigma}_G = 0.1540$			$\hat{\sigma}_T = 0.0616$							
<b>Data Splitting Statistic<sup>(a,e)</sup></b>		<b>DS1</b>	<b>DS2</b>	<b>DS3</b>	<b>DS4</b>	<b>DS5</b>	<b>Average</b>	<b>Data Partition Statistic, 86 Modeling &amp; 85 Validation<sup>(a,d)</sup></b>	<b>Value</b>	
R <sup>2</sup>		(f)	(f)	(f)	(f)	(f)	(f)	R <sup>2</sup>	0.989	
SSE		(f)	(f)	(f)	(f)	(f)	(f)	SSE	7.003	
RMSE		(f)	(f)	(f)	(f)	(f)	(f)	RMSE	0.148	
R <sup>2</sup> Validation (R <sup>2</sup> <sub>v</sub> )		(f)	(f)	(f)	(f)	(f)	(f)	R <sup>2</sup> Validation (R <sup>2</sup> <sub>v</sub> )	0.971	
RMSE Validation (RMSE <sub>v</sub> )		(f)	(f)	(f)	(f)	(f)	(f)	RMSE Validation (RMSE <sub>v</sub> )	0.210	

- (a) The model evaluation statistics are defined in Section C.3 of Appendix C. Model validation statistics are defined in Section C.5 of Appendix C. A negative value for R<sup>2</sup><sub>v</sub> means that the sum of squares of model prediction errors is larger than if the mean response value over the validation data set were used as the predicted value for each glass. In other words, the model predicts worse for the validation data than the mean response value does.
- (b) The “Others” component includes Ag<sub>2</sub>O, BaO, Br, CdO, Cs<sub>2</sub>O, I, La<sub>2</sub>O<sub>3</sub>, MnO, MoO<sub>3</sub>, NiO, PbO, Re<sub>2</sub>O<sub>7</sub>, SeO<sub>2</sub>, SrO, and “Unknown” as well as the reduced components Cl, Cr<sub>2</sub>O<sub>3</sub>, F, SO<sub>3</sub>, TiO<sub>2</sub>, and ZnO.
- (c) The 10 outlying LAW glass compositions are discussed in Section 8.1.4.
- (d) The partition of the viscosity modeling data set into modeling and validation subsets is described in Section 8.1.3.
- (e) The evaluation and validation statistics calculated for data-splits are defined the same as for separate modeling and validation sets. Section 8.1.2 describes how the data-splitting was accomplished.
- (f) These statistics require extra effort to calculate for GLS regression (see Section C.3.2 in Appendix C) and were only calculated for the recommended model.

**Table 8.7. Coefficients and Performance Summary for 22-Term Reduced Truncated T2-Linear Mixture Model on the Natural Logarithm of ILAW Viscosity.**

Mixture Terms ( $x_i$ )	Coefficient Estimate	Coefficient Stand. Dev.	Mixture-Temp. Terms [ $x_i/(T/1000)^2$ ]	Coefficient Estimate	Coefficient Stand. Dev.	t-value = Coeff/SD	p-value	Modeling Data Statistic, 171 Glasses <sup>(a)</sup>	Value	
Al <sub>2</sub> O <sub>3</sub>	0.0080	1.6909	Al <sub>2</sub> O <sub>3</sub> /(T/1000) <sup>2</sup>	24.5448	2.3201	10.58	< 0.0001	R <sup>2</sup>	0.982	
B <sub>2</sub> O <sub>3</sub>	-4.4384	1.1586	B <sub>2</sub> O <sub>3</sub> /(T/1000) <sup>2</sup>	-0.2172	1.5886	-0.14	< 0.0001	SSE	20.938	
CaO	-12.1245	0.9975	CaO/(T/1000) <sup>2</sup>	13.4850	1.3685	9.85	< 0.0001	RMSE	0.178	
Fe <sub>2</sub> O <sub>3</sub>	-6.1453	1.0872	Fe <sub>2</sub> O <sub>3</sub> /(T/1000) <sup>2</sup>	15.4329	1.4815	10.42	< 0.0001			
K <sub>2</sub> O	-1.2922	1.4124	K <sub>2</sub> O/(T/1000) <sup>2</sup>	-1.7053	1.9287	-0.88	< 0.0001			
Li <sub>2</sub> O	8.3350	2.2249	Li <sub>2</sub> O/(T/1000) <sup>2</sup>	-83.0236	3.0422	-27.29	< 0.0001			
MgO	-14.7521	2.1437	MgO/(T/1000) <sup>2</sup>	22.0746	2.9333	7.53	< 0.0001	<b>Extrapolative Validation Statistic, 10 Outlying Glasses<sup>(a,c)</sup></b>	<b>Value</b>	
Na <sub>2</sub> O	-0.5219	0.6569	Na <sub>2</sub> O/(T/1000) <sup>2</sup>	-14.6186	0.8993	-16.26	< 0.0001	R <sup>2</sup> Validation (R <sup>2</sup> <sub>v</sub> )	0.975	
SiO <sub>2</sub>	-0.5345	0.4724	SiO <sub>2</sub> /(T/1000) <sup>2</sup>	24.4325	0.6462	37.81	< 0.0001	RMSE Validation (RMSE <sub>v</sub> )	0.205	
ZrO <sub>2</sub>	-14.2247	2.2079	ZrO <sub>2</sub> /(T/1000) <sup>2</sup>	48.5047	3.0298	16.01	< 0.0001			
Others <sup>(b)</sup>	-8.4324	1.3807	Others/(T/1000) <sup>2</sup>	18.7292	1.8944	9.89	< 0.0001			
$\hat{\sigma}_G = 0.1693$			$\hat{\sigma}_T = 0.0617$							
<b>Data Splitting Statistic<sup>(a,e)</sup></b>		<b>DS1</b>	<b>DS2</b>	<b>DS3</b>	<b>DS4</b>	<b>DS5</b>	<b>Average</b>	<b>Data Partition Statistic, 86 Modeling &amp; 85 Validation<sup>(a,d)</sup></b>	<b>Value</b>	
R <sup>2</sup>		(f)	(f)	(f)	(f)	(f)	(f)	R <sup>2</sup>	0.988	
SSE		(f)	(f)	(f)	(f)	(f)	(f)	SSE	7.577	
RMSE		(f)	(f)	(f)	(f)	(f)	(f)	RMSE	0.153	
R <sup>2</sup> Validation (R <sup>2</sup> <sub>v</sub> )		(f)	(f)	(f)	(f)	(f)	(f)	R <sup>2</sup> Validation (R <sup>2</sup> <sub>v</sub> )	0.973	
RMSE Validation (RMSE <sub>v</sub> )		(f)	(f)	(f)	(f)	(f)	(f)	RMSE Validation (RMSE <sub>v</sub> )	0.205	

- (a) The model evaluation statistics are defined in Section C.3 of Appendix C. Model validation statistics are defined in Section C.5 of Appendix C. A negative value for R<sup>2</sup><sub>v</sub> means that the sum of squares of model prediction errors is larger than if the mean response value over the validation data set were used as the predicted value for each glass. In other words, the model predicts worse for the validation data than the mean response value does.
- (b) The “Others” component includes Ag<sub>2</sub>O, BaO, Br, CdO, Cs<sub>2</sub>O, I, La<sub>2</sub>O<sub>3</sub>, MnO, MoO<sub>3</sub>, NiO, PbO, Re<sub>2</sub>O<sub>7</sub>, SeO<sub>2</sub>, SrO, and “Unknown” as well as the reduced components Cl, Cr<sub>2</sub>O<sub>3</sub>, F, P<sub>2</sub>O<sub>5</sub>, SO<sub>3</sub>, TiO<sub>2</sub>, and ZnO.
- (c) The 10 outlying LAW glass compositions are discussed in Section 8.1.4.
- (d) The partition of the viscosity modeling data set into modeling and validation subsets is described in Section 8.1.3.
- (e) The evaluation and validation statistics calculated for data-splits are defined the same as for separate modeling and validation sets. Section 8.1.2 describes how the data-splitting was accomplished.
- (f) These statistics require extra effort to calculate for GLS regression (see Section C.3.2 in Appendix C) and were only calculated for the recommended model.

**Table 8.8. Coefficients and Performance Summary for 26-Term Reduced Truncated T2-Linear Mixture Model with Four Quadratic Terms on the Natural Logarithm of ILAW Viscosity.**

Mixture Terms ( $x_i$ )	Coefficient Estimate	Coefficient Stand. Dev.	Mixture-Temp. Terms [ $x_i/(T/1000)^2$ ]	Coefficient Estimate	Coefficient Stand. Dev.	t-value = Coeff/SD	p-value	Modeling Data Statistic, 171 Glasses <sup>(a)</sup>	Value	
Al <sub>2</sub> O <sub>3</sub>	5.5124	2.0960	Al <sub>2</sub> O <sub>3</sub> /(T/1000) <sup>2</sup>	24.6423	2.2683	10.86	< 0.0001	R <sup>2</sup>	0.988	
B <sub>2</sub> O <sub>3</sub>	-42.3772	6.8657	B <sub>2</sub> O <sub>3</sub> /(T/1000) <sup>2</sup>	(f)	(f)	(f)	(f)	SSE	14.291	
CaO	-10.6445	0.9836	CaO/(T/1000) <sup>2</sup>	13.7793	1.3498	10.21	< 0.0001	RMSE	0.147	
Fe <sub>2</sub> O <sub>3</sub>	-4.6220	1.0390	Fe <sub>2</sub> O <sub>3</sub> /(T/1000) <sup>2</sup>	15.2036	1.4269	10.66	< 0.0001			
K <sub>2</sub> O	-0.8689	0.9358	K <sub>2</sub> O/(T/1000) <sup>2</sup>	(f)	(f)	(f)	(f)			
Li <sub>2</sub> O	10.9390	4.5502	Li <sub>2</sub> O/(T/1000) <sup>2</sup>	-82.4815	2.9954	-27.54	< 0.0001			
MgO	-5.6188	5.5224	MgO/(T/1000) <sup>2</sup>	22.7608	2.8130	8.09	< 0.0001			
Na <sub>2</sub> O	0.9073	0.6740	Na <sub>2</sub> O/(T/1000) <sup>2</sup>	-14.5621	0.8958	-16.26	< 0.0001			
P <sub>2</sub> O <sub>5</sub>	-0.8081	2.8760	P <sub>2</sub> O <sub>5</sub> /(T/1000) <sup>2</sup>	24.0339	4.2324	5.68	< 0.0001			
SiO <sub>2</sub>	1.5575	0.5247	SiO <sub>2</sub> /(T/1000) <sup>2</sup>	24.4077	0.5709	42.75	< 0.0001			
ZrO <sub>2</sub>	-12.0741	2.0755	ZrO <sub>2</sub> /(T/1000) <sup>2</sup>	48.2286	2.9522	16.34	< 0.0001			
Others <sup>(b)</sup>	-9.3903	1.4313	Others/(T/1000) <sup>2</sup>	17.3800	2.0519	8.47	< 0.0001			
(B <sub>2</sub> O <sub>3</sub> ) <sup>2</sup>	198.7360	36.5259	→	→	→	5.44	< 0.0001			
(Li <sub>2</sub> O) <sup>2</sup>	133.6906	43.1873	→	→	→	3.10	0.0023			
Al <sub>2</sub> O <sub>3</sub> ×Li <sub>2</sub> O	-136.5095	56.0571	→	→	→	-2.44	0.0160			
(MgO) <sup>2</sup>	-179.8249	103.5284	→	→	→	-1.74	0.0844			
$\hat{\sigma}_G = 0.1375$			$\hat{\sigma}_T = 0.0615$							
<b>Data Splitting Statistic<sup>(a,e)</sup></b>			<b>DS1</b>	<b>DS2</b>	<b>DS3</b>	<b>DS4</b>	<b>DS5</b>	<b>Average</b>		
R <sup>2</sup>			0.988	0.987	0.989	0.986	0.989	0.988		
SSE			10.965	11.647	10.162	12.798	10.474	11.209		
RMSE			0.143	0.148	0.138	0.155	0.140	0.145		
R <sup>2</sup> Validation (R <sup>2</sup> <sub>v</sub> )			0.980	0.987	0.978	0.992	0.979	0.983		
RMSE Validation (RMSE <sub>v</sub> )			0.178	0.149	0.188	0.115	0.185	0.163		
								<b>Extrapolative Validation Statistic, 10 Outlying Glasses<sup>(a,c)</sup></b>		
								R <sup>2</sup> Validation (R <sup>2</sup> <sub>v</sub> )	0.976	
								RMSE Validation (RMSE <sub>v</sub> )	0.200	
								<b>Data Partition Statistic, 86 Modeling &amp; 85 Validation<sup>(a,d)</sup></b>		
								R <sup>2</sup>	0.990	
								SSE	6.222	
								RMSE	0.140	
								R <sup>2</sup> Validation (R <sup>2</sup> <sub>v</sub> )	0.980	
								RMSE Validation (RMSE <sub>v</sub> )	0.176	
(f) This term was not statistically significant and hence was omitted from the model.										

- (a) The model evaluation statistics are defined in Section C.3 of Appendix C. Model validation statistics are defined in Section C.5 of Appendix C. A negative value for R<sup>2</sup><sub>v</sub> means that the sum of squares of model prediction errors is larger than if the mean response value over the validation data set were used as the predicted value for each glass. In other words, the model predicts worse for the validation data than the mean response value does.
- (b) The “Others” component includes Ag<sub>2</sub>O, BaO, Br, CdO, Cs<sub>2</sub>O, I, La<sub>2</sub>O<sub>3</sub>, MnO, MoO<sub>3</sub>, NiO, PbO, Re<sub>2</sub>O<sub>7</sub>, SeO<sub>2</sub>, SrO, and “Unknown” as well as the reduced components Cl, Cr<sub>2</sub>O<sub>3</sub>, F, P<sub>2</sub>O<sub>5</sub>, SO<sub>3</sub>, TiO<sub>2</sub>, and ZnO.
- (c) The 10 outlying LAW glass compositions are discussed in Section 8.1.4.
- (d) The partition of the viscosity modeling data set into modeling and validation subsets is described in Section 8.1.3.
- (e) The evaluation and validation statistics calculated for data-splits are defined the same as for separate modeling and validation sets. Section 8.1.2 describes how the data-splitting was accomplished.

**Table 8.9. LAWA126 Composition in Formats Needed for Use in ILAW Viscosity Models.**

<b>Model Term<sup>(a)</sup></b>	<b>LAWA126 Composition<sup>(b)</sup> (wt%)</b>	<b>LAWA126 Composition (mass fractions) for Use in 24-Term Viscosity Model 3<sup>(c)</sup></b>	<b>LAWA126 Composition (mass fractions) for Use in 26-Term Viscosity Model 7<sup>(d)</sup></b>
Al <sub>2</sub> O <sub>3</sub>	0.05637	0.05637	0.05637
B <sub>2</sub> O <sub>3</sub>	0.09815	0.09815	0.09815
CaO	0.01989	0.01989	0.01989
Cl	0.00200	NA <sup>(e)</sup>	NA
Cr <sub>2</sub> O <sub>3</sub>	0.00020	NA	NA
F	0.00300	NA	NA
Fe <sub>2</sub> O <sub>3</sub>	0.05537	0.05537	0.05537
K <sub>2</sub> O	0.03878	0.03878	0.03878
Li <sub>2</sub> O	0	0	0
MgO	0.01479	0.01479	0.01479
Na <sub>2</sub> O	0.18451	0.18451	0.18451
P <sub>2</sub> O <sub>5</sub>	0.00080	0.00080	0.00080
SO <sub>3</sub>	0.00310	NA	NA
SiO <sub>2</sub>	0.44098	0.44098	0.44098
TiO <sub>2</sub>	0.01999	NA	NA
ZnO	0.02959	NA	NA
ZrO <sub>2</sub>	0.02989	0.02989	0.02989
Others	0.00260	0.06047	0.06047
(B <sub>2</sub> O <sub>3</sub> ) <sup>2</sup>	NA	NA	0.0096336
(Li <sub>2</sub> O) <sup>2</sup>	NA	NA	0
Al <sub>2</sub> O <sub>3</sub> ×Li <sub>2</sub> O	NA	NA	0
(MgO) <sup>2</sup>	NA	NA	0.0002188

- (a) The viscosity models contain  $x_i/(T/1000)^2$  terms in addition to the  $x_i$  and  $x_i x_j$  terms shown in this column. The purpose of this table is to show the compositional forms needed for model predictions, so the temperature-containing terms are not shown.
- (b) The composition in mass fractions is from Table 7.2.
- (c) See Table 8.6.
- (d) See Table 8.8.
- (e) NA = not applicable, because the model does not contain this term.



**Table 8.10. Predicted Viscosity, Standard Deviation, and Statistical Intervals for LAWA126 Composition Used in ILAW Viscosity Models.**

<b>Model<sup>(a)</sup></b>	<b>Predicted Viscosity <math>\ln(\eta)</math> [ln(P)]</b>	<b>Predicted Viscosity <math>\eta</math><sup>(c)</sup> [P]</b>	<b>Standard Deviation of Predicted Viscosity <math>\ln(\eta)</math><sup>(d)</sup> [ln(P)]</b>	<b>90% LCI<sup>(e)</sup> on Mean Viscosity <math>\ln(\eta)</math> [ln(P)]</b>	<b>90% LCI<sup>(e)</sup> on Median Viscosity <math>\eta</math> [P]</b>	<b>90% UCI<sup>(e)</sup> on Mean Viscosity <math>\ln(\eta)</math> [ln(P)]</b>	<b>90% UCI<sup>(e)</sup> on Median Viscosity <math>\eta</math> [P]</b>	<b>90% CI<sup>(e)</sup> on Mean Viscosity <math>\ln(\eta)</math> [ln(P)]</b>	<b>90% CI<sup>(e)</sup> on Median Viscosity <math>\eta</math> [P]</b>
24-Term Viscosity Model at 1161°C <sup>(b)</sup>	3.9501	51.94	0.0262	3.9164	50.22	3.9839	53.73	(3.9067, 3.9936)	(49.73, 54.25)
26-Term Viscosity Model at 1161°C <sup>(b)</sup>	3.8965	49.23	0.0267	3.8622	47.57	3.9309	50.95	(3.8523, 3.9407)	(47.10, 51.45)

- (a) The two models in this column are given in Tables 8.6 and 8.8, respectively.
- (b) The temperature of 1161°C was chosen because it was one of the temperatures at which the viscosity of LAWA126 was measured. This facilitates comparison of the predicted and measured values.
- (c) Of the two models, the one with the predicted viscosity value at 1161°C closest to the measured value of 55.81 P is the 24-term viscosity model.
- (d) The standard deviation is for the viscosity  $\ln(\eta)$  prediction at 1161°C considered to be the mean of such values for the LAWA126 glass.
- (e) UCI = upper confidence interval, LCI = lower confidence interval, and CI = two-sided confidence interval (see Section C.7 of Appendix C).
- (f) All calculations were performed using the LAWA126 glass composition, model coefficients, and variance-covariance matrix values given in tables of this report. The calculated  $\ln(\text{poise})$  values were rounded to four decimal places in this table. The poise values were calculated by exponentiating the  $\ln(\text{poise})$  values before rounding, then rounding the resulting values to two decimal places in this table

**Table 9.1. Minimums and Maximums of LAW Glass Components (in Mass Fractions) for Compositions in the Modeling Datasets for Each LAW Glass Property.**

LAW Glass Property	PCT		VHT		Viscosity & Electrical Conductivity <sup>(a)</sup>		Glasses in Any Property Modeling Dataset	
Number of Glasses in Modeling Set	244		165		171			
LAW Glass Component	Min (mf)	Max (mf)	Min (mf)	Max (mf)	Min (mf)	Max (mf)	Min (mf)	Max (mf)
Al <sub>2</sub> O <sub>3</sub>	0.03499	0.09044	0.03503	0.09044	0.03499	0.09043	0.03499	0.09044
B <sub>2</sub> O <sub>3</sub>	0.05999	0.13263	0.06008	0.13262	0.05999	0.13057	0.05999	0.13263
CaO	0	0.10463	0	0.10463	0	0.10462	0	0.10463
Cl	0	0.01171	0	0.00914	0	0.01171	0	0.01171
Cr <sub>2</sub> O <sub>3</sub>	0	0.00631	0	0.00631	0.00008	0.00592	0	0.00631
F	0	0.00471	0	0.00470	0	0.00351	0	0.00471
Fe <sub>2</sub> O <sub>3</sub>	0	0.08412	0	0.08039	0	0.08412	0	0.08412
K <sub>2</sub> O	0	0.05559	0	0.05413	0	0.05412	0	0.05559
Li <sub>2</sub> O	0	0.05825	0	0.05825	0	0.05825	0	0.05825
MgO	0	0.05019	0	0.05019	0	0.05019	0	0.05019
Na <sub>2</sub> O	0.02457	0.24007	0.02457	0.24007	0.02457	0.23002	0.02457	0.24007
P <sub>2</sub> O <sub>5</sub>	0	0.04752	0	0.03020	0	0.04023	0	0.04752 <sup>(b)</sup>
SiO <sub>2</sub>	0.38007	0.52148	0.38362	0.52148	0.38007	0.52147	0.38007	0.52148
SO <sub>3</sub>	0.00070	0.01060	0.00070	0.01021	0.00070	0.01060	0.00070	0.01060
TiO <sub>2</sub>	0	0.03015	0	0.03015	0	0.03014	0	0.03015
ZnO	0.00100	0.05366	0.00999	0.05366	0.00998	0.05365	0.00998	0.05366
ZrO <sub>2</sub>	0	0.05003	0	0.05003	0	0.05001	0	0.05003
Others	0	0.00451	0	0.00280	0	0.00280	0	0.00451
<b>Components in Others</b>								
BaO	0	0.00020	0	0.00010	0	0.01000	0	0.00020
Br	0	0.00079	0	0.00079	0	0	0	0.00079
CdO	0	0.00100	0	0.00010	0	0.00010	0	0.00100
Cs <sub>2</sub> O	0	0.00180	0	0.00180	0	0.00180	0	0.00180
I	0	0.00101	0	0	0	0	0	0.00101
MnO	0	0.00005	0	0	0	0	0	0.00005
MoO <sub>3</sub>	0	0.00012	0	0.00012	0	0.00010	0	0.00012
NiO	0	0.00036	0	0.00036	0	0.00031	0	0.00036
PbO	0	0.00031	0	0.00031	0	0.00031	0	0.00031
Re <sub>2</sub> O <sub>7</sub>	0	0.00111	0	0.00111	0	0.00111	0	0.00111
SeO <sub>2</sub>	0	0.00100	0	0	0	0	0	0.00100
SrO	0	0.00002	0	0	0	0	0	0.00002
Unknown	0	0.00264	0	0	0	0	0	0.00264

(a) Viscosity and electrical conductivity data were collected on exactly the same glasses, so their information is combined.

(b) Note the difference between this maximum value over all data and the maximum for VHT modeling data.

**Table 9.2. Lower and Upper Bounds on LAW Glass Components (in Mass Fractions) that Partially Define the Composition Validity Region for ILAW Property Models.**

LAW Glass Component	Lower Bound (mf) <sup>(a)</sup>	Upper Bound (mf) <sup>(a)</sup>
Al <sub>2</sub> O <sub>3</sub>	0.034	0.091
B <sub>2</sub> O <sub>3</sub>	0.059	0.133
CaO	0	0.105
Cl	0	0.012
Cr <sub>2</sub> O <sub>3</sub>	0	0.007
F	0	0.005
Fe <sub>2</sub> O <sub>3</sub>	0	0.085
K <sub>2</sub> O	0	0.056
Li <sub>2</sub> O	0	0.059
MgO	0	0.051
Na <sub>2</sub> O	0.024	0.241
P <sub>2</sub> O <sub>5</sub>	0	0.048
SiO <sub>2</sub>	0.380	0.522
SO <sub>3</sub>	0	0.011
TiO <sub>2</sub>	0	0.031
ZnO	0.009	0.054
ZrO <sub>2</sub>	0	0.051
Others	0	0.005
<b>Components in Others<sup>(b)</sup></b>		
BaO	0	0.0003
Br	0	0.0008
CdO	0	0.0011
Cs <sub>2</sub> O	0	0.0019
I	0	0.0011
MnO	0	0.0001
MoO <sub>3</sub>	0	0.0002
NiO	0	0.0004
PbO	0	0.0004
Re <sub>2</sub> O <sub>7</sub>	0	0.0012
SeO <sub>2</sub>	0	0.0011
SrO	0	0.0001
Unknown	0	0.0027

- (a) The lower and upper bound values for these components are the minimum and maximum values from the last two columns of Table 9.1, rounded down and up (respectively) to the third decimal place.
- (b) The lower and upper bound values for the components in Others are the minimum and maximum values from the last two columns of Table 9.1, rounded down and up (respectively) to the fourth decimal place.

Note: The lower and upper bounds in the table could be expanded by the WTP Project if it allows some extrapolation of LAW property models. Expansion of bounds could be different for the components listed in the top portion of the table (e.g., expansion by 10% relative) and the components in Others (e.g., a factor of 2 to 10 depending on the component).

**Table 9.3. Minimum and Maximum Temperatures at Which Electrical Conductivity and Viscosity were Measured for LAW Glass Compositions in the Modeling Datasets Along with the Lower and Upper Bounds on Temperature that Partially Define the Validity Region for ILAW Electrical Conductivity and Viscosity Models.**

<b>Temperature for Glass Property</b>	<b>Minimum</b>	<b>Maximum</b>
<i>T</i> (°C) for Electrical Conductivity	917	1278
<i>T</i> (°C) for Viscosity	903	1271
<b>Temperature for Glass Property</b>	<b>Lower Bound</b>	<b>Upper Bound</b>
<i>T</i> (°C) for EC & Viscosity	900	1280

**Table 9.4. Minimums and Maximums of LAW Glass Property Values for Compositions in the Modeling Dataset for Each LAW Glass Property.**

<b>LAW Glass Property</b>	<b>Minimum</b>		<b>Maximum</b>	
	<b>Measured</b>	<b>Predicted</b>	<b>Measured</b>	<b>Predicted</b>
PCT-B (g/L)	0.152	0.176	35.66	27.74
PCT-Na (g/L)	0.209	0.182	22.94	16.10
VHT Alteration Depth (μm)	1	1.36	980	1495.7
Electrical Conductivity (S/cm)	Functions of temperature, see Figure 9.1.			
Viscosity (poise)	Functions of temperature, see Figure 9.2.			

**Table 9.5. Multiple-Component and Multiple-Variable Constraints that Partially Define the Composition Validity Region for ILAW Property Models.**

LAW Glass Property	Lower Constraint <sup>(a)</sup>	Upper Constraint <sup>(a)</sup>
PCT-B (g/L)	None	2.7 <sup>(b)</sup>
PCT-Na (g/L)	None	2.7 <sup>(b)</sup>
VHT Alteration Depth (μm)	None	1100 <sup>(c)</sup>
EC as fct( <i>T</i> , °C) (S/cm)	$EC \geq \exp[3.75 - 7311.55 (1/T)]$	$EC \leq \exp[4.10 - 4869.65 (1/T)]$
Viscosity as fct( <i>T</i> , °C) (poise)	$\eta \geq \exp[-5.65 + 9259.90 (1/T)]$	$\eta \leq \exp[-7.75 + 14705.60 (1/T)]$
Composition Components	Lower Constraint	Upper Constraint
Li <sub>2</sub> O and Na <sub>2</sub> O	$Li_2O \geq 0.0466 - 0.5237 (Na_2O)$	$Li_2O \leq 0.0827 - 0.2839 (Na_2O)$
Cr <sub>2</sub> O <sub>3</sub> and P <sub>2</sub> O <sub>5</sub>	$Cr_2O_3 \geq -0.0018 + 0.2102 (P_2O_5)$	$Cr_2O_3 \leq 0.0017 + 0.3226 (P_2O_5)$
Na <sub>2</sub> O and CaO	$Na_2O \geq 0.1261 - 1.5048 (CaO)$	$Na_2O \leq 0.3191 - 1.5048 (CaO)$
Li <sub>2</sub> O and CaO	None	$Li_2O \leq 0.0282 + 0.4565 (CaO)$
Na <sub>2</sub> O and SO <sub>3</sub>	$Na_2O \geq 0.0947 - 18.8088 (SO_3)$	$Na_2O \leq 0.3161 - 18.8088 (SO_3)$
Li <sub>2</sub> O and SO <sub>3</sub>	$Li_2O \geq -0.0410 + 6.5263 (SO_3)$	$Li_2O \leq 0.0306 + 6.5263 (SO_3)$
Na <sub>2</sub> O and SiO <sub>2</sub>	$Na_2O \geq 0.6024 - 1.3287 (SiO_2)$	$Na_2O \leq 0.8050 - 1.3287 (SiO_2)$

- (a) These constraints (lower and upper bounds) on LAW glass property values are implemented using the LAW glass property models recommended in Sections 5 to 8. Thus, these are indirect constraints on LAW glass composition.
- (b) The maximum measured and predicted values of PCT-B and PCT-Na in Table 9.4 are much larger, but these limits are imposed because of the tendency of the recommended PCT-B and PCT-Na models to under-predict PCT releases above 2.7 g/L. See Section 5.6 for more discussion.
- (c) The maximum measured value in the VHT modeling dataset was 980 μm. The maximum predicted value by the recommended VHT model is 1900.7 μm. Because 1100 μm was used as the censoring value corresponding to complete alteration in the most recent version of the VHT used to generate data for the modeling dataset, the upper limit for VHT alteration was set to 1100 μm.

**Table 9.6. Summary of Constraints Specifying the Model Validity Region for each LAW Glass Property.**

Aspect of Model Validity Region	PCT-B	PCT-Na	VHT	Electrical Conductivity	Viscosity
Single-component lower & upper constraints	Same for all properties, as listed in Table 9.2				
Multiple-component constraints	Same for all properties, listed below.				
Li <sub>2</sub> O and Na <sub>2</sub> O	$0.0466 - 0.5237 (\text{Na}_2\text{O}) \leq \text{Li}_2\text{O} \leq 0.0827 - 0.2839 (\text{Na}_2\text{O})$				
Cr <sub>2</sub> O <sub>3</sub> and P <sub>2</sub> O <sub>5</sub>	$-0.0018 + 0.2102 (\text{P}_2\text{O}_5) \leq \text{Cr}_2\text{O}_3 \leq 0.0017 + 0.3226 (\text{P}_2\text{O}_5)$				
Na <sub>2</sub> O and CaO	$0.1261 - 1.5048 (\text{CaO}) \leq \text{Na}_2\text{O} \leq 0.3191 - 1.5048 (\text{CaO})$				
Li <sub>2</sub> O and CaO	$\text{Li}_2\text{O} \leq 0.0282 + 0.4565 (\text{CaO})$				
Na <sub>2</sub> O and SO <sub>3</sub>	$0.0947 - 18.8088 (\text{SO}_3) \leq \text{Na}_2\text{O} \leq 0.3161 - 18.8088 (\text{SO}_3)$				
Li <sub>2</sub> O and SO <sub>3</sub>	$-0.0410 + 6.5263 (\text{SO}_3) \leq \text{Li}_2\text{O} \leq 0.0306 + 6.5263 (\text{SO}_3)$				
Na <sub>2</sub> O and SiO <sub>2</sub>	$0.6024 - 1.3287 (\text{SiO}_2) \leq \text{Na}_2\text{O} \leq 0.8050 - 1.3287 (\text{SiO}_2)$				
Temperature constraints <sup>(b)</sup>	N/A <sup>(a)</sup>	N/A	N/A	900 – 1280°C	900 – 1280°C
Property constraints <sup>(c)</sup>	≤ 2.7 g/L	≤ 2.7 g/L	≤ 1100 μm	See Table 9.5	See Table 9.5

(a) N/A = not applicable.

(b) From Table 9.3.

(c) From Table 9.5. The property constraints for PCT-B, PCT-Na, and VHT are indirect multiple-component constraints on LAW glass composition. The property constraints for electrical conductivity and viscosity are indirect multiple-variable constraints on combinations of LAW glass composition and melt temperature. The property constraints are implemented using the recommended model for each property.

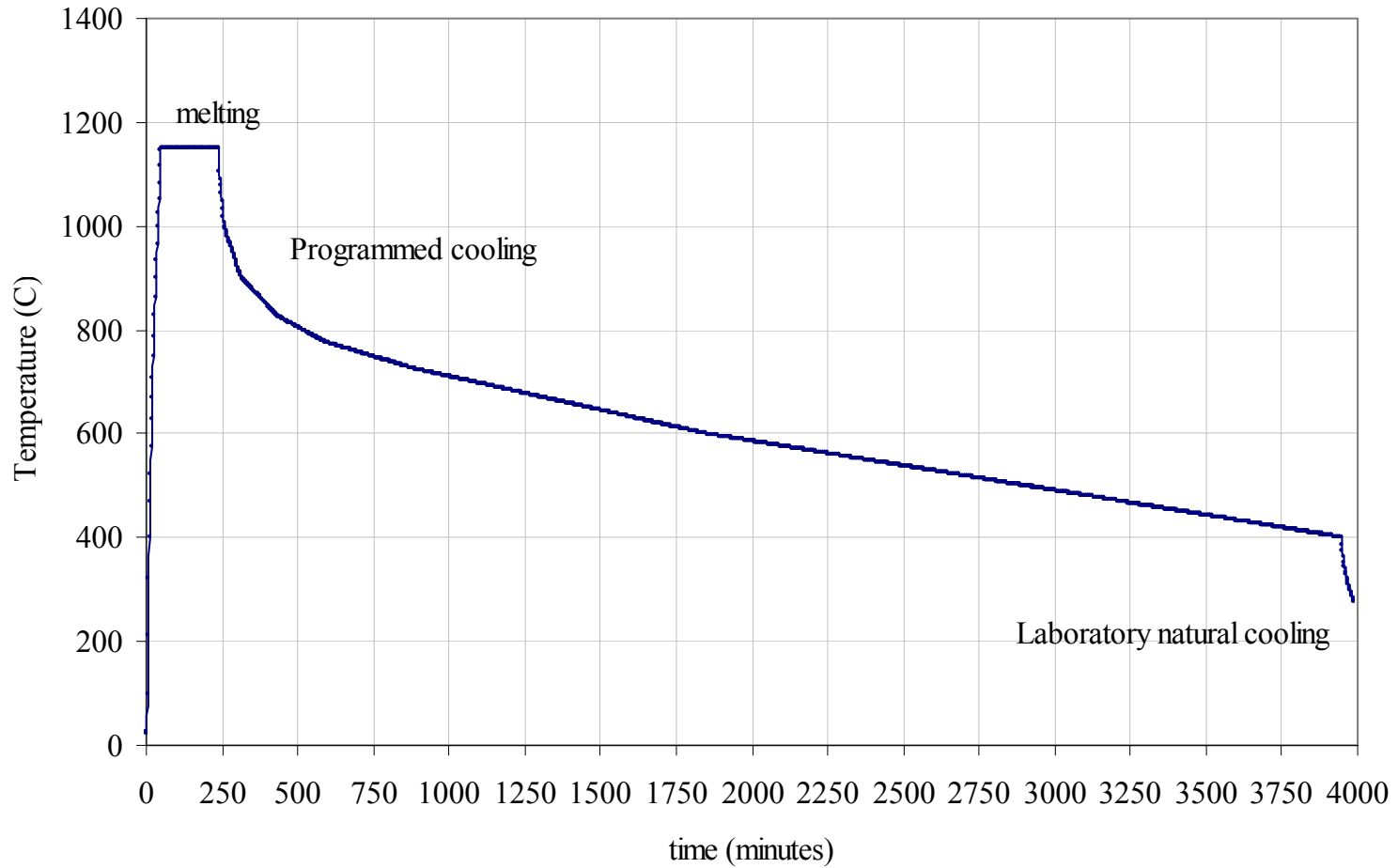


**Figure 3.1. Centerline Canister Cooling Curve Used for Heat Treatment of LA137SRCCC.**

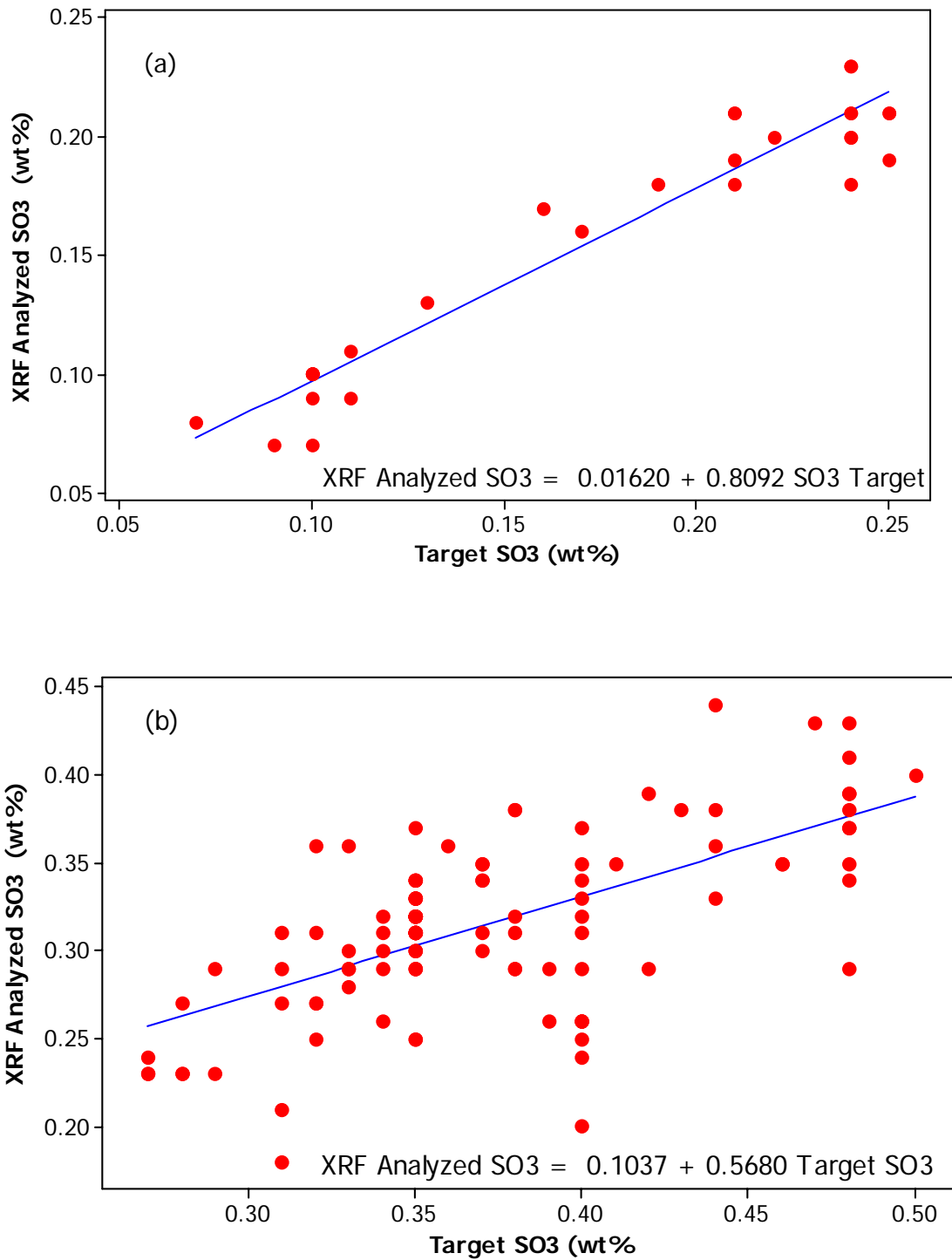


**Figure 3.2. Data and Regression Equations Relating Analyzed SO<sub>3</sub> to Target SO<sub>3</sub> ( $T_{SO_3}$ ) in LAW Glasses for (a)  $T_{SO_3} \leq 0.25$  wt% and (b)  $0.25$  wt%  $< T_{SO_3} \leq 0.50$  wt%.**



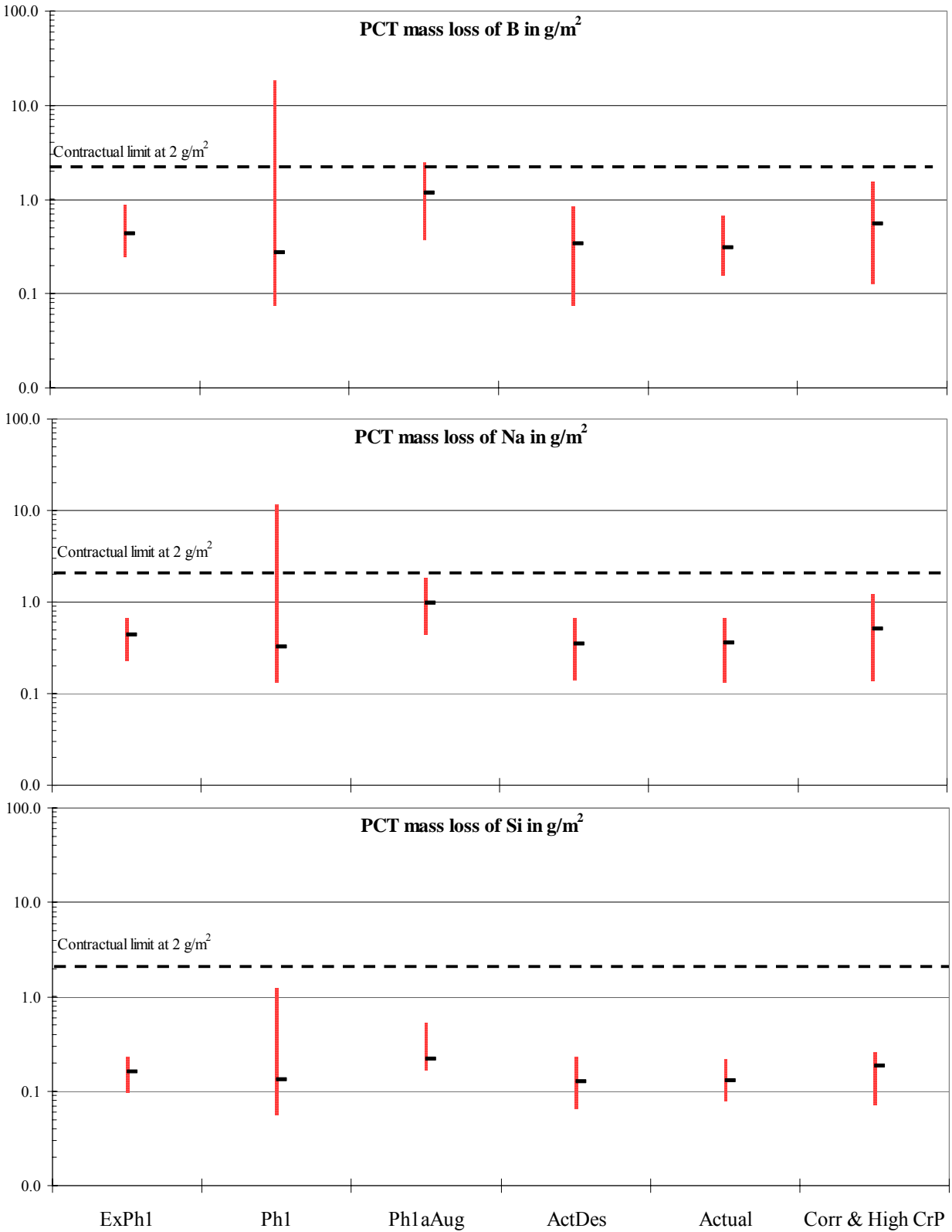


**Figure 4.1. Ranges of PCT Releases (B, Na, and Si, in g/m<sup>2</sup>) for the 264 LAW Glasses with PCT Data, by Sub-Groups of Glasses.**

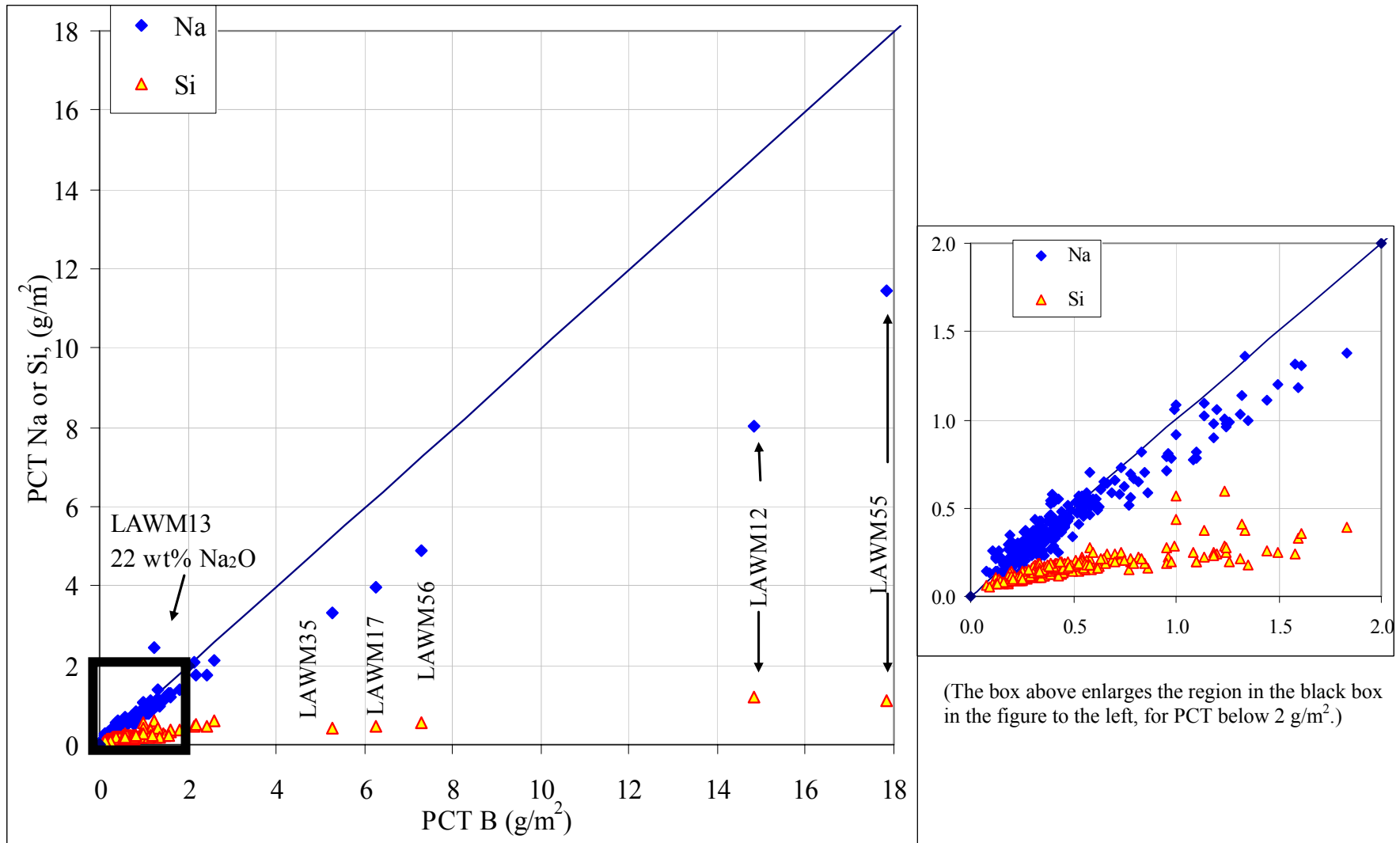


**Figure 4.2. PCT Sodium and Silicon Releases (g/m<sup>2</sup>) as a Function of PCT Boron Release for 264 LAW Glasses with PCT Data. Na and B leach nearly congruently in glasses with low leach rates, as shown in the enlarged figure on the right.**

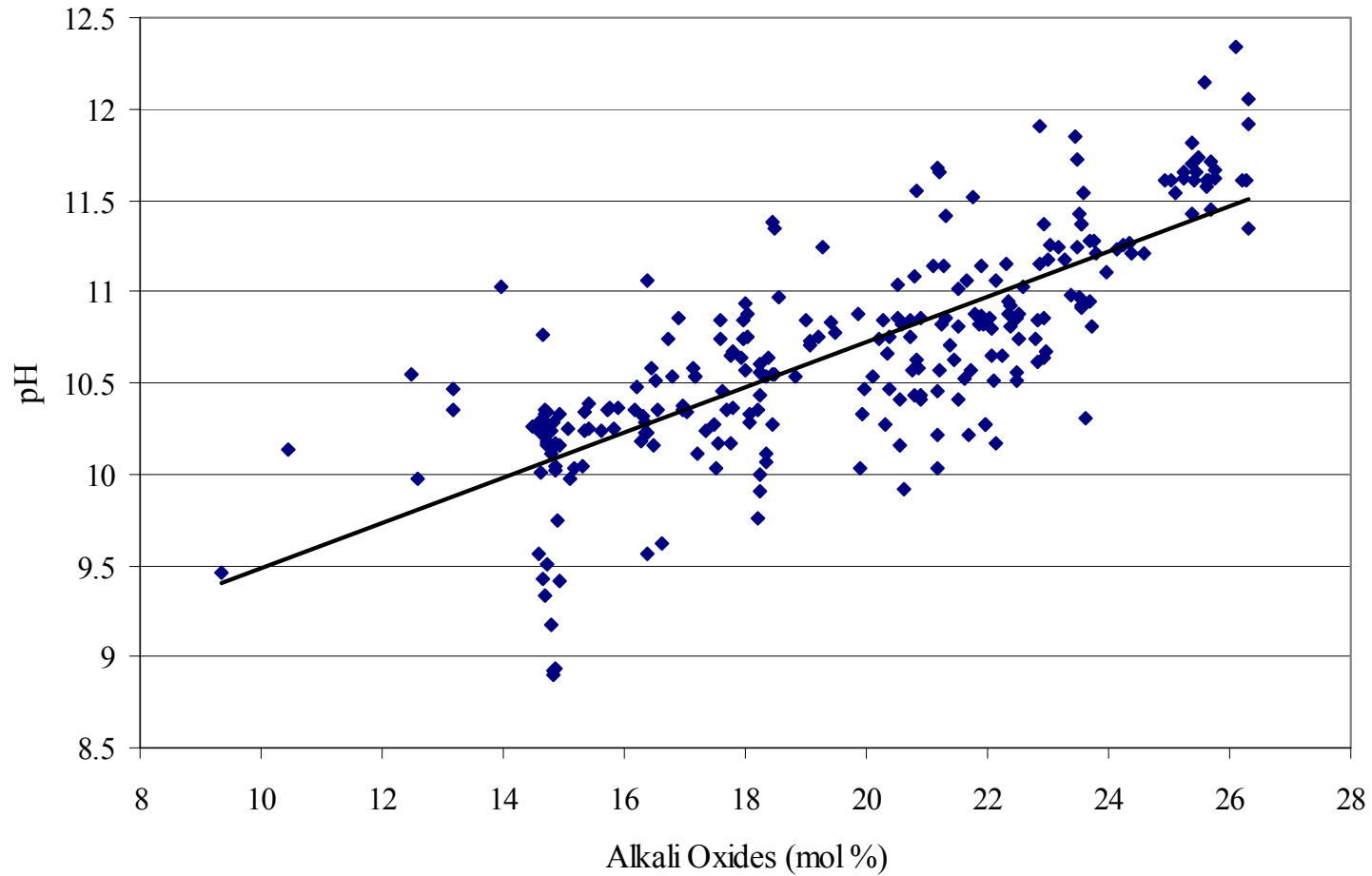


**Figure 4.3. Measured pH at 20°C in the 7-day PCT Leachate as a Function of the Sum of Alkali Oxides ( $\text{Li}_2\text{O}+\text{Na}_2\text{O}+\text{K}_2\text{O}$ ) in mol% for 262 LAW Glasses with PCT Data. Leachate pH values are not given for two actual waste glasses in test reports.**

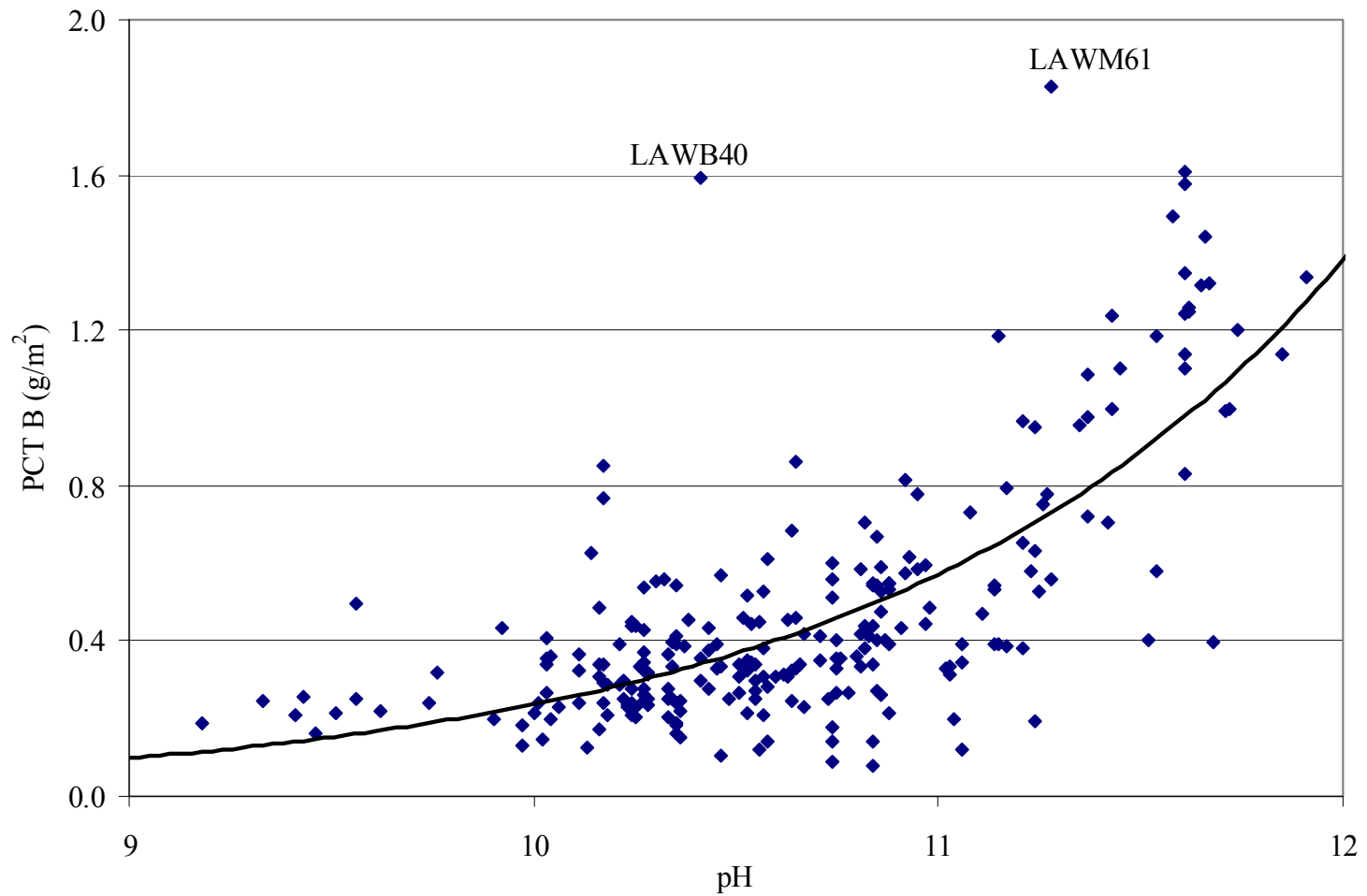


**Figure 4.4. Plot of the PCT Boron Release as a Function of the pH Measured at 20°C in the 7-day PCT Leachate for 264 LAW Glasses with PCT Data.**

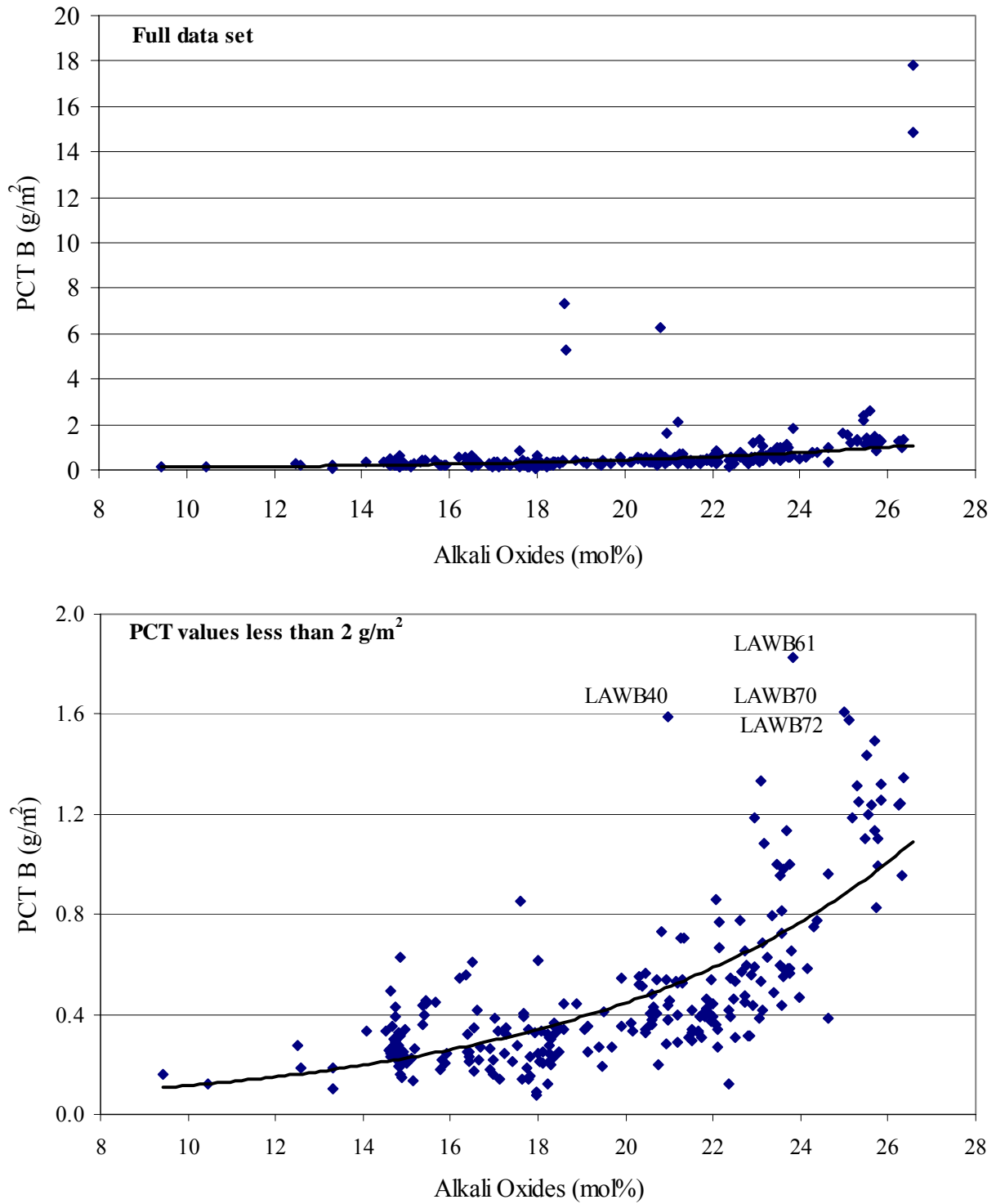


**Figure 4.5. PCT Boron Release as a Function of the Sum of Alkali Oxides ( $\text{Li}_2\text{O}+\text{Na}_2\text{O}+\text{K}_2\text{O}$ ) in mol% for 264 LAW Glasses with PCT Data.**

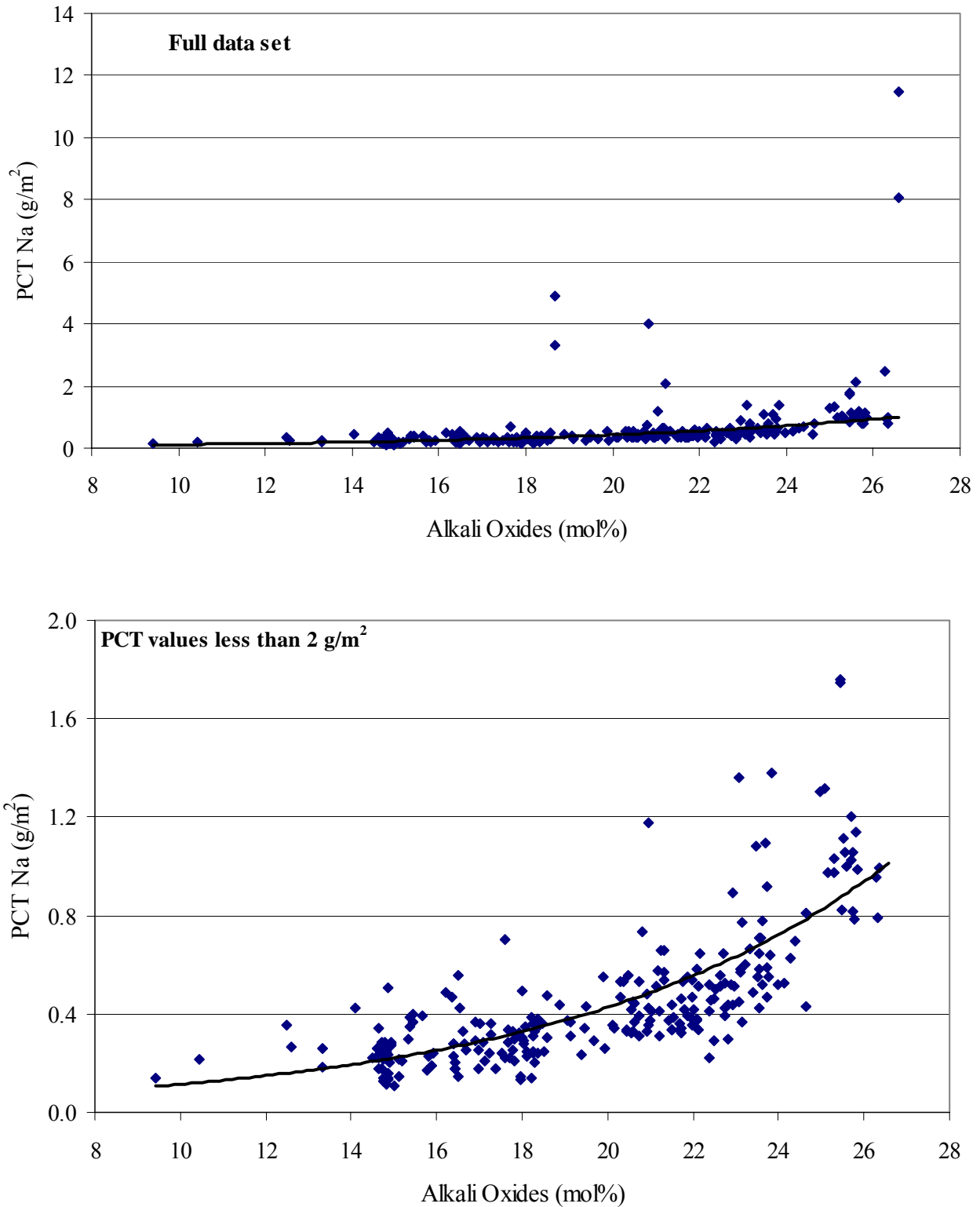


**Figure 4.6. PCT Sodium Release as a Function of the Sum of Alkali Oxides (Li<sub>2</sub>O+Na<sub>2</sub>O+K<sub>2</sub>O) in mol% for 264 LAW Glasses with PCT Data.**

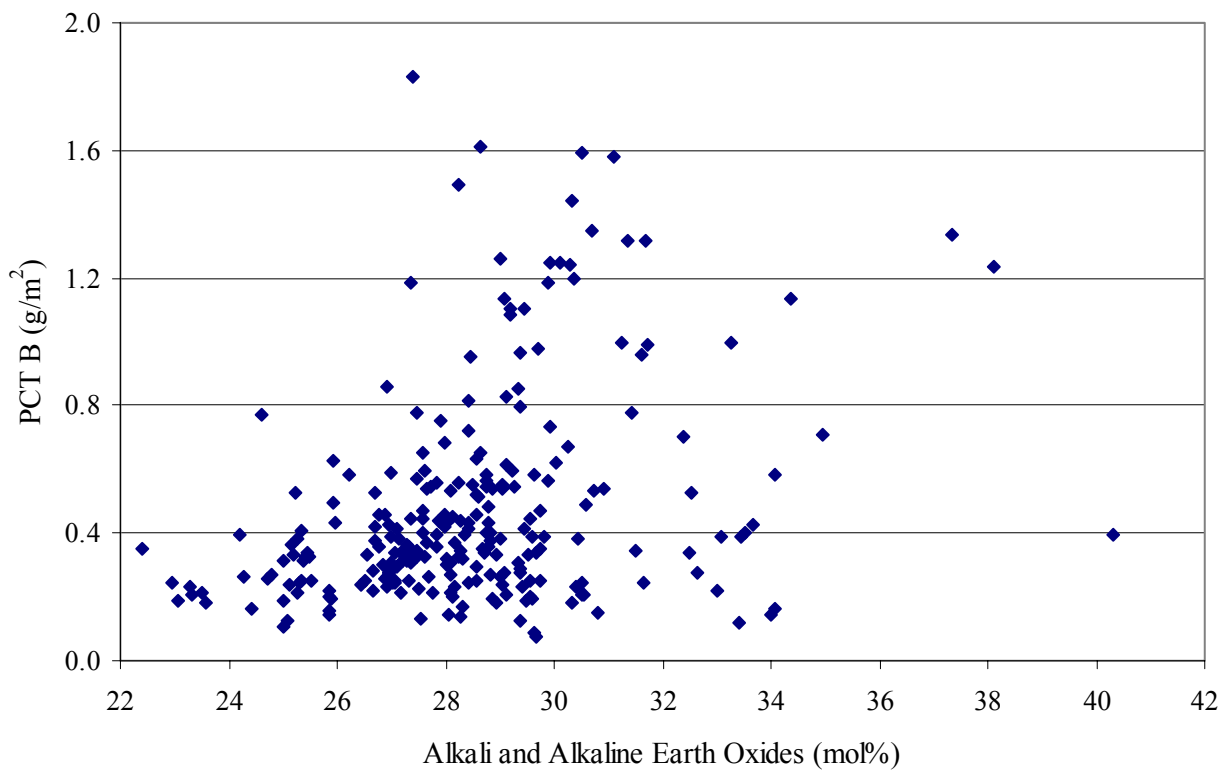
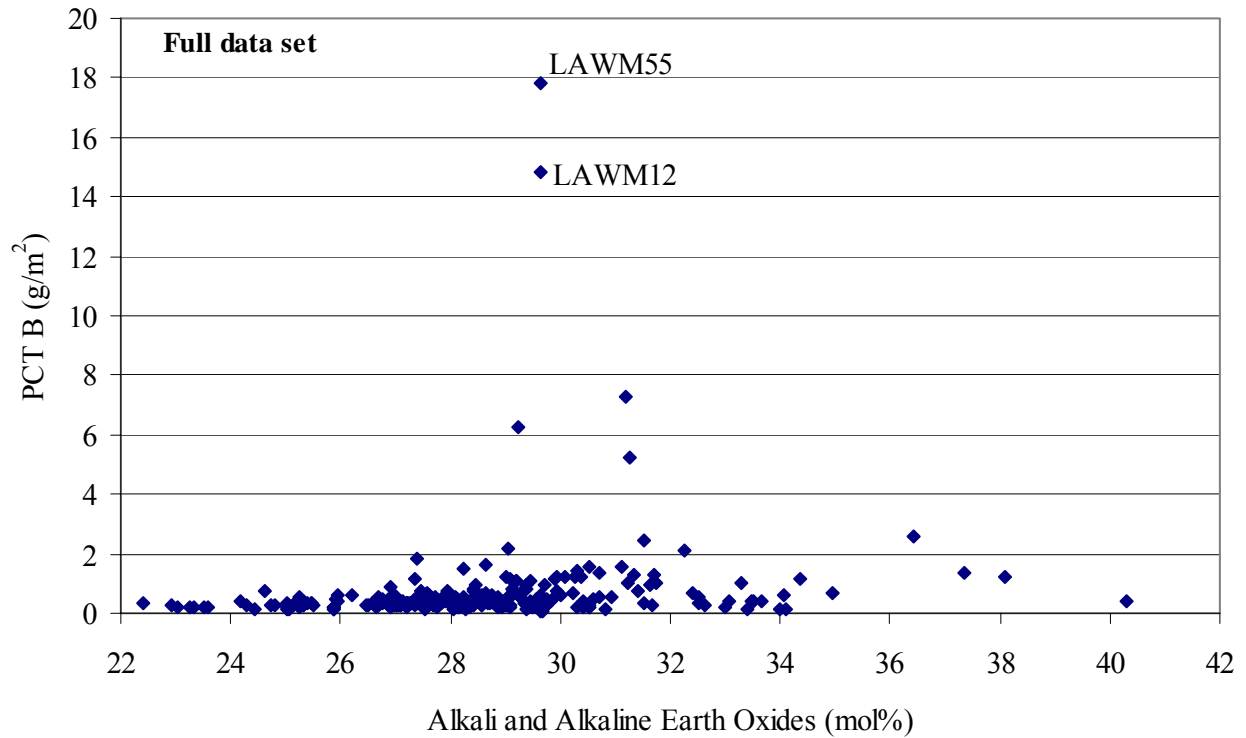


**Figure 4.7. PCT Boron Release as a Function of the Sum of Alkali and Alkaline Earth Oxides ( $\text{Li}_2\text{O}+\text{Na}_2\text{O}+\text{K}_2\text{O}+\text{CaO}+\text{MgO}$ ) in mol% for 264 LAW Glasses with PCT Data.**

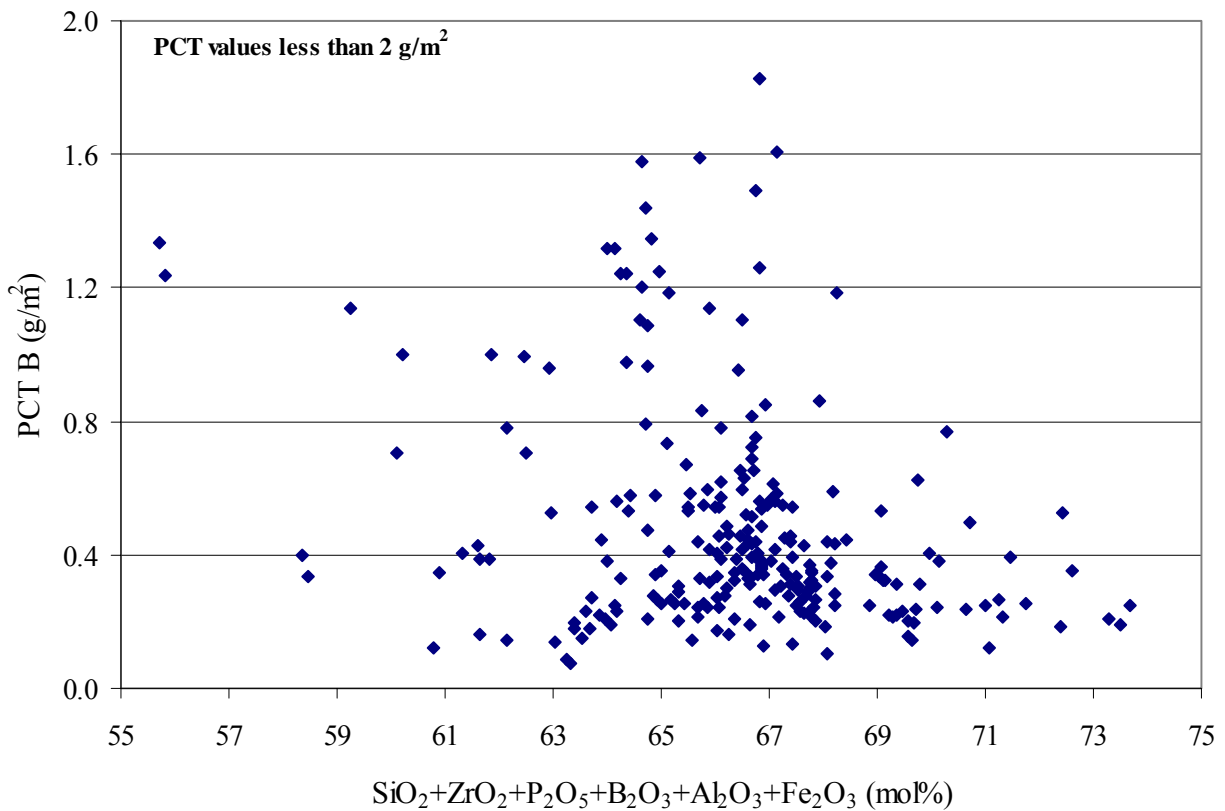
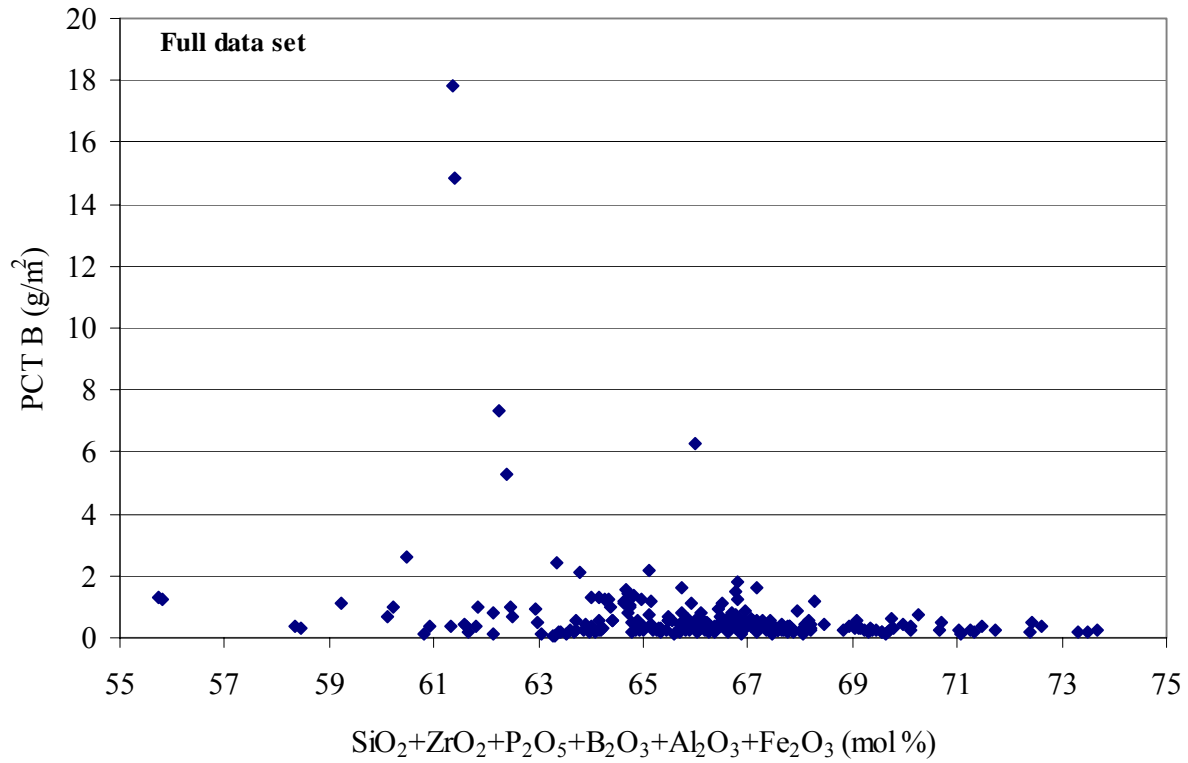


**Figure 4.8. PCT Boron Release as a Function of the Sum of Valence III, IV, and V Components ( $\text{SiO}_2+\text{ZrO}_2+\text{P}_2\text{O}_5+\text{B}_2\text{O}_3+\text{Al}_2\text{O}_3+\text{Fe}_2\text{O}_3$ ) in mol% for 264 LAW Glasses with PCT Data.**



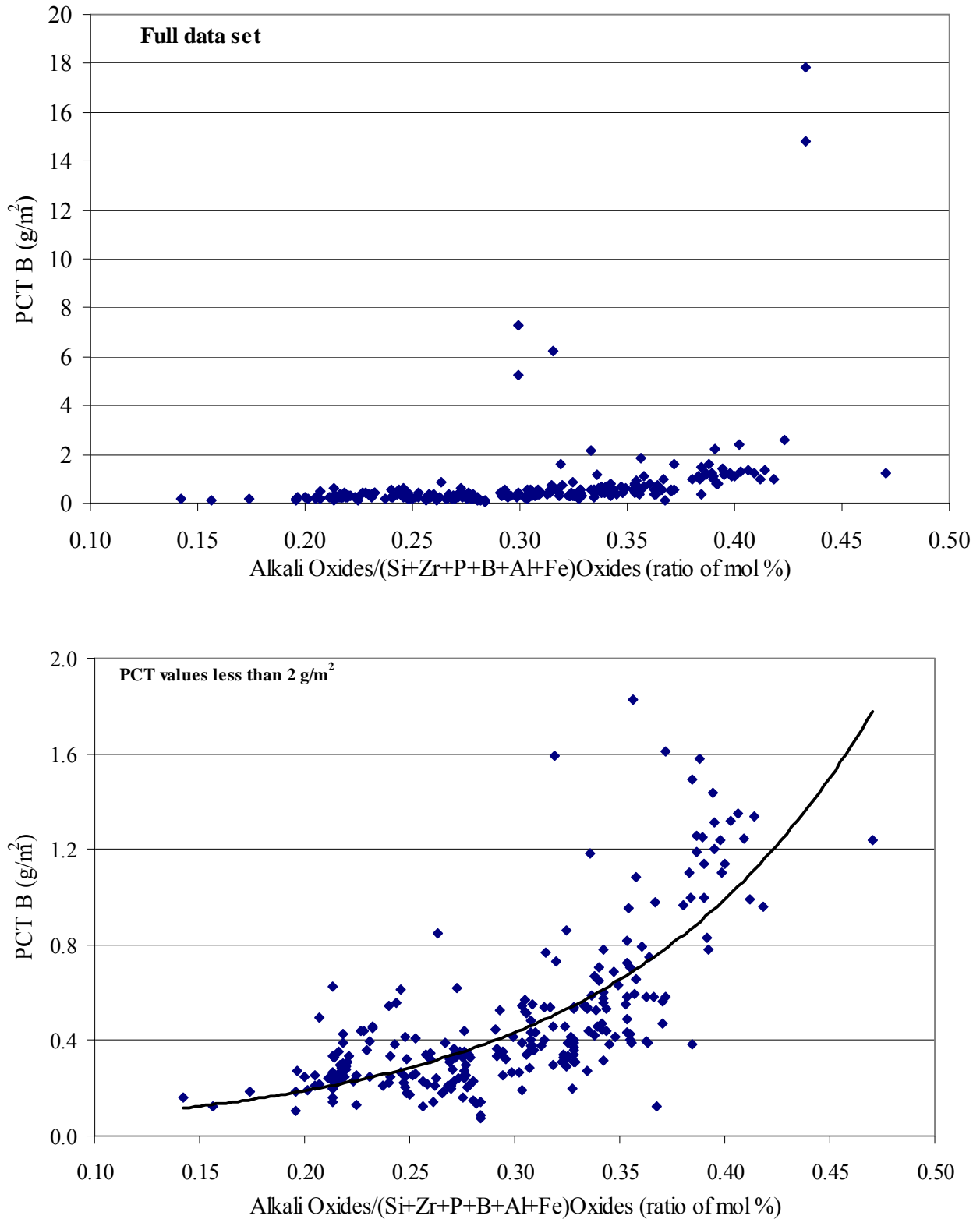


**Figure 4.9. PCT Boron Release as a Function of the Ratio of Alkali Oxides ( $\text{Li}_2\text{O}+\text{Na}_2\text{O}+\text{K}_2\text{O}$ ) to Glass Formers ( $\text{SiO}_2+\text{ZrO}_2+\text{P}_2\text{O}_5+\text{B}_2\text{O}_3+\text{Al}_2\text{O}_3+\text{Fe}_2\text{O}_3$ ) in mol% for 264 LAW Glasses with PCT Data.**

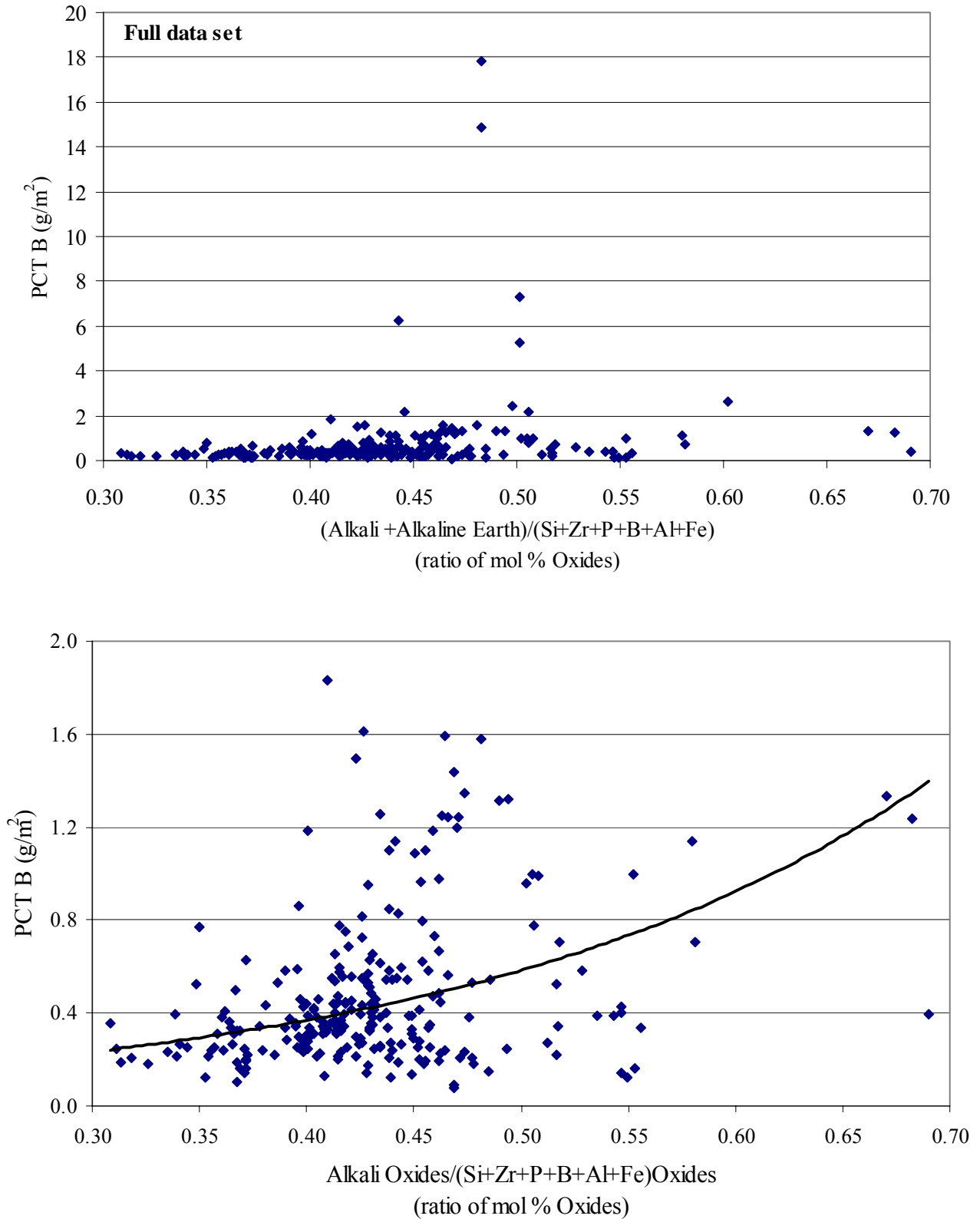


**Figure 4.10. PCT Boron Release as a Function of the Ratio of Alkali and Alkaline Earth Oxides ( $\text{Li}_2\text{O}+\text{Na}_2\text{O}+\text{K}_2\text{O}+\text{CaO}+\text{MgO}$ ) to Glass Formers ( $\text{SiO}_2+\text{ZrO}_2+\text{P}_2\text{O}_5+\text{B}_2\text{O}_3+\text{Al}_2\text{O}_3+\text{Fe}_2\text{O}_3$ ) in mol% for 264 LAW Glasses with PCT Data.**

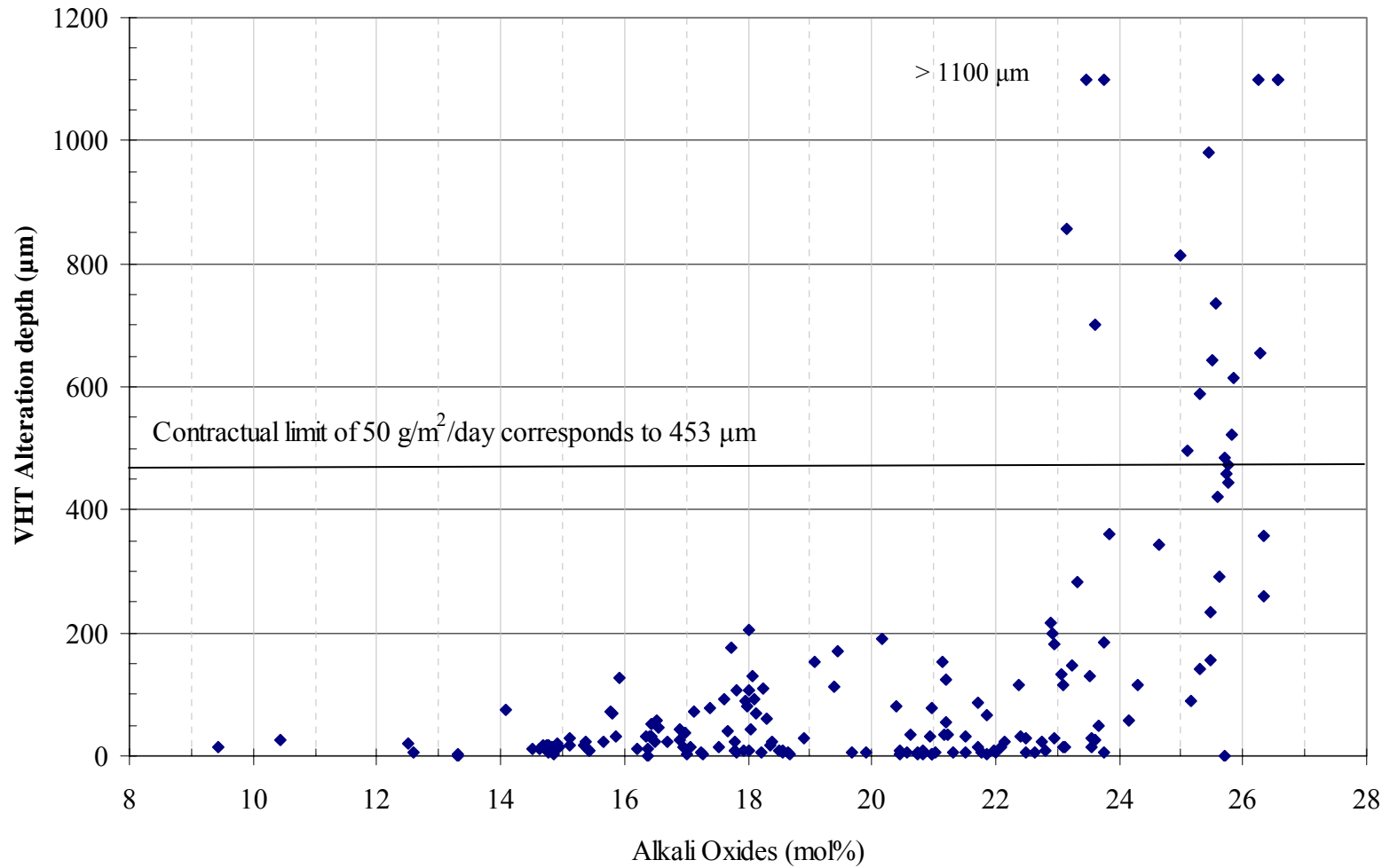


**Figure 4.11. VHT Alteration Depth (in µm) as a Function of the Sum of Alkali Oxides (Li<sub>2</sub>O+Na<sub>2</sub>O+K<sub>2</sub>O) in mol % for 181 LAW Glasses with VHT Data.**

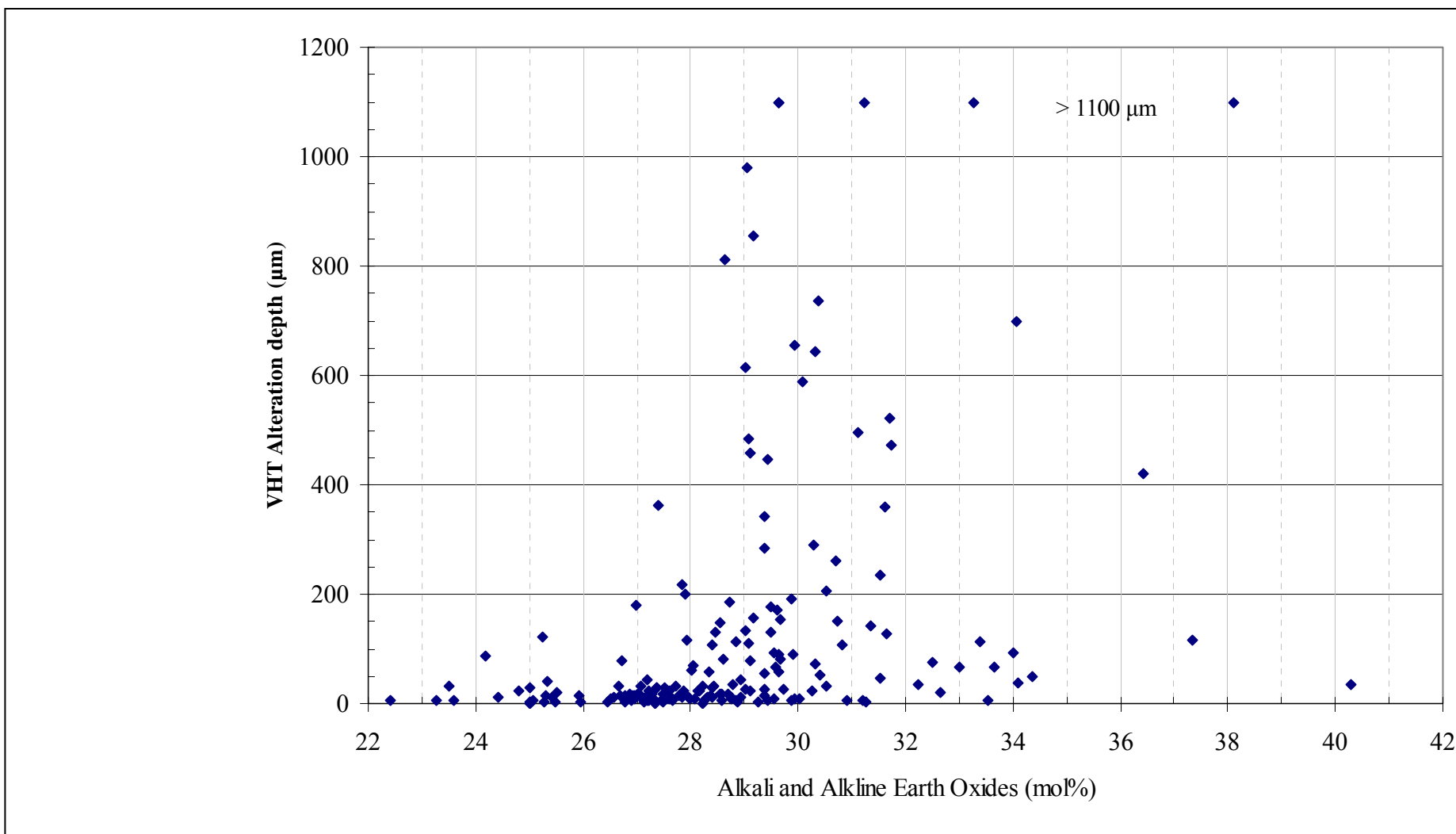


**Figure 4.12. VHT Alteration Depth (in μm) as a Function of the Sum of Alkali and Alkaline Earth Oxides ( $\text{Li}_2\text{O}+\text{Na}_2\text{O}+\text{K}_2\text{O}+\text{CaO}+\text{MgO}$ ) in mol% for 181 LAW Glasses with VHT Data.**

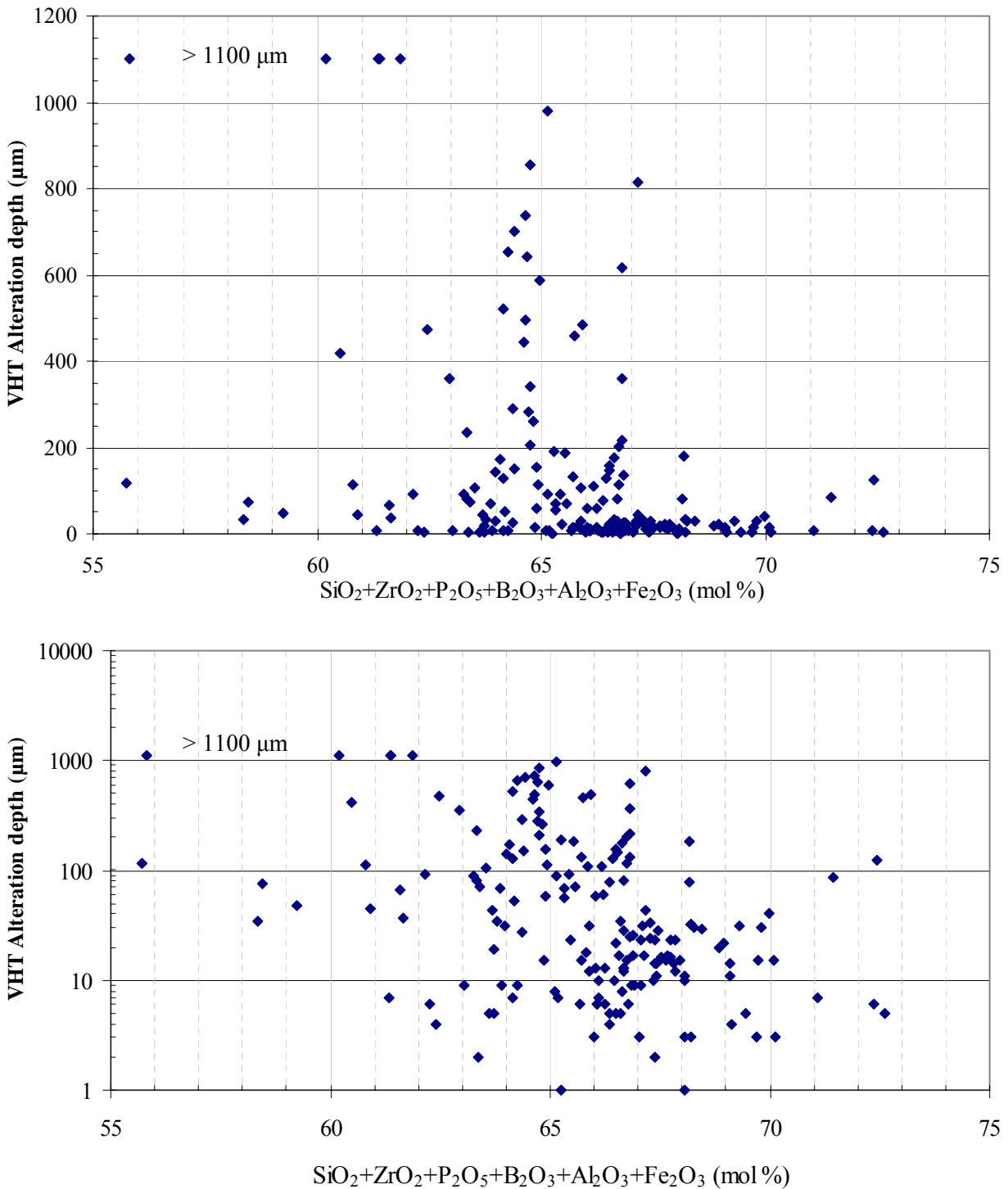


**Figure 4.13. VHT Alteration Depth (in µm) as a Function of the Sum of Valence III, IV, and V Components (SiO<sub>2</sub>+ZrO<sub>2</sub>+P<sub>2</sub>O<sub>5</sub>+B<sub>2</sub>O<sub>3</sub>+Al<sub>2</sub>O<sub>3</sub>+Fe<sub>2</sub>O<sub>3</sub>) in mol% for 181 LAW Glasses with VHT Data; linear scale (top) and log<sub>10</sub> scale (bottom).**

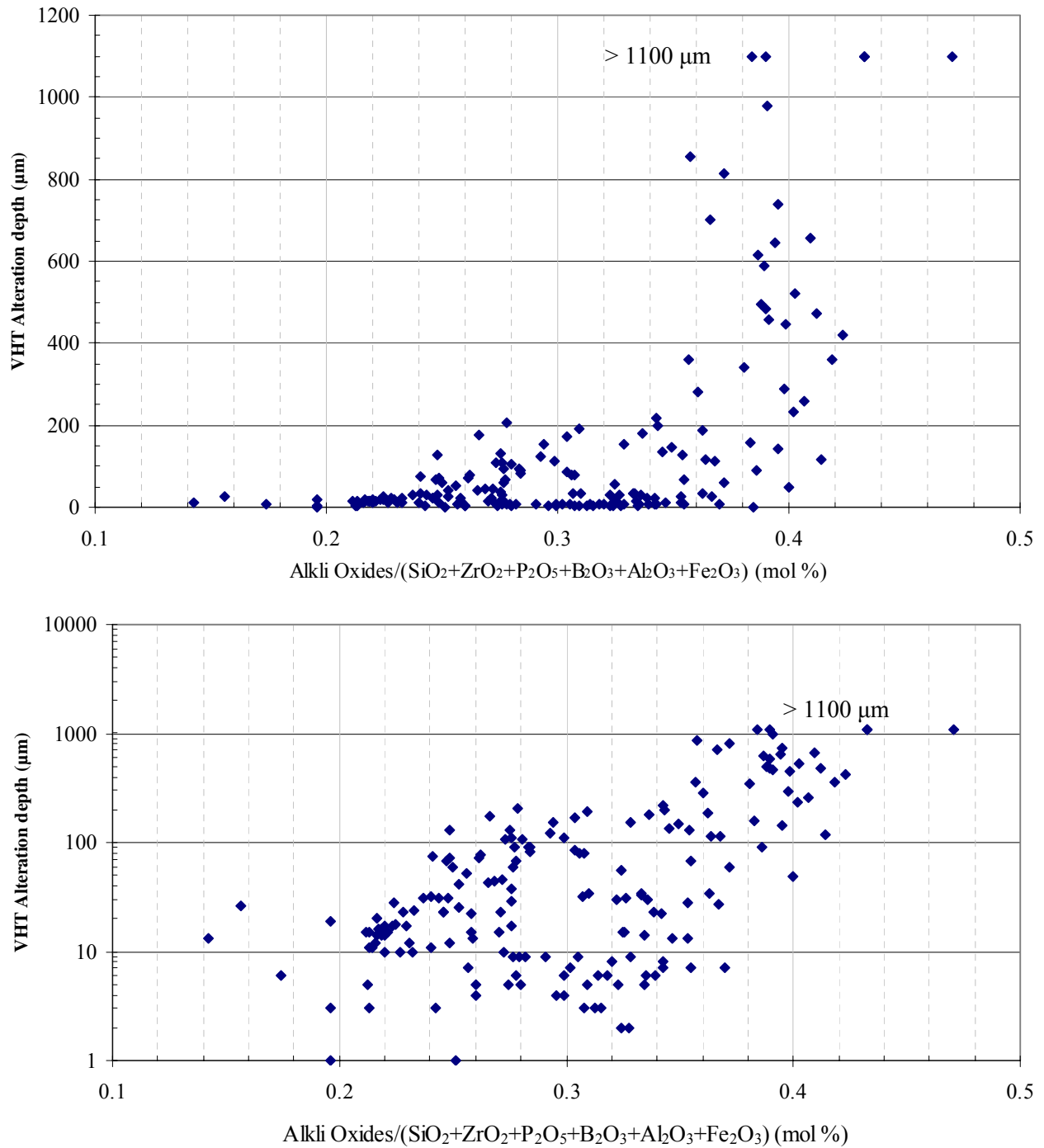


**Figure 4.14. VHT Alteration Depth (in µm) as a Function of the Ratio of Alkali Oxides (Li<sub>2</sub>O+Na<sub>2</sub>O+K<sub>2</sub>O) to Glass Formers (SiO<sub>2</sub>+ZrO<sub>2</sub>+P<sub>2</sub>O<sub>5</sub>+B<sub>2</sub>O<sub>3</sub>+Al<sub>2</sub>O<sub>3</sub>+Fe<sub>2</sub>O<sub>3</sub>) in mol% for 181 LAW Glasses with VHT Data; linear scale (top) and log<sub>10</sub> scale (bottom).**

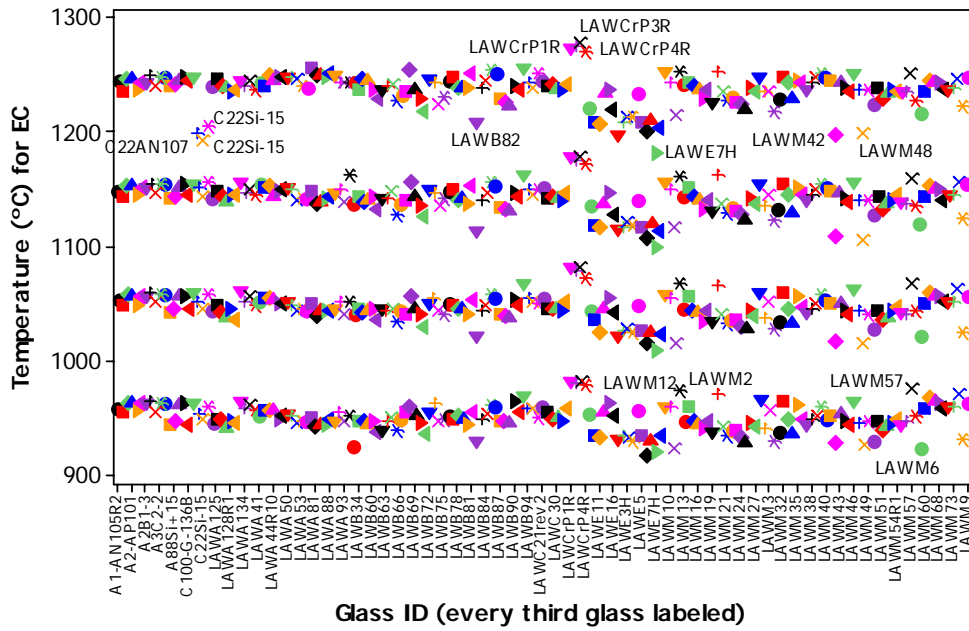


**Figure 4.15. Distribution of Temperature Values for Each of 181 LAW Glasses with Electrical Conductivity Data.**

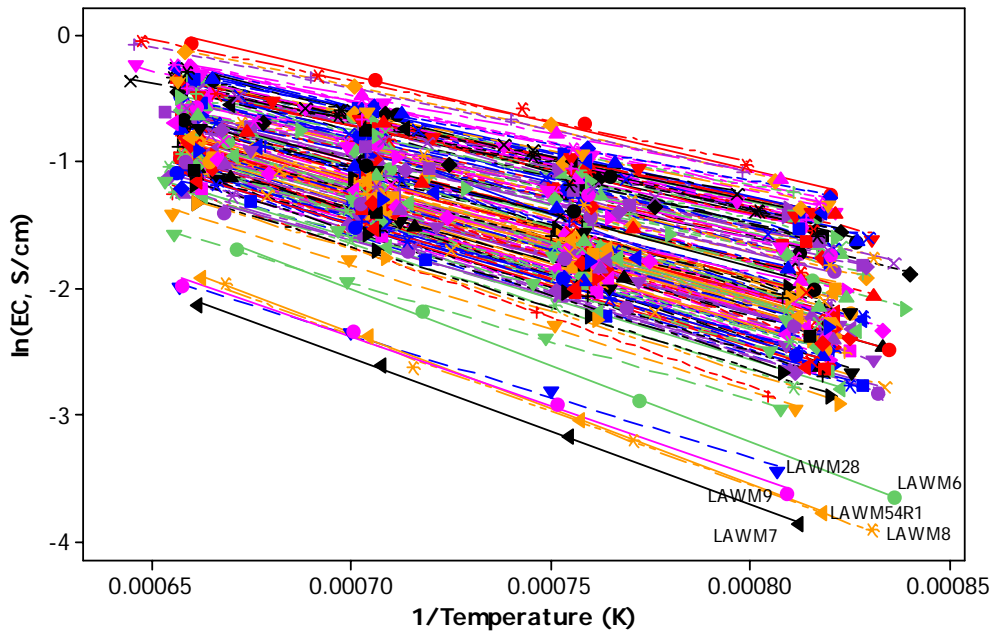


**Figure 4.16. Temperature Dependence of Electrical Conductivity for Each of 181 LAW Glasses with Electrical Conductivity Data. Also shown is an Arrhenius equation fit for each glass for comparison purposes.**

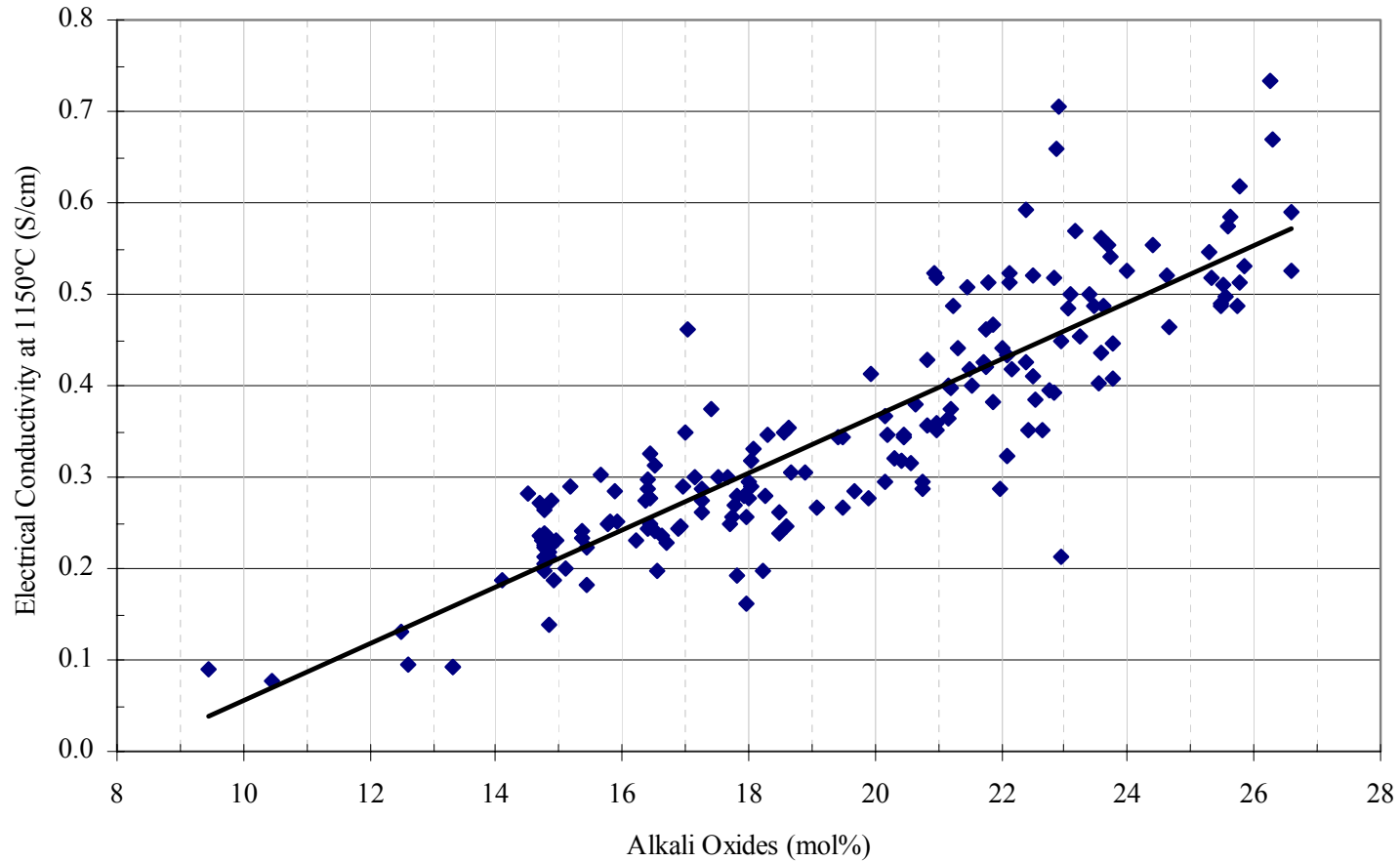


**Figure 4.17. Glass Melt Electrical Conductivity Calculated by Arrhenius Equation Fit (in S/cm) at 1150°C as a Function of the Sum of Alkali Oxides ( $\text{Li}_2\text{O}+\text{Na}_2\text{O}+\text{K}_2\text{O}$ ) in mol% for 181 LAW Glasses with Electrical Conductivity Data.**



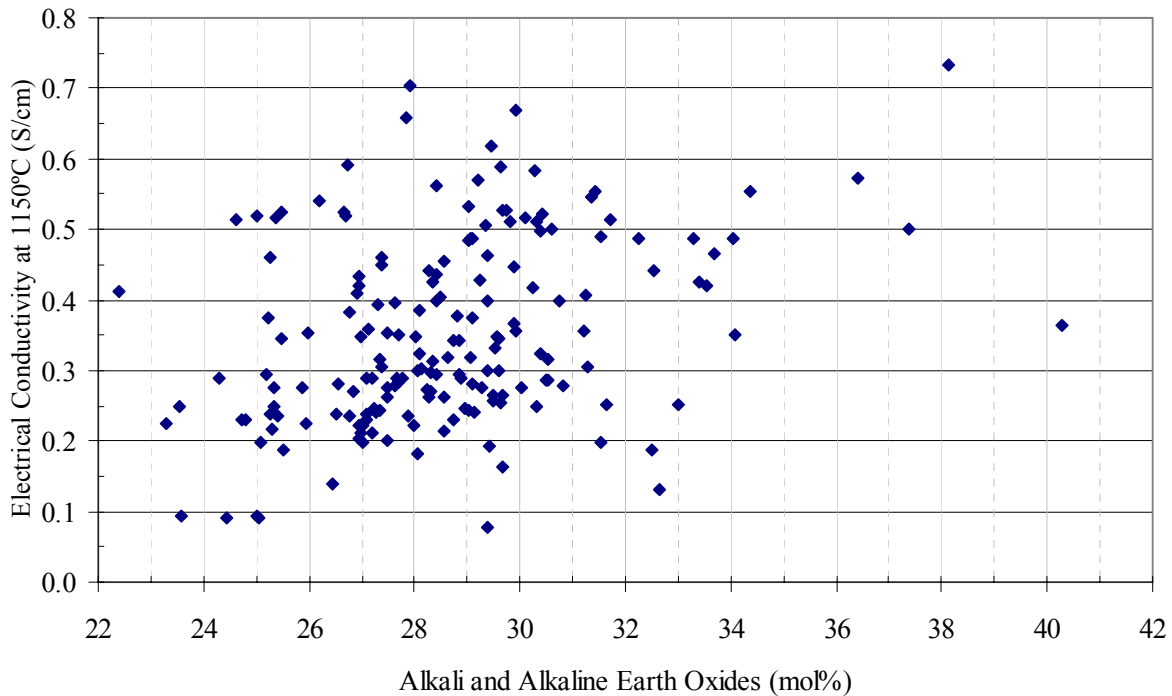


**Figure 4.18.** Glass Melt Electrical Conductivity Calculated by Arrhenius Equation Fit (in S/cm) at 1150°C as a Function of the Sum of Alkali and Alkaline Earth Oxides ( $\text{Li}_2\text{O}+\text{Na}_2\text{O}+\text{K}_2\text{O}+\text{CaO}+\text{MgO}$ ) in mol% for 181 LAW Glasses with Electrical Conductivity Data.

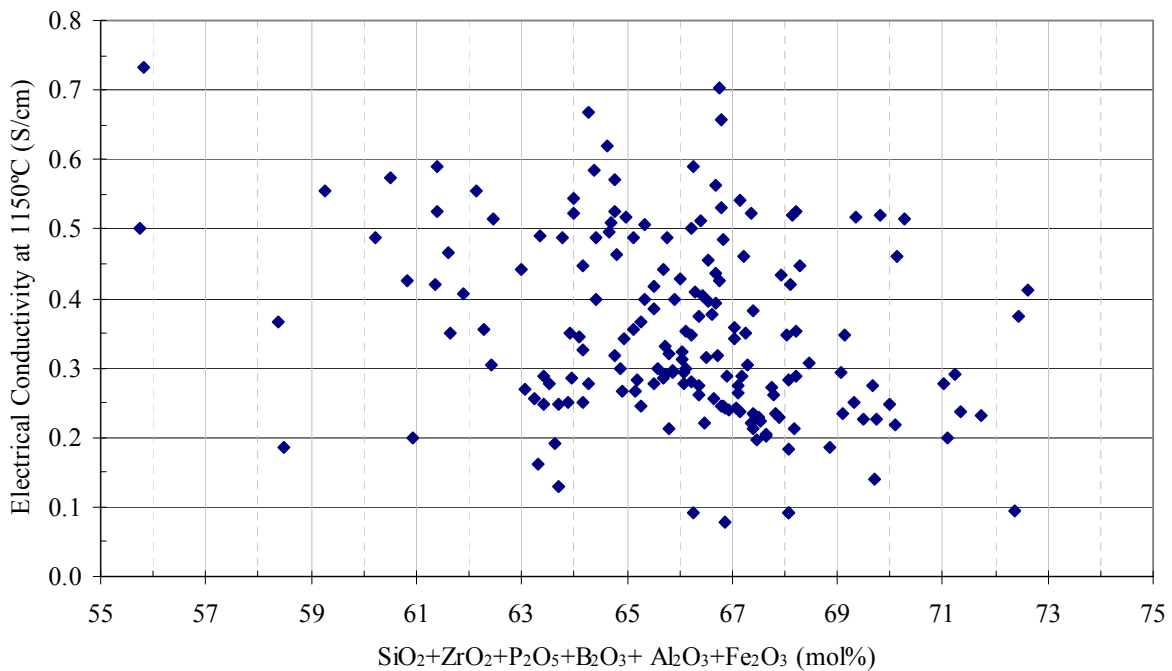


**Figure 4.19.** Glass Melt Electrical Conductivity Calculated by Arrhenius Equation Fit (in S/cm) at 1150°C as a Function of the Sum of Valence III, IV, and V Components ( $\text{SiO}_2+\text{ZrO}_2+\text{P}_2\text{O}_5+\text{B}_2\text{O}_3+\text{Al}_2\text{O}_3+\text{Fe}_2\text{O}_3$ ) in mol% for 181 LAW Glasses with Electrical Conductivity Data.

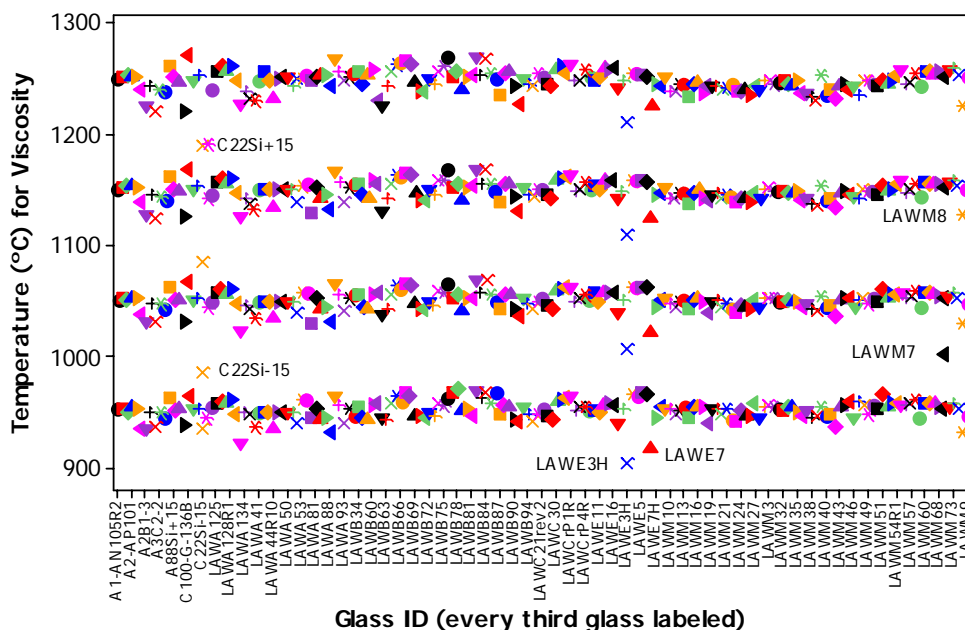


**Figure 4.20. Distribution of Temperature Values for Each of 181 LAW Glasses with Viscosity Data.**

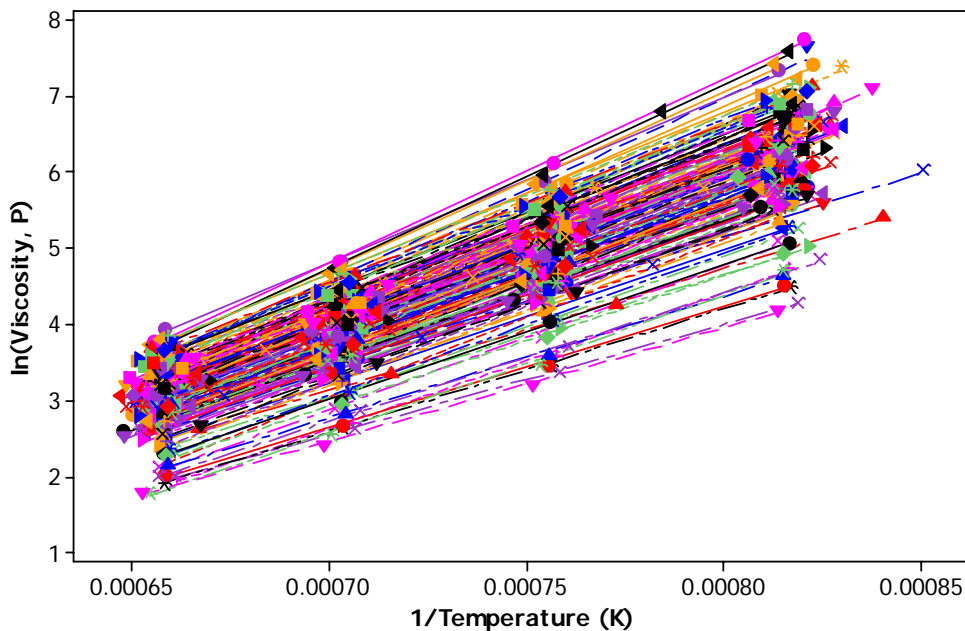


**Figure 4.21. Temperature Dependence of Viscosity for Each of 181 LAW Glasses with Viscosity Data. Also shown is an Arrhenius equation fit for each glass for comparison purposes.**

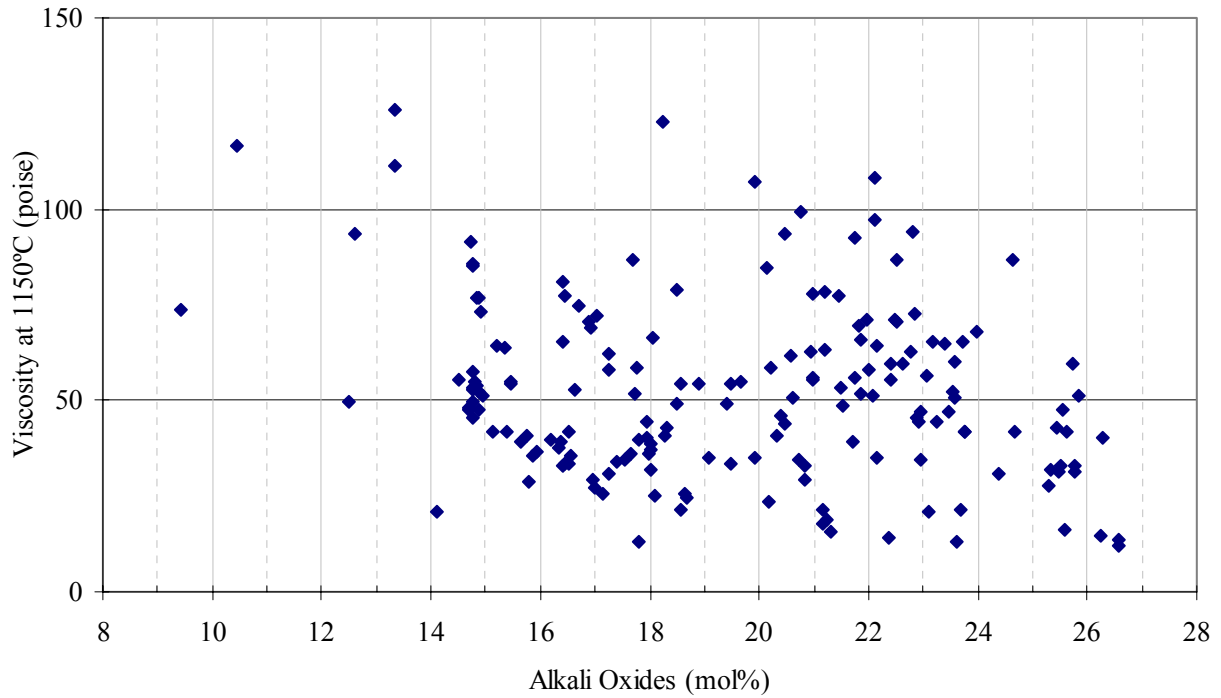


**Figure 4.22.** Glass Melt Viscosity Calculated by Arrhenius Equation Fit (in poise) at 1150°C as a Function of the Sum of Alkali Oxides (Li<sub>2</sub>O+Na<sub>2</sub>O+K<sub>2</sub>O) in mol% for 181 LAW Glasses with Melt Viscosity Data.

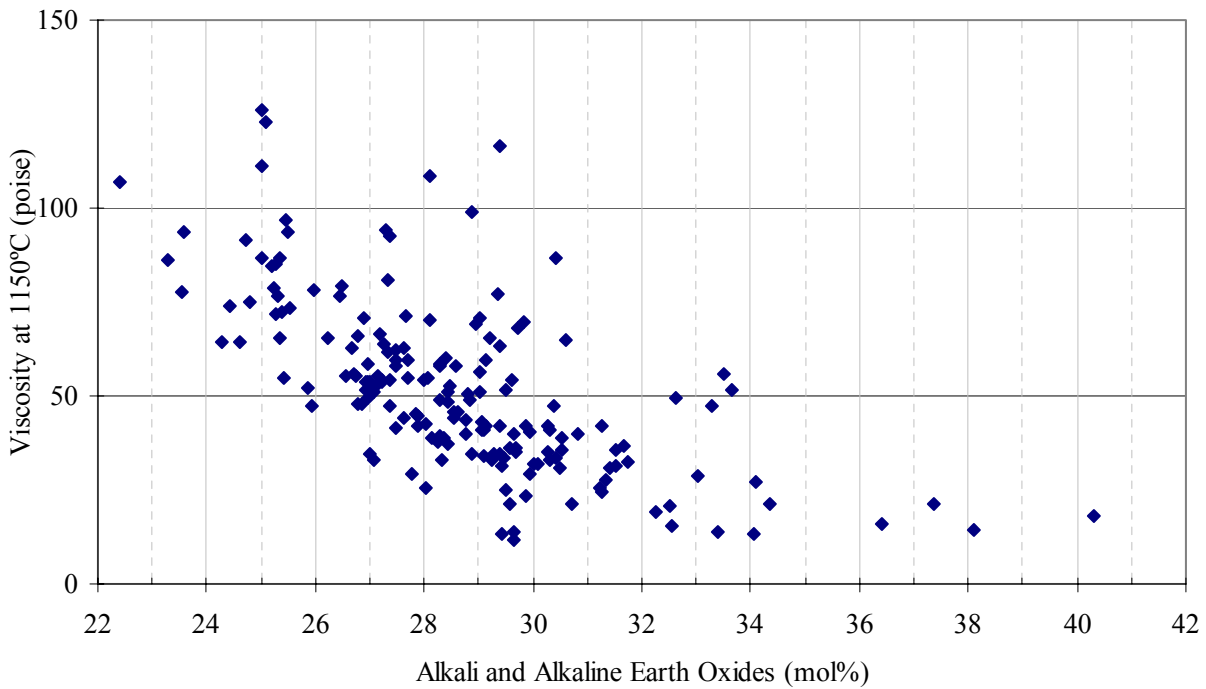


**Figure 4.23.** Glass Melt Viscosity Calculated by Arrhenius Equation Fit (in poise) at 1150°C as a Function of the Sum of Alkali and Alkaline Earth Oxides (Li<sub>2</sub>O+Na<sub>2</sub>O+K<sub>2</sub>O+CaO+MgO) in mol% for 181 LAW Glasses with Melt Viscosity Data.

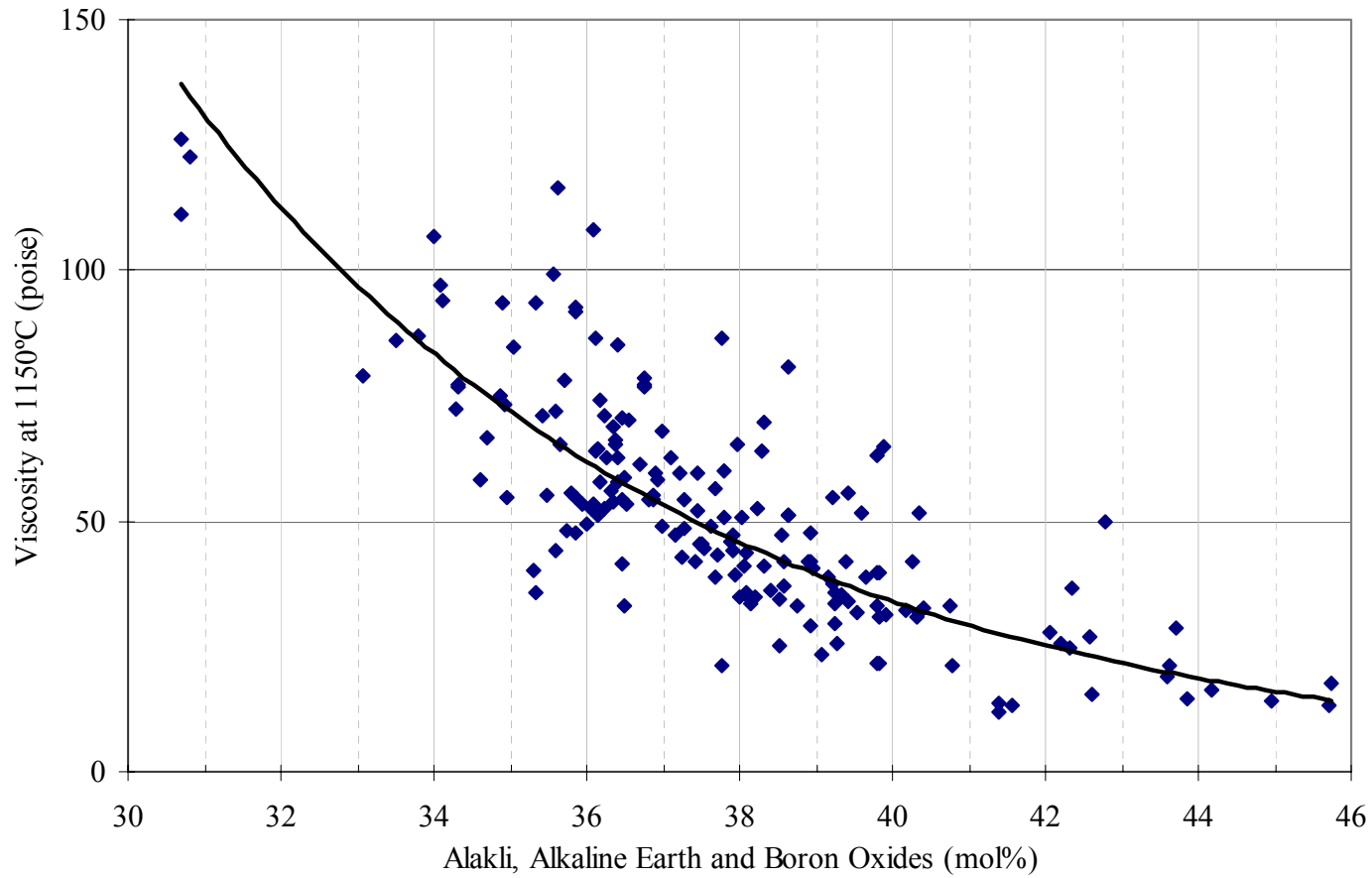


**Figure 4.24.** Glass Melt Viscosity Calculated by Arrhenius Equation Fit (in poise) at 1150°C as a Function of the Sum of Alkali, Alkaline Earth and Boron Oxides ( $\text{Li}_2\text{O}+\text{Na}_2\text{O}+\text{K}_2\text{O}+\text{CaO}+\text{MgO}+\text{B}_2\text{O}_3$ ) in mol% for 181 LAW Glasses with Melt Viscosity Data.

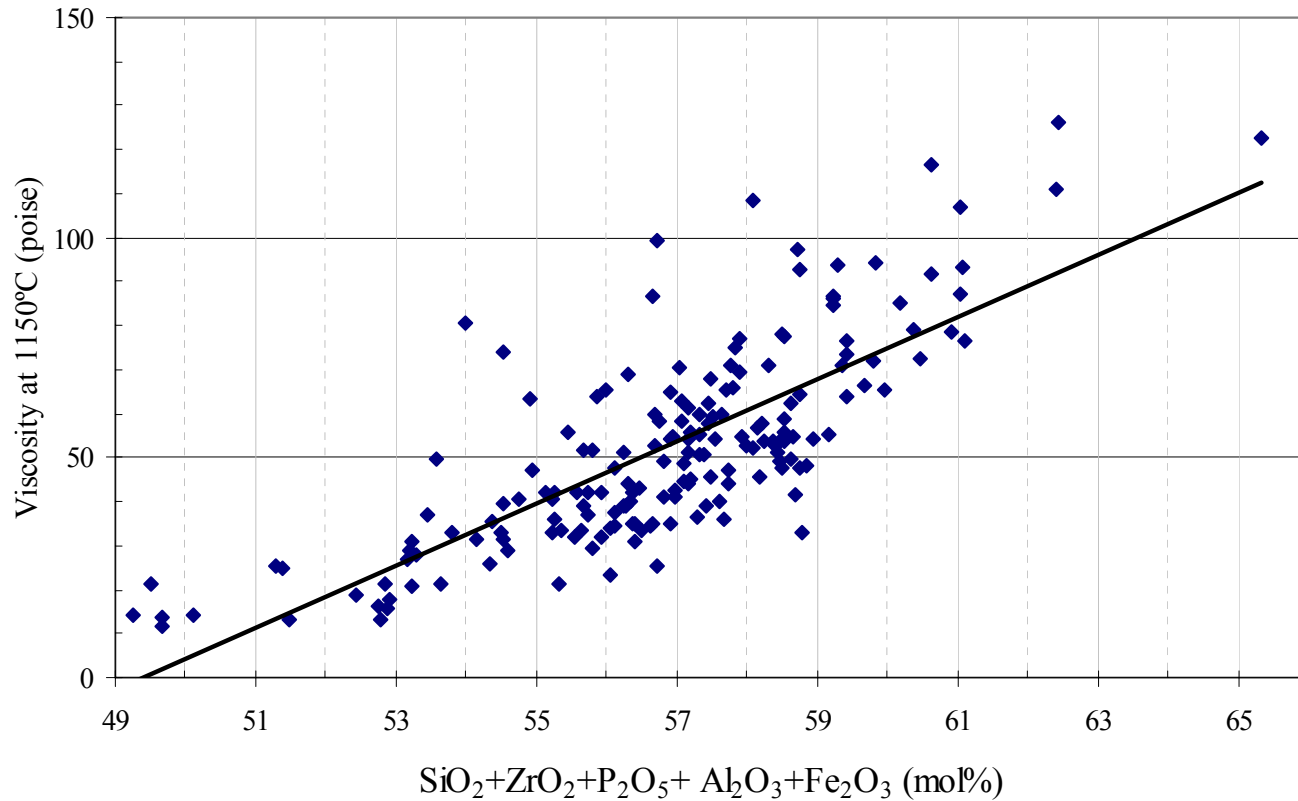


**Figure 4.25. Glass Melt Viscosity Calculated by Arrhenius Equation Fit (in poise) at 1150°C as a Function of SiO<sub>2</sub>+ZrO<sub>2</sub>+P<sub>2</sub>O<sub>5</sub>+B<sub>2</sub>O<sub>3</sub>+Al<sub>2</sub>O<sub>3</sub>+Fe<sub>2</sub>O<sub>3</sub> in mol% for 181 LAW Glasses with Melt Viscosity Data.**

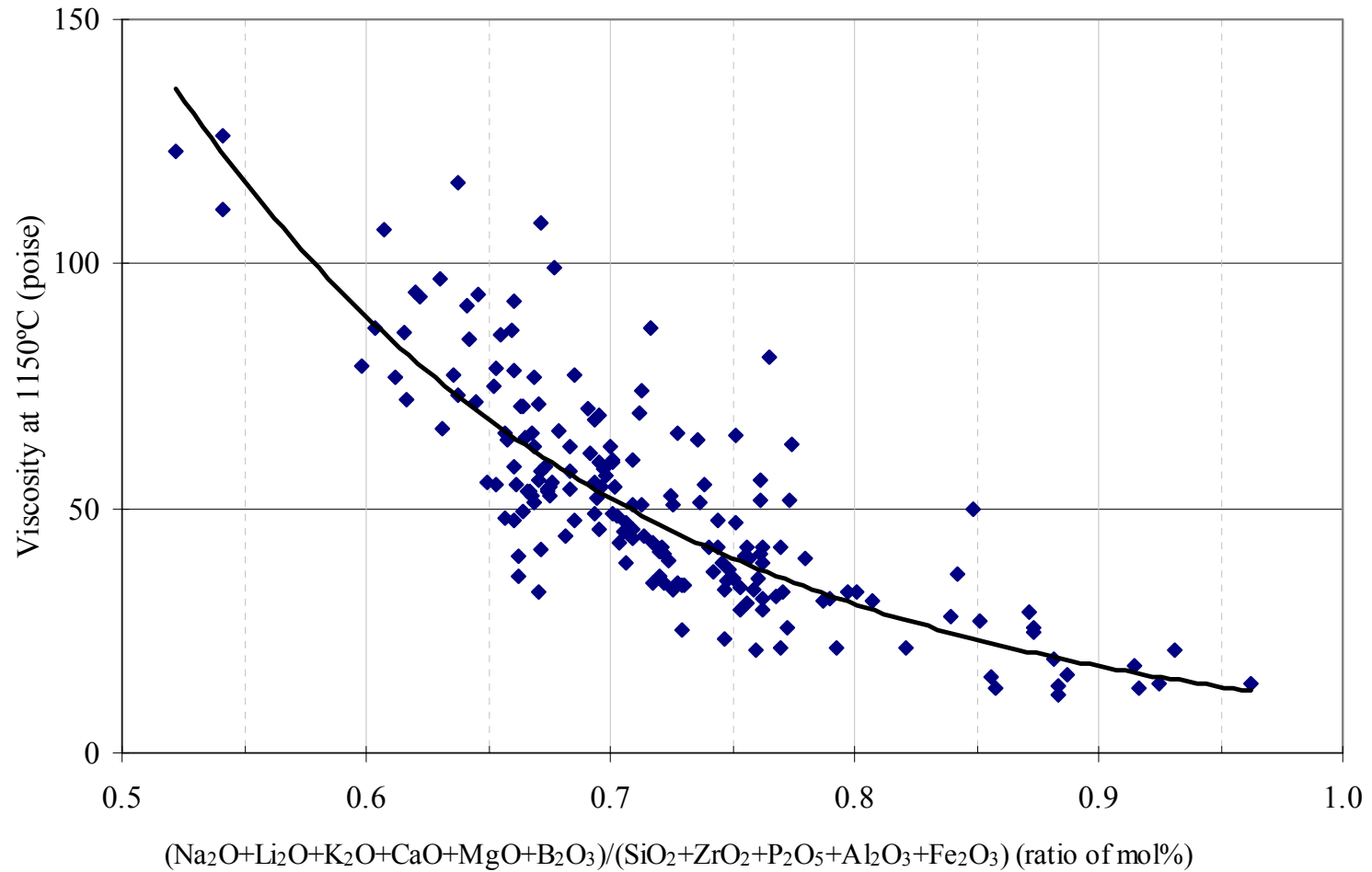


**Figure 4.26. Glass Melt Viscosity Calculated by Arrhenius Equation Fit (in poise) at 1150°C as a Function of the Ratio of Alkali and Alkaline Earth Oxides ( $\text{Li}_2\text{O}+\text{Na}_2\text{O}+\text{K}_2\text{O}+\text{CaO}+\text{MgO}+\text{B}_2\text{O}_3$ ) to Glass Former Oxides ( $\text{SiO}_2+\text{ZrO}_2+\text{P}_2\text{O}_5+\text{Al}_2\text{O}_3+\text{Fe}_2\text{O}_3$ ) in mol% for 181 LAW Glasses with Melt Viscosity Data.**

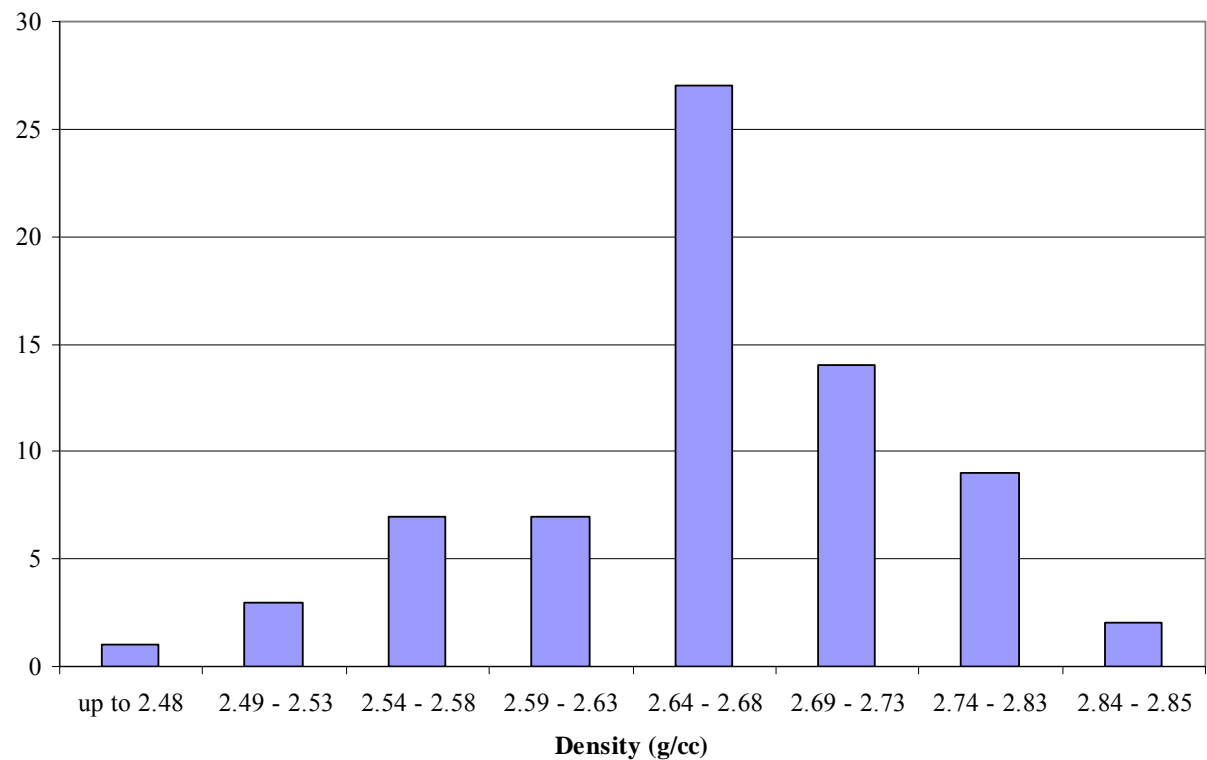


**Figure 4.27. Densities of LAW Glasses.**

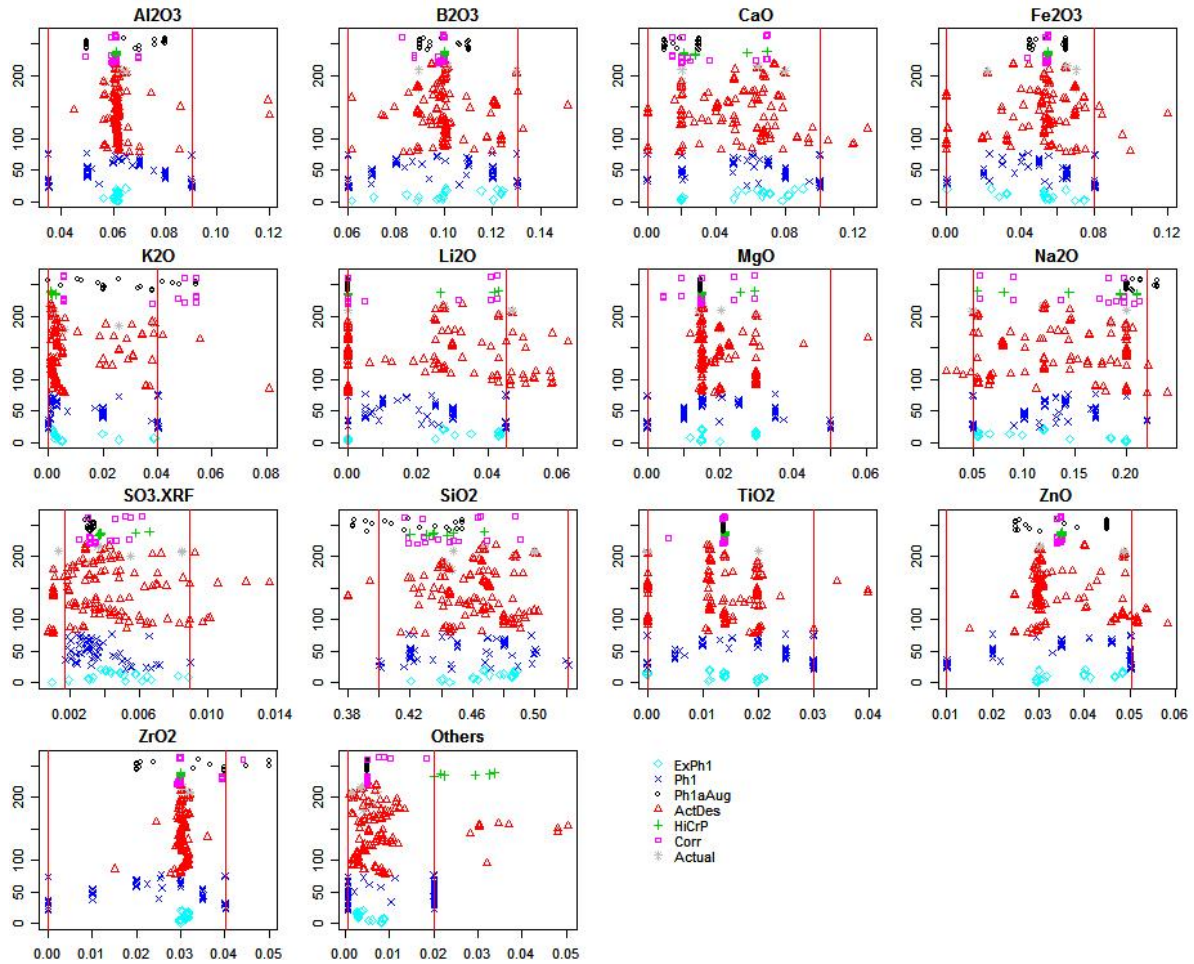


**Figure 5.1. Plots Showing Ranges and Distributions of Values (mass fractions) for 14 Main Components in 264 LAW Glasses with PCT Data. The vertical lines (when present) are the lower and upper limits for each component from the Phase 1 test matrix.**



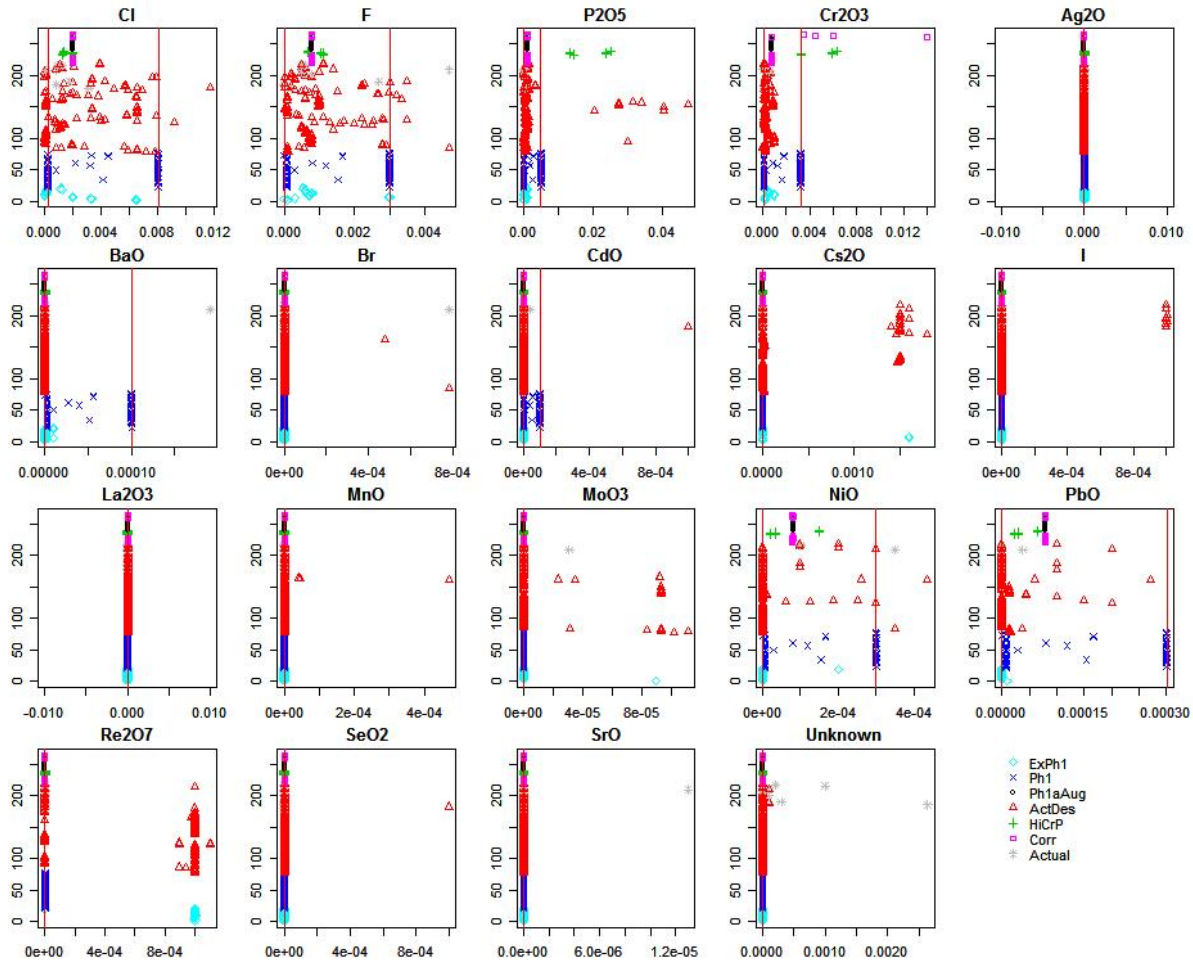


**Figure 5.2. Plots Showing Ranges and Distributions of Values (mass fractions) for 19 Minor Components in 264 LAW Glasses with PCT Data. The vertical lines (when present) are the lower and upper limits for each component from the Phase 1 test matrix.**

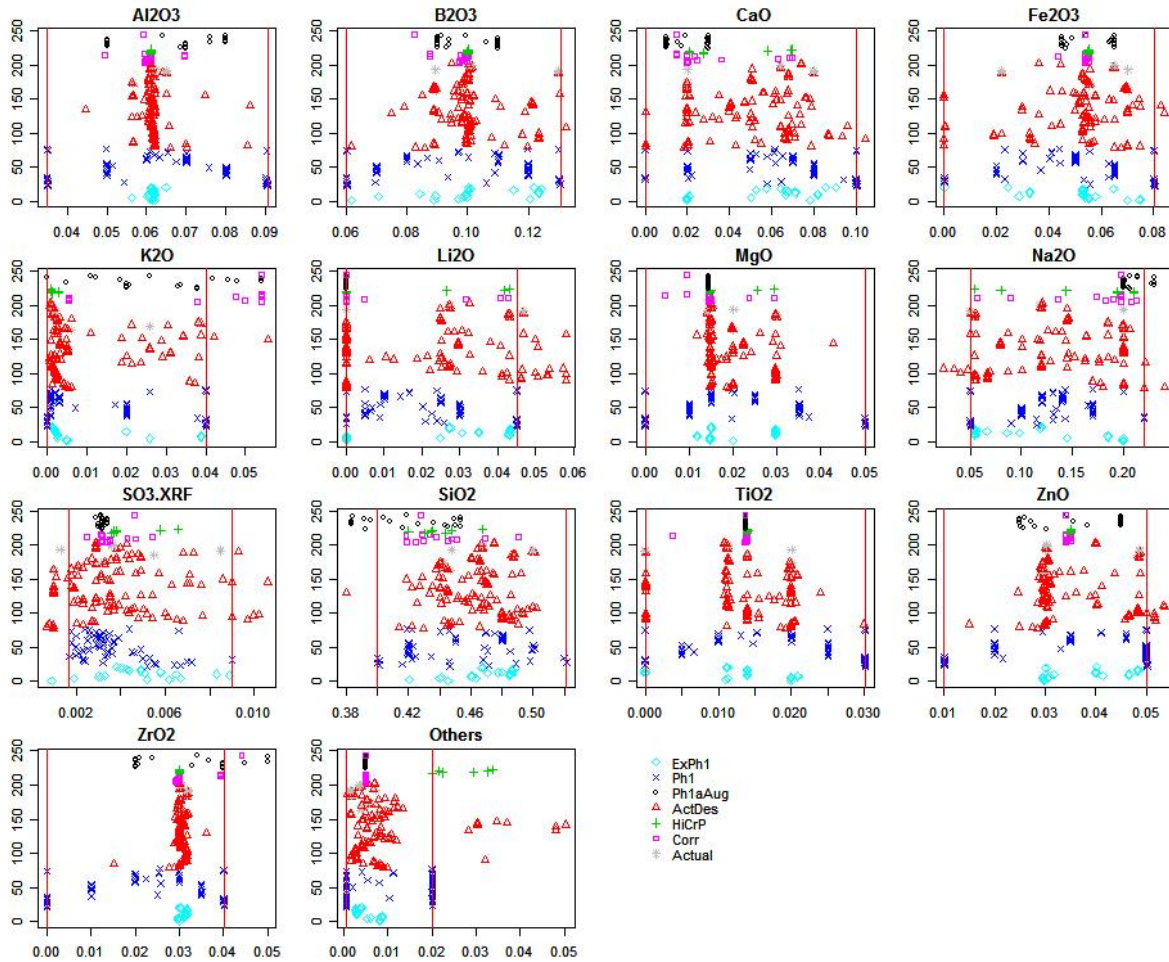


**Figure 5.3. Plots Showing Ranges and Distributions of Values (mass fractions) for 14 Main Components in 244 LAW Glasses Used for PCT Model Development (20 Outliers Excluded). The vertical lines (when present) are the lower and upper limits for each component from the Phase 1 test matrix.**

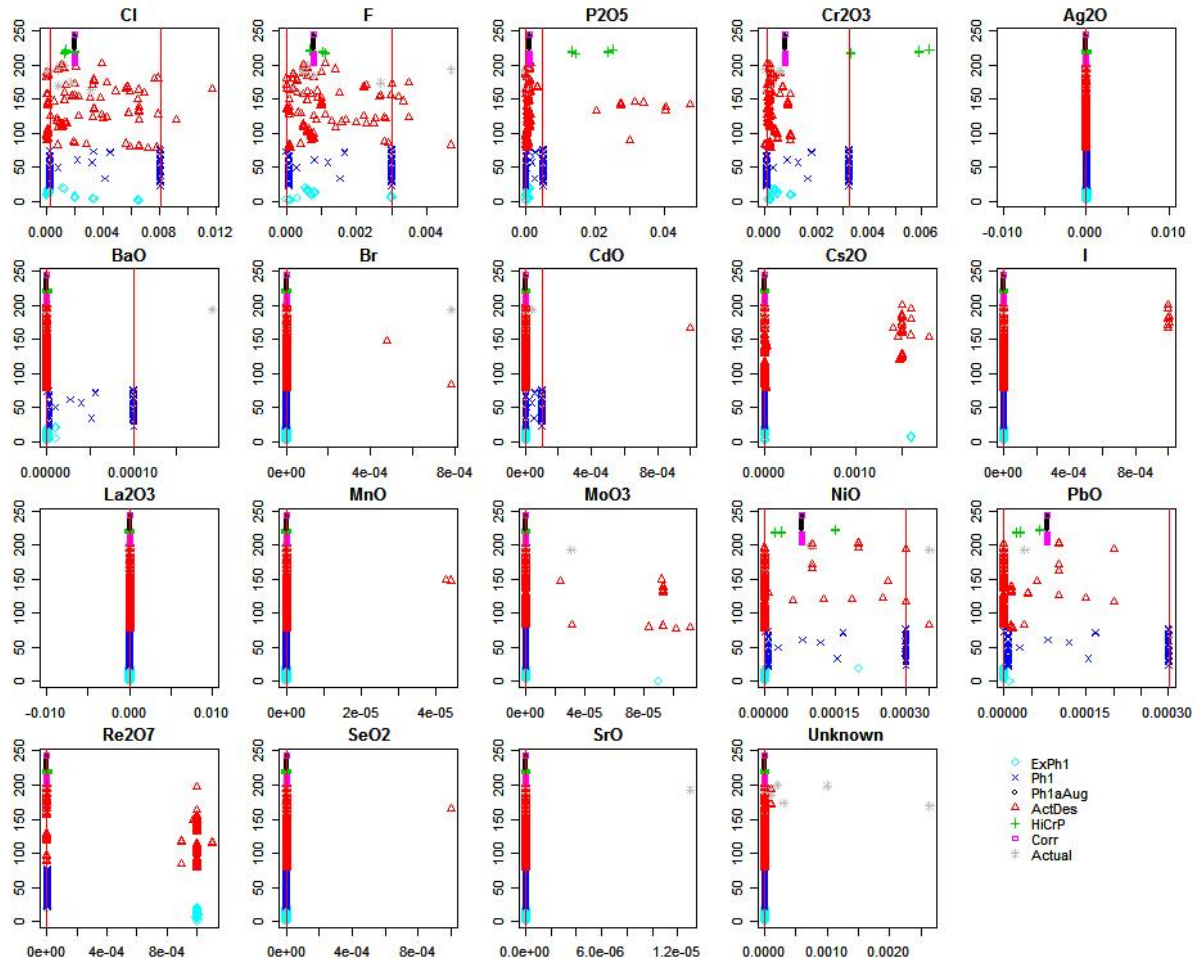


**Figure 5.4. Plots Showing Ranges and Distributions of Values (mass fractions) for 19 Minor Components in 244 LAW Glasses Used for PCT Model Development (20 Outliers Excluded). The vertical lines (when present) are the lower and upper limits for each component from the Phase 1 test matrix.**

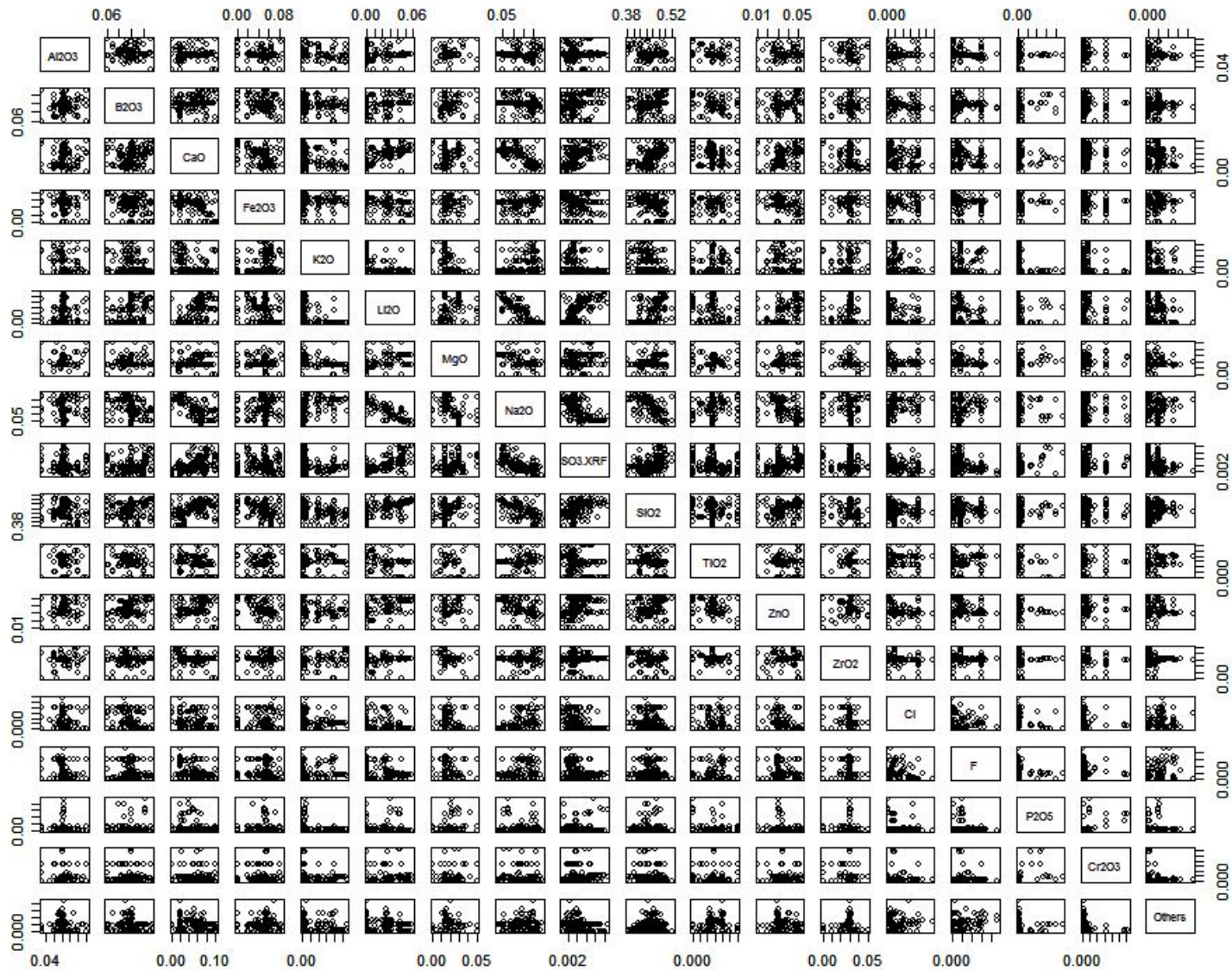
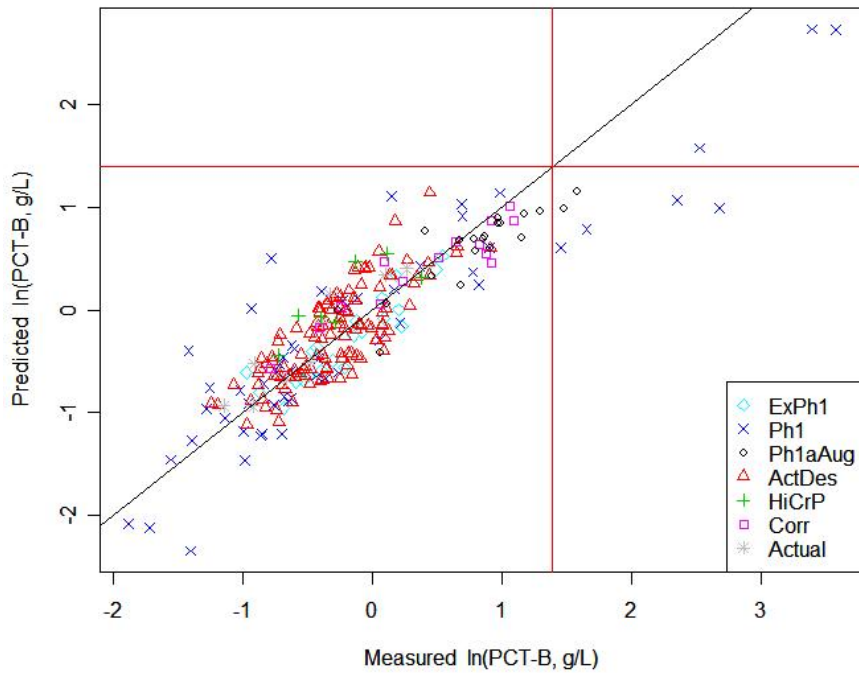
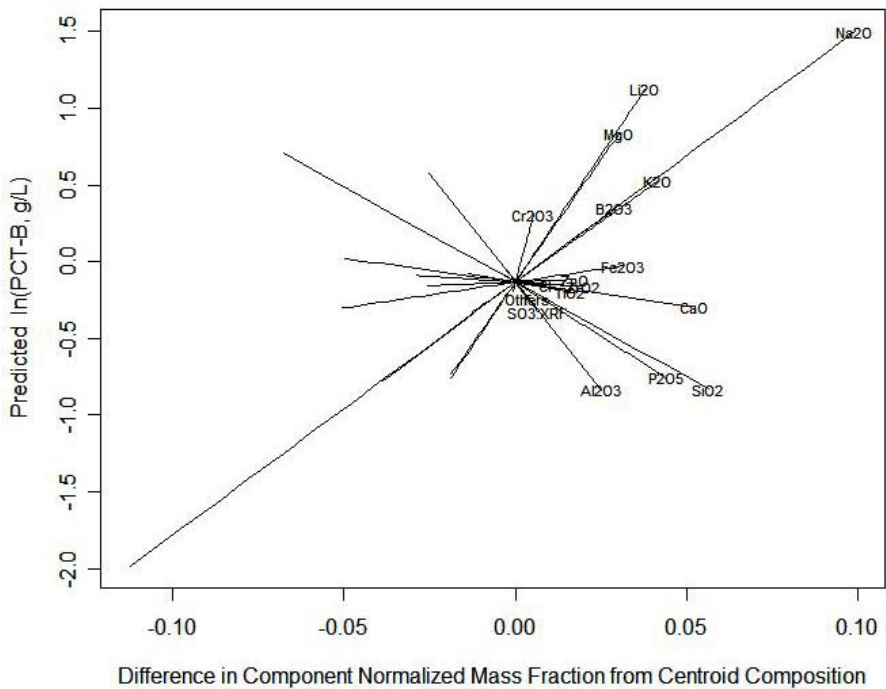


Figure 5.5. Scatterplot Matrix of 18 Components (mass fractions) for 244 LAW Glasses in the PCT Modeling Data Set



**Figure 5.6. Predicted Versus Measured Plot for 18-Component Full Linear Mixture Model on ILAW PCT-B. The red lines represent the WTP contract limit (4 g/L) for PCT-B release.**



**Figure 5.7. Response Trace Plot for 18-Component Full Linear Mixture Model on ILAW PCT-B.**

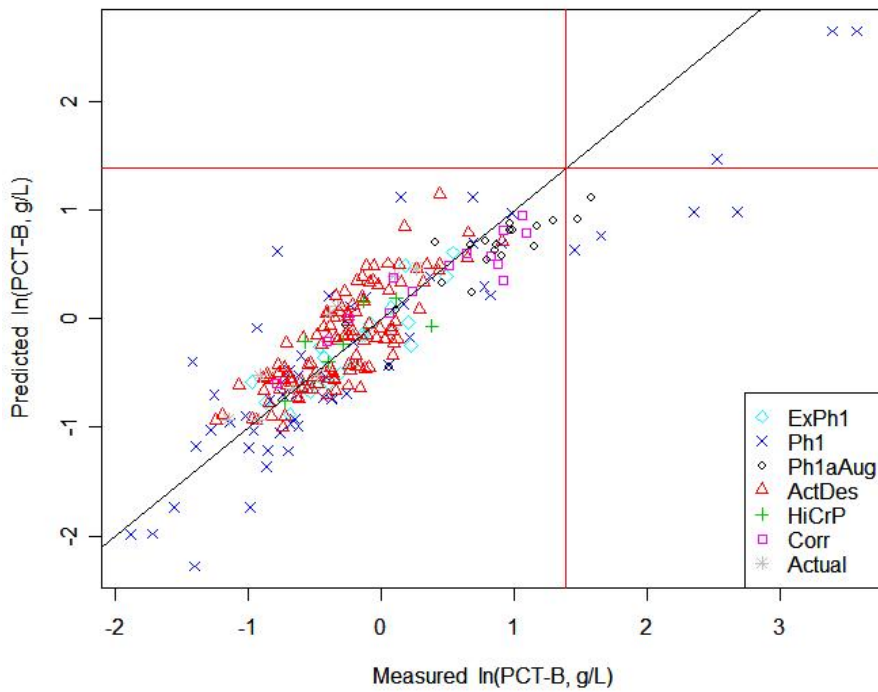


**Figure 5.8. Predicted Versus Measured Plot for 12-Component Reduced Linear Mixture Model on ILAW PCT-B. The red lines represent the WTP contract limit (4 g/L) for PCT-B release.**

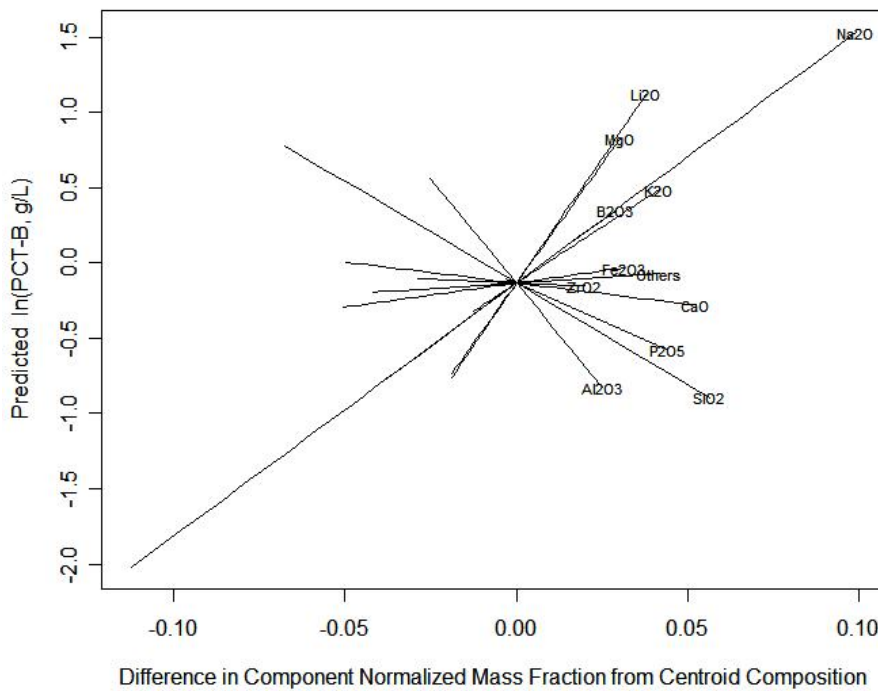


**Figure 5.9. Response Trace Plot for 12-Component Reduced Linear Mixture Model on ILAW PCT-B.**

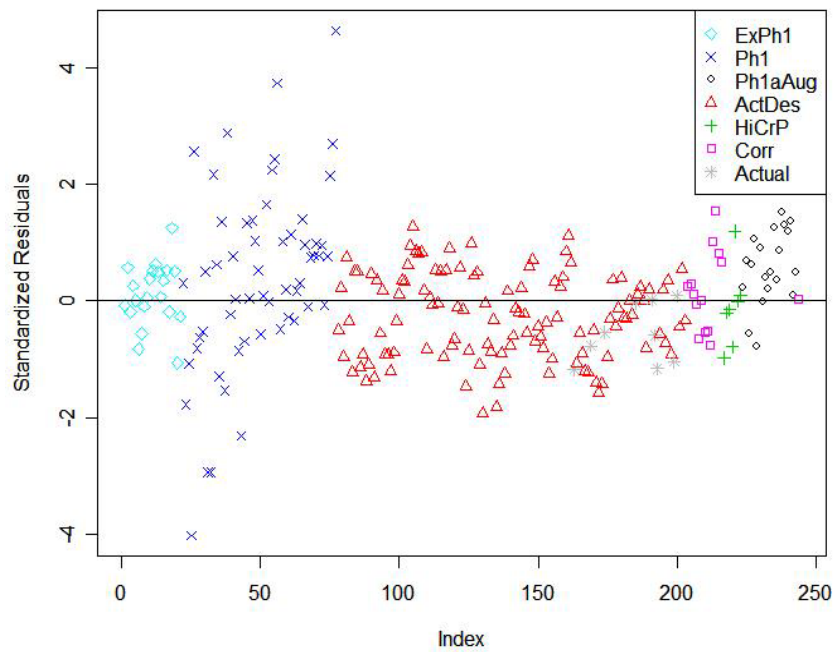


**Figure 5.10. Standardized Residuals Plot for 12-Component Reduced Linear Mixture Model on ILAW PCT-B.**

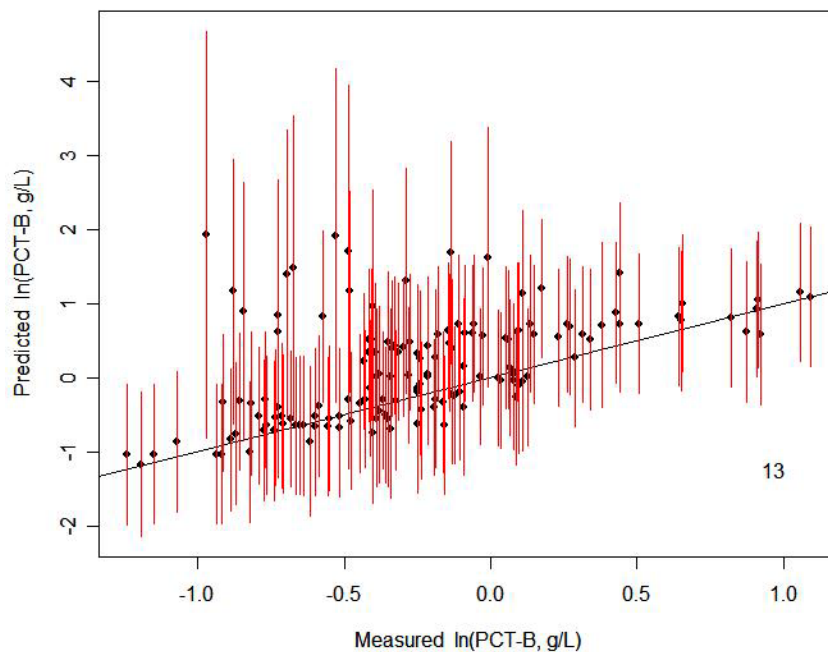


**Figure 5.11. Predicted Versus Measured Plot for 12-Component Reduced Linear Mixture Model on ILAW PCT-B Fitted to Modeling Subset of 97 Glasses and Applied to Validation Subset of 147 Glasses. Error bars are 95% prediction intervals (PIs). The number of glasses whose 95% PIs do not include the measured values (represented by the 45° line) is shown.**

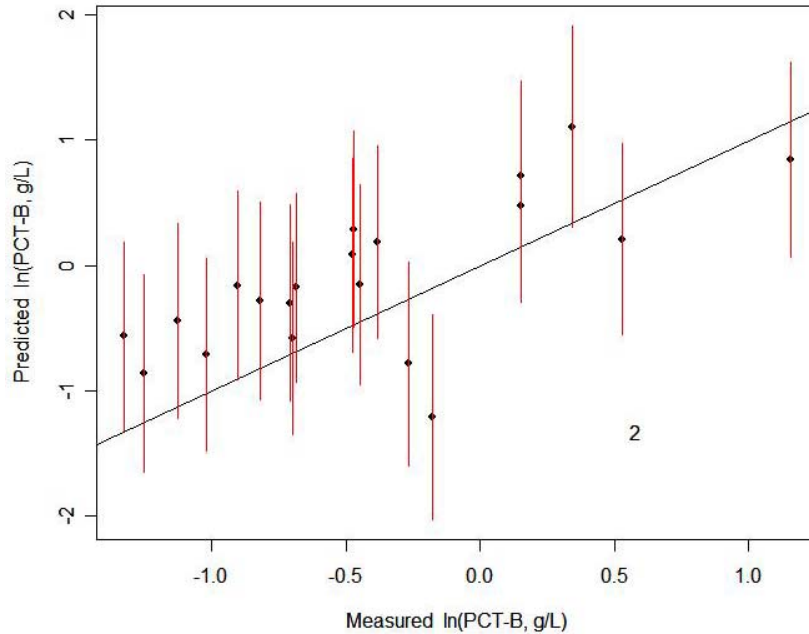


**Figure 5.12. Predicted Versus Measured Plot for 12-Component Reduced Linear Mixture Model on ILAW PCT-B Fitted to 244 Modeling Set Glasses and Applied to 20 Outlying Glasses. Error bars are 95% prediction intervals (PIs). The number of glasses whose 95% PIs do not include the measured values (represented by the 45° line) is shown.**

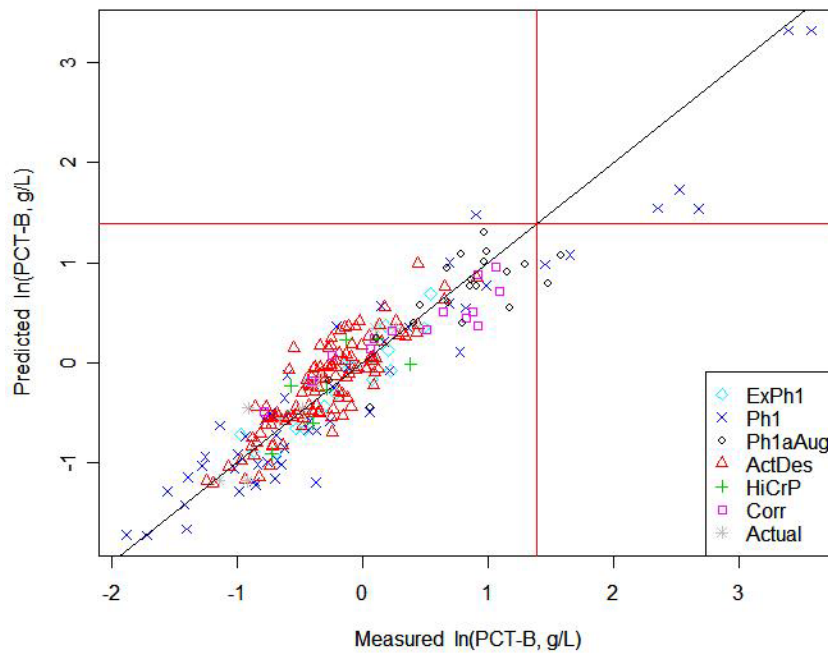


**Figure 5.13. Predicted Versus Measured Plot for 17-Term Reduced Partial Quadratic Mixture Model on ILAW PCT-B. The red lines represent the WTP contract limit (4 g/L) for PCT-B release.**



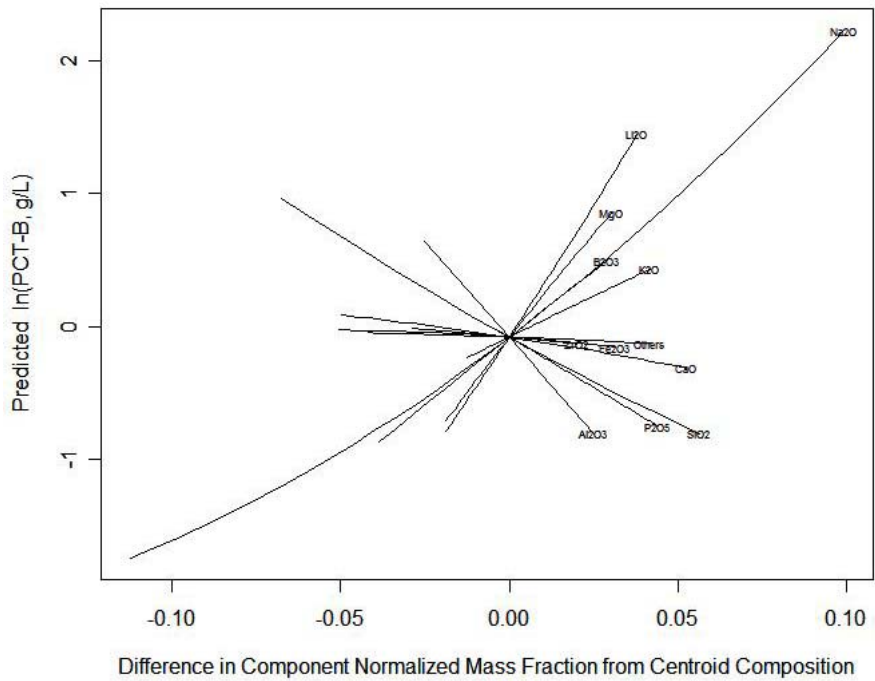


**Figure 5.14. Response Trace Plot for 17-Term Reduced Partial Quadratic Mixture Model on ILAW PCT-B.**

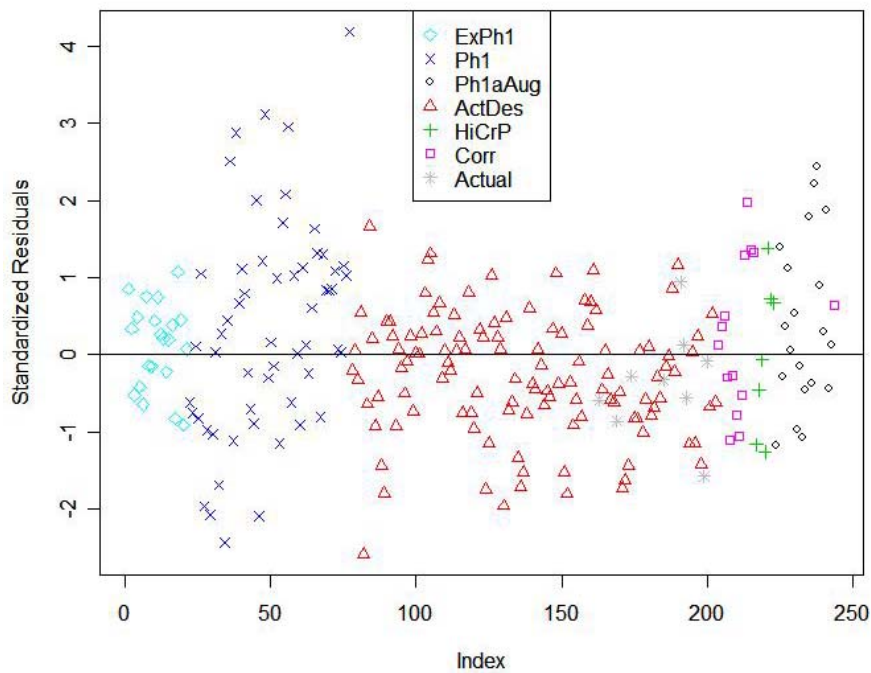


**Figure 5.15. Standardized Residuals Plot for 17-Term Reduced Partial Quadratic Mixture Model on ILAW PCT-B.**

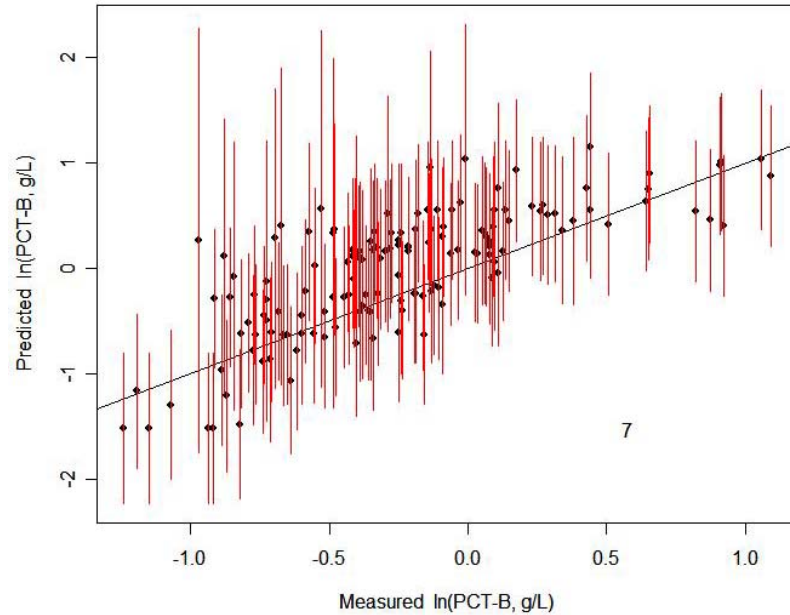


**Figure 5.16. Predicted Versus Measured Plot for 17-Term Reduced Partial Quadratic Mixture Model on ILAW PCT-B Fitted to Modeling Subset of 97 Glasses and Applied to Validation Subset of 147 Glasses. Error bars are 95% prediction intervals (PIs). The number of glasses whose 95% PIs do not include the measured values (represented by the 45° line) is shown.**

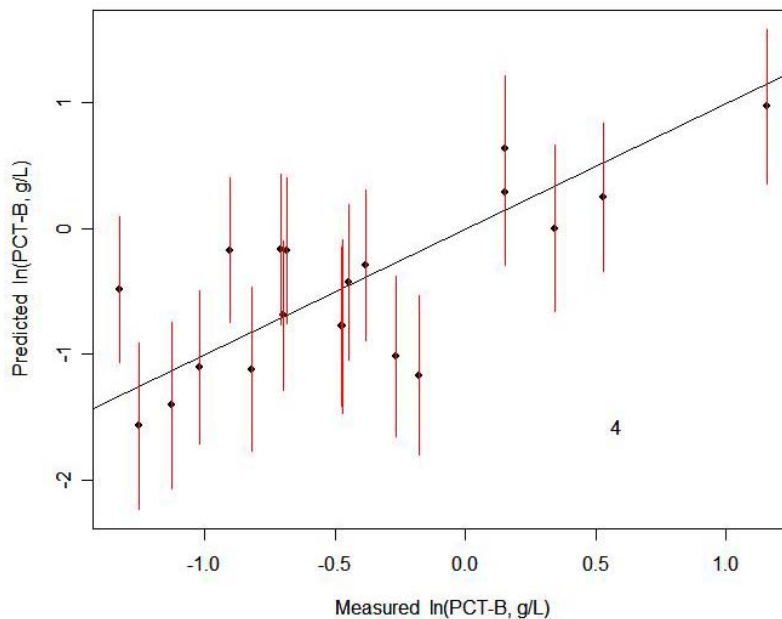


**Figure 5.17. Predicted Versus Measured Plot for 17-Term Reduced Partial Quadratic Mixture Model on ILAW PCT-B Fitted to 244 Modeling Set Glasses and Applied to 20 Outlying Glasses. Error bars are 95% prediction intervals (PIs). The number of glasses whose 95% PIs do not include the measured values (represented by the 45° line) is shown.**

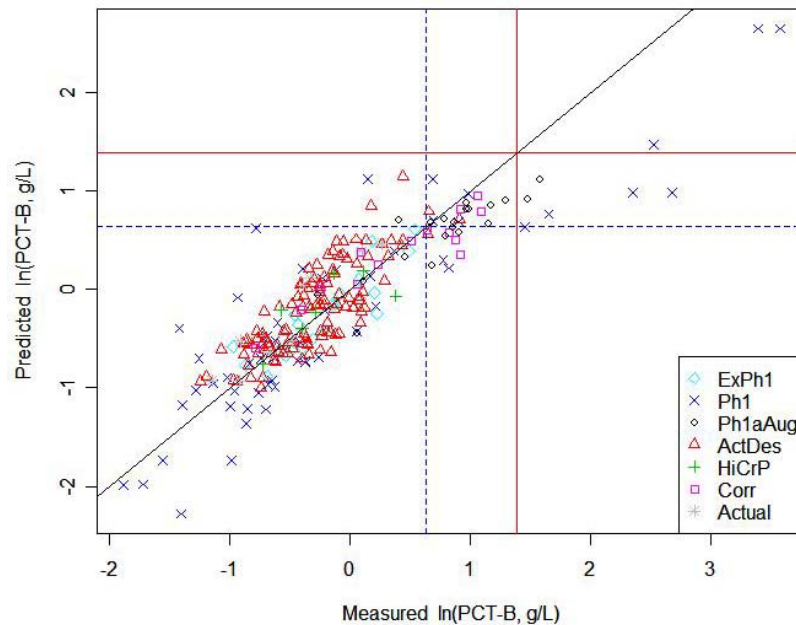


**Figure 5.18. Predicted Versus Measured Plot for 12-Term Reduced Linear Mixture Model on ILAW PCT-B Fitted to 244 Modeling Glasses. The WTP contract limit (4 g/L) is shown with solid red lines and the cutoff value (1.89 g/L) for the two-part reduced linear mixture model is shown with dashed blue lines.**

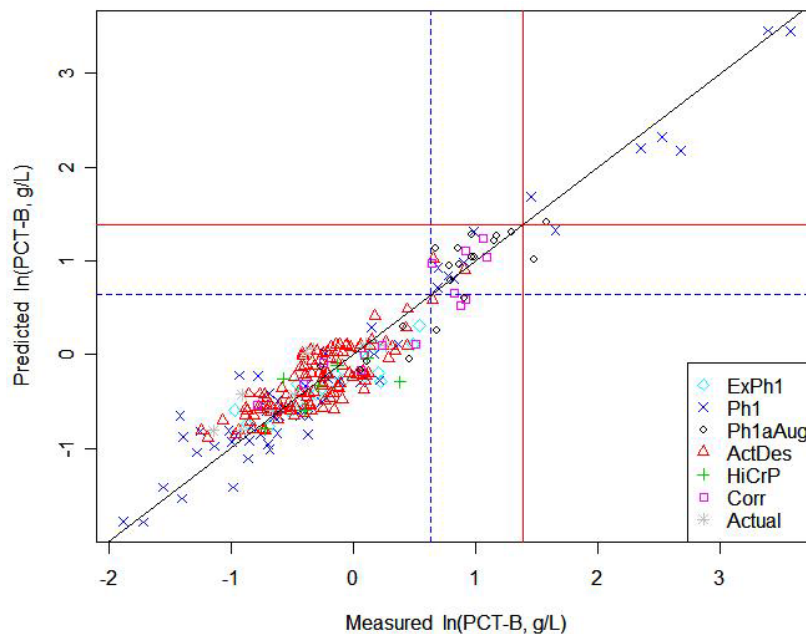


**Figure 5.19. Predicted Versus Measured Plot for 24-Term Two-Part Reduced Linear Mixture Model on ILAW PCT-B Fitted to 244 Modeling Glasses. The WTP contract limit (4 g/L) is shown with solid red lines and the cutoff value (1.89 g/L) for the two-part linear mixture model is shown with dashed blue lines.**

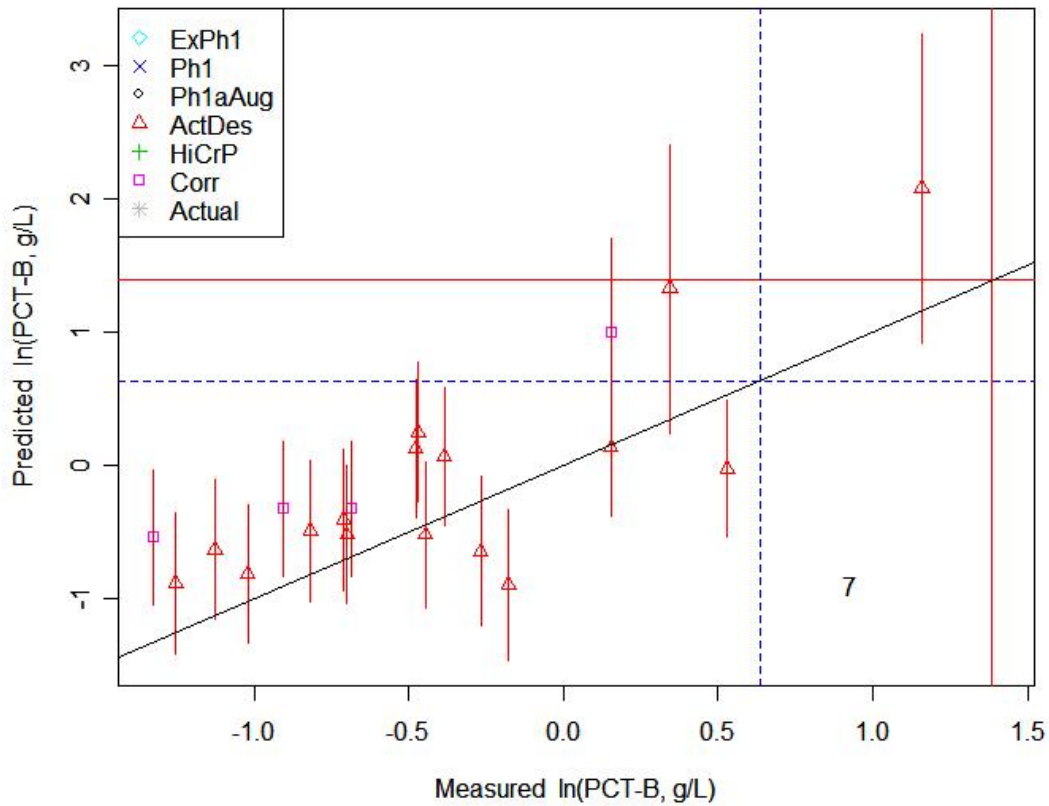


**Figure 5.20. Predicted Versus Measured Plot for 24-Term Two-Part Reduced Linear Mixture Model on ILAW PCT-B Fitted to 244 Modeling Set Glasses and Applied to 20 Outlying Glasses. The WTP contract limit (4 g/L) is shown with solid red lines and the cutoff value (1.89 g/L) for the two-part model is shown with dashed blue lines. Error bars are 95% prediction intervals (PIs). The number of glasses whose 95% PIs do not include the measured values (represented by the 45° line) is shown.**

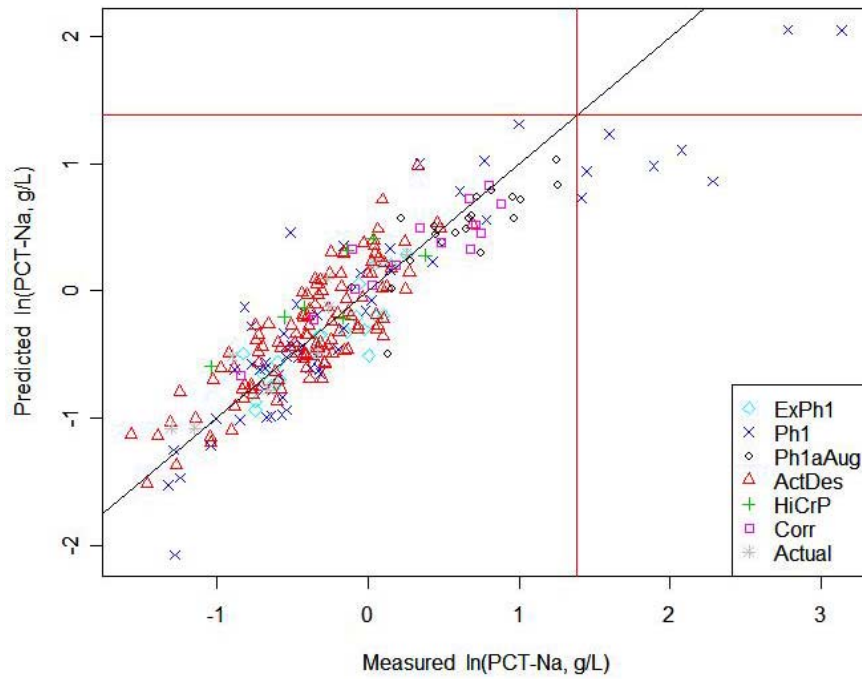


**Figure 5.21. Predicted Versus Measured Plot for 18-Component Full Linear Mixture Model on ILAW PCT-Na. The red lines represent the WTP contract limit (4 g/L) for PCT-Na release.**

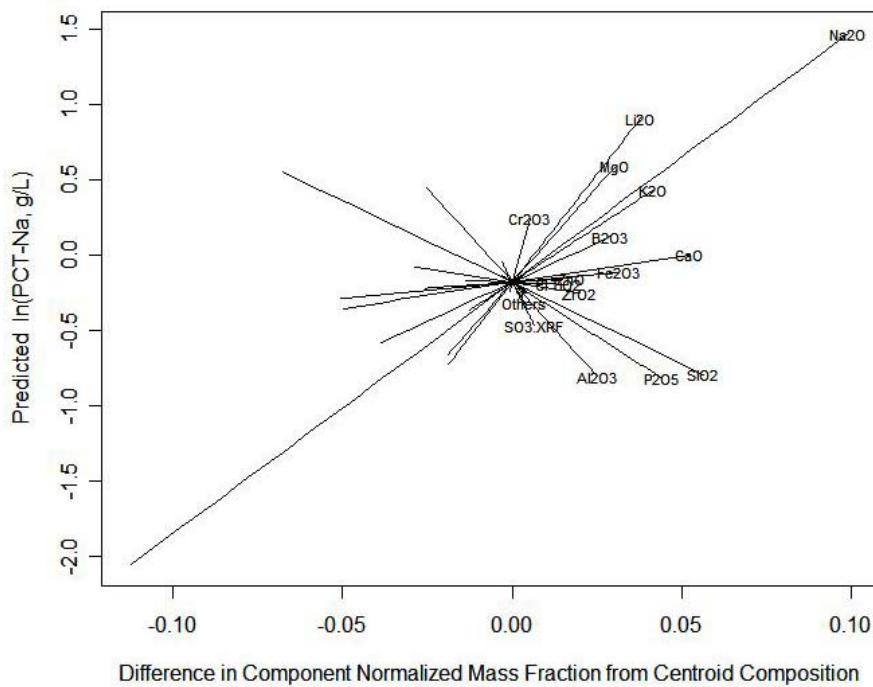


**Figure 5.22. Response Trace Plot for 18-Component Full Linear Mixture Model on ILAW PCT-Na.**

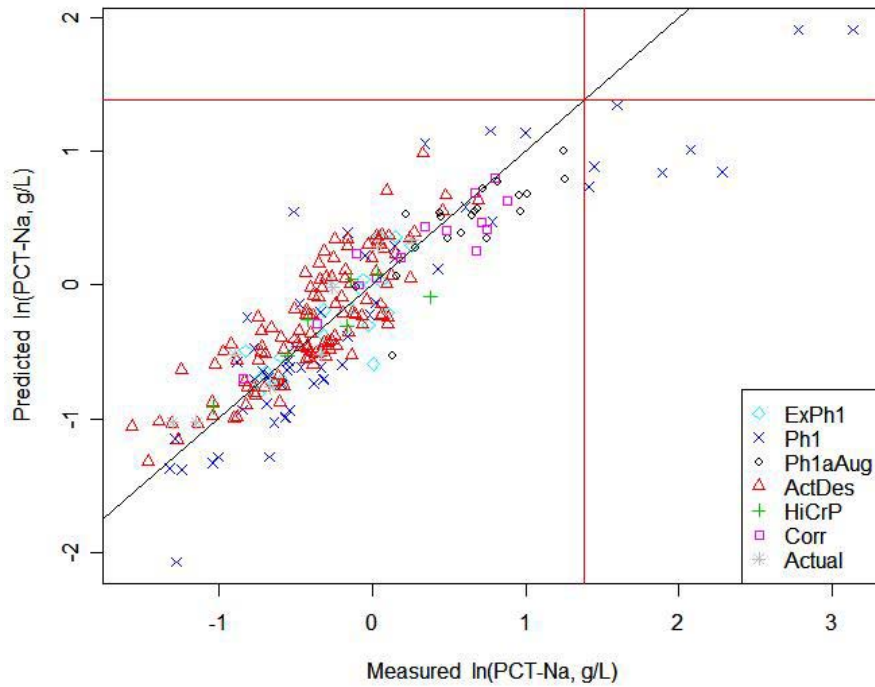


**Figure 5.23. Predicted Versus Measured Plot for 12-Component Reduced Linear Mixture Model on ILAW PCT-Na. The red lines represent the WTP contract limit (4 g/L) for PCT-Na release.**

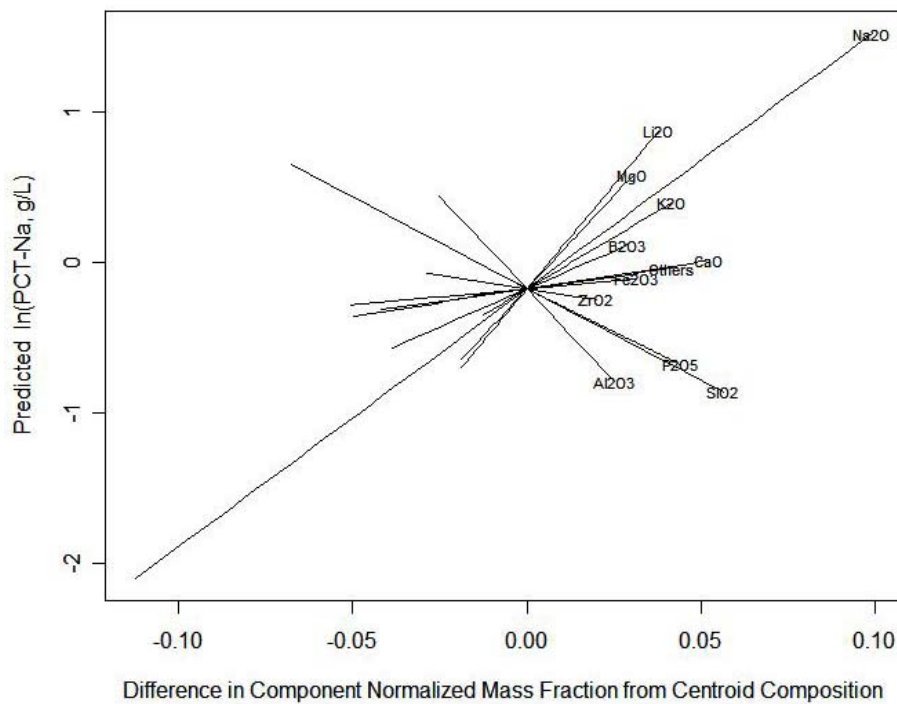


**Figure 5.24. Response Trace Plot for 12-Component Reduced Linear Mixture Model on ILAW PCT-Na.**

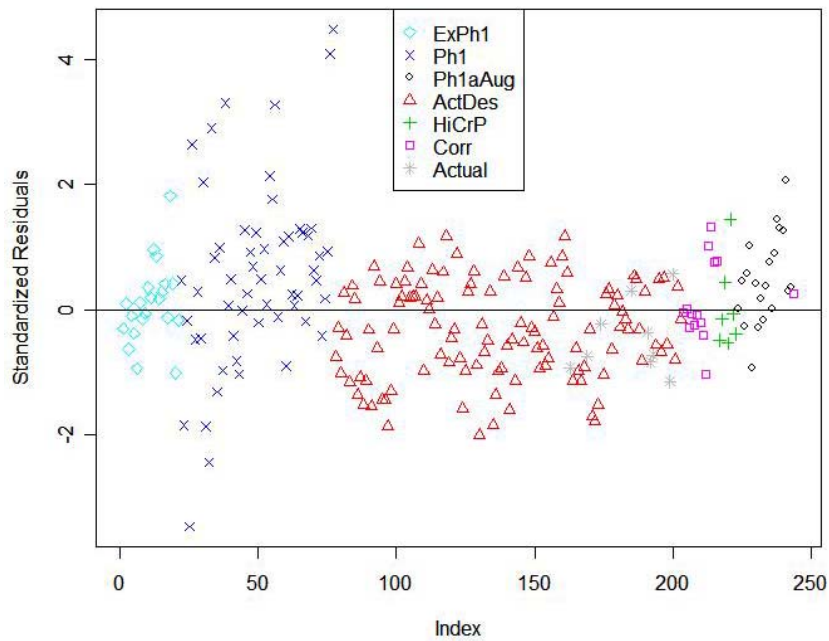


**Figure 5.25. Standardized Residuals Plot for 12-Component Reduced Linear Mixture Model on ILAW PCT-Na.**

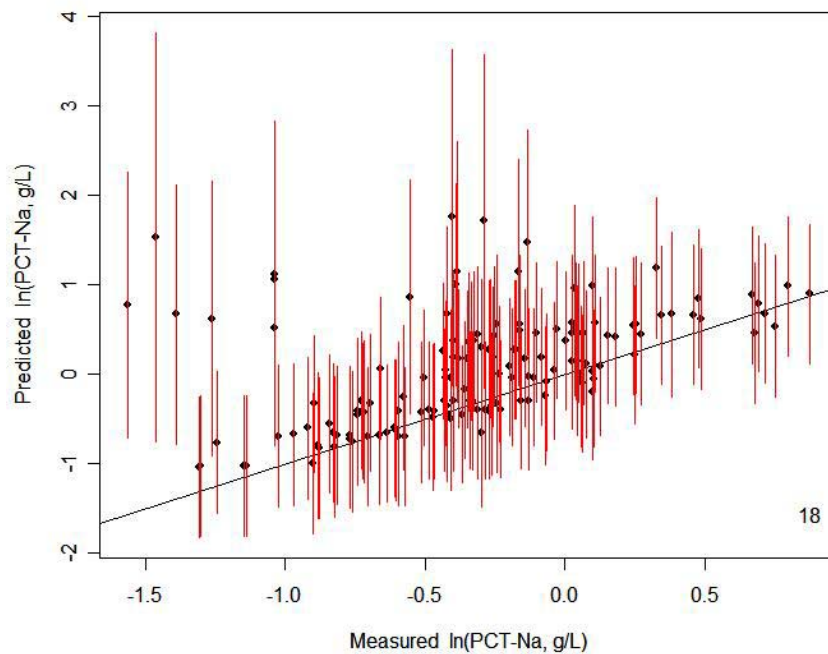


**Figure 5.26. Predicted Versus Measured Plot for 12-Component Reduced Linear Mixture Model on ILAW PCT-Na Fitted to Modeling Subset of 97 Glasses and Applied to Validation Subset of 147 Glasses. Error bars are 95% prediction intervals (PIs). The number of glasses whose 95% PIs do not include the measured values (represented by the 45° line) is shown.**

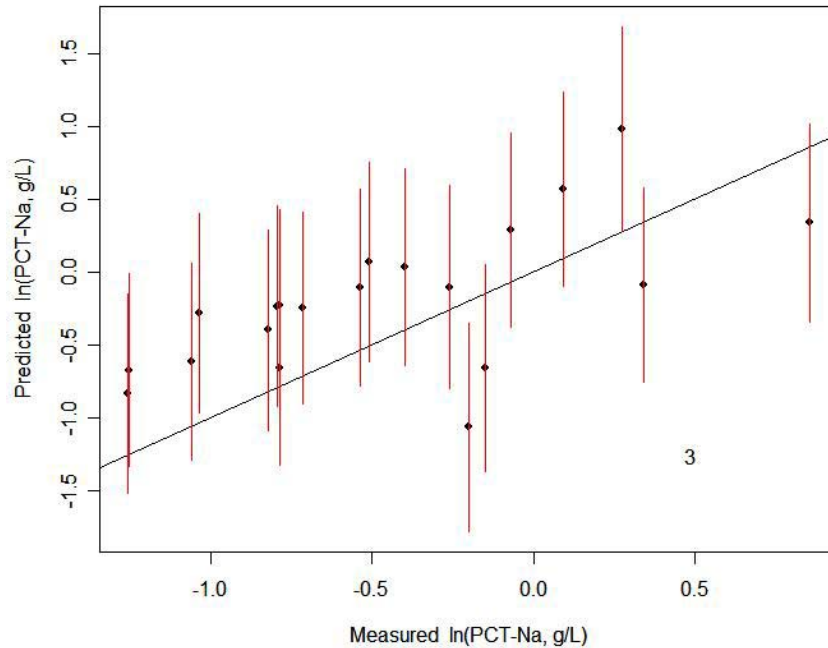


**Figure 5.27. Predicted Versus Measured Plot for 12-Component Reduced Linear Mixture Model on ILAW PCT-Na Fitted to 244 Modeling Set Glasses and Applied to 20 Outlying Glasses. Error bars are 95% prediction intervals (PIs). The number of glasses whose 95% PIs do not include the measured values (represented by the 45° line) is shown.**

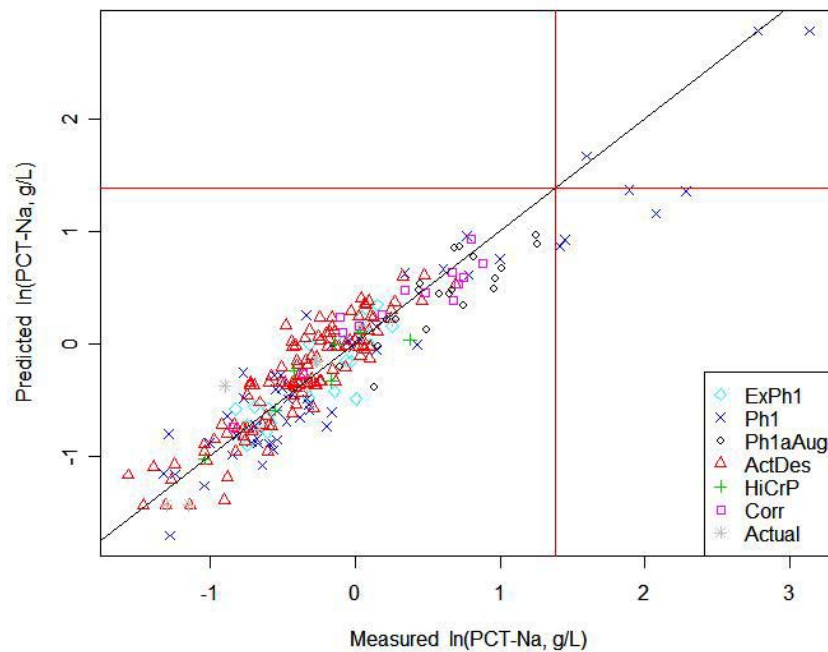


**Figure 5.28. Predicted Versus Measured Plot for 17-Term Reduced Partial Quadratic Mixture Model on ILAW PCT-Na. The red lines represent the WTP contract limit (4 g/L) for PCT-Na release.**



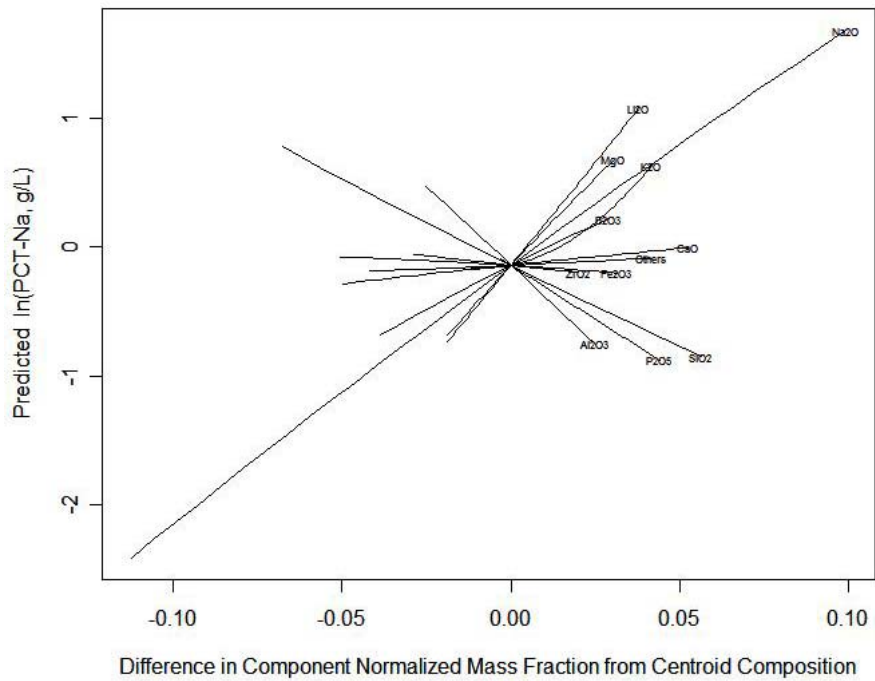


**Figure 5.29. Response Trace Plot for 17-Term Reduced Partial Quadratic Mixture Model on ILAW PCT-Na.**

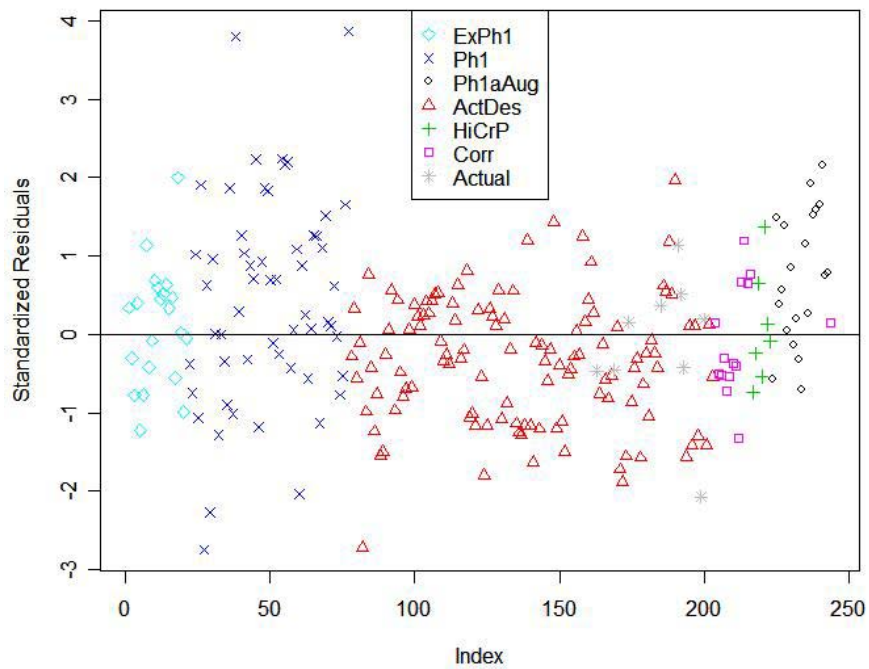


**Figure 5.30. Standardized Residuals Plot for 17-Term Reduced Partial Quadratic Mixture Model on ILAW PCT-Na.**

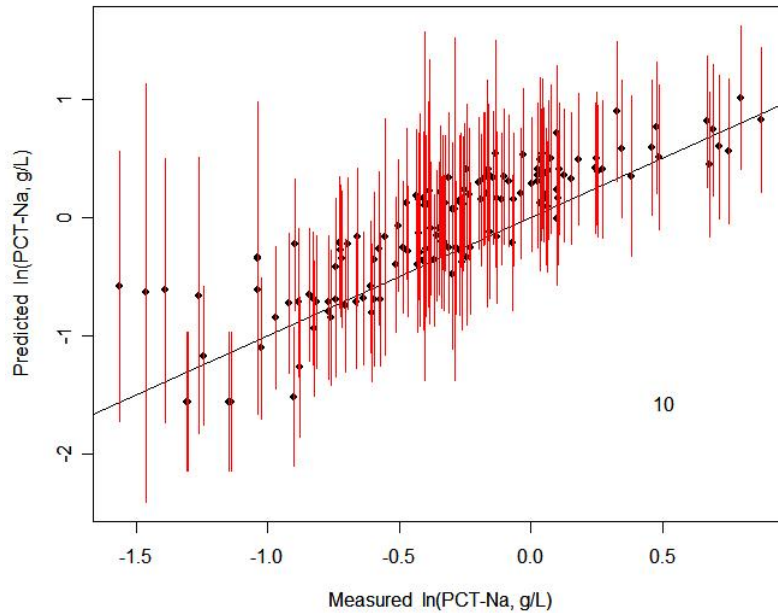


**Figure 5.31. Predicted Versus Measured Plot for 17-Term Reduced Partial Quadratic Mixture Model on ILAW PCT-Na Fitted to Modeling Subset of 97 Glasses and Applied to Validation Subset of 147 Glasses. Error bars are 95% prediction intervals (PIs). The number of glasses whose 95% PIs do not include the measured values (represented by the 45° line) is shown.**

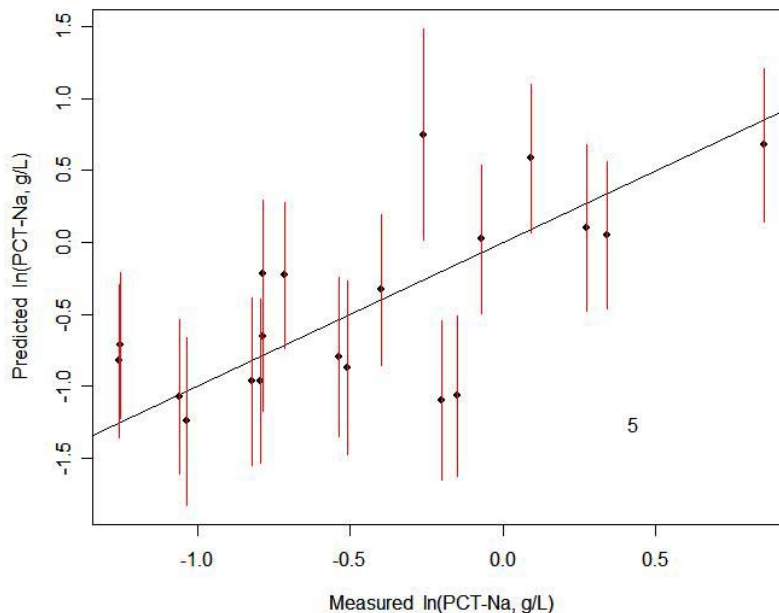


**Figure 5.32. Predicted Versus Measured Plot for 17-Term Reduced Partial Quadratic Mixture Model on ILAW PCT-Na Fitted to 244 Modeling Set Glasses and Applied to 20 Outlying Glasses. Error bars are 95% prediction intervals (PIs). The number of glasses whose 95% PIs do not include the measured values (represented by the 45° line) is shown.**

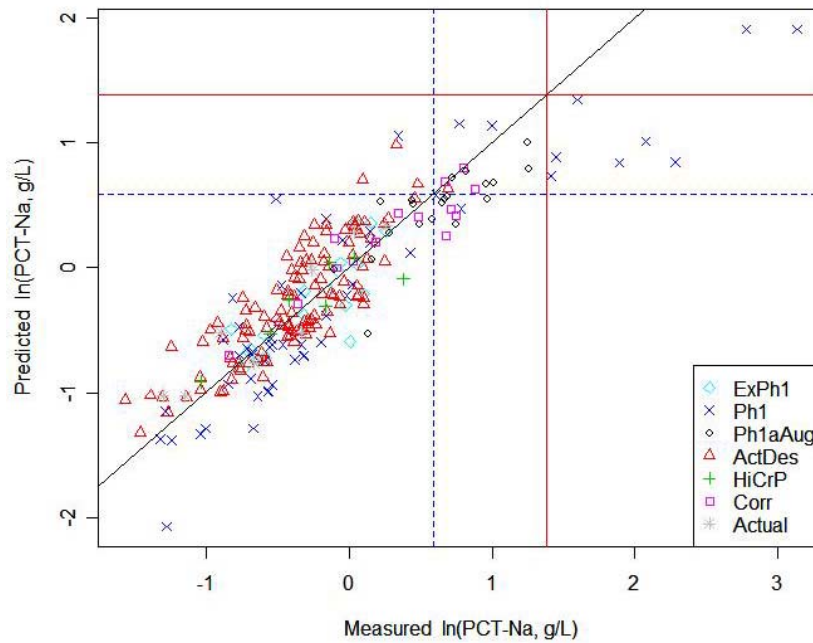


**Figure 5.33. Predicted Versus Measured Plot for 12-Component Reduced Linear Mixture Model on ILAW PCT-Na Fitted to 244 Modeling Glasses. The WTP contract limit (4 g/L) is shown with solid red lines and the cutoff value (1.80 g/L) for the two-part reduced linear mixture model is shown with dashed blue lines.**

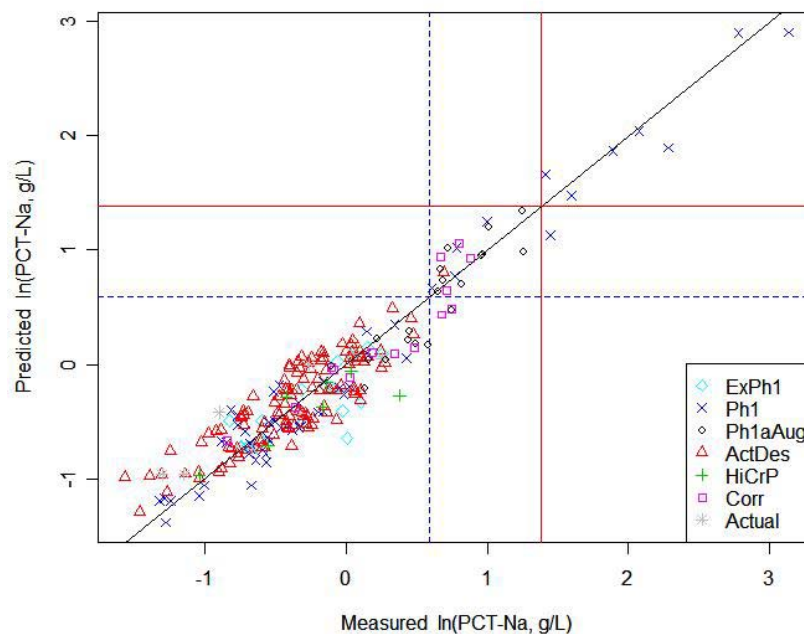


**Figure 5.34. Predicted Versus Measured Plot for 24-Term Two-Part Reduced Linear Mixture Model on ILAW PCT-Na Fitted to 244 Modeling Glasses. The WTP contract limit (4 g/L) is shown with solid red lines and the cutoff value (1.80 g/L) for the two-part linear mixture model is shown with dashed blue lines.**

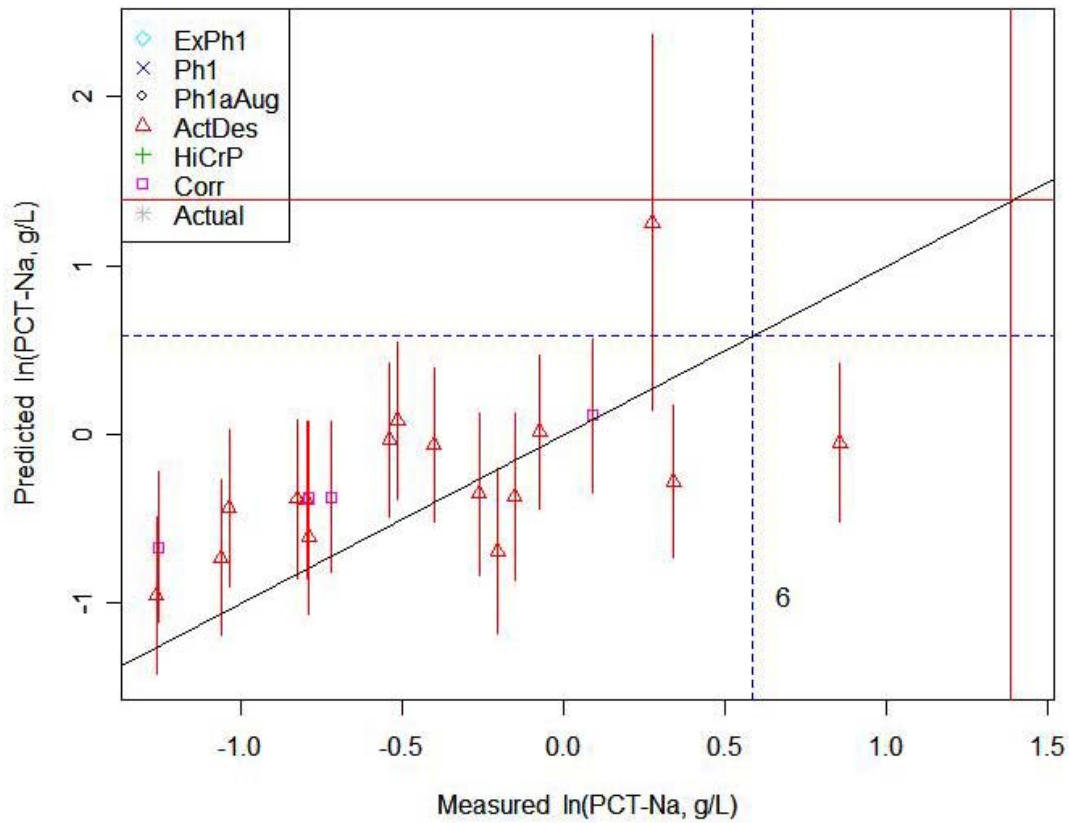


**Figure 5.35. Predicted Versus Measured Plot for 24-Term Two-Part Reduced Linear Mixture Model on ILAW PCT-Na Fitted to 244 Modeling Set Glasses and Applied to 20 Outlying Glasses. The WTP contract limit (4 g/L) is shown with solid red lines and the cutoff value (1.80 g/L) for the two-part linear mixture model is shown with dashed blue lines. Error bars are 95% prediction intervals (PIs). The number of glasses whose 95% PIs do not include the measured values (represented by the 45° line) is shown.**

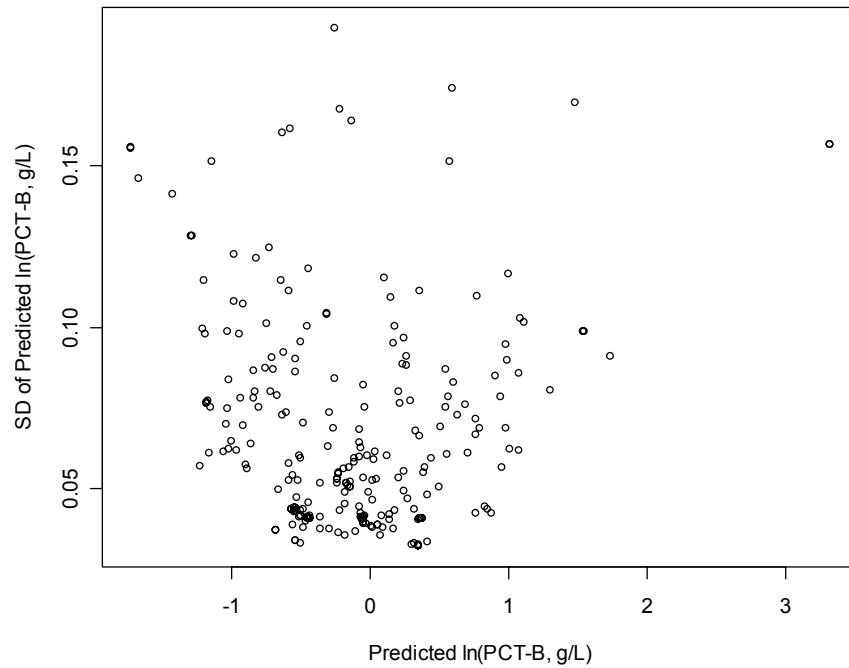


**Figure 5.36. Prediction Standard Deviations versus Predicted Values over the LAW Glass Compositions in the Modeling Dataset for the Recommended 17-Term PQM Model on PCT-B.**

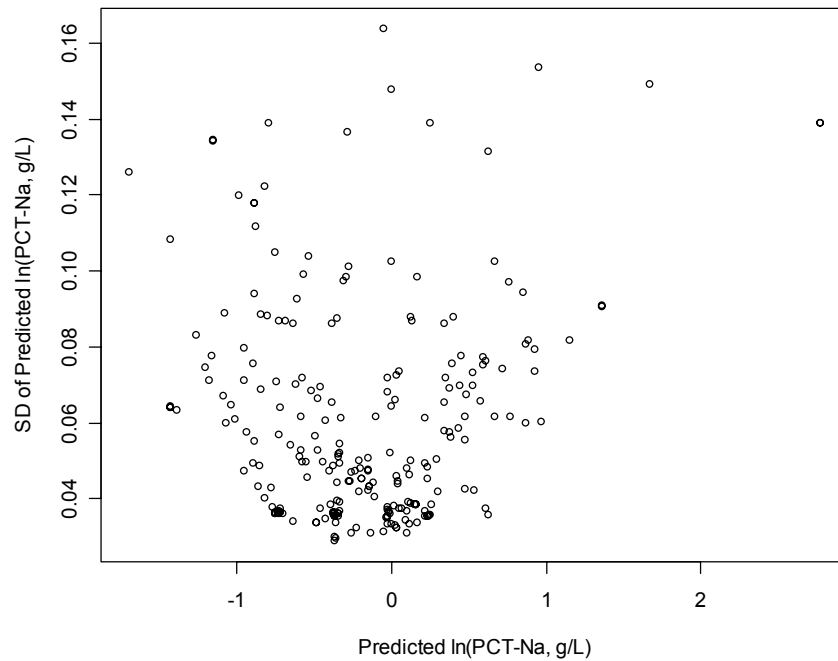


**Figure 5.37. Prediction Standard Deviations versus Predicted Values over the LAW Glass Compositions in the Modeling Dataset for the Recommended 17-Term PQM Model on PCT-Na.**

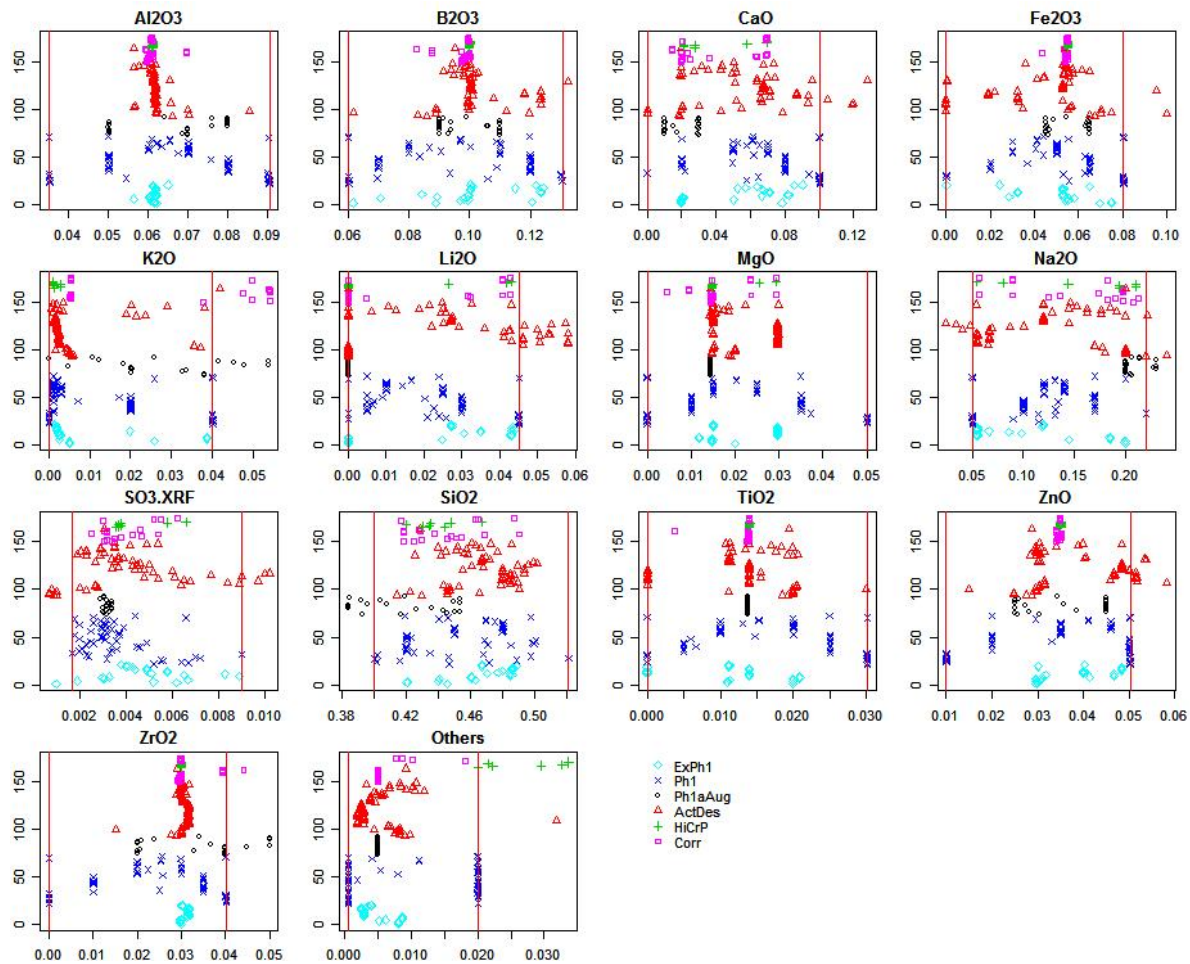


**Figure 6.1. Plots Showing Ranges and Distributions of Values (mass fractions) for 14 Main Components in 175 LAW Glasses with VHT Data. The six glasses with “greater than” VHT alteration depths are excluded. The vertical lines (when present) are the lower and upper limits for each component from the Phase 1 test matrix.**

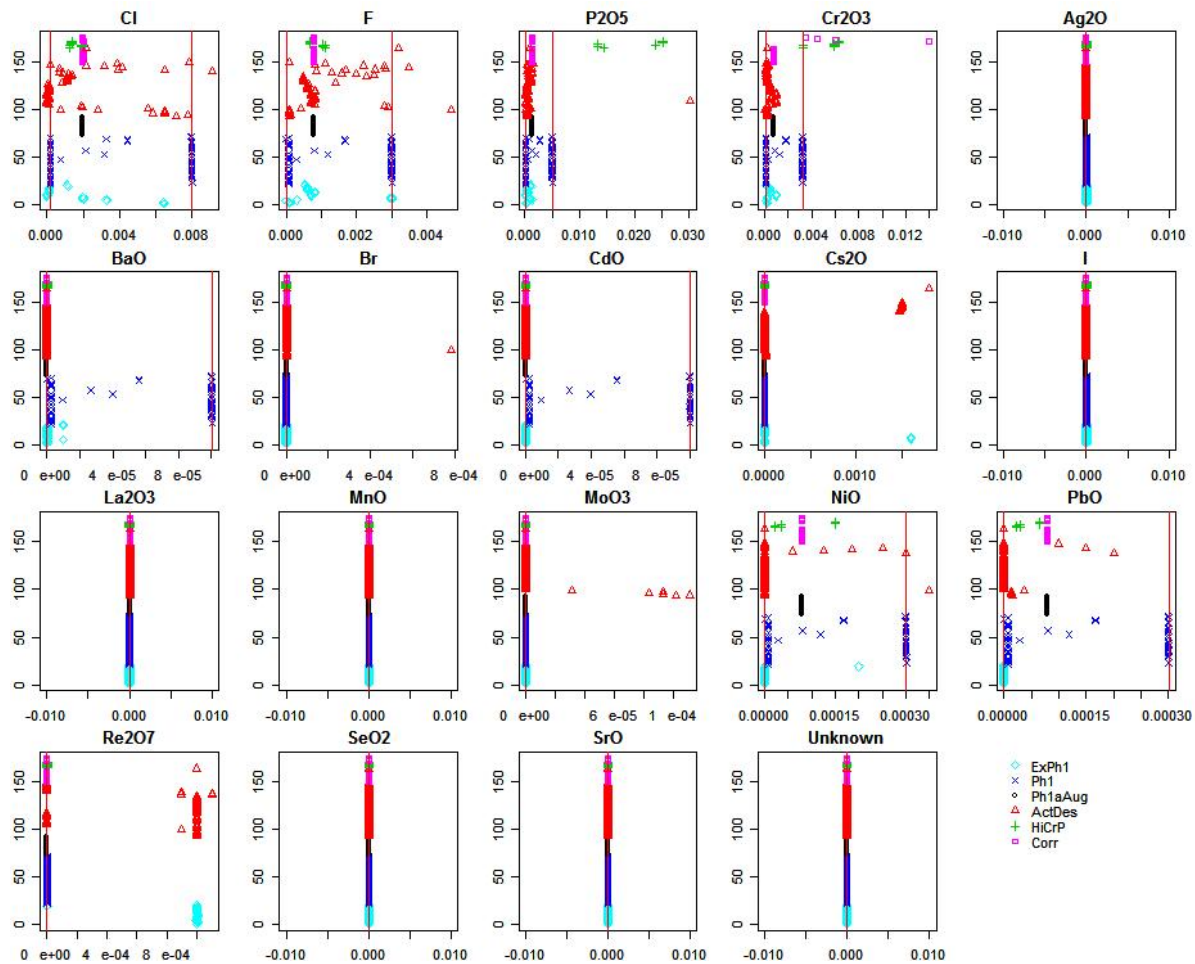


**Figure 6.2. Plots Showing Ranges and Distributions of Values (mass fractions) for 19 Minor Components in 175 LAW Glasses with VHT Data. The six glasses with “greater than” VHT alteration depths are excluded. The vertical lines (when present) are the lower and upper limits for each component from the Phase 1 test matrix.**

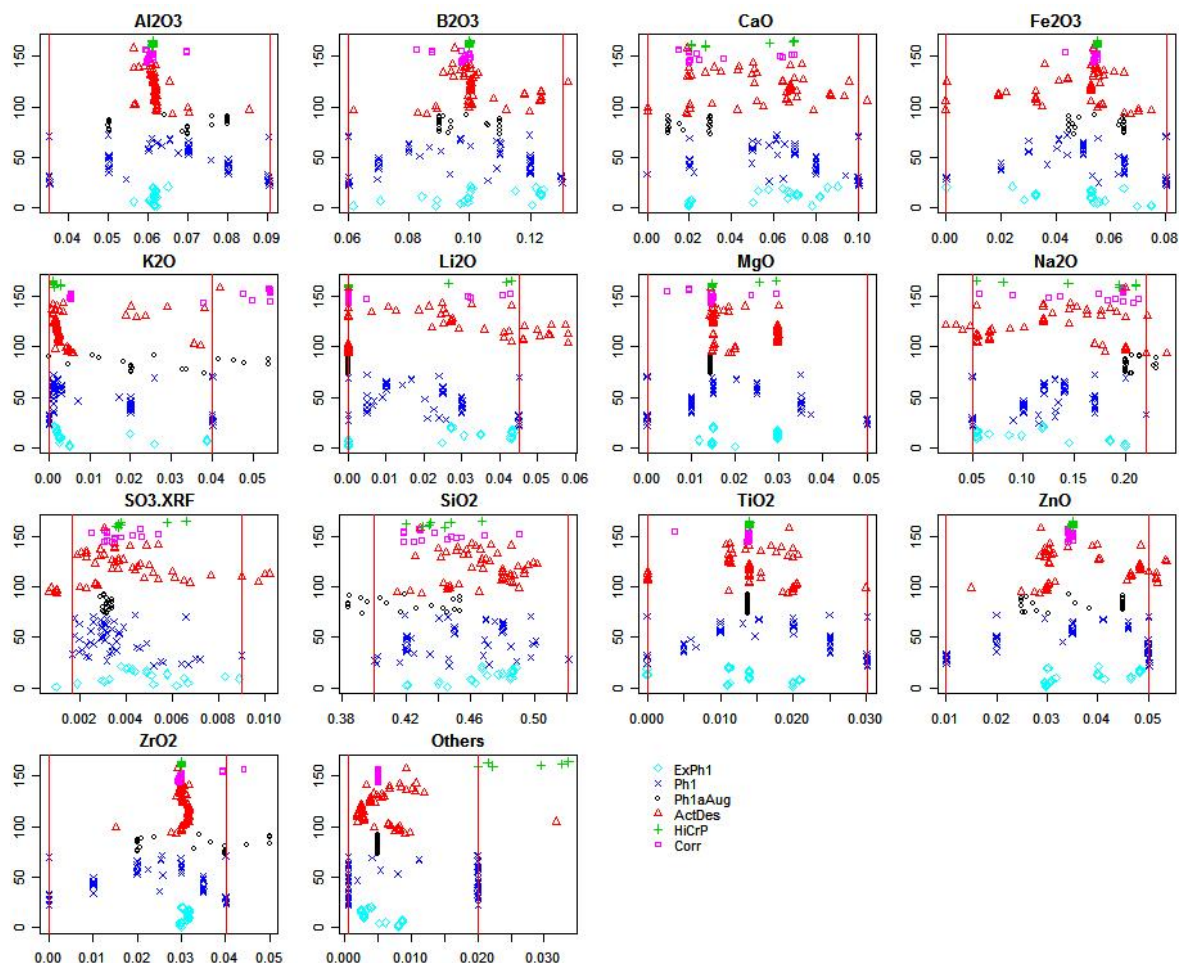


**Figure 6.3. Plots Showing Ranges and Distributions of Values (mass fractions) for 14 Main Components in 165 LAW Glasses Used for VHT Model Development (10 Outliers Excluded). The vertical lines (when present) are the lower and upper limits for each component from the Phase 1 test matrix.**



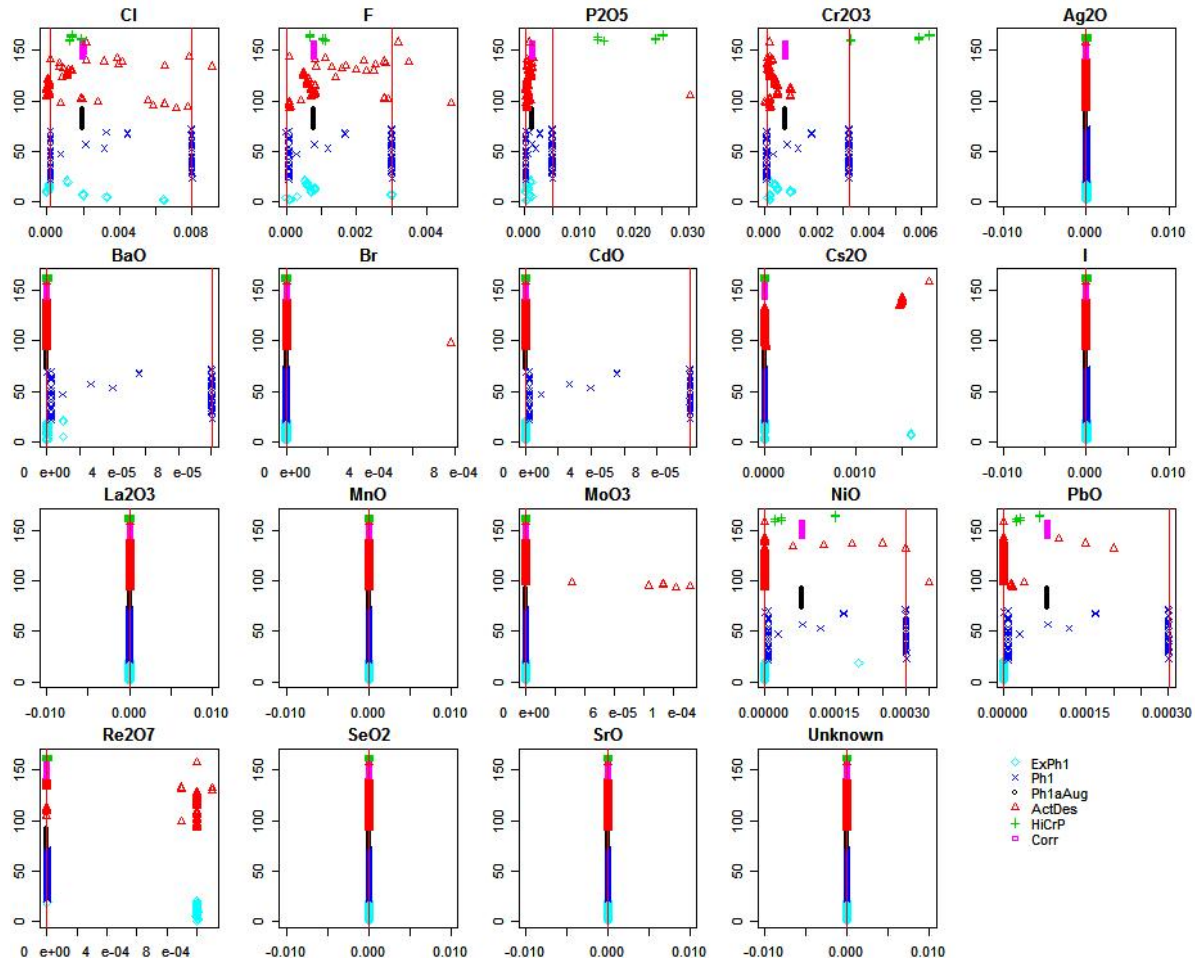


**Figure 6.4. Plots Showing Ranges and Distributions of Values (mass fractions) for 19 Minor Components in 165 LAW Glasses Used for VHT Model Development (10 Outliers Excluded). The vertical lines (when present) are the lower and upper limits for each component from the Phase 1 test matrix.**

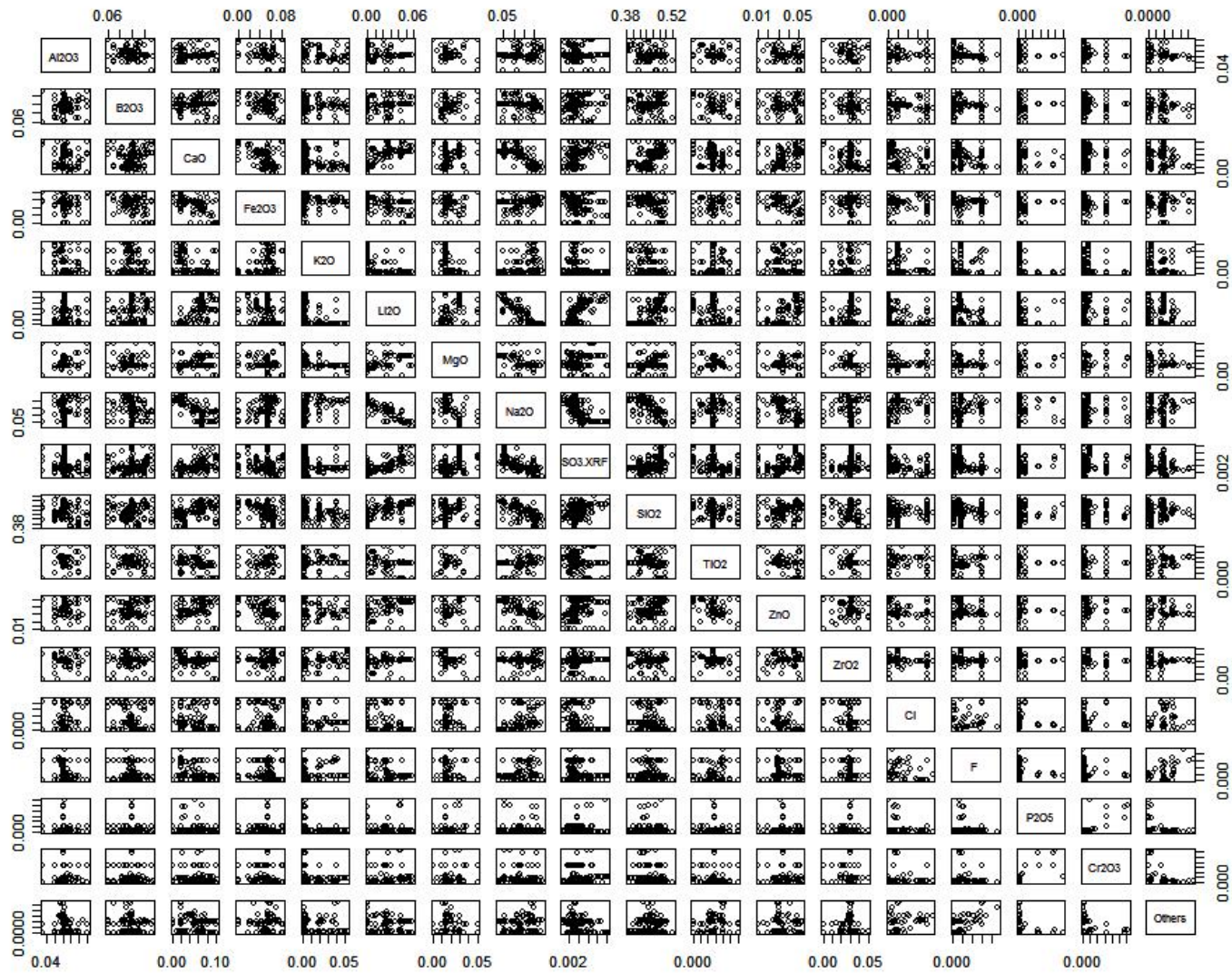
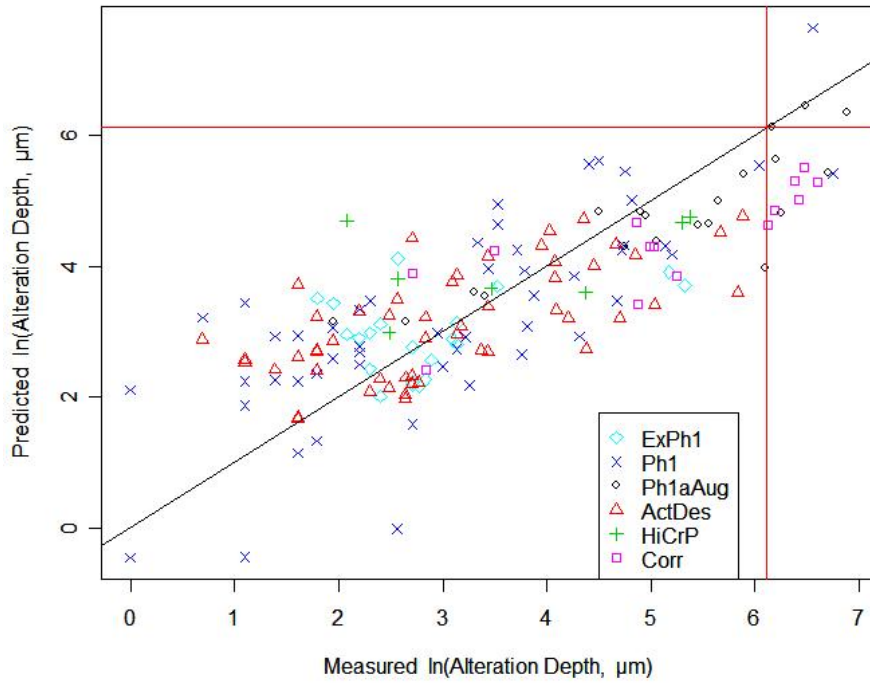
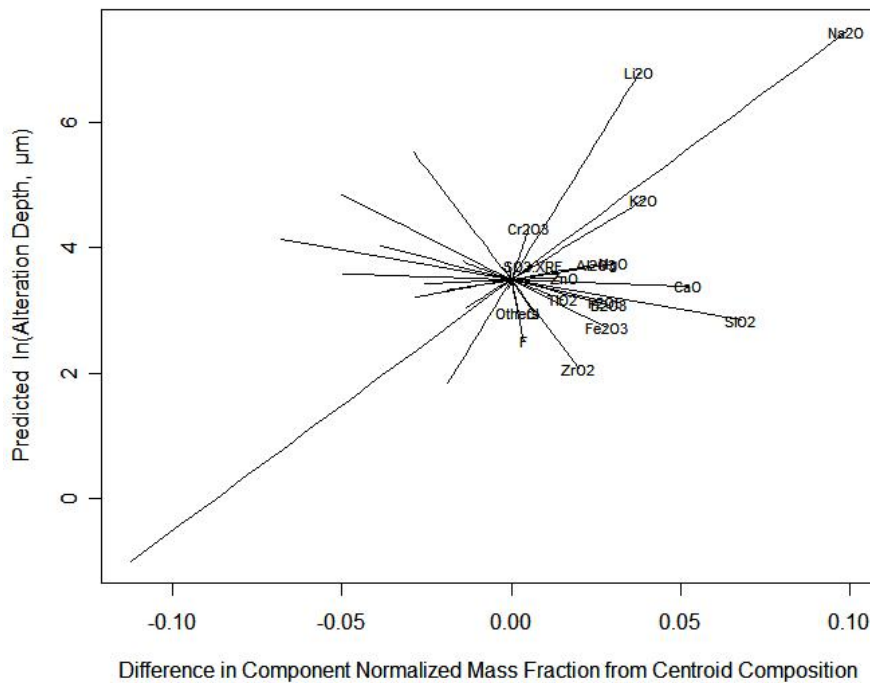


Figure 6.5. Scatterplot Matrix of 18 Components (mass fractions) for 165 LAW Glasses in the VHT Modeling Data Set.



**Figure 6.6. Predicted Versus Measured Plot for 18-Component Full Linear Mixture Model on ILAW VHT Alteration Depth ( $D$ ). The red lines represent the WTP contract limit corresponding to  $50 \text{ g/m}^2/\text{day}$  ( $D = 453 \text{ }\mu\text{m}$ ).**



**Figure 6.7. Response Trace Plot for 18-Component Full Linear Mixture Model on ILAW VHT Alteration Depth.**

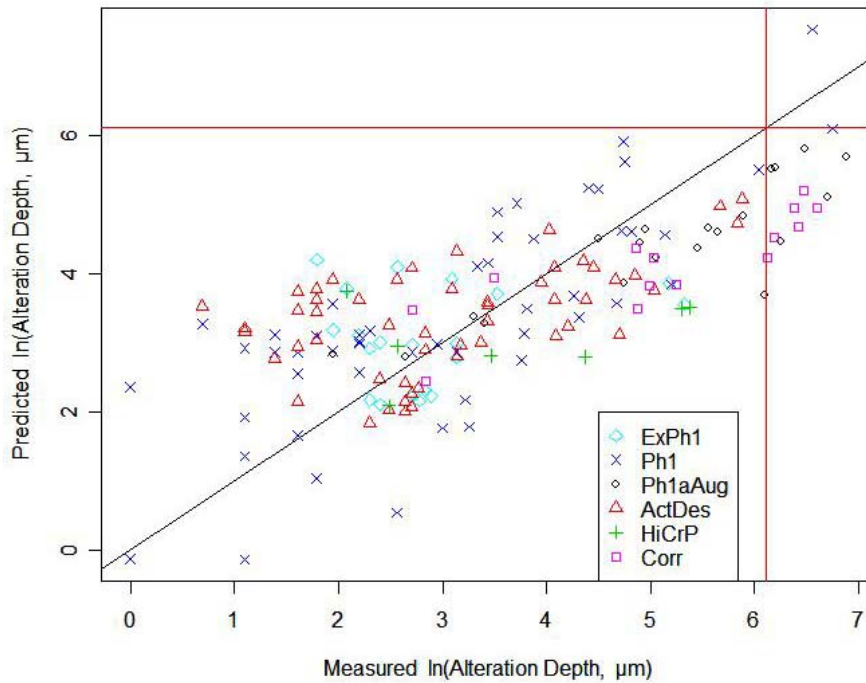


**Figure 6.8. Predicted Versus Measured Plot for 11-Component Reduced Linear Mixture Model on ILAW VHT Alteration Depth ( $D$ ). The red lines represent the WTP contract limit corresponding to  $50 \text{ g/m}^2/\text{day}$  ( $D = 453 \text{ } \mu\text{m}$ ).**

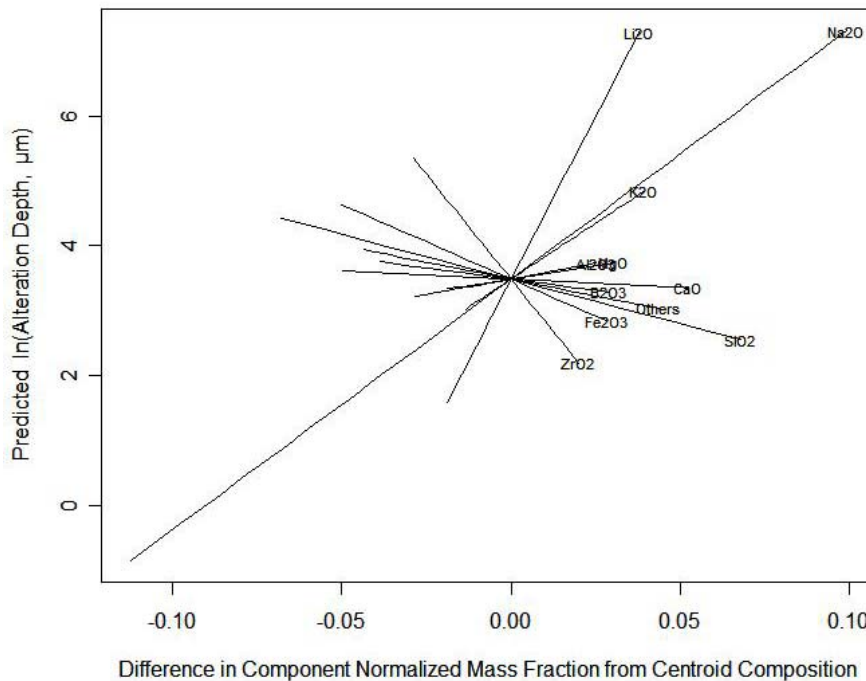


**Figure 6.9. Response Trace Plot for 11-Component Reduced Linear Mixture Model on ILAW VHT Alteration Depth.**

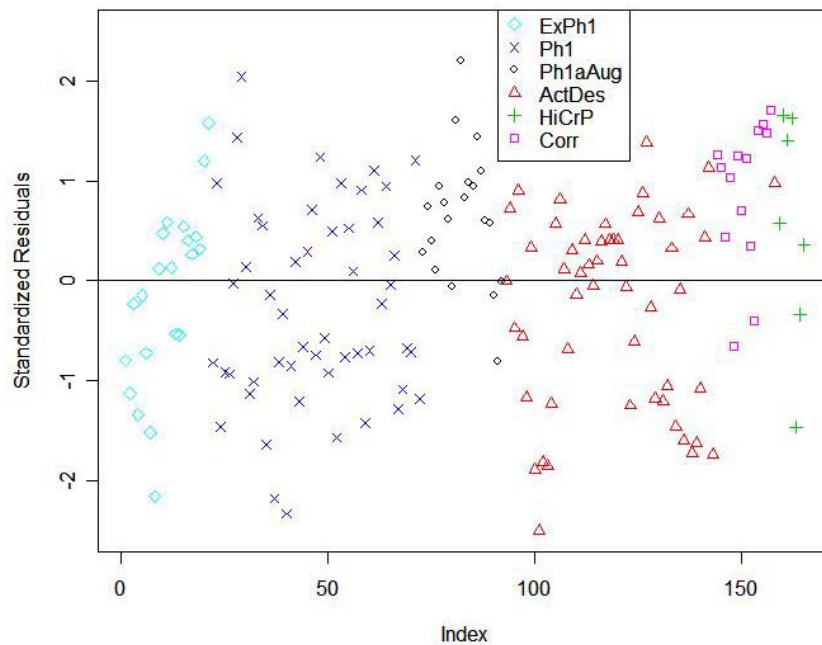


**Figure 6.10. Standardized Residuals Plot for 11-Component Reduced Linear Mixture Model on ILAW VHT Alteration Depth.**

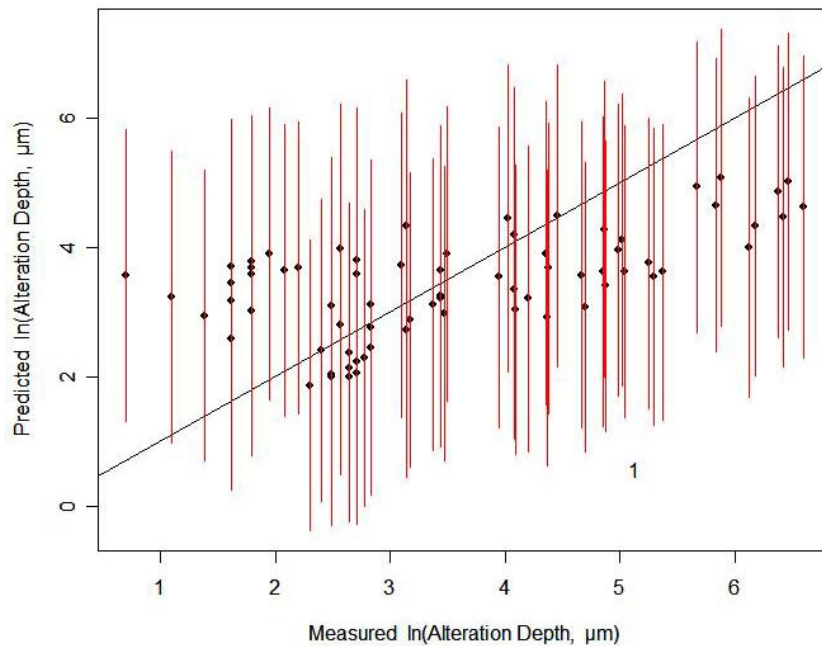


**Figure 6.11. Predicted Versus Measured Plot for 11-Component Reduced Linear Mixture Model on VHT Alteration Depth Fitted to Modeling Subset of 92 Glasses and Applied to Validation Subset of 73 Glasses. Error bars are 95% prediction intervals (PIs). The number of glasses whose 95% PIs do not include the measured values (represented by the 45° line) is shown.**

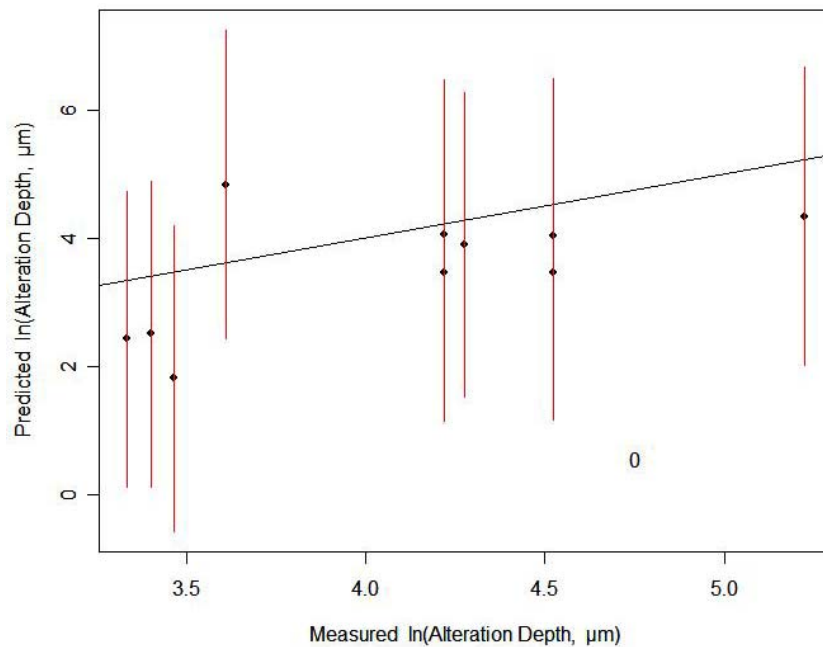


**Figure 6.12. Predicted Versus Measured Plot for 11-Component Reduced Linear Mixture Model on ILAW VHT Alteration Depth Fitted to 165 Modeling Set Glasses and Applied to 10 Outlying Glasses. Error bars are 95% prediction intervals (PIs). The number of glasses whose 95% PIs do not include the measured values (represented by the 45° line) is shown.**

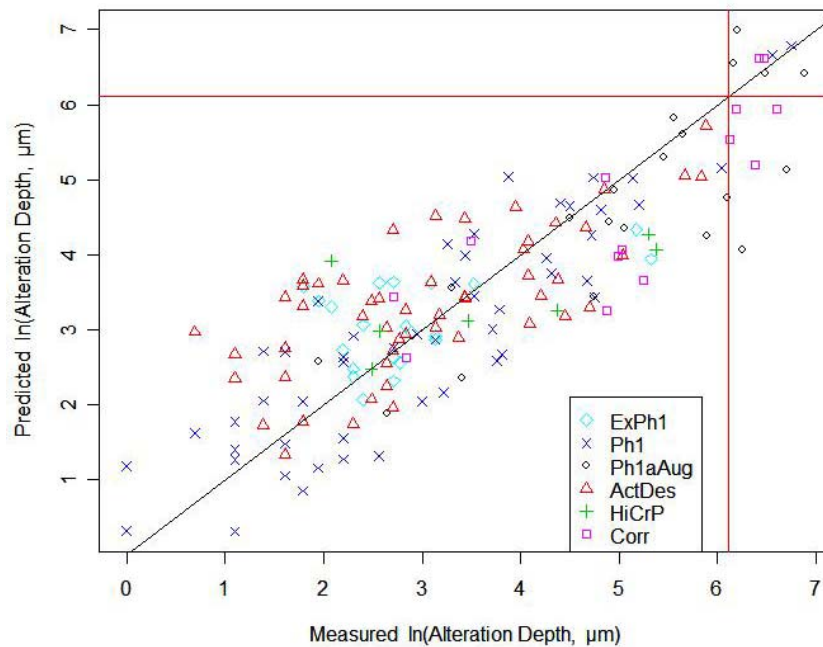


**Figure 6.13. Predicted Versus Measured Plot for 16-Term Reduced Partial Quadratic Mixture Model on ILAW VHT Alteration Depth ( $D$ ). The red lines represent the WTP contract limit corresponding to  $50 \text{ g/m}^2/\text{day}$  ( $D = 453 \text{ }\mu\text{m}$ ).**

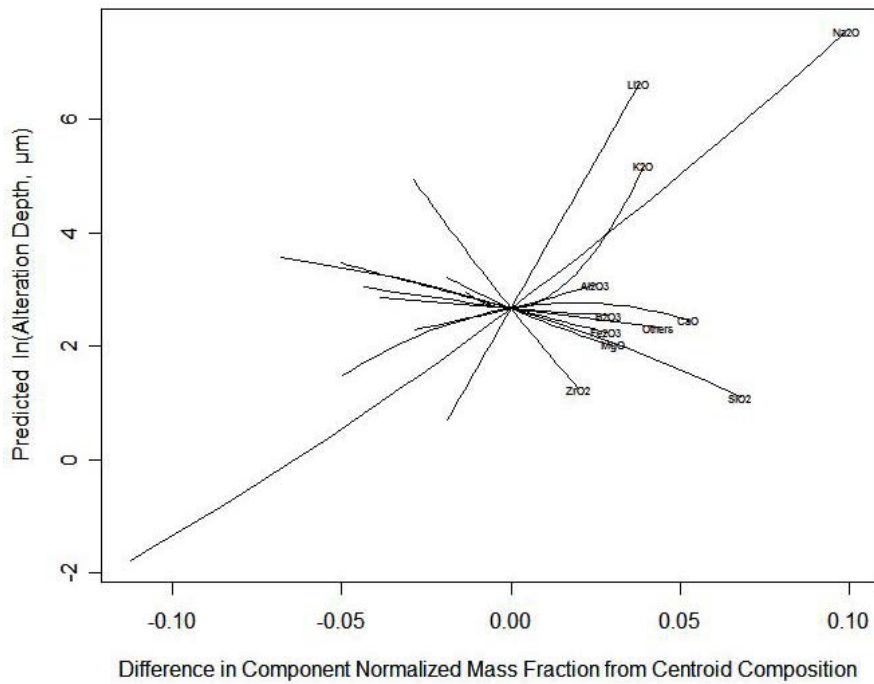


**Figure 6.14. Response Trace Plot for 16-Term Reduced Partial Quadratic Mixture Model on ILAW VHT Alteration Depth.**

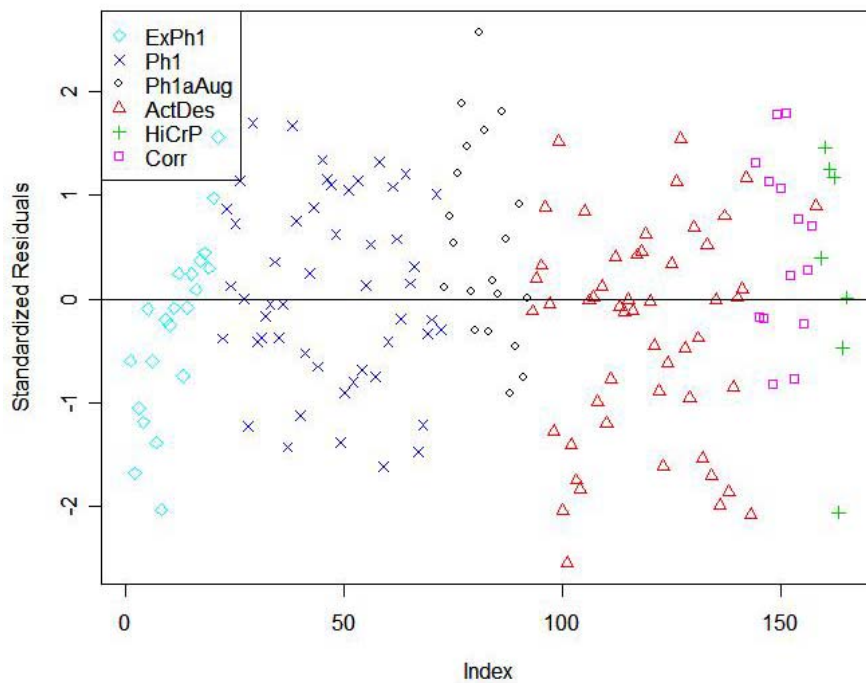


**Figure 6.15. Standardized Residuals Plot for 16-Term Reduced Partial Quadratic Mixture Model on ILAW VHT Alteration Depth.**

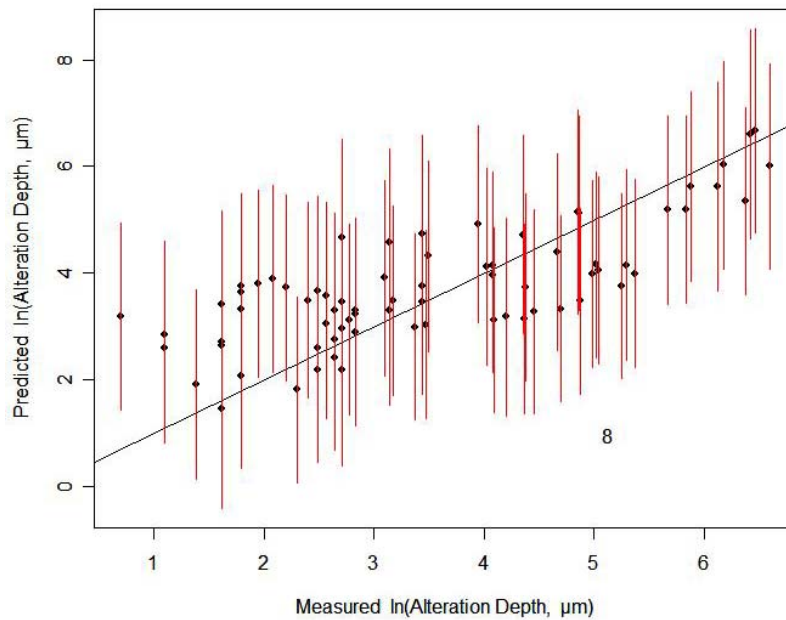


**Figure 6.16.** Predicted Versus Measured Plot for 16-Term Reduced Partial Quadratic Mixture Model on ILAW VHT Alteration Depth Fitted to Modeling Subset of 92 Glasses and Applied to Validation Subset of 73 Glasses. Error bars are 95% prediction intervals (PIs). The number of glasses whose 95% PIs do not include the measured values (represented by the 45° line) is shown.

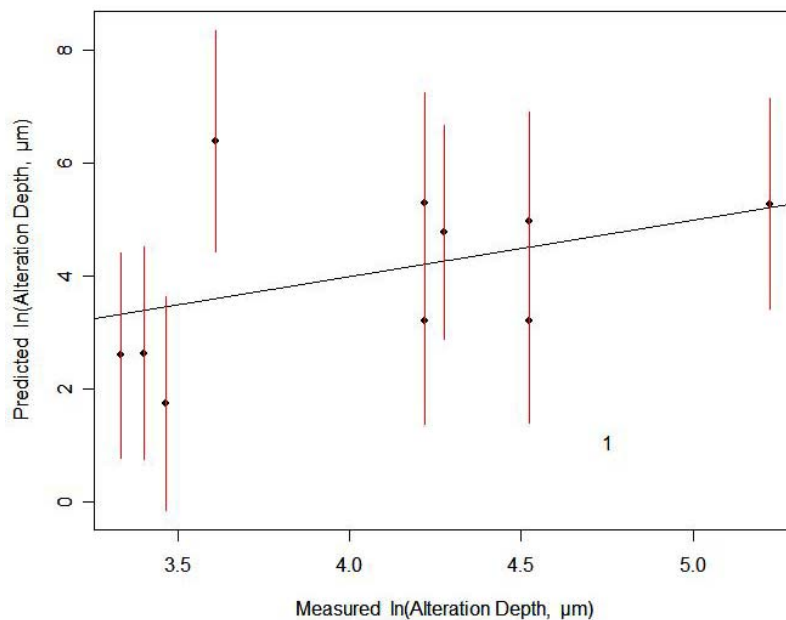


**Figure 6.17.** Predicted Versus Measured Plot for 16-Term Reduced Partial Quadratic Mixture Model on ILAW VHT Alteration Depth Fitted to 165 Modeling Set Glasses and Applied to 10 Outlying Glasses. Error bars are 95% prediction intervals (PIs). The number of glasses whose 95% PIs do not include the measured values (represented by the 45° line) is shown.



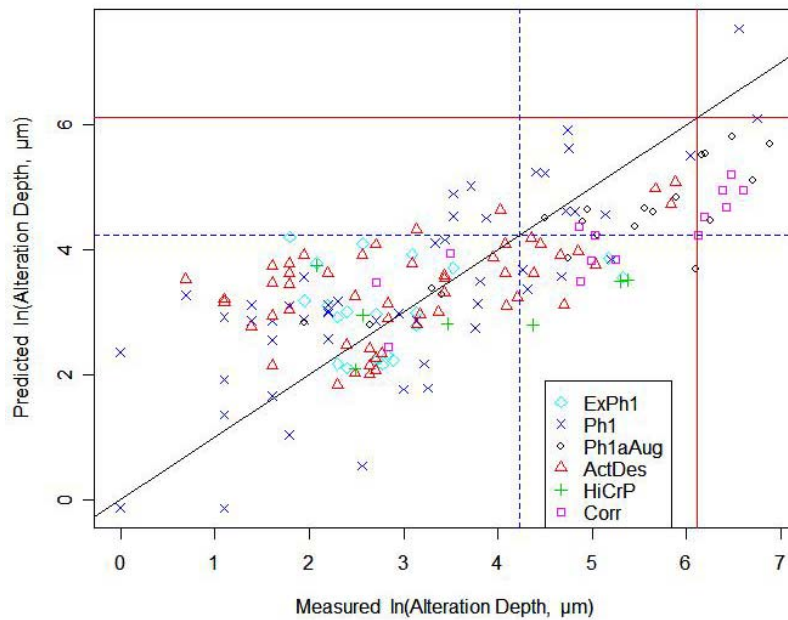


**Figure 6.18. Predicted Versus Measured Plot for 11-Term Reduced Linear Mixture Model on ILAW VHT Alteration Depth Fitted to 165 Modeling Glasses. The WTP contract limit ( $50 \text{ g/m}^2/\text{d} \sim 453 \text{ } \mu\text{m}$ ) is shown with solid red lines and the cutoff value ( $68.32 \text{ } \mu\text{m}$ ) for the two-part reduced linear mixture model is shown with dashed blue lines.**

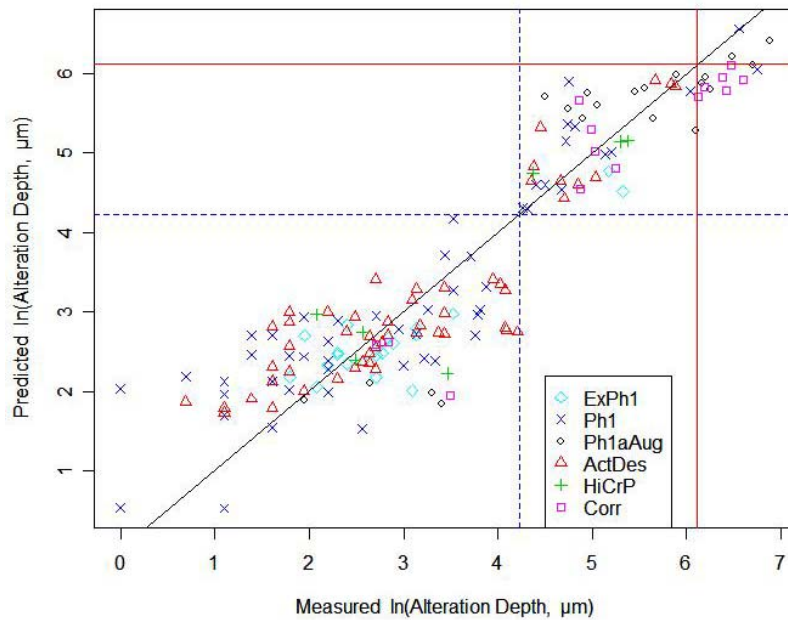


**Figure 6.19. Predicted Versus Measured Plot for 22-Term Two-Part Reduced Linear Mixture Model on ILAW VHT Alteration Depth Fitted to 165 Modeling Glasses. The WTP contract limit ( $50 \text{ g/m}^2/\text{d} \sim 453 \text{ } \mu\text{m}$ ) is shown with solid red lines and the cutoff value ( $68.32 \text{ } \mu\text{m}$ ) for the two-part linear mixture model is shown with dashed blue lines.**

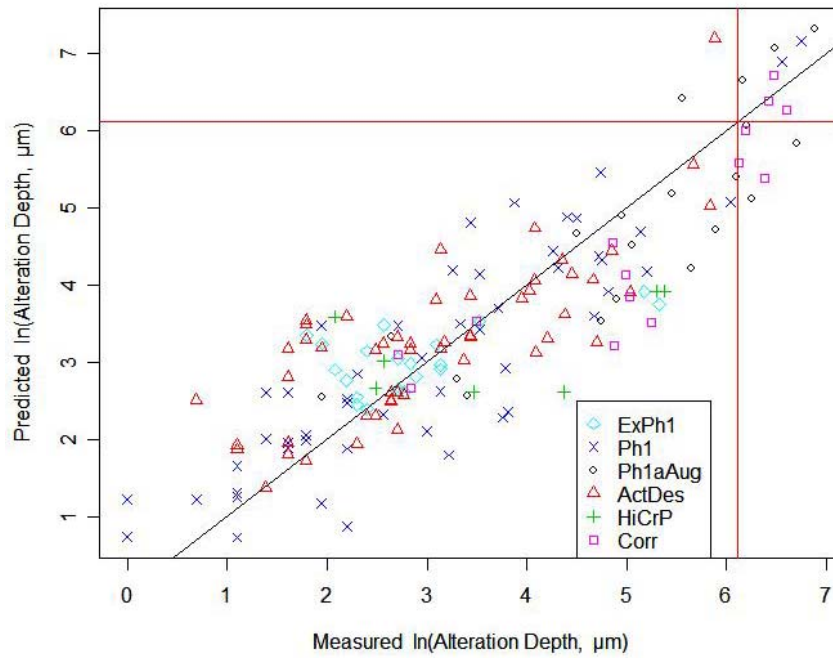


**Figure 6.20. Predicted Versus Measured Plot for 15-Term Reduced Partial Cubic Mixture Model on ILAW VHT Alteration Depth ( $D$ ). The red lines represent the WTP contract limit corresponding to  $50 \text{ g/m}^2/\text{day}$  ( $D = 453 \text{ }\mu\text{m}$ ).**

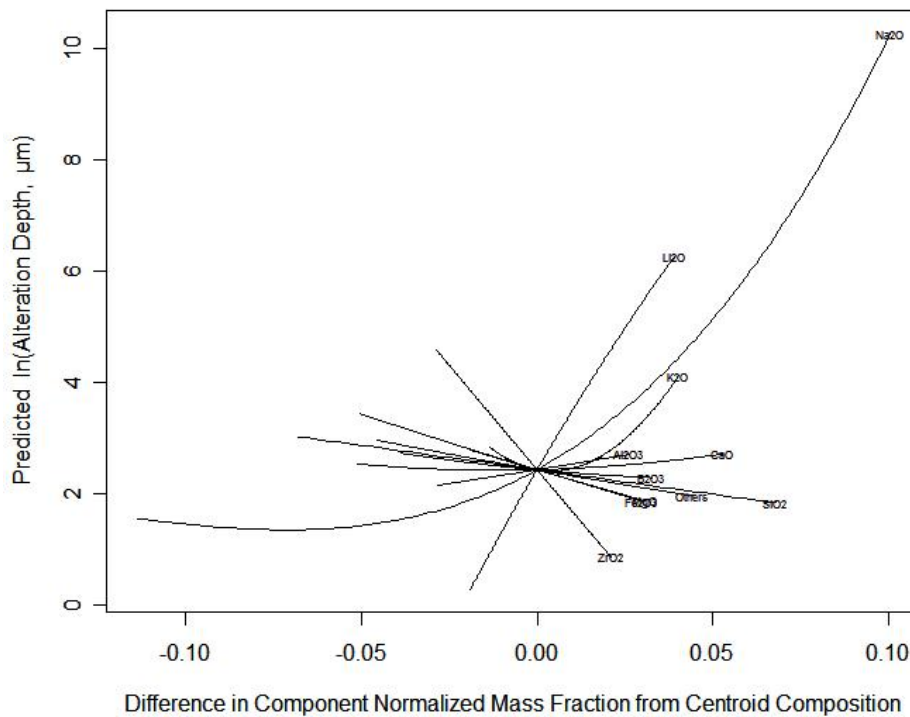


**Figure 6.21. Response Trace Plot for 15-Term Reduced Partial Cubic Mixture Model on ILAW VHT Alteration Depth.**

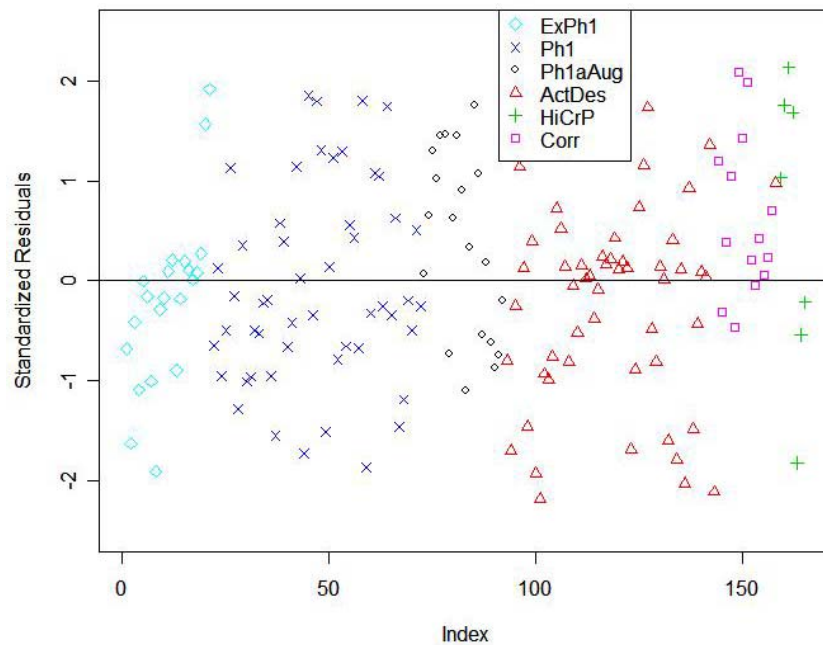


**Figure 6.22. Standardized Residuals Plot for 15-Term Reduced Partial Cubic Mixture Model on ILAW VHT Alteration Depth.**

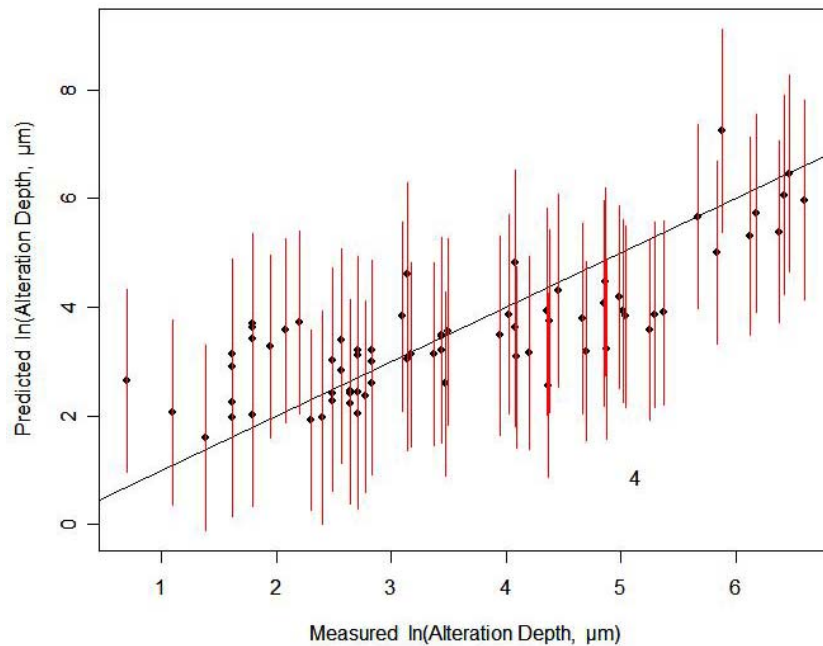


**Figure 6.23. Predicted Versus Measured Plot for 15-Term Reduced Partial Cubic Mixture Model on VHT Alteration Depth Fitted to Modeling Subset of 92 Glasses and Applied to Validation Subset of 73 Glasses. Error bars are 95% prediction intervals (PIs). The number of glasses whose 95% PIs do not include the measured values (represented by the 45° line) is shown.**

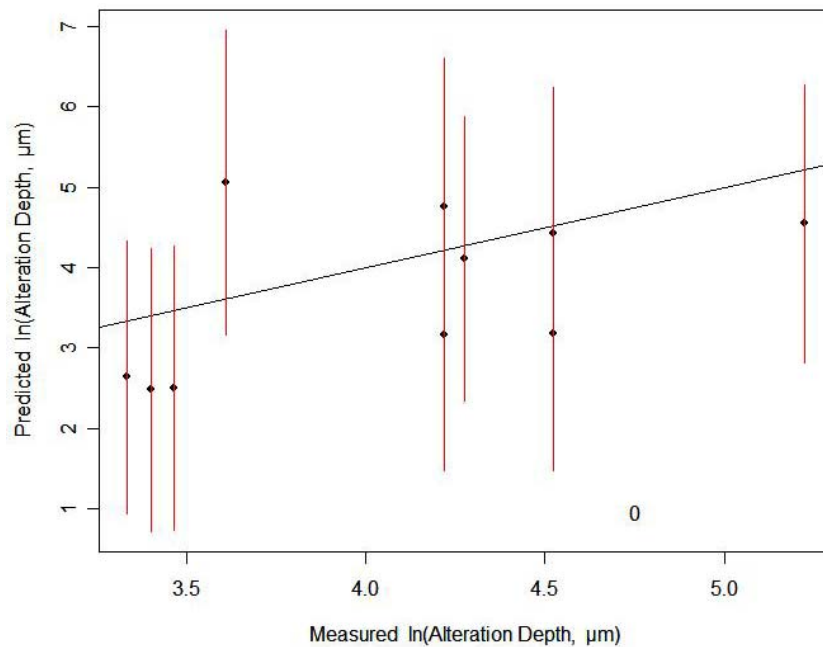


**Figure 6.24. Predicted Versus Measured Plot for 15-Term Reduced Partial Cubic Mixture Model on ILAW VHT Alteration Depth Fitted to 165 Modeling Set Glasses and Applied to 10 Outlying Glasses. Error bars are 95% prediction intervals (PIs). The number of glasses whose 95% PIs do not include the measured values (represented by the 45° line) is shown.**

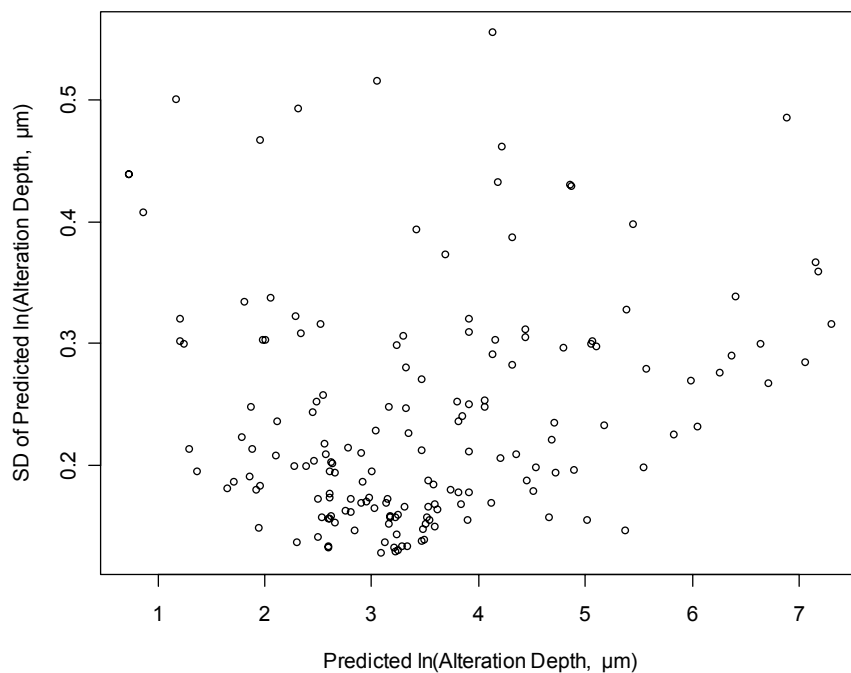


**Figure 6.25. Prediction Standard Deviations versus Predicted Values over the LAW Glass Compositions in the Modeling Dataset for the Recommended 15-Term PCM Model on VHT Alteration Depth.**

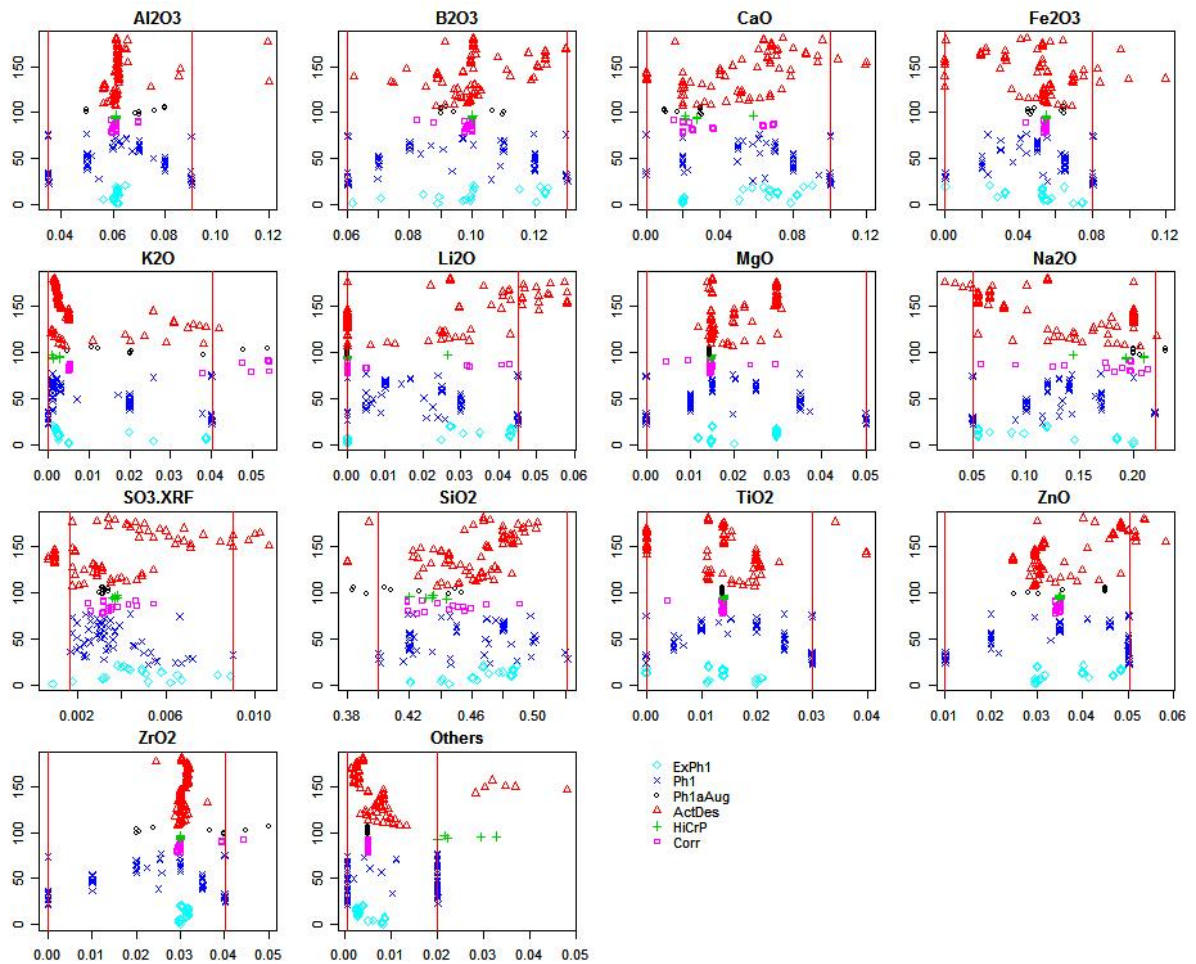


**Figure 7.1. Distributions of 14 Main Components (in mass fractions) for 181 LAW Glass Compositions with Viscosity and Electrical Conductivity Data. The vertical lines (when present) are the lower and upper limits for each component from the Phase 1 test matrix.**

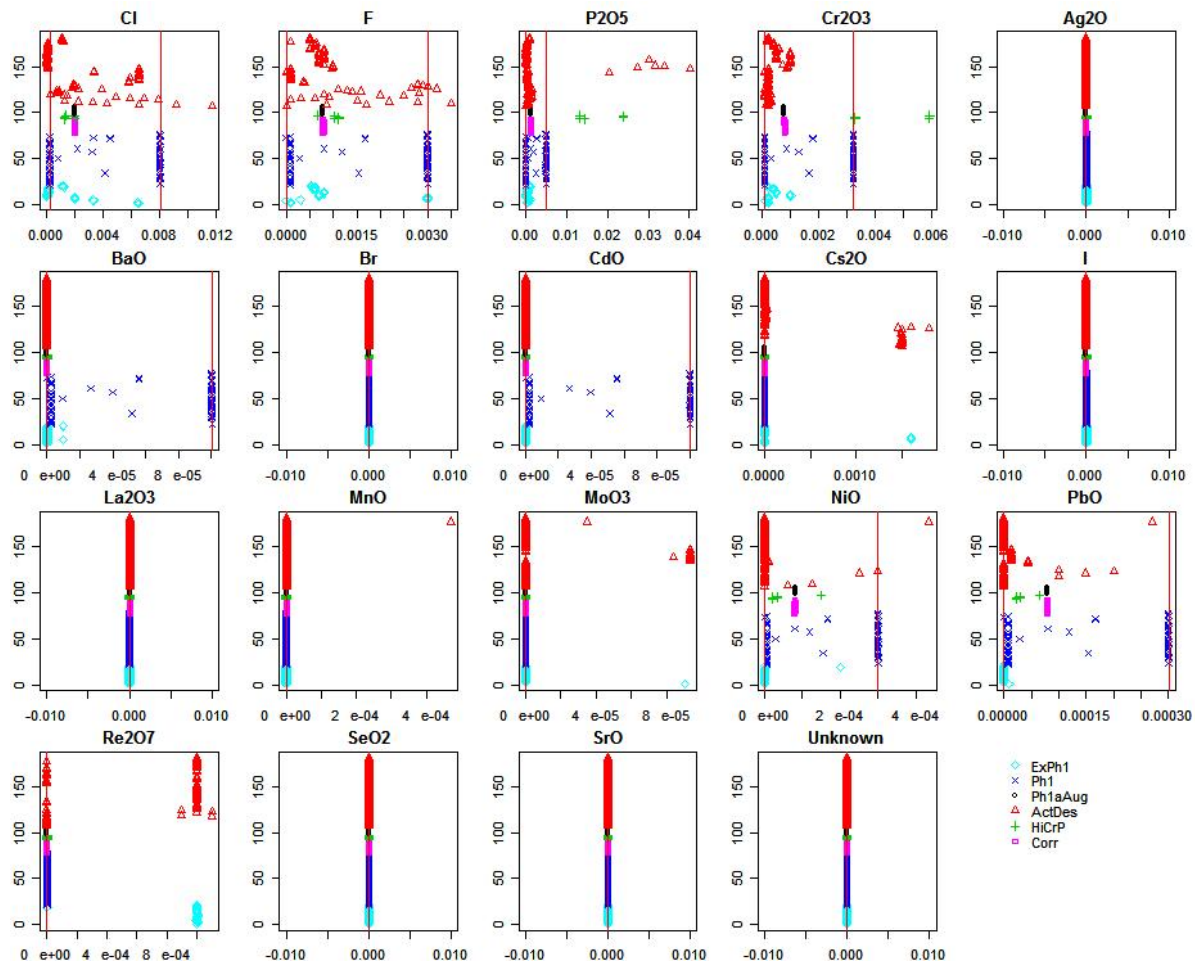


**Figure 7.2. Distributions of 19 Minor Components (in mass fractions) for 181 LAW Glass Compositions with Viscosity and Electrical Conductivity Data. The vertical lines (when present) are the lower and upper limits for each component from the Phase 1 test matrix.**

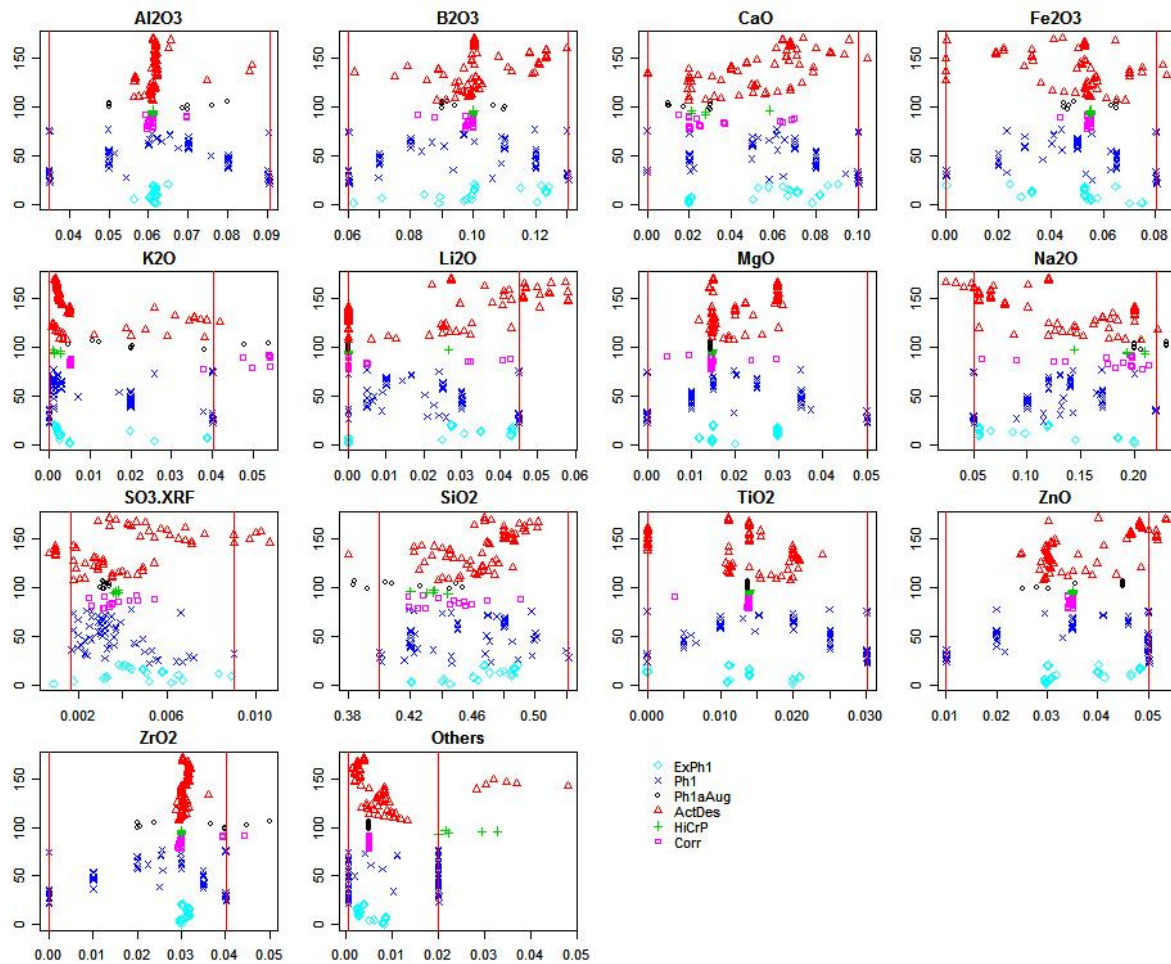


**Figure 7.3. Distributions of 14 Main Components (in mass fractions) for the 171 LAW Glass Compositions with Viscosity and Electrical Conductivity Data that Remain After Excluding 10 Glasses with “Outliers” in Individual Components. The vertical lines (when present) are the lower and upper limits for each component from the Phase 1 test matrix.**

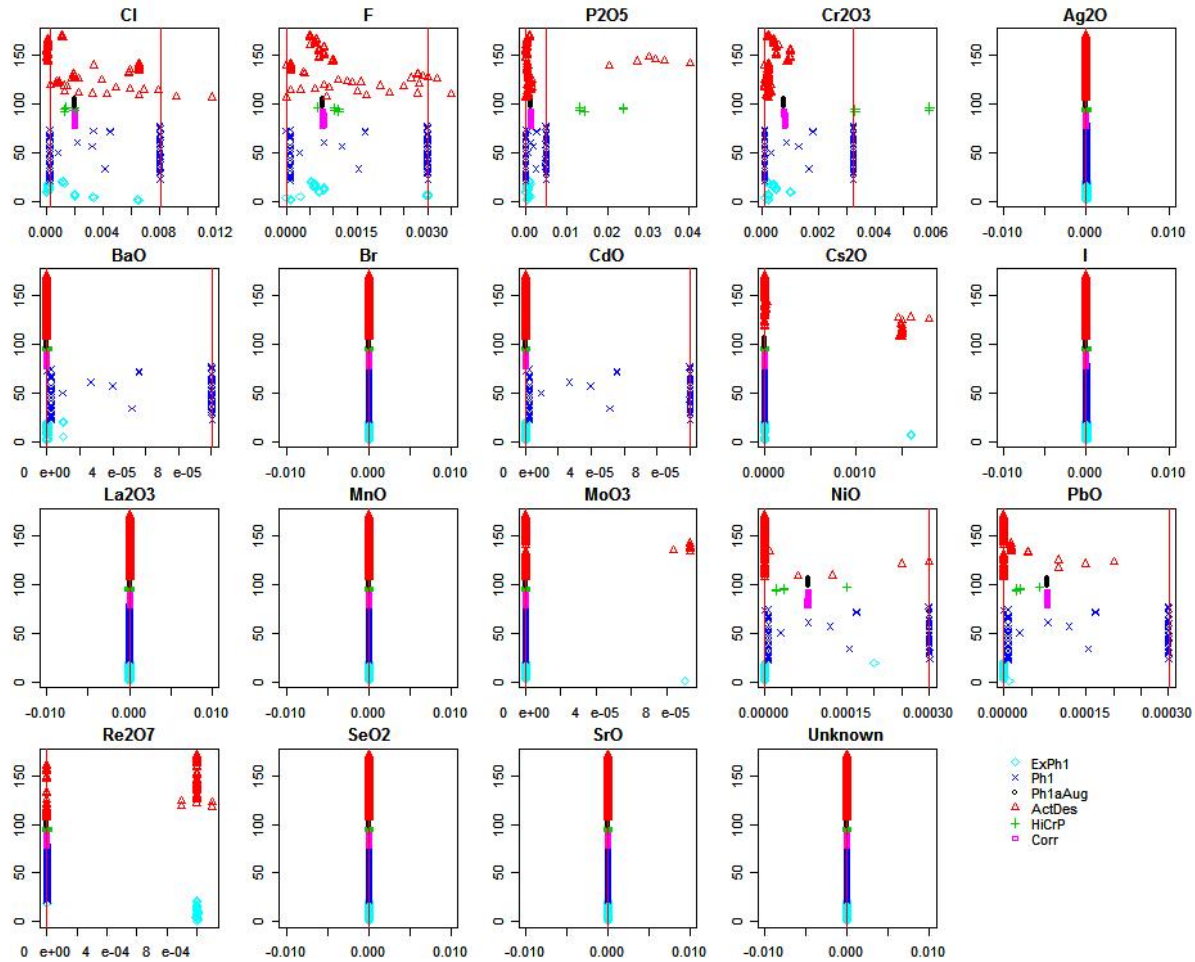


**Figure 7.4. Distributions of 19 Minor Components (in mass fractions) for the 171 LAW Glass Compositions with Viscosity and Electrical Conductivity Data that Remain After Excluding 10 Glasses with “Outliers” in Individual Components. The vertical lines (when present) are the lower and upper limits for each component from the Phase 1 test matrix.**



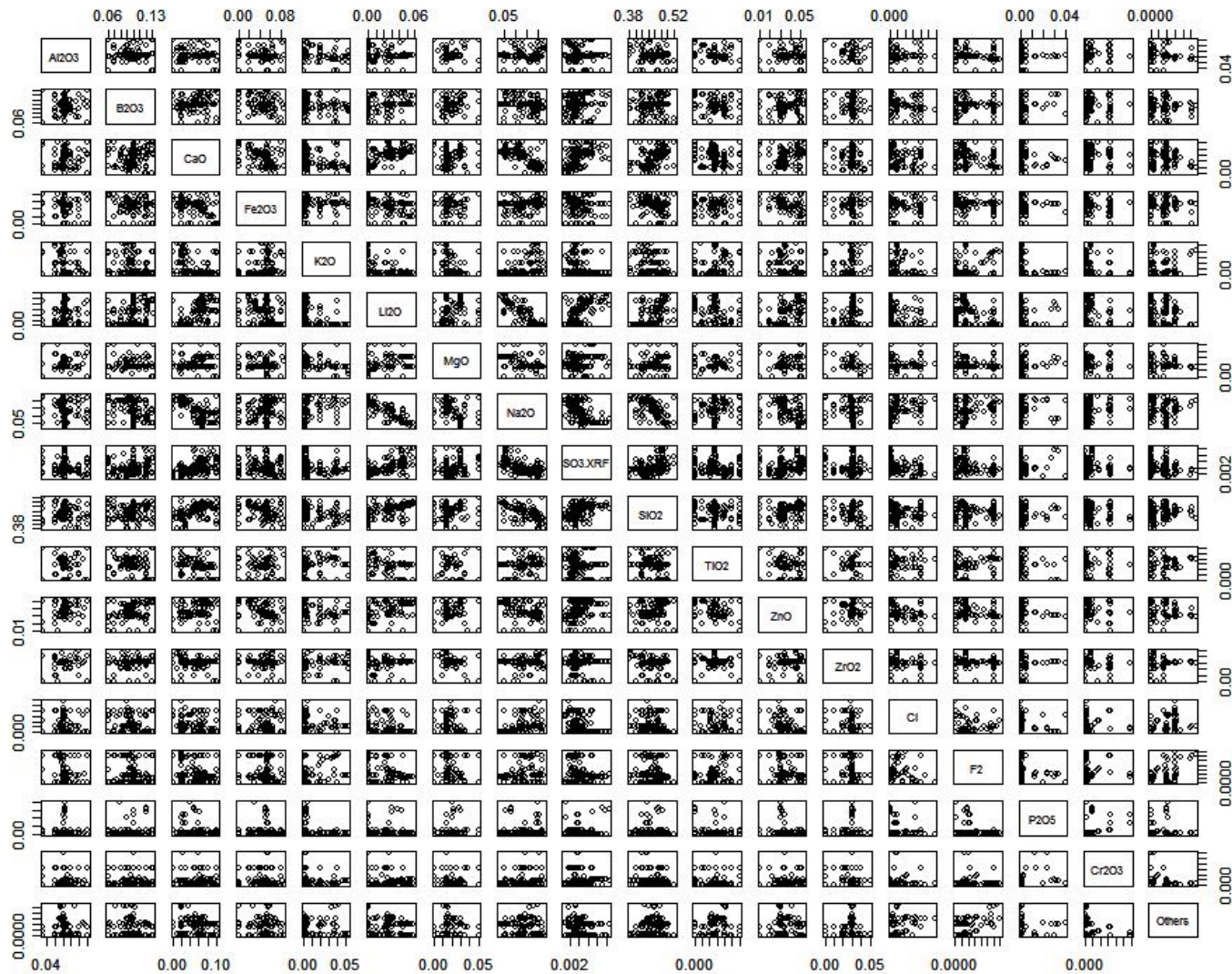


**Figure 7.5. Scatterplot Matrix of 18 Components (mass fractions) for 171 LAW Glasses with Viscosity and Electrical Conductivity Data that Remain After Excluding 10 Glasses with “Outliers” in Individual Components.**

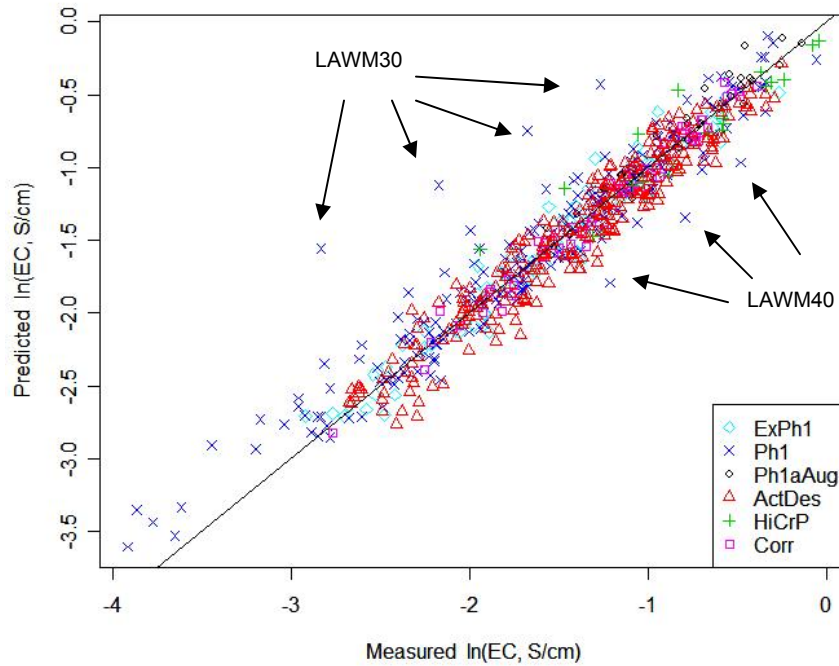


**Figure 7.6. Predicted Versus Measured Plot for 36-Term ILAW Electrical Conductivity Model with the Two Parameters of the Arrhenius Equation Expressed as 18-Component Linear Mixture Models.**

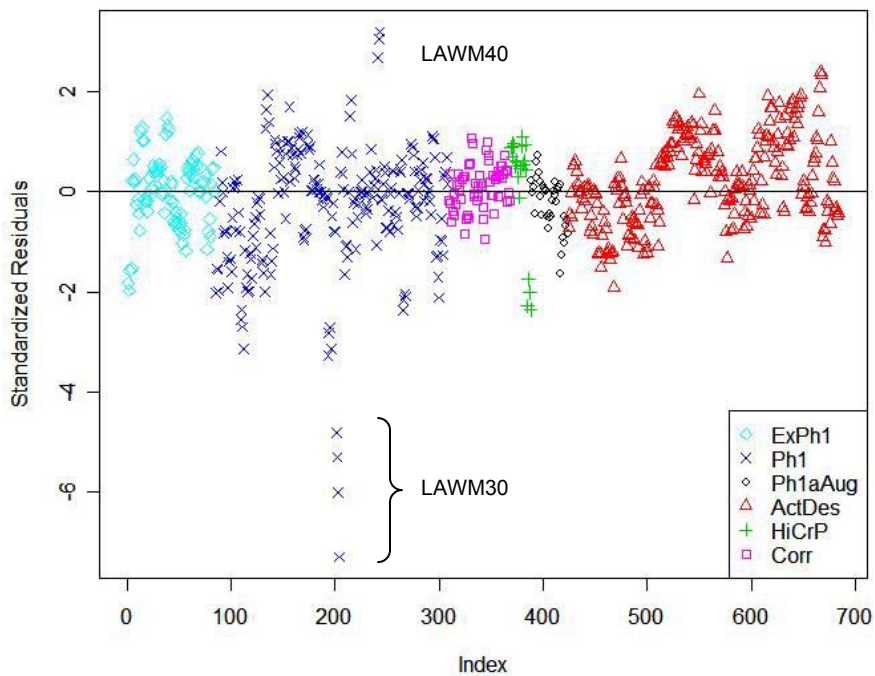


**Figure 7.7. Standardized Residuals Plot for 36-Term ILAW Electrical Conductivity Model with the Two Parameters of the Arrhenius Equation Expressed as 18-Component Linear Mixture Models.**

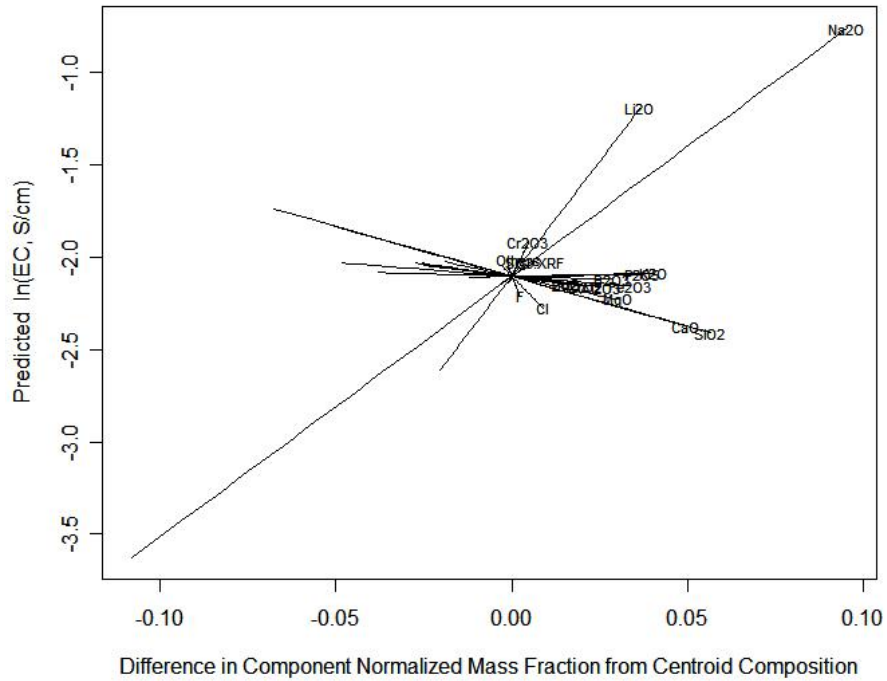


**Figure 7.8a. Response Trace Plot for ILAW Electrical Conductivity at 950°C Constructed Using the 36-Term Arrhenius-Linear Mixture Model.**

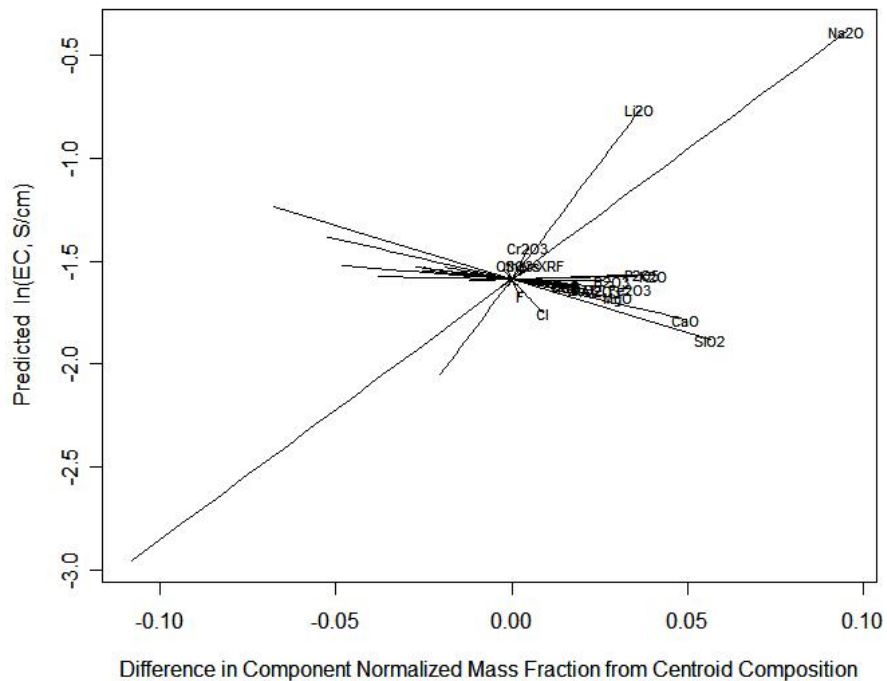


**Figure 7.8b. Response Trace Plot for ILAW Electrical Conductivity at 1050°C Constructed Using the 36-Term Arrhenius-Linear Mixture Model.**

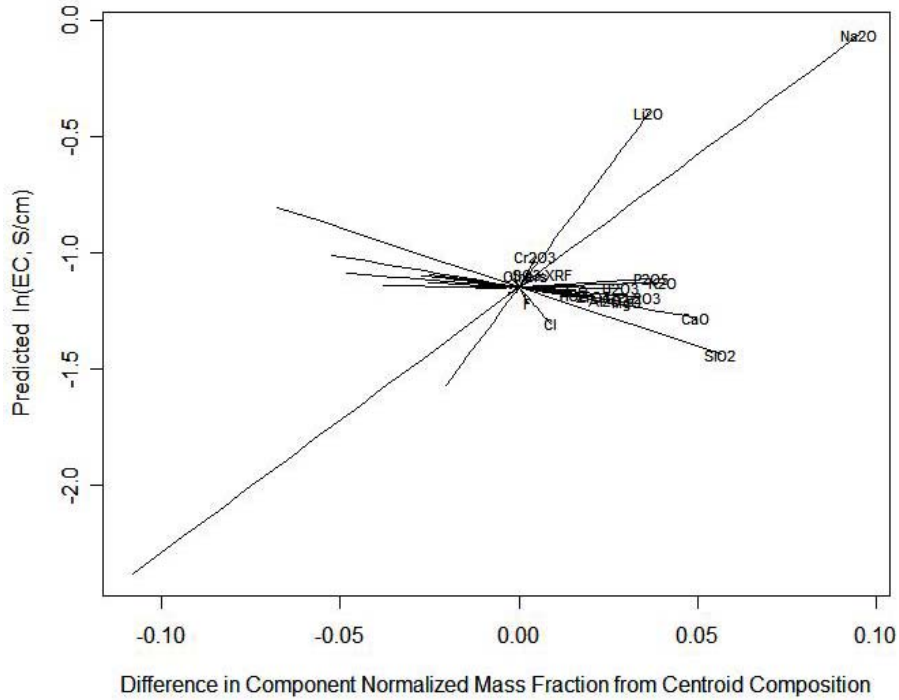


**Figure 7.8c.** Response Trace Plot for ILAW Electrical Conductivity at 1150°C Constructed Using the 36-Term Arrhenius-Linear Mixture Model.

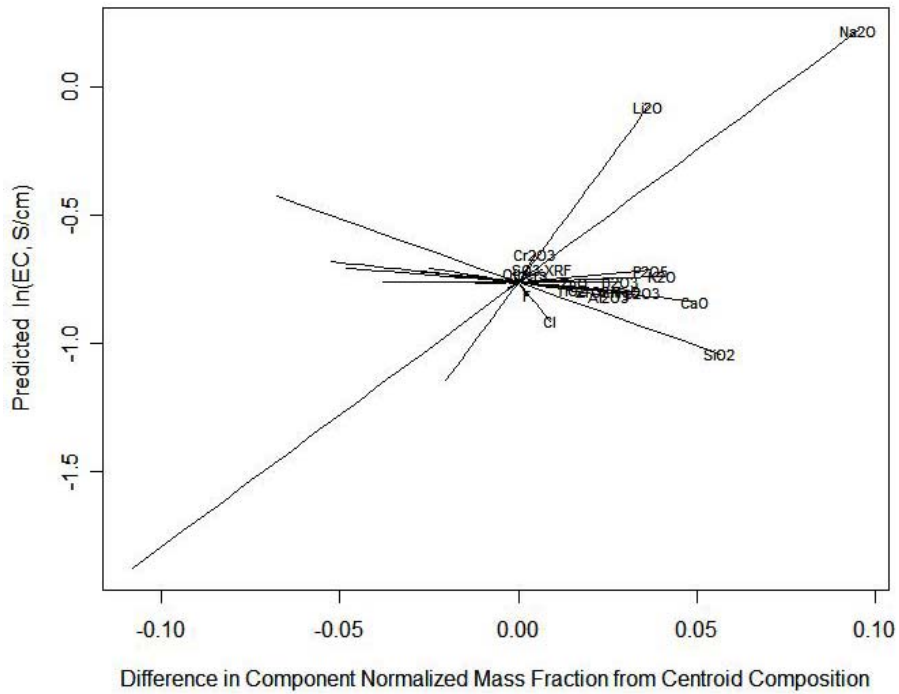


**Figure 7.8d.** Response Trace Plot for ILAW Electrical Conductivity at 1250°C Constructed Using the 36-Term Arrhenius-Linear Mixture Model.

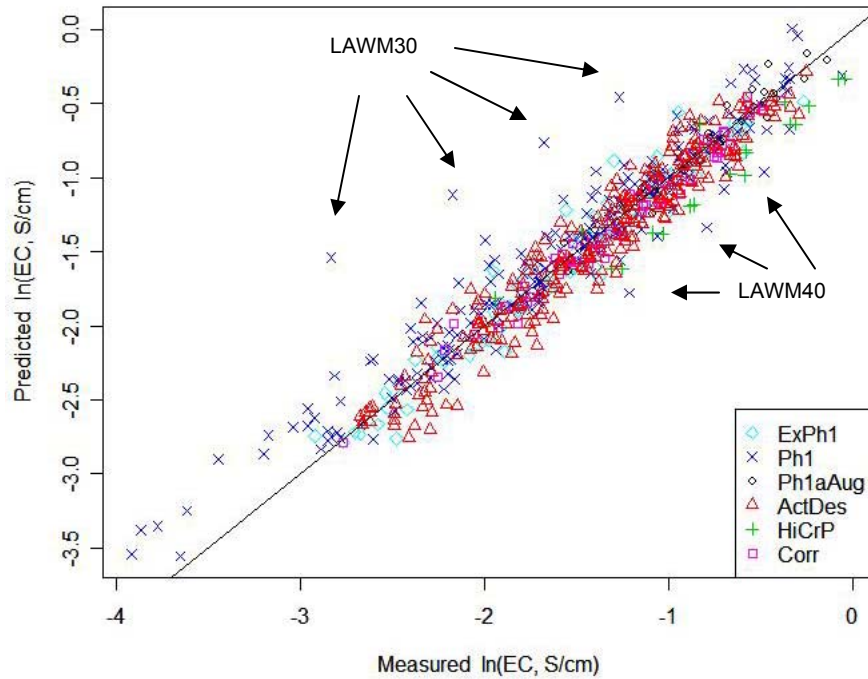


**Figure 7.9. Predicted Versus Measured Plot for 22-Term ILAW Electrical Conductivity Model with the Two Parameters of the Arrhenius Equation Expressed as Reduced 11-Component Linear Mixture Models.**

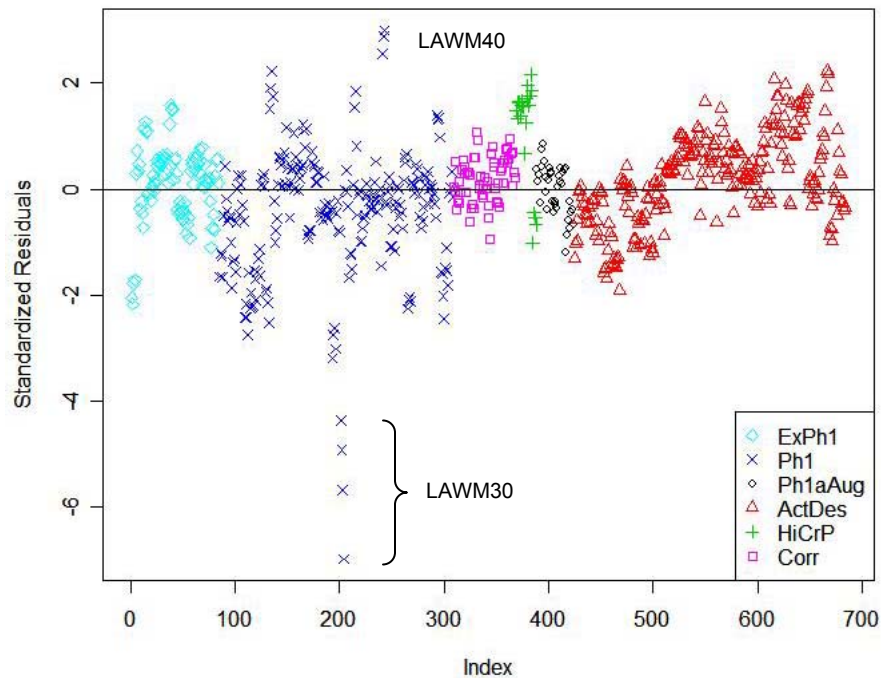


**Figure 7.10. Standardized Residuals Plot for 22-Term ILAW Electrical Conductivity Model with the Two Parameters of the Arrhenius Equation Expressed as Reduced 11-Component Linear Mixture Models.**

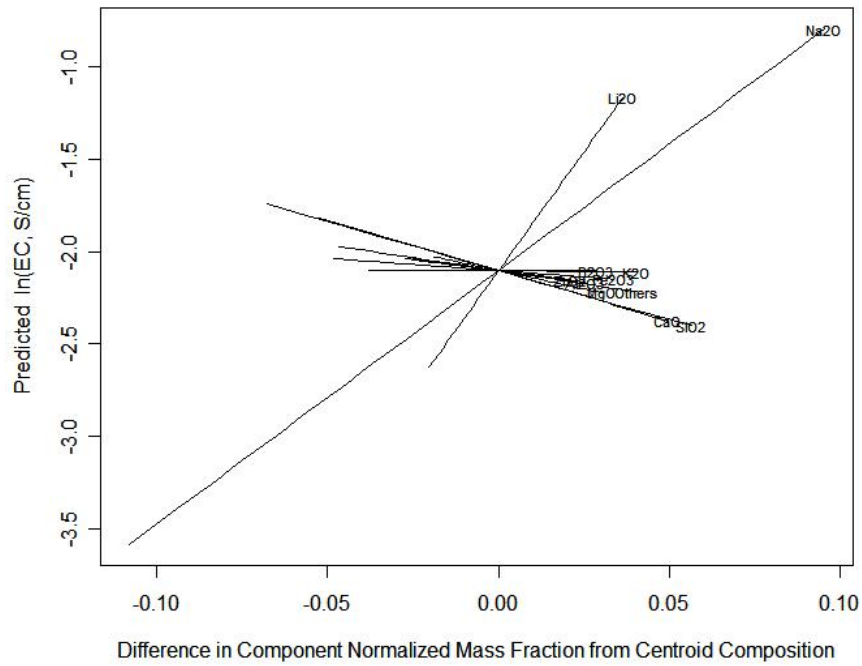


**Figure 7.11a. Response Trace Plot for ILAW Electrical Conductivity at 950°C Constructed Using the 22-Term Arrhenius-Linear Mixture Model.**

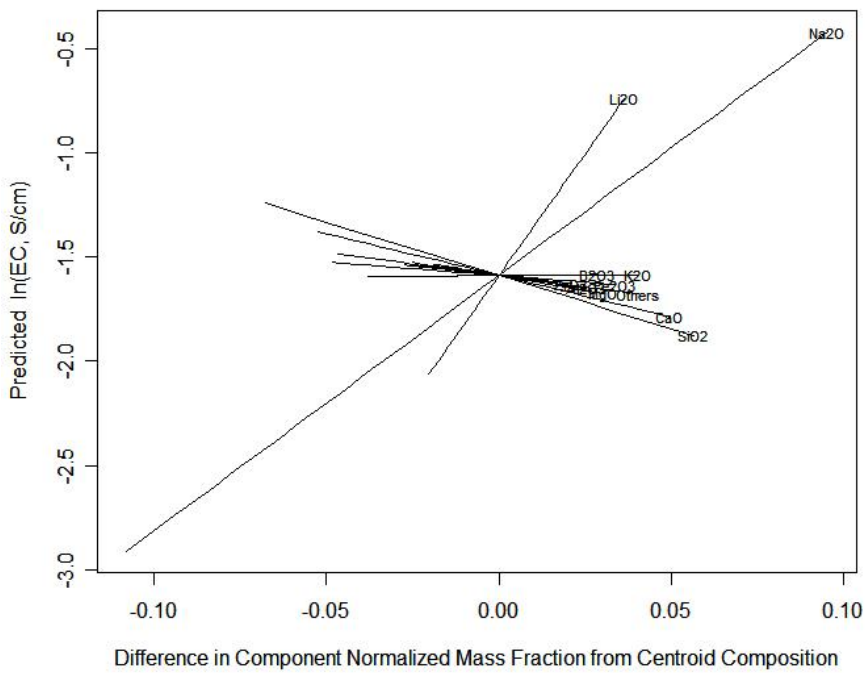


**Figure 7.11b. Response Trace Plot for ILAW Electrical Conductivity at 1050°C Constructed Using the 22-Term Arrhenius-Linear Mixture Model.**

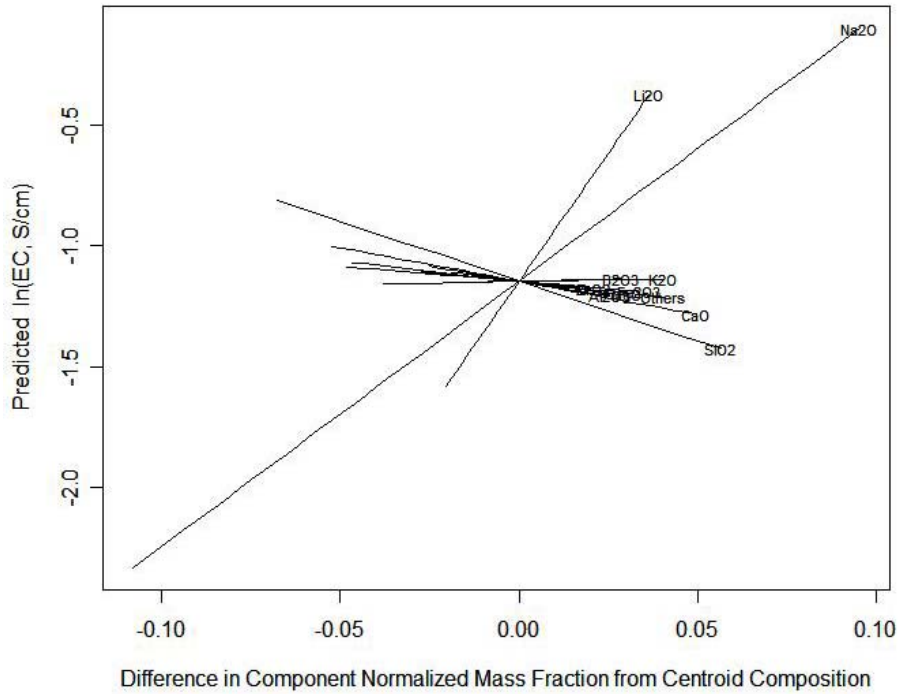


**Figure 7.11c. Response Trace Plot for ILAW Electrical Conductivity at 1150°C Constructed Using the 22-Term Arrhenius-Linear Mixture Model.**

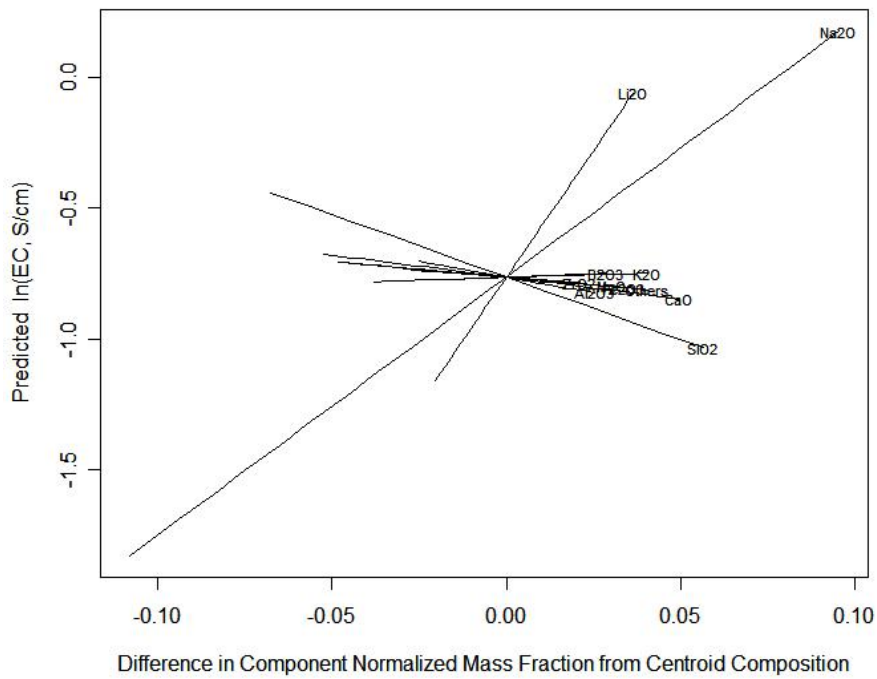


**Figure 7.11d. Response Trace Plot for ILAW Electrical Conductivity at 1250°C Constructed Using the 22-Term Arrhenius-Linear Mixture Model.**

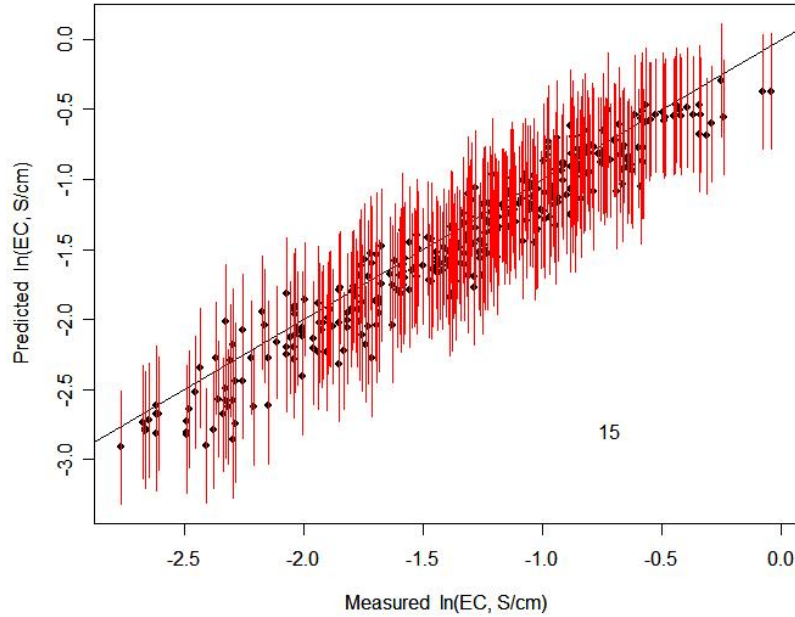


**Figure 7.12. Predicted Versus Measured Plot for 22-Term Arrhenius-Linear Model on ILAW Electrical Conductivity Fitted to Modeling Subset of 86 Glasses and Applied to Validation Subset of 85 Glasses. Error bars are 95% prediction intervals (PIs). The number of glasses whose 95% PIs do not include the measured values (represented by the 45° line) is shown.**

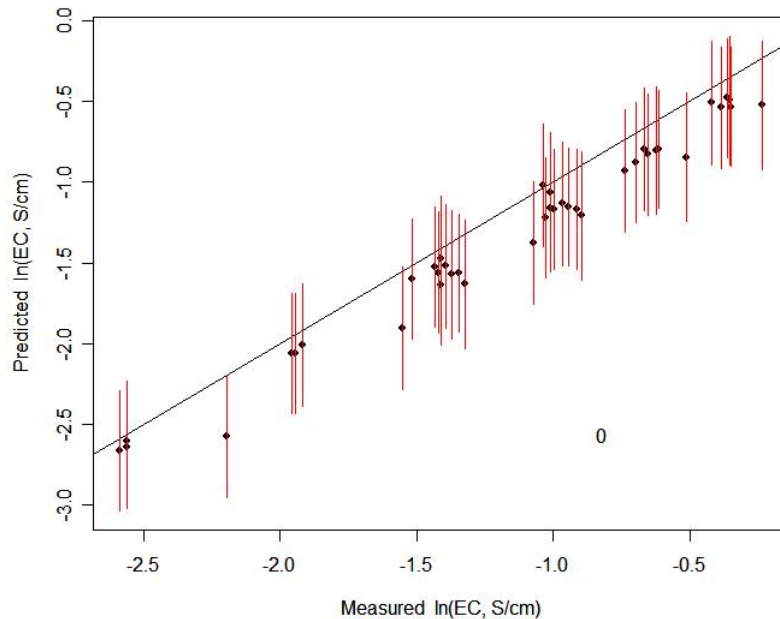


**Figure 7.13. Predicted Versus Measured Plot for 22-Term Arrhenius-Linear Model on ILAW Electrical Conductivity Fitted to 171 Modeling Set Glasses and Applied to 10 Outlying Glasses. Error bars are 95% prediction intervals (PIs). The number of glasses whose 95% PIs do not include the measured values (represented by the 45° line) is shown.**



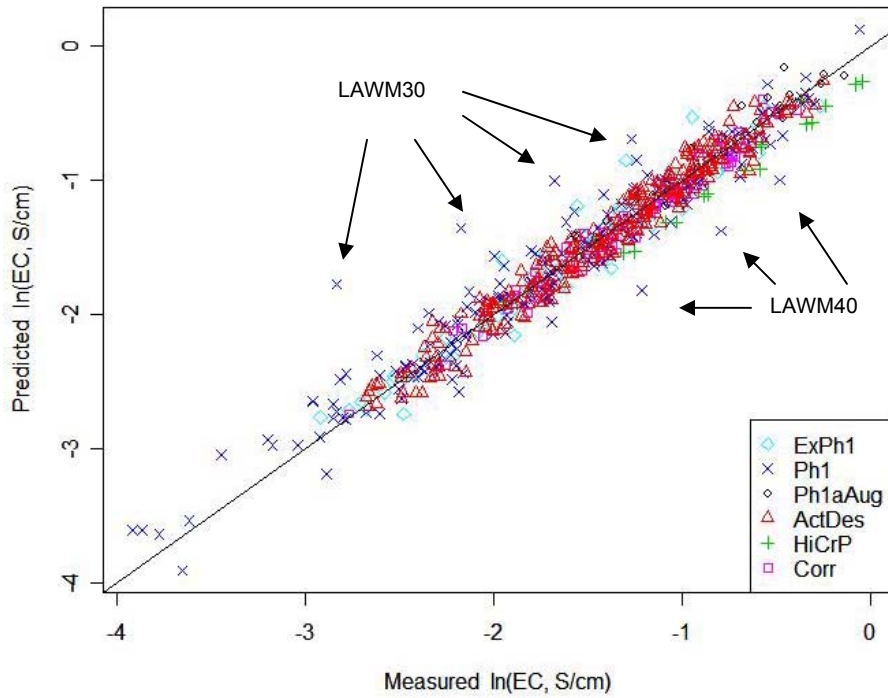


**Figure 7.14. Predicted Versus Measured Plot for 25-Term Arrhenius-Linear Mixture Model with Three Crossproduct Terms on ILAW Electrical Conductivity.**

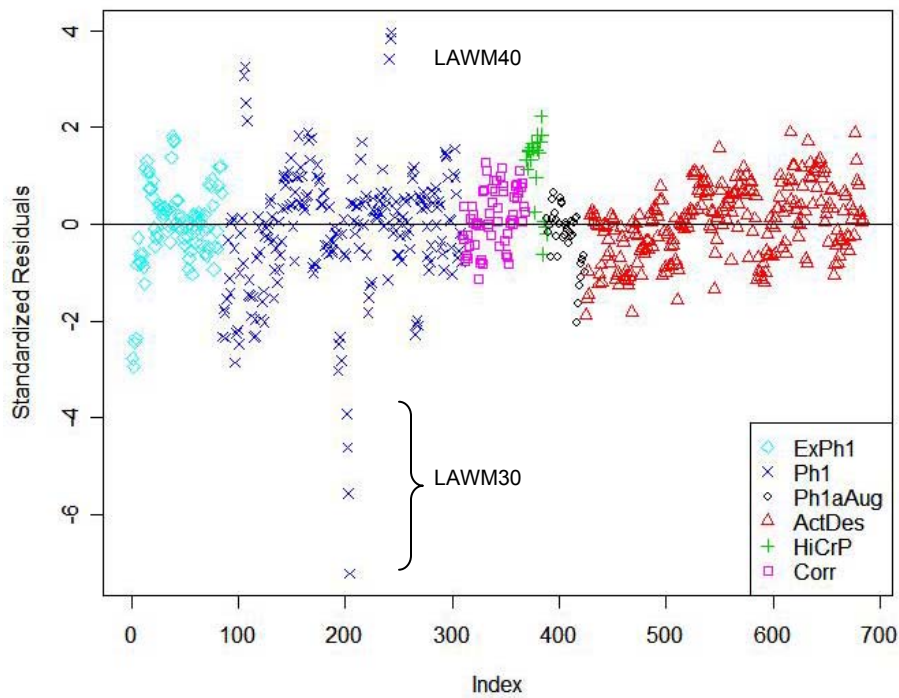


**Figure 7.15. Standardized Residuals Plot for 25-Term Arrhenius-Linear Mixture Model with Three Crossproduct Terms on ILAW Electrical Conductivity.**

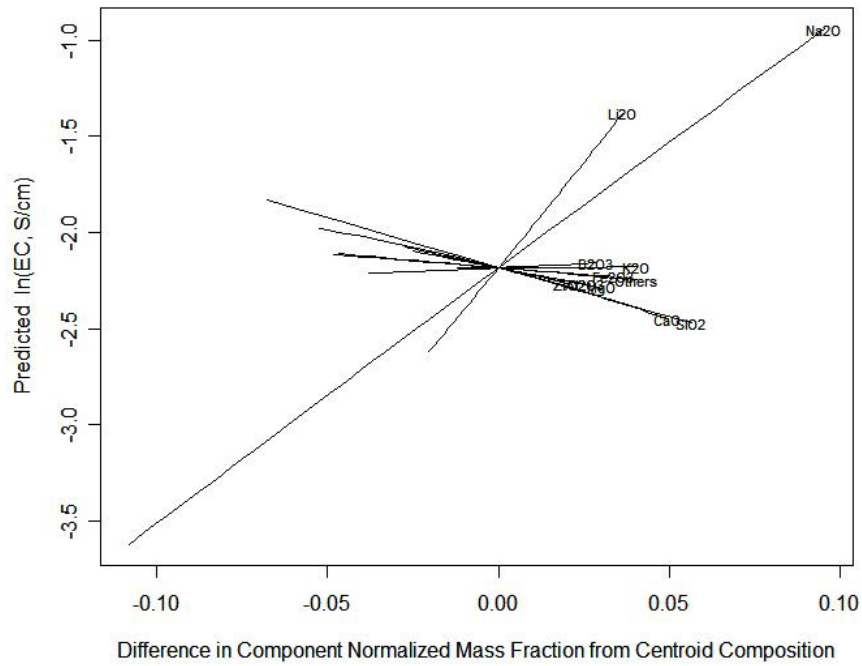


**Figure 7.16a. Response Trace Plot for ILAW Electrical Conductivity at 950°C Constructed Using the 25-Term Arrhenius-Linear Mixture Model with Three Crossproduct Terms.**

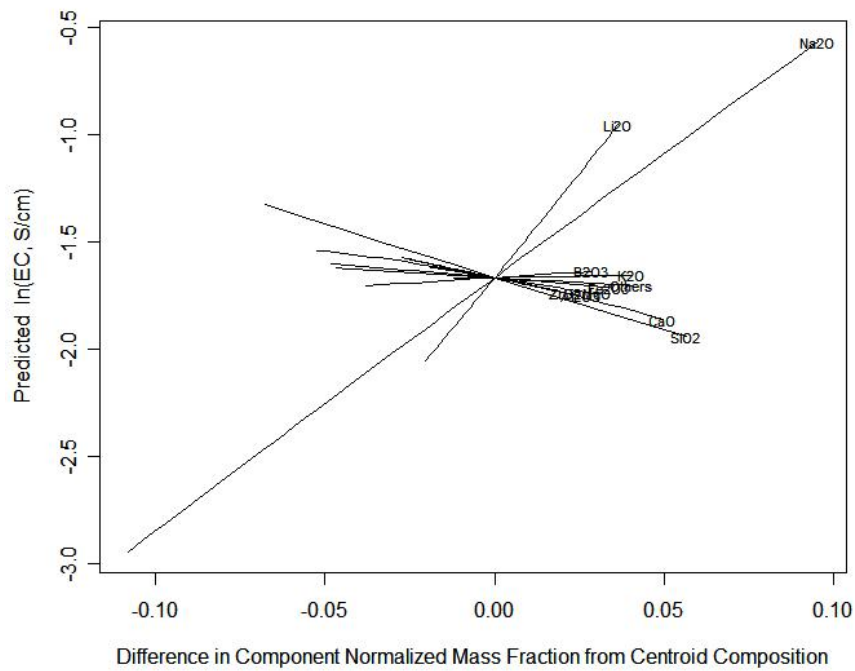


**Figure 7.16b. Response Trace Plot for ILAW Electrical Conductivity at 1050°C Constructed Using the 25-Term Arrhenius-Linear Mixture Model with Three Crossproduct Terms.**

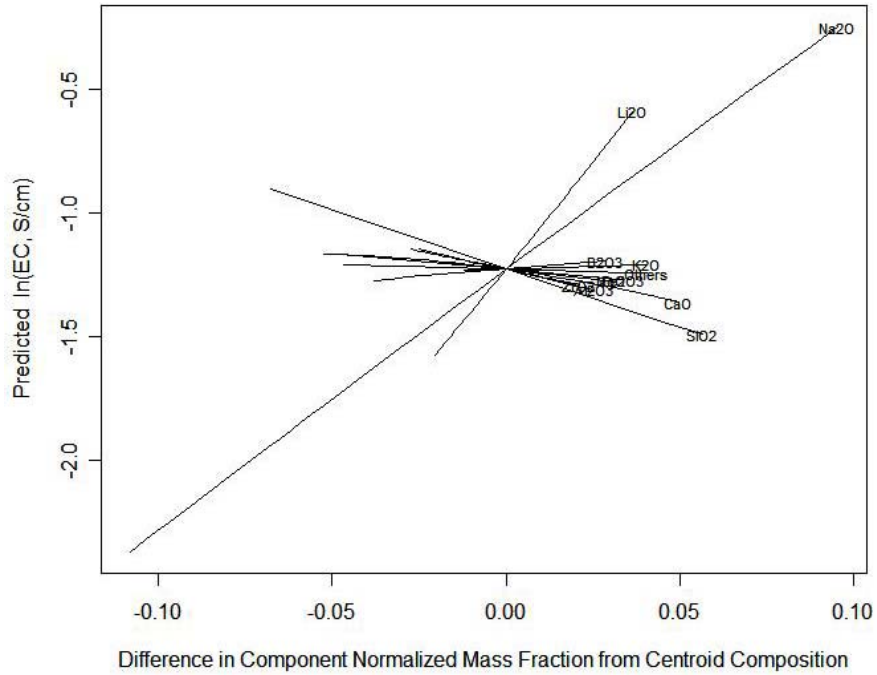


**Figure 7.16c. Response Trace Plot for ILAW Electrical Conductivity at 1150°C Constructed Using the 25-Term Arrhenius-Linear Mixture Model with Three Crossproduct Terms.**

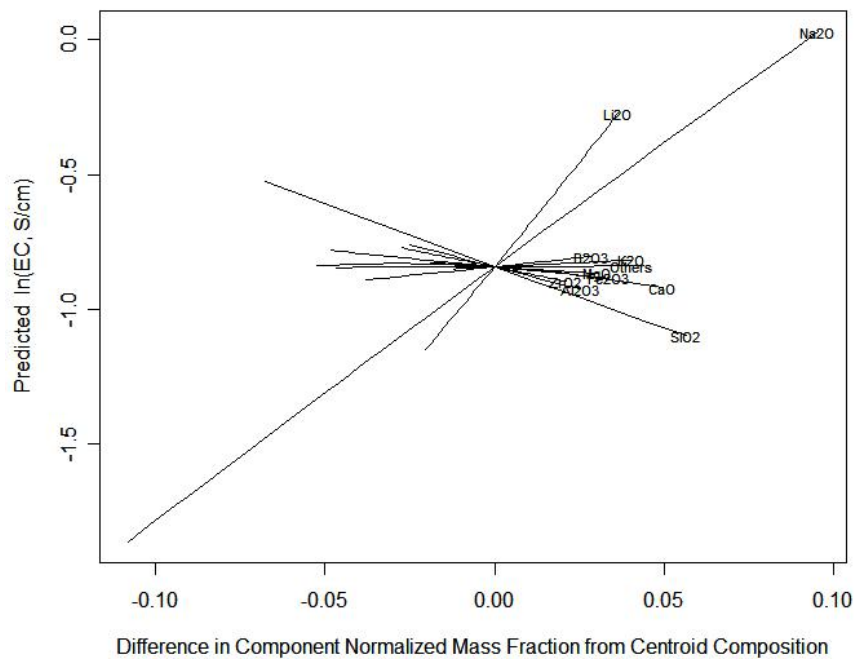


**Figure 7.16d. Response Trace Plot for ILAW Electrical Conductivity at 1250°C Constructed Using the 25-Term Arrhenius-Linear Mixture Model with Three Crossproduct Terms.**

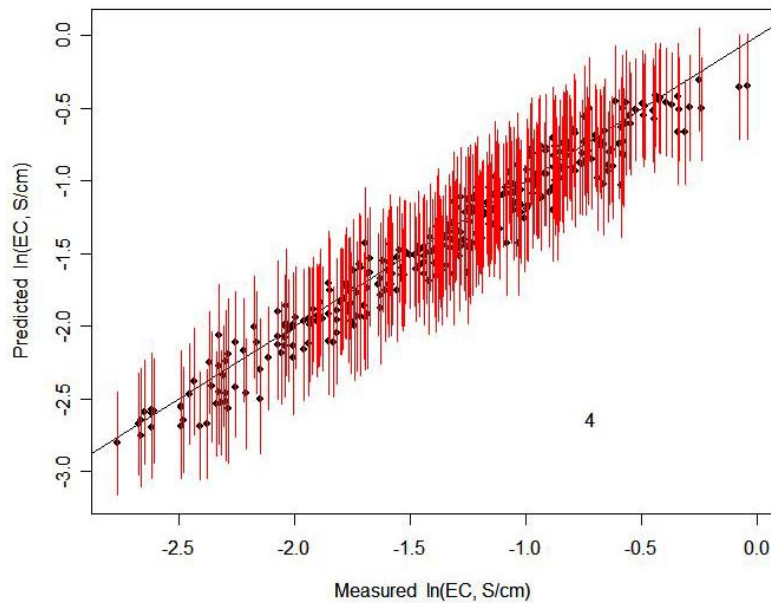


**Figure 7.17.** Predicted Versus Measured Plot for 25-Term Arrhenius-Linear Model with Three Crossproduct Terms on ILAW Electrical Conductivity Fitted to Modeling Subset of 86 Glasses and Applied to Validation Subset of 85 Glasses. Error bars are 95% prediction intervals (PIs). The number of glasses whose 95% PIs do not include the measured values (represented by the 45° line) is shown.

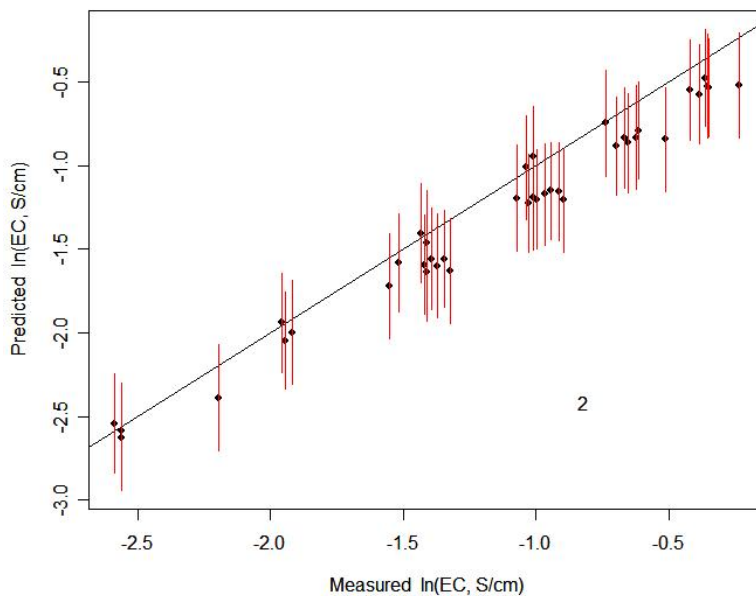


**Figure 7.18.** Predicted Versus Measured Plot for 25-Term Arrhenius-Linear Model with Three Crossproduct Terms on ILAW Electrical Conductivity Fitted to 171 Modeling Set Glasses and Applied to 10 Outlying Glasses. Error bars are 95% prediction intervals (PIs). The number of glasses whose 95% PIs do not include the measured values (represented by the 45° line) is shown.

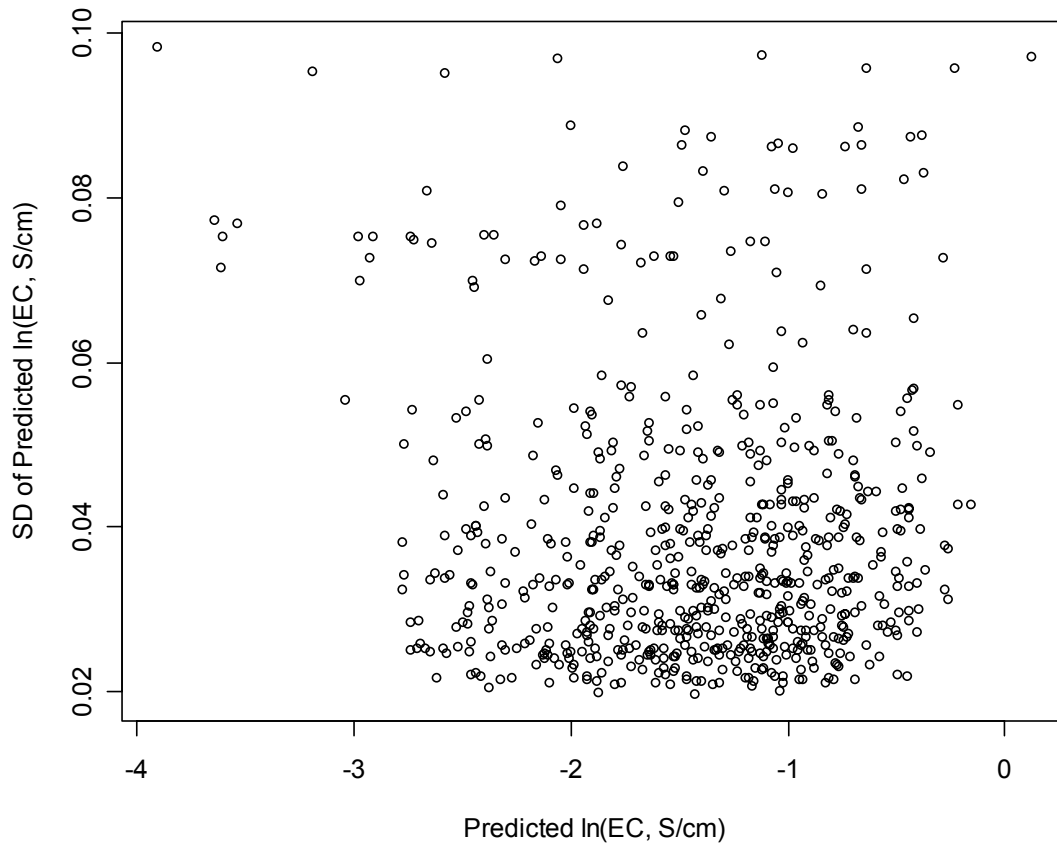


**Figure 7.19. Prediction Standard Deviations versus Predicted Values over the LAW Glass Compositions in the Modeling Dataset and Temperatures 950, 1050, 1150, and 1250°C for the Recommended 25-Term Electrical Conductivity Model.**

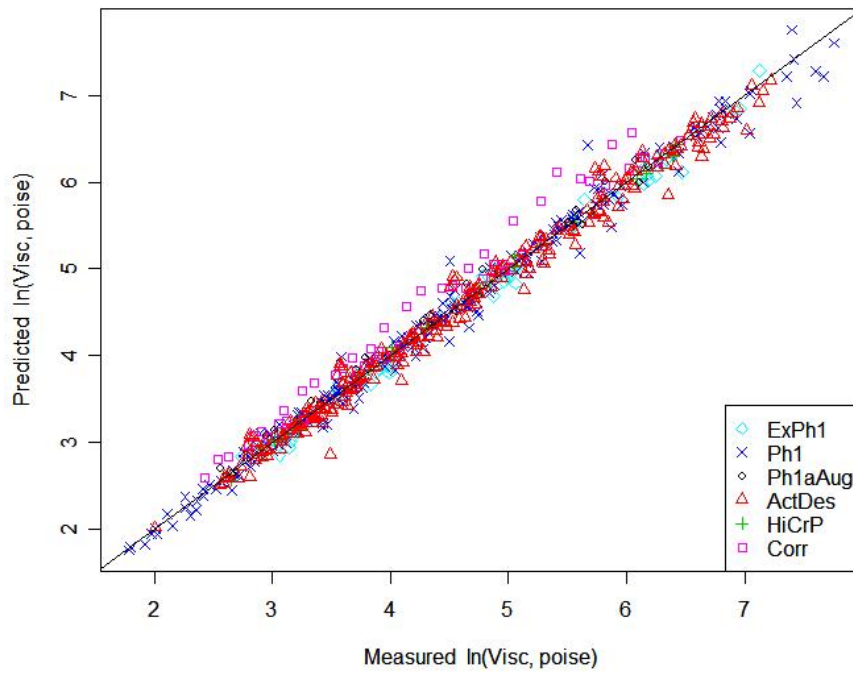


**Figure 8.1. Predicted Versus Measured Plot for 36-Term ILAW Viscosity Model with the Two Parameters of the Truncated-T2 Equation Expressed as 18-Component Linear Mixture Models.**

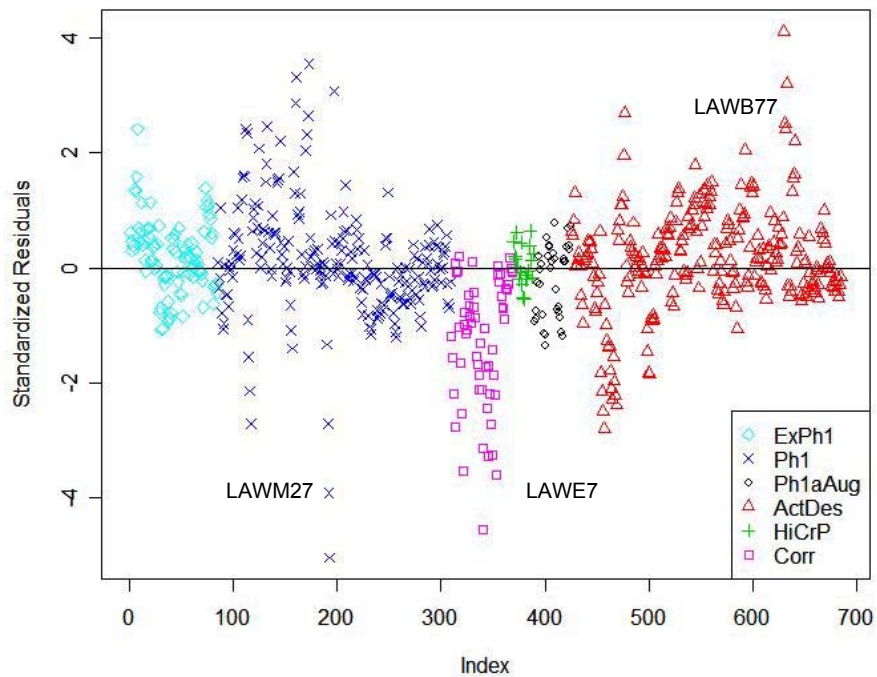


**Figure 8.2. Standardized Residuals Plot for 36-Term ILAW Viscosity Model with the Two Parameters of the Truncated-T2 Equation Expressed as 18-Component Linear Mixture Models.**

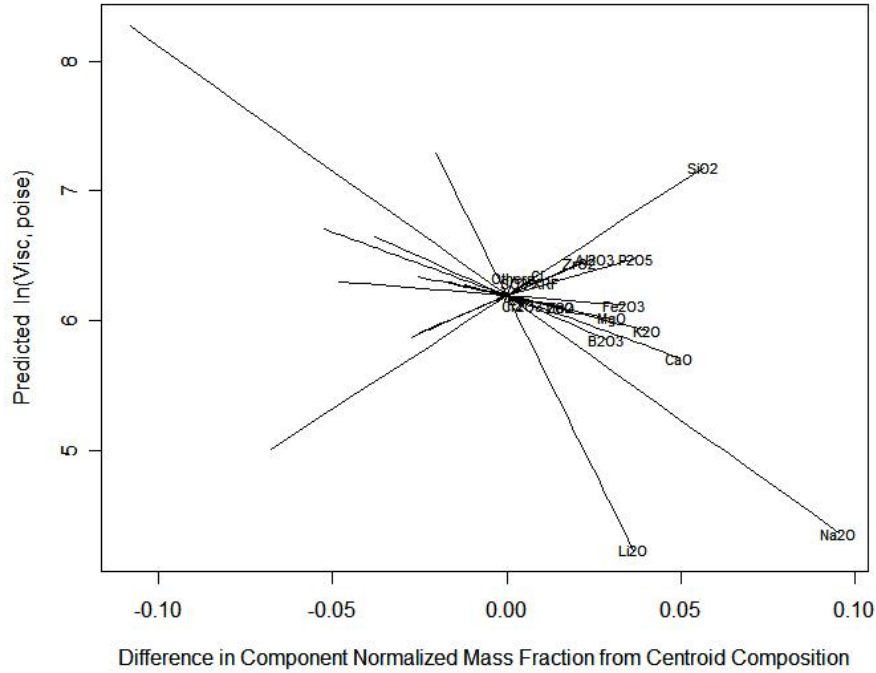


**Figure 8.3a. Response Trace Plot for ILAW Viscosity at 950°C Constructed Using the 36-Term Truncated T2-Linear Mixture Model.**

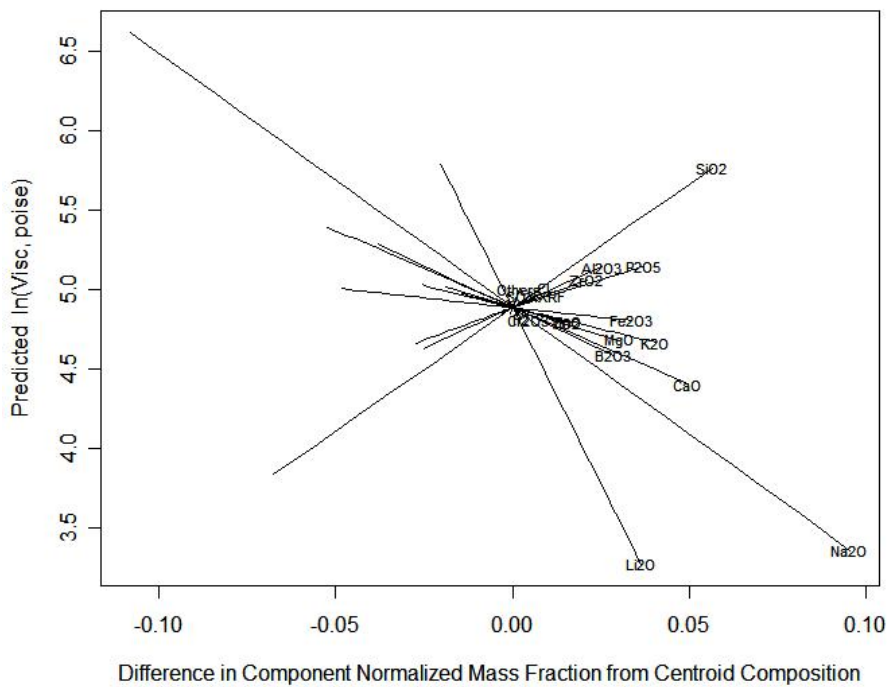


**Figure 8.3b. Response Trace Plot for ILAW Viscosity at 1050°C Constructed Using the 36-Term Truncated T2-Linear Mixture Model.**

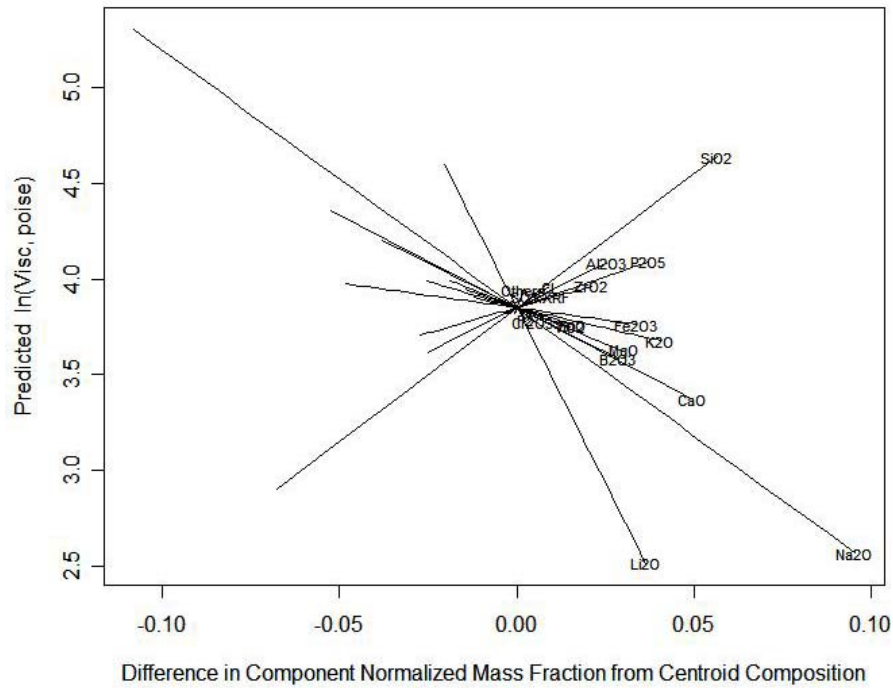


**Figure 8.3c. Response Trace Plot for ILAW Viscosity at 1150°C Constructed Using the 36-Term Truncated T2-Linear Mixture Model.**

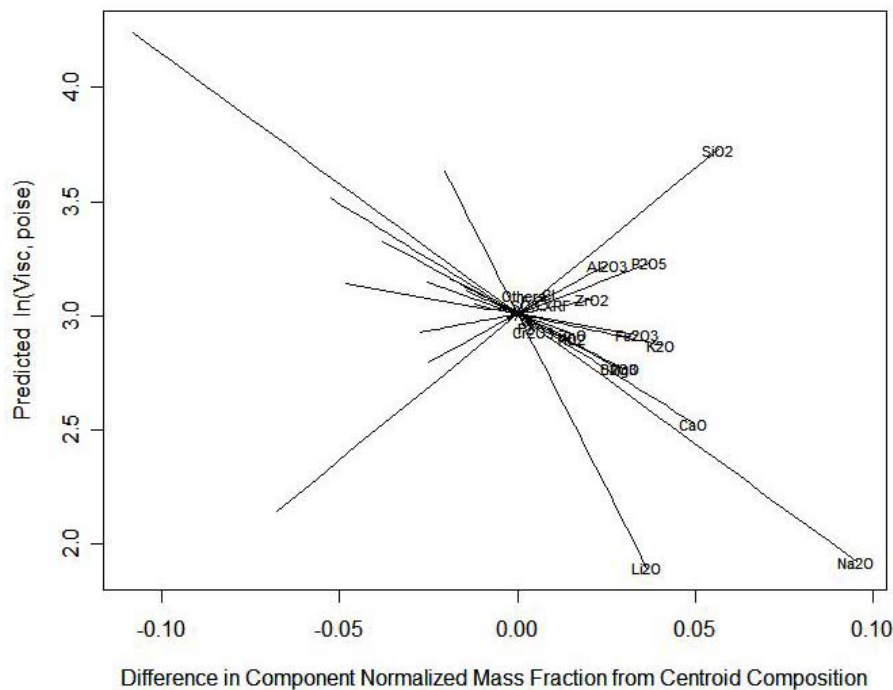


**Figure 8.3d. Response Trace Plot for ILAW Viscosity at 1250°C Constructed Using the 36-Term Truncated T2-Linear Mixture Model.**



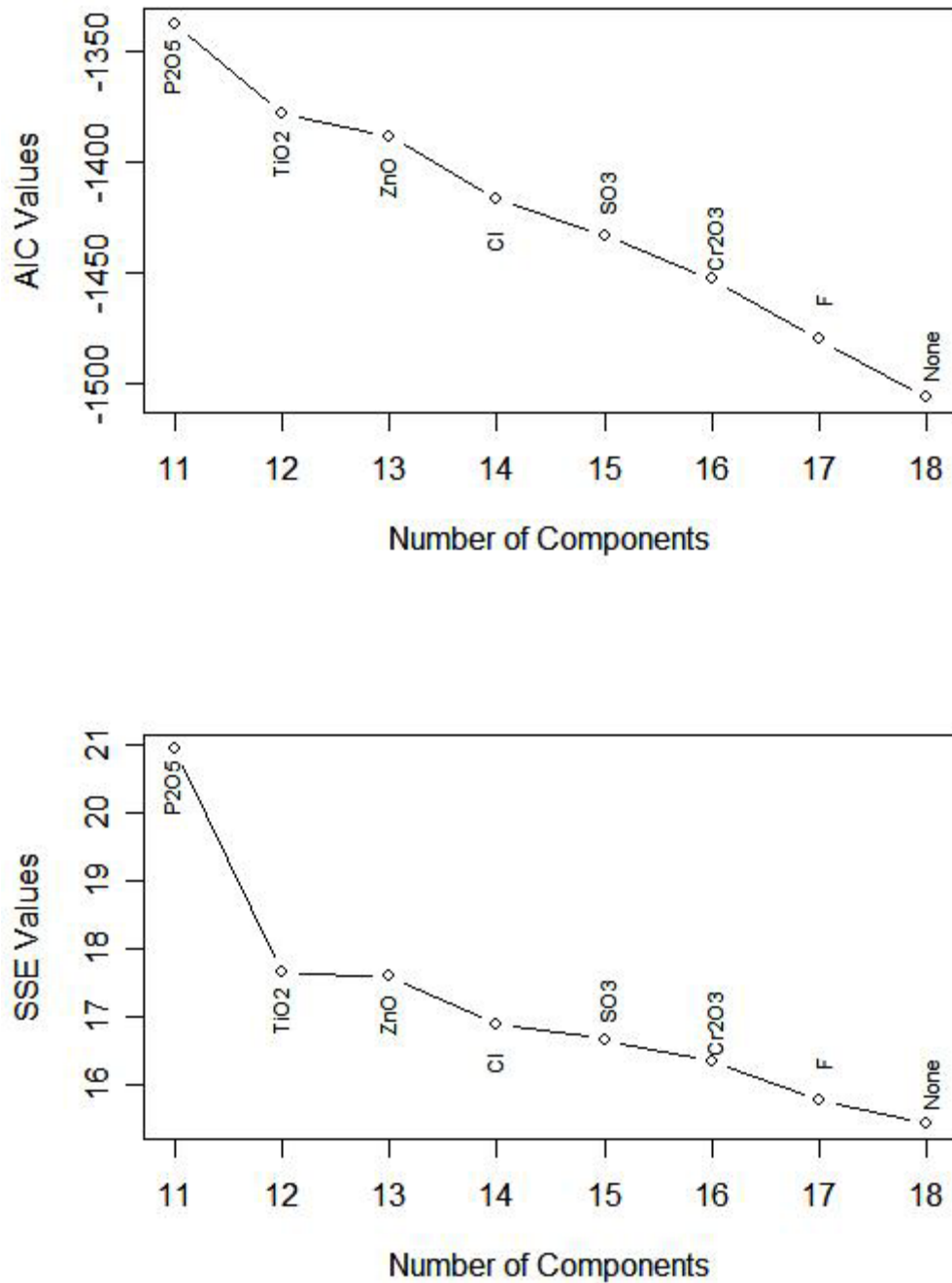


**Figure 8.4. Plots of the Akaike Information Criterion (AIC) and Sum-of-Squared Errors (SSE) Versus the Number of Mixture Components in Truncated T2-Linear Mixture Models for ILAW Viscosity. Reading from right to left, the components combined into Others are listed for each model reduction.**

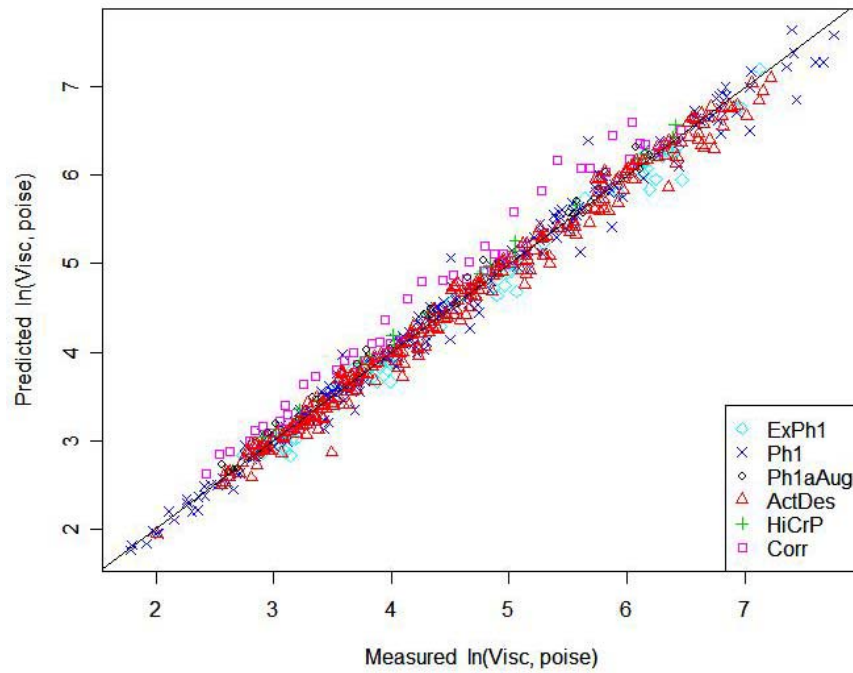


**Figure 8.5. Predicted Versus Measured Plot for 24-Term ILAW Viscosity Model with the Two Parameters of the Truncated-T2 Equation Expressed as Reduced 12-Component Linear Mixture Models.**

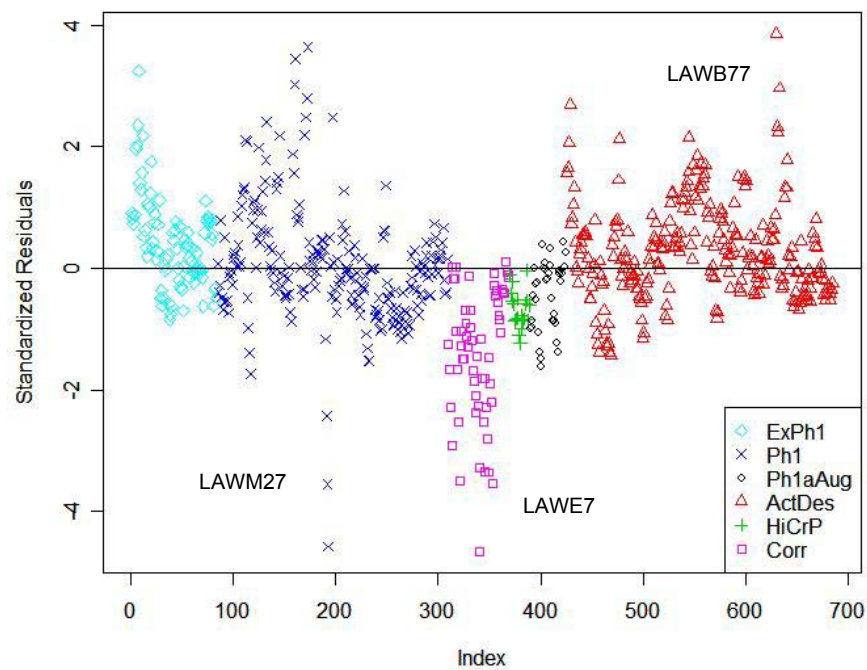


**Figure 8.6. Standardized Residuals Plot for 24-Term ILAW Viscosity Model with the Two Parameters of the Truncated-T2 Equation Expressed as Reduced 12-Component Linear Mixture Models.**

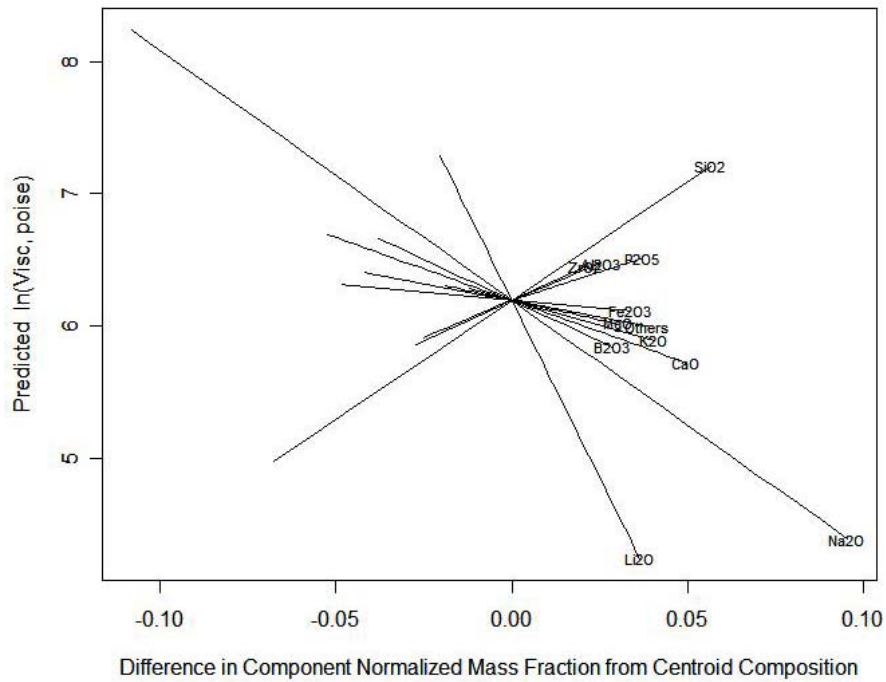


**Figure 8.7a. Response Trace Plot for ILAW Viscosity at 950°C Constructed Using the 24-Term Truncated T2-Linear Mixture Model.**

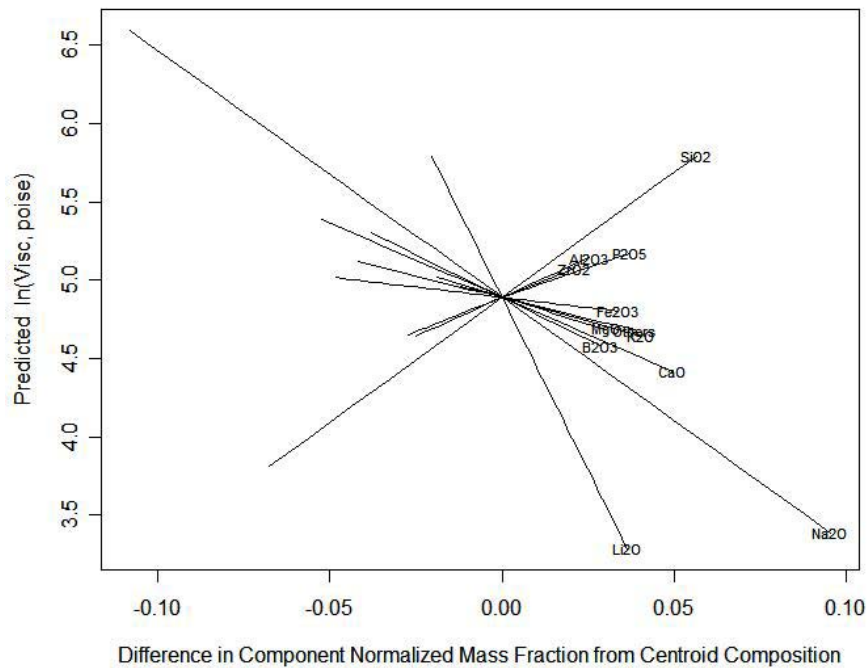


**Figure 8.7b. Response Trace Plot for ILAW Viscosity at 1050°C Constructed Using the 24-Term Truncated T2-Linear Mixture Model.**

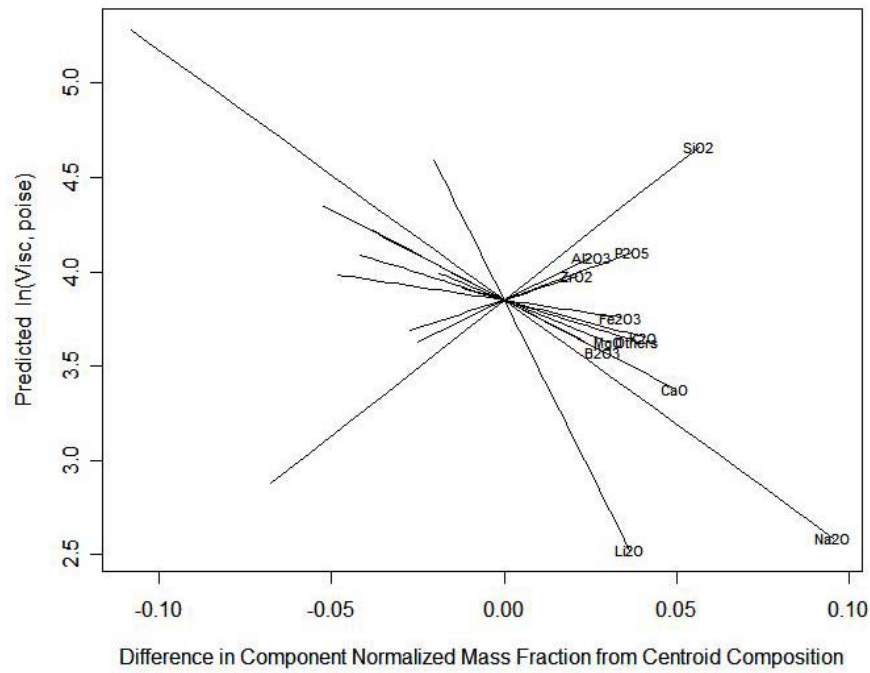


**Figure 8.7c. Response Trace Plot for ILAW Viscosity at 1150°C Constructed Using the 24-Term Truncated T2-Linear Mixture Model.**

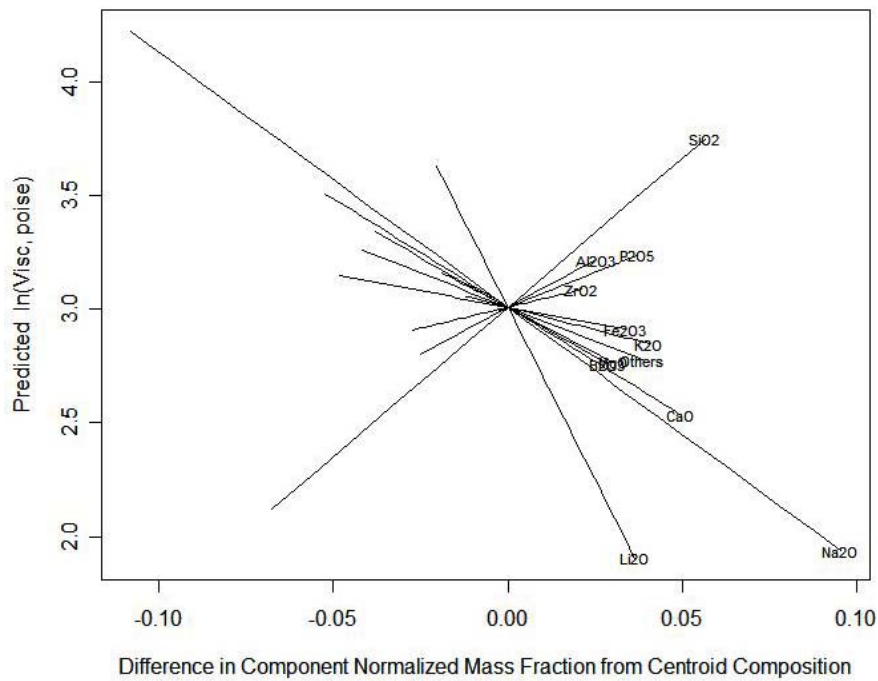


**Figure 8.7d. Response Trace Plot for ILAW Viscosity at 1250°C Constructed Using the 24-Term Truncated T2-Linear Mixture Model.**

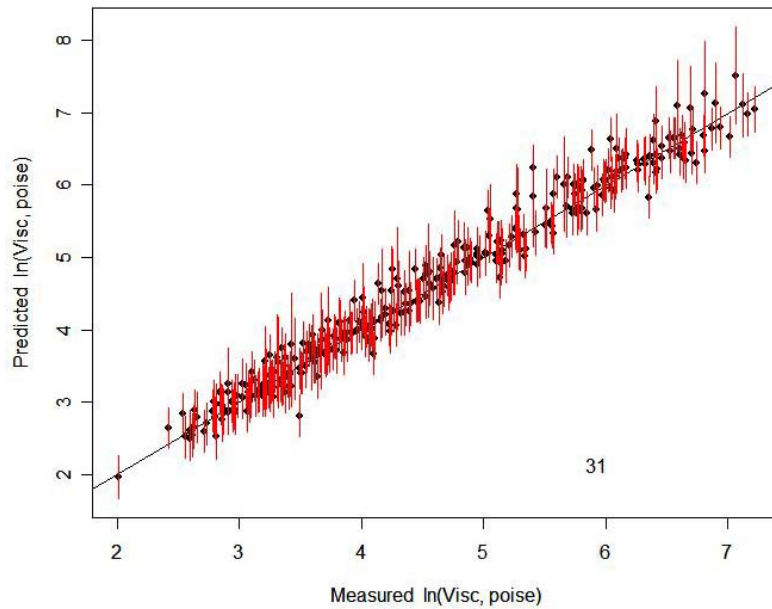


**Figure 8.8.** Predicted Versus Measured Plot for 24-Term Truncated T2-Linear Model on ILAW Viscosity Fitted to Modeling Subset of 86 Glasses and Applied to Validation Subset of 85 Glasses. Error bars are 95% prediction intervals (PIs). The number of glasses whose 95% PIs do not include the measured values (represented by the 45° line) is shown.

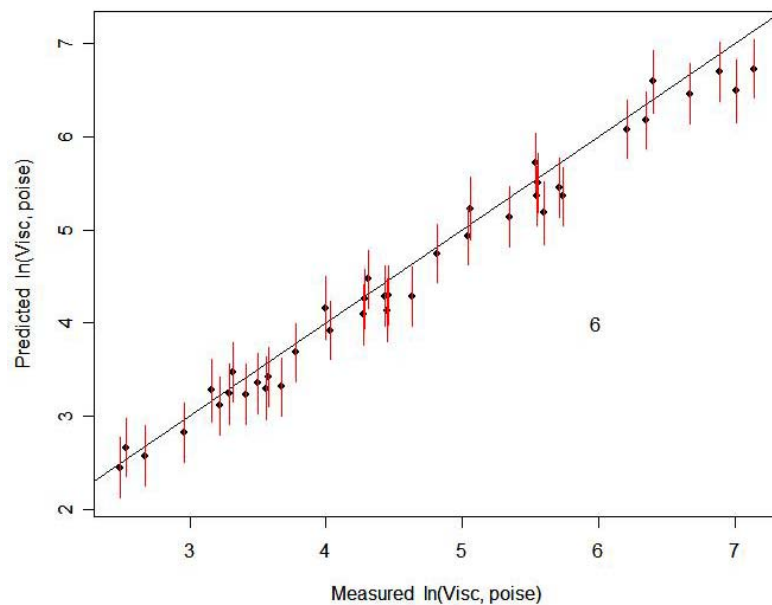


**Figure 8.9.** Predicted Versus Measured Plot for 24-Term Truncated T2-Linear Model on ILAW Viscosity Fitted to 171 Modeling Set Glasses and Applied to 10 Outlying Glasses. Error bars are 95% prediction intervals (PIs). The number of glasses whose 95% PIs do not include the measured values (represented by the 45° line) is shown.

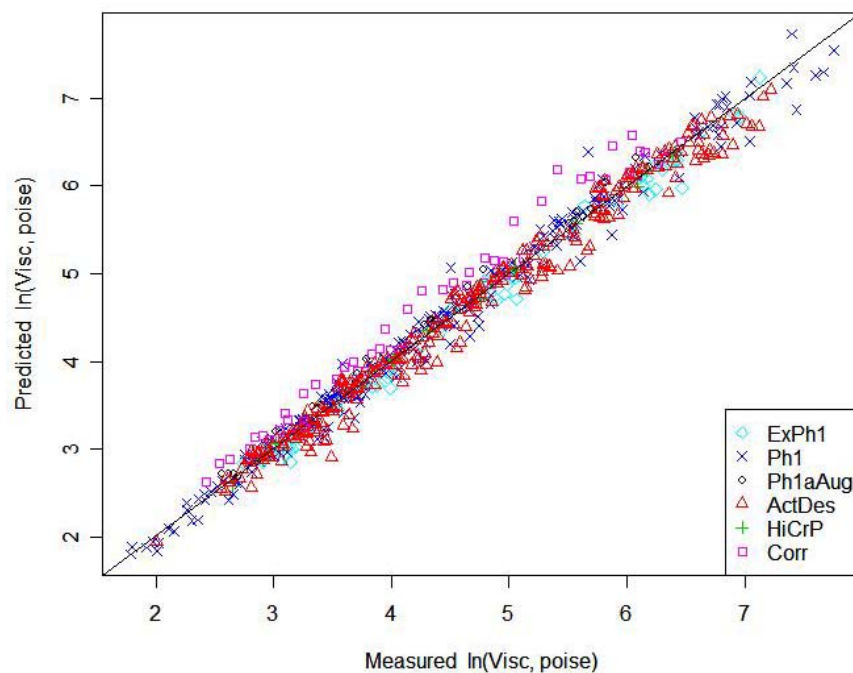


**Figure 8.10. Predicted Versus Measured Plot for 22-Term ILAW Viscosity Model with the Two Parameters of the Truncated-T2 Equation Expressed as Reduced 11-Component Linear Mixture Models.**

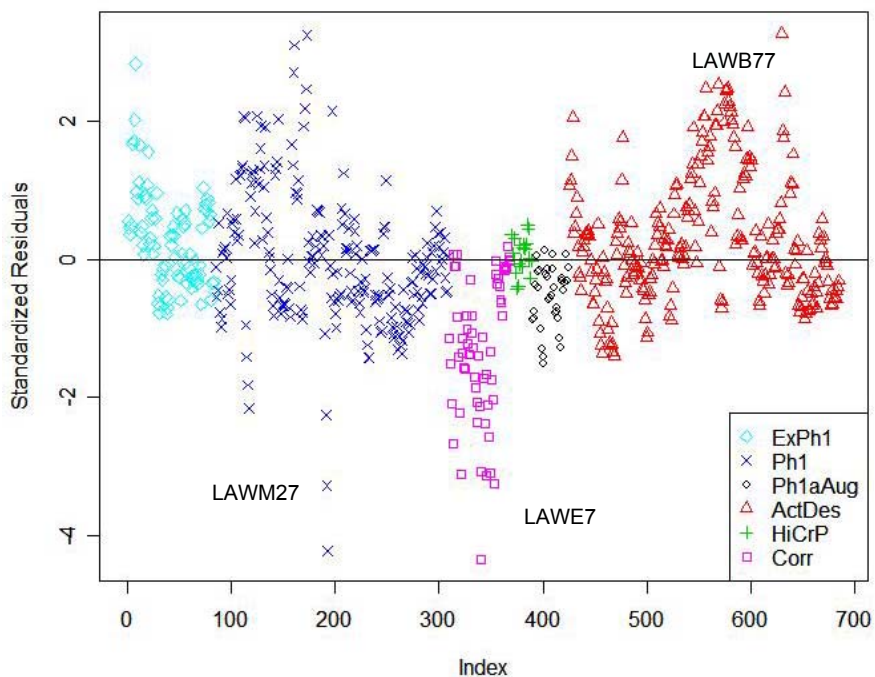


**Figure 8.11. Standardized Residuals Plot for 22-Term ILAW Viscosity Model with the Two Parameters of the Truncated-T2 Equation Expressed as Reduced 11-Component Linear Mixture Models.**

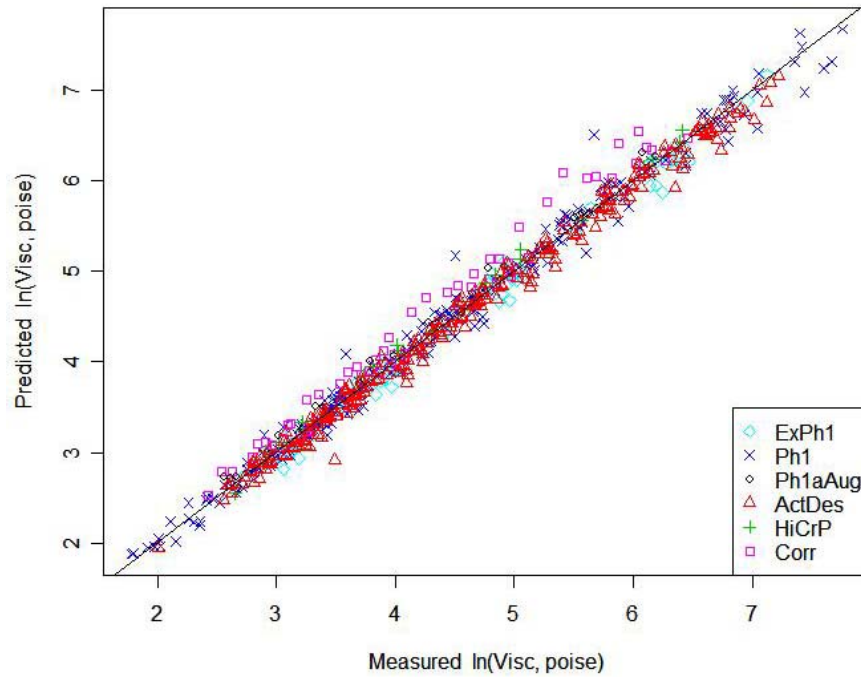


**Figure 8.12. Predicted Versus Measured Plot for 26-Term Reduced Truncated T2-Linear Mixture Model with Four Quadratic Terms on ILAW Viscosity.**

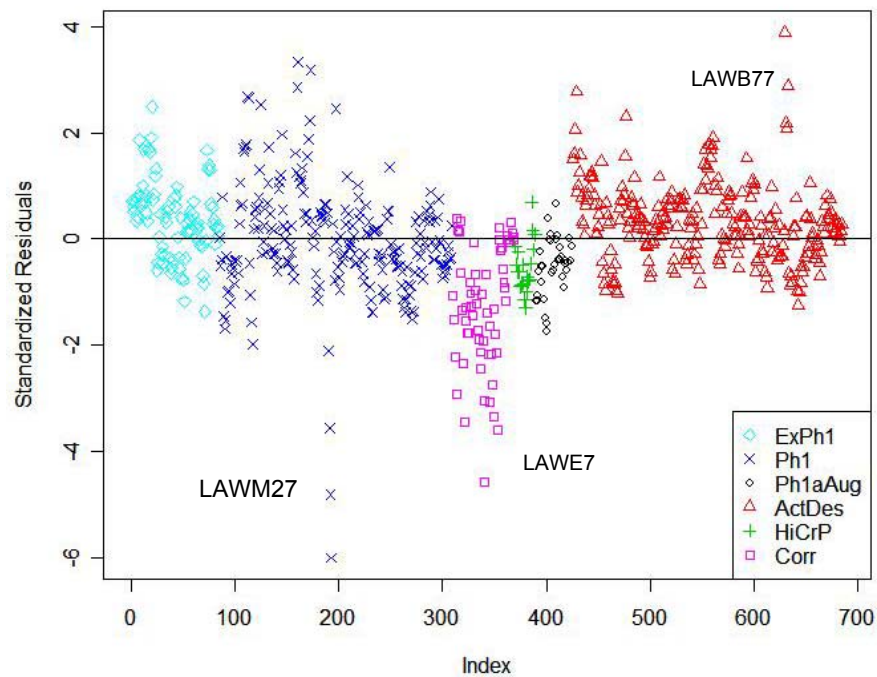


**Figure 8.13. Standardized Residuals Plot for 26-Term Reduced Truncated T2-Linear Mixture Model with Four Quadratic Terms on ILAW Viscosity.**

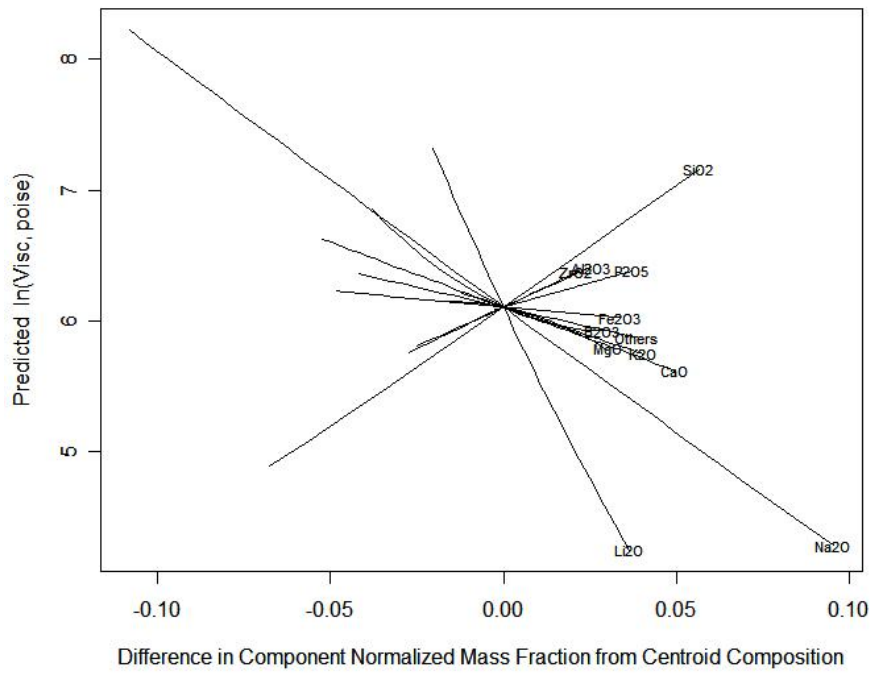


**Figure 8.14a. Response Trace Plot for ILAW Viscosity at 950°C Constructed Using the 26-Term Reduced Truncated T2-Linear Mixture Model with Four Quadratic Terms.**

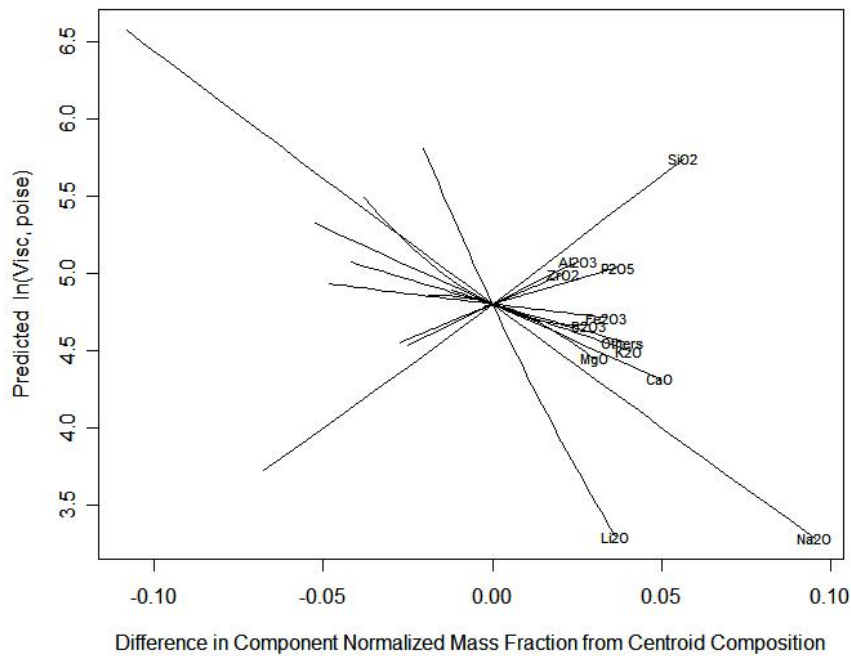


**Figure 8.14b. Response Trace Plot for ILAW Viscosity at 1050°C Constructed Using the 26-Term Reduced Truncated T2-Linear Mixture Model with Four Quadratic Terms.**



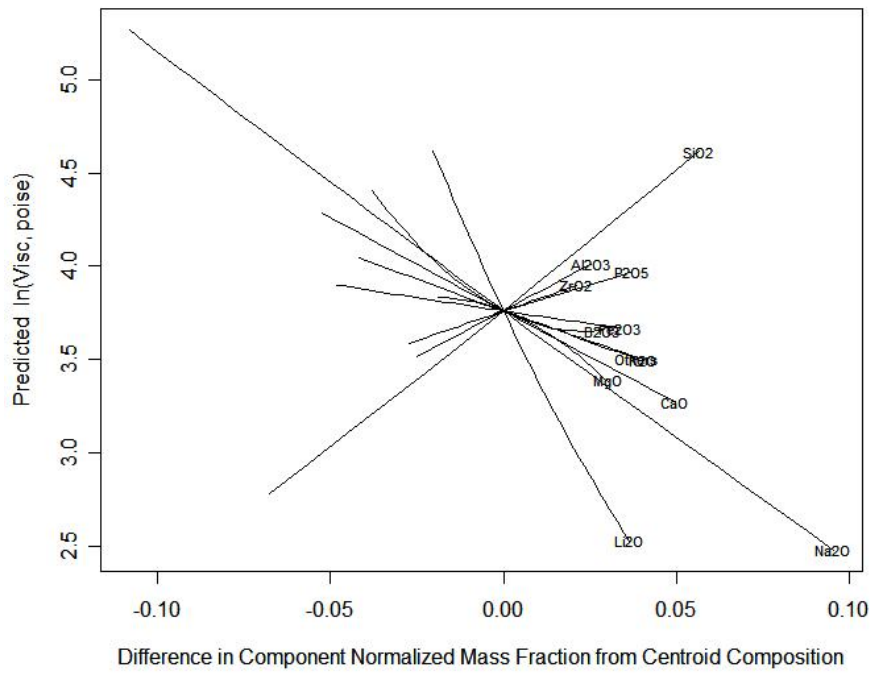


**Figure 8.14c. Response Trace Plot for ILAW Viscosity at 1150°C Constructed Using the 26-Term Reduced Truncated T2-Linear Mixture Model with Four Quadratic Terms.**

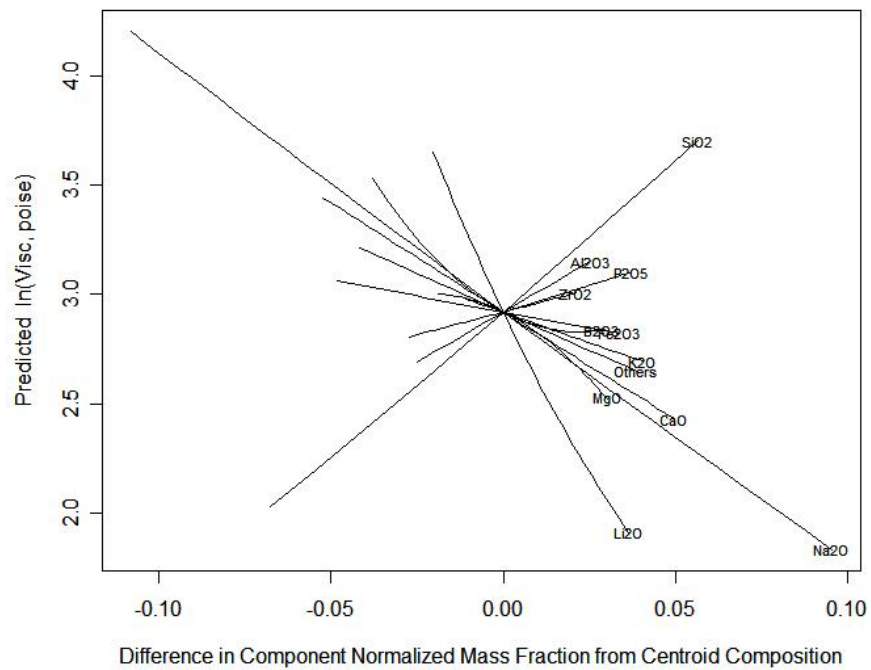


**Figure 8.14d. Response Trace Plot for ILAW Viscosity at 1250°C Constructed Using the 26-Term Reduced Truncated T2-Linear Mixture Model with Four Quadratic Terms.**

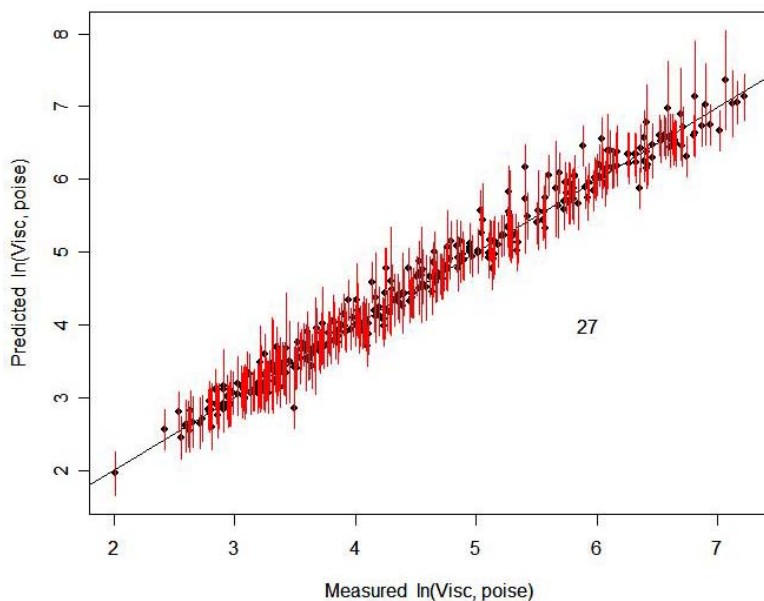


**Figure 8.15. Predicted Versus Measured Plot for the 26-Term Reduced Truncated T2-Linear Model with Four Quadratic Terms on ILAW Viscosity Fitted to Modeling Subset of 86 Glasses and Applied to Validation Subset of 85 Glasses. Error bars are 95% prediction intervals (PIs). The number of glasses whose 95% PIs do not include the measured values (represented by the 45° line) is shown.**

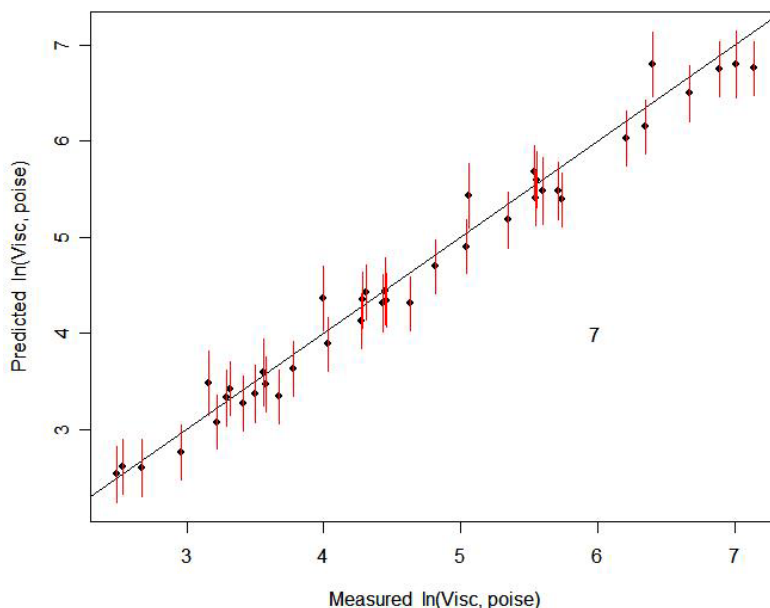


**Figure 8.16. Predicted Versus Measured Plot for the 26-Term Reduced Truncated T2-Linear Model with Four Quadratic Terms on ILAW Viscosity Fitted to 171 Modeling Set Glasses and Applied to 10 Outlying Glasses. Error bars are 95% prediction intervals (PIs). The number of glasses whose 95% PIs do not include the measured values (represented by the 45° line) is shown.**

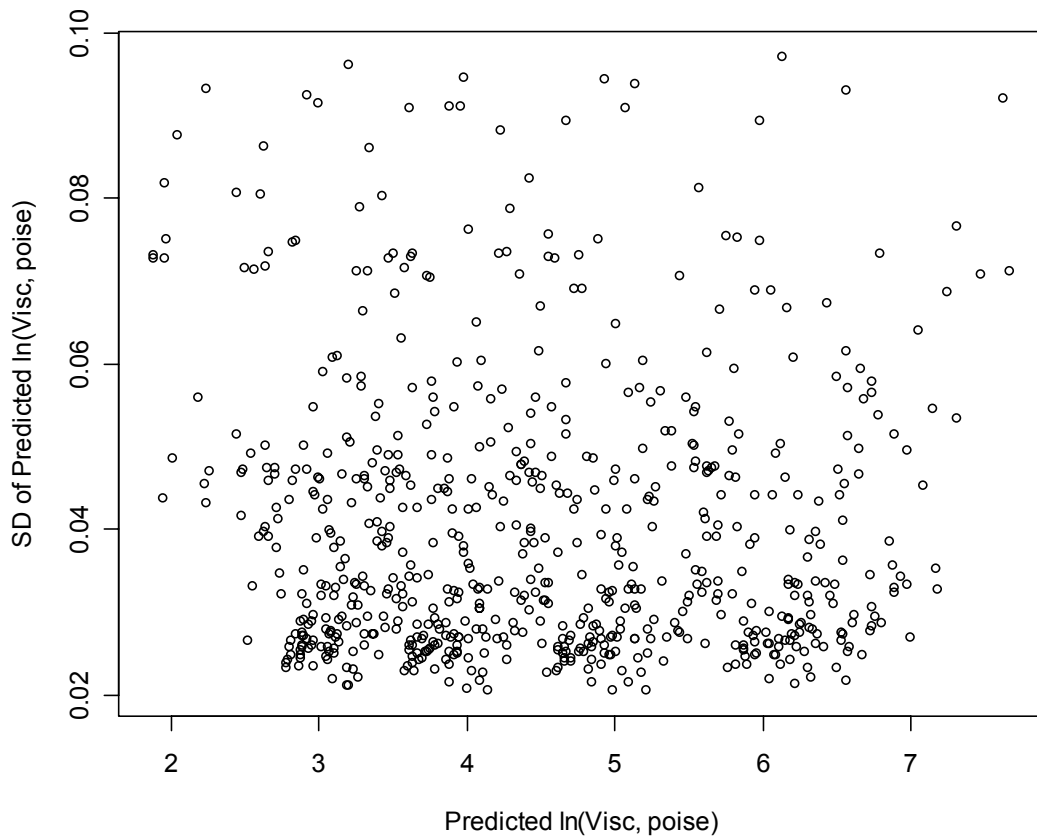


**Figure 8.17. Prediction Standard Deviations versus Predicted Values over the LAW Glass Compositions in the Modeling Dataset and Temperatures 950, 1050, 1150, and 1250°C for the Recommended 26-Term Viscosity Model.**

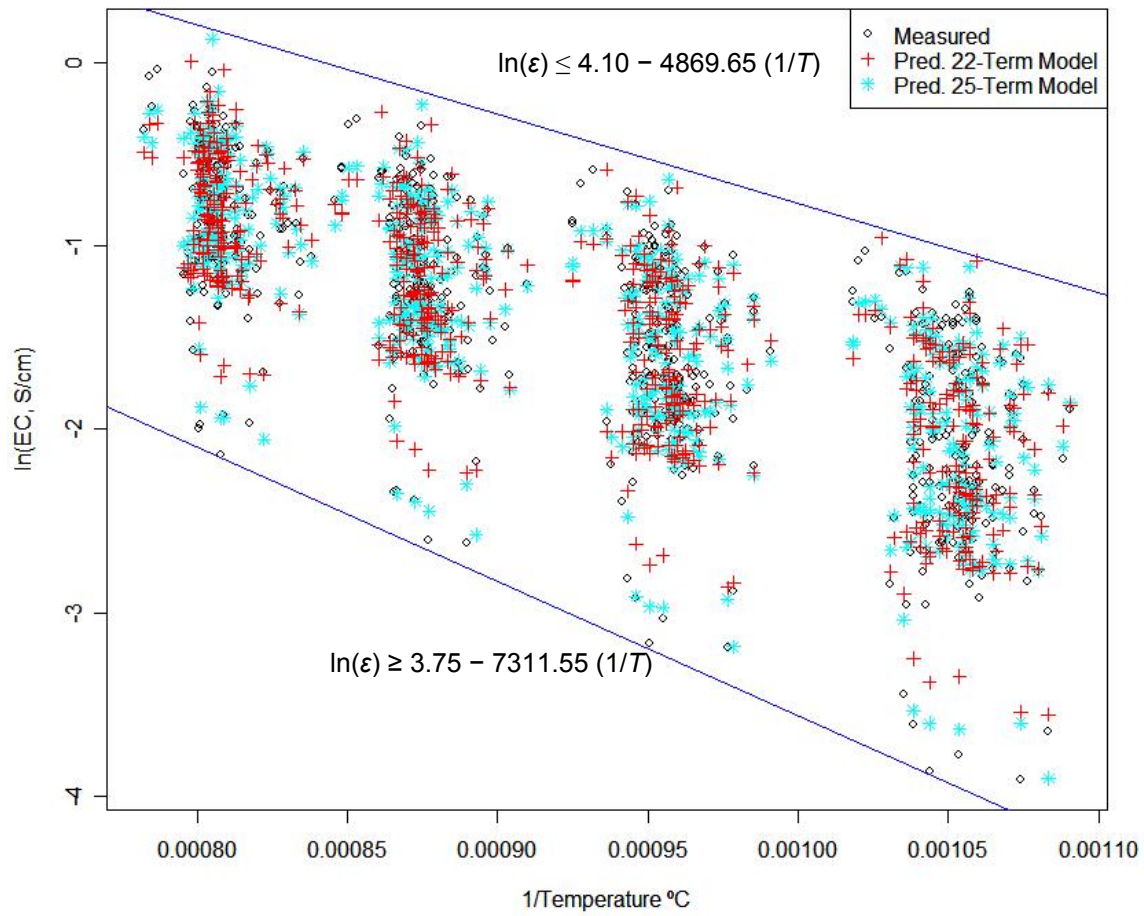


**Figure 9.1. Model Validity Constraints on LAW Glass Electrical Conductivity as Functions of Temperature. The constraints were determined to include all measured and predicted electrical conductivity values for glass-temperature combinations in the electrical conductivity modeling dataset.**

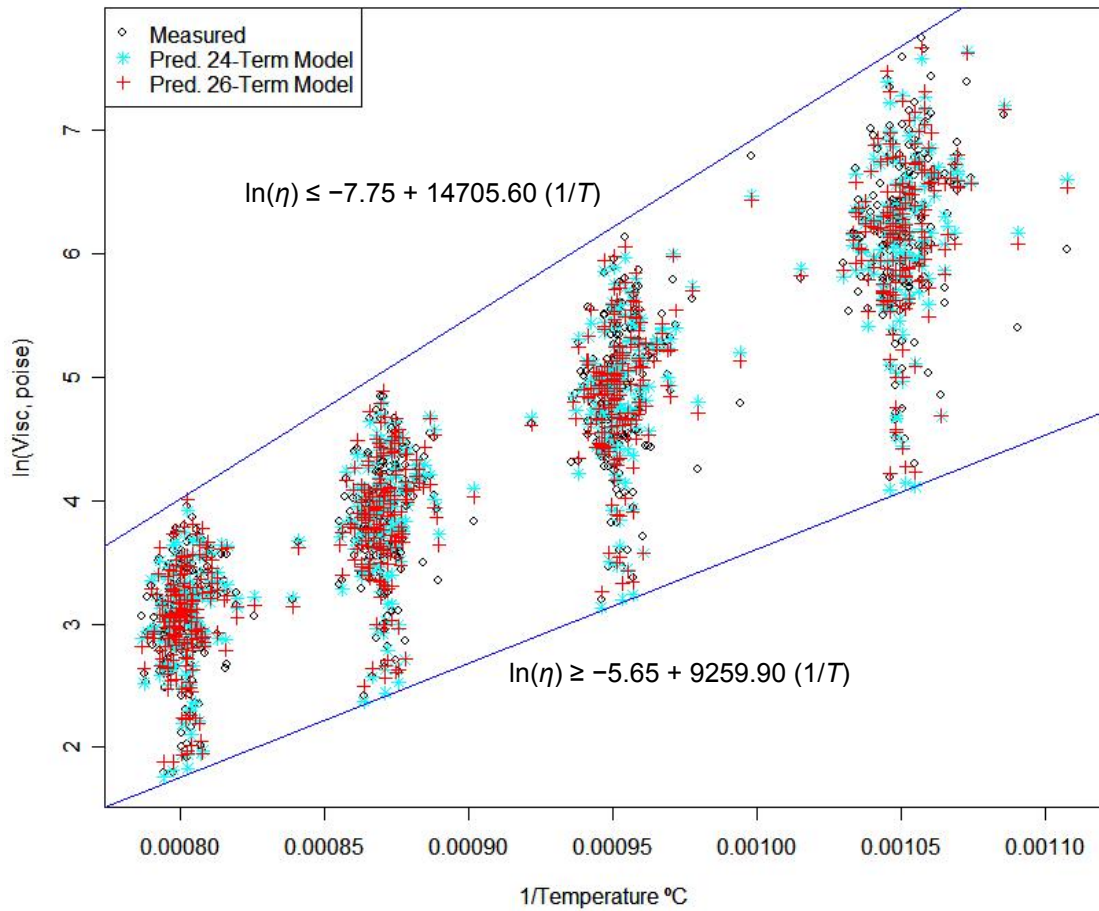


**Figure 9.2. Model Validity Constraints on LAW Glass Viscosity as Functions of Temperature. The constraints were determined to include all measured and predicted viscosity values for glass-temperature combinations in the viscosity modeling dataset.**

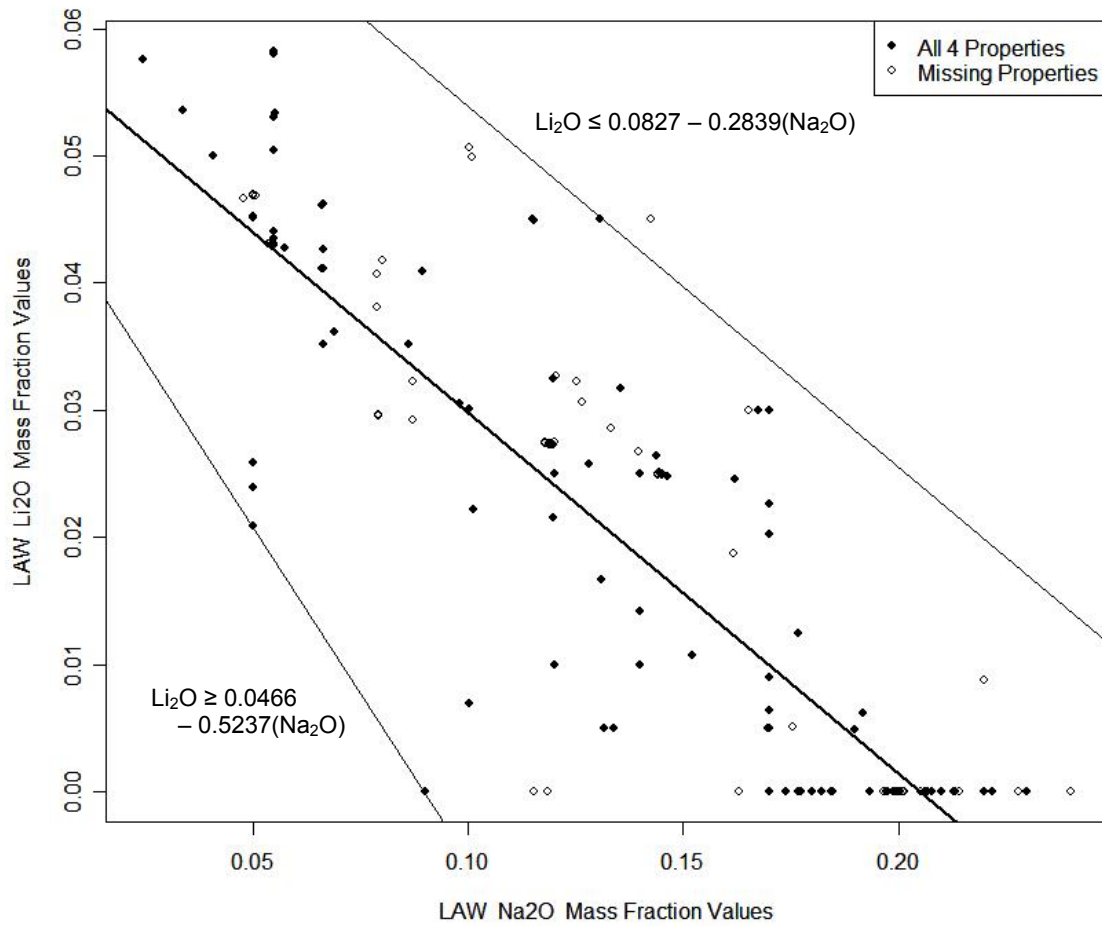


**Figure 9.3. Model Validity Constraints on LAW Glass Li<sub>2</sub>O and Na<sub>2</sub>O Values. The upper constraint line is parallel to the darker “best fit” line, while the lower constraint line was determined by two bounding points. The constraints were determined to include only those LAW glasses having values for all four LAW glass properties.**

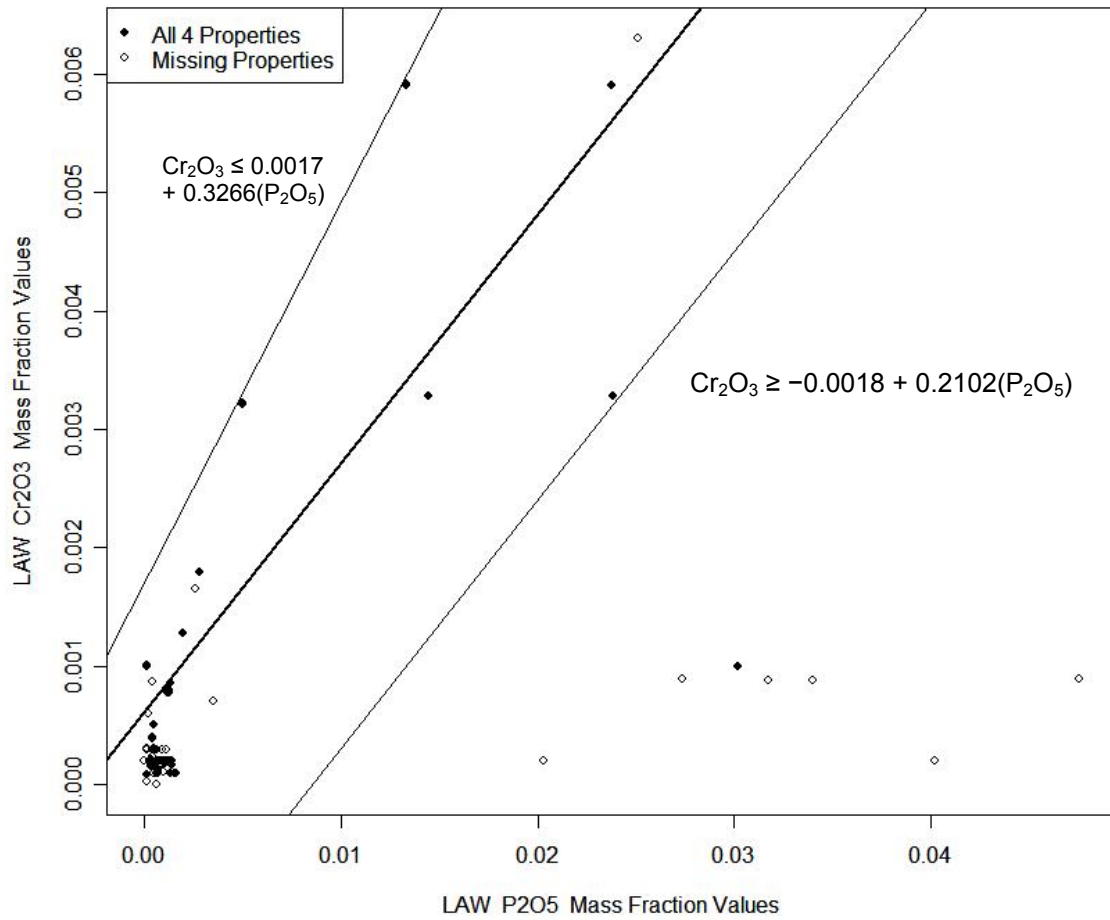


**Figure 9.4. Model Validity Constraints on LAW Glass Cr<sub>2</sub>O<sub>3</sub> and P<sub>2</sub>O<sub>5</sub> Values.** The lower constraint line is parallel to the darker “best fit” line, while the upper constraint line was determined by two bounding points. The upper constraint was determined to include only those LAW glasses having values for all four LAW glass properties, but it was decided to choose a lower constraint that excluded one outlying glass having all property values.

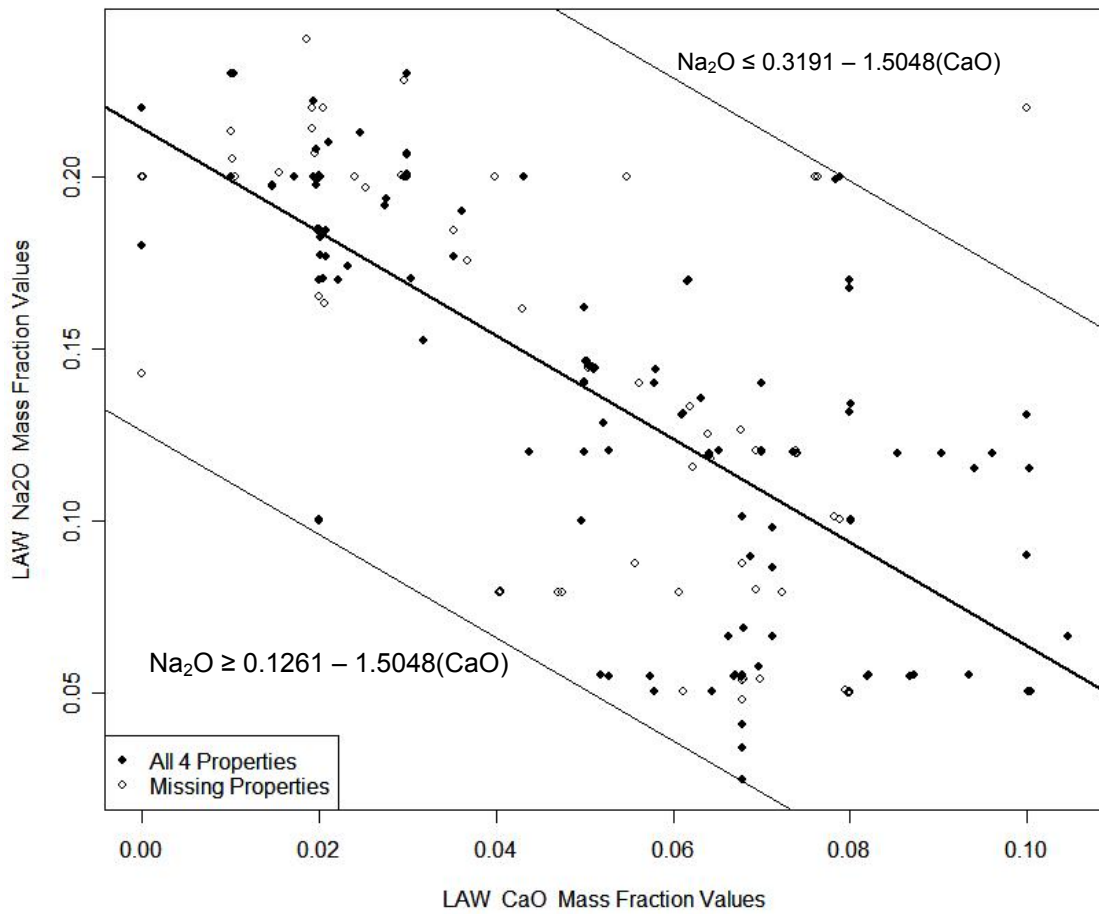


**Figure 9.5. Model Validity Constraints on LAW Glass Na<sub>2</sub>O and CaO Values. The constraint lines are parallel to the darker “best fit” line and were determined to include the LAW glasses having values for all four LAW glass properties.**



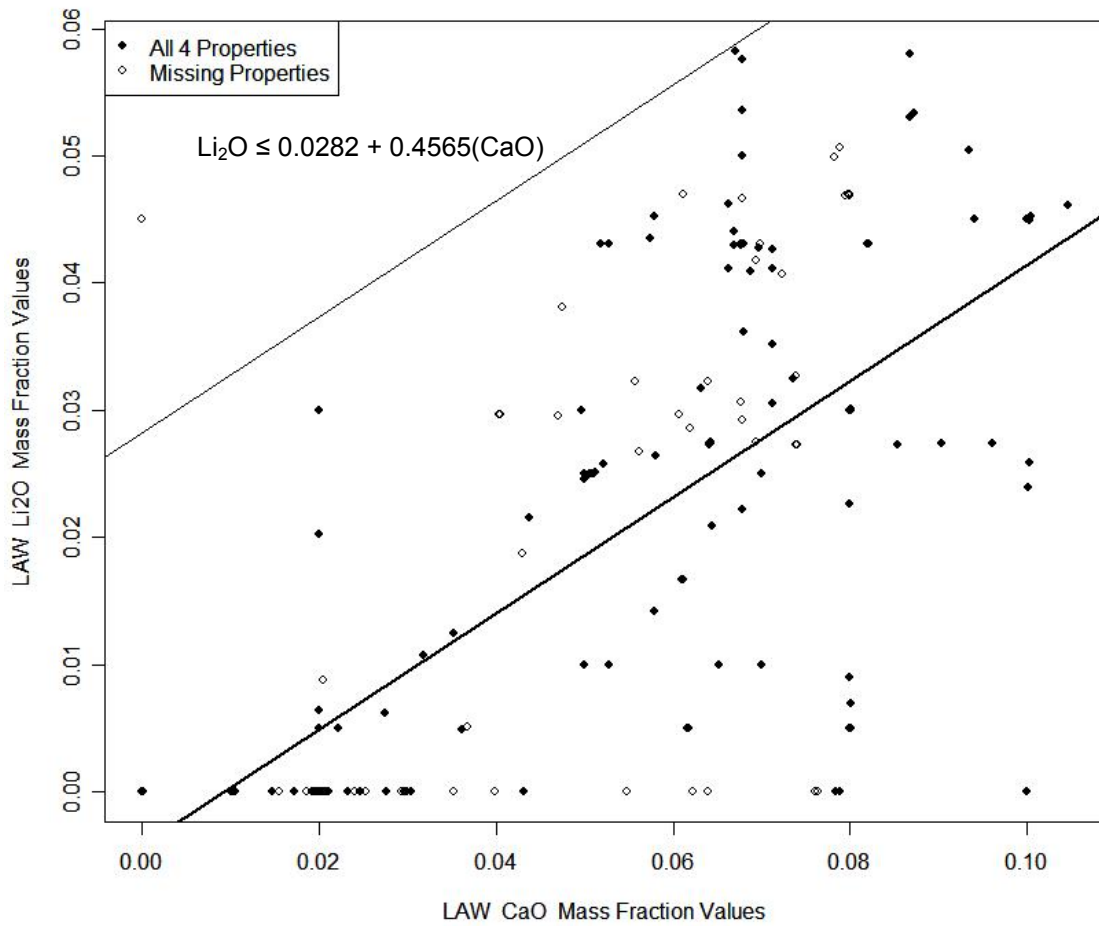


**Figure 9.6. Model Validity Constraint on LAW Glass  $\text{Li}_2\text{O}$  and  $\text{CaO}$  Values. The constraint line is parallel to the darker “best fit” line and was determined to include LAW glasses having values for all four LAW glass properties. There is no lower constraint for this pair of components.**

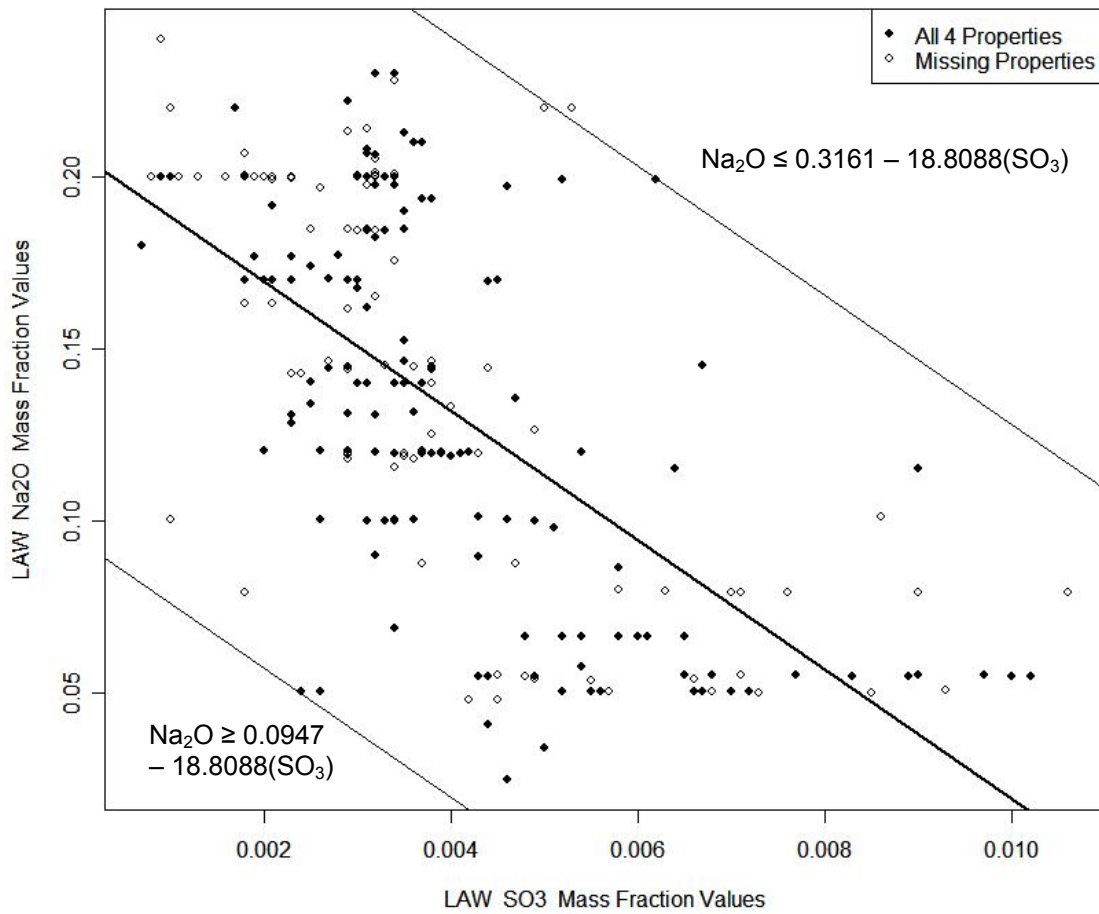


**Figure 9.7. Model Validity Constraints on LAW Glass Na<sub>2</sub>O and SO<sub>3</sub> Values. The constraint lines are parallel to the darker “best fit” line and were determined to include LAW glasses having values for all four LAW glass properties.**

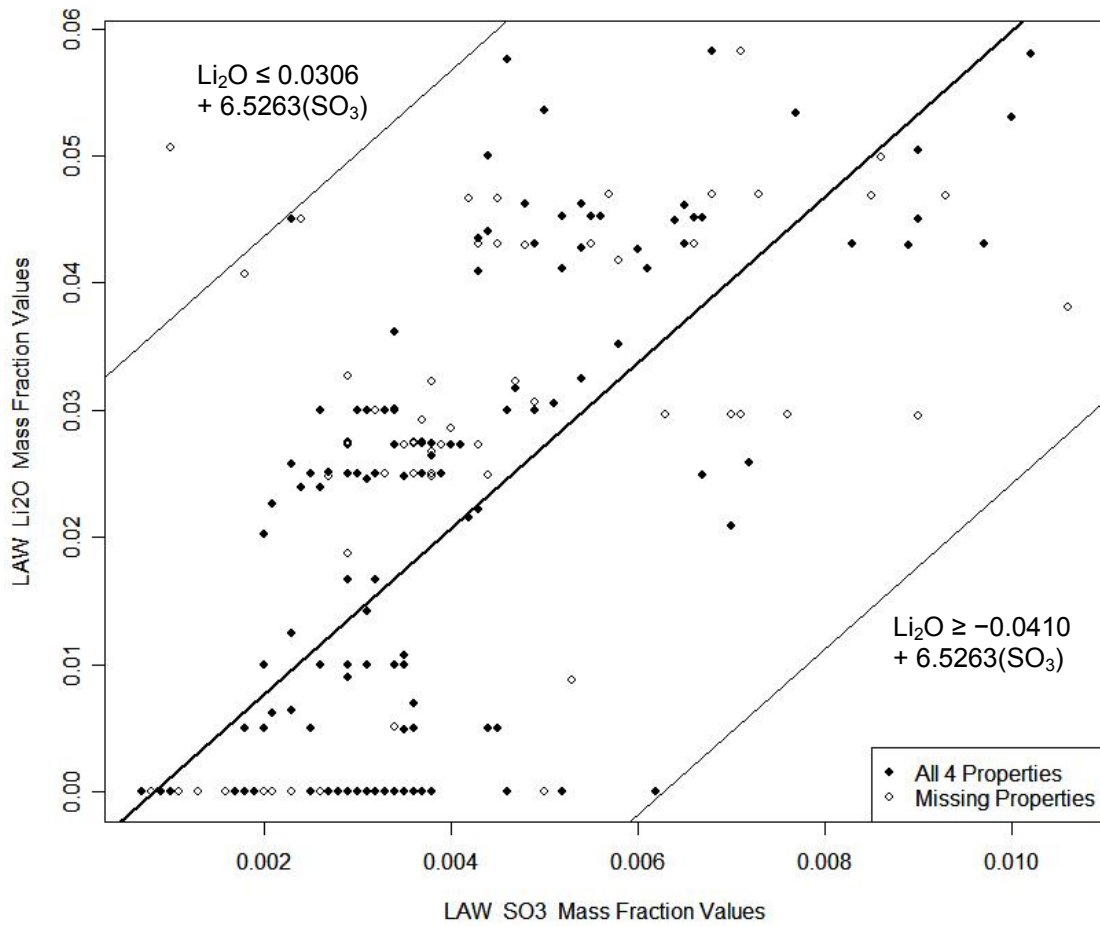


**Figure 9.8. Model Validity Constraints on LAW Glass Li<sub>2</sub>O and SO<sub>3</sub> Values.** The constraint lines are parallel to the darker “best fit” line and were determined to include the LAW glass compositions having data for all four LAW glass properties.

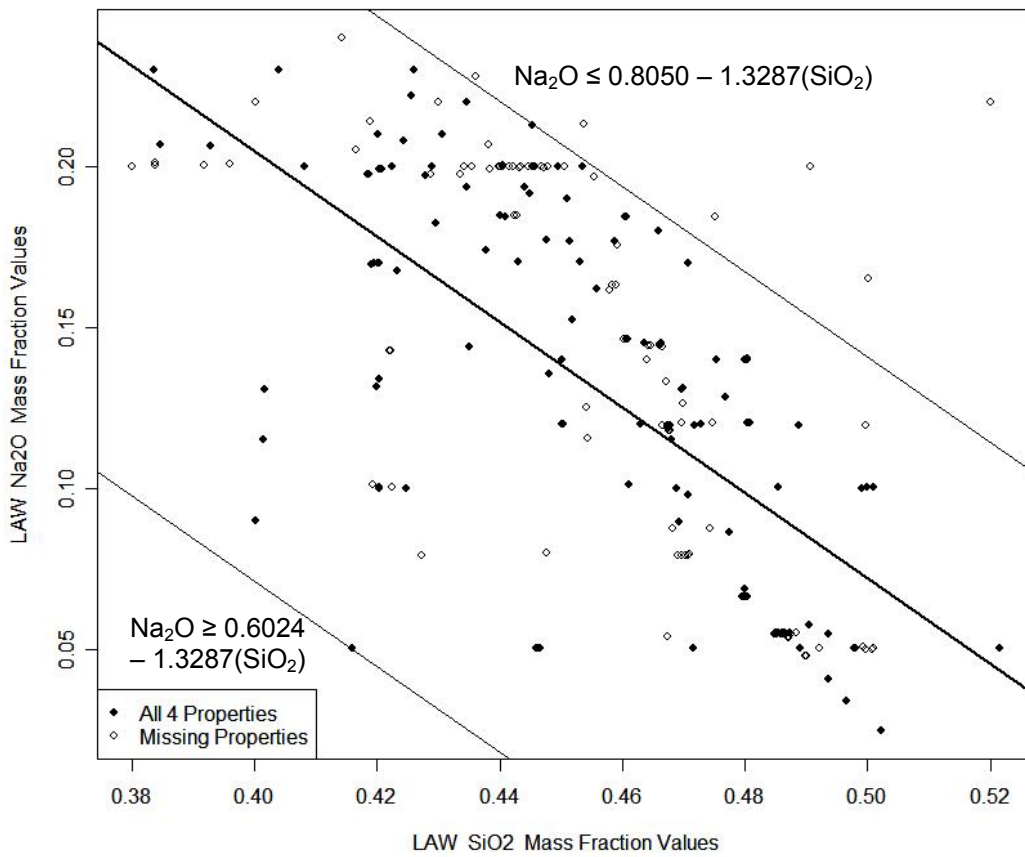


**Figure 9.9. Model Validity Constraints on LAW Glass Na<sub>2</sub>O and SiO<sub>2</sub> Values. The constraint lines are parallel to the darker “best fit” line and were determined to include the LAW glass compositions having data for all four LAW glass properties.**

## **Appendix A**

### **Normalized Compositions (in mol%) of 271 LAW Simulated and Actual Waste Glasses**

## **Appendix A**

### **Normalized Compositions (in mol%) of 271 LAW Simulated and Actual Waste Glasses**

This appendix contains tables of normalized mol% compositions of 271 LAW simulated and actual waste glasses calculated from the normalized wt% compositions given in Table 3.2. The normalized wt% compositions in Table 3.2 were based on XRF analyzed or estimated values of SO<sub>3</sub> and target values of the remaining components.

**Table A.1. Normalized Compositions (in mol%) of 271 LAW Simulated and Actual Waste Glasses.**

Glass ID	Al <sub>2</sub> O <sub>3</sub>	B <sub>2</sub> O <sub>3</sub>	CaO	Cl	Cr <sub>2</sub> O <sub>3</sub>	F	Fe <sub>2</sub> O <sub>3</sub>	K <sub>2</sub> O	Li <sub>2</sub> O	MgO	Na <sub>2</sub> O	P <sub>2</sub> O <sub>5</sub>	SO <sub>3</sub>	SiO <sub>2</sub>	TiO <sub>2</sub>	ZnO	ZrO <sub>2</sub>	Others	Sum
LAWA44R10	4.07	8.56	2.38	1.23	0.01	0.04	2.93	0.36	0.00	3.31	21.60	0.03	0.08	49.64	1.67	2.44	1.62	0.05	100
LAWA53	4.02	5.90	9.32	1.21	0.01	0.04	3.12	0.35	0.00	2.44	21.40	0.03	0.52	46.63	0.92	2.44	1.61	0.05	100
LAWA56	4.08	11.70	2.37	1.23	0.01	0.04	3.16	0.36	0.00	2.47	21.71	0.03	0.44	47.32	0.93	2.47	1.63	0.05	100
LAWA88	4.01	9.37	2.39	0.62	0.00	0.00	2.33	1.85	0.00	2.46	21.72	0.07	0.16	49.27	1.68	2.44	1.63	0.00	100
LAWA88R1	4.01	9.37	2.39	0.63	0.00	0.00	2.33	1.84	0.00	2.46	21.71	0.07	0.16	49.26	1.68	2.44	1.63	0.01	100
LAWA102R1	3.81	9.22	5.79	0.60	0.01	0.10	2.17	0.18	5.37	2.37	15.06	0.12	0.54	49.65	0.92	2.41	1.57	0.11	100
LAWA126	3.67	9.37	2.36	0.37	0.01	1.05	2.30	2.74	0.00	2.44	19.79	0.07	0.26	48.78	1.66	2.42	1.61	1.10	100
LAWA128	3.94	6.76	2.47	0.38	0.01	1.05	2.41	2.74	0.00	1.95	19.83	0.08	0.25	51.07	1.74	2.53	1.69	1.10	100
LAWA128R1	3.94	6.76	2.47	0.38	0.01	1.05	2.41	2.74	0.00	1.95	19.84	0.08	0.27	51.09	1.74	2.53	1.69	1.05	100
LAWA130	3.88	8.44	2.43	0.37	0.01	1.04	1.18	2.70	0.00	1.92	19.55	0.07	0.27	50.33	1.72	3.34	1.67	1.09	100
LAWB65	3.81	8.97	7.49	0.00	0.04	0.23	2.08	0.17	9.05	4.63	5.55	0.01	0.70	50.70	1.10	3.60	1.61	0.25	100
LAWB66	3.80	8.94	9.15	0.00	0.04	0.23	2.08	0.17	9.02	4.61	5.53	0.01	0.51	50.53	1.09	2.43	1.61	0.24	100
LAWB68	3.80	7.59	9.15	0.00	0.04	0.23	2.08	0.17	9.02	4.62	5.54	0.01	0.65	50.56	1.09	3.59	1.61	0.24	100
LAWB78	3.78	11.11	7.97	0.02	0.02	0.26	1.28	0.15	6.40	4.62	9.90	0.04	0.40	49.07	0.00	3.08	1.60	0.28	100
LAWB79	3.76	11.05	7.92	0.02	0.02	0.26	1.27	0.15	7.33	4.60	8.68	0.04	0.45	49.52	0.00	3.07	1.59	0.28	100
LAWB80	3.78	11.11	7.97	0.02	0.02	0.26	1.28	1.33	7.37	4.62	6.70	0.04	0.45	50.07	0.00	3.08	1.60	0.28	100
LAWB83	3.81	9.05	7.59	0.02	0.02	0.20	2.08	0.13	9.06	4.63	5.54	0.04	0.38	50.80	1.09	3.74	1.61	0.21	100
LAWB84	3.81	9.05	7.48	0.02	0.02	0.20	2.08	0.13	9.25	4.63	5.54	0.04	0.34	50.79	1.09	3.73	1.61	0.21	100
LAWB85	3.82	10.43	5.93	0.02	0.02	0.20	2.09	0.13	9.09	4.64	5.56	0.04	0.39	50.98	1.10	3.75	1.62	0.21	100
LAWB86	3.81	11.21	6.42	0.02	0.02	0.20	2.08	0.13	9.15	4.63	5.55	0.04	0.34	50.85	0.00	3.74	1.61	0.21	100
C100-G-136B	3.87	9.34	7.36	0.22	0.01	0.20	2.61	0.10	5.89	2.42	12.34	0.11	0.32	50.10	0.90	2.39	1.58	0.22	100
LAWC27	3.71	10.84	9.43	0.19	0.01	0.18	0.00	0.09	5.66	2.30	11.94	0.09	0.32	50.36	0.87	2.30	1.52	0.19	100
LAWC32	4.01	9.08	10.14	0.20	0.01	0.18	0.96	0.09	5.76	2.34	12.14	0.09	0.30	48.97	0.88	3.11	1.54	0.19	100
LAWM1	5.79	5.66	11.71	0.04	0.00	0.03	3.29	2.79	9.89	0.00	5.30	0.01	0.42	48.56	2.46	4.03	0.00	0.03	100
LAWM2	2.07	5.20	10.76	1.36	0.13	0.95	3.02	0.00	9.09	7.48	4.87	0.42	0.50	47.18	2.27	3.71	0.00	0.99	100
LAWM3	5.58	5.45	11.27	0.04	0.00	0.02	3.17	0.00	9.46	7.84	11.71	0.01	0.50	42.08	0.00	0.78	2.05	0.03	100
LAWM4	2.23	12.15	11.60	0.04	0.00	0.03	2.26	2.76	9.80	0.00	5.25	0.01	0.45	44.84	2.44	4.00	2.11	0.03	100
LAWM5	5.88	5.74	6.85	0.04	0.00	0.03	3.34	2.83	10.03	0.00	5.37	0.01	0.46	53.94	2.50	0.82	2.16	0.03	100
LAWM6	5.88	10.15	11.87	0.04	0.00	0.03	3.34	2.83	0.00	8.26	9.67	0.01	0.27	44.32	2.50	0.82	0.00	0.03	100
LAWM7	3.33	6.24	11.16	0.04	0.00	0.02	3.13	0.00	5.40	7.76	5.05	0.01	0.56	54.15	2.35	0.77	0.00	0.03	100
LAWM8	5.49	11.61	7.13	1.40	0.13	0.98	0.00	0.00	4.33	7.71	5.02	0.44	0.54	46.03	2.33	3.82	2.02	1.02	100
LAWM9	2.23	5.60	11.58	1.47	0.14	1.02	3.25	2.76	5.19	0.00	5.24	0.46	0.19	53.72	0.00	3.99	2.11	1.07	100
LAWM10	5.41	11.44	10.93	1.38	0.13	0.97	0.00	0.00	9.23	0.00	12.92	0.43	0.18	40.94	2.30	0.75	1.99	1.01	100

**Table A.1. Normalized Compositions (in mol%) of 271 LAW Simulated and Actual Waste Glasses (continued).**

Glass ID	Al <sub>2</sub> O <sub>3</sub>	B <sub>2</sub> O <sub>3</sub>	CaO	Cl	Cr <sub>2</sub> O <sub>3</sub>	F	Fe <sub>2</sub> O <sub>3</sub>	K <sub>2</sub> O	Li <sub>2</sub> O	MgO	Na <sub>2</sub> O	P <sub>2</sub> O <sub>5</sub>	SO <sub>3</sub>	SiO <sub>2</sub>	TiO <sub>2</sub>	ZnO	ZrO <sub>2</sub>	Others	Sum
LAWM11	2.14	11.65	10.46	0.04	0.00	0.02	2.07	2.65	9.39	0.00	11.55	0.01	0.70	48.53	0.00	0.77	0.00	0.03	100
LAWM12	2.13	11.61	0.00	1.40	0.13	0.98	0.90	2.64	9.37	3.04	14.30	0.44	0.18	43.68	2.34	3.82	2.02	1.02	100
LAWM13	2.27	5.70	11.79	0.77	0.07	0.54	3.31	2.66	0.00	0.00	23.46	0.24	0.41	44.00	2.48	1.76	0.00	0.56	100
LAWM14	2.10	5.26	2.23	0.03	0.00	0.02	0.00	0.00	1.80	7.57	21.67	0.01	0.40	52.83	2.29	3.75	0.00	0.03	100
LAWM15	5.70	8.68	0.00	1.46	0.14	1.02	2.54	0.00	0.00	5.97	22.92	0.45	0.14	46.71	2.42	0.79	0.00	1.06	100
LAWM16	5.11	11.23	9.29	0.04	0.00	0.03	2.65	0.07	6.54	1.62	10.51	0.01	0.27	46.03	2.04	4.00	0.53	0.03	100
LAWM17	3.27	11.49	2.63	0.04	0.00	0.03	2.71	1.42	1.12	5.79	18.29	0.01	0.17	46.60	0.42	4.10	1.89	0.03	100
LAWM18	5.01	11.01	9.11	1.44	0.14	1.01	2.60	0.07	6.42	1.59	10.31	0.45	0.27	44.66	2.00	1.57	1.30	1.05	100
LAWM19	5.08	11.16	9.23	1.46	0.14	1.02	0.81	1.37	1.08	1.61	13.76	0.46	0.29	45.25	0.41	3.98	1.84	1.06	100
LAWM20	3.02	6.19	8.78	1.39	0.13	0.97	0.77	1.31	4.66	5.35	16.88	0.43	0.16	43.03	0.39	3.78	1.75	1.01	100
LAWM21	3.22	10.26	9.36	0.04	0.00	0.03	2.67	1.39	6.59	1.63	10.59	0.01	0.38	45.86	2.05	4.03	1.86	0.03	100
LAWM22	5.16	6.61	2.34	1.48	0.14	1.04	2.68	1.40	1.10	5.71	18.03	0.46	0.37	45.95	0.55	4.04	1.87	1.08	100
LAWM23	3.05	6.25	8.87	1.40	0.13	0.98	0.78	1.32	6.24	1.54	10.03	0.44	0.26	50.13	1.95	3.82	1.77	1.02	100
LAWM24	5.25	11.52	2.38	0.04	0.00	0.03	2.72	1.42	1.43	1.66	18.34	0.01	0.19	52.37	0.42	1.64	0.54	0.03	100
LAWM25R1	4.85	10.66	2.21	1.40	0.13	0.97	1.43	1.31	6.21	5.37	9.98	0.44	0.20	51.40	0.39	1.52	0.50	1.02	100
LAWM26	4.86	10.67	5.48	1.40	0.13	0.98	0.78	0.07	6.22	1.54	9.99	0.44	0.38	51.38	0.39	3.80	0.50	1.02	100
LAWM27	5.07	6.49	9.21	1.46	0.14	1.02	2.63	1.37	1.08	5.61	13.93	0.45	0.20	45.12	2.02	2.62	0.52	1.06	100
LAWM28	3.22	11.31	9.36	0.04	0.00	0.03	2.67	0.49	1.51	1.63	10.59	0.01	0.29	54.61	2.05	1.61	0.53	0.03	100
LAWM29	4.84	6.56	2.33	0.14	0.01	0.10	2.66	1.39	6.56	5.67	10.53	0.04	0.25	50.90	2.04	4.01	1.85	0.10	100
LAWM30	5.25	11.53	2.39	0.04	0.00	0.03	2.72	0.07	4.53	1.66	18.34	0.01	0.17	46.74	0.50	4.11	1.90	0.03	100
LAWM31	3.09	6.34	9.00	1.42	0.13	0.99	2.57	0.07	6.33	1.57	17.05	0.44	0.24	44.41	1.97	1.55	1.79	1.04	100
LAWM32	3.06	6.09	2.16	1.37	0.13	0.96	0.76	1.29	6.09	5.26	16.15	0.43	0.24	50.43	0.38	3.72	0.49	1.00	100
LAWM33R1	3.23	11.34	9.38	0.04	0.00	0.03	2.68	1.20	1.98	1.63	18.04	0.01	0.24	45.97	2.06	1.62	0.53	0.03	100
LAWM34	3.17	7.75	9.22	0.04	0.00	0.03	2.55	1.37	6.49	1.60	17.72	0.01	0.24	45.17	1.19	1.59	1.84	0.03	100
LAWM35	3.10	10.91	6.97	1.43	0.13	1.00	1.75	0.07	1.06	5.50	17.36	0.45	0.14	44.24	1.98	1.56	1.32	1.04	100
LAWM36	4.39	10.10	7.98	0.57	0.05	0.40	2.00	0.20	5.35	2.38	12.38	0.18	0.30	47.89	1.60	2.75	1.04	0.42	100
LAWM37	4.25	10.15	8.02	0.04	0.00	0.03	2.01	0.20	5.37	3.98	12.43	0.01	0.26	48.09	0.80	2.76	1.56	0.03	100
LAWM38	4.25	7.12	7.73	1.40	0.13	0.98	1.16	0.10	5.18	2.31	13.99	0.44	0.29	49.47	0.78	2.66	1.01	1.02	100
LAWM39	4.25	8.04	5.51	1.40	0.13	0.97	1.16	0.07	5.17	3.84	13.97	0.43	0.19	49.40	0.77	2.66	1.00	1.02	100
LAWM40	3.83	10.30	5.81	0.39	0.04	0.27	2.04	0.07	2.18	2.43	14.72	0.12	0.25	52.05	0.82	2.80	1.59	0.29	100
LAWM41	4.38	7.33	7.96	1.44	0.13	1.00	2.00	0.20	2.13	3.96	14.40	0.45	0.27	47.75	0.80	3.60	1.16	1.05	100
LAWM42	3.69	7.21	5.59	1.42	0.13	0.99	1.58	0.07	5.25	2.33	14.16	0.44	0.23	50.09	1.57	2.70	1.53	1.03	100
LAWM43	4.35	7.89	5.64	1.43	0.13	1.00	1.98	0.20	5.30	3.93	12.26	0.45	0.31	47.40	1.58	3.58	1.54	1.04	100



**Table A.1. Normalized Compositions (in mol%) of 271 LAW Simulated and Actual Waste Glasses (continued).**

Glass ID	Al <sub>2</sub> O <sub>3</sub>	B <sub>2</sub> O <sub>3</sub>	CaO	Cl	Cr <sub>2</sub> O <sub>3</sub>	F	Fe <sub>2</sub> O <sub>3</sub>	K <sub>2</sub> O	Li <sub>2</sub> O	MgO	Na <sub>2</sub> O	P <sub>2</sub> O <sub>5</sub>	SO <sub>3</sub>	SiO <sub>2</sub>	TiO <sub>2</sub>	ZnO	ZrO <sub>2</sub>	Others	Sum
LAWM44	4.05	9.42	8.16	0.04	0.00	0.03	2.05	0.07	2.19	2.43	12.66	0.01	0.24	52.23	1.64	3.70	1.06	0.03	100
LAWM45	4.48	7.49	6.72	0.04	0.00	0.03	2.04	0.21	3.10	2.43	14.73	0.01	0.25	52.08	1.63	3.68	1.06	0.03	100
LAWM46	3.83	10.29	7.56	0.04	0.00	0.03	2.04	0.07	2.18	4.04	12.60	0.01	0.16	51.93	0.81	2.80	1.58	0.03	100
LAWM47	3.94	7.45	8.09	0.04	0.00	0.03	2.03	0.07	2.17	4.02	14.65	0.01	0.25	51.79	1.06	2.79	1.58	0.03	100
LAWM48	3.91	10.13	6.02	1.45	0.14	1.01	2.01	0.07	2.15	2.39	12.41	0.45	0.21	51.21	1.60	2.76	1.04	1.05	100
LAWM49	4.36	9.94	5.66	1.43	0.13	1.00	1.19	0.07	2.12	2.36	14.34	0.45	0.28	50.21	0.79	3.59	1.03	1.04	100
LAWM50	4.08	8.88	6.94	0.80	0.08	0.56	1.64	0.14	3.56	3.21	13.47	0.25	0.23	49.83	1.22	3.21	1.31	0.58	100
LAWM51	4.08	8.88	6.94	0.80	0.08	0.56	1.64	0.14	3.56	3.21	13.46	0.25	0.25	49.82	1.22	3.21	1.31	0.58	100
LAWM52	4.01	9.38	2.39	0.62	0.00	0.00	2.33	1.85	0.00	2.46	21.72	0.07	0.15	49.27	1.68	2.44	1.63	0.00	100
LAWM53	5.79	5.65	11.69	0.04	0.00	0.03	3.28	2.78	9.87	0.00	5.29	0.01	0.54	48.50	2.46	4.03	0.00	0.03	100
LAWM54R1	2.23	5.60	11.58	1.47	0.14	1.02	3.25	2.76	5.19	0.00	5.24	0.46	0.21	53.71	0.00	3.99	2.11	1.07	100
LAWM55	2.13	11.61	0.00	1.40	0.13	0.98	0.90	2.64	9.37	3.04	14.30	0.44	0.19	43.67	2.33	3.82	2.02	1.02	100
LAWM56	3.10	10.89	6.96	1.43	0.13	1.00	1.74	0.07	1.06	5.49	17.32	0.44	0.35	44.15	1.98	1.55	1.32	1.04	100
LAWM57	4.64	10.69	3.62	0.37	0.03	0.28	1.97	2.73	0.00	2.42	22.50	0.12	0.27	44.20	1.16	2.51	2.20	0.29	100
LAWM58	4.69	9.12	1.25	0.38	0.04	0.28	2.78	2.76	0.00	2.44	22.65	0.12	0.27	47.38	1.17	2.15	2.22	0.29	100
LAWM59	4.49	8.65	3.54	0.37	0.03	0.28	2.72	1.42	0.00	2.39	21.58	0.11	0.26	49.58	1.15	2.06	1.09	0.29	100
LAWM60	3.26	10.51	2.03	0.37	0.03	0.27	1.87	1.41	0.00	2.38	21.46	0.11	0.25	50.16	1.14	2.29	2.16	0.28	100
LAWM61	3.26	10.50	1.19	0.37	0.03	0.27	1.87	2.32	0.00	2.37	21.44	0.11	0.27	49.81	1.14	3.67	1.08	0.28	100
LAWM62	3.31	8.73	1.21	0.37	0.03	0.28	2.75	2.42	0.00	2.41	21.80	0.12	0.27	49.84	1.16	3.19	1.81	0.29	100
LAWM63	4.58	9.01	1.24	0.37	0.03	0.28	1.96	1.46	0.00	2.38	24.76	0.11	0.28	47.30	1.14	3.69	1.11	0.28	100
LAWM64	4.68	10.78	3.65	0.38	0.04	0.28	2.78	1.45	0.00	2.44	22.09	0.12	0.26	43.61	1.17	3.77	2.21	0.29	100
LAWM65	3.25	8.56	3.50	0.37	0.03	0.27	1.87	1.41	0.00	2.37	24.35	0.11	0.28	48.04	1.14	2.03	2.15	0.28	100
LAWM66	5.08	10.44	1.22	0.38	0.04	0.28	2.70	0.35	0.00	2.44	25.34	0.12	0.27	43.61	1.17	3.78	2.49	0.29	100
LAWM67	5.39	10.47	1.89	0.38	0.04	0.28	1.98	3.94	0.00	2.46	22.33	0.12	0.27	43.89	1.18	2.30	2.79	0.29	100
LAWM68	3.33	8.78	3.63	0.38	0.04	0.28	2.76	3.46	0.00	2.43	21.93	0.12	0.28	46.13	1.16	2.97	2.03	0.29	100
LAWM69	5.30	10.69	3.62	0.37	0.03	0.28	2.70	1.31	0.00	2.42	21.95	0.12	0.29	44.62	1.16	3.74	1.10	0.29	100
LAWM70	3.29	9.06	1.25	0.37	0.03	0.28	2.73	3.24	0.00	2.40	21.68	0.11	0.28	50.67	1.15	2.06	1.09	0.29	100
LAWM71	3.28	8.63	1.19	0.37	0.03	0.28	1.88	3.83	0.00	2.39	21.56	0.11	0.28	49.95	1.15	3.69	1.09	0.29	100
LAWM72	5.34	10.75	3.56	0.38	0.04	0.28	2.75	3.02	0.00	2.43	22.00	0.12	0.27	44.36	1.17	2.09	1.16	0.29	100
LAWM73	5.25	8.65	3.57	0.37	0.03	0.28	2.04	0.87	0.00	2.39	24.81	0.11	0.27	44.94	1.15	3.69	1.30	0.29	100
LAWM74	4.98	8.66	1.19	0.37	0.03	0.28	1.89	0.00	0.00	2.39	23.03	0.11	0.24	50.53	1.15	2.14	2.72	0.29	100
LAWM75	5.38	9.02	3.66	0.38	0.04	0.28	2.79	0.79	0.00	2.45	22.89	0.12	0.27	43.89	1.18	3.79	2.78	0.29	100
LAWM76	4.23	9.59	2.31	0.37	0.03	0.28	2.29	1.86	0.00	2.41	23.24	0.12	0.26	46.90	1.15	2.83	1.86	0.29	100

**Table A.1. Normalized Compositions (in mol%) of 271 LAW Simulated and Actual Waste Glasses (continued).**

Glass ID	Al <sub>2</sub> O <sub>3</sub>	B <sub>2</sub> O <sub>3</sub>	CaO	Cl	Cr <sub>2</sub> O <sub>3</sub>	F	Fe <sub>2</sub> O <sub>3</sub>	K <sub>2</sub> O	Li <sub>2</sub> O	MgO	Na <sub>2</sub> O	P <sub>2</sub> O <sub>5</sub>	SO <sub>3</sub>	SiO <sub>2</sub>	TiO <sub>2</sub>	ZnO	ZrO <sub>2</sub>	Others	Sum
LAWE2H	3.92	9.42	2.36	0.37	0.03	0.28	2.26	2.71	0.00	2.40	22.54	0.12	0.26	47.48	1.15	2.82	1.60	0.29	100
LAWE3	4.05	9.72	2.44	0.38	0.04	0.28	2.33	3.59	0.00	2.49	19.88	0.12	0.27	48.38	1.19	2.91	1.65	0.29	100
LAWE3H	3.94	9.47	2.38	0.37	0.03	0.28	2.27	3.89	0.00	2.42	21.55	0.12	0.29	47.12	1.15	2.83	1.60	0.29	100
LAWE4	3.98	9.56	2.99	0.38	0.04	0.28	2.29	0.35	0.00	2.44	21.08	0.12	0.22	50.35	1.17	2.86	1.62	0.28	100
LAWE4H	3.89	9.34	2.91	0.37	0.03	0.27	2.24	0.38	0.00	2.39	22.79	0.11	0.29	49.18	1.14	2.80	1.58	0.28	100
LAWE5	3.95	9.49	4.33	0.37	0.03	0.28	2.27	0.35	1.13	2.43	18.67	0.12	0.28	50.42	1.16	2.84	1.61	0.28	100
LAWE5H	3.88	9.30	4.25	0.36	0.03	0.27	2.23	0.38	1.08	2.37	20.20	0.11	0.29	49.47	1.13	2.78	1.57	0.28	100
LAWE7	3.82	9.18	7.28	0.36	0.03	0.27	2.20	0.34	6.89	2.40	12.89	0.11	0.30	48.22	1.12	2.75	1.56	0.27	100
LAWE7H	3.77	9.06	7.19	0.35	0.03	0.26	2.17	0.37	6.78	2.36	13.95	0.11	0.37	47.59	1.10	2.72	1.53	0.27	100
LAWE9H	3.74	8.97	7.70	0.35	0.03	0.26	2.15	0.36	8.60	3.69	9.08	0.11	0.34	49.05	1.10	2.69	1.52	0.27	100
LAWE10H	3.73	8.96	7.78	0.35	0.03	0.26	2.15	0.36	8.93	4.57	5.78	0.11	0.42	51.02	1.09	2.68	1.52	0.27	100
LAWE11	4.05	9.71	2.80	0.38	0.04	0.28	2.33	3.41	0.00	2.48	18.94	0.12	0.21	49.22	1.18	2.91	1.65	0.29	100
LAWE12	4.62	8.52	2.38	0.37	0.03	0.28	1.85	3.89	0.00	2.42	21.59	0.12	0.27	47.20	1.16	2.84	2.16	0.29	100
LAWE13	4.67	9.60	2.41	0.38	0.04	0.28	2.30	3.94	0.00	0.75	21.84	0.12	0.27	47.74	0.32	2.87	2.18	0.29	100
LAWE14	3.30	9.54	1.79	0.38	0.03	0.28	2.29	3.91	0.00	0.74	21.70	0.12	0.26	49.16	1.17	2.86	2.17	0.29	100
LAWE15	3.97	8.57	1.79	0.38	0.03	0.28	2.29	3.92	0.00	1.59	21.71	0.12	0.26	48.61	1.17	2.86	2.17	0.29	100
LAWE16	3.98	8.09	1.79	0.38	0.04	0.28	2.29	3.92	0.00	1.59	21.73	0.12	0.39	48.65	1.17	2.86	2.45	0.29	100
LAWCrP1R	3.98	9.55	3.27	0.23	0.14	0.39	2.29	0.09	0.00	2.44	20.76	1.35	0.31	49.14	1.17	2.86	1.62	0.39	100
LAWCrP2R	3.99	9.58	2.50	0.36	0.26	0.36	2.30	0.19	0.00	2.45	22.60	1.25	0.30	47.82	1.17	2.87	1.62	0.37	100
LAWCrP3R	3.99	9.57	3.28	0.23	0.14	0.39	2.29	0.09	0.00	2.45	20.79	2.23	0.32	48.18	1.17	2.86	1.62	0.39	100
LAWCrP4R	4.00	9.60	2.51	0.36	0.26	0.36	2.30	0.19	0.00	2.45	22.64	2.24	0.31	46.73	1.17	2.87	1.63	0.37	100
LAWCrP5	3.87	9.29	6.70	0.25	0.25	0.23	2.23	0.06	5.71	2.39	15.00	1.21	0.31	46.77	1.13	2.78	1.57	0.24	100
LAWCrP6	3.78	9.08	7.82	0.24	0.26	0.22	2.18	0.06	8.82	4.00	8.16	2.24	0.46	47.07	1.11	2.72	1.54	0.24	100
LAWCrP7	3.77	9.04	7.84	0.24	0.26	0.22	2.17	0.06	9.06	4.58	5.49	2.23	0.52	48.95	1.10	2.71	1.53	0.24	100
LAWE3Cr2CCC	4.09	9.81	2.46	0.39	0.63	0.29	2.35	3.62	0.00	2.51	20.07	0.12	0.26	47.32	1.20	2.94	1.66	0.30	100
LAWE9HCr1CCC	3.75	9.00	7.72	0.35	0.25	0.26	2.16	0.36	8.62	3.70	9.10	0.11	0.43	48.62	1.10	2.69	1.52	0.27	100
LAWE9HCr2CCC	3.74	8.99	7.72	0.35	0.19	0.26	2.15	0.36	8.61	3.69	9.09	0.11	0.41	48.74	1.10	2.69	1.52	0.27	100
LAWE10HCr3CCC	3.73	8.96	7.78	0.35	0.14	0.26	2.15	0.36	8.94	4.58	5.79	0.11	0.49	50.79	1.09	2.68	1.52	0.27	100
LAWA41	4.10	7.26	2.40	1.10	0.01	0.14	2.95	2.22	0.00	3.33	21.74	0.07	0.08	48.66	1.68	2.48	1.64	0.14	100
LAWA42	4.17	8.89	2.94	1.12	0.01	0.13	3.61	2.25	0.00	4.08	22.10	0.07	0.09	43.32	2.06	3.03	2.00	0.13	100
LAWA43-1	8.14	7.34	2.42	1.13	0.01	0.13	2.98	2.28	0.00	3.37	22.31	0.08	0.09	43.73	1.70	2.50	1.66	0.13	100
LAWA44	4.07	8.56	2.38	1.23	0.01	0.04	2.93	0.36	0.00	3.31	21.60	0.03	0.08	49.64	1.67	2.44	1.62	0.05	100
LAWA45	4.10	11.53	0.00	1.24	0.01	0.03	2.95	0.36	0.00	2.47	21.76	0.03	0.08	50.00	1.68	2.05	1.64	0.05	100

**Table A.1. Normalized Compositions (in mol%) of 271 LAW Simulated and Actual Waste Glasses (continued).**

Glass ID	Al <sub>2</sub> O <sub>3</sub>	B <sub>2</sub> O <sub>3</sub>	CaO	Cl	Cr <sub>2</sub> O <sub>3</sub>	F	Fe <sub>2</sub> O <sub>3</sub>	K <sub>2</sub> O	Li <sub>2</sub> O	MgO	Na <sub>2</sub> O	P <sub>2</sub> O <sub>5</sub>	SO <sub>3</sub>	SiO <sub>2</sub>	TiO <sub>2</sub>	ZnO	ZrO <sub>2</sub>	Others	Sum
LAWA49	4.17	8.77	0.00	1.26	0.01	0.03	4.29	0.36	0.00	2.51	22.13	0.03	0.06	50.85	1.71	2.09	1.67	0.05	100
LAWA50	4.23	8.89	0.00	1.28	0.01	0.04	5.22	0.37	0.00	2.55	22.44	0.03	0.09	49.25	1.74	2.12	1.69	0.05	100
LAWA51	4.10	11.60	0.00	1.12	0.01	0.03	2.96	0.32	0.00	2.48	19.59	0.03	0.06	52.27	1.68	2.06	1.64	0.05	100
LAWA52	4.04	5.92	9.36	1.22	0.01	0.03	3.13	0.35	0.00	2.44	21.49	0.03	0.08	46.83	0.92	2.45	1.62	0.05	100
LAWA60	5.40	10.42	4.98	1.19	0.01	0.03	0.00	0.34	0.00	3.20	20.84	0.03	0.08	47.89	1.61	2.35	1.57	0.05	100
LAWA65	3.94	5.78	3.83	1.20	0.01	0.03	3.06	0.35	0.00	9.77	20.98	0.03	0.39	45.71	0.90	2.39	1.58	0.05	100
LAWA76	3.81	9.94	8.84	1.16	0.01	0.03	2.96	0.33	10.58	2.31	10.33	0.03	0.68	44.23	0.87	2.31	1.53	0.05	100
LAWA81	4.04	8.50	4.73	1.22	0.01	0.03	2.90	0.35	0.00	3.29	21.45	0.03	0.08	49.28	0.00	2.42	1.61	0.05	100
LAWA82	4.10	8.62	0.00	1.24	0.01	0.03	2.95	0.36	0.00	3.34	21.75	0.03	0.08	49.98	3.37	2.46	1.64	0.05	100
LAWA83	4.03	8.47	2.36	1.22	0.01	0.03	2.07	0.35	0.00	3.28	21.37	1.89	0.08	49.11	1.65	2.41	1.61	0.05	100
LAWA84	3.99	8.38	2.33	1.21	0.01	0.03	1.23	0.35	0.00	3.24	21.16	3.72	0.08	48.61	1.64	2.39	1.59	0.05	100
LAWA87	2.95	8.56	2.39	0.62	0.00	0.00	2.93	1.84	0.00	3.32	21.68	0.07	0.16	49.71	1.67	2.44	1.63	0.01	100
LAWA88	4.01	9.37	2.39	0.62	0.00	0.00	2.33	1.84	0.00	2.46	21.71	0.07	0.16	49.26	1.68	2.44	1.63	0.01	100
LAWA89	4.04	9.44	0.00	0.63	0.00	0.00	2.35	1.86	0.00	2.48	21.87	0.07	0.16	49.61	3.38	2.46	1.64	0.01	100
LAWA90	3.98	9.31	4.74	0.62	0.00	0.00	2.31	1.83	0.00	2.45	21.56	0.07	0.16	48.91	0.00	2.42	1.62	0.01	100
LAWA93	3.83	10.08	8.89	1.16	0.01	0.03	2.97	0.34	10.73	2.32	10.24	0.03	0.08	44.49	0.88	2.33	1.54	0.05	100
LAWA96	3.98	7.42	4.65	1.20	0.01	0.03	1.22	0.35	0.00	3.23	21.09	3.70	0.08	47.38	1.63	2.38	1.59	0.05	100
LAWA104	4.34	8.25	2.30	1.35	0.01	0.04	2.82	0.39	0.00	3.19	23.75	0.03	0.08	47.86	1.61	2.35	1.57	0.06	100
LAWA105	4.61	7.95	2.21	1.47	0.01	0.04	2.72	0.43	0.00	3.08	25.89	0.04	0.08	46.09	1.55	2.26	1.51	0.06	100
LAWA112B14	3.82	9.06	8.72	0.68	0.01	0.34	0.00	1.28	0.00	2.35	20.62	0.09	0.13	47.07	1.60	2.33	1.56	0.35	100
LAWA112B15	3.87	9.03	8.70	0.56	0.00	0.30	0.00	1.64	0.00	2.35	20.68	0.05	0.09	46.94	1.60	2.32	1.55	0.32	100
LAWA125	3.67	9.10	2.30	0.41	0.01	1.12	2.24	2.97	0.00	2.37	21.41	0.08	0.26	47.37	1.61	2.35	1.57	1.17	100
LAWA127R1	3.69	9.76	2.46	0.34	0.01	0.93	2.40	2.43	0.00	2.54	17.53	0.07	0.15	50.80	1.73	2.51	1.68	0.98	100
LAWA127R2	3.69	9.76	2.45	0.34	0.01	0.95	2.40	2.42	0.00	2.54	17.50	0.07	0.17	50.80	1.73	2.52	1.68	0.96	100
LAWA129	4.72	7.89	4.06	0.36	0.01	1.02	0.00	2.66	0.00	1.89	19.21	0.07	0.25	51.02	1.69	2.45	1.64	1.07	100
LAWA133	3.96	8.32	6.37	1.03	0.01	0.14	1.42	0.30	0.00	3.23	20.99	0.09	0.16	48.25	1.63	2.37	1.58	0.15	100
LAWA134	3.68	9.51	2.39	0.37	0.01	1.01	2.34	2.63	0.00	2.47	19.00	0.07	0.23	49.48	1.69	2.45	1.64	1.03	100
LAWA135	3.69	9.64	2.43	0.36	0.01	0.98	2.37	2.52	0.00	2.51	18.25	0.07	0.22	50.12	1.70	2.48	1.66	0.99	100
LAWA136	3.68	9.63	3.61	0.36	0.01	0.98	2.37	2.52	0.00	2.50	18.24	0.07	0.22	48.98	1.70	2.48	1.66	0.99	100
LAWA170	4.00	9.34	2.38	0.62	0.00	0.00	2.32	2.18	0.00	2.46	21.62	0.07	0.18	49.11	1.67	2.43	1.63	0.00	100
LAWB30	5.43	9.28	8.30	0.01	0.04	0.33	3.34	0.22	8.77	4.91	8.20	0.03	0.14	45.77	0.00	3.25	1.63	0.34	100
LAWB31	3.93	11.30	4.67	0.01	0.04	0.34	2.92	0.22	6.43	3.61	8.29	2.50	0.51	50.78	0.00	2.47	1.63	0.35	100
LAWB32	3.87	13.87	4.60	0.01	0.04	0.33	1.67	0.22	6.33	3.56	8.16	2.46	0.54	49.97	0.00	2.43	1.61	0.35	100

**Table A.1. Normalized Compositions (in mol%) of 271 LAW Simulated and Actual Waste Glasses (continued).**

Glass ID	Al <sub>2</sub> O <sub>3</sub>	B <sub>2</sub> O <sub>3</sub>	CaO	Cl	Cr <sub>2</sub> O <sub>3</sub>	F	Fe <sub>2</sub> O <sub>3</sub>	K <sub>2</sub> O	Li <sub>2</sub> O	MgO	Na <sub>2</sub> O	P <sub>2</sub> O <sub>5</sub>	SO <sub>3</sub>	SiO <sub>2</sub>	TiO <sub>2</sub>	ZnO	ZrO <sub>2</sub>	Others	Sum
LAWB33	3.88	11.17	4.62	0.01	0.04	0.33	2.07	0.22	6.36	3.57	8.20	4.29	0.61	50.21	0.00	2.44	1.61	0.35	100
LAWB34	3.87	11.12	6.90	0.01	0.04	0.33	2.06	0.22	6.33	3.56	8.16	2.46	0.57	49.99	0.00	2.43	1.61	0.35	100
LAWB35	3.83	11.02	4.56	0.01	0.04	0.33	2.05	0.21	6.28	6.70	8.09	2.44	0.55	49.54	0.00	2.41	1.59	0.34	100
LAWB37	3.86	11.09	5.35	0.01	0.04	0.33	2.06	0.22	6.32	4.61	8.14	3.05	0.72	49.84	0.00	2.42	1.60	0.35	100
LAWB38	3.83	11.01	5.37	0.01	0.04	0.33	2.04	0.21	8.07	3.52	8.08	2.83	0.84	49.48	0.00	2.41	1.59	0.34	100
LAWB40	3.69	10.61	5.12	0.01	0.04	0.32	1.97	0.21	12.91	4.41	7.78	0.03	1.04	47.68	0.00	2.32	1.53	0.33	100
LAWB41	3.76	10.80	7.20	0.01	0.04	0.32	2.01	0.21	9.42	4.49	7.93	0.03	0.96	48.56	0.00	2.36	1.56	0.34	100
LAWB60	3.61	10.65	12.73	0.02	0.03	0.25	0.00	0.17	9.29	4.43	6.30	0.03	0.48	47.87	0.00	2.33	1.54	0.27	100
LAWB61	3.74	8.81	7.36	0.00	0.04	0.23	2.05	0.17	11.99	4.54	5.46	0.01	0.55	49.78	1.08	2.39	1.58	0.23	100
LAWB62	3.60	8.47	12.69	0.00	0.04	0.22	0.00	0.16	11.54	4.37	5.25	0.01	0.66	47.90	1.04	2.30	1.52	0.22	100
LAWB63	3.90	8.63	10.07	0.00	0.04	0.22	0.00	0.17	10.21	4.45	5.35	0.01	0.63	49.18	1.05	4.31	1.55	0.22	100
LAWB64	3.72	8.74	7.31	0.00	0.04	0.23	1.26	0.17	11.90	4.51	5.42	0.01	0.52	49.42	1.07	3.89	1.57	0.23	100
LAWB67	3.82	8.98	5.82	0.00	0.04	0.23	2.09	0.17	9.06	4.63	5.57	2.68	0.76	50.77	1.10	2.44	1.61	0.23	100
LAWB69	3.64	10.68	11.24	0.02	0.02	0.25	0.00	0.15	9.30	4.44	6.44	0.04	0.49	48.10	0.00	3.38	1.54	0.27	100
LAWB70	3.73	10.96	7.30	0.02	0.02	0.26	1.26	0.15	9.54	4.56	6.61	0.04	0.42	49.36	0.00	3.91	1.58	0.27	100
LAWB71	3.74	9.60	7.32	0.02	0.02	0.26	1.26	0.15	9.57	4.57	6.62	0.04	0.37	49.47	1.20	3.92	1.58	0.27	100
LAWB72	3.75	11.00	7.89	0.02	0.02	0.26	1.26	0.15	8.55	4.58	6.64	0.04	0.47	49.58	0.00	3.93	1.59	0.27	100
LAWB73	3.70	8.69	10.14	0.00	0.04	0.22	0.73	0.17	10.28	4.49	5.39	0.01	0.68	49.13	1.06	3.49	1.56	0.22	100
LAWB74	3.70	8.81	9.45	0.00	0.04	0.23	0.73	0.17	10.83	4.49	5.40	0.01	0.58	49.22	1.06	3.49	1.56	0.23	100
LAWB75	3.72	10.39	9.49	0.00	0.04	0.23	0.73	0.17	10.89	2.29	5.43	0.01	0.77	49.47	1.07	3.51	1.57	0.23	100
LAWB76	3.69	10.29	9.41	0.00	0.04	0.22	0.73	0.17	11.81	2.27	5.38	0.01	0.77	49.94	0.00	3.48	1.56	0.22	100
LAWB77	3.74	10.98	7.32	0.02	0.02	0.26	0.85	0.15	8.53	4.57	6.62	0.04	0.40	49.49	1.20	3.92	1.59	0.27	100
LAWB81	3.74	10.98	7.87	0.02	0.02	0.26	1.26	0.15	8.84	4.57	6.62	0.04	0.46	49.48	0.00	3.81	1.59	0.27	100
LAWB82	3.92	9.41	8.25	0.02	0.02	0.27	3.86	0.16	9.26	2.39	6.94	0.05	0.39	49.13	0.00	3.99	1.66	0.29	100
LAWB87	4.02	11.80	6.88	0.02	0.02	0.17	1.99	0.13	9.93	2.21	5.10	0.02	0.45	51.67	0.00	3.79	1.64	0.17	100
LAWB88	3.94	11.56	8.82	0.02	0.02	0.16	0.85	0.13	9.72	2.17	5.00	0.02	0.53	51.59	0.00	3.71	1.60	0.16	100
LAWB89	3.78	8.98	7.54	0.02	0.02	0.20	2.07	0.13	10.43	4.60	4.10	0.04	0.34	51.16	1.08	3.71	1.60	0.21	100
LAWB90	3.84	9.13	7.66	0.02	0.02	0.20	2.10	0.13	7.66	4.67	7.03	0.04	0.27	50.53	1.10	3.77	1.63	0.21	100
LAWB91	3.87	9.20	7.72	0.02	0.02	0.20	2.12	0.13	6.24	4.71	8.99	0.04	0.29	49.69	1.11	3.80	1.64	0.21	100
LAWB92	3.90	9.27	7.78	0.02	0.02	0.20	2.13	0.13	4.78	4.74	10.50	0.04	0.35	49.32	1.12	3.83	1.65	0.22	100
LAWB93	3.79	9.02	7.57	0.02	0.02	0.20	2.07	0.13	9.76	4.61	4.83	0.04	0.35	50.98	1.09	3.72	1.61	0.21	100
LAWB93R1	3.80	9.02	7.57	0.02	0.02	0.20	2.07	0.13	9.76	4.61	4.83	0.04	0.33	50.99	1.09	3.72	1.61	0.20	100
LAWB94	3.76	8.94	7.50	0.01	0.02	0.21	2.06	0.13	11.13	4.58	3.39	0.03	0.39	51.28	1.08	3.69	1.59	0.22	100

**Table A.1. Normalized Compositions (in mol%) of 271 LAW Simulated and Actual Waste Glasses (continued).**

Glass ID	Al <sub>2</sub> O <sub>3</sub>	B <sub>2</sub> O <sub>3</sub>	CaO	Cl	Cr <sub>2</sub> O <sub>3</sub>	F	Fe <sub>2</sub> O <sub>3</sub>	K <sub>2</sub> O	Li <sub>2</sub> O	MgO	Na <sub>2</sub> O	P <sub>2</sub> O <sub>5</sub>	SO <sub>3</sub>	SiO <sub>2</sub>	TiO <sub>2</sub>	ZnO	ZrO <sub>2</sub>	Others	Sum
LAWB95	3.75	8.90	7.47	0.01	0.02	0.21	2.05	0.13	11.91	4.56	2.45	0.03	0.35	51.61	1.08	3.67	1.58	0.22	100
LAWC12	8.10	9.05	1.96	0.23	0.01	0.03	2.47	0.10	0.00	2.37	22.27	0.03	0.15	45.17	2.95	3.62	1.37	0.13	100
LAWC15	3.99	8.39	2.34	0.14	0.00	1.62	2.87	0.10	0.00	3.26	21.06	0.01	0.19	48.67	1.64	2.40	1.59	1.73	100
LAWC21	3.88	9.35	7.37	0.22	0.01	0.20	2.62	0.10	5.91	2.42	12.36	0.11	0.23	50.13	0.90	2.39	1.58	0.20	100
LAWC21rev2	3.87	9.32	7.38	0.20	0.01	0.17	2.60	0.10	5.90	2.40	12.45	0.10	0.23	50.20	0.90	2.39	1.58	0.18	100
LAWC22	3.77	9.15	5.77	0.09	0.01	1.12	2.15	0.06	5.31	2.38	14.72	0.06	0.23	49.15	0.91	2.39	1.56	1.20	100
LAWC23	4.03	9.72	7.67	0.23	0.01	0.21	2.72	2.05	0.00	2.51	12.85	0.11	0.29	52.28	0.94	2.49	1.64	0.23	100
LAWC24	3.95	9.54	7.52	0.23	0.01	0.21	2.67	4.00	0.00	2.47	12.61	0.11	0.29	51.19	0.92	2.44	1.61	0.23	100
LAWC25	3.87	9.34	7.37	0.22	0.01	0.20	2.61	5.85	0.00	2.41	12.34	0.11	0.45	50.12	0.90	2.39	1.58	0.22	100
LAWC26	3.73	11.83	7.10	0.19	0.01	0.16	0.00	0.09	5.68	2.31	11.99	0.10	0.27	51.65	0.87	2.31	1.52	0.18	100
LAWC28	3.69	8.88	14.07	0.19	0.01	0.16	0.00	0.09	5.62	2.29	11.87	0.10	0.33	47.86	0.86	2.28	1.51	0.17	100
LAWC29	4.00	8.98	10.66	0.20	0.01	0.18	0.00	0.09	5.69	2.32	12.00	0.09	0.29	48.82	0.87	4.10	1.52	0.19	100
LAWC30	3.84	9.23	7.31	0.20	0.01	0.17	1.64	0.10	5.84	2.38	12.34	0.10	0.27	49.73	0.90	4.20	1.57	0.18	100
LAWC31	3.83	9.21	8.43	0.20	0.01	0.17	1.77	0.09	5.83	2.37	12.31	0.10	0.31	49.60	0.89	3.15	1.56	0.18	100
LAWC31R1	3.83	9.21	8.43	0.20	0.01	0.17	1.77	0.09	5.83	2.37	12.31	0.10	0.27	49.63	0.89	3.15	1.56	0.17	100
LAWC33	3.85	9.26	7.90	0.20	0.01	0.17	1.78	0.09	5.88	2.39	12.37	0.10	0.29	49.89	0.90	3.17	1.57	0.18	100
TFA-BASE	4.56	9.53	0.01	0.52	0.00	0.03	2.29	0.29	0.00	2.47	21.41	0.06	0.07	54.19	2.49	1.22	0.81	0.05	100
C22AN107	3.84	9.28	5.84	0.14	0.01	0.47	2.24	0.06	5.39	2.40	14.92	0.11	0.22	49.70	0.91	2.41	1.57	0.49	100
A88AP101R1	3.97	9.38	2.37	0.24	0.01	0.79	2.31	1.51	0.00	2.44	21.44	0.07	0.19	48.79	1.66	2.42	1.62	0.81	100
A88Si+15	3.99	9.02	2.28	0.26	0.01	0.87	2.22	1.67	0.00	2.35	23.72	0.07	0.24	46.93	1.60	2.32	1.55	0.89	100
A88Si-15	3.95	9.77	2.46	0.23	0.00	0.70	2.40	1.33	0.00	2.54	18.98	0.06	0.16	50.79	1.73	2.51	1.68	0.71	100
C22Si+15	3.79	9.03	5.69	0.16	0.01	0.54	2.15	0.06	5.26	2.35	16.71	0.12	0.25	48.50	0.90	2.36	1.54	0.58	100
C22Si-15	3.87	9.47	5.96	0.13	0.01	0.43	2.23	0.05	5.52	2.47	13.24	0.12	0.18	50.84	0.94	2.47	1.61	0.45	100
A1C1-1	3.93	8.62	3.21	1.69	0.01	0.30	2.68	0.24	1.37	3.02	20.33	0.03	0.17	48.66	1.45	2.38	1.58	0.34	100
A1C1-2	3.87	8.78	4.07	1.20	0.01	0.58	2.49	0.18	2.71	2.79	18.50	0.06	0.19	48.75	1.26	2.38	1.57	0.62	100
A1C1-3	3.81	8.93	4.91	0.71	0.00	0.85	2.31	0.11	4.01	2.57	16.72	0.09	0.23	48.82	1.08	2.37	1.56	0.90	100
C1-AN107	3.78	9.15	5.77	0.12	0.00	0.95	2.16	0.05	5.33	2.38	14.82	0.12	0.23	49.29	0.91	2.39	1.56	1.01	100
A2-AP101	3.64	9.32	2.34	0.78	0.01	1.22	2.29	2.67	0.00	2.43	19.68	0.07	0.29	48.38	1.65	2.39	1.59	1.25	100
A2B1-1	3.68	9.26	3.70	0.59	0.01	0.96	2.24	2.01	2.34	3.00	16.02	0.06	0.29	49.02	1.50	2.74	1.59	1.00	100
A2B1-2	3.72	9.16	5.02	0.40	0.01	0.75	2.18	1.37	4.63	3.56	12.43	0.05	0.34	49.56	1.36	3.08	1.60	0.78	100
B1-AZ101	3.80	9.03	7.57	0.04	0.01	0.26	2.07	0.12	9.04	4.65	5.54	0.04	0.38	50.70	1.09	3.74	1.61	0.30	100
C2-AN102C35	3.74	8.49	8.22	0.69	0.00	0.36	1.41	0.06	6.83	2.32	12.12	0.14	0.42	49.33	0.85	3.08	1.53	0.40	100

**Table A.1. Normalized Compositions (in mol%) of 271 LAW Simulated and Actual Waste Glasses (continued).**

Glass ID	Al <sub>2</sub> O <sub>3</sub>	B <sub>2</sub> O <sub>3</sub>	CaO	Cl	Cr <sub>2</sub> O <sub>3</sub>	F	Fe <sub>2</sub> O <sub>3</sub>	K <sub>2</sub> O	Li <sub>2</sub> O	MgO	Na <sub>2</sub> O	P <sub>2</sub> O <sub>5</sub>	SO <sub>3</sub>	SiO <sub>2</sub>	TiO <sub>2</sub>	ZnO	ZrO <sub>2</sub>	Others	Sum
A3-AN104	3.81	9.15	5.76	1.43	0.01	0.03	2.16	0.22	5.33	2.36	15.17	0.10	0.28	49.25	0.91	2.40	1.56	0.07	100
A2B1-3	3.76	9.10	6.32	0.22	0.01	0.50	2.13	0.74	6.85	4.10	8.95	0.04	0.37	50.14	1.23	3.41	1.60	0.54	100
A3C2-1	3.80	8.98	6.39	1.24	0.01	0.10	1.97	0.18	5.71	2.35	14.40	0.11	0.30	49.30	0.90	2.57	1.56	0.13	100
A3C2-2	3.77	8.82	7.01	1.06	0.01	0.20	1.78	0.14	6.08	2.33	13.64	0.13	0.32	49.31	0.88	2.74	1.55	0.23	100
A3C2-3	3.75	8.65	7.62	0.87	0.00	0.30	1.60	0.10	6.46	2.33	12.87	0.13	0.39	49.30	0.86	2.91	1.54	0.34	100
A1-AN105R2	3.99	8.46	2.33	2.20	0.01	0.00	2.87	0.31	0.00	3.24	22.21	0.00	0.15	48.59	1.63	2.39	1.59	0.04	100
12U-G-86A	4.05	8.62	2.37	1.06	0.01	0.07	2.91	0.31	0.00	3.29	21.60	0.07	0.19	49.46	1.66	2.43	1.62	0.28	100
LA44PNCC	4.00	8.42	2.33	1.06	0.03	0.77	2.88	0.18	0.00	3.23	21.33	0.33	0.17	48.90	1.63	2.36	1.60	0.77	100
LA44CCCR2	4.00	8.42	2.33	1.06	0.03	0.77	2.88	0.18	0.00	3.23	21.33	0.33	0.17	48.90	1.63	2.36	1.60	0.77	100
WVF-G-21B	3.96	9.35	2.36	0.24	0.01	0.80	2.30	1.50	0.00	2.44	21.45	0.07	0.27	48.65	1.65	2.41	1.61	0.90	100
PNLA126CC	3.68	9.39	2.37	0.37	0.01	1.05	2.31	2.73	0.00	2.44	19.76	0.07	0.24	48.83	1.66	2.41	1.62	1.05	100
LA126CCC	3.68	9.39	2.37	0.37	0.01	1.05	2.31	2.73	0.00	2.44	19.76	0.07	0.24	48.83	1.66	2.41	1.62	1.05	100
WVM-G-142C	3.64	9.33	2.35	0.78	0.01	1.22	2.29	2.68	0.00	2.41	19.69	0.07	0.21	48.39	1.64	2.39	1.59	1.31	100
LAWA102R2	3.82	9.24	5.80	0.60	0.01	0.10	2.18	0.18	5.38	2.39	15.03	0.12	0.26	49.87	0.92	2.42	1.58	0.10	100
A100G115A	3.82	9.24	5.80	0.60	0.01	0.10	2.18	0.18	5.38	2.38	15.01	0.12	0.31	49.86	0.92	2.43	1.58	0.10	100
A100CC	3.82	9.24	5.80	0.60	0.01	0.10	2.18	0.18	5.38	2.38	15.01	0.12	0.29	49.86	0.92	2.43	1.58	0.10	100
WVB-G-124B	3.81	9.22	5.80	0.60	0.01	0.10	2.18	0.18	5.37	2.38	14.98	0.12	0.35	49.79	0.92	2.42	1.58	0.19	100
LA137SRCCC	3.81	9.13	5.76	1.38	0.01	0.07	2.15	0.42	5.33	2.36	15.16	0.10	0.22	49.18	0.91	2.40	1.56	0.07	100
WVR-G-127A	3.81	9.15	5.75	1.43	0.01	0.00	2.16	0.23	5.33	2.36	15.17	0.10	0.31	49.24	0.91	2.40	1.56	0.08	100
LB83PNCC	3.82	9.04	7.59	0.00	0.01	0.26	2.08	0.12	9.05	4.65	5.43	0.04	0.38	50.80	1.10	3.74	1.61	0.26	100
LB83CCC-1	3.82	9.04	7.59	0.00	0.01	0.26	2.08	0.12	9.05	4.65	5.43	0.04	0.38	50.80	1.10	3.74	1.61	0.26	100
WVJ-G-109D	3.80	9.04	7.59	0.02	0.02	0.20	2.08	0.13	9.06	4.64	5.55	0.04	0.34	50.78	1.10	3.74	1.61	0.28	100
LAWB96	3.81	9.06	7.60	0.02	0.01	0.07	2.08	0.08	9.05	4.65	5.56	0.01	0.38	51.05	1.10	3.76	1.62	0.10	100
GTSD-1126	3.81	9.06	7.60	0.02	0.01	0.07	2.09	0.08	9.06	4.64	5.57	0.01	0.35	51.09	1.10	3.75	1.62	0.07	100
LB88CCC	3.95	11.54	8.80	0.02	0.02	0.16	0.85	0.13	9.72	2.17	5.00	0.02	0.56	51.58	0.00	3.71	1.60	0.16	100
AZ-102 Surr SRNL	3.89	11.51	8.76	0.00	0.02	0.32	0.85	0.13	9.67	2.16	5.05	0.02	0.72	51.28	0.00	3.70	1.60	0.32	100
12S-G-85C	3.83	9.26	5.82	0.14	0.01	0.47	2.23	0.05	5.37	2.40	14.94	0.11	0.30	49.57	0.92	2.41	1.57	0.59	100
C100GCC	3.87	9.34	7.36	0.22	0.01	0.20	2.61	0.10	5.89	2.42	12.34	0.11	0.32	50.10	0.90	2.39	1.58	0.22	100
AN-102 Surr LC Melter	3.88	9.38	7.37	0.38	0.01	0.20	2.62	0.05	5.92	2.43	12.26	0.07	0.23	50.10	0.91	2.40	1.58	0.21	100
WVH-G-57B	3.82	9.19	8.41	0.20	0.01	0.17	1.77	0.09	5.83	2.38	12.29	0.09	0.34	49.55	0.90	3.15	1.56	0.26	100
GTSD-1437	3.74	8.51	8.24	0.69	0.00	0.36	1.42	0.06	6.85	2.32	12.15	0.14	0.23	49.44	0.85	3.08	1.53	0.38	100
PLTC35CCC	3.74	8.51	8.24	0.69	0.00	0.36	1.42	0.06	6.85	2.32	12.15	0.14	0.23	49.44	0.85	3.08	1.53	0.38	100

**Table A.1. Normalized Compositions (in mol%) of 271 LAW Simulated and Actual Waste Glasses (continued).**

Glass ID	Al <sub>2</sub> O <sub>3</sub>	B <sub>2</sub> O <sub>3</sub>	CaO	Cl	Cr <sub>2</sub> O <sub>3</sub>	F	Fe <sub>2</sub> O <sub>3</sub>	K <sub>2</sub> O	Li <sub>2</sub> O	MgO	Na <sub>2</sub> O	P <sub>2</sub> O <sub>5</sub>	SO <sub>3</sub>	SiO <sub>2</sub>	TiO <sub>2</sub>	ZnO	ZrO <sub>2</sub>	Others	Sum
AN-103 Actual	4.09	8.62	2.40	0.59	0.00	0.07	2.95	0.43	0.00	3.34	21.64	0.05	0.08	49.86	1.69	2.47	1.64	0.07	100
AW-101 Actual	4.02	9.41	2.39	0.15	0.00	0.00	2.34	1.85	0.00	2.48	21.77	0.07	0.18	49.46	1.68	2.45	1.64	0.10	100
AP-101 Actual	3.69	9.40	2.37	0.32	0.01	0.94	2.31	2.70	0.00	2.46	19.80	0.08	0.26	48.97	1.67	2.43	1.62	0.96	100
AZ-101 Actual	3.82	9.04	7.59	0.00	0.01	0.26	2.08	0.12	9.04	4.65	5.41	0.04	0.43	50.80	1.10	3.73	1.61	0.27	100
AZ-102 Actual	3.94	11.55	8.83	0.02	0.02	0.16	0.85	0.14	9.71	2.16	4.99	0.02	0.66	51.48	0.00	3.70	1.60	0.16	100
AZ-102 Actual CCC	3.94	11.55	8.83	0.02	0.02	0.16	0.85	0.14	9.71	2.16	4.99	0.02	0.66	51.48	0.00	3.70	1.60	0.16	100
AN-107 Actual (LAWC15)	3.99	8.39	2.34	0.14	0.00	1.62	2.87	0.10	0.00	3.26	21.09	0.01	0.11	48.70	1.64	2.40	1.60	1.73	100
AN-102 Actual LC Melter	3.89	9.35	7.39	0.16	0.01	0.17	2.62	0.05	5.93	2.43	12.28	0.07	0.29	50.22	0.91	2.41	1.59	0.22	100
AN-102 Actual	3.89	9.37	7.38	0.22	0.01	0.20	2.62	0.06	5.91	2.43	12.27	0.12	0.29	50.13	0.91	2.40	1.58	0.22	100

## **Appendix B**

### **Glass Melt Electrical Conductivity and Viscosity Values Calculated by Arrhenius Regression at a Temperature of 1150°C**



## **Appendix B**

### **Glass Melt Electrical Conductivity and Viscosity Values Calculated by Arrhenius Regression at a Temperature of 1150°C**

This appendix contains tables of electrical conductivity and viscosity values calculated at a temperature of 1150°C using Arrhenius regression. Specifically, the Arrhenius equation (Equation (4.1) in Section 4.3.1) was fitted to the electrical conductivity-at-temperature and viscosity-at-temperature data for each LAW glass. Then, the fitted Arrhenius equation was used to calculate the electrical conductivity or viscosity value at 1150°C for each glass.

**Table B.1. Glass Melt Electrical Conductivity and Viscosity Values Calculated by Arrhenius Regression at a Temperature of 1150°C.**

Glass ID	Viscosity at 1150°C	Electrical Conductivity at 1150°C
LAWA44R10	71.17	0.288
LAWA53	55.78	0.421
LAWA56	51.39	0.433
LAWA88	59.87	0.562
LAWA102R1	50.58	0.378
LAWA126	62.66	0.395
LAWA128R1	94.04	0.393
LAWA130	71.00	0.410
LAWB65	53.48	0.222
LAWB66	45.62	0.263
LAWB68	57.73	0.214
LAWB78	41.98	0.241
LAWB79	39.91	0.231
LAWB80	54.92	0.183
LAWB83	53.54	0.223
LAWB84	51.24	0.230
LAWB85	54.86	0.235
LAWB86	47.38	0.225
C100-G-136B	56.09	0.310
LAWC27	51.50	0.256
LAWC32	38.78	0.317
LAWM1	35.95	0.162
LAWM2	20.97	0.187
LAWM3	17.85	0.365
LAWM4	13.25	0.192
LAWM5	122.87	0.198
LAWM6	49.65	0.130
LAWM7	116.59	0.077
LAWM8	73.95	0.090
LAWM9	126.10	0.091
LAWM10	14.05	0.424
LAWM11	13.04	0.487
LAWM12	13.58	0.526
LAWM13	14.39	0.733
LAWM14	47.27	0.488
LAWM15	65.49	0.570
LAWM16	25.65	0.299
LAWM17	32.91	0.428
LAWM18	29.06	0.290
LAWM19	80.77	0.244
LAWM20	21.10	0.501
LAWM21	21.40	0.349
LAWM22	99.15	0.288
LAWM23	58.32	0.269
LAWM24	78.63	0.375

Glass ID	Viscosity at 1150°C	Electrical Conductivity at 1150°C
LAWM25R1	86.51	0.248
LAWM26	77.41	0.249
LAWM27	35.55	0.198
LAWM28	93.49	0.094
LAWM29	79.17	0.239
LAWM30	34.50	0.212
LAWM31	21.29	0.554
LAWM32	42.05	0.407
LAWM33R1	18.98	0.488
LAWM34	16.21	0.574
LAWM35	24.66	0.304
LAWM36	37.00	0.294
LAWM37	32.05	0.276
LAWM38	54.34	0.344
LAWM39	49.10	0.342
LAWM40	71.99	0.461
LAWM41	68.98	0.247
LAWM42	54.87	0.283
LAWM43	44.19	0.278
LAWM44	73.27	0.186
LAWM45	66.52	0.289
LAWM46	76.67	0.139
LAWM47	70.71	0.245
LAWM48	85.91	0.225
LAWM49	74.92	0.229
LAWM50	57.82	0.274
LAWM51	62.45	0.261
LAWM52	50.83	0.437
LAWM53	40.02	0.255
LAWM54R1	111.10	0.093
LAWM55	11.83	0.589
LAWM56	25.46	0.355
LAWM57	27.90	0.545
LAWM59	56.58	0.484
LAWM60	47.24	0.448
LAWM63	40.45	0.668
LAWM66	31.25	0.619
LAWM68	31.61	0.490
LAWM71	43.12	0.487
LAWM73	32.71	0.514
LAWM75	42.03	0.447
LAWE2H	31.78	0.517
LAWE3	52.47	0.404
LAWE3H	33.05	0.510
LAWE4	53.55	0.419

**Table B.1. Glass Melt Electrical Conductivity and Viscosity Values Calculated by Arrhenius Regression at a Temperature of 1150°C (continued).**

Glass ID	Viscosity at 1150°C	Electrical Conductivity at 1150°C
LAW4E4H	44.23	0.455
LAW4E5	58.64	0.347
LAW4E5H	39.04	0.426
LAW4E7	23.51	0.366
LAW4E7H	21.41	0.400
LAW4E9H	25.26	0.331
LAW4E10H	41.60	0.201
LAW4E11	59.42	0.350
LAW4E12	47.53	0.496
LAW4E13	50.98	0.531
LAW4E16	59.57	0.487
LAW4CrP1R	62.52	0.524
LAW4CrP2R	45.24	0.658
LAW4CrP3R	55.89	0.519
LAW4CrP4R	44.59	0.704
LAW4CrP5	29.40	0.356
LAW4A41	68.06	0.526
LAW4A42	30.87	0.554
LAW4A45	64.48	0.514
LAW4A49	86.97	0.520
LAW4A50	72.45	0.517
LAW4A51	106.92	0.412
LAW4A52	51.70	0.466
LAW4A60	63.23	0.398
LAW4A81	69.54	0.512
LAW4A82	97.06	0.523
LAW4A83	92.49	0.461
LAW4A88	59.87	0.562
LAW4A89	65.34	0.542
LAW4A90	64.78	0.501
LAW4A93	15.60	0.442
LAW4A96	77.25	0.507
LAW4A125	41.97	0.464
LAW4A127R1	84.69	0.295
LAW4A129R1	108.26	0.323
LAW4A134	66.00	0.382
LAW4A135	78.00	0.352
LAW4A136	55.37	0.358
LAW4B30	30.69	0.287
LAW4B34	85.36	0.238
LAW4B37	91.58	0.231
LAW4B38	65.48	0.277
LAW4B60	28.89	0.250
LAW4B61	36.24	0.300
LAW4B62	27.08	0.350
LAW4B63	40.79	0.248

Glass ID	Viscosity at 1150°C	Electrical Conductivity at 1150°C
LAWB64	34.43	0.300
LAWB67	76.66	0.217
LAWB69	36.75	0.250
LAWB70	37.72	0.274
LAWB71	39.22	0.297
LAWB72	41.92	0.234
LAWB73	35.77	0.285
LAWB74	33.52	0.325
LAWB75	33.20	0.312
LAWB76	33.95	0.374
LAWB77	63.84	0.242
LAWB81	38.94	0.303
LAWB82	33.11	0.288
LAWB87	64.10	0.290
LAWB88	52.07	0.275
LAWB89	47.76	0.271
LAWB90	53.83	0.212
LAWB92	54.44	0.222
LAWB93R1	49.60	0.204
LAWB94	48.05	0.235
LAWB95	55.32	0.282
LAWC12	55.51	0.591
LAWC21rev2	49.01	0.262
LAWC29	39.63	0.279
LAWC30	42.79	0.347
LAWC31R1	40.90	0.280
C22AN107	43.86	0.343
A88Si+15	41.88	0.584
A88Si-15	93.53	0.346
C22Si+15	35.09	0.418
C22Si-15	54.45	0.306
A1C1-1	58.17	0.440
A1C1-2	48.53	0.400
C1-AN107	45.76	0.318
A2-AP101	59.68	0.353
A2B1-1	61.44	0.316
A2B1-2	54.17	0.245
B1-AZ101	52.69	0.198
C2-AN102C35	34.97	0.265
A3-AN104	34.75	0.295
A2B1-3	52.54	0.237
A3C2-1	40.94	0.320
A3C2-2	34.79	0.277
A3C2-3	33.31	0.265
A1-AN105R2	70.32	0.385

## **Appendix C**

### **Statistical Methods Used to Develop, Evaluate, and Validate Property-Composition Models**

## Appendix C

### Statistical Methods Used to Develop, Evaluate, and Validate Property-Composition Models

This appendix presents various statistical methods used for developing, evaluating, and validating waste glass property-composition models. Section C.1 discusses mixture experiments, introduces two general forms of mixture experiment models, and two variants of one of the model forms appropriate for assessing the presence of “block effects”. Section C.2 discusses mixture-temperature model forms appropriate for glass properties such as viscosity and electrical conductivity that depend on temperature as well as composition. Section C.3 discusses the least squares regression methods used to fit models to data and corresponding assumptions. Section C.4 discusses the statistical methods and summary statistics used for model evaluation based on the data used to fit a model. Section C.5 discusses statistical methods for model augmentation (i.e., adding terms to a model) and model reduction (i.e., removing unneeded terms from a model). Section C.6 discusses the statistical methods and summary statistics used for model validation based on data not used to fit a model. Section C.7 discusses several statistical intervals used to quantify uncertainties in model predictions.

#### C.1 Mixture Experiments, Model Forms, and Assessing Block Effects

A *mixture experiment* involves mixing two or more components in various proportions, and then measuring one or more response variables for the resulting end-product mixtures. If the proportions of  $q$  mixture components are denoted  $x_i$ ,  $i = 1, 2, \dots, q$ , then these proportions are subject to the basic mixture constraints

$$0 \leq x_i \leq 1 \quad \text{and} \quad \sum_{i=1}^q x_i = 1. \quad (\text{C.1})$$

Often in practice, the component proportions will be subject to additional single-component constraints

$$0 \leq L_i \leq x_i \leq U_i \leq 1 \quad (\text{C.2})$$

and/or multiple-component constraints that can be written in the general form

$$\sum_{i=1}^q A_{ki} x_i + A_{k0} \geq 0, \quad k = 1, 2, \dots, K. \quad (\text{C.3})$$

In Equation (C.2)  $L_i$  and  $U_i$  denote, respectively, the lower and upper constraints on the  $i^{\text{th}}$  component ( $i = 1, 2, \dots, q$ ). In Equation (C.3), the  $A_{ki}$  ( $i = 1, 2, \dots, q$ ) and  $A_{k0}$  denote the coefficients of the  $k^{\text{th}}$  multiple-component constraint. Cornell (2002) provides a comprehensive

discussion of statistical methods for the design, modeling, and data analysis of mixture experiments.

Section C.1.1 introduces the linear mixture (LM) model and partial quadratic mixture (PQM) model forms for mixture experiment data. Section C.1.2 discusses two variations of the LM model that can be used to assess modeling data collected in two or more blocks (e.g., at different times or under different conditions) for “block effects”.

### C.1.1 Linear and Partial Quadratic Mixture Model Forms

The LM model form is given by

$$f(y) = \sum_{i=1}^q b_i x_i + E \quad (C.4)$$

while the PQM model form is given by

$$f(y) = \sum_{i=1}^q b_i x_i + \text{Selected} \left\{ \sum_{i=1}^q b_{ii} x_i^2 + \sum_{i < j}^{q-1} b_{ij} x_i x_j \right\} + E . \quad (C.5)$$

In Equations (C.4) and (C.5),  $y$  is a property or response variable that can be measured for each end-product mixture;  $f(y)$  is some mathematical transformation of  $y$  (which could be the identity transformation); the  $x_i$  ( $i = 1, 2, \dots, q$ ) are proportions of  $q$  components subject to the constraints in Equation (C.1) and possibly constraints of the forms in Equations (C.2) and/or (C.3); the  $b_i$  ( $i = 1, 2, \dots, q$ ), the  $b_{ii}$  (selected), and the  $b_{ij}$  (selected) are coefficients to be estimated from data; and  $E$  is a random experimental and property measurement error for each data point. Many statistical methods exist for the case where the  $E$  are independent (i.e., not correlated) and normally distributed with mean 0 and standard deviation  $\sigma$ . In Equation (C.5), “Selected” means that only some of the terms in curly brackets are included in the model. The subset is selected using standard stepwise regression or related methods (Draper and Smith 1998; Montgomery et al. 2001). LM models and PQM models are discussed in more detail and illustrated, respectively, by Cornell (2002) and Piepel et al. (2002).

Cornell (2002) discusses many other empirical mixture model forms that can be more appropriate than models of the forms in Equations (C.4) and (C.5) in certain specialized conditions. However, models of the form in Equations (C.4) and (C.5) are widely used in many application areas (including waste glass property modeling) and have been shown to perform very well.

### C.1.2 Variants of the Linear Mixture Model for Assessing Block Effects

Two variants of the LM model, useful in assessing the presence or absence of “block effects” in a modeling dataset comprised of two subsets of data collected at different times and/or locations (i.e., “blocks”), are presented in this section. These LM model variants can easily be extended for use with modeling datasets comprised of three or more subsets of data.

The following model form is applicable if: (1) the LM model accounts for the majority of the compositional dependence of  $f(y)$  and (2) there is a constant difference in  $f(y)$  values for one subset of data (i.e., block) compared to the other:

$$f(y) = b_0 B + \sum_{i=1}^q b_i x_i + E, \quad (C.6)$$

where  $B = 0$  for one of the two subsets of modeling data and  $B = 1$  for the other subset. The remaining notation is as described previously. If there is a reason to believe one subset is unbiased and the other biased, then  $B = 0$  should be used for the subset believed to be unbiased. In Equation (C.6),  $b_0$  is a coefficient estimated from the modeling data that gives the estimated magnitude of the constant difference in  $f(y)$  values between the two subsets. If the  $b_0$  coefficient is statistically different from zero, then that is an indication there is a significant constant difference between the  $f(y)$  values for one subset of the modeling data compared to the other.

The following model form is applicable if: (1) the LM model accounts for the majority of the compositional dependence of  $f(y)$  and (2) the difference in  $f(y)$  values for one subset of data compared to the other depends on the composition of the mixture:

$$f(y) = \sum_{i=1}^q b_i^0 x_i + \sum_{i=1}^q b_i^1 x_i B + E, \quad (C.7)$$

where the choice of  $B = 0$  or  $B = 1$  and the remaining notation is the same as previously discussed. In Equation (C.7), the  $b_i^0$  coefficient represents the linear blending effect of the  $i^{\text{th}}$  component for the subset of modeling data represented by  $B = 0$ . The  $b_i^1$  coefficient represents the change or bias in the linear blending effect of the  $i^{\text{th}}$  component for the subset of modeling data represented by  $B = 1$ . If any of the  $b_i^1$  coefficients ( $i = 1, 2, \dots, q$ ) are statistically different from zero, that is an indication that there are compositionally-dependent differences in the  $f(y)$  values for one subset of the modeling data compared to the other.

The model forms in Equations (C.6) and (C.7) are intended for use in assessing whether data collected at different times, locations, or conditions are subject to effects (biases) related to the change in time, location, or conditions of data collection. If significant bias is indicated by such models, it should ideally be confirmed by other means (e.g., results on a standard collected at different times, locations, and conditions). It is beyond the scope of this discussion to address what to do when biased data are detected and confirmed. The appropriate steps will depend on

the specific situation, the intended use of the data, and any requirements or limitations regarding the use of biased (or bias-corrected) data.

Equations (C.6) and (C.7) are for cases where a LM model accounts for the majority of the compositional dependence of  $f(y)$ . This will usually be the case for most waste glass property models. It is possible to include block effect terms similar to those in Equations (C.6) and (C.7) in cases where there is substantial non-linear compositional dependence. However, doing this can have added complications for some waste glass property-composition databases, and so is not discussed further.

Ultimately, investigation of block effects was not performed in conjunction with property-composition modeling work discussed in this report. The use of Equations (C.6) and (C.7) to assess block effects is complicated if different glass components vary, or vary over different ranges for groups of data in the property-composition modeling dataset. These factors can cause block effects to appear significant even though there is no systematic bias in property values across groups. Hence, investigation of block effects is often not performed in such cases. Further, because (i) procedures for batching, melting, and testing of waste glasses are well established, (ii) no block effects have been identified in previous phases of the WTP property-composition modeling work, and (iii) assessment of replicate data over groups showed no sign of block effects, investigation of block effects was deemed unnecessary for the property-composition modeling work discussed in this report.

## C.2 Mixture-Temperature Models for Viscosity and Electrical Conductivity

Viscosity and electrical conductivity of glass melts depend on the melt temperatures as well as the compositions of the glasses. Equations for representing the temperature dependence of viscosity or electrical conductivity for a given glass composition are discussed in Section C.2.1. Then, Section C.2.2 discusses using the temperature-dependence equations as a basis for developing property-composition-temperature model forms for viscosity and electrical conductivity.

### C.2.1 Equations for Temperature Dependence of Viscosity and Electrical Conductivity

The temperature dependence for a given glass can be represented by the *Arrhenius equation*

$$\ln(y) = A + \frac{B}{T} + E \quad (\text{C.8})$$

where  $y$  = viscosity or electrical conductivity for a given glass,  $\ln(y)$  denotes the natural logarithm of  $y$ ,  $A$  and  $B$  are coefficients specific to a given glass, and  $T$  is temperature in Kelvin.



Sometimes there is curvature in the relationship between  $\ln(y)$  and  $1/T$ , which can be represented by the *T2 equation*

$$\ln(y) = A + \frac{B}{T} + \frac{C}{T^2} + E \quad (\text{C.9})$$

or the *truncated-T2 equation*

$$\ln(y) = A + \frac{C}{T^2} + E \quad (\text{C.10})$$

In these two equations,  $B$  and  $C$  represent coefficients specific to a given glass. The T2 equation is a second-order Taylor series expansion of the Vogel-Fulcher equation

$$\ln(y) = A + \frac{B}{T - T_0} + E \quad (\text{C.11})$$

with coefficients  $A$ ,  $B$ , and  $T_0$ . However, the Vogel-Fulcher equation is non-linear in its coefficients (specifically  $T_0$ ). Hence, iterative nonlinear least squares methods are required to fit the Vogel-Fulcher equation to data rather than the single-step solution of linear least squares methods. Feng et al. (2004) showed that the T2 and truncated-T2 equations can provide adequate approximations of the Vogel-Fulcher equation, while requiring only linear least squares fitting methods.

In each of Equations (C.8) to (C.11), the  $E$  denotes a random error for each data point. When these errors are independent (i.e., not correlated) and have equal variance across the data set, ULS regression can be used to fit the equation.

### **C.2.2 Models for Temperature and Compositions Dependence of Viscosity and Electrical Conductivity**

The equations for temperature dependence in Section C.2.1 are applicable to specific glasses, with the equation coefficients differing from glass to glass. Hence, the temperature dependence equations can be converted to models representing the effects of both temperature and glass composition on viscosity or electrical conductivity by writing the coefficients as functions of glass composition. For viscosity and electrical conductivity, linear functions of glass composition (specifically, linear mixture models) may be sufficient. Thus, expanding the coefficients of the Arrhenius equation using LM models yields

$$\ln(y) = \sum_{i=1}^q a_i x_i + E_G + \sum_{i=1}^q b_i \frac{x_i}{T} + E_T, \quad (\text{C.12})$$

where  $a_i$  and  $b_i$  are coefficients for the  $i^{\text{th}}$  glass component estimated from data,  $x_i$  is the mass fraction of the  $i^{\text{th}}$  glass component such that  $\sum x_i = 1$ ,  $E_G$  is a random error associated with determining  $y$  for each LAW glass, and  $E_T$  is a random error associated with determining  $y$  at the temperature values for a given glass. The random errors  $E_G$  and  $E_T$  are assumed to be normally distributed with zero means and standard deviations  $\sigma_G$  and  $\sigma_T$ . Further, the  $E_G$  and  $E_T$  are assumed to be statistically independent (i.e., not correlated).

In a similar manner, expanding the coefficients of the  $T2$  equation using LM models yields

$$\ln(y) = \sum_{i=1}^q a_i x_i + E_G + \sum_{i=1}^q b_i \frac{x_i}{T} + \sum_{i=1}^q c_i \frac{x_i}{T^2} + E_T, \quad (\text{C.13})$$

while expanding the coefficients of the truncated-T2 equation yields

$$\ln(y) = \sum_{i=1}^q a_i x_i + E_G + \sum_{i=1}^q c_i \frac{x_i}{T^2} + E_T, \quad (\text{C.14})$$

where  $c_i$  is the coefficient of the corresponding component-temperature model term for the  $i^{\text{th}}$  glass component, and all other notations have been defined previously. In some cases it may be required to expand one or more coefficients in a temperature-dependence equation using a PQM model. Such models for viscosity or electrical conductivity are discussed in the main body of the report where appropriate.

The two error terms,  $E_G$  and  $E_T$ , in Equations (C.12) to (C.14) are a result of a “restriction on randomization” in measuring  $y$  (viscosity or EC). Specifically, the property  $y$  is measured at multiple temperatures on each glass before moving on to the next glass. This is a natural way to measure viscosity or EC, because glass is a “hard-to-change” factor while temperature is an “easy-to-change” factor. Thus, it is infeasible to completely randomize all combinations of glass composition and temperature in measuring viscosity or EC. Hence, the way in which viscosity or EC is measured is a “restriction on randomization” that requires a proper analysis of the data. Experiments with this sort of restriction are referred to as *split-plot experiments* in the statistical literature, because of their early use in agricultural experiments. However, this type of restricted-randomization data collection is common in engineering and other experiments where there is at least one hard-to-change factor and at least one easy-to-change factor. The main consequence of the split-plot nature of the data is that there are two uncertainty standard deviations, one related to whole plots (WPs) and one related to sub-plots (SPs). For viscosity and EC, glasses are the WP “treatments” and the associated uncertainty standard deviation is denoted  $\sigma_G$ . Temperature values are the SP “treatments” and the associated uncertainty standard deviation is denoted  $\sigma_T$ . The observations within a WP (e.g.,  $y$  values at four temperatures) are correlated. Thus, it is improper to use ordinary least squares (OLS) regression, which has only one uncertainty standard deviation and assumes observations are uncorrelated. Generalized least squares (GLS) regression modeling is needed for the split-plot data structure present with viscosity and EC data.

GLS regression modeling simultaneously estimates the model coefficients as well as  $\sigma_G$  and  $\sigma_T$ . See Section C.3.3 for further discussion and references on these topics.

Investigation of block effects by adding block effect terms to the models in Equations (C.12) to (C.14) is an added complication on top of the split-plot structure of the data for such models. Assessing block effects is further complicated if different glass components vary, or vary over different ranges for groups of data in the property-composition-temperature modeling dataset. These factors can cause block effects to appear significant even though there is no systematic bias in property values across groups. Hence, investigation of block effects is often not performed in such cases. Further, because (i) procedures for batching, melting, and testing of waste glasses are well established, (ii) no block effects have been identified in previous phases of the WTP property-composition modeling work, and (iii) assessment of replicate data over groups showed no sign of block effects, investigation of block effects was deemed unnecessary for the property-composition-temperature modeling work discussed in this report.

### **C.3 Least Squares Regression Methods and Assumptions for Fitting Models**

Empirical or semi-empirical property-composition models are typically fitted to data sets using unweighted least squares (ULS) or weighted least squares (WLS) regression. However, in some cases generalized least squares (GLS) regression is required. Section C.3.1 discusses ULS and WLS regression, while Section C.3.2 discusses GLS regression. Section C.3.3 discusses the case of GLS regression for data with a split-plot structure such as occurs when measuring viscosity and electrical conductivity of glasses at various temperatures. Draper and Smith (1998) and Montgomery et al. (2001) provide additional discussion of the ULS, WLS, and GLS topics.

#### **C.3.1 Unweighted and Weighted Least Squares Regression**

The underlying assumptions of ULS and WLS regression are:

- (i) The predictor variable values (e.g., mass fractions of glass components) are known or measured without uncertainty, or at least that the uncertainty is small relative to the uncertainty in response variable (glass property) values
- (ii) The testing and/or measurement errors in a response variable (glass property) over a model development data set are independently distributed (i.e., the errors are not correlated). For ULS regression, the additional assumption is made that the errors are identically distributed (i.e., with zero mean and the same variance). For WLS regression, the errors are also assumed to have zero mean, but the variance can be different for different data points.
- (iii) The errors from (ii) are normally (Gaussian) distributed.

Regarding assumption (i), the true composition of glasses in a model development data set are generally not known, and so any representation of glass composition selected (e.g., target compositions, analyzed compositions, or adjusted and normalized versions of analyzed compositions) will be subject to uncertainty. Weier and Piepel (2002) discuss a procedure for performing adjustments and weighted normalization of analyzed glass compositions that corrects for biases and reduces uncertainties in analyzed glass compositions. As long as representations of glass composition do not have significant biases (or those biases are appropriately corrected), it is generally expected that uncertainties will be small compared to uncertainties in glass property values. Further, uncertainties in glass compositions are expected to be small compared to errors in using empirical or semi-empirical model forms to approximate the true (but unknown) property-composition relationships. Hence, assumption (i) is sufficiently satisfied for most waste glass property-composition modeling situations.

The portion of assumption (ii) having to do with the independence of errors in testing and measuring properties may not be completely satisfied when model development data sets are comprised of subsets of data generated at different times or locations (e.g., different laboratories). There is the potential for errors in testing and measuring properties to vary for different subsets of data, and be more alike within the same subset of data. However, this issue has generally not been a problem in many past property-composition modeling efforts. If needed, GLS methods that account for correlations among data points could be applied.

The “identically distributed” portion of assumption (ii) for ULS regression is not valid for some properties, because the variance of errors in testing and measurement of properties depends on the value of the property. For example, the variances of viscosity and durability results for waste glasses tend to increase as the values of these properties increase. In cases where the identically distributed (equal variance) assumption is violated, it can often be remedied by applying an appropriate mathematical transformation to the property values (e.g., a logarithmic transformation). The Box-Cox family of transformations contains transformations (including the logarithmic transformation) appropriate for many models (see Draper and Smith 1998). Such transformations also often yield better fitting empirical or semi-empirical property-composition models. In some cases, a property transformation used in a particular model form may be preferred for some reason (e.g., provides a better fit), but does not satisfy the constant variance assumption of (ii). Or, it may be that the difference in variances across response values in the modeling data set cannot be rectified by a response transformation. In such cases, other regression methods such as WLS regression or generalized linear models (Myers et al. 2002) could be applied.

The assumption of normally distributed measurement and testing errors in the measured response variable values allows the use of normal theory regression tests and uncertainty equations associated with the fitted regression model. For example, normal theory confidence intervals and prediction intervals can be used (see Section C.7).

As discussed in preceding text, ULS regression requires that all response values for the modeling data have constant variance (i.e., uncertainty). WLS regression accounts for response values having different variations by using a weight for each data point ( $w_i$ ). Often,  $w_i$  is chosen

to be proportional to the reciprocal of the variance (squared standard deviation) of the response for the  $i^{\text{th}}$  data point ( $y_i$ ).

$$w_i = \frac{\lambda}{\text{Var}(y_i)} = \frac{\lambda}{[\text{SD}(y_i)]^2} \quad (\text{C.15})$$

where  $\lambda$  is a proportionality constant (which could be 1). Thus, in such a WLS regression the weighted response values  $\sqrt{w_i} y_i$  then have equal variance. However, other methods for selecting weights can be applicable for various situations.

In summary, assumptions of ULS regression may not be completely satisfied for typical property-composition data sets and models. Violations of the constant variance assumption for property values over a modeling data set can sometimes be addressed by appropriate property transformations so that ULS regression may be used. Other violations may be small enough that ULS regression methods can still be used without significant consequence. However, if there are large enough differences in variances of property values across a modeling data set that cannot be addressed by a property transformation, then WLS regression methods should be used. If there are correlations among data points in a regression set, GLS methods are needed as discussed in the following subsection.

### **C.3.2 Generalized Least Squares Regression**

The underlying assumptions of GLS regression are:

- (i) The predictor variable values (e.g., mass fractions of glass components) are known or measured without uncertainty, or at least that the uncertainty is small relative to the uncertainty in response variable (glass property) values
- (ii) The testing and/or measurement errors in a response variable (glass property) over a model development data set are normally distributed with a mean vector of zeros and a variance-covariance matrix  $V$ .

Under these assumptions, the data to be modeled by GLS regression can be written in the general form

$$\mathbf{y} \sim N(\boldsymbol{\mu}(\mathbf{x}, \boldsymbol{\beta}), \mathbf{V}), \quad (\text{C.16})$$

which denotes that the vector of property values  $\mathbf{y}$  is normally distributed with mean vector  $\boldsymbol{\mu}(\mathbf{x}, \boldsymbol{\beta})$  and variance-covariance matrix  $\mathbf{V}$ . The mean vector is a function of the vector of predictor variables  $\mathbf{x}$  and the unknown model parameter vector  $\boldsymbol{\beta}$ . Most commonly, functions linear in the parameters  $\boldsymbol{\mu}(\mathbf{x}, \boldsymbol{\beta}) = \boldsymbol{\beta}' \mathbf{a}$  are used, where  $\mathbf{a}$  is an expansion of  $\mathbf{x}$  in the form of the model. Note that such functions can still be linear as well as nonlinear in the predictor variables. If the variance-covariance matrix  $\mathbf{V}$  is known, the estimate of the parameter vector obtained by GLS can be written as

$$\hat{\boldsymbol{\beta}} = (\mathbf{A}'\mathbf{V}^{-1}\mathbf{A})^{-1} \mathbf{A}'\mathbf{V}^{-1}\mathbf{y} \quad (\text{C.17})$$

with the variance of the parameter estimates denoted by

$$\text{Var}(\hat{\boldsymbol{\beta}}) = (\mathbf{A}'\mathbf{V}^{-1}\mathbf{A})^{-1} \quad (\text{C.18})$$

(see Montgomery et al. 2001, Section 5.5.1). In both of these equations,  $\mathbf{A}$  is the matrix of data used to fit the model, expanded in the form of the model. If the variance-covariance matrix  $\mathbf{V}$  is not known in advance, for some problems it can be estimated at the same time as the model parameters are estimated (see Section C.3.3 for further discussion). In such a case, Equation (C.18) is only approximate.

Note that ULS and WLS regression are special cases of GLS regression. ULS applies when the diagonal elements of  $\mathbf{V}$  (the variances of the data points) are all the same, and the off-diagonal elements (covariances) are all zero. WLS applies when the diagonal elements of  $\mathbf{V}$  differ and the off-diagonal elements are all zero.

### C.3.3 Generalized Least Squares Regression for Split-Plot Data Structures

Viscosity and electrical conductivity are examples of glass properties for which GLS regression is required when data are collected using the approach typical for those properties. Specifically, viscosity (or electrical conductivity) is measured at each of several temperatures for one glass, then another glass, etc. This is referred to in the statistical literature as a “restriction on randomization” because the property is not measured on composition-temperature combinations in a completely random order. The glass composition is referred to as a hard-to-change factor, and temperature is referred to as an easy-to-change factor. It is easier to make viscosity or electrical conductivity measurements at various temperatures for one glass, then the next glass, etc., but it results in a restriction on randomization. Experimental data collected in this way are referred to as having a split-plot structure. The terminology originally came from agricultural experiments with restrictions on randomization, where fields were split into “whole plots” and

“sub plots”. However, this terminology is also used for experiments in various non-agricultural application areas.

Every viscosity (or electrical conductivity)-at-temperature data point is subject to one uncertainty related to batching and melting a glass, as well as the uncertainty associated with the set-up and property measurement of a given glass. The associated standard deviation is denoted  $\sigma_G$ . The data points for a given glass are also subject to a second uncertainty related to measuring the property at various temperatures. The associated standard deviation is denoted  $\sigma_T$ . The property-at-temperature values for each given glass are correlated. The variance-covariance matrix for the split-plot structure typical for viscosity or electrical conductivity data on several glasses is given by

$$V = \begin{bmatrix} T_1 & 0 & \dots & \dots & 0 \\ 0 & T_2 & 0 & \dots & 0 \\ 0 & 0 & \ddots & \dots & 0 \\ \vdots & \vdots & \vdots & \ddots & \vdots \\ 0 & 0 & 0 & \dots & T_g \end{bmatrix}, \quad (C.19)$$

where  $g$  denotes the number of glasses in a modeling dataset and a  $T_i$  matrix is given by

$$T_i = \begin{bmatrix} \sigma_G^2 + \sigma_T^2 & \sigma_G^2 & \sigma_G^2 & \sigma_G^2 \\ \sigma_G^2 & \sigma_G^2 + \sigma_T^2 & \sigma_G^2 & \sigma_G^2 \\ \sigma_G^2 & \sigma_G^2 & \sigma_G^2 + \sigma_T^2 & \sigma_G^2 \\ \sigma_G^2 & \sigma_G^2 & \sigma_G^2 & \sigma_G^2 + \sigma_T^2 \end{bmatrix}. \quad (C.20)$$

These equations are based on ones given by Myers and Montgomery (1995, Section 9.6.3). This form of  $T_i$  assumes viscosity or electrical conductivity is measured at four temperatures for each glass. The  $T_i$  matrix would expand or contract accordingly if the number of temperatures at which a property is measured for a given glass would increase or decrease.

If  $\sigma_G$  and  $\sigma_T$  were known, then  $V$  in (C.19) could be used in Equations (C.17) and (C.18) to estimate viscosity or electrical conductivity model coefficients and their uncertainties. However,  $\sigma_G$  and  $\sigma_T$  generally are not known and must be estimated from data. Statistical software is available for fitting so-called *mixed models*, that is, models that require simultaneous estimation of data uncertainties (e.g.,  $\sigma_G$  and  $\sigma_T$ ) and model coefficients. The PROC MIXED routine in SAS (2005) was used to fit the viscosity and electrical conductivity models presented in this report.

## C.4 Statistical Methods for Model Evaluation

There are many statistical methods (both numerical and graphical) for assessing models. *Evaluation methods* assess a model with the data used to develop the model. Such data are referred to as *model development data*. The goals of model evaluation are to assess: (1) how well a model fits the data used to develop it, (2) how well the least squares or other regression method assumptions are satisfied (see Section C.3), and (3) whether there are any outlying or influential data points that significantly affect the fitted model. Problems detected by model evaluation such as violation of assumptions, detection of outlying data points, or detection of model inadequacy require implementing various remedies in the model development process until the problem(s) are corrected. When the model being evaluated acceptably fits the data used to develop the model, *model validation* methods should be applied using data not used to develop the model. Such data are referred to as *model validation data*. If model validation data are not available, *crossvalidation methods* can be applied using the model development data. Crossvalidation methods leave out one or more data points at a time, so that some of the data are used for model development and some for model validation. Such methods are also referred to as data-splitting validation methods, where part of the data is used for model development and evaluation, while the other part is used for validation. Draper and Smith (1998) and Montgomery et al. (2001) discuss statistical methods for evaluating and validating models.

Model evaluation techniques include predicted versus measured (PvM) property plots, standardized residual plots, outlier diagnostics, three  $R^2$  statistics, root mean squared error (*RMSE*), and statistical lack-of-fit (LOF) tests. Each of these is explained briefly below. The following notation is used in the subsequent descriptions and definitions:

- $n$  = the number of data points used to fit a model,
- $p$  = the number of parameters (coefficients) in a model form estimated via regression on the data,
- $y_i$  = the measured property value (mathematically transformed, if appropriate for the model form used) for the  $i^{th}$  data point,
- $\hat{y}_i$  = the predicted property value (mathematically transformed, if appropriate for the model form used) for the  $i^{th}$  data point made using the model fitted to all  $n$  data points,
- $r_i$  = the residual for the  $i^{th}$  data point =  $y_i - \hat{y}_i$ ,
- $\hat{y}_{(i)}$  = the predicted property value (mathematically transformed, if appropriate for the model form used) for the  $i^{th}$  data point made using a model fitted to all  $n$  data points except the  $i^{th}$ ,



- $w_i$  = the weight applied to the  $i^{th}$  data point in cases where WLS regression is used. Typically,  $w_i$  is proportional to the reciprocal of the variance of the response variable for the  $i^{th}$  data point,
- $\bar{y}$  = the unweighted average (mean) of the  $n$  measured property values (mathematically transformed, if appropriate for the model form used),
- $\bar{y}_w$  = the weighted average (mean) of the  $n$  measured property values (mathematically transformed, if appropriate for the model form used)

$$\bar{y}_w = \frac{\sum_{i=1}^n w_i y_i}{\sum_{i=1}^n w_i} \quad (C.19)$$

The model evaluation methods are now briefly described.

- Predicted versus measured (PvM) property plots show how well model predicted values  $\hat{y}_i$  compare to the measured values  $y_i$  for the glasses in the model development data set. Predicted property values  $\hat{y}_i$  are plotted on the  $y$ -axis and measured property values  $y_i$  are plotted on the  $x$ -axis. A line with slope one is included in the plot for reference purposes, and represents the ideal of predicted values equaling measured values. Plotted points falling above this line correspond to glasses for which the model over-predicts the property, while plotted points falling below this line represent glasses for which the model under-predicts the property. A preponderance of plotted points in a portion of the plot falling above or below the line indicates that the model tends to yield biased predictions for that range of property values. Plotted points far from the line are outlying or potentially influential data points.

For WLS regression, an *ordinary (unweighted) PvM plot* of  $\hat{y}_i$  versus  $y_i$  could be viewed as is done for ULS regression. Or, a *weighted PvM plot* of  $\sqrt{w_i} \hat{y}_i$  versus  $\sqrt{w_i} y_i$  could be viewed. The ordinary (unweighted) PvM plot has the advantage of retaining the units of the response (or its transformation), but the disadvantage that points with smaller weights (i.e., higher uncertainties) may appear farther from the line with slope one. However, rather than considering this a disadvantage, it may be better thought of as showing the penalty paid in obtaining predictions having more uncertainty for modeling data points with smaller weights (i.e., higher uncertainty). The weighted PvM plot would show the model predictive performance for the modeling data points after accounting for (i.e., removing the scatter due to) the differing weights (i.e., uncertainties).

For GLS regression, an ordinary PvM plot could be viewed as is done for ULS regression. Or, a modified version could be viewed that accounts for the variance-covariance structure of the data. Because such modified PvM plots are more complicated,

they are not discussed or used in this report. In this report, ordinary PvM plots are viewed regardless of whether ULS, WLS, or GLS regression is employed to fit models.

- RMSE is given by

$$RMSE_U = \sqrt{\frac{\sum_{i=1}^n (\hat{y}_i - y_i)^2}{n - p}} \quad (\text{C.20a})$$

for ULS regression, and by

$$RMSE_W = \sqrt{\frac{\sum_{i=1}^n w_i (\hat{y}_i - y_i)^2}{n - p}} \quad (\text{C.20b})$$

for WLS regression. If the fitted model is adequate and does not have a statistically significant lack-of-fit, this statistic provides an estimate of the experimental and measurement uncertainty standard deviation associated with melting glasses and measuring the associated property. The statistic  $RMSE$  is included as standard output in most regression software, and has units the same as the property values  $y_i$  (including any mathematical transformation of the property in the model form) for ULS regression and the units of  $\sqrt{w_i} y_i$  for WLS regression.

RMSE values are not traditionally calculated and reported by software implementing GLS regression because of the more complicated uncertainty structure of the data. In this report we have opted for using  $RMSE_U$  to provide an overall summary measure of GLS fitted models. Note that  $RMSE_U$  will not directly give proper estimates of  $\sigma_G$ ,  $\sigma_T$ , or  $\sqrt{\sigma_G^2 + \sigma_T^2}$  and should not be interpreted as such.

- Standardized residual plots display standardized residuals ( $s_i$ , differences in predicted and measured property values divided by their standard deviations) versus various quantities, such as: glass component mass fractions ( $x_i$ ), predicted property values ( $\hat{y}_i$ ), or an index associated with each data point. The formula for a standardized residual is given by

$$s_i = \frac{r_i}{RMSE_U \left[ 1 - \mathbf{a}_i^T (\mathbf{A}^T \mathbf{A})^{-1} \mathbf{a}_i \right]^{0.5}} \quad (\text{C.21a})$$

for ULS regression, by

$$s_i = \frac{\sqrt{w_i} r_i}{RMSE_W \left[ 1 - w_i \mathbf{a}_i^T (\mathbf{A}^T \mathbf{W} \mathbf{A})^{-1} \mathbf{a}_i \right]^{0.5}} \quad (\text{C.21b})$$

for WLS regression, and by

$$s_i = \frac{r_i}{\left[1 - \mathbf{a}_i^T (\mathbf{A}^T \mathbf{V}^{-1} \mathbf{A})^{-1} \mathbf{a}_i\right]^{0.5}} \quad (\text{C.21c})$$

for GLS regression. In Equations (C.21a), (C.21b), and (C.21c):  $s_i$ ,  $w_i$ , and  $r_i$  are as previously described;  $RMSE_U$  and  $RMSE_W$  are respectively given by Equations (C.20a) and (C.20b);  $\mathbf{a}_i$  is the composition (column) vector for the  $i^{\text{th}}$  modeling data point expanded in the form of the model;  $\mathbf{A}$  is an  $n \times p$  matrix of the compositions (and temperatures in the case of viscosity or electrical conductivity) in the modeling data set expanded in the form of the model;  $\mathbf{W}$  is an  $n \times n$  matrix with the weights  $w_i$  along the main diagonal, and zeros elsewhere; and  $\mathbf{V}$  is an  $n \times n$  matrix representing the variance-covariance structure of the modeling dataset.

Patterns in the  $s_i$  versus  $\hat{y}_i$  plot can indicate a violation of the least squares regression assumptions and suggest a property transformation to remedy the situation. Patterns in the  $s_i$  versus  $x_i$  plots can indicate inadequacies of the model or least squares assumptions. Patterns in  $s_i$  versus data indices can indicate subsets of the data for which a model may be inadequate. Standardized residuals are typically used in residual plots because the majority should fall within the range of  $\pm 2.0$  and almost all should fall within  $\pm 3.0$ . Comparing standardized residuals to such a range provides an easy criterion for judging whether a data point is outlying.

- Normality plots display normal scores versus the ordered (from smallest to largest) standardized residuals (from Equations (C.21a), (C.21b), or (C.21c) for ULS, WLS, and GLS regression, respectively) for the  $n$  data points used to fit the model being assessed. Normal scores are the expected values of a sample of size  $n$  from standard normal distribution (with mean 0 and standard deviation 1). The plotted points are compared to the ideal of a straight line corresponding to a normal distribution. A straight middle portion of the plot with curved “tails” on each end of the plot indicate the presence of outlying data points, which cause a heavier-tailed distribution than the normal distribution.
- Outlier diagnostics and plots indicate data points that are outlying or influential with respect to property value or composition. There are too many of these diagnostics and plots to discuss here, but several produced by the R software (Ihaka and Gentleman 1996, R Core Development Team 2006) and the SAS software (2005) were considered in this work. Draper and Smith (1998) and Montgomery et al. (2001) discuss outlier diagnostics and plots for ULS regression, but software such as R and SAS produce the appropriate versions of diagnostics and plots for WLS and GLS as well as ULS regression.
- $R^2$  statistics quantify the proportion of variation in the property values  $y_i$  (for ULS regression) or weighted property values  $\sqrt{w_i} y_i$  (for WLS regression) accounted for by the

fitted model. Three  $R^2$  statistics are used, as discussed later in this section. Typically  $R^2$  type statistics are not calculated and reported by software that performs GLS regression. This is because of the more complicated uncertainty structure of the data. It may be possible to develop such statistics for GLS regression, but the interpretations would be modified.

- A statistical lack-of-fit (LOF) test checks whether the differences (for ULS regression) or weighted differences (for WLS regression) between measured and predicted property values from a fitted model are larger than expected based on the experimental and measurement uncertainty in the data. If the predicted versus measured differences are larger than data uncertainty at a high enough statistical confidence (e.g., greater than 90%), the model is said to have a statistically significant LOF. Replicate data points containing all applicable sources of experimental and measurement uncertainty<sup>1</sup> are required to perform statistical LOF tests. This process is conducted using a LOF F-test given by

$$F = \frac{(SSE - SSPE)/(n - p - f)}{SSPE/f} = \frac{\left[ \left( \sum_{i=1}^n (\hat{y}_i - y_i)^2 - \sum_{k=1}^K \sum_{j=1}^{m_k} (y_{kj} - \bar{y}_k)^2 \right) / (n - p - f) \right]}{\sum_{k=1}^K \sum_{j=1}^{m_k} (y_{kj} - \bar{y}_k)^2 / f} \quad (C.22a)$$

for ULS regression, and by

$$F = \frac{(SSE - SSPE)/(n - p - f)}{SSPE/f} = \frac{\left[ \left( \sum_{i=1}^n w_i (\hat{y}_i - y_i)^2 - \sum_{k=1}^K \sum_{j=1}^{m_k} w_j (y_{kj} - \bar{y}_k)^2 \right) / (n - p - f) \right]}{\sum_{k=1}^K \sum_{j=1}^{m_k} w_j (y_{kj} - \bar{y}_k)^2 / f} \quad (C.22b)$$

for WLS regression. In Equations (C.22a) and C.22b): SSE = sum of squares error; SSPE = sum of squared pure error (i.e., from replicates);  $n$  and  $p$  are as described previously such that  $n-p$  is the degrees of freedom for SSE; and the degrees of freedom for pure error is given by  $f = \sum_{k=1}^K (m_k - 1)$ , where  $m_k$  is the number of replicate data points in the  $k^{th}$  replicate set,  $k = 1, 2, \dots, K$ . In practice, if the F-test is statistically significant at a significance level (often referred to as a *p-value*) of 0.05 or smaller (i.e., 95% confidence or higher), then it

<sup>1</sup> To be appropriate replicate data points, two or more glass samples of the same composition must be batched and melted at different times, and have their properties measured at different times. It is insufficient, for example, to batch and melt a glass once, and measure its properties several times (because the batching and melting sources of uncertainty are not included in the data). Similarly, replicate samples should not be measured at the same time (or close in time) because all sources of measurement uncertainty will not be included in the data.

would be concluded that the fitted model has a statistically significant LOF for the modeling dataset. See Draper and Smith (1998) or Montgomery et al. (2001) for additional discussion of the statistical test for model LOF.

Statistical tests of LOF for GLS-fitted models have not been provided in the statistics literature. An ad hoc assessment of LOF for GLS-fitted viscosity and electrical conductivity models (see Section C.3.3) is provided by considering

$$\frac{\hat{\sigma}_G^2 + \hat{\sigma}_T^2}{\text{Pure Error Estimate of } \sigma_G^2 + \sigma_T^2} \quad (\text{C.22c})$$

where  $\hat{\sigma}_G^2$  and  $\hat{\sigma}_T^2$  are estimates of the whole-plot (glasses) and sub-plot (temperatures) variance components that are outputs of the GLS software used to fit viscosity and electrical conductivity models. The denominator of Equation (C.22c) is a “pure error” estimate of  $\sigma_G^2 + \sigma_T^2$  based on viscosity or electrical conductivity data on replicate glasses. Developing the theory for the ratio in Equation (C.22c) was beyond the scope of the work in this report. However, a ratio as large as 1.5 to 2.0 provides evidence of a possible model LOF.

Even when a fitted model has a statistically significant LOF, the LOF may not be “practically significant”. An example of such a situation is when a fitted model yields biased predictions for higher and/or lower values of a property or in a particular subregion of compositions, but the model will not be applied to such areas in practice. Another example is when the model fits the data very well (e.g.,  $R^2 > 0.95$ ) without bias over the model’s region of validity, but the LOF is statistically significant because the experimental and measurement uncertainty is very small (e.g., because glasses can be batched, melted, and properties measured with excellent repeatability). Finally, a statistically significant LOF may not be practically significant if the uncertainty in model predictions is considerably smaller than uncertainty that can be tolerated and still meet requirements.

The model evaluation techniques discussed in the preceding bullets are included in, or can be obtained from, the output of the R software (Ihaka and Gentleman 1996, R Core Development Team) and SAS software (2005). See Draper and Smith (1998) or Montgomery et al. (2001) for further discussion of the concepts.

Three different  $R^2$  statistics are useful in evaluating models fitted to glass property-composition data. These are denoted as  $R^2$ ,  $R_A^2$ , and  $R_P^2$ , which are discussed subsequently. Formulas for these statistics are given when models are fitted by ULS or WLS. It may be possible to develop formulas for these statistics in the case of GLS regression, but doing so was beyond the scope of work in this report. Hence, only  $R^2$  values as calculated by the ULS formula are given in this report for models fitted by GLS.

The (*ordinary*)  $R^2$  statistic is given by

$$R^2 = 1 - \frac{\sum_{i=1}^n (\hat{y}_i - y_i)^2}{\sum_{i=1}^n (y_i - \bar{y})^2} \quad (\text{C.23a})$$

for ULS regression, and by

$$R^2 = 1 - \frac{\sum_{i=1}^n w_i (\hat{y}_i - y_i)^2}{\sum_{i=1}^n w_i (y_i - \bar{y}_w)^2} \quad (\text{C.23b})$$

for WLS regression, where  $\bar{y}_w$  in Equation (C.23b) is the weighted mean whose formula is given in Equation (C.19).  $R^2$  is interpreted as the fraction of variability in the unweighted (for ULS regression) or weighted (for WLS regression) property data (transformed if appropriate) accounted for by the fitted model. The *adjusted  $R^2$  statistic* is given by

$$R_A^2 = 1 - \frac{\sum_{i=1}^n (\hat{y}_i - y_i)^2 / (n - p)}{\sum_{i=1}^n (y_i - \bar{y})^2 / (n - 1)} \quad (\text{C.24a})$$

for ULS regression, and by

$$R_A^2 = 1 - \frac{\sum_{i=1}^n w_i (\hat{y}_i - y_i)^2 / (n - p)}{\sum_{i=1}^n w_i (y_i - \bar{y}_w)^2 / (n - 1)} \quad (\text{C.24b})$$

for WLS regression.  $R_A^2$  is interpreted as the adjusted fraction of variability in the unweighted or weighted property data (transformed if appropriate) accounted for by the fitted model. The adjustment is for the number of parameters ( $p$ ) and number of data points ( $n$ ) used in fitting the model. A version of  $R_A^2$  for GLS regression has not been proposed in the literature, and so this statistic is not calculated and reported for models fitted by GLS regression.

The *predicted  $R^2$  statistic* is given by

$$R^2 = 1 - \frac{\sum_{i=1}^n w_i (\hat{y}_i - y_i)^2}{\sum_{i=1}^n w_i (y_i - \bar{y}_w)^2}, \quad (\text{C.25a})$$

for ULS regression, and by

$$R_p^2 = 1 - \frac{\sum_{i=1}^n w_i (\hat{y}_{(i)} - y_i)^2}{\sum_{i=1}^n w_i (y_i - \bar{y}_w)^2}, \quad (\text{C.25b})$$

for WLS regression.  $R_p^2$  is interpreted as the leave-one-out crossvalidation fraction of variability in the unweighted or weighted property data (transformed if appropriate) accounted for by the fitted model. This statistic is calculated by a method equivalent to leaving each data point out of the model fit, and then evaluating how well the model predicts the property for that data point.  $R_p^2$  estimates the fraction of variability that would be explained in predicting new observations drawn from the same composition space. However, computational simplifications for ULS and WLS regression do not require re-fitting a model with each data point removed. Unfortunately, no such simplification exists for GLS regression. Thus,  $R_p^2$  is not calculated in this report for models fitted by GLS.

Generally  $R^2$  statistics take values between 0 and 1. However,  $R_A^2$  and  $R_p^2$  can take negative values for a poor fitting model, a model that contains many more terms than needed to fit the data, or a model fitted to data with one or more very influential data points. Among the three  $R^2$  statistics, typically  $R^2 > R_A^2 > R_p^2$ . More than a minor difference between  $R^2$  and  $R_A^2$  indicates that the model may contain more terms than needed to achieve the same goodness of fit. A substantial difference between  $R^2$  and  $R_p^2$  is indicative of one or more data points being very influential in determining the fit of the model. Some reduction from  $R^2$  to  $R_p^2$  is expected because  $R^2$  corresponds to using all data to fit the model, whereas  $R_p^2$  corresponds to leaving each data point out of the fit when evaluating the performance of the model for that point. In general, a model will tend to predict better for data used to fit it than for data not used to fit it.  $R_p^2$  is a crossvalidation evaluation method.

## C.5 Statistical Methods for Model Reduction and Augmentation

Section C.5.1 discusses methods for identifying and removing unnecessary terms from mixture experiment models. Section C.5.2 discusses methods for augmenting linear mixture models with quadratic terms or other nonlinear blending terms.

### C.5.1 Statistical Methods for Reducing Mixture Experiment Models

In evaluating a fitted regression model, it may often be determined that there are unnecessary terms in the model. Such terms may not improve, and can even degrade, the predictive performance of the model in applications to data not used to develop the model.

The most basic statistical method to identify unnecessary terms in a model is a *t-test* to perform a hypothesis test of whether the coefficient of a model term is statistically different from zero. The *t-test* computes a *t-statistic* equal to a model coefficient divided by the standard deviation of the coefficient. The *t-statistic* is then compared to the Student-*t* probability distribution to determine the probability of getting a *t-statistic* at least that large. The resulting probability is referred to as a *p-value*, and represents the probability of incorrectly deciding a

coefficient is significantly different than zero. Most regression software outputs estimated model coefficients, coefficient standard deviations, t-statistics, and p-values. Typically, practitioners require a p-value to be smaller than 0.05 or 0.01 as strong evidence that the coefficient is significantly different than zero, and thus that the corresponding model term is needed. If there are not too many potentially unnecessary terms in a model, a practitioner can assess the t-statistics and p-values for the coefficients in a “full” model, and remove the model term whose coefficient is least statistically significant. Then, the model would be refitted without that term, and the t-statistics and p-values again considered, deleting the model term with the least statistically significant coefficient. This process continues until all terms in the model have p-values lower than 0.05, say. *Backward elimination* (Draper and Smith 1998, Montgomery et al. 2001) is a widely used statistical method for removing unneeded terms from a model. This method basically automates the process just described, where the practitioner sets a stopping criterion.

Unfortunately, there are some model forms for which the model reduction methods just described are inappropriate. In general, these are model forms where a model coefficient being small (e.g., near zero) does not imply the corresponding model term is unneeded. That, is some model forms may have terms with significant effects even though the coefficients of those terms are small. One class of models in this category relevant to this work is the class of *mixture experiment models* (Cornell 2002), of which LM and PQM models are given in Section C.1.1.

The LM model (or the linear blending portion of a PQM model) is of the form  $\sum_{i=1}^q b_i x_i$ , where the  $b_i$  are coefficients and the  $x_i$  are proportions of the mixture components (e.g., mass fractions of waste glass components) that must sum to one (i.e.,  $\sum_{i=1}^q x_i = 1$ ). When each  $x_i$  can vary from zero to one, the coefficient  $b_i$  represents the estimated response variable value for pure component  $i$  [i.e., when  $x_i = 1$  and  $x_j = 0$  ( $j \neq i$ )]. When the ranges of the mixture component proportions  $x_i$  are constrained, each  $b_i$  represents extrapolated response values for pure component  $i$ . Because hypotheses concerning LM model coefficients (or the coefficients of linear terms in PQM models) equaling zero are not related to the importance or non-importance of a given component, it is inappropriate to use t-tests or the standard backward elimination method to reduce the linear portion of a mixture experiment model. However, mixture models can contain nonlinear terms in the components (such as in the PQM model form discussed in Section C.1.1), and it is appropriate to use t-tests or the standard stepwise, forward, or backward elimination *variable selection methods* (see Draper and Smith 1998 or Montgomery et al. 2001) on such terms.

*Component response trace plots* (Cornell 2002) provide for graphically assessing the effects of mixture components on a response variable of interest. These plots are generally produced using a fitted mixture model. The model is used to predict, for each component, the response for a series of compositions lying along an *effect direction* for that component. The most commonly used effect direction corresponds to subtracting or adding a component to a reference (or baseline) mixture. Along such a direction, the component of interest is varied within the allowable composition region of interest. The changes in the component of interest are offset by changes in the remaining components, such that they remain in the same relative proportions as in the reference mixture. The predicted response values along the effect direction



for a given component form a *component response trace*. The response traces for the components varied in a mixture experiment plotted together form the *component response trace plot*. The predicted response values are plotted on the y-axis and changes in each component from its reference mixture value are plotted on the x-axis. Components with steeper response traces have stronger effects on the response. A response trace that is nearly horizontal indicates the corresponding component has little or no effect on the response. Components whose response traces are very close may have similar effects on the response. Thus, component response trace plots can be used to guide the reduction of components appearing in a mixture experiment model (e.g., see Piepel and Redgate 1997).

A special backward elimination method for mixture experiments has been developed to reduce linear mixture models and linear portions of mixture models (Piepel and Cooley 2006). The reduction method is performed in stages. In general at the end of each stage, either (i) a mixture component is dropped and the remaining components are renormalized, or (ii) two components are combined. As an option, model reductions of the form (i) can be skipped and only reductions of the form (ii) considered. For each stage, the process occurs as follows.

- If reductions of the form (i) are allowed, each mixture component still in the model is in turn dropped from the model, the remaining mixture component proportions are renormalized to sum to one. Then a linear mixture model without the dropped component is fitted to the data. The dropped mixture component that causes the smallest increase in the error sums of squares (the quantity being minimized in ULS regression) is then the component permanently dropped from the model at the current stage. After each component is dropped, the remaining components are renormalized according to the mixture experiment definition that a response variable depends only on the relative proportions of the mixture components that affect the response variable (Cornell 2002).
- For reductions of the form (ii), each allowable pair of components is combined and the corresponding reduced linear mixture model is fitted. The pair of components causing the smallest increase in the error sum of squares is then permanently combined at the current stage.

Similar stages continue, with either one component dropped [option (i)] or one pair of components combined [option (ii)], until the stage in which a model reduction causes the full-reduced model F-test (Draper and Smith 1998, Montgomery et al. 2001) to declare a statistically significant increase in the error sum of squares. This then signals the stopping point for the backward elimination algorithm. Note that the algorithm allows for the user specifying the components (if any) that can be dropped, and components that can be combined. These options provide for incorporating glass science knowledge into the model reduction process.

### **C.5.2 Statistical Methods for Adding Terms to Models**

It is often of interest to add additional terms onto a starting model in the hopes of improving the predictive performance of the starting model. For example, a linear mixture model

may be considered as a starting model. However, if it has a significant LOF, adding nonlinear composition terms may be considered in hopes of improving the predictive performance of the model. *Stepwise regression* is the most commonly used method to add terms to an existing starting model. In stepwise regression, certain terms can be forced into the model, and a candidate list of possible terms to add is identified. The procedure identifies the term from the candidate list that, if added to the model, would yield the greatest reduction in the error sum of squares (i.e., the sum of squared differences in measured and model-predicted values across the modeling data set). If the reduction is statistically significant, that term is added to the model. Stepwise regression proceeds in stages, with one additional term being added at each stage unless the user-selected stopping criterion is reached. After adding a term, stepwise regression checks all other terms in the model to assess if they are still statistically significant. If not, a term can be removed during a stage.

The stepwise regression algorithm requires that a significance level be specified for terms to enter the model, and that a significance level be specified for terms to remain in the model. In each iteration of a stepwise regression application, t-tests are conducted for each term already in the model and for terms being considered for inclusion in the model. To describe the results of these t-tests, a p-value is calculated for each of the terms. Loosely speaking, the p-values represent the probability that the respective model terms do not make a significant contribution to the predictive ability of the model. Terms whose corresponding p-values are small (often <0.05 is considered sufficiently small) are considered important in the model. The significance levels specified for the stepwise regression algorithm indicate how small p-values must be for the corresponding terms to be included in the model. The statistical literature generally indicates that the stepwise algorithm is somewhat liberal in allowing terms into models. Yet, models containing unnecessary terms are undesirable because they tend to have inflated prediction variance. Thus, it is typically advisable to use tight significance levels such as 0.05 or 0.01 when applying the stepwise regression algorithm.

One particular variation of stepwise regression that can be used to select terms for model building is what the SAS statistical software package (SAS 2005) refers to as the Maximum R-squared Improvement (MAXR) selection method. For the MAXR criterion (as with other criteria for stepwise regression), terms can enter and leave (being replaced by another term) the model. Sequential changes to the model are based on maximal increases to the model's  $R^2$  value, and MAXR tries to find the "best" model having a specified numbers of terms. However, MAXR is not the same as the "best subsets" algorithm because it does not consider all possible models with a given number of terms. Therefore, MAXR is not guaranteed to find the model with the highest  $R^2$  value among all models having a given number of terms. This method tends to have a better chance of finding more nearly optimal models than does the stepwise selection method using other criteria (Freund and Littell 1995). The MAXR method does not require significance levels to control term selection, but does require the user to identify any terms to force into the model and to specify the number of terms to include in models being considered.

The standard stepwise regression procedure (regardless of the criterion used for model term selection) is not appropriate for linear mixture models or linear portions of other mixture experiment models for similar reasons as described previously with regard to the standard

backward elimination method. However, it is appropriate for adding nonlinear mixture terms or non-mixture terms to mixture models.

## C.6 Statistical Methods for Model Validation

Model validation methods assess how well a fitted model predicts property values for glasses not used in fitting the model. The glasses used for validation ideally should be in the same composition region as the data used to fit the property-composition models, because (in general) fitted empirical and semi-empirical models should not be used to extrapolate much beyond the region covered by the modeling data. Also, ideally the validation data should be evenly distributed over the model composition region of model validity to properly assess predictive ability over the region. However, this is difficult to achieve in practice because validation data are typically not designed, but often consists of whatever extra data are available.

Validation generally consists of using a fitted model to predict property values for a set of validation data, and then comparing the predicted property values to the measured values from the validation database. The following subsections describe several methods for comparing predicted and measured values of properties.

### C.6.1 Validation $R^2$

Statistical summary comparisons of predicted and measured property values are also useful to see if differences are larger than their expected uncertainties. One such comparison is the *validation*  $R^2$  statistic, which in general is given by

$$R_V^2 = 1 - \frac{\sum_{i=1}^n (\hat{y}_i - y_i)^2}{\sum_{i=1}^n (y_i - \bar{y})^2} . \quad (\text{C.26a})$$

However, in cases where WLS regression is used to fit the model and corresponding weights are available, a weighted version of the *validation*  $R^2$  statistics is given by

$$R_V^2 = 1 - \frac{\sum_{i=1}^n w_i (\hat{y}_i - y_i)^2}{\sum_{i=1}^n w_i (y_i - \bar{y}_w)^2} . \quad (\text{C.26b})$$

$R_V^2$  is interpreted as the fraction of variability in the unweighted or weighted property values (transformed if appropriate) in the validation data accounted for by the fitted model. Note that  $R_V^2$  is defined exactly the same as the ordinary  $R^2$  defined in Equations (C.23a) and (C.23b), except that model validation data are used to assess model predictive performance instead of the

model development data. Hence, the  $y_i$ ,  $\hat{y}_i$ ,  $\bar{y}$ ,  $w_i$ , and  $\bar{y}_w$  values in Equations (C.26a) and (C.26b) correspond to the model validation data. Because it was beyond the scope of the work in this report to develop formulas for validation statistics on models fitted by GLS regression, the ULS formulas are used for such models in this report.

Generally  $R_V^2 \leq R_p^2 \leq R_A^2 \leq R^2 \leq 1$ . However,  $R_V^2$  can take negative values (when a model predicts a validation set very poorly) and can take values larger than  $R_p^2$ ,  $R_A^2$ , or  $R^2$  (when a model predicts a particular validation dataset better than estimated by these statistics based on the modeling data).

### C.6.2 Validation RMSE

Another useful summary statistic for model validation is *validation RMSE* (RMSE<sub>V</sub>). This statistic is calculated the same as given in Equation (C.20a) for ULS-fitted models and as given in Equation (C.20b) for WLS-fitted models. For GLS-fitted models, the ULS formula is used in this report.

### C.6.3 Predicted Versus Measured Plots

Predicted and measured values for a model validation data set can be compared by plotting the predicted versus the measured property values for each data point. Such *predicted versus measured plots* are the same as described in Section C.4, except model validation data are used instead of model development data. Also, similarly as described in Section C.4, *unweighted PvM plots* or *weighted PvM plots* may be produced and viewed to validate models fitted by WLS regression.

Optionally, error bars consisting of 95% two-sided prediction intervals (95% PIs) on the predicted values can be included in the predicted versus measured plot for validation. Then, if the error bar for a given validation data point overlaps a line with slope one superimposed on the PvM plot, the model is validated for that data point. Draper and Smith (1998) and Montgomery et al. (2001) provide additional discussion of 95% PIs for regression models. The formulas for a 95% two-sided PI in the ULS, WLS, and GLS cases are given in Section C.7 following.

## C.7 Statistical Intervals for Describing Uncertainties in Model Predictions

Several types of statistical intervals are available to describe the uncertainty associated with model predictions. Each type of statistical interval has a particular interpretation. A common assumption for all statistical intervals based on regression models is that the model represents the true underlying response surface (property-composition or property-composition-temperature relationship for waste glasses) without a statistically significant lack-of-fit.

The following subsections present the formulas for one-sided upper (or lower) confidence intervals (Section C.7.1), two-sided confidence intervals (Section C.7.2), and two-sided prediction intervals (Section C.7.3). These types of statistical intervals are used to describe the uncertainty associated with model predictions at a single specific composition, or at single specific composition and temperature for properties such as viscosity and electrical conductivity that depend on temperature as well as composition. Section C.7.4 presents the formulas for simultaneous upper confidence intervals, which are used to describe the uncertainty associated with model predictions at many glass compositions, or at many composition-temperature combinations for properties such as viscosity and electrical conductivity. The formulas for these types of statistical intervals are given in each subsection for the ULS, WLS, and GLS cases. Section C.7.5 discusses aspects of using the statistical intervals.

### C.7.1 One-Sided Confidence Interval

A  $100(1-\alpha)\%$  upper confidence interval (UCI) for the true mean response value for a given glass composition  $\mathbf{x} = (x_1, x_2, \dots, x_q)$  is given by

$$\begin{aligned} \hat{y}(\mathbf{x}) + t_{1-\alpha}(n-p)\sqrt{\mathbf{a}^T \mathbf{C}_U \mathbf{a}} &= \hat{y}(\mathbf{x}) + t_{1-\alpha}(n-p)\sqrt{\mathbf{a}^T [(\mathbf{A}^T \mathbf{A})^{-1} MSE_U] \mathbf{a}} \\ &= \hat{y}(\mathbf{x}) + t_{1-\alpha}(n-p)RMSE_U \sqrt{\mathbf{a}^T (\mathbf{A}^T \mathbf{A})^{-1} \mathbf{a}} \end{aligned} \quad (\text{C.27a})$$

for ULS regression, and by

$$\begin{aligned} \hat{y}(\mathbf{x}) + t_{1-\alpha}(n-p)\sqrt{\mathbf{a}^T \mathbf{C}_W \mathbf{a}} &= \hat{y}(\mathbf{x}) + t_{1-\alpha}(n-p)\sqrt{\mathbf{a}^T [(\mathbf{A}^T \mathbf{W} \mathbf{A})^{-1} MSE_W] \mathbf{a}} \\ &= \hat{y}(\mathbf{x}) + t_{1-\alpha}(n-p)RMSE_W \sqrt{\mathbf{a}^T (\mathbf{A}^T \mathbf{W} \mathbf{A})^{-1} \mathbf{a}} \end{aligned} \quad (\text{C.27b})$$

for WLS regression. The formula is similar for properties such as viscosity and electrical conductivity that depend on glass composition and melt temperature and have models fitted by GLS regression. A  $100(1-\alpha)\%$  UCI for the true mean response value for a given glass composition  $\mathbf{x} = (x_1, x_2, \dots, x_q)$  and temperature  $T$  (in Kelvin) is given by

$$\begin{aligned} \hat{y}(\mathbf{x}, T) + t_{1-\alpha}(n_g - p_g)\sqrt{\mathbf{a}^T \mathbf{C}_G \mathbf{a}} &= \hat{y}(\mathbf{x}, T) + t_{1-\alpha}(n_g - p_g)\sqrt{\mathbf{a}^T [(\mathbf{A}^T \hat{\mathbf{V}}^{-1} \mathbf{A})^{-1}] \mathbf{a}} \\ &= \hat{y}(\mathbf{x}, T) + t_{1-\alpha}(n_g - p_g)\sqrt{\mathbf{a}^T (\mathbf{A}^T \hat{\mathbf{V}}^{-1} \mathbf{A})^{-1} \mathbf{a}} \end{aligned} \quad (\text{C.27c})$$

In Equations (C.27a), (C.27b), and (C.27c), the superscript  $T$  notation indicates a vector or matrix transpose, not temperature. Only the  $T$  appearing in  $\hat{y}(\mathbf{x}, T)$  denotes temperature. Otherwise, the vector  $\mathbf{a}$  is a function of both composition and temperature as explained following. The other notations in Equations (C.27a), (C.27b), and (C.27c) are defined as follows.

$$\hat{y}(\mathbf{x}) \quad = \quad \text{model predicted value at composition } \mathbf{x},$$

- $\hat{y}(\mathbf{x}, T)$  = model predicted value at composition  $\mathbf{x}$  and temperature  $T$ ,
- $100(1-\alpha)$  = desired confidence (e.g., 90%) for the confidence interval, where  $\alpha$  denotes the significance level (e.g.,  $\alpha = 0.10$  for 90% confidence),
- $t_{1-\alpha}(n-p)$  =  $100(1-\alpha)$ -percentile of the Student's  $t$ -distribution with  $n-p$  degrees of freedom,
- $t_{1-\alpha}(n_g - p_g)$  =  $100(1-\alpha)$ -percentile of the Student's  $t$ -distribution with  $n_g - p_g$  degrees of freedom,
- $n$  = number of data points used to fit the model,
- $p$  = number of parameters estimated in the model,
- $n_g$  = number of glasses used to fit a viscosity or electrical conductivity model,
- $p_g$  = number of parameters estimated in the composition-only portion of the model (as differentiated from the composition-temperature portion of the model).
- $C_U$  = estimated variance-covariance matrix for the estimated coefficients of a model fitted by ULS regression =  $(A^T A)^{-1} MSE_U$ ,
- $C_W$  = estimated variance-covariance matrix for the estimated coefficients of a model fitted by WLS regression =  $(A^T W A)^{-1} MSE_W$ ,
- $C_G$  = estimated variance-covariance matrix for the estimated coefficients of a model fitted by GLS regression, which is approximated by  $(A^T \hat{V}^{-1} A)^{-1}$ ,
- $\mathbf{a}^T$  = the vector transpose of the glass composition vector  $\mathbf{x}$  and temperature (if involved in the model) expanded in the form of the model,
- $A^T$  = the matrix transpose of the data matrix (consisting of glass compositions and temperatures, if involved in the model) expanded in the form of the model,
- $W$  = an  $n \times n$  diagonal weight matrix with entries  $w_i, i = 1, 2, \dots, n$  (i.e., the weights associated with the model development set of  $n$  data points),
- $MSE$  = mean squared error, which is obtained from the ULS ( $MSE_U$ ) or WLS ( $MSE_W$ ) regression fit of the model,
- $RMSE$  = the root mean squared error =  $\sqrt{MSE}$ , with  $RMSE_U$  and  $RMSE_W$  resulting from ULS and WLS regression fits of a model, respectively.

A  $100(1-\alpha)\%$  UCI, as given by Equations (C.27a), (C.27b), and (C.27c) is appropriate when an uncertainty statement is desired about the true mean response for a given composition  $\mathbf{x}$  and temperature  $T$  (for properties that also depend on temperature).

Equation (C.27c) is approximate because of using an estimate  $\hat{V}$  of  $V$  (the variance-covariance matrix for the vector of viscosity or electrical conductivity-at-temperature data used to fit the model—see Sections C.3.2 and C.3.3). Further, the number of degrees of freedom ( $n_g - p_g$ ) associated with the t-distribution multiplier is approximate. However, there is no practical consequence to using this approximate number of degrees of freedom because of the large number of glasses used to develop viscosity and electrical conductivity models. In such cases, the t-distribution multiplier will essentially be a z-distribution (standard normal) multiplier, and thus there is no practical consequence.

The formulas for a one-sided lower confidence interval are the same as in Equations (C.27a), (C.27b), and (C.27c) except the plus signs following  $\hat{y}(\mathbf{x}, T)$  are changed to minus signs. Thus, a  $100(1-\alpha)\%$  lower confidence interval (LCI) for the true mean response value for a given glass composition  $\mathbf{x} = (x_1, x_2, \dots, x_q)$  is given by

$$\begin{aligned} \hat{y}(\mathbf{x}) - t_{1-\alpha}(n-p)\sqrt{\mathbf{a}^T \mathbf{C}_U \mathbf{a}} &= \hat{y}(\mathbf{x}) - t_{1-\alpha}(n-p)\sqrt{\mathbf{a}^T [(\mathbf{A}^T \mathbf{A})^{-1} \text{MSE}_U] \mathbf{a}} \\ &= \hat{y}(\mathbf{x}) - t_{1-\alpha}(n-p) \text{RMSE}_U \sqrt{\mathbf{a}^T (\mathbf{A}^T \mathbf{A})^{-1} \mathbf{a}} \end{aligned} \quad (\text{C.28a})$$

for ULS regression, and by

$$\begin{aligned} \hat{y}(\mathbf{x}) - t_{1-\alpha}(n-p)\sqrt{\mathbf{a}^T \mathbf{C}_W \mathbf{a}} &= \hat{y}(\mathbf{x}) - t_{1-\alpha}(n-p)\sqrt{\mathbf{a}^T [(\mathbf{A}^T \mathbf{W} \mathbf{A})^{-1} \text{MSE}_W] \mathbf{a}} \\ &= \hat{y}(\mathbf{x}) - t_{1-\alpha}(n-p) \text{RMSE}_W \sqrt{\mathbf{a}^T (\mathbf{A}^T \mathbf{W} \mathbf{A})^{-1} \mathbf{a}} \end{aligned} \quad (\text{C.28b})$$

for WLS regression. The formula is similar for properties such as viscosity and electrical conductivity that depend on glass composition and melt temperature and have models fitted by GLS regression. A  $100(1-\alpha)\%$  LCI for the true mean response value for a given glass composition  $\mathbf{x} = (x_1, x_2, \dots, x_q)$  and temperature  $T$  is given by

$$\begin{aligned} \hat{y}(\mathbf{x}, T) - t_{1-\alpha}(n_g - p_g)\sqrt{\mathbf{a}^T \mathbf{C}_G \mathbf{a}} &= \hat{y}(\mathbf{x}, T) - t_{1-\alpha}(n_g - p_g)\sqrt{\mathbf{a}^T [(\mathbf{A}^T \hat{V}^{-1} \mathbf{A})^{-1}] \mathbf{a}} \\ &= \hat{y}(\mathbf{x}, T) - t_{1-\alpha}(n_g - p_g)\sqrt{\mathbf{a}^T (\mathbf{A}^T \hat{V}^{-1} \mathbf{A})^{-1} \mathbf{a}} \end{aligned} \quad (\text{C.28c})$$

where the notation is as previously defined. Equation (C.28c) is approximate for the same reasons given following Equation (C.27c).

### C.7.2 Two-Sided Confidence Interval

A  $100(1-\alpha)\%$  two-sided confidence interval (CI) for the true mean response value for a given glass composition  $\mathbf{x} = (x_1, x_2, \dots, x_q)$  is given by

$$\begin{aligned}\hat{y}(\mathbf{x}) \mp t_{1-\alpha/2}(n-p)\sqrt{\mathbf{a}^T \mathbf{C}_U \mathbf{a}} &= \hat{y}(\mathbf{x}) \mp t_{1-\alpha/2}(n-p)\sqrt{\mathbf{a}^T [(\mathbf{A}^T \mathbf{A})^{-1} \text{MSE}_U] \mathbf{a}} \\ &= \hat{y}(\mathbf{x}) \mp t_{1-\alpha/2}(n-p) \text{RMSE}_U \sqrt{\mathbf{a}^T (\mathbf{A}^T \mathbf{A})^{-1} \mathbf{a}},\end{aligned}\quad (\text{C.29a})$$

for ULS regression, and by

$$\begin{aligned}\hat{y}(\mathbf{x}) \mp t_{1-\alpha/2}(n-p)\sqrt{\mathbf{a}^T \mathbf{C}_W \mathbf{a}} &= \hat{y}(\mathbf{x}) \mp t_{1-\alpha/2}(n-p)\sqrt{\mathbf{a}^T [(\mathbf{A}^T \mathbf{W} \mathbf{A})^{-1} \text{MSE}_W] \mathbf{a}} \\ &= \hat{y}(\mathbf{x}) \mp t_{1-\alpha/2}(n-p) \text{RMSE}_W \sqrt{\mathbf{a}^T (\mathbf{A}^T \mathbf{W} \mathbf{A})^{-1} \mathbf{a}},\end{aligned}\quad (\text{C.29b})$$

for WLS regression. The formula is similar for properties such as viscosity and electrical conductivity that depend on glass composition and melt temperature and have models fitted by GLS regression. A  $100(1-\alpha)\%$  CI for the true mean response value for a given glass composition  $\mathbf{x} = (x_1, x_2, \dots, x_q)$  and temperature  $T$  is given by

$$\begin{aligned}\hat{y}(\mathbf{x}, T) \mp t_{1-\alpha/2}(n_g - p_g)\sqrt{\mathbf{a}^T \mathbf{C}_G \mathbf{a}} &= \hat{y}(\mathbf{x}, T) \mp t_{1-\alpha/2}(n_g - p_g)\sqrt{\mathbf{a}^T [(\mathbf{A}^T \hat{\mathbf{V}}^{-1} \mathbf{A})^{-1}] \mathbf{a}} \\ &= \hat{y}(\mathbf{x}, T) \mp t_{1-\alpha/2}(n_g - p_g)\sqrt{\mathbf{a}^T (\mathbf{A}^T \hat{\mathbf{V}}^{-1} \mathbf{A})^{-1} \mathbf{a}}\end{aligned}\quad (\text{C.29c})$$

In Equations (C.29a), (C.29b), and (C.29c), the notation is all the same as described in Section C.7.1, except that  $t_{1-\alpha/2}(n-p)$  denotes the  $100(1-\alpha/2)$ -percentile of the Student's  $t$ -distribution with  $n-p$  degrees of freedom. Similarly,  $t_{1-\alpha/2}(n_g - p_g)$  denotes the  $100(1-\alpha/2)$ -percentile of the Student's  $t$ -distribution with  $n_g - p_g$  degrees of freedom. Equation (C.29c) is approximate for the same reasons given following Equation (C.27c).

### C.7.3 Two-Sided Prediction Interval

A  $100(1-\alpha)\%$  two-sided prediction interval (PI) for an individual response value for a given composition  $\mathbf{x}$  is given by

$$\begin{aligned}\hat{y}(\mathbf{x}) \mp t_{1-\alpha/2}(n-p)\sqrt{\text{MSE}_U + \mathbf{a}^T \mathbf{C}_U \mathbf{a}} \\ = \hat{y}(\mathbf{x}) \mp t_{1-\alpha/2}(n-p) \text{RMSE}_U \sqrt{1 + \mathbf{a}^T (\mathbf{A}^T \mathbf{A})^{-1} \mathbf{a}},\end{aligned}\quad (\text{C.30a})$$

for ULS regression, and by

$$\begin{aligned}\hat{y}(\mathbf{x}) \mp t_{1-\alpha/2}(n-p)\sqrt{\frac{\text{MSE}_W}{w_i} + \mathbf{a}^T \mathbf{C}_W \mathbf{a}} \\ = \hat{y}(\mathbf{x}) \mp t_{1-\alpha/2}(n-p) \text{RMSE}_W \sqrt{\frac{1}{w_i} + \mathbf{a}^T (\mathbf{A}^T \mathbf{W} \mathbf{A})^{-1} \mathbf{a}},\end{aligned}\quad (\text{C.30b})$$



for WLS regression. The formula is similar for properties such as viscosity and electrical conductivity that depend on glass composition and melt temperature and have models fitted by GLS regression. A  $100(1-\alpha)\%$  two-sided PI for an individual response value for a given composition  $\mathbf{x}$  and temperature  $T$  is given by

$$\begin{aligned} \hat{y}(\mathbf{x}, T) \mp t_{1-\alpha/2}(n_g - p_g) \sqrt{\hat{\sigma}_y^2 + \mathbf{a}^T \mathbf{C}_G \mathbf{a}} \\ = \hat{y}(\mathbf{x}, T) \mp t_{1-\alpha/2}(n_g - p_g) \sqrt{(\hat{\sigma}_G^2 + \hat{\sigma}_T^2) + \mathbf{a}^T (\mathbf{A}^T \hat{\mathbf{V}}^{-1} \mathbf{A})^{-1} \mathbf{a}} \end{aligned} \quad (\text{C.30c})$$

where

$\hat{\sigma}_y^2$  = estimate of the variance of a response variable observation  $y$ . For the split-plot structure associated with viscosity and electrical conductivity data, as discussed in Sections C.2.2 and C.3.3,  $\hat{\sigma}_y^2 = \hat{\sigma}_G^2 + \hat{\sigma}_T^2$ .

The remaining notations in Equations (C.30a), (C.30b), and (C.30c) are defined as given following the UCI formulas in Section C.7.1. Equation (C.30c) is approximate for the same reasons given following Equation (C.27c).

The preceding equations for  $100(1-\alpha)\%$  two-sided PIs are easily converted to  $100(1-\alpha)\%$  one-sided PIs by replacing “ $\mp$ ” with “ $-$ ” or “ $+$ ”, replacing  $t_{1-\alpha/2}(n-p)$  with  $t_{1-\alpha}(n-p)$ , and replacing  $t_{1-\alpha/2}(n_g - p_g)$  with  $t_{1-\alpha}(n_g - p_g)$ .

Note in Equation (C.30b) that the  $w_i$  under the square root applies when PIs are calculated for modeling data, validation data, or application data (i.e., data used in applying the models and PIs) with weights. In situations where validation or application data do not have weights,  $w_i$  should be set to 1.

A  $100(1-\alpha)\%$  PI is appropriately used when comparing a model predicted response value for a given composition to an individual measurement of the response for that composition. This type of application arises in validating the predictive performance of a model for one or more glass compositions not used to fit the model. Specifically, Equations (C.30a), (C.30b), and (C.30c) can be used to produce 95% PIs displayed as error bars in PvM plots, as described at the end of Section C.6.

#### C.7.4 Simultaneous Upper Confidence Intervals

At times it is desirable to describe the uncertainty associated with predictions obtained for a specified group of compositions. For example, a statement may be desired that indicates with high confidence that the predicted response value for every composition  $\mathbf{x}$  in a specified group of compositions (or composition region) is below a particular regulatory limit. Such a

confidence statement requires a statistical interval called a simultaneous upper confidence interval. The formula for a  $100(1-\alpha)\%$  simultaneous upper confidence interval (SUCI) associated with predictions on an unlimited number of compositions  $\mathbf{x}$  is given by

$$\begin{aligned} \hat{y}(\mathbf{x}) + \sqrt{pF_{1-2\alpha}(p, n-p)} \sqrt{\mathbf{a}^T \mathbf{C}_U \mathbf{a}} \\ = \hat{y}(\mathbf{x}) + RMSE_U \sqrt{pF_{1-2\alpha}(p, n-p)} \sqrt{\mathbf{a}^T (\mathbf{A}^T \mathbf{A})^{-1} \mathbf{a}} \end{aligned} \quad (\text{C.31a})$$

for ULS regression, and by

$$\begin{aligned} \hat{y}(\mathbf{x}) + \sqrt{pF_{1-2\alpha}(p, n-p)} \sqrt{\mathbf{a}^T \mathbf{C}_W \mathbf{a}} \\ = \hat{y}(\mathbf{x}) + RMSE_W \sqrt{pF_{1-2\alpha}(p, n-p)} \sqrt{\mathbf{a}^T (\mathbf{A}^T \mathbf{W} \mathbf{A})^{-1} \mathbf{a}} \end{aligned} \quad (\text{C.31b})$$

for WLS regression. The formula is similar for properties such as viscosity and electrical conductivity that depend on glass composition and melt temperature and have models fitted by GLS regression. The formula for a  $100(1-\alpha)\%$  SUCI associated with predictions on an unlimited number of combinations of composition  $\mathbf{x}$  and temperature  $T$  is given by

$$\begin{aligned} \hat{y}(\mathbf{x}, T) + \sqrt{pF_{1-2\alpha}(p, n_g - p_g)} \sqrt{\mathbf{a}^T \mathbf{C}_G \mathbf{a}} \\ = \hat{y}(\mathbf{x}, T) + \sqrt{pF_{1-2\alpha}(p, n_g - p_g)} \sqrt{\mathbf{a}^T (\mathbf{A}^T \hat{\mathbf{V}}^{-1} \mathbf{A})^{-1} \mathbf{a}} \end{aligned} \quad (\text{C.31c})$$

In Equations (C.31a) and (C.31b)

$$F_{1-2\alpha}(p, n-p) = 100(1-2\alpha)\text{-percentile of the } F\text{-distribution with } p \text{ and } n-p \text{ degrees of freedom}$$

while in Equation (C.31c)

$$\sqrt{pF_{1-2\alpha}(p, n_g - p_g)} = 100(1-2\alpha)\text{-percentile of the } F\text{-distribution with } p_g \text{ and } n_g - p_g \text{ degrees of freedom.}$$

The remaining notations are the same as defined previously. Equation (C.31c) is approximate because of using an estimate  $\hat{\mathbf{V}}$  of  $\mathbf{V}$  (the variance-covariance matrix for the vector of viscosity or electrical conductivity-at-temperature data used to fit the model—see Sections C.3.2 and C.3.3). Further, the numbers of degrees of freedom for the numerator ( $p_g$ ) and denominator ( $n_g - p_g$ ) of the F-distribution multiplier are approximate.

### C.7.5 Statistical Intervals in Transformed and Untransformed Units

Equations (C.27), (C.28), (C.29), (C.30), and (C.31) yield statistical intervals in transformed units when a transformed property is modeled. For example, a natural logarithm transformation of a response  $y$  [i.e.,  $\ln(y)$ ] is often used for property-composition models. Hence, the statistical intervals calculated using the preceding equations would be in  $\ln(y)$  units. The statistical intervals can be transformed back to the original units of  $y$  by exponentiating the endpoint(s) of the statistical interval. However, the process of back-transforming (exponentiating) a statistical interval can change its interpretation. For example, if a 90% UCI in  $\ln(y)$  units has the value “ $v$ ”, the back-transformed 90% UCI in the original units of  $y$  is given by  $e^v$ . The 90% UCI in units of  $\ln(y)$  is a statement about the true mean response in  $\ln(y)$  units for a given glass composition  $x$  (at a given temperature for properties that also depend on temperature). However, the resulting back-transformed interval is a 90% UCI on the true median response value for the given composition  $x$  (and temperature, if applicable), under the assumption that experimental errors in the data used to develop the model are lognormally distributed. This assumption corresponds to the assumption of the natural-log-transformed response data being normally distributed. This change in interpretation occurs because the mean and median of a normal distribution are the same, but the mean of a lognormal distribution is larger than the median of a lognormal distribution.

Hence, back-transforming a 90% UCI on a mean response for a given composition  $x$  and temperature (if applicable) in  $\ln$ -units yields a 90% UCI on the median response for a given composition  $x$  in original units. This then underestimates a 90% UCI on the mean response for a given composition  $x$  and temperature (if applicable) in original units. Back-transforming 100(1- $\alpha$ )% SUCIs given by Equation (C.31) in log-transformed units has a similar change in interpretation. Whereas the original 100(1- $\alpha$ )% SUCIs are statements about the true mean values of responses in log-transformed response units for multiple compositions  $x$  and temperatures (if applicable), the back-transformed 100(1- $\alpha$ )% SUCIs are statements about the true median values of responses in original response units for multiple compositions  $x$  and temperatures (if applicable). However, a 100(1- $\alpha$ )% PI given by Equation (C.30) in log-transformed units does not have a change in interpretation when back-transforming, because the original statement (in log-transformed units) and the back-transformed statement (in original units) are both about a true individual response value.

Alternatives exist to using normal-theory-based Equations (C.27) through (C.31) and back-transforming them when a transformed response variable is modeled. One alternative is to modify the statistical interval equations so that the statistical statement is about the true mean response value in the original units for a given composition  $x$  and temperature (where applicable) [e.g., Equation C.27) for an UCI] or a set of compositions  $x$  and temperature combinations (where applicable) [e.g., Equation (C.31) for a SUCI]. Although this type of alternative is discussed in the literature for non-regression problems (e.g., Gilbert 1987), no references were found for the regression context. Another alternative, the *generalized linear model* regression approach (Myers et al. 2002), avoids directly transforming the response variable and instead uses the transformation indirectly. These alternative approaches were not pursued in this work. However, the interested reader may refer to the references given.

Note that Equations (C.27) through (C.31) require knowledge of the variance-covariance matrix  $\mathbf{C}_U = MSE_U(\mathbf{A}^T\mathbf{A})^{-1}$  for ULS regression,  $\mathbf{C}_W = MSE_W(\mathbf{A}^T\mathbf{W}\mathbf{A})^{-1}$  for WLS regression, and  $\mathbf{C}_G = (\mathbf{A}^T\hat{\mathbf{V}}^{-1}\mathbf{A})^{-1}$  for GLS regression. The  $MSE_U$  and  $MSE_W$  are mean squared errors equal to the squares of  $RMSE_U$  and  $RMSE_W$  given by Equations (C.20a) and (C.20b). This information is included in the ULS, WLS, or GLS regression software output that comes with the estimates of the  $p$  model coefficients. A variance-covariance matrix is a  $p \times p$  matrix with coefficient variances along the diagonal, and covariances between coefficient pairs in the off-diagonal entries.

## **APPENDIX D**

### **Variance-Covariance Matrices Associated with the Coefficients of ILAW PCT, VHT, Electrical Conductivity, and Viscosity Models**

## APPENDIX D

### **Variance-Covariance Matrices Associated with the Coefficients of ILAW PCT, VHT, Electrical Conductivity, and Viscosity Models**

This appendix contains the variance-covariance matrices for selected property models for LAW glasses discussed in this report. Included are variance-covariance matrices for PCT and VHT models, which are functions of LAW glass composition. Also included are variance-covariance matrices for electrical conductivity and viscosity models, which are functions of LAW glass composition and glass melt temperature. Variances and covariances are listed to four decimal places, which was determined to be sufficient to obtain appropriate precision in calculated values of statistical intervals (see Section C.7).

Tables D.1 and D.2, respectively, contain the variance-covariance matrices for two  $\ln(\text{PCT-B, g/L})$  models: (1) the 12-component reduced linear mixture (LM) model given in Table 5.8, and (2) the 17-term reduced partial quadratic mixture (PQM) model given in Table 5.9. The 12-component reduced LM model was identified as providing a baseline for comparison to the 17-term PQM model (which is the recommended model for PCT-B).

Tables D.3 and D.4, respectively, contain the variance-covariance matrices for two  $\ln(\text{PCT-Na, g/L})$  models: (1) the 12-component reduced LM model given in Table 5.13, and (2) the 17-term reduced PQM model given in Table 5.14. The 12-component reduced LM model was identified as providing a baseline for comparison to the 17-term PQM model (which is the recommended model for PCT-Na).

Tables D.5, D.6, and D.7, respectively, contain the variance-covariance matrices for three  $\ln(\text{VHT Alteration Depth, } \mu\text{m})$  models: (1) the 11-component reduced LM model given in Table 6.8, (2) the 16-term PQM model given in Table 6.9, and (3) the 15-term partial cubic mixture (PCM) model given in Table 6.11. The 11-component reduced LM was judged as inadequate for predicting VHT alteration depth, but provides a baseline for comparison to the other two models. The 15-term PCM model is the recommended model for predicting VHT alteration depth, with the 16-term PQM model a second-choice alternative if a model without cubic terms is desired.

Tables D.8 and D.9, respectively, contain the variance-covariance matrices for two  $\ln(\text{Electrical Conductivity, S/cm})$  models: (1) the 22-term Arrhenius-LM model given in Table 7.8, and (2) the 25-term given in Table 7.9, which adds to the 22-term Arrhenius-LM model three crossproduct terms. The 25-term model is the one recommended for use, but the 22-term model provides a baseline for comparison.

Tables D.10 and D.11, respectively, contain the variance-covariance matrices for two  $\ln(\text{Viscosity, poise})$  models: (1) the 24-term truncated T2-LM model given in Table 8.6 and (2) the 20-term truncated T2-LM model given in Table 8.8. The 20-term model is the one recommended for use, but the 24-term model includes terms for  $\text{P}_2\text{O}_5$  and serves as a basis for comparison.

**Table D.1. Variance-Covariance Matrix Associated With the Estimated Coefficients of Terms in the 12-Component Reduced Linear Mixture Model for ln(PCT-B, g/L) of LAW Glasses.**

<b>Term</b>	<b>Al<sub>2</sub>O<sub>3</sub></b>	<b>B<sub>2</sub>O<sub>3</sub></b>	<b>CaO</b>	<b>Fe<sub>2</sub>O<sub>3</sub></b>	<b>K<sub>2</sub>O</b>	<b>Li<sub>2</sub>O</b>	<b>MgO</b>	<b>Na<sub>2</sub>O</b>	<b>P<sub>2</sub>O<sub>5</sub></b>	<b>SiO<sub>2</sub></b>	<b>ZrO<sub>2</sub></b>	<b>Others</b>
<b>Al<sub>2</sub>O<sub>3</sub></b>	5.5710	-0.8279	-0.5109	-0.5529	0.2492	0.0114	-0.9110	-0.3677	0.0616	-0.2532	-0.3757	-0.3273
<b>B<sub>2</sub>O<sub>3</sub></b>	-0.8279	2.6238	0.2240	0.4863	-0.0908	-0.6521	0.2508	-0.0762	-0.3520	-0.4983	-0.9063	0.4833
<b>CaO</b>	-0.5109	0.2240	1.7926	0.0114	0.2697	-0.8099	0.7190	0.2898	0.5065	-0.2904	0.5131	-0.0985
<b>Fe<sub>2</sub>O<sub>3</sub></b>	-0.5529	0.4863	0.0114	1.9282	-0.3949	-0.0127	-0.1257	-0.1152	-0.0213	-0.2513	0.0120	0.4355
<b>K<sub>2</sub>O</b>	0.2492	-0.0908	0.2697	-0.3949	3.2828	1.2402	1.4557	0.1178	0.8567	-0.1175	-0.5288	-0.7447
<b>Li<sub>2</sub>O</b>	0.0114	-0.6521	-0.8099	-0.0127	1.2402	9.3575	0.5050	2.0180	0.6469	-0.5963	-1.9346	-0.9453
<b>MgO</b>	-0.9110	0.2508	0.7190	-0.1257	1.4557	0.5050	9.0188	0.5248	-0.7339	-0.4902	0.6458	-1.0917
<b>Na<sub>2</sub>O</b>	-0.3677	-0.0762	0.2898	-0.1152	0.1178	2.0180	0.5248	0.7677	0.2239	-0.2339	-0.4860	-0.2504
<b>P<sub>2</sub>O<sub>5</sub></b>	0.0616	-0.3520	0.5065	-0.0213	0.8567	0.6469	-0.7339	0.2239	12.0577	-0.1680	-0.4337	0.3157
<b>SiO<sub>2</sub></b>	-0.2532	-0.4983	-0.2904	-0.2513	-0.1175	-0.5963	-0.4902	-0.2339	-0.1680	0.3986	-0.1396	-0.4812
<b>ZrO<sub>2</sub></b>	-0.3757	-0.9063	0.5131	0.0120	-0.5288	-1.9346	0.6458	-0.4860	-0.4337	-0.1396	9.1085	-0.2191
<b>Others</b>	-0.3273	0.4833	-0.0985	0.4355	-0.7447	-0.9453	-1.0917	-0.2504	0.3157	-0.4812	-0.2191	4.4428

**Table D.2. Variance-Covariance Matrix Associated With the Estimated Coefficients of Terms in the 17-Term Reduced Partial Quadratic Mixture Model for ln(PCT-B, g/L) of LAW Glasses.**

Term	Al <sub>2</sub> O <sub>3</sub>	B <sub>2</sub> O <sub>3</sub>	CaO	Fe <sub>2</sub> O <sub>3</sub>	K <sub>2</sub> O	Li <sub>2</sub> O	MgO	Na <sub>2</sub> O	P <sub>2</sub> O <sub>5</sub>	SiO <sub>2</sub>
Al <sub>2</sub> O <sub>3</sub>	4.5411	-0.8535	-0.0978	0.0909	0.9952	-4.5759	-0.0689	-4.8201	0.6100	-0.9005
B <sub>2</sub> O <sub>3</sub>	-0.8535	6.5050	-0.4167	-0.6563	-0.0878	10.2294	11.4075	-2.3603	0.0070	-1.0301
CaO	-0.0978	-0.4167	9.0851	8.3041	2.1673	6.1810	1.3799	-5.4011	1.5476	-1.5567
Fe <sub>2</sub> O <sub>3</sub>	0.0909	-0.6563	8.3041	10.3431	2.0919	3.0053	0.5102	-7.1887	1.8056	-1.7741
K <sub>2</sub> O	0.9952	-0.0878	2.1673	2.0919	3.0456	0.4433	0.6721	-5.0192	1.3508	-1.0531
Li <sub>2</sub> O	-4.5759	10.2294	6.1810	3.0053	0.4433	72.0621	-0.5370	2.9757	-0.8300	-1.5044
MgO	-0.0689	11.4075	1.3799	0.5102	0.6721	-0.5370	68.0494	-1.9809	-0.1016	-1.2803
Na <sub>2</sub> O	-4.8201	-2.3603	-5.4011	-7.1887	-5.0192	2.9757	-1.9809	27.1863	-4.0699	4.9330
P <sub>2</sub> O <sub>5</sub>	0.6100	0.0070	1.5476	1.8056	1.3508	-0.8300	-0.1016	-4.0699	7.9409	-0.9021
SiO <sub>2</sub>	-0.9005	-1.0301	-1.5567	-1.7741	-1.0531	-1.5044	-1.2803	4.9330	-0.9021	1.2395
ZrO <sub>2</sub>	1.2709	0.5252	-0.5915	-0.6713	0.6179	-3.7898	2.2079	-6.7996	0.5266	-1.2130
Others	0.6941	0.1474	0.7187	1.4425	0.4403	-2.8944	-1.3257	-4.6686	0.9485	-1.0866
CaO×Li <sub>2</sub> O	3.9237	-5.0328	-82.4567	-50.8286	-6.5335	-198.0406	-87.7450	-26.7093	17.4291	0.6220
B <sub>2</sub> O <sub>3</sub> ×MgO	5.7135	-125.6845	0.4841	10.4487	13.4220	-18.4379	-703.1255	-33.3977	6.7145	0.4196
B <sub>2</sub> O <sub>3</sub> ×Li <sub>2</sub> O	50.1661	-109.6279	-0.4991	20.5465	17.2896	-538.7395	4.6201	-49.6081	9.8905	2.2332
Na <sub>2</sub> O×SiO <sub>2</sub>	11.8034	4.2468	13.4194	17.4395	12.8827	-6.2908	-2.2819	-67.5964	10.5893	-12.6902
CaO×Fe <sub>2</sub> O <sub>3</sub>	11.6489	7.9481	-122.4661	-130.7800	-21.6787	-107.5801	-26.9959	33.8730	-16.7213	12.3915

Term	ZrO <sub>2</sub>	Others	CaO×Li <sub>2</sub> O	B <sub>2</sub> O <sub>3</sub> ×MgO	B <sub>2</sub> O <sub>3</sub> ×Li <sub>2</sub> O	Na <sub>2</sub> O×SiO <sub>2</sub>	CaO×Fe <sub>2</sub> O <sub>3</sub>
Al <sub>2</sub> O <sub>3</sub>	1.2709	0.6941	3.9237	5.7135	50.1661	11.8034	11.6489
B <sub>2</sub> O <sub>3</sub>	0.5252	0.1474	-5.0328	-125.6845	-109.6279	4.2468	7.9481
CaO	-0.5915	0.7187	-82.4567	0.4841	-0.4991	13.4194	-122.4661
Fe <sub>2</sub> O <sub>3</sub>	-0.6713	1.4425	-50.8286	10.4487	20.5465	17.4395	-130.7800
K <sub>2</sub> O	0.6179	0.4403	-6.5335	13.4220	17.2896	12.8827	-21.6787
Li <sub>2</sub> O	-3.7898	-2.8944	-198.0406	-18.4379	-538.7395	-6.2908	-107.5801
MgO	2.2079	-1.3257	-87.7450	-703.1255	4.6201	-2.2819	-26.9959
Na <sub>2</sub> O	-6.7996	-4.6686	-26.7093	-33.3977	-49.6081	-67.5964	33.8730
P <sub>2</sub> O <sub>5</sub>	0.5266	0.9485	17.4291	6.7145	9.8905	10.5893	-16.7213
SiO <sub>2</sub>	-1.2130	-1.0866	0.6220	0.4196	2.2332	-12.6902	12.3915
ZrO <sub>2</sub>	7.7654	0.9872	22.7654	-6.3621	20.6910	16.5233	32.4518
Others	0.9872	3.4495	13.2488	18.5875	24.3367	11.6207	-3.4768
CaO×Li <sub>2</sub> O	22.7654	13.2488	2855.3392	1162.9848	343.3240	86.3608	1009.9195
B <sub>2</sub> O <sub>3</sub> ×MgO	-6.3621	18.5875	1162.9848	8018.1830	227.1726	175.8912	225.1001
B <sub>2</sub> O <sub>3</sub> ×Li <sub>2</sub> O	20.6910	24.3367	343.3240	227.1726	5204.8656	138.6761	301.8835
Na <sub>2</sub> O×SiO <sub>2</sub>	16.5233	11.6207	86.3608	175.8912	138.6761	172.0205	-71.7517
CaO×Fe <sub>2</sub> O <sub>3</sub>	32.4518	-3.4768	1009.9195	225.1001	301.8835	-71.7517	2124.8909



**Table D.3. Variance-Covariance Matrix Associated With the Estimated Coefficients of Terms in the 12-Component Reduced Linear Mixture Model for ln(PCT-Na, g/L) of LAW Glasses.**

<b>Term</b>	<b>Al<sub>2</sub>O<sub>3</sub></b>	<b>B<sub>2</sub>O<sub>3</sub></b>	<b>CaO</b>	<b>Fe<sub>2</sub>O<sub>3</sub></b>	<b>K<sub>2</sub>O</b>	<b>Li<sub>2</sub>O</b>	<b>MgO</b>	<b>Na<sub>2</sub>O</b>	<b>P<sub>2</sub>O<sub>5</sub></b>	<b>SiO<sub>2</sub></b>	<b>ZrO<sub>2</sub></b>	<b>Others</b>
<b>Al<sub>2</sub>O<sub>3</sub></b>	4.2585	-0.6328	-0.3905	-0.4226	0.1905	0.0087	-0.6964	-0.2810	0.0471	-0.1935	-0.2872	-0.2502
<b>B<sub>2</sub>O<sub>3</sub></b>	-0.6328	2.0056	0.1712	0.3717	-0.0694	-0.4985	0.1917	-0.0583	-0.2691	-0.3809	-0.6928	0.3694
<b>CaO</b>	-0.3905	0.1712	1.3703	0.0087	0.2061	-0.6191	0.5496	0.2216	0.3872	-0.2220	0.3922	-0.0753
<b>Fe<sub>2</sub>O<sub>3</sub></b>	-0.4226	0.3717	0.0087	1.4739	-0.3019	-0.0097	-0.0961	-0.0880	-0.0163	-0.1921	0.0092	0.3329
<b>K<sub>2</sub>O</b>	0.1905	-0.0694	0.2061	-0.3019	2.5093	0.9480	1.1127	0.0901	0.6548	-0.0898	-0.4042	-0.5693
<b>Li<sub>2</sub>O</b>	0.0087	-0.4985	-0.6191	-0.0097	0.9480	7.1529	0.3860	1.5426	0.4945	-0.4558	-1.4788	-0.7226
<b>MgO</b>	-0.6964	0.1917	0.5496	-0.0961	1.1127	0.3860	6.8940	0.4011	-0.5610	-0.3747	0.4937	-0.8345
<b>Na<sub>2</sub>O</b>	-0.2810	-0.0583	0.2216	-0.0880	0.0901	1.5426	0.4011	0.5868	0.1712	-0.1788	-0.3715	-0.1914
<b>P<sub>2</sub>O<sub>5</sub></b>	0.0471	-0.2691	0.3872	-0.0163	0.6548	0.4945	-0.5610	0.1712	9.2169	-0.1284	-0.3315	0.2413
<b>SiO<sub>2</sub></b>	-0.1935	-0.3809	-0.2220	-0.1921	-0.0898	-0.4558	-0.3747	-0.1788	-0.1284	0.3047	-0.1067	-0.3678
<b>ZrO<sub>2</sub></b>	-0.2872	-0.6928	0.3922	0.0092	-0.4042	-1.4788	0.4937	-0.3715	-0.3315	-0.1067	6.9626	-0.1675
<b>Others</b>	-0.2502	0.3694	-0.0753	0.3329	-0.5693	-0.7226	-0.8345	-0.1914	0.2413	-0.3678	-0.1675	3.3961

**Table D.4. Variance-Covariance Matrix Associated With the Estimated Coefficients of Terms in the 17-Term Reduced Partial Quadratic Mixture Model for ln(PCT-Na, g/L) of LAW Glasses.**

Term	Al <sub>2</sub> O <sub>3</sub>	B <sub>2</sub> O <sub>3</sub>	CaO	Fe <sub>2</sub> O <sub>3</sub>	K <sub>2</sub> O	Li <sub>2</sub> O	MgO	Na <sub>2</sub> O	P <sub>2</sub> O <sub>5</sub>	SiO <sub>2</sub>
Al <sub>2</sub> O <sub>3</sub>	2.6367	-0.2222	-0.7385	-0.9214	0.3894	0.0726	0.0444	-0.2025	-0.0847	-0.0931
B <sub>2</sub> O <sub>3</sub>	-0.2222	7.6234	-1.8619	-1.2119	0.0080	-2.1700	8.3156	2.8308	-0.9891	-0.8349
CaO	-0.7385	-1.8619	6.5491	5.5974	-0.3900	4.5648	1.3215	-0.8383	0.7250	-0.3090
Fe <sub>2</sub> O <sub>3</sub>	-0.9214	-1.2119	5.5974	6.7804	-0.7335	3.5350	0.5885	-0.5800	0.6211	-0.3470
K <sub>2</sub> O	0.3894	0.0080	-0.3900	-0.7335	15.7842	0.2329	1.0913	-0.1269	0.6935	0.0011
Li <sub>2</sub> O	0.0726	-2.1700	4.5648	3.5350	0.2329	12.5785	0.1544	0.0640	-0.0688	-0.4073
MgO	0.0444	8.3156	1.3215	0.5885	1.0913	0.1544	52.5669	-2.6874	0.1514	-1.0574
Na <sub>2</sub> O	-0.2025	2.8308	-0.8383	-0.5800	-0.1269	0.0640	-2.6874	2.8123	-0.5161	-0.4047
P <sub>2</sub> O <sub>5</sub>	-0.0847	-0.9891	0.7250	0.6211	0.6935	-0.0688	0.1514	-0.5161	5.7728	-0.0060
SiO <sub>2</sub>	-0.0931	-0.8349	-0.3090	-0.3470	0.0011	-0.4073	-1.0574	-0.4047	-0.0060	0.2645
ZrO <sub>2</sub>	0.0893	-0.2650	-1.4150	-1.8620	0.5222	-1.8244	1.9660	-0.6056	-0.2731	0.0507
Others	-0.1842	-0.0865	-0.0130	0.2671	-0.9330	-0.6020	-0.9052	-0.2447	0.2061	-0.1846
B <sub>2</sub> O <sub>3</sub> ×MgO	-2.8191	2.1879	-70.6074	-48.1835	7.4888	-130.1176	-66.8946	7.1486	9.1275	4.6965
Li <sub>2</sub> O×ZrO <sub>2</sub>	10.9332	22.0585	-93.0576	-98.1200	4.8711	-59.0421	-22.4845	9.7084	-10.6784	4.0376
Fe <sub>2</sub> O <sub>3</sub> ×K <sub>2</sub> O	-5.5808	-105.5970	-7.7365	-4.3021	-8.5036	-0.2581	-540.0123	22.8696	-2.1734	10.8288
Fe <sub>2</sub> O <sub>3</sub> ×Li <sub>2</sub> O	0.3251	-40.8666	9.5918	4.2261	-1.1662	9.1771	5.6624	-29.0184	7.2277	4.3856
B <sub>2</sub> O <sub>3</sub> ×K <sub>2</sub> O	-7.5665	-13.1053	30.6658	30.2914	-313.1547	24.6694	-8.6805	-2.7077	-4.3109	-1.1330

Term	ZrO <sub>2</sub>	Others	CaO×Li <sub>2</sub> O	CaO×Fe <sub>2</sub> O <sub>3</sub>	B <sub>2</sub> O <sub>3</sub> ×MgO	B <sub>2</sub> O <sub>3</sub> ×Na <sub>2</sub> O	K <sub>2</sub> O×K <sub>2</sub> O
Al <sub>2</sub> O <sub>3</sub>	0.0893	-0.1842	-2.8191	10.9332	-5.5808	0.3251	-7.5665
B <sub>2</sub> O <sub>3</sub>	-0.2650	-0.0865	2.1879	22.0585	-105.5970	-40.8666	-13.1053
CaO	-1.4150	-0.0130	-70.6074	-93.0576	-7.7365	9.5918	30.6658
Fe <sub>2</sub> O <sub>3</sub>	-1.8620	0.2671	-48.1835	-98.1200	-4.3021	4.2261	30.2914
K <sub>2</sub> O	0.5222	-0.9330	7.4888	4.8711	-8.5036	-1.1662	-313.1547
Li <sub>2</sub> O	-1.8244	-0.6020	-130.1176	-59.0421	-0.2581	9.1771	24.6694
MgO	1.9660	-0.9052	-66.8946	-22.4845	-540.0123	5.6624	-8.6805
Na <sub>2</sub> O	-0.6056	-0.2447	7.1486	9.7084	22.8696	-29.0184	-2.7077
P <sub>2</sub> O <sub>5</sub>	-0.2731	0.2061	9.1275	-10.6784	-2.1734	7.2277	-4.3109
SiO <sub>2</sub>	0.0507	-0.1846	4.6965	4.0376	10.8288	4.3856	-1.1330
ZrO <sub>2</sub>	4.8825	-0.1335	11.8234	30.3392	-17.9346	4.3044	-21.3201
Others	-0.1335	2.0567	4.2279	-0.8944	5.6599	2.0542	13.3522
CaO×Li <sub>2</sub> O	11.8234	4.2279	2181.7928	819.1763	810.6713	-25.9923	-398.1906
CaO×Fe <sub>2</sub> O <sub>3</sub>	30.3392	-0.8944	819.1763	1633.1939	203.0666	-73.5093	-408.6876
B <sub>2</sub> O <sub>3</sub> ×MgO	-17.9346	5.6599	810.6713	203.0666	6060.0432	59.3798	202.3782
B <sub>2</sub> O <sub>3</sub> ×Na <sub>2</sub> O	4.3044	2.0542	-25.9923	-73.5093	59.3798	361.3491	102.0262
K <sub>2</sub> O×K <sub>2</sub> O	-21.3201	13.3522	-398.1906	-408.6876	202.3782	102.0262	6928.8404

**Table D.5. Variance-Covariance Matrix Associated With the Estimated Coefficients of Terms in the 11-Component Reduced Linear Mixture Model for ln(VHT Alteration Depth,  $\mu\text{m}$ ) of LAW Glasses.**

<b>Term</b>	<b>Al<sub>2</sub>O<sub>3</sub></b>	<b>B<sub>2</sub>O<sub>3</sub></b>	<b>CaO</b>	<b>Fe<sub>2</sub>O<sub>3</sub></b>	<b>K<sub>2</sub>O</b>	<b>Li<sub>2</sub>O</b>	<b>MgO</b>	<b>Na<sub>2</sub>O</b>	<b>SiO<sub>2</sub></b>	<b>ZrO<sub>2</sub></b>	<b>Others</b>
<b>Al<sub>2</sub>O<sub>3</sub></b>	65.4457	-7.7270	-2.2023	-3.6416	-1.8669	-16.0019	-14.8636	-8.5703	-1.9340	6.3549	-9.2850
<b>B<sub>2</sub>O<sub>3</sub></b>	-7.7270	32.4279	0.7454	10.1316	0.3777	-4.1659	-1.7967	-2.6418	-6.5586	-3.2100	4.3297
<b>CaO</b>	-2.2023	0.7454	23.3747	-0.5010	2.4306	-15.4380	4.0744	2.7878	-2.8182	5.1994	-2.8452
<b>Fe<sub>2</sub>O<sub>3</sub></b>	-3.6416	10.1316	-0.5010	31.2795	-8.0986	-0.5539	-4.5747	-3.1055	-4.3545	7.0856	1.3940
<b>K<sub>2</sub>O</b>	-1.8669	0.3777	2.4306	-8.0986	40.6817	15.5158	19.2872	2.3002	-2.0541	-8.7240	0.2596
<b>Li<sub>2</sub>O</b>	-16.0019	-4.1659	-15.4380	-0.5539	15.5158	140.5426	14.2002	30.7589	-9.9163	-34.0278	4.8870
<b>MgO</b>	-14.8636	-1.7967	4.0744	-4.5747	19.2872	14.2002	103.8143	8.4833	-4.9975	-2.0470	-3.7618
<b>Na<sub>2</sub>O</b>	-8.5703	-2.6418	2.7878	-3.1055	2.3002	30.7589	8.4833	11.5770	-2.9348	-11.0216	1.4296
<b>SiO<sub>2</sub></b>	-1.9340	-6.5586	-2.8182	-4.3545	-2.0541	-9.9163	-4.9975	-2.9348	5.0307	-1.8786	-5.7186
<b>ZrO<sub>2</sub></b>	6.3549	-3.2100	5.1994	7.0856	-8.7240	-34.0278	-2.0470	-11.0216	-1.8786	102.6413	-7.5869
<b>Others</b>	-9.2850	4.3297	-2.8452	1.3940	0.2596	4.8870	-3.7618	1.4296	-5.7186	-7.5869	45.0501

**Table D.6. Variance-Covariance Matrix Associated With the Estimated Coefficients of Terms in the 16-Term Reduced Partial Quadratic Mixture Model for ln(VHT Alteration Depth,  $\mu\text{m}$ ) of LAW Glasses.**

Term	Al <sub>2</sub> O <sub>3</sub>	B <sub>2</sub> O <sub>3</sub>	CaO	Fe <sub>2</sub> O <sub>3</sub>	K <sub>2</sub> O	Li <sub>2</sub> O	MgO	Na <sub>2</sub> O	SiO <sub>2</sub>
Al <sub>2</sub> O <sub>3</sub>	179.3480	-3.8133	-186.2479	-4.5506	-12.2610	2.3651	78.2069	14.7232	-27.2363
B <sub>2</sub> O <sub>3</sub>	-3.8133	28.1471	-90.3403	12.5652	5.5638	4.9309	-18.2350	-2.2279	-9.4030
CaO	-186.2479	-90.3403	1571.2221	-87.3928	-131.7677	-115.1655	-74.9925	-112.1934	125.6311
Fe <sub>2</sub> O <sub>3</sub>	-4.5506	12.5652	-87.3928	26.0197	-3.2596	5.4462	-7.9369	4.0042	-8.7405
K <sub>2</sub> O	-12.2610	5.5638	-131.7677	-3.2596	297.6795	22.1497	20.9783	7.0081	-8.4621
Li <sub>2</sub> O	2.3651	4.9309	-115.1655	5.4462	22.1497	95.9600	0.1856	21.4094	-13.8206
MgO	78.2069	-18.2350	-74.9925	-7.9369	20.9783	0.1856	333.9251	70.2445	-25.5950
Na <sub>2</sub> O	14.7232	-2.2279	-112.1934	4.0042	7.0081	21.4094	70.2445	41.9994	-16.5252
SiO <sub>2</sub>	-27.2363	-9.4030	125.6311	-8.7405	-8.4621	-13.8206	-25.5950	-16.5252	15.4631
ZrO <sub>2</sub>	364.0642	-27.1081	-303.0949	-11.6834	-75.7002	-12.2663	275.3123	98.4232	-69.4503
Others	-14.9326	8.5169	-70.7047	6.7332	5.5544	7.8562	-11.2806	3.9674	-7.3919
CaO×SiO <sub>2</sub>	419.6613	214.4029	-3675.5772	207.6296	313.4053	247.8674	187.4004	273.9175	-300.2441
K <sub>2</sub> O×K <sub>2</sub> O	17.5107	3.4578	1472.1284	82.4346	-5660.4111	-167.9266	-509.6079	-53.2509	77.8437
MgO×Na <sub>2</sub> O	-752.6094	231.7518	-67.7613	96.3626	-42.5917	155.1178	-2794.7710	-635.3253	161.9452
Al <sub>2</sub> O <sub>3</sub> ×ZrO <sub>2</sub>	-5424.6006	249.4261	2533.7792	406.4922	1167.7523	-184.8774	-3258.3465	-363.6708	667.7530
Na <sub>2</sub> O×ZrO <sub>2</sub>	-11.6988	92.9758	821.3928	-68.2544	41.6825	52.5762	-591.7715	-651.5548	175.9120

Term	ZrO <sub>2</sub>	Others	CaO×SiO <sub>2</sub>	K <sub>2</sub> O×K <sub>2</sub> O	MgO×Na <sub>2</sub> O	Al <sub>2</sub> O <sub>3</sub> ×ZrO <sub>2</sub>	Na <sub>2</sub> O×ZrO <sub>2</sub>
Al <sub>2</sub> O <sub>3</sub>	364.0642	-14.9326	419.6613	17.5107	-752.6094	-5424.6006	-11.6988
B <sub>2</sub> O <sub>3</sub>	-27.1081	8.5169	214.4029	3.4578	231.7518	249.4261	92.9758
CaO	-303.0949	-70.7047	-3675.5772	1472.1284	-67.7613	2533.7792	821.3928
Fe <sub>2</sub> O <sub>3</sub>	-11.6834	6.7332	207.6296	82.4346	96.3626	406.4922	-68.2544
K <sub>2</sub> O	-75.7002	5.5544	313.4053	-5660.4111	-42.5917	1167.7523	41.6825
Li <sub>2</sub> O	-12.2663	7.8562	247.8674	-167.9266	155.1178	-184.8774	52.5762
MgO	275.3123	-11.2806	187.4004	-509.6079	-2794.7710	-3258.3465	-591.7715
Na <sub>2</sub> O	98.4232	3.9674	273.9175	-53.2509	-635.3253	-363.6708	-651.5548
SiO <sub>2</sub>	-69.4503	-7.3919	-300.2441	77.8437	161.9452	667.7530	175.9120
ZrO <sub>2</sub>	1271.2145	-43.2389	687.6426	771.0181	-2606.6833	-14517.3249	-2019.6240
Others	-43.2389	33.8521	165.2029	2.1562	124.7127	642.4658	-15.2290
CaO×SiO <sub>2</sub>	687.6426	165.2029	8682.7411	-3398.8206	100.8389	-5218.9300	-2061.1857
K <sub>2</sub> O×K <sub>2</sub> O	771.0181	2.1562	-3398.8206	120145.9135	4848.8986	-10516.6315	-2258.2496
MgO×Na <sub>2</sub> O	-2606.6833	124.7127	100.8389	4848.8986	29555.1637	29992.1262	6229.7570
Al <sub>2</sub> O <sub>3</sub> ×ZrO <sub>2</sub>	-14517.3249	642.4658	-5218.9300	-10516.6315	29992.1262	229896.7963	-4486.4866
Na <sub>2</sub> O×ZrO <sub>2</sub>	-2019.6240	-15.2290	-2061.1857	-2258.2496	6229.7570	-4486.4866	18464.9259

**Table D.7. Variance-Covariance Matrix Associated With the Estimated Coefficients of Terms in the 15-Term Reduced Partial Cubic Mixture Model for ln(VHT Alteration Depth,  $\mu\text{m}$ ) of LAW Glasses.**

Term	Al <sub>2</sub> O <sub>3</sub>	B <sub>2</sub> O <sub>3</sub>	CaO	Fe <sub>2</sub> O <sub>3</sub>	K <sub>2</sub> O	Li <sub>2</sub> O	MgO	Na <sub>2</sub> O
Al <sub>2</sub> O <sub>3</sub>	37.0274	-6.1959	-7.5969	0.8362	-3.8661	-21.7084	-7.1062	-16.2542
B <sub>2</sub> O <sub>3</sub>	-6.1959	35.0847	34.8292	1.0209	-6.1880	-37.0646	-6.2560	6.5622
CaO	-7.5969	34.8292	89.2636	-12.8816	-23.1870	-31.9473	-14.3315	42.1681
Fe <sub>2</sub> O <sub>3</sub>	0.8362	1.0209	-12.8816	22.3018	-11.4926	-19.7243	-0.8794	-19.7161
K <sub>2</sub> O	-3.8661	-6.1880	-23.1870	-11.4926	114.6504	11.3336	33.6888	-3.7296
Li <sub>2</sub> O	-21.7084	-37.0646	-31.9473	-19.7243	11.3336	402.6862	-3.1993	150.0097
MgO	-7.1062	-6.2560	-14.3315	-0.8794	33.6888	-3.1993	64.6618	-7.0818
Na <sub>2</sub> O	-16.2542	6.5622	42.1681	-19.7161	-3.7296	150.0097	-7.0818	109.7369
SiO <sub>2</sub>	0.7085	-7.7598	-12.6605	0.5479	0.5948	-14.3494	-0.4710	-15.6511
ZrO <sub>2</sub>	4.4076	-3.1717	-4.0153	5.4465	3.7883	-33.6196	2.6589	-15.8112
Others	-2.6630	-0.3724	-11.9223	5.1363	-0.2410	-22.2422	0.9723	-16.6912
(K <sub>2</sub> O) <sup>2</sup> ×Na <sub>2</sub> O	771.0153	163.3330	859.1075	1630.2301	-10990.5144	-4461.2830	-2212.0420	-2639.7226
(Na <sub>2</sub> O) <sup>3</sup>	136.0406	-21.6663	-349.6870	195.3939	60.2046	-1792.6212	115.1066	-1302.7253
Li <sub>2</sub> O×Na <sub>2</sub> O×SiO <sub>2</sub>	276.5747	673.4985	310.5460	424.0416	230.0304	-6956.0025	343.3545	-2825.3603
B <sub>2</sub> O <sub>3</sub> ×CaO×Na <sub>2</sub> O	640.1299	-3014.8798	-6657.9092	1204.3237	1358.4667	1732.9326	1224.0790	-4182.2868

Term	SiO <sub>2</sub>	ZrO <sub>2</sub>	Others	(K <sub>2</sub> O) <sup>2</sup> ×Na <sub>2</sub> O	(Na <sub>2</sub> O) <sup>3</sup>	Li <sub>2</sub> O×Na <sub>2</sub> O×SiO <sub>2</sub>	B <sub>2</sub> O <sub>3</sub> ×CaO×Na <sub>2</sub> O
Al <sub>2</sub> O <sub>3</sub>	0.7085	4.4076	-2.6630	771.0153	136.0406	276.5747	640.1299
B <sub>2</sub> O <sub>3</sub>	-7.7598	-3.1717	-0.3724	163.3330	-21.6663	673.4985	-3014.8798
CaO	-12.6605	-4.0153	-11.9223	859.1075	-349.6870	310.5460	-6657.9092
Fe <sub>2</sub> O <sub>3</sub>	0.5479	5.4465	5.1363	1630.2301	195.3939	424.0416	1204.3237
K <sub>2</sub> O	0.5948	3.7883	-0.2410	-10990.5144	60.2046	230.0304	1358.4667
Li <sub>2</sub> O	-14.3494	-33.6196	-22.2422	-4461.2830	-1792.6212	-6956.0025	1732.9326
MgO	-0.4710	2.6589	0.9723	-2212.0420	115.1066	343.3545	1224.0790
Na <sub>2</sub> O	-15.6511	-15.8112	-16.6912	-2639.7226	-1302.7253	-2825.3603	-4182.2868
SiO <sub>2</sub>	5.2310	0.3491	-0.6156	279.1963	164.8064	197.3669	1064.2436
ZrO <sub>2</sub>	0.3491	57.6249	-1.8627	-614.7721	112.1162	368.3748	527.1768
Others	-0.6156	-1.8627	28.6027	786.0088	195.0451	561.4452	927.7819
(K <sub>2</sub> O) <sup>2</sup> ×Na <sub>2</sub> O	279.1963	-614.7721	786.0088	1436442.3984	29221.3465	65274.7345	24923.3397
(Na <sub>2</sub> O) <sup>3</sup>	164.8064	112.1162	195.0451	29221.3465	17067.2975	37209.8730	40016.3557
Li <sub>2</sub> O×Na <sub>2</sub> O×SiO <sub>2</sub>	197.3669	368.3748	561.4452	65274.7345	37209.8730	150236.7297	-25688.2830
B <sub>2</sub> O <sub>3</sub> ×CaO×Na <sub>2</sub> O	1064.2436	527.1768	927.7819	24923.3397	40016.3557	-25688.2830	598088.4681

**Table D.8. Variance-Covariance Matrix Associated With the Estimated Coefficients of Terms in the 22-Term Arrhenius-Linear Mixture Model for ln(Electrical Conductivity, S/cm) of LAW Glasses.**

Term	Al <sub>2</sub> O <sub>3</sub>	B <sub>2</sub> O <sub>3</sub>	CaO	Fe <sub>2</sub> O <sub>3</sub>	K <sub>2</sub> O	Li <sub>2</sub> O	MgO	Na <sub>2</sub> O	SiO <sub>2</sub>	ZrO <sub>2</sub>	Others
Al <sub>2</sub> O <sub>3</sub>	6.9806	-0.8322	-0.5154	-0.7157	0.3315	0.1088	-1.0788	-0.3722	-0.4435	-0.2462	-0.2681
B <sub>2</sub> O <sub>3</sub>	-0.8322	3.2800	0.3018	0.5718	0.2392	-0.7475	0.2597	-0.1504	-0.6201	-1.2655	0.4479
CaO	-0.5154	0.3018	2.4215	-0.2545	0.4256	-1.1271	0.9113	0.3665	-0.4018	0.7425	0.0141
Fe <sub>2</sub> O <sub>3</sub>	-0.7157	0.5718	-0.2545	2.9180	-0.6916	0.2549	0.0078	-0.1685	-0.3405	-0.0477	0.6079
K <sub>2</sub> O	0.3315	0.2392	0.4256	-0.6916	5.0192	0.8422	2.0979	-0.0078	-0.2401	-0.4515	-0.4880
Li <sub>2</sub> O	0.1088	-0.7475	-1.1271	0.2549	0.8422	12.2679	0.4126	2.6863	-0.9032	-2.5228	-0.5756
MgO	-1.0788	0.2597	0.9113	0.0078	2.0979	0.4126	11.3328	0.5865	-0.6920	0.9306	-0.8566
Na <sub>2</sub> O	-0.3722	-0.1504	0.3665	-0.1685	-0.0078	2.6863	0.5865	1.0680	-0.3360	-0.6024	-0.1914
SiO <sub>2</sub>	-0.4435	-0.6201	-0.4018	-0.3405	-0.2401	-0.9032	-0.6920	-0.3360	0.5559	-0.1658	-0.6147
ZrO <sub>2</sub>	-0.2462	-1.2655	0.7425	-0.0477	-0.4515	-2.5228	0.9306	-0.6024	-0.1658	11.9599	-0.5936
Others	-0.2681	0.4479	0.0141	0.6079	-0.4880	-0.5756	-0.8566	-0.1914	-0.6147	-0.5936	4.6944
Al <sub>2</sub> O <sub>3</sub> /(T/1000)	-7.4729	0.8875	0.5394	0.7728	-0.3472	-0.1538	1.1874	0.3809	0.4814	0.2369	0.3045
B <sub>2</sub> O <sub>3</sub> /(T/1000)	0.8874	-3.5068	-0.3188	-0.6120	-0.2485	0.8022	-0.2504	0.1626	0.6644	1.3235	-0.4897
CaO/(T/1000)	0.5394	-0.3188	-2.5868	0.2722	-0.4483	1.2101	-0.9639	-0.3880	0.4279	-0.8063	-0.0073
Fe <sub>2</sub> O <sub>3</sub> /(T/1000)	0.7728	-0.6120	0.2722	-3.1291	0.7479	-0.2489	-0.0098	0.1868	0.3634	0.0430	-0.6638
K <sub>2</sub> O/(T/1000)	-0.3475	-0.2485	-0.4484	0.7479	-5.3937	-0.9099	-2.2413	0.0078	0.2568	0.4524	0.5152
Li <sub>2</sub> O/(T/1000)	-0.1532	0.8022	1.2100	-0.2491	-0.9101	-13.1588	-0.5000	-2.8850	0.9798	2.6940	0.5841
MgO/(T/1000)	1.1872	-0.2505	-0.9640	-0.0098	-2.2410	-0.5002	-12.1426	-0.6409	0.7335	-0.9785	0.9269
Na <sub>2</sub> O/(T/1000)	0.3811	0.1626	-0.3880	0.1867	0.0077	-2.8850	-0.6409	-1.1462	0.3632	0.6432	0.1989
SiO <sub>2</sub> /(T/1000)	0.4813	0.6644	0.4279	0.3634	0.2568	0.9798	0.7335	0.3632	-0.5980	0.1862	0.6607
ZrO <sub>2</sub> /(T/1000)	0.2369	1.3237	-0.8063	0.0431	0.4520	2.6944	-0.9787	0.6433	0.1861	-12.8166	0.6725
Others/(T/1000)	0.3046	-0.4896	-0.0072	-0.6635	0.5152	0.5842	0.9267	0.1989	0.6606	0.6723	-5.0384

Term	Al <sub>2</sub> O <sub>3</sub> /(T/1000)	B <sub>2</sub> O <sub>3</sub> /(T/1000)	CaO/(T/1000)	Fe <sub>2</sub> O <sub>3</sub> /(T/1000)	K <sub>2</sub> O/(T/1000)	Li <sub>2</sub> O/(T/1000)
Al <sub>2</sub> O <sub>3</sub>	-7.4729	0.8874	0.5394	0.7728	-0.3475	-0.1532
B <sub>2</sub> O <sub>3</sub>	0.8875	-3.5068	-0.3188	-0.6120	-0.2485	0.8022
CaO	0.5394	-0.3188	-2.5868	0.2722	-0.4484	1.2100
Fe <sub>2</sub> O <sub>3</sub>	0.7728	-0.6120	0.2722	-3.1291	0.7479	-0.2491
K <sub>2</sub> O	-0.3472	-0.2485	-0.4483	0.7479	-5.3937	-0.9101
Li <sub>2</sub> O	-0.1538	0.8022	1.2101	-0.2489	-0.9099	-13.1588
MgO	1.1874	-0.2504	-0.9639	-0.0098	-2.2413	-0.5000
Na <sub>2</sub> O	0.3809	0.1626	-0.3880	0.1868	0.0078	-2.8850
SiO <sub>2</sub>	0.4814	0.6644	0.4279	0.3634	0.2568	0.9798
ZrO <sub>2</sub>	0.2369	1.3235	-0.8063	0.0430	0.4524	2.6940
Others	0.3045	-0.4897	-0.0073	-0.6638	0.5152	0.5841
Al <sub>2</sub> O <sub>3</sub> /(T/1000)	10.1481	-1.2061	-0.7273	-1.0549	0.4644	0.2362
B <sub>2</sub> O <sub>3</sub> /(T/1000)	-1.2061	4.7568	0.4283	0.8329	0.3293	-1.0853
CaO/(T/1000)	-0.7273	0.4283	3.5090	-0.3697	0.6046	-1.6437
Fe <sub>2</sub> O <sub>3</sub> /(T/1000)	-1.0549	0.8329	-0.3697	4.2556	-1.0179	0.3256
K <sub>2</sub> O/(T/1000)	0.4644	0.3293	0.6046	-1.0179	7.3152	1.2486
Li <sub>2</sub> O/(T/1000)	0.2362	-1.0853	-1.6437	0.3256	1.2486	17.8554
MgO/(T/1000)	-1.6373	0.3230	1.2962	0.0130	3.0260	0.7202
Na <sub>2</sub> O/(T/1000)	-0.5065	-0.2213	0.5246	-0.2577	-0.0096	3.9144
SiO <sub>2</sub> /(T/1000)	-0.6554	-0.9022	-0.5787	-0.4938	-0.3475	-1.3384
ZrO <sub>2</sub> /(T/1000)	-0.3180	-1.7719	1.1016	-0.0535	-0.5984	-3.6618
Others/(T/1000)	-0.4268	0.6708	0.0052	0.9119	-0.6918	-0.7631

**Table D.8. Variance-Covariance Matrix Associated With the Estimated Coefficients of Terms in the 22-Term Arrhenius-Linear Mixture Model for ln(Electrical Conductivity, S/cm) of LAW Glasses (continued).**

Term	MgO/(T/1000)	Na <sub>2</sub> O/(T/1000)	SiO <sub>2</sub> /(T/1000)	ZrO <sub>2</sub> /(T/1000)	Others/(T/1000)
Al <sub>2</sub> O <sub>3</sub>	1.1872	0.3811	0.4813	0.2369	0.3046
B <sub>2</sub> O <sub>3</sub>	-0.2505	0.1626	0.6644	1.3237	-0.4896
CaO	-0.9640	-0.3880	0.4279	-0.8063	-0.0072
Fe <sub>2</sub> O <sub>3</sub>	-0.0098	0.1867	0.3634	0.0431	-0.6635
K <sub>2</sub> O	-2.2410	0.0077	0.2568	0.4520	0.5152
Li <sub>2</sub> O	-0.5002	-2.8850	0.9798	2.6944	0.5842
MgO	-12.1426	-0.6409	0.7335	-0.9787	0.9267
Na <sub>2</sub> O	-0.6409	-1.1462	0.3632	0.6433	0.1989
SiO <sub>2</sub>	0.7335	0.3632	-0.5980	0.1861	0.6606
ZrO <sub>2</sub>	-0.9785	0.6432	0.1862	-12.8166	0.6723
Others	0.9269	0.1989	0.6607	0.6725	-5.0384
Al <sub>2</sub> O <sub>3</sub> /(T/1000)	-1.6373	-0.5065	-0.6554	-0.3180	-0.4268
B <sub>2</sub> O <sub>3</sub> /(T/1000)	0.3230	-0.2213	-0.9022	-1.7719	0.6708
CaO/(T/1000)	1.2962	0.5246	-0.5787	1.1016	0.0052
Fe <sub>2</sub> O <sub>3</sub> /(T/1000)	0.0130	-0.2577	-0.4938	-0.0535	0.9119
K <sub>2</sub> O/(T/1000)	3.0260	-0.0096	-0.3475	-0.5984	-0.6918
Li <sub>2</sub> O/(T/1000)	0.7202	3.9144	-1.3384	-3.6618	-0.7631
MgO/(T/1000)	16.4672	0.8787	-0.9890	1.3212	-1.2647
Na <sub>2</sub> O/(T/1000)	0.8787	1.5557	-0.4948	-0.8737	-0.2632
SiO <sub>2</sub> /(T/1000)	-0.9890	-0.4948	0.8129	-0.2551	-0.8990
ZrO <sub>2</sub> /(T/1000)	1.3212	-0.8737	-0.2551	17.3951	-0.9429
Others/(T/1000)	-1.2647	-0.2632	-0.8990	-0.9429	6.8462

**Table D.9. Variance-Covariance Matrix Associated With the Estimated Coefficients of Terms in the 25-Term Arrhenius-Linear Mixture Model with Three Crossproduct Terms for ln(Electrical Conductivity, S/cm) of LAW Glasses.**

Term	Al <sub>2</sub> O <sub>3</sub>	B <sub>2</sub> O <sub>3</sub>	CaO	Fe <sub>2</sub> O <sub>3</sub>	K <sub>2</sub> O	Li <sub>2</sub> O	MgO	Na <sub>2</sub> O	SiO <sub>2</sub>
Al <sub>2</sub> O <sub>3</sub>	6.4799	-0.7687	-0.5444	-0.6502	0.3336	0.1030	-0.9935	-0.3862	-0.4047
B <sub>2</sub> O <sub>3</sub>	-0.7687	3.0753	-0.2350	0.5775	0.2775	-1.2268	0.3064	-0.2836	-0.5409
CaO	-0.5444	-0.2350	9.0967	-0.8749	-0.4213	4.9678	-0.0479	2.2997	-0.8098
Fe <sub>2</sub> O <sub>3</sub>	-0.6502	0.5775	-0.8749	2.7741	-0.5565	-0.6301	0.1079	-0.3634	-0.2683
K <sub>2</sub> O	0.3336	0.2775	-0.4213	-0.5565	4.7674	0.0410	2.0530	-0.2676	-0.1665
Li <sub>2</sub> O	0.1030	-1.2268	4.9678	-0.6301	0.0410	25.2917	-0.8496	4.5557	-1.3387
MgO	-0.9935	0.3064	-0.0479	0.1079	2.0530	-0.8496	10.6342	0.2676	-0.5761
Na <sub>2</sub> O	-0.3862	-0.2836	2.2997	-0.3634	-0.2676	4.5557	0.2676	1.6011	-0.4465
SiO <sub>2</sub>	-0.4047	-0.5409	-0.8098	-0.2683	-0.1665	-1.3387	-0.5761	-0.4465	0.5453
ZrO <sub>2</sub>	-0.2125	-1.1722	0.7554	-0.0338	-0.4077	-2.5711	0.8667	-0.5657	-0.1535
Others	-0.2443	0.5012	-1.0702	0.6758	-0.3242	-1.8311	-0.6353	-0.4966	-0.4958
CaO×Li <sub>2</sub> O	-1.2238	8.2817	-97.2024	10.3567	9.9114	-144.7756	15.5091	-27.7001	6.6834
CaO×Na <sub>2</sub> O	0.6257	2.6594	-37.2667	3.2215	4.5760	-23.1400	4.3607	-10.5266	2.2859
Li <sub>2</sub> O×Na <sub>2</sub> O	0.7076	0.4980	-3.8171	2.3793	1.5515	-49.3728	3.0783	-4.2848	1.0436
Al <sub>2</sub> O <sub>3</sub> /(T/1000)	-7.5254	0.8973	0.4993	0.7818	-0.3460	-0.2022	1.2016	0.3729	0.4873
B <sub>2</sub> O <sub>3</sub> /(T/1000)	0.8936	-3.5307	-0.3263	-0.6165	-0.2495	0.8258	-0.2525	0.1631	0.6690
CaO/(T/1000)	0.5428	-0.3195	-2.6215	0.2754	-0.4498	1.2059	-0.9684	-0.3947	0.4317
Fe <sub>2</sub> O <sub>3</sub> /(T/1000)	0.7772	-0.6154	0.2666	-3.1503	0.7529	-0.2586	-0.0089	0.1873	0.3662
K <sub>2</sub> O/(T/1000)	-0.3493	-0.2504	-0.4489	0.7530	-5.4297	-0.9151	-2.2564	0.0078	0.2585
Li <sub>2</sub> O/(T/1000)	-0.1538	0.8038	1.2660	-0.2552	-0.9205	-13.1967	-0.5100	-2.8923	0.9836
MgO/(T/1000)	1.1952	-0.2491	-1.0073	-0.0067	-2.2522	-0.5340	-12.2210	-0.6549	0.7407
Na <sub>2</sub> O/(T/1000)	0.3837	0.1629	-0.3799	0.1868	0.0067	-2.8888	-0.6470	-1.1510	0.3650
SiO <sub>2</sub> /(T/1000)	0.4850	0.6685	0.4366	0.3658	0.2583	0.9848	0.7382	0.3665	-0.6023
ZrO <sub>2</sub> /(T/1000)	0.2397	1.3326	-0.8151	0.0439	0.4558	2.7148	-0.9854	0.6460	0.1876
Others/(T/1000)	0.3050	-0.4933	0.0014	-0.6695	0.5157	0.5978	0.9315	0.2048	0.6643

Term	ZrO <sub>2</sub>	Others	CaO×Li <sub>2</sub> O	CaO×Na <sub>2</sub> O	Li <sub>2</sub> O×Na <sub>2</sub> O	Al <sub>2</sub> O <sub>3</sub> /(T/1000)	B <sub>2</sub> O <sub>3</sub> /(T/1000)
Al <sub>2</sub> O <sub>3</sub>	-0.2125	-0.2443	-1.2238	0.6257	0.7076	-7.5254	0.8936
B <sub>2</sub> O <sub>3</sub>	-1.1722	0.5012	8.2817	2.6594	0.4980	0.8973	-3.5307
CaO	0.7554	-1.0702	-97.2024	-37.2667	-3.8171	0.4993	-0.3263
Fe <sub>2</sub> O <sub>3</sub>	-0.0338	0.6758	10.3567	3.2215	2.3793	0.7818	-0.6165
K <sub>2</sub> O	-0.4077	-0.3242	9.9114	4.5760	1.5515	-0.3460	-0.2495
Li <sub>2</sub> O	-2.5711	-1.8311	-144.7756	-23.1400	-49.3728	-0.2022	0.8258
MgO	0.8667	-0.6353	15.5091	4.3607	3.0783	1.2016	-0.2525
Na <sub>2</sub> O	-0.5657	-0.4966	-27.7001	-10.5266	-4.2848	0.3729	0.1631
SiO <sub>2</sub>	-0.1535	-0.4958	6.6834	2.2859	1.0436	0.4873	0.6690
ZrO <sub>2</sub>	11.0901	-0.5539	0.0352	-0.5814	2.1222	0.2378	1.3316
Others	-0.5539	4.5320	18.0251	5.4664	2.3364	0.3140	-0.4931
CaO×Li <sub>2</sub> O	0.0352	18.0251	1955.4791	445.9270	279.7517	0.8392	-0.0833
CaO×Na <sub>2</sub> O	-0.5814	5.4664	445.9270	214.7187	-20.8270	0.2132	0.0547
Li <sub>2</sub> O×Na <sub>2</sub> O	2.1222	2.3364	279.7517	-20.8270	295.9502	-0.0160	-0.1174
Al <sub>2</sub> O <sub>3</sub> /(T/1000)	0.2378	0.3140	0.8392	0.2132	-0.0160	10.2181	-1.2142
B <sub>2</sub> O <sub>3</sub> /(T/1000)	1.3316	-0.4931	-0.0833	0.0547	-0.1174	-1.2142	4.7895
CaO/(T/1000)	-0.8125	-0.0048	0.2714	0.0903	-0.0290	-0.7321	0.4311
Fe <sub>2</sub> O <sub>3</sub> /(T/1000)	0.0427	-0.6668	0.2092	0.0305	-0.0398	-1.0621	0.8387
K <sub>2</sub> O/(T/1000)	0.4556	0.5178	-0.0760	-0.0100	0.0342	0.4675	0.3314
Li <sub>2</sub> O/(T/1000)	2.7133	0.5798	-0.8599	-0.2373	-0.0166	0.2379	-1.0927
MgO/(T/1000)	-0.9862	0.9390	0.5694	0.1969	-0.0226	-1.6484	0.3250
Na <sub>2</sub> O/(T/1000)	0.6476	0.1982	-0.2141	-0.0500	-0.0316	-0.5099	-0.2228
SiO <sub>2</sub> /(T/1000)	0.1879	0.6645	-0.0733	-0.0355	0.0541	-0.6600	-0.9084
ZrO <sub>2</sub> /(T/1000)	-12.9040	0.6778	-0.0523	0.0289	0.0110	-0.3207	-1.7838
Others/(T/1000)	0.6765	-5.0739	-0.0016	-0.0585	-0.0907	-0.4295	0.6754



**Table D.9. Variance-Covariance Matrix Associated With the Estimated Coefficients of Terms in the 25-Term Arrhenius-Linear Mixture Model with Three Crossproduct Terms for ln(Electrical Conductivity, S/cm) of LAW Glasses (continued).**

Term	CaO/(T/1000)	Fe <sub>2</sub> O <sub>3</sub> /(T/1000)	K <sub>2</sub> O/(T/1000)	Li <sub>2</sub> O/(T/1000)	MgO/(T/1000)
Al <sub>2</sub> O <sub>3</sub>	0.5428	0.7772	-0.3493	-0.1538	1.1952
B <sub>2</sub> O <sub>3</sub>	-0.3195	-0.6154	-0.2504	0.8038	-0.2491
CaO	-2.6215	0.2666	-0.4489	1.2660	-1.0073
Fe <sub>2</sub> O <sub>3</sub>	0.2754	-3.1503	0.7530	-0.2552	-0.0067
K <sub>2</sub> O	-0.4498	0.7529	-5.4297	-0.9205	-2.2522
Li <sub>2</sub> O	1.2059	-0.2586	-0.9151	-13.1967	-0.5340
MgO	-0.9684	-0.0089	-2.2564	-0.5100	-12.2210
Na <sub>2</sub> O	-0.3947	0.1873	0.0078	-2.8923	-0.6549
SiO <sub>2</sub>	0.4317	0.3662	0.2585	0.9836	0.7407
ZrO <sub>2</sub>	-0.8125	0.0427	0.4556	2.7133	-0.9862
Others	-0.0048	-0.6668	0.5178	0.5798	0.9390
CaO×Li <sub>2</sub> O	0.2714	0.2092	-0.0760	-0.8599	0.5694
CaO×Na <sub>2</sub> O	0.0903	0.0305	-0.0100	-0.2373	0.1969
Li <sub>2</sub> O×Na <sub>2</sub> O	-0.0290	-0.0398	0.0342	-0.0166	-0.0226
Al <sub>2</sub> O <sub>3</sub> /(T/1000)	-0.7321	-1.0621	0.4675	0.2379	-1.6484
B <sub>2</sub> O <sub>3</sub> /(T/1000)	0.4311	0.8387	0.3314	-1.0927	0.3250
CaO/(T/1000)	3.5331	-0.3723	0.6086	-1.6551	1.3049
Fe <sub>2</sub> O <sub>3</sub> /(T/1000)	-0.3723	4.2851	-1.0248	0.3279	0.0132
K <sub>2</sub> O/(T/1000)	0.6086	-1.0248	7.3644	1.2568	3.0460
Li <sub>2</sub> O/(T/1000)	-1.6551	0.3279	1.2568	17.9774	0.7249
MgO/(T/1000)	1.3049	0.0132	3.0460	0.7249	16.5800
Na <sub>2</sub> O/(T/1000)	0.5282	-0.2595	-0.0097	3.9412	0.8847
SiO <sub>2</sub> /(T/1000)	-0.5827	-0.4972	-0.3498	-1.3476	-0.9958
ZrO <sub>2</sub> /(T/1000)	1.1093	-0.0539	-0.6020	-3.6868	1.3306
Others/(T/1000)	0.0053	0.9181	-0.6959	-0.7680	-1.2733

Term	Na <sub>2</sub> O/(T/1000)	SiO <sub>2</sub> /(T/1000)	ZrO <sub>2</sub> /(T/1000)	Others/(T/1000)
Al <sub>2</sub> O <sub>3</sub>	0.3837	0.4850	0.2397	0.3050
B <sub>2</sub> O <sub>3</sub>	0.1629	0.6685	1.3326	-0.4933
CaO	-0.3799	0.4366	-0.8151	0.0014
Fe <sub>2</sub> O <sub>3</sub>	0.1868	0.3658	0.0439	-0.6695
K <sub>2</sub> O	0.0067	0.2583	0.4558	0.5157
Li <sub>2</sub> O	-2.8888	0.9848	2.7148	0.5978
MgO	-0.6470	0.7382	-0.9854	0.9315
Na <sub>2</sub> O	-1.1510	0.3665	0.6460	0.2048
SiO <sub>2</sub>	0.3650	-0.6023	0.1876	0.6643
ZrO <sub>2</sub>	0.6476	0.1879	-12.9040	0.6765
Others	0.1982	0.6645	0.6778	-5.0739
CaO×Li <sub>2</sub> O	-0.2141	-0.0733	-0.0523	-0.0016
CaO×Na <sub>2</sub> O	-0.0500	-0.0355	0.0289	-0.0585
Li <sub>2</sub> O×Na <sub>2</sub> O	-0.0316	0.0541	0.0110	-0.0907
Al <sub>2</sub> O <sub>3</sub> /(T/1000)	-0.5099	-0.6600	-0.3207	-0.4295
B <sub>2</sub> O <sub>3</sub> /(T/1000)	-0.2228	-0.9084	-1.7838	0.6754
CaO/(T/1000)	0.5282	-0.5827	1.1093	0.0053
Fe <sub>2</sub> O <sub>3</sub> /(T/1000)	-0.2595	-0.4972	-0.0539	0.9181
K <sub>2</sub> O/(T/1000)	-0.0097	-0.3498	-0.6020	-0.6959
Li <sub>2</sub> O/(T/1000)	3.9412	-1.3476	-3.6868	-0.7680
MgO/(T/1000)	0.8847	-0.9958	1.3306	-1.2733
Na <sub>2</sub> O/(T/1000)	1.5664	-0.4982	-0.8797	-0.2651
SiO <sub>2</sub> /(T/1000)	-0.4982	0.8185	-0.2568	-0.9051
ZrO <sub>2</sub> /(T/1000)	-0.8797	-0.2568	17.5140	-0.9500
Others/(T/1000)	-0.2651	-0.9051	-0.9500	6.8928

**Table D.10. Variance-Covariance Matrix Associated With the Estimated Coefficients of Terms in the 24-Term Truncated T2-Linear Mixture Model for ln(Viscosity, poise) of LAW Glasses.**

Term	Al <sub>2</sub> O <sub>3</sub>	B <sub>2</sub> O <sub>3</sub>	CaO	Fe <sub>2</sub> O <sub>3</sub>	K <sub>2</sub> O	Li <sub>2</sub> O	MgO	Na <sub>2</sub> O	P <sub>2</sub> O <sub>5</sub>	SiO <sub>2</sub>	ZrO <sub>2</sub>	Others
Al <sub>2</sub> O <sub>3</sub>	2.6478	-0.3308	-0.2044	-0.2713	0.1488	0.0346	-0.4034	-0.1540	0.0754	-0.1553	-0.1284	-0.1303
B <sub>2</sub> O <sub>3</sub>	-0.3308	1.2482	0.1096	0.2230	0.0650	-0.3027	0.1085	-0.0590	-0.0655	-0.2363	-0.4893	0.2160
CaO	-0.2044	0.1096	0.9270	-0.1034	0.1946	-0.3986	0.3573	0.1479	0.2426	-0.1508	0.2718	-0.0379
Fe <sub>2</sub> O <sub>3</sub>	-0.2713	0.2230	-0.1034	1.0974	-0.2717	0.0963	-0.0098	-0.0624	0.0269	-0.1320	-0.0221	0.2701
K <sub>2</sub> O	0.1488	0.0650	0.1946	-0.2717	1.9508	0.4002	0.8097	0.0106	0.7117	-0.0767	-0.2074	-0.3981
Li <sub>2</sub> O	0.0346	-0.3027	-0.3986	0.0963	0.4002	4.6269	0.1475	1.0056	0.3725	-0.3175	-0.9762	-0.3899
MgO	-0.4034	0.1085	0.3573	-0.0098	0.8097	0.1475	4.2597	0.2202	-0.0272	-0.2603	0.3823	-0.3755
Na <sub>2</sub> O	-0.1540	-0.0590	0.1479	-0.0624	0.0106	1.0056	0.2202	0.4004	0.0280	-0.1215	-0.2326	-0.1001
P <sub>2</sub> O <sub>5</sub>	0.0754	-0.0655	0.2426	0.0269	0.7117	0.3725	-0.0272	0.0280	9.1543	-0.1067	-0.2857	-0.0415
SiO <sub>2</sub>	-0.1553	-0.2363	-0.1508	-0.1320	-0.0767	-0.3175	-0.2603	-0.1215	-0.1067	0.2084	-0.0550	-0.2608
ZrO <sub>2</sub>	-0.1284	-0.4893	0.2718	-0.0221	-0.2074	-0.9762	0.3823	-0.2326	-0.2857	-0.0550	4.5090	-0.1982
Others	-0.1303	0.2160	-0.0379	0.2701	-0.3981	-0.3899	-0.3755	-0.1001	-0.0415	-0.2608	-0.1982	2.2032
Al <sub>2</sub> O <sub>3</sub> /(T/1000) <sup>2</sup>	-2.9186	0.3739	0.2285	0.2964	-0.1650	-0.0489	0.4610	0.1695	-0.0859	0.1678	0.1484	0.1491
B <sub>2</sub> O <sub>3</sub> /(T/1000) <sup>2</sup>	0.3739	-1.3746	-0.1207	-0.2440	-0.0674	0.3375	-0.1177	0.0643	0.0788	0.2589	0.5379	-0.2405
CaO/(T/1000) <sup>2</sup>	0.2284	-0.1207	-1.0216	0.1146	-0.2147	0.4338	-0.3922	-0.1653	-0.2715	0.1669	-0.3002	0.0394
Fe <sub>2</sub> O <sub>3</sub> /(T/1000) <sup>2</sup>	0.2964	-0.2440	0.1146	-1.1976	0.2958	-0.0997	0.0125	0.0695	-0.0257	0.1441	0.0244	-0.3021
K <sub>2</sub> O/(T/1000) <sup>2</sup>	-0.1650	-0.0673	-0.2147	0.2957	-2.1338	-0.4517	-0.8820	-0.0133	-0.7859	0.0851	0.2270	0.4356
Li <sub>2</sub> O/(T/1000) <sup>2</sup>	-0.0488	0.3375	0.4339	-0.0997	-0.4516	-5.0752	-0.1794	-1.1018	-0.4102	0.3482	1.0753	0.4313
MgO/(T/1000) <sup>2</sup>	0.4609	-0.1176	-0.3922	0.0126	-0.8821	-0.1794	-4.6799	-0.2479	0.0270	0.2867	-0.4375	0.4121
Na <sub>2</sub> O/(T/1000) <sup>2</sup>	0.1695	0.0643	-0.1653	0.0694	-0.0133	-1.1018	-0.2479	-0.4400	-0.0331	0.1339	0.2563	0.1103
P <sub>2</sub> O <sub>5</sub> /(T/1000) <sup>2</sup>	-0.0859	0.0788	-0.2715	-0.0257	-0.7859	-0.4101	0.0269	-0.0332	-9.9955	0.1183	0.3198	0.0347
SiO <sub>2</sub> /(T/1000) <sup>2</sup>	0.1678	0.2589	0.1669	0.1440	0.0851	0.3482	0.2867	0.1339	0.1183	-0.2285	0.0584	0.2868
ZrO <sub>2</sub> /(T/1000) <sup>2</sup>	0.1483	0.5379	-0.3002	0.0243	0.2271	1.0752	-0.4374	0.2563	0.3199	0.0585	-4.9718	0.2380
Others/(T/1000) <sup>2</sup>	0.1490	-0.2406	0.0393	-0.3020	0.4355	0.4314	0.4119	0.1104	0.0349	0.2868	0.2381	-2.4273

Term	Al <sub>2</sub> O <sub>3</sub> /(T/1000) <sup>2</sup>	B <sub>2</sub> O <sub>3</sub> /(T/1000) <sup>2</sup>	CaO/(T/1000) <sup>2</sup>	Fe <sub>2</sub> O <sub>3</sub> /(T/1000) <sup>2</sup>	K <sub>2</sub> O/(T/1000) <sup>2</sup>	Li <sub>2</sub> O/(T/1000) <sup>2</sup>
Al <sub>2</sub> O <sub>3</sub>	-2.9186	0.3739	0.2284	0.2964	-0.1650	-0.0488
B <sub>2</sub> O <sub>3</sub>	0.3739	-1.3746	-0.1207	-0.2440	-0.0673	0.3375
CaO	0.2285	-0.1207	-1.0216	0.1146	-0.2147	0.4339
Fe <sub>2</sub> O <sub>3</sub>	0.2964	-0.2440	0.1146	-1.1976	0.2957	-0.0997
K <sub>2</sub> O	-0.1650	-0.0674	-0.2147	0.2958	-2.1338	-0.4516
Li <sub>2</sub> O	-0.0489	0.3375	0.4338	-0.0997	-0.4517	-5.0752
MgO	0.4610	-0.1177	-0.3922	0.0125	-0.8820	-0.1794
Na <sub>2</sub> O	0.1695	0.0643	-0.1653	0.0695	-0.0133	-1.1018
P <sub>2</sub> O <sub>5</sub>	-0.0859	0.0788	-0.2715	-0.0257	-0.7859	-0.4102
SiO <sub>2</sub>	0.1678	0.2589	0.1669	0.1441	0.0851	0.3482
ZrO <sub>2</sub>	0.1484	0.5379	-0.3002	0.0244	0.2270	1.0753
Others	0.1491	-0.2405	0.0394	-0.3021	0.4356	0.4313
Al <sub>2</sub> O <sub>3</sub> /(T/1000) <sup>2</sup>	5.3847	-0.7000	-0.4233	-0.5424	0.3045	0.1062
B <sub>2</sub> O <sub>3</sub> /(T/1000) <sup>2</sup>	-0.7000	2.5360	0.2214	0.4483	0.1182	-0.6185
CaO/(T/1000) <sup>2</sup>	-0.4233	0.2214	1.8849	-0.2116	0.3946	-0.7986
Fe <sub>2</sub> O <sub>3</sub> /(T/1000) <sup>2</sup>	-0.5424	0.4483	-0.2116	2.2038	-0.5460	0.1782
K <sub>2</sub> O/(T/1000) <sup>2</sup>	0.3045	0.1182	0.3946	-0.5460	3.9351	0.8417
Li <sub>2</sub> O/(T/1000) <sup>2</sup>	0.1062	-0.6185	-0.7986	0.1782	0.8417	9.3461
MgO/(T/1000) <sup>2</sup>	-0.8538	0.2154	0.7192	-0.0218	1.6194	0.3556
Na <sub>2</sub> O/(T/1000) <sup>2</sup>	-0.3089	-0.1159	0.3058	-0.1286	0.0249	2.0267
P <sub>2</sub> O <sub>5</sub> /(T/1000) <sup>2</sup>	0.1541	-0.1503	0.4999	0.0486	1.4509	0.7568
SiO <sub>2</sub> /(T/1000) <sup>2</sup>	-0.3075	-0.4769	-0.3072	-0.2659	-0.1558	-0.6461
ZrO <sub>2</sub> /(T/1000) <sup>2</sup>	-0.2842	-0.9953	0.5534	-0.0442	-0.4136	-1.9791
Others/(T/1000) <sup>2</sup>	-0.2844	0.4477	-0.0752	0.5646	-0.8042	-0.7806

**Table D.10. Variance-Covariance Matrix Associated With the Estimated Coefficients of Terms in the 24-Term Truncated T2-Linear Mixture Model for ln(Viscosity, poise) of LAW Glasses (continued).**

Term	MgO/(T/1000) <sup>2</sup>	Na <sub>2</sub> O/(T/1000) <sup>2</sup>	P <sub>2</sub> O <sub>5</sub> /(T/1000) <sup>2</sup>	SiO <sub>2</sub> /(T/1000) <sup>2</sup>	ZrO <sub>2</sub> /(T/1000) <sup>2</sup>	Others/(T/1000) <sup>2</sup>
Al <sub>2</sub> O <sub>3</sub>	0.4609	0.1695	-0.0859	0.1678	0.1483	0.1490
B <sub>2</sub> O <sub>3</sub>	-0.1176	0.0643	0.0788	0.2589	0.5379	-0.2406
CaO	-0.3922	-0.1653	-0.2715	0.1669	-0.3002	0.0393
Fe <sub>2</sub> O <sub>3</sub>	0.0126	0.0694	-0.0257	0.1440	0.0243	-0.3020
K <sub>2</sub> O	-0.8821	-0.0133	-0.7859	0.0851	0.2271	0.4355
Li <sub>2</sub> O	-0.1794	-1.1018	-0.4101	0.3482	1.0752	0.4314
MgO	-4.6799	-0.2479	0.0269	0.2867	-0.4374	0.4119
Na <sub>2</sub> O	-0.2479	-0.4400	-0.0332	0.1339	0.2563	0.1104
P <sub>2</sub> O <sub>5</sub>	0.0270	-0.0331	-9.9955	0.1183	0.3199	0.0349
SiO <sub>2</sub>	0.2867	0.1339	0.1183	-0.2285	0.0585	0.2868
ZrO <sub>2</sub>	-0.4375	0.2563	0.3198	0.0584	-4.9718	0.2381
Others	0.4121	0.1103	0.0347	0.2868	0.2380	-2.4273
Al <sub>2</sub> O <sub>3</sub> /(T/1000) <sup>2</sup>	-0.8538	-0.3089	0.1541	-0.3075	-0.2842	-0.2844
B <sub>2</sub> O <sub>3</sub> /(T/1000) <sup>2</sup>	0.2154	-0.1159	-0.1503	-0.4769	-0.9953	0.4477
CaO/(T/1000) <sup>2</sup>	0.7192	0.3058	0.4999	-0.3072	0.5534	-0.0752
Fe <sub>2</sub> O <sub>3</sub> /(T/1000) <sup>2</sup>	-0.0218	-0.1286	0.0486	-0.2659	-0.0442	0.5646
K <sub>2</sub> O/(T/1000) <sup>2</sup>	1.6194	0.0249	1.4509	-0.1558	-0.4136	-0.8042
Li <sub>2</sub> O/(T/1000) <sup>2</sup>	0.3556	2.0267	0.7568	-0.6461	-1.9791	-0.7806
MgO/(T/1000) <sup>2</sup>	8.6165	0.4625	-0.0501	-0.5286	0.8154	-0.7708
Na <sub>2</sub> O/(T/1000) <sup>2</sup>	0.4625	0.8107	0.0605	-0.2484	-0.4716	-0.2001
P <sub>2</sub> O <sub>5</sub> /(T/1000) <sup>2</sup>	-0.0501	0.0605	18.5226	-0.2162	-0.5928	-0.0668
SiO <sub>2</sub> /(T/1000) <sup>2</sup>	-0.5286	-0.2484	-0.2162	0.4212	-0.1036	-0.5289
ZrO <sub>2</sub> /(T/1000) <sup>2</sup>	0.8154	-0.4716	-0.5928	-0.1036	9.1693	-0.4603
Others/(T/1000) <sup>2</sup>	-0.7708	-0.2001	-0.0668	-0.5289	-0.4603	4.4768

**Table D.11. Variance-Covariance Matrix Associated With the Estimated Coefficients of Terms in the Recommended 26-Term Truncated T2-Linear Mixture Model with Four Quadratic Terms for ln(Viscosity, P) of LAW Glasses.**

Term	Al <sub>2</sub> O <sub>3</sub>	B <sub>2</sub> O <sub>3</sub>	CaO	Fe <sub>2</sub> O <sub>3</sub>	K <sub>2</sub> O	Li <sub>2</sub> O	MgO	Na <sub>2</sub> O	P <sub>2</sub> O <sub>5</sub>	SiO <sub>2</sub>
Al <sub>2</sub> O <sub>3</sub>	4.3931	-4.2122	-0.1233	-0.0843	0.0498	4.6732	0.6928	-0.1107	-0.0789	-0.0429
B <sub>2</sub> O <sub>3</sub>	-4.2122	47.1379	-1.8275	-2.2280	-1.7454	-3.3764	-20.4729	-1.9214	-0.5171	-2.2502
CaO	-0.1233	-1.8275	0.9674	0.0108	0.1916	-0.7363	1.9764	0.2159	0.2320	-0.0453
Fe <sub>2</sub> O <sub>3</sub>	-0.0843	-2.2280	0.0108	1.0795	0.0179	0.1230	1.2104	0.0502	0.1245	0.0050
K <sub>2</sub> O	0.0498	-1.7454	0.1916	0.0179	0.8756	0.2793	2.5447	0.0852	0.2515	0.0266
Li <sub>2</sub> O	4.6732	-3.3764	-0.7363	0.1230	0.2793	20.7045	-0.1117	0.7659	-0.3392	-0.4024
MgO	0.6928	-20.4729	1.9764	1.2104	2.5447	-0.1117	30.4968	1.0138	0.2125	0.4123
Na <sub>2</sub> O	-0.1107	-1.9214	0.2159	0.0502	0.0852	0.7659	1.0138	0.4543	0.0486	-0.0246
P <sub>2</sub> O <sub>5</sub>	-0.0789	-0.5171	0.2320	0.1245	0.2515	-0.3392	0.2125	0.0486	8.2711	-0.0620
SiO <sub>2</sub>	-0.0429	-2.2502	-0.0453	0.0050	0.0266	-0.4024	0.4123	-0.0246	-0.0620	0.2754
ZrO <sub>2</sub>	-0.0615	-2.1771	0.2763	0.1063	-0.1280	-0.8618	-0.5144	-0.1311	-0.2324	0.0220
Others	-0.2520	-1.2726	0.0602	0.2731	-0.0457	-1.0501	0.5974	-0.0078	0.1048	-0.1523
(B <sub>2</sub> O <sub>3</sub> ) <sup>2</sup>	20.3262	-249.5197	9.9237	12.3605	9.4277	13.5252	107.9026	10.2913	2.7664	11.6977
(Li <sub>2</sub> O) <sup>2</sup>	0.0997	-12.1963	4.2240	-0.1684	-9.1920	-93.4991	-10.9375	-0.4836	4.7339	2.5586
Al <sub>2</sub> O <sub>3</sub> ×Li <sub>2</sub> O	-75.9624	50.2923	2.8455	1.3714	5.7603	-190.3501	17.3764	3.3875	5.5647	-0.1315
(MgO) <sup>2</sup>	-27.1251	390.6125	-33.5639	-21.9405	-44.4567	-8.3165	-534.4482	-14.7794	-7.7473	-11.2139
Al <sub>2</sub> O <sub>3</sub> /(T/1000) <sup>2</sup>	-2.7928	-0.0012	0.2130	0.2020	0.0001	0.0764	0.5136	0.1879	0.0040	0.2319
CaO/(T/1000) <sup>2</sup>	0.2113	-0.0023	-0.9869	0.1058	0.0003	0.4454	-0.2894	-0.1686	-0.2004	0.1368
Fe <sub>2</sub> O <sub>3</sub> /(T/1000) <sup>2</sup>	0.2016	-0.0045	0.1043	-1.1063	-0.0008	-0.2253	-0.1139	0.0560	-0.1533	0.1090
Li <sub>2</sub> O/(T/1000) <sup>2</sup>	0.0822	0.0065	0.4475	-0.2271	-0.0005	-4.8829	-0.0575	-1.0790	-0.2152	0.3947
MgO/(T/1000) <sup>2</sup>	0.5041	-0.0094	-0.2921	-0.0913	0.0014	-0.0124	-4.2316	-0.2458	0.3431	0.2332
Na <sub>2</sub> O/(T/1000) <sup>2</sup>	0.1874	0.0016	-0.1692	0.0557	-0.0009	-1.0799	-0.2568	-0.4355	-0.0234	0.1449
P <sub>2</sub> O <sub>5</sub> /(T/1000) <sup>2</sup>	-0.0002	0.0554	-0.2028	-0.1564	-0.0020	-0.2204	0.3159	-0.0256	-9.6661	0.1036
SiO <sub>2</sub> /(T/1000) <sup>2</sup>	0.2305	0.0005	0.1368	0.1083	0.0001	0.3919	0.2358	0.1450	0.1060	-0.1768
ZrO <sub>2</sub> /(T/1000) <sup>2</sup>	0.2824	0.0072	-0.3680	-0.0435	-0.0013	1.1774	-0.5962	0.2783	0.2752	0.1662
Others/(T/1000) <sup>2</sup>	0.0521	-0.0081	0.0177	-0.1935	0.0019	0.2932	0.2725	0.0950	-0.1446	0.2553

**Table D.11. Variance-Covariance Matrix Associated With the Estimated Coefficients of Terms in the Recommended 26-Term Truncated T2-Linear Mixture Model with Four Quadratic Terms for ln(Viscosity, P) of LAW Glasses (continued).**

Term	ZrO <sub>2</sub>	Others	(B <sub>2</sub> O <sub>3</sub> ) <sup>2</sup>	(Li <sub>2</sub> O) <sup>2</sup>	Al <sub>2</sub> O <sub>3</sub> ×Li <sub>2</sub> O	(MgO) <sup>2</sup>
Al <sub>2</sub> O <sub>3</sub>	-0.0615	-0.2520	20.3262	0.0997	-75.9624	-27.1251
B <sub>2</sub> O <sub>3</sub>	-2.1771	-1.2726	-249.5197	-12.1963	50.2923	390.6125
CaO	0.2763	0.0602	9.9237	4.2240	2.8455	-33.5639
Fe <sub>2</sub> O <sub>3</sub>	0.1063	0.2731	12.3605	-0.1684	1.3714	-21.9405
K <sub>2</sub> O	-0.1280	-0.0457	9.4277	-9.1920	5.7603	-44.4567
Li <sub>2</sub> O	-0.8618	-1.0501	13.5252	-93.4991	-190.3501	-8.3165
MgO	-0.5144	0.5974	107.9026	-10.9375	17.3764	-534.4482
Na <sub>2</sub> O	-0.1311	-0.0078	10.2913	-0.4836	3.3875	-14.7794
P <sub>2</sub> O <sub>5</sub>	-0.2324	0.1048	2.7664	4.7339	5.5647	-7.7473
SiO <sub>2</sub>	0.0220	-0.1523	11.6977	2.5586	-0.1315	-11.2139
ZrO <sub>2</sub>	4.3076	-0.1032	11.0765	0.1008	-0.7979	21.0534
Others	-0.1032	2.0486	7.4392	1.5422	11.7642	-15.3621
(B <sub>2</sub> O <sub>3</sub> ) <sup>2</sup>	11.0765	7.4392	1334.1445	61.0130	-199.7892	-2044.9113
(Li <sub>2</sub> O) <sup>2</sup>	0.1008	1.5422	61.0130	1865.1464	-51.5337	113.7300
Al <sub>2</sub> O <sub>3</sub> ×Li <sub>2</sub> O	-0.7979	11.7642	-199.7892	-51.5337	3142.4026	-64.0502
(MgO) <sup>2</sup>	21.0534	-15.3621	-2044.9113	113.7300	-64.0502	10718.1194
Al <sub>2</sub> O <sub>3</sub> /(T/1000) <sup>2</sup>	0.2772	0.0446	-0.0209	0.0292	0.0986	-0.2344
CaO/(T/1000) <sup>2</sup>	-0.3660	0.0170	0.0117	-0.0295	0.0783	-0.1081
Fe <sub>2</sub> O <sub>3</sub> /(T/1000) <sup>2</sup>	-0.0387	-0.1942	0.0219	-0.0963	0.0713	0.4542
Li <sub>2</sub> O/(T/1000) <sup>2</sup>	1.1620	0.2724	-0.0139	0.2143	-0.0200	0.8846
MgO/(T/1000) <sup>2</sup>	-0.5703	0.2492	0.0437	-0.0437	-0.0298	-1.3377
Na <sub>2</sub> O/(T/1000) <sup>2</sup>	0.2795	0.0955	0.0009	0.0233	-0.0073	0.2273
P <sub>2</sub> O <sub>5</sub> /(T/1000) <sup>2</sup>	0.2737	-0.1465	-0.3035	0.0376	0.0266	0.5350
SiO <sub>2</sub> /(T/1000) <sup>2</sup>	0.1657	0.2560	-0.0007	0.0171	0.0282	-0.0353
ZrO <sub>2</sub> /(T/1000) <sup>2</sup>	-4.7238	0.1832	-0.0509	-0.0321	-0.2577	0.6372
Others/(T/1000) <sup>2</sup>	0.1827	-2.2841	0.0410	-0.0521	-0.2877	-0.5317

**Table D.11. Variance-Covariance Matrix Associated With the Estimated Coefficients of Terms in the Recommended 26-Term Truncated T2-Linear Mixture Model with Four Quadratic Terms for ln(Viscosity, P) of LAW Glasses (continued).**

Term	Al <sub>2</sub> O <sub>3</sub> /(T/1000) <sup>2</sup>	CaO/(T/1000) <sup>2</sup>	Fe <sub>2</sub> O <sub>3</sub> /(T/1000) <sup>2</sup>	Li <sub>2</sub> O/(T/1000) <sup>2</sup>	MgO/(T/1000) <sup>2</sup>
Al <sub>2</sub> O <sub>3</sub>	-2.7928	0.2113	0.2016	0.0822	0.5041
B <sub>2</sub> O <sub>3</sub>	-0.0012	-0.0023	-0.0045	0.0065	-0.0094
CaO	0.2130	-0.9869	0.1043	0.4475	-0.2921
Fe <sub>2</sub> O <sub>3</sub>	0.2020	0.1058	-1.1063	-0.2271	-0.0913
K <sub>2</sub> O	0.0001	0.0003	-0.0008	-0.0005	0.0014
Li <sub>2</sub> O	0.0764	0.4454	-0.2253	-4.8829	-0.0124
MgO	0.5136	-0.2894	-0.1139	-0.0575	-4.2316
Na <sub>2</sub> O	0.1879	-0.1686	0.0560	-1.0790	-0.2458
P <sub>2</sub> O <sub>5</sub>	0.0040	-0.2004	-0.1533	-0.2152	0.3431
SiO <sub>2</sub>	0.2319	0.1368	0.1090	0.3947	0.2332
ZrO <sub>2</sub>	0.2772	-0.3660	-0.0387	1.1620	-0.5703
Others	0.0446	0.0170	-0.1942	0.2724	0.2492
(B <sub>2</sub> O <sub>3</sub> ) <sup>2</sup>	-0.0209	0.0117	0.0219	-0.0139	0.0437
(Li <sub>2</sub> O) <sup>2</sup>	0.0292	-0.0295	-0.0963	0.2143	-0.0437
Al <sub>2</sub> O <sub>3</sub> ×Li <sub>2</sub> O	0.0986	0.0783	0.0713	-0.0200	-0.0298
(MgO) <sup>2</sup>	-0.2344	-0.1081	0.4542	0.8846	-1.3377
Al <sub>2</sub> O <sub>3</sub> /(T/1000) <sup>2</sup>	5.1453	-0.3937	-0.3688	-0.1387	-0.9292
CaO/(T/1000) <sup>2</sup>	-0.3937	1.8219	-0.1946	-0.8270	0.5412
Fe <sub>2</sub> O <sub>3</sub> /(T/1000) <sup>2</sup>	-0.3688	-0.1946	2.0360	0.4119	0.1716
Li <sub>2</sub> O/(T/1000) <sup>2</sup>	-0.1387	-0.8270	0.4119	8.9724	0.0513
MgO/(T/1000) <sup>2</sup>	-0.9292	0.5412	0.1716	0.0513	7.9128
Na <sub>2</sub> O/(T/1000) <sup>2</sup>	-0.3424	0.3119	-0.1034	1.9851	0.4583
P <sub>2</sub> O <sub>5</sub> /(T/1000) <sup>2</sup>	-0.0127	0.3693	0.2845	0.3957	-0.6325
SiO <sub>2</sub> /(T/1000) <sup>2</sup>	-0.4263	-0.2516	-0.2002	-0.7304	-0.4320
ZrO <sub>2</sub> /(T/1000) <sup>2</sup>	-0.5259	0.6740	0.0786	-2.1333	1.0470
Others/(T/1000) <sup>2</sup>	-0.0898	-0.0334	0.3652	-0.4870	-0.4692

**Table D.11. Variance-Covariance Matrix Associated With the Estimated Coefficients of Terms in the Recommended 26-Term Truncated T2-Linear Mixture Model with Four Quadratic Terms for ln(Viscosity, P) of LAW Glasses (continued).**

Term	Na <sub>2</sub> O/(T/1000) <sup>2</sup>	P <sub>2</sub> O <sub>5</sub> /(T/1000) <sup>2</sup>	SiO <sub>2</sub> /(T/1000) <sup>2</sup>	ZrO <sub>2</sub> /(T/1000) <sup>2</sup>	Others/(T/1000) <sup>2</sup>
Al <sub>2</sub> O <sub>3</sub>	0.1874	-0.0002	0.2305	0.2824	0.0521
B <sub>2</sub> O <sub>3</sub>	0.0016	0.0554	0.0005	0.0072	-0.0081
CaO	-0.1692	-0.2028	0.1368	-0.3680	0.0177
Fe <sub>2</sub> O <sub>3</sub>	0.0557	-0.1564	0.1083	-0.0435	-0.1935
K <sub>2</sub> O	-0.0009	-0.0020	0.0001	-0.0013	0.0019
Li <sub>2</sub> O	-1.0799	-0.2204	0.3919	1.1774	0.2932
MgO	-0.2568	0.3159	0.2358	-0.5962	0.2725
Na <sub>2</sub> O	-0.4355	-0.0256	0.1450	0.2783	0.0950
P <sub>2</sub> O <sub>5</sub>	-0.0234	-9.6661	0.1060	0.2752	-0.1446
SiO <sub>2</sub>	0.1449	0.1036	-0.1768	0.1662	0.2553
ZrO <sub>2</sub>	0.2795	0.2737	0.1657	-4.7238	0.1827
Others	0.0955	-0.1465	0.2560	0.1832	-2.2841
(B <sub>2</sub> O <sub>3</sub> ) <sup>2</sup>	0.0009	-0.3035	-0.0007	-0.0509	0.0410
(Li <sub>2</sub> O) <sup>2</sup>	0.0233	0.0376	0.0171	-0.0321	-0.0521
Al <sub>2</sub> O <sub>3</sub> ×Li <sub>2</sub> O	-0.0073	0.0266	0.0282	-0.2577	-0.2877
(MgO) <sup>2</sup>	0.2273	0.5350	-0.0353	0.6372	-0.5317
Al <sub>2</sub> O <sub>3</sub> /(T/1000) <sup>2</sup>	-0.3424	-0.0127	-0.4263	-0.5259	-0.0898
CaO/(T/1000) <sup>2</sup>	0.3119	0.3693	-0.2516	0.6740	-0.0334
Fe <sub>2</sub> O <sub>3</sub> /(T/1000) <sup>2</sup>	-0.1034	0.2845	-0.2002	0.0786	0.3652
Li <sub>2</sub> O/(T/1000) <sup>2</sup>	1.9851	0.3957	-0.7304	-2.1333	-0.4870
MgO/(T/1000) <sup>2</sup>	0.4583	-0.6325	-0.4320	1.0470	-0.4692
Na <sub>2</sub> O/(T/1000) <sup>2</sup>	0.8025	0.0422	-0.2683	-0.5126	-0.1727
P <sub>2</sub> O <sub>5</sub> /(T/1000) <sup>2</sup>	0.0422	17.9128	-0.1942	-0.5139	0.2648
SiO <sub>2</sub> /(T/1000) <sup>2</sup>	-0.2683	-0.1942	0.3259	-0.3022	-0.4711
ZrO <sub>2</sub> /(T/1000) <sup>2</sup>	-0.5126	-0.5139	-0.3022	8.7153	-0.3605
Others/(T/1000) <sup>2</sup>	-0.1727	0.2648	-0.4711	-0.3605	4.2105